Assessment of the potential interactions of an oil spill with sediments on the west coast of New Zealand

A thesis

submitted in partial fulfilment

of the requirements for the degree

of

Master of Science

in Earth Sciences

at

The University of Waikato

by

JUSTINE ARIKI PARK

THE UNIVERSITY OF

WAIKATO

Te Whare Wānanga o Waikato

2016

For Olive and Louise.

You were always there for me.

I love you.

ABSTRACT

There are limited data available on the interaction of spilt oil and sediment commonly found on New Zealand beaches and the data available have been obtained for intermediate state east coast beaches. The west coast of New Zealand's north island generally has higher energy dissipative to ultra-dissipative beaches.

Physical mixing of oil with beach sediment depends on both the depth of penetration into sediment and surface elevation changes. This study assessed physical mixing depths on three contrasting beaches; a highly dissipative open coast beach, a tidally controlled beach and a sheltered estuarine beach. Estimated and measured forcing conditions were correlated with vertical maxima of disturbance. The use of spatially discrete, non-averaged measurements of the depth of disturbance allowed spatial variation to be interpreted. Surface elevation changes were evaluated in conjunction with depth of disturbance measurements which allowed morphological features to be correlated with mixing depths alongshore and crosshore. Measurement of large scale morphological change also allowed interpretation of maximum potential oil burial depths. Oil settling experiments were carried out to evaluate oil settling times and behaviours.

Morphological response is a function of changing incident wave regimes, currents, pre-existing morphology and tidal range. Large-scale erosive events have been recorded and observed at Ngarunui Beach that change the bed elevation in excess of 5 m, while small bed level variation occurs on the scale of decimetres during each tidal cycle. It was found that disturbance depths varied substantially in the cross-shore and longshore during all experiments. Wave breaking was determined to be the main mechanism for sediment mixing. Hence, the significant variation across the beach is attributed to the complex morphology of the beach.

The areas most exposed to wave breaking exhibited the most disturbance at Ngarunui Beach; larger values of disturbance in the mid intertidal zone at

Ngarunui Beach correspond with the zone that is most exposed to wave breaking. Cross-shore bimodal distributions of mixing were not observed. Swash processes dominated in the high intertidal zone with accretion occurring during spring tides however swash processes have limited effects on this beach, with mixing values greatly reduced under these processes. A tidally controlled beach located within the estuary close to the harbour entrance experienced significantly larger mixing depth values when no waves were present due in part to stronger currents and greater inundation during spring tides. The sheltered estuarine beach within the harbour experienced minimal mixing depths.

Values for the vertical limits of the mixing layer exceed 40 % of the breaking wave height, Hb, for reflective beaches, while on dissipative beaches, theory predicts that the values will be extremely reduced as wave energies are dispersed across wide surf zones. However, in this study, disturbance values were higher than those previously reported in the literature for dissipative beaches. Using parameters for wave obliquity and beach slope, the average mixing depths could be somewhat predicted using the method of Bertin et al. (2008). Significant variation between and within locations means that use of this model could significantly underestimate depths of disturbance and hence oil burial on the west coast of New Zealand's North Island.

Assessment of the interactions between oil and sediment in the laboratory indicated preferential bonding of oil with heavy minerals common on west coast New Zealand beaches. This implies that oil is more likely to form stable oil-mineral aggregates on west coast beaches compared to east coast beaches with low heavy mineral content.

ACKNOWLEDGEMENTS

I would like to extend my deepest gratitude to my supervisor, Willem de Lange, for his on-going support, his concise feedback and his continued responses to my multitude of questions. I wish also to extend my thanks to Karin Bryan, for providing another perspective and for the rectification software.

I would like to acknowledge the financial support I have received from Ngati Rarua Ati Awa Iwi Trust over the duration of my studies, from the New Horizons for Women Trust and from the OMV group. Without this assistance life would have been exceedingly difficult.

Big thanks to Dean Sandwell for his consistent interest; an excellent field technician and a great help with scripts, data auditing and keeping me in-the-loop. Thanks to Ron Ovenden and Andrew Wood for sharing with me their intellectual property; both the beach profiles and Ron's comprehensive knowledge of the Ngarunui Beach system. Thank you to Tex Rickard and the Rickard whanau for allowing me direct access to the Wainamu Beach site.

I wish to thank Shawn Harrison for being so approachable and helping with the rectification software when he had so much on his plate. I would also like to thank Dougal Greer at eCoast for helping me with MATLAB and for providing the numerical modelling. I am grateful to Amir Emami, Shari Gallop and Karin Bryan for allowing me access to VRS data and Rafael Guedes for rectification software. A special mention to Renat Radionsky for making me extra rods, to Annette Rodgers and Janine Ryburn for instruction on the use of the Mastersizer and to Cheryl Ward for so much help with formatting.

Thank you to Joseph Coyle at OMV and Chris Battershill from the University of Waikato for providing oil samples for me to test. For allowing me use of and giving me instruction on the Cawthron Institute's stereoscope, I would like to acknowledge Fiona Gower and Brett Thompson.

Thanks too to all the other friends and family who stood in as field assistants and provided support over the past two years; Wainui Witika-Park, Finn Kingi, Jahvik Leng-Ware, Zahara Leng-Ware, Charlotte Ashton, Denise Fort, Ben Galloway, Suzette Drew, Asha Rodger, Alisha Hosking, Sascha Philips and Sarah Corner aka ‘The Snaz’. You all provided great usefulness, laughs and lunch sometimes.

I would also like to thank my family; my mum Wendy, Mike, Ems, Wainui,and aunty Vik, for all their support, time and love. For eating toast for dinner while I was busy, I must acknowledge my son, Sam (Bug) Park. I love you.

Last, but not least, I would like to thank my wonderful partner, Daza Fraza, who spent numerous early mornings on the beach cold, wet and thirsty. Without you this project would never have been completed. Your tremendous help and ongoing support is so very much appreciated. I love you too!!

TABLE OF CONTENTS

LIST OF FIGURES

LIST OF TABLES

CHAPTER ONE: INTRODUCTION

1.0 PROBLEM BACKGROUND

Determination of sediment fluxes during tidal cycles or storm events and longshore sediment transport is essential for the; design of beach replenishment schemes; prediction of bed scouring at the base of structures; estimation of erosion of buried underwater bedrocks in coastal engineering; viability of substrate as marine faunal egg laying grounds; and importantly for contaminant depth of burial and dispersal (Anfuso, 2005, Ciavola et al, 1997).

Spilled oil may drift large distances before impacting a long length of coast remote from the original spill site (Lewis, 2002). When a spill occurs, heavier weight components will agglomerate, sink and/or float depending on the characteristics of the spilt oil (de Groot, 2014). The response to spills of heavier oils often becomes a shoreline clean-up operation with high compensation and clean-up costs (Lewis, 2002). Human intervention for clean-up of spills can result in impacts that are greater than those of the spill, such as damage to vulnerable dune areas (ITOPF, 2014c). The environmental toll of spilled oil is a function of the oil type, the specific sensitivity of the area affected and the time of exposure (NRC, 2003).

Persistence of buried oil is viewed as concerning as major pollutant source (Bernabeu et al., 2006). Baseline data can aid in rapid decision making and improves the effectiveness of any oil spill response (Andrade et al., 2012). Understanding of the cross-shore patterns of oil burial is integral for limiting environmental damage and in reducing costs (Wang and Roberts, 2010). Temporal shifts in depths of disturbance related to storm and fair weather conditions will also help to elucidate potential burial pathways/depths.

New Zealand’s current permissive climate for oil exploration permits means there is a need for effective safety procedures and comprehensive understanding of the processes involved in dispersion and depth of burial of oil in the oceans and around the coasts of New Zealand. The potential for oil spills is expected to increase with increased exploration (Maritime New Zealand, 2015). In light of the recent foundering of the cargo ship *Rena* upon the Astrolabe Reef in the Bay of Plenty, examination of depth of activity on New Zealand beaches is pertinent, particularly as oil residuals may be exhumed periodically (NRC, 2003). Little is known about how high energy, titanomagnetite rich sand beaches such as those on New Zealand's west coast could be affected by an oil spill. Ngarunui Beach is a popular recreational beach on the west coast(Patel, 2015), which could be adversely affected by an oil spill.

There are over 100,000 organic and inorganic hydrocarbons of various molecular weights contained in crude oil (NRC, 2003). Because of physical and chemical transformations in spilled oil characteristics due to weathering, the National Oceanic and Atmospheric Administration Office of Response and Restoration (NOAA OR&R) has developed an Automated Data Inquiry for Oil Spills (ADIOS). This model is used by the Maritime NZ to predict changes in spilled oil characteristics such as evaporation, dispersion and mousse formation, density, viscosity, and water content of an oil or product (Taranaki Regional Council, 2008). Hence, the package also estimates when the effectiveness of dispersants will be reduced. The oil types transported around New Zealand coastal waters are registered in the ADIOS library.

When oil comes into contact with beach sediments it may form oil sheets, clump into tar globules or smaller patches and it may become coated around the surface of the individual sediment grains (Delvigne, 2002). Wave action then disturbs the sediment and has the potential to bury the oil either by shifting the relative position of entrained sediment grains or by deposition under freshly accreted sediment (Bernabeu et al., 2006). In this way oil can be buried far deeper than by simple gravity induced seepage and swash infiltration especially when it is of high viscosity and high wave and current energies are present. Chemical and physical processes remove oil from the environment. This study focuses on the mechanical burial of oil. The deeper oil is buried on beaches, the longer it can remain and during large storm events with strong onshore winds and associated wave and wind energy it may resurface, having potential catastrophic consequences for marine flora and fauna and their habitats. The recreational value of beaches is also adversely affected by the highly toxic nature of oil (NRC, 2003).

Because of the cohesion of oil within pore spaces of sand and the subsequent stabilisation of sediment parcels, the morphological behaviour within beach profiles is modified. Conversely intergranular friction between grains of sand may be reduced due to lubrication by oil residue, which may destabilise the sediment parcels (Bernabeu et al., 2006). Previous research on the effects of oil on sediment cohesion of sand grains has focused on deltaic sediments. Limited work has been done on the effect of oil on cohesion on fine-medium sands and those with high concentrations of titaniferous oxide sands. Understanding of beach morphology, wave climate and the nature of cohesion/intergranular friction of oil sands is fundamental for establishing anticipated mixing and burial pathways.

Figure 1.1: **Photograph of Ngarunui Beach during a storm event illustrating the energetic conditions of the beach.**

After Bertin et al. (2008) the mixing depths for dissipative sandy beaches is ~ 2 – 4 % of significant wave height. However, this determination may not apply to ultra-dissipative West Coast beaches in New Zealand, and storm events, groundwater, and swash infiltration may also modify mixing depths. Further, the interactions between oil and sediments can vary depending on the type of sediment, particularly the mineral composition. An evaluation of mixing depths on a high energy dissipative titanomagnetite beach such as at Raglan is therefore pertinent.

1.1 AIMS AND OBJECTIVES

The aim of my research thesis is to assess the depth of burial and sediment/oil interactions on a high energy, ultra-dissipative beach in New Zealand. The *Bertin et al, 2008* model results for depth of activation on a dissipative beach will also be tested with field observations from an ultradissipative beach, and oil-sediment interactions will be assessed in the lab.

Hence, this thesis is subdivided into two separate phases that correspond to the two main areas of research. The specific objectives of the first phase dealing with the depth of disturbance are:

1. Survey Raglan beaches using *Trimble VX* and Total Station to ascertain whether and how beaches respond to wave climate/tidal conditions and to ascertain longer term sediment fluctuations that may have an effect on oil burial and exhumation.
2. Obtain 3-D profiles of Ngarunui Beach to ascertain spatial and temporal variations along and cross shore.
3. Use a network of ~ 5 mm diameter depth disturbance rods to monitor bathymetric evolution and physical mixing in the surf/swash zone. Groundwater and swash infiltration are beyond the scope of this study.
4. Collate daily camera footage (*Cam-Era* Network Project). Link to storm and fair weather conditions and morphological features present on Ngarunui Beach.
5. The *Bertin et al.* (2008) mixing depth relationships derived for the French coast will be tested for Ngarunui Beach in Raglan.

This will be followed by the second phase of the study, which will examine the interactions between oil and typical sediments found in a range of environments (open coast high energy beach, and high and low energy estuarine beaches). The specific objective of the second aim is:

6. To create oil-sediment mixtures in the laboratory and assess their characteristics.

The overall results and interpretations for both phases will be reported in this thesis.

1.2 STUDY LOCATION

Raglan is located on the west coast of the North Island of New Zealand, approximately 48 km west of Hamilton. The area extends from Mount Karioi, an extinct basaltic andesite volcano, in the south-west to the dunes and dune-dammed lakes in the north. The township of Raglan is located on the southern shore of Whaingaroa Harbour, a 35 km^2 estuary (Waikato Regional Council, n.d.) with two main arms; the Waingaro-Ohautira arm and the Waitetuna arm to the south, separated by Paritata Peninsula.

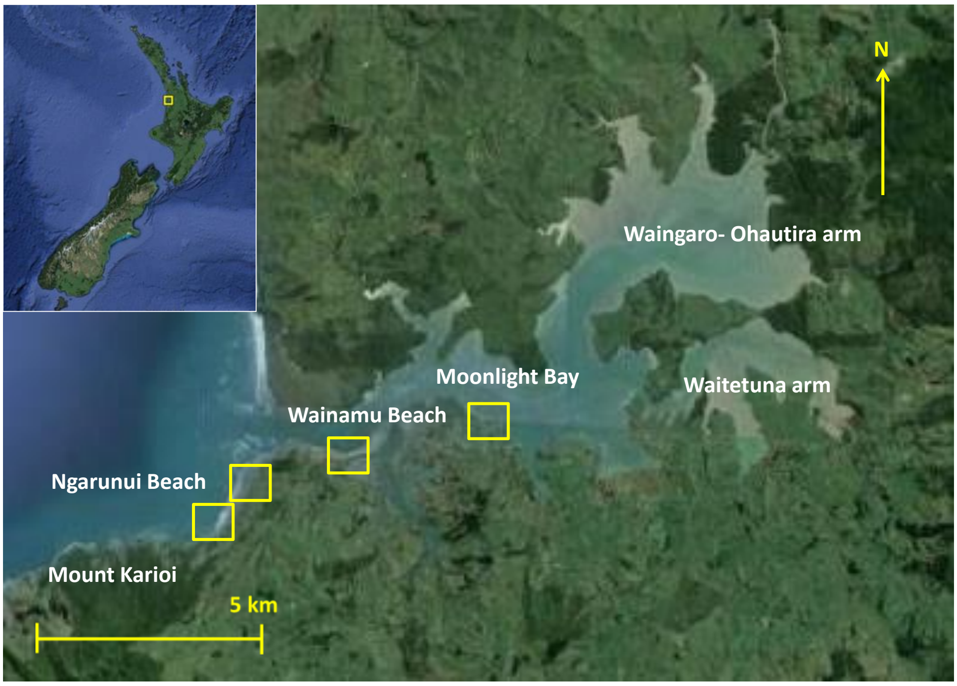

Figure 1.2: **Map of the Raglan (Whaingaroa) area illustrating the location of the three study sites; Ngarunui Beach (high energy open coast beach), Wainamu Beach (high energy estuarine beach) inside the harbour entrance and Moonlight Bay (low energy estuarine beach).**

1.3 GEOLOGICAL SETTING, SEDIMENTS AND HYDRODYNAMICS

The geology of Raglan (Whaingaroa) is dominated by Upper Pliocene Lower Pleistocene Alexandra Volcanics andesites and basalts in the south. In the east and north sandstones and mudstones dominate; Te Kuiti Group soft, calcareous and muddy of the Oligocene in the north and indurated Mesozoic in the east A mantle of volcanic ash from the Quaternary thinly covers most of the area Te Kuiti Group mudstones form most of the shoreline with extensive shore platforms offshore (Sherwood and Nelson, 1979).

The estuary was formed by the drowning of a river valley during the post-glacial rise in sea level, 15,000 years ago (Sherwood and Nelson, 1979).The estuary was largely infilled 8000-6000 years BP by physical weathering of soft mudstone cliffs and 700 m wide intertidal shore platforms that were 10 m below present day sea level (Swales et al., 2005). Little or no infilling over the last 150 years has occurred in the Waingaro arm of the harbour. This is likely to be the result of transportation waves driven by the prevailing southwest winds and tidal currents within the estuary to long term sheltered sinks such as inlets, bays and tidal creeks (Swales et al., 2005). Sands in the lower harbour are progressively replaced by more muddy sediments in the upper reaches. The estuary sedimentation rates have been altered by extensive land use with 50-80% of the sediment in the harbour from catchment sources while erosion of the mudstone shoreline through wetting and drying is likely to be a significant input (Sherwood and Nelson, 1979).

The area of the estuary is 33 km^2 at high tide (Sherwood and Nelson, 1979). Raglan Harbour has a large tidal prism of 46 x 10^6 m^3 during spring tides and 29 x 10^6 m^3 during neap tides (Heath, 1976). Large volumes of water pass through the deep channels of the small inlet throats, with associated high current velocities. Annually, average runoff is 0.034 m^3s^{-1} km^{-2} with only a small (18 m^3s^{-1}) freshwater inflow in to the estuary. This allows effective near daily flushing of the estuary during spring tides (Heath, 1976). Catchment yields are in the order of 123,000 tonnes/year (Mead and Moores, 2004).

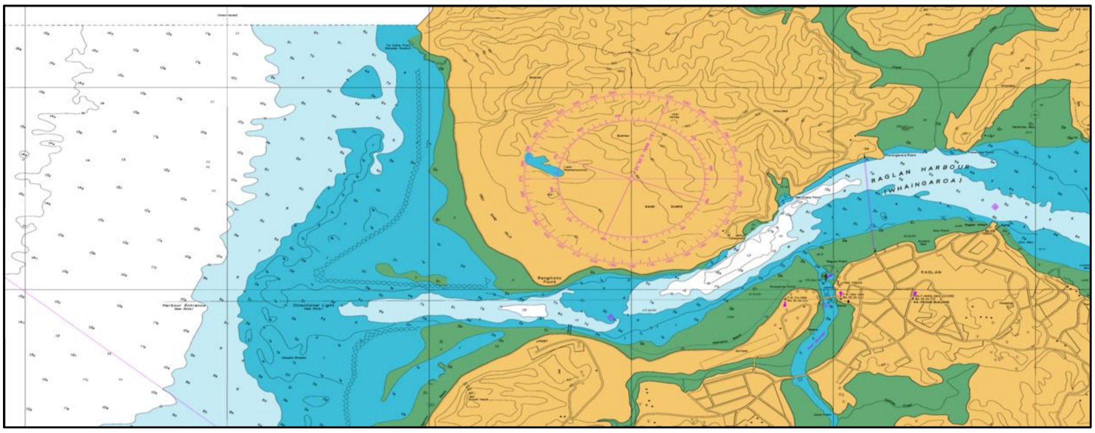

Figure 1.3: **Bathymetric map of Raglan Harbour entrance. Source: *LINZ chart-nz-4421 (2014).***

Bedrock and rocky headlands control the orientation of the main ebb channel (R. Ovenden, personal communication, November 8, 2014). The harbour entrance is tidally dominated and a stable, free form ebb tidal delta with a single spit is apparent offshore. The sand volume of the ebb delta was estimated to be 7.10 x 10^{6} m^3 by Hicks and Hume (1996). At the mouth of the harbour, the channel is bounded by channel margin linear bars, which are visible at low tide (Harrison, 2015) (Figures 1.3 and 1.4). The throat of the harbour at mid tide has an area of 3600 m^2, a width of 640 m^2 and a depth of 5.63 m^2 (Figure 1.3). Large shore normal bedforms such as deep megaripples and tide pools indicate strong flow regimes at this location with implications for depths of disturbance (R. Ovenden, personal communication, November 8, 2014).

The shallow depth of the shore platform on the southern side of the harbour entrance also has implications for mixing limits. Monitoring surveys carried out in 2003 and 2010 for Vodafone New Zealand showed little change in offshore bathymetry near Raglan and the shoreline has remained relatively stable since 1987 possibly due to soft engineering programmes close to the harbour entrance (Patel, 2015).

The ‘Raglan Bar’ is part of the ebb-tidal delta as it relates to the longshore sediment drift; the result of wave action and tidal currents. The longshore, elongate near symmetric terminal lobe of the ebb-tidal delta is 4 m below mean sea level and approximately 2 km offshore of the mouth of the harbour (Figure 1.3). The position of the 3 km wide sand bar shifts with wave energy and strength of the ebb-tide jet (Harrison, 2015).. The sand bar position oscillates from inshore to offshore with northerly and southerly winds respectively, forming near symmetry of the terminal lobe during high-energy erosive winter waves and storm events (Harrison, 2015). Seasonal transitions cause the most rapid swash bar migrations.

The high-energy swell dominated coast is meso-tidal with an average 2-4 m springs range (Wood, 2010). Tides are semi-diurnal with significant spring-neap variations. Average maximum tidal ranges for spring tides and neap tides are 2.8 m and 2.0 m respectively within the estuary (Wood, 2010) however maxima of 3.1 m have been observed on the open coast (Guedes, 2000) and minima of 1.8 m noted within the estuary (Heath, 1976).

A Wave Energy Factor (H^2T^2) of 159 m^2s^2 was calculated by Hicks and Hume (1996) signifying an energetic wave environment. According to the wave hindcast modelling of Scarfe (2008), the average deepwater significant wave height (H_o) is 1.6 m, with a corresponding peak period (T_m) of 7.4 s. However Harrison (2015), found higher values of 2.1 m and 12 s respectively. Mean wave approach direction was given by Scarfe (2008) as 68.3^o.

Raglan’s coastline is positioned within a major ‘sediment cell’ of titanomagnetite sand, the source of which is Mount Taranaki, 180 km south of Raglan. This ‘sediment cell’ exhibits large scale sediment transport, referred to as a ‘river of sand’ which, as it progresses north from the Taranaki region is augmented through localised cliff erosion, river and estuary input, as well as off shore deposits (Hart and Bryan, 2008). Because of the high concentrations of sand that bypass the west coast, the morphology of the coastline is controlled by this ‘river of sand’; embayments fill easily (Wood, 2010).This sand, under persistent high wave energies from the Southern Ocean becomes more well-sorted and rounder the further from the sediment source, with heavier fractions preferentially removed and remaining as placers along the coast (Hart and Bryan, 2008).

Longshore sediment drift can be seen as substantial, elongate sand bars (> 100 m) that pulse northward around the southern headland. Large slugs of sand occasionally are visible at the northern end of Ngarunui Beach (Figure 1.4), which then disperse northwards or into the harbour (Phillips and Mead, 2009). The annual littoral drift has been estimated at 175, 000 m^3 towards the north (Hicks and Hume, 1996).

In the southwest of Ngarunui Beach, boulders of basaltic andesite armour the shoreline around the headland to Ruapuke Beach on the southern side of Mount Karioi (Phillips and Mead, 2009) (Figure 1.2). Strong currents travel easterly around the headland with burst-averaged velocities of up to 0.8 m s^{-1} and 2.0 m s^{-1} in the breaking wave zone and at the bed respectively. Re-circulating gyres direct flow back up the headland further offshore (Phillips et al., 2003).

Figure 1.4: **Aerial photograph of Raglan Harbour entrance and the northern end of Ngarunui Beach with the large shore-welded bar and channel margin linear bars.** ***Source: Noel Bailey.***

Ngarunui Beach is a gently sloping, exposed (open coast), high energy, swell dominated beach located on the southern side of the estuary mouth, constrained by a headland in the south and the inlet to the north (Figures 1.1 and 1.2) (Hart & Bryan, 2008). Ngarunui Beach is approximately 1800 m in length (Huisman et al., 2011). A single ridge of large (some heights in excess of 15 m), ephemeral, steep dunes (~1:5) forms the landward limit of the littoral zone, while the headland behind constrains the beach system (Huisman et al., 2011). A large flood channel at the northern end of the beach contributes to onshore/offshore sediment exchange (Figure 1.4) (R. Ovenden, personal communication, November 8, 2014).

Ngarunui Beach consists of predominantly well-sorted, rounded, dense, fine grained (average grain size of 293 µm), black titanomagnetite and quartz sand (Wood, 2010). The width of the beach is ~200 m at low tide. Current and wave action are the primary mechanisms for shifting sand, while surficial winds are present but are estimated to contribute only negligible amounts to total bed level changes, and water drainage even smaller amounts (R. Ovenden, personal communication, November 8, 2014). Aeolian processes have a significant effect in the entrance to the harbour, however, as the winds are directed around the headland and transport sand into the harbour. Groundwater seepage is frequently visible above the swash zone on Ngarunui Beach (Huisman, et al., 2011). The average beach slope has been recorded as 0.014 over the intertidal region (Guedes, 2012) to as low as 0.0081 (to -10 m) (Hicks and Hume, 1996).

Ngarunui Beach is an ultra-highly dissipative beach according to the Wright and Short (1984) classification scheme, with a Dean dimensionless fall parameter (Ω) of ≥ 6 (Figure 1.5). Characteristically, dissipative beaches are associated with high energies from large (> 2-3 m) waves, gentle low gradients ($\tan \beta = 0.01 – 0.02$) and wide (> 100s) differentiated surf zones (100s m), typical of storm profiles. Wave energies are dissipated across the entire surf zone. Persistently high wave energy maintains the low mobility dissipative states. Dissipative beaches are generally flat, shallow and have large subaqueous sand storage in the inner surf zone; currents associated with infragravity standing waves dominate. In the outer surf zone shoreward decay of incident waves is accompanied by shoreward growth of infragravity energy (Wright, Guza and Short, 1982 and Wright and Short, 1984). Spilling waves with Surf Similarity values of $\xi < 0.4$ according to the classification of Deigaard (1992 as cited in Anfuso, 2005) are common as are multi-barred surf zones with straight, shore-parallel bars. Longshore rhythms are rare. These fine sand beaches dominate the west coast of New Zealand (Hart and Bryan, 2008).

The low gradient, large width and significant tidal range present, results in features consistent with the ultradissipative beaches of Northern Australia, even though Ngarunui Beach has a higher wave energy. Ngarunui Beach also displays features commonly associated with the longshore bar and trough beach types according to the classification of Wright and Short (1984), as rips are present approximately every 250-500 m. The presence of the ebb tidal delta in Raglan possibly causes sediment recirculation offshore and affects especially the northern end of Ngarunui Beach (R. Ovenden, personal communication, November 8, 2014).

As well as storm-driven events, seasonal and decadal-scale variations in wave climate meteorological conditions have been shown to modify the landscape of the beach, altering erosion rates and sediment transport pathways (Bryan, Kench and Hart, 2008). Although New Zealand beaches do not have distinctive seasonal shifts, storm and fair weather conditions exist throughout the year. Large scale erosion caused by fluidisation during heavy rainfall has occurred at Ngarunui Beach; an entrance to a large enclosed swale close to the boardwalk at the northern end of Ngarunui Beach was formed over a large rainfall event at Ngarunui Beach and it has been noted that streams moved location during these event (R. Ovenden, personal communication, November 8, 2014).

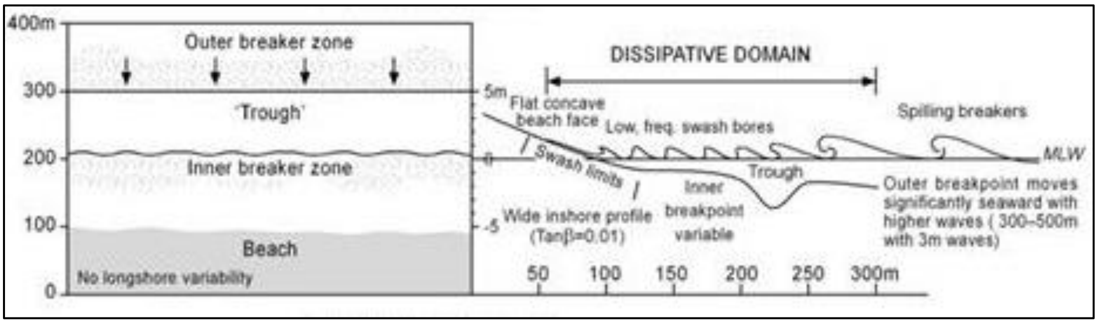

Figure 1.5: **Schematic diagram of a dissipative beach. *Source: Short (2006).***

The other sites studied in this research do not fit in to the classification scheme of Wright and Short. Wainamu Beach is tidally dominated and is located close to the main estuary channel, near the mouth of the estuary (Figures 1.2 and 1.6). Currents scour inside the harbour, with a spit beginning to form with a west-east aspect (Figure 1.6). Bedforms which are oriented perpendicular to the channel can be seen along the beach (Figure 1.7). As well as strong currents, aeolian processes are significant at Wainamu Beach (R. Ovenden, personal communication, November 8, 2014). The area of Wainamu Beach is dynamic and large amounts of erosion are occurring due to a southerly shift in the position of the channel.

Figure 1.6: **Wainamu Beach, Raglan. *Source: Noel Bailey.***

Figure 1.7: **Deep 3-4 mm ripples at Wainamu Beach on the 16th of July, 2014. 19/11 18:51**

Raglan model output showing the peak magnitude and direction of ebb and flood tidal currents during mean tidal conditions around the Harbour entrance and Wainamu Beach. Raglan harbour a flooded river valley (ria). At the entrance there is an ebb tidal delta (the Raglan Bar) and a flood tidal delta (which is entirely submerged). The magnitude of current exiting the harbour on the ebb tide can clearly be seen in Figures 1.8 and 1.9. Although the area directly to the east of the experimental site at Wainamu Beach shows reduced currents on both the ebb and flood tides, the area where experiments were undertaken shows moderate amounts of current, 0.6 – 0.8 m/s. As a result, Wainamu Beach is considered a high energy estuarine beach.

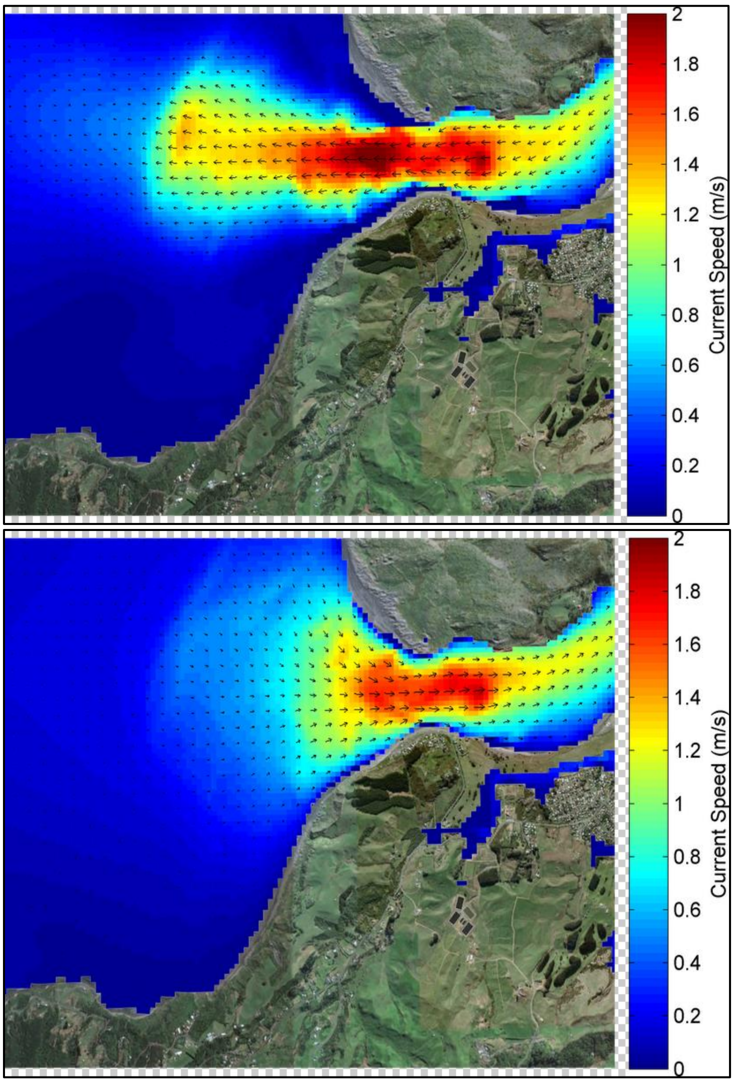

Figures 1.8 and 1.9:* Current magnitude and direction during peak ebb tide and peak flood tide respectively. *Source: eCoast, 2015.

Predominantly tidally controlled, Moonlight Bay consists of a coarse sandy upper littoral area, with mud flats further down the intertidal zone. A rock platform is exposed at low tide level. Wave refraction of small waves entering or generated within the harbour occurs around the western headland of the beach, and modify the beach as observed by the author. Two small boulder groynes have been emplaced on the eastern side of the beach to provided protection from waves generated within the harbour that cause sediment recirculation and loss. As Moonlight Bay is exposed to a large fetch area of approximately 5 km, resuspension by waves can also cause modification of sediment. Short, steep waves which overtop the~1 m rock wall at Moonlight Bay occur with north-easterly winds. The area experiences erosive/accretionary events as large changes in bed level, ± 40 cm at Okete Bay, 2.5 km away with a similar aspect have been recorded (Swales et al., 2005).

1.4 THESIS OUTLINE

The thesis structure for the remaining chapters is as follows:

Chapter Two describes the collection, analysis and results of sediment sampling and analysis using the *Malvern Mastersizer 2000*. The spatial distribution and temporal variation of beach grain size and morphology are examined.

Chapter Three provides a review and synthesis of previous literature pertaining to depth of disturbance (DoD) processes, influences, measurement methods. The chapter also describes the depth of disturbance (DoD) experiments and results. Spatial and temporal patterns of DoD are extrapolated and variations of DoD are linked to weather conditions including significant wave height and period. The larger scale morphological changes associated with erosion/accretion events and their influence on depth of burial are also investigated here.

Chapter Four summarises the properties and classification of oils and provides a review of the literature pertaining to oil spills. The behaviour of oil following a spill, with focus on the interactions that occur in the coastal environment, is considered.

Chapter Five outlines the methods and results of laboratory experiments on mixtures of distinctive oil samples, beach sediment and sea water. Observations of sediment and oil settling velocity, in settling flasks, among oil samples with dissimilar API° values and wax contents were documented. These observations were replicated for two distinct beach sediments; the titanomagnetite sands of Ngarunui Beach and the more biogenic sediments of Moonlight Bay. Microscopic analysis of the sediment/oil mixtures allowed observations of sediment/oil interactions.

Chapter Six summarises the major findings and conclusions of this study. Recommendations for future research into measurements of depth of disturbance on high energy, highly dissipative to ultra-dissipative beaches are also given.

CHAPTER TWO: SEDIMENT CHARACTERISTICS

2.0 INTRODUCTION

Beaches possess characteristic compositions and textures; the consequence of the source rocks and weathering conditions. Within these bounds natural variation can be considerable; resulting in a breadth of grain shapes and sizes (Larson et al, 1997). Sediment characteristics, including their nature and distribution, provide information about the energy of the depositional environment, provenance and transport history of sediment grains (Folk, 1980; Larson et al, 1997; Zeeman, 2008). Spatial and temporal patterns of sediment grain size distribution and minerology are important indicators of direction of littoral drift, depositional energy variability and the stability of the intertidal zone (Larson et al, 1997).

This chapter examines the textural characteristics of subaerial sediments from all four study locations; northern and southern Ngarunui Beach, eastern Wainamu Beach and Moonlight Bay (Figure 1.2). Grain size distributions were determined using the University of Waikato's *Malvern Mastersizer-2000*. Logarithmic statistical and graphical parameters were then derived for enquiry of possible sediment transport pathways and for use in investigations of controls on depths of disturbance. Sediment composition and complimentary sediment textural properties such as angularity were evaluated under stereo-microscope.

2.1 RESEARCH METHODS

2.1.1 SEDIMENT SAMPLE COLLECTION

Sediment samples were obtained at specific zones on the beach face; the high intertidal zone, the mid intertidal zone and the low intertidal zone. The sediment samples were taken in conjunction with disturbance rod experiments and beach surveys to allow spatial referencing and correlation to hydrodynamic zones and morphology. Surficial samples of approximately 100-150 grams (dependent on water content) were taken by hand from within the top 25 cm of beach sediments and within a 30 cm radius of each disturbance rod before extraction. Samples were collected at each rod location during each of the field experiments, except when rods were lost or removed or tidal conditions prevented it.

On Ngarunui Beach, sediment samples were gathered from three transects located on the northern end of the beach, spaced approximately 250 m apart (Figure 4.1) except on the 10th of February 2015 when samples were collected from four provisional transects on the southern end of Ngarunui Beach spaced approximately 8-10 m apart (Figure 4.2). The transect lines at the northern end of the beach were established during a doctoral research experiment by Amir Emami of the University of Waikato in September, 2013. At Wainamu Beach three transect lines were established in July, 2014 with separation distances of 150 m (Figure 4.3). A total of six samples were gathered along two profile lines at Moonlight Bay during one experiment on the 22nd and 23rd of September, 2014 (Figure 4.4). All transects were shore-normal. Grain size analysis was not carried out on the dune sediments.

2.1.2 GRAIN SIZE ANALYSIS

For each discrete sediment sample obtained during all field experiments, grain size analysis was undertaken using the University of Waikato *Malvern Mastersizer-2000.* The Mastersizer is highly accurate for spherical particles between 0.02 – 2000 µm (Malvern Instruments Ltd, 2015). Sources of error relate to the presence of non-spherical grains and as the Mastersizer is an ensemble analyser; the results are not a true count. The sediments were not analysed in the Rapid Sediment Analyser (RSA) as non-spherical shapes common in particles less than 2 µm in size (clay sediments) result in slow settling times due to a predominance of Brownian motion (Malvern Instruments Ltd, 2015; Morelock et al, 2005). Likewise particles greater than 50 µm in size give rise to errors as settling is turbulent (Malvern Instruments Ltd, 2015). The laser sizer is also faster at analysing sediments.

The *Malvern Mastersizer-2000* calculates particle size using laser diffraction theory or *Mie theory* of light scattering (Malvern Instruments Ltd, 2015). The *Mastersizer-2000* measures the angle at which dispersed particulate samples vary the intensity of the light from a laser beam passing through them. By assuming a volume equivalent sphere diameter, the De Brouckere volume or mass moment mean is obtained by,

$$D[4,3] = \frac{\sum_1^n D^4{}_{i_v i}}{\sum_1^n D^3{}_{i_v i}} \tag{2-1}$$

where, D_v is volume diameter commonly in µm , ∑ is summation of all diameters of the i^{th} particle. Because a volume-based distribution is biased toward coarser sediments, the presence of fine sediment particles is indicative of a large relative amount of fines and the lack of fines does not truly indicate their absence (Wolfram, 2011). The Mie theory is satisfied if the sediment particles are isotropic, spherical, smooth and homogenous, which is not the case for the sediments analysed. The known refractive index (RI) and absorption coefficient for quartz (S_iO_2) grains were used; RI = 1.5 and particle absorption = 0.2. A significant proportion of the sample consisted of other minerals with different properties. However, the purpose of the analysis was to obtain a comparison between samples, and an indication of the size ranges, so the deviations from the assumed characteristics were not considered an issue.

Sub-samples of approximately 4 g were placed into the dispersion unit with the suspension medium; water. Obscuration levels were adjusted to be below 30 %, which ensured enough detectable light from the laser passed through the sample, without the risk of multiple scattering (Malvern Instruments Ltd, 1997). As the samples contained less than 2 % organic matter and the particles were not aggregated, hydrogen peroxide treatment was not carried out prior to analysis. Sieve analysis of samples from Moonlight Bay that contained shell fragments larger than 2 mm allowed larger fractions to be included in the particle size analysis. The results of sieve analysis are included in Appendix II.

The mastersizer generates relative volume size distributions with pre-defined size classes. Frequency distributions (histograms) and cumulative frequency curves were generated from these outputs, highlighting any apparent distribution patterns. Statistical moment and graphical parameters were also manually calculated using the following equations:

Table 2.1: ***Logarithmic graphical measures (after Folk, 1957) and method of moments formulas where ϕx are grain size diameters at the cumulative percentile value of x, f is the frequency weight percent and m is the class interval mid-point. Adapted from Blott and Pye (2001).***

Parameter	***Graphical Method After Folk (1957)***	***Method of Moments***
Mean	$M_z = \frac{(\phi_{16} + \phi_{50} - \phi_{84})}{3}$	$\bar{x}_\phi = \frac{\sum f m_\phi}{\sum 100}$
Standard deviation	$\sigma_1 = \frac{\phi_{84} + \phi_{16}}{4} + \frac{\phi_{95} + \phi_5}{6.6}$	$\sigma_\phi = \sqrt{\frac{\sum f(m_\phi - \bar{x}_\phi)^2}{100}}$
Skewness	$Sk_1 = \frac{\phi_{16} + \phi_{84} - 2\phi_{50}}{2(\phi_{84} - \phi_{16})} + \frac{\phi_5 + \phi_{95} - 2\phi_{50}}{2(\phi_{95} - \phi_5)}$	$Sk_\phi = \frac{\sum f(m_\phi - \bar{x}_\phi)^3}{100\sigma_\phi{}^3}$
Kurtosis	$K_G = \frac{\phi_{95} - \phi_5}{2.44\,(\phi_{75} - \phi_{25})}$	$K_\phi = \frac{\sum f(m_\phi - \bar{x}_\phi)^4}{100\sigma_\phi{}^4}$

Because statistical moments methods are affected by the entire spread, they produce superior values (Folk, 1980; Larson et al, 1997); however graphical measures are the convention and are therefore easily comparable (Larson et al, 1997; Maher, 1989). Both the graphical and method of moments formulae (Table 2.1) use logarithmic scales. Repeat samples were not included in the statistical analysis.

Mean grain size classifications are based on the Wentworth Grade Scale (after Wentworth, 1922) (Figure 2.1). The phi value (after Krumbein, 1937) is the base

2 negative logarithm of the diameter of a particle in mm calculated as follows;

$$\phi = -log_2 d = -\left(\frac{log_{10} d}{log_{10} 2}\right) \tag{2.2}$$

where ϕ is particle size in ϕ units and d is diameter of particle in mm (Folk, 1980; Pfannkuch and Paulson, n.d.; Zeeman, 2008). Mean is the average grain size of a sample distribution constrained by the sediment source (Folk, 1980; Maher, 1989; Zeeman, 2008). It is commonly used as it is directly comparable to the applied stress required to set a grain in motion by wind or water (Brown et al, 1999; Lancaster, 2009; Wilcock, 1988). The most inclusive graphically derived mean values include the 16^{th}, 50^{th}, and 84^{th} percentile values of the sample by weight (Folk, 1980).

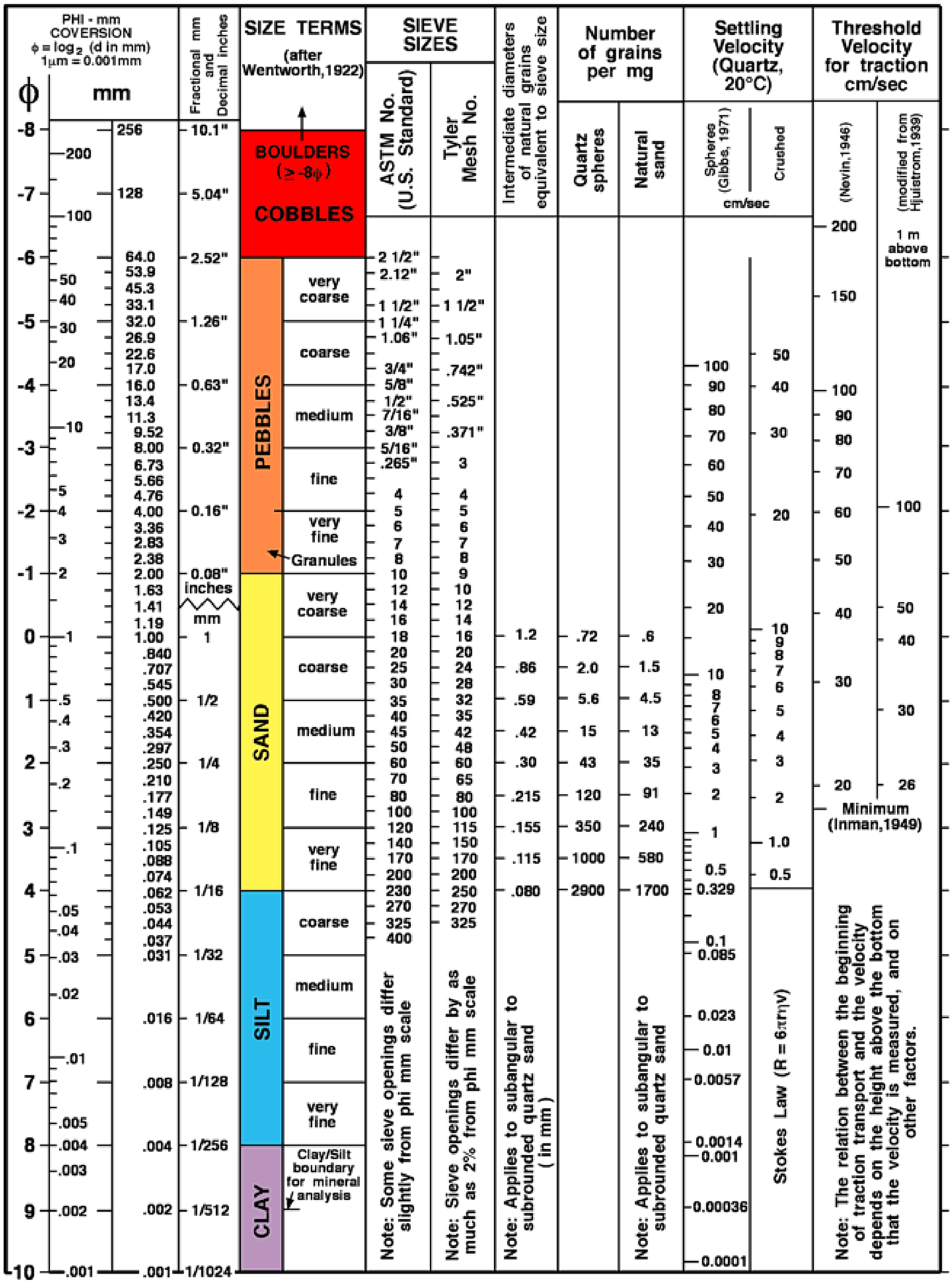

Figure 2.1: **Wentworth grade scale. After Wentworth (1922). Source: USGS Open-File Report 2006-1195 (2011).**

Sorting or the standard deviation is the measure of spread of a distribution or the grain-size variation in a sample (Folk, 1980; Larson et al, 1997; Maher, 1989). The inclusive graphic standard deviation is inclusive of 90 % of the distribution (Folk, 1980). Skewness and kurtosis (measures of uniformity of distributions) values are used to test the uniformity of the grain size distribution i.e. how close it approximates a normal Gaussian probability curve (Brown, 2015). The median (M_d or D_{50}) of the sample or distribution corresponds to the grain size diameter of the 50th percentile on the cumulative curve (Folk, 1980; Larson et al, 1997; Maher, 1989; Pfannkuch and Paulson, n.d.; Zeeman, 2008). Mode is the most frequently occurring grain size (Pfannkuch and Paulson, n.d.; Zeeman, 2008). Textural descriptions for graphic and moment sorting, skewness, and kurtosis were determined using the classification given in Tables 2.2 – 2.4.

Table 2.2: ***Verbal description limits of graphic sorting (σ_1) (after Folk, 1968) and method of moment sorting limits (σ_ϕ). All units are in phi (ϕ). Source: Blott and Pye (2001).***

Graphical measure range (σ_1)	Method of moments range (σ_ϕ)	Description
< 0.35	< 0.35	*very well sorted*
0.35 - 0.50	0.35 - 0.50	*well sorted*
0.50 - 0.70	0.50 - 0.70	*moderately well sorted*
0.70 - 1.00	0.70 - 1.00	*moderately sorted*
1.00 - 2.00	0.00 - 2.00	*poorly sorted*
2.00 - 4.00	2.00 - 4.00	*very poorly sorted*
> 4.00	> 4.00	*extremely poorly sorted*

Table 2.3: ***Verbal description limits of graphic skewness (Sk_1) (after Folk, 1968) and method of moments skewness limits (Sk_ϕ). All units are in phi (ϕ). Source: Blott and Pye (2001).***

Graphical measure range (Sk_1)	Method of moments range (Sk_ϕ)	Description
0.30 - 1.00	> 1.30	*strongly fine skewed*
0.10 - 0.30	0.43 - 1.30	*fine skewed*
0.10 – -0.10	-0.43 - 0.43	*near symmetrical*
-0.10 – -0.30	-1.3 - -0.43	*coarsely skewed*
-0.30 – -1.00	< -1.30	*strongly coarsely skewed*

Table 2.4: ***Verbal description limits of graphic kurtosis (KG) (after Folk, 1968) and method of moments kurtosis limits (Kϕ). All units are in phi (ϕ). Source: Blott and Pye (2001).***

Graphical measure range (K_G)	Method of moments range (K_ϕ)	Description

< 0.67	< 1.70	very platykurtic
0.67 - 0.90	1.70 - 2.55	Platykurtic
0.90 - 1.11	2.55 - 3.70	Mesokurtic
1.11 - 1.50	3.70 - 7.40	Leptokurtic
1.50 - 3.00	> 7.40	very leptokurtic
> 3.00		extremely leptokurtic

The relative abundance of grain size fractions in the sediment samples were used to classify the sediments using Folk's classification system (after Folk, 1974) (Figure 2.5).

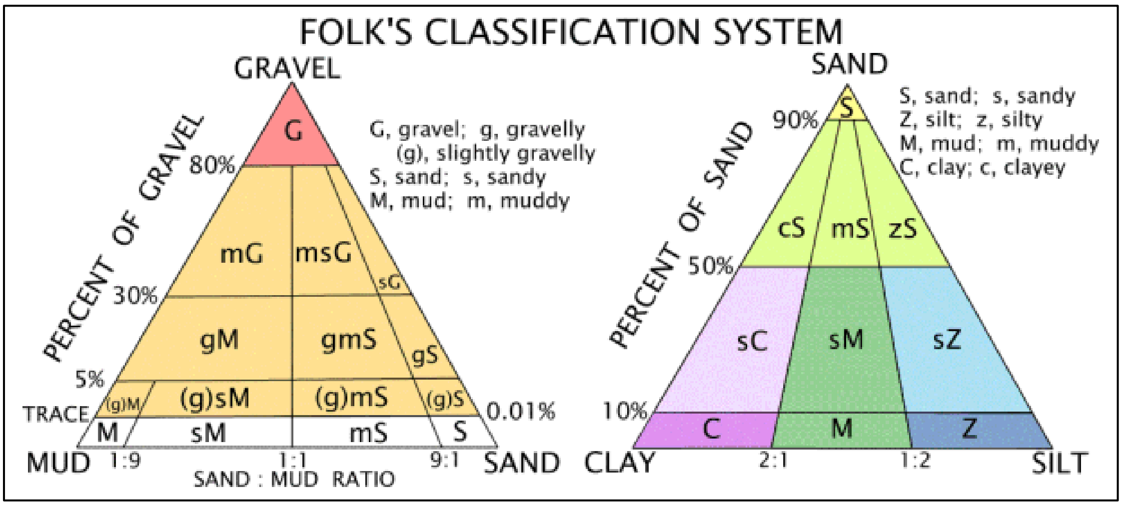

Figure 2.2: **Folk classification scheme showing approximate relationship between the sediment size fractions. After Folk (1974). Source: USGS Open-File Report 2006-1195 (2011).**

2.1.3 PARTICLE MORPHOLOGY

Complementary sediment textural properties including sphericity, form and curvature were visually evaluated under stereo - microscope at between 10x and 63x magnification and classified according to the scale of Powers (1953) (Figure 2.5). Shape is qualified by how much a sediment grain approximates a sphere (sphericity) and the curvature of the corners of the particle (angularity/roundness) (Figure 2.5) (Folk, 1980; Morelock et al, 2005; Nichols, 2009; Persaud, n.d.). Form is also numerically specified by the ratio of the dimensions of the grain (Folk, 1980; Morelock et al, 2005; Persaud, n.d.). Sediment grains are therefore classified as equidimensional (compact and spherical), elongate (rod and blades), platy (discs); smooth, round, subangular and angular.

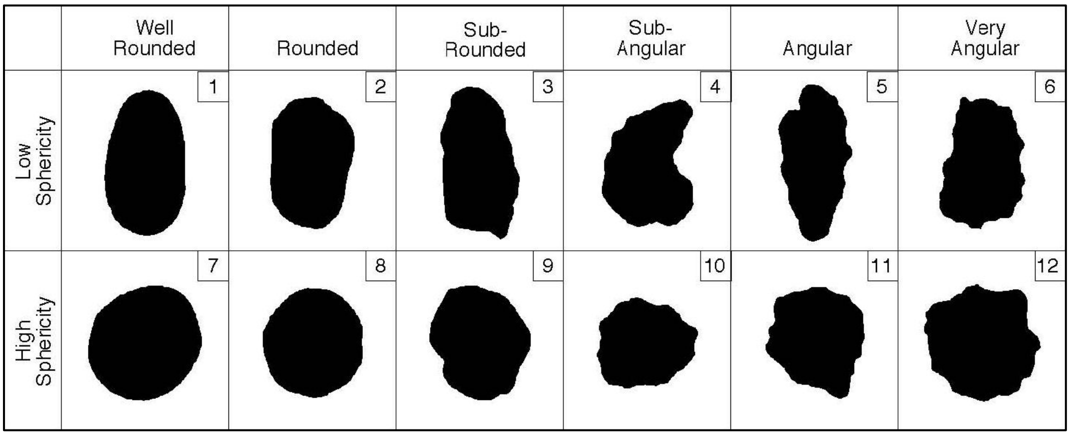

Figure 2.3: **Visual comparison chart of known reference particles. After Powers (1953). Source: MacLeod (2002). Note: Numbers are arbitrary identification numbers.**

The curvature of the sediment grain corners and their sphericity is indicative of the duration and energy of transport processes and the grain's inherent hardness (Folk, 1980). Lengthy transport as suspended load and bed load in high energy environs will cause abrasion to polish and then round the edges of sediment grains, particularly softer sediment grains, and to cause grains to become more equidimensional (Folk, 1980). However sphericity and form are constrained by the shape and composition of the source fragments (Folk, 1980; Nichols, 2009). Preferential sorting of grains will also result in variations of sphericity and angularity/roundness (Folk, 1980).

2.2 SEDIMENT TEXTURAL RESULTS

Sediment size analysis results from the University of Waikato's *Malvern Mastersizer-2000* are presented in tables in Appendix I. Derived logarithmic graphical parameters following the method of Folk (1980) including mean (M_z), sorting (σ_1), skewness (Sk_1), kurtosis (K_G) and grain size percentile statistics are also given. Tables of summary statistics including textural size class and description, Wentworth size class, logarithmic method of moments parameters and logarithmic graphical measures after Folk (1980) are presented in Appendix II. Derived grain size distribution histograms and cumulative frequency (both

arithmetic and probability scale) plots of ‘percent finer than’ are also presented Appendix II. Because the method of moments is statistically more robust (Larson et al., 1997), grain-size parameters calculated using the method of moments as well as graphically derived values are both reported.
Sieve analysis to determine particle size distribution was conducted on the sub-sample from Moonlight Bay (used in the oiling experiments) as it contained grain sizes larger than 2 mm.

Table 2.5 presents a summary of the sediment characteristic parameters obtained from all samples collected during this study. The results from the separate samples at each site (Appendix I) were averaged to provide the summary values in Table 2.5, which are therefore indicative of the overall average sediment texture. Ranges of textural characteristic values (shown in brackets) are presented alongside averaged statistics from discreet samples. Tables 2.6 and 2.7 summarise the sediment characteristic parameters in averaged cross-shore and longshore samples with similar depositional energy levels and processes. The ranges of values for the separate samples collected at these locations are also included. All units are in phi (ϕ). For mean grain size and standard deviation, mm equivalents are also presented. Textural characteristics were derived using the logarithmic graphical method of Folk (1980).

Table 2.5: ***Summary of grain size analysis using laser diffraction for particle sizing. ms = medium sand, fs = fine sand, vfs = very fine sand.***

Site location	**Mean grain size (M_z) (ϕ)**	**Sorting (SI) (ϕ)**	**Skewness (Sk_I) (ϕ)**	**Kurtosis (K_G) (ϕ)**	**Mean grain size (mm)**	**Standard devation (mm)**	**Wright and Short beach classification (1984)**	**Wentworth Scale size class (1922)**
Ngarunui Beach North	**1.77** (0.92 - 2.34)	**0.63** (0.45 - 0.74)	**-0.05** (0.07 - 0.03)	**0.99** (0.93 - 0.97)	**0.29** (0.22 – 0.27)	**0.65** (0.73 – 0.60)	*D*	*ms*
Ngarunui Beach South	**1.83** (1.30 - 2.11)	**0.57** (0.46 - 0.85)	**-0.05** (-0.11 - 0.01)	**0.99** (0.95 - 0.98)	**0.28** (0.23 – 0.41)	**0.67** (0.56 – 0.72)	*I – D*	*ms*
Wainamu Beach	**2.40** (2.09 - 2.91)	**0.58** (0.40 - 1.05)	**0.00** (-0.09 - 0.35)	**0.98** (0.94 - 2.17)	**0.19** (0.13 – 0.24)	**0.67** (0.64 – 0.76)	*I*	*fs*
Moonlight Bay	**2.23** (0.82 - 5.03)	**2.19** (0.66 - 3.34)	**0.51** (-0.02 - 0.65)	**2.02** (0.73 - 2.83)	**0.21** (0.04 – 0.57)	**0.22** (0.10 – 0.63)	*R & TMF*	*fs*

Note: Tables 2.5 – 2.7 present averaged statistics from discreet samples with the range of textural characteristic values shown in brackets. All units are in phi (ϕ). For mean grain size and standard deviation, mm equivalents are also presented. Textural characteristics were derived using the logarithmic graphical method of Folk (1980).

Table 2.6: ***Summary of the range of graphical textural characteristics for crosshore profiles. ms = medium sand, fs = fine sand, vfs = very fine sand.***

Site location	Intertidal position	Mean grain size (M_z) (ϕ)	Sorting (SI) (ϕ)	Skewness (Sk_I) (ϕ)	Kurtosis (K_G) (ϕ)	Mean grain size (mm)	Standard devation (mm)	Wentworth Scale size class (1922)
Ngarunui Beach North	*High*	**2.06** (1.66 - 2.34)	**0.55** (0.45 - 0.64)	**0.01** (-0.03 - 0.01)	**0.98** (0.95 - 0.98)	**0.24** (0.20 – 0.32)	**0.68** (0.64 – 0.73)	*fs*
Ngarunui Beach North	*Mid*	**1.69** (1.13 - 1.99)	**0.57** (0.46 - 0.66)	**-0.03** (-0.03 - 0.02)	**0.97** (0.93 - 0.97)	**0.31** (0.25 – 0.46)	**0.67** (0.63 – 0.73)	*ms*
Ngarunui Beach North	*Low*	**1.53** (0.92 - 2.02)	**0.67** (0.51 - 0.74)	**-0.05** (-0.07 - 0.03)	**0.98** (0.93 - 0.99)	**0.35** (0.25 – 0.53)	**0.63** (0.60 – 0.70)	*ms*
Ngarunui Beach South	*High*	**2.05** (2.00 - 2.11)	**0.49** (0.46 - 0.51)	**0.00** (-0.00 - 0.01)	**0.96** (0.95 - 0.98)	**0.24** (0.23 – 0.25)	**0.71** (0.70 – 0.72)	*fs*
Ngarunui Beach South	*Mid*	**1.67** (1.61 - 1.71)	**0.54** (0.53 -0.59)	**-0.01** (-0.01 - -0.01)	**0.95** (0.95 - 0.96)	**0.31** (0.31 – 0.33)	**0.69** (0.67 – 0.70)	*ms*
Ngarunui Beach South	*Low*	**1.75** (1.30 - 2.05)	**0.64** (0.50 - 0.85)	**-0.11** (-0.11 - 0.01)	**1.05** (0.95 - 0.98)	**0.30** (0.24 – 0.41)	**0.64** (0.556 – 0.71)	*ms*
Wainamu Beach	*High*	**2.46** (2.26 - 2.63)	**0.56** (0.51 - 0.64)	**0.00** (-0.08 - 0.01)	**0.96** (0.94 - 1.03)	**0.18** (0.16 – 0.21)	**0.68** (0.64 – 0.70)	*fs*
Wainamu Beach	*Mid*	**2.49** (2.17 - 2.91)	**0.60** (0.40 - 0.85)	**-0.02** (-0.09 - 0.29)	**0.96** (0.94 - 1.93)	**0.18** (0.13 – 0.22)	**0.66** (0.55 – 0.76)	*fs*
Wainamu Beach	*Low*	**2.26** (2.09 - 2.40)	**0.57** (0.50 - 1.05)	**0.02** (-0.00 - 0.35)	**0.97** (0.95 - 2.17)	**0.21** (0.19 – 0.24)	**0.68** (0.48 – 0.71)	*fs*
Moonlight Bay	*High*	**1.02** (0.82 - 1.14)	**0.81** (0.66 - 1.19)	**0.00** (-0.01 - 0.21)	**0.97** (0.93 - 1.41)	**0.50** (0.45 – 0.57)	**0.57** (0.45 – 0.57)	*ms*
Moonlight Bay	*Mid*	**1.72** (1.22 - 2.65)	**1.57** (1.39 - 1.74)	**0.29** (0.31 - 0.65)	**2.33** (2.14 - 2.83)	**0.30** (0.16 – 0.43)	**0.34** (0.16 – 0.43)	*ms*
Moonlight Bay	*Low*	**3.72** (2.12 - 5.03)	**2.88** (1.51 - 3.34)	**0.52** (0.03 - 0.49)	**0.91** (0.73 - 2.34)	**0.08** (0.03 – 0.23)	**0.14** (0.03 – 0.23)	*vfs*

Table 2.7: ***Summary of the range of graphical textural characteristics for long-shore profiles at all study locations. ms = medium sand, fs = fine sand.***

Site location	Intertidal position	Mean grain size (M_z) (ϕ)	Sorting (SI) (ϕ)	Skewness (Sk_I) (ϕ)	Kurtosis (K_G) (ϕ)	Mean grain size (mm)	Standard devation (mm)	Wentworth Scale size class (1922)
Ngarunui Beach North	*North*	**1.84** (1.31 - 2.34)	**0.58** (0.45 - 0.69)	**-0.02** (-0.07 - 0.01)	**0.99** (0.93 - 0.99)	**0.28** (0.20 – 0.40)	**0.67** (0.62 – 0.73)	*ms*
Ngarunui Beach North	*Mid*	**1.74** (0.92 - 2.30)	**0.66** (0.46 - 0.65)	**-0.06** (-0.03 - 0.03)	**0.99** (0.93 - 0.98)	**0.30** (0.20 – 0.53)	**0.63** (0.64 – 0.73)	*ms*
Ngarunui Beach North	*South*	**1.74** (1.04 - 2.19)	**0.64** (0.48 - 0.74)	**-0.05** (-0.01 - 0.01)	**0.99** (0.94 - 0.98)	**0.30** (0.22 – 0.49)	**0.64** (0.60 – 0.72)	*ms*
Ngarunui Beach South	*Transect 1*	**1.66** (1.30 - 2.00)	**0.70** (0.51 - 0.85)	**-0.12** (-0.10 - -0.00)	**1.04** (0.96 - 0.98)	**0.32** (0.25 – 0.41)	**0.79** (0.56 – 0.70)	*ms*
Ngarunui Beach South	*Transect 2*	**1.84** (1.66 - 2.01)	**0.54** (0.47 - 0.54)	**-0.02** (-0.01 - -0.00)	**0.97** (0.95 - 0.96)	**0.28** (0.25 – 0.32)	**0.83** (0.69 – 0.72)	*ms*
Ngarunui Beach South	*Transect 3*	**1.86** (1.70 - 2.11)	**0.54** (0.47 - 0.53)	**-0.02** (-0.01 - 0.01)	**0.96** (0.95 - 0.98)	**0.28** (0.23 – 0.31)	**0.83** (0.69 – 0.72)	*ms*
Ngarunui Beach South	*Transect 4*	**1.94** (1.71 - 2.06)	**0.53** (0.50 - 0.53)	**-0.02** (-0.01 - 0.01)	**0.96** (0.95 - 0.95)	**0.26** (0.24 – 0.31)	**0.82** (0.69 – 0.71)	*ms*
Wainamu Beach	*West*	**2.49** (2.09 - 2.91)	**0.57** (0.40 - 0.64)	**-0.02** (-0.08 - 0.02)	**0.95** (0.94 - 1.03)	**0.18** (0.13 – 0.24)	**0.67** (0.64 – 0.76)	*fs*
Wainamu Beach	*Mid*	**2.39** (2.17 - 2.63)	**0.58** (0.52 - 0.64)	**0.00** (-0.09 - 0.01)	**0.97** (0.95 - 1.04)	**0.19** (0.16 – 0.22)	**0.67** (0.64 – 0.70)	*fs*
Wainamu Beach	*East*	**2.33** (2.17 - 2.61)	**0.59** (0.51 - 1.05)	**0.04** (-0.01 - 0.35)	**1.00** (0.94 - 2.17)	**0.20** (0.16 – 0.22)	**0.66** (0.48 – 0.70)	*fs*
Moonlight Bay	*West*	**1.79** (1.09 - 2.68)	**1.45** (0.66 - 1.86)	**0.28** (-0.02 - 0.65)	**2.20** (0.93 - 2.83)	**0.29** (0.16 – 0.47)	**0.37** (0.16 – 0.47)	*ms*
Moonlight Bay	*East*	**2.56** (0.82 - 5.03)	**2.76** (0.93 - 3.34)	**0.61** (0.03 - 0.38)	**1.17** (0.73 - 2.39)	**0.17** (0.03 – 0.57)	**0.15** (0.03 – 0.57)	*fs*

2.2.1 MEAN GRAIN SIZE

According to the size range classification of Folk (1974) (Figure 2.1), the dominant sediment texture was medium sand at northern Ngarunui Beach with average grain sizes of 1.77 ϕ (0.65 s.d.) and a range of 0.92 – 2.34 ϕ (fine – coarse) (Table 2.5). Once on the 27th of September, 2014, a small fraction (< 0.01 %) of silt was present (refer Appendix II). At the southern end of Ngarunui Beach during the February 10th experiment, sediment sizes were all within the fine – medium sand fraction also, with an average grain size of 1.83 ϕ (0.67 s.d.) and a range of 1.30 – 2.11 ϕ (Table 2.5).

At Moonlight Bay on the 22nd and 23rd of September, 2014, a larger fraction of fines (silts and clay sized particles) were present, especially at the eastern low tide position (~62 % fine sediment) (refer Appendix II). The average grain size ranged from coarse sand to medium silt (0.82 ϕ – 5.03 ϕ), with an average grain size of 2.23 ϕ and a standard deviation of 0.22 ϕ (Table 2.5). All Wainamu Beach sediment samples were classified as fine sands (average grain size of 2.40 ϕ and 0.67 s.d.), within the size range of 2.09 – 2.91 ϕ (Table 2.5).

2.2.2 LONGSHORE AND CROSS-SHORE VARIATION

In the foreshore zone, temporal and spatial variations in deposition occur due to ever changing wave climates and tidal conditions and their effect on swash processes. These influence grain sizes and morphology temporally and spatially (Larson et al., 1997). Stauble and Hoel (1986 as cited in Larson et al., 1997) found that foreshore composites containing samples along profile sub-environments with similar depositional energy levels and processes (such as the mean high water, mid-tide, and low water) are the most useful in the analysis of grain size distributions as they reduce some of the high variability. The lower energy environment of the nearshore has less variability while energetic bar systems and the beachface experience active sorting and sediment transport. Aeolian processes dominate in the dune areas, limiting grain sizes to smaller fractions, unless extreme events carry larger fractions into the backshore (Larson et al., 1997).

The values of sediment characteristic parameters (mean grain size, sorting, skewness and kurtosis) in composite longshore and cross-shore groupings from the intertidal zone are given in Tables 2.6 and 2.7. The longshore variation at all four sites is illustrated in Figures 2.4 – 2.8. All mean values are graphically derived and are shown as black dashed lines in Figures 2.4 – 2.8. Confidence Limits (error bars) of one standard deviation from the mean are also shown in Figures 2.4 – 2.8. Average values and standard deviations are for composite groups not the entire spread.

Much finer average grains predominated in the upper intertidal at northern Ngarunui Beach during February, July, September and October and were present in the lower intertidal once in February and once in October (refer Appendix I and II). Average grain sizes become coarser offshore (Table 2.6 and Figure 2.4). On one occasion, the 25th of October, 2014, a sample with coarse average grain size was obtained at the most northern transect at the high intertidal position (refer Appendix I and II). Little variation occurred in the longshore at northern Ngarunui Beach.

At the southern end of Ngarunui Beach, average sediment sizes were finer at higher positions on the beach except at Transect 1 where medium fractions were obtained at this position. All other samples gathered were medium sand sized except at Transect 4 where finer average grain sizes were recorded in the low intertidal zone (Figure 2.5). There was coarsening alongshore of average grain size toward Transect 1 (in a southerly direction) (Table 2.7).

At Moonlight Bay, coarsening occurred in an onshore direction (Figure 2.6). The eastern transect contained finer average grain sizes however the grain size range was far greater (Table 2.7). Average sizes of coarse sands were present at the high intertidal while average sizes of fine and medium silts were present at the low intertidal position (Table 2.6 and Figure 2.6).

Average grain size was fine sand at all locations on all dates at Wainamu Beach (refer Appendix II). Trace fractions (< 1 %) of silt and clay sized particles were found predominantly in the mid intertidal and at the eastern transect (refer

Appendix II). Greater amounts (< 10 %) of fine sized particles were found twice at the mid intertidal and once at the low intertidal positions on the eastern transect on the 12th of December, 2014 and the 15th and 16th of July, 2014 respectively.

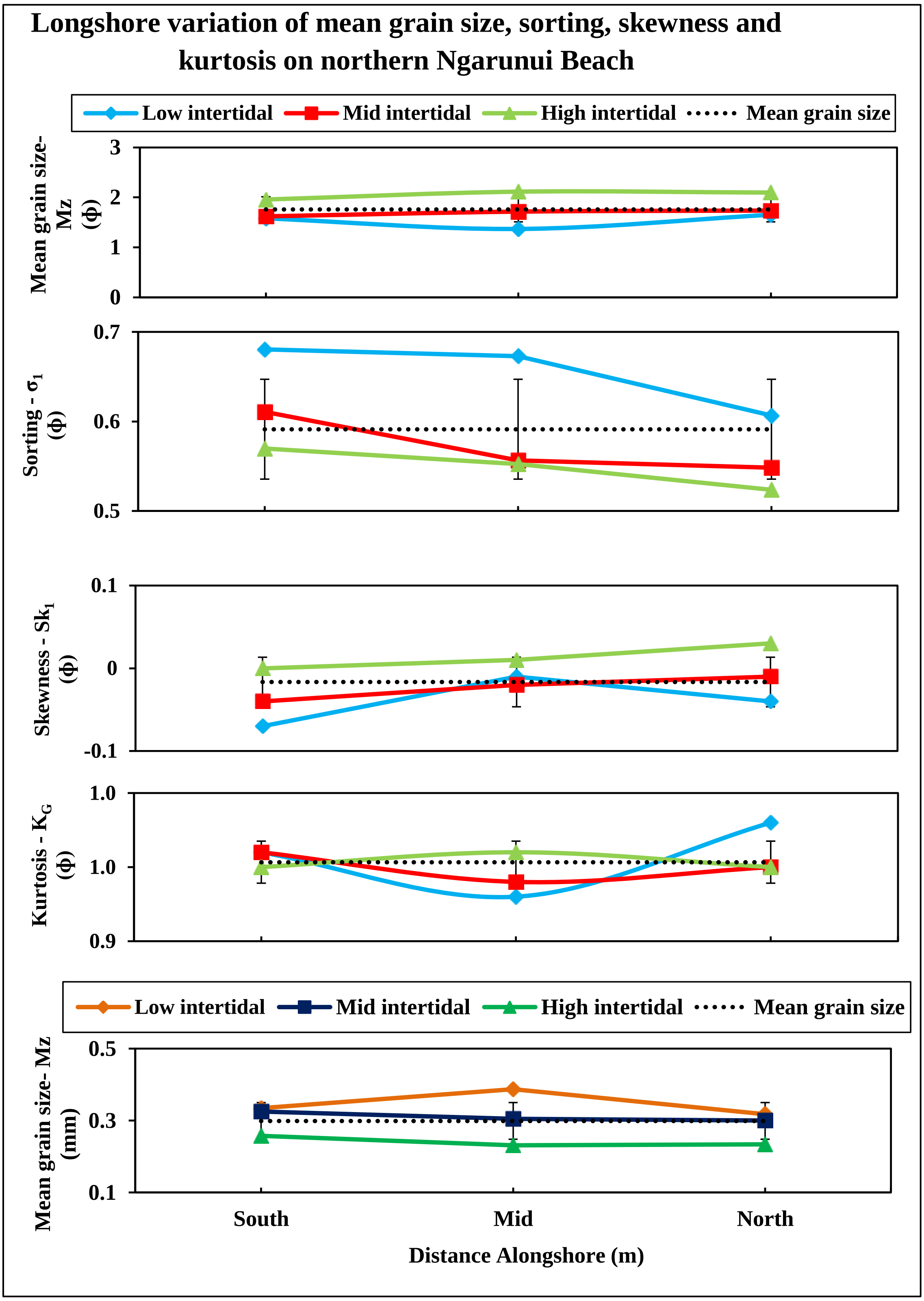

Figure 2.4: **Longshore variation of mean grain size, sorting, kurtosis and skewness for different cross-shore locations on northern Ngarunui Beach (Table 2.7).**

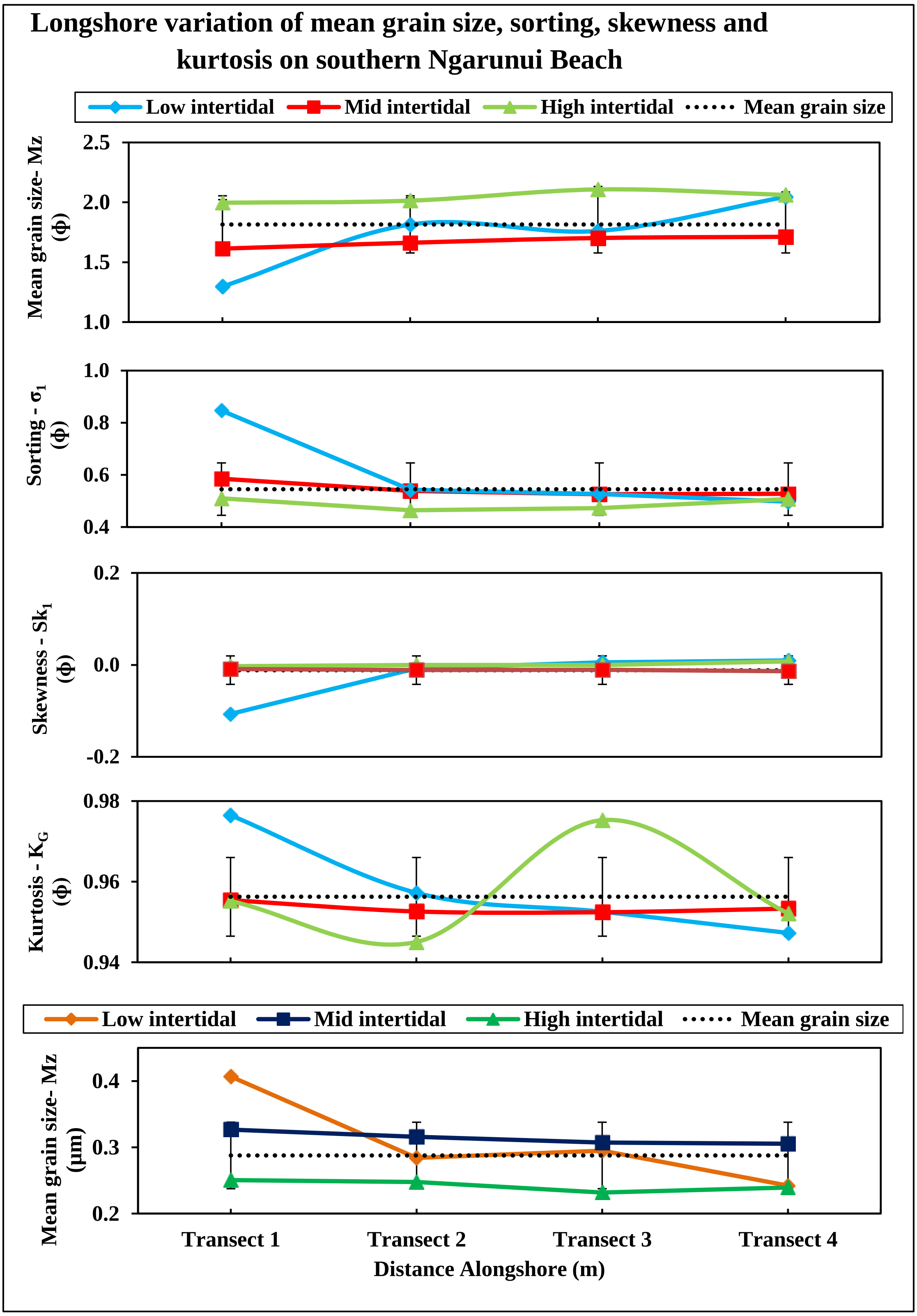

Figure 2.5: **Longshore variation of mean grain size, sorting, kurtosis and skewness for different cross-shore locations on southern Ngarunui Beach (Table 2.7).**

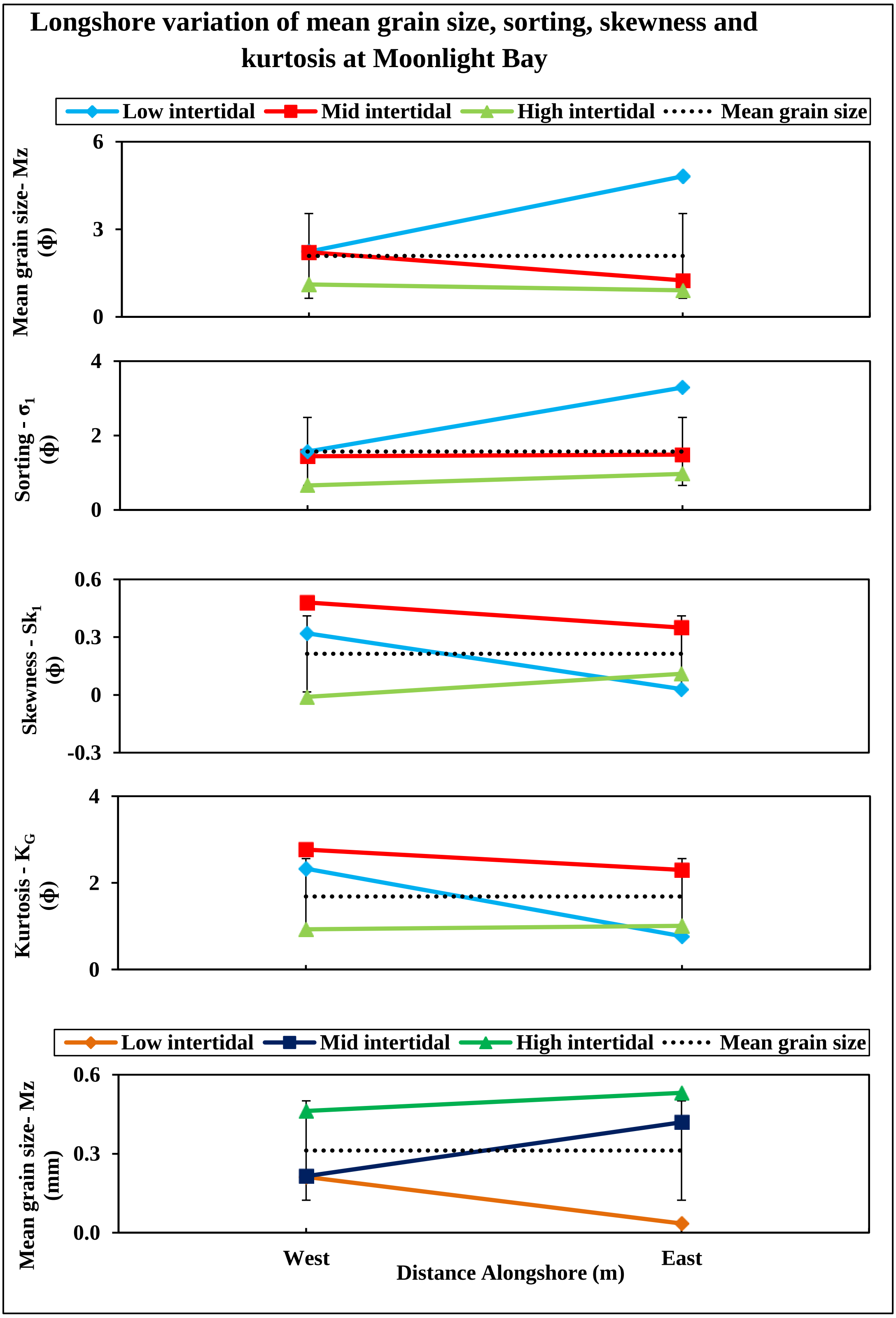

Figure 2.6: **Longshore variation of mean grain size, sorting, kurtosis and skewness for different cross-shore locations at Moonlight Bay (Table 2.7).**

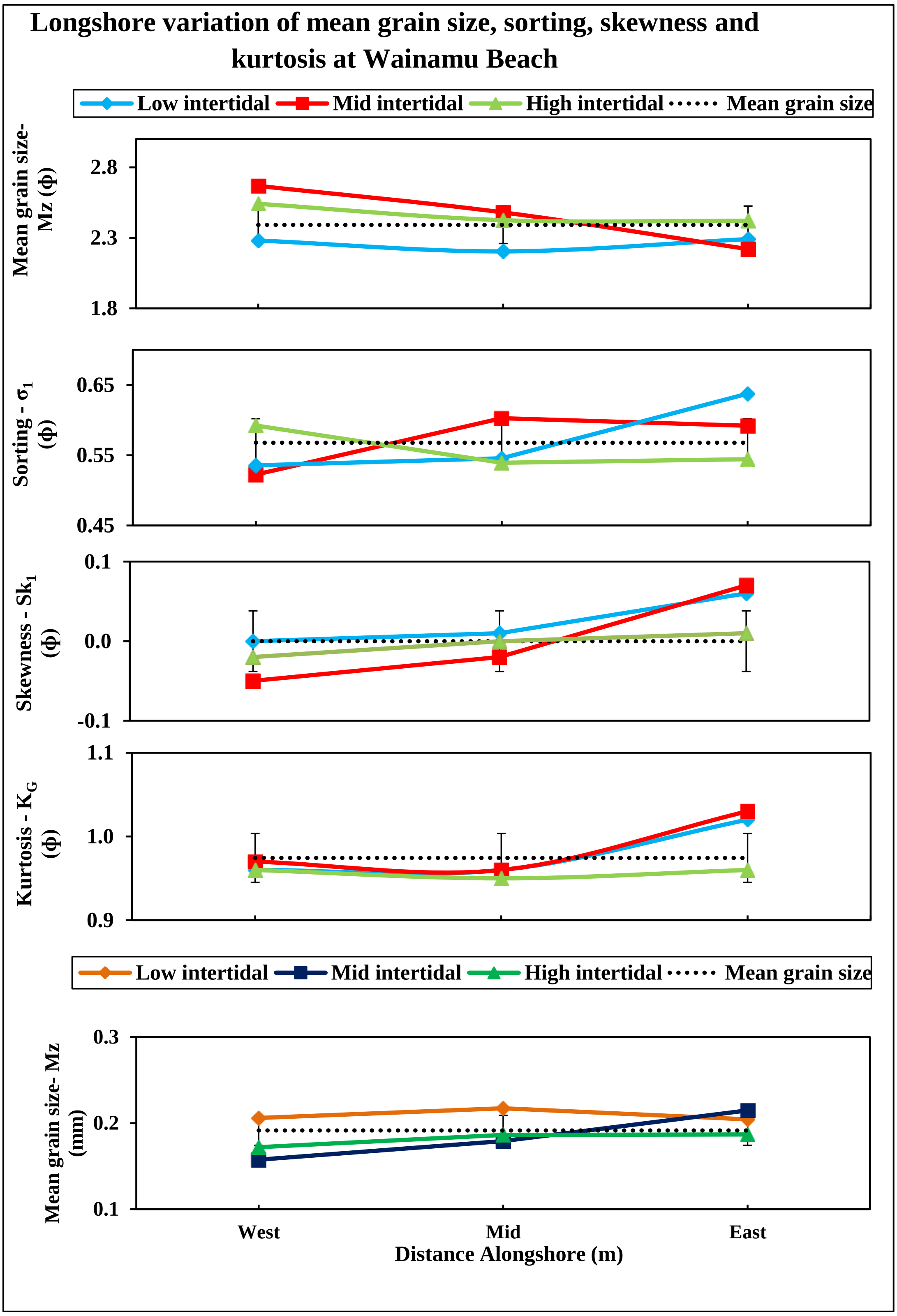

Figure 2.7: **Longshore variation of mean grain size, sorting, kurtosis and skewness for different cross-shore locations at Wainamu Beach (Table 2.7).**

2.2.3 SORTING

As the samples deviate from normal distributions, the standard deviations acquire greater error however standard deviations better represent bimodal distributions than the mean. Sorting is determined by both the size and density of the material transported. Permeability increases with poor sorting due to variable surface areas. When turbulent energy decreases, heavier gravel and larger particles settle due to their relative settling velocities while lighter, smaller particles, silts and clays, remain in suspension and are transported further from their source (Evans, 2003; Folk, 1980; Larson et al, 1997). Particle size, density, shape and the surrounding media affect settling velocities (Larson et al, 1997). The size fraction is a function of the source rock and amount of weathering. Well sorted samples are unimodal with relatively peaked (leptokurtic) distributions. Bimodal or less distinct modes (platykurtic) represent poorer sorting (Morelock et al., 2005). Poor sorting is indicative of wide bands of depositional energy, weak or undeveloped sediment transport and diverse sediment sources (Larson et al., 1997). Bimodal, multimodal or less distinct modes represent poorer sorting, common in carbonate sediments (Morelock, 2005).

Sediment samples from northern Ngarunui Beach were predominantly moderately well sorted as expected for an open coast beach in which the processes of uprush and backwash are the principal transport mechanisms. During all seven experiments, apart from the moderately well-sorted samples, seven samples were well sorted and one moderately sorted. On the 20th of July, 2014, 4 of the 6 samples were well sorted corresponding to a large storm event. All well sorted samples were obtained from the mid and high intertidal positions; the moderately sorted sample was from the low intertidal position on the southern Transect. Slightly poorer sorting was found at the low intertidal position, with better sorting in a northerly direction along the foreshore.

Sediment samples from southern Ngarunui Beach were mostly well sorted to moderately well sorted (refer Appendix II). Sediment was consistently less well sorted in an offshore direction (Figure 2.6 and Table 2.5). Sorting showed little variation alongshore except at the low intertidal site of Transect 1 that showed less sorting (Figure 2.7 and Table 2.5).

Moonlight Bay was mostly poorly sorted, indicative of low energy environments with weak transport energies and multiple sediment sources. Extremely poor sorting predominated at low intertidal, especially on the eastern transect (Figure 2.6, Tables 2.6 and 2.7), corresponding to the coarser average grain sizes and the presence of large fractions of fine sediment in this location. The high intertidal zone on the western transect was moderately well sorted (refer Appendix II). The Moonlight Bay samples display bimodal frequency curves, with sub equal amounts in the two peaks (refer Appendix II).

Wainamu Beach consistently produced moderately well sorted averages for grain size. Only twice, both at the mid-intertidal site on the western transect were averages well sorted (refer Appendix II). One moderately sorted sample and one poorly sorted sample came from the eastern transect, at the mid intertidal and low intertidal respectively.

2.2.4 SKEWNESS

Skewness indicates the degree of asymmetry of a distribution curve (Folk, 1980). Symmetrical curves have skewness values of 0 and reflect a state of dynamic equilibrium between the dominant wave and energy conditions during sampling (Beamsley, 1996). A negatively skewed distribution (left skewed) indicates a large proportion of coarse grained material and a positively skewed distribution (right skewed) indicates finer sediment fractions dominate (Folk, 1980). The inclusive graphic skewness (Sk_G) is commonly used as it incorporates the values in the tails of the distribution curves and is independent of sorting (Folk, 1980; Maher, 1989).

All sediment sample size distributions were near symmetrical skewed at Ngarunui Beach, indicative of dynamic equilibrium conditions during all experiments over a four month period in 2014 (Table 2.5). The variations in sorting at these sites were therefore insufficient to affect the skewness. A single low intertidal sample taken from southern Ngarunui Beach on the 10th of February, 2015, was coarsely skewed (refer Appendix II). Wainamu Beach also exhibited near symmetrical skewness during all experiments although on three occasions along the eastern profile values diverged; twice at the mid-intertidal position and once in the low intertidal zone (refer Appendix II). Moonlight Bay samples indicated a predominance of strongly fine, fine and near symmetrical skewness values (refer Appendix II). All mid intertidal samples at Moonlight Bay exhibited strongly fine skewness, while the high intertidal zone on the eastern profile exhibited fine skewness during both samplings (refer Appendix II). Along the western profile, the low intertidal zone displayed strongly fine skewness on the 22nd of September, 2014 and became finely skewed overnight. This may be due to sampling methods. During both experiments, samples from the high intertidal zone of the western transect and low intertidal zone on the eastern transect were near symmetrical skewed indicating dynamic equilibrium.

2.2.5 KURTOSIS

Kurtosis implies how tall and sharp the central peak of the size distribution curve is, relative to a normal Gaussian curve (Folk, 1980; Maher, 1989; Wolfram, 2011). Increasing kurtosis is associated with larger probability mass in the centre of the distribution (more of the variability of the distribution curve is due to a few extreme differences from the mean) and is said to be leptokurtic or excessively peaked (Brown, 2015). Extreme values of kurtosis imply multiple sediment sources (Folk, 1980) while variation reflects the medium's flow characteristics (Baruah et al., 1997; Ray et al., 2006 as cited in Rajganapathi, Jitheshkumar, Sundararajan, Bhat and Velusamy, 2012). Platykurtic distributions with less distinct modes occur as the probability mass shifts to the tails and flattens the distribution curve; the results of a larger number of modest differences from the mean over time (Maher, 1989). Carbonate sediments often display multiple or less distinct modes. Normal Gaussian distributions have graphic kurtosis (KG) values of 1.00 (Folk, 1980; Maher, 1989; Pfannkuch and Paulson, n.d.).

All samples from Ngarunui Beach during in all experiments displayed mesokurtic grain size distributions consistent with the near symmetrical skewness of the distributions and moderately well sorted average grain sizes. Only two samples from Wainamu Beach displayed very leptokurtic grain size distributions. Both samples were from the eastern profile; one in the mid-intertidal zone on the 12th of December, 2014 and the other from the low intertidal zone on the 16th of July, 2014. Moonlight Bay showed greater variation, with most samples being very leptokurtic and leptokurtic (Table 2.5). Mesokurtic samples were gathered from the high intertidal and samples from the low intertidal on the eastern transect were platykurtic on both days (Figure 2.6), corresponding with the larger fraction of smaller particle sizes at these locations.

2.2.6 SEDIMENT TEXTURAL PROPERTIES

Unconsolidated clastic sediments including detrital quartz grains and other resistant minerals such as feldspars comprise most coastal deposits (Zeeman, 2008). These siliclastic sediments are eroded to equidimensional shapes during long periods of transportation. Settling rates of platy grains are slower than for rounded grains (Morelock, 2005). Preferential entrainment and transportation of angular, platy and lighter sediment occurs and preferential erosion of platy sediment also occurs (Larson et al., 1997; Morelock et al, 2005). Clay and silt cohesive particle aggregates can also form producing larger grain sizes.

From visual analysis of sediment samples from the low intertidal, mid-intertidal and high intertidal from each experiment site; Ngarunui Beach, Wainamu Beach and Moonlight Bay (Figures 2.8 – 2.13), it was considered that mostly particles were rounded and well-rounded according to the classification of Powers (1953) (Figure 2.5), common for siliclastic sediments that are far from source. Sediment from Ngarunui and Wainamu beaches possessed considerable amounts of euhedral shaped particles with lower sphericity (Figures 2.9 and 2.13) while the sediments from Moonlight Bay displayed greater sphericity and were well rounded and rounded with some more platy grains (Figure 2.11 and 2.12) as well as smaller fractions with shapes not visible under microscope (Figure 2.14). Bioclastic fractions were much greater in Moonlight Bay samples from visual approximation (Figure 2.8 and 2.10).


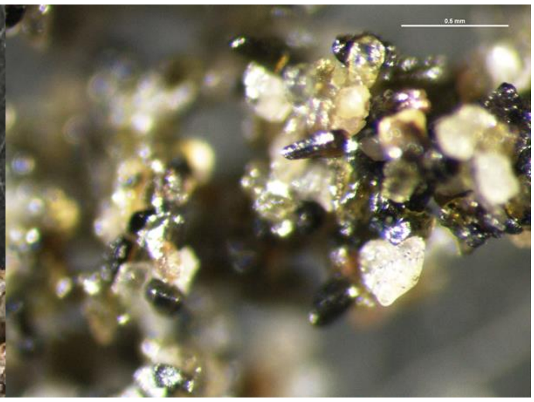

***Figure 2.8:* Sediment containing bioclasts from the mid intertidal zone of the southern transect on northern Ngarunui Beach on the 27th of September, 2014. *Figure 2.9:* Sediment taken from the high intertidal zone on the eastern transect of Wainamu Beach on the 15th of July, 2014.**

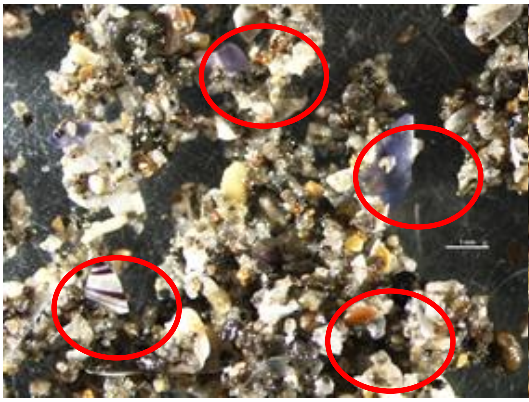


***Figure 2.10:* Bioclastic rich sediment from the low intertidal zone of the southern transect on southern Ngarunui Beach on the 10th of February, 2015. *Figure 2.11:* Sediment from the low intertidal on the eastern transect at Moonlight Bay collected on the 23rd of September, 2014.**

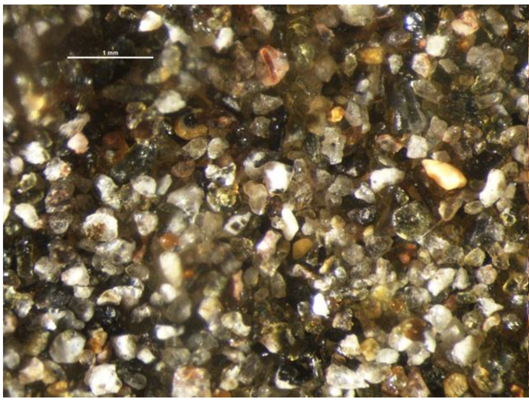


***Figure 2.12:* Sediment grains from eastern transect at Moonlight Bay collected on the 23rd of July, 2015. *Figure 2.13:* Sediment grains from southern Ngarunui Beach collected on the 23rd of July, 2015.**

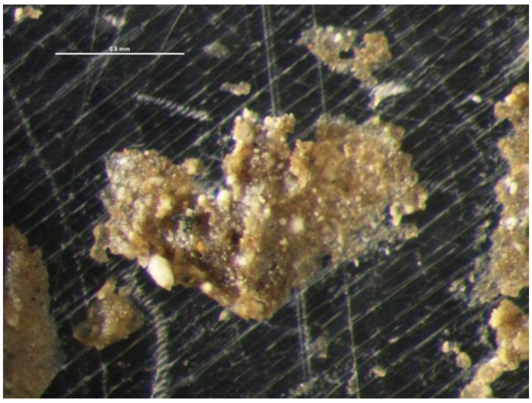

Figure 2.14: **Fine sized particles collected from the low intertidal on the eastern transect at Moonlight Bay on the 23rd of September, 2014.**

The significant distinction in morphology between the estuary sediments from Moonlight Bay, open coast Ngarunui Beach and the inner harbour entrance sediments is likely due to both the significant differences in processes acting on the sediments and selective sorting of the fractions by wind and wave energy particularly on the open coast. High wave and tidal energies respectively at Ngarunui and Wainamu Beaches would effectively erode the grains that are present, while low energy estuarine processes at Moonlight Bay and further in the estuary result in more angular grains. The rounder grains present in the estuary have likely undergone substantial transport and deposition and the smaller clay fractions are likely to have been transported from catchment sources. Elongate, darker grains on the coast and in the harbour entrance are likely to be minerals such as hornblende eroded from Mt Karioi lavas and lahars.

2.2.7 FAIR WEATHER AND STORM EVENTS

Grain size distribution is often affected by variations between fair weather and storm conditions on New Zealand beaches occurring throughout the year. Characteristic accretionary/erosive profiles are representative of fair weather and high wave periods due to increased frequency of storm events, respectively. Fair weather profiles commonly consist of finer grained, well sorted sediment, while storm profiles typically exhibit coarser, poorly sorted sediment (Larson et al., 1997). However, at Ngarunui Beach, storm conditions are reflected by an increase in finer, but much denser titanomagnetite and other heavy minerals. These form a very dark lag surface. It is common for lag deposits of coarser and denser grains to remain on beaches after high energy storm events due to decreasing energy gradients that are no longer able to entrain the sediment (Larson et al., 1997).

The quasi-periodic cycles (2-7 years) of El Nino Southern Oscillation (ENSO) and the Pacific Decadal Oscillation (PDO) also influence beach morphodynamic behaviour and sediment properties on longer time scales (de Lange, 2001). Higher fractions of shells were observed at Ngarunui Beach on the 15th and 30th of August, 2014, the 27th of September, 2014 and the 10th of February, 2015, during and following storm conditions, especially in the low intertidal zone. Wainamu Beach showed less variation with storm forcing although a small shell fraction could be seen on the 28th of November, 2014. Moonlight Bay was not sampled enough to allow any inferences to be made although large shells and fragments were observed during sampling at most locations on Moonlight Bay.

The presence of rare, heavy minerals or placer deposits in the nearshore can exhibit pronounced seasonal variations with lag deposits associated with storm events. These heavy minerals also provide information regarding sediment source geomorphic variability in the coastal zone (Larson et al., 1997). Darker, fine sediments, thought to be titanomagnetite placers were found in the high intertidal zone at Ngarunui Beach during experiments on the 27th of September, 2014 associated with a large erosive storm event.

Figures 2.15 and 2.16: **Placer deposits exposed on the 19th of October, 2014 at 1.05 pm and the 8th of August, 2014 at 9.39 am respectively.**

The presence of titanomagnetite placer deposits were observed around the southern end of the harbour entrance at Ngarunui Beach after large storm events and high winds aided in exposing the placers (Figures 2.14 and 2.15). Titanomagnetite placer deposits within facies stratigraphy were also exposed directly adjacent to the harbour entrance on the 26th of October, 2014 after a large erosive storm event which caused a new scarp to form (Figure 2.16).

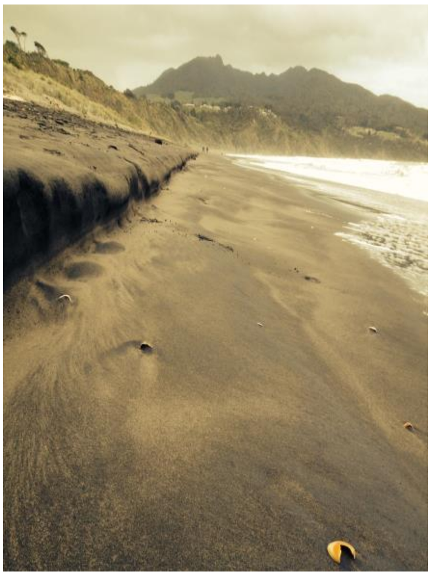

Figure 2.17: **Placer deposits exposed on the 26th of October, 2014 at 12.40 pm.**

2.3 DISCUSSION

The single source sediments and higher energy at Ngarunui Beach and Wainamu Beach is consistent, with both displaying fairly normal curves. However, multiple sediment sources and low energy conditions at Moonlight Bay resulted in sediment displaying pronounced skewness and kurtosis and poorer sorting. Distinctive variations in grain size distributions were found at different locations within Moonlight Bay due to the sheltering effects of the local morphology; coarse fractions were found at the high intertidal area and at the mid intertidal area of the eastern transect. Fine sediments (clays and silts) were present at the low intertidal and the mid intertidal due to low energies within the estuary. Size fractions were slightly smaller in the low intertidal zone and at the mid intertidal in the eastern transect at Wainamu Beach as this is the area closest to the channel experiencing the greatest tidal currents in the case of the low intertidal. The mid intertidal area on the eastern transect is most exposed to the greater currents associated with the ebb tide as this area is sub-aqueous for longer periods due to reduced elevations (Figure 1.3).

Low wave energies associated with fine conditions caused the foreshore means to become slightly finer and more well sorted at Ngarunui Beach. Storm conditions resulted in medium sized foreshore mean particle sizes with poorer sorting. Lag deposits of shell fragments and placers were observed after storms however larger variations in median grain sizes and sorting were not observed such as granule lags.

Grain geometry was not investigated further than a few grains. Both subaerial and subaqueous samples are necessary to adequately interpret coastal zone environments however only subaerial samples were attainable. Variations of grain properties with depth were also not investigated due to time limitations with approaching tides.

CHAPTER THREE: DEPTH OF DISTURBANCE

3.0 INTRODUCTION

Determination of sediment activation depths during tidal cycles or storm events is essential in design of beach replenishment schemes, estimation of transport rates in the active bed layer, for viability of substrate as marine faunal egg laying grounds and in modelling nearshore processes (Anfuso, 2005, Ciavola et al, 1997). Because depths of disturbance values approximate the initial vertical borrow of hydrocarbon contaminants, interpretation of cross-shore variability is essential for effective oil excavation and efficacy of clean-up operations. Interpretation of morphodynamic variability on shorelines is likewise essential for estimation of oil burial depths and locations as relatively unweathered, highly toxic residual oil can re-emerge on beaches after years due to exhumation (Bernabeu et al., 2006).

This chapter examines the depths of disturbance on three significantly different beaches; Ngarunui Beach, an exposed open coast beach; Wainamu Beach, a tidally dominated beach on the channel of the main estuary in Raglan and; Moonlight Bay, a sheltered beach within the Raglan Harbour. A network of depth of disturbance rods was used to monitor bathymetric evolution and the transitory layer of mixing in the surf/swash zone. Depth of disturbance was recorded during storm and fair weather conditions and related to breaking wave height (H_b) (as representative of wave and swash/backwash energies), beach face slope (β), and breaking wave angle (α) through the model of *Bertin* et al. (2008). An attempt to relate grain size variation to mixing depths was also carried out. Images of Ngarunui Beach were geo-rectified and rod positions were located within images and exposure to wave conditions was observed. Beach surveys carried out on Ngarunui Beach provided information data for the estimation of rates of morphological change.

3.1 REVIEW AND SYNTHESIS OF THE LITERATURE

3.1.1 DEPTH OF DISTURBANCE (DOD)

Depth of disturbance (DoD) is the vertical thickness of the active bed layer in which the physical mixing of sediment by wave action and currents occurs. Waves in the surf zone exert strong shear stress on the sea floor, fluidizing the upper layer of sediment to some depth and in this state the sediment grains can move laterally and vertically. However there are many factors which can cause disturbance of sediment including scouring, mixing under plunging breakers, turbulence caused by the collision of run-up and rundown in swash and the pressure gradient at the bottom of the water column associated with sheet flow (Sunamura and Kraus, 1985).

Depth of activity or sediment activation depth is defined as a "river of sand moving upon an unaffected substratum and is related to wave and wave induced current action in the breaker, surf and swash zones" (Anfuso, 2000; Sherman, 1993) and "the thickness of bottom sediment layer affected by hydrodynamic processes, essentially waves and currents, during a time span varying from a few minutes or hours to a tidal cycle or several days" by many authors including Gómez-Pujol et al. (2011), Ciavola et al., (1997), Kraus, (1985), Greenwood and Hale, (1980) and Anfuso, (2005). It has been assumed that the depth to which sand mixes vertically, DoD, is equal to thickness to the laterally moving active layer. This is based on the premise that grains which exchange positions vertically will also participate in the lateral motion (Kraus, 1985).

Activation depth is an altitude difference measured commonly within intertidal periods. The spatial distribution of activation depth has been investigated by Kraus (1985) Ciavola et al. (1997) and others. Activation depth is therefore often ascribed no temporal connotation or specific methodology, but applies to a generic process (Anfuso, 2005).

Depth of disturbance has been defined by King (1951), Williams (1971) and Anfuso (2005) as the layer of sand affected by hydrodynamic processes during a single tidal cycle or multiple tidal cycles and storm events. Restrictions on the use of "depth of disturbance" as being only representative of small scale topographic changes, excluding those of accretionary/erosive events and large scale bed-form migration during only a single tidal cycle were given by Williams (1971). However, commonly in contemporary literature is it considered the longer term component of activation depth reflecting landward and seaward surf and swash zones migration; in contrast to a concrete moment in recording hydrodynamic processes (Anfuso et al, 2000; Anfuso, 2005).

Mixing depths are defined by Anfuso (2000), Kraus (1985) and Kraus and Sunamura (1985) as the "depth of activity measured over time scales of a few hours and during the passage of a few waves, not affected by waves, seasonal cycles of beach profiles, or tidal action or large - scale tidal bedform migration" and thus it is conceptually different to disturbance depth. With the passage of the tide and cross-shore transport, substantial surface level changes may result. However, other authors such as Ciavola et al. (1997) and Ferreira et al. (1998; 2000) used mixing depths to describe sediment activation over tidal cycles and used similar methodology for determination of intertidal activation depths to those of intra-tidal temporal scales. The ambiguity of this means that lots of different approaches to measurement of DoD exist, and their results may be conceptually different.

Limitations of tide scale measurements are that altitude differences measured by topographical surveys at low tide, whilst providing an overview of intertidal domain changes, lack in their ability to continuously record bed level changes or evolution through the tidal cycle i.e. perturbations due to wave action, as noted by Arnaud et al. (2009) and Jackson and Malvarez (2002).

Sediment characteristics, beach grain size, breaker height, Shield's parameters, beach slope, bedform migration, wind strength and direction, bottom currents, energy fluctuation, and pressure gradients have all been explored to varying degrees as variables affecting DoD (Malvarez, 2002; Williams, 1971).

King (1951) pioneered research into the relationship between wave breaker heights, H_b, wave periods, T, and beach slopes with depth of disturbance of beach sediments using pegs and dyed sands. Transient zones of coloured sand tracts (6-9 inches deep) were emplaced along beach profiles. After a complete tidal cycle, sediment disturbance depths are determined as the distance from the sharp contact of the remaining coloured grains to the sediment surface. It is within this zone that sediment undergoes scattering and dispersion by waves (King, 1951). Pegs placed close to the coloured sand tracts were used to identify any surface elevation variation that had occurred. By including only samples which displayed nil or negligible surface level variation (in equilibrium) it could be assured that the actual disturbance readings were not confounded by any surface elevation change that occurred post maximum disturbance (King, 1951).

Correlation of the different parts of the wave profile with maximum DoD are confounded by the succession of the different parts of the wave profile, and associated different processes, traversing the width of the beach during the tidal cycle. The duration each of the processes acts on the beach sediment, controls DoD, particularly at the low and mid tide zones (King, 1951).

Values of disturbance depth were observed by King to be in the order of a few centimetres at four beaches in the British Isles, with greatest values in relatively shallow water, at and inside the breakpoint of waves. Outside of this breakpoint orbital velocities are unlikely to extend from the water surface to the floor (King, 1951). King determined that a linear relationship exists between wave height and depth of disturbance (DoD) with values of between 3 - 4 % of average breaking wave height, H_b. These small values of DoD have implications for the protection of bedrock from wave scour action; sand removal by this method must be relatively small so abrasion of bedrock will only occur where sand cannot accumulate i.e. at exposed headlands, under storm conditions, or where littoral drift removes large quantities of sand.

King made an attempt to relate the wave energy, E, to DoD, through equation;

$$E = 0.64\ \omega\ H^2 T^2 \tag{3-1}$$

where E is the wave energy in foot-lbs., H, is the wave height in deep water in feet, and T is the wave period in s, again presented a linear relationship. King found no correlation between wave length and DoD however she suggested that wave length, L, and period, T, may play a secondary role in sand disturbance with wave height being the primary mechanism of sediment disturbance.

Using an angular distance to the nearest second of arc between wave crests and troughs, after *Williams* (1971) method, King was able to determine wave heights at offshore positions which replicate deep water wave stages i.e. non-shoaling waves. Good correlation between this proxy deep-water wave height and DoD was obtained, although this was on a dissipative beach.

At Rhosili Beach under long swells and large tidal ranges, it was noted that values in the swash zone were comparable to those at the wave breakpoint as a result of dissipation of energy across a wide cross-shore zone (King, 1951). Conversely at Druridge Beach in South Wales, a narrow, concentrated zone of turbulence at the breakpoint, led to greater values of DoD under similar breaking wave conditions. King asserted that because of the mobility in coarser grained beaches, water may percolate more readily, creating steeper and more turbulent swash slopes, however other authors such as Williams (1971), Kraus (1985), and Sunamura and Kraus (1982), have maintained that it was related to the position of the breaker line. Both beaches displayed similar magnitudes of DoD.

In contrast to King's earlier work, Otvos (1965) and Williams (1971) observed that sediment size had little or no effect on disturbance depths. Williams in the summer of 1971, researched sediment fluxes over single tidal cycles on three bays on Hong Kong Island, concentrating on median grain size and position on beach face, as constraints on and in addition to breaker height, H_b, beach face slope (°)

and wave period, *T*. Using control sedimentation stations with dissimilar median grain sizes, Williams was able to determine that disturbance depths and erosional rates were analogous between different grain sizes under similar wave conditions and beach morphologies. Likewise, Otvos, from evaluation of differential erosion rates on two Long Island Sound, Connecticut, beaches in 1965 found no statistical correlation between breaker heights, H_b, as representative of wave and swash/backwash energies, and median grain size diameter or between breaker heights, H_b, and ratios of differing grain sizes. Sediment variation was determined to be the result of pre-tide distribution and coincidental encounters of discreet sediment fractions with waves and swash/backwash and their associated mixing processes, consequently breaker height variation does affect sediment distribution, although averaging of breaker height values makes any variation in breaker energy illusive (Otvos, 1965).

As the sediment composition varied greatly on the beaches observed by both Williams (1971) and Otvos (1965), dual, single and multiple sedimentation units formed as the consequence of substantial erosion or deposition of previously deposited beds. Sedimentation sequences show initial flood tide brings deposition in the swash zone, followed by strong erosion in the surf zone with the progressing tide, which may or may not completely erode the initially deposited layer. During the ebb tide, deposition under both the breaker zone and the swash zone results in accumulation of coarser (lower) and finer (upper) sedimentation units respectively (Otvos, 1965). Some variations in energy regimes within the tidal cycle resulted in reversed sequences of beds and quadruple beds (Williams, 1971). Grain size analysis of median diameters of discreet sediment beds, indicated coarser grained lower units, exhibiting poorer sorting ($\sigma 1$ = up to 2.2) and negative skewness (SK_G = -0.68-+0.26); the result of effective winnowing of smaller sized grains in the highest-energy breaker zone during ebb tide (Otvos, 1965). Some of this winnowed-out material is recaptured as the fine surface layer deposited during the ebbing tide atop of the coarser fraction, which was deported during the energetic breaking on the ebbing tide (Williams, 1971). In the swash zone, symmetric size distribution and good sorting exists as only a constrained range of sediment is carried by the swash current and only the finer fraction is transported back to the breaker zone by backwash (Otvos, 1965).

Highly variable heavy mineral assemblages over small beach surface areas were understood to be the function of; varying hydraulic conditions (energy from waves); the mixing of adjoining sand bodies; original source rock grain sizes and natural 'panning' with heavy minerals left behind on the sand surface while lighter fractions are removed (Otvos, 1965). Deposition depths of heavy mineral laminations are determined by breaker heights and associated hydraulic energies.

Values of DoD were distinctly inconsistent with King's reported 2-4 % H_b, being in the range of 40% H_b, on the Hong Kong islands and 20-40% H_b, on the U.S. beaches (from 342 measurements) (Otvos, 1964 and Williams, 1971). Both authors noted greater disturbance in the foreshore zones at the breakpoint of waves, than in the upper swash/backwash zones. Some measurements at low water were absent but Williams noted that measurements in the mid-tide position replicated those at lower low water.

Differences between the large values of DoD given by Otvos (1965) and Williams (1971) and those of King (1951) are attributed to variations in the bottom profiles and incomparable waves and therefore beach types (Williams, 1971). King's studies were done in spilling conditions on dissipative beaches with various breaker lines, while the three Hong Kong beaches exhibited lower frequencies than surf waves, mostly < 2, with plunging waves and large ripples dominating. Plunging waves dominated on the Long Island Sound beaches. The variable breaker lines in King's study lead to dissipation of energy over the entire beach width and no variance in disturbance depth with position on the beach face.

On the Connecticut beaches large variation of disturbance depth under the same wave heights was considered to be the consequence of scouring or protection by pebbles, littoral drift direction and time within the breaking wave zone (Otvos, 1965). Bottom currents, energy fluctuations, wind strength and direction contributed to the variation in DoD values by Williams in Hong Kong (1971).

For equilibrium purposes, Williams rejected values of surface elevation change greater than ½ an inch in statistical correlation analysis of breaker height with depth of erosion. Williams found that breaker height determines 82% (0.001 significance level) of the depth of disturbance in the mid/low tide zone, while slope is a more significant factor in the higher high-tide zone, where poor correlation between wave heights and DoD exists (Williams, 1971). This area of second energy maxima is also where other complex swash processes dominate; according to Williams (1971) only 61 % of DoD can be explained by the breaker height, slope and wave period, in this zone (0.01 significance level). Wave period was found to have little effect on both beach slope and DoD anywhere on the beach, as backwash generally returns to the breaker point before the approach of the subsequent wave except on reflective beach profiles, where waves do not break or surge (Kemp and Plinston, 1968 as cited in Williams, 1971).

Often the breaker zone is coupled with the breaker zone step "a sudden steepening of the foreshore in a relatively narrow zone parallel with the shore" as it moves landward (Miller, 1958 in Otvos, 1965). Otvos (1965) stated that these steps form not only by the collision of swash/backwash sediment loads with material transported by the incoming wave, but also through piling up of coarse, poorly sorted sand and pebbles with wave action, moved landward by the transgression of the tide and supplemented with backwash material. Breaker zone steps can form on low slope beaches (<5 °), and with negligible breaker activity, during the turning of the tide and subsequent ebbing tide, when backwash energy is great enough to shift fine-grained sediment downslope, where the balancing forces of small breakers keep the ridge in place until the step is formed by accumulation by backwash currents. Breaker heights, H_b, with a range of 10-25 cm were attributed with 3.75-15 cm high steps, while smaller wave heights produced smaller steps (Otvos, 1965). Finer grains are usually associated with high steps.

On a Pacific Ocean beach in Ensenada, Mexico, Gaughan (1978) used a mid-tide single point source to release 20-50 kg of fluorescent sand tracer grains, to interpret the depth of vertical mixing, b_m, as the vertical layer between the sediment surface and the lower limit of observed tracer grains. By inserting transparent sampling tubes inside coring pipes at 0.2 and 0.32 of an ebbing tide, Gaughan was able to obtain concentration weighted 0.4 cm core slices to determine vertical mixing for a 4 hour period. For this typically dissipative, (ξ= 30), gentle sloping (tangent s= 0.012), wide beach with characteristic spilling waves, fine grained sediment and moderate tidal ranges (~2 m), DoDs were distinctively smaller than those of King (1951), Otvos (1965) and Williams (1971). These greatly reduced DoD values were likely the result of short time exposures of passing surf bores and the associated bottom stresses as well as differing breaking processes (Gaughan, 1978).

Gaughan quantified the relationship between DoD and the incident wave conditions by extricating the spring/summer and autumn/winter profiles. Histograms of DoD show average DoD values and wave heights, H_b, doubled during the winter/autumn season; 1.1 cm (range 0.2 – 1.6 cm) (s.d. = 0.5) for winter conditions and during the spring/summer months when average DoD was 0.5 (s.d. = 0.5) for wave heights, H_b, of 75 and 150 cm respectively. Grain size distribution, heavy mineral concentration, beach surface levels and beach transport mechanisms transform with seasonal cycles. However this seasonal aspect had not been apparent in the earlier studies at Long Island Sound (Otvos, 1965).

During the autumn/winter regime experiment, when large waves pervade, maximum concentration of tracers are found at the bed surface shoreward of the mid-tide zone; the result of swash deposited sediment that is continually receding seaward during the ebbing tide. Maximum concentration is one layer below the surface seaward of the mid tide and alongshore of it, 0.4 – 1.2 cm and 0.4 – 1.6 cm respectively (Gaughan, 1978). Maximum concentrations of tracers were predominantly found in a shore parallel line, at the mid tide position. Few DoD samples showed dependence on distance from injection site and none showed any dependence on wave exposure after 3 hours (Gaughan, 1978).

Complex morphologies have been found to result in proportionality constants of 0.05 for the relationship between mixing and breaking wave height (Kato et al, 1985 as cited in Sherman, 1993). Sherman and Greenwood (1984) established that with megaripple migration, vertical mixing exceeded 0.16 m for maximum breaking wave heights of 2 m. Sherman et al. (1993) found predicted disturbance values were twice as high in a bar-trough system and four times as high in megaripples associated with rip-feeder channels, than on planar beaches as mixing depths associated with bedforms is dominated by longshore currents and not direct wave action. The bedform migration rate of 0.275 mm/s (0.99 m/hr) found by Sherman et al. (1993) was considered as reasonably representative of the surf zone conditions for intermediate beach states and compared well with other megaripple migration rates. Bedforms such as ripples and megaripples are associated with bar troughs and feeder channels and can be found offshore of breakers on high-energy beaches (Clifton, 1976 as cited in Sherman et al., 1993). Because mobile bedforms can occur across the beach face, and enhanced sediment mixing occurs at these locations, it is likely that mixing across, especially dissipative and intermediate beaches and post storm morphologies, will be highly variable (Sherman et al. 1993).

To determine the relationship between the thickness of the beach active layer, associated morphological change and Lagrangian and temporal patterns of sediment transport during high energy conditions, Greenwood and Hale (1980) and Greenwood and Mittler (1984) focused on discrete storm events of known frequency, on submerged, crescentic nearshore bar system in Kouchibouguac Bay, New Brunswick, southern gulf of St. Lawrence. Using 62 depth of disturbance rods (0.5 cm width x 1-2 m in length) emplaced by scuba, determination of net surface changes and sediment flux (total and net transport) was attained by Greenwood and Hale (1980). Greenwood and Mittler (1984) intensified rod measurements at the outer bar, every 10 m within a 100 x 150 m grid, in which control volumes were generated for sub-sections of the grid and a mean profile was assumed. The use of control volumes produces time-integrated estimates of transport rates or *integrated total volume flux* (ITVF) while surface elevation change during the storm event is expressed as *integrated net volume flux* (INVF).

Fluorescent tracers with a concentration cut-off of 10 grains per 30 grams and epoxy peels of box cores were also used by Greenwood and Hale (1980). Structural indices produced by bedforms; truncation of bioturbation phenomena, structural or textural changes and scour planes appear in epoxy peels providing direction, rate of transport and calibration for rod and washer results. Good correlation between rods and box core characteristics, including fluorescent tracer distributions was established (Greenwood and Hale, 1980).

During a large storm on the 11th of June, 1976, with a return period of 1.3 years (~ annual maximum storm), with wave periods, T, of 6 s and significant deep water wave heights, H_{bs}, of 2 m, a bimodal distribution of depth of activity was observed within a single bar profile. From disturbance rod experiments, maximum values for both depth of activity (43-70 cm, decreasing with distance along slope) and net elevation change (35 cm) were detected on the seaward side of the crest of the bar (Greenwood and Hale, 1980).

Crest maxima can be related to the seaward migration of lunate megaripples in 'rip-type' currents generated by intense wave breaking with decreases in water depth during the storm event or intense asymmetric wave oscillatory flows at the bed (Greenwood and Hale, 1980). Minimum (6 cm) depth of activity was on the landward side of the crest with negligible values or no net surface elevation change seaward of crest in all profiles (Greenwood and Hale, 1980; Greenwood and Mittler, 1984). The second disturbance maxima (43 cm, erosion = 37 cm, is positioned in the trough landward of the bar, due to scour by longshore currents which are generally short-lived and have high rates of unidirectional sediment flux. Disturbance and elevation change indicate that in this instance surface lowering was prevalent and the crest of the bar was moving seaward, the trough was deepening and the seaward slope steepening, a general bar response to storm events (Greenwood and Hale, 1980). This was further validated by structural indices reflecting increased landward transport; lunate megaripples, ripples and sheet flows increasing with elevation up the seaward slope and associated shallowing on the seaward slope.

Much larger values of disturbance and net bed change appear in the shoaling zone of a two bar profile, to the south of the single bar profile. The depth of activity doubled during the storm event, from 28 cm to 60 cm inclusive of 32 cm of erosion. This is because there is a larger area of the bar form in shallower water intensifying of wave and current activity (Greenwood and Hale, 1980).

Kraus (1985) emphasised the bimodal conditions of the cross-shore mixing depth profiles, with maxima near the breaker line and outer half of surf zone and in the swash zone though this varied locally. Increases in mixing with time were nominal except when tidal influences were present reflecting equilibrium. Average mixing depths of 2.9 cm (range of 2-4 cm), representing 1-3% of breaking wave height were in contrast to Gaughan's (1978) findings on beaches displaying bedform morphologies. With smaller wave conditions, the maxima for mixing shifted to just inside the breaker line, decreasing shoreward however Kraus (1985) found the largest DoD values at locations seaward of the breaker line, in the region of larger but more infrequent waves. The largest average mixing depth of 3.8 cm was on a steep beach featuring high, collapsing waves, producing intense swash over the full width of the surf zone. During this experiment, tracer sand was deposited into the beach face and not transported longshore with the strong longshore current. Mixing depths did not vary for distances up to 200 m on these high energy, medium grained, micro tidal beaches.

Kraus investigated mixing depths on the east coast of Japan using tracers over a period long enough for equilibrium across the beach to be reached but that was not affected by tidal and wave condition variations. Average mixing depth is quantitatively found by separating out core samples with higher and lower tracer amounts than 80 % of the total number of grains recorded in a core, $\bar{Z}80$ (Ciavola et al, 1997; Kraus, 1985 and Sunamura and Kraus, 1985). This method was found to be the most robust in a comparison of concentration weighted procedures for mixing depths including those used by Gaughan (1978), Inman and Crickmore (1967) and $\bar{Z}_{max.}$ Erosion/accretion events are excluded in this method i.e. cores with layers containing no tracers are considered suspect and eliminated. Longshore transport may be calculated from these experiments. Variations on this method used by Ciavola e t al, (1997); Kraus (1985) and Ferreira (2000) include the use of PVC tubes for coring and larger sample sizes. At equilibrium cores should display uniform distributions however wave induced flows, pressure fields and turbulence produced varying concentration gradients (mostly monotonic decreases under steady wave conditions) with depth, reflecting different mixing events or bed level change (Kraus, 1985).

Kraus, 1985 and Sunamura and Kraus (1985) also using 80 % cut-off rates for tracer distributions in both the cross-shore and longshore, were able to conceive average mixing depths (within tidal cycles) for the surf zone from a large range of sites around the islands of Honshu, Japan. Averaged mixing depth ($\bar{\bar{Z}}$) was found to be linearly related to breaker height on these high energy, micro tidal (~1 m), dissipative beaches by;

$$\bar{\bar{Z}} = 0.027\, H_b \tag{3-2}$$

where $\bar{\bar{Z}}$ is the averaged sediment mixing depth in the surf zone. Sunamura and Kraus, 1985, validated this result using a predictive model for average mixing depths in the surf zone relating wave period, T, wavelength, L, and height, H_b, to bed stress (wave-induced shear on the bottom), τ_b. τ_b is a function of maximum near-bottom orbital velocity of breaking waves, u_b, and the wave friction factor, f_w, (after Jonsson, 1966) which accounts for roughness length, r, substituted for the sediment grain diameter, D, in the case of smooth bottom i.e. no ripples and the horizontal semi-excursion distance of the wave orbit at the bottom, ^{a}b. Collectively these parameters relate through the Shields Parameter,

$$\psi_b = \frac{\tau_b}{(\rho s - \rho) g D} \tag{3-3}$$

Dilation of the bottom surface layer caused by fluid-to-grain interactions is accounted for through the introduction of a non-dimensional constant, k. Normalisation by the sediment grain size, r, gives

$$K = \frac{k}{1 - \epsilon}$$

(3-4)

and

$$\frac{\bar{Z}}{D} = K'(\psi_b - \psi_c)$$

(3-5)

where *K'* is a constant, Ψ_b is the Shield's parameter at the wave breaking point, Ψ_c is the critical Shield's number for oscillatory flow and Є is porosity. Ψ_c is estimated using empirical observations of the initiation of sediment movement in oscillatory flow (after Madsen and Grant, 1976) for a given fall velocity,

$$S* = \frac{D}{4v}[(\frac{\rho_s}{\rho - 1)}gD]$$

(3-6)

where v is the kinematic viscosity of the fluid (≈0.01 $cm^2 s^{-1}$) (Sunamura and Kraus, 1985).

The relation between the normalised average mixing depth, $\bar{Z}$/D and the effective Shields parameter, $\Psi_b - \Psi_c$, gives the line;

$$\frac{\bar{Z}}{D} = 81.4\ (\psi_b - \psi_c)$$

(3-7)

The mixing depth is predicted to increase linearly with breaking wave heights, H_b, up to ~1.5 m. The rate of increase of mixing, decreases for larger waves (>1.5 m) as the shear stress lessens. Wave periods are relevant at wave heights in excess of 1.5 – 2 m, when mixing becomes an increasing function of wave period, *T*. Anfuso et al, 2000 corroborated these findings. Only a weak positive correlation between mean mixing depth and sediment grain size existed under the wave conditions present, breaker heights, H_b, of 0.63-1.61 m and wave periods, *T*, of 4.9 – 10.2 s (Ciavola, 1997). Therefore wave induced stress on the bottom varies with bottom roughness, *r*, wave height, H_b, and period, *T*, in conditions with moderate wave H_b and large ranges of *T*, and fine to coarse grained sediments.

Ciavola et al. (1997), did similar experiments under plunging waves on reflective, moderate energy, meso-tidal (~4 m maximum tidal range) beaches near to and along the barrier islands of the Ria Formosa system on the Algarve region of Southern Portugal, with steep upper slopes of between tanβ = 0.10 – 0.14 and gentle low tide terraces. The beaches differ in their aspects; Faro Beach is situated on the 100 x 300 m wide Ancào sand spit which is prone to overwash, has limited sediment supply on it's western slopes, has a high degree of sediment exchange in the onshore/offshore and buffers incoming wave energy on it's eastern shore; Garrào Beach is adjusted by people shifting material from the lower beach to the upper to avoid notch formation (narrow beach width supports wave attack); and Culatra Beach on one of the barrier islands. Average grain sizes were 0.26 – 0.38 mm and consisted mainly of quartzitic sands. Regression analysis gives statistical significance at the 95% confidence interval for the empirical relationship between breaker height and mean sediment mixing depth;

$$Z_m = 0.27\, H_b \tag{3-8}$$

Ciavola et al. (1997) found that mixing depths for reflective beaches were ten times (one order of magnitude) greater than the proportion of breaker height found by Kraus (1985) and Sunamura and Kraus (1985) for dissipative, flat beaches but were in agreeance with the earlier work of King (1951) and Williams (1971) on reflective beaches. Consequently the empirical relationship implied by Kraus (1985) cannot be applied to beaches with slopes larger than tanβ = 0.08. Ciavola et al. (1997) averaged mixing depth values along composite cross-shore lines and then averaged over distance between measurements to garner continuous values of DoD.

Contrary to the findings of Kraus (1985) and Sunamura and Kraus (1985) and in accordance with King (19), Ciavola et al. (1997) found that on reflective beaches with steep slopes, the distribution of mixing depths in the shore-normal direction is uni-modal (maximum at wave break and minimum at swash), the result of the direct transformation of plunging breakers to swash that occurs on reflective/steep beaches especially during small wave conditions. Other work by Kraus (1985), Komar and Inman (1972), Sherman et al. (1984) and Sherman et al. (1994) specifically relates to reflective beach states with different tidal ranges. Zero-up crossing periods, *T's*, are associated with large waves and as such affect mixing depths. Ciavola et al. (1997) could not establish an empirical relationship between mean grain size and mixing depths though the large pebble clasts present may have caused armouring.

Jackson and Malvarez, 2002 had similar findings from different methods, SAM:

$$Z_m = 0.24\, H_b \tag{3-9}$$

which like Ciavola et al.s'(1997) findings is significantly different to the values of Sunamura and Kraus (1985) and Kraus (1985). The significant variation is likely the result of different beach morphodynamics and hydrodynamic processes acting on individual beaches.

On the same medium to coarse grained beaches as Ciavola et al. (1997), using rods/washers, tracers and marked sand, Ferreira et al. (2000) found values of;

$$Z_m = 0.23 H_{bs} \quad r = 0.94,\ p < 0.01 \tag{3-10}$$

for average mixing depths and Z_{max} values of;

$$Z_m = 0.39 H_{bs} \quad r = 0.96,\ p < 0.01 \tag{3-11}$$

which correlate well to those values for steep beaches and 8 - 8.5 times larger than for gentle beaches. A ratio of 1:8 for maximum and mean sediment activation depths ($Z_{max/}Z_m$) of 1:8 was found as mean values ranged from 10 cm - 22 cm and maximum values from 12.5 cm – 35 cm. Fair weather conditions prevailed during the experiments with wave heights of 0.34 m – 0.8 m. Ferreira et al. (2000) refined the formula for the estimation of activation depth by including a beach gradient, *tanβ*;

$$Z_m = 1.86\, H_b \tan\beta \tag{3-12}$$

and

$$Z_{max} = 3.33H_{bs} \tan\beta \tag{3-13}$$

This improved accuracy in predicting activity depths over a range of beach slopes and wave heights. Ferreira et al. (2000) attempted to correlate surf scaling and surf similarity parameters to activation depths but found that wave period, *T*, and wave length, *L*, increased the scatter of points.

In response to the widespread use of temporally constrained, spatially averaged mixing depth parameters for nearshore studies, Gonzalez et al. (2002) researched spatial variations of mixing depth on a fine grained, extremely dissipative beach. The study used marked rods to elucidate erosion/accretion profiles and dyed sand was injected into holes of known depth, 0.3 m from the rods, rotated 90° between tides. With excavation of the sand, the relative position of marked sand to the surface equated to accretion, while erosion could be deduced from the height difference of the marked grains after the tide had passed. Mixing depth was equated to the largest of two values. Mixing depth at different locations was correlated to tidally callibrated wave height statistics.

Gonzalez et al. (2002) tested the empirical relationship of Ferreira et al. (2002), relating mixing depth with significant breaking wave height H_{bs}, and a beach face slope parameter $\tan\beta$. Mixing depth maxima of 0.15 m and 0.1 m were recorded during two storms in breaking wave heights of 1-2.6 m and 0.7 m – 1.1 m respectively. When compared with the Ferreira et al. (2000) formula, values were found to be within 0.05 m (s.d. = 0.022 m and 0.028 m for each storm) but consistently overerestimated mixing however discrete values of beach slope ($\tan\beta$) and wave breaking height (H_{bs}) were slightly better fitted. Larger variations between the observed and predicted values were also found for the larger wave heights associated with the larger storm possbily as wave height statistics were predicted during this storm. Differences were also apparent at the high intertidal with no significant morphological variation i.e. the berm had been dispersed. Although spilling breakers dominated during the larger of the two storms, according to the Irrabaren number (ξ), plunging breakers were present in the upper interidal and lower terarace during the smaller storm. Bottom currents created by horizontal circulatory gyres were observed every 50-70 m which may account for these large standard deviations.

Importantly, Gonzalez et al. (2002) observed that mixing depths decreased with increasing wave height in contrast to the majority of the research on mixing depths. It was postured that rising tides may negate the influence of increasing wave height. It was considered that as beach slope decreased shoreward, this characteristic controlled mixing on this type of beach. Mixing depth maxima were found at wave breaking point during high tide and at the maxima of wave run-up. Gonzalez et al. (2002) stated that the time that sediment was exposed to certain beach processes had a great effect on the maxima. Gonzalez et al. (2002) also observed large amounts of sediment transported into the run-up maxima area by sea foam.

Saini et al. (2009) studied depth of activation on an estuarine pebble beach over nearly a month and found that in purely pebble substrates, activation depths are reduced. This is because the critical transport threshold for larger grain sizes is higher. Once pure pebble beaches are reworked to include a sand fraction, activation depths resemble those on sand beaches. Under breaking wave heights of 0.18 m - 0.14 m and net elevation change of < 0.02 m, mixing depths of 0.02 m - 0.12 m were observed. Proportionality coefficients of 0.22 to 0.23 (0.24 in the pebble plot) were found for activation depth to wave height on this low energy beach, though higher rates of 0.30–0.31 were observed with experimental fill.

Anfuso et al. (2000) looked at a single tidal cycle on exposed, meso tidal beaches along an energetically homogeneous coastline with differing morphodynamic characteristics. Through use of uniform measurement techniques (rods and plugs of marked sand), direct comparison of experiment results was possible. Net elevation was measured by a diver during the tidal cycle. As incident waves approached the beach at small angles, longshore currents were produced. Anfuso et al. (2000) recorded values of between 0.4 and 16.3 % H_b and averaged DoD values of between 3 and 8.5 cm. The larger values on the intermediate beach were attributed to short period ‘seas’.

Anfuso’s (2005) paper analyses techniques and terminologies for vertical cross and longshore distribution of sediment-activation depth from a large array of field assessments. In this paper, Anfuso (2005) also analysed data sets of disturbance depths, beach face slopes ($\tan^2\beta$) and period (T) on steep beach faces with plunging breakers and gently sloping beaches with large surf zones, compiled from the work of Ciavola et al. (1997); Ferreira et al. (1998); Sunamura and Kraus (1985), Anfuso et al. (2000); Anfuso et al. (2003); Anfuso and Ruiz. (2004). Anfuso (2005) recognised that although activation depth was determined by breaking wave height in similar beach systems; morphodynamic beach state and beach slope induce large variations in activation depth when different beach types are considered. Morphological changes are a function of changing incident wave regimes, currents, pre-existing morphology and tidal range. Steep beach slope ($\tan^2\beta$) created disturbance depths of between 20-40 % of significant breaker wave height from the research from the compiled research. Gentle beach slopes had ranges of disturbance depths between 1-4 %. Anfuso found good correlation between beach slope and depth of disturbance though steeper beaches had larger depths of disturbance and subsequently larger standard deviations. As slope is a function of grain size, Anfuso acknowledged that more work was required to quantify the effects of sand grain density, which may result in armouring effects and also sediment cohesion and packaging.

Bellido et al. (2011) also observed that disturbance varied with morphology and beach slope across the beach face. On a steep, reflective beach during low energy conditions, average DoD values of 3.3 cm – 4.3 cm were recorded under wave heights of 0.16 m and 0.20 m with 7-9 s periods. Shore parallel currents were also present. The beach was experiencing beach recovery (erosion in the low intertidal and accretion in the upper intertidal). Disturbance increased shoreward to the high tide berm and decreased shoreward of that. Plunging breakers caused a maximum of 10 cm of disturbance.

Jackson and Malvarez (2002) were the first able to take instantaneous measurements of sediment mixing, deposition or erosion in the surf zone, within the tidal cycle, and to make realistic inferences of bed change in response to the system's forcing parameters, i.e. wave height and water depth with tidal level. Using a mechanical Sediment Activity Meter (SAM) they were able to locate the bed approximately every 2 minutes, providing a high-resolution measuring system. The instrument itself consists of an automated, shifting vertical bar, attached to a central mast (fixed to the beach at low tide) which surveys micro-topographic, 1 mm in the vertical (Gómez-Pujol et al, 2011) beach variation, even in energetic surf zones (Jackson and Malvarez, 2002). A pulley lowers a retractable suspension cord with a conical contact pad and tension sensor attached, which automatically retracts one second after the bed surface is contacted; height above bed is measured by voltmeter. The robustness of the mechanism meant that deployment and measurements were not limited to the intertidal domain. From approximately 144 samples from SAM over a period of ~5.36 hours on a micro tidal, high energy, swell dominated beach in Ireland with an average significant wave height H_s of 45.2 cm, a constant of 0.24 was empirically incorporated into the equation;

$$\bar{\bar{z}} = 0.24\, H_s, \qquad (3\text{-}14)$$

comparing well with earlier reflective beach constants of Ciavola et al. (1997).

Jackson and Malvarez (2002) established that although bed height increased linearly (studies were carried out during a beach rebuilding phase related to seasonal adjustment post winter erosion) with corresponding increases in water level (incoming tide) and significant wave height, H_{bs}, large bed level variations were present within the tidal cycle. Total net surface change was measured by *DGPS* as 7.8 cm while bed elevation changes were recorded at 11 cm using SAM. Wave height, H_{bs}, and wave period, T, are more significant in beach modification at this site due to high refraction that occurs within the bay (Jackson and Malvarez, 2002).

Jackson and Malvarez (2002) also confirmed that in low water phases (beginning of rising or end of falling tides) with typically high frequency waves, the relationship between significant wave height and depth of disturbance fails and swash development and processes dominate. In the swash zone, reduced disturbance occurs, as waves may fail to penetrate the seabed, possibly because of an inability of waves (and associated energy and stress), to reach an optimum level where orbital speed penetrates the water column, thus reducing sediment entrainment. Outside of shallow water phases, the relationship between water depth (and corresponding significant wave height) and DoD increases linearly up to the point where wave length, λ, is greater than twice the significant wave height, wave orbital velocities are shorter than wave amplitude when depth becomes less than 1.3 times their height; then this relationship also fails. A lag was found between bed disturbance response and an increase in significant wave height and specifically the moment wave orbital velocities are large enough to penetrate the water column (Jackson and Malvarez, 2002).

The high temporal resolution of SAM allows investigation of the relationship between water depth variation, wave action and sediment disturbance in a range of environments however issues exist with this technique as the sampling period is higher than the high frequency bed evolution (Berni et al, 2009). There is minimal scour due to emplacement of SAM as time on the bed surface is limited to~1 s (Jackson and Malvarez, 2002). Deployment of SAM into lower intertidal beach zones and in greater numbers will ensure that spatial patterns of bedform change can be better understood as there is a current need for further research into the effects of wave groupiness, length scales of waves and the characterisation of morphodynamic systems (Gómez-Pujol et al., 2011).

Gómez-Pujol et al. (2011) used the SAM device in conjunction with DoD rods and washers and high resolution *DGPS* (Trimble 5800 series) to determine the sediment activation depth and depth of disturbance consecutively under storm wave conditions (forcings) on the same coast as Jackson and Malvarez (2002). The experiments were carried out during a neap to spring transitional period, with tidal range variation of 0.5 m over 4 days, on the high energy, dissipative, microtidal (~1.3 m), fine grained quartz sand beach at Whitepark Bay. A large swell event with offshore deep-water wave heights of 6 m occurred during the experiment causing 0.6 m waves with 6 s periods at the intertidal zone near the location of SAM, while wave heights under normal conditions (no storm event) were 0.3 m with 5 s periods. 48 rods were deployed to determine spatial variation in bedform change (Gómez-Pujol et al., 2011).

Like Jackson and Malvarez (2002), Gómez-Pujol et al. (2011) found complex variability in bed surface elevation. Erosion of 0.1 m occurred during the storm event, while accretionary events were recorded pre and post storm with corresponding sediment activation values for SAM of 0.04 m, 0.24 m and 0.06 m and from rods and washers of 0.03, 0.23 and 0.11 m. These values yield ratios of;

$$\bar{\bar{Z}} = 0.28\ H_b \tag{3-15}$$

and

$$\bar{\bar{Z}} = 0.25\ H_b, \tag{3-16}$$

for SAM measurements and rod experiments respectively. For similar beach slopes (tanβ = 0.03). As stated previous, Jackson and Malvarez (2002) and Anfuso et al (2005) found similar ratios for Z_m/H_b and on steep slopes and under reflective wave conditions. Ciavola et al. (1997) produced similar ratios for Z_m/H_b.

Although DoD values doubled during energetic wave conditions, cut-and-fill sequences in the swash zone forced by tides appear to be main processes contributing to the DoD changes, with waves accentuating these values and the effects of DoD (Gómez-Pujol et al., 2011). Values of DoD for individual energetic waves were larger than entire net intertidal elevation differences during a storm event. Cross shore and alongshore variation of DoD was determined by variation with mean water level and the relative time spent under the influence of breaking wave processes. It was discovered that the unimodal distribution of DoD was extended and moved up-slope during larger tides i.e. spring tides. Wave height was found to explain 80 % of the variance in DoD corroborating much of the findings of earlier research. Wave period was regarded as not having an effect on DoD values (Gómez-Pujol et al., 2011).

Modern ideas in surf zone morphodynamics have elucidated the role of water levels on wave action and thus as a mechanism for sediment transport and distribution level through initiation and modes of sediment transport and induced morphodynamics (Masselink and Short, 1993 and Masselink et al., 2007). From the research of Jackson and Malvarez (2002) and Gómez-Pujol et al. (2011), it was highlighted that tidal level and corresponding water depth determines significant wave height and therefore sediment transport and effective beach state (Green and MacDonald, 2001, in Jackson and Malvarez, 2002).

Arnaud et al. (2009) describe an intra-tidal technique for bed-level measurement in the surf/swash zone involving the use of local electrical resistivity rods to monitor bathymetric evolution. Measurements are possible because of the resistivity contrasts of seawater and the beach sediment layer and conductivity contrasts within sediment layers; resistivity in saturated sediment is approximately three times greater than water. Likewise no resistivity exists in air and so the air/water interface can be found. The resistivity recorders have a 2-3 cm radius around each electrode, are spaced > 3 cm along ten ~3-5 m vertical poles which are partially submerged in the sediment at distances of 20 m in the cross-shore. The sediment surface is located in real time as sampling frequency is at 10 Hz for each electrode (Arnaud et al., 2009).

Arnaud et al. (2009) were able to take continuous time series of bed level changes over 10 tidal cycles, at the gently sloping ($\tan\beta = 0.04$), macro-meso beach of Truc-Vert and then to analyse sediment activation depth distribution along the cross shore during tidal events. Arnaud et al. (2009) were able to apply threshold values to determine upper and lower boundaries of sheet flow; 0.16 – 0.18 Ω.m is the minimum and represents sea water, 0.18 Ω.m – 0.3 Ω.m represents highly concentrated water (bubbles and undifferentiated sand) and 0.3 – 0.55 Ω.m is saturated sand (ranging from unstable to stable). In air or dry sand, 1.3 Ω.m of resistivity applies. The altitude difference between these threshold limits may represent flow parameters in bed level change (Arnaud et al., 2009).

From representation of an entire rod's sensors, it is clear that erosion and deposition phases occur successively, with erosion initiating at commencement of submergence in water (Arnaud et al., 2009). Using the earlier thresholds averaged over a minute in the processing, the data provides defined characterisation of the medium. The sediment/water interface is difficult to discern however as the water and sediment are in a constant state of flux: The threshold parameter, 0.3 Ω.m, for highly concentrated water, is used to determine the interface. The stable bed surface is likewise difficult to discern and determined threshold values, 0.55 Ω.m, were proven too high.

Intuitively, bed level change obtained from resistivity rods, when compared with *DGPS*, shows greater variation and frequency. Greatest frequency of bed level change coincided with 2 m deep-water wave height, H_b, and period, T, of 12 s, on the lower beach which may have been the consequence of bedform migration. Maximum DoD values, 47 and 84 cm, were detected at the upper beach zone with high frequency bed level change during the low water phases (Arnaud et al., 2009). These rapid bed level changes may have been the result of sampling error. Near high water, a large erosion event reaches a rate of ~1 $cm.min^{-1}$ with maximum disturbance of 18 cm. Sequential deposition replenishes the bed to a final surface elevation at the end of the tide, 3 cm below initial surface level (Arnaud et al., 2009).

Other methods for determining intra-tidal morphological changes were introduced by Erlingson (as cited in Arnaud et al., 2009) using high frequency optical backscatter devices attached to poles to determine the sediment/water interface. However like Arnaud's resistivity rod experiment the sediment/water interface proves elusive. Lawler (as cited in Berni, 2009) directly computed the surrounding light though the soil using photovoltaic cells. Ridd, (as cited in Berni, 2009) used a set of current electrodes and a current source within the sediment to locate conductivity differences within the bed. Acoustic backscatter profilers have been used by Battisto et al. (1999) but have problematic calibration due to the presence of organic matter in the water column. Accuracy was shown to be high for the acoustic instruments of Jestin et al. by Gallagher et al. (1996) and Gallagher et al. (2005) (as cited in Arnaud et al., 2009) even when reflected signals were degraded by bubbles and suspended sediments. An acoustic method for use in the swash zone, outside fluid flow, was developed by Turner (2008) to detect continuous bed level change (as cited in Arnaud et al., 2009). The benefit of this method is that the sediment/water interface is viewed as a vertical rather seen as not threshold continuous medium with layering.

Berni et al., (2009) published a paper on the diversity of bed evolution at wave and tidal scales on Truc-Vert beach in southern France. Using an Acoustic Doppler Velocity Profiler and optical fibres with pressure sensors they were able to detect bed elevation, velocity field, thickness of sheetflow layer and the state (stability and concentration) of the medium in front of the sensors. The experiment showed that under energetic high tide conditions, symmetric deposition and erosion exists but under contrasting calm conditions, periodic oscillations occur that are characteristic of ripple propagation. During energetic periods, Berni et al. (2009) found that excess pore pressure, being negative under wave troughs and positive under crests, promotes sheet flow. The relationships for the two tidal conditions were given as:

$$Z_m = 0.2\, H_s \tag{3-17}$$

$$Z_m = 0.17\, H_b \tag{3-18}$$

Brook and Lemckert (2010) introduced a new technique for measuring intra-tidal ‘mixing depth. Coloured tracers were injected into the beach sediments and after a few swash waves have passed, coring samples were extracted and were frozen for detailed research of DoD and sediment transport patterns. Offshore pressure transducer results were related to nearshore wave heights using a Simulating Waves Nearshore Model (SWAN). In this way it is hoped that estimates of DoD may be determined from only offshore wave buoy data combined with modelled nearshore wave climate information. Results for mixing depths were on average~ 98 mm and using the Ferreira et al. (1998) relationship for breaking wave height and DoD, values of $Zm = 0.14\ H_{bs}$ were obtained. They found that the DoD increases with the number of swash waves a core/ area is exposed to and thus the low tide cores that are exposed more often show display a higher amount of disturbance and that accretion will be less than DoD on accreting beach as subsurface mixing occurs. Brook and Lemckert (2010) found that DoD was on average 30 mm greater than accretion on the accretionary beach that they studied.

Bosnic et al. (2011) extended research into the textural form of the beach active layer which had traditionally only been considered a homogeneous stratum (as observed by Williams, 1971). Bosnic et al. (2011) developed a unprecedented high resolution, effective in situ method for vertical sediment image data, modifying existing digital image algorithms of Barnard (as cited in Bosnic et al., 2011) for vertical profiling, illumination homogeneity and restriction of analysis to median grain size using the autocorrelation method. 50 cm x 45 cm (internal diameter) PVC cores were emplaced systematically across the beach profile, upon retrieval they were split and photographed with a 14 megapixel camera fixed to a portable wooden box, to achieve 3059 x 1841 pixel photographs. Median grain size was determined for each 1 cm core slice within the active layer, which in turn was determined from rods and washers emplaced near the core locations on the beach. The diameter of the cores imposed limits to the area of analysis as did location of the water table; saturation eliminated cohesion of sediment and necessitated samples were taken above the water table (Bosnic et al., 2011). From experiments on steep (~0.12 and ~0.09), mesotidal beaches with median grain sizes of 0.57 – -0.84 ϕ and 0.97 – 0.48 ϕ; Lagoa de Ablufeira and Salgado Beach, on the Portugese south and west coasts they discovered that rather than the displaying positive graded sedimentary sequences, vertical variation of median grain size demonstrated random cyclic variations linked to infragravity wave energy oscillations during a tidal cycle (Bosnic et al., 2011). A continuous coarsening offshore of median grain size at both beaches was also revealed although at Salgado the grain size distinctions were small and not in continuous increments like Lagoa de Ablufeira. DoD maximum values were >15 cm at both beaches detected in the mid-upper slope at Salgado and the upper slope region at Lagoa de Ablufeira. Minimum values were 10 cm at Lagoa de Ablufeira and 5 cm at Salgado l in the upper slope region. Erosion profiles illustrated accretion at the upper and lower areas of Lagoa de Ablufeira with erosion in the mid-slope zones of both beaches at the end of a tidal cycle; significant amounts at Salgado (Bosnic et al., 2011). A necessity to link beach forcings to the textural variability was alluded to by Bosnic et al. (2011).

3.1.2 MORPHODYNAMIC VARIABILITY AND SUBSURFACE CONTAMINATION MORPHOLOGY

In the days and weeks that follow an oil spill, subsurface contamination of beaches by percolation results in oil penetration within the surface few centimetres of sediment (Bernabeu et al., 2006, Bernabeu et al., 2009). This type of passive burial is regulated by features of the sediment and oil; such as sediment porosity and the viscosity of the oil, as well as the depth of water table. The porosity of the sediment is in turn controlled by the sediment grain size; larger grains sizes result in larger intergranular pore spaces and faster percolation (Bernabeu et al., 2006). Percolation mainly occurs on gravel beaches where oil is embedded on fine sediment layers below the gravel to approximately 0.5 m (Bernabeu et al., 2006; Fernández-Fernández et al, 2011).

The November, *2002 Prestige* oil spill off the NW Galician coast of Spain, caused almost 7,000 tonnes of oil contamination; stretching more than 1000 km of coastline (Bernabeu et al., 2006). The high viscosity, high density oil was discovered in layers several metres thick, at depths exceeding 2.38 m from 20 cores with maximum extraction depths of the same. It was established that oil contamination was not merely restricted to the surface layers of sediment above the water table but that oil had become buried deeper within the beach profile due to beach morphodynamic shifts (Bernabeu et al., 2006).

During storm events, (which often engender oil spills) (Fernández-Fernández et al., 2011), a net bedload movement of sediment from the high intertidal zone to the subtidal zone produces flatter beach slope profiles, upon which the oil is deposited (Bernabeu et al., 2006). Extremely turbulent mixing of residual oil within the surf zone disintegrates the oil and actively mixes it with sediment, generating tar balls of up to several centimetres in diameter. Dispersion of tar balls and burial during low energy phases, in which mass transport of sediment from the subtidal to the higher intertidal areas occurs, results in significant oil burial depths (Bernabeu et al., 2006). As limited moderation by evaporation and biodegradation (due to oxygen deprivation and nutrient deficiency) occurs at depth (Venosa and Zhu, 2003), the evolutionary expression of the oil is principally due to physical mixing, deformation and ancillary fragmentation, directly controlled by morphological processes, particularly wave action and wave-induced currents especially in the early stages of oiling (Bernabeu et al., 2006).

The conceptual model developed by Bernabeu et al (2006) defines the burial, subsequent reworking of oil-sediment mixtures and exhumation during storm conditions (Figure 3.1) however a time scale for natural beach recovery based on morphodynamic changes remains illusory. The influence of continental shelf oil on sediment regeneration has also not been resolved.

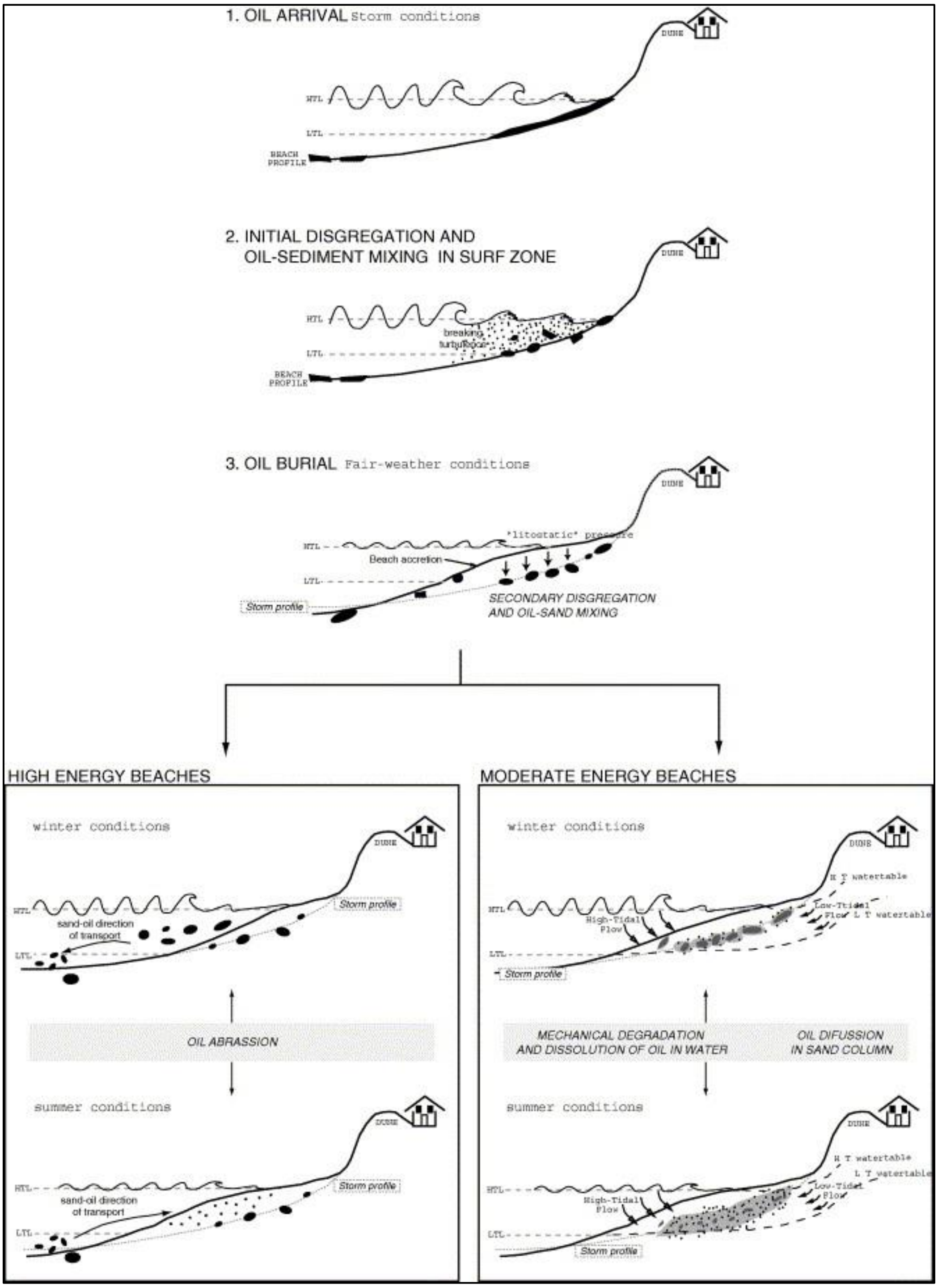

Figure 3.1: Conceptual model of oil burial on beaches. Source: Bernabeu et al. (2006).

It is especially important for assessment of wave conditions on dissipative beaches where low waves energies may prevent burial and mixing of oil with sand, making extraction easier. Conversely high wave energies result in increased DoD and will bury mats and tar balls and higher tides with high run-up caused by storms can deposit oil above the intertidal. With burial, persistence is likely and emulsified oil microparticles become more bioavailable (Bernabeu et al., 2009). Storm conditions can free some buried oil but most will require mechanical removal. It is therefore important to know for clean-up procedures whether wave climates will result in exhumation/burial and where oil will become emplaced. Oil distribution or extent is a function of the maximum energy over the course of the spill (Bernabeu et al., 2009). Complex morphologies, bars and rips, alter circulations patterns and high wave and current energies associated with these morphologies result in thick matrices of shell, gravel and sand, making extraction difficult. Longshore currents can transport tar balls into embayments. Offshore in deep water oil is likely to remain embedded.

Oil spill research carried out 14 months after the *Prestige* oil spill and yearly since has focused on two contrasting macro tidal beaches; O Rostro Beach, a high energy, intermediate bayed beach (González et al., 2010), featuring symmetrically skewed distributions of moderately well sorted coarse grains (Bernabeu et al., 2006); the other Nemiña Beach, a sheltered beach with moderately well to moderately sorted, medium grained sediment, displaying asymmetrical skewness toward coarser grain sizes (Bernabeu et al, 2006; Bernabeu et al., 2010). The morphodynamic behaviour of the juxtaposed beaches is that one favours a short burial and subsequent exhumation cycle at O Rostro Beach and intermittent morphological shifts promoting extensive burial periods (years) at Nemiña Beach (Bernabeu et al., 2006; Bernabeu et al., 2010). During the 2002 storm event with 9.34 m maximum wave height and 15.5 s periods, the normally sheltered Nemiña Beach was exposed to energetic wave conditions from the WNW promoting exceedingly deep burial. O Rostro was not exposed during the initial spill, however, 4 subsequent storms with > 5 m waves over more than 3 days from the WSW to NW deposited sedimented oil there. Oil contamination decreased abruptly during the first years after the oil spill but remained constant after that, as both surficial and buried oil deposits.

In a subsequent study at O Rostro and Nemiña Beaches in 2009, 7 years after the spill, both physical morphology and distribution of oil were comparable to studies in the years subsequent to the spill. Depths of oil burial were however in excess of 286 cm due to lengthened core samples in these studies (Bernabeu et al., 2009; Fernández-Fernández et al, 2011). Is it possible that under favourable oceanographic conditions, ongoing migration of tar balls from oiled rocky outcrops on the inner shelf occurs, as particles have been observed to not mix offshore (Fernández-Fernández et al, 2011). Low PAH concentrations were found but could not be linked with morphology, the highest of which were at the lowest points of coated grains (Bernabeu et al., 2009). Nemiña Beach expressed longer burial times as greater concentrations of oil coatings were present buried under 250 cm of clean sand.

On O Rostro Beach it was observed that oil was deposited where circulation stops in an offshore secondary current system during storm events. Tar balls were also found in the rip current channels buried up to 1-2 m and 1-2.5 m on the sides of transversal bar-salient systems. Tar balls were also found in the intertidal zones of embayments. During storm events on exposed beaches, oil penetrates the high-tide berms up to a metre but the top 10-25 cm is re-worked through normal erosion/deposition following this.

Cross-shore distributions of surface and subsurface oil were examined with respect to beach morphodynamics and wave climate by Roberts and Wang (2013). Wang and Roberts deduced that the landward limit of heavy particulate residue contamination is controlled by the most energetic states, particularly the high tide maxima run-up and individual wave run-up over the duration of the oil spill. At maximum high tide, the longer temporal scale (of~1 hour) causes higher concentrations of contaminant with a larger range of forms. The terminus of individual wave run-up deposits smaller scale oil contamination on the beach surface; tar balls, oil stains and sometimes tar balls with oil stains. At maximum high tide, the longer temporal scale (of~1 hour) causes higher concentrations of contaminant with a larger range of forms. Width of the dynamic zone is a function of incident wave, *h* or period, *t*, which in turn equals wave run-up maximum. Oil contamination is constrained between the active berm crest and the maximum wave run-up (Wang and Roberts, 2013).

Guza and Thornton (1982 as cited in Wang and Roberts, 2013) estimated that significant wave run-up, R_s (swash run-up and wave setup), is linearly proportional to the deep-water wave height (H_o) using the equation:

$$R_s = 3.48 + 0.71\ H_0 \tag{3-19}$$

However according to Holman (1986 as cited in Wang and Roberts, 2013), for intermediate beaches, a more accurate estimation of wave run-up (based on field measurements) can be obtained using the surf similarity parameter, ξ:

$$\xi = \frac{\tan\beta}{\sqrt{H_0/L_0}} \tag{3-20}$$

Integrating the surf similarity parameter, ξ, with the deepwater significant wave height, the 2 % exceedance of run-up, R_2, is determined:

$$R_2 = (0.83\xi + 0.2)\ H_0 \tag{3-21}$$

Significant breaking wave height, H_{bs}, has been empirically related to maximum wave run-up, R_{tw}, and therefore maximum elevation by Roberts, Wang and Kraus (2010):

$$R_{tw} = 1.0\ H_{bs} \tag{3-22}$$

The landward limit of oil-contamination is therefore directly related to the significant breaking-wave height (Wang and Roberts, 2013).

One month after the initial DWH beach oiling, Hurricane Alex produced high wave energy for a four day period, oil was deposited landward of the active berm, in the back-beach trough. Limited interaction with waves and swash in these areas can induce long residence times of months to years (Wang and Roberts, 2013). In the more active foreshore, contamination is usually limited to a few tidal cycles;

swash motions moved tar balls around depositing them in piles of shell hash for a few tidal cycles. Subsurface contamination of oil during the DWH spill dominated in the foreshore. A large-scale oil sheet was deposited at maximum wave run-up, buried up to 25 cm shortly after or during emplacement, preserving the sheet structure within the sediment column. Although the swash energy was unable to break apart the viscous oil sheet at the time of deposition, it had eroded within a month (Wang and Roberts, 2013). Deposition by wave run-up was overlain by multiple contaminated layers and also an 18 cm clean surface layer. A storm berm or ridge and runnel forms during beach recovery after storm events erode the foreshore and parts of the back-beach. Oil was also buried deeply under the active berm and landward of it, in multiple laminations of tar balls and stained sand. Oil was buried 50 cm below the active berm crest in a 15 cm thick layer which was inclusive of all oil forms; tar balls, cakes, patties and stains. Burial depth decreased in both the landward and seaward direction away from the berm. Parham and Gundlach (2015) observed, like Wang and Roberts (2013), that oil was buried deeply under the intertidal berm, up to 1 m with averages of between 20 and 50 cm. Burial depths were found by Parham and Gundlach (2015) to be amplified by high energy wave conditions due to periodic storms and higher high-tides. Processes that drive surficial oil contamination drive buried oil contamination on an equivalent temporal scale (Wang and Roberts, 2013).

Seasonal variations in aeolian, weathering and clean-up efforts were also observed by Parham and Gundlach (2015) in the years following the DWH spill. In winter, aeolian processes dominated in the backshore, exposing buried oil due to reduced water levels. During the summer of the active oiling phase, broadening of beaches during net sediment transport landward in the nearshore also occurred. Higher water levels extended oil deposition into the supratidal zone above the higher high water mark (HHWM), through overwash and backshore flooding, sometimes depositing up to a metre of sand. Under the sun’s heat, oil submerged in supratidal pools rose to the water surface where it was blown to the lee side of the pool. Concentric rings formed and remained after the pools evaporated (Parham and Gundlach, 2015). In subsequent years, storm events transported oil and sediment from the berm to the backshore and reburied previously emplaced backshore oil sheets. Large storm events also eroded large tracts of beachface, reworking and transporting oil alongshore into swales with shell hash. Rebuilding phases reburied this oil however patties (~6 cm) were commonly exposed as lag in the nearshore with changes in spit configuration (Parham and Gundlach, 2015). Burial of tar balls aided in the breakup of tar balls.

Although natural dispersion through energetic pathways will alleviate some of the oiling, it is essential for an understanding of the surface and subsurface cross-shore distribution of oil. The distribution and movement of oil offshore dictates longshore distribution of surficial and buried oil and can be found in the Operation Science Advisory Team (OSAT-2) reports (OSAT-2, 2011 as cited in Wang and Roberts, 2013).

Buried oil has traditionally not been included in contamination classification schemes such as those based on the NOAA Shoreline assessment Manual. It is necessary to include buried oil in such schemes so as not to underestimate levels of contamination. It is however inherently difficult to determine the specific spatial scale of buried oil and oil can be buried under layers of unoiled sand (Wang and Roberts, 2013). Incident wave conditions affect the characteristic morphodynamics of the discreet morphological zones.

Only combustion, biodegradation and physical removal can reduce oil in the environment. The small surface area to volume ratio and strong chemical bonds of tar balls limits the ability of bacteria to break them down (Leahy and Colwell 1990; Atlas 1981 as cited in Warnock, 2015). Physical removal burial, offshore submersion and manual/mechanical removal is therefore required although the sand sized MTB are difficult to separate (Bernabeu et al. 2013). Manual removal of beached tars is effective but labour intensive. Methods that are effective for floating oil and tars such as skimming are not useful once the oil has sunk or been stranded ashore. Mechanical methods such as those implemented in the DWH clean-up involved using beach equipment to sieve the sand and filter out tar aggregates. Initial use of these vehicles during the DWH clean-up resulted in the breaking up of the tar residues into smaller pieces that passed through the sifting mechanism slowing it down (Hayworth and Clement 2011; Owens et al. 2011).

3.2 RESEARCH METHODS

As sediments were mostly unconsolidated sands, it was decided against using a shear vane to test the shear strength of the sediment. It has been found previously that results from this method are ineffective for unconsolidated sediment (de Groot, 2014). Due to financial constraints and an understanding that the presence of placers would be of limited value, coring was not carried out during this study. It was evident from the presence of placers at > 3 m depth in newly cut scarps that mixing depths did not confine placer deposits.

3.2.1 BEACH PROFILES

Temporary control points (TCPs) were set up along the length of Ngarunui Beach to Wainamu Beach during the early topographic beach profile surveys and 3-D laser scans in summer 2013 (refer Appendix IV). The location of the profile benchmarks are identified in Appendix III.

Known primary and secondary surveyed temporary benchmarks (TBM’s) emplaced by Environment Waikato in conjunction with NIWA were also used. The profile benchmarks and control points at Ngarunui Beach were surveyed using a real time kinetic global positioning system (RTK-GPS) to determine the location and elevation of benchmarks and were surveyed to *Mount Eden Circuit 2000 Transverse Mercator* meridional circuit Chart Datum with vertical reference to *Moturiki Vertical Datum 1953* for mean sea level, *msl*. Control points were re-checked periodically using the RTK-GPS to provide consistency of the data i.e. that no vertical movement had occurred throughout the survey. Topographic checks were carried out on survey control points on 7/02/2013, 28/07/2014 and 29/08/2014.

Three beach profile lines were constructed at the northern end of Ngarunui Beach, with spacing between them of approximately 200 m. Established Waikato Regional Council (WRC) and newly emplaced benchmark locations can be found in Appendix III. The location of the profile lines was established based on:

- Proximity to location of WRC benchmarks;
- Beach access locations;
- Distance from Surf Life Saving flag locations and other areas of high pedestrian/swimmer volumes;
- Rip locations (swimmer numbers are less in areas of high rip numbers);
- The harbour entrance impact upon physical processes;
- Apparent presence of noteworthy physical processes such as the large slug of sand that is sometimes present at northern Ngarunui Beach;
- Visibility in any submerged areas;
- Location of the two EW/NIWA cam-ERA cameras;
- Area of reduced human impact.

Three beach profile lines were established in the inner harbour, at Wainamu Beach, based on similar factors and to encompass the spit forming at this location. The Moonlight Bay location included only two transects due to the limited extent of the beach.

Beach profiles of the intertidal zone were constructed from surveyed data obtained with a DTM-322 Nikon Total Station and optical prism before and after most disturbance rod experiments, except when weather conditions prevented it. The Total Station has an accuracy of +/-3+2 ppm x D mm and a precision of ±10 mm up to 500 m. The Total Station was set up over temporary control points (TCPs) established by Amir Emami and Dean Sandwell and the author and Dean Sandwell, and levelled using the optical instruments. During all transect surveys at northern Ngarunui Beach, the Total Station was set up over benchmark *T2* (*Transect 2*), except once when the Total Station was set up on the boardwalk at

CP7 as *T2* could not be located because it had become buried under the sand. Benchmark control point locations are in given in Appendix III). Backsights to a fixed reference benchmark *BM3-Front* (a secondary benchmark set up by EW/NIWA) were conducted for all survey experiments at northern Ngarunui Beach. On the 10th of February, 2015, at the southern end of the beach, surveys were carried out using a free form survey arrangement (no coordinate system). Likewise surveys at Moonlight Bay used a free form arrangement. At Wainamu Beach the Total Station was set up over *CP18* and a backsight onto *CP19* was used on the 11th and 12th of December, 2014. Free form arrangements were used otherwise.

Survey profiles extended the width of the intertidal zone beginning at either the low tide zone or the high tide zone and in some cases from the beach berm in the foredune area. Measurements were taken approximately every 2 metres (3 steps), though fewer measurements were taken on flat featureless areas and measurement intervals were increased where changes in slope occurred and where features of interest were present. Surveying was carried out as close to the low tide as possible (within an hour either side of low tide) to achieve maximum coverage of the intertidal zone. The beach transects covered cross-shore distances of around 200 m. Notable features were recorded along the profile lines and included a channel that was present in 29th of August, 2014, the location of the high water mark and any other bedforms that were present. The extent of any groundwater seepage was usually confounded by the ebbing tide so was not included.

Coordinates for the Nikon Total Station are given in Transverse Mercator meridional, thus elevations are coincident to the *New Zealand Geodetic Datum 2000 (NZGD).* As the beach profiling was carried out in concurrence with the depth of disturbance experiments, no additional sampling methodology was required for this activity.

A *Trimble VX* beach scan was carried out on the 5th February 2015 by Dean Sandwell, using the real time kinetic global positioning system (GPS) affixed to the back of the University quad bike and 3-D beach profiles are included in

Appendix .Another total survey was carried out in 2013 on foot. The methodology used for beach scale topographic surveys was to start with the longshore and then to cover the cross-shore from low tide to the foredune and sometimes dune areas.

3-D laser scanning was undertaken using the *Trimble VX* at Ngarunui Beach in the Summer of 2013. However, as the data were not downloaded correctly the 3-D profiles could not be included. It was also found that on wet sand the 3-D laser scanner would not work effectively and on the dry black titanomagnetite sand, errors were greatly increased, making it unproductive to proceed with this method. 3-D profiles were however generated from the GPS referenced coordinates by interpolation and fitting of a continuous linear (co-continuous function) surface to the topographic survey data. Tri-scattered interpolation in *Matlab* was used to interpolate the 3-D surface between the points. This function uses a triangulation method (Delaunay triangulation) to fit a continuous linear surface to the GPS referenced coordinates and generate a meshgrid of the surface. Triangulation is a matrix representing the set of vertices that make up the triangulation.

Monthly erosion profiles were obtained by Ron Ovenden and Andrew Wood for Environment Waikato between 2009 and 2014 and more recently by Ron Ovenden using the fixed origin Emery Method. They have been used here to provide background information on the surface elevation changes at Ngarunui Beach. The Emery Method requires two people to locate the lower position of the land relative to the horizon. A line-of-sight of the horizon and the top of one of two marked vertical rods along a transect between known control points is used to determine the elevation difference from the point of intersection between the two.

Photographs taken from transects at 6 locations along Ngarunui Beach were evaluated for surf zone width, scarp development, rip channel locations, water table locations etc. These photographs combined with the beach profiles from the past five years enabled interpretation of hydrodynamics, movement and mixing of sand on Ngarunui Beach and in the harbour entrance.

3.2.2 DEPTH OF DISTURBANCE EXPERIMENTS

Depth of disturbance was measured at three locations; Ngarunui Beach, Wainamu Beach inside the harbour entrance and Moonlight Bay (Figure 1.2). Transects were spaced approximately 150 m apart at northern Ngarunui Beach (Figure 3.2) and 150 m apart at Wainamu Beach (Figure 3.3).

Figure 3.2: **Subaerial rod locations and sediment sampling locations at northern Ngarunui Beach (Site 1).**

Figure 3.3: **Rod locations and control points (*CP18* and *CP19* in blue) at Wainamu Beach.**

Southern Ngarunui Beach has four profile sites with separation distances between the four sites of 245 m, 205 m, and 251 m (Figure 3.4).

Figure 3.4: **Plan view of subaerial rod and sediment sampling locations at southern Ngarunui Beach.**

Along each of the transects, stainless steel rods, 1.5 m long and 10 mm in diameter were driven into the beach sediment at the mid, low and high intertidal zones; placed into position using a Garmin eTrex handheld GPS. The position of the rods allowed measurement in each of the distinct beach process areas. The depth of distribution during tidal events at discrete locations and along the cross-shore and longshore beach profile could then be determined. The rods were marked with a reference line at 500 mm to allow the direct measurement of erosion/accretion profiles and depths of disturbance. A 50 x 50 x 6 cm, square loose fitting washer with a 16 mm hole was placed over the top of each rod and permitted to fall to the beach surface level. The locations of the mid, low and high tide rods were modified during some experiments due to variances in tidal range and sea level fluctuations associated with storm surges and tidal variations.

At the low tide following the deployment; after a full semi diurnal tidal cycle (~12.5 hours) had elapsed, the washer was dug up, taking care not to disturb the relative position of the washer to the rod. The distance from the washer to the 500 mm mark was recorded to ascertain disturbance depth. Surface elevation changes, due to sand accumulation and erosion, were also determined, through the position of the sand with respect to the demarcation line. Erosion is not considered part of the disturbance depth as the rod and washer technique allowed direct measurement of both, however the addition of accretion allows quantification of the total disturbed bed layer. There are inherent limitations with this method, due to non-continuous measurement of bed level change. The relative time of any modification of surface elevation (erosion/accretion) cannot be ascertained with respect to the pattern of DoD.

During large storms however the lines would often be removed by wave action and the distance from the sand to the base of the rod was used as a proxy for distance by taking into account the 500 mm at which the rod was driven into the beach sediment at deposition. The Moonlight Bay transects were spaced approximately 15 m apart at this location (Figure 3.5). The dates of the field experiments were selected to represent storm conditions and the associated above average significant wave heights, however, fair weather episodes were included to provide a comparison. Sediment samples were obtained for each discreet rod location during all experiments except when rods were lost, removed or interfered with.

Figure 3.5: **Transect locations at Moonlight Bay.**

As Ngarunui is a popular recreational beach, it was deemed hazardous to carry out experiments during the daylight hours when surfers and swimmers use the beach; most experiments were run overnight. It was also considered to be less hazardous at the most unused northern part of the beach. When rods were emplaced on the beach outside of night time hours, warning cones and verbal warnings alerted people to the presence of the rods extruding from the ground (Figure 3.6).

Figure 3.6: Disturbance rod with hazard warning sign to avoid risk to the public and deter interference with rods.

The use of cores was also determined to be somewhat redundant as placers were exposed at depths well below the average DoD on Ngarunui Beach, inferring burial during storm events. It was therefore more prudent to gather data on bed elevation changes and morphodynamic variability at this location and at Wainamu Beach. As it was unlikely that mineral placers would be present at Moonlight Bay, coring would have also been irrelevant at this location.

As the direction of transport along Ngarunui Beach was evident from rectified Cam-ERA images and from previous estimates of littoral drift, sediment tracers were not utilised in this study. It has also been observed that under high-energy conditions that maximum mixing depths do not reflect average transport conditions and determination of tracer counts are highly subjective (Komar, 1969 as cited in Kraus, 1985).

The water table is also often exposed at Ngarunui Beach. Groundwater and swash infiltration is likely to occur on this beach, which would affect the transportation of any oil during a spill.

Sediment movement is controlled by grain characteristics such as shape, size and sorting and these features are important in the movement of oil on the shoreline (Owens et al., 2008). Variation in grain size cross-shore has been discussed in Chapter Two and has been used here to evaluate differences in DOD across the beach.

3.2.3 HYDRODYNAMICS

The source for the majority of the wave conditions and meteorological data observations was estimates of sea state from SwellMap.co.nz, owned and operated by MetOcean Solutions Ltd. Wave conditions were calculated from the nearest grid cell of the National Oceanographic and Atmospheric Administration (NOAA) Wavewatch III wave hindcast model. Both the WWIII model and the MetOcean model have been calibrated. The angle of wave approach during some of the experiments was taken from the averaged georectified Cam-ERA digital footage. Tide data is from Metservice and available from http://www.metservice.com/national/home.

3.2.4 CAM-ERA RECTIFICATION

Cam-ERA is a network of computer-controlled cameras operated by NIWA and Environment Waikato (EW) that monitor New Zealand beaches including Ngarunui Beach. The two cameras at Ngarunui Beach are placed at the southern end of the beach, mounted approximately 95 m above mean sea level). The digital cameras take continuous pictures at 2 Hz during daylight hours generating high-resolution (1528 x 2016 pixels) digital photographs (Guedes, 2012).

Georectification turns image coordinates into real world coordinates. Georectification of the Cam-Era images was generated by manipulating the date appropriate images from the WRC Cameras with a 1.5 km alongshore and 150-800 m cross-shore range (Huisman et al., 2011) and using the predicted tides from a tide gauge at Manu Bay in Raglan. The 2-D images are first normalised to amend radial and tangential distortions. The true optical centre/principle point is found and then rotated using a tilt, swing and azimuth (aligning the images on the same plane). The images are then translated taking into account the calibration coefficient. A skew adjustment enables image pixel rows to be synchronised and finally scaled to ensure image size parity. A check for camera position produces a set of georectified images. These rectified pixels are then interpolated with colour schemes enabling interpretation of the physical features within them. Georectification of Cam-ERA photos produce good, accurate measurements with high spatial and temporal resolution of nearshore bathymetry. The hourly averaged footage is part of the Cam-Era Network Project and has been used to create the geo-rectified images in this project.

I have used the georectified images to establish the position of the DoD rods and the digital footage has been analysed for the wave approach direction, beach width, location of wave run-up with respect to the rods, the presence of any rip channels and sand banks, general patterns of sediment movement and location of wave breaking with respect to the rods. The extent of the saturated surface (groundwater seepage) was also observed.

3.2.5 BERTIN ET AL. (2008) MODEL AND BEACH CLASSIFICATION

As previous prediction formulae underestimated sediment activation depth (SAD) by 40-60 %, Bertin et al's (2008) numerical model looked to incorporate wave incidence angle as a part of bed shear stress is due to wave induced longshore currents. As wave incidence angles are often smaller than the margin of error there is inherent difficulty in studying them and so the literature is deficient.

Two contrasting wave dominated beaches along the Atlantic coast of France were studied; one gently and one steeply sloping beach with low and high oblique angles respectively. Published data was incorporated with results from fluorescent tracers and plughole experiments to establish activation depths. 10/20 % differences between methods were found and averages were used for numerical modelling and so for theoretical relations.

Bertin et al. (2008) used the spectral wave model SWAN to drive the time and depth averaged coastal model MORPHODYN. Maximum computed bed shear stress (*T*) along the beach profile was determined at subsequent low tides as several bed shear stress events occurred during a tidal cycle. Bertin et al. (2008) initially ran the model under boundary conditions that were present at the time of measurement campaigns and then undertook to determine variation in activation depths by fixing wave period and wave incidence angle and restricting wave parameters to approximate steady currents (after Liu and Dalrymple, 1978 as cited in Bertin et al., 2008).

Results from the field experiments were sediment activation depths of 0.015 +/- 0.003 m with wave heights (H_s) of 0.4 m and 0.05 +/- 0.01 m for higher wave energy conditions, H_s = 2.0 m. These were in agreement with Ferreira et al. (2000). Calibration was only carried out on one of the beaches, as the data was available at that time. Results from the numerical modelling correlated activation depth and total bed stress as well as wave incidence at breaking and total bottom shear stress. Testing for the relative influences of wave parameters, Bertin et al. (2008) ascertained that quasi-linear relationships exist between *SAD* and wave height (in normal and mildly oblique wave breaking conditions) and *SAD* and wave obliquity. The new empirical formula for *SAD* (Z_o) prediction includes; wave height (H_s), beach face slope (β) as well as the breaking wave angle (α) and is as follows:

$$Z_o = 1.6 \tan(\beta) H_s^{0.5} \sqrt{1+\sin(2\alpha)} \tag{3-23}$$

where 1.6 is a constant which has been empirically adjusted.

Battjes (1974) expressed the relationship of beach slope and significant wave height to beach morphodynamic state through the surf similarity parameter, ξ, as;

$$\xi = \tan\beta / \sqrt{H_b / L_o} \tag{3-24}$$

where L_o is the deep water wave condition for the wavelength, L and H_b is root mean square wave height. The predicted wave types are determined from the following ranges from Fredscoe and Deigaard, 1992 (as cited in Anfuso, 2005) and Vincent et al. (2003) respectively; ($\xi>2$) = surging breakers, ($0.4<\xi<2$) = plunging breakers, ($\xi<0.4$) = spilling breakers and ($\xi>3.3$) = surging breakers, ($0.5<\xi<3.3$) = plunging breakers, ($\xi<0.5$) = spilling breakers.

The surf scaling parameter, Ω, introduced by Guza and Inman in 1975 is used to characterize morphodynamic beach state from wave period (T), significant breaker height (H_b), and slope ($\tan^2\beta$). It is related to the surf similarity index through the expression;

$$e = \pi E_b^{-2} \tag{3-25}$$

The equation

$$\varepsilon = 2\pi^2 H_b / 2gT^2 \tan^2\beta \tag{3-26}$$

producing an index of beach state; ($\varepsilon < 2.5$) corresponding to reflective conditions, ($2.5 < \varepsilon < 30$) corresponding to intermediate beach types and ($\varepsilon > 30$) corresponding to dissipative beach types (Anfuso, 2000).

Dissipative beach states are commonly associated with spilling breakers and large surf zones; while plunging breakers with free falling wave jets dominate in intermediate to reflective conditions; resulting in condensed. The migration of a constrained, energetic breaking line, from plunging breakers; results in high disturbance values (Anfuso et al., 2005).

3.3 RESULTS

3.3.1 DEPTH OF DISTURBANCE MEASUREMENTS

Summary tables for both the longshore and cross-shore DoD values are given below to allow any variations to be observed. Results from depth of disturbance experiments are given in Appendix VI while meteorological and wave conditions are given in Appendix VII. Data were not available for some locations when rods were lost, interfered with, were bent or it was deemed unsafe to retrieve the rods. Values of discrete DoD were presented as it has been postured that averaging values of DoD does not provide adequate assessment of variation of DoD. Averages were also presented to make direct comparisons between beaches possible. Composite averages in the longshore and cross-shore also provide comparative ability. Standard deviations were also given for all averages. Beach profiles are presented in Appendix V.

According to the Bertin et al. (2008) model, Z_o of 0.0522 was established under fair weather conditions on the 27th of September and Z_o of 0.084708 under 3 m wave conditions on the 14th of August, 2014. Measurements of average profiles show that Ngarunui Beach can be classified as an ultra-dissipative beach according to Wright and Short (1984) model and dissipative according the surf scaling parameter. Breaking conditions were dominated by spilling waves with a wide surf zone. In this instance all measurements are directly comparable as all waves are spilling and dissipative.

Table 3.1: ***Summary table of DoD values. Averaged statistics from discreet samples are presented. Note: All units are in mm. Standard deviations are shown in brackets.***

Site location	**Average DOD (mm)**	**Wentworth Scale size class (1922)**
Ngarunui Beach North	**86 (73.21)**	*ms*
Ngarunui Beach South	**62** (24.84)	*ms*
Wainamu Beach	**13** (13.14)	*fs*
Moonlight Bay	**1** (2.04)	*fs*

Average DoD at Ngarunui Beach was moderate, however total variation across Ngarunui Beach was quite large, which is reflected in the large standard deviation (Table 3.1). Variation was much less at Wainamu Beach and southern Ngarunui Beach. However, this was during one experiment. DoD was negligible at Moonlight Bay and only one experiment was carried out here. All localised surface elevation changes at DoD rods were less than 500 mm (refer Appendix VI) as were all DoD measurements (Table 3.1).

Table 3.2: ***DOD values for cross-shore profiles at northern Ngarunui Beach. Note: All mean values are whole numbers as data was collected in whole numbers. Standard deviations are given in top brackets while discrete values of DoD are given in lower brackets. nd = no data available.***

Position	19th August 2013	20/21st July 2014	14/15th August 2014	29/30th August 2014	26/27th September 2014	24/25th October 2014	26/27th November 2014	5/6th February 2015	μ & s.d.
Low	**61 (17.24)** (64 76 42)	**130 (177.55)** (335 30 25)	**157 (26.87)** (176 138 nd)	**49 (11.02)** (44 62 42)	**132 (72.51)** (59 134 204)	Nd (51 nd nd)	**70 (35.53)** (56 110 43)	**233 (46.67)** (200 nd 266)	**108** **(84.80)**
Mid	**39 (14.05)** (40 24 52)	**81 (54.26)** (143 44 55)	**252 (44.55)** (230 283 nd)	**54 (14.53)** (68 55 39)	**88 (55.64)** (43 70 150)	**54 (32.35)** (80 65 18)	**40 (27.54)** (60 55 10)	**143 (15.89)** (158 159 131)	**88** **(69.82)**
High	Nd	Nd	**89 (30.51)** (98 114 55)	**12 (6.08)** (+5 +15 +16)	**42 (41.04)** (+2 40 84)	**18 (9.29)** (28 10 +15)	**33 (7.78)** (29 nd 40)	**128 (39.34)** (92 122 170)	**55** **(49.27)**

Maxima of DoD were found both in the low and mid intertidal zones on different days. Generally DoD values decreased shoreward; maximum average values of DoD were found in the low intertidal during all experiments except on the 14/15th of August and on the 29/30th of August. Average values were found to be the same at the low and mid intertidal on the 24/25th of October however data was limited in the low intertidal on this date. Standard deviations associated with DoD decreased shoreward also, as larger DoD values became less present. Values within each zone were found to vary significantly alongshore however in July and early August, the cross-shore values maintained their relative proportions between the low and mid and mid and high intertidal positions respectively.

The July dates were associated with moderate wave conditions (1.6-1.8 H_b approaching from the SW and T of 12-16 s) however from real world observation, the model considerably underestimated the wave heights on this day. The largest DoD value collected during any experiment was taken on this day. Beach profiles showed a relatively linear descending profile at the southern end of the beach, with small micro-topographic changes in elevation elsewhere. A hole was apparent just landward of the outer rod at the northern transect which had a distinctive accreted area just seaward of it (refer Appendix V). Erosion was recorded by the disturbance rods across the mid to low intertidal area of the beach (refer Appendix VI). Larger amounts of erosion corresponded to the larger northern transect DoD values (Table 3.2). The significantly larger values of DoD on the northern transect in July signify that morphological features were present at these locations and were controlling DoD. These values did not display a uniform increase in a southerly or northerly direction and cannot therefore be associated with the prevailing southerly longshore drift. They are possibly due to rip currents in this area and/or a high water table. In the preceding week footage from Cam-ERA showed elevated zones just north of the mid and low intertidal rods on the northern transect (Figure 3.7).

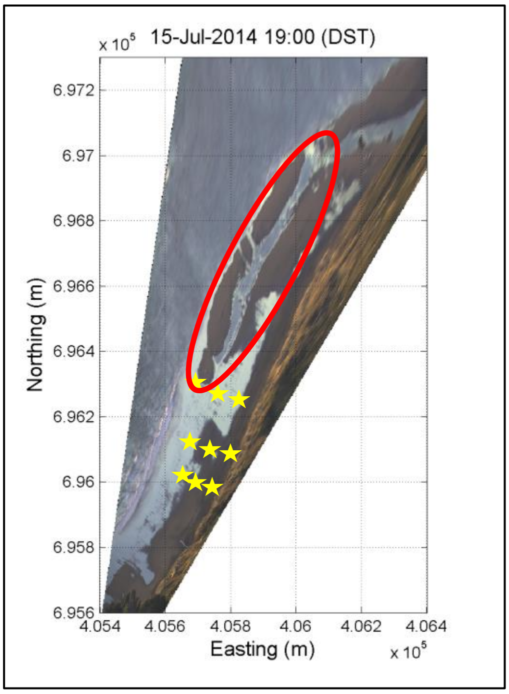

Figure 3.7: **Ngarunui Beach on the 15th of July at 7 pm showing emerging bars ad groundwater seepage. *Source: Cam-ERA.***

The 14/15th of August had significantly larger waves forecast, 3.2 H_b, and T of 10-15 s. Waves approached from the west. The Beach profiles were only available for the mid and north transect on the 14th and showed some very small scale (< 10 mm) variation in elevation cross-shore (refer Appendix V). The largest values of DoD were recorded on this day. Two rods were knocked over along the southern transect in the high wave conditions. These conditions prevailed over the 14th and 15th (Figures 3.8 and 3.9). The rods consistently recorded erosion on this date also however along the high intertidal accretion occurred (refer Appendix VI). The northern transect was in a rip on August the 14th and 15th, 2014 while the mid transect was also exposed to a rip as seen on the 14th at 15:00 (Figures 3.10 and 3.11). There was also a longshore channel that was present just seaward of the most seaward rods and another that was apparent beneath the most seaward rods (Figure 3.12). These channels were not visible during the other experiments. Consistently smaller values of DoD in the low intertidal (relative to the mid intertidal) were apparent during both August experiments that may have been the result of the waves failing to penetrate the sediment in the deeper water of the trough. Significantly large tides occurred on this date (3.5 m), which may have contributed to the large effect of the swash at the high intertidal area.

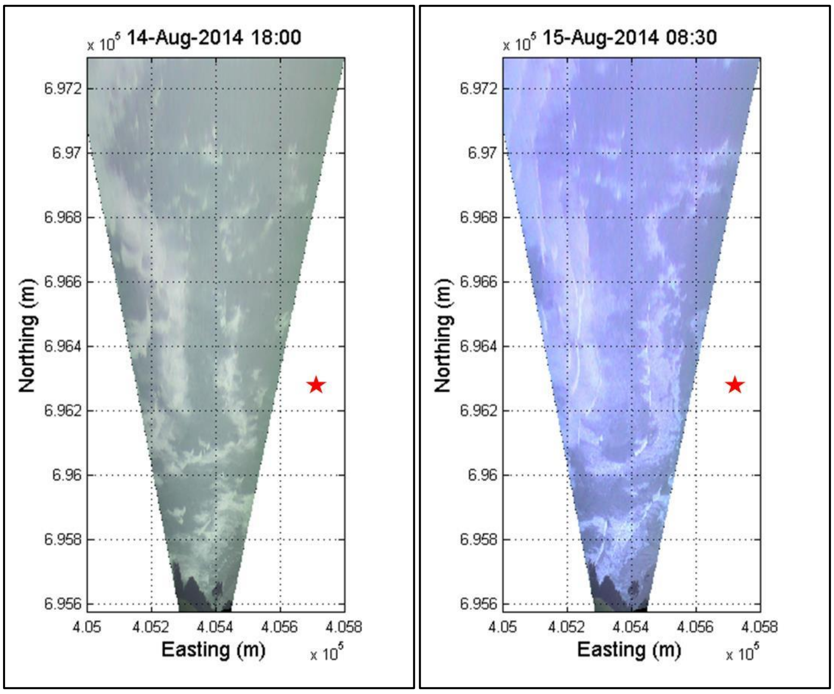

***Figures 3.8 and 3.9:* Wave conditions at Ngarunui Beach on the 14th and 15th of August, 2014. Note: Red star in experiment location.**

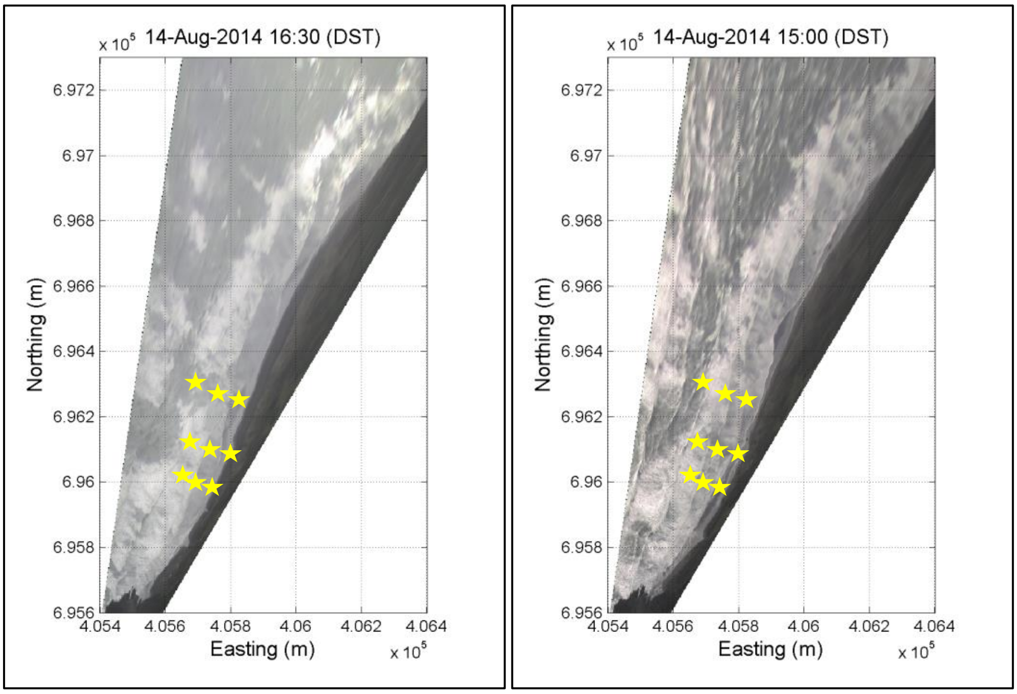

Figures 3.10 and 3.11: **Rips visible at the northern and mid transects respectively.**

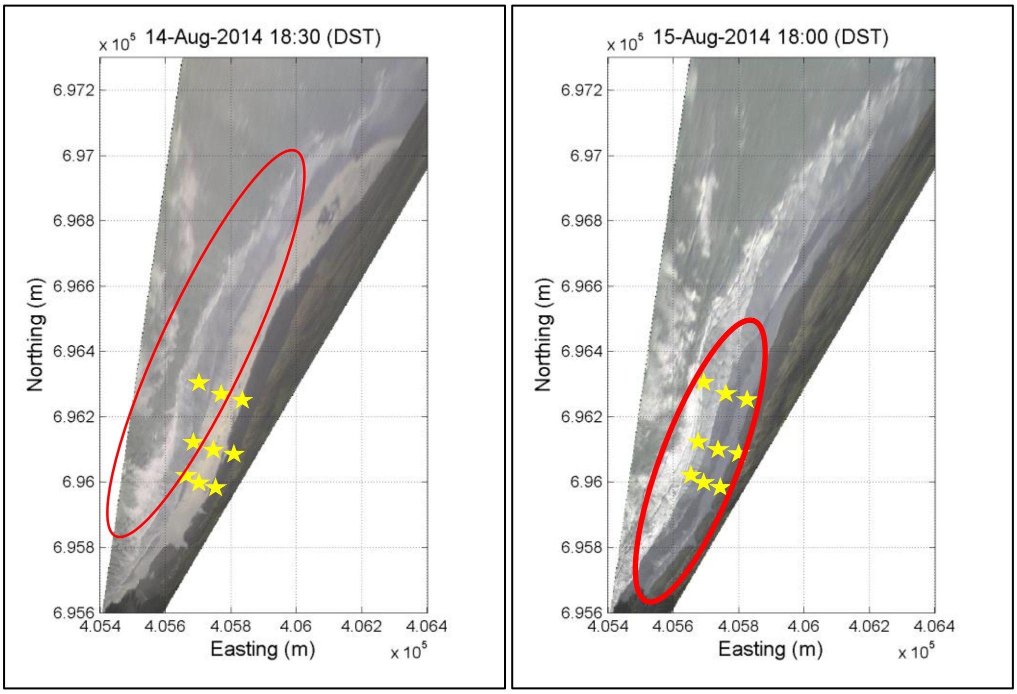

Figures 3.12 and 3.13: **Longshore channels at northern Ngarunui Beach and sand bar.**

Less variation occurred alongshore on August the 29/30th, reflected by low standard deviations. This was during a beach recovery phase with significant accretion recorded at the low and high intertidal. Large values of positive DoD were recorded in the upper intertidal zone (refer Appendix VI). The northern transect displayed a hole at the bottom, landward of the disturbance rod (Figure 3.14). This was similar to the profile taken in July at the same location. DoD values were relatively small on this day and were associated with small Hb values of 1.1 m and long periods of 14-18 s. A small breaker zone was apparent and low tide rods were not exposed once this narrow band had moved shoreward (Figure 3.15). Non-uniform areas of elevated sand and channels were present on the 29th (Figures 3.16 and 3.17) which were still visible on the 30th of August and in mid-September. The low tide disturbance rod was positioned just seaward of this channel, however, no distinct variation in DoD at this rod could be correlated to this feature. As previously mentioned however the mid intertidal zone displayed distinctively larger values of DoD during August.

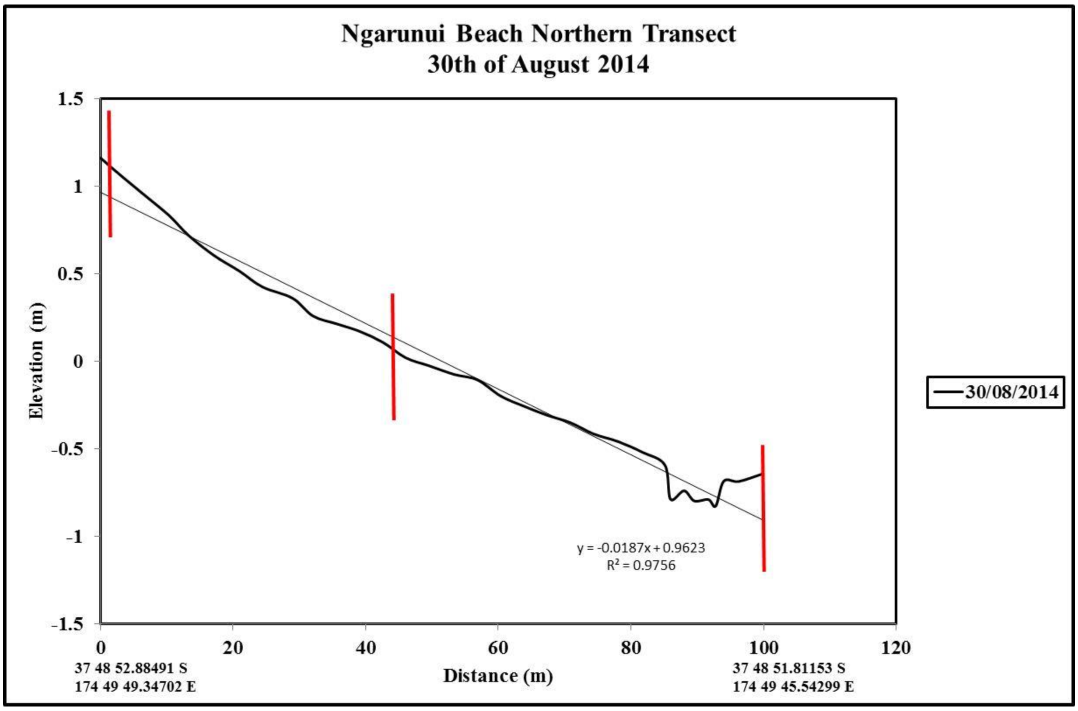

Figure 3.14: Beach profile at the northern most transect on Ngarunui Beach.

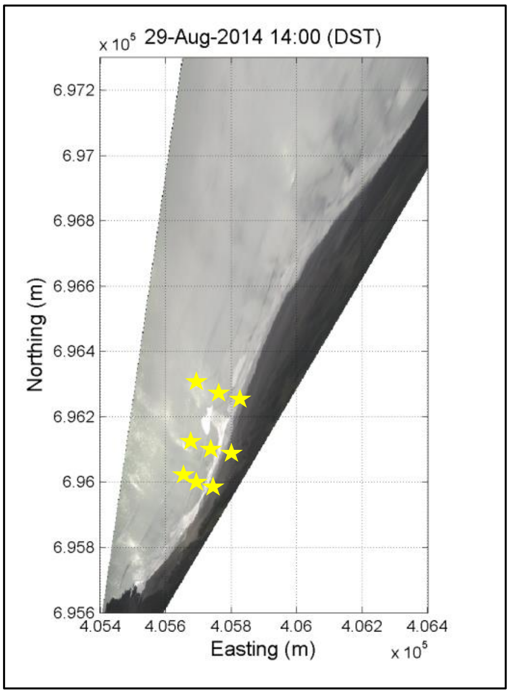

re

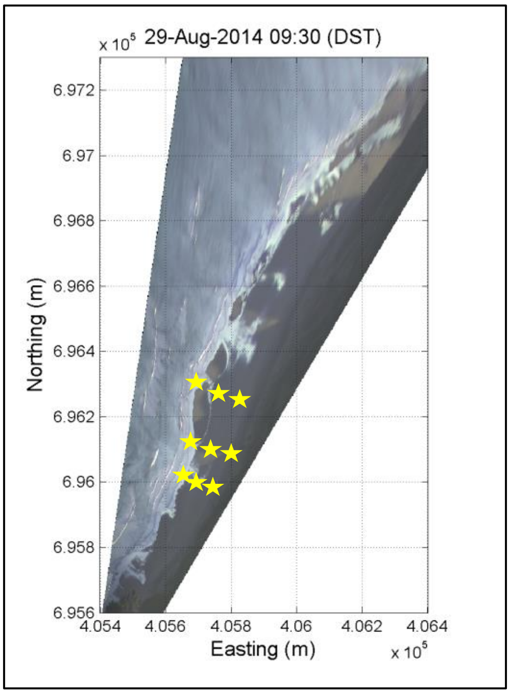

Figures 3.15 and 3.16: **Negligible breaker zone close to high tide and sand humps at exposed during low tide at northern Ngarunui Beach.**

Figure 3.17: **Channel visible on northern Ngarunui Beach on the 29th of August, 2014 at 17:34.**

Figure 3.18: Groundwater seepage on the 30th of August, 2014.

The high intertidal zone did not seem to follow the same pattern as the other zones, with much greater variation (range of 2 – 170 mm) and often mixing depths were positive. The smallest DoD value not associated with these accretionary events at the high intertidal was 10 mm on Ngarunui Beach. The significantly larger values in the high intertidal were associated with large storm events on the 5/6th of February and on the 14/15th of August. In fact on these dates, disturbance and rods had been forced over under the heavy seas. Because tidal heights on these days (refer Appendix VII) were higher, the relative positions of the beach moved shoreward, thus the mid intertidal and high intertidal zones were exposed to larger breaking wave energies. It is interesting to note that during experiments in February, 2015, the rods on the northern transect in the upper intertidal zone were only submerged to around 600 mm of water and were within 500 mm of the swash limit. However, large values of DoD were still recorded at his location. No profiles were available for February the 5/6th.

All other wave conditions were significantly smaller than this during experiments except those in October, which did have moderate DoD values at the high intertidal. No data were available on July the 14th/15th for the high intertidal zone during these experiments; although it is likely that large DoD values would have been recorded at these positions.

On the 20/21st of July an extremely large standard deviation associated with a DoD value of 335 mm was recorded at the low intertidal. This corresponds to a large value (relative to the other locations in this zone) in the mid intertidal. Smaller standard deiviations were associated with fair weather conditions. The mid intertidal zone also showed a large variation of DoD, with a difference of 273 mm.

Large DoD values were observed on the 26/27th of September, 2014 when waves were between 1.1 m and 1.3 m with 13-15 s periods. Tides were also high (3.2 m) on this day corresponding to moderate disturbance values in the upper part of the beach. The southern transect showed up to 50 mm of accretion in places (refer Appendix V) and disturbance rods consistently recorded accretion (refer Appendix VI). A uniform decrease in DoD in a northerly direction was not correlated with similar elevation change patterns. This was the only time that uniformity alongshore was observed. Wave refraction around an area of elevated sediment could be distinguished on both the 26th and 27th of September, however, this did not have a clear effect on DoD.

Small scale variation at the bottom of the mid transect on the 26th of November occurred. A large (> 2 m) scale shift in the profile line was established also but may have been due to faulty measurement.

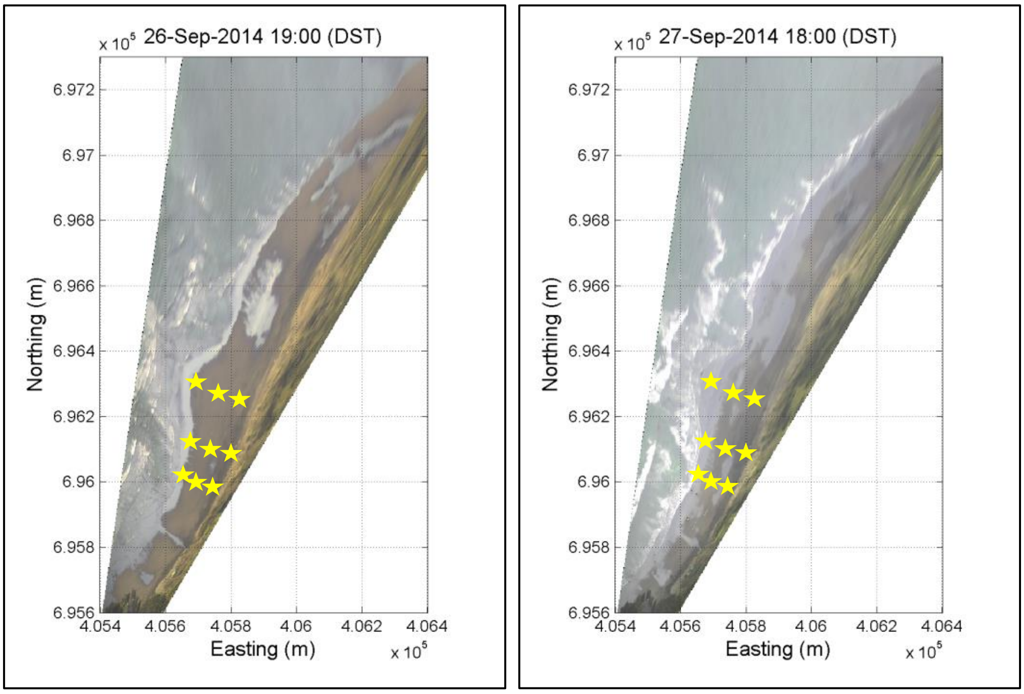

***Figure 3.19 and 3.20:* Wave refraction around a sediment slug on the 26th and 27th of September respectively.**

Table 3.3: ***Summary of the DOD for long-shore profiles at northern Ngarunui Beach.***

Position	19th August 2013	20/21st July 2014	14/15th August 2014	29/30th August 2014	26/27th September 2014	24/25th October 2014	26/27th November 2014	5/6th February 2015	μ & s.d.
North	**52 (16.97)** (64 40 nd)	**239 (135.76)** (335 143 nd)	**165 (62)** (176 230 98)	**39 (31.80)** (44 68 +5)	**25 (29)** (59 43 +2)	**53 (26.06)** (51 80 28)	**48 (17)** (56 60 29)	**150 (54.44)** (200 158 92)	**94 (84.11)**
Mid	**50 (36.77)** (76 24 nd)	**37 (9.90)** (30 44 nd)	**178 (91)** (138 283 114)	**44 (25.36)** (62 55 +15)	**81 (48)** (134 70 40)	**38 (38.89)** (nd 65 10)	**83 (39)** (110 55 nd)	**141 (26.16)** (nd 159 122)	**85 (65.29)**
South	**47 (7.07)** (42 52 nd)	**40 (21.21)** (25 55 nd)	**55 (nd)** (nd nd 55)	**32 (14.22)** (42 39 +16)	**146 (60)** (204 150 84)	**16.5 (2.12)** (nd 18 +15)	**31 (18)** (43 10 40)	**189 (69.48)** (266 131 170)	**77 (72.66)**

By averaging values of DoD in the cross-shore, it was possible to see that average DoD increased slightly in a northerly direction. Although the mid and southern in particular had lower DoD values; during the larger storms of August 15th 2014 and February 2015, rods were bent and fallen in the low and high intertidal at these transects the missing data possibly skews this distribution. Removing the equivalent positions of discrete locations where data were missing, the same increasing pattern could be seen.

Table 3.4: ***Summary of the DOD for long-shore profiles at southern Ngarunui Beach.***

Position	10th February 2015
Transect 1	**58 (27)** (30 83 60)
Transect 2	**56 (30)** (23 81 65)
Transect 3	**64 (35)** (28 98 65)
Transect 4	**74 (9)** (nd 80 67)

The range of DoD values at southern Ngarunui Beach on the 10th of February, 2015 varied significantly between 23 cm and 98 cm (Tables 3.4 and 3.5). There was an apparent increase in average DoD in a northerly direction. However, the range of values did not differ greatly along the different intertidal zones; values were within 7 cm of each other except in one instance; at the mid intertidal on transect 3; DoD was 18 cm greater than the lowest value in this intertidal zone. Moderate conditions prevailed on this day with 1.1 – 1.3 m wave heights and 13 s periods on Ngarunui Beach. Holes can consistently be seen across the low intertidal zone in all beach profiles (Figure 3.21 and Appendix V). The low intertidal rods were however within the holes at the lower beach face and the mid intertidal rods were on the concave gradient apparent at the middle of the beach (Figure 3.21 and Appendix V). This increase in slope may also have contributed to the higher values of DoD at this position as waves break with shallower bathymetry.

Morphological changes in the longshore were not observed possibly as there was a smaller spatial scale between the rods at this location. The most notable feature at northern Ngarunui Beach was the cross-shore pattern; consistently high values of DoD were found in the mid intertidal with moderate values in the low intertidal and much smaller values in the swash zone.

When compared with the northern part of the beach, this location displays a smaller distribution of DoD, but this experiment was done during fair weather conditions.

Table 3.5: ***Summary of the DOD for cross-shore profiles at southern Ngarunui Beach.***

Position	10th February 2015
Low	**27 (3.61)** (30 23 28 nd)
Mid	**86 (8.43)** (83 81 98 80)
High	**64 (2.99)** (60 65 65 67)

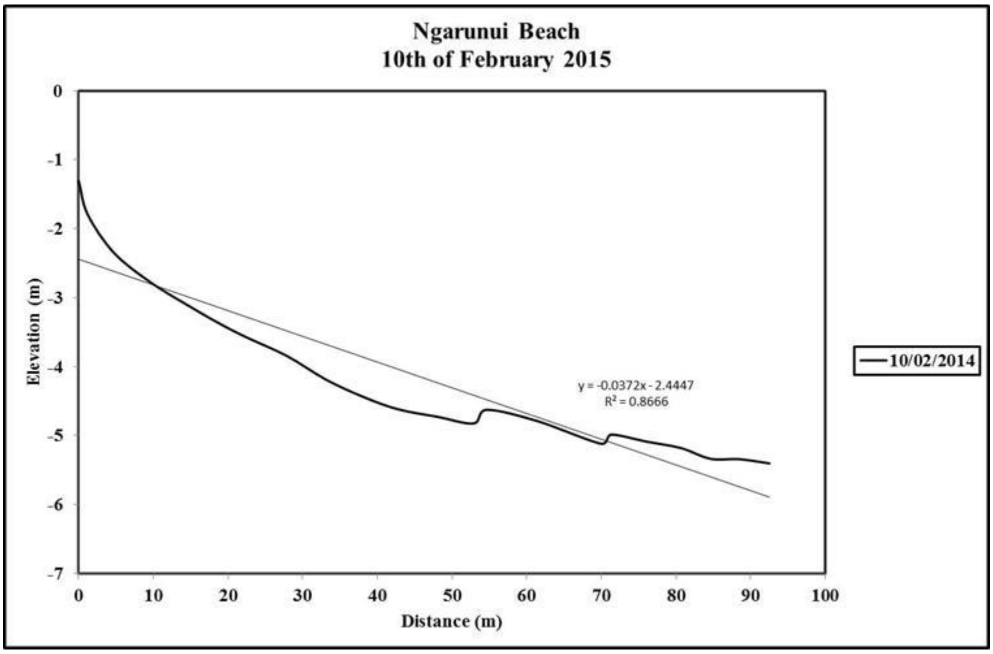

Figure 3.21: **Beach profile from southern Ngarunui Beach on the 10th of February, 2015.**

Fair weather conditions were present during all of the experiments at Wainamu Beach with average breaking wave height, H_b, of between 1 m and 1.8 m with wave periods, *T*, ranging from 8 and 15 s (refer Appendix VII). Prevailing winds were westerly and south-westerly, but were more variable and light in July. Swells consistently approached from the southwest and but were slightly more westerly on December the 11th. Disturbance only occurred at the mid profile line and at the low intertidal on the western transect on the 11/12th of December. Otherwise no disturbance was recorded (Tables 3.6 and 3.7).

The values in the low intertidal were much larger in November 2014, related to the 3.1 m tide overnight on this date; a 2.8 m tide was predicted for the night of the 11 and 12th of December (refer Appendix VII). Likewise tidal ranges were large during July 2014, with a 3.5 m tide predicted for the evening of the 15th. The nil values on the western transect on the 11/12th of December were areas that were not exposed to the tide on this date. They were on the flat, higher section of the beach. The nil values on the eastern transect may also have been related to the smaller tides on this day as current scour at this location may be less on the ebbing tide under a smaller tidal prism. A large DoD value at the high intertidal zone on the western transect on 15/16th of July and 27/28th of November can be related to the large area of shallower bathymetry at this location during the high tide.

Comparatively larger DoD values were recorded on the 14th/15th of July, although wave conditions were comparable. On this day, the rod in the high intertidal position at the western transect was knocked over; possibly by the force of the tidal current. Values were, similar to those in November, larger in the middle transect at the low tide level. This location is not only the most exposed to the channel and the ebbing current but also has a significantly gentler slope than the lower section of the western transect and mid transect (refer Appendix V). At the western transect, the largest value was recorded at the mid intertidal zone on the 14/15th of July. The rod was placed close to the abrupt change in slope at this location (refer Appendix V). At this point the rod was most exposed to tidal and wave processes as it has shallow bathymetry and is the first and longest exposed part of the upper intertidal zone. Values were not recorded for this slope but would have been useful.

On the 11/12th of December, a large (~0.5 m) amount of accretion was recorded in the profiles at lower intertidal zone of the western transect (refer Appendix V).

This was not visible at other locations on this date. This area also experienced nearly the same amount of accretion on the 15/16th of July. On this date in the beach profiles accretion was recorded at the low intertidal zone of the mid transect also. However, none of these profiles changes were recorded by the rods (refer Appendix VI). This may be due to the rods not being on the profile lines (this was the case in the July western transect profile) or may be due to movement in the total station causing the vertical assessment to be imprecise. The rods act as micro-erosion meters recording small changes. It is possible that the profiling was not carried out correctly at these locations i.e. the rod with prism attached was held off the ground.

Table 3.6: ***Summary of the DOD for long-shore profiles at Wainamu Beach.***

Position	14/15th July 2014	15/16th July 2014	27/28th November 2014	11/12th December 2014	µ & s.d.
West	**22 (19)** (8 35 nd)	**16 (5.66)** (12 20)	**10 (14.14)** (nd 0 20)	**3 (5)** (8 0 0)	**14 (11.27)**
Mid	**17 (10)** (20 6 26)	**11 (1.41)** (12 10)	**24 (31.43)** (60 10 2)	**9 (6)** (16 6 5)	**16 (16.30)**
East	**17 (18)** (nd 4 30)	**10 (8.49)** (4 16)	**10 (9.19)** (nd 16 3)	**0 (0)** (0 0 0)	**8 (10.37)**

Table 3.7: ***Summary of the DOD for cross-shore profiles at southern Wainamu Beach.***

Position	14/15th July 2014	15/16th July 2014	27/28th November 2014	11/12th December 2014	µ & s.d.
Low	**14 (8.49)** (8 20 nd)		**60 (nd)** (nd 60 nd)	**8 (8)** (8 16 0)	**19 (21.42)**
Mid	**12 (17.35)** (35 6 4)	**9 (4.62)** (12 12 4)	**9 (8.08)** (0 10 16)	**2 (3.46)** (0 6 0)	**8.75 (9.79)**
High	**28 (2.83)** (nd 26 30)	**15 (5.03)** (20 10 16)	**8.33 (10.12)** (20 2 3)	**2 (2.89)** (0 5 0)	**12 (10.89)**

DoD was negligible at Moonlight Bay however~5 cm of disturbance was apparent in the coarse sand at the top of the beach on the 23rd of September (Tables 3.8 and 3.9) with a corresponding 5 cm of accretion. Disturbance was not noted elsewhere. Negligible bed level change was observed during this experiment (refer Appendix V). There was large scour present around the disturbance rod at the mid intertidal zone. Scour effects were often observed at Wainamu Beach and Ngarunui Beach also but were not included in DoD measurements. The pools found around obstacles are the result of wave scour, mostly during backwash. Quite substantial scour occurred around the rod in the low intertidal zone (Figure 3.22).

Table 3.8: ***Summary of the DOD for long-shore profiles at Moonlight Bay.***

Position	22/23rd September 2014
West	**0 (0)** (0 0 0)
East	**2 (2.89)** (0 0 5)

Table 3.9: ***Summary of the DOD for cross-shore profiles at Moonlight Bay.***

Position	22/23rd September 2014
Low	**0 (0)** (0 0)
Mid	**0 (0)** (0 0)
High	**2.5 (3.54)** (0 5)

Figure 3.22: **Scour around the disturbance rod and seepage collapse at the mid intertidal zone at Moonlight Bay.**

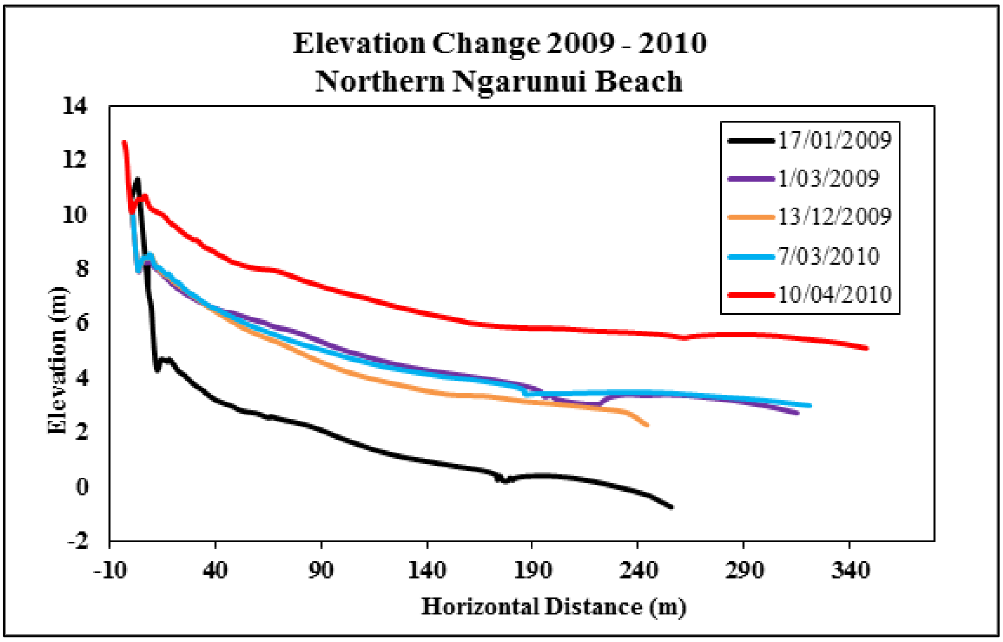

Figure 3.23: **Bed elevation change between 17th of January, 2009 and the 10th of April, 2010. Source: Ron Ovenden and Andrew Wood.**

Although it has been observed that the beach elevation at Ngarunui Beach generally remains stable with limited spatial or temporal variation, 1.8 m – 2 m (±10 %) in previous studies (Huisman et al., 2011; Patel, 2015), a maximum elevation change of ~5 m occurred between 17th of January, 2009 and the 10th of April, 2010, associated with a large increase in the beach scarp (Figure 3.23). Beach survey profiles produced during experiments are provided in Appendix V.

VRS beach surveys show bed elevation differences of ~80 m to the top of the dunes at the harbour entrance. Beach survey profiles show negligible variation within tidal cycles however some bed level change did occur and was in excess of 300 mm. Large (> 0.5 m) bedforms are present on Ngarunui Beach particularly near the harbour entrance and show bed level variation on small scales. Tidal pools near the entrance are sometimes in excess of 1.5 m deep (Figure 3.25).

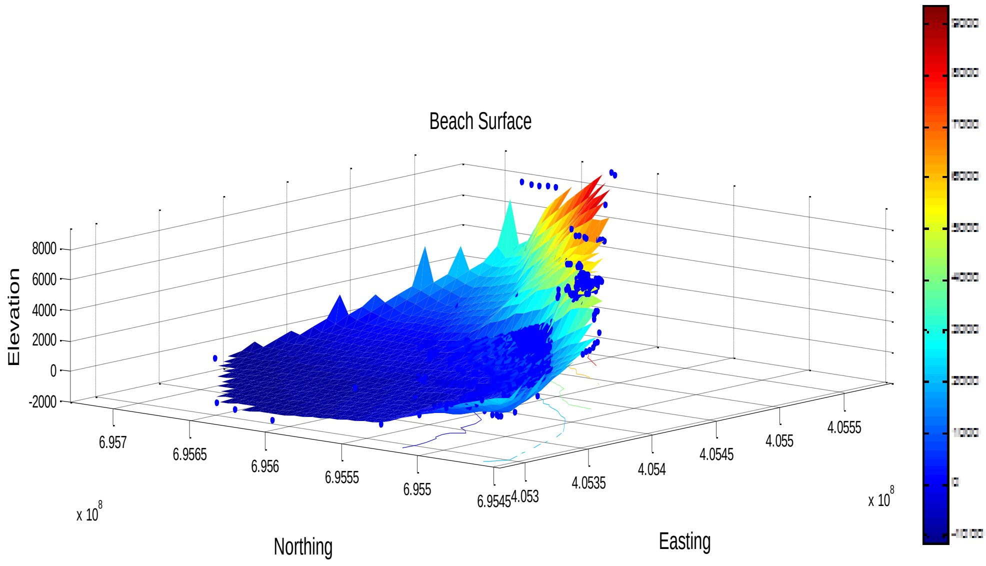

Figure 3.24: **3-D plot of Ngarunui Beach. Vertical scale is in mm.**

Figure 3.25: **Large tidal pool near the northern transect at Ngarunui Beach on the 15th of September, 2014.** ***Source: Ron Ovenden.***

3.4 DISCUSSION

New Zealand beaches tend to show variation between fair weather and storm conditions at any time of the year. During storms, beaches become narrower, erode, and are prone to overwash. Eroded sediment is transported into the offshore. During fair weather conditions, net sediment transport is landward. As oil spills are often associated with storm events and the high wave energies and changes in beach slope that occur because of storms can cause larger mixing depths and increased groundwater seepage. There is a fundamental need for evaluation of maximum mixing depths distributions at the shoreline to assess the maximum potential depth of oil burial.

The intertidal zone is the most active area of the littoral zone. Therefore disturbance rod experiments and beach profiling was carried out here. Discrete observations of DoD provided observation of morphodynamic drivers of DoD and variation both in the longshore and cross-shore. It has been suggested that this method is superior in the estimation of DoD.

Large variations of DoD between sites were observed in this study. On the exposed coast, values of DoD were found to be above 300 mm while less than 100 mm was observed at Wainamu Beach. Insignificant mixing occurred at Moonlight Bay essentially due to bedrock that occurred close to the surface.

Studies of beach morphodynamic behaviour have consistently emphasised the influence of waves, currents, tidal undulation, rainfall on groundwater levels, pre-existing morphology as well as beach sediment characteristics including porosity, grain size and distribution (Masselink and Turner, 2000). Relating morphology and the activation regime is a key concept to explain spatial variation of sediment activation in different beaches as it reflects the distribution and relative intensity of wave processes across the beach profile (Anfuso, 2000).

A general sequence of disturbance was observed by Otvos (1965); deposition in the swash zone on the flood tide followed by erosion in the surf zone during the ebbing tide. This may lead to the formation of discrete sedimentation units. However, these were not observed on Ngarunui or Wainamu Beaches. Layers of shell hash were deposited in the swash zone on several occasions. Coarser-grained lower units were observed by Otvos (1965) in the highest energy breaker zone on the ebb tide as the finer fractions had been winnowed out. Otvos (1965) also emphasized that as backwash may only carry finer fractions on the return flow; good sorting and symmetric size distribution in the upper intertidal zone occurs. This was observed at Ngarunui Beach as well as slightly better sorting in a northerly direction.

Kraus (1985); Sunamura and Kraus (1985); Ciavola (1997) and Inman et al. (1980) found that mixing depths were constant alongshore in contrast with the observations of Sherman et al. (1994) and Gaughan (1978); that mixing distribution varied unsystematically. In this study disturbance depths varied substantially in both the cross-shore and longshore. This variation was determined by bed morphology predominantly. No large gradient changes were visible at Ngarunui Beach so this could not account for cross-shore differences. Only once, during moderate wave conditions and large tides did a linear decrease in DoD occur alongshore in a northerly direction. On this date Ngarunui Beach was experiencing net accretion in fair weather conditions. Average DoD values displayed slightly larger DoD in a northerly direction.

Mixing depth maxima were found at wave breaking point during high tide and at the maxima of wave run-up by many authors. Bi-modal maxima were not apparent though measurements were not continuous cross-shore. In the swash zone, reduced disturbance occurred possibly as waves may fail to penetrate the water column and therefore to penetrate the seabed at this location (Jackson and Malvarez, 2002). Gonzalez et al. (2002) observed large amounts of sediment transported into the run-up maxima area by sea foam.

Generally DoD decreased onshore however the presence of a trough created by the high water table in August, 2014 resulted in larger values of DoD in the mid intertidal zone. Values of DoD have been found to be twice as high in bar-troughs and four times as high in megaripples associated with rip-feeder channels. This was possibly observed in July when a rip was visible. The bedform migration rate of 0.275 mm/s was estimated by Sherman et al. (1993) for surf zone conditions on intermediate beaches. Because Ngarunui Beach displays a high number of rip channels, the complex morphology makes mixing highly variable across the beach.

A bimodal distribution of depth of activity was observed within a single bar profile in studies by Greenwood and Hale (1980) and Greenwood and Mittler (1984). A maximum is associated with rip currents and the other in the trough landward of the bar due to longshore current scour. High erosion values are associated with these. Although no measurements were taken at the bar, smaller scale troughs were present on intertidal zone. Unfortunately rods were not well positioned to obtain values over around the patterns of troughs and channels apparent on Ngarunui Beach, so this could not be established.

Gonzalez et al. (2002) stated that the time that sediment was exposed to certain beach processes had a great effect on the maximum disturbance. Correlation of the different parts of the wave profile with maximum DoD are confounded by the succession of the different parts of the wave profile, however.

Scouring or protection by pebbles, littoral drift direction, bottom currents, energy fluctuations, wind strength and direction and time within the breaking wave zone have all be observed to contribute to the variation in DoD values. On Ngarunui Beach, morphological features such as rips and the longshore troughs have all affected DoD values both in the longshore and the cross-shore.

Gonzalez et al. (2002) observed that mixing depths decreased with increasing wave height in contrast to the majority of the research on mixing depths. It was proposed that rising tides may negate the influence of increasing wave height. This was not observed on Ngarunui Beach; however, the tides did play a role in the high intertidal zone. Tidal conditions were found to have a large effect on swash processes in the high intertidal zone, increasing it. Tidal currents also played a significant role at Wainamu Beach. For significantly smaller waves, (waves are not generally present at this location), DoD was large.

Sunamura and Kraus (1985) proposed that mixing depth is predicted to increase linearly with breaking wave heights, H_{b}, up to ~1.5 m. The rate of increase of mixing, decreases for larger waves (>1.5 m) as the shear stress lessens. Wave periods are relevant at wave heights in excess of 1.5 – 2 m, when mixing becomes an increasing function of wave period, T. Anfuso et al. (2000) corroborated these findings. However, wave period has been observed to have little effect on dissipative beaches as backwash reaches the breaker point before the incoming waves.

The largest DoD in the low intertidal was associated with a large storm event with successively smaller average DoD onshore. The largest average values of DoD were however in the mid intertidal on the 15/16th of August during an even bigger storm event. On this day tides were larger and the breaker zone was wider and encroached on the shoreline.

Averaged DoD maxima were observed on Ngarunui Beach in the low and mid intertidal regions and not at the high tide zone exposed to the run-up maxima; unlike the findings of Gonzalez et al. (2002) and many more authors. The decreasing shoreward DoD values were in contrast to the work of many previous authors including King (1951) who, on dissipative beaches, found that DoD was comparative cross-shore.

DoD in the high intertidal zone did not seem to be driven by the same processes as lower in the intertidal zone. Values were significantly smaller and varied alongshore significantly. Positive DoD values represent areas of accretion where the washer moved upward during the tide. This only occurred at the high intertidal zone and only on Ngarunui Beach. This was likely caused by vibrations as the swash zone approached, piling sand beneath and the lifting the washer as the sand accreted. Large erosion values were measured elsewhere by rods and profiles on these dates. Large values were associated with large tidal conditions. The positive values for DoD at the high tide maxima may be associated with sea foam during swash run-up. This transport has been observed on dissipative beaches (Gonzalez et al., 2002). Under larger wave conditions, disturbance was greater at the mid position in the high intertidal. In fairer conditions, there was no apparent pattern.

Small consistent increases in values of DoD alongshore at southern Ngarunui Beach were in contrast to many findings that cross-shore DoD values do not vary alongshore. The larger values of DoD in the mid intertidal zone correspond with the zone that is exposed to wave breaking, as at high tide it is directly beneath the breakers at a depth where the waves reach the bed; offshore from this the depth of the water was observed to be greater than the wave height and inshore from this run-up processes dominate as waves have already broken in the outer zones. This zone is also more exposed to swash processes. It can be deduced that as the areas most exposed to wave breaking exhibit the most disturbance, swash processes have limited effects on this beach during fair weather conditions.

DoD was much more varied at Wainamu Beach than on Ngarunui Beach and values were larger in the mid transect. When the flat high intertidal area on the western transect was exposed to the tide, moderate values of disturbance were found at this position however the largest values at this transect were recorded near the break in slope. The eastern transect showed little variation and was therefore less affected by current scour.

The slightly higher DoD values that were measured at the eastern transect at the high intertidal at Moonlight Bay were possibly due to wave refraction around the eastern headland, causing currents which would be greatest when they reach the groyne at the opposite side of the beach (location of the rod which experienced disturbance). There also happened to be a large amount of seepage at this location due to a storm water drain and at the opposite side of the beach due to a high water table. The wind and wave approach on this day was from the S and SW respectively so the beach was not exposed to incident waves. 2.8 – 3.8 m waves were forecast for the open coast, at Ngarunui Beach with a 12-14 s period (refer Appendix VII).

Morphological changes are a function of changing incident wave regimes, currents, pre-existing morphology and tidal range. Large-scale erosive events have been recorded and observed at Ngarunui Beach, which are in excess of 5 m while small scale bed level variation occurs on the scale of hundreds of millimetres. This complex morphology at Ngarunui Beach, rip currents and offshore channels, will have an effect on predicting DoD. At the high intertidal, the swash, run-up, morphology, slope, energy and shear stress differ and also have implications for the Bertin et al. (2008) model. Most small scale morphological change occurred in the mid intertidal region.

An indirect relationship between grain size and DoD exists as beach slope is determined by grain size. The average sediment grain size on the open coast beach is consistently fine – medium with finer fractions in the upper intertidal zones. The longshore distribution shows little variation; thus the changes in beach morphology along the beach had little impact on the average sediment grains size. The slightly finer grains at the southern end of the beach may be due to the current gyres that are prevalent along the headlands.

Oil penetration on Ngarunui Beach has the potential to be deep, especially when considering potential burial pathways. As groundwater and swash infiltration causes oil to migrate below initial mixing depths and there is a high water table present at Ngarunui, exfiltration is likely to occur rapidly at this location. The exposed beach however undergoes large amounts of erosion frequently and so it is likely that oil would be not remain buried for long periods.

Comparisons with Moonlight Bay were not possible due to lack of data. However it was anticipated that DoD would be negligible at least under fair weather conditions. Storm events have been observed to cause up to a metre of change at the shore implying that oil burial at this location could potentially be > 1 m, with possible groundwater infiltration increasing burial. Due to the high concentrations of fine clay and silt-sized particles, at Moonlight Bay, it would be expected that oil-mineral aggregates would form if oil were transported into this type of low energy environment. The coarse sands in the upper intertidal at Moonlight Bay are indicative of greater wave/current energies within these zones however bedrock at this location would prevent deep penetration or percolation.

According to the Bertin et al. (2008) model, Z_o of 0.0522 was established under fair weather conditions and 1.2 m waves on the 27th of September and Z_o of 0.084708 under 3 m wave conditions on the 14th of August, 2014. These values were not in good agreement with the measured data as the formula underestimated depths of disturbance on Ngarunui Beach during fair weather conditions. It is however important to note that wave heights were predicted and can therefore have inherent error. Mixing was up to 13 % of the wave heights during large storm events and even larger proportion coefficients were obtained in fair weather conditions up to 18% especially in the low intertidal zone. The addition of incidence angle and beach slope did not account for these large values of DoD. As wave heights were not known at Moonlight Bay or Wainamu Beach, it was not appropriate to determine proportionality coefficients at these locations.

The results found here do not compare well with others from dissipative beaches. Recorded values range from 3 % to 8 % however Anfuso observed values of 16.3 % H_b under significantly smaller wave heights on an intermediate beach. Variation between locations has been estimated at 1500 % mostly due to differing morphologies (Ferreira et al., 1998). Differences in reported values may also be due to inherent differences in measurement techniques.

3.5 LIMITATIONS OF RESEARCH

Traditional techniques for estimating mixing depths and depth of disturbance are not generally comparable and care must be taken when relating mixing depths and depth of disturbance because of discrepancies with temporal limits. For example cores containing fluorescent tracers are strictly representative of mixing depths; cores containing accretionary layers are excluded from analysis as stated above.

Results from different beach types cannot be compared. Where comparable results are found it is often in dissipative conditions where single breaker lines which migrate are not present.

The high water table at Ngarunui Beach may have interfered with mixing depths produced by physical mixing processes. As the rod experiments were carried out overnight, it was only possible to gather the antecedent wave and tidal conditions from the rectified images of the preceding day.

CHAPTER FOUR: REVIEW AND SYNTHESIS OF LITERATURE

4.0 INTRODUCTION

There are over 100,000 organic and inorganic hydrocarbons of various molecular weights contained in crude oil (NRC, 2003). By the times oil reaches the shoreline, it has undergone significant changes due to weathering processes. Oil behaviour therefore varies greatly at the shore with consequences for marine organisms, plants and shoreline recreational use. The sensitivity of species and coastal morphology to oil spills is classified according to the Environmental Sensitivity Index, *ESI* with open coast beaches ranking as low priority and soft sediment low energy environments as highly sensitive areas. Oil has however been found buried deeply within coarse/boulder beaches, protected by the boulder armouring. Coarser sediments allow oil to percolate more readily.

Chapter five introduces the second phase of the study which examines the interactions between oil and sediment. Crude oil composition and characteristics are outlined as well as the influence of weathering. Oil spills and their effects are discussed with focus on marine tar residues. Aspects of oil-mineral-aggregate (OMA) formation are reviewed.

4.1 CRUDE OIL COMPOSITION

Petroleum bearing formations (oil pools and reservoir rocks), are the result of pressure and heat applied to the decayed remains of marine organisms. The oils, waxes and fats of decaying organisms settle on the sea floor, become buried under sediment and are transformed into kerogen over hundreds of thousands of years to millions of years depending on the geothermal gradient. The kerogen oil becomes trapped in porous rock formations by cap rocks, such as salt deposits, providing an impervious cover (Tissot and Welte, 1978).

Diffuse and point sources of petroleum oil contribute to the ocean's hydrocarbon loadings. Discharges from vessels and operational discharges are restricted to areas 50 nautical miles offshore but pose environmental risk when dense sea traffic is near sensitive areas. Likewise volatile hydrocarbons from two stroke vessels, pose a threat as they are often concentrated near the coast. Diffuse sources from land runoff and gross atmospheric deposition are among the larger contributors to hydrocarbons in the ocean (NRC, 2003). Naturally occurring oil seeps also contribute considerably to the hydrocarbons in the ocean. The oil from the seeps is often heavily biodegraded by a unique few species of benthic animals using the hydrocarbons as a source of metabolic energy. These microorganisms are however limited to areas adjacent to seeps where chronic exposure causes some microorganisms to adapt, making them capable of metabolising oil (Wood Hole Oceanographic Institution, 2015). High volume inputs of oil and refined hydrocarbon products into the world's oceans in areas lacking natural defences however make many coastlines vulnerable. Moreover natural oil seeps are significant contributors to the PAH budget, enriching the waters with dissolved PAH and causing net volatilisation to the unsaturated atmosphere (NRC, 2003).

In addition to the naturally occurring seepage of oil from below the seafloor to the water column above; during extraction, transportation, loading/unloading and consumption of oil, spills are a frequent occurrence (ITOPF, 2015). Although there has been a decline in major oil spills and total volume of oil spilt over the last decade; thicker, viscous, more persistent fuel oils (similar in nature to crude) carried in container ships and bulk carriers (such as those spilt from the *Rena)* are now more frequently observed (Andrade, K., Buckley, H.L., Rubin, L.K., Shill, K. and Mulvihill, M.J., 2012; Lewis, 2002). From 2009 to 2014, spills greater than 7 tonnes due to oil tankers accidents more than halved with corresponding lower volumes spilt; while cargo tankers spills increased due to the increased seabourne trade (Rogowska and Namieśnik, 2010; ITOPF, 2015) albeit with smaller volumes of oil spilt (Andrade et al., 2012). Heavy fuel oils, produced through blending lower viscosity distillates with heavier residues (from distillation or cracking) are increasingly consumed for sea transportation. Of the 140 million tonnes of marine bunker fuel consumed annually, most is heavy fuel oil (Lewis, 2002).

Three major types of hydrocarbons are generally found in the environment; petrogenic, i.e. crude oil and its refined products; biogenic, i.e. hydrocarbons generated by biological processes or in the early stages of diagenesis in marine sediments; and pyrogenic, i.e. compounds generated in combustion processes (Stogiannidis and Laane, 2015).

Crude oil is the naturally occurring liquid form of petroleum. Crude oil contains both organic compounds (hydrocarbons) of various molecular weights and inorganic compounds (metals and salts - NaCl, $CaCl_2$) (NRC, 2003), often concentrated in the heavier fractions (Barth, 2002). There are between 100,000 and 1,000,000 types of hydrocarbons present in crude oil, constituting up to 97 % of the total oil (NRC, 2003).

The elemental composition of crude oil is relatively comparable throughout the world though the exact molecular composition varies considerably with the source of the oil. Typical ranges of crude oil composition are given in Table 4.1.

Crude oils are usually complex mixtures of hydrocarbons. The unique properties of individual compositions of oil mean that their behaviour in oceans and on coasts is distinctive, having different effects on marine life and ecosystems (NRC, 2003). Classification of oil hydrocarbon compounds is based on the structure of the hydrocarbons molecules present.

Table 4.1: Crude oil composition by relative weight (Adapted from Hyne, 2001).

Chemical element	**Percentage weight (%)**
Carbon (C)	83 – 87
Hydrogen (H)	10 – 14
Sulphur (S)	0.05 – 6
Nitrogen (N)	0.1 – 2
Oxygen (O)	0.05 – 1.5
Metals	

Nickel (Ni)	trace
Vanadium (V)	trace
Chromium (Cr)	trace
Mineral salts	0 – 0.1

The *saturate* group of hydrocarbons includes the aliphatic single bond *n*-alkanes or paraffins. These stable, non-reactive compounds, have the general formula C_nH_{2n+2}, starting with the simplest form; methane gas (CH_4) (Figure 4.1), possessing one carbon atom; shifting into liquid states when between 5 and 19 carbon atoms are present and solid state heavier waxes with carbon atoms in excess of 20 (Society of Petroleum Engineers, 2015b; Occupational Safety & Health Administration, n.d.). The largest constituent of crude oil, alkanes include the rarer, higher octane, branched (iso) *i*-alkanes (Figure 5.1), found in the heavier fractions of crude oil, and the no-charge alkyl group including ethyl CH_3CH_2 (Et) and propyl, $CH_3CH_2CH_2$ (Packer and Scott, n.d.). The light end fraction (C_{6-}) of petroleum includes all pure hydrocarbon components and hydrogen sulfide (H_2S), nitrogen (N_2) and carbon dioxide (CO_2); the heavy end (C_{6+}) includes components with carbon numbers of 6 or more (Society of Petroleum Engineers, 2015a).

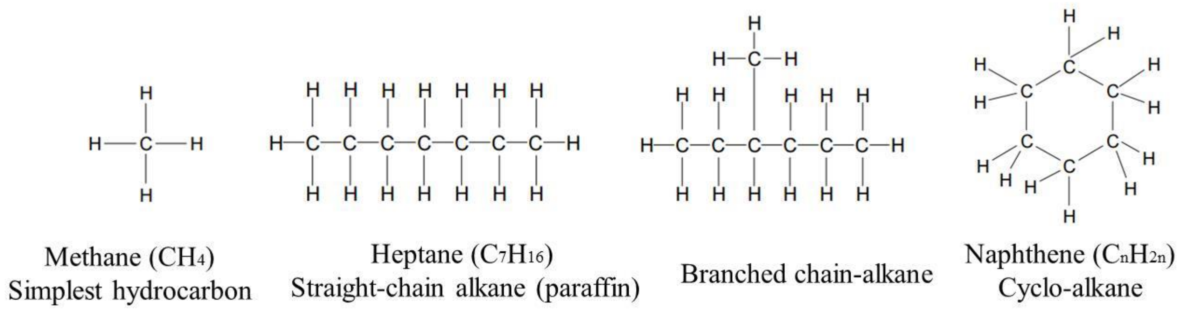

Figure 4.1: Examples of molecular structure of alkanes and cycloalkanes present in crude oil. Figure adapted from Barth (2002).

Waxes are high molecular weight saturates, having between 18 and 65 carbon molecules (Society of Petroleum Engineers, 2015a). They are solid (in crystal form) when oils are below their pour point (Scholz et al., 1999) and they dictate the pour point (the lowest temperature at which oil will flow) of oils; higher concentrations of wax result in higher pour points. Waxes also affect evaporation, dispersion and promote emulsification (Jokuty, Whiticar, Wang, Fingas, Lambert, Fieldhouse and Mullin (n.d). Two distinct forms of wax exist; microcrystalline waxes crystallize as small needle structures, with melting points greater than 50° C and are iso-alkanes and cycloalkanes. Paraffin waxes are normal alkanes with macrocrystalline structures (large flat plates) with melting points above 20°C (Society of Petroleum Engineers, 2015a).

Naphthenes or cycloparaffins (Figure 4.1), the ring bonded, high molecular weight compounds such as cyclohexane, are also saturated hydrocarbons with the formula C_nH_{2n+2} (Penn State University Information Technology Services, 2010). Monocycloparaffins (single ring naphthenes) dominate, with dicycloparaffins (two-ring naphthenes) in the heavier ends of naphtha (Occupational Safety & Health Administration, n.d.). Proportionally, naphthenes are the second largest constituent of crude oil (Society of Petroleum Engineers, 2015b), are liquid under standard conditions and are relatively stable (International Human Resources Development Corporation, n.d).

Double and triple carbon bonded, unsaturated hydrocarbons; (cyclo)alkenes or olefins such as ethylene; diolefins such as 1,2-butadiene and isoprene; aliphatic alkynes such as acetylene are produced during refinement, are highly reactive and are generally only present in crude oil in small amounts (NRC, 2003).

Aromatic compounds constitute a large percentage (1-20%) of the hydrocarbons present in crude oil and pose severe health effects due to high toxicity and produce the serious environmental impacts (NRC, 2003). Aromatic compounds are based on the the basic benzene ring structure of C_6H_6 with conjugated double bonds.

Monoaromatic (single ring compounds) are the most volatile. Specified as Volatile Organic Compounds (VOCs) this group includes benzene and the alkyl group (with one or more alkyl, CH_3, attached to the ring structure through substitution of alkane for hydrogen); toluene, ethylbenzene, and xylene collectively named the BTEX group (NRC, 2003). Under normal conditions solid or liquid states exist (International Human Resources Development Corporation, n.d.); with concentrations of 1,000 in lighter oils to 10,000 mg/kg present in heavier crude oil; toluene being of the highest proportion (NRC, 2003). The solubility and volatility of the BTEX group (Figure 4.2) make them the most mobile compounds present in oil and as they are carcinogenic and neurotoxic, they are priority pollutants (Boyd, Kucklick, Scholz, Walker, Pond and Bostrom, 2001).

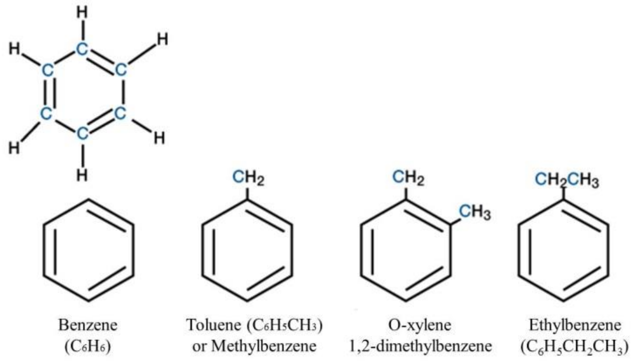

Figure 4.2: Molecular structure of the BTEX compounds. Figure adapted from International Human Resources Development Corporation IPIMS (n.d.).

Polyaromatic Hydrocarbons, PAH or polynuclear aromatic hydrocarbons (PNAs) are those aromatics containing more than 1 benzene ring (Figure 4.3). Concentrations in crude oils are between 0.2 to > 7 % (NRC, 2003). They are persistent due to being notably stable and pose the most serious environmental risk effects (NRC, 2003) and include:

- Naphthalene ($C_{10}H_8$) – 2 rings
- Anthracene ($C_{14}H_{10}$) – 3 rings
- Pyrene ($C_{16}H_{10}$) – 4 rings

One – three ring aromatics and heterocyclic aromatics make up 90% of aromatics present. Four – six ring aromatics are known mammalian carcinogens but are usually in trace amounts in crude oil (NRC, 2003; Penn State University Information Technology Services, 2010). PAH’s include aromatic compounds exhibiting elemental substitution through alkyl, methyl and ethyl for carbon, which are generally more abundant than the parent components (NRC, 2003). Larger aromatics are insoluble and don’t evaporate readily.

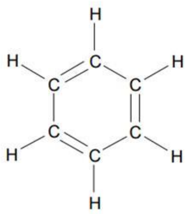

Benzene (C_6H_1)
Simplest aromatic
hydrcarbon

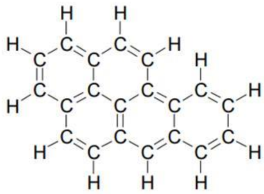

Benzopyrene ($C_{20}H_{12}$)
Polycyclic aromatic
hydrocarbon (PAH)

Figure 4.3: Examples of molecular structure of aromatic hydrocarbons present in crude oil. Figure adapted from Barth (2002).

Large polar compounds, asphaltenes, gain polarity from bonding with sulphur, nitrogen, or oxygen elements (NRC, 2003). These non-volatile, aromatic, polycyclic compounds exist in a colloidal suspension in crude oil, are insoluble in n-alkanes such as n-heptane or n-pentane yet soluble in benzene or toluene and significantly affect oil behaviour by stabilising water-in-oil-emulsions (especially in solid state) (Spiecker and Kilpatrick, 2004; Fingas, 2011). Asphaltenes have molecular weights of between 500 and 10,000 with carbon numbers greater than 30 (Clayton, Payne and Farlow, 1993).

The smallest polar compounds, resins, have molecular weights between 800 and 1,500, are soluble in oil and are typically responsible for the adhesion of oil due to strong adsorption tendencies toward surface active material (Clayton et al., 1993; Fingas, 2011; Society of Petroleum Engineers, 2014).

Heteroatoms are contained within the alkyl and alicyclic systems in the condensed aromatic nuclei of both the asphaltenes and the resins (Clayton et al, 1993). Both groups do not appreciably evaporate, disperse, or degrade, and both groups stabilise water-in-oil emulsions when they are present in higher quantities (Fingas and Fieldhouse, 2003). These heteroatom compounds include:

- Dibenzylthiophene (2 benzene rings separated by 1 sulphur atom).
- Carbazole (2 benzene rings separated by 1 nitrogen atom) – neutral.
- Quinoline (2 benzene rings with 1 nitrogen atom on 1 ring) – basic.
- Carboxylic (OH-C=O bonded to a benzene ring).

- Phenolic (OH bonded to a benzene ring).

Metal compounds, porphyrins, containing nickel, vanadium or chromium and also impurities from other trace elements including iron, aluminium, copper, sodium, calcium are also associated with asphaltenes and aid in the stabilisation of emulsions (NRC, 2003; Scholz et al., 1999).

4.2 CRUDE OIL CHARACTERISTICS

Crude oils are usually complex mixtures of hydrocarbons and can be characterised by the proportion of paraffins-naphthenes-aromatics present along with the geological region of origin (PNAS) (Figure 4.2). Most oils are paraffinic, paraffinic-naphthenic or aromatic-intermediate. Because of the differences in composition, correlations developed from regional samples may not be accurate for oils of other regions (Society of Petroleum Engineers, 2015b).

Table 4.2: Hydrocarbon composition by average weight of constituents and general characteristics of constituents. Adapted from Hyne (2001), Venkata Ramana (2010) and Jokuty et al. (n.d.).

	Weight percent	**Percent Range**	**Characteristics**
Paraffins	30	15 - 60	waxy, less asphaltic, low sulphur, high pour point, small saturate dispersable waxes, anomalous weathering
Naphthenes	49	30 - 60	less wax, less asphaltic, low pour point
Aromatics	15	3 – 30	high sulphur, small aromatic, volatile and soluble
Asphaltics	6	remainder	high sulphur and nitrogen, don’t weather, stabilise water-oil emulsions

The properties of oil viscosity, density or specific gravity, pour point, volatility (distillation characteristics), vapour pressure and solubility are used to determine the behaviour of spilled oil and therefore the effects of spilled oil (ITOPF, 2011a).

These variables are a function of the chemical composition of the oil and will dictate oil persistence.

Often densities of oil are used to determine whether oils will float and also as a proxy for the rate of weathering of spilled oil (NRC, 2003). Although temperature dependent, the density of most oils ranges from 0.7 to 0.99 g/F (at 15° C) even after weathering and the density of seawater is 1.03 g/cm^3 (at 15° C), therefore most oils float on water (Fingas, 2011; NRC, 2003). Exceptions are Bunker C oils, which have been known to sink (Fingas, 2011). Most light oils are easily degraded though microbial action and lost through evaporation, leaving heavier fractions, thus increasing density over time. Specific gravity or relative density, the ratio of the mass of a substance to the mass of freshwater at corresponding temperatures, is commonly used to classify oil 'weights'. Values above 1 correspond to oils that may sink or become submerged due to neutral buoyancy (Scholz et al., 1999).

Viscosity dictates the rate of oil spread and the depth of penetration into the substrate (Penn State University Information Technology Services, 2010). It is a function of the weight of the components present (NRC, 2003). Higher viscosity is associated with heavier fractions such as asphaltenes and often results in tar balls and thicker deposits which may remain for decades on beaches, as weathering is slow (Scholz et al., 1999). Viscosity is inversely proportional to temperature with variation due to individual compositions (ITOPF, 2011a). Weathering increases viscosity (Scholz et al., 1999).

Viscosity, the resistance to flow is usually measured as kinematic viscosity @ 100 ^{o}F in centistokes (cSt = mm^{2}s-1) for Newtonian flow (independent of rate of shear) but may also be calculated by the dynamic viscosity divided by the density (dynamic viscosity being the shear stress divided by the shear rate) (Real Services, n.d.). A higher specific gravity will have a higher viscosity. Viscosity will dictate the type of mechanical equipment that is used during spill clean-up (Rowson, 2014b).

As a rule, the viscosity, the carbon chain length and the sulphur content of fuel oils increase as the oil classification number increases. Heating of the heaviest oils is required for them to flow. The flash point, the temperature at which the vapours ignite, and the pour point, the lowest temperature at which oil will flow, also increase with classification number (Scholz et al., 1999). Flash points are also higher for weathered oils as the lighter fractions have evaporated. Viscosity expands pour point along with asphaltenes, wax concentration and the thermal history of residual fuel oil (ITOPF, 2011a; Jokuty et al., n.d). Separation of waxes and asphaltenes into crystalline structures occurs at cloud point, slowing fluid flow, until at pour point oil the oil becomes a semi-solid (ITOPF, 2011a). The waxes in diesel have the potential to solidify in lower temperatures. Low pour point is associated with aromatic content while the paraffinic composition of high pour point oils is related to higher asphaltic concentrations and more nitrogen (Khalaf, 2008-2009). Crude oils pour points are between 125° and -75°F (52°and -60°C) (Hyne, 2001).

Solubility of oil in water is generally very low, < 100 parts per million (ppm) however the toxicity of the water-soluble fractions of oil are often high causing harm to marine life (NRC, 2003). The water-soluble fraction of oil is controlled by the temperature and weathering conditions and is expressed as the cumulative concentration of the individually dissolved components (Jokuty et al., n.d.). Increasing molecular weight of oil components and alkyl substituents decreases aqueous solubilities; in order of descending solubility: aromatics, cycloalkanes, isoalkanes and n-alkanes (McAuliffe, 1966 and Tissot and Welte, 1984 as cited in The American Petroleum Institute Petroleum HPV Testing Group, 2011). Aqueous concentrations are dictated by the amounts and ratio of aqueous and petroleum phases, the partition coefficient between phases and the maximum water solubility of each constituent. In saltwater, aqueous concentrations ranged from 7.75 to 25.5 mg/L for 12 crude oils (The American Petroleum Institute Petroleum HPV Testing Group, 2011).

Distillation characteristics are an indication of the volatility of oil components and are expressed as the relative amount of oil that distils within given temperature ranges (ITOPF, 2011a). Even though temperatures range from -1°C to over 720°C

(30 – 1328 °F) at 1013 Pa, some asphaltenic, waxy or bituminous residues will remain (ITOPH, 2011a; The American Petroleum Institute Petroleum HPV Testing Group, 2011).

Vapour pressure is determined by the kinetic energy of the molecules within a liquid, the liquid's volatility or ability to vaporise and is the pressure that a vapour exerts on it' surroundings (Ornitz and Champ, 2002). Vapour pressure is also an indirect measurement of evaporation rates for volatile petroleum products. Evaporation occurs above 3 kPa (23 mmHg) vapour pressure; above 100 kPa (760 mmHg) gaseous states dominate (ITOPF, 2011a). As vapour pressure is determined by chemical structure, molecular weight and temperature (Ornitz and Champ, 2002), it alters with weathering state (Fingas, 2013).

4.3 MARINE TAR RESIDUES

Occurring worldwide from both anthropogenic (> 50%) and natural oil releases, marine tar residues are the result of weathering, sedimentation and other processes acting on heavy crude oils in the marine environment (Warnock, Hagen and Passeri, 2015). Reductions in operational discharges of oil (deliberate, routine releases of oil and tar from ballast tanks and from the washing out of tanker bilges) since the MARPOL 73/78 International Convention have decreased the incidence of oil pollution in the marine environment (NAS 2003 as cited in Warnock, 2015) however sizable oil spills such as the DWH and the Gulf War oil spill have resulted in significant amounts of pelagic and benthic tar residues.

Tar balls, persistent oil/sediment aggregates, black and spherical, are usually between a few millimeters to tens of centimeters, which can be transported over hundreds of square kilometers rapidly (Goodman, 2003; Warnock, 2015). Although not considered a serious health hazard to humans, they jeopardise the aesthetics amenity beaches and if ingested by marine animals they pose a serious health threat (Goodman, 2003). Tar balls are difficult to remove from the environment and require specialised equipment and manual labour. Their physical distribution spans from one to hundreds per square metre. The density of tar balls is used by shoreline clean-up assessment teams (SCAT) to determine the impact of a marine oil spill (Goodman, 2003).

Formation of tar balls is poorly understood (Goodman, 2003). Theories pertaining to formation include the; Lump Theory - Tar balls are fragments or lumps of weathered oil with a semi-solid consistency; Sand Theory - sediment sand and oil adhere together forming lumps or tar balls with uniform grain structure with small pieces of debris.; Oxidizing Theory - partial oxidation of thick slick fragments creates tar balls which can have a soft gooey centres with consolidated, encrusted outer layers; Glob Theory - large droplets resurface and reform as surface slicks and tar balls (Goodman, 2003).; Flocculation Theory - flocculation causes tar ball formation (Omotoso et al., 2002); Emulsion theory – tar balls are the final stage of water-in-emulsion (Goodman, 2003).

In the flocculation theory, large globules of oil and clay fines form, which gradually decrease in size due to collisions to uniform particle sizes of < 1 mm. The clay fines prevent the globules from adhering. These particles have a similar composition to tar balls found in nature, but are much smaller in size. While this process is consistent with the laboratory observations, there is no data to support this formation mechanism in the open ocean situation (Omotoso et al., 2002).

According to Warnock et al. (2015) the best explanation for the presence of pelagic tar residues is surface-weathering. Weathered, heavy, viscous water-in-oil-emulsion breaks apart, forming pelagic tar balls or patties. With increased specific gravity (*SG*) (through weathering, barnacles and isopods colonisation, sediment accumulation and temperature shifts) these tar balls may become benthic. The adherence of sediment/particulate matter to tar balls/tar lumps renders the hard outer layer even more resistant to turbulent energy. Evaporation rates for tar balls are unknown as simulation of the resistant outer surface of tar balls has been unsuccessful; the energy required to degrade these tar balls by physical mechanisms is therefore also undetermined. With increased temperature, time and available sediment, tar balls are more likely to become hardened (Office of Response and Restoration (NOAA, 2015). With temperature increases it is possible for these tar balls to reliquify (Scholz et al., 1999) and droplets have been observed to reform tar balls and mats (Fingas, 2011). During the *Prestige* oil spill, dense fragments of the 60,000 tonnes of emulsified oil, sank off the shore of Costa de Morte, leaving tar balls of 1 - 20 cm in diameter with densities of nearly 300 kg/km^2 (Rogowska and J. Namiesnik, 2010).

Other than surface-weathering, sedimentation of eroded oiled sands and entrainment of sediment and shell particles and aggregates formed by the sinking of heavy oils also produce tar balls (Michel et al., 1993 as cited in Warnock et al., 2015). Large agglomerations (tar mats or submerged oil mats, SOMs) of oil, shell and sediment, rest in depressions on the sea floor in nearshore, intertidal and subtidal zones as these high energy environments readily entrain sediment within the oil (OSAT, 2010 and OSAT, 2011 as cited in Warnock et al., 2015; OSAT, 2013; Wang and Roberts, 2013); a kilogram of suspended fine particles can effectively adsorb 120-300 mg of petroleum hydrocarbons (Neff, 1990 as cited in Scholz, 1999). The increased *SG* of oil, with as little as 2 % sediment, promotes sinking. More fragile than directly weathered tar residues, tar balls /patties break off these agglomerations and wash ashore (Michel et al., 1993 as cited in Warnock et al., 2015). These tar balls and patties were prevalent after the DWH spill along with high sand content tar balls formed from direct erosion of oiled sand and were collectively referred to as surface residual balls (SRBs) (OSAT, 2010 and OSAT, 2011 as cited in Warnock et al., 2015; OSAT, 2013; Wang and Roberts, 2013). Sedimentation of subsurface oil from natural seeps occurs as the result of separation of heavy components which are deposited in troughs on the sea floor.

Temporal envelopes for tar ball formation are unknown but reports of 2 days to 2 months have been recorded; in the laboratory, pelagic tar balls formed after 2 weeks under baseline conditions, others have taken months to form. MacGregor and McLean (1977 as cited in Warnock et al., 2015) determined that weathering is not solely responsible for the formation of tar balls and that emulsification processes increased *SG* however sedimentation and microbial activity were neglected in their experiments. 1-2 cm spherical tar balls formed around debris that act as nuclei after 5 days in an experiment by Heaton et al. (1980 as cited in Warnock et al., 2015) however no comparison with real tar balls were made. The aggregation of weathered oil flakes and resultant growth of tar balls was shown by Payne (1982 as cited in Warnock et al., 2015) after agitation. Synthetic tar balls from four crude oils were successfully created by Savage and Ward (1984).

The increased viscosity of water-in-oil emulsion stimulates the formation of lumps, patties, tar mats and tar balls from the heavy components of oil (Scholz et al., 1999). High densities and viscosities and the presence of waxes, resins and asphaltenes promote the formation of emulsion which with agitation and photo-oxidation will form petroleum particulate residues (tar balls) (Goodman, 2003). Stable mousses generally involve 65–85 % water incorporation (Fingas and Fieldhouse 2009), and the size of the water droplets in the most stable emulsions is typically less than 10 μm in diameter (Payne 1982).

The physical appearance and distribution of oil is also defined by the morphodynamic variability of the beach system (Bernabeu et al, 2006). During the 2004 research of the *Prestige* oil spill, tar balls of centimetre size (CTB), tar balls of millimetre size (MTB) and iridescences on the surface of the sediment (oil in water emulsion) all occurred as surface contaminations. Sub surface oil morphology was equivalent but continuous layers of oil coatings on sediment grains were also present. These coatings, microns thick and discontinuous, colour the sand a distinctive grey tone but do not alter the structure of the sediment (Bernabeu et al., 2006; Fernández-Fernández et al., 2011; Bernabeu et al., 2010; Fernández-Fernández et al., 2014). Oil coatings were largely attracted to the flat, angular, bioclastic grains present on the Galician coast thus physical forms of oil are also determined by the mineralogical composition of the sediment, in contrast to the findings of Delvigne (2002). Oil in water emulsion, identified through higher than normal mineral concentrations of vanadium (V), nickel (Ni) and sulphur (S), was found to be continuous with depth (Bernabeu et al, 2006).

Persistent transport on the frequently oscillating O Rostro beach effectively abrades the tar balls to mean grain size (millimeters), allowing sedimentation (selective transportation and deposition) of oil particles, predominantly onto bioclastic sediment (Bernabeu et al., 2006). As well as moderating biodegradation rates, lengthy burial at Nemiña Beach reduced direct abrasion and dispersion of residual oil, nevertheless, wave climate indirectly affected dissolution and fragmentation rates, through groundwater fluctuation (Bernabeu et al., 2006).

A flow of water due to groundwater oscillation, results in an interchange of filtrated seawater moving shoreward and exfiltrated freshwater moving seaward. Diffusion of oil through the sediment column is permitted as the resettling of oil grains in response to groundwater movement and promotes disintegration of entrenched oil, from tar ball size to particle size (Bernabeu et al., 2006). Direct dissolution of oil by water to form stable oil in water emulsions, pumping and diffusion of hydrocarbons laterally along the sedimentary column also occurs as the direct result of water flowing through the sediment. Layers of oil coatings up to metres in thickness (Bernabeu et al., 2009; Bernabeu et al, 2010; Fernández-Fernández et al., 2011) at Nemiña Beach were treated as indicative of this phenomenon.
Stable emulsions form by direct contact seawater and oil surface of tar ball. Releasing particles mainly in emulsion; the volume and speed of formation controlled by confinement.

In an attempt to quantify the temporal scale of oil degradation at depth, microcosm experiments with controlled degradation factors; flow regimes, organic matter content, salinity and recirculation of sea water were carried out over 130 days using bioclastic-siliclastic sediment from Nemiña Beach (Bernabeu et al, 2010). To emulate burial, light (a source of photo-oxidation) was eliminated. Spectrophotometric colour determinations of tar balls, areas 5 cm to the left and right of the tar balls and each centimetre vertically, were produced, in addition to photographic reporting. After 20 days grey “halos” were visible in static water and after 34 days were well defined and increasing in size at a steady rate of 6.45 cm/year. With constant water flow however the halo did not form until day 46 and did not appear in the freshwater treatment at all. “Halo” appearance was considered to be proportional to flow rate (expansion rates between of 8.4 cm/year and 14.1 cm/year for faster and slower flow rates respectively) except in the highest flow rate which had the earliest appearance of a grey “halo”. Likewise expansion increased laterally with flow velocity (Bernabeu et al, 2010). Physical degradation of oil by these mechanisms is therefore limited to sheltered and low energy environments due to temporal requirements (Bernabeu, 2010).

Residual oil particles were found in filtered outflowing sea water, with size being dependent on the effective porosity of the sediment. As the fastest flow was also recirculated, millimetre scale oil particles were additionally recirculated, contributing to the concentration of oil coatings (Bernabeu et al., 2010). The reduction in emulsion formation and therefore degradation rates due to reduced salinity has implications for beaches with freshwater inputs and brackish environments (Bernabeu et al., 2010).

The experiments of Bernabeu et al. (2010) demonstrated a sequence of degradation that occur over weeks and months; emulsification (oil in water), diffusion of oil particles away from tar balls, advection of particles with water flow away from the microcosm causing particles to expand and retention through adsorption of oil onto sediment grains (grey coating). Relative amounts of advected and adsorbed oil are likely dependent on the oil particle concentrations and are only possible if oil particles are smaller than the intergranular porosity (Bernabeu et al., 2010).

In contrast with other studies which infer low degradation rates of buried oil due to limited abrasion and dispersion from mechanical energy (Hayes et al., 1993), limited photo-oxidation at depth and oxygen and nutrient scarcity especially in low energy environments (Venosa and Zhu, 2003); Bernabeu et al. (2006) and González et al. (2010) substantiated the rapid degradation of oil at depth through physicochemical factors. Biomarkers, sterane and triterpane, also indicated biodegradation within the grey layers of sand during *Prestige* spill investigations, as water flows provide microorganisms, oxygen and nutrients to the sand column (Bernabeu et al., 2009). PAH indices also indicated weathering and degradation at 3 m depths while PAH and aliphatic hydrocarbons levels indicative of oil in emulsion (Bernabeu et al., 2009) were distributed homogeneously along the sedimentary column (Bernabeu et al., 2006).

Further investigation by Fernández-Fernández et al. (2014) into the sequence of degradation for buried oil focused on compositional factors. It was established that carbonate concentrations of bioclastic sediments with altered, rough surfaces may enhance the halo development of oil coatings at depth, staining the grains (10-15 µm thick) and retaining the oil within the sediment column. Conversely siliciclastic sediments generate oil microparticles generally, enabling rapid permeation and dispersion. Concentrated oil microparticles rich in TPH appeared as a black layer on the surface of the sediment away from the buried tar balls in siliclastic microcosm experiments. The containment of oil coated onto bioclastic sediments has consequences for bioremediation; possibly forming a constricted environment in which to employ bioremediation measures (Fernández-Fernández et al, 2014). Expansion rates of 4.5 cm/year and 18 cm/year were established with similar microbial numbers. The results indicate that the mineralogical composition is important for the physical appearance of the oil (tar-balls or oil coatings).

It has been deduced from field studies that tar ball distribution is dictated by the oil properties, proximity to transport pathways (where discharge rates are highest) and natural oil seeps, winds, currents and circulation patterns (with seasonal and temporal variation) and geology and geomorphology of the coast, whereas surface floating oil is mostly affected by winds (Warnock et al., 2015). Peak tar concentrations are associated with subtropical waters and windward beaches. Convergent mesoscale and small-scale eddies surface circulation features (cyclonic eddies result in surface convergence, whereas anticyclonic eddies produce surface divergence). Longshore currents have been shown to transport tar balls into estuaries or other gap in cliffs where they were weathered and dispersed by wind or became buried within the sediment (Golik, 1982 as cited in Warnock et al., 2015). Wave refraction, offshore overtopping and wave breaking processes were also observed to affect rates of tar ball deposition along the Mediterranean coast (Tsouk et al., 1985 as cited in Warnock, 2015). High concentrations of tar balls have been recorded mainly windward of sand cusps and along the high-tide water lines (Badawy et al., 1993 as cited in Warnock et al., 2015). During storms and spring tides, overtopping causes removal of tar balls from the littoral zone and deposition in the supralittoral zone (Golik, 1982 as cited in Warnock et al., 2015;

Bernabeu et al., 2006; Wang and Roberts, 2013). Depositional cycles can also lead to permanent stranding (Bernabeu et al., 2006).

As well as spatial variability, distributions of residues have been found to be temporally variable. Hydrodynamic factors and meteorological conditions change consistently affecting the distribution of residues; oiling of beaches can occur in very short-times (hours) and can last for months (Gundlach et al, 1981). Coles and Riyami (1996 as cited in Warnock et al., 2015) observed a two week delay in peak tar concentrations after a storm event. Pelagic tar balls were still present eight months after an oil spill where slack currents dominated (Eagle et al., 1979 as cited in Warnock et al., 2015). Seasonal monsoons were correlated with high concentrations of tar residues in the Indian Ocean (Sen Gupta, Fondekar and Alagarsamy, 1993 as cited in Warnock et al., 2015). Del Sontro et al. (2007 as cited in Warnock et al., 2015) found that during winter, quantities of oil accumulation were an order of magnitude less than in summer, due to seasonal trends in advection (in an onshore direction via wind and low swell heights) that maintained the oil slick. As transition seasons cause significant shifts in morphology, it is likely that movement of tar balls will occur at these times. Owens (2002) also reported higher values of tar residues in winter (1999/2000). Concentrations of tar balls are highly variable temporally. The spatial and temporal distribution of tar balls is dependent on previous deposition, sediment redistribution and tidal or wind-induced water levels; distribution of residues in the supratidal zone is also affected by aeolian processes (Owens, 2002).

Sandy beaches such as Ngarunui Beach are susceptible to the accumulation of pelagic tar balls. A SCAT observation program focused on stranded tar ball frequency after the *New Carissa* grounded in 1999 on the Pacific coast of North America (Owens, 2002). Using systematic beach surveys between March 1999 to April 2001 time-series plots were used to identify trends. Using GC/MS 48% of the tar balls were found not to have come from the *New Carissa* which confounded clean-up efforts. 48 barrels (2000 gal) of oil were released on the high energy coast. 8.9 million tar balls (< 0.25 inches to two inches in diameter and with < 3.4 grams of oil) were estimated to have formed (Owens et al., 2000). Sediment cores oil penetrated to as much as 20 cm in cores, decreasing concentrations with depth. Oil that was buried deeply, biodegraded relatively slowly, due to the anoxic conditions. Wong et al. (2002) studied sediment contamination levels in a mangrove swamp after the spillage of 60,720 gallons of crude oil in Hong Kong. Wong et al. (2002) report average pelagic tar ball concentrations in the order of 0.03 mg/m2 at 25 N and 0.4 mg/m2 at 35 N, for the Northeast Pacific.

Marine tar residues have been described as tar balls, tar patties, tar cakes, oil sheets and oil stains by Wang and Roberts (2013). Tar patties are discreet accumulations of oil and sand, greater than 10 cm in diameter while tar balls are less than 10 cm. Continuous accumulations greater than 5 m in length or width, partially or completely submerged by water, are defined as tar sheets. Tar cakes are tar patties thicker than three cm while staining occurs due to oil coating sediment grains in a thin veneer. Staining was observed after the DWH spill by Wang and Roberts as white quartz sand was coloured brown. Bernabeu, Rey, Lago and Vilas (2010) generated staining in the laboratory.

As well as tar balls, oil may become stranded in intertidal zones as large visible accumulations, submerged tar mats (SOMs) (OSAT-1 2010), when oil type, persistency, currents, tidal position, winds, wave conditions and proximity to the shoreline are favourable (Parham and Gundlach, 2015). The blowout and subsequent 87 day leak from the Deepwater Horizon platform on April the 20th, 2010, was one of the worst oil spills to date, with 648,000 tons (using average density of 0.832 g/cm) spilt into the Gulf of Mexico (Parham and Gundlach, 2015). During the active oiling period large amounts of floating mousse patties (emulsified oil) became stranded on 1,773 km of shoreline, mostly in the oiling phase, during June and July, 2010. Both individual mousse patties and continuous sheets of coalescences were observed. As oil settled, sand adhered to it, increasing it’s density leading to burial and breaking up of the patties to oil/sand aggregates. Heavy build ups resulted in subtidal mats consisting of 9.4 to 10.7 % oil and 70 to 90 % sand, plant material and shell hash which sank into depressions in the surf zone (Mulabagal et al., 2013 as cited in Warnock, 2015; Parham and Gundlach, 2015). These SOMs remained relatively unweathered even after 2 years. Due to the high energy environment of the surf zone where the SOMs tended to be found, it was difficult to discover and remove them (OSAT-2 2011) so oil remained in the subtidal and intertidal regions following the initial clean-up, leading to frequent reoccurrences of tar ball deposition on the coasts (OSAT-2 2011; OSAT-3 2013). Chronic re-oiling occurred from SOMs breaking apart under hydrodynamic forces, lead to the repeated transport of SRBs on shore, particularly after heavy storm events (Hayworth et al. 2011; Clement et al. 2012). Tar balls were described as fragile, soft, sticky and brownish indicative of residues that formed due to sinking and sedimentation not surface weathering. BP's active DWH clean-up operations were discontinued in June 2013 in Florida, Alabama, Mississippi, and Louisiana, citing "the extraordinary progress that Coast Guard and BP had made in restoring the Gulf of Mexico coastline to pre-spill conditions" (BP, 2013 as cited in Warnock, 2015). However, significant quantities of tar SOMs are still present in the Gulf region. A large, 40,000 lb SOM was discovered in later in 2013, south of New Orleans (Buskey 2013 as cited in Warnock, 2015) and the Coast Guard recovered 450 lb of tar over two weeks in Pensacola after cessation of active cleaning. There are still an unknown number of SOMs in the Gulf region however enough SOMs have been found to close fisheries in the Louisiana area (Louisiana Department of Wildlife and Fisheries 2013 as cited in Warnock, 2015).

During the 2010 Deep Water Horizon spill in the NE coast of the Gulf of Mexico, due to the massive economic cost to tourism and health concerns for the densely populated coast, aggressive mechanical clean up measures were undertaken as well as natural beach recovery. Eleven field investigations examined crosshore distributions of subsurface oil from trenches dug into the sediment and contaminant distribution patterns were documented. Wang and Roberts (2013) identified two new morphological forms of oil; tar cakes, "discreet accumulations of oil and sand mixture greater than 10 cm diameters" and tar patties, accretions of tar cakes (> 3 cm thick). It was noted that thicker accumulations of oil may have different effects for burrowing beach fauna.

An investigative study of the DWH spill tar residues, by Clement et al. (2012), observed that after storm events, there was a prevalence of tar balls (SRBs) in shell hash piles at the maximum high-tide water line and landward of the berm crest in the trough; controlled by hydrodynamic and morphological factors, including incident wave conditions. Parham and Gundlach (2015) and Wang and Roberts (2013) had similar findings. It is posited that the physical shape of the shell hash influences deposition and transport of tar balls.

Weathering processes became more evident with time. Oxidation of submerged subtidal oil was visible, lamination of surface patties and disaggregation of tar patties in the supratidal due to winds and scouring, heat and gravity occurred. Interior pockets developed in surficially buried patties due to oil capillary migration into sand pore spaces and tar patties were incorporated into algal mats in periodically flooded backshore swales. Some inner portions of aggregates were unweathered in the supratidal zone after a year (Parham and Gundlach, 2015).

Hydrodynamic properties of tar balls i.e. settling velocity, drag coefficient, entrainment velocity and break-down have only been examined minimally because often tar balls become buried or submerged and disappear from view (Iliffe and Knap, 1979 as cited in Warnock, 2015). Tracking of benthic tar balls in Bermuda showed that in 24 days tar balls move up to 40–50 m to the subtidal and offshore, in the direction of circular currents within the bay. Lower specific gravities and onshore winds resulted in greater distances. Golik (1982 as cited in Warnock et al., 2015) observed painted tar balls released in the swash zone for 5 days in calm conditions. The tar balls were transported up to 43 m alongshore.

The nearshore region is a high energy environment, requiring reconnaissance methods such as diver searching and autonomous underwater vehicles (AUVs). The difficulties in detecting and observing benthic tar balls or tar mats, as well as the common assumption that beached tar is the direct result of pelagic tar balls, have meant that transport mechanisms for benthic, beached and pelagic tar residues are not well understood. Chemistries and densities of tar balls were measured by Balkas et al. (1982 as cited in Warnock et al., 2015) in order to estimate the state of weathering. Both benthic and pelagic tar balls had similar density to sea water however. Iliffe and Knap (1979 as cited in Warnock, 2015) found that pelagic tar balls were lighter than beached and benthic tar balls, which had similar specific gravities. This allows the deposition of the lighter pelagic tar balls further into the supralittoral zone, where they may remain. Benthic tar balls were noted as irregularly shaped and flattened while pelagic tar balls are near spherical.

Residence times have been estimated at 6 -12 months based on the half-life of tars which are undoubtedly different from marine tars (Morris, 1971 as cited in Warnock, 2015); 1-4 months using a mass balance approach which is limited as input and stock quantities are unknown Sleeter and Butler (1982 as cited in Warnock, 2015); and 1-2 tidal cycles using visual inspections by Hartman and Hammond (1981 as cited in Warnock, 2015). Biodegradation and sedimentation have been found to be the primary means of removal of tar residues Albaiges and Cuberes (1980 as cited in Warnock, 2015) but rates are dependent on the source oil and climate variability i.e. warmer weather promotes faster biodegradation for specific microbes (Wang and Fingas, 1995). Growth profiles of microbes have been correlated with tar ball degradation (Itah and Essien, 2005 as cited in Warnock, 2015).

Grain size affects the ability of oil to percolate into beach sediment (Hayes and Michel, 2001). Gravel beaches have high porosity and permeability that allow deep penetration from the surface especially in the upper swash. Coarse-grained gravel beaches can form armours, though oil can penetrate the subsurface sediments below with slow natural removal rates. Oil may be removed readily (days to weeks) from rounded clast gravel beaches but remains for months to years in more angular clasted gravel sediments. Fine and medium grained sediments and bioclastic beaches allow deep penetration because of their wide gentle slopes, especially at the high intertidal where the water table is deeest. These environments typically recover quickly (Barth, 2002). Oil does not readily penetrate very fine grained, well packed sediments, such as muds unless infaunal burrows and vegetation are present resulting in better drainage characteristics (Edrick, 2007). Slow removal from these environments would be expected (Hayes). Penetration into vegetation root channels, animal burrows and desiccation cracks in the clay soils of depths of up to up to 60 cm have been reported by Zengel et al. (2001 as cited in Edrick, 2007). Depth of penetration is also dependent on oil properties, concentration and temperature. Small amounts of lighter oils within the active surf zone of erosional beaches or impermeable bedrock are less likely to persist (Owens, 2008).

Stranded oil penetrates the sediment, to below the depth of sediment reworking through large pore spaces and either adheres to the surface of the sediments or fills the voids. The coated surfaces of coarse-sediments or the surface of an oil layer may weather to form a hard crust that resists further attenuation and effectively seal the oil within that layer (Owens et al., 2008). Although bioavailability is reduced with formation of pavements, there can be deleterious impacts for habitats, especially if they are migratory routes or areas of larvae cycling (Barth, 2002). Tar mats (or cyanobacteria) mats reduce oxygen, slowing biodegradation (Barth, 2002). Especially on coarse grained shores, oil can persist for decades (with associated toxicity) until physically removed by storm or erosion events (Owens et al., 2008). Because this oil is relatively unweathered, release may have devastating effects for marine organisms (Edrick et al., 2007).

Once oil has penetrated the shoreline substrate it may become incorporated into the groundwater system of the beach. During the *Prestige* spill of 2002, it was observed that oil could penetrate past surface sediments. Tar balls were found in cores at depths of 3.75-m by Bernabeu et al. (2013). The degree to which oil is retained and/or transported within the sediment is dependent on; the depth of the water table, the depth of oil penetration, the porosity of the shoreline substrate and beach morphology, oil viscosity and wave conditions (Bernabeu et al., 2013; Edrick et al., 2007). Wave exposure and oil concentration become less important with time. When pore spaces are filled with oil above a confining impermeable layer such as bedrock, the water table, peat or fine sediments, the loading capacity of the beach is reached (Owens, 2008). High concentrations of oil are found just above the impermeable layer, above which, oil flows freely (Owens, 1978).

4.4 OIL BREAKUP

Early pouring experiments by Delvigne and Hulsen (1994) gave low dispersion coefficient values for high oil viscosities, while viscosities <1 cm^2/s had no affect (Khelifa et al., 2002. While large eddies diffuse oil, small scale eddies with large velocity gradients break up oil droplet and increase collision efficiency. In a study of the natural dispersion of oil, Delvigne and Sweeny (1988) Breaking-wave experiments at three different scales (to generate scaling factors), a small-scale wave flume (15 m long, 0.5 m wide, water depth of 0.43 m), a ten times larger 'Delta Flume' (200 m long, 5 m wide, water depth of 4.3 m) and a 4 m high, 0.3 m wide grid-stirred column were undertaken to examine oil droplet size distributions, entrainment rate (vertical dispersion of oil mass per unit surface area with time) and oil concentration profile. These are important parameters dictating horizontal diffusion, reduction of oil and sediment processes. Droplet size infers dispersion stability.

Delvigne and Sweeny (1988) found that the mean d_{50} and maximum d_{max} are a function of the oil's viscosity, dictated by oil type, weathering and temperature for Newtonian-type oil as given by equation (4-1);

$$d_{50}, d_{max} \sim {\nu_o}^{0.34(\pm 0.05)} \tag{4-1}$$

For highly turbulent conditions ($e \geq 100$ J/m^{3}s) and submerged oil, with limited breakup of rising droplets due to shear;

$$d_{50}, d_{max} \sim e^{-0.50(\pm 0.1)} \tag{4-2}$$

Droplet size was found to be independent of salinity and oil input location and dependent on the duration of turbulence and energy dissipation rate, e. At 5 minutes a steady-state droplet size distribution was reached, where physicochemical changes, soluble component dissolution, migration of specific oil components to the interface, and adsorption of compounds onto the oil droplets. This implies that a single wave will not produce a steady-state distribution. In the flume experiments, larger aggregations and droplets of oil resurfaced immediately, therefore d_{max} decreased with time. D_{max} is thus actually determined by the resurfacing parameters. Droplet size is known to be a function of interfacial tension (σ_{ow}) (Delvigne and Sweeny, 1988). Droplet size distributions were found to follow the of relationship;

$$N_u(d_o) \sim d_o^{-2.30(\pm 0.06)}$$

(4-3)

where d_o is droplet size and $N_u(d_o)$ is the number of droplets in a unit size interval, Δd around d_o, regardless of temperature, weathering state or oil layer thickness. Oil entrainment (Q (kg/m^2) is determined by the time after the passage of the breaking wave as large droplets resurface. To avoid distortion by resurfacing droplets, size classes < 200 µm were used to find the empirical relation;

$$Q \sim D_{ba}^{-2.300.57\ (\pm 0.06)}$$

(4-4)

valid for small and large scale experiments where D_{ba} is the dissipated energy per unit surface area (J/m^2). Stability of dispersed oil droplets is a function of intrusion depth, z_i, vertical diffusion coefficient in the ambient water, ε_z and rise velocity, *W*(do). Oil entrainment and droplet size distribution were found to be independent of oil layer thickness (h_o). Intrusion depth was found to be 1.15 to 1.85 times the breaking wave height.

Hinze (1955 as cited in Khelifa et al., 2002) postulated that the mechanism of droplet break-up could be described by the dimensionless Weber number (N_{we}) and Capillary number (N_{ca}):

$$N_{we} = \frac{\rho_c u^2 D}{\sigma}$$

(4-5)

and

$$N_{ca} = \frac{\mu_d}{\sqrt{\rho_d}\sigma D}$$

(4-6)

where u is the velocity difference in the flow over a distance of droplet diameter D, σ is the oil-water interfacial tension and ρ_c and ρ_d are the densities of the continuous and droplet phases. These ratios express the dynamic pressure viscous shear (external disturbing forces induced by flow) and internal resisting force due to the interfacial tension respectively. According to equation (4-7), when the Capillary number is very small, viscosity effects are negated and interfacial tension, density of the continuous phase and rate of dissipation of turbulent energy influence oil droplet size. Maximum size of droplets (D_{max}) is related to minimum value of N_{we}, defined as the critical Weber number $(N_{we})_{crit}$;

$$(N_{we})_{crit} = \frac{\rho_c u^2 D_{max}}{\sigma}$$

(4-7)

$(N_{we})_{crit}$ is related to N_{ca} by equation;

$$(N_{we})_{crit} = \chi(1 + \varphi(N_{ca}))$$

(4-8)

where χ and ϕ are two functions of turbulence intensity and viscosity of the continuous phase (external conditions); ϕ decreasing to zero with values of zero for N_{ca} goes to zero. Critical Weber $(N_{we})_{crit}$ number has been used to investigate maximum size of droplets under various flow conditions and to show variations of the critical velocity for droplet entrainment with oil viscosity from a boomed oil slick (Calabrese et al., 1986; Fraser & Wicks, 1995; Li & Garrett, 1998; van der Zande & van den Broek, 1998; Delvigne, 1991 as cited in Khelifa et al., 2002). A dimensionless relationship incorporating oil and continuous phase properties and the energy dissipation rate, ε due to turbulence is given by;

$$\frac{D}{\eta} = f\left(\frac{\mu_d}{\mu_c}, \frac{\rho_d}{\rho_c}, \frac{\sigma}{\mu_c v}\right)$$

(4-9)

where η and v are the length and velocity Kolmogorov microscales respectively (Hinze, 1975 as cited in Khelifa et al., 2002); the first two terms being the viscosity and density ratios, respectively. The effects of variables, η and v, were however not addressed in this study as the shaking energy was kept constant. A modified critical Weber number after Sleicher (1962);

$$(N_{we})_{crit} N_{\sigma}^{-0.5} = \chi(1 + \varphi(N_{ca}))$$

(4-10)

includes a dimensionless variable similar to Nσ (σ/(μc ν) to account for low viscosity effects. Density effects are limited by narrow ranges of variation.

Volume concentration of droplets and oil density determine stabilisation of OMA. The dimensionless mass concentration (the ratio of mass of oil stabilized by OMA to initial mass of oil introduced in the system) of oil droplets, W_o, when normalized with ARC (W_{ar}) is shown to correlate well with the viscosity ratio regardless of temperature. The correlation function;

$$\frac{W_0}{W_{ar}} = 0.3\mathrm{e}^{3.23\left(\frac{\mu_d}{\mu_c}\right)^{-0.22}} \tag{4-11}$$

estimates that OMA traps oils with high ARC more effectively for a given viscosity ratio in agreeance with many other authors (Menon and Wasan, 1986; Bragg and Owens, 1994; Owens et al., 1994; Bragg and Yang, 1995; Guyomarch et al., 1999; Owens, 1999 as cited in Khelifa et al., 2002). Mineral concentrations were not considered in this work even though they are fundamental to the process of OMA formation, nor were the effects of turbulent energy; at low rates of turbulent energy, viscosity controls the rate of OMA formation however with higher energies, after formation of droplets, chemistry determines the rate of OMA formation. Trends in number concentration of oil droplets with oil-water interfacial tension were not observed by Khelifa et al. (2002) however data was limited in this area and it was postured that droplet concentration decreases with oil-water interfacial tension.

Temperature effects could be seen in mean oil droplet size (mean size was greater at higher temperature). Although spherical droplets prevailed, elongate droplets were present; more at 20° C and less at 0° C.

Viscosity was however found by Khelifa et al. (2002) to have negligible effect on mean and maximum droplet size in contrast to the earlier study of Delvigne et al. (1987 as cited in Khelifa et al., 2002) and Delvigne and Sweeney (1988). Importantly Delvigne et al.'s (1987 and 1988) experiments excluded a mineral phase, a grid was used to generate turbulent energy and sampling methods may have allowed droplet coalescence. Van der Zande and van den Broek (1998 as cited in Khelifa et al., 2002) had similar findings; viscosity affected droplet size minimally and the authors maintained that the rapidity of the break-up mechanism in the orifice was responsible. Li and Garrett (1998 as cited in Khelifa et al., 2002) showed that the maximum size of droplets due to viscous shear is proportional to the ratio $(\mu_d/\mu_c)n$, where μ_d is the viscosity of the droplet, μ_c the viscosity of continuous phase and *n* equals to 3/8 if the size of the droplet is larger than half the Kolmogorov length (Hinze, 1975) and 1/8 otherwise. Guyomarch, (2002) also found the average droplet size to be a function of viscosity (except the Forties Blend) in experiments without a mineral phase.

4.5 OMA FORMATION

Primarily termed "clay-oil flocs" after a study by Lee et al. (1988 as cited in Lee, 2002) with specific reference to glacially derived phyllosilicates in association with large molecule and polymer mineral flocculations, oil- mineral-aggregates (OMA) can potentially incorporate a larger mineral fraction than 2 microns and minerals other than phyllosilicates and by definition include a distinct oil component (Stoffyn-Egli and Lee, 2002). The significance of these aggregates as a mechanism affecting the rate of natural cleansing of oil residues from shorelines was not recognised until after the 1989 *Exxon Valdez* spill in Prince William Sound, Alaska, by Bragg and Yang (1993 as cited in Stoffyn-Egli and Lee, 2002) however over the past three decades, significant research into the ecological significance of oil-particle interactions has been undertaken, including: the mechanisms for oil-particle interactions; the effects of oil-particle interaction on the persistence of oil in the environment; and the application of interaction mechanisms to oil spill countermeasures. OMA formation has now been identified as an important process that facilitates the natural removal of oil stranded in coastal sediments, particularly in low energy intertidal environments such as estuaries (Bragg and Owens, 1995).

Persistence of oil in the marine environment can be extended by the interactions of oil with sediment (Boehm et al., 2007; Lee, 2002). Through aggregations of dispersed oil droplets with suspended particulate matter (both inorganic and organic) and adsorption of hydrocarbons to the surface of mineral particles, spilled oil is physically transported from the sea water surface to the benthic environment where residence times are prolonged, decreasing degradation rates and increasing toxicity exposure for marine organisms (Muschenheim and Lee, 2002). Settling rates of fine and pollutant particles are increased with flocculation of fine particulate matter into larger aggregates (Muschenheim and Lee, 2002). Large quantities of oil and associated PAH compounds are transported in this way (Payne et al., 2003). PAH concentrations have been associated with both finer clay sizes and larger grains (Viñas et al., 2010; Wang, et al., 2001). As the free surface of natural waters incorporates fine sized particles (< 2 microns) that bind hydrophobic compounds there is a significant potential for oil sedimentation (Hargrave and Kranck, 1976 as cited in Lee, 2002). Sedimentation also occurs readily in localised regions along coastlines where higher suspended sediment loads occur (Payne, 2003). Inputs of sediment occur as a result of resuspension of bottom sediments, physical scouring of shorelines, aeolian transport and advective input from rivers, streams and glaciers (Payne et al., 2003).

OMA also increase oil dispersion by augmenting buoyancy and therefore duration of suspension, allowing currents to transport oil further (Lee, 2002). OMA also behaves as a surfactant, reducing the surface tension of the oil (and therefore the adhesion) and therefore mitigating coalescence into and sedimentation of larger flocs (Ajijolaiya et al., 2006). Oil therefore adheres less to shoreline sediment once flocculated (Bragg and Owens, 1995). Additionally, sedimentation through agglomeration enlarges the surface area to volume ratio, increasing the capacity of weathering process such as evaporation, biodegradation, photo-oxidation and dissolution (Stoffyn-Egli and Lee, 2002). The increased weathering of oil lowers the concentration of toxic components that can be taken up by marine biota. It has recently been noted that oil biodegradation may also be enhanced by OMA formation due to the flux of nutrient and oxygen to droplet surfaces (Ajijolaiya, Hill, Khelifa, Islam and Lee, 2006). UV radiation however has also been recently identified as causing increased PAH toxicity by a factor of 2 – 1000 through phototoxicity (Barron et al., 2003). The stranded oil on the exposed shoreline is also influenced by the formation of OMA, transporting oil to the littoral zone and beyond (Lunel et al., 1996; Wolfe et al., 1994; Ballschmiter et al., 1997 all cited in Muschenheim and Lee, 2002). This has been observed on a large range of shoreline types (Bragg & Owens, 1995).

Early estimates indicating that 30 g of sand was required to sediment 10 ml of oil (a sediment: oil ratio of approximately 3:1) were made by Chipman and Galtsoff (1949 as cited in Muschenheim and Lee, 2002) while sediment:oil ratios of 0.1- 1 were required for diatomaceous earth to effectively remove oil (Hartung & Klingler, 1967 as cited in Muschenheim and Lee, 2002). Estimates of nearly 35% particulate interaction were given by Davies (1994 as cited in Muschenheim and Lee, 2002) in high energy conditions during the *Braer* spill, with Total Petroleum Hydrocarbons (TPH) as high as 2000-10000 ppm in some places. Other estimates of natural removal of spilled oil by sedimentation include; 10-15 % from the mass balance equations of *Tsesis* spilt oil in the Baltic Sea due to turbulent resuspension of bottom sediments (Johansson et al., 1980 as cited in Lee, 2002 and Payne et al., 2003); up to 50 % of the insoluble hydrocarbon fraction during mesocosm studies (Gearing et al., 1980; Wade & Quinn, 1980 as cited in Lee, 2002); 50 % of oil released from cobble shores dispersed in associated fines causing enhanced biodegradation rates after the 1996 *Sea Empress* spill, due to high turbidity in the water column and remediation though mechanical transportation of oiled sediment from the high-water mark into the intertidal zone over four days (Lee 1997 as cited in Lee, 2002); 87-98% in particulate form as either mineral free globules or adsorbed to or incorporated within mineral aggregates (Gordon et al., 1973 as cited in Lee, 2002).

For concentrations greater than 100 mg/l, the potential for oil sequestering was estimated to be significantly high for open-ocean and nearshore oil/SPM interactions; at 1-10 mg/l SPM, negligible amounts of transport of particle-associated oil to the seabed occurs and with 10–100 mg/l, large amounts of sedimentation are possible with sufficient turbulent mixing (Boehm, 1987 as cited in Lee, 2002; Payne, 2003). An 80-90% contribution to dispersion was observed within 20-40 minutes, dependent on viscosity (24% for viscous oils at 20 °C) in seawater containing 200 mg/l of mineral fines (Khelifa et al., 2005). Rates of oil removal from the water surface by OMA have been estimated at between 0.017% and 22.6% for 0.1 – 10 mg/l concentrations. Sedimented oil is estimated by

mineral concentration (mg/l) x 0.183 (i.e. 18 %) per day approximately in the study by F.F. Slaney & Co. for Canadian
Marine Drilling of Calgary (Duval & McDonald, 1978 as cited in Muschenheim and Lee, 2002). Anecdotal estimates of the rate of sedimentation of hydrocarbons have been rapid, between 16 hours and a few days (DiSalvo & Guard, 1975; Spooner, 1970 and 1978 as cited in Muschenheim and Lee, 2002), or continual sedimentation has been detectable for 6–12 months. Settling velocities between 0.22 and 1.04 cm s^{-1} were observed for large (100–200 μm) clay–oil flocs in the laboratory by Muschenheim and Lee (2002), implying that settling could occur within a day within continental shelf settings. Settling rates for OMAs are usually approximated to the range between fine sand and silt (Gebelein, 1973; Spooner, 1978 as cited in Muschenheim and Lee, 2002) which would allow shallow water transportation offshore. Oil concentration of 10 to 100 mg/l represents the typical range in coastal waters affected by spills (Payne et al. 1989).

Huang and Elliott (1977) identified the 'armouring' effect of oil droplets adhered to by fine particles of alumina, silica and kaolinite. Stabilisation of the suspension occurred with up to 100 mg/l of suspended sediment. Suspensions larger than this destabilized and settled due to the increased density from adhered inorganics. Oil spill remediation studies have used the knowledge of this effect to clean up oiled shorelines (Bragg & Yang, 1995; Lunel et al., 1996; Owens et al., 1994 as cited in Muschenheim and Lee, 2002; Bragg & Owens, 1995) and to enhance biodegradation (Lee et al., 1997; Weise et al., 1999 as cited in Muschenheim and Lee, 2002). OMA formation is enhanced by physical processes such as wave, energy, tides or currents (Khelifa et al., 2005; Payne et al., 2003; Stoffyn-Egli and Lee, 2002).. Sediment is therefore mechanically moved to the surf zone and naturally self-cleaned although oil loss from the surf zone is also attributed to physical erosion of the residual oil from coastal sediments (Lee, 2002). Oil is lost in this process due to solution and erosion of visible droplets or soluble aromatics (Cloutier et al., 2002 as cited in Lee, 2002). Some lower molecular weight 2–3 ring PAH (logK_{ow} values of 3.7 - 4.8) and monocyclic aromatics (benzene and alkyl-substituted benzenes) (log K_{ow} values between 2.1 and 3.7) are partitioned into the water column where they can be evaporated or biodegraded during the initial stages of oil-mineral interaction. Heavier alkyl-substituted 2–5 ring PAH compounds (log K_{ow}>4) and aliphatic (C_{10}–C_{40+}) compounds sink with the particles when turbulence is insufficient to keep the particles in suspension (Payne et al., 2003). Mechanical clean-up and surf washing of oil stains from No. 6 fuel oil on Tampa Bay was highly successful after a large oil spill in 1993. A notable absence of clays and high shell content was present on this fine to coarse sand (Owens et al., 1995 as cited in Lee, 2002). Surf washing also accelerated natural removal of oil through enhanced formation of OMA during a large scale field experiment in 1997 in Svalbard, Norway; biodegradation occurred in oil dispersed in nearshore waters and sediments in association with OMA (Lee, 2002; Owens, 2002). Buoyant OMA dispersed over a large area. Nearshore sediments were tested and found to be within Canadian regulatory toxicity limits for dredged spoils destined for ocean disposal (Lee, 2002).

OMA were found to result from interactions among oil residues (physically or chemically dispersed oil droplets), suspended particulate matter (SPM), and seawater or from adsorption of dissolved components to SPM on a molecular level with subsequent flocculation (Payne, Clayton Jr. and Kirstein, 2003). Poirier and Thiel (1941 as cited in Muschenheim and Lee, 2002) also observed oil adhering to mineral grains as globules and irregular stingers in early tests using ten sediment types and mid-continent crude oil. In the first instance, micro-sized mineral fines coat small oil droplets surrounded by seawater (Lee, 2002). These floccules may aggregate, forming solid-stabilised emulsions which are inherently different to the highly viscous emulsions, the shape of which, depend on hydraulic energy (Bragg and Owens, 1995). This coating of oil droplets is well researched and occurs as ‘cation bridges’ stabilise the electrical charges between the polar oil components and cations in seawater (Bragg and Owens, 1995; Bragg and Yang, 1995 as cited in Lee, 2002). Mineral surfaces which have positive edge charges due to isomorphic substitution and uptake of H^- and OH^- form flocculants with the oil also (Weise, 1997). Clay flocculation occurs as the electrostatic repulsion between mineral and oil particles in water are balanced with the attractive Van der Waals forces. Electrolytes in seawater cause the formation of electric double layers around the particles which are ‘thinned’ with increases in salinity (negative charges are moderated), making interaction between particles easier (Le Floch et al., 2002). In the second instance, a discrete phase of oil-mineral interaction, OMA may also occur as oil is incorporated into the mineral solid phase through adsorption. Bassin & Ichiye (1977 as cited in Lee, 2002) observed the presence of thin monolayers of light crude oil adsorbed onto the smectite-rich marine clay minerals (association colloids) and coagulation of dissolved salts. Excess oil is wetted onto the thin organic film as oil globules forming flocs. Smectites have expandable interlayer spaces and swell in water dependent on their isomorphous substitution and associated negative charges. These organo-clays have a large capacity to bind petroleum hydrocarbons.

OMA form readily with smaller grain sizes, smaller sized particles (clay sized) have the largest ratio of surface electrical charge/particle mass, a function of larger mineral surface areas (Ajijolaiya et al., 2006; Guyomarch et al., 1999; Khelifa et al., 2002; Omotoso et al., 2002). Larger sized fractions (up to silts) can also be found in the flocs. Particles sizes less than 4-5 µm have been asserted as the optimal range for OMA formation (Bragg and Owens, 1995; Zhang et al., 2010). Larger grain sizes promote rapid OMA formation while smaller particles result in consistent formation (Sun et al., 2010). Omotoso (2002) observed that mineral surface area is a more important marker for OMA formation than particle size while Bragg and Owens (1995) tested OMA formation with pure minerals and concluded that the size fractions determined flocculation efficiency more than the mineral properties.

Stoffyn-Egli and Lee (2002) outlined three structurally unique forms of OMA including; dispersed oil droplets (< µm - tens of µm; larger size fractions are in floating droplet OMA) with discreet or aggregate mineral particles affixed to their surface; larger (tens to 100s of µm) solid mineral aggregates of irregular shape (a function of mineral inclusions) which may or may not have particles affixed to their surface and; thin sheet flake aggregates with dendritic microstructure. Solid OMA can be up to 200 – 300 µm and may be branched, curved or elongated. Droplet formation is turbulence-limited and will occur with most oils and minerals. The large (mm scale) flake aggregates formed out of an Intermediate Fuel Oil (IFO 30) mixed with montmorillonite clay as oil penetrates the interlayer spaces of swelling clays.

Flake aggregates (which have only been found in the lab) are generally neutrally buoyant or floating but sink readily when disintegrated with increased turbulence (high shear strength) to form compact OMA (Stoffyn-Egli and Lee, 2002). Identification may be possible by the preferential orientation of the minerals even with compaction. Although flake aggregates form most readily with smectites, mineral bound oil at the particle scale may also occur with high concentrations of oil and low oil/mineral ratios using different clay minerals, including mica, illite and chlorite (Stoffyn-Egli and Lee, 2002). Lee et al. (1998 as cited in Omotoso et al., 2002) had previously identified droplet flocs and solid flocs from shaker laboratory experiments.

A validated quantitative image analysis study Stoffyn-Egli and Lee (2002 concluded that OMA formation was a function of the minerals present; kaolinite and quartz results in droplet aggregates that, with high oil concentration or low mineral content, are in the floating phase; montmorillonite results only in flake aggregates which are neutrally buoyant or float unless compacted. Concentrations of kaolinite above 80% form droplet OMA. Montmorillonite is therefore more effective at scavenging oil. Large silica grains (0.14 μm) result in large mineral flocs with some trapped oil. Solid OMA in the floating phase predominates with larger concentrations of oil Stoffyn-Egli and Lee (2002). Using Svalbard sediment (only 2-3% smectite by weight) and above 0.2 g/l of oil and low ratios of oil/minerals, flake OMA big enough to be seen with the naked eye were the result of mineral-bound oil at the particle scale controlling the shape of the OMA. Omotoso (2002) observed that low-surface-area calcite (an oleophilic, hydrophobic mineral) flocculates crude oils more than hydrophilic, low-surface-area quartz and kaolinite, which interact strongly with low-viscosity oils only. Omotoso (2002) stated that particle size and surface area are not limiting factors but are important when substantial variations are present. Low hydrophobicity minerals have grain sizes less than 20 μm (Zhang et al., 2010). The average size of the OMA formed with the hydrophobic mineral, modified kaolin was 25.180 μm (up to 100 μm) in a study by Zhang et al. (2010).

Polar and ionic hydrocarbon quantities (which increase with weathering) were also found to affect OMA formation as they increase the lipophilicity of the minerals. The shear energy of waves was determined to be an integral part of OMA formation and as highly viscous oils are harder to disperse, viscosity is inversely related to OMA formation. The average size of OMA and width of size distribution increases with decreased mixing energy and long sedimentation periods however oil droplet size decreases (Khelifa et al., 2002; Zhang et al., 2010). Also as the dispersed droplets are larger in more viscous slicks, the resultant OMA is likely to be in the solid form (Stoffyn-Egli and Lee, 2002). Thicker oil slicks will not readily disperse and as the slick becomes coated in mineral grains, it shears off, coils due to hydrophobicity of oil and forms solid OMA with irregular shapes (Bragg and Yang, 1995 as cited in Stoffyn-Egli and Lee, 2002). Physical dispersion of lower concentrations of oil is easier, resulting in increased droplet concentrations. Alternatively large globules of oils can engulf hydrophobic mineral grains. Droplet OMA do not readily break down because the mineral coating protects the oil and because there is a threshold for oil droplet size below which turbulence cannot break up the droplets (Delvigne et al., 1987; Stoffyn-Egli and Lee, 2002). As viscosity increases with weathering, OMA formation is usually (except in extremely high turbulence) limited to the first two days after a spill (Payne, 2003).

OMA have also been categorized as positively, negatively and neutrally buoyant (Lee et al. 2001, 2008; Stoffyn-Egli and Lee, 2002). Negatively buoyant OMA does not readily biodegrade while neutrally buoyant OMA degrades rapidly (Gearing et al. 1980 and Wade and Quinn 1980 as cited in Loh et al., 2014). The oil-sediment ratio in agglomerates control the buoyancy (positive, neutral or negative) and subsequent behaviour of the agglomerate. Once oil is bound to a mineral it’s density is generally less than sediment, it’s stability increases and it is more easily transported out of a low energy environment by currents, especially as these environments have prolific small grain sizes (Lee, 2002).

An equilibrium time for OMA formation in seawater; 20 minutes using kaolinite clay and > 3 hours using Waddensea silt was estimated by Delvigne et al. (1987 as cited in Sun et al. 2010). A laboratory study on the explicit measurements of the time scale of OMA formation was done by Khelifa (2005b) using a reciprocating shaker and two engineered sediments (bentonite and chalk) viscosity in brackish and cold water. Using relatively high mixing energy and a reaction time of 3 hours (much longer period than in Payne et al., 1989), data showed that the equilibrium (reach of maxima) of OMA formation was reached after 20 min of mixing for Heidrun crude oil and 40 min for IFO 30 oil with chuck sediment. In contrast to Payne et al. (1989), this showed that oil types have a strong influence on the kinetics of OMA formation.

Most research has concluded that hydrophobic compounds (hydrocarbons, pesticides and nutrients) adsorp onto the organic coating of mainly marine and estuarine fine and sand particles (Muschenheim and Lee, 2002). However Meyers and Quinn (1973a as cited in Muschenheim and Lee, 2002), found that sorption of oil was hindered by organic coatings on clays and marine sediments. The organic content of the sediment determines differences in adsorption coefficients and low molecular weight organic compounds do not readily adsorb hydrophobics (Hargrave & Phillips, 1975 and Murray, 1973 as cited in Muschenheim and Lee, 2002). Increased temperature also decreases sorption of hydrocarbons (likely due to increases in aqueous solubility (Meyers and Quinn, 1973a as cited in Muschenheim and Lee, 2002). Marine humic and fulvic acids and microbial cells (yeasts and bacteria) are more effective sorbants than clays however clays alter the chemistry of the dissolved phase, increasing availability to microbiota (Boehm & Quinn, 1973; Pierce et al., 1974; Button, 1969 and Button, 1976; Herbes, 1977 as cited in Muschenheim and Lee, 2002).

It has been determined that high viscosity oil fails to form OMA (Bragg and Yang, 1993, 1995 as cited in Stoffyn-Egli and Lee, 2002; Kepkay, 2002; Khelifa, 2002; Lee et al., 1998 as cited in Loh et al., 2014; Le Floch et al., 2002; Omotoso, 2002). Bragg & Owens (1994) developed a field spectroscopy technique based on the fluorescence characteristics of different oils and OMA confirmed that highly viscous oils are less likely to form OMA than low-viscosity oils. Stoffyn-Egli and Lee (2002) found lower rates of OMA were obtained from higher viscosity oils and lower temperatures however OMA did form. Lee et al. (1998 as cited in Loh et al., 2014) determined that 9500 mPa.s is the threshold value of viscosity above which no OMAs could form. Significant amounts of OMA do not form with high viscosity oils such as Bunker C (Bragg and Yang 1993, 1995; Bragg and Owens

1994; Lee et al. 1998 as cited in Loh et al., 2014; Omotoso et al. 2002). Data from UVF analysis (450 nm emission) and microscopical observations of seven reference oils (covering a 3600-fold range in viscosity) suggested that higher-viscosity oils with mineral fines are less likely to form fluorescent particles (optically-thick suspensions of crude oils and OMAs) (Kepkay, 2002).

Concentrations of oil droplets stabilized by clay particles were observed by Khelifa et al. (2002) to have an inverse relationship with viscosity and temperature which is more pronounced at low viscosity ratios (Newtonian flow) possibly due to differences in rheological properties. This was observed for both number and volume concentration. Asphaltenes-resins content (ARC) had a similar inverse relationship with droplet concentration, with temperature affecting these relationships. This is because higher viscosities are associated with asphaltenes; therefore more energy is required for breakup (Khelifa et al., 2002). Viscosity ratios were found to increase exponentially with ARC and are affected by temperature.

Settling of mineral flocs was slowed by the addition of viscous oil, even more so with less viscous crudes. This is because the highly viscous oils rise quickly, avoiding sedimentation. Low viscosity oils are generally associated with the floc structure. Chemistry was not shown to have an effect on the degree of interaction of oil and kaolin however the flocculation index (degree of interaction) decreases with viscosity.

Two types of OMA were identified by Omotoso (2002); trapping of minerals in an oil-continuous phase and minerals stabilizing oil droplets in a water-continuous phase. Negatively buoyant flocs associated with hydrophilic minerals and low-viscosity oils were comprised of minerals stabilizing oil droplets in a water-continuous phase. Positively buoyant flocs containing oleophilic minerals such as calcite have both water-continuous (with calcite intrusions) and oil-continuous sections which are mineral-rich. Oil slicks contain some quartz particles or water droplets dispersed in the oil-continuous phase. Some negatively buoyant flocs IFO 30 oil droplets in seawater are stabilised by clay minerals and calcite and to a lesser degree quartz.

With respect to sediments, Delvigne (2002) used direct microscopic observation of experiments using natural, artificial and spiked sediment to describe three distinct phases for the presence of oil in the sediment; oil droplets, oil-coated (about 0.3 microns thick) sediment particles and oil patches (which only form with high oil concentration) are tens of microns thick, and have no defined shape due to sediment grain inclusion. Oil droplets are present either as oil droplets incorporated in sediment flocs or oil droplets coated with sediment particles which are negatively, positively or neutrally buoyant dependent on the oil-mineral ratio. The division of oil into these phases was found to be the result of mineral and oil type and concentration, weathering state and oil-mineral interactions. All visible oil in OMA was discrete and was between 1 – 60 µm in negatively buoyant OMA. Size distribution of oil droplets did not vary with oil, sediment or turbulence. Droplet phase was found to be linearly dependent on oil concentration in the sediment and size distributions of droplets were also determined by oil concentration; larger droplet sizes are present with increased concentrations. The lower surface tension oil used in spiked sediment experiments resulted in lower concentrations of oil droplets and in the only visible oil patches regardless of grain size. With weathering of oil no changes to oil droplet distribution nor physical appearance was observed.

Sediment size was found to have an inverse relationship with OMA formation by Ajijolaiya, Hill, Khelifa, Islam and Lee (2006). Sediment concentration, contrastingly, has a positive relationship with OMA formation; with increased concentrations, oil trapped in OMA abruptly increases and stabilisation is extensive. It was determined that a critical threshold of sediment concentration therefore exists for OMA formation based on sediment particle diameter, shape, density, packing on droplet surfaces and oil concentration, density and droplet size. An expression for critical sediment mass concentration, C_s,

$$C_s = \frac{\beta \rho_s D_{s32}}{\rho_o D_{o32}} C_o \tag{4-12}$$

where ρS and ρO are sediment and oil density, β is a dimensionless packing factor, D_{S32} is the sediment Sauter mean diameter (m), D_{O32} is the oil Sauter mean diameter (m), and C_O is the oil mass concentration (kg/m^3). Critical sediment concentrations for 1 μm droplet size were approximately 200 mg/l and for 16 μm sediment size, 490 mg/l. The coefficient β accounted for variability in critical concentrations caused by shape and the assumption that grains were spherical.

Payne et al. (1989) and Payne et al. (2003) studied the kinetics of OMA formation using the equation derived by Kirstein;

$$\frac{dC}{dt} = -1.3\alpha[\varepsilon/\nu]^{1/2}CS \tag{4-13}$$

which characterises the rate of loss of free oil droplets due to collision and adherence to SPM in high energy conditions and high sediment concentrations. C is the concentration of oil droplets in mg/l, S is the concentration of SPM in mg/l, α is a coefficient for "shape, size, and stickiness" of the SPM, ν is the kinematic viscosity of the water and ε is the energy dissipation rate (per mass of fluid). Derivations for sediment starved concentrations and when oil and SPM are source terms were also created by Kirstein. The work of Payne et al. (1989 and 2003) aimed to establish values for the removal rate of free oil droplets due to the interaction with SPM particles. Using a propeller with variable speed motor and in-line torque meter in a turbulent mixing chamber, energy dissipation rates were maintained. Microscopic analysis of 50 μL samples at varying times allowed quantification of free oil droplets which were presumed not attached to any SPM/OMA. Payne et al. (1989) reported that OMA formation was independent of the type of oil and SPM concentration but that sediment type (particle number density), salinity and mixing energy have strong controlling effect on the reaction rate. Payne et al. (2003) also observed an exponential decrease in free oil-droplet concentration with time (a proxy for OMA formation). When the shaking rate increased from 2.0 to 2.3 Hz, the maximum oil trapping efficiency, OTE (the ratio of mass of oil trapped in negatively buoyant OMA and mass of total oil) representing magnitude of OMA formation, increased from 19.8% to 42% and the required shaking time decreased from 3.7 to 0.7 hours. Adsorption of hydrocarbons onto the surfaces of particulate matter is considered negligible for removal rates in contrast to the high values estimated by Gordon et al. (1973 as cited in Muschenheim and Lee, 2002).

Hill et al. (2002) simplified the population balance equation, relating time of OMA formation to the properties of the droplet and sediment suspensions as well and the mixing (turbulent-kinetic-energy) to formulate a predictive model for intertidal oil; the size ratios of oil droplets and sediment grains and the ratio of oil to sediment being controlling factors:

$$t_c = \frac{In\left(1 - \frac{2\pi}{\sqrt{3}}\right)\left(\frac{D_o}{Ds}\right)^2\left(\frac{N_o}{Ns(0)}\right)}{\beta} \tag{4-14}$$

where t_c is the critical time for OMA formation, D_s is the mean sediment diameter and D_o is droplet diameter in µm. N_s and N_o are number concentrations of sediment particles and oil droplets respectively (m^{-3}). Coalescence efficiencies between 10^{-3}–10^{-2} were found. The rate at which small sediment particles adsorb to larger oil droplets varies with oil volume concentration in suspension. The model showed that stabilization and coating of OMA is within 5 minutes to one day, 50 % of the time, and within an hour, 25 % of the time, dependent on sedimentation concentration and mixing.

Sun, Khelifa, Zheng, Wang, So, Wong, Yang and Fieldhouse (2010) also investigated the kinetics of OMA formation as a function of mixing energy and the sediment-to-oil ratio using the standard reference material 1941b. OSR, oil-to-sediment ratios, were determined using the ratio of oil mass (mg) to sediment mass (mg) in the settled oil-sediment mixture. Trapping efficiencies of different sediments and relative percentages of sediment mass into settling, floating and neutrally buoyant OMA can be assessed with OSR. Similar to OTE, OSR increased exponentially with time and converged toward a maximum. Higher than previously reported values of McCourt and Shier (1999 and 2001 as cited in Sun et al., 2010), maximum OSR (R_{max}) ranged from 0.21 to 1.13 (mg oil/ mg sediment). Maximum OSR between 0.01 and 0.45 g oil/g sediment (average 0.13 g oil/g sediment) were found by McCourt and Shier (2001) with high mixing energy and between 30 and 60 minutes mixing time. R_{max} decreased with increases in sediment concentration as the excess sediment settles on the bottom of the reaction chamber.

The fitting function;

$$E = \frac{E_{max}}{1 + e^{-\frac{(t - t_o)}{b}}} \tag{4-15}$$

can be used to predict the kinetics of OSA formation with known maximum OTE in percent, E_{max} (known from previous literature), t_0, the critical time for OSA formation when the oil trapping efficiency E is 50% of E_{max} (varies with mixing energy and sediment concentration) and parameter b which controls the shape of the curve (related to sediment concentration). t_0 is correlated with equilibrium time t_e (during which E reaches its maximum value E_{max}) and can be estimated using the theoretical model proposed by Hill et al. (2002) . E is the OTE in percent and t is the shaking time in minutes.

Results showed that formation of OMAs increased exponentially with the mixing time and reached saturation within 4 hours. Akin to the work of Hill et al. (2002), the sediment size in suspension was shown to determine OMA formation times, with ranges from minutes to days. These observations are in accordance with the population balance equation in which the aggregation rate is proportional to the product of concentrations and the energy dissipation rate (mixing) and also the conceptual model proposed by Hill et al. (2002). Mixing energy is also an integral control on the kinetics of OMA formation, enhancing efficiency in formation and equilibrium maximum of OTE. This effect predominated with lower sediment concentrations and had been observed earlier by Payne et al. (1989 and 2003) and Khelifa et al. (2005). Sediment concentration also enhanced efficiency of OMA formation and accelerated the process. This was similar to the findings of Payne et al. (1989 and 2003), Guyomarch et al. (1999), Khelifa et al. (2002 and 2005) and Ajijolaiya et al. (2006) among others. Stabilisation of droplets occurred as either trapping of droplets in sediment flocs (nesting) or by coating of the droplet surface in a sediment layer and was augmented with increased sediment. The oil type was also shown to have an effect on OMA formation kinetics as they varied considerably from those reported by Payne et al. (1989 as cited in Sun et al., 2010).

Østgaard & Jensen (1983) observed that UVF of oil suspensions in seawater is readily detected at concentrations < 10 ppb by measuring emissions between 300 and 500 nm and since then UV epi-fluorescence has been widely used to study OMA. UV epi-fluorescence microscopy was also used by Kepkay et al. (2000 as cited in Omotoso, 2002) to observe the nature of flocculants. A test for formation of OMA using a thinly coated (in oil) glass slide shaken with a suspension of sediment was also developed. Kepkay (2002) proposed that direct UVF spectroscopy of dispersed/dissolved oil, measurements of emission at 355 and 450 nm, in response to an excitation wavelength of 320 nm at a spill site could be used to assess the distribution and calculate the onset of OMA using normalised aggregate fluorescence ratios. These are the result of correlation of aggregate area and OMA fluorescence; < 1 are unlikely to form aggregates, 2-4 would aggregate to an intermediate extent and ratios between 8 and 10 are highly likely to form aggregates. Direct UVF spectroscopy allows observation of changes in oil fluorescence characteristics during OMAs formation and avoids the problems associated with extracted sea water samples resulting from the three phase system. Fluorescence at 355 nm was determined to be the result of the soluble components, which was all similar in the oils used.

Wang, Zheng, Li and Lee (2011) used particle image velocimetry (PIV) to study the oil–mineral interactions and the formation of OMAs in situ. Flow fields of stationary and moving oil droplets were captured as two successive exposures on two separate frames as a pair using a CCD camera. The mean velocity of the particle flow was then calculated by dividing the frames into interrogation areas where correlation algorithms were used to generate velocity vectors. Opposite interaction between oil and Kaolin particles in the area close to the surface of the oil droplet were observed and interaction between oil and mineral particles becomes weak further from the surface of oil droplet. The vector intensity, size of the tail (extended area of interaction behind the oil droplet) and duration of velocity increased using hydrophobic modified Kaolin with Alaska North Slope

(ANS) crude oil suggesting that hydrophobic minerals interact more and for longer with oil; with the likelihood of producing more OMA. The hydrophilic property of minerals caused stronger repulsion with oils, especially the more polar (richer in asphaltenes) Medium South American (MESA) crude oil. This was in contrast to the findings of Omotoso et al. (2002) who determined that polar content had little effect on interactions with Fisher kaolin but similar to the observations of Stoffyn-Egli and Lee (2002) and Bragg and Yang (1995). Oil droplets that form in brine solution are irregular as reverse micelles of dispersant form as hydrophobic tails maintain contact with oil. As the oil droplets rise, the hydrophilic heads of the core make contact with the salt water contorting the droplet shape and dispersing the oil into smaller oil droplets. When dispersant was introduced directly to the brine solution, a surface film was generated by surface agents, repelling the oil and mitigating oil droplet formation; with implications for the introduction of dispersant into oil spills; dispersant introduced to oil does not have this result.

The lower ionic strength (100x lower than seawater) of fresh water allows the mineral surface properties (charge) to become important (Omotoso, 2002). As the interfacial tensions of the crude oils are by 3–6 orders of magnitude lower in seawater than in fresh water, spreading coefficients are higher and oil droplets will be more stable in seawater, favouring formation of droplet flocs. Quartz and calcite both interact with crude oil more in fresh water than seawater. High-surface-area montmorillonite interacts more than quartz and kaolin but only in seawater solutions due to it's negative charge.

Effects of salinity are complex and depend on nature of solid particles, the oil composition, the pH and ionic strength of the aqueous phase. Minimum salinity required for OSA formation has been identified as between 1.2 to 3.5 ppt (Khelifa et al. 2005; Le Floch et al. 2002). Bassin and Ichiye (1977 as cited in Khelifa et al., 2005) observed that adsorption of South Louisiana crude oils onto clay occurred only in brackish water (10 ppt saline solution) and concluded that electrolytic flocculation of the clay particles was primarily responsible for sedimentation of oil with clay; high electrolyte concentrations reducing oil presence in clay flocculations due to coagulation of oil and agglomeration of clay particles individually. Payne et al. (1989 and 2003) found high rates of reaction (number of oil droplets stabilized by SPM per minute) at salinities of 15 and 30 ppt and reduced rates with lower salinities while Delvigne, van der Stel and Sweeney (1987 as cited in Khelifa et al., 2005) determined that salinity had no effect on droplet size. Kerebel and Khelifa et al. (1997 and 2003a respectively as cited in Khelifa et al., 2005) observed that salinity increases between 0 and 0.2 ppt and 0 and 3.5 ppt respectively resulted in sharp increases in OMA formation. Concentrations above these values had little effect. Guyomarch et al. (1999 as cited in Khelifa et al., 2002 and 2005) however ascertained that increased salinity reduced OMA concentration; an increase of 10 to 35 ppt doubled the amount of clay required to stabilise 40% of the oil. Abend, Bonnke, Gutschner, and Lagaly (1998 as cited in Khelifa et al., 2005) found that the addition of sodium chloride stabilised oil-in-water emulsions with paraffin oil. Tambe and Sharma (1993 as cited in Khelifa et al., 2005) observed the opposite with barium sulphate as the solid phase; 5 wt% of sodium chloride reduced emulsion stability however with increased pH levels, this effect was negated. Earlier work by Huang and Elliot (1977 as cited in Khelifa et al., 2005) established that increased sodium chloride concentration reduced Cabosil (sub-micron SiO_2) particles' ability to stabilise emulsions. The Nigerian oil used was more negatively charged at lower salinities. Liu, Zhou, Xu, and Masliyah (2002 as cited in Khelifa et al., 2005) showed that calcium is important in the adsorption of clay particles on the surface of bitumen droplets which is also dependent on the type of clay; montmorillonite clay being adsorbed more readily than kaolinite clay.

Le Floch et al. (2002) established that salinity is only significant to the formation of OMA at values below a critical threshold; itself determined by the mineral and oil characteristics but around a salinity of approximately 2 (0.2 for BAL110 and 1.5 for IF30). OMA formation above this threshold is uniform but linearly decreases with diminishing salinity below, until the formation of OMA is prevented at freshwater phases (Le Floch et al., 2002). This threshold correlates to a critical thickness of the electrical double layer around the mineral and oil caused by ionic solution, which decreases with increased salinity. This is in contrast to earlier studies that found the highest rates of flocculation were at lower intermediate salinity ranges (Muschenheim and Lee, 2002). Le Floch et al. (2002)

also found that higher viscosity oils in low salinity ranges were less likely to form OMA in agreement with Bragg and Owens, 1994; Bragg and Yang, 1995; Lee et al., 1998 as cited in Le Floch et al., 2002 and Stoffyn-Egli & Lee, 2002). An anomaly with intermediate viscosity BAL110 oil was attributed to higher vermiculite and smectite concentrations in the sample.

The effects of salinity and clay type on the characteristics of oil droplets (shape, size and concentration) stabilized by the OMA were investigated by Khelifa et al. (2005) with various oil/sediment ratios under constant mixing energy. OMA formed in moderately energetic conditions even with only 200 mg/l of minerals and varying oil types. Droplets larger than 45 μm were rarely observed and large droplets remained stable for several days only in seawater. The shape of oil droplets stabilized by mineral particles was investigated using the shape factor variable, Φ. In all experiments, most oil droplets were spherical however, elongation of oil droplets increased with salinity; maxima occurring between 1.2 and 3.5 ppt salinity (exception of BAL110 oil combined with Conrod Beach (CBS) sediment which had a maxima at 34 ppt showing little influence from salinity) after which values remain constant. The effect of salinity on the size distribution of BAL/CBS was negligible too, possibly as abundant organic matter weakened the effect of salinity on clay flocculation. The size distributions otherwise increased substantially with increased salinity, in line with the findings of Khelifa et al., (2002), Delvigne and Sweeney (1988) and Muzzio et al. (1991 as cited in Khelifa et al., 2005). Median size of the mineral-stabilized droplets was independent of oil type and temperature in seawater (35 ppt) paralleling earlier findings of Khelifa et al., (2002). Maximum grain size values were observed at 1.2 ppt (maxima), minima at 3.5 ppt and at 35 ppt the median size is around 6 μm regardless of oil/sediment used. .. With salinity increases, the ability of clay particles to flocculate and form particle networks also increased. Reduced electrokinetic potential indirectly affects droplet size also through increased droplet collision efficiency and ability of minerals particles to adsorb onto the surface of oil droplets (Khelifa et al., 2005).

Droplet concentration showed abrupt salinity increases between zero and 3.5 ppt and then steady values (no increases with salinity above 35 ppt). BAL 110 oil and

Bolivia sediment (BS) displayed decreases in concentration at <1 ppt and around 3.5 ppt salinity, followed by a steep increase with maxima at 35 ppt (the highest tested salinity). Equivalent decreases in median and maximum droplet size at 3.5 ppt were observed for BAL 110 and BS. High values at 35 ppt were associated with positively buoyant OMA. Mass concentrations of droplets trapped in OMA could be compared using $N_* = N_t /(N_t)_{max}$ and $S_* = S/S_{cas}$, normalised salinity (S) and critical aggregation salinity (S_{cas}) (above which there is no significant increase in N_t) with the fitting function;

$$N* = \frac{S_*^{\,1.97} + 0.01}{S_*^{\,1.97} + 0.12}$$

(4-16)

The variables $(Nt)_{max}$ and Scas are a function of oil properties, mineral types and environmental factors. Reduced concentrations of droplets at high salinity (less than asymptotic value of 1) were recorded for the experimental data of Khelifa et al. (2005), Guyomarch et al. (1999) with a mixture of HFO/BAL110 oil and montmorillonite clay and by Bassin and Ichiye (1977). Normalised numbers were used to plot the data of Meyers and Quinn (1978) and Kerebel (1977 as cited in Khelifa et al., 2005) which were likewise well fitted and showed the same reductions at high salinity. The data of Kerebel however gave S_{cas} values of 0.2 ppt using BAL110 oil using different clay minerals and longer and more turbulent mixing regimes. S_{cas} is more affected by the composition of the sediment, and possibly the mixing energy, than by the type of oil. For a given salinity, sediment type and then oil type strongly influence magnitude of droplet concentration for a given salinity. The effects of turbulence on characteristics of oil droplets were not addressed by Khelifa et al. in associated studies (2005).

Measurement of the zeta (electrokinetic) potential of minerals and oil-in-water emulsions have consistently reported negative charges associated with freshwaters and positive charges in seawater. Charge reversal for minerals has been recorded at salinity values of between 2 and 6 ppt (Pravdic, 1970 as cited in Khelifa et al., 2005) and 0.1 to 1 ppt (Sondi, Biscan and Pravdic, 1996 as cited in Khelifa et al., 2005). At neutral pH, negative zeta potential decreases with increased salinity. The collision efficiency factor was found to increase with salinity increases from

0 and 5 ppt (range at which OMA formation also occurs) and then stabilised at higher salinities; maxima a function of the mineral clay Gibbs (1983, as cited in Khelifa et al., 2005).

The pH of sea water is marginally alkaline and studies have shown that optimum biodegradation occurs in slightly alkaline conditions (7-9). High energy shorelines require a constant or frequent nutrient supply and have a lower carrying capacity than low energy (estuarine) environments which are more likely to become anoxic or anaerobic (Venosa & Zhu, 2003).

Sedimented oil flocs containing particulate material of biological origin have been observed in nature. In Bermuda, subtidal deposits of marine algae with oil were observed (Sleeter et al., 1980 as cited in Muschenheim and Lee, 2002). Organic-oil aggregates generated by flocculation of phytoplankton with dispersed oil droplets and fecal pellets from zooplankton which have grazed actively grazed on spilled oil may also transport oil to the sea floor (NRC, 2003; Payne, 2003). Although temperature dependent, microbial utilisation of hydrocarbon substrates in the water column has been found as nearly 80% at 25 °C to 0% at 4 °C (Ludzack & Kinkead, 1956 as cited in Muschenheim and Lee, 2002); values being far greater than for sedimented sand which is normally O_2 limited except in surf zones (Gebelein, 1973 as cited in Muschenheim and Lee, 2002). Rates of microbial degradation of nearly 1% in 4 hours were found by Johnston (1970 as cited in Muschenheim and Lee, 2002) in well-oxygenated sand columns. Detrimental effects of oil on zooplankton are generally small however they can be biomagnified. Microbial and metazoan mats induce oil sinking and are due to organism's preferential utilisation of lighter components of oil and resultant increased densities (Voroshilova and Dianova, 1950 as cited in Muschenheim and Lee, 2002).

Guyomarch et al. (1999 and 2002) investigated the formation and size distribution of OMA with a chemically dispersed (using Inipol IP 90 CECA) oil fraction and illite and montmorillonite (bentonite). Stabilisation of OMA was enhanced by dispersant more than any other factor (Guyomarch et al., 1999; Guyomarch et al., 2002; Lee et al., 2008) and the resultant positively buoyant OMA remained in suspension in the water column, promoting dispersion and sedimentation. This was again found by Zhang et al. (2010). Results showed that a minimum particle concentration of 400 to 800 mg/l and a ratio of oil to particles of 3:1 were required for effective OMA formation regardless of their types which was similar to Muschenheim and Lee, 2002; Stoffyn-Egli and Lee 2002). For lower suspended mineral concentrations and dispersed oil, the average OMA size was significantly large, 800 µm for as the OMA were predominantly mineral. Although distinctive behaviours were observed with the new pollutant formed, both minerals were equivalent in their ability to form OMA. This was also found by Muschenheim and Lee (2002) in contrast to the findings of Omotoso et al. (2002).

Increased clay concentrations were required to form the largest aggregates with increasing salinity and the minimum clay concentration required to form aggregates at increased salinities, above 10 g/l, increased from 0.4 to 0.8 g/l (Guyomarch, 2002). For low oil–mineral ratios, the smaller average OMA size is the result of fewer multiple droplet aggregates possibly due to saturation of the oil droplet by mineral particles (Guyomarch, 2002). Multiple-droplet aggregates (up to 15 droplets) were observed more with dispersant than in previous studies without it (Lee et al., 1998 as cited in Guyomarch, 2002). Dispersant alone was found to trap oil effectively.

4.6 OIL SPILL IMPACTS

Highly volatile, light component oils such as diesel and kerosene spread on the surface of the sea water as thin slicks which are readily evaporated (ITOPF, 2011a). These spills do not require any remediation. Medium crude oils spread somewhat and when weathered become more viscous (ITOPF, 2014b). Crude oils contain both the lighter (C_4) fraction and the heavier ($> C_{17}$) fractions of hydrocarbons (Table 4.5). Relatively unweathered crudes contain between 20-40 % light components which are lost to evaporation/volatilisation and dissolution (in minor amounts) during the initial 24 hour period after a spill, leaving the medium and heavier compound residues (NRC, 2003). Medium weight compounds are biodegraded and photoxidised over the following weeks and may be emulsified or adsorbed to sediments. The remaining heavy molecular weight compounds may also adhere to the sediment, agglomerate or float or sink in the water column depending on their specific gravities (The American Petroleum Institute Petroleum HPV Testing Group, 2011). Aromatics and polyaromatics are also present, with small amounts of asphaltenes, resins and waxes. Light components can become trapped in the water column with sub-surface release, resulting in weathered oil at the surface (Andrade et al., 2012). The presence of waxes, resins and asphaltenes increases the likelihood of formation of water-in-oil emulsions which are extremely difficult to clean up. Although there are immediate dangers from lighter weight component due to flammability and vapour toxicity, their volatility means they evaporate relatively quickly ITOPF, 2011a).

Unlike lighter oils which evaporate quickly, the heavier oils and the heavier residues left after the evaporation of volatiles, are extremely persistent; gasoline has a persistence value of 1 while No. 6 Bunker oil has a value of 400 (Boyd et al, 2001). Even relatively small concentrations of persistent oils can cause substantial damage and are a challenge for clean-up projects (Andrade et al., 2012; Lewis, 2002). Skimmers, burning and the use of dispersants are not effective on these oils and it is rare to recover 10-15% at sea (ITOPF, 2011a; ITOPF, 2014b). As much of the volume of oil spilled at sea (approximately 48 % by volume) is highly viscous bunker oil and crude oil heavy residues (29 % by volume) (Andrade et al., 2012), the required mechanical and manual clean-up using equipment such as scrapers and grabs, can create large amounts of waste and damage sensitive shores (ITOPF, 2014c). The remaining oil spilt at sea is waste refined products and mixed oil (Andrade et al., 2012).

Table 4.3: Composition of crude oil and residual oils. Adapted from Fingas (2011).

Group	Compound Class	Light Crude (%)	Heavy Crude (%)	IFO (%)	Bunker C (%)
Saturates		55-90	25-80	25-35	20-30
	Alkanes				
	cyclo-alkanes				
	Waxes	0-20	0-10	2-10	5-15
Olefins					
Aromatics		10-35	15-40	40-60	30-50
	BTEX	0.1-2.5	0.01-2	0.05-1	0-1
	PAHs	10-35	15-40	30-50	30-50
Polar Compounds		1-15	5-40	15-25	10-30
	Resins	0-10	2-25	10-15	10-20
	Asphaltenes	0-10	0-20	5-10	5-20
Metals (ppm)		30-250	100-500	100-1000	100-2000
Sulphur		0-2	0-5	0.5-2	2-4

Crude oil becomes denser, more viscous and more adhesive with weathering therefore less penetration and permeation will occur at the shoreline however this depends on the tidal stage and wave energy at deposition (Etkin et al., 2007). Wave action also affects contamination as waves mix dispersed oil causing it to take on water. It can then emulsify or sink to the seabed at large tar mats. Oil thickness on the shoreline is determined by the amount of oil spilt, the spill trajectory, the characteristics of the oil (viscosity and adhesiveness), shoreline steepness, tidal and wave conditions during the spill and the porosity of the sediment surface (Etkin et al., 2007). The sinking of the *Erika* in off the coast of resulted in a viscous emulsion with sedimentation in shallow water due to high wave energy (Kerambrun, 2003 as cited in Etkin, 2007). Oil has also been observed as high as 35 meters up steep and craggy cliffs in large (10s of metres) patches and trapped in caves at the foot of cliffs (Etkin, 2007).

Heavy Fuel Oil (HFO) or Heavy Bunker Oil (HBO) has less than 3 % light components (Andrade et al., 2012) resulting in thick viscous oil that does not evaporate nor disperse generally, instead; large thick, semi-solid slicks form that persist for long periods, traveling hundreds of kilometres over days (Lewis, 2002). These slicks smother coastal habitats, wildlife and amenities at the shore while residues form tar balls which are difficult to clean up and extremely hazardous (NRC, 2003). Annual use of HFO is in excess of 4 billion tonnes (ITOPF, 2014a). Asphaltenes, resins and waxes are in significant amounts in bunker oil (Table 4.5) (Andrade et al., 2012). Spilled HFO tends to float very low in the water, often semi-submerged by wave action, so it's position in the water column can be determined by variability in water density. Due to it's high relative density, HFO can also sink to below any less dense fresher inputs of water (1-10 m below the sea surface) (Fingas, 2013). Rarely HFO forms an emulsion. Due to it's high viscosity HFO generally sits on the surface of sediments and is only buried through sediment accretion. Light accumulations are often visible at the high tide line while heavier accumulations occur as bathtub rims around tidal pools (Office of Response and Restoration (NOAA), 2016a).

Although HFO can result in smothering of organisms; it's low water solubility makes it less bioavailable so it is not as toxic. Asphalt pavements (conglomerates of highly weathered oil and shingle are not readily bioavailable, irrespective of time on shore though their presence may affect the habitats of marine organisms. Tar balls also have low bioavailability.

During large storm events, it is likely that weathering processes will be intensified and that if prevailing wind and wave conditions favour onshore deposition, any contamination will be spatially extensive. This may be extenuated by wave and tidal conditions that result in overwashing and deposition of oil in the supratidal zone.

Petroleum transportation by pipeline and supertankers can carry up to 50 million barrels of oil and results of spills can be catastrophic. Modern large ships use ~150 tonnes/day and carry as much as 4000 tonnes of fuel (Lewis, 2002). Most (> 70 %) of marine bunker fuel oil is Intermediate Fuel Oil (IFO 380) grade (equivalent to Bunker C fuel oil or a No. 6 fuel oil) consisting of a blend of heavy fuel oil and gasoil with maximum viscosity of 380 cSt at 50 ºC and <3.5% sulphur. Number 6 fuel oil is also referred to as Residual Fuel Oil (RFO), Bunker C (navy specification) or PS-400(Pacific Specification) and is a high-viscosity residual oil which requires preheating to (104 – 127 °C), 220 – 260 °F. Heavy Fuel Oil (HFO), a near pure residual oil, is similar to IFO 380 but maximum viscosity is 420 cSt at 50ºC. IFO 180 is also widely used in marine diesel engines; smaller ships use lower viscosity grades. The ISO 8217 : 1996 designation, which has replaced the earlier intermediate fuel oil classification uses RM 35 (RMG-, RMH- or RMK-35) which is roughly equivalent to IFO 380 but has a maximum viscosity of 35 cSt at 100 ºC (Lewis, 2002). Viscosities for classifications of oils cannot be used to determine the viscosity of the oil after a spill as the low temperatures will induce non-Newtonian flow.

Increasingly heavy and more viscous oils are being created and used through “cracking” Unsaturated and aromatic fractions are greater in cracked residues. RMK is a cracked fuel oil with maximum density 1010 kg/m^3; making submergence in heavy seas likely. The straight-run oils are more likely to remain on the surface due to lower densities. Although asphaltene concentrations are greater in the cracked fuels, emulsification is slow due to the high viscosity of the oil (Lewis, 2002). The release of a heavy fuel oil or residual fuel oil (No. 6, Bunker C) would likely result in a water-oil emulsion. The ineffectiveness of dispersants and mechanical burning on these heavy oils would mean that oil would most likely reach the shoreline due to wave energy, winds and currents where they can persist for decades. Table 4.6 provides a summary of oil behaviour during an oil spill. Refer to Maritime New Zealand’s Oil Spill Operation Manual (2014) for a more comprehensive list of general crude oil characteristics that influence the behaviour and likely effects of spilt oil. The ADIOS library also provides information on weathering and changes to oil behaviour and individual oil types with weathering.

Table 4.4: ***Oil properties and their characteristic behaviour in a spill. Adapted from and Maritime New Zealand (n.d.) and Scholz et al. (1999) .***

Types of Oil/ C number	Volatility	Viscosity (mPa.s at 15 ° C)	API Gravity	Density (g/ml at 15 °C)	Solubility (ppm)	Emulsification	Interfacial Tension (mN/m)	Persistence	Pour point (°C)	Impacts
Very Light Oils **C_1 - C_{10}** Jet Fuels, Gasoline	H (1-2 days)	0.5	50-65	0.72	H	L	27	Non-persistent	N/A	Localised and severe
Light Oils **C_1 - C_{10}** Diesel, No. 2 Fuel Oil, Light Crudes	M (days) residue of 1/3 original oil amount	2-50	30-50	0.78-0.88	M	L	10-30	Persistent, clean-up effective	-60-0	Oils intertidal zone, long-term contamination. Adverse effects for esp. invertebrates in low energy environments. Bioavailable through respiratory system.
Medium Oils **C_{11} - C_{22}** Most Crude Oils	VL 1/3 evaporates in 24 hour period	50-50000	10-30	0.88-1	S/LT	M - H	15-30	Persistent, effective clean-up if rapid	-30-30	Toxic components but not bioavailable. Impacts to waterfowl and fur-bearing mammals
Heavy Oils **> C_{23}** Heavy Crude, No. 6, Bunker C	VL < 3% light components so doesn’t evaporate readily	10000-50000	5-15	0.96-1.04	S/LT	H	25-35	Persistent, shoreline clean-up difficult	5-20	Weathers slowly, long term contamination (chronic exposures of carcinogens through topical contact).

Although New Zealand is not a large producer of oil, crude oil from the Taranaki oil fields and offshore, is shipped to Marsden Point refinery in Northland which is turn is carried to ports nationwide as refined oil (Maritime New Zealand, 2013). Cargo tankers, mainly international freight, carrying marine fuel oils and heavy fuel oils in their bunkers also regularly transport goods around New Zealand's coast (Statistics New Zealand Te Tari Tatou, 2000). Not only are the numbers of bulk, container and cruise ships voyages increasing with corresponding increases in median vessel size in New Zealand (from 20,867 to 25,049 gross tons between 2011 and 2013) but activity in offshore mining and oil and gas exploration will necessitate greater risk of wellhead and extraction leaks with larger and more sea vessels involved (Maritime New Zealand, 2015; Rogowska and Namieśnik, 2010). Increased extraction and exploration and deeper wells all increase the potential for oil spills to occur. Temporal scales of exploration and the type of oil rig also influences oil spill probabilities. The aging of reservoirs also means increasingly large amounts of produced water discharges from existing production facilities, the impacts of which are unclear (NRC, 2003).

The massive Deep Water Horizon (DWH) well blow out significantly amplified the amount and proportion of oil released from platform leaks. In April 2010, the explosion and subsequent sinking of the Deepwater Horizon/BP MC252 drilling platform resulted in 87 days of oil leaking from the Macondo wellhead, 5000 feet below the sea surface (Smithsonian Institute, n.d.). 134 million gallons (3.19 million barrels) were estimated to have been released into the Gulf of Mexico (Smithsonian Institute, n.d.). During the DWH wellhead leak, capping and containment equipment was devised (Maritime New Zealand, 2015).

Since 1990, notable oil spills in New Zealand include the loss of 400 tonnes of automotive gas oil from the *Don Wong 529* in 1998 off Stewart Island, 60 tonnes of diesel off the Chatham Islands in 2000, 25 tonnes of fuel oil from the *Jody F Millennium* near Gisborne and a discharge of 7 tonnes of oily bilge near the Poor Knights by the *Rotoma* (Maritime New Zealand, n.d.). A discharge from the Umuroa FPSO in the Tui Oil Field released 23,000 litres of crude oil in October 2007 resulting in a large area of coastline being affected and an eight month cleanup operation although parts of rocky shoreline were left to self-clean (Taranaki Regional Council, 2008). New Zealand's largest oil spill to date was the result of the grounding of a cargo tanker; the *MV Rena* ran aground on the Astrolabe Reef (Otaiti) in the Bay of Plenty area in October, 2011. 350 tonnes of heavy fuel oil HFO, Bunker C was released into the environment during the weeks that followed. Six months later small amounts of oil were still being released into the sea (Bay of Plenty Regional Council, n.d.).

Table 4.5: PAH concentrations in a crude oil and two distillate fuel oils (Nagpal, 1993 adapted from Neff, 1979).

Compound	Kuwait Crude (µg/g)	No. 2 fuel oil (µg/g)	Bunker C residual oil (µg/g)
Naphthalene	400	4000	1000
1-Methylnaphthalene	500	8200	2800
2-Methylnaphthalene	700	18900	4700
Dimethylnaphthalenes	2000	31100	12300
Trimethylnaphthalenes	1900	18400	8800
Fluorenes	<100	3600	2400
Phenanthrene	26	429	482
1-Methylphenanthrene	-	173	43
2-Methylphenanthrene	89	7677	828
Fluoranthene	2.9	37	240
Pyrene	4.5	41	23
Benz[a]anthracene	2.3	1.2	90
Chrysene	6.9	2.2	196
Triphenylene	2.8	1.4	31
Benzo[ghi]fluoranthene	<1		
Benzo[b]fluoranthene	<1		
Benzo[j]fluoranthene	<1		
Benzo[k]fluoranthene	<1		
Benzo[a]pyrene	2.8	0.6	44
Benzo[e]pyrene	0.5	0.1	10
Perylene	<0.1	-	22
Benzo[ghi]perylene	<1		

Aside from obvious consequential damage to the shoreline, it is difficult to determine marine and ecotoxicological responses. The sensitivity of marine organisms to harmful hydrocarbons is variable, even within the same taxa, while the bioavailability and toxicity of the oil is determined by the weathering processes acting on the oil (NRC, 2003). PAH concentrations are relevant, as the volatility of the BTEX group compounds (monoaromatics) promotes evaporation during the initial stages of an oil spill, leaving heavier PAH compounds; both groups being extremely toxic. The resilience of heavier aromatic hydrocarbon components such as alkylated phenanthrenes and alkylated dibenzothiophenes means that they are not only the most persistent compounds in sediment but also in animal tissue (Capuzzo, 1987 as cited in NRC, 2003).

Confounding this, underlying natural fluctuations (due to decadal and multidecadal climate variability) and the altered compositions of functioning populations and communities post spill, on large spatial and temporal scales, makes recovery of ecosystems somewhat incalculable (ITOPF, 2011b; NRC, 2003). While four levels of biological organisation exist; biochemical and cellular, organismal, population and community; variation in population and community dynamics is still relatively unexplored (ITOPF, 2011b; NRC, 2003). Chronic physiological and behavioural disturbances may alter population and community dynamics. For example high fecundity species such as plankton show rapid recovery after oil spills however multi-generational effects in these mobile communities and altered population age distributions may occur (NRC, 2003).

Exposure times also govern the effects of oil spills on marine organisms; acute exposure by physical smothering or exposure to chemicals may have limited impact or may alter community or population numbers and/or makeup (NRC, 2003). When oil is dispersed in high concentrations in shallow inshore waters then mass mortalities may occur, especially of invertebrates. Light toxic components of crude oil cause bivalve molluscs to eject, leaving them gaping and vulnerable to predators (Rowson, 2014c). Chronic exposure due to pipeline bursts, discharges from offshore production, land run-off and exhumation of buried oil can result in sublethal effects even at concentrations several orders of magnitude lower than acutely toxic concentrations (Vandermeulen and Capuzzo, 1983 as cited in NRC, 2003). Loss of habitat or shelter, sustained reduction of prey populations, elimination of key species and ingestion of oil via prey can lead to delayed responses of marine bird and mammal populations to sub-lethal amounts of petroleum hydrocarbons in the sea (NRC, 2003). Sublethal effects are poorly understood.

The acute and chronic toxicity of petroleum hydrocarbons to marine organisms and seabirds is dependent on the amount, persistence and bioavailability of specific hydrocarbons (NRC, 2003). The abilities' of organisms to accumulate and metabolise various hydrocarbons, the fate of metabolised products, the interference of specific hydrocarbons (or metabolites) with normal metabolic processes (that may alter an organism's chances for survival and reproduction in the environment) and the narcotic effects on nerve transmission (especially of the lighter, volatile, hydrocarbons) are major biological factors in determining the ecologic impact of any release (NRC, 2003). Specifically sublethal effects of hydrocarbon exposure (especially PAH) may impair the reproductive output; growth, development and recruitment rates; feeding mechanisms and energetics of marine organisms while increasing their susceptibility to histopathological disorders especially when exposure occurs during important breeding times and in migratory routes (Capuzzo, 1987 as cited in NRC, 2003). Marine birds and mammals' mortality and reproductive rates may also be affected by the effects of hydrocarbons on distribution, abundance, or availability of prey (NRC, 2003). Indirect and delayed effects on structural development and biological composition are of ecological importance especially for shallow sediment species and other sensitive organisms (Peterson et al., 2003 as cited in Rogowska and Namieśnik, 2010). A period of twelve years was reported by Southward and Southward (1978 as cited in Barth, 2002) to remedy massive predatory-prey imbalances and shifts in species population dynamics after the *Torrey Canyon* oil spill. Most spill sites require 2-5 years for recovery of characteristic species (ITOPH, 2011b). Recolonization will depend on the time of year, the availability of recolonizing forms, biological interactions, and climatic and other factors (Kingston, 2002). Monitoring shellfish toxicity months after the sinking of *Rena* shows that oil is still present (de Groot, 2014).

Benthic sediment serves as sources of nutrients for aquatic organisms (Rogowska and Namieśnik, 2010). Oil products are rather severe pollutants because they accumulate in bottom deposits as a result of the high sorption capacity of the sediment-forming particulates and biochemically they are highly stable and can accumulate PAH. Tar products that settle on the bottom sediments may also destroy organism habitats including fish and shellfish nursing grounds (Global Marine Oil Pollution Information Gateway, n.d.). The accumulation of oil in the benthic environment allows secondary water pollution (Belkina, 2006 as cited in Rogowska and Namieśnik, 2010). Persistence of benthic oil depends on the oil characteristics, the sediment characteristics, temperature, the concentration of nutrients and the rate of biodegradation (Nikanorov and Stradomskaya 2003, as cited in Rogowska and Namieśnik, 2010). In 1990, over a year after the *Exxon Valdez* oil spill, mean TPAH (total polycyclic aromatic hydrocarbons) concentrations were 4–8 times higher in sediments collected from sites adjacent to heavily oiled shorelines than at reference sites (Rogowska and J. Namiesnik).

Communities of benthic dwelling species crabs, bivalves, and plants including plants are most affected in shallow areas with greatest exposure to oil. Intertidal invertebrates (infauna and epifauna) can be killed outright by heavy coatings or smothering, especially sessile species such as barnacles, which cannot escape the oil. Mobile invertebrates can become embedded in the oil, which may smother them or make them easy prey for birds and other predators (Rogowska and Namieśnik, 2010). As oil slicks hinder gas exchange with the air and limit penetration of solar radiation, catastrophic declines in benthic fauna from anoxia a heavily oiled fjord several months after an oil spill have been observed (Page et al. 2000). The intertidal area is a habitat for many juvenile and adult organisms during certain times of the year providing shelter for developing bacteria, unicellular algae and other microorganisms, gastropods, polychaetes and crustaceans (Rogowska and Namieśnik, 2010). Biological recovery of the intertidal habitat is largely a function of the nature of the habitat and the degree to which the shore has been cleaned.

The *Hebei Spirit* oil spill occurred in December 2007,~10 km off the coast of Taean, South Korea, on the Yellow Sea collided when a crane barge spilled ∼10 800 tons of Iranian heavy crude oil, primarily consisting of aliphatic/aromatic hydrocarbons and polar compounds as well as heavy metals and some volatile organic compounds. In one of the first studies to apply a combination of both instrumental and bioanalytical assessment to evaluate the potential toxic effects of oil-contaminated sediments, Hong et al. (2011) determined the concentration, distribution, composition of residual crudes in surface and sub-surface sediment along the Taean coast two years after the *Hebei Spirit* oil spill. Potential toxic effects of residual crudes were determined by use of the in vitro H4IIE-luc bioassay and mass balance analysis. The macrobenthic communities of the intertidal areas were analysed using the habitat mapping technique, which facilitates the understanding of community level responses to oil spills.

Detectable concentrations of residual crude hydrocarbons from the oil spill were found in all samples but were concentrated in muddy bottoms and in small bays, particularly in subsurface layers of muck, where flushing was negligible. Concentrations in these areas exceeded suggested sediment quality guidelines, potentially causing toxic effects for benthic organisms. Unidentified toxic substances, such as unverified PAHs, alkylated PAHs, alkylated phenols, and organic sulphur compounds are suspected to occur in crude oils which can be toxic to benthic organisms and humans following long-term exposure. Large amounts of dioxin-like compounds were found. Deeply buried oil appeared to be resistant to weathering and could cause long-term biological effects. Deposit feeding gastropods *Batillaria* were present in areas of high PAH concentration through tidal current immigration or egg capsules. After two years, the macrobenthic populations had almost completely recovered.

Bioavailability is the "extent to which a chemical can be absorbed or adsorbed by a living organism by active (biological) or passive (physical or chemical) processes" (NRC, 2003). Bioavailability is limited by the morphological form and properties of the chemical, the organism's ability to metabolise the chemical through the permeable epithelia surface area and the duration of exposure (NRC, 2003). Bioavailability is highest in solubilised oil (in water), followed by oil in tissues of marine organisms after consumption, or liquid unweathered droplets. The hydrophobic nature of petroleum hydrocarbons contribute to high lipid solubility. When rates of absorption into and desorption from the lipid phase of the organism are not in equilibrium and a critical concentration occurs with the lipid phase, a toxic response follows. The equilibrium of partitioning is approximated by the octanol/ water partition coefficient (K_{ow}) which increases with increasing molecular weight (NRC, 2003). Limited uptake by organisms, lower solubility in lipid phases and rapid metabolism leaves higher molecular weight compounds less bioavailable. Particulate and fine grained PAH are not bioavailable in highly weathered and buried hydrocarbons. Temporally, only a fraction of oil is bioavailable at a point in time. The bioaccumulation of hydrocarbons is influenced by bioavailability of the compounds, the solubility (morphodynamic form), the amount of lipids an organism has, their position in the food chain and metabolic transformations which may increase toxicity (NRC, 2003). Biomagnification increases concentrations of toxins by 3-5 times, two or more levels up the food chain, though some may be metabolised. Disease or mortality is measured by the concentration based on the water-accommodated fraction (WAF) of the oil, which is the fraction of an oil product that remains in the water phase after mixing and settling to measure toxicity.

Bioaccumulation and biomagnification of hydrocarbons are not believed to be of great concern to vertebrates such as fish and mammals since they are able to metabolize them

(NRC, 2003). Some invertebrates i.e. filtering organisms such as shellfish accumulate petroleum components in their tissue. Some contaminated shellfish however are be able to eliminate (depurate) hydrocarbons over time in uncontaminated waters. Mussels have been shown to depurate hydrocarbons within 16 days (Kingston, 2002). The effects (if any) of oil on these organisms have not been clearly established (Rogowska and Namieśnik, 2010).

Direct mortality for marine mammals and birds can occur when migration pathways intersect oiled zones and when populations are concentrated in small areas. Reduced and contaminated prey can also have an effect (Office of Response and Restoration (NOAA), 2016a). Many marine mammals have shown resilience to chronic exposures to petroleum hydrocarbons however some sea otters have shown sensitivity (Geraci and Williams, 1990; Monson et al., 2000 as cited in NRC, 2003).

A study by Heintz et al. (1999 as cited in NRC, 2003) on exposures of fish eggs and embryos (pink salmon) to relatively modest amounts of PAH (1 ppb total PAH) corroborated field observations of embryo mortality of pink salmon after the *Exxon Valdez* spill. About 2.3% of the approximately 1300 wild-stock pink salmon streams suffered significant oiling in tidally influenced reaches after the spill. Even smaller concentrations of PAH (0.7 ppb total PAH) were observed to increase mortality and impaired physical function of Pacific herring when eggs were exposed to ANS crude for 16 days. Equivalent responses to unweathered oil were found at higher exposure concentrations (9.1 ppb) (Carls et al., 1999 as cited in NRC, 2003). It has been postured that high concentrations of other compounds present with PAH in weathered oils contribute to the increased toxicity (Heintz et al., 1999 and Carls et al., 1999 in NRC, 2003). Impairment of behavioural, developmental, and physiological processes may occur at concentrations significantly lower than acutely toxic levels. Although wild herring and salmon larvae and fry individuals (a few percent were negatively affected with exposure to oils during the *Exxon Valdez* spill, the concentration were not high enough and exposure duration did not persist long enough to cause lethal and sublethal effects to pelagic life stages of fish populations in PWS (Boehm et al, 2007). Fish are at risk from spilt oil during spawning, when eggs are attached to intertidal and shallow subtidal macroalgae and during migration to spawning shores.

The presence of aromatic compounds has been correlated to the stress indices (scope for growth and lysosomal properties) and tissue concentration in *Mytilus edulis* bivalve molluscs.

The depuration of PAH negated some of these effects (Widdows et al. 1982 as cited in NRC, 2003). Scope for growth in *M. edulis* deficiency has also been linked to the effect on ciliary feeding mechanisms of accumulation of two- and three-ring aromatic hydrocarbons (Donkin et al. as cited in NRC, 2003). Benthic fauna, amphipods and cetaceans have all shown negative long term effects from No. 2 fuel oil; mortality, recruitment and population densities have all been affected (NRC, 2003).

The individual populations of the amphipod, *Ampelisca*, were killed off immediately after the 1978 *Amoco Cadiz* oil spill. It took ten years for population density of *Ampelisca* to recover although standing crop biomass and productivity had recovered rapidly as opportunistic species had taken the amphipods niche (Kingston, 2002). Populations of the bivalve *Abra alba* in the Bay of Morlaix, Brittany had recovered after only two years. Within 8 years of the *Amoco Cadiz* oil spill, the Brittany area had returned to normal except the most heavily oiled areas (Kingston, 2002).

Buried oil and residue is also directly toxic to plant life, reducing germination and leading to poor seeds. Plants occupying intertidal areas are most at risk (compared to subtidal plants) as they can be directly coated by stranded oil for long periods of time. Loss of plant-covered areas may impact the community at large, because many organisms use plants as habitat and a source of food. Although the faunal community may recover within a year or two, final return of the entire ecosystem to non-oiled condition can take up to a decade (NRC, 1985).

Salt marshes are generally associated with temperate climates and mangroves with the tropical regions (Allen, J.R.L, Pye, K, 1992; Morrisey, D., Beard, C., Morrison, M., Craggs, R., Lowe, M., 2007). Mangroves provide shoreline protection through stabilisation of the sediments (Graeme, 2012; NRC, 2003). Most damage is done when oil smothers the leaves and blocks lenticels for oxygen uptake in aerial root systems. Oil is also translocated from the roots to the leaf stomata affecting transpiration and disruption to root membranes allowing salt to accumulate in tissue. The degree of damage is dictated by the oil characteristics including toxicity, residence times and concentrations; the degree of oiling to exposed roots and substrate; tidal heights and ranges; and the season and life stage of the plants. Recovery is usually timely, dictated by the amount of damage to the ecosystem including clean-up, persistence of the oil and the ability for the system to recover. Recovery can occur if the impact is not severe, during plant dormancy phases, when plants are mature and when oil is not mixed into the sediment (Boyd et al., 2001). Levels of nutrients, bacteria and oxygen as well as sediment type all influence the recovery. The feedback of biogenically-structured communities lengthens the time required for recovery; biological communities are dependent on the physical structures of the plants while the structures rely on structure forming species to stabilise the habitat. Loss of key species could result in permanent effects for the habitat; mortality, unstable habitats (NRC, 2003). Sediment erosion may result which can potentially transport contamination ((NRC, 2003). Osmoregulation by some mangroves, including the black mangrove *Avicennia germinans,* renders them capable of uptaking oil through the roots to the vascular system.

In February 1969, in Milford Haven, Wales, deposits of heavy fuel oil on parts of the Martinshaven marsh resulted in the smothering and subsequent death of the marsh plants. Recovery however had begun 1 year after the spill and within 15 years only heavily degraded oil persisted. Fresh oil was found in the salt marshes near Puerto Espora, Tierra del Fuego, 17 years after the *Metula* spill of light Arabian crude in the Strait of Magellan, Chile (Baker et al., 1993). Recovery times will be reduced with light to moderate oiling of oils with higher fractions of light components, warmer temperatures, mineral rich soils, less intrusive clean-up methods, small tidal heights at time of oiling and larger tidal ranges (NRC, 2003). It was observed that after a spill in the northern Puget Sound, Washington, most salt marsh plants had begun to recover within the first year however where heavy oiling occurred, no recovery was observed (Hoff et al., 1993 as cited in Barth, 2002). With continued exposure and damage to their root systems, marshes can be severely affected. In post DWH studies of Louisiana salt marshes, recovery within 1.5 years had occurred, except in areas where erosion had exposed substrate and permanent loss resulted. Erosion rates were twice as high at oiled sites. Mass mortality of mussels, snails and plant material had occurred with exposure to PAHs levels more than 100x higher than in the non-oiled. The oil had heavily coated the marsh plants preventing photosynthesis. The mortality of the stabilising root matrix caused a geomorphic response (Silliman et al., 2012).

Seagrass provides erosion protection by tempering turbulent energy and increasing sedimentation. Spilled oil usually floats over seagrass but with large concentrations, oil may smother the woody perennial. Seagrass mortality within the tidal zone is higher within the first year after an oil spill due to direct exposure to oil. Leaves are affected in the subtidal areas. Rhizomes of seagrasses are not exposed. It has been shown that the density of shoots and flowering shoots *Zostera marina* decreased after > 5 years after the *Exxon Valdez* disaster though no change to the biomass of seagrass meadows was found; likewise after the Gulf spill (NRC, 2003). This is suggested to occur because of the lateral root growth of seagrass. Estuaries are often located proximal to oil transports routes or storage (NRC, 2003).

The low energy environments of kelp and mussel beds are often holdfasts for oil and fine sediments, trapped in the pore spaces (e.g. after the Macquarie island spill) (Irvine, 2006; NRC, 2003). Corals if in direct contact with oil over large temporal scales will take a long times to recover i.e. in mangroves near reefs. Reef organisms exhibit reduced or suspended growth and reproduction, and abnormal behaviour or death (Boyd et al., 2001). Sublethal effects observed in the laboratory include tissue death and decreased calcium uptake (Boyd et al., 2001). Macroalgae such as kelp, have large exposed surface areas and can perish from exposure to oil. Reduced reproduction also occurs and these canopy plants can experience bleaching. However if organisms feed off contaminated kelp, then the kelp can rejuvenate itself (Boyd, 2001).

Soft sediment shorelines (fine sands and mud), such as Moonlight Bay, are biologically productive habitats, with large numbers of sediment dwelling invertebrates, migratory birds and bivalves; they are also nursery grounds for coral reefs and near shore fish stocks (ITOPF, 2011b). These low energy environments are extremely sensitive to oil pollution. Sedimentation of stable oil-mineral-aggregates occurs in these systems with no known practical clean up methods (Kingston, 2002). Limited water movement in these sheltered zones allows oil to become buried in the fine sediments, sometimes persistent for decades. As these areas are sensitive and vulnerable they rank highest on the Environmental Sensitivity Index (ESI) (Table 4.7) (Rowson, 2014c); a classification scale designed for ranking shorelines according to sensitivity, natural persistence of oil, and ease of clean-up, based on exposure to shoreline wave and tidal energy, slope, substrate type, biological productivity and sensitivity (Andrade et al., n.d.; NOAA, 2002; NRC, 2003; Wang and Roberts, 2013). Clean-up can cause such extensive physical damage in these areas that they are often left to self-clean (ITOPF, 2011b).

Table 4.6: Simplified ESI classification system. After Michel, Hayes and Brown, 1978. Adapted from NOAA, 2002.

ESI Code	ESTUARINE ENVIRONMENTS
1A	Exposed rocky shores
2A	Exposed wave cut platforms in bedrock, mud or clay
3A	Fine to medium grained sand beaches
4	Coarse grained sand beaches
5	Mixed sand and gravel beaches
6A	Gravel beaches
7	Exposed tidal flats
8A (impermeable)	Sheltered scarps in bedrock, mud or clay & sheltered rocky shores
9A	Sheltered tidal flats
10A	Salt and brackish water marshes
10B	Freshwater marshes
10C	Swamps
10D	Mangroves
10E	Inundated low lying tundra

On low energy shorelines oil is commonly highly weathered (Scholz et al., 1999) and remains on the surface due to lack of turbulent mixing however during storm events oil can mix with suspended sediment and become buried. Oil can also become bioturbated into the sediment, through such things as worm burrows and open plant stems. Oil can remain buried in soft sediments for years while the anaerobic conditions within the sediment prevent further degradation (ITOPF, 2011a).

New Zealand's mangrove (*Avicennia marina subsp. australasica*) incidence terminates just south of Raglan Harbour at 38 ° S (Morrisey et al., 2007), while salt marshes are common throughout New Zealand, generally at the heads of estuaries though species vary geographically (Wassilieff, 2012). Stunted shrublands of mangrove subsist in Raglan harbour with prevalence in the arms of the Waingaro River arm. Seagrass (*Zostera muelleri*; previously *Z. novazelandica* and/or *Z. capricorni*) beds are extensive around the township of

Raglan, near Moonlight Bay and into the Opotoru River and Waingaro River arms. Salt marsh rushes and sedges; sea rush *Juncus krausii subsp. australiensis* and oioi *Apodasmia similis,* along with saltmarsh ribbonwood *Plagianthus divaricatus* are extensive in the Ohautira and Waitetuna arms, in pockets in the exposed parts of the harbour and at the head of Waingaro River arm (Graeme, 2012).

In the Waitetuna River arm, bittern and fernbird dwell, associated with the saltmarsh ribbonwood and remnant freshwater wetland vegetation. Thin bands of sea meadow communities exist in the more exposed parts of Raglan harbour (Graeme, 2012). Though New Zealand mangroves display moderate abundance and species diversity, two species fully depend on and are endemic to mangrove habitats; an eriophyid mite *Aceria avicenniae* and a tortricid moth, the mangrove leafroller *Planotortrix avicenniae*. *Ctenopseustis obliquana, Oemona hirta* (lemon tree borer) and the pyralid *Ptyomaxia* sp. are also ubiquitous. Terrestrial invertebrate fauna of New Zealand's mangroves forests is relatively unknown and the benthic invertebrate fauna distributions and numbers appear modest. Ant colonies and geckos are also found within New Zealand mangrove ecosystems. On the west coast, grey mullet *Mugil cephalus* and nationwide; yellow-eyed mullet *Aldrichetta forsteri*, short-finned eels *Anguilla australis* and parore *Girella tricuspidata* use the mangrove habitats as nursery grounds for juvenile fish. Mangroves are also frequently used for roosting, feeding and breeding of many species of birds including white-faced heron, harriers, grey warblers, kingfishers, welcome swallows, pukeko and silvereyes, pied and little black shags, bitterns, royal spoonbills and banded rails (Morrisey et al., 2007).

In a study for the Aqualink project off the west coast of New Zealand, no infaunal animals were observed on Ngarunui Beach (Patel, 2015), due to the intensity of the wave action (preventing settlement) however Beca (2000 as cited in Patel, 2015) reported patchy distributions of tuatua (*Pahies subtriangulatum*), toheroa (*Paphies oentricosa*), paddle crabs (*Ovalipes catharus*) and small concentrations of other amphipods (*Haustorus sp*.), ghost shrimps (*Callianassa filholi*), bivalves and occasional gastropod species in similarly exposed shorelines north of Raglan (Manukau heads to Kariotahi). Flounder, skates and rays are known to feed on the seabed in the area. Trough shells *(Scalpomactra scalpellum – Maorimactra ordinaria* and the bivalve shellfish assemblage *Nemocardium pulchellum – Pleuromeris zelandica* are widespread on the offshore open shelf at depths of 20-98 m while in the nearshore zone it was concluded that communities of marine life are limited and dominated either by deep burrowing bivalve shellfish or species readily able to burrow into the seabed (e.g. tube dwelling polychaete). Cetaceans including humpback whales, orca and Maui's Dolphin are known to frequent the area. Fine to medium grained, high energy sand beaches such as Ngarunui Beach are considered less sensitive to marine oil contamination, while the sheltered rock shore with exposed tidal flat at Moonlight Bay represents one of the most sensitive ecosystems according to National Oceanographic and Atmospheric Administration's (NOAA) Environmental Sensitivity Index (ESI) (Table 4.7).

Rocky shorelines are commonly where oil spills are likely to occur (NRC, 2003). Well adapted to the scouring effects of pounding waves, the flushing of tides and drying winds, these ecosystems rapidly self-clean. Ephemeral plant and animal communities recover quickly (Kingston, 2002; Rowson, 2014c). Direct smothering of *Fucus*, mussels, periwinkles, starfish and barnacles has been observed oil spills of North America (NRC, 2003). Severity of disturbance at rocky intertidal shores is determined by the (type and amount) wave and tidal energy with shoreline geomorphology for recovery ecological structure of the shoreline important, but the type of oil, the weather conditions following the spill, the thickness and lateral continuity of the slick, the time of year, and the recent history of disturbance of the biological communities are all important factors affecting severity (Rowson, 2014c). Bivalves can be flushed out of rocky environs by clean up processes. Toxicity soluble fractions of oil may occur in small pools of water and on the wetted surfaces of rocks from contaminated sea water (NRC, 2003).

The process of surf washing, clean up by mechanically depositing oiled sediment from the higher intertidal zones into the energetic surf zone) is most effective on high energy beaches where strong wave energies can flush oil from the sediment (ITOPF, n.d.). wind and tidal currents need to be right so not offshore and not sensitive.

Not only do oils spills have adverse effects on aquiculture and mariculture resources; the physical contamination of high amenity areas can have long term economic effects through loss of tourism, loss of recreational amenities, clean-up costs which can reach several billion (the *Exxon Valdez* supertanker spill), local property values and regional business (NRC, 2003). Though prospects for recovery are generally good, limited evaluation of chronic effects of oil spills exist as it falls outside of the scope of oil spill clean-up.

Estimates of shoreline recovery have been between five years to decades (Hayes et al. 1993). Some estimates have exceeded 170 years (Vandermeulen and Gordon (1976 as cited in Edrick et al., 2007). Alkylated benzene and alkylated PAH distribution and *N*-alkane analysis was carried out by Wang et al. (1999) on samples from the Northern Alberta wetland after the Nipisi pipeline spill in the early 1970s. Twenty five years after the spill, residual subsurface is relatively unweathered due to acidic conditions, extremely low temperatures (annual temperatures of 1.7 °C) and water saturation in the peat. Oil deposited on muds near Punta Espora after the 1974 *Metula* spill has not been reworked by wave action and was still mobile in places 30 years later (Owens and Sergy, 2005). Oil pavements at depths > 1m with unweathered cores were still present 36 years after the *Arrow* spill on affected beaches (Kingston, 2002). Persistent and toxic alkyl PAH homologues were present at the spill site after 22 years (Lee et al., 2003).

CHAPTER FIVE: SETTLING EXPERIMENTS

5.0 INTRODUCTION

To simulate the effects of oil on sediment settling time and behaviour, microcosm experiments using settling flasks and varying sediment/oil ratios were undertaken. Two distinctive sediment compositions were tested in order to observe any distinctive characteristics and behaviours; one dark, titaniferous magnetite rich sand from an open coast beach, typical of New Zealand's west coast (Brander, R.W., Osborne, P.D., Parnell, K., 2003 as cited in Goff, Nichol and Rouse, 2003); the other from a low energy estuarine environment. Additionally two distinct oil types were tested with each sediment; one a Heavy Fuel Oil sample with high viscosity and medium density, the other a high wax, medium density co-mingled crude oil.

Recorded video and photographic imagery was used to observe settling times and behaviours. Observational analysis of the interactions of Maari/Moki co-mingled crude oil and Heavy Fuel Oil (HFO) (in varying amounts of 10 ml and 20 ml) with representative Ngarunui Beach and Moonlight Bay sediments was undertaken using a stereo - microscope at between 10x and 63x magnification.

This chapter presents the results from settling experiments, including settling times, distributions and behaviours. Observational investigations of the sediment/oil/water interactions at varying depths in the water column are also summarised. Settling behaviour and oil and sediment interactions are then analysed in the context of the wider literature on oil-sediment interactions.

5.1 RESEARCH METHODS

5.1.1 SETTLING EXPERIMENTS

The Heavy Fuel Oil sample from aboard the Awanuia ship on the 13th of March, 2013 had similar properties to those of the HBFO aboard the container ship *Rena*. The Awanuia oil sample is likely to be either a RMF 380 or RMK 380 – 700 with a kinematic viscosity at 50 °C of < 380 or < 700 mm^2/s and a density of < 0.991 or <1.010 (Bunker Oil - Marine Fuel Oil, n.d.) although the average kinematic viscosity is likely to be between 154 – 176 mm^2/s at 50 °C (Table 5.1). The release of a persistent, heavy fuel oil or residual fuel oil (No. 6, Bunker C) would likely result in a thick dark slick. Some dense, viscous residual fuels can float below the water surface and some break into discreet patches or balls and sink or become sedimented into tar mats. Tar balls can disperse for hundreds of kilometres. Water-oil emulsions may form with time. HFO is not likely to disperse into the water column however. The high viscosity of HFO prevents permeation into beach sediments so it often remains on the surface of beaches unless morphological variation results in burial (Office of Response and Restoration, NOAA, 2016a).

Table 5.1: Maari/Moki crude oil and Heavy Fuel Oil (HFO), No. 6 Fuel Oil, Bunker C characteristics. Adapted from Maritime New Zealand (2014) and OMV New Zealand (2015).

Oil Characteristics	HFO No. 6 Bunker C	Maari/Moki crude oil
Density at 15 °C kg/l	0.947 – 0.952	0.836
Flash Point °C	107 – 111	< 23
Kinematic viscosity mm^2/s at 50 °C	154 – 176	3.73
Pour Point °C	-3 – 3	24
Total Sulphur % mass	2.16 – 2.48	
Hydrogen sulphide		< 1 ppm

The Maari/Moki co-mingled crude oil is a highly flammable, medium density, very low sulphur, waxy crude oil for use as refinery feedstock (Table 5.1). It is immiscible in water. It is a Class 3 hazardous chemical with carcinogenic and mutagenic properties and is very toxic to aquatic life with long lasting effects (OMV New Zealand, 2015). Crude oils are likely to remain on the water surface, forming slicks. As crude oils become more adhesive and viscous with weathering, increased adhesion precludes penetration. The presence of waxes, resins and asphaltenes increases the likelihood of formation of water-in-oil emulsions (Etkin et al., 2007).

Beach sand was compacted into the bases of 1 litre settling flasks (class A+) up to 150 ml and subsequently filled to the 1 litre mark with seawater from Ngarunui Beach. The mean initial temperature of the seawater was 16°. Beach sand was sourced from the low-tide zone on Ngarunui Beach and in the low tide zone at Moonlight Bay. This allowed observation and comparison of the effects of oil on a medium grained sediment sample and a clay type sediment with a larger grain size distribution from the inner estuary. Mean grain sizes was 1.789 φ (0.289 mm) for the Ngarunui Beach sediment with sorting, skewness and kurtosis values of 0.528 φ, 0.007 φ, 0.951 φ respectively. Mean grain size for the Moonlight Bay sediment for the size fraction under 3 mm was 1.367 φ (0.388 mm) with sorting, skewness and kurtosis values of 0.638 φ, -0.049 φ and 0.955 φ respectively. The fraction above this size was 32.07 % in the Moonlight Bay sediment. Although detailed analysis of beach composition was not available, it is plausible that a high percentage of the sand from both Ngarunui Beach and Moonlight Bay is siliclastic, with a major portion being quartz and lime-soda feldspars while the black sand from Ngarunui beach islikely to contain more titaniferous oxide (New Zealand Steel, 2016). Bioclastic fractions were much greater in Moonlight Bay samples from visual approximation (very little shell was found in Ngarunui Beach sediments except during storm events).

Two control experiments after de Groot (2014) were prepared and used as baselines for the settling velocity and behaviour of sediment without the addition of any oil; the first containing sediment from Moonlight Bay and the other using Ngarunui Beach sediment. Together with absolute settling times, the relative amounts of settling at various times during the control experiment were observed and applied as a baseline for comparison with the oil coated sediment. 10 ml and 20 ml of HBFO 380 were added to two more flasks respectively and the settling behaviour and times were gauged. To a fourth and fifth flask, 10 ml and 20 ml of Maari/Moki co-mingled crude oil were added and the same experimental procedure was followed. The concentration of oil resembled heavy oiling conditions.

To simulate the turbulent conditions of the intertidal zone caused by the process of breaking waves and interactions of waves and currents, the sediment/oil mixture was agitated for approximately 30 seconds using a metal stirrer after the method of de Groot (2014). Settling behaviour was examined from visual recordings taken during the experiments. Photographs were also obtained at 5 - 10 second intervals during settling. Sediment settling was easily observed as sand grains were visibly distinguishable from oil and the surrounding medium. Oil settling was defined as the point at which > 95 % of the oil has settled and is often nearly stationary. In some experiments large amounts of oil adhered to the metal stirrer and sides of the flasks, especially those using Maari/Moki crude oil. The experiments were repeated a minimum of 6 times. However some experiments were repeated more than this as settling was hard to observe in the initial experiments. These experiments were included in the final analysis as they did not affect the spread of the data.

5.1.2 MICROSCOPIC INVESTIGATION

Following the methodology of de Groot (2014) after completion of sediment settling experiments, sub-samples were taken from the water surface, the sediment surface (or close to) and the top, middle and base of the water column and observed under 10x – 63x magnification. Aliquots were pipetted from each 1 litre graduated cylinder however in this method, oil, especially HFO, adhered to the plastic pipettes and contamination could not be avoided in a few of the samplings. The aggregations and/or flocculations of particles or colloids in suspension are referred to as an aggregation for the purposes of this study as the prevalent mechanism of formation is unknown. No differentiation between oil-mineral-aggregates and mineral aggregates is made, due to magnification limitations, except with the obvious presence of sediment and oil.

It was not possible to utilise a microscope with polarising filters for observation of the experiment sub-samples, so a stereo-scope with 10x - 63x magnification was used. The use of episcopic illumination with reflected light rather than diascopic illumination allowed examination of some opaque oil forms. Sample containers were placed directly on the object space of the microscope. Photomicrographs were collected for all sub-samples. Quantitative image analysis is possibly most effective using one of the following methods; x-ray fluorescence, environmental scanning electron microscopy (SEM), confocal scanning laser microscopy, UV epi-fluorescence microscopy (UVS) (Stoffyn- Egli and Lee, 2002) and particle image velocimetry (PIV) (Wang et al., 2011). As quantitative microscopical observations were not made within one week after sub-sampling, residual oil concentrations and florescence were likely reduced by chemical and biological processes. Examination under diascopic microscope was more appropriate for this reason also.

5.2 RESULTS

5.2.1 SETTLING FLASK EXPERIMENTS

5.2.1.1 Control Experiments

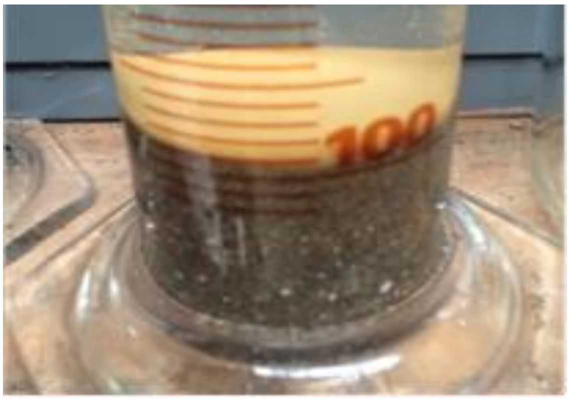

Figure 5.1: Fine sediment surface layer on the Moonlight Bay sample.

Settling was distinctive between sediment from the different sites. The mean settling times for the Ngarunui and Moonlight Bay sediments control experiments were 23.594 seconds and 11.571 seconds respectively (Table 5.2). The water became more turbid in the Moonlight Bay sample after mixing. Settling of both sediment types resulted in a surface layer flocculated particles with a distinctive yellow hue (Figure 5.1).

5.2.1.2 Sediment Settling

The average time for Moonlight Bay sediment to settle in oiled samples ranged from 14.618 to 16.406 seconds, while the average time for Ngarunui Beach sediment to settle in oiled samples ranged from 18.660 to 21.683 seconds (Table 5.2 and Figure 5.3). Interestingly, all sediment settling experiments with Ngarunui Beach sediments were between 0.99 and 7.018 seconds faster than the average control time while all experiments using Moonlight Bay sediments were between 0.093 and 9.564 seconds slower (Table 5.2). One outlier was 0.249 seconds slower than the Moonlight Bay control average.

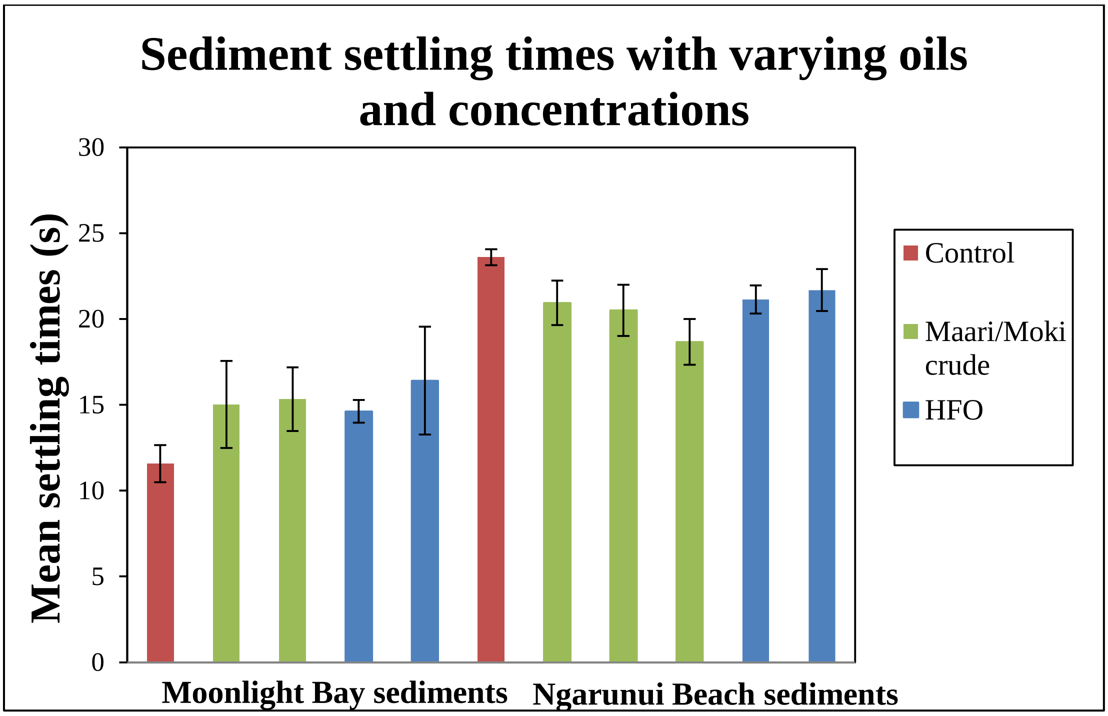

Figure 5.2: **Variation in sediment settling times with different oil concentrations and types.**

Table 5.2: ***Sediment settling times during settling flask experiments using both HFO and Maari/Moki co-mingled crude oils), in varying amounts of 10 ml and 20 ml with Moonlight Bay and Ngarunui Beach sediments respectively. The results from experiment 10 ml Maari marked with ** were performed outside in temperatures exceeding 15 °C.***

	Moonlight Bay sediments					*Ngarunui Beach Sediments*					
Experiment	**Control**	**10 ml Maari (%)**	**20 ml Maari (%)**	**10 ml HBFO (%)**	**20 ml HBFO (%)**	**Control**	**10 ml Maari (%)**	****10 ml Maari (%)**	**20 ml Maari (%)**	**10 ml HBFO (%)**	**20 ml HBFO (%)**
1	10.198	16.422	14.337	14.268	21.135	23.670	19.471	21.755	17.560	21.651	19.419
2	11.436	16.659	16.531	14.357	15.460	23.696	20.807	21.303	16.576	21.998	20.265
3	13.241	15.603	14.980	13.807	16.767	24.257	20.459	20.565	17.756	21.334	21.030
4	12.369	17.246	16.975	14.951	13.556	23.015	21.573	18.395	19.450	21.590	22.685
5	10.846	19.398	18.275	15.741	13.188	23.332	18.566		17.502	20.384	21.835
6	11.337	14.480	15.126	14.582	20.152		20.437		18.306	19.888	22.279
7		13.734	17.394		14.582		20.646		21.151		21.538
8		13.692	16.959				21.940		19.380		22.705
9		11.322	12.569				21.476		19.577		23.495
10		11.664	14.000				19.831		18.248		21.580
11			13.462				22.429		19.839		
12			13.355				23.460		19.663		
13							21.105		18.673		
14									20.878		
15									18.644		
16									18.215		
17									15.931		
18									*		
19									17.943		
20									19.250		
Mean settling times (s)	**11.571**	**15.022**	**15.330**	**14.618**	**16.406**	**23.594**	**20.938**	**20.505**	**18.660**	**21.141**	**21.683**

5.2.1.3 Oil Settling

Oil settling times were comparatively longer than settling times for sediments, mean oil settling times were between 72 and 129 seconds for HFO and 36.25 and 46.428 for Maari/Moki crude (oil settling times were much faster, 21.25 seconds with higher temperatures). HFO settling times were consistently higher than Maari/Moki crude; approximately 3 times as high (Table 5.3 and Figure 5.4). Settling times for Maari/Moki crude were relatively uniform with both sediment types (Table 5.3 and Figure 5.4). HFO settling times showed greater variation; settling was protracted with greater sediment concentrations, averages were nearly twice as much for Ngarunui and percentage increase of 14 %for Moonlight Bay sediments. The large standard deviations from most of the Moonlight Bay samples (especially using HFO) shows how highly variable the results are, probably due to poor visibility.

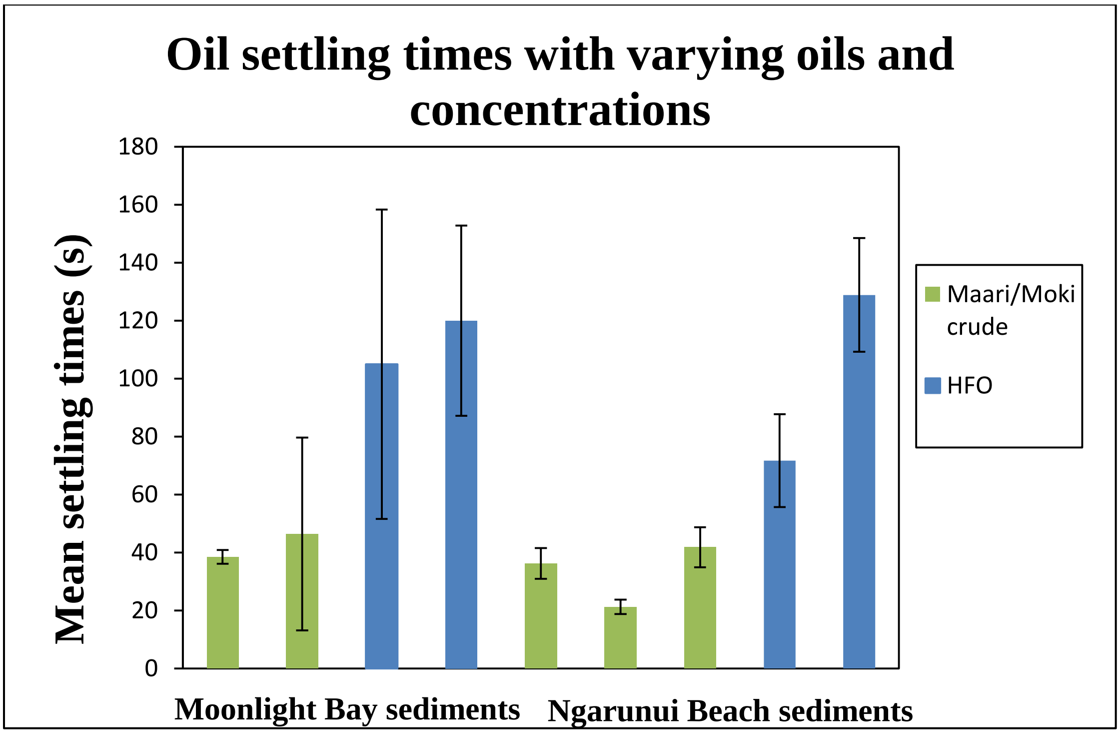

Figure 5.3: **Variation in oil settling times with different oil concentrations and types.**

Table 5.3: ***Oil settling times during settling flask experiments using both HFO and Maari/Moki co-mingled crude oil, in varying amounts of 10 ml and 20 ml with Moonlight Bay and Ngarunui Beach sediments respectively. These values are rounded to the nearest whole number for simplification. Note: *'s denote experiments in which settling times were unable to be determined. The results from experiment 10 ml Maari marked with ** were performed outside in temperatures exceeding 15 °C.***

	Moonlight Bay sediments				*Ngarunui Beach sediments*				
Experiment	**10 ml Maari (%)**	**20 ml Maari (%)**	**10 ml HBFO (%)**	**20 ml HBFO (%)**	**10 ml Maari (%)**	****10 ml Maari (%)**	**20 ml Maari (%)**	**10 ml HBFO (%)**	**20 ml HBFO (%)**
1	35-45	35	150	*	30	25	55	50	150
2	35-45	85	75	>120	35	20	40	60	120
3	35-45	*	*	80	45	20	40	70	150
4	35-45	*	150	80	35	20	55	90	150
5	35-45	30	>45	>120	35		40	70	130
6	40	30	*	80	45		40	90	120
7	35	30		>120	40		40		90
8	35	120			35		45		120
9	35	*			35		50		130
10	40	*			*		35		*
11		*			40		35		
12		50			30		40		
13					30		40		
14							45		
15							45		
16							30		
17							*		
18							35		
19							50		
20							35		
Mean settling times (s)	**37**	**49**	**125**	**>120**	**36**	**21**	**42**	**72**	**129**

Table 5.4: ***Average percentage of settling for oil at varying time intervals.***

	Moonlight Bay sediments				*Ngarunui Beach sediments*			
Time elapsed (s)	**10 ml Maari (%)**	**20 ml Maari (%)**	**10 ml HBFO (%)**	**20 ml HBFO (%)**	**10 ml Maari (%)**	**20 ml Maari (%)**	**10 ml HBFO (%)**	**20 ml HBFO (%)**
~ 5	48	50	20	40	50	40	50	49
~ 10	56	60	35	45	55	50	58	57
~ 15	63	72	45	48	63	60	60	62
~ 20	70	72	50	55	74	70	68	67
~ 25	77	73	55	55-60	79	78	70	70
~ 30	85	77	55	50-60	85	84	74	72
~ 35	88	77	60	60	92	88	77	74
~ 40	95	80	70	65	90	90	80	77
~ 45		85	73	50-65	95	91	83	80
~ 50		87.5	78	50-70	95	93	84	82
~ 55			80		95	93	87	84
~ 60		90	80			95	88	85
~ 70		95	>90			95	94	88
~ 90							85-95	89
~ 120		95					90	92
~ 150			95					95
~ 240								95

Note: These are averaged settling percentages; most but not all experiments followed a characteristic progression.

The relative percentages of oil settling during the initial stages of the experiments are high (Table 5.4). Within the first 5 seconds, an average on 43 % has settled. Average settling of oiled Moonlight Bay sediment at 15 seconds is 57 % and for Ngarunui Beach sediments at 25 seconds is 74 %. The low averages for Moonlight Bay sediment reflects the slower settling of the HFO. Equivalent settling percentages of Ngarunui Beach sediments are apparent at 25 seconds however HFO settling slows after this time. As the sand fraction settled, oil settling slowed (Table 5.4), especially for Ngarunui Beach sediment with HFO oil.

5.2.2 EXPERIMENT OBSERVATIONS

The descriptions below outline the important events that occurred during settling experiments.

5.2.2.1 *Experiments using Moonlight Bay sediments and 10 ml of Heavy Fuel Oil (HFO)*

- Cloudy, turbid water in most experiments.
- Spherical droplets were between < 1mm and 10 mm with most 2 - 3 mm in diameter (Figure 5.4). Larger droplets resurfaced immediately due to buoyancy and proximity to the surface.

Figure 5.4: **Spherical and oblate droplets resurface within the first 10 seconds.**

- Settling slowed substantially after the sand has settled at around 15 seconds and again at 40 seconds.
- Most oil moved toward the water surface in these experiments to form a thick slick, > 15 - 20 mm, on the water surface. This slick was highly aerated and contained 60-90 % of total oil by volume in all experiments (Figure 5.5).

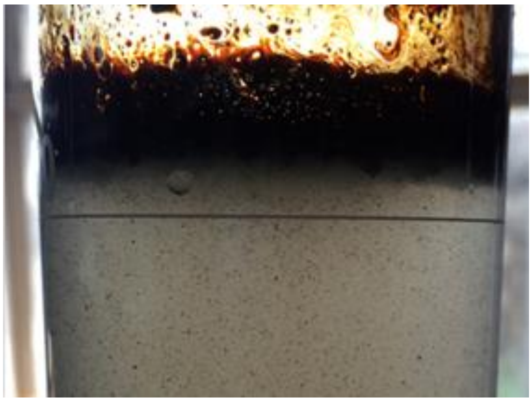

Figure 5.5: **Thick aerated slick that formed at the water/air interface.**

- A smaller proportion of oil descended to the bottom of the flask to become buried within the sediments.
- After 15 seconds, most oil droplets were between~1 mm and 2 mm; mostly solitary droplets though some coalesce.
- Droplets and grains were well distributed throughout the water column.
- After 30 seconds more than half the oil had settled.
- Fine sediment and small oil droplets were present but were moving very slowly or were stationary at > 1 minute.
- Oil and larger grains were sparse after 3 minutes (< 5 % by volume) however fine clay sediments and small oil droplets were still in suspension.
- Water remained cloudy after 6 minutes due to the fine sediment contained in the Moonlight Bay sample.
- The thick surface oil layer had a very cohesive form in this sample after settling of~36 hours. The convex shapes of spherical tar balls can be seen protruding below the slick. Grains are not able to be seen in the slick (Figure 5.6).
- At 45 seconds, large aggregations can be seen on the surface of the bottom sediments (Figure 5.7).

***Figure 5.6 (left)*: Thick surface oil layer with distinctive convex shapes distended from it's base after 36 hours. *Figure 5.7 (right):* Tar balls and aggregations were just visible on the surface of the sediment.**

- Spherical, dark tar balls (up to < 5 mm in diameter but predominantly smaller) were visible on the surface of the bottom sediments after approximately 60 hours (Figures 5.8 and 5.9).
- A thin yellow layer of fine sediment flocs coated the sediment surface and tar balls after settling (Figure 5.9).

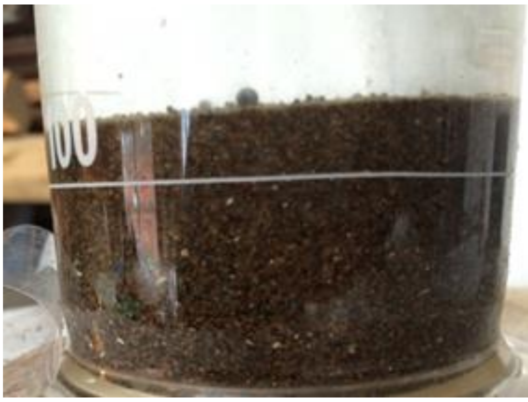
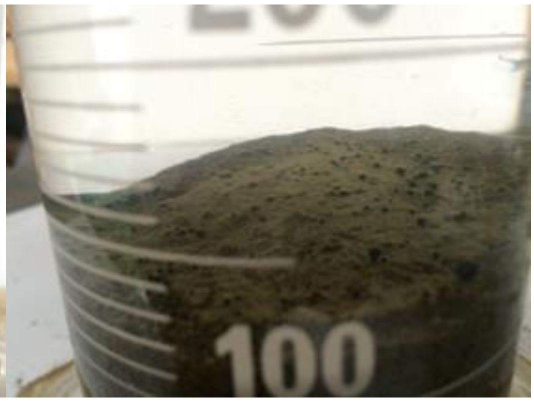

***Figures 5.8 (left) and 5.9 (right):* Tar balls on the sediment surface after approximately 60 hours and 36 hours respectively.**

5.2.2.2 Experiments using Moonlight Bay sediments and 20 ml of Heavy Fuel Oil (HFO)

- Most experiments were too turbid to accurately account for oil settling times and proportions.
- 1 – 2 or 3 mm dark, spherical oil droplets and aggregations resurfaced immediately due to buoyancy and proximity to the surface; after 15 seconds only smaller droplets were visible.
- Most oil moved toward the water surface in these experiments.
- Oil settling slowed a lot after 20 seconds in all of these experiments and again at 90 seconds and the water did not clear.
- The water cleared a little at 1 minute 30 seconds and at around 2 minutes became stationary. The water column was still turbid after 3 minutes and did not clear within an hour.
- A distinctive lighter layer near the base of the water column was apparent in two experiments at around 1 minute (Figure 5.10 and 5.11).

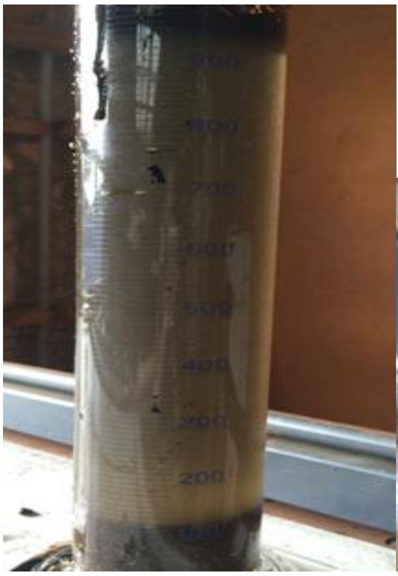


Figures 5.10 (left) and 5.11 (right): After 1 minute, there is a distinctive lighter layer near the base of the water column.

- A 15 mm slick on the water surface was highly aerated during the experiments and contained 50 - 90 % of total oil by volume in all experiments. After 36 hours, very fine oil flakes were seen toward the top of the water column, which, after agitation (by moving the flask), became redistributed throughout the water column. There was a distinct lack of convex outlines of tar balls distended from the underside of the oil slick (Figure 5.12). The presence of these flakes may be due to differences in the mineral/clay composition/proportions between the experiments as the sediment samples may not have been homogenised well.

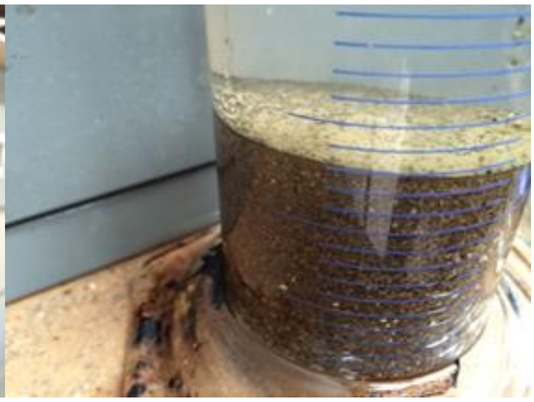

Figure 5.12 (left): **Oil flakes distended from the surface oil slick.** ***Figure 5.13 (right)*****: Yellow layer of flocs coated the sediment surface after settling; oil flakes were visible on top.**

- Fine oil flakes were also present on top of the fine sediment on the surface of the bottom sediments, no tar balls were present (Figure 5.13).
- Yellow layer of flocculated particles covers the sediment surface after settling (5.14).

5.2.2.3 Experiments using Ngarunui Beach sediments and 10 ml of Heavy Fuel Oil (HFO)

- A highly aerated oil slick (~10 mm) formed within the initial seconds, which, after settling contained > 85 % of total oil by volume (Figures 6.14 and 6.15).
- No tar balls were visible on the underside of the slick however tiny convex shapes or could be made out (Figure 5.15).
- Initial resurfacing within the first 5 seconds of large (> 3 mm) oil droplets and aggregations/tar balls. Some oil droplets coalesced; one aggregation was > 10 mm.

- With time, progressively smaller oil droplets and aggregations were visible within the water column; within 10 seconds, forms > 2 mm settled at both the top and bottom of the flask leaving droplets, 1-2 mm forms settled out before ~35 seconds, 1 mm forms before 60 seconds, leaving mostly < 1 mm forms.
- Droplets mostly rose in the first 5-10 seconds, though a few droplets descended and became buried in the sediment, some > 1 mm.
- Oil droplets were dark, spherical and sub-rounded with an average size = 2 mm in diameter, largest = 5 mm); some larger lighter coloured spherical droplets were also visible (5 mm in diameter).
- Most samples slowed at 1 minute, 30 seconds and became stationary at 2 minutes.
- Between 15 and 30 seconds there was a predominance of larger aggregations towards the bottom of the water column.
- After ~ 48 hours the water was totally clear.

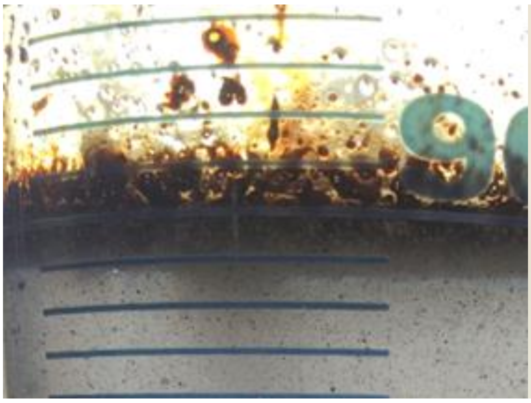


Figure 5.14 (left): **Initial slick that formed on the water surface, aerated and non-cohesive.** ***Figure 5.15 (right):*** **A more cohesive slick after 40 hours of settling.**

- Small spherical tar balls (< 5 mm in diameter) were visible on the surface of the bottom sediments and buried deeply within the sediment after settling (Figure 5.16).

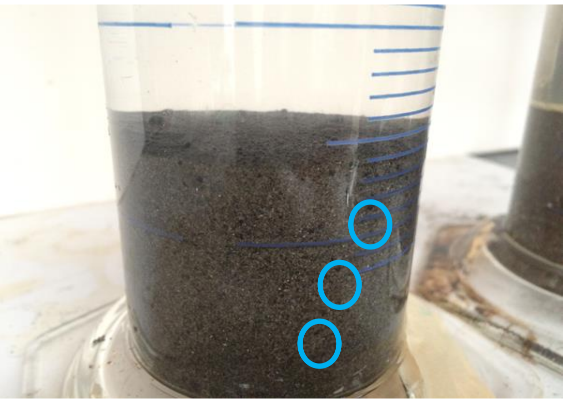

Figure 5.16: **Small tar balls (< 5 mm) on the surface of and buried within the sediment.**

5.2.2.4 Experiments using Ngarunui Beach sediments and 20 ml of Heavy Fuel Oil (HFO)

- Initial resurfacing within the first 5 seconds of large, 2/3 mm to >5 mm (some > 15 mm), dark, mostly spherical oil droplets and aggregations.
- Oil mostly rose in the first 5-10 seconds, although a few droplets were visible descending to become buried in the sediment. Some > 1 mm. After this oil rose and descended in equal amounts.
- Aggregations still surfaced at 10 seconds and very occasionally after 1 minute although most of the oil was in large droplets after 10 seconds.
- Decreasing size distribution with time; > 2 mm oil droplets and aggregations settled before 5 secs, 1-2 mm before 10 secs, < 1 mm after 30 seconds and small < 0.5 mm oil droplets and grains at around 2 minutes with a few exceptions of larger forms.
- The oil was well distributed throughout the water column.
- Some large aggregations broke off the surface oil slick and descended slowly at 2 minutes, likely due to the discharge of air.
- It took ~77 seconds for a droplet to rise to the surface.
- More rigorous stirring (> 30 seconds) resulted in greater amounts of individual oil droplets and fewer aggregations.
- Lots of oil settled before the sediment in these experiments.

- The water column was stationary at between 2 minutes and 3 minutes, 45 seconds and had cleared within an hour and a half. No yellow hue was visible.
- Aggregations, tar balls and air bubbles were visible on the sediment surface after 2 minutes (Figure 5.17).
- Approximately 50% of the oil present was tar balls on the bottom sediment and 50% as oil slick. The oil slick was 15 mm thick and large tar balls were distended from the bottom of the slick (Figure 5.18).
- Experiments using Ngarunui Beach sediments and 20 ml HFO were mostly too turbid to accurately account for settling times and proportions however it was noted that larger sized forms settled out earlier leaving smaller sized droplets and aggregations.


Figure 5.17 (left): **Air bubbles and oil droplets on the sediment surface.** ***Figure 5.18 (right):*** **Tar balls distended from the base of the surface slick.**

- Large relative amounts and large sized tar balls were visible on the surface of the bottom sediments (5 - 10 mm in diameter); tar balls appeared dusted in flocculated particles (Figures 5.19 and 5.20).
- Tar balls or oil droplets were seen buried within the bottom sediments though they were smaller and close to the surface at a depth of 4 mm (Figure 5.20).

Figures 5.19 (left) and 5.20 (right): **Tar balls on the sediment surface and buried within the sediment.**

5.2.2.5 Experiments using Moonlight Bay sediments and 10 ml of Maari/Moki co-mingled oil

- The water was turbid and settling was hard to define.
- Large amounts of oil adhered to the metal stirrer in this experiment causing a loss of oil in experiments performed on the 28th of July, 2015. This reduced the size and amount of aggregations. Large amounts of oil also remained on the flask walls above the water line after mixing; tar balls can be seen on the walls of the cylinder, close to 10 mm in diameter.
- Most oil rose to the surface of the water and formed a 5 mm thick slick (> 90% of oil). The slick was formed of large oil patches (5 -10 mm in diameter) (Figure 5.21). With settling of 18 hours, the slick became more cohesive (continuous instead of patchy) (Figure 5.22).
- Complex shaped patches of oil were seen near the top of the water column, ~ 2.5 mm in diameter.

Figures 5.21 (left): **Complex surface slick made up of large globs of oil during settling experiments.** ***Figure 5.22 (right):*** **Surface slick with distinctive globs distended from the base of the surface slick after settling.**

- On average, large aggregations of oil (< 20 mm) resurfaced immediately and within 5 seconds due to buoyancy and proximity to the surface followed by 1 mm – 2mm in diameter droplets before 15 seconds with small (< 1mm) droplets remaining.
- Droplets were semi spherical and light coloured.
- Negligible oil was present after 30 seconds, with remaining oil < 0.5 mm.
- Within 50 seconds the bottom of the water column had cleared, with grains/droplets (< 0.5 mm) toward the top of the water column in one experiment. Within 1 minute, 45 seconds the water had cleared.
- In all other experiments the water remained turbid.
- In most experiments the water column became stationary between 1 minute, 30 seconds and 2 minutes with neutrally buoyant grains, droplets and aggregations visible.

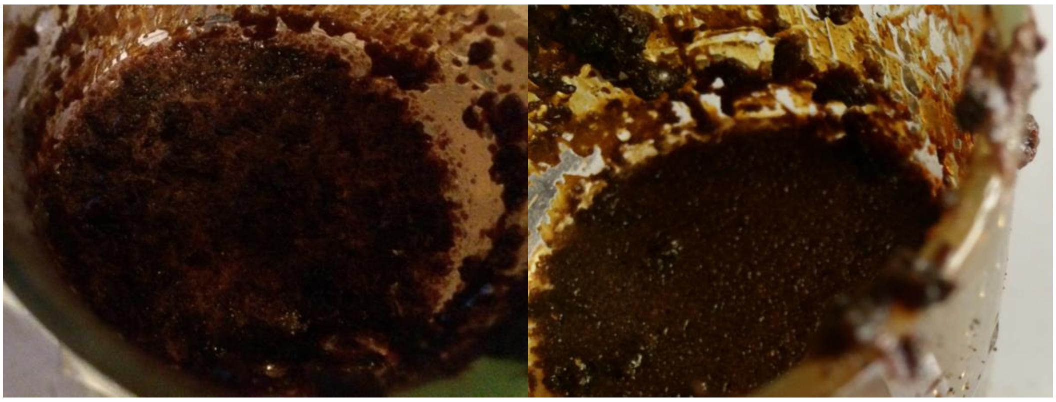

Figures 5.23 (left) and 5.24 (right): **Surface oil slicks after~1 minute and 18 hours respectively.**

- The surface slick appeared to show little change after 18 hours, air bubbles were still visible and oil remained on the flask walls (Figures 5.23 and 5.24).
- Tar balls did not form on the bottom sediments however air bubbles could be seen at after 2 minutes on the surface of the bottom sediments in some experiments (Figures 5.25).
- A distinctive thick yellow layer of flocs coated the bottom sediments between settling and 18 hours (Figure 5.26).
- It was difficult to determine if tar balls or droplets were buried within the bottom sediments in these experiments but it did not appear so.

Figure 5.25 (left): **Photograph of settled sediment after~2 minutes with no visible oil in the water column or the sediment.** ***Figure 5.26 (right):*** **Yellow layer of flocs atop of sediment after more than 18 hours settling.**

5.2.2.6 Experiments using Moonlight Bay sediments and 20 ml of Maari/Moki co-mingled oil

Figures 5.27 (left) and 5.28 (right): **Cohesive surface slick with fuzzy contours at the base of oil slick.**

- Water was turbid possibly due to the presence of fine clay minerals.
- A 10 mm slick formed at the water/air interface with > 90% of total oil (Figures 5.27).
- A fuzzy contour is visible on the base of the surface slick which is probably due to grains adhered to the bottom of the slick (Figure 5.28).
- Oil patches were seen on the flask walls above the slick.
- Again large amounts of oil adhered to the metal stirrer.
- Larger aggregations and oil patches cleared within the first 5-7 seconds and decreasing size distributions occurred with time.
- After 25 seconds, the water column began to clear at the bottom in the earliest experiment.
- After 1 minute, grains were still clearly visible (Figure 5.28).
- The sea water in the initial experiments had cleared significantly after only 1 minute, 30 seconds however the sea water in experiments performed the following day remained cloudy during the experiments.
- Oil cleared quickly during these experiments however neutrally bouyant grains and small aggregations were visible until about 1 minute, 30 seconds in the intial experiments.
- Suspended yellow particles were visible again after 5 and 8 hours of settling. The sediment that was in suspension has flocculated and is settling.
- Tar balls did not form within 32 hours in these experiments and it appeared that oil was not present within the sediment.

- A distinctive yellow layer of flocculated particles coated the bottom sediments between settling and 18 hours (Figure 5.29).

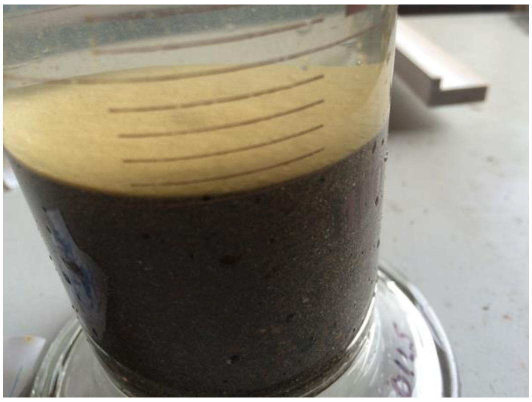

Figure 5.29: **Yellow surface layer of flocs after approximately 5 hours with suspended flocs.**

5.2.2.7 Experiments using Ngarunui Beach sediments and 10 ml of co-mingled Maari/Moki crude oil

- During one experiment the metal stirrer was inadvertently left in the flask; large amounts of oil in the form of aggregations (>30 mm) adhered to it.
- Very large (some > 50 mm) complex shaped, aerated aggregations containing sediment grains settled on the water surface before 5 seconds usually, as they were buoyant (Figure 5.30).
- 5 - 10 mm aggregations settled out usually before 10 seconds, then 2-3 mm aggregations before 15 seconds. A few remained after 25 seconds which were neutrally buoyant. After 60 seconds only minimal grains and a little oil remained in the water column. The water was slightly opaque, white and cloudy. After 2 minutes, no changes in distributions were visible however the remaining oil and sediment grains were stationary.

Figure 5.30: **Large aggregations rising in the initial few seconds.**

- Lots air bubbles were present in the water column.
- Most of the oil had settled before the sand.
- Most oil rose to the surface of the water and formed a slick (> 90% of oil). The slick was not a cohesive unit but made up of individual tar patches that made up large aerated, aggregations of oil and sediment. The slick was approximately 10 mm thick (Figures 5.30, 5.31 and 5.32).
- Aggregations that formed on the surface of the bottom sediments were aerated, complex forms made up of rounded aggregations, between 2-3 mm and 5 mm in diameter (Figure 5.33).
- Tar balls and aggregations were seen distended from the surface slick (Figure 5.31).
- It was evident that after the initial settling period and before 12.5 hours, large tar balls detached from the slick and distended to the bottom of the water column. Tar balls can also be seen dropping (Figure 5.34) from the slick to the bottom of the flask during settling.


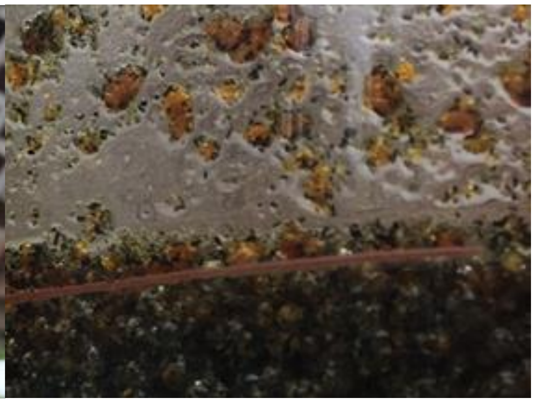

Figure 5.31 (left): **Oil slick at the water surface after 2 minutes and 40 secs.** ***Figure 5.32 (right):*** **Close up of the individual tar patches that form the slick.**

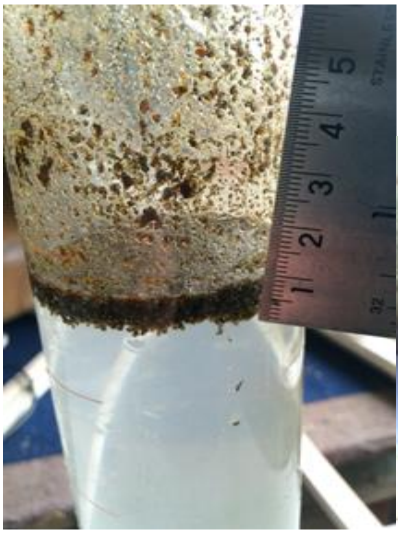


Figure 5.33 (left)**: Oil and sediment aggregations breaking away from the surface slick.** ***Figure 5.34 (right):*** **Aerated tar balls on the sediment surface after 3 minutes.**

- Tar balls were present after 12.5 hours and were covered in a characteristic yellow later of flocs. Tar balls have therefore formed after the initial sediment settling but before the settling of silt-sized particles (Figures 5.35 and 5.36).

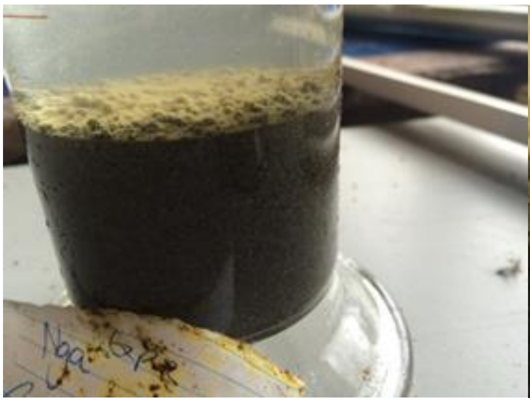 

Figure 5.35 (left): **Tar balls at the bottom of the flask covered in flocs after 12.5 hours.** ***Figure 5.36 (right):*** **Dark sediment grains are clearly visible.**

- Dark black elongated grains and green grains were visible within the patches (Figure 5.36). These are likely to be titanomagnetite and hornblende.
- Oil was also buried within the sediment.
- Not many individual oil droplets were visible in these experiments; though some tiny patches and smears either with or without sediment grains adsorbed to and absorbed within were seen.
- Small quantities of apparently medium to coarse "grains" were suspended within the water column forming oil-mineral-aggregates with neutral buoyancy (Figure 5.37).
- With less oil, the concentrations were decreased for each of the size fractions within each time parcel.

Figure 5.37: **Individual and coalesced sand grains displaying neutral buoyancy after 2 minutes.**

5.2.2.8 Experiments using Ngarunui Beach sediments and 20 ml of co-mingled Maari/Moki crude oil

- Lots of oil adhered to the metal stirrer.
- Initial dispersion of surface layer oil followed by immediate resurfacing of oil droplets and sediment/oil aggregations. Some of these were very large aggregations, > 10 mm, with an average size of 5 mm. These coalescences had complex, non-spherical shapes, were aerated, dark and contained sediment grains; they surfaced within the first 3 - 5 seconds due their buoyancy.
- Other large 20 - 30 mm aggregations settled out usually before 5 seconds and then 5 mm aggregations had settled within 10-15 seconds. A few aggregations remained after 25 seconds which were neutrally buoyant but the water column was mostly clear with an opaque, white, cloudy hue.
- The water column became stationary after about 1 minute however it sometimes took up to 4 minutes for the last few grains to settle.
- Most of the oil descended to the bottom of the flask in these experiments except in two experiments where the largest concentration of oil rose to the surface and formed a 15 - 25 mm slick. In other experiments the surface slick was < 4 mm.
- The oil droplets and aggregations were predominantly non-spherical in shape (Figure 5.38).
- Lots of tar balls and aggregations were distended from the surface slick (Figure 5.39).

Figure 5.38 (left): **Angular aggregations were visible in the water column after < 5 seconds.** ***Figure 5.39 (right):*** **Aggregations distended from the surface slick after 18 hours.**

- The settling of the aggregations on the bottom of the flask was the result of higher densities and possibly less air or oil being trapped.
- A large amount of oil was buried within the sediments.
- Individual sand grains were seen in the water column.
- The oil had nearly settled by the time the sediment had settled.
- Air bubbles were visible in the aggregations on the surface of the sediment which were present after approximately 3 minutes (Figure 5.40).
- More spherical and larger tar balls (> 10 mm) were visible on the sediment surface after nearly 18 hours. These aggregations were covered in a characteristic yellow surface layer of flocs. Some were 'fresher' i.e. not covered in the yellow layer. The fresh tar balls obviously formed or separated from the surface slick after the flocs had settled (Figure 5.41).

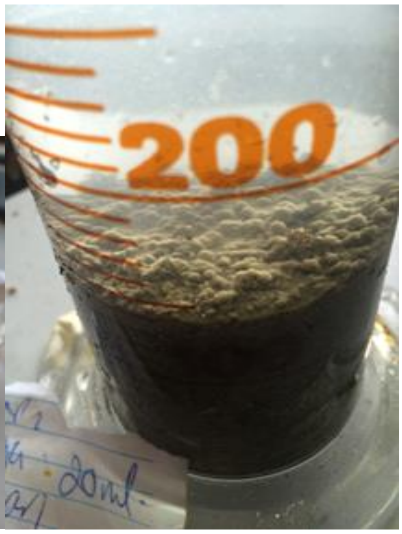

Figure 5.40 (left): **Visible aggregations formed after 3 minutes. Figure 5*.41 (right):*** **Aggregations were larger, more spherical and covered in a yellow veneer of flocculated particles after nearly 18 hours.**

5.2.3 MICROSCOPIC OBSERVATIONS

Results and interpretation of microscopic observations are outlined below.

5.2.3.1 Sea water surface

The surface samples from Moonlight Bay experiments with treatment of Maari/Moki oil contained an abundance of flocs with a distinct absence of larger grain sizes (Figure 5.42). Maari/Moki crude oil maintained a complex, cohesive structure, which fine grains readily adhered to in some surface samples (Figure 5.43).

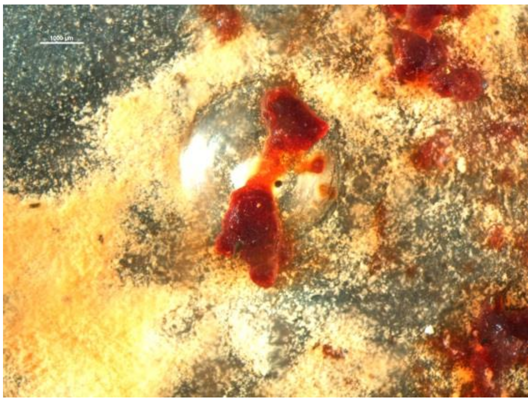 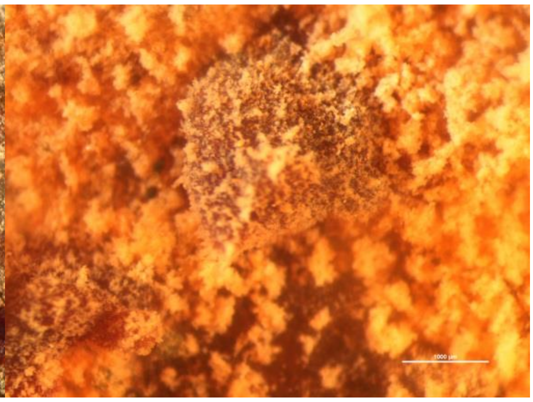

Figure 5.42 (left): **Maari/Moki co-mingled oil in the water surface sample.** ***Figure 5.43 (right):*** **Fine grained sediment adsorbed and adhered to the surface of the Maari/Moki oil.**

Surface samples from Maari/Moki treatment of Ngarunui Beach sediment contained profuse amounts of both sediment and tar balls (Figures 5.44 and 5.45). Tar balls were densely covered in grains and had grains absorbed into them. Small oil patches were also present with grains absorbed within them (Figures 5.45 and 5.46).

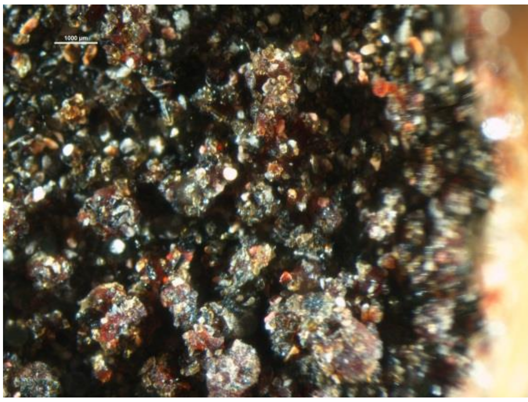 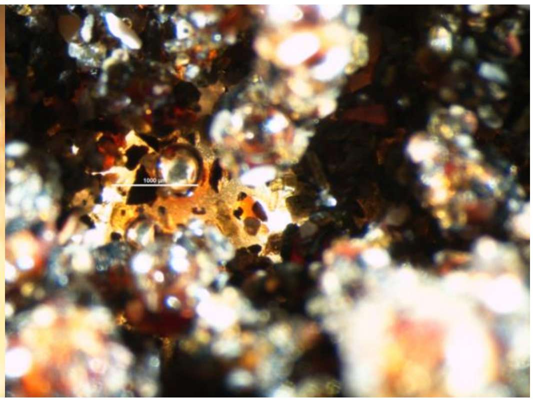

Figure 5.44 (left): **Abundant tar balls in the surface samples.** ***Figure 5.45 (right):*** **Close-up of tar patch with visible grains adsorbed to them and absorbed within them.**

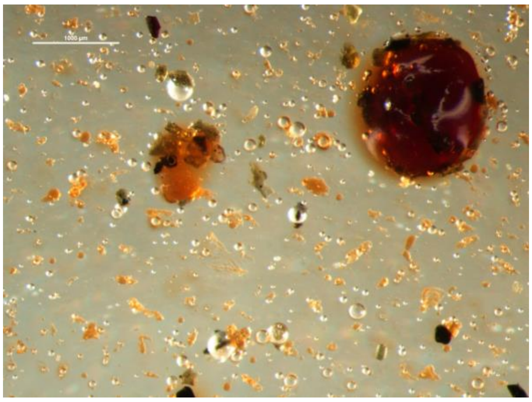

Figure 5.46: **Suspended oil patches with visible grains absorbed within.**

Moonlight Bay surface samples containing HFO consisted of thick, opaque oil, limiting analysis. Negligible grains were visible within the sub-sample (Figure 5.47). Isolated grains upon the lid of the container were visibly coated in a thin veneer of oil (Figure 5.48).

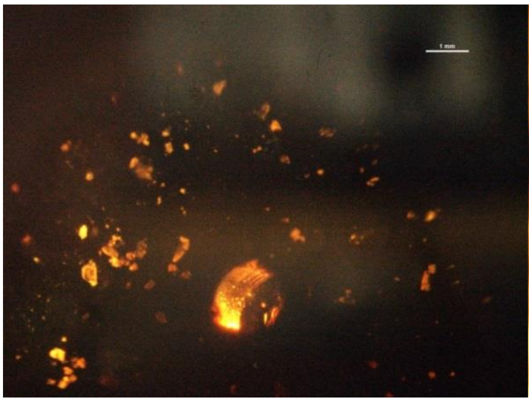

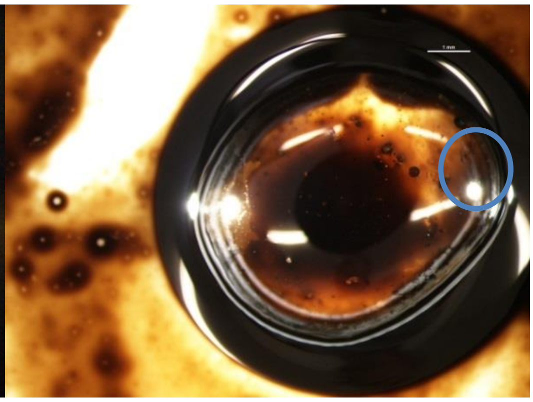

Figure 5.47 (left): **Subsample from the surface of HFO experiment using Moonlight Bay sediment in which oil is thick and cohesive.** *Figure 5.48 (right):* **A veneer of oil was visible on individual grains upon the lid of the container.**

HFO in the Ngarunui Beach samples consistently adhered into the walls and base of the plastic container and was not visible in the water except as a thin surface veneer. An emulsion had started to form around the walls of the container in the 10 ml experiments. (Figures 5.49 and 5.50).

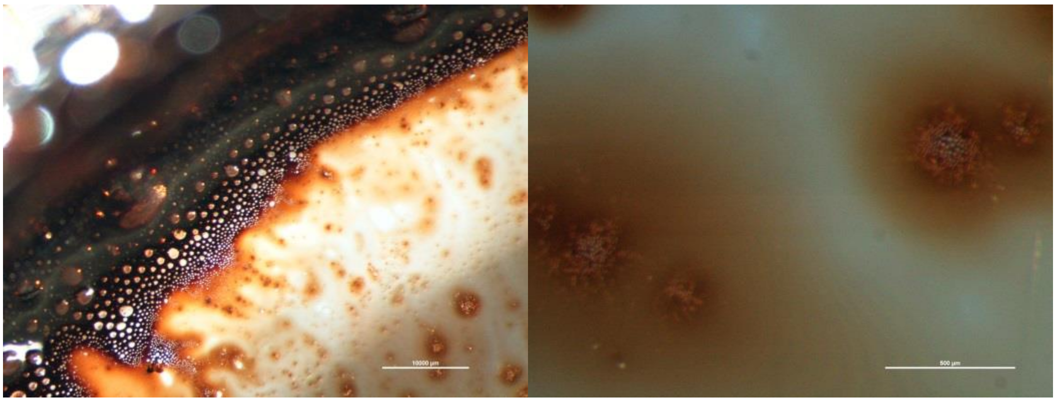

Figure 5.49 (left) and 5.50 (right): **Water-in-oil-emulsion formed in the surface sample using 10 ml of HFO oil.**

20 ml experiments revealed larger concentrations of oil which were adsorbed to the plastic bottom of the container. No water was present in this sample at the time of examination. Sparse, scattered grains were visible atop of the oil but were not absorbed within it, nor was any oil visible coating the grains (Figure 5.51). Some very large, elongate grains were visible and an unidentified aggregation was present possibly organic matter in the sediment. Interspersed throughout the oil patches, non-oiled areas also showed grains within them. A second sampling from the Ngarunui Beach surface sample showed a thicker oil slick which displayed needle-like features (Figure 5.52). Grains were visibly coated in oil in these samples.

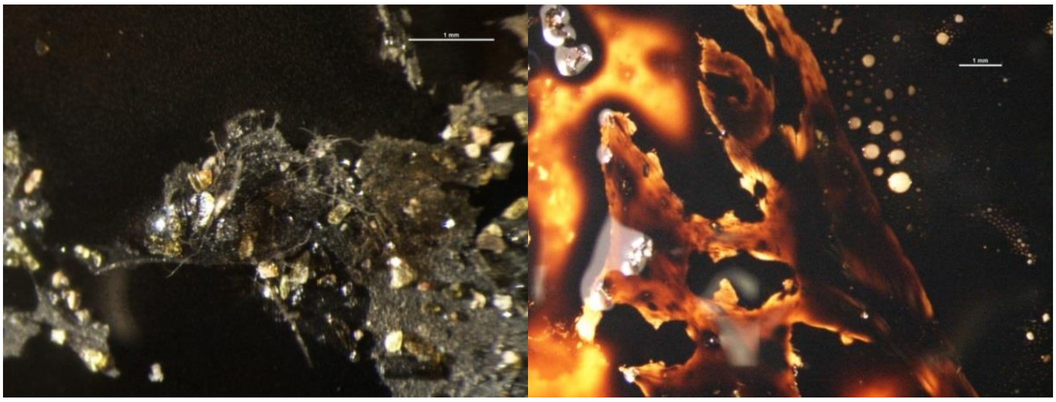

Figure 5.51 (left): **Unidentified object in HFO treatment of Ngarunui Beach sediment.** ***Figure 5.52 (right):*** **Needle-like structures revealed in the surface sub-sample from 20 ml HFO treatment of Ngarunui Beach sediment.**

5.2.3.2 Sediment surface near the base of the flask

Tar balls were not present in the bottom Moonlight Bay sediment samples with treatment of Maari/Moki oil, consistent with flask settling observations. Tar patches were visible on the walls and container lids of the samples and as a thin surface veneer in the 10 ml treatment however these patches contained very sparse grains.


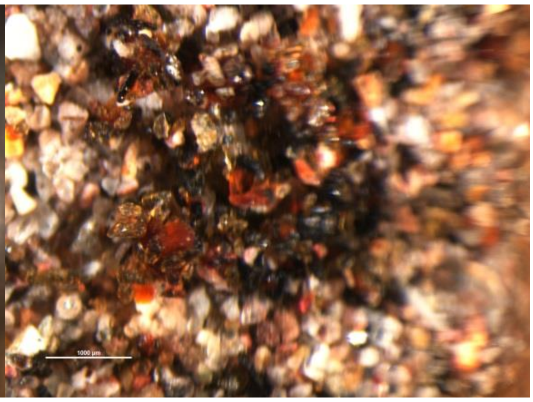

Figures 5.53 (left) and 5.54 (right): **Dark grains adhered to tar patches along container walls.**

Large tar patches/balls (> 1 mm) were apparent in the Maari/Moki, Ngarunui Beach sediment samples, positioned close to the container walls (Figures 5.53 and 5.54). These patches are distinctively darker than the surrounding sediment as a predominance of dark grains have adsorbed to them. Tar patches had sediment grains adsorbed to their surface and absorbed within them however denser oil patches apparently contained less sediment.


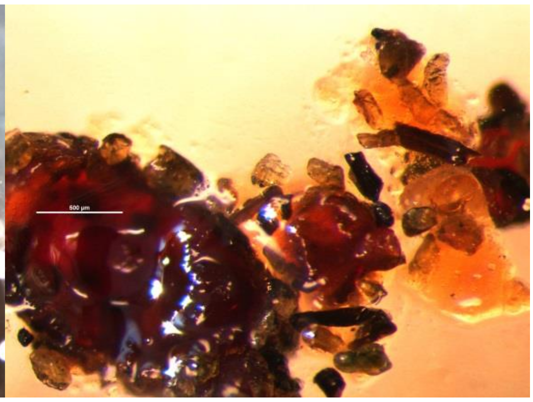

Figure 5.55 (left): **Numerous tar balls covered in sediment close to the container walls.** ***Figure 5.56 (right):*** **Tar patches with visible grains.**

Droplets were not present in the bottom sediment of the 10 ml HFO, Moonlight Bay sample and only two oil droplets were visible in the 20 ml HFO sample, again near the container wall (Figure 5.57); droplets in the 20 ml sample were ~1 mm in diameter. A thin emulsion had also begun to form in this experiment (Figure 5.58).

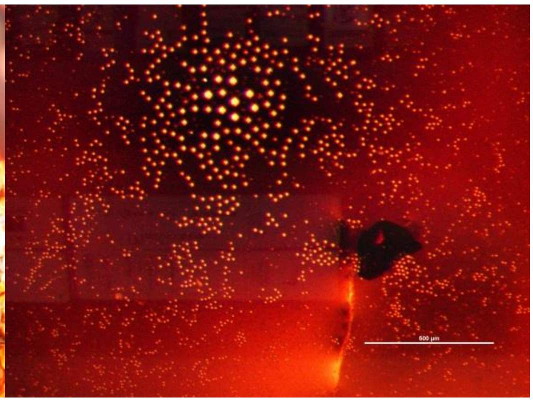

Figure 5.57 (left): **Moonlight Bay sediment with negligible (<1 mm) oil droplets.**
Figure 5.58 (right): **A thin water-in-oil emulsion on the water surface.**

Numerous spherical droplets were present in the 10 ml HFO sample with Ngarunui Beach sediment (Figure 5.59). These droplets were all in one area along the side of the container, possibly due to electric attraction to the thick, plastic container walls. Negligible droplet OMA appeared in the sediment from the Ngarunui Beach sample with 20 ml HFO. Those present were large (> 1 mm) and sediment grains could be seen adsorbed to the tar ball surfaces (Figure 5.60).

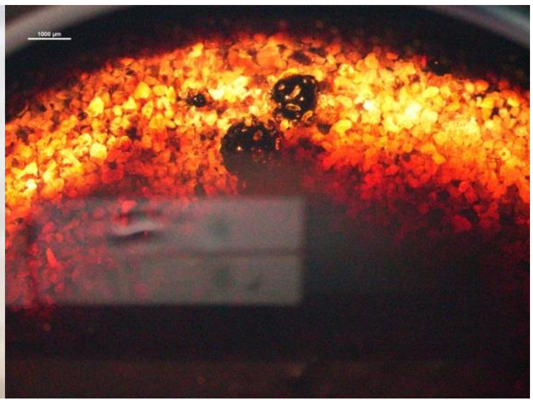

Figure 5.59 (left) and 5.60 (right): **Spherical oil droplets present in the Ngarunui sediment with 10 ml and 20 ml HFO respectively.**

Oil visibly coated the sediment grains on the container lid (Figure 5.61) and an unknown solid object was visible in the 20 ml HFO, Ngarunui sub-sample (Figure 5.62).

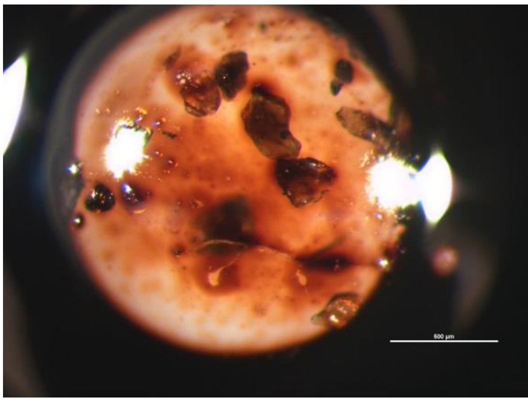
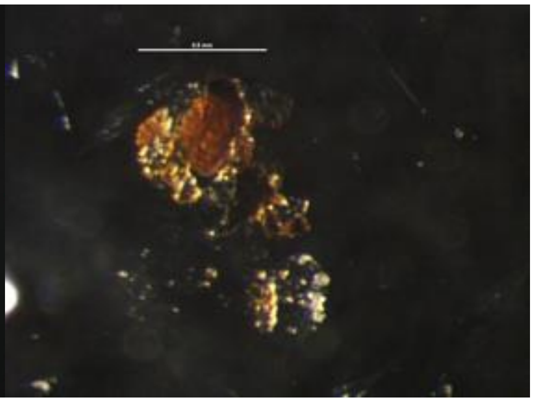

Figure 5.61 (left): **Close-up of oil coated sediment grains within an air bubble.**
Figure 5.62 (right): **Unknown solid object.**

5.2.3.3 Sediment/oil in the water column

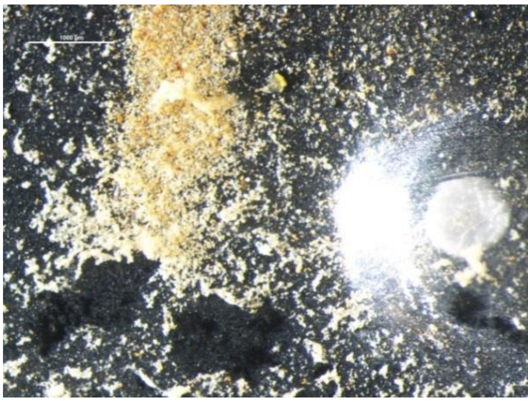


Figures 5.63 (left) and 5.64 (right): **Flocculations in the upper and middle part of the water column respectively.**

Throughout the water column of the Moonlight Bay, Maari/Moki samples, profuse amounts of flocculations were visible (Figures 5.63, 5.64 and 5.68). Tar patches (0.5 mm - 1 mm) were present at the top and bottom of the water column (Figures 5.65 and 5.66). An unknown solid object from the middle of the water column could not be disaggregated (Figure 5.67).


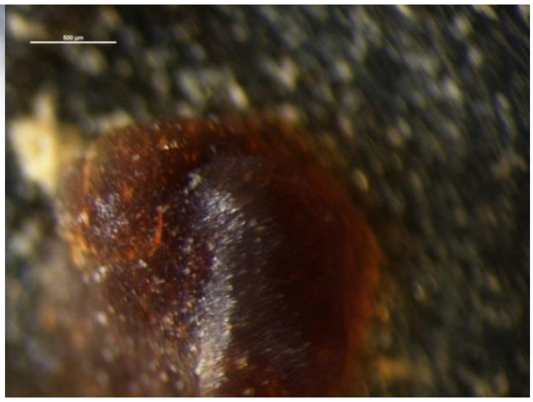

Figures 5.65 (left) and 5.66 (right): **Isolated tar balls from the top of the water column.**

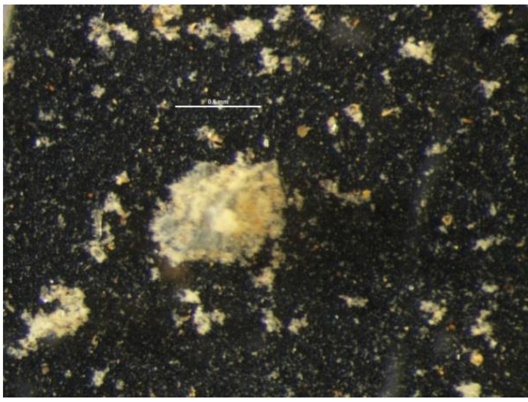
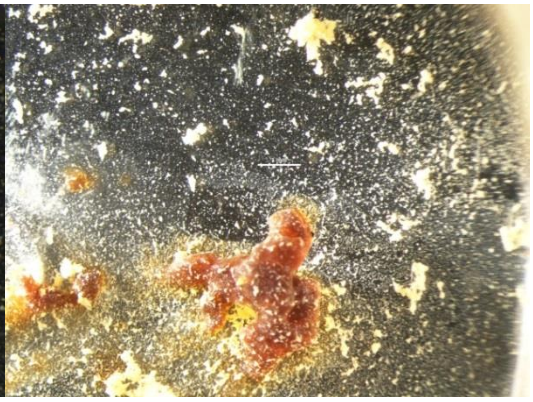

Figure 5.67 (left): **Negatively buoyant solid OMA from the middle of the water column.** ***Figure 5.68 (right):*** **Tar balls at the base of the water column.**

Abundant larger grained Moonlight Bay sediment and large tar patches are present in the sub-samples from the bottom of the water column in the 20 ml Maari/Moki oil experiment (Figures 5.69 and 5.70). Dark, elongate sediment grains predominate on the surface of the oil though lighter coloured platy grains are also visible (Figure 5.70). Negligible oil is present on the container lids.

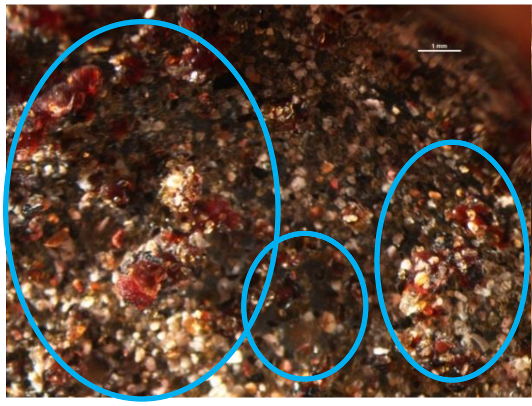
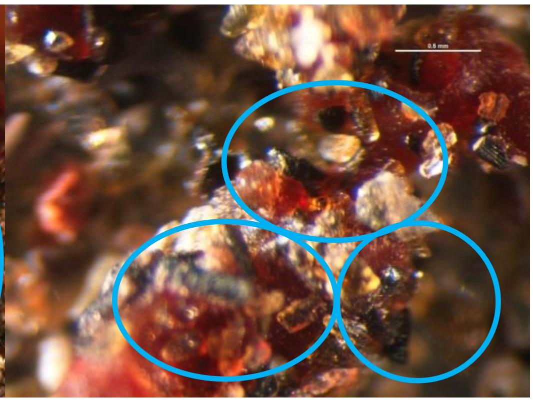

Figure 5.69 (left): **Abundant sediment adsorbed to large tar patches.** ***Figure 5.70 (right):*** **Dark, elongate and platy lighter grains adsorbed to the tar balls surface.**

In treatment of Ngarunui sediment with Maari/Moki oil, tar balls and patches (~ 0.5 - ~1 mm in diameter) displayed moderate amounts of sediment adsorbed to their surface and absorbed within, with a predominance of large (~0.5 mm in length) elongate, dark grains and green, round grains so heavy minerals were preferentially incorporated into the oil (Figure 5.71, 5.72 and 5.74). The tar balls are again attracted to the container walls and air bubbles are prevalent within them (Figure 5.72).

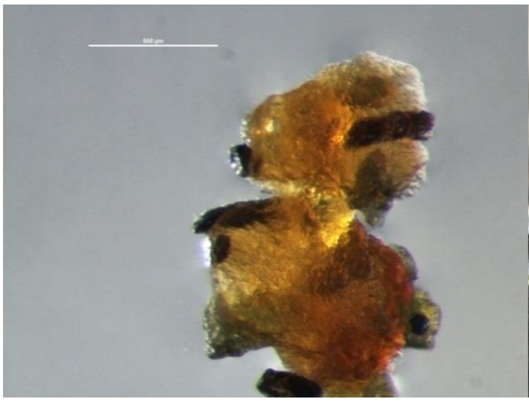
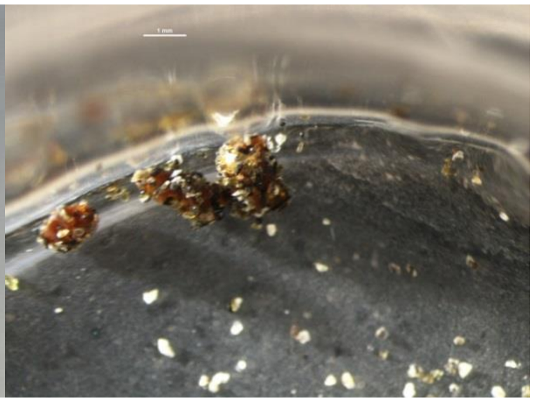

Figure 5.71 (left): **Close-up of an oil globule, complex in shape, with large, dark grains adsorbed to and absorbed within.** ***Figure 5.72 (right):*** **Negligible light coloured grains and in 20 ml Maari/Moki surface sample.**

Negligible oil was visible at the top of the water column however progressively more oil and sediment was present with depth (Figure 5.73). Flocculations are absent from all samples containing Maari/Moki oil and Ngarunui Beach sediments however fine particles very lightly coat the bottoms of the containers (Figure 5.72).

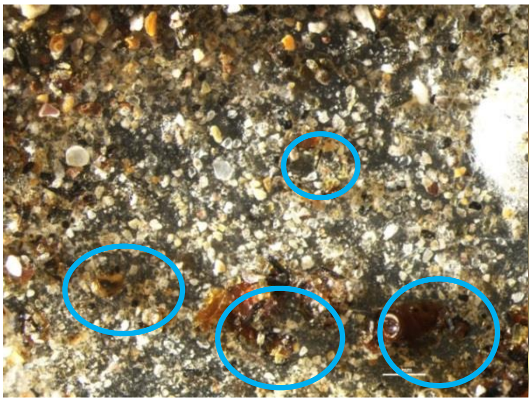
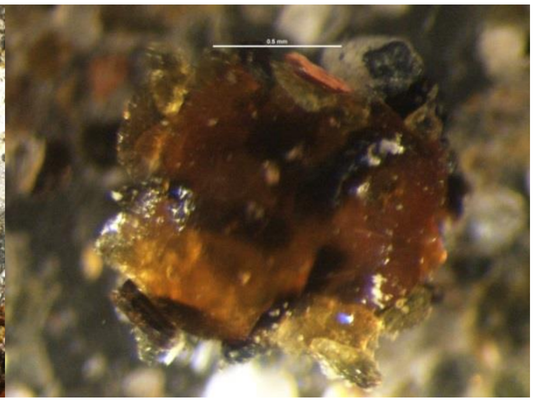

***Figure 5.73 (left):* A moderate amount of sediment with oil patches from the base of the water column in treatment of Ngarunui sediment with 10 ml Maari/Moki oil.**
***Figure 5.74 (right):* An obvious predominance of dark, elongate grains within the tar ball.**

Sediment grains on the container lid were coated in a thin veneer of oil and absorbed into large tar patches from the top and bottom of the water column and with 10 ml and 20 ml of Maari/Moki with Ngarunui sediments (Figures 5.75 and 5.76). More solid patches contained more particles at the edges.

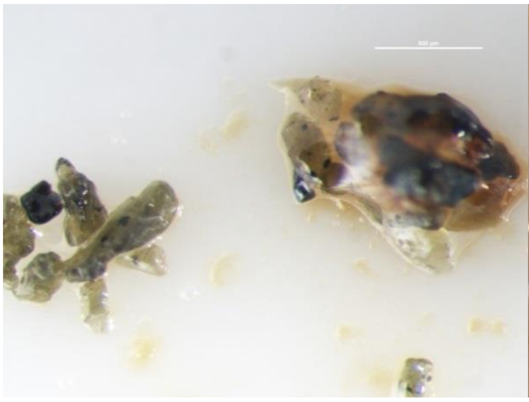
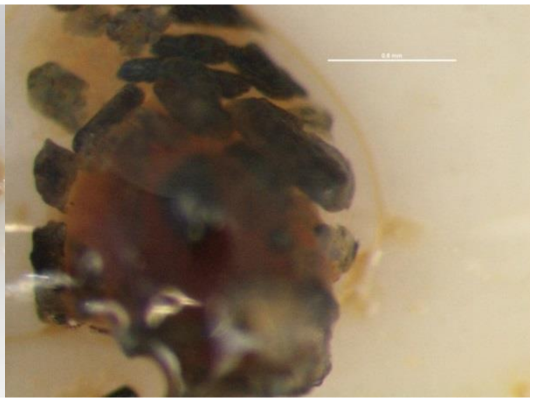

***Figure 5.75 (left) and 5.76 (right):* Sediment grains on the container lid coated in a thin veneer of oil and absorbed into a large tar patch from the top and bottom of the water column and with 10 ml and 20 ml of Maari/Moki with Ngarunui sediments respectively.**

In experiments using HFO and Moonlight Bay sediments, oil is only apparent at the surface of the water column (Figure 5.77) and as an emulsified surface slick in the bottom column sub-samples (Figure 5.78). The oil in the surface sub-sample also exhibits some early emulsification (Figure 5.77).

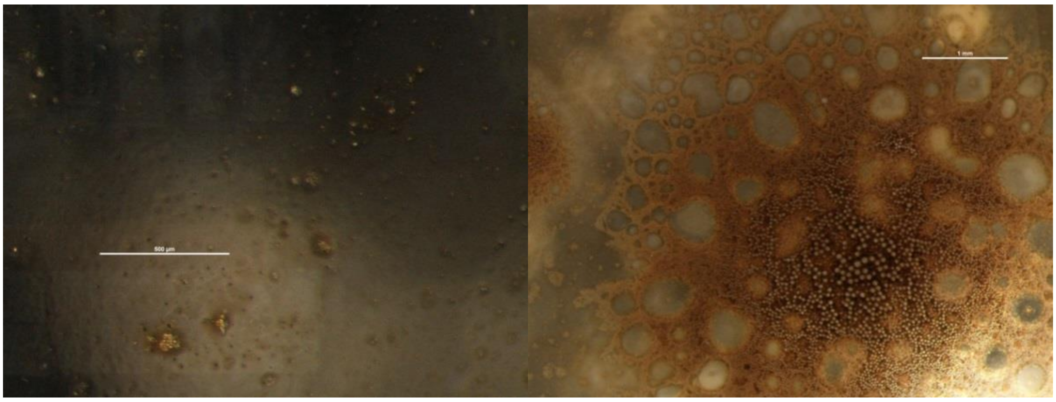

Figure 5.77 (left) and 5.78 (right): **Water-in-oil emulsion formed in the sub-samples from the surface and bottom of the water column respectively.**

The oil in the sub-sample from near the surface seems to have adhered to the plastic container base, with distinct and fuzzy edges at different locations (Figure 5.79, 5.80 and 5.81). The oil does not appear to coat the sediment, nor does it seem to have adhered to it. There is an observable increase in concentration of particles in the oil patch however.

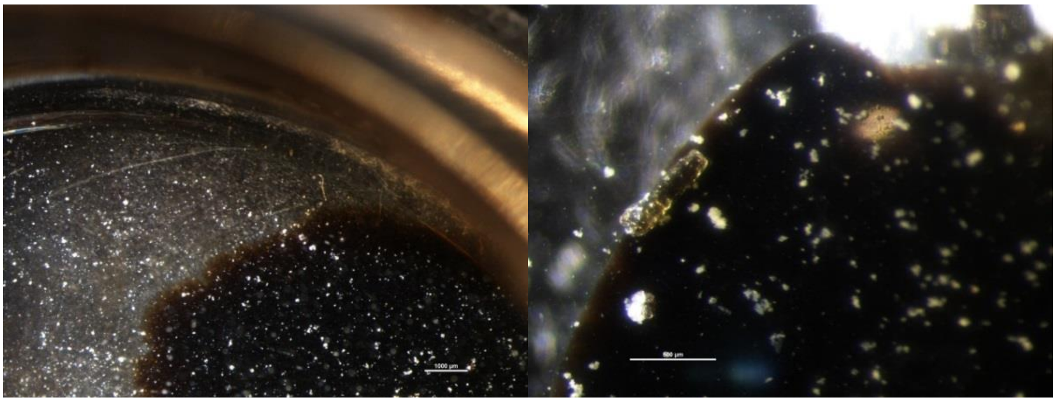

Figure 5.79 (left): **Oil adsorbed to the floor of the plastic container.** ***Figure 5.80 (right):*** **Dark oil patch with high concentration of grains sitting atop.**

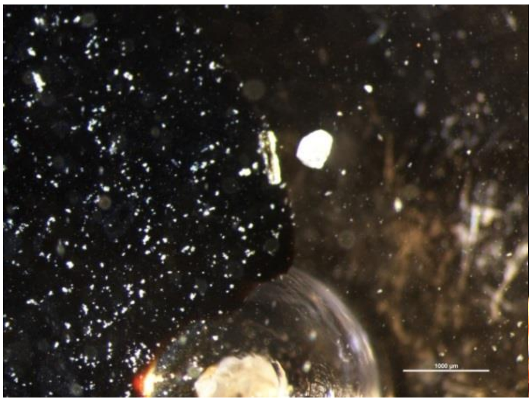
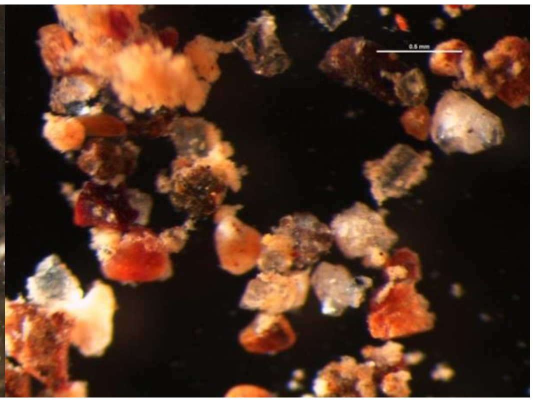

Figure 5.81 (left): **Dark oil patch.** ***Figure 5.82 (right):*** **Sediment grains and flocculations at the bottom of the water column.**

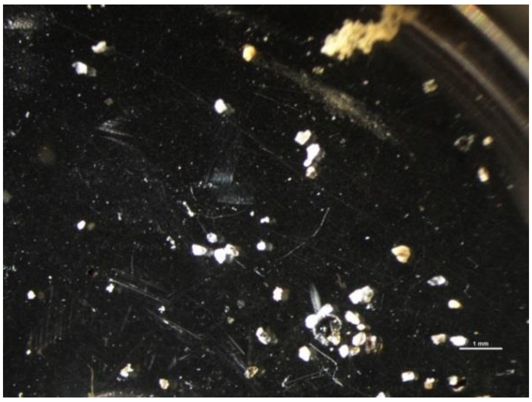

Figure 5.83 : **Neutrally buoyant OMA in the water column.**

Neutrally buoyant OMA are visible in the 10 ml sub-samples from the middle and bottom of the water column (Figures 5.82 and 5.83) and an unknown complex formation is present in the 20 ml sub-sample (Figure 5.84). A similar outline is present on the container lid (Figure 5.85).

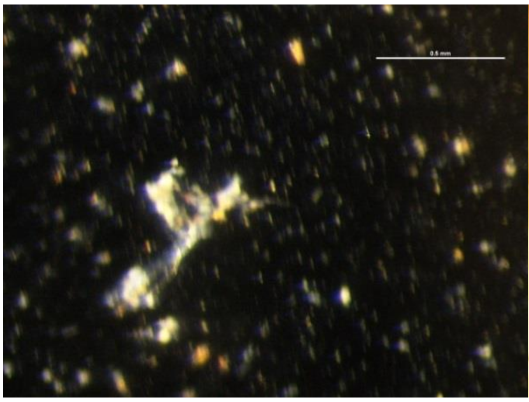
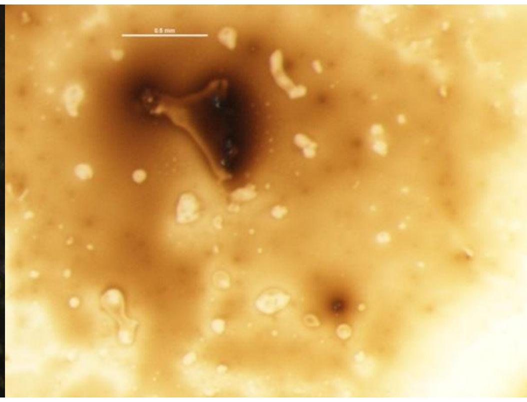

Figures 5.84 (left) and 5.85 (right): **Unknown complex formation and outline on container lid.**

In the sub-samples from the water column of the HFO, Ngarunui Beach sediment experiments, very little oil was apparent except as faint staining on the plastic container bases and as concentric rings on the lids of the containers (Figure 5.86), which were likely caused by bubbles of oil that burst. An exception to this was the sub-sample from the top of the water column with 20 ml of HFO, which exhibited a thick surface slick however it was likely that this sample was contaminated by surface oil. The presence of bubbles within the slick signified the onset of emulsion (Figure 5.87). Grains were visible within the water/air bubbles. Large grains were sparse in the samples taken from the water column however finer grained particles coated the bottom of all containers. Concentrations of fine grains increased with depth.


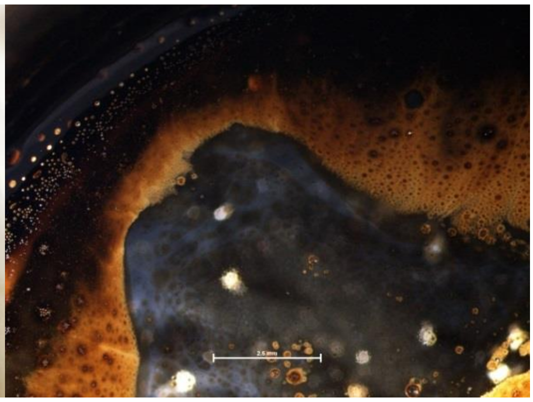

Figure 5.86 (left): **Concentric rings coating the container lid.** ***Figure 5.87 (right):*** **Surface slick exhibiting early stages of emulsification.**

An isolated fluffy object was visible at the bottom of the water column in the 20 ml experiment (Figure 5.88) otherwise only negatively buoyant flocculations formed in the bottom water column sub-samples with 20 ml. An isolated spherical oil droplet (< 0.5 mm) was present in the sub-sample from the top of the water column using 20 ml HFO (Figure 5.89). Oil droplets, particles and a larger solid complex object could clearly be seen on the water surface at the top of the water column sub-sample with 20 ml HFO (Figure 6.90) while oil seems to have adsorbed onto a grain in the same sample (Figure 5.91).

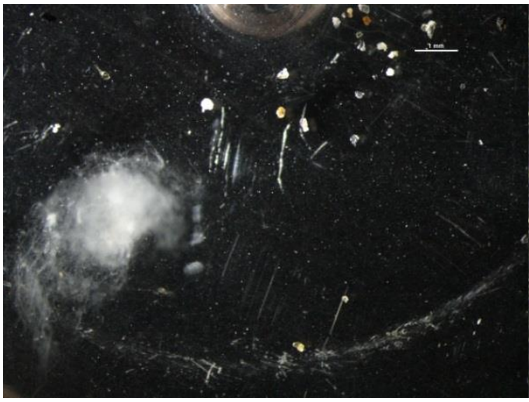
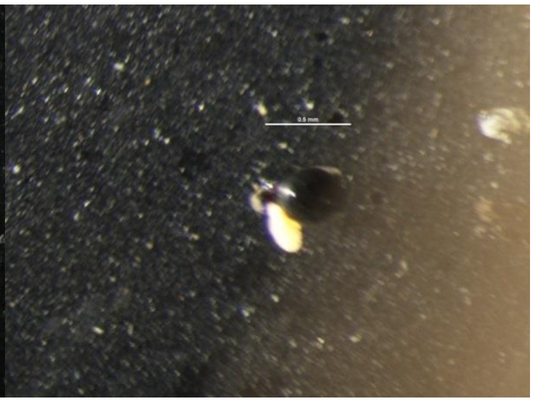

Figure 5.88 (left): **Suspended fluffy object.** ***Figure 5.89 (right):*** **Spherical oil droplet.**

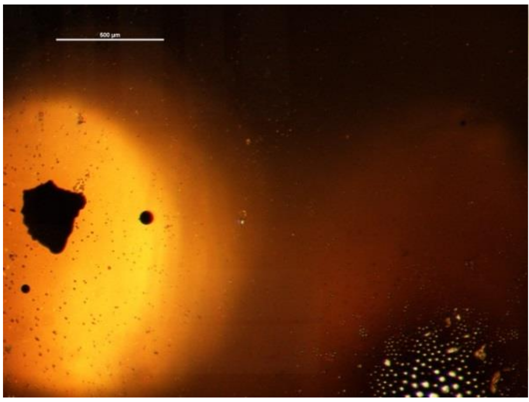
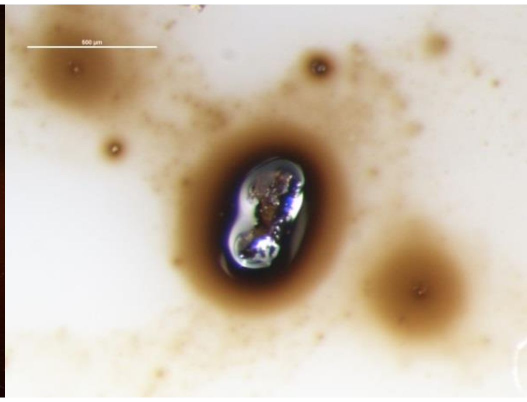

Figure 5.90 (left): **Visible opaque spherical oil droplets and complex oil shape.**
Figure 5.91 (right): **Oil coated grain in the surface samples**

5.3 DISCUSSION

OMA aid in the removable of stranded oil from contaminated shorelines, especially low energy shorelines, due to their increased ability to transport oil through augmented buoyancy and to reduce oil adhesion (Stoffyn-Egli and Lee, 2002). OMA can act as a surfactant, reducing oil coalescence, increasing the surface to volume ratios of oil and causing a flux of nutrients to the oil surface, facilitating amplified biodegradation and other weathering processes. Persistence of oil within the beach profile has been linked to the presence of OMA; transporting oil and associated toxic compounds from the water surface to the benthic environment where is can reside for decades (Barth, 2002; Bragg and Owens, 1995; Hayes et al., 1993; Scholz et al., 1999; Warnock et al., 2015). Understanding OMA formation and characteristics is paramount to estimates of residual oil transport and natural removal of stranded/buried oil, for predictive models of their environmental significance and for measuring efficacy of oil spill remediation such as surf washing (Stoffyn) and natural self-cleaning processes (Lee, 2002).

Due to limited research on the interactions of oil and titaniferous magnetite rich sediments, laboratory experiments were carried out to determine interaction and settling behaviours using two distinct oils; one ubiquitous HFO oil and the other a locally sourced crude oil, and two distinct sediment types; one with a characteristically high concentration of titaniferous magnetite. As there is also limited data on flocculation rates, settling velocities of mineral-oil flocs and the rate at which oil is removed from the environment, i.e. how rapidly the water column will clear, this research will contribute to some of these questions and aid in modelling timeframes of oil slick reduction.

The purpose of the current study was to observe the oil-sediment interactions, specifically oil-sediment aggregations, with respect to concentration, buoyancy, size and physical structure. Previous experiments carried out on OMAs found that different forms of oil were a result of sediment characteristics such as organic matter content, grain size and distribution, density and concentration, surface qualities and mineralogy, oil mineral ratios and oil properties including oil composition and viscosity, droplet size, density and concentration and environmental conditions such as the amount of turbulent energy, temperature and water pH and salinity (Delvigne et al, 1997; Delvigne, 2002; Payne et al., 1989 as cited in Stoffyn-Egli and Lee, 2002; Stoffyn-Egli and Lee, 2002; Khelifa et al., 2005).

OMA were found to result from interactions among oil residue (physically or chemically dispersed oil droplets), suspended particulate matter (SPM), and seawater or from adsorption of dissolved components to SPM on a molecular level with subsequent flocculation (Payne, Clayton Jr. and Kirstein, 2003). Poirier and Thiel (1941 as cited in Muschenheim and Lee, 2002) also observed oil adhering to mineral grains as globules and irregular stringers.

Different structures of OMA were identified by Stoffyn-Egli and Lee (2002); dispersed oil droplets (< µm - tens of µm; larger size fractions are in floating droplet OMA) with discreet or aggregate mineral particles affixed to their surface formed using kaolinite and quartz, larger (tens to hundreds of µm), solid mineral aggregates of irregular shape (a function of mineral inclusions) which may or may not have particles affixed to their surface and thin sheet flake aggregates with dendritic microstructure. These classifications were used in the current study. Solid OMA can be up to 200 – 300 µm and may be branched, curved or elongated. The large (mm scale) flake aggregates formed out of an Intermediate Fuel Oil (IFO 30) with montmorillonite clay due to intercalation complexes of swelling clays. When smaller concentrations (< 20%) were used, droplet OMA formed. Flake aggregates (which have only been found in the lab) are generally neutrally buoyant or floating but sink readily when disintegrated with increased turbulence (high shear strength) to form compact OMA (Stoffyn-Egli and Lee, 2002). Although flake aggregates form most readily with smectites, mineral bound oil may also occur with high concentrations of oil and low oil/mineral ratios using different clay minerals, including mica, illite and chlorite; using Svalbard sediment (2-3% smectite by weight) and above 0.2 g/l of oil and low ratios of oil/minerals, flake OMA of several mm were the result of mineral-bound oil at the particle scale controlling the shape of the OMA (Stoffyn-Egli and Lee, 2002). Large silica grains (0.14 µm) resulted in large mineral flocs with some trapped oil; although sediment became absorbed into the surface slick during these experiments, so they were unable to form discreet OMA. Both droplet and solid OMA were prevalent however with larger concentrations of oil, solid OMA predominated and oil was mostly in the floating phase (Stoffyn-Egli and Lee, 2002).

Polar and ionic hydrocarbon quantities (which increase with weathering) were also found to affect OMA formation as they increase the lipophilicity of the minerals (Stoffyn-Egli and Lee, 2002; Wang et al., 2011). Asphaltenes, resins and waxes are in significant amounts in bunker oil (Andrade et al., 2012) while Maari/Moki crude has a very high wax content. Lee et al. (1998 as cited in Loh et al., 2014) determined that 9500 mPa.s is the threshold value of viscosity above which no OMAs could form. Significant amounts of OMA do not form with high viscosity oils such as Bunker C (Bragg and Owens 1994; Bragg and Yang, 1993, 1995 as cited in Stoffyn-Egli and Lee, 2002; Kepkay, 2002; Khelifa, 2002; Lee et al., 1998 as cited in Loh et al., 2014; Le Floch et al., 2002; Omotoso, 2002) however OMA did form using a wide variety of oils and viscosities in experiments by Stoffyn-Egli and Lee (2002).

The shear energy of waves was determined to be an integral part of OMA formation and as highly viscous oils are harder to disperse, viscosity is inversely related to OMA formation however with higher energies and once droplets have formed, chemistry controls the rate of OMA formation (Khelifa, 2002). Also as the dispersed droplets are larger in more viscous slicks, the resultant OMA is likely to be in the solid form (Stoffyn-Egli and Lee, 2002). Physical dispersion of lower concentrations of oil is easier, resulting in increased droplet concentrations (Delvigne et al., 1987). Thicker oil slicks will not readily disperse and as the slick becomes coated in mineral grains, it shears off, coils due to hydrophobicity of oil and forms solid OMA (Bragg and Yang, 1995 as cited in Stoffyn-Egli and Lee, 2002). Alternatively large globules of oils can engulf hydrophobic mineral grains.

Hydrophobicity enhances OMA formation, particle sizes and size distributions (Zhang et al., 2010). The specific surface properties of minerals also influence the shape of OMA. Minerals remained at the outer layer of spherical positively buoyant OMA formed with hydrophilic minerals, while irregular shaped OMA were observed with hydrophobic minerals that had minerals penetrated into the oil phase (Stoffyn-Egli and Lee, 2002; Zhang et al., 2010). At higher temperatures, more elongated OSAs were observed by Khelifa et al. (2002). Mixing energy was found to have an effect on the dispersion and stabilisation of oil and OMA. The smaller droplets associated with increased turbulence (250 rpm) increased stabilisation, formed smaller OMA and increased the width of the size distribution (Zhang et al., 2010).

Two types of OMA were identified by Omotoso (2002); trapping of minerals in an oil-continuous phase and minerals stabilising oil droplets in a water-continuous phase. Negatively buoyant flocs associated with hydrophilic minerals and low-viscosity oils were comprised of minerals stabilizing oil droplets in a water-continuous phase. Positively buoyant flocs containing oleophilic minerals such as calcite have both water-continuous (with calcite intrusions) and oil-continuous sections which are mineral-rich. Oil slicks contain some quartz particles or water droplets dispersed in the oil-continuous phase. Omotoso (2002) also determined that OMA formation was controlled by the viscosity of the crude oil, the type of mineral present, water chemistry and droplet formation by shearing action and stability of droplets (prevention of coalescence). Omotoso (2002) stated that particle size and surface area are not limiting factors but are important when substantial variations are present.

Payne et al. (1989) reported that OMA formation was independent of the type of oil and SPM concentration but that sediment type (particle number density), salinity and mixing energy have a strong controlling effect on the reaction rate. OMA form readily with smaller grain sizes, smaller sized particles (clay sized) have the largest ratio of surface electrical charge/particle mass, a function of larger mineral surface areas (Ajijolaiya et al., 2006; Guyomarch et al., 1999; Khelifa et al., 2002; Omotoso et al., 2002). Particles sizes less than 4-5 μm have been asserted as the optimal range for OMA formation (Bragg and Owens, 1995; Zhang et al., 2010). Larger sized fractions (up to silts) can also be found in the flocs. Omotoso (2002) observed that mineral surface area is a more important marker for OMA formation than particle size while Bragg and Owens (1995) tested OMA formation with pure minerals and concluded that the size fractions determined flocculation efficiency more than the mineral properties.

Sun et al. (2010) observed that sediment size in suspension was shown to determine OMA formation times, with ranges from minutes to days. OMA formation increased exponentially with the mixing time and reached saturation within 4 hours. Huang and Elliott (1977) identified that stabilisation of a suspension occurred with up to 100 mg/l of suspended sediment. Suspensions larger than this destabilized and settled due to the increased density from adhered inorganics.

Delvigne (2002) identified the structures of three oil phases in experiments; oil droplets which may be coated with sediment particles or may be incorporated into sediment flocs, oil-coated sediment particles (~0.3 microns thick) and patches in high oil concentration samples, larger (μs to tens of μ) with no defined shape due to incorporation of sediment. The division of oil into these phases is the result of mineral and oil type and concentration, weathering state and oil-mineral interactions. OMA were categorised as positively, negatively and neutrally buoyant (Delvigne, 2002; Omotoso et al., 2002; Stoffyn-Egli and Lee, 2002; Zhang et al., 2010). The classifications of Delvigne (2002) were also used in this study. Negatively buoyant OMA do not readily biodegrade while neutrally buoyant OMA degrade rapidly (Gearing et al. 1980 and Wade and Quinn 1980 as cited in Loh et al., 2014). Droplet OMA do not readily break down because the mineral coating protects the oil and because there is a threshold for oil droplet size below which turbulence cannot break up the droplets (Delvigne et al., 1987; Stoffyn-Egli and Lee, 2002). Size distribution of oil droplets did not vary with oil, sediment or turbulence however size and concentrations of droplets increased iwthi increased concentrations. Lower surface tension oil results in lower concentrations of oil droplets and in oil patches (Delvigne, 2002).

The oil-sediment ratios in agglomerates control the buoyancy and subsequent behaviour of the aggregations. Once oil is bound to a mineral, it's density is generally less than sediment, it's stability increases and it is more easily transported out of a low energy environment by currents, especially as these environments have prolific small grain sizes (Lee, 2002). Biodegradation rates and levels of photo-oxidation, dissolution and evaporation can also increase due to the increased surface area of OMA, further mitigating toxicity (Stoffyn-Egli & Lee, 2002). It has recently been noted that oil biodegradation may be enhanced by OMA formation due to the flux of nutrient and oxygen to droplet surfaces (Ajijolaiya et al., 2006). Conversely the toxic components of oil can be retained in the bottom sediments for decades.

Wang and Roberts (2013) described marine tar residues as; tar balls, tar patties, tar cakes, oil sheets and oil stains. Tar balls are discreet accumulations of oil and sand, less than 10 cm in diameter while patties are greater than 10 cm. Continuous accumulations greater than 5 m in length or width, partially or completely submerged by water, are defined as tar sheets. Tar cakes are tar patties thicker than three cm while staining occurs due to oil coating sediment grains in a thin veneer. Staining was observed after the DWH spill by Wang and Roberts (2013) as white quartz sand was coloured brown. Bernabeu et al. (2006) described tar balls of a centimetre in size as CTB and tar balls of a millimetre size as MTB. Bernabeu et al. (2006) also observed microns thick staining after the *Prestige* spill, and postured that is was an indicator of diffusion and emulsion processes and noted that it was preferentially adhered to the flat, angular, bioclastic fraction. Bernabeu, Rey, Lago and Vilas (2010) generated coating in the laboratory with tar balls placed 10-12 cm deep in sand columns and exposed to varying speeds of water flow over 130 days. No staining effects were observed in the core samples from the Bay of Plenty after the *Rena* spill according to de Groot (2014).

Tar balls can form due to surface-weathering of oil but can also form as pieces of submerged oil mats (SOMs) break off and wash ashore and through sedimentation of eroded oiled sands (Michel et al., 1993 as cited in Warnock et al., 2015). More fragile than directly weathered tar residues, these tar balls and patties have a high sand content and are collectively referred to as surface residual balls (SRBs) (OSAT, 2010 and OSAT, 2011 as cited in Warnock et al., 2015; OSAT, 2013; Wang and Roberts, 2013). SRBs are frequently found in shell hash piles along the maximum high-tide water line and landward of the berm crest in the trough especially after storms (Parham and Gundlach, 2015; Clement et al., 2012). Experiments on characterization of clay–oil interactions have resulted in the production of tar balls when the suspension is heavily agitated.

5.3.1 SETTLING BEHAVIOURS

The results of the Ngarunui Beach control treatment was analogous with those results of de Groot (2014) however settling times for Moonlight Bay control experiments were almost half that time (Figure 5.2 and Table 5.2). Faster settling times for HFO oiled sediment was in contrast to the findings of de Groot (2014) who consistently obtained lengthened (albeit small) sediment settling values with the addition of HFO using fine sediments. The relative magnitude of variation between the control and HFO oiled experiments was also significantly different to variations found by de Groot (2014). de Groot (2014) found the average sediment settling times were only 1.1 seconds and 1.2 seconds longer than the control experiments while the range found in this research was significantly larger. Moonlight Bay sediment settling times were lengthened by up to 3.8 s and 4.8 s with the addition of Maari/Moki crude and HFO respectively; Ngarunui Beach sediment settling times decreased by 2.5 s and 3.1 s respectively (Table 5.2). Sediment settling times were therefore affected by the different treatments.

Numerous authors have asserted that higher-viscosity oils were less likely to form aggregates with mineral fines. Omotoso (2002) found that the addition of highly viscous oils will increase the settling times of mineral flocs, while low viscous oils will increase them further. This is because viscous oils will immediately resurface, avoiding sedimentation. Both oils in this case increased the settling times for Moonlight Bay sediments while reducing them further for Ngarunui sediments. Large aggregations settled out early in all experiments with the viscous oils. It is likely that the different densities of the particles had an effect on the settling behaviours of the oiled sediment. It is also possible that the clay size range, particle size, organic concentrations or surface areas were limiting factors in the mineral-oil interactions. This has been observed by many authors. The reduced settling times of oiled grains from Ngarunui Beach is likely to have resulted as dense aggregates formed from the Ngarunui Beach sediments which are expected to have heavy minerals present. Settling was slowed in Maari/Moki crude experiments as flocs containing material less dense than seawater were present. The oil types (lighter crude or heavier fuel oil) did not seem to differ in their effect on sediment settling times; settling was consistently faster for Ngarunui sediment and consistently slower for Moonlight Bay sediment with oiling from both types. The quantity of oil did not have significantly different effects on sediment settling times either. Values were within 2.5 seconds of each other for each individual sediment type (Table 5.2 and Figure 5.2).

Oil settling times were protracted especially for HFO samples. Similarly to the results of de Groot (2014) whose times were 124.6 and 126.2 for 10 ml and 20 ml HFO samples respectively, the mean values for HFO settling in these experiments was above 105 seconds except for the 10 ml sample with Ngarunui beach sediments which seemed to settle earlier (Figure 5.3 and Table 5.3). Maari/Moki oil settling times showed less variation but much lower values for settling time (Figure 5.3 and Table 5.3) due to the insolubility and relative density (0.836) of the crude oil and it's propensity for forming large aggregates which settled quickly, rising to the surface with Moonlight Bay sediment and some sinking to the bottom of the water column with Ngarunui Beach sediment (due to the increased density of Ngarunui Beach sediment). The insolubility of the Maari/Moki crude may also have affected the amount of oil suspended in the water column. The larger aggregates/patches that were present in the crude oil experiments may also have had larger wakes, dragging other aggregates down. HFO settling slowed significantly once the sand had settled probably as drag decreased.

There was initial break-up of the surface layer oil and rapid vertical dispersion due to turbulence followed by immediate resurfacing of large oil droplets (some > 2 mm) and sediment/oil aggregations (> 10 mm) with an average size of 5 mm due to buoyancy and proximity to the surface. In the first 3 seconds, proportionally more oil rises to the surface than descends to the bottom of the flask. Some oil settles within the bottom sediments as tar balls (< 10 mm in diameter) though in all experiments more than 85 % of the oil settled at the sea water surface as a cohesive surface slick due to high oil viscosities. The original thickness of the surface slick was therefore roughly equivalent to the post experiment slick. The surface oil slick was generally highly aerated. Convex shapes of spherical tar balls distended from the oil slick before 36 hours of settling in all HFO experiments except the 10 ml, Ngarunui Beach sample and the 20 ml Moonlight Bay sample which at 36 hours still had flake aggregates near the top of the water column (Figure 5.12) and by 48 hours only had visible particles at the base of the slick. In Maari/Moki experiments with Ngarunui Beach sediment, large dangling aggregates distend from the base of the slick immediately after experimentation which remained after 18 hours (Figures 5.31, 5.33 and 5.39). Although the water has almost cleared, a few grains are present near the top of the water column (Figure 5.37) and air bubbles can be seen trapped within and rising from the aggregates on the bottom sediments (Figures 5.34 and 5.40). Similar dangling shapes and large blobs were visible at the base of the 10 ml Moonlight Bay slick (Figure 5.21 and 5.22) while only particles were visible on the base of the 20 ml slick after 17 hours settling (Figure 5.27 and 5.28). Flocs were present in the water column in both of these experiments at 17 hours which were not visible earlier. No samples dispersed through the water column without mixing.

After the initial resurfacing, oil within the water column remains generally evenly distributed though in the Moonlight Bay experiments with crude oil, the lower water column cleared after~15 seconds in both the 10 ml and 20 ml experiments (Figure 5.25). The Moonlight Bay, 20 ml, HFO experiment also showed a distinctive lighter layer near the base of the water column in two experiments; perhaps due a fluid density increase relative to the rest of the water column. The oil rich water further up in the water column may be limiting mixing also (Figures 5.11 and 5.11). As the sand fraction settles, oil settling slows due to a decrease in associated turbulent energy. Cessation of vertical mixing currents may also enable the specific gravity of oil droplets to offset their neutral buoyancy, resulting in descent of droplets that have been suspended. Thirty seconds of mixing would not have resulted in equilibrium for droplet formation nor would it have resulted in equilibrium for tar ball and OMA formation according to Delvigne and Sweeney (1998) who stated that 5 minutes was required however 5 seconds is appropriate for simulation of a breaking wave. The equilibrium time for OMA formation in seawater was found by Delvigne et al. (1987 as cited in Sun et al. 2010) as 20 minutes using kaolinite clay and > 3 hours for Wadden Sea silt.

Direction of movement becomes both upward and downward though lots of horizontal movement occurs due to the remaining turbulent eddies. Droplet size and position within the water column did not determine the direction of migration of the oil droplets; this was likely the result of density differences within the droplets associated with bound air (droplets ascend) and/or sediment (droplets descend) (de Groot, 2014). Likewise air discharging from the droplets may explain the occurrence of oil droplets descending from the water surface after initial ascension. After 2 minutes in the Ngarunui Beach, 20 ml HFO experiment, some large and presumably some smaller oil droplets and tar balls broke off the surface layer and descended slowly to settle atop of the bottom sediments (Figure 5.33). It was assumed that sedimented oil continued to break off the surface slick after this time in all experiments that resulted in tar balls.

Few observable differences were identified between the oil-sediment particle interactions using different proportions (10 ml and 20 ml) of the individual oil samples with the exception of the 20 ml HFO, Moonlight Bay experiment which formed negatively buoyant flake aggregates (< 1 mm), while the 10 ml sample formed negatively buoyant tar balls. The negative buoyancy of the tar balls is likely to be caused by the density of the minerals present. In this experiment, flakes of oil were also visible still in suspension near the top of the water column after approximately 36 hours which became remobilised after movement of the flask but which had settled by 48 hours (Figure 5.12). It was difficult to determine whether flakes were buried within the bottom sediments. The flakes produced in the experiments are similar to those found by Stoffyn-Egli and Lee (2002) which formed with Using Svalbard sediment (only 2-3% smectite by weight and 50% mica, illite and chlorite) and above 0.2 g/l of oil and low ratios of oil/minerals as the flake OMA were big enough to be seen with the naked eye. These were the result of mineral-bound oil at the particle scale controlling the shape of the OMA.

Oil droplet, tar ball and aggregate concentrations and sizes increased with oil concentration. As small oil droplets were not visible to the naked eye during the mixing experiments and as oil droplets less than 0.5 microns were not visible using the microscope, it is difficult to make exact inferences about the size distributions of oil droplets and to estimate the fraction of oil in the different phases in the experiments without being biased toward larger fractions. It was also not possible to observe oil droplets behaviour and characteristics under the microscope using the current technique, either as oil had changed phase before observation (i.e. had formed a surface slick within the sub-sample or negatively buoyant OMA) or because reflected light did not allow it. It was therefore not possible to make inferences about the phase distributions of oil in the experiments. However even though a portion of oil was not visible using the current method, the amounts of oil in small (< 5 microns) droplets and oil coatings are quite small, some inferences about the distribution of oil were made.

All experiments displayed reduced size distributions with time. Generally the larger sized fractions of sediment settled out earlier, due to increased densities and droplets became progressively smaller with time until they were no longer visible. Sphericity of oil droplets increased with time in the HFO experiments (due to fewer coalescences), while size distribution decreased. Crude oil droplets were always spherical. Oil droplets were present throughout the water column during most of the experiments and showed no obvious distribution patterns in HFO sub-samples however concentrations of particle grains increased with depth using HFO. Sediment and oil concentration increased with depth in Maari/Moki sub-samples.

Oil droplets are spherical and generally dark while aggregations have complex forms. The Maari/Moki sample displayed a much greater propensity for large (< 20 mm), complex form aggregations whereas the HFO samples showed mainly smaller aggregations (10 mm) of spherical oil droplets or isolated spherical droplets and particles. Oil droplets sizes were between < 0.5 mm and 10 mm. Aggregations settled on the surface of the bottom sediments as soon as sediment had settled and were mixed in with the sediment as it settled in many experiments. The form of the aggregations at this time was complex and non-spherical however after further settling more spherical tar balls were emplaced. Ngarunui Beach sediment interacted more than the Moonlight Bay sediments with oil, producing large tar balls with both HFO and crude oil possibly due to increased polarity of the heavier minerals present or the elongate shape of the grain, with larger surface area to volume ratio.

Between 12.5 and 48 hours, large spherical tar balls (5 – >10 mm) formed on the surface of the bottom sediments in all experiments except those with Maari/Moki crude oil and Moonlight Bay sediments and Ngarunui Beach sediment with 20 ml HFO (as flakes formed). It is plausible therefore that before 48 of settling, these tar balls broke off the oil slick and descended to rest on the sediment at the bottom of the flask, due to increased density from incorporated sediment. The high sphericity of the HFO tar balls follows the description of pelagic SRB tar balls as determined by Iliffe and Knap (1979 as cited in Warnock, 2015) which are less tarry and softer than surface weathered tar balls. The crude oil tar balls were less spherical in shape and it was not possible to determine whether the aggregates that were present immediately after cessation of mixing where incorporated within them.

Tar balls that formed from the Maari/Moki oil differed significantly from those formed with HFO. Maari/Moki tar balls were semi-spherical and non-spherical with obvious sediment grains adsorbed to the surface of and engulfed within especially darker, elongate grains; the mineral grains were in the oil phase. HFO tar balls were highly spherical with sediment in the oil phase despite high levels of sedimentation on the tar balls. Quantities of minerals attached to droplets and tar balls seem to be determined by oil, with larger amounts of sediment adhered to the tar balls with treatment of HFO. As tar balls were not the result of weathering and were generated through sedimentation of oiled sands they are considered to be surface residual tar balls (SRBs) according to OSAT classification (2013). Tar balls are 10 millimetres and less in size and are therefore classified as millimetre tar balls (MTB) according to the scheme of Bernabeu et al. (2006). Although tar balls were present on the sediment during settling in the experiment, these were not observed during the microscopic observations of HFO oil; rather spherical oil droplets were present. The processes required for tar ball formation were therefore not present after the experiments. It is likely that without turbulent energy, tar balls will not form.

With increasing proportions of oil, an increased size distribution and increase in number of tar balls on the surfaces of the bottom sediments was identified. Tar balls were generally less than 10 mm in experiments using 10 ml of HFO and Ngarunui Beach sediments while tar balls were greater than 10 mm using 20 ml of HFO and Ngarunui Beach sediments. Likewise the size of the tar balls formed in the Ngarunui Beach sediment using 20 ml of Maari/Moki oil was > 10 mm in diameter; double that of the 10 ml samples which were between 2 - 5 mm in diameter. With 10 ml of HFO added to Moonlight Bay sediment, small (< 5 mm) tar balls formed.

Tar balls did not form on the bottom sediments in any of the Moonlight Bay experiments using Maari/Moki co-mingled oil even after more than 18 hours. The density of the Maari/Moki oil in combination with the fine sediment from

Moonlight Bay may have been insufficient to produce tar balls dense enough to descend to the bottom of the flasks. Individual grains were visible at the base of the oil slick but using the method available it was not possible to ascertain the presence or amount of sediment within the oil. The presence of sediment within the sub-sample from the slick suggests that there was a large amount of sediment in the slick. The presence of negatively buoyant tar balls in the Ngarunui sediments using Maari/Moki co-mingled oil and absence in the Moonlight Bay sediments verified that the density, morphology or chemistry of the sediment contributed to the formation and sinking of tar balls.

A layer of flocs coated the sediment surface and any tar balls that were present in all experiments except the 10 ml HFO sample with Ngarunui Beach sediments (Figures 5.16, 5.19 and 5.20). Reduced amounts were present in the 20 ml sample also. This yellow layer is silt-sized flocculations have formed due to agitation and the clay fraction present in the sediments. This settling has been observed by many authors. As these flocs were also present during control experiments, it is difficult to ascertain oil concentrations within these flocs however as Ngarunui Beach samples had very different floc concentrations with the different oils, it is conceivable that oil was a determining factor in the flocculation process.

The presence of oil patches in the Moonlight Bay surface samples with treatment of Maari/Moki oil is consistent with the significant concentration of Maari/Moki oil that remained in the surface slick after settling. The relative density of the oil and light grains ensured that the oil remained buoyant even with the addition of grains. Oil was also present in the water column samples.

5.3.2 MICROSCOPIC OBSERVATIONS

Due to the presence of fine clay minerals and particles, the water was turbid in the Moonlight Bay experiments and some of the Ngarunui Beach experiments and settling was hard to see The water did not remain cloudy after 12.5 - 48 hours however, in contrast to de Groot’s (2014) findings; indicating that the clay minerals had formed large silt-sized particles that settle within hours to days.

Emulsions only formed in the HFO experiments. Emulsions formed in all surface and top of water column sub samples and at the bottom of the water column and on the sediments in the 20 ml experiments. A thin veneer of oil was present with sediment grains incorporated in the surface sub-samples and bottom sediment sub-samples from the Ngarunui, Maari/Moki experiments.

Oil type was shown to have an effect on OMA formation kinetics, as OMA varied considerably between the two oils, large tar balls and flakes formed with HFO, while oil globules engulfing grains (some spherical) (Figures 5.74, 5.76) formed with the crude oil. The presence of large amounts of flocs in the Maari/Moki, Moonlight Bay sub-samples is possibly due to the high clay particle concentrations that are assumed at Moonlight Bay and would corroborate the presence of flake OMA during experiments. Flocs were not visible in the bottom sediment samples with crude oil however. This was possibly due to the negligible amounts of oil and finer sized particles in these sub-samples and because any buoyant OMA would not have been sampled at these positions in the water column. The fine minerals/OMA may also be present but unseen in these samples because of the larger mineral fractions. Neutrally buoyant, solid OMA were present in two of the sub-samples from the water column of the Moonlight Bay sediment and 10 ml HFO; one from the middle section and one from the bottom section (Figures 5.82 and 5.83). The presence of large solid OMA in the water column with HFO and Moonlight Bay sediments backs up the assumption that clay minerals are present. These large (0.5-1 mm) aggregations contain more trapped oil resulting in more buoyant OMA and have been observed using smectite clays. An unknown neutrally buoyant white flocculation was present in the sample from the bottom of the water column with Ngarunui sediments with 20 ml HFO (Figure 5.88).

Although viscous oils normally form solid OMA, a predominance of droplet OMA formed in the HFO experiments in the bottom sediments with mineral particles at their peripheries (Figure 5.60 and 5.61). These do not contain mineral particles according to Stoffyn-Egli and Lee, 2002). These droplets are probably due to the surface properties/chemistry of the minerals present and the time for settling, as the droplets were very large, up to a millimetre in diameter. More droplets formed with Ngarunui Beach sediment in general, though the 20 ml sub-sample had fewer and larger droplets. Only two droplets were visible in the 20 ml HFO, Moonlight Bay sub-sample (Figure 5.57). These treatments produced flakes during the experiments. As droplet OMA were found only in the bottom sediment samples and once in the water column, it is evident that the heavier, larger, hydrophilic grains settled earlier during the experiments and resulted in droplet OMA. These heavier fractions may also have caused the formation of the large (silt-sized) OMA. The position of the droplet OMA in the water column may be the result of the mineral particles absorbed to them or the heavier HFO. The presence of flake like structures in the surface sub-sample with Ngarunui, HFO (Figure 5.53) might indicate water-in-oil-emulsion. It is possible that the absence of water in the sample resulted in diminished hydrophobicity, producing an effective medium for flake aggregation without the necessary strength to produce solid aggregates. The sphericity of the droplet OMA in the HFO experiments in both sediments was indicative of hydrophilic minerals present, perhaps kaolinite and likely quartz. However the formation of solid OMA and tar patches which engulfed mineral grains within Maari/Moki experiments is indicative of the presence of hydrophobic minerals also and the insolubility of the crude oil.

The HFO oil did not readily coat the sediment grains in any of the experiments, in fact in some experiments; it seemed to sit atop of the oil (Figures 5.52, 5.80, 5.81 and 5.82). This was also found by de Groot (2014). On one occasion a grain on the container lid was saturated by oil (Figure 5.92) and grains within an air bubble appeared to have a thin veneer (Figure 5.62). In contrast, the crude oil visibly coats, absorbs and has grains adsorbed to it’s surface. Sediment coatings were clearly distinguishable in crude oil sub-samples under episcopic light, resembling those found by Delvigne (2002). The irregular shape of the oil patches is possibly the result of the absorbed sediment grains. Semi-spherical tar balls formed in the sub-samples using Maari/Moki oil however they were not present in any of the HFO sub-samples (only during the experiments). Tar balls that formed in the sub-samples with Maari/Moki (Figure 5.72) were much larger (1 mm) than those formed during the experiments and contained more sediment grains. These tar balls may indicate the effect of the grains on the oil especially as these tar balls were heavily coated in surface grains. The absence of HFO tar balls in the sub-samples means that the processes causing the formation of tar balls with HFO were not present i.e. turbulent energy and that the tar balls readily broke down.

There was a distinct attraction of darker, elongate grains to the waxy Maari/Moki oil, possibly due to electrostatic attractive forces between the oil and grains or the elongate shape of the grain, with larger surface area to volume ratio. The elongate, darker grains are possibly heavy mineral grains of hornblende with increased polarity. The large charge differentials of metals make their binding properties stronger. The presence of elongate grains in the water column in tar patches was due to the buoyancy of the tar balls; the dense grains would otherwise have sunk to the bottom of the flask. Although particles were not as attracted to the HFO oil in some samples (instead sitting above it), grains were visible on the droplet OMA and darker, elongate grains covered tar balls during the experiments (Figure 5.20).

The absence of larger grain sizes in Moonlight Bay surface samples with treatment of Maari/Moki crude suggested that fine clay sediments had preferentially adhered to the sediment while heavier, larger grains had sunk to the bottom due to their relative densities. The water column was turbid at this time during experimentation. The abundance of oil and sediment in the Maari/Moki, Ngarunui Beach surface samples suggested that the sediment had adhered to the waxy oil. The increased density however was not enough to make the oiled particles sink. It is likely that these OMA/patches contained more oil. The thick surface slick apparent in Moonlight Bay surface samples with HFO substantiated that the oil had not degraded significantly; it’s density remaining lighter than the surrounding medium.

Intuitively, all sub-samples from the bottom sediments contained abundant sediment. The presence of prevalent sediment in the lower water column samples could have been due to human error during sampling as grains may have been inadvertently picked up from the bottom with the pipettes; likewise high concentrations of oil and/or sediment in water column sub-samples are likely due to human error.

Air bubbles were present in Maari/Moki samples in all positions within the flask. Air bubbles were not visible within the spherical HFO droplets however they were present on the container lids, in emulsions and in the negatively buoyant aggregations that formed during experiments.

A long term study by Bernabeu et al. (2010) ascertained that ‘halos’ or the staining of the sand around near-surface tar balls (10 -12 cm from the surface) occurred in saline conditions at a stable temperature of 14 °C; with shorter time frames for appearances of ‘halos’ for decreased flow rates. It was established that carbonate concentrations of bioclastic sediments may enhance the halo development of oil coatings at depth, retaining the oil within the sediment column. Conversely siliciclastic sediments generate oil microparticles generally, enabling rapid permeation and dispersion. The tar balls and sediment used in the study by Bernabeu et al. (2010) were from weathered crude oil with similar characteristics to HFO, with a high concentration of bioclastic grains (50%) and asphaltenes and resins (28%). Stained testifiers due to water in oil emulsion were not found in the current study although the timeframe between sampling and observation was over a month at similar temperatures and the sea water was kept static and a significant fraction of bioclastic grains were visible in the Moonlight Bay sediments. However tar balls were not deeply buried in the sediment and thus were not exposed to the same pressures as during the previous study. Anaerobic conditions also prevailed in the current study therefore emulsification, the primary mechanism for separation of oil from tar balls, could not exist.

Due to the stirrer transferring oil up the flask walls during repetitive agitation, it is likely some losses occurred during successive experiments although these were considered negligible. More rigorous stirring or lengthier stirring (> 30 seconds) resulted in greater amounts of individual oil droplets and fewer aggregations in experiment using 20 ml HFO and Ngarunui sediment. This is agreement with the work of Delvigne and Sweeney (1998) and Zhang et al., (2010). The arrangement of tar balls and patches close to the walls of the container in all of the Ngarunui Beach samples (using both treatment of HFO and Maari/Moki oil) is indicative of electrostatic attraction between the oil and thick plastic walls of the container. The

HFO adsorbed to the base of the container in the Ngarunui Beach sub-samples. This phenomenon was also observed by de Groot (2014).

5.4 LIMITATIONS OF RESEARCH

Maari/Moki experiments were carried out immediately after the oil was introduced into the seawater. Although the Heavy Fuel Oil (HFO) was added to the flask more than 30 hours before settling experiments were undertaken, the lack of light distillates in HFO meant that it is unlikely that significant losses through evaporation and dissolution occurred. Losses of 3 % over 2 days through weathering have been found previously (Fingas, 2013).

As the only mechanism for measuring settling times and percentages were visual approximations it was difficult to accurately predict the point at which sediment grains and oil had settled. It is likely there are inherent errors in the measurements. Other sources of error arise from the single observer with inherent bias. It must be noted that only a limited number of replicates were performed due to the number of experiments carried out.

Sub-samples were kept in air tight plastic containers to minimise oxidation and biodegradation however some samples showed signs of weathering, such as water in oil emulsion. Although samples are considered fresh after one month, it is possible that some samples underwent a degree of degradation especially as sea water samples were not fixed using mercuric chloride (200 ppm) or refrigerated to minimise oil biodegradation. Subsamples were kept at temperatures between 5 – 10 °C and not in excess of 12 °C.

Immediate observations of sub-samples from settling experiments and use of polarising filters would have aided in distinguishing the oil from sediment as fresh oil is fluorescent and enabled more accurate assessment of any OMA and characterisation of oil droplets. Oil coatings would have been visible on the sediment grains.

For future research, detailed analysis of the beach composition would provide useful information on the binding characteristics of the sediment particularly the clay fractions. Settling experiments using a low density, less viscous, low wax oil sample could also provide additional comparative information.

SUMMARY AND CONCLUSIONS

Ngarunui Beach is an ultra- or highly dissipative, gently sloping, 200 m wide (at low tide), open coast beach. It's morphology is controlled by high wave energies, the ebb tidal delta at the harbour entrance and by littoral drift of large slugs of titaniferous rich sediment that have travelled from Taranaki, 180 km away. The presence of the ebb tidal delta at the Raglan Harbour entrance possibly causes sediment recirculation offshore and affects the northern end of Ngarunui Beach. Placer deposits of titanomagnetite are often exposed along Ngarunui Beach and in the harbour entrance. A large flood channel at the northern end of the beach contributes to onshore/offshore sediment exchange. Ngarunui Beach also has rips present approximately every 250-500 m. Mean wave approach is from the SW. Although New Zealand beaches do not have distinctive seasonal shifts, oscillations between storm and fair weather conditions exist throughout the year. No infaunal species have been observed on this high energy beach, however cetaceans are known to frequent the offshore area.

Wainamu Beach, inside the harbour entrance is characterised by strong ebb tidal currents that scour out the channel edges with a spit beginning to form with a west-east aspect and erosion occurring just west of this. Bedforms that are oriented perpendicular to the channel can be seen along the beach. The area of Wainamu Beach is dynamic and large amounts of erosion are presently occurring due to a southerly shift in the position of the main tidal channel.

Predominantly tidally controlled, Moonlight Bay consists of a coarse sandy upper littoral area, with mud flats in the lower parts of the intertidal zone. A rock platform is exposed at low tide level, indicating the beach is a veneer deposit. Wave refraction of small waves entering or generated within the harbour occurs around the western headland of the beach, and modify the beach. Two small boulder groynes have been emplaced on the eastern side of the beach to provided protection from waves generated within the harbour that cause sediment recirculation and loss. As Moonlight Bay is exposed to a large fetch area of approximately 5 km, resuspension by waves can also cause modification of sediment. Short, steep waves that overtop the~1 m rock wall at Moonlight Bay occur with north-easterly winds. The area experiences erosive/accretionary events as large changes in bed level, ± 40 cm at Okete Bay, 2.5 km away with a similar aspect have been recorded.

Sediment samples from Ngarunui Beach showed coarsening offshore. Low wave energy associated with fine weather conditions caused the foreshore means to become slightly finer and more well sorted at Ngarunui Beach. Storm conditions resulted in medium sized foreshore mean particle sizes with poorer sorting. Samples from southern Ngarunui Beach contained slightly finer fractions with coarsening in a southerly direction. Average grain sizes from Wainamu Beach sediment samples were consistently fine. This is possibly linked to the high current velocities in this area. Large fractions of fine particles (< 10 %) were found in the east of the beach, at the mid and low intertidal zones. This area is not as close to the main channel and is likely to be a sink for finer fractions as it is also sheltered from the prevailing SW winds. Moonlight Bay samples contained larger fractions of clay and silt sized particles typical of sheltered estuarine environments. Coarse samples were found in the upper intertidal and were indicative of areas of higher wave and current energy. The eastern transect and low intertidal areas have predominantly fine sediment distributions with large clay and silt concentrations.

Slightly poorer sorting was found at the low intertidal position, with better sorting in a northerly direction along the foreshore though all samples displayed mesokuritc grain size distributions. Sediment samples from northern Ngarunui Beach were predominantly moderately well sorted as expected for an open coast beach in which the processes of uprush and backwash are the principal transport mechanisms. Poorer sorting was found in the low intertidal at the southern end of Ngarunui Beach. Wainamu Beach showed slightly less sorting than Ngarunui Beach which suggests reduced energies during experiments at this location. Moonlight Bay sediment samples displayed bimodal, leptokurtic frequency curves, typical for sheltered estuarine environments with weak transport energies and multiple sediment sources. The poorest sorting and most platykurtic distributions were associated with the coarse fractions present on the eastern transect and the presence of fine sediment at the low intertidal. Only Wainamu Beach displayed highly asymmetrical skewness, predominantly in the mid intertidal zone.

Elongate, darker grains on the coast and in the harbour entrance are likely to be minerals such as hornblende eroded from Mt Karioi lavas and lahars. Rounded grains were present on the open coast beach while more angular grains were observed in the sheltered estuarine bays. Considerable amounts of euhedral shaped particles were also present. Bioclastic fractions were much greater at Moonlight Bay and only Moonlight Bay had grain sizes above 2 mm. At Ngarunui Beach, storm conditions are reflected by an increase in finer, but much denser titanomagnetite and other heavy minerals. These form a very dark lag surface. Shell hash is also deposited with the ebbing tide.

Interpretation of the depths of the transitory sediment/water layer on beaches is essential for estimation of initial depth of penetration of spilled oil, for sediment transport rates and nearshore process modelling. Because of differing methodologies and definitions for measurement of the active bed layer on beaches, comparisons of values recorded are not always beneficial. Measurement techniques have included coloured sands, sediment tracers and rods and washers. Temporal scales have varied from a few waves to whole tidal periods. Measurements have both excluded bed level change and included it. Averaging of disturbance values is not ideal as bedforms can have extreme effects on these averages.

A network of ~ 5 mm diameter depth of disturbance rods were used to monitor bathymetric evolution in the surf/swash zone in this study. These stainless steel rods had loose fitting washers attached to gather data on the depth of the transitory sediment/water layer and net accretion and erosion. Large variations of DoD within and between sites were observed in this study. On the exposed coast, values of DoD were found to be > 300 mm while < 100 mm was observed at Wainamu Beach. Insignificant mixing occurred at Moonlight Bay essentially due to the thin veneer of sediment over a bedrock surface, and to sheltering.

It was found that disturbance depths varied substantially in the cross-shore and longshore during all experiments. This variation was determined by bed morphology predominantly. Only once, during moderate wave conditions and large tides did a linear decrease in DoD occur alongshore in a northerly direction. On this date Ngarunui Beach was experiencing net accretion in fair weather conditions. Averaged DoD values displayed slightly larger DoD in a northerly direction.

Morphological changes are a function of changing incident wave regimes, currents, pre-existing morphology and tidal range. Large scale erosive events which exceeded 5 m have been recorded and observed at Ngarunui Beach while small scale bed level variation occurs on the scale of decimetres. This complex morphology at Ngarunui Beach, rip currents and offshore channels affect prediction of DoD.

Generally DoD decreased onshore with swash processes dominating the high intertidal region. The presence of a trough created by the high water table in August, 2014 resulted in larger values of DoD in the mid intertidal zone. The largest values of DoD were during large storm events when erosion occurred in the mid and low intertidal and accretion occurred in the high intertidal except during a large storm event in February. However, it is possible that high tidal elevations at this time caused deposition further inshore. Most small scale morphologlical change occurred in the mid intertidal region.

Swash processes dominated in the high intertidal zone. Values of DoD were comparatively smaller and varied alongshore significantly. Under larger wave conditions, disturbance was greater at the mid position in the high intertidal. In fairer conditions, there was no apparent pattern. Tidal conditions were found to have a large increasing effect on swash processes in the high intertidal zone. Tidal currents also played a significant role at Wainamu Beach. For significantly smaller waves, (waves are not generally present at this location), DoD was large. Positive DoD values represent areas of accretion when the washer moved upward during the tide. This was caused by vibrations as the swash zone approached, piling sand beneath and the lifting the washer as the sand accreted.

Small consistent increases in values of DoD alongshore at southern Ngarunui Beach were possibly associated with longshore drift. The larger values of DoD in the mid intertidal zone at Southern Ngarunui Beach correspond with the zone that is most exposed to wave breaking. At high tide it is directly beneath the breakers at a depth where the waves reach the bed. Offshore from this the depth of the water was observed to be greater than the wave height and inshore from this run-up processes dominate as waves have already broken in the outer zones. This zone is also more exposed to swash processes. It can be deduced that as the areas most exposed to wave breaking exhibit the most disturbance, that swash processes have limited effects on this beach.

DoD was much more varied at Wainamu Beach than on Ngarunui Beach and values were largest in the mid transect. When the flat high intertidal area on the western transect was exposed to the tide (during spring tides), moderate values of disturbance were found at this position. However, the largest values at this transect were recorded near the break in slope at this western transect. The eastern transect showed little variation and was therefore less affected by current scour.

The slightly higher DoD values that were measured at the high intertidal on the eastern transect at Moonlight Bay were possibly due to wave refraction around the eastern headland, causing currents which would be greatest when they reach the groyne at the opposite side of the beach (location of the rod which experienced disturbance). There also happened to be a large amount of seepage at this location due to a storm water drain and at the opposite side of the beach due to a high water table.

Values of DoD have been found to be small on dissipative beaches and comparable across the shore face. This is because of dissipation of energy across a wide crosshore zone. On reflective beaches, a concentrated zone of turbulence is associated with the breakpoint and results in much higher values of DoD under similar wave conditions. Values of DoD have been given as ~3 - 4 % of the average breaking wave height, H_b, on a dissipative beach.

Significant wave height, deep water wave height, wave period, average grain size, beach slope and tidal variations have all been shown to affect. Groundwater and swash infiltration may also modify mixing depths. Models that incorporate these statistics have been used to predict mixing depths.

After Bertin et al. (2008), the mixing depths for dissipative sandy beaches is ~ 2 – 4 % of significant wave height. Following the Bertin et al. (2008) model, Z_o of 0.0522 was established under fair weather conditions and 1.2 m waves on the 27th of September and Z_o of 0.084708 under 3 m wave conditions on the 14th of August, 2014. These values were not in good agreement with the measured data as the formula underestimated depths of disturbance on Ngarunui Beach especially during fair weather conditions. It is, however, important to note that wave heights were predicted and can therefore have inherent error. Mixing was up to 13 % of the wave heights during large storm events and even larger proportion coefficients were obtained in fair weather conditions, up to 18% in the low intertidal zone. As wave heights were not known at Moonlight Bay or Wainamu Beach, it was not appropriate to determine proportionality coefficients at these locations.

The results found here do not compare well with others from dissipative beaches. Recorded values range from 3 % to 8 % generally. However Anfuso observed values of 16.3 % H_b under significantly smaller wave heights on an intermediate beach. Variation between locations has been estimated at 1500 % mostly due to differing morphologies (Ferreira et al., 1998). Differences in reported values may also be due to inherent differences in measurement techniques.

Oil penetration on Ngarunui Beach has the potential to be deep, especially when considering potential burial. Groundwater and swash infiltration cause oil to migrate below initial mixing depths and as there is a high water table present at Ngarunui, exfiltration is likely to occur rapidly at this location. The exposed beach however undergoes large amounts of erosion frequently and so it is likely that oil would be not remain buried for long periods.

Comparisons with Moonlight Bay were not possible due to lack of data. However it was anticipated that DoD would be negligible at Moonlight Bay at least under fair weather conditions. Storm events have been observed to cause 0.4 m of change at the shore implying that oil burial at this location could potentially be this deep, with possible groundwater infiltration increasing the depth of oil contamination. However bedrock at this location would prevent deep penetration or percolation. Due to the high concentrations of fine clay and silt sized particles at Moonlight Bay, it would be expected that OMA would form if oil were transported into this low energy environment.

Oil settling experiments were carried out to evaluate oil settling times and behaviours. Settling times for clay rich fine sediments of Moonlight Bay were close to half the time of the Ngarunui Beach's sediment settling times. Both oils increased the settling times for Moonlight Bay sediments while reducing them further for Ngarunui sediments. Moonlight Bay sediment settling times were lengthened by up to 3.8 s and 4.8 s with the addition of Maari/Moki crude and HFO respectively. Ngarunui Beach sediment settling times decreased by 2.5 s and 3.1 s respectively. Settling was clearly determined by the sediment type. It is likely that the different densities or surface areas of the particles had an effect on the settling behaviours of the oiled sediment. The reduced settling times of oiled grains from Ngarunui Beach is likely to have resulted as dense aggregates formed from the Ngarunui Beach sediments which are expected to have heavy minerals present. Settling was slowed in Maari/Moki crude experiments as flocs containing material less dense than seawater were present. The oil types (lighter crude or heavier fuel oil) did not differ in their effect on sediment settling times. Settling was consistently faster for Ngarunui sediment and consistently slower for Moonlight Bay sediment. The quantity of oil did not significantly affect sediment settling times either. Values were within 2.5 seconds using different concentrations. Oil droplet, tar ball and aggregate concentrations and sizes increased with oil concentration.

Oil settling times were protracted especially for HFO samples. The mean values for HFO settling in these experiments was above 105 seconds except for the 10 ml sample with Ngarunui beach sediments which seemed to settle earlier.

Maari/Moki oil settling times showed less variation but much lower values for settling time due to the insolubility and relative density (0.836) of the crude oil and it's propensity for forming large aggregates which settled quickly, rising to the surface with Moonlight Bay sediment and some sinking to the bottom of the water column with Ngarunui Beach sediment (due to the increased density of Ngarunui Beach sediment). The insolubility of the Maari/Moki crude may also have affected the amount of oil suspended in the water column. The larger aggregates/patches that were present in the crude oil experiments may also have had larger wakes, dragging other aggregates down. HFO settling slowed significantly once the sand had settled, probably as drag decreased.

Rapid vertical dispersion occurred due to turbulence followed by immediate resurfacing of large oil droplets (some > 2 mm) and sediment/oil aggregations (> 5 mm) due to buoyancy and proximity to the surface. Most (~85%) of the oil rose to the surface forming thick aerated slicks. Oil did not disperse through the water column without mixing during the experiments. Reduced size distributions occurred with time (due to fewer aggregations) and shericity of oil droplets increased. Larger aggregates formed in the crude oil experiments. The oil in the experiments was generally evenly distributed (droplets less than 0.5 μm were not visible so are not included). In one experiment, fluid density increases were apparent near the base of the water column. Oil rich water higher in the water column may be limiting mixing also. Although 5 minutes has been shown to provide equilibrium for droplet dispersion, the 30 seconds chosen for these experiments imitated the passage of a wave.

Eddies caused horizontal movement of oil and particles. Droplet size and position within the water column did not determine the direction of migration of the oil droplets; this was likely the result of density differences within the droplets associated with bound air (droplets ascend) and/or sediment (droplets descend). Likewise air discharging from the droplets may explain the occurrence of oil droplets descending from the water surface after initial ascension. Mixing introduces vertical turbulence that can offset the negative buoyancy of some droplets. When the turbulence dissipates, then the droplets are no longer supported and sink.

During the experiments convex shapes (HFO) and large aggregates (Maari/Moki crude) could be seen distended from the slicks which later broke off and settled on the bottom sediments as tar balls (5 – >10 mm). These tar balls resemble pelagic SRBs that are soft, non-tarry and readily break apart. The 20 ml HFO experiment with Moonlight Bay experiment resulted in large (< 1mm) flake aggregates which stayed in suspension for 36 hours but had settled by 48 hours. Ngarunui Beach sediment interacted more than the crude oil producing larger tar balls possibly due to increased polarity or larger surface to volume ratio. The tar balls that formed in the crude oil experiments were less spherical, had less sediment adhered to their surface and replaced the complex shaped aggregates that had settled earlier in the experiments. Tar balls did not form with crude oil and Moonlight Bay sediment and in the 20 ml experiment, particles not convex tar ball shapes were visible at the bottom of the slick. The density of the Maari/Moki oil in combination with the fine sediment from Moonlight Bay may have been insufficient to produce tar balls dense enough to descend to the bottom of the flasks.

Floccules formed in both the control experiments and oiled experiments and were large silt-sized particles that sank readily, allowing the water column to clear within 12.5-48 hours. As Ngarunui Beach samples had very different floc concentrations with the different oils; (much higher concentrations of flocs were associated with crude oil), it is conceivable that oil was a determining factor in the flocculation process. Emulsification had occurred in some of the HFO experiments and dendritic structures were present in the Ngarunui/HFO sub-sample that might be indicative of water-in-oil emulsion.

Oil type dictated the type of OMA that formed; HFO produced large tar balls and flakes during experiments and droplet OMA in sub-samples. Large oil patches, tar balls and large (0.5-1 mm), neutrally buoyant, solid OMA were present in crude oil sub-samples that have been associated with smectite clays.

A predominance of large (~mm), droplet OMA (with mineral particles at their peripheries) formed in the HFO experiments in the bottom sediments. The size of the droplets may be due to lengthy settling times. The presence of the OMA at the bottom of the water column indicates that large, heavy hydrophilic minerals may be present which may also have caused the predominance of large (silt-sized) flocs. The higher concentrations in Ngarunui Beach sediments in combination with the shape of the OMA (hydrophilic minerals produce droplet OMA), suggests that mineral surface properties/chemistry affect droplet OMA formation. Conversely, the presence of tar patches in the crude oil sub-samples indicates hydrophobic minerals (and insolubility of the crude oil). Air bubbles were not visible in the solid and droplet OMA.

The crude oil tar patches visibly coat, adsorb to and have grains absorbed within them possibly causing the irregular shape of the patches. Generally, HFO did not seem to coat the grains. Grains in fact it seemed to float above the oil patches in these sub-samples. Spherical tar balls/patches were present within the crude oil sub-samples but were larger than those formed during the experiments. These tar balls may indicate the effect of the grains on the oil especially as these tar balls were heavily coated in surface grains. Air bubbles were visible in most oil patches/tar balls.

Dark, elongate grains (possibly hornblende) were preferentially attracted to the crude oil due to electrostatic attractive forces between the oil or the larger surface area to volume ratio. These grains also showed preferential attraction to the surface of droplet OMA formed in HFO experiments. Oil was also electrostatically attracted to the walls and bases of the plastic containers.

The absence of larger grains in the Moonlight Bay surface sub-samples and presence in the Ngarunui Beach sub-samples suggested that the larger minerals at Ngarunui Beach resulted in larger OMA/patches; that were buoyant because of large concentrations of oil. The oil in the Moonlight Bay experiments had preferentially adhered to the smaller clay particles.

Stains due to water in oil emulsions were not found in the current study however tar balls were not exposed to high pressure and anaerobic conditions prevailed. Immediate observations of sub-samples from settling experiments and use of polarising filters would have enabled more accurate assessment of any OMA and characterisation of oil droplets.

RECOMMENDATIONS FOR FUTURE RESEARCH

Future research in disturbance depths on dissipative beaches should include measurements of DoD before and after storm events and during tidal cycles. Variation in the distribution of DoD can then be monitored and correlated to any morphodynamic features present.

Use of continuous measurements would allow more accurate quantification of the transitory bed surface layer. Measurement of currents to establish drift patterns and use of underwater cameras for assessment of bedform migration would all elucidate the distribution of disturbance on the shoreline.

More detailed study of the sheltered estuary beaches would also be of value. Assessment of the aerated zone and concentrations of animal burrows could aid in establishing possible oil burial transport pathways.

Settling experiments using a low density, less viscous, low wax oil sample could also provide additional comparative information

Detailed analysis of the mineral grains would provide useful information on the binding characteristics of the sediment particularly the clay fractions. Settling experiments using a low density, less viscous, low wax oil sample could also provide additional comparative information on oil/sediment settling. Use of UV epi-fluorescence microscopy or particle image velocimetry would enable better evaluation of OMA.

REFERENCES

Ajijolaiya, L, O., Hill, P.S., Khelifa, A., Islam, R.M. and Lee, K. (2006). Laboratory investigation of the effects of mineral size and concentration on the formation of oil–mineral aggregates. *Marine Pollution Bulletin, 52* (8), 920-927. http://doi.org/10.1016/j.marpolbul.2005.12.006

Allen, J.R.L, and Pye, K (1992). *Saltmarshes - Morphodynamics, Conservation and Engineering Significance*. Cambridge, UK.: Cambridge University Press.

Anderson, C.M., Mayes, M., and LaBelle, R. (2012). *Update of Occurrence Rates for Offshore Oil Spills.* (OCS Report BOEM 2012-069 BSEE 2012-069). USA: Department of the Interior Bureau of Ocean Energy Management [BOEM] and the Department of the Interior Bureau of Safety and Environmental Enforcement [BSEE]. Retrieved from http://www.boem.gov/uploadedFiles/BOEM/Environmental_Stewardship/Environmental_Assessment/Oil_Spill_Modeling/AndersonMayesLabelle2012.pdf

Andrade, K., Buckley, H.L., Rubin, L.K., Shill, K. and Mulvihill, M.J. (2012). *Understanding Marine Oil Spills: Improving Decision-making and Identifying Research Needs.* California, U.S.A.: Systems Approach to Green Energy (SAGE). The Berkely Center for Green Chemistry. Retrieved from http://sage-bcgc.berkeley.edu/sites/default/files/pages/docs/OTTERS%20FINAL.pdf

Anfuso, G. and Ruiz, N. (2004). Morphodynamics of a mesotidal, exposed, low tide terrace beach (Faro, southern Portugal). *Ciencias Marinas,*30 (4). http://dx.doi.org/10.7773/cm.v30i4.341

Anfuso, G., Benavente, J., Del Rio, L., Castiglione, E., Ventorre, M., (2003). Sand transport and disturbance depth during a single tidal cycle in a dissipative beach: La Barrosa (SW Spain). *Proceeding of the 3rd IAHR Symposium on River, Coastal and Estuarine Morphodynamics*, *2*, 1176-1186.

Anfuso, G. (2005). Sediment-activation depth values for gentle and steep beaches. *Marine Geology, 220* (1-4), 101-112. http://doi.org/10.1016/j.margeo.2005.06.027

Anfuso, G., Gracia, F.J., Andres, J., Sanchez, F., Del Rio, L. and Lopez-Aguayo, F. (2000). Depth of disturbance in Mesotidal Beaches during a Single Tidal Cycle. *Journal of Coastal Research, 16* (2), 446-457.

Anthoni, J.F. (2000). Soil Erosion and Conservation – part 2. Retrieved on 17/04/2015, from http://www.seafriends.org.nz/enviro/soil/erosion2.htm#gravity

Arnaud, G., Mory, M., Abadie, S, and Cassen, M. (2009). Use of a resistive rods network to monitor baythymetric evolution in the surf/swash zone. *Journal of Coastal Research, SI 56*, 1781-1785.

Baker, J.M., Guzman, L.M., Bartlett, P.D., Little, D.I. and Wilson, C.M. (1993). Long-Term Fate and Effects of Untreated Thick Oil Deposits on Salt Marshes. *International Oil Spill Conference Proceedings, 1993* (1), 395-399. http://dx.doi.org/10.7901/2169-3358-1993-1-395

Bunker Oil - Marine Fuel Oil. (n.d.) in *Viscopedia. A free encyclopedia for viscosity.* Retrieved on 28/11/2015, from http://www.viscopedia.com/viscosity-tables/substances/bunker-oil-marine-fuel-oil/

Barron, M.G., Carls, M., Short, J., Rice, S, Heintz, R. Rau, M. and Di Giulio, R. (2003). *Assessment of the Phototoxicity of Weathered Alaska North Slope Crude Oil to Juvenile Pink Salmon.* Anchorage, Alaska: P.E.A.K. Research. Retrieved from http://www.arlis.org/docs/vol1/191100560.pdf

Barth, H-J. (2002). The 1991 Gulf War Oil Spill Its ecological effects and recovery rates of intertidal ecosystems at the Saudi Arabian Gulf coast - results of a 10-year monitoring period. *The University of Regensburg.kempten.* Retrieved from http://www.jubail-wildlife-sanctuary.info/pdf/Barth2002.pdf

Bay of Plenty Regional Council in partnership with Tauranga City Council; Whakatāne, Western Bay of Plenty, and Ōpōtiki District Councils; and the Department of Conservation. (n.d.). *Life's a Beach, Education Resource: Section 6 – Management and Action.* Retrieved from http://www.boprc.govt.nz/media/293882/lab-6n.pdf

Bellido, C., Anfuso, G., Plomaritis, T.A., and Rangel-Buitrago, N. (2011). Morphodynamic behavior, disturbance depth and longshore transport at

Camposoto Beach (Cadiz, SW Spain). *Journal of Coastal Research, SI 64*, 35-39.

Bernabeu, A.M., Fernández-Fernández, S., Bouchette, F., Rey, D., Arcos, A., Bayonad, J.M. and Albaiges, J. (2013). Recurrent arrival of oil to Galician coast: The final step of the Prestige deep oil spill. *Journal of Hazardous Materials, 250–251*, 82–90. http://doi.org/10.1016/j.jhazmat.2013.01.057

Bernabeu, A.M., Nuez de la Fuente, M., Rey, D., Rubio, B.; Vilas, F.; Medina, R. and González, M.E. (2006). Beach morphodynamics forcements in oiled shorelines: coupled physical and chemical processes during and after fuel burial. *Marine Pollution Bulletin, 52* (10), 1156-1168. http://doi.org/10.1016/j.marpolbul.2006.01.013

Bernabeu, A.M., Rey, D., Lago, A. and Vilas, F. (2010). Simulating the influence of physicochemical parameters on subsurface oil on beaches: Preliminary results. *Marine Pollution Bulletin*, *60* (8), 1170–1174. http://doi.org/10.1016/j.marpolbul.2010.04.001

Bernabeu, A.M.; Rey, D.; Rubio, B.; Vilas, F.; Domínguez, C.; Bayona, J.M. and Albaigés, J. (2009). Assessment of Cleanup Needs of Oiled Sandy Beaches: Lessons from the Prestige Oil Spill. *Environmental Science Technology*, *43* (7), 2470-2475. http://doi.org/10.1021/es803209h

Berni, C., Mignot, E., Michallet, H., Dalla-Costa, C., Grasso, F., and Lagauzère, M. (2009). Diversity of bed evolution at wave and tidal scales on Truc-Vert beach. *Journal of Coastal Research, SI 56*, 1726-1730.

Bertin, X., Castell, B., Anfuso, G., Ferreira, O. (2008). Improvement of sand activation depth prediction under conditions of oblique wave breaking. *Geo-Marine Letters*: 28 (2), 65-75. http://doi.org/10.1007/s00367-007-0090-2.

Blott, S. J. and Pye, K. (2001). Gradistat: A grain size distribution and statistics package for the analysis of unconsolidated sediments. *Earth Surface Processes and Landforms 26*, 1237-1248. http://doi.org/10.1002/esp.261

Boehm, P.D., Neff, J.M. and Page, D.S. (2007). Assessment of polycyclic aromatic hydrocarbon exposure in the waters of Prince William Sound after the Exxon Valdez oil spill: 1989–2005. *Marine Pollution Bulletin, 54* (3), 339-356. http://doi.org/10.1016/j.marpolbul.2006.11.025

Bosnic, I., Casaclho,J., Taborda, R., Ribeiro, M., Oliveira, A., Rodrigues, A., and Lira, C. (2011). Textural Characterisation of the Beach Active Layer. *Journal of Coastal Research, SI 64*, 40-44.

Boyd, J.N., Kucklick, J.H., Scholz, D.K., Walker, A.H., Pond, R.G. and Bostrom, A. (2001). *Effects of Oil and Chemically Dispersed Oil in the Environment* [Information Booklet Publication Number 4693]. Washington, D.C.: Health and Environmental Sciences Department American Petroleum Institute [API]. Retrieved from http://www.api.org/environment-health-and-safety/clean-water/oil-spill-prevention-and-response/~/media/CE3C1A19E5B54C2B9D757C59CF303B27.ashx

Bragg, J.R. and Owens, E.H. (1995). Shoreline Cleansing By Interactions Between Oil And Fine Mineral Particles. *International Oil Spill Conference Proceedings:* 1995 (1), 219-227. http://doi/pdf/10.7901/2169-3358-1995-1-219

Brander, R.W., Osborne, P.D., Parnell, K. (2003). High-energy beach and nearshore processes. In Goff, R.R., Nichol, S.L, Rouse, H.L, The New Zealand Coast: Te Tai O Aotearoa. Dunmore Press and Whitireia Publishing, Palmerston North, 119-142.

Brook, A., and Lemckert, C. (2010). *A new technique for measuring depth of disturbance in the swash zone*. (Master's thesis, Griffith University, Gold Coast, Australia). Retrieved from https://www120.secure.griffith.edu.au/rch/file/e6c956ad-ef86-6e5f-da37-d6870b844681/1/Brook_2011_01Abstract.pdf

Brown, S. (2015). *Measures of Shape: Skewness and Kurtosis*. Retrieved on 27/11/2015, from http://brownmath.com/stat/shape.htm#WhatsNew

Brown, E., Wright, J., Colling, A. and Park, D. (1999). *Waves, tides and shallow-water processes* (2nd ed., Vol. 4). Oxford, United Kingdom: Butterworth Heinemann. Retrieved from http://www.sisal.unam.mx/labeco/LAB_ECOLOGIA/OF_files/54211042-Ocean-Circulation-Open-University.pdf

Bryan, K.R., Kench, P.S. and Hart, D.E. (2008). Multi-decadal coastal change in New Zealand: Evidence, mechanisms and implications. *New Zealand Geographer, 64* (2), 117-128. http://dx.doi.org/10.1111/j.1745-7939.2008.00135.x

Ciavola, P., Taborda, R., Ferreira, O, Dias, J.A. (1997). Field observations of sand-mixing depths on steep beaches, *Marine geology, 141* (1-4), 147-156. http://dx.doi.org/10.1016/S0025-3227(97)00054-6

Clayton, Jr. J.R., Payne, J.R., Farlow, J.S. and Sarwar, C. (1993). *Oil Spill Dispersants Mechanisms of Action and Laboratory Tests* (1st ed.). Boca Raton, The United States of America: C.K. Smoley–CRC Press, Inc.

Clement, T. P., Hayworth, J. S., Mulabagal, V., Yin, F., and John, G. F. (2012). Research brief II: impact of Hurricane Isaac on mobilizing Deepwater Horizon oil spill residues along Alabama's coastline—a physicochemical characterization study. Retrieved from Samuel Ginn College of Engineering, Auburn University. http://www.eng.auburn.edu/files/acad_depts/civil/oil-research-hurricane-isaac.pdf

de Groot, N. (2014). *The Extent of Burial of the Rena Oil Spill Within Bay of Plenty Coastal Sediments.* (Master's thesis, University of Waikato, Hamilton, Waikato, New Zealand). Retrieved from http://researchcommons.waikato.ac.nz/handle/10289/8648

de Lange, W.P. (2001). Interdecadal Pacific Oscillation (IPO): a mechanism for forcing decadal scale coastal change on the Northeast coast of NZ? *Journal of Coastal Research, SI 34*, 657-664. http://www.jstor.org/stable/25736331

Delvigne, G.A.L. (2002). Physical Appearance of Oil in Oil-Contaminated Sediment. *Spill Science and Technology Bulletin, 8* (1), 55-63. http://dx.doi.org/10.1016/S1353-2561(02)00121-4

Delvigne, G.A.L. and Sweeney, C.E. (1988). Natural Dispersion of Oil. *Oil & Chemical Pollution, 4* (4), 281-310. http://dx.doi.org/10.1016/S0269-8579(88)80003-0

Etkin, D.S., McCay, D.F. and Michel, J. (2007). *Review of the State-Of-The-Art on Modeling Interactions Between Spilled Oil and Shorelines for the Development of Algorithms for Oil Spill Risk Analysis Modeling* (OCS Study MMS 2007-063). U.S.A.: U.S. Department of the Interior Minerals Management Service.

Evans, M.A. (2003). *Pittsburgh Area Geologic Sites.* Retrieved on 30/3/2015, from http://www.geology2.pitt.edu/GeoSites/sedstructures.htm

Fernández-Fernández, S., Bernabeu, A.M., Rey, D., Mucha, A.P., Almeida, C.M.R. and Bouchette, F. (2014). The effect of sand composition on the degradation of buried oil. *Marine Pollution Bulletin, 86* (1-2), 15, 391-401. http://doi.org/10.1016/j.marpolbul.2014.06.040

Fernández-Fernández, S., Bernabeu, A.M., Bouchette, F., Rey, D. and Vilas, F. (2011). Beach morphodynamic influence on long-term oil pollution: The Prestige oil spill. *Journal of Coastal Research, SI 64*, 890-893.

Fernández-Fernández, S., Bernabeu, A.M., Bouchette, F., Rey, D. and Vilas, F. (2011, January). Persistence of 7- years- old Prestige Oil Spill on Sandy Beaches (NW Spain). Paper presented at the 2011 International Oil Spill Conference. http://dx.doi.org/10.7901/2169-3358-2011-1-209

Ferreira, O., Bairros, M., Pereira, H., Ciavola, P., Dias, J.A. (1998). Mixing depth levels and distribution on steep foreshores. *Journal of Coastal Research, SI 26:* 292-296.

Ferreira, O., Ciavola, P., Tarborda, R., Bairros, M., Dias, J.A. (2000). Sediment mixing depth determination steep and gentle foreshores. *Journal of Coastal Research, 16* (3). 830-839.

Fingas, M. (2011). *Oil Spill Science and Technology*. Burlington, MA, USA, Oxford, UK. Elsevier Inc. http://doi.org/10.1016/B978-1-85617-943-0.10041-3

Fingas, M. (2013). *The Basics of Oil Spill Cleanup* (3rd ed.). Boca Raton: CRC Press Taylor and Francis Group.

Fingas, M. and Fieldhouse, B. (2009). Studies on crude oil and petroleum product emulsions: Water resolution and rheology. *Colloids and Surfaces A: Physicochemical and Engineering Aspects, 333* (1-3), 67-81. http://doi.org/10.1016/j.colsurfa.2008.09.029

Folk, R.L. (1980). *Petrology of Sedimentary Rocks* (2nd ed.). Austin, Texas: Hemphill Publishing Company. Retrieved from http://www.lib.utexas.edu/geo/folkready/entirefolkpdf.pdf

Gaughan, M., K. (1978). Depth of disturbance of sand in surf zones. *Proceeding of the 16th Coastal Engineering Proceedings, 16*, 1513-1530. http://dx.doi.org/10.9753/icce.v16.%25p

Global Marine Oil Pollution Information Gateway. (n.d.). *What happens to oil in the water?* Retrieved on 3/12/2015, from http://oils.gpa.unep.org/facts/fate.htm

Gómez-Pujol, L., Jackson, D.W.T., Cooper, J.A.G., Málvarez, G., Navas, F., Loureiro, C., and Smith, T.A. (2011). Spatial and temporal patterns of sediment activation on a high-energy microtidal beach. *Journal of Coastal Research, SI 64*, 85-89.

Gonzalez, M., Medina, R., Bernabeu, A.M., and Novoa, X. (2004). Mixing depth on an estuarine dissipative beach; St. Georges Beach, Gironde (France). *Journal of Coastal Research, SI 41*, 43-52.

Gonzalez, M., Medina, R., Bernabeu, A.M., and Novoa, X. (2009). Influence of beach morphodynamics in the deep burial of fuel in beaches. *Journal of Coastal Research, 25* (4), 799-818. http://dx.doi.org/10.2112/08-1033.1

Goodman, R. (2003). Tar Balls: The End State. *Spill Science & Technology Bulletin, 8* (2), 117-121. http://dx.doi.org/10.1016/S1353-2561(03)00045-8

Graeme, M. (2012). *Estuarine vegetation survey – Raglan (Whaingaroa) Harbour. Waikato Regional Council Technical Report 2012/35 (Document #: 2298302).* Hamilton, New Zealand: Waikato Regional Council.

Greenwood, B., and Hale, P.B. (1980). Depth of activity, sediment flux, and morphological change in a barred nearshore environment. *Geological Survey of Canada*, *80* (10), 89-109.

Greenwood, B., and Mittler, P.R. (1984). Sediment flux and equilibrium slopes in a barred nearshore. *Marine Geology, 60*, 79-98. http://dx.doi.org/10.1016/0025-3227(84)90145-2

Guedes, R.M. (2012). Effects of surfzone wave transformation on swash dynamics. (PHD thesis, University of Waikato, Waikato, New Zealand). Retrieved from http://hdl.handle.net/10289/6964

Guedes, R.M. (2010). *Raglan Field Experiment 2010* [Unpublished report]. Hamilton New Zealand: NIWA and The University of Waikato.

Guyomarch, J., Le Floch, S. and Merlin, F.X. (2002). Effect of Suspended Mineral Load, Water Salinity and Oil Type on the Size of Oil–Mineral Aggregates in the Presence of Chemical Dispersant. *Spill Science & Technology Bulletin, 8* (1), 95-100. http://dx.doi.org/10.1016/S1353-2561(02)00118-4

Hart, D. and Bryan, K.R. (2008). New Zealand coastal system boundaries, connections and management. *New Zealand Geographer, 64* (2), 129-143. http://dx.doi.org/10.1111/j.1745-7939.2008.00133.x

Hayes, M.O., Michel, J., Montello, T.M., Aurand, D.V., Al-Mansi, A., Al-Moamen, A.H., Sauer, T.C., Thayer, G.W. (1993). Distribution and weathering of shoreline oil one year after Gulf War oil spill. *Marine Pollution Bulletin, 27*, 135-142. http://dx.doi.org/10.1016/0025-326X(93)90017-E

Heath, R.A. (1976). Broad classification of New Zealand inlets with emphasis on residence times. *Journal of Marine and Freshwater Research, 10* (3), 429 – 44. http://dx.doi.org/10.1080/00288330.1976.9515628

Hicks, D.M. and Hume, T.M. (1996). Morphology and Size of Ebb Tidal Deltas at Natural Inlets on Open-sea and Pocket-bay Coasts, North Island, New Zealand. *Journal of Coastal Research, 12* (1), 47-63.

Hill, P.S., Khelifa, A. and Lee, K. (2002). Time Scale for Oil Droplet Stabilization by Mineral Particles in Turbulent Suspensions. *Spill Science & Technology Bulletin, 8*, (1), 73–81. http://dx.doi.org/10.1016/S1353-2561(03)00008-2

Hong, S., Khim, J.S., Ryu, J., Park, J., Song, S.J., Kwon, B., Choi, K., Ji, K., Seo, J., Lee, S., Park, J., Lee, W., Choi, Y., Lee, K.T., Kim, C., Shim, W.J., Naile, J.E. and Giesy, J.P. (2011). Two Years after the Hebei Spirit Oil Spill: Residual Crude-Derived Hydrocarbons and Potential AhR-Mediated Activities in Coastal Sediments. *Environmental Science and Technology, 46* (3), 1406−1414. http://dx.doi.org/10.1021/es203491b

Huisman, C.E., Bryan, K.R., Coco, G. and Ruessink, B.G. (2011). The use of video imagery to analyse groundwater and shoreline dynamics on a dissipative beach. *Continental Shelf Research, 31* (16), 1728–1738. http://dx.doi.org/10.1016/j.csr.2011.07.013

Hyne, N.J. (2001). Nontechnical Guide to Petroleum Geology, Exploration, Drilling and Production (3rd ed.). Oklahoma, USA: Pennwell Corporation.

Inman, D., Zampol, J.A., White, T.E., Hanes, D.M., Walton Waldorf, B. and Kastens, K.A. (1980). Field Measurements of Sand Motion in the Surf Zone. *Coastal Engineering Proceedings, 17*. http://dx.doi.org/10.9753/icce.v17.%25p

International Human Resources Development Corporation [IPIMS]. (n.d.). *Chemistry of Hydrocarbons*. Retrieved on 27/11/2015, from http://www.ipims.com/data/fe31/E3102.asp?UserID=

Irvine, G.V., Mann, D.H. and Short, J.W. (2006). Persistence of 10-year old Exxon Valdez oil on Gulf of Alaska beaches: The importance of boulder-armoring. *Marine Pollution Bulletin, 52.* 1011-1022. http://dx.doi.org/10.1016/j.marpolbul.2006.01.005

Jackson, D. W. T., and Malvarez, G. (2002). A new, high-resolution 'depth of disturbance' instrument (SAM) for use in the surf zone. *Journal of Coastal Research, SI 36,* 406-413.

Jokuty, P., Whiticar, S., Wang, Z., Fingas, M., Lambert, P., Fieldhouse, B. and Mullin, J. (n.d). *A Catalogue of Crude Oil and Oil Product Properties. Environmental Technology Advancement Directorate* [Unpublished manuscript]. Retrieved on 1/12/2015, from http://www.labo-analytika.com/html/oilproducts.html

Kepkay, P.E., Bugden, J.B.C., Lee, K. and Stoffyn-Egli, P. (2002). Application of Ultraviolet Fluorescence Spectroscopy to Monitor Oil–Mineral Aggregate Formation. *Spill Science & Technology Bulletin, 8* (1), 101-108. http://dx.doi.org/10.1016/S1353-2561(02)00122-6

Khalaf, I.H. (2008-2009). *Chapter two – Petroleum & petroleum product* [Course notes]. Retrieved on 29/11/2015, from Ministy of Higher Education and Scientific Research University of Chemical Engineering Department. University of Iraq: http://uotechnology.edu.iq/dep-chem-eng/second%20year/Fuels%20Technology%20Dr.%20Intisar/lect2.pdf

Khelifa, A., Ajijolaiya, L.O., MacPherson, P., Lee, K., Hill, P.S., Gharbi, S., Blouin, M., (2005b). *Validation of OMA formation in cold brackish and sea waters. In: Proceedings of 28th Arctic and Marine Oil spill Program Technical Seminar, Environment Canada, Ottawa, ON*, 527–538. https://www.researchgate.net/publication/264727806_Validation_of_OMA_formation_in_cold_brackish_and_sea_waters

Khelifa, A., Stoffyn-Egli, P., Hill, P.S. and Lee, K. (2002). Characteristics of Oil Droplets Stabilized by Mineral Particles: Effects of Oil Type and Temperature. *Spill Science & Technology Bulletin, 8* (1), 19-30. http://doi.org/10.1016/S1353-2561(02)00117-2

Khelifa, A., Stoffyn-Egli, P., Hill, P.S. and Lee, K. (2005). Effects of salinity and clay type on oil–mineral aggregation. *Marine Environmental Research, 59* (3), 235-254. http://doi.org/10.1016/j.marenvres.2004.05.003

King, C.A.M. (1951). Depth of disturbance of sand on sea beaches by waves. *Journal of Sedimentary Research*, 21, 131 -140. http://dx.doi.org/10.1306/D4269445-2B26-11D7-8648000102C1865D

Kingston, P. (2002). Long-term Environmental Impact of Oil Spills. *Spill Science & Technology Bulletin, 7* (1-2), 53–61. http://doi.org/10.1016/S1353-2561(02)00051-8

Kraus, N. (1985). Field experiments on vertical mixing of sand in the surf zone. Journal of Sedimentary Petrology, *55* (1), 3-14.

Lancaster, N. (2009). Aeolian features and processes. In Young, R. and Norby, L. (Eds.), *Geological Monitoring* (1-25). Boulder, Colorado: The Geological Society of America. http://doi.org/10.1130/2009

Land Information New Zealand (LINZ). (2014). LINZ Data Service [Hydrographic chart]. Retrieved on 10/09/2014, from http://data.linz.govt.nz/

Larson, R., Morang, A. and Gorman, L. (1997). Monitoring the Coastal Environment; Part II: Sediment Sampling and Geotechnical Methods. *Journal of Coastal Research, 13* (2), 308-330. http://www.jstor.org/stable/4298628

Le Floch, S., Guyomarch, J., Merlin, F., Stoffyn-Egli, S., Dixon, J. and Lee, K. (2002). The influence of salinity on oil–mineral aggregate formation. *Spill Science & Technology Bulletin, 8* (1), 65-71. http://dx.doi.org/10.1016/S1353-2561(02)00124-X

Lee, K. (2002). Oil–Particle Interactions in Aquatic Environments: Influence on the Transport, Fate, Effect and Remediation of Oil Spills. *Spill Science and Technology Bulletin, 8* (1), 3-8. http://doi.org/10.1016/S1353-2561(03)00006-9

Lee, K., Stoffyn-Egli, P., Tremblay, G.H., Owens, E.H., Sergy, G.A., Guénette, C.G. and Prince, R.C. (2003). Oil–Mineral Aggregate Formation on Oiled Beaches: Natural Attenuation and Sediment Relocation. *Spill Science & Technology Bulletin, 8* (3), 285-296. http://dx.doi.org/10.1016/S1353-2561(03)00042-2

Lerda, D. (2011). Polycyclic Aromatic Hydrocarbons (PAHs) Factsheet 4th edition. *European Commission Joint Research Centre Technical Notes*. Retrieved on 27/11/2015, from https://ec.europa.eu/jrc/sites/default/files/Factsheet%20PAH_0.pdf

Lewis, A. (2002). Composition, properties and classification of heavy fuel oils. Third R&D Forum on High-density Oil Spill Response [Intype]. Retrieved on 27/11/2015, from http://www.imo.org/en/OurWork/Environment/PollutionResponse/OtherIMOFora/Documents/Proceedings%20final-EN.pdf

Loh, A., Shim, W.J., Sung, Y.H. and Yim, U.H. (2014). Oil-Suspended Particulate Matter Aggregates: Formation Mechanism and Fate in the Marine Environment. *Ocean Science Journal, 49* (4), 329-341. http://dx.doi.org/10.1007/s12601-014-0031-8

MacLeod, N. (2002). Geometric morphometrics and geological shape-classification systems. *Earth-Science Reviews, 59* (1-4), 27-47. http://dx.doi.org/10.1016/S0012-8252(02)00068-5

Maher, N.M., Karl, H.A., Chin, J.L. and Schwab, W.C. (1989). Station Locations and Grain-Size Analysis of Surficial Sediment Samples collected on the Continental Shelf, Gulf of the Farallones during Cruise F2-89-NC, January 1989. Preliminary report. (U.S. Department of the Interior U.S. Geological Survey. Open-File Report 91-375-A). U.S.A.: Department of the Interior U.S. Geological Survey. Retrieved from http://pubs.usgs.gov/of/1991/0375a/report.pdf

Malvern Instruments Limited. (2015). *Basic principles of particle size analysis.* Retrieved from http://www.malvern.com/en/support/resource-center/application-notes/AN020710BasicPrinciplesPSA.aspx

Malvern Instruments Limited. (2015b). *Laser Diffraction. Particle size distributions from nanometers to millimeters*. Retrieved from http://www.malvern.com/en/products/technology/laser-diffraction/

Malvern Instruments Limited. (1997). *Mastersizer Micro/Microplus getting started manual* (MAN0106-1-1). Retrieved from http://www.malvern.com/en/support/resource-center/user-manuals/MAN0106EN.aspx

Marine Pollution Response Service Maritime New Zealand (n.d.).Fact Sheet All About Oil. Retrieved on 1/112/2015, from http://www.maritimenz.govt.nz/Publications-and-forms/Environmental-protection/All-about-oil.pdf

Marine Pollution Response Service Maritime New Zealand (2013). *National Oil Spill Contingency Plan*. Retrieved on 1/12/2015, from http://www.maritimenz.govt.nz/Environmental/Responding-to-spills-and-pollution/The-national-plan.asp

Maritime New Zealand Nō te rere moana Aotearoa. (n.d.). *Major oil spills around New Zealand*. Retrieved on 12/12/2015, from http://www.maritimenz.govt.nz/Environmental/Responding-to-spills-and-pollution/Past-spill-responses/

Maritime New Zealand Nō te rere moana Aotearoa. (2015). *New Zealand Marine Oil Spill Response Strategy 2015–2019*. Retrieved on 12/12/2015, from https://www.maritimenz.govt.nz/Publications-and-forms/Environmental-protection/Oil-spill-response-strategy.pdf

Mead, S. and Moores, A. (2004). *Estuary Sedimentation: a Review of Estuarine Sedimentation in the Waikato Region* (Environment Waikato Technical Report Series Document #:989833). Hamilton, New Zealand. Retrieved from http://www.waikatoregion.govt.nz/PageFiles/3355/tr05-13.pdf

Morelock, J., Ramirez, W., Hallock, P. and Hubbard, D. (2005). *Sediment Character* [Course notes]. Retrieved on 29/11/2015, from Geological Oceanography Program, University of Puerto Rico: http://geology.uprm.edu/Morelock/character.htm

Morrisey, D., Beard, C., Morrison, M., Craggs, R. and Lowe, M. (2007). *The New Zealand mangrove: review of the current state of knowledge* (Auckland Regional Council Technical Publication No. TP325). Auckland, New Zealand: National Institute of Water & Atmospheric Research Ltd [NIWA]. Retrieved from http://www.aucklandcouncil.govt.nz/EN/planspoliciesprojects/plansstrategies/unitaryplan/Documents/Section32report/Appendices/Appendix%203.32.2.pdf

Moustafa, Y.M. and Morsi, R.E. (2012). Biomarkers. In Dhanarasu, S. (Ed.), *Chromatography and Its Applications* (165-186). InTech. Retrieved from http://doi.org/10.5772/1961

Muschenheim, D.K. and Lee, K. (2002). Removal of Oil from the Sea Surface through Particulate Interactions: Review and Prospectus. *Spill Science & Technology Bulletin, 8* (1), 9-18. http://doi.org/10.1016/S1353-2561(02)00129-9

Nagpal, N.K. (1993). *Ambient Water Quality Criteria For Polycyclic Aromatic Hydrocarbons (PAHs).* British Columbia: Ministry of Environment, Lands and Parks Province of British Columbia. Water Quality Branch Water Management Division. http://www.env.gov.bc.ca/wat/wq/BCguidelines/pahs/pahs_over.html

National Institute of Weather and Atmosphere [NIWA]. *Cam-Era*. Retrieved on 20/10/2012, from http://www.niwa.co.nz/our-services/online-services/cam-era

National Research Council [NRC] (2003). *Oil in the sea III: Inputs, fates, and effects*. Washington, D.C.: National Academies Press (US).

New Zealand Steel. (2016). *The History of Ironsand*. Retrieved on 12/2/2016, from http://www.nzsteel.co.nz/new-zealand-steel/the-story-of-steel/the-history-of-ironsand

Nichols, G. (2009). *Sedimentology and Stratigraphy* (2nd ed.). West Sussex, UK: Wiley-Blackwell.

NIWA. (n.d.). *Sea levels* [online service]. Retrieved on 20/10/2012, from https://www.niwa.co.nz/our-science/coasts/tools-and-resources/sea-levels/raglan

NIWA. (2012). *Cam-Era* [online service]. Retrieved on 20/10/2012, from http://www.niwa.co.nz/our-services/online-services/cam-era

Northwest Research Obsidian Studies Laboratory. *Obsidian Terminology*. Retrieved on 1/1/2015, from http://www.obsidianlab.com/terminology.html

Occupational Safety & Health Administration [OSHA]. (n.d.). *OSHA Technical Manual*. Retrieved from U.S. Department of Labor website. https://www.osha.gov/dts/osta/otm/index.html Retrieved on 29/11/2015.

Ocean Portal Find Your Blue Smithsonian Institute National Museum of Natural History. (n.d.). *Gulf Oil Spill*. Retrieved on, from http://ocean.si.edu/gulf-oil-spill

Office of Response and Restoration [NOAA]. (2015). *Tar Balls.* Retrieved on 2/12/2015, from http://response.restoration.noaa.gov/oil-and-chemical-spills/oil-spills/resources/tarballs.html

Office of Response and Restoration [NOAA]. (2016a). *No. 6 Fuel oil (Bunker C) Spills.* Retrieved on 14/1/2016, from http://response.restoration.noaa.gov/oil-and-chemical-spills/oil-spills/oil-types.html

Office of Response and Restoration [NOAA]. (2016b). *Oil Types.* Retrieved on 14/1/2016, from http://response.restoration.noaa.gov/oil-and-chemical-spills/oil-spills/oil-types.html

Omotoso, O.E., Munoz, V.A. and Mikula, R.J. (2002). Mechanisms of crude oil–mineral interactions. *Spill Science and Technology Bulletin*, *8* (1), 45– 54. http://doi.org/10.1016/S1353-2561(02)00116-0

Statistics New Zealand. (n.d.). *Shipping*. Retrieved on 23/04/2016, from http://www2.stats.govt.nz/domino/external/web/nzstories.nsf/0/aa5cd290e1cd9810cc256b1f00040811?OpenDocument

Ornitz, B. and Champ, M. (Eds.). (2002). *Oil Spills First Principles: Prevention and Best Response.* Oxford, UK: Elsevier Science Ltd.

Operational Science Advisory Team (OSAT-3). (2013). *Unified Command Investigation of Recurring Residual Oil in Discrete Shoreline Areas in the Eastern Area of Responsibility.* Retrieved from https://www.restorethegulf.gov/sites/default/files/u372/OSAT%20III%20Eastern%20States.pdf

Otvos, E. G. (1965). Sedimentation-erosion Cycles of Single Tidal Periods on Long Island Sound Beaches. *Journal of Sedimentary Research*, *35* (3), 604-604. http://dx.doi.org/10.1306/74D71307-2B21-11D7-8648000102C1865D

Owens, E.H., Mauseth, G.S.,Martin, C.A., Lamarche, A. and Brown, J. (2002). Tar ball frequency data and analytical results from a long-term beach monitoring program. *Marine Pollution Bulletin*, *44* (8), 770–780. http://dx.doi.org/10.1016/S0025-326X(02)00057-7

Owens, E.H., Taylor, E. and Humphrey. B. (2008).The persistence and character of stranded oil on coarse-sediment beaches. *Marine Pollution Bulletin, 56* (1), 14-26. http://dx.doi.org/10.1016/j.marpolbul.2007.08.020

Packer, J. and Scott, B. (n.d.). *The Basic Language and Vocabulary of Chemistry. Section 6. Nomenclature and Structure of Organic Compounds* [Course notes]. Retrieved on 29/11/2015, from The University of Canterbury: http://www.chem.canterbury.ac.nz/LetsTalkChemistry/ElectronicVersion/ElectronicVersionNew/chapter06/section6.shtml

Page, D.S. Boehm, P.D., Douglas, G.S., Bence, A.E., Burns, W.A. and Mankiewicz, P.J. (1996). The natural petroleum hydrocarbon background in subtidal sediments of Prince William Sound, Alaska, USA. *Environmental Toxicology and Chemistry, 15* (8), 1266-1281. http://doi.org/10.1002/etc.5620150804

Parham, P.R. and Gundlach, E. (2015). Sedimentary Evolution of Deepwater Horizon/Macondo Oil on Sand Beaches of the Northern Gulf of Mexico, USA. *Open Journal Of Ocean And Coastal Sciences, 2* (1), 34-47. http://doi.org/10.15764/OCS.2015.01003

Patel, S. (2015). *Assessment of Environmental Effects. Vodafone New Zealand Limited. TGA Cable, Ngarunui Beach, Raglan. Tasman Global Access Cable*. New Zealand: Vodafone New Zealand Limited. Retrieved from http://www.waikatoregion.govt.nz/PageFiles/37578/Vodafone%20cable.pdf

Payne, J.R., Clayton Jr, J.R. and Kirstein, B.E. (2003). Oil/Suspended Particulate Material Interactions and Sedimentation. *Spill Science & Technology Bulletin, 8* (2), 201–221. http://doi.org/10.1016/S1353-2561(03)00048-3

Penn State University Information Technology Services (2010). *Lecture 4 – Crude Oil Properties* [Course notes]. Retrieved on 20/10/2012, from http://www.personal.psu.edu/rtw1/lecture_topics/physprop.htm

Persaud, N. (n.d.). *Integrating effect of grain size and shape distribution on selected physical properties of aggregate industry sands used for constructed root zone profiles*. Virginia Tech, Blacksburg, Virginia: Scieneering associates. Retrieved from http://www.scieneeringassociates.com/home/grain_proposal.pdf

Petersen, J., Michel, J., Zengel, S., White, M., Lord, C and Plank, C. (2002). *NOAA, Environmental Sensitivity Index Guidelines, Version 3.0* (NOAA

Technical Memorandum NOS ORR 11) NOAA Office of Response and Restoration: Seattle, Washington. Retrieved from http://response.restoration.noaa.gov/sites/default/files/ESI_Guidelines.pdf

Pfannkuch, H.O. and Paulson, R. (n.d.). *Grain Size Distribution and Hydraulic Properties*. [Course notes]. Retrieved on 5/1/2016, from New Jersey City University: http://faculty.njcu.edu/wmontgomery/Coastal_Zone/Grain%20Size%20Distribution.htm

Phillips, D.J. and Mead, S.T. (2009). Investigation of a Large Sandbar at Raglan New Zealand: Project Overview and Preliminary Results. Reef Journal, 1, (1), 267-278. http://www.thereefjournal.com/files/20._Phillips_and_Mead.pdf

Phillips, D., Mead, S., Black, K. and Healy, T. (2003). Surf Zone Currents and Influence on Surfability. *Proceedings of the 3 rd International Surfing Reef Symposium, Raglan, New Zealand*. 60-82. http://hdl.handle.net/10289/190

Pontes, J., Mucha, A.P., Santos, H., Reis, I., Bordalo, A., Basto, M.C., Bernabeu, A., Almeida, C.M. (2013). Potential of bioremediation for buried oil removal in beaches after an oil spill. *Marine Pollution Bulletin, 76* (1-2), 258-265. http://doi.org/10.1016/.marpolbul.2013.08.029

Prince, R.C., Garrett, R.M., Bare, R.E., Grossman, M.J., Townsend, T., Suflita, J.M., Lee, K., Owens, E.H., Sergy, G.A., Braddock, J.F., Lindstrom, J.E. and Lessard, R.R. (2003). The Roles of Photooxidation and Biodegradation in Long-term Weathering of Crude and Heavy Fuel Oils. *Spill Science & Technology Bulletin, 8* (2), 145–156. http://doi.org/10.1016/S1353-2561(03)00017-3

Rajganapathi, V.C., Jitheshkumar, N, Sundararajan, M, Bhat, K.H. and Velusamy, S. (2012). Grain size analysis and characterization of sedimentary environment along Thiruchendur coast, Tamilnadu, India. *Arabian Journal of Geosciences, 6* (12). http://doi.org/10.1007/s12517-012-0709-0

Reliability Evaluation Analytical Laboratory [REAL Services]. (n.d.). *Viscosity-gravity constant (VGC) Analytical Almanac Application Notes* copyright date. Retrieved on 2/12/2015, from http://www.realservices.com/Technical/Analytical-Almanac/viscosity-gravity_constant.html

Rogowska, J. and Namieśnik, J. (2010). Environmental Implications of Oil Spills from Shipping Accidents. In Whitacre, D.M. (Ed.), *Reviews of Environmental Contamination and Toxicolog*y (206, 95-114). New York London: Springer. http://doi.org/10.1007/978-1-4419-6260-7

Rowson, W. (Producer). (2014a, May 16). *Introduction to oil spills* [Video file]. London: The International Tanker Owners Pollution Federation Limited [ITOPF Ltd]. Retrieved on 11/11/2015, from http://www.itopf.com/knowledge-resources/library/video-library/video/1-introduction-to-oil-spills/

Rowson, W. (Producer). (2014b, May 16). *At-sea response* [Video file]. London: The International Tanker Owners Pollution Federation Limited [ITOPF Ltd]. Retrieved on 11/11/2015, from http://www.itopf.com/knowledge-resources/library/video-library/video/3-at-sea-response/

Rowson, W. (Producer). (2014c, July 3). *Environmental Impacts* [Video file]. London: The International Tanker Owners Pollution Federation Limited [ITOPF Ltd]. Retrieved on 11/11/2015, from http://www.itopf.com/knowledge-resources/library/video-library/video/6environmental-impacts/

Saini, S., Jackson, N. and Nordstrom, K.F. (2009). Depth of activation on a mixed sediment beach. *Coastal Engineering, 12* (4), 381-385. http://doi.org/10.1016/j.coastaleng.2009.02.002

Scarfe, B.E. (2008). Oceanographic considerations for the management and prediction of surfing breaks [Unpublished PhD thesis]. University of Waikato, Hamilton, New Zealand.

Scholz, D.K., Kucklick, J.H., Pond, R., Walker, A.H., Bostrom, A. and Fischbeck, P. (1999). Fate of Spilled Oil in Marine Waters Where Does It Go? What Does It Do? How Do Dispersants Affect It? An Information Booklet for Decision-Makers [Information Booklet Publication Number 4691]. Washington, D.C.: Health and Environmental Sciences Department American Petroleum Institute. Retrieved from http://www.api.org/environment-health-and-safety/clean-water/oil-spill-prevention-and-response/~/media/0C4E212C65DE4A3D9C2EEE1A9E604A05.ashx

Sherman, D., Nordstrom, K.F., Jackson, N.L., Allen, J.R. (1994). Sediment mixing-depths on a low-energy reflective beach. .*Journal of Coastal Research, 10* (20), 297-305.

Sherman, D,J., Short, A.D and Takeda, I. (1993). Sediment Mixing-Depth and Bedform Migration in RIP channels. .*Journal of Coastal Research, SI 15*, 39-48.

Sherwood, A.M. and Nelson, C.S. (1979). Surficial sediments of Raglan Harbour. *New Zealand Journal of Marine and Freshwater Research, 13* (4), 475-496. http://doi.org/10.1080/00288330.1979.9515825

Short, A.D. (2006). Australian Beach Systems—Nature and Distribution. *Journal of Coastal Research, 22* (1), 11-27. http://doi.org/10.2112/05A-0002

Silliman, B.R., van de Koppel, J., . McCoy, M.W., Diller, J., Kasozi, G.N., Earl, K., Adams, P.N..and Zimmerman, A.R. (2012). Degradation and resilience in Louisiana salt marshes after the BP–Deepwater Horizon oil spill. *Proceedings of the National Academy of Sciences, 109* (28), 11234-11239. http://www.pnas.org/content/109/28/11234

Society of Petroleum Engineers [SPE] (2015a). *Petrowiki Asphaltenes and waxes.* Retrieved on 29/11/2015, from http://petrowiki.org/Asphaltenes_and_waxes

Society of Petroleum Engineers [SPE] (2015b). *Petrowiki Crude oil characterisation.* Retrieved on 29/11/2015, from http://petrowiki.org/Crude_oil_characterization

Society of Petroleum Engineers [SPE] (2015c). *Petrowiki Oil emulsions*. Retrieved on 29/11/2015, from http://petrowiki.org/Oil_emulsions

Society of Petroleum Engineers [SPE] (2014). *Petrowiki Stability of oil emulsions*. Retrieved on 29/11/2015, from http://petrowiki.org/Stability_of_oil_emulsions#cite_note-r2-1

Statistics New Zealand Te Tari Tatou (2000). *New Zealand Official Yearbook 2000* . Retrieved on 14/08/2015, from http://www2.stats.govt.nz/domino/external/web/nzstories.nsf/0/aa5cd290e1cd9810cc256b1f00040811

Stogiannidis, E. and Remi Laane, R. (2015). Source Characterization of Polycyclic Aromatic Hydrocarbons by Using Their Molecular Indices: An Overview of Possibilities. In Whitacre, D.M. (Ed.), *Reviews of*

Environmental Contamination and Toxicology (234, 49-133). New York London: Springer http://doi.org/10.1007/978-3-319-10638-0_2.

Spiecker, P.M. and Kilpatrick, P.K. (2004). Interfacial Rheology of Petroleum Asphaltenes at the Oil-Water Interface. *Langmuir, 20*, 4022-4032. http://doi.org/10.1021/la035635

Stoffyn-Egli, P., and Lee, K. (2002). Formation and characterization of oil mineral aggregates. *Spill Science and Technology, 8* (1), 31-44. http://doi.org/10.1016/S1353-2561(02)00128-7

Sun, J., Khelifa, A., Zheng, X., Wang, Z., So, L.L., Wong, S., Yang, C. and Fieldhouse, B. (2010). A laboratory study on the kinetics of the formation of oil-suspended particulate matter aggregates using the NIST-1941b sediment. *Marine Pollution Bulletin, 60* (10), 1701-1707. http://doi.org/10.1016/j.marpolbul.2010.06.044

Sunamura, T. and Kraus, N.C. (1985). Prediction of average mixing depth of sediment in the surf zone. *Marine Geolog,: 62* (1-2), 1-12. http://doi.org/10.1016/0025-3227(84)90051-3

Swales, A., Ovenden, R., Budd, R., Hawken, J., McGlone, M.S., Hermanspahn, N. and Okey, M.J. (2005). *Whaingaroa (Raglan) Harbour: Sedimentation and the Effects of Historical Catchment Landcover Changes*. Document#: 1036467. Hamilton, New Zealand: Environment: Waikato Technical Report 2005/36 (ISSN 1172-4005). Retrieved from http://www.waikatoregion.govt.nz/PageFiles/3585/tr05-36.pdf

Sykes, R.; Zink, K.-G. (2012). The New Zealand Oils Geochemistry Database. GNS Science Data Series 14a. Retrieved from http://www.gns.cri.nz/Home/Our-Science/Energy-Resources/Oil-and-Gas/Products/NZ-Petroleum-Geochemistry

Taranaki Regional Council (2008). *Taranaki Regional Council Marine Oil Spill Contingency Plan. Annex 4 Sensitive Site and Coastal Information*. Retrieved on 29/11/2015, from http://www.trc.govt.nz/assets/Publications/guidelines-procedures-and-publications/marine-oil-spill-contingency-plan-2/moscp2012-nx4.pdf

Taranaki Regional Council (2009). *Effectiveness and Efficiency of the Regional Coastal Plan for Taranaki*. (Document # 609786). Taranaki, New Zealand.

Retrieved on, from http://www.trc.govt.nz/assets/Publications/policies-plans-strategies/regional-plans-and-guides/regional-coastal-plan/eercp09.pdf

Taylor, E. and Reimer, D. (2008). Oil persistence on beaches in Prince William Sound – A review of SCAT surveys conducted from 1989 to 2002. *Marine Pollution Bulletin, 56* (3), 458-474. http://doi.org/10.1016/j.marpolbul.2007.11.008

The American Petroleum Institute Petroleum HPV Testing Group (2011). *Crude Oil Category Assessment Document* (High Production Volume (Hpv) Chemical Challenge Program Submission). Retrieved from http://www.petroleumhpv.org/petroleum-substances-and-categories/~/media/0DA0EA3771174E9DB6F5B43B73857842.ashx

The International Tanker Owners Pollution Federation Limited [ITOPF Ltd] (2011a). *Fate of Marine Oil Spills* (Technical Information Paper). Canterbury, UK: Impact PR & Design Limited. Retrieved on 11/11/2015, from file:///C:/Users/User/Downloads/TIP2FateofMarineOilSpills%20(4).pdf

The International Tanker Owners Pollution Federation Limited [ITOPF Ltd] (2011b). *Effects of Oil Pollution on the Marine Environment* (Technical Information Paper). Canterbury, UK: Impact PR & Design Limited. Retrieved on 11/11/2015, from http://www.itopf.com/fileadmin/data/Documents/TIPS%20TAPS/TIP13EffectsofOilPollutionontheMarineEnvironment.pdf

The International Tanker Owners Pollution Federation Limited [ITOPF Ltd] (2015). *Oil Tanker Spill Statistics 2014*. (Technical Information Paper). Canterbury, UK. Impact PR & Design Limited. Retrieved on 11/11/2015, from http://www.itopf.com/fileadmin/data/Documents/Company_Lit/Oil_Spill_Stats_2014FINALlowres.pdf

The Pennsylvania State University (2010). *Chemical composition of crude oil* [Course notes]. Retrieved on 20/10/2012, from http://www.personal.psu.edu/faculty/r/t/rtw1/lecture_topics/classifications.htm

Tissot, B.P. and Welte, D.H. (1978). Petroleum Formation and Occurrence A New Approach to Oil and Gas Exploration (1st ed). New York, NY: Springer-Verlag

Venkata Ramana, U. (2010, August). *Presentation on crude oil characteristics and refinery products.* Paper presented at the workshop on "Refining & Petrochemicals", Kerela, Andhra Pradesh,Tamil Nadu & Karnataka. Retrieved from http://petrofed.winwinhosting.net/upload/25-28Aug10/2.pdf

Venosa, A.D., and Zhu, X. (2003). Biodegradation of Crude Oil Contaminating Marine Shorelines and Freshwater Wetlands. *Spill Science & Technology Bulletin, 8* (2), 163-178. http://doi.org/10.1016/S1353-2561(03)00019-7

Viñas, L., Franco M.A, Soriano J A., Gonzalez J.J., Pon, J. and Albaigés, J. (2010). Sources and distribution of polycyclic aromatic hydrocarbons in sediments from the Spanish northern continental shelf. Assessment of spatial and temporal trends. *Environmental Pollution. (158),* 1551 – 1560. http://doi.org/10.1016/j.envpol.2009.12.023

Waikato Regional Council (n.d.). Improving Whaingaroa Harbour (Raglan) water quality. http://www.waikatoregion.govt.nz/Environment/Natural-resources/coast/Coastal-case-studies/Improving-Whaingaroa-Harbour-Raglan-water-quality/

Wang, Z. and Fingas, M.F. (2003). Development of oil hydrocarbon fingerprinting and identification techniques. *Marine Pollution Bulletin, 47* (9-12), 423 452. http://dx.doi.org/10.1016/S0025-326X(03)00215-7

Wang, P. and Roberts, T.M. (2010). Distribution of Surficial and Buried Oil Contaminants across Sandy Beaches along NW Florida and Alabama Coasts Following the Deepwater Horizon Oil Spill in 2010. *Journal of Coastal Research, 29 (6A),* 144-155. http://dx.doi.org/10.2112/JCOASTRES-D-12-00198.1

Wang, Z., Stout, S.A. and Fingas, M. (2006). Forensic Fingerprinting of Biomarkers for Oil Spill Characterization and Source Identification. *Environmental Forensics, 7* (2), 105-146. http://dx.doi.org/10.1080/15275920600667104

Wang, X., Zhang, Y., and Chen, R.F. (2001). Distribution and partitioning of polycylcic aromatic hydrocarbons (PAHs) in different size fractions in sediments from Boston Harbor, United States. *Marine Pollution Bulletin, 42*, 1139-1149. http://doi.org/10.1016/S0025-326X(01)00129-1

Wang, W., Zheng, Y., Li, Z. and Lee, K. (2011). PIV investigation of oil–mineral interaction for an oil spill application. *Chemical Engineering Journal, 170* (1), 241-249. http://doi.org/10.1016/j.cej.2011.03.062

Warnock, A.M., Hagen, S.C. and Passeri, D.L. (2015). Marine Tar Residues: a Review. Water, Air, & Soil Pollution, 226-268. http://doi.org/10.1007/s11270-015-2298-5

Wassilieff, M. (2012). 'Estuaries - Plants of the estuary'. *Te Ara - the Encyclopedia of New Zealand*. Retrieved on 28/11/2015, from http://www.TeAra.govt.nz/en/estuaries/page-3

Weise, A.M. (1997). *The Significance of Clay-Oil Flocculation Processes to Oil Biodegradation*. (Master's thesis, University of Toronto, Toronto, Ontario, Canada). Retrieved from https://tspace.library.utoronto.ca/bitstream/1807/11594/1/MQ28738.pdf

White, I.C. (2000, August). *Oil Spill Response- Experience, Trends and Challenges*. Technical Information Paper. Paper presented at SPILLCON 2000, 8th International Oil Spill Conference, Darwin, Australia. Retrieved from http://www.itopf.com/fileadmin/data/Documents/Papers/spillcon.pdf

Wilcock, P. R. (1988). Methods for estimating the critical shear stress of individual fractions in mixed-size sediment. *Water Resources Research, 24* (7), 1127-1135. http://doi.org/10.1029/WR024i007p01127

Williams, A.T. (1971). An analysis of some factors involved in the depth of disturbance of beach sand by waves. *Marine Geology, 11*,145-158. http://doi.org/10.1016/0025-3227(71)90003-X

Williams, J., Arsenault, M. A., Buczkowski, B. J., Reid, J.A., Flocks, J.G., Kulp, M. A., Penland, S. and Jenkins, C.J. (2011). *Surficial sediment character of the Louisiana offshore continental shelf region: A GIS Compilation* (United States Geological Survey Open-File Report 2006-1195). Retrieved from http://pubs.usgs.gov/of/2006/1195/htmldocs/images/chart.pdf open file report

Wolfram, R. (2011). Fine Particle Technology The Language of Particle Size. *Journal of GXP Compliance, 15* (2). Retrieved from http://www.ivtnetwork.com/sites/default/files/LanguageParticleSize.pdf

Wood Hole Oceanographic Institution [WHOI]. (2015). *Natural Oil Seeps.* Retrieved on 27/11/2015, from http://www.whoi.edu/main/topic/natural-oil-seeps

Wood, A. (2010). *Episodic, seasonal, and long term morphological changes of Coromandel Beaches*. (Master's thesis, University of Waikato, Hamilton, New Zealand). Retrieved from http://researchcommons.waikato.ac.nz/bitstream/handle/10289/4345/thesis.pdf?sequence=1

Wright, L.D., Guza, R.T., Short, A.D. (1982). Dynamics of a high-energy dissipative surf zone. *Marine Geology, 45* (1-2), 41-62. http://doi.org/10.1016/0025-3227(82)90179-7

Wright, L.D., Short, A.D. (1984). Morphodynamic variability of surf zones and beaches: a synthesis. *Marine Geology, 56* (1-4), 93-118. http://doi.org/10.1016/0025-3227(84)90008-2

Zakaria, M.P., Okudab, T. and Takadab, H. (2001). Polycyclic Aromatic Hydrocarbon (PAHs) and Hopanes in Stranded Tar-balls on the Coasts of Peninsular Malaysia: Applications of Biomarkers for Identifying Sources of Oil Pollution. *Marine Pollution Bulletin, 42* (12), 1357-1366. http://doi.org/10.1016/S0025-326X(01)00165-5

Zeeman, S. (2008). *Sand Grain Size Analysis.* [Course notes]. Retrieved on 27/11/2015, from University of New England: http://faculty.une.edu/cas/szeeman/oce/lab/sediment_analysis.pdf

Zhang, H., Khatibi, M.,Ying, Z., Lee, K. Zhengkai, L. and Mullin, J.V. (2010). Investigation of OMA formation and the effect of minerals. *Marine Pollution Bulletin, 60* (9), 1433-1441. http://doi.org/10.1016/j.marpolbul.2010.05.014

APPENDIX I: SEDIMENT TEXTURAL RESULTS

I.0 SEDIMENT TEXTURAL ANALYSIS

Sediment size analysis results from the University of Waikato's Malvern *Mastersizer-2000* are presented below.

Derived logarithmic graphical parameters following the method of Folk (1974) including mean (Mz), sorting (σ_1), skewness (Sk_1), kurtosis (K_G) and grain size percentile statistics are also given.

Table I.1: *Results summary for sample 1: Mid intertidal zone, mid transect, Northern Ngarunui Beach. Sample collected on the 20th of July, 2014.*

Column: 2 **Density:** 2650
Volume: 0.010
Sample ID: 20-7-2014 mm

Malvern data Phi	**Malvern data Micron**	**Vol %**	**Equivalent Cum wt (g)**
-1.00	2000.00	0	0.0
-0.75	1680.00	0	0.0
-0.50	1410.00	0	0.0
-0.25	1190.00	0	0.0
0.00	1000.00	0	0.0
0.25	840.00	0	0.0
0.49	710.00	0	0.0
0.76	590.00	0.642174	0.2
1.00	500.00	3.389974	0.9
1.25	420.00	10.397636	2.8
1.51	350.00	23.448093	6.2
1.74	300.00	38.518257	10.2
2.00	250.00	58.399382	15.5
2.25	210.00	75.823525	20.1
2.50	177.00	88.542476	23.5
2.75	149.00	96.070396	25.5
3.00	125.00	99.320737	26.3
3.25	105.00	99.968873	26.5
3.51	88.00	100	26.5
3.76	74.00	100	26.5
3.99	63.00	100	26.5
4.24	53.00	100	26.5
4.51	44.00	100	26.5
4.76	37.00	100	26.5
5.01	31.00	100	26.5
6.00	15.60	100	26.5
6.64	10.00	100	26.5
7.00	7.80	100	26.5
8.00	3.90	100	26.5
8.97	2.00	100	26.5
9.99	0.98	100	26.5
10.48	0.70	100	26.5
10.99	0.49	100	26.5
12.02	0.24	100	26.5
13.02	0.12	100	26.5
14.02	0.06	100	26.5
14.29	0.05	100	26.5
		Total weight:	26.5

	mm	**phi**	**Cum wt (g)**	**Int wt (g)**	**Int wt%**	**Cum % finer**	**Modes**
1	2.0000	-1.00	0.000000	0.000000	0.000000	100.000000	
2	1.6800	-0.75	0.000000	0.000000	0.000000	100.000000	
3	1.4100	-0.50	0.000000	0.000000	0.000000	100.000000	
4	1.1900	-0.25	0.000000	0.000000	0.000000	100.000000	
5	1.0000	0.00	0.000000	0.000000	0.000000	100.000000	8
6	0.8400	0.25	0.000000	0.000000	0.000000	100.000000	
7	0.7100	0.49	0.000000	0.000000	0.000000	100.000000	
8	0.5900	0.76	0.642174	0.642174	0.642174	99.357826	
9	0.5000	1.00	3.389974	2.747800	2.747800	96.610026	
10	0.4200	1.25	10.397636	7.007662	7.007662	89.602364	
11	0.3500	1.51	23.448093	13.050457	13.050457	76.551907	
12	0.3000	1.74	38.518257	15.070164	15.070164	61.481743	
13	0.2500	2.00	58.399382	19.881125	19.881125	41.600618	mode at 1.868483
14	0.2100	2.25	75.823525	17.424143	17.424143	24.176475	
15	0.1770	2.50	88.542476	12.718951	12.718951	11.457524	
16	0.1490	2.75	96.070396	7.527920	7.527920	3.929604	
17	0.1250	3.00	99.320737	3.250341	3.250341	0.679263	
18	0.1050	3.25	99.968873	0.648136	0.648136	0.031127	
19	0.0880	3.51	100.000000	0.031127	0.031127	0.000000	
20	0.0740	3.76	100.000000	0.000000	0.000000	0.000000	
21	0.0630	3.99	100.000000	0.000000	0.000000	0.000000	
22	0.0530	4.24	100.000000	0.000000	0.000000	0.000000	
23	0.0440	4.51	100.000000	0.000000	0.000000	0.000000	
24	0.0370	4.76	100.000000	0.000000	0.000000	0.000000	
25	0.0310	5.01	100.000000	0.000000	0.000000	0.000000	
26	0.0156	6.00	100.000000	0.000000	0.000000	0.000000	
27	0.0100	6.64	100.000000	0.000000	0.000000	0.000000	
28	0.0078	7.00	100.000000	0.000000	0.000000	0.000000	
29	0.0039	8.00	100.000000	0.000000	0.000000	0.000000	
30	0.0020	8.97	100.000000	0.000000	0.000000	0.000000	
31	0.0010	9.99	100.000000	0.000000	0.000000	0.000000	
32	0.0007	10.48	100.000000	0.000000	0.000000	0.000000	
33	0.0005	10.99	100.000000	0.000000	0.000000	0.000000	
34	0.0002	12.02	100.000000	0.000000	0.000000	0.000000	
35	0.0001	13.02	100.000000	0.000000	0.000000	0.000000	
36	0.0001	14.02	100.000000	0.000000	0.000000	0.000000	
37	0.0001	14.29	100.000000	0.000000	0.000000	0.000000	
	Sums:			100.00	100.00		

Grainsize Statistics
Percentiles

	phi	***mm***
5	1.06	0.480
16	1.36	0.388
25	1.54	0.344
50	1.89	0.270
75	2.24	0.212
84	2.41	0.188
95	2.71	0.153

Column: 2
Sample ID: 20-7-2014 mm

Folks' Graphic Statistics

	Mean (Mz)	Sorting (σI)	Skewness (SkI)	Kurtosis (KG)	Mean ***mm***
phi	1.888	0.512	-0.004	0.965	0.270

Table I.2: *Results summary for sample 2: High intertidal zone, mid transect, Northern Ngarunui Beach. Sample collected on the 20th of July, 2014.*

Column: 3 **Density:** 2650
Volume: 0.010
Sample ID: 20-7-2014hm

Malvern data Phi	Malvern data Micron	Vol %	Equivalent Cum wt (g)
-1.00	2000.00	0	0.0
-0.75	1680.00	0	0.0
-0.50	1410.00	0	0.0
-0.25	1190.00	0	0.0
0.00	1000.00	0	0.0
0.25	840.00	0	0.0
0.49	710.00	0	0.0
0.76	590.00	0.005389	0.0
1.00	500.00	0.257925	0.1
1.25	420.00	2.244799	0.6
1.51	350.00	8.677496	2.3
1.74	300.00	19.391852	5.1
2.00	250.00	38.15001	10.1
2.25	210.00	59.018394	15.6
2.50	177.00	77.492468	20.5
2.75	149.00	90.526885	24.0
3.00	125.00	97.391719	25.8
3.25	105.00	99.700811	26.4
3.51	88.00	100	26.5
3.76	74.00	100	26.5
3.99	63.00	100	26.5
4.24	53.00	100	26.5
4.51	44.00	100	26.5
4.76	37.00	100	26.5
5.01	31.00	100	26.5
6.00	15.60	100	26.5
6.64	10.00	100	26.5
7.00	7.80	100	26.5
8.00	3.90	100	26.5
8.97	2.00	100	26.5
9.99	0.98	100	26.5
10.48	0.70	100	26.5
10.99	0.49	100	26.5
12.02	0.24	100	26.5
13.02	0.12	100	26.5
14.02	0.06	100	26.5
14.29	0.05	100	26.5
	Total weight:		26.5

	mm	phi	Cum wt (g)	Int wt (g)	Int wt%	Cum % finer	Modes	
1	2.0000	-1.00	0.000000	0.000000	0.000000	100.000000		
2	1.6800	-0.75	0.000000	0.000000	0.000000	100.000000		
3	1.4100	-0.50	0.000000	0.000000	0.000000	100.000000		
4	1.1900	-0.25	0.000000	0.000000	0.000000	100.000000		
5	1.0000	0.00	0.000000	0.000000	0.000000	100.000000		8
6	0.8400	0.25	0.000000	0.000000	0.000000	100.000000		
7	0.7100	0.49	0.000000	0.000000	0.000000	100.000000		
8	0.5900	0.76	0.005389	0.005389	0.005389	99.994611		
9	0.5000	1.00	0.257925	0.252536	0.252536	99.742075		
10	0.4200	1.25	2.244799	1.986874	1.986874	97.755201		
11	0.3500	1.51	8.677496	6.432697	6.432697	91.322504		
12	0.3000	1.74	19.391852	10.714356	10.714356	80.608148		
13	0.2500	2.00	38.150010	18.758158	18.758158	61.849990		
14	0.2100	2.25	59.018394	20.868384	20.868384	40.981606	mode at 2.125769	
15	0.1770	2.50	77.492468	18.474074	18.474074	22.507532		
16	0.1490	2.75	90.526885	13.034417	13.034417	9.473115		
17	0.1250	3.00	97.391719	6.864834	6.864834	2.608281		
18	0.1050	3.25	99.700811	2.309092	2.309092	0.299189		
19	0.0880	3.51	100.000000	0.299189	0.299189	0.000000		
20	0.0740	3.76	100.000000	0.000000	0.000000	0.000000		
21	0.0630	3.99	100.000000	0.000000	0.000000	0.000000		
22	0.0530	4.24	100.000000	0.000000	0.000000	0.000000		
23	0.0440	4.51	100.000000	0.000000	0.000000	0.000000		
24	0.0370	4.76	100.000000	0.000000	0.000000	0.000000		
25	0.0310	5.01	100.000000	0.000000	0.000000	0.000000		
26	0.0156	6.00	100.000000	0.000000	0.000000	0.000000		
27	0.0100	6.64	100.000000	0.000000	0.000000	0.000000		
28	0.0078	7.00	100.000000	0.000000	0.000000	0.000000		
29	0.0039	8.00	100.000000	0.000000	0.000000	0.000000		
30	0.0020	8.97	100.000000	0.000000	0.000000	0.000000		
31	0.0010	9.99	100.000000	0.000000	0.000000	0.000000		
32	0.0007	10.48	100.000000	0.000000	0.000000	0.000000		
33	0.0005	10.99	100.000000	0.000000	0.000000	0.000000		
34	0.0002	12.02	100.000000	0.000000	0.000000	0.000000		
35	0.0001	13.02	100.000000	0.000000	0.000000	0.000000		
36	0.0001	14.02	100.000000	0.000000	0.000000	0.000000		
37	0.0001	14.29	100.000000	0.000000	0.000000	0.000000		
	Sums:			100.00	100.00			

Grainsize Statistics
Percentiles

	phi	*mm*
5	1.36	0.388
16	1.67	0.315
25	1.82	0.284
50	2.14	0.226
75	2.46	0.181
84	2.62	0.162
95	2.91	0.133

Column: 3
Sample ID: 20-7-2014hm

Folks' Graphic Statistics

	Mean (Mz)	Sorting (σI)	Skewness (SkI)	Kurtosis (KG)	Mean *mm*
phi	2.144	0.473	-0.002	0.977	0.226

Table I.3: *Results summary for sample 3: Mid intertidal zone, northern transect, Northern Ngarunui Beach. Sample collected on the 20th of July, 2014.*

Column: 4 **Density:** 2650
Volume: 0.010
Sample ID: 20-7-2014mn

Malvern data Phi	Malvern data Micron	Vol %	Equivalent Cum wt (g)
-1.00	2000.00	0	0.0
-0.75	1680.00	0	0.0
-0.50	1410.00	0	0.0
-0.25	1190.00	0	0.0
0.00	1000.00	0	0.0
0.25	840.00	0	0.0
0.49	710.00	0.023743	0.0
0.76	590.00	1.054167	0.3
1.00	500.00	5.01914	1.3
1.25	420.00	14.778569	3.9
1.51	350.00	31.941855	8.5
1.74	300.00	50.129115	13.3
2.00	250.00	71.274609	18.9
2.25	210.00	86.689427	23.0
2.50	177.00	95.479851	25.3
2.75	149.00	99.134843	26.3
3.00	125.00	99.948479	26.5
3.25	105.00	100	26.5
3.51	88.00	100	26.5
3.76	74.00	100	26.5
3.99	63.00	100	26.5
4.24	53.00	100	26.5
4.51	44.00	100	26.5
4.76	37.00	100	26.5
5.01	31.00	100	26.5
6.00	15.60	100	26.5
6.64	10.00	100	26.5
7.00	7.80	100	26.5
8.00	3.90	100	26.5
8.97	2.00	100	26.5
9.99	0.98	100	26.5
10.48	0.70	100	26.5
10.99	0.49	100	26.5
12.02	0.24	100	26.5
13.02	0.12	100	26.5
14.02	0.06	100	26.5
14.29	0.05	100	26.5

Total weight: 26.5

	mm	phi	Cum wt (g)	Int wt (g)	Int wt%	Cum % finer	Modes
1	2.0000	-1.00	0.000000	0.000000	0.000000	100.000000	
2	1.6800	-0.75	0.000000	0.000000	0.000000	100.000000	
3	1.4100	-0.50	0.000000	0.000000	0.000000	100.000000	
4	1.1900	-0.25	0.000000	0.000000	0.000000	100.000000	
5	1.0000	0.00	0.000000	0.000000	0.000000	100.000000	8
6	0.8400	0.25	0.000000	0.000000	0.000000	100.000000	
7	0.7100	0.49	0.023743	0.023743	0.023743	99.976257	
8	0.5900	0.76	1.054167	1.030424	1.030424	98.945833	
9	0.5000	1.00	5.019140	3.964973	3.964973	94.980860	
10	0.4200	1.25	14.778569	9.759429	9.759429	85.221431	
11	0.3500	1.51	31.941855	17.163286	17.163286	68.058145	
12	0.3000	1.74	50.129115	18.187260	18.187260	49.870885	
13	0.2500	2.00	71.274609	21.145494	21.145494	28.725391	mode at 1.868483
14	0.2100	2.25	86.689427	15.414818	15.414818	13.310573	
15	0.1770	2.50	95.479851	8.790424	8.790424	4.520149	
16	0.1490	2.75	99.134843	3.654992	3.654992	0.865157	
17	0.1250	3.00	99.948479	0.813636	0.813636	0.051521	
18	0.1050	3.25	100.000000	0.051521	0.051521	0.000000	
19	0.0880	3.51	100.000000	0.000000	0.000000	0.000000	
20	0.0740	3.76	100.000000	0.000000	0.000000	0.000000	
21	0.0630	3.99	100.000000	0.000000	0.000000	0.000000	
22	0.0530	4.24	100.000000	0.000000	0.000000	0.000000	
23	0.0440	4.51	100.000000	0.000000	0.000000	0.000000	
24	0.0370	4.76	100.000000	0.000000	0.000000	0.000000	
25	0.0310	5.01	100.000000	0.000000	0.000000	0.000000	
26	0.0156	6.00	100.000000	0.000000	0.000000	0.000000	
27	0.0100	6.64	100.000000	0.000000	0.000000	0.000000	
28	0.0078	7.00	100.000000	0.000000	0.000000	0.000000	
29	0.0039	8.00	100.000000	0.000000	0.000000	0.000000	
30	0.0020	8.97	100.000000	0.000000	0.000000	0.000000	
31	0.0010	9.99	100.000000	0.000000	0.000000	0.000000	
32	0.0007	10.48	100.000000	0.000000	0.000000	0.000000	
33	0.0005	10.99	100.000000	0.000000	0.000000	0.000000	
34	0.0002	12.02	100.000000	0.000000	0.000000	0.000000	
35	0.0001	13.02	100.000000	0.000000	0.000000	0.000000	
36	0.0001	14.02	100.000000	0.000000	0.000000	0.000000	
37	0.0001	14.29	100.000000	0.000000	0.000000	0.000000	
	Sums:			100.00	100.00		

Column: 4
Sample ID: 20-7-2014mn

Folks' Graphic Statistics

	Mean (Mz)	Sorting (σI)	Skewness (SkI)	Kurtosis (KG)	Mean *mm*
phi	1.738	0.459	0.008	0.933	0.300

Grainsize Statistics
Percentiles

	phi	*mm*
5	1.00	0.500
16	1.27	0.415
25	1.41	0.377
50	1.74	0.300
75	2.06	0.240
84	2.21	0.216
95	2.48	0.179

Table I.4: *Results summary for sample 4: High intertidal zone, southern transect, Northern Ngarunui Beach. Sample collected on the 20th of July, 2014.*

Column: 5 **Density:** 2650
Volume: 0.010
Sample ID: 20-7-2014hs

Malvern data Phi	Malvern data Micron	Vol %	Equivalent Cum wt (g)
-1.00	2000.00	0	0.0
-0.75	1680.00	0	0.0
-0.50	1410.00	0	0.0
-0.25	1190.00	0	0.0
0.00	1000.00	0	0.0
0.25	840.00	0	0.0
0.49	710.00	0	0.0
0.76	590.00	0.005241	0.0
1.00	500.00	0.254775	0.1
1.25	420.00	2.249381	0.6
1.51	350.00	8.675242	2.3
1.74	300.00	19.338827	5.1
2.00	250.00	37.977033	10.1
2.25	210.00	58.726219	15.6
2.50	177.00	77.157592	20.4
2.75	149.00	90.253061	23.9
3.00	125.00	97.239963	25.8
3.25	105.00	99.655777	26.4
3.51	88.00	99.991677	26.5
3.76	74.00	100	26.5
3.99	63.00	100	26.5
4.24	53.00	100	26.5
4.51	44.00	100	26.5
4.76	37.00	100	26.5
5.01	31.00	100	26.5
6.00	15.60	100	26.5
6.64	10.00	100	26.5
7.00	7.80	100	26.5
8.00	3.90	100	26.5
8.97	2.00	100	26.5
9.99	0.98	100	26.5
10.48	0.70	100	26.5
10.99	0.49	100	26.5
12.02	0.24	100	26.5
13.02	0.12	100	26.5
14.02	0.06	100	26.5
14.29	0.05	100	26.5
		Total weight:	26.5

	mm	phi	Cum wt (g)	Int wt (g)	Int wt%	Cum % finer	Modes
1	2.0000	-1.00	0.000000	0.000000	0.000000	100.000000	
2	1.6800	-0.75	0.000000	0.000000	0.000000	100.000000	
3	1.4100	-0.50	0.000000	0.000000	0.000000	100.000000	
4	1.1900	-0.25	0.000000	0.000000	0.000000	100.000000	
5	1.0000	0.00	0.000000	0.000000	0.000000	100.000000	8
6	0.8400	0.25	0.000000	0.000000	0.000000	100.000000	
7	0.7100	0.49	0.000000	0.000000	0.000000	100.000000	
8	0.5900	0.76	0.005241	0.005241	0.005241	99.994759	
9	0.5000	1.00	0.254775	0.249534	0.249534	99.745225	
10	0.4200	1.25	2.249381	1.994606	1.994606	97.750619	
11	0.3500	1.51	8.675242	6.425861	6.425861	91.324758	
12	0.3000	1.74	19.338827	10.663585	10.663585	80.661173	
13	0.2500	2.00	37.977033	18.638206	18.638206	62.022967	
14	0.2100	2.25	58.726219	20.749186	20.749186	41.273781	mode at 2.125769
15	0.1770	2.50	77.157592	18.431373	18.431373	22.842408	
16	0.1490	2.75	90.253061	13.095469	13.095469	9.746939	
17	0.1250	3.00	97.239963	6.986902	6.986902	2.760037	
18	0.1050	3.25	99.655777	2.415814	2.415814	0.344223	
19	0.0880	3.51	99.991677	0.335900	0.335900	0.008323	
20	0.0740	3.76	100.000000	0.008323	0.008323	0.000000	
21	0.0630	3.99	100.000000	0.000000	0.000000	0.000000	
22	0.0530	4.24	100.000000	0.000000	0.000000	0.000000	
23	0.0440	4.51	100.000000	0.000000	0.000000	0.000000	
24	0.0370	4.76	100.000000	0.000000	0.000000	0.000000	
25	0.0310	5.01	100.000000	0.000000	0.000000	0.000000	
26	0.0156	6.00	100.000000	0.000000	0.000000	0.000000	
27	0.0100	6.64	100.000000	0.000000	0.000000	0.000000	
28	0.0078	7.00	100.000000	0.000000	0.000000	0.000000	
29	0.0039	8.00	100.000000	0.000000	0.000000	0.000000	
30	0.0020	8.97	100.000000	0.000000	0.000000	0.000000	
31	0.0010	9.99	100.000000	0.000000	0.000000	0.000000	
32	0.0007	10.48	100.000000	0.000000	0.000000	0.000000	
33	0.0005	10.99	100.000000	0.000000	0.000000	0.000000	
34	0.0002	12.02	100.000000	0.000000	0.000000	0.000000	
35	0.0001	13.02	100.000000	0.000000	0.000000	0.000000	
36	0.0001	14.02	100.000000	0.000000	0.000000	0.000000	
37	0.0001	14.29	100.000000	0.000000	0.000000	0.000000	
	Sums:			100.00	100.00		

Grainsize Statistics
Percentiles

	phi	*mm*
5	1.36	0.388
16	1.67	0.315
25	1.82	0.284
50	2.15	0.226
75	2.47	0.181
84	2.63	0.162
95	2.92	0.132

Column: 5
Sample ID: 20-7-2014hs

Folks' Graphic Statistics

	Mean (Mz)	Sorting (σI)	Skewness (SkI)	Kurtosis (KG)	Mean *mm*
phi	2.147	0.476	-0.001	0.977	0.226

Table I.5: *Results summary for sample 5: High intertidal zone, northern transect, Northern Ngarunui Beach. Sample collected on the 20th of July, 2014.*

Column: 6 **Density:** 2650
Volume: 0.010
Sample ID: 20-7-2014hn

Malvern data Phi	Malvern data Micron	Vol %	Equivalent Cum wt (g)
-1.00	2000.00	0	0.0
-0.75	1680.00	0	0.0
-0.50	1410.00	0	0.0
-0.25	1190.00	0	0.0
0.00	1000.00	0	0.0
0.25	840.00	0	0.0
0.49	710.00	0	0.0
0.76	590.00	0	0.0
1.00	500.00	0.50191	0.1
1.25	420.00	3.46461	0.9
1.51	350.00	12.132688	3.2
1.74	300.00	25.288317	6.7
2.00	250.00	46.29754	12.3
2.25	210.00	67.405452	17.9
2.50	177.00	84.120089	22.3
2.75	149.00	94.422528	25.0
3.00	125.00	98.911751	26.2
3.25	105.00	99.959153	26.5
3.51	88.00	100	26.5
3.76	74.00	100	26.5
3.99	63.00	100	26.5
4.24	53.00	100	26.5
4.51	44.00	100	26.5
4.76	37.00	100	26.5
5.01	31.00	100	26.5
6.00	15.60	100	26.5
6.64	10.00	100	26.5
7.00	7.80	100	26.5
8.00	3.90	100	26.5
8.97	2.00	100	26.5
9.99	0.98	100	26.5
10.48	0.70	100	26.5
10.99	0.49	100	26.5
12.02	0.24	100	26.5
13.02	0.12	100	26.5
14.02	0.06	100	26.5
14.29	0.05	100	26.5
		Total weight:	26.5

	mm	phi	Cum wt (g)	Int wt (g)	Int wt%	Cum % finer	Modes
1	2.0000	-1.00	0.000000	0.000000	0.000000	100.000000	
2	1.6800	-0.75	0.000000	0.000000	0.000000	100.000000	
3	1.4100	-0.50	0.000000	0.000000	0.000000	100.000000	
4	1.1900	-0.25	0.000000	0.000000	0.000000	100.000000	
5	1.0000	0.00	0.000000	0.000000	0.000000	100.000000	8
6	0.8400	0.25	0.000000	0.000000	0.000000	100.000000	
7	0.7100	0.49	0.000000	0.000000	0.000000	100.000000	
8	0.5900	0.76	0.000000	0.000000	0.000000	100.000000	
9	0.5000	1.00	0.501910	0.501910	0.501910	99.498090	
10	0.4200	1.25	3.464610	2.962700	2.962700	96.535390	
11	0.3500	1.51	12.132688	8.668078	8.668078	87.867312	
12	0.3000	1.74	25.288317	13.155629	13.155629	74.711683	
13	0.2500	2.00	46.297540	21.009223	21.009223	53.702460	
14	0.2100	2.25	67.405452	21.107912	21.107912	32.594548	mode at 2.125769
15	0.1770	2.50	84.120089	16.714637	16.714637	15.879911	
16	0.1490	2.75	94.422528	10.302439	10.302439	5.577472	
17	0.1250	3.00	98.911751	4.489223	4.489223	1.088249	
18	0.1050	3.25	99.959153	1.047402	1.047402	0.040847	
19	0.0880	3.51	100.000000	0.040847	0.040847	0.000000	
20	0.0740	3.76	100.000000	0.000000	0.000000	0.000000	
21	0.0630	3.99	100.000000	0.000000	0.000000	0.000000	
22	0.0530	4.24	100.000000	0.000000	0.000000	0.000000	
23	0.0440	4.51	100.000000	0.000000	0.000000	0.000000	
24	0.0370	4.76	100.000000	0.000000	0.000000	0.000000	
25	0.0310	5.01	100.000000	0.000000	0.000000	0.000000	
26	0.0156	6.00	100.000000	0.000000	0.000000	0.000000	
27	0.0100	6.64	100.000000	0.000000	0.000000	0.000000	
28	0.0078	7.00	100.000000	0.000000	0.000000	0.000000	
29	0.0039	8.00	100.000000	0.000000	0.000000	0.000000	
30	0.0020	8.97	100.000000	0.000000	0.000000	0.000000	
31	0.0010	9.99	100.000000	0.000000	0.000000	0.000000	
32	0.0007	10.48	100.000000	0.000000	0.000000	0.000000	
33	0.0005	10.99	100.000000	0.000000	0.000000	0.000000	
34	0.0002	12.02	100.000000	0.000000	0.000000	0.000000	
35	0.0001	13.02	100.000000	0.000000	0.000000	0.000000	
36	0.0001	14.02	100.000000	0.000000	0.000000	0.000000	
37	0.0001	14.29	100.000000	0.000000	0.000000	0.000000	
		Sums:		100.00	100.00		

Grainsize Statistics
Percentiles

	phi	*mm*
5	1.30	0.407
16	1.58	0.334
25	1.73	0.301
50	2.04	0.242
75	2.36	0.194
84	2.50	0.177
95	2.78	0.146

Column: 6
Sample ID: 20-7-2014hn

Folks' Graphic Statistics

	Mean (Mz)	Sorting (σI)	Skewness (SkI)	Kurtosis (KG)	Mean *mm*
phi	2.040	0.454	-0.010	0.961	0.243

Table I.6: *Results summary for sample 6: Mid intertidal zone, southern transect, Northern Ngarunui Beach. Sample collected on the 20th of July, 2014.*

Column: 7 **Density:** 2650
Volume: 0.010
Sample ID: 20-7-2014ms

Malvern data Phi	Malvern data Micron	Vol %	Equivalent Cum wt (g)
-1.00	2000.00	0	0.0
-0.75	1680.00	0	0.0
-0.50	1410.00	0	0.0
-0.25	1190.00	0	0.0
0.00	1000.00	0	0.0
0.25	840.00	0	0.0
0.49	710.00	0	0.0
0.76	590.00	0.785736	0.2
1.00	500.00	3.965762	1.1
1.25	420.00	11.727308	3.1
1.51	350.00	25.620359	6.8
1.74	300.00	41.13596	10.9
2.00	250.00	60.977269	16.2
2.25	210.00	77.835046	20.6
2.50	177.00	89.781652	23.8
2.75	149.00	96.633017	25.6
3.00	125.00	99.469528	26.4
3.25	105.00	99.986186	26.5
3.51	88.00	100	26.5
3.76	74.00	100	26.5
3.99	63.00	100	26.5
4.24	53.00	100	26.5
4.51	44.00	100	26.5
4.76	37.00	100	26.5
5.01	31.00	100	26.5
6.00	15.60	100	26.5
6.64	10.00	100	26.5
7.00	7.80	100	26.5
8.00	3.90	100	26.5
8.97	2.00	100	26.5
9.99	0.98	100	26.5
10.48	0.70	100	26.5
10.99	0.49	100	26.5
12.02	0.24	100	26.5
13.02	0.12	100	26.5
14.02	0.06	100	26.5
14.29	0.05	100	26.5
	Total weight:		26.5

	mm	phi	Cum wt (g)	Int wt (g)	Int wt%	Cum % finer	Modes	
1	2.0000	-1.00	0.000000	0.000000	0.000000	100.000000		
2	1.6800	-0.75	0.000000	0.000000	0.000000	100.000000		
3	1.4100	-0.50	0.000000	0.000000	0.000000	100.000000		
4	1.1900	-0.25	0.000000	0.000000	0.000000	100.000000		
5	1.0000	0.00	0.000000	0.000000	0.000000	100.000000		8
6	0.8400	0.25	0.000000	0.000000	0.000000	100.000000		
7	0.7100	0.49	0.000000	0.000000	0.000000	100.000000		
8	0.5900	0.76	0.785736	0.785736	0.785736	99.214264		
9	0.5000	1.00	3.965762	3.180026	3.180026	96.034238		
10	0.4200	1.25	11.727308	7.761546	7.761546	88.272692		
11	0.3500	1.51	25.620359	13.893051	13.893051	74.379641		
12	0.3000	1.74	41.135960	15.515601	15.515601	58.864040		
13	0.2500	2.00	60.977269	19.841309	19.841309	39.022731	mode at 1.868483	
14	0.2100	2.25	77.835046	16.857777	16.857777	22.164954		
15	0.1770	2.50	89.781652	11.946606	11.946606	10.218348		
16	0.1490	2.75	96.633017	6.851365	6.851365	3.366983		
17	0.1250	3.00	99.469528	2.836511	2.836511	0.530472		
18	0.1050	3.25	99.986186	0.516658	0.516658	0.013814		
19	0.0880	3.51	100.000000	0.013814	0.013814	0.000000		
20	0.0740	3.76	100.000000	0.000000	0.000000	0.000000		
21	0.0630	3.99	100.000000	0.000000	0.000000	0.000000		
22	0.0530	4.24	100.000000	0.000000	0.000000	0.000000		
23	0.0440	4.51	100.000000	0.000000	0.000000	0.000000		
24	0.0370	4.76	100.000000	0.000000	0.000000	0.000000		
25	0.0310	5.01	100.000000	0.000000	0.000000	0.000000		
26	0.0156	6.00	100.000000	0.000000	0.000000	0.000000		
27	0.0100	6.64	100.000000	0.000000	0.000000	0.000000		
28	0.0078	7.00	100.000000	0.000000	0.000000	0.000000		
29	0.0039	8.00	100.000000	0.000000	0.000000	0.000000		
30	0.0020	8.97	100.000000	0.000000	0.000000	0.000000		
31	0.0010	9.99	100.000000	0.000000	0.000000	0.000000		
32	0.0007	10.48	100.000000	0.000000	0.000000	0.000000		
33	0.0005	10.99	100.000000	0.000000	0.000000	0.000000		
34	0.0002	12.02	100.000000	0.000000	0.000000	0.000000		
35	0.0001	13.02	100.000000	0.000000	0.000000	0.000000		
36	0.0001	14.02	100.000000	0.000000	0.000000	0.000000		
37	0.0001	14.29	100.000000	0.000000	0.000000	0.000000		
		Sums:		100.00	100.00			

Grainsize Statistics
Percentiles

	phi	*mm*
5	1.03	0.489
16	1.33	0.397
25	1.50	0.353
50	1.85	0.277
75	2.21	0.216
84	2.38	0.192
95	2.69	0.155

Column: **7**
Sample ID: 20-7-2014ms

Folks' Graphic Statistics

	Mean (Mz)	Sorting (σI)	Skewness (SkI)	Kurtosis (KG)	Mean *mm*
phi	1.855	0.512	0.005	0.960	0.276

Table II.7: *Results summary for sample 7: High intertidal zone, eastern transect, Wainamu Beach. Sample collected on the 16th of July, 2014.*

Column:	8	**Density:**	2650
		Volume:	0.010
Sample ID:	16-7-2014he		

Malvern data Phi	**Malvern data** Micron	Vol %	Equivalent Cum wt (g)
-1.00	2000.00	0	0.0
-0.75	1680.00	0	0.0
-0.50	1410.00	0	0.0
-0.25	1190.00	0	0.0
0.00	1000.00	0	0.0
0.25	840.00	0	0.0
0.49	710.00	0	0.0
0.76	590.00	0	0.0
1.00	500.00	0.013113	0.0
1.25	420.00	0.896468	0.2
1.51	350.00	4.535091	1.2
1.74	300.00	11.31112	3.0
2.00	250.00	24.590858	6.5
2.25	210.00	41.692744	11.0
2.50	177.00	59.974056	15.9
2.75	149.00	76.579981	20.3
3.00	125.00	89.05868	23.6
3.25	105.00	96.258118	25.5
3.51	88.00	99.320077	26.3
3.76	74.00	99.989008	26.5
3.99	63.00	100	26.5
4.24	53.00	100	26.5
4.51	44.00	100	26.5
4.76	37.00	100	26.5
5.01	31.00	100	26.5
6.00	15.60	100	26.5
6.64	10.00	100	26.5
7.00	7.80	100	26.5
8.00	3.90	100	26.5
8.97	2.00	100	26.5
9.99	0.98	100	26.5
10.48	0.70	100	26.5
10.99	0.49	100	26.5
12.02	0.24	100	26.5
13.02	0.12	100	26.5
14.02	0.06	100	26.5
14.29	0.05	100	26.5
		Total weight:	26.5

	mm	phi	Cum wt (g)	Int wt (g)	Int wt%	Cum % finer	Modes	
1	2.0000	-1.00	0.000000	0.000000	0.000000	100.000000		
2	1.6800	-0.75	0.000000	0.000000	0.000000	100.000000		
3	1.4100	-0.50	0.000000	0.000000	0.000000	100.000000		
4	1.1900	-0.25	0.000000	0.000000	0.000000	100.000000		
5	1.0000	0.00	0.000000	0.000000	0.000000	100.000000		8
6	0.8400	0.25	0.000000	0.000000	0.000000	100.000000		
7	0.7100	0.49	0.000000	0.000000	0.000000	100.000000		
8	0.5900	0.76	0.000000	0.000000	0.000000	100.000000		
9	0.5000	1.00	0.013113	0.013113	0.013113	99.986887		
10	0.4200	1.25	0.896468	0.883355	0.883355	99.103532		
11	0.3500	1.51	4.535091	3.638623	3.638623	95.464909		
12	0.3000	1.74	11.311120	6.776029	6.776029	88.688880		
13	0.2500	2.00	24.590858	13.279738	13.279738	75.409142		
14	0.2100	2.25	41.692744	17.101886	17.101886	58.307256		
15	0.1770	2.50	59.974056	18.281312	18.281312	40.025944	mode at 2.374859	
16	0.1490	2.75	76.579981	16.605925	16.605925	23.420019		
17	0.1250	3.00	89.058680	12.478699	12.478699	10.941320		
18	0.1050	3.25	96.258118	7.199438	7.199438	3.741882		
19	0.0880	3.51	99.320077	3.061959	3.061959	0.679923		
20	0.0740	3.76	99.989008	0.668931	0.668931	0.010992		
21	0.0630	3.99	100.000000	0.010992	0.010992	0.000000		
22	0.0530	4.24	100.000000	0.000000	0.000000	0.000000		
23	0.0440	4.51	100.000000	0.000000	0.000000	0.000000		
24	0.0370	4.76	100.000000	0.000000	0.000000	0.000000		
25	0.0310	5.01	100.000000	0.000000	0.000000	0.000000		
26	0.0156	6.00	100.000000	0.000000	0.000000	0.000000		
27	0.0100	6.64	100.000000	0.000000	0.000000	0.000000		
28	0.0078	7.00	100.000000	0.000000	0.000000	0.000000		
29	0.0039	8.00	100.000000	0.000000	0.000000	0.000000		
30	0.0020	8.97	100.000000	0.000000	0.000000	0.000000		
31	0.0010	9.99	100.000000	0.000000	0.000000	0.000000		
32	0.0007	10.48	100.000000	0.000000	0.000000	0.000000		
33	0.0005	10.99	100.000000	0.000000	0.000000	0.000000		
34	0.0002	12.02	100.000000	0.000000	0.000000	0.000000		
35	0.0001	13.02	100.000000	0.000000	0.000000	0.000000		
36	0.0001	14.02	100.000000	0.000000	0.000000	0.000000		
37	0.0001	14.29	100.000000	0.000000	0.000000	0.000000		
	Sums:			100.00	100.00			

Column: 8
Sample ID: 16-7-2014he

Folks' Graphic Statistics

	Mean (Mz)	Sorting (σI)	Skewness (SkI)	Kurtosis (KG)	Mean *mm*
phi	2.364	0.521	0.003	0.959	0.194

Grainsize Statistics
Percentiles

	phi	*mm*
5	1.53	0.346
16	1.83	0.281
25	2.01	0.249
50	2.36	0.194
75	2.72	0.151
84	2.90	0.134
95	3.21	0.108

Table II.8: *Results summary for sample 8: Mid intertidal zone, western transect, Wainamu Beach. Sample collected on the 16th of July, 2014.*

Column: 9 | Density: 2650 | Volume: 0.010

Sample ID: 16-7-2014mw

Malvern data Phi	Malvern data Micron	Vol %	Equivalent Cum wt (g)
-1.00	2000.00	0	0.0
-0.75	1680.00	0	0.0
-0.50	1410.00	0	0.0
-0.25	1190.00	0	0.0
0.00	1000.00	0	0.0
0.25	840.00	0	0.0
0.49	710.00	0	0.0
0.76	590.00	0	0.0
1.00	500.00	0.012093	0.0
1.25	420.00	0.337615	0.1
1.51	350.00	2.565075	0.7
1.74	300.00	7.308809	1.9
2.00	250.00	17.740238	4.7
2.25	210.00	32.653007	8.7
2.50	177.00	50.283367	13.3
2.75	149.00	68.078244	18.0
3.00	125.00	83.110721	22.0
3.25	105.00	93.075679	24.7
3.51	88.00	98.193939	26.0
3.76	74.00	99.869233	26.5
3.99	63.00	100	26.5
4.24	53.00	100	26.5
4.51	44.00	100	26.5
4.76	37.00	100	26.5
5.01	31.00	100	26.5
6.00	15.60	100	26.5
6.64	10.00	100	26.5
7.00	7.80	100	26.5
8.00	3.90	100	26.5
8.97	2.00	100	26.5
9.99	0.98	100	26.5
10.48	0.70	100	26.5
10.99	0.49	100	26.5
12.02	0.24	100	26.5
13.02	0.12	100	26.5
14.02	0.06	100	26.5
14.29	0.05	100	26.5
		Total weight:	26.5

	mm	phi	Cum wt (g)	Int wt (g)	Int wt%	Cum % finer	Modes
1	2.0000	-1.00	0.000000	0.000000	0.000000	100.000000	
2	1.6800	-0.75	0.000000	0.000000	0.000000	100.000000	
3	1.4100	-0.50	0.000000	0.000000	0.000000	100.000000	
4	1.1900	-0.25	0.000000	0.000000	0.000000	100.000000	
5	1.0000	0.00	0.000000	0.000000	0.000000	100.000000	8
6	0.8400	0.25	0.000000	0.000000	0.000000	100.000000	
7	0.7100	0.49	0.000000	0.000000	0.000000	100.000000	
8	0.5900	0.76	0.000000	0.000000	0.000000	100.000000	
9	0.5000	1.00	0.012093	0.012093	0.012093	99.987907	
10	0.4200	1.25	0.337615	0.325522	0.325522	99.662385	
11	0.3500	1.51	2.565075	2.227460	2.227460	97.434925	
12	0.3000	1.74	7.308809	4.743734	4.743734	92.691191	
13	0.2500	2.00	17.740238	10.431429	10.431429	82.259762	
14	0.2100	2.25	32.653007	14.912769	14.912769	67.346993	
15	0.1770	2.50	50.283367	17.630360	17.630360	49.716633	
16	0.1490	2.75	68.078244	17.794877	17.794877	31.921756	mode at 2.622397
17	0.1250	3.00	83.110721	15.032477	15.032477	16.889279	
18	0.1050	3.25	93.075679	9.964958	9.964958	6.924321	
19	0.0880	3.51	98.193939	5.118260	5.118260	1.806061	
20	0.0740	3.76	99.869233	1.675294	1.675294	0.130767	
21	0.0630	3.99	100.000000	0.130767	0.130767	0.000000	
22	0.0530	4.24	100.000000	0.000000	0.000000	0.000000	
23	0.0440	4.51	100.000000	0.000000	0.000000	0.000000	
24	0.0370	4.76	100.000000	0.000000	0.000000	0.000000	
25	0.0310	5.01	100.000000	0.000000	0.000000	0.000000	
26	0.0156	6.00	100.000000	0.000000	0.000000	0.000000	
27	0.0100	6.64	100.000000	0.000000	0.000000	0.000000	
28	0.0078	7.00	100.000000	0.000000	0.000000	0.000000	
29	0.0039	8.00	100.000000	0.000000	0.000000	0.000000	
30	0.0020	8.97	100.000000	0.000000	0.000000	0.000000	
31	0.0010	9.99	100.000000	0.000000	0.000000	0.000000	
32	0.0007	10.48	100.000000	0.000000	0.000000	0.000000	
33	0.0005	10.99	100.000000	0.000000	0.000000	0.000000	
34	0.0002	12.02	100.000000	0.000000	0.000000	0.000000	
35	0.0001	13.02	100.000000	0.000000	0.000000	0.000000	
36	0.0001	14.02	100.000000	0.000000	0.000000	0.000000	
37	0.0001	14.29	100.000000	0.000000	0.000000	0.000000	
	Sums:			100.00	100.00		

Column: 9

Sample ID: 16-7-2014mw

Folks' Graphic Statistics

	Mean (Mz)	Sorting (σI)	Skewness (SkI)	Kurtosis (KG)	Mean *mm*
phi	2.491	0.527	-0.008	0.951	0.178

Grainsize Statistics

Percentiles

	phi	*mm*
5	1.63	0.323
16	1.96	0.258
25	2.12	0.230
50	2.49	0.177
75	2.86	0.137
84	3.02	0.123
95	3.35	0.098

Table II.9: *Results summary for sample 9: Low intertidal zone, mid transect, Northern Ngarunui Beach. Sample collected on the 6th of February, 2015.*

Column: 10 **Density:** 2650
Volume: 0.010
Sample ID: 6-2-2015lm

Malvern data Phi	Malvern data Micron	Vol %	Equivalent Cum wt (g)
-1.00	2000.00	0	0.0
-0.75	1680.00	0	0.0
-0.50	1410.00	0	0.0
-0.25	1190.00	0	0.0
0.00	1000.00	0	0.0
0.25	840.00	0	0.0
0.49	710.00	0	0.0
0.76	590.00	0.435107	0.1
1.00	500.00	2.647037	0.7
1.25	420.00	8.68229	2.3
1.51	350.00	20.466479	5.4
1.74	300.00	34.610059	9.2
2.00	250.00	54.027429	14.3
2.25	210.00	71.865921	19.0
2.50	177.00	85.633168	22.7
2.75	149.00	94.414157	25.0
3.00	125.00	98.666149	26.1
3.25	105.00	99.914172	26.5
3.51	88.00	100	26.5
3.76	74.00	100	26.5
3.99	63.00	100	26.5
4.24	53.00	100	26.5
4.51	44.00	100	26.5
4.76	37.00	100	26.5
5.01	31.00	100	26.5
6.00	15.60	100	26.5
6.64	10.00	100	26.5
7.00	7.80	100	26.5
8.00	3.90	100	26.5
8.97	2.00	100	26.5
9.99	0.98	100	26.5
10.48	0.70	100	26.5
10.99	0.49	100	26.5
12.02	0.24	100	26.5
13.02	0.12	100	26.5
14.02	0.06	100	26.5
14.29	0.05	100	26.5
		Total weight:	26.5

	mm	phi	Cum wt (g)	Int wt (g)	Int wt%	Cum % finer	Modes	
1	2.0000	-1.00	0.000000	0.000000	0.000000	100.000000		
2	1.6800	-0.75	0.000000	0.000000	0.000000	100.000000		
3	1.4100	-0.50	0.000000	0.000000	0.000000	100.000000		
4	1.1900	-0.25	0.000000	0.000000	0.000000	100.000000		
5	1.0000	0.00	0.000000	0.000000	0.000000	100.000000		8
6	0.8400	0.25	0.000000	0.000000	0.000000	100.000000		
7	0.7100	0.49	0.000000	0.000000	0.000000	100.000000		
8	0.5900	0.76	0.435107	0.435107	0.435107	99.564893		
9	0.5000	1.00	2.647037	2.211930	2.211930	97.352963		
10	0.4200	1.25	8.682290	6.035253	6.035253	91.317710		
11	0.3500	1.51	20.466479	11.784189	11.784189	79.533521		
12	0.3000	1.74	34.610059	14.143580	14.143580	65.389941		
13	0.2500	2.00	54.027429	19.417370	19.417370	45.972571	mode at 1.868483	
14	0.2100	2.25	71.865921	17.838492	17.838492	28.134079		
15	0.1770	2.50	85.633168	13.767247	13.767247	14.366832		
16	0.1490	2.75	94.414157	8.780989	8.780989	5.585843		
17	0.1250	3.00	98.666149	4.251992	4.251992	1.333851		
18	0.1050	3.25	99.914172	1.248023	1.248023	0.085828		
19	0.0880	3.51	100.000000	0.085828	0.085828	0.000000		
20	0.0740	3.76	100.000000	0.000000	0.000000	0.000000		
21	0.0630	3.99	100.000000	0.000000	0.000000	0.000000		
22	0.0530	4.24	100.000000	0.000000	0.000000	0.000000		
23	0.0440	4.51	100.000000	0.000000	0.000000	0.000000		
24	0.0370	4.76	100.000000	0.000000	0.000000	0.000000		
25	0.0310	5.01	100.000000	0.000000	0.000000	0.000000		
26	0.0156	6.00	100.000000	0.000000	0.000000	0.000000		
27	0.0100	6.64	100.000000	0.000000	0.000000	0.000000		
28	0.0078	7.00	100.000000	0.000000	0.000000	0.000000		
29	0.0039	8.00	100.000000	0.000000	0.000000	0.000000		
30	0.0020	8.97	100.000000	0.000000	0.000000	0.000000		
31	0.0010	9.99	100.000000	0.000000	0.000000	0.000000		
32	0.0007	10.48	100.000000	0.000000	0.000000	0.000000		
33	0.0005	10.99	100.000000	0.000000	0.000000	0.000000		
34	0.0002	12.02	100.000000	0.000000	0.000000	0.000000		
35	0.0001	13.02	100.000000	0.000000	0.000000	0.000000		
36	0.0001	14.02	100.000000	0.000000	0.000000	0.000000		
37	0.0001	14.29	100.000000	0.000000	0.000000	0.000000		
	Sums:			100.00	100.00			

Grainsize Statistics
Percentiles

	phi	*mm*
5	1.10	0.467
16	1.41	0.375
25	1.59	0.333
50	1.95	0.260
75	2.31	0.202
84	2.47	0.181
95	2.78	0.145

Column: 10
Sample ID: 6-2-2015lm

Folks' Graphic Statistics

	Mean (Mz)	Sorting (σI)	Skewness (SkI)	Kurtosis (KG)	Mean *mm*
phi	1.943	0.519	-0.007	0.956	0.260

Table II.10: *Results summary for sample 10: High intertidal zone, mid transect, Northern Ngarunui Beach. Sample collected on the 6th of February, 2015.*

Column: 11 **Density:** 2650
Volume: 0.010
Sample ID: 6-2-2015hm

Malvern data Phi	Malvern data Micron	Vol %	Equivalent Cum wt (g)
-1.00	2000.00	0	0.0
-0.75	1680.00	0	0.0
-0.50	1410.00	0	0.0
-0.25	1190.00	0	0.0
0.00	1000.00	0	0.0
0.25	840.00	0	0.0
0.49	710.00	0	0.0
0.76	590.00	0	0.0
1.00	500.00	0.590926	0.2
1.25	420.00	3.405094	0.9
1.51	350.00	10.765539	2.9
1.74	300.00	21.483051	5.7
2.00	250.00	38.838436	10.3
2.25	210.00	57.586288	15.3
2.50	177.00	74.574008	19.8
2.75	149.00	87.552333	23.2
3.00	125.00	95.526181	25.3
3.25	105.00	99.041478	26.2
3.51	88.00	99.966817	26.5
3.76	74.00	100	26.5
3.99	63.00	100	26.5
4.24	53.00	100	26.5
4.51	44.00	100	26.5
4.76	37.00	100	26.5
5.01	31.00	100	26.5
6.00	15.60	100	26.5
6.64	10.00	100	26.5
7.00	7.80	100	26.5
8.00	3.90	100	26.5
8.97	2.00	100	26.5
9.99	0.98	100	26.5
10.48	0.70	100	26.5
10.99	0.49	100	26.5
12.02	0.24	100	26.5
13.02	0.12	100	26.5
14.02	0.06	100	26.5
14.29	0.05	100	26.5
		Total weight:	26.5

	mm	phi	Cum wt (g)	Int wt (g)	Int wt%	Cum % finer	Modes	
1	2.0000	-1.00	0.000000	0.000000	0.000000	100.000000		
2	1.6800	-0.75	0.000000	0.000000	0.000000	100.000000		
3	1.4100	-0.50	0.000000	0.000000	0.000000	100.000000		
4	1.1900	-0.25	0.000000	0.000000	0.000000	100.000000		
5	1.0000	0.00	0.000000	0.000000	0.000000	100.000000		8
6	0.8400	0.25	0.000000	0.000000	0.000000	100.000000		
7	0.7100	0.49	0.000000	0.000000	0.000000	100.000000		
8	0.5900	0.76	0.000000	0.000000	0.000000	100.000000		
9	0.5000	1.00	0.590926	0.590926	0.590926	99.409074		
10	0.4200	1.25	3.405094	2.814168	2.814168	96.594906		
11	0.3500	1.51	10.765539	7.360445	7.360445	89.234461		
12	0.3000	1.74	21.483051	10.717512	10.717512	78.516949		
13	0.2500	2.00	38.838436	17.355385	17.355385	61.161564		
14	0.2100	2.25	57.586288	18.747852	18.747852	42.413712	mode at 2.125769	
15	0.1770	2.50	74.574008	16.987720	16.987720	25.425992		
16	0.1490	2.75	87.552333	12.978325	12.978325	12.447667		
17	0.1250	3.00	95.526181	7.973848	7.973848	4.473819		
18	0.1050	3.25	99.041478	3.515297	3.515297	0.958522		
19	0.0880	3.51	99.966817	0.925339	0.925339	0.033183		
20	0.0740	3.76	100.000000	0.033183	0.033183	0.000000		
21	0.0630	3.99	100.000000	0.000000	0.000000	0.000000		
22	0.0530	4.24	100.000000	0.000000	0.000000	0.000000		
23	0.0440	4.51	100.000000	0.000000	0.000000	0.000000		
24	0.0370	4.76	100.000000	0.000000	0.000000	0.000000		
25	0.0310	5.01	100.000000	0.000000	0.000000	0.000000		
26	0.0156	6.00	100.000000	0.000000	0.000000	0.000000		
27	0.0100	6.64	100.000000	0.000000	0.000000	0.000000		
28	0.0078	7.00	100.000000	0.000000	0.000000	0.000000		
29	0.0039	8.00	100.000000	0.000000	0.000000	0.000000		
30	0.0020	8.97	100.000000	0.000000	0.000000	0.000000		
31	0.0010	9.99	100.000000	0.000000	0.000000	0.000000		
32	0.0007	10.48	100.000000	0.000000	0.000000	0.000000		
33	0.0005	10.99	100.000000	0.000000	0.000000	0.000000		
34	0.0002	12.02	100.000000	0.000000	0.000000	0.000000		
35	0.0001	13.02	100.000000	0.000000	0.000000	0.000000		
36	0.0001	14.02	100.000000	0.000000	0.000000	0.000000		
37	0.0001	14.29	100.000000	0.000000	0.000000	0.000000		
	Sums:			100.00	100.00			

Grainsize Statistics
Percentiles

	phi	*mm*
5	1.31	0.404
16	1.62	0.325
25	1.79	0.289
50	2.15	0.225
75	2.51	0.176
84	2.68	0.156
95	2.98	0.126

Column: 11
Sample ID: 6-2-2015hm

Folks' Graphic Statistics

	Mean (Mz)	Sorting (σI)	Skewness (SkI)	Kurtosis (KG)	Mean *mm*
phi	2.151	0.518	-0.001	0.959	0.225

Table II.11: *Results summary for sample 11: High intertidal zone, southern transect, Northern Ngarunui Beach. Sample collected on the 6th of February, 2015.*

Column: 12 **Density:** 2650
Volume: 0.010
Sample ID: 6-2-2015sh

Malvern data Phi	Malvern data Micron	Vol %	Equivalent Cum wt (g)
-1.00	2000.00	0	0.0
-0.75	1680.00	0	0.0
-0.50	1410.00	0	0.0
-0.25	1190.00	0	0.0
0.00	1000.00	0	0.0
0.25	840.00	0	0.0
0.49	710.00	0	0.0
0.76	590.00	0.101581	0.0
1.00	500.00	1.42395	0.4
1.25	420.00	5.889674	1.6
1.51	350.00	15.778994	4.2
1.74	300.00	28.675755	7.6
2.00	250.00	47.666267	12.6
2.25	210.00	66.326549	17.6
2.50	177.00	81.693015	21.6
2.75	149.00	92.219789	24.4
3.00	125.00	97.817942	25.9
3.25	105.00	99.776385	26.4
3.51	88.00	100	26.5
3.76	74.00	100	26.5
3.99	63.00	100	26.5
4.24	53.00	100	26.5
4.51	44.00	100	26.5
4.76	37.00	100	26.5
5.01	31.00	100	26.5
6.00	15.60	100	26.5
6.64	10.00	100	26.5
7.00	7.80	100	26.5
8.00	3.90	100	26.5
8.97	2.00	100	26.5
9.99	0.98	100	26.5
10.48	0.70	100	26.5
10.99	0.49	100	26.5
12.02	0.24	100	26.5
13.02	0.12	100	26.5
14.02	0.06	100	26.5
14.29	0.05	100	26.5
		Total weight:	26.5

	mm	phi	Cum wt (g)	Int wt (g)	Int wt%	Cum % finer	Modes
1	2.0000	-1.00	0.000000	0.000000	0.000000	100.000000	
2	1.6800	-0.75	0.000000	0.000000	0.000000	100.000000	
3	1.4100	-0.50	0.000000	0.000000	0.000000	100.000000	
4	1.1900	-0.25	0.000000	0.000000	0.000000	100.000000	
5	1.0000	0.00	0.000000	0.000000	0.000000	100.000000	8
6	0.8400	0.25	0.000000	0.000000	0.000000	100.000000	
7	0.7100	0.49	0.000000	0.000000	0.000000	100.000000	
8	0.5900	0.76	0.101581	0.101581	0.101581	99.898419	
9	0.5000	1.00	1.423950	1.322369	1.322369	98.576050	
10	0.4200	1.25	5.889674	4.465724	4.465724	94.110326	
11	0.3500	1.51	15.778994	9.889320	9.889320	84.221006	
12	0.3000	1.74	28.675755	12.896761	12.896761	71.324245	
13	0.2500	2.00	47.666267	18.990512	18.990512	52.333733	mode at 1.868483
14	0.2100	2.25	66.326549	18.660282	18.660282	33.673451	
15	0.1770	2.50	81.693015	15.366466	15.366466	18.306985	
16	0.1490	2.75	92.219789	10.526774	10.526774	7.780211	
17	0.1250	3.00	97.817942	5.598153	5.598153	2.182058	
18	0.1050	3.25	99.776385	1.958443	1.958443	0.223615	
19	0.0880	3.51	100.000000	0.223615	0.223615	0.000000	
20	0.0740	3.76	100.000000	0.000000	0.000000	0.000000	
21	0.0630	3.99	100.000000	0.000000	0.000000	0.000000	
22	0.0530	4.24	100.000000	0.000000	0.000000	0.000000	
23	0.0440	4.51	100.000000	0.000000	0.000000	0.000000	
24	0.0370	4.76	100.000000	0.000000	0.000000	0.000000	
25	0.0310	5.01	100.000000	0.000000	0.000000	0.000000	
26	0.0156	6.00	100.000000	0.000000	0.000000	0.000000	
27	0.0100	6.64	100.000000	0.000000	0.000000	0.000000	
28	0.0078	7.00	100.000000	0.000000	0.000000	0.000000	
29	0.0039	8.00	100.000000	0.000000	0.000000	0.000000	
30	0.0020	8.97	100.000000	0.000000	0.000000	0.000000	
31	0.0010	9.99	100.000000	0.000000	0.000000	0.000000	
32	0.0007	10.48	100.000000	0.000000	0.000000	0.000000	
33	0.0005	10.99	100.000000	0.000000	0.000000	0.000000	
34	0.0002	12.02	100.000000	0.000000	0.000000	0.000000	
35	0.0001	13.02	100.000000	0.000000	0.000000	0.000000	
36	0.0001	14.02	100.000000	0.000000	0.000000	0.000000	
37	0.0001	14.29	100.000000	0.000000	0.000000	0.000000	
		Sums:		100.00	100.00		

Column: 12
Sample ID: 6-2-2015sh

Folks' Graphic Statistics

	Mean (Mz)	Sorting (σI)	Skewness (SkI)	Kurtosis (KG)	Mean *mm*
phi	2.034	0.512	0.007	0.955	0.244

Grainsize Statistics
Percentiles

	phi	*mm*
5	1.20	0.435
16	1.52	0.349
25	1.67	0.313
50	2.03	0.245
75	2.39	0.191
84	2.55	0.170
95	2.87	0.137

Table II.12: *Results summary for sample 12: High intertidal zone, northern transect, Northern Ngarunui Beach. Sample collected on the 6th of February, 2015.*

Column: 13 **Density:** 2650
Volume: 0.010
Sample ID: 6-2-2015nh

Malvern data Phi	Malvern data Micron	Vol %	Equivalent Cum wt (g)
-1.00	2000.00	0	0.0
-0.75	1680.00	0	0.0
-0.50	1410.00	0	0.0
-0.25	1190.00	0	0.0
0.00	1000.00	0	0.0
0.25	840.00	0	0.0
0.49	710.00	0	0.0
0.76	590.00	0	0.0
1.00	500.00	0.049216	0.0
1.25	420.00	1.126552	0.3
1.51	350.00	5.140994	1.4
1.74	300.00	12.327276	3.3
2.00	250.00	26.059694	6.9
2.25	210.00	43.394176	11.5
2.50	177.00	61.611871	16.3
2.75	149.00	77.883858	20.6
3.00	125.00	89.885075	23.8
3.25	105.00	96.651511	25.6
3.51	88.00	99.435218	26.4
3.76	74.00	100	26.5
3.99	63.00	100	26.5
4.24	53.00	100	26.5
4.51	44.00	100	26.5
4.76	37.00	100	26.5
5.01	31.00	100	26.5
6.00	15.60	100	26.5
6.64	10.00	100	26.5
7.00	7.80	100	26.5
8.00	3.90	100	26.5
8.97	2.00	100	26.5
9.99	0.98	100	26.5
10.48	0.70	100	26.5
10.99	0.49	100	26.5
12.02	0.24	100	26.5
13.02	0.12	100	26.5
14.02	0.06	100	26.5
14.29	0.05	100	26.5
		Total weight:	26.5

	mm	phi	Cum wt (g)	Int wt (g)	Int wt%	Cum % finer	Modes	
1	2.0000	-1.00	0.000000	0.000000	0.000000	100.000000		
2	1.6800	-0.75	0.000000	0.000000	0.000000	100.000000		
3	1.4100	-0.50	0.000000	0.000000	0.000000	100.000000		
4	1.1900	-0.25	0.000000	0.000000	0.000000	100.000000		
5	1.0000	0.00	0.000000	0.000000	0.000000	100.000000		8
6	0.8400	0.25	0.000000	0.000000	0.000000	100.000000		
7	0.7100	0.49	0.000000	0.000000	0.000000	100.000000		
8	0.5900	0.76	0.000000	0.000000	0.000000	100.000000		
9	0.5000	1.00	0.049216	0.049216	0.049216	99.950784		
10	0.4200	1.25	1.126552	1.077336	1.077336	98.873448		
11	0.3500	1.51	5.140994	4.014442	4.014442	94.859006		
12	0.3000	1.74	12.327276	7.186282	7.186282	87.672724		
13	0.2500	2.00	26.059694	13.732418	13.732418	73.940306		
14	0.2100	2.25	43.394176	17.334482	17.334482	56.605824		
15	0.1770	2.50	61.611871	18.217695	18.217695	38.388129	mode at 2.374859	
16	0.1490	2.75	77.883858	16.271987	16.271987	22.116142		
17	0.1250	3.00	89.885075	12.001217	12.001217	10.114925		
18	0.1050	3.25	96.651511	6.766436	6.766436	3.348489		
19	0.0880	3.51	99.435218	2.783707	2.783707	0.564782		
20	0.0740	3.76	100.000000	0.564782	0.564782	0.000000		
21	0.0630	3.99	100.000000	0.000000	0.000000	0.000000		
22	0.0530	4.24	100.000000	0.000000	0.000000	0.000000		
23	0.0440	4.51	100.000000	0.000000	0.000000	0.000000		
24	0.0370	4.76	100.000000	0.000000	0.000000	0.000000		
25	0.0310	5.01	100.000000	0.000000	0.000000	0.000000		
26	0.0156	6.00	100.000000	0.000000	0.000000	0.000000		
27	0.0100	6.64	100.000000	0.000000	0.000000	0.000000		
28	0.0078	7.00	100.000000	0.000000	0.000000	0.000000		
29	0.0039	8.00	100.000000	0.000000	0.000000	0.000000		
30	0.0020	8.97	100.000000	0.000000	0.000000	0.000000		
31	0.0010	9.99	100.000000	0.000000	0.000000	0.000000		
32	0.0007	10.48	100.000000	0.000000	0.000000	0.000000		
33	0.0005	10.99	100.000000	0.000000	0.000000	0.000000		
34	0.0002	12.02	100.000000	0.000000	0.000000	0.000000		
35	0.0001	13.02	100.000000	0.000000	0.000000	0.000000		
36	0.0001	14.02	100.000000	0.000000	0.000000	0.000000		
37	0.0001	14.29	100.000000	0.000000	0.000000	0.000000		
	Sums:			100.00	100.00			

Grainsize Statistics
Percentiles

	phi	*mm*
5	1.51	0.352
16	1.81	0.286
25	1.98	0.254
50	2.34	0.197
75	2.70	0.154
84	2.88	0.136
95	3.19	0.110

Column: 13
Sample ID: 6-2-2015nh

Folks' Graphic Statistics

	Mean (Mz)	Sorting (σI)	Skewness (SkI)	Kurtosis (KG)	Mean *mm*
phi	2.341	0.522	0.005	0.955	0.197

Table II.13: *Results summary for sample 13: Mid intertidal zone, mid transect, Northern Ngarunui Beach. Sample collected on the 6th of February, 2015.*

Column:	14	**Density:**	2650
		Volume:	0.010
Sample ID:	6-2-2015mm		

Malvern data Phi	**Malvern data** Micron	Vol %	Equivalent Cum wt (g)
-1.00	2000.00	0	0.0
-0.75	1680.00	0	0.0
-0.50	1410.00	0	0.0
-0.25	1190.00	0	0.0
0.00	1000.00	0	0.0
0.25	840.00	0	0.0
0.49	710.00	0	0.0
0.76	590.00	0.064965	0.0
1.00	500.00	1.107221	0.3
1.25	420.00	5.298894	1.4
1.51	350.00	15.64711	4.1
1.74	300.00	29.883517	7.9
2.00	250.00	51.047913	13.5
2.25	210.00	71.113763	18.8
2.50	177.00	86.30116	22.9
2.75	149.00	95.312951	25.3
3.00	125.00	99.12965	26.3
3.25	105.00	99.932851	26.5
3.51	88.00	100	26.5
3.76	74.00	100	26.5
3.99	63.00	100	26.5
4.24	53.00	100	26.5
4.51	44.00	100	26.5
4.76	37.00	100	26.5
5.01	31.00	100	26.5
6.00	15.60	100	26.5
6.64	10.00	100	26.5
7.00	7.80	100	26.5
8.00	3.90	100	26.5
8.97	2.00	100	26.5
9.99	0.98	100	26.5
10.48	0.70	100	26.5
10.99	0.49	100	26.5
12.02	0.24	100	26.5
13.02	0.12	100	26.5
14.02	0.06	100	26.5
14.29	0.05	100	26.5
		Total weight:	26.5

	mm	phi	Cum wt (g)	Int wt (g)	Int wt%	Cum % finer	Modes	
1	2.0000	-1.00	0.000000	0.000000	0.000000	100.000000		
2	1.6800	-0.75	0.000000	0.000000	0.000000	100.000000		
3	1.4100	-0.50	0.000000	0.000000	0.000000	100.000000		
4	1.1900	-0.25	0.000000	0.000000	0.000000	100.000000		
5	1.0000	0.00	0.000000	0.000000	0.000000	100.000000		8
6	0.8400	0.25	0.000000	0.000000	0.000000	100.000000		
7	0.7100	0.49	0.000000	0.000000	0.000000	100.000000		
8	0.5900	0.76	0.064965	0.064965	0.064965	99.935035		
9	0.5000	1.00	1.107221	1.042256	1.042256	98.892779		
10	0.4200	1.25	5.298894	4.191673	4.191673	94.701106		
11	0.3500	1.51	15.647110	10.348216	10.348216	84.352890		
12	0.3000	1.74	29.883517	14.236407	14.236407	70.116483		
13	0.2500	2.00	51.047913	21.164396	21.164396	48.952087	mode at 1.868483	
14	0.2100	2.25	71.113763	20.065850	20.065850	28.886237		
15	0.1770	2.50	86.301160	15.187397	15.187397	13.698840		
16	0.1490	2.75	95.312951	9.011791	9.011791	4.687049		
17	0.1250	3.00	99.129650	3.816699	3.816699	0.870350		
18	0.1050	3.25	99.932851	0.803201	0.803201	0.067149		
19	0.0880	3.51	100.000000	0.067149	0.067149	0.000000		
20	0.0740	3.76	100.000000	0.000000	0.000000	0.000000		
21	0.0630	3.99	100.000000	0.000000	0.000000	0.000000		
22	0.0530	4.24	100.000000	0.000000	0.000000	0.000000		
23	0.0440	4.51	100.000000	0.000000	0.000000	0.000000		
24	0.0370	4.76	100.000000	0.000000	0.000000	0.000000		
25	0.0310	5.01	100.000000	0.000000	0.000000	0.000000		
26	0.0156	6.00	100.000000	0.000000	0.000000	0.000000		
27	0.0100	6.64	100.000000	0.000000	0.000000	0.000000		
28	0.0078	7.00	100.000000	0.000000	0.000000	0.000000		
29	0.0039	8.00	100.000000	0.000000	0.000000	0.000000		
30	0.0020	8.97	100.000000	0.000000	0.000000	0.000000		
31	0.0010	9.99	100.000000	0.000000	0.000000	0.000000		
32	0.0007	10.48	100.000000	0.000000	0.000000	0.000000		
33	0.0005	10.99	100.000000	0.000000	0.000000	0.000000		
34	0.0002	12.02	100.000000	0.000000	0.000000	0.000000		
35	0.0001	13.02	100.000000	0.000000	0.000000	0.000000		
36	0.0001	14.02	100.000000	0.000000	0.000000	0.000000		
37	0.0001	14.29	100.000000	0.000000	0.000000	0.000000		
		Sums:		100.00	100.00			

Grainsize Statistics
Percentiles

	phi	*mm*
5	1.23	0.425
16	1.52	0.349
25	1.66	0.316
50	1.99	0.252
75	2.31	0.201
84	2.46	0.182
95	2.74	0.150

Column: 14
Sample ID: 6-2-2015mm

Folks' Graphic Statistics

	Mean (Mz)	Sorting (σI)	Skewness (SkI)	Kurtosis (KG)	Mean *mm*
phi	1.989	0.463	0.003	0.943	0.252

Table II.14: *Results summary for sample 14: High intertidal zone, northern transect, Northern Ngarunui Beach. Sample collected on the 27th of November, 2014.*

Column: 15 **Density:** 2650
Volume: 0.010
Sample ID: 2014-11-27nh

Malvern data Phi	Malvern data Micron	Vol %	Equivalent Cum wt (g)
-1.00	2000.00	0	0.0
-0.75	1680.00	0	0.0
-0.50	1410.00	0	0.0
-0.25	1190.00	0	0.0
0.00	1000.00	0	0.0
0.25	840.00	0	0.0
0.49	710.00	0	0.0
0.76	590.00	0	0.0
1.00	500.00	0.469034	0.1
1.25	420.00	3.213647	0.9
1.51	350.00	11.359992	3.0
1.74	300.00	23.933329	6.3
2.00	250.00	44.415798	11.8
2.25	210.00	65.492831	17.4
2.50	177.00	82.647386	21.9
2.75	149.00	93.592457	24.8
3.00	125.00	98.612258	26.1
3.25	105.00	99.923864	26.5
3.51	88.00	100	26.5
3.76	74.00	100	26.5
3.99	63.00	100	26.5
4.24	53.00	100	26.5
4.51	44.00	100	26.5
4.76	37.00	100	26.5
5.01	31.00	100	26.5
6.00	15.60	100	26.5
6.64	10.00	100	26.5
7.00	7.80	100	26.5
8.00	3.90	100	26.5
8.97	2.00	100	26.5
9.99	0.98	100	26.5
10.48	0.70	100	26.5
10.99	0.49	100	26.5
12.02	0.24	100	26.5
13.02	0.12	100	26.5
14.02	0.06	100	26.5
14.29	0.05	100	26.5
		Total weight:	26.5

	mm	phi	Cum wt (g)	Int wt (g)	Int wt%	Cum % finer	Modes	
1	2.0000	-1.00	0.000000	0.000000	0.000000	100.000000		
2	1.6800	-0.75	0.000000	0.000000	0.000000	100.000000		
3	1.4100	-0.50	0.000000	0.000000	0.000000	100.000000		
4	1.1900	-0.25	0.000000	0.000000	0.000000	100.000000		
5	1.0000	0.00	0.000000	0.000000	0.000000	100.000000		8
6	0.8400	0.25	0.000000	0.000000	0.000000	100.000000		
7	0.7100	0.49	0.000000	0.000000	0.000000	100.000000		
8	0.5900	0.76	0.000000	0.000000	0.000000	100.000000		
9	0.5000	1.00	0.469034	0.469034	0.469034	99.530966		
10	0.4200	1.25	3.213647	2.744613	2.744613	96.786353		
11	0.3500	1.51	11.359992	8.146345	8.146345	88.640008		
12	0.3000	1.74	23.933329	12.573337	12.573337	76.066671		
13	0.2500	2.00	44.415798	20.482469	20.482469	55.584202		
14	0.2100	2.25	65.492831	21.077033	21.077033	34.507169	mode at 2.125769	
15	0.1770	2.50	82.647386	17.154555	17.154555	17.352614		
16	0.1490	2.75	93.592457	10.945071	10.945071	6.407543		
17	0.1250	3.00	98.612258	5.019801	5.019801	1.387742		
18	0.1050	3.25	99.923864	1.311606	1.311606	0.076136		
19	0.0880	3.51	100.000000	0.076136	0.076136	0.000000		
20	0.0740	3.76	100.000000	0.000000	0.000000	0.000000		
21	0.0630	3.99	100.000000	0.000000	0.000000	0.000000		
22	0.0530	4.24	100.000000	0.000000	0.000000	0.000000		
23	0.0440	4.51	100.000000	0.000000	0.000000	0.000000		
24	0.0370	4.76	100.000000	0.000000	0.000000	0.000000		
25	0.0310	5.01	100.000000	0.000000	0.000000	0.000000		
26	0.0156	6.00	100.000000	0.000000	0.000000	0.000000		
27	0.0100	6.64	100.000000	0.000000	0.000000	0.000000		
28	0.0078	7.00	100.000000	0.000000	0.000000	0.000000		
29	0.0039	8.00	100.000000	0.000000	0.000000	0.000000		
30	0.0020	8.97	100.000000	0.000000	0.000000	0.000000		
31	0.0010	9.99	100.000000	0.000000	0.000000	0.000000		
32	0.0007	10.48	100.000000	0.000000	0.000000	0.000000		
33	0.0005	10.99	100.000000	0.000000	0.000000	0.000000		
34	0.0002	12.02	100.000000	0.000000	0.000000	0.000000		
35	0.0001	13.02	100.000000	0.000000	0.000000	0.000000		
36	0.0001	14.02	100.000000	0.000000	0.000000	0.000000		
37	0.0001	14.29	100.000000	0.000000	0.000000	0.000000		
		Sums:		100.00	100.00			

Grainsize Statistics
Percentiles

	phi	*mm*
5	1.31	0.404
16	1.60	0.331
25	1.75	0.297
50	2.07	0.239
75	2.39	0.191
84	2.53	0.173
95	2.82	0.142

Column: 15
Sample ID: 2014-11-27nh

Folks' Graphic Statistics

	Mean (Mz)	Sorting (σI)	Skewness (SkI)	Kurtosis (KG)	Mean *mm*
phi	2.064	0.462	-0.006	0.970	0.239

Table II.15: *Results summary for sample 15: Mid intertidal zone, northern transect, Northern Ngarunui Beach. Sample collected on the 27th of November, 2014.*

Column: 16 **Density:** 2650
Volume: 0.010
Sample ID: 2014-11-27nm

Malvern data Phi	Malvern data Micron	Vol %	Equivalent Cum wt (g)
-1.00	2000.00	0	0.0
-0.75	1680.00	0	0.0
-0.50	1410.00	0	0.0
-0.25	1190.00	0	0.0
0.00	1000.00	0	0.0
0.25	840.00	0	0.0
0.49	710.00	0.150591	0.0
0.76	590.00	1.930366	0.5
1.00	500.00	6.701104	1.8
1.25	420.00	16.555101	4.4
1.51	350.00	32.356613	8.6
1.74	300.00	48.626423	12.9
2.00	250.00	67.960038	18.0
2.25	210.00	83.153137	22.0
2.50	177.00	93.036734	24.7
2.75	149.00	98.10487	26.0
3.00	125.00	99.825428	26.5
3.25	105.00	100	26.5
3.51	88.00	100	26.5
3.76	74.00	100	26.5
3.99	63.00	100	26.5
4.24	53.00	100	26.5
4.51	44.00	100	26.5
4.76	37.00	100	26.5
5.01	31.00	100	26.5
6.00	15.60	100	26.5
6.64	10.00	100	26.5
7.00	7.80	100	26.5
8.00	3.90	100	26.5
8.97	2.00	100	26.5
9.99	0.98	100	26.5
10.48	0.70	100	26.5
10.99	0.49	100	26.5
12.02	0.24	100	26.5
13.02	0.12	100	26.5
14.02	0.06	100	26.5
14.29	0.05	100	26.5
		Total weight:	26.5

	mm	phi	Cum wt (g)	Int wt (g)	Int wt%	Cum % finer	Modes	
1	2.0000	-1.00	0.000000	0.000000	0.000000	100.000000		
2	1.6800	-0.75	0.000000	0.000000	0.000000	100.000000		
3	1.4100	-0.50	0.000000	0.000000	0.000000	100.000000		
4	1.1900	-0.25	0.000000	0.000000	0.000000	100.000000		
5	1.0000	0.00	0.000000	0.000000	0.000000	100.000000		8
6	0.8400	0.25	0.000000	0.000000	0.000000	100.000000		
7	0.7100	0.49	0.150591	0.150591	0.150591	99.849409		
8	0.5900	0.76	1.930366	1.779775	1.779775	98.069634		
9	0.5000	1.00	6.701104	4.770738	4.770738	93.298896		
10	0.4200	1.25	16.555101	9.853997	9.853997	83.444899		
11	0.3500	1.51	32.356613	15.801512	15.801512	67.643387		
12	0.3000	1.74	48.626423	16.269810	16.269810	51.373577		
13	0.2500	2.00	67.960038	19.333615	19.333615	32.039962	mode at 1.868483	
14	0.2100	2.25	83.153137	15.193099	15.193099	16.846863		
15	0.1770	2.50	93.036734	9.883597	9.883597	6.963266		
16	0.1490	2.75	98.104870	5.068136	5.068136	1.895130		
17	0.1250	3.00	99.825428	1.720558	1.720558	0.174572		
18	0.1050	3.25	100.000000	0.174572	0.174572	0.000000		
19	0.0880	3.51	100.000000	0.000000	0.000000	0.000000		
20	0.0740	3.76	100.000000	0.000000	0.000000	0.000000		
21	0.0630	3.99	100.000000	0.000000	0.000000	0.000000		
22	0.0530	4.24	100.000000	0.000000	0.000000	0.000000		
23	0.0440	4.51	100.000000	0.000000	0.000000	0.000000		
24	0.0370	4.76	100.000000	0.000000	0.000000	0.000000		
25	0.0310	5.01	100.000000	0.000000	0.000000	0.000000		
26	0.0156	6.00	100.000000	0.000000	0.000000	0.000000		
27	0.0100	6.64	100.000000	0.000000	0.000000	0.000000		
28	0.0078	7.00	100.000000	0.000000	0.000000	0.000000		
29	0.0039	8.00	100.000000	0.000000	0.000000	0.000000		
30	0.0020	8.97	100.000000	0.000000	0.000000	0.000000		
31	0.0010	9.99	100.000000	0.000000	0.000000	0.000000		
32	0.0007	10.48	100.000000	0.000000	0.000000	0.000000		
33	0.0005	10.99	100.000000	0.000000	0.000000	0.000000		
34	0.0002	12.02	100.000000	0.000000	0.000000	0.000000		
35	0.0001	13.02	100.000000	0.000000	0.000000	0.000000		
36	0.0001	14.02	100.000000	0.000000	0.000000	0.000000		
37	0.0001	14.29	100.000000	0.000000	0.000000	0.000000		
		Sums:		100.00	100.00			

Column: 16
Sample ID: 2014-11-27nm

Folks' Graphic Statistics

	Mean (Mz)	Sorting (σI)	Skewness (SkI)	Kurtosis (KG)	Mean *mm*
phi	1.755	0.513	-0.001	0.950	0.296

Grainsize Statistics
Percentiles

	phi	***mm***
5	0.91	0.530
16	1.24	0.424
25	1.39	0.381
50	1.76	0.296
75	2.12	0.231
84	2.27	0.207
95	2.59	0.166

Table II.16: *Results summary for sample 16: High intertidal zone, southern transect, Northern Ngarunui Beach. Sample collected on the 27th of November, 2014.*

Column: 17 **Density:** 2650
Volume: 0.010
Sample ID: 2014-11-27sh

Malvern data Phi	Malvern data Micron	Vol %	Equivalent Cum wt (g)
-1.00	2000.00	0	0.0
-0.75	1680.00	0	0.0
-0.50	1410.00	0	0.0
-0.25	1190.00	0	0.0
0.00	1000.00	0	0.0
0.25	840.00	0	0.0
0.49	710.00	0.146181	0.0
0.76	590.00	1.695095	0.4
1.00	500.00	6.063724	1.6
1.25	420.00	15.311234	4.1
1.51	350.00	30.444022	8.1
1.74	300.00	46.324553	12.3
2.00	250.00	65.601953	17.4
2.25	210.00	81.182996	21.5
2.50	177.00	91.711893	24.3
2.75	149.00	97.445719	25.8
3.00	125.00	99.656976	26.4
3.25	105.00	100	26.5
3.51	88.00	100	26.5
3.76	74.00	100	26.5
3.99	63.00	100	26.5
4.24	53.00	100	26.5
4.51	44.00	100	26.5
4.76	37.00	100	26.5
5.01	31.00	100	26.5
6.00	15.60	100	26.5
6.64	10.00	100	26.5
7.00	7.80	100	26.5
8.00	3.90	100	26.5
8.97	2.00	100	26.5
9.99	0.98	100	26.5
10.48	0.70	100	26.5
10.99	0.49	100	26.5
12.02	0.24	100	26.5
13.02	0.12	100	26.5
14.02	0.06	100	26.5
14.29	0.05	100	26.5

Total weight: 26.5

	mm	phi	Cum wt (g)	Int wt (g)	Int wt%	Cum % finer	Modes	
1	2.0000	-1.00	0.000000	0.000000	0.000000	100.000000		
2	1.6800	-0.75	0.000000	0.000000	0.000000	100.000000		
3	1.4100	-0.50	0.000000	0.000000	0.000000	100.000000		
4	1.1900	-0.25	0.000000	0.000000	0.000000	100.000000		
5	1.0000	0.00	0.000000	0.000000	0.000000	100.000000		8
6	0.8400	0.25	0.000000	0.000000	0.000000	100.000000		
7	0.7100	0.49	0.146181	0.146181	0.146181	99.853819		
8	0.5900	0.76	1.695095	1.548914	1.548914	98.304905		
9	0.5000	1.00	6.063724	4.368629	4.368629	93.936276		
10	0.4200	1.25	15.311234	9.247510	9.247510	84.688766		
11	0.3500	1.51	30.444022	15.132788	15.132788	69.555978		
12	0.3000	1.74	46.324553	15.880531	15.880531	53.675447		
13	0.2500	2.00	65.601953	19.277400	19.277400	34.398047	mode at 1.868483	
14	0.2100	2.25	81.182996	15.581043	15.581043	18.817004		
15	0.1770	2.50	91.711893	10.528897	10.528897	8.288107		
16	0.1490	2.75	97.445719	5.733826	5.733826	2.554281		
17	0.1250	3.00	99.656976	2.211257	2.211257	0.343024		
18	0.1050	3.25	100.000000	0.343024	0.343024	0.000000		
19	0.0880	3.51	100.000000	0.000000	0.000000	0.000000		
20	0.0740	3.76	100.000000	0.000000	0.000000	0.000000		
21	0.0630	3.99	100.000000	0.000000	0.000000	0.000000		
22	0.0530	4.24	100.000000	0.000000	0.000000	0.000000		
23	0.0440	4.51	100.000000	0.000000	0.000000	0.000000		
24	0.0370	4.76	100.000000	0.000000	0.000000	0.000000		
25	0.0310	5.01	100.000000	0.000000	0.000000	0.000000		
26	0.0156	6.00	100.000000	0.000000	0.000000	0.000000		
27	0.0100	6.64	100.000000	0.000000	0.000000	0.000000		
28	0.0078	7.00	100.000000	0.000000	0.000000	0.000000		
29	0.0039	8.00	100.000000	0.000000	0.000000	0.000000		
30	0.0020	8.97	100.000000	0.000000	0.000000	0.000000		
31	0.0010	9.99	100.000000	0.000000	0.000000	0.000000		
32	0.0007	10.48	100.000000	0.000000	0.000000	0.000000		
33	0.0005	10.99	100.000000	0.000000	0.000000	0.000000		
34	0.0002	12.02	100.000000	0.000000	0.000000	0.000000		
35	0.0001	13.02	100.000000	0.000000	0.000000	0.000000		
36	0.0001	14.02	100.000000	0.000000	0.000000	0.000000		
37	0.0001	14.29	100.000000	0.000000	0.000000	0.000000		
		Sums:		100.00	100.00			

Grainsize Statistics
Percentiles

	phi	*mm*
5	0.94	0.521
16	1.26	0.417
25	1.42	0.374
50	1.79	0.290
75	2.15	0.225
84	2.32	0.201
95	2.64	0.160

Column: 17
Sample ID: 2014-11-27sh

Folks' Graphic Statistics

	Mean (Mz)	Sorting (σI)	Skewness (SkI)	Kurtosis (KG)	Mean *mm*
phi	1.789	0.521	0.006	0.951	0.289

Table II.17: *Results summary for sample 17: Mid intertidal zone, southern transect, Northern Ngarunui Beach. Sample collected on the 27th of November, 2014.*

Column: 18 **Density:** 2650
Volume: 0.010
Sample ID: 2014-11-27sm

Malvern data Phi	Malvern data Micron	Vol %	Equivalent Cum wt (g)
-1.00	2000.00	0	0.0
-0.75	1680.00	0	0.0
-0.50	1410.00	0	0.0
-0.25	1190.00	0	0.0
0.00	1000.00	0	0.0
0.25	840.00	0.024494	0.0
0.49	710.00	0.602263	0.2
0.76	590.00	3.513818	0.9
1.00	500.00	9.673907	2.6
1.25	420.00	20.95406	5.6
1.51	350.00	37.601385	10.0
1.74	300.00	53.761713	14.2
2.00	250.00	72.067522	19.1
2.25	210.00	85.826885	22.7
2.50	177.00	94.40835	25.0
2.75	149.00	98.596698	26.1
3.00	125.00	99.89852	26.5
3.25	105.00	100	26.5
3.51	88.00	100	26.5
3.76	74.00	100	26.5
3.99	63.00	100	26.5
4.24	53.00	100	26.5
4.51	44.00	100	26.5
4.76	37.00	100	26.5
5.01	31.00	100	26.5
6.00	15.60	100	26.5
6.64	10.00	100	26.5
7.00	7.80	100	26.5
8.00	3.90	100	26.5
8.97	2.00	100	26.5
9.99	0.98	100	26.5
10.48	0.70	100	26.5
10.99	0.49	100	26.5
12.02	0.24	100	26.5
13.02	0.12	100	26.5
14.02	0.06	100	26.5
14.29	0.05	100	26.5

Total weight: 26.5

	mm	phi	Cum wt (g)	Int wt (g)	Int wt%	Cum % finer	Modes
1	2.0000	-1.00	0.000000	0.000000	0.000000	100.000000	
2	1.6800	-0.75	0.000000	0.000000	0.000000	100.000000	
3	1.4100	-0.50	0.000000	0.000000	0.000000	100.000000	
4	1.1900	-0.25	0.000000	0.000000	0.000000	100.000000	
5	1.0000	0.00	0.000000	0.000000	0.000000	100.000000	
6	0.8400	0.25	0.024494	0.024494	0.024494	99.975506	
7	0.7100	0.49	0.602263	0.577769	0.577769	99.397737	
8	0.5900	0.76	3.513818	2.911555	2.911555	96.486182	
9	0.5000	1.00	9.673907	6.160089	6.160089	90.326093	
10	0.4200	1.25	20.954060	11.280153	11.280153	79.045940	
11	0.3500	1.51	37.601385	16.647325	16.647325	62.398615	mode at 1.383056
12	0.3000	1.74	53.761713	16.160328	16.160328	46.238287	
13	0.2500	2.00	72.067522	18.305809	18.305809	27.932478	mode at 1.868483
14	0.2100	2.25	85.826885	13.759363	13.759363	14.173115	
15	0.1770	2.50	94.408350	8.581465	8.581465	5.591650	
16	0.1490	2.75	98.596698	4.188348	4.188348	1.403302	
17	0.1250	3.00	99.898520	1.301822	1.301822	0.101480	
18	0.1050	3.25	100.000000	0.101480	0.101480	0.000000	
19	0.0880	3.51	100.000000	0.000000	0.000000	0.000000	
20	0.0740	3.76	100.000000	0.000000	0.000000	0.000000	
21	0.0630	3.99	100.000000	0.000000	0.000000	0.000000	
22	0.0530	4.24	100.000000	0.000000	0.000000	0.000000	
23	0.0440	4.51	100.000000	0.000000	0.000000	0.000000	
24	0.0370	4.76	100.000000	0.000000	0.000000	0.000000	
25	0.0310	5.01	100.000000	0.000000	0.000000	0.000000	
26	0.0156	6.00	100.000000	0.000000	0.000000	0.000000	
27	0.0100	6.64	100.000000	0.000000	0.000000	0.000000	
28	0.0078	7.00	100.000000	0.000000	0.000000	0.000000	
29	0.0039	8.00	100.000000	0.000000	0.000000	0.000000	
30	0.0020	8.97	100.000000	0.000000	0.000000	0.000000	
31	0.0010	9.99	100.000000	0.000000	0.000000	0.000000	
32	0.0007	10.48	100.000000	0.000000	0.000000	0.000000	
33	0.0005	10.99	100.000000	0.000000	0.000000	0.000000	
34	0.0002	12.02	100.000000	0.000000	0.000000	0.000000	
35	0.0001	13.02	100.000000	0.000000	0.000000	0.000000	
36	0.0001	14.02	100.000000	0.000000	0.000000	0.000000	
37	0.0001	14.29	100.000000	0.000000	0.000000	0.000000	
		Sums:		100.00	100.00		

Column: 18
Sample ID: 2014-11-27sm

Folks' Graphic Statistics

	Mean (Mz)	Sorting (σI)	Skewness (SkI)	Kurtosis (KG)	Mean *mm*
phi	1.681	0.529	-0.011	0.952	0.312

Grainsize Statistics
Percentiles

	phi	*mm*
5	0.82	0.567
16	1.14	0.453
25	1.32	0.402
50	1.69	0.311
75	2.05	0.241
84	2.22	0.215
95	2.53	0.173

Table II.18: *Results summary for sample 18: Low intertidal zone, mid transect, Northern Ngarunui Beach. Sample collected on the 27th of November, 2014.*

Column: 19 **Density:** 2650
Volume: 0.010
Sample ID: 2014-11-27ml

Malvern data Phi	Malvern data Micron	Vol %	Equivalent Cum wt (g)
-1.00	2000.00	0	0.0
-0.75	1680.00	0.070654	0.0
-0.50	1410.00	0.451319	0.1
-0.25	1190.00	1.637188	0.4
0.00	1000.00	4.591957	1.2
0.25	840.00	10.381365	2.8
0.49	710.00	19.360914	5.1
0.76	590.00	33.053553	8.8
1.00	500.00	47.560177	12.6
1.25	420.00	63.224926	16.8
1.51	350.00	77.742527	20.6
1.74	300.00	87.232353	23.1
2.00	250.00	94.645404	25.1
2.25	210.00	98.338179	26.1
2.50	177.00	99.740542	26.4
2.75	149.00	100	26.5
3.00	125.00	100	26.5
3.25	105.00	100	26.5
3.51	88.00	100	26.5
3.76	74.00	100	26.5
3.99	63.00	100	26.5
4.24	53.00	100	26.5
4.51	44.00	100	26.5
4.76	37.00	100	26.5
5.01	31.00	100	26.5
6.00	15.60	100	26.5
6.64	10.00	100	26.5
7.00	7.80	100	26.5
8.00	3.90	100	26.5
8.97	2.00	100	26.5
9.99	0.98	100	26.5
10.48	0.70	100	26.5
10.99	0.49	100	26.5
12.02	0.24	100	26.5
13.02	0.12	100	26.5
14.02	0.06	100	26.5
14.29	0.05	100	26.5

Total weight: 26.5

	mm	phi	Cum wt (g)	Int wt (g)	Int wt%	Cum % finer	Modes
1	2.0000	-1.00	0.000000	0.000000	0.000000	100.000000	
2	1.6800	-0.75	0.070654	0.070654	0.070654	99.929346	
3	1.4100	-0.50	0.451319	0.380665	0.380665	99.548681	
4	1.1900	-0.25	1.637188	1.185869	1.185869	98.362812	
5	1.0000	0.00	4.591957	2.954769	2.954769	95.408043	8
6	0.8400	0.25	10.381365	5.789408	5.789408	89.618635	
7	0.7100	0.49	19.360914	8.979549	8.979549	80.639086	
8	0.5900	0.76	33.053553	13.692639	13.692639	66.946447	
9	0.5000	1.00	47.560177	14.506624	14.506624	52.439823	
10	0.4200	1.25	63.224926	15.664749	15.664749	36.775074	mode at 1.125769
11	0.3500	1.51	77.742527	14.517601	14.517601	22.257473	
12	0.3000	1.74	87.232353	9.489826	9.489826	12.767647	
13	0.2500	2.00	94.645404	7.413051	7.413051	5.354596	
14	0.2100	2.25	98.338179	3.692775	3.692775	1.661821	
15	0.1770	2.50	99.740542	1.402363	1.402363	0.259458	
16	0.1490	2.75	100.000000	0.259458	0.259458	0.000000	
17	0.1250	3.00	100.000000	0.000000	0.000000	0.000000	
18	0.1050	3.25	100.000000	0.000000	0.000000	0.000000	
19	0.0880	3.51	100.000000	0.000000	0.000000	0.000000	
20	0.0740	3.76	100.000000	0.000000	0.000000	0.000000	
21	0.0630	3.99	100.000000	0.000000	0.000000	0.000000	
22	0.0530	4.24	100.000000	0.000000	0.000000	0.000000	
23	0.0440	4.51	100.000000	0.000000	0.000000	0.000000	
24	0.0370	4.76	100.000000	0.000000	0.000000	0.000000	
25	0.0310	5.01	100.000000	0.000000	0.000000	0.000000	
26	0.0156	6.00	100.000000	0.000000	0.000000	0.000000	
27	0.0100	6.64	100.000000	0.000000	0.000000	0.000000	
28	0.0078	7.00	100.000000	0.000000	0.000000	0.000000	
29	0.0039	8.00	100.000000	0.000000	0.000000	0.000000	
30	0.0020	8.97	100.000000	0.000000	0.000000	0.000000	
31	0.0010	9.99	100.000000	0.000000	0.000000	0.000000	
32	0.0007	10.48	100.000000	0.000000	0.000000	0.000000	
33	0.0005	10.99	100.000000	0.000000	0.000000	0.000000	
34	0.0002	12.02	100.000000	0.000000	0.000000	0.000000	
35	0.0001	13.02	100.000000	0.000000	0.000000	0.000000	
36	0.0001	14.02	100.000000	0.000000	0.000000	0.000000	
37	0.0001	14.29	100.000000	0.000000	0.000000	0.000000	
		Sums:		100.00	100.00		

Grainsize Statistics
Percentiles

	phi	*mm*
5	0.02	0.988
16	0.40	0.756
25	0.60	0.658
50	1.04	0.487
75	1.46	0.362
84	1.66	0.316
95	2.02	0.246

Column: 19
Sample ID: 2014-11-27ml

Folks' Graphic Statistics

	Mean (Mz)	Sorting (σI)	Skewness (SkI)	Kurtosis (KG)	Mean *mm*
phi	1.035	0.618	-0.015	0.955	0.488

Table II.19: *Results summary for sample 19: Low intertidal zone, southern transect, Northern Ngarunui Beach. Sample collected on the 27th of November, 2014.*

Column: 20 **Density:** 2650
Volume: 0.010
Sample ID: 2014-11-27sl

Malvern data Phi	Malvern data Micron	Vol %	Equivalent Cum wt (g)
-1.00	2000.00	0	0.0
-0.75	1680.00	0	0.0
-0.50	1410.00	0	0.0
-0.25	1190.00	0	0.0
0.00	1000.00	0.010508	0.0
0.25	840.00	0.410439	0.1
0.49	710.00	2.184325	0.6
0.76	590.00	6.884471	1.8
1.00	500.00	14.433758	3.8
1.25	420.00	26.130814	6.9
1.51	350.00	41.658652	11.0
1.74	300.00	55.974688	14.8
2.00	250.00	72.049905	19.1
2.25	210.00	84.555716	22.4
2.50	177.00	93.017828	24.6
2.75	149.00	97.783023	25.9
3.00	125.00	99.724424	26.4
3.25	105.00	100	26.5
3.51	88.00	100	26.5
3.76	74.00	100	26.5
3.99	63.00	100	26.5
4.24	53.00	100	26.5
4.51	44.00	100	26.5
4.76	37.00	100	26.5
5.01	31.00	100	26.5
6.00	15.60	100	26.5
6.64	10.00	100	26.5
7.00	7.80	100	26.5
8.00	3.90	100	26.5
8.97	2.00	100	26.5
9.99	0.98	100	26.5
10.48	0.70	100	26.5
10.99	0.49	100	26.5
12.02	0.24	100	26.5
13.02	0.12	100	26.5
14.02	0.06	100	26.5
14.29	0.05	100	26.5
	Total weight:		26.5

	mm	phi	Cum wt (g)	Int wt (g)	Int wt%	Cum % finer	Modes	
1	2.0000	-1.00	0.000000	0.000000	0.000000	100.000000		
2	1.6800	-0.75	0.000000	0.000000	0.000000	100.000000		
3	1.4100	-0.50	0.000000	0.000000	0.000000	100.000000		
4	1.1900	-0.25	0.000000	0.000000	0.000000	100.000000		
5	1.0000	0.00	0.010508	0.010508	0.010508	99.989492		8
6	0.8400	0.25	0.410439	0.399931	0.399931	99.589561		
7	0.7100	0.49	2.184325	1.773886	1.773886	97.815675		
8	0.5900	0.76	6.884471	4.700146	4.700146	93.115529		
9	0.5000	1.00	14.433758	7.549287	7.549287	85.566242		
10	0.4200	1.25	26.130814	11.697056	11.697056	73.869186		
11	0.3500	1.51	41.658652	15.527838	15.527838	58.341348	mode at 1.383056	
12	0.3000	1.74	55.974688	14.316036	14.316036	44.025312		
13	0.2500	2.00	72.049905	16.075217	16.075217	27.950095	mode at 1.868483	
14	0.2100	2.25	84.555716	12.505811	12.505811	15.444284		
15	0.1770	2.50	93.017828	8.462112	8.462112	6.982172		
16	0.1490	2.75	97.783023	4.765195	4.765195	2.216977		
17	0.1250	3.00	99.724424	1.941401	1.941401	0.275576		
18	0.1050	3.25	100.000000	0.275576	0.275576	0.000000		
19	0.0880	3.51	100.000000	0.000000	0.000000	0.000000		
20	0.0740	3.76	100.000000	0.000000	0.000000	0.000000		
21	0.0630	3.99	100.000000	0.000000	0.000000	0.000000		
22	0.0530	4.24	100.000000	0.000000	0.000000	0.000000		
23	0.0440	4.51	100.000000	0.000000	0.000000	0.000000		
24	0.0370	4.76	100.000000	0.000000	0.000000	0.000000		
25	0.0310	5.01	100.000000	0.000000	0.000000	0.000000		
26	0.0156	6.00	100.000000	0.000000	0.000000	0.000000		
27	0.0100	6.64	100.000000	0.000000	0.000000	0.000000		
28	0.0078	7.00	100.000000	0.000000	0.000000	0.000000		
29	0.0039	8.00	100.000000	0.000000	0.000000	0.000000		
30	0.0020	8.97	100.000000	0.000000	0.000000	0.000000		
31	0.0010	9.99	100.000000	0.000000	0.000000	0.000000		
32	0.0007	10.48	100.000000	0.000000	0.000000	0.000000		
33	0.0005	10.99	100.000000	0.000000	0.000000	0.000000		
34	0.0002	12.02	100.000000	0.000000	0.000000	0.000000		
35	0.0001	13.02	100.000000	0.000000	0.000000	0.000000		
36	0.0001	14.02	100.000000	0.000000	0.000000	0.000000		
37	0.0001	14.29	100.000000	0.000000	0.000000	0.000000		
		Sums:		100.00	100.00			

Column: 20
Sample ID: 2014-11-27sl

Folks' Graphic Statistics

	Mean (Mz)	Sorting (σI)	Skewness (SkI)	Kurtosis (KG)	Mean *mm*
phi	1.639	0.597	-0.014	0.959	0.321

Grainsize Statistics
Percentiles

Percentile	*phi*	*mm*
5	0.65	0.635
16	1.03	0.488
25	1.23	0.427
50	1.64	0.320
75	2.06	0.240
84	2.24	0.212
95	2.60	0.165

Table II.20*: Results summary for sample 20: Low intertidal zone, northern transect, Northern Ngarunui Beach. Sample collected on the 27th of November, 2014.*

Column: 21 **Density:** 2650
Volume: 0.010
Sample ID: 2014-11-27nl

Malvern data Phi	Malvern data Micron	Vol %	Equivalent Cum wt (g)
-1.00	2000.00	0	0.0
-0.75	1680.00	0.123016	0.0
-0.50	1410.00	0.421423	0.1
-0.25	1190.00	0.888245	0.2
0.00	1000.00	1.669087	0.4
0.25	840.00	3.063108	0.8
0.49	710.00	5.531074	1.5
0.76	590.00	10.428166	2.8
1.00	500.00	17.496478	4.6
1.25	420.00	28.109008	7.4
1.51	350.00	42.232343	11.2
1.74	300.00	55.499718	14.7
2.00	250.00	70.821002	18.8
2.25	210.00	83.187453	22.0
2.50	177.00	91.932445	24.4
2.75	149.00	97.157263	25.7
3.00	125.00	99.521125	26.4
3.25	105.00	99.993029	26.5
3.51	88.00	100	26.5
3.76	74.00	100	26.5
3.99	63.00	100	26.5
4.24	53.00	100	26.5
4.51	44.00	100	26.5
4.76	37.00	100	26.5
5.01	31.00	100	26.5
6.00	15.60	100	26.5
6.64	10.00	100	26.5
7.00	7.80	100	26.5
8.00	3.90	100	26.5
8.97	2.00	100	26.5
9.99	0.98	100	26.5
10.48	0.70	100	26.5
10.99	0.49	100	26.5
12.02	0.24	100	26.5
13.02	0.12	100	26.5
14.02	0.06	100	26.5
14.29	0.05	100	26.5
	Total weight:		26.5

	mm	phi	Cum wt (g)	Int wt (g)	Int wt%	Cum % finer	Modes
1	2.0000	-1.00	0.000000	0.000000	0.000000	100.000000	
2	1.6800	-0.75	0.123016	0.123016	0.123016	99.876984	
3	1.4100	-0.50	0.421423	0.298407	0.298407	99.578577	
4	1.1900	-0.25	0.888245	0.466822	0.466822	99.111755	
5	1.0000	0.00	1.669087	0.780842	0.780842	98.330913	8
6	0.8400	0.25	3.063108	1.394021	1.394021	96.936892	
7	0.7100	0.49	5.531074	2.467966	2.467966	94.468926	
8	0.5900	0.76	10.428166	4.897092	4.897092	89.571834	
9	0.5000	1.00	17.496478	7.068312	7.068312	82.503522	
10	0.4200	1.25	28.109008	10.612530	10.612530	71.890992	
11	0.3500	1.51	42.232343	14.123335	14.123335	57.767657	mode at 1.383056
12	0.3000	1.74	55.499718	13.267375	13.267375	44.500282	
13	0.2500	2.00	70.821002	15.321284	15.321284	29.178998	mode at 1.868483
14	0.2100	2.25	83.187453	12.366451	12.366451	16.812547	
15	0.1770	2.50	91.932445	8.744992	8.744992	8.067555	
16	0.1490	2.75	97.157263	5.224818	5.224818	2.842737	
17	0.1250	3.00	99.521125	2.363862	2.363862	0.478875	
18	0.1050	3.25	99.993029	0.471904	0.471904	0.006971	
19	0.0880	3.51	100.000000	0.006971	0.006971	0.000000	
20	0.0740	3.76	100.000000	0.000000	0.000000	0.000000	
21	0.0630	3.99	100.000000	0.000000	0.000000	0.000000	
22	0.0530	4.24	100.000000	0.000000	0.000000	0.000000	
23	0.0440	4.51	100.000000	0.000000	0.000000	0.000000	
24	0.0370	4.76	100.000000	0.000000	0.000000	0.000000	
25	0.0310	5.01	100.000000	0.000000	0.000000	0.000000	
26	0.0156	6.00	100.000000	0.000000	0.000000	0.000000	
27	0.0100	6.64	100.000000	0.000000	0.000000	0.000000	
28	0.0078	7.00	100.000000	0.000000	0.000000	0.000000	
29	0.0039	8.00	100.000000	0.000000	0.000000	0.000000	
30	0.0020	8.97	100.000000	0.000000	0.000000	0.000000	
31	0.0010	9.99	100.000000	0.000000	0.000000	0.000000	
32	0.0007	10.48	100.000000	0.000000	0.000000	0.000000	
33	0.0005	10.99	100.000000	0.000000	0.000000	0.000000	
34	0.0002	12.02	100.000000	0.000000	0.000000	0.000000	
35	0.0001	13.02	100.000000	0.000000	0.000000	0.000000	
36	0.0001	14.02	100.000000	0.000000	0.000000	0.000000	
37	0.0001	14.29	100.000000	0.000000	0.000000	0.000000	
		Sums:		100.00	100.00		

Grainsize Statistics
Percentiles

	phi	*mm*
5	0.44	0.736
16	0.95	0.518
25	1.18	0.442
50	1.64	0.320
75	2.09	0.236
84	2.27	0.207
95	2.64	0.160

Column: 21
Sample ID: 2014-11-27nl

Folks' Graphic Statistics

	Mean (Mz)	Sorting (σI)	Skewness (SkI)	Kurtosis (KG)	Mean *mm*
phi	1.623	0.665	-0.071	0.995	0.325

Table II.21: *Results summary for sample 21: Mid intertidal zone, mid transect, Northern Ngarunui Beach. Sample collected on the 27th of November, 2014.*

Column: 22 **Density:** 2650
Volume: 0.010
Sample ID: 2014-11-27mm

Malvern data Phi	Malvern data Micron	Vol %	Equivalent Cum wt (g)
-1.00	2000.00	0	0.0
-0.75	1680.00	0	0.0
-0.50	1410.00	0	0.0
-0.25	1190.00	0	0.0
0.00	1000.00	0	0.0
0.25	840.00	0.01447	0.0
0.49	710.00	0.406391	0.1
0.76	590.00	2.540537	0.7
1.00	500.00	7.405641	2.0
1.25	420.00	16.984545	4.5
1.51	350.00	32.186871	8.5
1.74	300.00	47.941461	12.7
2.00	250.00	66.947763	17.7
2.25	210.00	82.209273	21.8
2.50	177.00	92.4004	24.5
2.75	149.00	97.810262	25.9
3.00	125.00	99.767394	26.4
3.25	105.00	100	26.5
3.51	88.00	100	26.5
3.76	74.00	100	26.5
3.99	63.00	100	26.5
4.24	53.00	100	26.5
4.51	44.00	100	26.5
4.76	37.00	100	26.5
5.01	31.00	100	26.5
6.00	15.60	100	26.5
6.64	10.00	100	26.5
7.00	7.80	100	26.5
8.00	3.90	100	26.5
8.97	2.00	100	26.5
9.99	0.98	100	26.5
10.48	0.70	100	26.5
10.99	0.49	100	26.5
12.02	0.24	100	26.5
13.02	0.12	100	26.5
14.02	0.06	100	26.5
14.29	0.05	100	26.5
		Total weight:	26.5

	mm	phi	Cum wt (g)	Int wt (g)	Int wt%	Cum % finer	Modes	
1	2.0000	-1.00	0.000000	0.000000	0.000000	100.000000		
2	1.6800	-0.75	0.000000	0.000000	0.000000	100.000000		
3	1.4100	-0.50	0.000000	0.000000	0.000000	100.000000		
4	1.1900	-0.25	0.000000	0.000000	0.000000	100.000000		
5	1.0000	0.00	0.000000	0.000000	0.000000	100.000000		8
6	0.8400	0.25	0.014470	0.014470	0.014470	99.985530		
7	0.7100	0.49	0.406391	0.391921	0.391921	99.593609		
8	0.5900	0.76	2.540537	2.134146	2.134146	97.459463		
9	0.5000	1.00	7.405641	4.865104	4.865104	92.594359		
10	0.4200	1.25	16.984545	9.578904	9.578904	83.015455		
11	0.3500	1.51	32.186871	15.202326	15.202326	67.813129		
12	0.3000	1.74	47.941461	15.754590	15.754590	52.058539		
13	0.2500	2.00	66.947763	19.006302	19.006302	33.052237	mode at 1.868483	
14	0.2100	2.25	82.209273	15.261510	15.261510	17.790727		
15	0.1770	2.50	92.400400	10.191127	10.191127	7.599600		
16	0.1490	2.75	97.810262	5.409862	5.409862	2.189738		
17	0.1250	3.00	99.767394	1.957132	1.957132	0.232606		
18	0.1050	3.25	100.000000	0.232606	0.232606	0.000000		
19	0.0880	3.51	100.000000	0.000000	0.000000	0.000000		
20	0.0740	3.76	100.000000	0.000000	0.000000	0.000000		
21	0.0630	3.99	100.000000	0.000000	0.000000	0.000000		
22	0.0530	4.24	100.000000	0.000000	0.000000	0.000000		
23	0.0440	4.51	100.000000	0.000000	0.000000	0.000000		
24	0.0370	4.76	100.000000	0.000000	0.000000	0.000000		
25	0.0310	5.01	100.000000	0.000000	0.000000	0.000000		
26	0.0156	6.00	100.000000	0.000000	0.000000	0.000000		
27	0.0100	6.64	100.000000	0.000000	0.000000	0.000000		
28	0.0078	7.00	100.000000	0.000000	0.000000	0.000000		
29	0.0039	8.00	100.000000	0.000000	0.000000	0.000000		
30	0.0020	8.97	100.000000	0.000000	0.000000	0.000000		
31	0.0010	9.99	100.000000	0.000000	0.000000	0.000000		
32	0.0007	10.48	100.000000	0.000000	0.000000	0.000000		
33	0.0005	10.99	100.000000	0.000000	0.000000	0.000000		
34	0.0002	12.02	100.000000	0.000000	0.000000	0.000000		
35	0.0001	13.02	100.000000	0.000000	0.000000	0.000000		
36	0.0001	14.02	100.000000	0.000000	0.000000	0.000000		
37	0.0001	14.29	100.000000	0.000000	0.000000	0.000000		
		Sums:		100.00	100.00			

Column: 22
Sample ID: 2014-11-27mm

Folks' Graphic Statistics

	Mean (Mz)	Sorting (σI)	Skewness (SkI)	Kurtosis (KG)	Mean *mm*
phi	1.762	0.530	-0.014	0.958	0.295

Grainsize Statistics
Percentiles

	phi	*mm*
5	0.88	0.543
16	1.23	0.428
25	1.39	0.382
50	1.77	0.294
75	2.13	0.228
84	2.29	0.204
95	2.62	0.163

Table II.22: *Results summary for sample 22: Mid intertidal zone, eastern transect, Wainamu Beach. Sample collected on the 15th of July, 2014.*

Column: 23 **Density:** 2650
Volume: 0.010
Sample ID: 2014-7-15me

Malvern data Phi	Malvern data Micron	Vol %	Equivalent Cum wt (g)
-1.00	2000.00	0	0.0
-0.75	1680.00	0	0.0
-0.50	1410.00	0	0.0
-0.25	1190.00	0	0.0
0.00	1000.00	0	0.0
0.25	840.00	0	0.0
0.49	710.00	0	0.0
0.76	590.00	0	0.0
1.00	500.00	0.449033	0.1
1.25	420.00	2.746483	0.7
1.51	350.00	8.995699	2.4
1.74	300.00	18.375554	4.9
2.00	250.00	34.026908	9.0
2.25	210.00	51.503774	13.6
2.50	177.00	67.931734	18.0
2.75	149.00	81.063781	21.5
3.00	125.00	89.66144	23.8
3.25	105.00	93.878619	24.9
3.51	88.00	95.309921	25.3
3.76	74.00	95.49162	25.3
3.99	63.00	95.489193	25.3
4.24	53.00	95.489193	25.3
4.51	44.00	95.495507	25.3
4.76	37.00	95.654615	25.3
5.01	31.00	96.060463	25.5
6.00	15.60	97.543281	25.8
6.64	10.00	98.029986	26.0
7.00	7.80	98.385217	26.1
8.00	3.90	99.514236	26.4
8.97	2.00	100	26.5
9.99	0.98	100	26.5
10.48	0.70	100	26.5
10.99	0.49	100	26.5
12.02	0.24	100	26.5
13.02	0.12	100	26.5
14.02	0.06	100	26.5
14.29	0.05	100	26.5

Total weight: 26.5

	mm	phi	Cum wt (g)	Int wt (g)	Int wt%	Cum % finer	Modes
1	2.0000	-1.00	0.000000	0.000000	0.000000	100.000000	
2	1.6800	-0.75	0.000000	0.000000	0.000000	100.000000	
3	1.4100	-0.50	0.000000	0.000000	0.000000	100.000000	
4	1.1900	-0.25	0.000000	0.000000	0.000000	100.000000	
5	1.0000	0.00	0.000000	0.000000	0.000000	100.000000	8
6	0.8400	0.25	0.000000	0.000000	0.000000	100.000000	
7	0.7100	0.49	0.000000	0.000000	0.000000	100.000000	
8	0.5900	0.76	0.000000	0.000000	0.000000	100.000000	
9	0.5000	1.00	0.449033	0.449033	0.449033	99.550967	
10	0.4200	1.25	2.746483	2.297450	2.297450	97.253517	
11	0.3500	1.51	8.995699	6.249216	6.249216	91.004301	
12	0.3000	1.74	18.375554	9.379855	9.379855	81.624446	
13	0.2500	2.00	34.026908	15.651354	15.651354	65.973092	
14	0.2100	2.25	51.503774	17.476866	17.476866	48.496226	mode at 2.125769
15	0.1770	2.50	67.931734	16.427960	16.427960	32.068266	
16	0.1490	2.75	81.063781	13.132047	13.132047	18.936219	
17	0.1250	3.00	89.661440	8.597659	8.597659	10.338560	
18	0.1050	3.25	93.878619	4.217179	4.217179	6.121381	
19	0.0880	3.51	95.309921	1.431302	1.431302	4.690079	
20	0.0740	3.76	95.491620	0.181699	0.181699	4.508380	
21	0.0630	3.99	95.489193	-0.002427	-0.002427	4.510807	
22	0.0530	4.24	95.489193	0.000000	0.000000	4.510807	
23	0.0440	4.51	95.495507	0.006314	0.006314	4.504493	
24	0.0370	4.76	95.654615	0.159108	0.159108	4.345385	
25	0.0310	5.01	96.060463	0.405848	0.405848	3.939537	
26	0.0156	6.00	97.543281	1.482818	1.482818	2.456719	mode at 5.506949
27	0.0100	6.64	98.029986	0.486705	0.486705	1.970014	
28	0.0078	7.00	98.385217	0.355231	0.355231	1.614783	
29	0.0039	8.00	99.514236	1.129019	1.129019	0.485764	mode at 7.50231
30	0.0020	8.97	100.000000	0.485764	0.485764	0.000000	
31	0.0010	9.99	100.000000	0.000000	0.000000	0.000000	
32	0.0007	10.48	100.000000	0.000000	0.000000	0.000000	
33	0.0005	10.99	100.000000	0.000000	0.000000	0.000000	
34	0.0002	12.02	100.000000	0.000000	0.000000	0.000000	
35	0.0001	13.02	100.000000	0.000000	0.000000	0.000000	
36	0.0001	14.02	100.000000	0.000000	0.000000	0.000000	
37	0.0001	14.29	100.000000	0.000000	0.000000	0.000000	
		Sums:		100.00	100.00		

Column: 23
Sample ID: 2014-7-15me

Folks' Graphic Statistics

	Mean (Mz)	Sorting (σI)	Skewness (SkI)	Kurtosis (KG)	Mean *mm*
phi	2.248	0.607	0.104	1.101	0.211

Grainsize Statistics
Percentiles

	phi	*mm*
5	1.35	0.393
16	1.68	0.312
25	1.85	0.278
50	2.23	0.213
75	2.63	0.161
84	2.83	0.140
95	3.45	0.091

Table II.23: *Results summary for sample 23: High intertidal zone, mid transect, Wainamu Beach. Sample collected on the 15th of July, 2014.*

Column: 24 **Density:** 2650
Volume: 0.010
Sample ID: 2014-7-15hm

Malvern data Phi	Malvern data Micron	Vol %	Equivalent Cum wt (g)
-1.00	2000.00	0	0.0
-0.75	1680.00	0	0.0
-0.50	1410.00	0	0.0
-0.25	1190.00	0	0.0
0.00	1000.00	0	0.0
0.25	840.00	0	0.0
0.49	710.00	0	0.0
0.76	590.00	0	0.0
1.00	500.00	0	0.0
1.25	420.00	0.534918	0.1
1.51	350.00	3.256301	0.9
1.74	300.00	8.79341	2.3
2.00	250.00	20.388711	5.4
2.25	210.00	36.238721	9.6
2.50	177.00	54.170673	14.4
2.75	149.00	71.475189	18.9
3.00	125.00	85.434754	22.6
3.25	105.00	94.264652	25.0
3.51	88.00	98.584016	26.1
3.76	74.00	99.913045	26.5
3.99	63.00	100	26.5
4.24	53.00	100	26.5
4.51	44.00	100	26.5
4.76	37.00	100	26.5
5.01	31.00	100	26.5
6.00	15.60	100	26.5
6.64	10.00	100	26.5
7.00	7.80	100	26.5
8.00	3.90	100	26.5
8.97	2.00	100	26.5
9.99	0.98	100	26.5
10.48	0.70	100	26.5
10.99	0.49	100	26.5
12.02	0.24	100	26.5
13.02	0.12	100	26.5
14.02	0.06	100	26.5
14.29	0.05	100	26.5
		Total weight:	26.5

	mm	phi	Cum wt (g)	Int wt (g)	Int wt%	Cum % finer	Modes	
1	2.0000	-1.00	0.000000	0.000000	0.000000	100.000000		
2	1.6800	-0.75	0.000000	0.000000	0.000000	100.000000		
3	1.4100	-0.50	0.000000	0.000000	0.000000	100.000000		
4	1.1900	-0.25	0.000000	0.000000	0.000000	100.000000		
5	1.0000	0.00	0.000000	0.000000	0.000000	100.000000		8
6	0.8400	0.25	0.000000	0.000000	0.000000	100.000000		
7	0.7100	0.49	0.000000	0.000000	0.000000	100.000000		
8	0.5900	0.76	0.000000	0.000000	0.000000	100.000000		
9	0.5000	1.00	0.000000	0.000000	0.000000	100.000000		
10	0.4200	1.25	0.534918	0.534918	0.534918	99.465082		
11	0.3500	1.51	3.256301	2.721383	2.721383	96.743699		
12	0.3000	1.74	8.793410	5.537109	5.537109	91.206590		
13	0.2500	2.00	20.388711	11.595301	11.595301	79.611289		
14	0.2100	2.25	36.238721	15.850010	15.850010	63.761279		
15	0.1770	2.50	54.170673	17.931952	17.931952	45.829327	mode at 2.374859	
16	0.1490	2.75	71.475189	17.304516	17.304516	28.524811		
17	0.1250	3.00	85.434754	13.959565	13.959565	14.565246		
18	0.1050	3.25	94.264652	8.829898	8.829898	5.735348		
19	0.0880	3.51	98.584016	4.319364	4.319364	1.415984		
20	0.0740	3.76	99.913045	1.329029	1.329029	0.086955		
21	0.0630	3.99	100.000000	0.086955	0.086955	0.000000		
22	0.0530	4.24	100.000000	0.000000	0.000000	0.000000		
23	0.0440	4.51	100.000000	0.000000	0.000000	0.000000		
24	0.0370	4.76	100.000000	0.000000	0.000000	0.000000		
25	0.0310	5.01	100.000000	0.000000	0.000000	0.000000		
26	0.0156	6.00	100.000000	0.000000	0.000000	0.000000		
27	0.0100	6.64	100.000000	0.000000	0.000000	0.000000		
28	0.0078	7.00	100.000000	0.000000	0.000000	0.000000		
29	0.0039	8.00	100.000000	0.000000	0.000000	0.000000		
30	0.0020	8.97	100.000000	0.000000	0.000000	0.000000		
31	0.0010	9.99	100.000000	0.000000	0.000000	0.000000		
32	0.0007	10.48	100.000000	0.000000	0.000000	0.000000		
33	0.0005	10.99	100.000000	0.000000	0.000000	0.000000		
34	0.0002	12.02	100.000000	0.000000	0.000000	0.000000		
35	0.0001	13.02	100.000000	0.000000	0.000000	0.000000		
36	0.0001	14.02	100.000000	0.000000	0.000000	0.000000		
37	0.0001	14.29	100.000000	0.000000	0.000000	0.000000		
		Sums:		100.00	100.00			

Grainsize Statistics
Percentiles

	phi	*mm*
5	1.58	0.333
16	1.90	0.268
25	2.07	0.238
50	2.44	0.184
75	2.81	0.143
84	2.97	0.127
95	3.29	0.102

Column: 24
Sample ID: 2014-7-15hm

Folks' Graphic Statistics

	Mean (Mz)	Sorting (σI)	Skewness (SkI)	Kurtosis (KG)	Mean *mm*
phi	2.438	0.528	-0.004	0.951	0.184

Table II.24: *Results summary for sample 24: Mid intertidal zone, mid transect, Wainamu Beach. Sample collected on the 15th of July, 2014.*

Column: 25 **Density:** 2650
Volume: 0.010
Sample ID: 2014-7-15mm

Malvern data Phi	Malvern data Micron	Vol %	Equivalent Cum wt (g)
-1.00	2000.00	0	0.0
-0.75	1680.00	0	0.0
-0.50	1410.00	0	0.0
-0.25	1190.00	0	0.0
0.00	1000.00	0	0.0
0.25	840.00	0	0.0
0.49	710.00	0	0.0
0.76	590.00	0	0.0
1.00	500.00	0.558563	0.1
1.25	420.00	3.067047	0.8
1.51	350.00	9.279611	2.5
1.74	300.00	18.144619	4.8
2.00	250.00	32.676292	8.7
2.25	210.00	49.152542	13.0
2.50	177.00	65.422471	17.3
2.75	149.00	79.592758	21.1
3.00	125.00	90.162784	23.9
3.25	105.00	96.437823	25.6
3.51	88.00	99.296994	26.3
3.76	74.00	99.987207	26.5
3.99	63.00	100	26.5
4.24	53.00	100	26.5
4.51	44.00	100	26.5
4.76	37.00	100	26.5
5.01	31.00	100	26.5
6.00	15.60	100	26.5
6.64	10.00	100	26.5
7.00	7.80	100	26.5
8.00	3.90	100	26.5
8.97	2.00	100	26.5
9.99	0.98	100	26.5
10.48	0.70	100	26.5
10.99	0.49	100	26.5
12.02	0.24	100	26.5
13.02	0.12	100	26.5
14.02	0.06	100	26.5
14.29	0.05	100	26.5
		Total weight:	26.5

	mm	phi	Cum wt (g)	Int wt (g)	Int wt%	Cum % finer	Modes
1	2.0000	-1.00	0.000000	0.000000	0.000000	100.000000	
2	1.6800	-0.75	0.000000	0.000000	0.000000	100.000000	
3	1.4100	-0.50	0.000000	0.000000	0.000000	100.000000	
4	1.1900	-0.25	0.000000	0.000000	0.000000	100.000000	
5	1.0000	0.00	0.000000	0.000000	0.000000	100.000000	8
6	0.8400	0.25	0.000000	0.000000	0.000000	100.000000	
7	0.7100	0.49	0.000000	0.000000	0.000000	100.000000	
8	0.5900	0.76	0.000000	0.000000	0.000000	100.000000	
9	0.5000	1.00	0.558563	0.558563	0.558563	99.441437	
10	0.4200	1.25	3.067047	2.508484	2.508484	96.932953	
11	0.3500	1.51	9.279611	6.212564	6.212564	90.720389	
12	0.3000	1.74	18.144619	8.865008	8.865008	81.855381	
13	0.2500	2.00	32.676292	14.531673	14.531673	67.323708	
14	0.2100	2.25	49.152542	16.476250	16.476250	50.847458	mode at 2.125769
15	0.1770	2.50	65.422471	16.269929	16.269929	34.577529	
16	0.1490	2.75	79.592758	14.170287	14.170287	20.407242	
17	0.1250	3.00	90.162784	10.570026	10.570026	9.837216	
18	0.1050	3.25	96.437823	6.275039	6.275039	3.562177	
19	0.0880	3.51	99.296994	2.859171	2.859171	0.703006	
20	0.0740	3.76	99.987207	0.690213	0.690213	0.012793	
21	0.0630	3.99	100.000000	0.012793	0.012793	0.000000	
22	0.0530	4.24	100.000000	0.000000	0.000000	0.000000	
23	0.0440	4.51	100.000000	0.000000	0.000000	0.000000	
24	0.0370	4.76	100.000000	0.000000	0.000000	0.000000	
25	0.0310	5.01	100.000000	0.000000	0.000000	0.000000	
26	0.0156	6.00	100.000000	0.000000	0.000000	0.000000	
27	0.0100	6.64	100.000000	0.000000	0.000000	0.000000	
28	0.0078	7.00	100.000000	0.000000	0.000000	0.000000	
29	0.0039	8.00	100.000000	0.000000	0.000000	0.000000	
30	0.0020	8.97	100.000000	0.000000	0.000000	0.000000	
31	0.0010	9.99	100.000000	0.000000	0.000000	0.000000	
32	0.0007	10.48	100.000000	0.000000	0.000000	0.000000	
33	0.0005	10.99	100.000000	0.000000	0.000000	0.000000	
34	0.0002	12.02	100.000000	0.000000	0.000000	0.000000	
35	0.0001	13.02	100.000000	0.000000	0.000000	0.000000	
36	0.0001	14.02	100.000000	0.000000	0.000000	0.000000	
37	0.0001	14.29	100.000000	0.000000	0.000000	0.000000	
	Sums:			100.00	100.00		

Grainsize Statistics
Percentiles

	phi	*mm*
5	1.33	0.397
16	1.68	0.311
25	1.86	0.275
50	2.26	0.208
75	2.67	0.158
84	2.85	0.138
95	3.19	0.109

Column: 25
Sample ID: 2014-7-15mm

Folks' Graphic Statistics

	Mean (Mz)	Sorting (σI)	Skewness (SkI)	Kurtosis (KG)	Mean *mm*
phi	2.267	0.574	0.002	0.947	0.208

Table II.25: *Results summary for sample 25: Mid intertidal zone, western transect, Wainamu Beach. Sample collected on the 15th of July, 2014.*

Column: 26 **Density:** 2650
Volume: 0.010
Sample ID: 2014-7-15mw

Malvern data Phi	Malvern data Micron	Vol %	Equivalent Cum wt (g)
-1.00	2000.00	0	0.0
-0.75	1680.00	0	0.0
-0.50	1410.00	0	0.0
-0.25	1190.00	0	0.0
0.00	1000.00	0	0.0
0.25	840.00	0	0.0
0.49	710.00	0	0.0
0.76	590.00	0	0.0
1.00	500.00	0.014142	0.0
1.25	420.00	0.370719	0.1
1.51	350.00	2.688653	0.7
1.74	300.00	7.562706	2.0
2.00	250.00	18.187398	4.8
2.25	210.00	33.25119	8.8
2.50	177.00	50.918346	13.5
2.75	149.00	68.610702	18.2
3.00	125.00	83.446334	22.1
3.25	105.00	93.219927	24.7
3.51	88.00	98.221	26.0
3.76	74.00	99.863072	26.5
3.99	63.00	100	26.5
4.24	53.00	100	26.5
4.51	44.00	100	26.5
4.76	37.00	100	26.5
5.01	31.00	100	26.5
6.00	15.60	100	26.5
6.64	10.00	100	26.5
7.00	7.80	100	26.5
8.00	3.90	100	26.5
8.97	2.00	100	26.5
9.99	0.98	100	26.5
10.48	0.70	100	26.5
10.99	0.49	100	26.5
12.02	0.24	100	26.5
13.02	0.12	100	26.5
14.02	0.06	100	26.5
14.29	0.05	100	26.5

Total weight: 26.5

	mm	phi	Cum wt (g)	Int wt (g)	Int wt%	Cum % finer	Modes	
1	2.0000	-1.00	0.000000	0.000000	0.000000	100.000000		
2	1.6800	-0.75	0.000000	0.000000	0.000000	100.000000		
3	1.4100	-0.50	0.000000	0.000000	0.000000	100.000000		
4	1.1900	-0.25	0.000000	0.000000	0.000000	100.000000		
5	1.0000	0.00	0.000000	0.000000	0.000000	100.000000		8
6	0.8400	0.25	0.000000	0.000000	0.000000	100.000000		
7	0.7100	0.49	0.000000	0.000000	0.000000	100.000000		
8	0.5900	0.76	0.000000	0.000000	0.000000	100.000000		
9	0.5000	1.00	0.014142	0.014142	0.014142	99.985858		
10	0.4200	1.25	0.370719	0.356577	0.356577	99.629281		
11	0.3500	1.51	2.688653	2.317934	2.317934	97.311347		
12	0.3000	1.74	7.562706	4.874053	4.874053	92.437294		
13	0.2500	2.00	18.187398	10.624692	10.624692	81.812602		
14	0.2100	2.25	33.251190	15.063792	15.063792	66.748810		
15	0.1770	2.50	50.918346	17.667156	17.667156	49.081654		
16	0.1490	2.75	68.610702	17.692356	17.692356	31.389298	mode at 2.622397	
17	0.1250	3.00	83.446334	14.835632	14.835632	16.553666		
18	0.1050	3.25	93.219927	9.773593	9.773593	6.780073		
19	0.0880	3.51	98.221000	5.001073	5.001073	1.779000		
20	0.0740	3.76	99.863072	1.642072	1.642072	0.136928		
21	0.0630	3.99	100.000000	0.136928	0.136928	0.000000		
22	0.0530	4.24	100.000000	0.000000	0.000000	0.000000		
23	0.0440	4.51	100.000000	0.000000	0.000000	0.000000		
24	0.0370	4.76	100.000000	0.000000	0.000000	0.000000		
25	0.0310	5.01	100.000000	0.000000	0.000000	0.000000		
26	0.0156	6.00	100.000000	0.000000	0.000000	0.000000		
27	0.0100	6.64	100.000000	0.000000	0.000000	0.000000		
28	0.0078	7.00	100.000000	0.000000	0.000000	0.000000		
29	0.0039	8.00	100.000000	0.000000	0.000000	0.000000		
30	0.0020	8.97	100.000000	0.000000	0.000000	0.000000		
31	0.0010	9.99	100.000000	0.000000	0.000000	0.000000		
32	0.0007	10.48	100.000000	0.000000	0.000000	0.000000		
33	0.0005	10.99	100.000000	0.000000	0.000000	0.000000		
34	0.0002	12.02	100.000000	0.000000	0.000000	0.000000		
35	0.0001	13.02	100.000000	0.000000	0.000000	0.000000		
36	0.0001	14.02	100.000000	0.000000	0.000000	0.000000		
37	0.0001	14.29	100.000000	0.000000	0.000000	0.000000		
		Sums:		100.00	100.00			

Grainsize Statistics
Percentiles

	phi	*mm*
5	1.62	0.325
16	1.95	0.260
25	2.11	0.231
50	2.49	0.179
75	2.86	0.138
84	3.01	0.124
95	3.34	0.099

Column: 26
Sample ID: 2014-7-15mw

Folks' Graphic Statistics

	Mean (Mz)	Sorting (σI)	Skewness (SkI)	Kurtosis (KG)	Mean *mm*
phi	2.482	0.528	-0.007	0.951	0.179

Table II.26: *Results summary for sample 26: Low intertidal zone, mid transect, Wainamu Beach. Sample collected on the 15th of July, 2014.*

Column:	27	**Density:**	2650
		Volume:	0.010
Sample ID:	2014-7-15lm		

Malvern data Phi	Malvern data Micron	Vol %	Equivalent Cum wt (g)
-1.00	2000.00	0	0.0
-0.75	1680.00	0	0.0
-0.50	1410.00	0	0.0
-0.25	1190.00	0	0.0
0.00	1000.00	0	0.0
0.25	840.00	0	0.0
0.49	710.00	0	0.0
0.76	590.00	0	0.0
1.00	500.00	0.55662	0.1
1.25	420.00	3.213788	0.9
1.51	350.00	9.769716	2.6
1.74	300.00	19.021053	5.0
2.00	250.00	33.978321	9.0
2.25	210.00	50.679121	13.4
2.50	177.00	66.914522	17.7
2.75	149.00	80.81838	21.4
3.00	125.00	90.988918	24.1
3.25	105.00	96.875397	25.7
3.51	88.00	99.452293	26.4
3.76	74.00	100	26.5
3.99	63.00	100	26.5
4.24	53.00	100	26.5
4.51	44.00	100	26.5
4.76	37.00	100	26.5
5.01	31.00	100	26.5
6.00	15.60	100	26.5
6.64	10.00	100	26.5
7.00	7.80	100	26.5
8.00	3.90	100	26.5
8.97	2.00	100	26.5
9.99	0.98	100	26.5
10.48	0.70	100	26.5
10.99	0.49	100	26.5
12.02	0.24	100	26.5
13.02	0.12	100	26.5
14.02	0.06	100	26.5
14.29	0.05	100	26.5
		Total weight:	26.5

	mm	phi	Cum wt (g)	Int wt (g)	Int wt%	Cum % finer	Modes
1	2.0000	-1.00	0.000000	0.000000	0.000000	100.000000	
2	1.6800	-0.75	0.000000	0.000000	0.000000	100.000000	
3	1.4100	-0.50	0.000000	0.000000	0.000000	100.000000	
4	1.1900	-0.25	0.000000	0.000000	0.000000	100.000000	
5	1.0000	0.00	0.000000	0.000000	0.000000	100.000000	8
6	0.8400	0.25	0.000000	0.000000	0.000000	100.000000	
7	0.7100	0.49	0.000000	0.000000	0.000000	100.000000	
8	0.5900	0.76	0.000000	0.000000	0.000000	100.000000	
9	0.5000	1.00	0.556620	0.556620	0.556620	99.443380	
10	0.4200	1.25	3.213788	2.657168	2.657168	96.786212	
11	0.3500	1.51	9.769716	6.555928	6.555928	90.230284	
12	0.3000	1.74	19.021053	9.251337	9.251337	80.978947	
13	0.2500	2.00	33.978321	14.957268	14.957268	66.021679	
14	0.2100	2.25	50.679121	16.700800	16.700800	49.320879	mode at 2.125769
15	0.1770	2.50	66.914522	16.235401	16.235401	33.085478	
16	0.1490	2.75	80.818380	13.903858	13.903858	19.181620	
17	0.1250	3.00	90.988918	10.170538	10.170538	9.011082	
18	0.1050	3.25	96.875397	5.886479	5.886479	3.124603	
19	0.0880	3.51	99.452293	2.576896	2.576896	0.547707	
20	0.0740	3.76	100.000000	0.547707	0.547707	0.000000	
21	0.0630	3.99	100.000000	0.000000	0.000000	0.000000	
22	0.0530	4.24	100.000000	0.000000	0.000000	0.000000	
23	0.0440	4.51	100.000000	0.000000	0.000000	0.000000	
24	0.0370	4.76	100.000000	0.000000	0.000000	0.000000	
25	0.0310	5.01	100.000000	0.000000	0.000000	0.000000	
26	0.0156	6.00	100.000000	0.000000	0.000000	0.000000	
27	0.0100	6.64	100.000000	0.000000	0.000000	0.000000	
28	0.0078	7.00	100.000000	0.000000	0.000000	0.000000	
29	0.0039	8.00	100.000000	0.000000	0.000000	0.000000	
30	0.0020	8.97	100.000000	0.000000	0.000000	0.000000	
31	0.0010	9.99	100.000000	0.000000	0.000000	0.000000	
32	0.0007	10.48	100.000000	0.000000	0.000000	0.000000	
33	0.0005	10.99	100.000000	0.000000	0.000000	0.000000	
34	0.0002	12.02	100.000000	0.000000	0.000000	0.000000	
35	0.0001	13.02	100.000000	0.000000	0.000000	0.000000	
36	0.0001	14.02	100.000000	0.000000	0.000000	0.000000	
37	0.0001	14.29	100.000000	0.000000	0.000000	0.000000	
	Sums:			100.00	100.00		

Grainsize Statistics
Percentiles

	phi	*mm*
5	1.32	0.400
16	1.66	0.315
25	1.84	0.279
50	2.24	0.211
75	2.64	0.160
84	2.83	0.141
95	3.17	0.111

Column: 27
Sample ID: 2014-7-15lm

Folks' Graphic Statistics

	Mean (Mz)	Sorting (σI)	Skewness (SkI)	Kurtosis (KG)	Mean *mm*
phi	2.244	0.570	0.007	0.946	0.211

Table II.27: *Results summary for sample 27: High intertidal zone, eastern transect, Wainamu Beach. Sample collected on the 15th of July, 2014.*

Column: 28 **Density:** 2650
Volume: 0.010
Sample ID: 2014-7-15he

Malvern data Phi	Malvern data Micron	Vol %	Equivalent Cum wt (g)
-1.00	2000.00	0	0.0
-0.75	1680.00	0	0.0
-0.50	1410.00	0	0.0
-0.25	1190.00	0	0.0
0.00	1000.00	0	0.0
0.25	840.00	0	0.0
0.49	710.00	0	0.0
0.76	590.00	0	0.0
1.00	500.00	0.080216	0.0
1.25	420.00	1.539003	0.4
1.51	350.00	6.592199	1.7
1.74	300.00	15.167053	4.0
2.00	250.00	30.697223	8.1
2.25	210.00	49.187738	13.0
2.50	177.00	67.444786	17.9
2.75	149.00	82.636135	21.9
3.00	125.00	92.916642	24.6
3.25	105.00	98.075621	26.0
3.51	88.00	99.842785	26.5
3.76	74.00	100	26.5
3.99	63.00	100	26.5
4.24	53.00	100	26.5
4.51	44.00	100	26.5
4.76	37.00	100	26.5
5.01	31.00	100	26.5
6.00	15.60	100	26.5
6.64	10.00	100	26.5
7.00	7.80	100	26.5
8.00	3.90	100	26.5
8.97	2.00	100	26.5
9.99	0.98	100	26.5
10.48	0.70	100	26.5
10.99	0.49	100	26.5
12.02	0.24	100	26.5
13.02	0.12	100	26.5
14.02	0.06	100	26.5
14.29	0.05	100	26.5
		Total weight:	26.5

	mm	phi	Cum wt (g)	Int wt (g)	Int wt%	Cum % finer	Modes	
1	2.0000	-1.00	0.000000	0.000000	0.000000	100.000000		
2	1.6800	-0.75	0.000000	0.000000	0.000000	100.000000		
3	1.4100	-0.50	0.000000	0.000000	0.000000	100.000000		
4	1.1900	-0.25	0.000000	0.000000	0.000000	100.000000		
5	1.0000	0.00	0.000000	0.000000	0.000000	100.000000		8
6	0.8400	0.25	0.000000	0.000000	0.000000	100.000000		
7	0.7100	0.49	0.000000	0.000000	0.000000	100.000000		
8	0.5900	0.76	0.000000	0.000000	0.000000	100.000000		
9	0.5000	1.00	0.080216	0.080216	0.080216	99.919784		
10	0.4200	1.25	1.539003	1.458787	1.458787	98.460997		
11	0.3500	1.51	6.592199	5.053196	5.053196	93.407801		
12	0.3000	1.74	15.167053	8.574854	8.574854	84.832947		
13	0.2500	2.00	30.697223	15.530170	15.530170	69.302777		
14	0.2100	2.25	49.187738	18.490515	18.490515	50.812262	mode at 2.125769	
15	0.1770	2.50	67.444786	18.257048	18.257048	32.555214		
16	0.1490	2.75	82.636135	15.191349	15.191349	17.363865		
17	0.1250	3.00	92.916642	10.280507	10.280507	7.083358		
18	0.1050	3.25	98.075621	5.158979	5.158979	1.924379		
19	0.0880	3.51	99.842785	1.767164	1.767164	0.157215		
20	0.0740	3.76	100.000000	0.157215	0.157215	0.000000		
21	0.0630	3.99	100.000000	0.000000	0.000000	0.000000		
22	0.0530	4.24	100.000000	0.000000	0.000000	0.000000		
23	0.0440	4.51	100.000000	0.000000	0.000000	0.000000		
24	0.0370	4.76	100.000000	0.000000	0.000000	0.000000		
25	0.0310	5.01	100.000000	0.000000	0.000000	0.000000		
26	0.0156	6.00	100.000000	0.000000	0.000000	0.000000		
27	0.0100	6.64	100.000000	0.000000	0.000000	0.000000		
28	0.0078	7.00	100.000000	0.000000	0.000000	0.000000		
29	0.0039	8.00	100.000000	0.000000	0.000000	0.000000		
30	0.0020	8.97	100.000000	0.000000	0.000000	0.000000		
31	0.0010	9.99	100.000000	0.000000	0.000000	0.000000		
32	0.0007	10.48	100.000000	0.000000	0.000000	0.000000		
33	0.0005	10.99	100.000000	0.000000	0.000000	0.000000		
34	0.0002	12.02	100.000000	0.000000	0.000000	0.000000		
35	0.0001	13.02	100.000000	0.000000	0.000000	0.000000		
36	0.0001	14.02	100.000000	0.000000	0.000000	0.000000		
37	0.0001	14.29	100.000000	0.000000	0.000000	0.000000		
		Sums:		100.00	100.00			

Column: 28
Sample ID: 2014-7-15he

Folks' Graphic Statistics

	Mean (Mz)	Sorting (σI)	Skewness (SkI)	Kurtosis (KG)	Mean *mm*
phi	2.265	0.510	0.006	0.953	0.208

Grainsize Statistics
Percentiles

	phi	*mm*
5	1.43	0.371
16	1.75	0.297
25	1.90	0.267
50	2.26	0.208
75	2.62	0.162
84	2.78	0.146
95	3.10	0.117

Table II.28: *Results summary for sample 28: Low intertidal zone, western transect, Wainamu Beach. Sample collected on the 15th of July, 2014.*

Column: 29 **Density:** 2650
Volume: 0.010
Sample ID: 2014-7-15lw

Malvern data Phi	Malvern data Micron	Vol %	Equivalent Cum wt (g)
-1.00	2000.00	0	0.0
-0.75	1680.00	0	0.0
-0.50	1410.00	0	0.0
-0.25	1190.00	0	0.0
0.00	1000.00	0	0.0
0.25	840.00	0	0.0
0.49	710.00	0	0.0
0.76	590.00	0	0.0
1.00	500.00	0	0.0
1.25	420.00	0.500126	0.1
1.51	350.00	3.382616	0.9
1.74	300.00	9.374831	2.5
2.00	250.00	21.938875	5.8
2.25	210.00	38.900924	10.3
2.50	177.00	57.623301	15.3
2.75	149.00	75.008283	19.9
3.00	125.00	88.260504	23.4
3.25	105.00	95.969793	25.4
3.51	88.00	99.262909	26.3
3.76	74.00	99.987751	26.5
3.99	63.00	100	26.5
4.24	53.00	100	26.5
4.51	44.00	100	26.5
4.76	37.00	100	26.5
5.01	31.00	100	26.5
6.00	15.60	100	26.5
6.64	10.00	100	26.5
7.00	7.80	100	26.5
8.00	3.90	100	26.5
8.97	2.00	100	26.5
9.99	0.98	100	26.5
10.48	0.70	100	26.5
10.99	0.49	100	26.5
12.02	0.24	100	26.5
13.02	0.12	100	26.5
14.02	0.06	100	26.5
14.29	0.05	100	26.5

Total weight: 26.5

	mm	phi	Cum wt (g)	Int wt (g)	Int wt%	Cum % finer	Modes
1	2.0000	-1.00	0.000000	0.000000	0.000000	100.000000	
2	1.6800	-0.75	0.000000	0.000000	0.000000	100.000000	
3	1.4100	-0.50	0.000000	0.000000	0.000000	100.000000	
4	1.1900	-0.25	0.000000	0.000000	0.000000	100.000000	
5	1.0000	0.00	0.000000	0.000000	0.000000	100.000000	8
6	0.8400	0.25	0.000000	0.000000	0.000000	100.000000	
7	0.7100	0.49	0.000000	0.000000	0.000000	100.000000	
8	0.5900	0.76	0.000000	0.000000	0.000000	100.000000	
9	0.5000	1.00	0.000000	0.000000	0.000000	100.000000	
10	0.4200	1.25	0.500126	0.500126	0.500126	99.499874	
11	0.3500	1.51	3.382616	2.882490	2.882490	96.617384	
12	0.3000	1.74	9.374831	5.992215	5.992215	90.625169	
13	0.2500	2.00	21.938875	12.564044	12.564044	78.061125	
14	0.2100	2.25	38.900924	16.962049	16.962049	61.099076	
15	0.1770	2.50	57.623301	18.722377	18.722377	42.376699	mode at 2.374859
16	0.1490	2.75	75.008283	17.384982	17.384982	24.991717	
17	0.1250	3.00	88.260504	13.252221	13.252221	11.739496	
18	0.1050	3.25	95.969793	7.709289	7.709289	4.030207	
19	0.0880	3.51	99.262909	3.293116	3.293116	0.737091	
20	0.0740	3.76	99.987751	0.724842	0.724842	0.012249	
21	0.0630	3.99	100.000000	0.012249	0.012249	0.000000	
22	0.0530	4.24	100.000000	0.000000	0.000000	0.000000	
23	0.0440	4.51	100.000000	0.000000	0.000000	0.000000	
24	0.0370	4.76	100.000000	0.000000	0.000000	0.000000	
25	0.0310	5.01	100.000000	0.000000	0.000000	0.000000	
26	0.0156	6.00	100.000000	0.000000	0.000000	0.000000	
27	0.0100	6.64	100.000000	0.000000	0.000000	0.000000	
28	0.0078	7.00	100.000000	0.000000	0.000000	0.000000	
29	0.0039	8.00	100.000000	0.000000	0.000000	0.000000	
30	0.0020	8.97	100.000000	0.000000	0.000000	0.000000	
31	0.0010	9.99	100.000000	0.000000	0.000000	0.000000	
32	0.0007	10.48	100.000000	0.000000	0.000000	0.000000	
33	0.0005	10.99	100.000000	0.000000	0.000000	0.000000	
34	0.0002	12.02	100.000000	0.000000	0.000000	0.000000	
35	0.0001	13.02	100.000000	0.000000	0.000000	0.000000	
36	0.0001	14.02	100.000000	0.000000	0.000000	0.000000	
37	0.0001	14.29	100.000000	0.000000	0.000000	0.000000	
	Sums:			100.00	100.00		

Grainsize Statistics
Percentiles

	phi	*mm*
5	1.57	0.336
16	1.88	0.273
25	2.05	0.242
50	2.40	0.190
75	2.75	0.149
84	2.92	0.132
95	3.22	0.107

Column: 29
Sample ID: 2014-7-15lw

Folks' Graphic Statistics

	Mean (Mz)	Sorting (σI)	Skewness (SkI)	Kurtosis (KG)	Mean *mm*
phi	2.397	0.510	-0.001	0.962	0.190

Table II.29: *Results summary for sample 29: Low intertidal zone, Transect 1, Southern Ngarunui Beach. Sample collected on the 10th of February, 2015.*

Column: 30 **Density:** 2650
Volume: 0.010
Sample ID: 2015-2-101L

Malvern data Phi	Malvern data Micron	Vol %	Equivalent Cum wt (g)
-1.00	2000.00	0	0.0
-0.75	1680.00	0	0.0
-0.50	1410.00	0	0.0
-0.25	1190.00	0	0.0
0.00	1000.00	0	0.0
0.25	840.00	0	0.0
0.49	710.00	0	0.0
0.76	590.00	0.028819	0.0
1.00	500.00	1.039256	0.3
1.25	420.00	5.020906	1.3
1.51	350.00	14.495618	3.8
1.74	300.00	27.327321	7.2
2.00	250.00	46.63615	12.4
2.25	210.00	65.833036	17.4
2.50	177.00	81.678364	21.6
2.75	149.00	92.445441	24.5
3.00	125.00	98.026052	26.0
3.25	105.00	99.845122	26.5
3.51	88.00	100	26.5
3.76	74.00	100	26.5
3.99	63.00	100	26.5
4.24	53.00	100	26.5
4.51	44.00	100	26.5
4.76	37.00	100	26.5
5.01	31.00	100	26.5
6.00	15.60	100	26.5
6.64	10.00	100	26.5
7.00	7.80	100	26.5
8.00	3.90	100	26.5
8.97	2.00	100	26.5
9.99	0.98	100	26.5
10.48	0.70	100	26.5
10.99	0.49	100	26.5
12.02	0.24	100	26.5
13.02	0.12	100	26.5
14.02	0.06	100	26.5
14.29	0.05	100	26.5
	Total weight:		26.5

	mm	phi	Cum wt (g)	Int wt (g)	Int wt%	Cum % finer	Modes	
1	2.0000	-1.00	0.000000	0.000000	0.000000	100.000000		
2	1.6800	-0.75	0.000000	0.000000	0.000000	100.000000		
3	1.4100	-0.50	0.000000	0.000000	0.000000	100.000000		
4	1.1900	-0.25	0.000000	0.000000	0.000000	100.000000		
5	1.0000	0.00	0.000000	0.000000	0.000000	100.000000		8
6	0.8400	0.25	0.000000	0.000000	0.000000	100.000000		
7	0.7100	0.49	0.000000	0.000000	0.000000	100.000000		
8	0.5900	0.76	0.028819	0.028819	0.028819	99.971181		
9	0.5000	1.00	1.039256	1.010437	1.010437	98.960744		
10	0.4200	1.25	5.020906	3.981650	3.981650	94.979094		
11	0.3500	1.51	14.495618	9.474712	9.474712	85.504382		
12	0.3000	1.74	27.327321	12.831703	12.831703	72.672679		
13	0.2500	2.00	46.636150	19.308829	19.308829	53.363850	mode at 1.868483	
14	0.2100	2.25	65.833036	19.196886	19.196886	34.166964		
15	0.1770	2.50	81.678364	15.845328	15.845328	18.321636		
16	0.1490	2.75	92.445441	10.767077	10.767077	7.554559		
17	0.1250	3.00	98.026052	5.580611	5.580611	1.973948		
18	0.1050	3.25	99.845122	1.819070	1.819070	0.154878		
19	0.0880	3.51	100.000000	0.154878	0.154878	0.000000		
20	0.0740	3.76	100.000000	0.000000	0.000000	0.000000		
21	0.0630	3.99	100.000000	0.000000	0.000000	0.000000		
22	0.0530	4.24	100.000000	0.000000	0.000000	0.000000		
23	0.0440	4.51	100.000000	0.000000	0.000000	0.000000		
24	0.0370	4.76	100.000000	0.000000	0.000000	0.000000		
25	0.0310	5.01	100.000000	0.000000	0.000000	0.000000		
26	0.0156	6.00	100.000000	0.000000	0.000000	0.000000		
27	0.0100	6.64	100.000000	0.000000	0.000000	0.000000		
28	0.0078	7.00	100.000000	0.000000	0.000000	0.000000		
29	0.0039	8.00	100.000000	0.000000	0.000000	0.000000		
30	0.0020	8.97	100.000000	0.000000	0.000000	0.000000		
31	0.0010	9.99	100.000000	0.000000	0.000000	0.000000		
32	0.0007	10.48	100.000000	0.000000	0.000000	0.000000		
33	0.0005	10.99	100.000000	0.000000	0.000000	0.000000		
34	0.0002	12.02	100.000000	0.000000	0.000000	0.000000		
35	0.0001	13.02	100.000000	0.000000	0.000000	0.000000		
36	0.0001	14.02	100.000000	0.000000	0.000000	0.000000		
37	0.0001	14.29	100.000000	0.000000	0.000000	0.000000		
	Sums:			100.00	100.00			

Column: 30
Sample ID: 2015-2-101L

Folks' Graphic Statistics

	Mean (Mz)	Sorting (σI)	Skewness (SkI)	Kurtosis (KG)	Mean *mm*
phi	2.045	0.497	0.010	0.947	0.242

Grainsize Statistics
Percentiles

	phi	***mm***
5	1.25	0.420
16	1.54	0.344
25	1.70	0.309
50	2.04	0.242
75	2.39	0.190
84	2.55	0.171
95	2.86	0.137

Table II.30: *Results summary for sample 30: Low intertidal zone, Transect 2, Southern Ngarunui Beach. Sample collected on the 10th of February, 2015.*

Column: 31 **Density:** 2650
Volume: 0.010
Sample ID: 2015-2-102L

Malvern data Phi	Malvern data Micron	Vol %	Equivalent Cum wt (g)
-1.00	2000.00	0	0.0
-0.75	1680.00	0	0.0
-0.50	1410.00	0	0.0
-0.25	1190.00	0	0.0
0.00	1000.00	0	0.0
0.25	840.00	0	0.0
0.49	710.00	0.183889	0.0
0.76	590.00	2.070706	0.5
1.00	500.00	6.954767	1.8
1.25	420.00	16.842167	4.5
1.51	350.00	32.463925	8.6
1.74	300.00	48.409634	12.8
2.00	250.00	67.325027	17.8
2.25	210.00	82.311259	21.8
2.50	177.00	92.282065	24.5
2.75	149.00	97.643066	25.9
3.00	125.00	99.686602	26.4
3.25	105.00	100	26.5
3.51	88.00	100	26.5
3.76	74.00	100	26.5
3.99	63.00	100	26.5
4.24	53.00	100	26.5
4.51	44.00	100	26.5
4.76	37.00	100	26.5
5.01	31.00	100	26.5
6.00	15.60	100	26.5
6.64	10.00	100	26.5
7.00	7.80	100	26.5
8.00	3.90	100	26.5
8.97	2.00	100	26.5
9.99	0.98	100	26.5
10.48	0.70	100	26.5
10.99	0.49	100	26.5
12.02	0.24	100	26.5
13.02	0.12	100	26.5
14.02	0.06	100	26.5
14.29	0.05	100	26.5
	Total weight:		26.5

	mm	phi	Cum wt (g)	Int wt (g)	Int wt%	Cum % finer	Modes
1	2.0000	-1.00	0.000000	0.000000	0.000000	100.000000	
2	1.6800	-0.75	0.000000	0.000000	0.000000	100.000000	
3	1.4100	-0.50	0.000000	0.000000	0.000000	100.000000	
4	1.1900	-0.25	0.000000	0.000000	0.000000	100.000000	
5	1.0000	0.00	0.000000	0.000000	0.000000	100.000000	8
6	0.8400	0.25	0.000000	0.000000	0.000000	100.000000	
7	0.7100	0.49	0.183889	0.183889	0.183889	99.816111	
8	0.5900	0.76	2.070706	1.886817	1.886817	97.929294	
9	0.5000	1.00	6.954767	4.884061	4.884061	93.045233	
10	0.4200	1.25	16.842167	9.887400	9.887400	83.157833	
11	0.3500	1.51	32.463925	15.621758	15.621758	67.536075	
12	0.3000	1.74	48.409634	15.945709	15.945709	51.590366	
13	0.2500	2.00	67.325027	18.915393	18.915393	32.674973	mode at 1.868483
14	0.2100	2.25	82.311259	14.986232	14.986232	17.688741	
15	0.1770	2.50	92.282065	9.970806	9.970806	7.717935	
16	0.1490	2.75	97.643066	5.361001	5.361001	2.356934	
17	0.1250	3.00	99.686602	2.043536	2.043536	0.313398	
18	0.1050	3.25	100.000000	0.313398	0.313398	0.000000	
19	0.0880	3.51	100.000000	0.000000	0.000000	0.000000	
20	0.0740	3.76	100.000000	0.000000	0.000000	0.000000	
21	0.0630	3.99	100.000000	0.000000	0.000000	0.000000	
22	0.0530	4.24	100.000000	0.000000	0.000000	0.000000	
23	0.0440	4.51	100.000000	0.000000	0.000000	0.000000	
24	0.0370	4.76	100.000000	0.000000	0.000000	0.000000	
25	0.0310	5.01	100.000000	0.000000	0.000000	0.000000	
26	0.0156	6.00	100.000000	0.000000	0.000000	0.000000	
27	0.0100	6.64	100.000000	0.000000	0.000000	0.000000	
28	0.0078	7.00	100.000000	0.000000	0.000000	0.000000	
29	0.0039	8.00	100.000000	0.000000	0.000000	0.000000	
30	0.0020	8.97	100.000000	0.000000	0.000000	0.000000	
31	0.0010	9.99	100.000000	0.000000	0.000000	0.000000	
32	0.0007	10.48	100.000000	0.000000	0.000000	0.000000	
33	0.0005	10.99	100.000000	0.000000	0.000000	0.000000	
34	0.0002	12.02	100.000000	0.000000	0.000000	0.000000	
35	0.0001	13.02	100.000000	0.000000	0.000000	0.000000	
36	0.0001	14.02	100.000000	0.000000	0.000000	0.000000	
37	0.0001	14.29	100.000000	0.000000	0.000000	0.000000	
		Sums:		100.00	100.00		

Grainsize Statistics
Percentiles

	phi	*mm*
5	0.90	0.534
16	1.23	0.426
25	1.39	0.382
50	1.76	0.295
75	2.13	0.229
84	2.29	0.204
95	2.62	0.162

Column: 31
Sample ID: 2015-2-102L

Folks' Graphic Statistics

	Mean (Mz)	Sorting (σI)	Skewness (SkI)	Kurtosis (KG)	Mean *mm*
phi	1.761	0.526	0.005	0.953	0.295

Table II.31: *Results summary for sample 31: High intertidal zone, Transect 4, Southern Ngarunui Beach. Sample collected on the 10th of February, 2015.*

Column: 32 **Density:** 2650
Volume: 0.010
Sample ID: 2015-2-104H

Malvern data Phi	Malvern data Micron	Vol %	Equivalent Cum wt (g)
-1.00	2000.00	0	0.0
-0.75	1680.00	0	0.0
-0.50	1410.00	0	0.0
-0.25	1190.00	0	0.0
0.00	1000.00	0	0.0
0.25	840.00	0	0.0
0.49	710.00	0	0.0
0.76	590.00	0.17844	0.0
1.00	500.00	1.765323	0.5
1.25	420.00	6.741471	1.8
1.51	350.00	17.341889	4.6
1.74	300.00	30.801786	8.2
2.00	250.00	50.150989	13.3
2.25	210.00	68.685733	18.2
2.50	177.00	83.531426	22.1
2.75	149.00	93.353405	24.7
3.00	125.00	98.312585	26.1
3.25	105.00	99.874451	26.5
3.51	88.00	100	26.5
3.76	74.00	100	26.5
3.99	63.00	100	26.5
4.24	53.00	100	26.5
4.51	44.00	100	26.5
4.76	37.00	100	26.5
5.01	31.00	100	26.5
6.00	15.60	100	26.5
6.64	10.00	100	26.5
7.00	7.80	100	26.5
8.00	3.90	100	26.5
8.97	2.00	100	26.5
9.99	0.98	100	26.5
10.48	0.70	100	26.5
10.99	0.49	100	26.5
12.02	0.24	100	26.5
13.02	0.12	100	26.5
14.02	0.06	100	26.5
14.29	0.05	100	26.5

Total weight: 26.5

	mm	phi	Cum wt (g)	Int wt (g)	Int wt%	Cum % finer	Modes	
1	2.0000	-1.00	0.000000	0.000000	0.000000	100.000000		
2	1.6800	-0.75	0.000000	0.000000	0.000000	100.000000		
3	1.4100	-0.50	0.000000	0.000000	0.000000	100.000000		
4	1.1900	-0.25	0.000000	0.000000	0.000000	100.000000		
5	1.0000	0.00	0.000000	0.000000	0.000000	100.000000		8
6	0.8400	0.25	0.000000	0.000000	0.000000	100.000000		
7	0.7100	0.49	0.000000	0.000000	0.000000	100.000000		
8	0.5900	0.76	0.178440	0.178440	0.178440	99.821560		
9	0.5000	1.00	1.765323	1.586883	1.586883	98.234677		
10	0.4200	1.25	6.741471	4.976148	4.976148	93.258529		
11	0.3500	1.51	17.341889	10.600418	10.600418	82.658111		
12	0.3000	1.74	30.801786	13.459897	13.459897	69.198214		
13	0.2500	2.00	50.150989	19.349203	19.349203	49.849011	mode at 1.868483	
14	0.2100	2.25	68.685733	18.534744	18.534744	31.314267		
15	0.1770	2.50	83.531426	14.845693	14.845693	16.468574		
16	0.1490	2.75	93.353405	9.821979	9.821979	6.646595		
17	0.1250	3.00	98.312585	4.959180	4.959180	1.687415		
18	0.1050	3.25	99.874451	1.561866	1.561866	0.125549		
19	0.0880	3.51	100.000000	0.125549	0.125549	0.000000		
20	0.0740	3.76	100.000000	0.000000	0.000000	0.000000		
21	0.0630	3.99	100.000000	0.000000	0.000000	0.000000		
22	0.0530	4.24	100.000000	0.000000	0.000000	0.000000		
23	0.0440	4.51	100.000000	0.000000	0.000000	0.000000		
24	0.0370	4.76	100.000000	0.000000	0.000000	0.000000		
25	0.0310	5.01	100.000000	0.000000	0.000000	0.000000		
26	0.0156	6.00	100.000000	0.000000	0.000000	0.000000		
27	0.0100	6.64	100.000000	0.000000	0.000000	0.000000		
28	0.0078	7.00	100.000000	0.000000	0.000000	0.000000		
29	0.0039	8.00	100.000000	0.000000	0.000000	0.000000		
30	0.0020	8.97	100.000000	0.000000	0.000000	0.000000		
31	0.0010	9.99	100.000000	0.000000	0.000000	0.000000		
32	0.0007	10.48	100.000000	0.000000	0.000000	0.000000		
33	0.0005	10.99	100.000000	0.000000	0.000000	0.000000		
34	0.0002	12.02	100.000000	0.000000	0.000000	0.000000		
35	0.0001	13.02	100.000000	0.000000	0.000000	0.000000		
36	0.0001	14.02	100.000000	0.000000	0.000000	0.000000		
37	0.0001	14.29	100.000000	0.000000	0.000000	0.000000		
		Sums:		100.00	100.00			

Grainsize Statistics
Percentiles

	phi	*mm*
5	1.16	0.446
16	1.48	0.358
25	1.64	0.321
50	2.00	0.250
75	2.36	0.195
84	2.51	0.176
95	2.83	0.141

Column: 32
Sample ID: 2015-2-104H

Folks' Graphic Statistics

	Mean (Mz)	Sorting (σI)	Skewness (SkI)	Kurtosis (KG)	Mean *mm*
phi	1.996	0.510	-0.003	0.955	0.251

Table II.32: *Results summary for sample 32: High intertidal zone, Transect 1, Southern Ngarunui Beach. Sample collected on the 10th of February, 2015.*

Column: 33 **Density:** 2650
Volume: 0.010
Sample ID: 2015-2-101H

Malvern data Phi	Malvern data Micron	Vol %	Equivalent Cum wt (g)
-1.00	2000.00	0	0.0
-0.75	1680.00	0	0.0
-0.50	1410.00	0	0.0
-0.25	1190.00	0	0.0
0.00	1000.00	0	0.0
0.25	840.00	0	0.0
0.49	710.00	0	0.0
0.76	590.00	0.050897	0.0
1.00	500.00	1.121224	0.3
1.25	420.00	5.067394	1.3
1.51	350.00	14.250913	3.8
1.74	300.00	26.645696	7.1
2.00	250.00	45.428952	12.0
2.25	210.00	64.379162	17.1
2.50	177.00	80.347013	21.3
2.75	149.00	91.51648	24.3
3.00	125.00	97.575221	25.9
3.25	105.00	99.741791	26.4
3.51	88.00	100	26.5
3.76	74.00	100	26.5
3.99	63.00	100	26.5
4.24	53.00	100	26.5
4.51	44.00	100	26.5
4.76	37.00	100	26.5
5.01	31.00	100	26.5
6.00	15.60	100	26.5
6.64	10.00	100	26.5
7.00	7.80	100	26.5
8.00	3.90	100	26.5
8.97	2.00	100	26.5
9.99	0.98	100	26.5
10.48	0.70	100	26.5
10.99	0.49	100	26.5
12.02	0.24	100	26.5
13.02	0.12	100	26.5
14.02	0.06	100	26.5
14.29	0.05	100	26.5
		Total weight:	26.5

	mm	phi	Cum wt (g)	Int wt (g)	Int wt%	Cum % finer	Modes	
1	2.0000	-1.00	0.000000	0.000000	0.000000	100.000000		
2	1.6800	-0.75	0.000000	0.000000	0.000000	100.000000		
3	1.4100	-0.50	0.000000	0.000000	0.000000	100.000000		
4	1.1900	-0.25	0.000000	0.000000	0.000000	100.000000		
5	1.0000	0.00	0.000000	0.000000	0.000000	100.000000		8
6	0.8400	0.25	0.000000	0.000000	0.000000	100.000000		
7	0.7100	0.49	0.000000	0.000000	0.000000	100.000000		
8	0.5900	0.76	0.050897	0.050897	0.050897	99.949103		
9	0.5000	1.00	1.121224	1.070327	1.070327	98.878776		
10	0.4200	1.25	5.067394	3.946170	3.946170	94.932606		
11	0.3500	1.51	14.250913	9.183519	9.183519	85.749087		
12	0.3000	1.74	26.645696	12.394783	12.394783	73.354304		
13	0.2500	2.00	45.428952	18.783256	18.783256	54.571048		
14	0.2100	2.25	64.379162	18.950210	18.950210	35.620838	mode at 2.125769	
15	0.1770	2.50	80.347013	15.967851	15.967851	19.652987		
16	0.1490	2.75	91.516480	11.169467	11.169467	8.483520		
17	0.1250	3.00	97.575221	6.058741	6.058741	2.424779		
18	0.1050	3.25	99.741791	2.166570	2.166570	0.258209		
19	0.0880	3.51	100.000000	0.258209	0.258209	0.000000		
20	0.0740	3.76	100.000000	0.000000	0.000000	0.000000		
21	0.0630	3.99	100.000000	0.000000	0.000000	0.000000		
22	0.0530	4.24	100.000000	0.000000	0.000000	0.000000		
23	0.0440	4.51	100.000000	0.000000	0.000000	0.000000		
24	0.0370	4.76	100.000000	0.000000	0.000000	0.000000		
25	0.0310	5.01	100.000000	0.000000	0.000000	0.000000		
26	0.0156	6.00	100.000000	0.000000	0.000000	0.000000		
27	0.0100	6.64	100.000000	0.000000	0.000000	0.000000		
28	0.0078	7.00	100.000000	0.000000	0.000000	0.000000		
29	0.0039	8.00	100.000000	0.000000	0.000000	0.000000		
30	0.0020	8.97	100.000000	0.000000	0.000000	0.000000		
31	0.0010	9.99	100.000000	0.000000	0.000000	0.000000		
32	0.0007	10.48	100.000000	0.000000	0.000000	0.000000		
33	0.0005	10.99	100.000000	0.000000	0.000000	0.000000		
34	0.0002	12.02	100.000000	0.000000	0.000000	0.000000		
35	0.0001	13.02	100.000000	0.000000	0.000000	0.000000		
36	0.0001	14.02	100.000000	0.000000	0.000000	0.000000		
37	0.0001	14.29	100.000000	0.000000	0.000000	0.000000		
	Sums:			100.00	100.00			

Column: 33
Sample ID: 2015-2-101H

Folks' Graphic Statistics

	Mean (Mz)	Sorting (σI)	Skewness (SkI)	Kurtosis (KG)	Mean *mm*
phi	2.062	0.508	0.007	0.952	0.239

Grainsize Statistics
Percentiles

	phi	*mm*
5	1.25	0.421
16	1.55	0.342
25	1.71	0.306
50	2.06	0.240
75	2.42	0.187
84	2.58	0.167
95	2.89	0.135

Table II.33: *Results summary for sample 33: High intertidal zone, Transect 2, Southern Ngarunui Beach. Sample collected on the 10th of February, 2015.*

Column: 34 **Density:** 2650
Volume: 0.010
Sample ID: 2015-2-102H

Malvern data Phi	Malvern data Micron	Vol %	Equivalent Cum wt (g)
-1.00	2000.00	0	0.0
-0.75	1680.00	0	0.0
-0.50	1410.00	0	0.0
-0.25	1190.00	0	0.0
0.00	1000.00	0	0.0
0.25	840.00	0	0.0
0.49	710.00	0	0.0
0.76	590.00	0	0.0
1.00	500.00	0.364581	0.1
1.25	420.00	2.717613	0.7
1.51	350.00	9.995628	2.6
1.74	300.00	21.583549	5.7
2.00	250.00	41.087324	10.9
2.25	210.00	61.958504	16.4
2.50	177.00	79.759289	21.1
2.75	149.00	91.833534	24.3
3.00	125.00	97.900212	25.9
3.25	105.00	99.798239	26.4
3.51	88.00	100	26.5
3.76	74.00	100	26.5
3.99	63.00	100	26.5
4.24	53.00	100	26.5
4.51	44.00	100	26.5
4.76	37.00	100	26.5
5.01	31.00	100	26.5
6.00	15.60	100	26.5
6.64	10.00	100	26.5
7.00	7.80	100	26.5
8.00	3.90	100	26.5
8.97	2.00	100	26.5
9.99	0.98	100	26.5
10.48	0.70	100	26.5
10.99	0.49	100	26.5
12.02	0.24	100	26.5
13.02	0.12	100	26.5
14.02	0.06	100	26.5
14.29	0.05	100	26.5
		Total weight:	26.5

	mm	phi	Cum wt (g)	Int wt (g)	Int wt%	Cum % finer	Modes
1	2.0000	-1.00	0.000000	0.000000	0.000000	100.000000	
2	1.6800	-0.75	0.000000	0.000000	0.000000	100.000000	
3	1.4100	-0.50	0.000000	0.000000	0.000000	100.000000	
4	1.1900	-0.25	0.000000	0.000000	0.000000	100.000000	
5	1.0000	0.00	0.000000	0.000000	0.000000	100.000000	8
6	0.8400	0.25	0.000000	0.000000	0.000000	100.000000	
7	0.7100	0.49	0.000000	0.000000	0.000000	100.000000	
8	0.5900	0.76	0.000000	0.000000	0.000000	100.000000	
9	0.5000	1.00	0.364581	0.364581	0.364581	99.635419	
10	0.4200	1.25	2.717613	2.353032	2.353032	97.282387	
11	0.3500	1.51	9.995628	7.278015	7.278015	90.004372	
12	0.3000	1.74	21.583549	11.587921	11.587921	78.416451	
13	0.2500	2.00	41.087324	19.503775	19.503775	58.912676	
14	0.2100	2.25	61.958504	20.871180	20.871180	38.041496	mode at 2.125769
15	0.1770	2.50	79.759289	17.800785	17.800785	20.240711	
16	0.1490	2.75	91.833534	12.074245	12.074245	8.166466	
17	0.1250	3.00	97.900212	6.066678	6.066678	2.099788	
18	0.1050	3.25	99.798239	1.898027	1.898027	0.201761	
19	0.0880	3.51	100.000000	0.201761	0.201761	0.000000	
20	0.0740	3.76	100.000000	0.000000	0.000000	0.000000	
21	0.0630	3.99	100.000000	0.000000	0.000000	0.000000	
22	0.0530	4.24	100.000000	0.000000	0.000000	0.000000	
23	0.0440	4.51	100.000000	0.000000	0.000000	0.000000	
24	0.0370	4.76	100.000000	0.000000	0.000000	0.000000	
25	0.0310	5.01	100.000000	0.000000	0.000000	0.000000	
26	0.0156	6.00	100.000000	0.000000	0.000000	0.000000	
27	0.0100	6.64	100.000000	0.000000	0.000000	0.000000	
28	0.0078	7.00	100.000000	0.000000	0.000000	0.000000	
29	0.0039	8.00	100.000000	0.000000	0.000000	0.000000	
30	0.0020	8.97	100.000000	0.000000	0.000000	0.000000	
31	0.0010	9.99	100.000000	0.000000	0.000000	0.000000	
32	0.0007	10.48	100.000000	0.000000	0.000000	0.000000	
33	0.0005	10.99	100.000000	0.000000	0.000000	0.000000	
34	0.0002	12.02	100.000000	0.000000	0.000000	0.000000	
35	0.0001	13.02	100.000000	0.000000	0.000000	0.000000	
36	0.0001	14.02	100.000000	0.000000	0.000000	0.000000	
37	0.0001	14.29	100.000000	0.000000	0.000000	0.000000	
	Sums:			100.00	100.00		

Column: 34
Sample ID: 2015-2-102H

Folks' Graphic Statistics

	Mean (Mz)	Sorting (σI)	Skewness (SkI)	Kurtosis (KG)	Mean *mm*
phi	2.108	0.473	0.000	0.975	0.232

Grainsize Statistics
Percentiles

	phi	*mm*
5	1.33	0.397
16	1.63	0.323
25	1.78	0.291
50	2.11	0.232
75	2.43	0.185
84	2.59	0.167
95	2.88	0.136

Table II.34: *Results summary for sample 34: High intertidal zone, Transect 3, Southern Ngarunui Beach. Sample collected on the 10th of February, 2015.*

Column: 35 **Density:** 2650
Volume: 0.010
Sample ID: 2015-2-103H

Malvern data Phi	Malvern data Micron	Vol %	Equivalent Cum wt (g)
-1.00	2000.00	0	0.0
-0.75	1680.00	0	0.0
-0.50	1410.00	0	0.0
-0.25	1190.00	0	0.0
0.00	1000.00	0	0.0
0.25	840.00	0	0.0
0.49	710.00	0	0.0
0.76	590.00	0.035155	0.0
1.00	500.00	0.890596	0.2
1.25	420.00	4.632855	1.2
1.51	350.00	14.286326	3.8
1.74	300.00	27.963209	7.4
2.00	250.00	48.820979	12.9
2.25	210.00	69.115516	18.3
2.50	177.00	84.900147	22.5
2.75	149.00	94.583839	25.1
3.00	125.00	98.866308	26.2
3.25	105.00	99.941333	26.5
3.51	88.00	100	26.5
3.76	74.00	100	26.5
3.99	63.00	100	26.5
4.24	53.00	100	26.5
4.51	44.00	100	26.5
4.76	37.00	100	26.5
5.01	31.00	100	26.5
6.00	15.60	100	26.5
6.64	10.00	100	26.5
7.00	7.80	100	26.5
8.00	3.90	100	26.5
8.97	2.00	100	26.5
9.99	0.98	100	26.5
10.48	0.70	100	26.5
10.99	0.49	100	26.5
12.02	0.24	100	26.5
13.02	0.12	100	26.5
14.02	0.06	100	26.5
14.29	0.05	100	26.5

Total weight: 26.5

	mm	phi	Cum wt (g)	Int wt (g)	Int wt%	Cum % finer	Modes	
1	2.0000	-1.00	0.000000	0.000000	0.000000	100.000000		
2	1.6800	-0.75	0.000000	0.000000	0.000000	100.000000		
3	1.4100	-0.50	0.000000	0.000000	0.000000	100.000000		
4	1.1900	-0.25	0.000000	0.000000	0.000000	100.000000		
5	1.0000	0.00	0.000000	0.000000	0.000000	100.000000		8
6	0.8400	0.25	0.000000	0.000000	0.000000	100.000000		
7	0.7100	0.49	0.000000	0.000000	0.000000	100.000000		
8	0.5900	0.76	0.035155	0.035155	0.035155	99.964845		
9	0.5000	1.00	0.890596	0.855441	0.855441	99.109404		
10	0.4200	1.25	4.632855	3.742259	3.742259	95.367145		
11	0.3500	1.51	14.286326	9.653471	9.653471	85.713674		
12	0.3000	1.74	27.963209	13.676883	13.676883	72.036791		
13	0.2500	2.00	48.820979	20.857770	20.857770	51.179021	mode at 1.868483	
14	0.2100	2.25	69.115516	20.294537	20.294537	30.884484		
15	0.1770	2.50	84.900147	15.784631	15.784631	15.099853		
16	0.1490	2.75	94.583839	9.683692	9.683692	5.416161		
17	0.1250	3.00	98.866308	4.282469	4.282469	1.133692		
18	0.1050	3.25	99.941333	1.075025	1.075025	0.058667		
19	0.0880	3.51	100.000000	0.058667	0.058667	0.000000		
20	0.0740	3.76	100.000000	0.000000	0.000000	0.000000		
21	0.0630	3.99	100.000000	0.000000	0.000000	0.000000		
22	0.0530	4.24	100.000000	0.000000	0.000000	0.000000		
23	0.0440	4.51	100.000000	0.000000	0.000000	0.000000		
24	0.0370	4.76	100.000000	0.000000	0.000000	0.000000		
25	0.0310	5.01	100.000000	0.000000	0.000000	0.000000		
26	0.0156	6.00	100.000000	0.000000	0.000000	0.000000		
27	0.0100	6.64	100.000000	0.000000	0.000000	0.000000		
28	0.0078	7.00	100.000000	0.000000	0.000000	0.000000		
29	0.0039	8.00	100.000000	0.000000	0.000000	0.000000		
30	0.0020	8.97	100.000000	0.000000	0.000000	0.000000		
31	0.0010	9.99	100.000000	0.000000	0.000000	0.000000		
32	0.0007	10.48	100.000000	0.000000	0.000000	0.000000		
33	0.0005	10.99	100.000000	0.000000	0.000000	0.000000		
34	0.0002	12.02	100.000000	0.000000	0.000000	0.000000		
35	0.0001	13.02	100.000000	0.000000	0.000000	0.000000		
36	0.0001	14.02	100.000000	0.000000	0.000000	0.000000		
37	0.0001	14.29	100.000000	0.000000	0.000000	0.000000		
	Sums:			100.00	100.00			

Column: 35
Sample ID: 2015-2-103H

Folks' Graphic Statistics

	Mean (Mz)	Sorting (σI)	Skewness (SkI)	Kurtosis (KG)	Mean *mm*
phi	2.014	0.464	0.000	0.945	0.248

Grainsize Statistics
Percentiles

	phi	*mm*
5	1.26	0.417
16	1.54	0.343
25	1.69	0.310
50	2.01	0.247
75	2.34	0.197
84	2.48	0.179
95	2.77	0.146

Table II.35: *Results summary for sample 35: Low intertidal zone, Transect 3, Southern Ngarunui Beach. Sample collected on the 10th of February, 2015.*

Column: 36 **Density:** 2650
Volume: 0.010
Sample ID: 2015-2-103L

Malvern data Phi	Malvern data Micron	Vol %	Equivalent Cum wt (g)
-1.00	2000.00	0	0.0
-0.75	1680.00	0	0.0
-0.50	1410.00	0	0.0
-0.25	1190.00	0	0.0
0.00	1000.00	0	0.0
0.25	840.00	0	0.0
0.49	710.00	0.28691	0.1
0.76	590.00	2.141326	0.6
1.00	500.00	6.515312	1.7
1.25	420.00	15.281902	4.0
1.51	350.00	29.4504	7.8
1.74	300.00	44.467398	11.8
2.00	250.00	63.164786	16.7
2.25	210.00	78.886458	20.9
2.50	177.00	90.066137	23.9
2.75	149.00	96.5825	25.6
3.00	125.00	99.387	26.3
3.25	105.00	99.965157	26.5
3.51	88.00	100	26.5
3.76	74.00	100	26.5
3.99	63.00	100	26.5
4.24	53.00	100	26.5
4.51	44.00	100	26.5
4.76	37.00	100	26.5
5.01	31.00	100	26.5
6.00	15.60	100	26.5
6.64	10.00	100	26.5
7.00	7.80	100	26.5
8.00	3.90	100	26.5
8.97	2.00	100	26.5
9.99	0.98	100	26.5
10.48	0.70	100	26.5
10.99	0.49	100	26.5
12.02	0.24	100	26.5
13.02	0.12	100	26.5
14.02	0.06	100	26.5
14.29	0.05	100	26.5
		Total weight:	26.5

	mm	phi	Cum wt (g)	Int wt (g)	Int wt%	Cum % finer	Modes
1	2.0000	-1.00	0.000000	0.000000	0.000000	100.000000	
2	1.6800	-0.75	0.000000	0.000000	0.000000	100.000000	
3	1.4100	-0.50	0.000000	0.000000	0.000000	100.000000	
4	1.1900	-0.25	0.000000	0.000000	0.000000	100.000000	
5	1.0000	0.00	0.000000	0.000000	0.000000	100.000000	8
6	0.8400	0.25	0.000000	0.000000	0.000000	100.000000	
7	0.7100	0.49	0.286910	0.286910	0.286910	99.713090	
8	0.5900	0.76	2.141326	1.854416	1.854416	97.858674	
9	0.5000	1.00	6.515312	4.373986	4.373986	93.484688	
10	0.4200	1.25	15.281902	8.766590	8.766590	84.718098	
11	0.3500	1.51	29.450400	14.168498	14.168498	70.549600	
12	0.3000	1.74	44.467398	15.016998	15.016998	55.532602	
13	0.2500	2.00	63.164786	18.697388	18.697388	36.835214	mode at 1.868483
14	0.2100	2.25	78.886458	15.721672	15.721672	21.113542	
15	0.1770	2.50	90.066137	11.179679	11.179679	9.933863	
16	0.1490	2.75	96.582500	6.516363	6.516363	3.417500	
17	0.1250	3.00	99.387000	2.804500	2.804500	0.613000	
18	0.1050	3.25	99.965157	0.578157	0.578157	0.034843	
19	0.0880	3.51	100.000000	0.034843	0.034843	0.000000	
20	0.0740	3.76	100.000000	0.000000	0.000000	0.000000	
21	0.0630	3.99	100.000000	0.000000	0.000000	0.000000	
22	0.0530	4.24	100.000000	0.000000	0.000000	0.000000	
23	0.0440	4.51	100.000000	0.000000	0.000000	0.000000	
24	0.0370	4.76	100.000000	0.000000	0.000000	0.000000	
25	0.0310	5.01	100.000000	0.000000	0.000000	0.000000	
26	0.0156	6.00	100.000000	0.000000	0.000000	0.000000	
27	0.0100	6.64	100.000000	0.000000	0.000000	0.000000	
28	0.0078	7.00	100.000000	0.000000	0.000000	0.000000	
29	0.0039	8.00	100.000000	0.000000	0.000000	0.000000	
30	0.0020	8.97	100.000000	0.000000	0.000000	0.000000	
31	0.0010	9.99	100.000000	0.000000	0.000000	0.000000	
32	0.0007	10.48	100.000000	0.000000	0.000000	0.000000	
33	0.0005	10.99	100.000000	0.000000	0.000000	0.000000	
34	0.0002	12.02	100.000000	0.000000	0.000000	0.000000	
35	0.0001	13.02	100.000000	0.000000	0.000000	0.000000	
36	0.0001	14.02	100.000000	0.000000	0.000000	0.000000	
37	0.0001	14.29	100.000000	0.000000	0.000000	0.000000	
		Sums:		100.00	100.00		

Grainsize Statistics
Percentiles

	phi	*mm*
5	0.92	0.530
16	1.26	0.416
25	1.43	0.371
50	1.81	0.284
75	2.19	0.219
84	2.36	0.194
95	2.69	0.155

Column: 36
Sample ID: 2015-2-103L

Folks' Graphic Statistics

	Mean (Mz)	Sorting (σI)	Skewness (SkI)	Kurtosis (KG)	Mean *mm*
phi	1.815	0.543	-0.008	0.957	0.284

Table II.36: *Results summary for sample 36: Mid intertidal zone, Transect 3, Southern Ngarunui Beach. Sample collected on the 10th of February, 2015.*

Column: 37 **Density:** 2650
Volume: 0.010
Sample ID: 2015-2-103M

Malvern data Phi	Malvern data Micron	Vol %	Equivalent Cum wt (g)
-1.00	2000.00	0	0.0
-0.75	1680.00	0	0.0
-0.50	1410.00	0	0.0
-0.25	1190.00	0	0.0
0.00	1000.00	0	0.0
0.25	840.00	0.09661	0.0
0.49	710.00	0.919338	0.2
0.76	590.00	4.300009	1.1
1.00	500.00	10.909786	2.9
1.25	420.00	22.496521	6.0
1.51	350.00	39.130248	10.4
1.74	300.00	55.019164	14.6
2.00	250.00	72.848285	19.3
2.25	210.00	86.184269	22.8
2.50	177.00	94.501429	25.0
2.75	149.00	98.585907	26.1
3.00	125.00	99.886909	26.5
3.25	105.00	100	26.5
3.51	88.00	100	26.5
3.76	74.00	100	26.5
3.99	63.00	100	26.5
4.24	53.00	100	26.5
4.51	44.00	100	26.5
4.76	37.00	100	26.5
5.01	31.00	100	26.5
6.00	15.60	100	26.5
6.64	10.00	100	26.5
7.00	7.80	100	26.5
8.00	3.90	100	26.5
8.97	2.00	100	26.5
9.99	0.98	100	26.5
10.48	0.70	100	26.5
10.99	0.49	100	26.5
12.02	0.24	100	26.5
13.02	0.12	100	26.5
14.02	0.06	100	26.5
14.29	0.05	100	26.5
		Total weight:	26.5

	mm	phi	Cum wt (g)	Int wt (g)	Int wt%	Cum % finer	Modes
1	2.0000	-1.00	0.000000	0.000000	0.000000	100.000000	
2	1.6800	-0.75	0.000000	0.000000	0.000000	100.000000	
3	1.4100	-0.50	0.000000	0.000000	0.000000	100.000000	
4	1.1900	-0.25	0.000000	0.000000	0.000000	100.000000	
5	1.0000	0.00	0.000000	0.000000	0.000000	100.000000	8
6	0.8400	0.25	0.096610	0.096610	0.096610	99.903390	
7	0.7100	0.49	0.919338	0.822728	0.822728	99.080662	
8	0.5900	0.76	4.300009	3.380671	3.380671	95.699991	
9	0.5000	1.00	10.909786	6.609777	6.609777	89.090214	
10	0.4200	1.25	22.496521	11.586735	11.586735	77.503479	
11	0.3500	1.51	39.130248	16.633727	16.633727	60.869752	mode at 1.383056
12	0.3000	1.74	55.019164	15.888916	15.888916	44.980836	
13	0.2500	2.00	72.848285	17.829121	17.829121	27.151715	mode at 1.868483
14	0.2100	2.25	86.184269	13.335984	13.335984	13.815731	
15	0.1770	2.50	94.501429	8.317160	8.317160	5.498571	
16	0.1490	2.75	98.585907	4.084478	4.084478	1.414093	
17	0.1250	3.00	99.886909	1.301002	1.301002	0.113091	
18	0.1050	3.25	100.000000	0.113091	0.113091	0.000000	
19	0.0880	3.51	100.000000	0.000000	0.000000	0.000000	
20	0.0740	3.76	100.000000	0.000000	0.000000	0.000000	
21	0.0630	3.99	100.000000	0.000000	0.000000	0.000000	
22	0.0530	4.24	100.000000	0.000000	0.000000	0.000000	
23	0.0440	4.51	100.000000	0.000000	0.000000	0.000000	
24	0.0370	4.76	100.000000	0.000000	0.000000	0.000000	
25	0.0310	5.01	100.000000	0.000000	0.000000	0.000000	
26	0.0156	6.00	100.000000	0.000000	0.000000	0.000000	
27	0.0100	6.64	100.000000	0.000000	0.000000	0.000000	
28	0.0078	7.00	100.000000	0.000000	0.000000	0.000000	
29	0.0039	8.00	100.000000	0.000000	0.000000	0.000000	
30	0.0020	8.97	100.000000	0.000000	0.000000	0.000000	
31	0.0010	9.99	100.000000	0.000000	0.000000	0.000000	
32	0.0007	10.48	100.000000	0.000000	0.000000	0.000000	
33	0.0005	10.99	100.000000	0.000000	0.000000	0.000000	
34	0.0002	12.02	100.000000	0.000000	0.000000	0.000000	
35	0.0001	13.02	100.000000	0.000000	0.000000	0.000000	
36	0.0001	14.02	100.000000	0.000000	0.000000	0.000000	
37	0.0001	14.29	100.000000	0.000000	0.000000	0.000000	
	Sums:			100.00	100.00		

Grainsize Statistics
Percentiles

	phi	*mm*
5	0.79	0.580
16	1.11	0.463
25	1.29	0.409
50	1.67	0.315
75	2.04	0.243
84	2.21	0.216
95	2.53	0.173

Column: 37
Sample ID: 2015-2-103M

Folks' Graphic Statistics

	Mean (Mz)	Sorting (σI)	Skewness (SkI)	Kurtosis (KG)	Mean *mm*
phi	1.663	0.539	-0.011	0.953	0.316

Table II.37: *Results summary for sample 37: Mid intertidal zone, Transect 1, Southern Ngarunui Beach..*
Sample collected on the 10th of February, 2015.

Column: 38 **Density:** 2650
Volume: 0.010
Sample ID: 2015-2-101M

Malvern data Phi	Malvern data Micron	Vol %	Equivalent Cum wt (g)
-1.00	2000.00	0	0.0
-0.75	1680.00	0	0.0
-0.50	1410.00	0	0.0
-0.25	1190.00	0	0.0
0.00	1000.00	0	0.0
0.25	840.00	0	0.0
0.49	710.00	0.457534	0.1
0.76	590.00	2.991194	0.8
1.00	500.00	8.595773	2.3
1.25	420.00	19.201994	5.1
1.51	350.00	35.336275	9.4
1.74	300.00	51.419498	13.6
2.00	250.00	70.099631	18.6
2.25	210.00	84.50385	22.4
2.50	177.00	93.7176	24.8
2.75	149.00	98.348573	26.1
3.00	125.00	99.862404	26.5
3.25	105.00	100	26.5
3.51	88.00	100	26.5
3.76	74.00	100	26.5
3.99	63.00	100	26.5
4.24	53.00	100	26.5
4.51	44.00	100	26.5
4.76	37.00	100	26.5
5.01	31.00	100	26.5
6.00	15.60	100	26.5
6.64	10.00	100	26.5
7.00	7.80	100	26.5
8.00	3.90	100	26.5
8.97	2.00	100	26.5
9.99	0.98	100	26.5
10.48	0.70	100	26.5
10.99	0.49	100	26.5
12.02	0.24	100	26.5
13.02	0.12	100	26.5
14.02	0.06	100	26.5
14.29	0.05	100	26.5

Total weight: 26.5

	mm	phi	Cum wt (g)	Int wt (g)	Int wt%	Cum % finer	Modes
1	2.0000	-1.00	0.000000	0.000000	0.000000	100.000000	
2	1.6800	-0.75	0.000000	0.000000	0.000000	100.000000	
3	1.4100	-0.50	0.000000	0.000000	0.000000	100.000000	
4	1.1900	-0.25	0.000000	0.000000	0.000000	100.000000	
5	1.0000	0.00	0.000000	0.000000	0.000000	100.000000	8
6	0.8400	0.25	0.000000	0.000000	0.000000	100.000000	
7	0.7100	0.49	0.457534	0.457534	0.457534	99.542466	
8	0.5900	0.76	2.991194	2.533660	2.533660	97.008806	
9	0.5000	1.00	8.595773	5.604579	5.604579	91.404227	
10	0.4200	1.25	19.201994	10.606221	10.606221	80.798006	
11	0.3500	1.51	35.336275	16.134281	16.134281	64.663725	mode at 1.383056
12	0.3000	1.74	51.419498	16.083223	16.083223	48.580502	
13	0.2500	2.00	70.099631	18.680133	18.680133	29.900369	mode at 1.868483
14	0.2100	2.25	84.503850	14.404219	14.404219	15.496150	
15	0.1770	2.50	93.717600	9.213750	9.213750	6.282400	
16	0.1490	2.75	98.348573	4.630973	4.630973	1.651427	
17	0.1250	3.00	99.862404	1.513831	1.513831	0.137596	
18	0.1050	3.25	100.000000	0.137596	0.137596	0.000000	
19	0.0880	3.51	100.000000	0.000000	0.000000	0.000000	
20	0.0740	3.76	100.000000	0.000000	0.000000	0.000000	
21	0.0630	3.99	100.000000	0.000000	0.000000	0.000000	
22	0.0530	4.24	100.000000	0.000000	0.000000	0.000000	
23	0.0440	4.51	100.000000	0.000000	0.000000	0.000000	
24	0.0370	4.76	100.000000	0.000000	0.000000	0.000000	
25	0.0310	5.01	100.000000	0.000000	0.000000	0.000000	
26	0.0156	6.00	100.000000	0.000000	0.000000	0.000000	
27	0.0100	6.64	100.000000	0.000000	0.000000	0.000000	
28	0.0078	7.00	100.000000	0.000000	0.000000	0.000000	
29	0.0039	8.00	100.000000	0.000000	0.000000	0.000000	
30	0.0020	8.97	100.000000	0.000000	0.000000	0.000000	
31	0.0010	9.99	100.000000	0.000000	0.000000	0.000000	
32	0.0007	10.48	100.000000	0.000000	0.000000	0.000000	
33	0.0005	10.99	100.000000	0.000000	0.000000	0.000000	
34	0.0002	12.02	100.000000	0.000000	0.000000	0.000000	
35	0.0001	13.02	100.000000	0.000000	0.000000	0.000000	
36	0.0001	14.02	100.000000	0.000000	0.000000	0.000000	
37	0.0001	14.29	100.000000	0.000000	0.000000	0.000000	
		Sums:		100.00	100.00		

Column: 38
Sample ID: 2015-2-101M

Folks' Graphic Statistics

	Mean (Mz)	Sorting (σI)	Skewness (SkI)	Kurtosis (KG)	Mean *mm*
phi	1.712	0.527	-0.014	0.953	0.305

Grainsize Statistics
Percentiles

	phi	*mm*
5	0.85	0.556
16	1.18	0.443
25	1.35	0.393
50	1.72	0.304
75	2.09	0.236
84	2.24	0.211
95	2.57	0.169

Table II.38: *Results summary for sample 38: Mid intertidal zone, Transect 2, Southern Ngarunui Beach. Sample collected on the 10th of February, 2015.*

Column: 39 **Density:** 2650
Volume: 0.010
Sample ID: 2015-2-102M

Malvern data Phi	Malvern data Micron	Vol %	Equivalent Cum wt (g)
-1.00	2000.00	0	0.0
-0.75	1680.00	0	0.0
-0.50	1410.00	0	0.0
-0.25	1190.00	0	0.0
0.00	1000.00	0	0.0
0.25	840.00	0	0.0
0.49	710.00	0.445589	0.1
0.76	590.00	3.042037	0.8
1.00	500.00	8.804854	2.3
1.25	420.00	19.662673	5.2
1.51	350.00	36.048653	9.6
1.74	300.00	52.234389	13.8
2.00	250.00	70.845268	18.8
2.25	210.00	85.034802	22.5
2.50	177.00	94.005187	24.9
2.75	149.00	98.453242	26.1
3.00	125.00	99.877233	26.5
3.25	105.00	100	26.5
3.51	88.00	100	26.5
3.76	74.00	100	26.5
3.99	63.00	100	26.5
4.24	53.00	100	26.5
4.51	44.00	100	26.5
4.76	37.00	100	26.5
5.01	31.00	100	26.5
6.00	15.60	100	26.5
6.64	10.00	100	26.5
7.00	7.80	100	26.5
8.00	3.90	100	26.5
8.97	2.00	100	26.5
9.99	0.98	100	26.5
10.48	0.70	100	26.5
10.99	0.49	100	26.5
12.02	0.24	100	26.5
13.02	0.12	100	26.5
14.02	0.06	100	26.5
14.29	0.05	100	26.5
		Total weight:	26.5

	mm	phi	Cum wt (g)	Int wt (g)	Int wt%	Cum % finer	Modes	
1	2.0000	-1.00	0.000000	0.000000	0.000000	100.000000		
2	1.6800	-0.75	0.000000	0.000000	0.000000	100.000000		
3	1.4100	-0.50	0.000000	0.000000	0.000000	100.000000		
4	1.1900	-0.25	0.000000	0.000000	0.000000	100.000000		
5	1.0000	0.00	0.000000	0.000000	0.000000	100.000000		8
6	0.8400	0.25	0.000000	0.000000	0.000000	100.000000		
7	0.7100	0.49	0.445589	0.445589	0.445589	99.554411		
8	0.5900	0.76	3.042037	2.596448	2.596448	96.957963		
9	0.5000	1.00	8.804854	5.762817	5.762817	91.195146		
10	0.4200	1.25	19.662673	10.857819	10.857819	80.337327		
11	0.3500	1.51	36.048653	16.385980	16.385980	63.951347	mode at 1.383056	
12	0.3000	1.74	52.234389	16.185736	16.185736	47.765611		
13	0.2500	2.00	70.845268	18.610879	18.610879	29.154732	mode at 1.868483	
14	0.2100	2.25	85.034802	14.189534	14.189534	14.965198		
15	0.1770	2.50	94.005187	8.970385	8.970385	5.994813		
16	0.1490	2.75	98.453242	4.448055	4.448055	1.546758		
17	0.1250	3.00	99.877233	1.423991	1.423991	0.122767		
18	0.1050	3.25	100.000000	0.122767	0.122767	0.000000		
19	0.0880	3.51	100.000000	0.000000	0.000000	0.000000		
20	0.0740	3.76	100.000000	0.000000	0.000000	0.000000		
21	0.0630	3.99	100.000000	0.000000	0.000000	0.000000		
22	0.0530	4.24	100.000000	0.000000	0.000000	0.000000		
23	0.0440	4.51	100.000000	0.000000	0.000000	0.000000		
24	0.0370	4.76	100.000000	0.000000	0.000000	0.000000		
25	0.0310	5.01	100.000000	0.000000	0.000000	0.000000		
26	0.0156	6.00	100.000000	0.000000	0.000000	0.000000		
27	0.0100	6.64	100.000000	0.000000	0.000000	0.000000		
28	0.0078	7.00	100.000000	0.000000	0.000000	0.000000		
29	0.0039	8.00	100.000000	0.000000	0.000000	0.000000		
30	0.0020	8.97	100.000000	0.000000	0.000000	0.000000		
31	0.0010	9.99	100.000000	0.000000	0.000000	0.000000		
32	0.0007	10.48	100.000000	0.000000	0.000000	0.000000		
33	0.0005	10.99	100.000000	0.000000	0.000000	0.000000		
34	0.0002	12.02	100.000000	0.000000	0.000000	0.000000		
35	0.0001	13.02	100.000000	0.000000	0.000000	0.000000		
36	0.0001	14.02	100.000000	0.000000	0.000000	0.000000		
37	0.0001	14.29	100.000000	0.000000	0.000000	0.000000		
	Sums:			100.00	100.00			

Column: 39
Sample ID: 2015-2-102M

Folks' Graphic Statistics

	Mean (Mz)	Sorting (σI)	Skewness (SkI)	Kurtosis (KG)	Mean ***mm***
phi	1.702	0.526	-0.011	0.952	0.307

Grainsize Statistics
Percentiles

	phi	***mm***
5	0.84	0.558
16	1.17	0.445
25	1.34	0.396
50	1.71	0.306
75	2.07	0.238
84	2.23	0.213
95	2.55	0.170

Table II.39: *Results summary for sample 39: Mid intertidal zone, Transect 4, Southern Ngarunui Beach. Sample collected on the 10th of February, 2015.*

Column: 40 **Density:** 2650
Volume: 0.010
Sample ID: 2015-2-104M

Malvern data Phi	Malvern data Micron	Vol %	Equivalent Cum wt (g)
-1.00	2000.00	0	0.0
-0.75	1680.00	0	0.0
-0.50	1410.00	0	0.0
-0.25	1190.00	0	0.0
0.00	1000.00	0	0.0
0.25	840.00	0.318695	0.1
0.49	710.00	2.124275	0.6
0.76	590.00	7.083353	1.9
1.00	500.00	15.06947	4.0
1.25	420.00	27.348973	7.2
1.51	350.00	43.432592	11.5
1.74	300.00	58.014983	15.4
2.00	250.00	74.047059	19.6
2.25	210.00	86.171808	22.8
2.50	177.00	94.083624	24.9
2.75	149.00	98.307938	26.1
3.00	125.00	99.842253	26.5
3.25	105.00	100	26.5
3.51	88.00	100	26.5
3.76	74.00	100	26.5
3.99	63.00	100	26.5
4.24	53.00	100	26.5
4.51	44.00	100	26.5
4.76	37.00	100	26.5
5.01	31.00	100	26.5
6.00	15.60	100	26.5
6.64	10.00	100	26.5
7.00	7.80	100	26.5
8.00	3.90	100	26.5
8.97	2.00	100	26.5
9.99	0.98	100	26.5
10.48	0.70	100	26.5
10.99	0.49	100	26.5
12.02	0.24	100	26.5
13.02	0.12	100	26.5
14.02	0.06	100	26.5
14.29	0.05	100	26.5
		Total weight:	26.5

	mm	phi	Cum wt (g)	Int wt (g)	Int wt%	Cum % finer	Modes	
1	2.0000	-1.00	0.000000	0.000000	0.000000	100.000000		
2	1.6800	-0.75	0.000000	0.000000	0.000000	100.000000		
3	1.4100	-0.50	0.000000	0.000000	0.000000	100.000000		
4	1.1900	-0.25	0.000000	0.000000	0.000000	100.000000		
5	1.0000	0.00	0.000000	0.000000	0.000000	100.000000		8
6	0.8400	0.25	0.318695	0.318695	0.318695	99.681305		
7	0.7100	0.49	2.124275	1.805580	1.805580	97.875725		
8	0.5900	0.76	7.083353	4.959078	4.959078	92.916647		
9	0.5000	1.00	15.069470	7.986117	7.986117	84.930530		
10	0.4200	1.25	27.348973	12.279503	12.279503	72.651027		
11	0.3500	1.51	43.432592	16.083619	16.083619	56.567408	mode at 1.383056	
12	0.3000	1.74	58.014983	14.582391	14.582391	41.985017		
13	0.2500	2.00	74.047059	16.032076	16.032076	25.952941	mode at 1.868483	
14	0.2100	2.25	86.171808	12.124749	12.124749	13.828192		
15	0.1770	2.50	94.083624	7.911816	7.911816	5.916376		
16	0.1490	2.75	98.307938	4.224314	4.224314	1.692062		
17	0.1250	3.00	99.842253	1.534315	1.534315	0.157747		
18	0.1050	3.25	100.000000	0.157747	0.157747	0.000000		
19	0.0880	3.51	100.000000	0.000000	0.000000	0.000000		
20	0.0740	3.76	100.000000	0.000000	0.000000	0.000000		
21	0.0630	3.99	100.000000	0.000000	0.000000	0.000000		
22	0.0530	4.24	100.000000	0.000000	0.000000	0.000000		
23	0.0440	4.51	100.000000	0.000000	0.000000	0.000000		
24	0.0370	4.76	100.000000	0.000000	0.000000	0.000000		
25	0.0310	5.01	100.000000	0.000000	0.000000	0.000000		
26	0.0156	6.00	100.000000	0.000000	0.000000	0.000000		
27	0.0100	6.64	100.000000	0.000000	0.000000	0.000000		
28	0.0078	7.00	100.000000	0.000000	0.000000	0.000000		
29	0.0039	8.00	100.000000	0.000000	0.000000	0.000000		
30	0.0020	8.97	100.000000	0.000000	0.000000	0.000000		
31	0.0010	9.99	100.000000	0.000000	0.000000	0.000000		
32	0.0007	10.48	100.000000	0.000000	0.000000	0.000000		
33	0.0005	10.99	100.000000	0.000000	0.000000	0.000000		
34	0.0002	12.02	100.000000	0.000000	0.000000	0.000000		
35	0.0001	13.02	100.000000	0.000000	0.000000	0.000000		
36	0.0001	14.02	100.000000	0.000000	0.000000	0.000000		
37	0.0001	14.29	100.000000	0.000000	0.000000	0.000000		
	Sums:			100.00	100.00			

Column: 40
Sample ID: 2015-2-104M

Folks' Graphic Statistics

	Mean (Mz)	Sorting (σI)	Skewness (SkI)	Kurtosis (KG)	Mean *mm*
phi	1.613	0.585	-0.009	0.955	0.327

Grainsize Statistics
Percentiles

	phi	*mm*
5	0.65	0.638
16	1.02	0.493
25	1.20	0.434
50	1.61	0.327
75	2.02	0.247
84	2.21	0.217
95	2.55	0.171

Table II.40: *Results summary for sample 40: Low intertidal zone, Transect 4, Southern Ngarunui Beach. Sample collected on the 10th of February, 2015.*

Column: 41 **Density:** 2650
Volume: 0.010
Sample ID: 2015-2-104L

Malvern data Phi	Malvern data Micron	Vol %	Equivalent Cum wt (g)
-1.00	2000.00	0	0.0
-0.75	1680.00	0.71904	0.2
-0.50	1410.00	2.246442	0.6
-0.25	1190.00	4.514637	1.2
0.00	1000.00	7.76667	2.1
0.25	840.00	12.173994	3.2
0.49	710.00	17.7826	4.7
0.76	590.00	25.803476	6.8
1.00	500.00	34.684783	9.2
1.25	420.00	45.565307	12.1
1.51	350.00	57.918173	15.3
1.74	300.00	68.332632	18.1
2.00	250.00	79.528665	21.1
2.25	210.00	88.191602	23.4
2.50	177.00	94.256201	25.0
2.75	149.00	97.943521	26.0
3.00	125.00	99.686108	26.4
3.25	105.00	100	26.5
3.51	88.00	100	26.5
3.76	74.00	100	26.5
3.99	63.00	100	26.5
4.24	53.00	100	26.5
4.51	44.00	100	26.5
4.76	37.00	100	26.5
5.01	31.00	100	26.5
6.00	15.60	100	26.5
6.64	10.00	100	26.5
7.00	7.80	100	26.5
8.00	3.90	100	26.5
8.97	2.00	100	26.5
9.99	0.98	100	26.5
10.48	0.70	100	26.5
10.99	0.49	100	26.5
12.02	0.24	100	26.5
13.02	0.12	100	26.5
14.02	0.06	100	26.5
14.29	0.05	100	26.5
		Total weight:	26.5

	mm	phi	Cum wt (g)	Int wt (g)	Int wt%	Cum % finer	Modes	
1	2.0000	-1.00	0.000000	0.000000	0.000000	100.000000		
2	1.6800	-0.75	0.719040	0.719040	0.719040	99.280960		
3	1.4100	-0.50	2.246442	1.527402	1.527402	97.753558		
4	1.1900	-0.25	4.514637	2.268195	2.268195	95.485363		
5	1.0000	0.00	7.766670	3.252033	3.252033	92.233330		8
6	0.8400	0.25	12.173994	4.407324	4.407324	87.826006		
7	0.7100	0.49	17.782600	5.608606	5.608606	82.217400		
8	0.5900	0.76	25.803476	8.020876	8.020876	74.196524		
9	0.5000	1.00	34.684783	8.881307	8.881307	65.315217		
10	0.4200	1.25	45.565307	10.880524	10.880524	54.434693		
11	0.3500	1.51	57.918173	12.352866	12.352866	42.081827	mode at 1.383056	
12	0.3000	1.74	68.332632	10.414459	10.414459	31.667368		
13	0.2500	2.00	79.528665	11.196033	11.196033	20.471335	mode at 1.868483	
14	0.2100	2.25	88.191602	8.662937	8.662937	11.808398		
15	0.1770	2.50	94.256201	6.064599	6.064599	5.743799		
16	0.1490	2.75	97.943521	3.687320	3.687320	2.056479		
17	0.1250	3.00	99.686108	1.742587	1.742587	0.313892		
18	0.1050	3.25	100.000000	0.313892	0.313892	0.000000		
19	0.0880	3.51	100.000000	0.000000	0.000000	0.000000		
20	0.0740	3.76	100.000000	0.000000	0.000000	0.000000		
21	0.0630	3.99	100.000000	0.000000	0.000000	0.000000		
22	0.0530	4.24	100.000000	0.000000	0.000000	0.000000		
23	0.0440	4.51	100.000000	0.000000	0.000000	0.000000		
24	0.0370	4.76	100.000000	0.000000	0.000000	0.000000		
25	0.0310	5.01	100.000000	0.000000	0.000000	0.000000		
26	0.0156	6.00	100.000000	0.000000	0.000000	0.000000		
27	0.0100	6.64	100.000000	0.000000	0.000000	0.000000		
28	0.0078	7.00	100.000000	0.000000	0.000000	0.000000		
29	0.0039	8.00	100.000000	0.000000	0.000000	0.000000		
30	0.0020	8.97	100.000000	0.000000	0.000000	0.000000		
31	0.0010	9.99	100.000000	0.000000	0.000000	0.000000		
32	0.0007	10.48	100.000000	0.000000	0.000000	0.000000		
33	0.0005	10.99	100.000000	0.000000	0.000000	0.000000		
34	0.0002	12.02	100.000000	0.000000	0.000000	0.000000		
35	0.0001	13.02	100.000000	0.000000	0.000000	0.000000		
36	0.0001	14.02	100.000000	0.000000	0.000000	0.000000		
37	0.0001	14.29	100.000000	0.000000	0.000000	0.000000		
	Sums:			100.00	100.00			

Grainsize Statistics
Percentiles

	phi	*mm*
5	-0.21	1.160
16	0.42	0.749
25	0.73	0.601
50	1.35	0.393
75	1.89	0.269
84	2.13	0.228
95	2.55	0.171

Column: 41
Sample ID: 2015-2-104L

Folks' Graphic Statistics

	Mean (Mz)	Sorting (σI)	Skewness (SkI)	Kurtosis (KG)	Mean *mm*
phi	1.298	0.847	-0.107	0.976	0.407

Table II.41: *Results summary for sample 41: Mid intertidal zone, mid transect, Wainamu Beach. Sample collected on the 12th of December, 2014.*

Column: 42 **Density:** 2650
Volume: 0.010
Sample ID: 2014-12-12mm

Malvern data Phi	Malvern data Micron	Vol %	Equivalent Cum wt (g)
-1.00	2000.00	0	0.0
-0.75	1680.00	0	0.0
-0.50	1410.00	0	0.0
-0.25	1190.00	0	0.0
0.00	1000.00	0	0.0
0.25	840.00	0	0.0
0.49	710.00	0	0.0
0.76	590.00	0	0.0
1.00	500.00	0.005259	0.0
1.25	420.00	0.515516	0.1
1.51	350.00	2.916693	0.8
1.74	300.00	7.557864	2.0
2.00	250.00	17.116414	4.5
2.25	210.00	30.422225	8.1
2.50	177.00	46.276061	12.3
2.75	149.00	62.928562	16.7
3.00	125.00	78.089986	20.7
3.25	105.00	89.386866	23.7
3.51	88.00	96.326645	25.5
3.76	74.00	99.348507	26.3
3.99	63.00	99.99335	26.5
4.24	53.00	100	26.5
4.51	44.00	100	26.5
4.76	37.00	100	26.5
5.01	31.00	100	26.5
6.00	15.60	100	26.5
6.64	10.00	100	26.5
7.00	7.80	100	26.5
8.00	3.90	100	26.5
8.97	2.00	100	26.5
9.99	0.98	100	26.5
10.48	0.70	100	26.5
10.99	0.49	100	26.5
12.02	0.24	100	26.5
13.02	0.12	100	26.5
14.02	0.06	100	26.5
14.29	0.05	100	26.5
		Total weight:	26.5

	mm	phi	Cum wt (g)	Int wt (g)	Int wt%	Cum % finer	Modes	
1	2.0000	-1.00	0.000000	0.000000	0.000000	100.000000		
2	1.6800	-0.75	0.000000	0.000000	0.000000	100.000000		
3	1.4100	-0.50	0.000000	0.000000	0.000000	100.000000		
4	1.1900	-0.25	0.000000	0.000000	0.000000	100.000000		
5	1.0000	0.00	0.000000	0.000000	0.000000	100.000000		8
6	0.8400	0.25	0.000000	0.000000	0.000000	100.000000		
7	0.7100	0.49	0.000000	0.000000	0.000000	100.000000		
8	0.5900	0.76	0.000000	0.000000	0.000000	100.000000		
9	0.5000	1.00	0.005259	0.005259	0.005259	99.994741		
10	0.4200	1.25	0.515516	0.510257	0.510257	99.484484		
11	0.3500	1.51	2.916693	2.401177	2.401177	97.083307		
12	0.3000	1.74	7.557864	4.641171	4.641171	92.442136		
13	0.2500	2.00	17.116414	9.558550	9.558550	82.883586		
14	0.2100	2.25	30.422225	13.305811	13.305811	69.577775		
15	0.1770	2.50	46.276061	15.853836	15.853836	53.723939		
16	0.1490	2.75	62.928562	16.652501	16.652501	37.071438	mode at 2.622397	
17	0.1250	3.00	78.089986	15.161424	15.161424	21.910014		
18	0.1050	3.25	89.386866	11.296880	11.296880	10.613134		
19	0.0880	3.51	96.326645	6.939779	6.939779	3.673355		
20	0.0740	3.76	99.348507	3.021862	3.021862	0.651493		
21	0.0630	3.99	99.993350	0.644843	0.644843	0.006650		
22	0.0530	4.24	100.000000	0.006650	0.006650	0.000000		
23	0.0440	4.51	100.000000	0.000000	0.000000	0.000000		
24	0.0370	4.76	100.000000	0.000000	0.000000	0.000000		
25	0.0310	5.01	100.000000	0.000000	0.000000	0.000000		
26	0.0156	6.00	100.000000	0.000000	0.000000	0.000000		
27	0.0100	6.64	100.000000	0.000000	0.000000	0.000000		
28	0.0078	7.00	100.000000	0.000000	0.000000	0.000000		
29	0.0039	8.00	100.000000	0.000000	0.000000	0.000000		
30	0.0020	8.97	100.000000	0.000000	0.000000	0.000000		
31	0.0010	9.99	100.000000	0.000000	0.000000	0.000000		
32	0.0007	10.48	100.000000	0.000000	0.000000	0.000000		
33	0.0005	10.99	100.000000	0.000000	0.000000	0.000000		
34	0.0002	12.02	100.000000	0.000000	0.000000	0.000000		
35	0.0001	13.02	100.000000	0.000000	0.000000	0.000000		
36	0.0001	14.02	100.000000	0.000000	0.000000	0.000000		
37	0.0001	14.29	100.000000	0.000000	0.000000	0.000000		
	Sums:			100.00	100.00			

Column: 42
Sample ID: 2014-12-12mm

Folks' Graphic Statistics

	Mean (Mz)	Sorting (σI)	Skewness (SkI)	Kurtosis (KG)	Mean ***mm***
phi	2.552	0.570	-0.012	0.945	0.171

Grainsize Statistics
Percentiles

	phi	***mm***
5	1.61	0.327
16	1.97	0.255
25	2.15	0.225
50	2.55	0.170
75	2.95	0.130
84	3.13	0.114
95	3.46	0.091

Table II.42: *Results summary for sample 42: Low intertidal zone, western transect, Wainamu Beach. Sample collected on the 12th of December, 2014.*

Column: 43 **Density:** 2650
Volume: 0.010
Sample ID: 2014-12-12lw

Malvern data Phi	Malvern data Micron	Vol %	Equivalent Cum wt (g)
-1.00	2000.00	0	0.0
-0.75	1680.00	0	0.0
-0.50	1410.00	0	0.0
-0.25	1190.00	0	0.0
0.00	1000.00	0	0.0
0.25	840.00	0	0.0
0.49	710.00	0	0.0
0.76	590.00	0.114077	0.0
1.00	500.00	1.26006	0.3
1.25	420.00	5.123829	1.4
1.51	350.00	13.896792	3.7
1.74	300.00	25.698208	6.8
2.00	250.00	43.726339	11.6
2.25	210.00	62.243397	16.5
2.50	177.00	78.280982	20.7
2.75	149.00	89.964234	23.8
3.00	125.00	96.719609	25.6
3.25	105.00	99.461746	26.4
3.51	88.00	99.971789	26.5
3.76	74.00	100	26.5
3.99	63.00	100	26.5
4.24	53.00	100	26.5
4.51	44.00	100	26.5
4.76	37.00	100	26.5
5.01	31.00	100	26.5
6.00	15.60	100	26.5
6.64	10.00	100	26.5
7.00	7.80	100	26.5
8.00	3.90	100	26.5
8.97	2.00	100	26.5
9.99	0.98	100	26.5
10.48	0.70	100	26.5
10.99	0.49	100	26.5
12.02	0.24	100	26.5
13.02	0.12	100	26.5
14.02	0.06	100	26.5
14.29	0.05	100	26.5
		Total weight:	26.5

	mm	phi	Cum wt (g)	Int wt (g)	Int wt%	Cum % finer	Modes	
1	2.0000	-1.00	0.000000	0.000000	0.000000	100.000000		
2	1.6800	-0.75	0.000000	0.000000	0.000000	100.000000		
3	1.4100	-0.50	0.000000	0.000000	0.000000	100.000000		
4	1.1900	-0.25	0.000000	0.000000	0.000000	100.000000		
5	1.0000	0.00	0.000000	0.000000	0.000000	100.000000		8
6	0.8400	0.25	0.000000	0.000000	0.000000	100.000000		
7	0.7100	0.49	0.000000	0.000000	0.000000	100.000000		
8	0.5900	0.76	0.114077	0.114077	0.114077	99.885923		
9	0.5000	1.00	1.260060	1.145983	1.145983	98.739940		
10	0.4200	1.25	5.123829	3.863769	3.863769	94.876171		
11	0.3500	1.51	13.896792	8.772963	8.772963	86.103208		
12	0.3000	1.74	25.698208	11.801416	11.801416	74.301792		
13	0.2500	2.00	43.726339	18.028131	18.028131	56.273661		
14	0.2100	2.25	62.243397	18.517058	18.517058	37.756603	mode at 2.125769	
15	0.1770	2.50	78.280982	16.037585	16.037585	21.719018		
16	0.1490	2.75	89.964234	11.683252	11.683252	10.035766		
17	0.1250	3.00	96.719609	6.755375	6.755375	3.280391		
18	0.1050	3.25	99.461746	2.742137	2.742137	0.538254		
19	0.0880	3.51	99.971789	0.510043	0.510043	0.028211		
20	0.0740	3.76	100.000000	0.028211	0.028211	0.000000		
21	0.0630	3.99	100.000000	0.000000	0.000000	0.000000		
22	0.0530	4.24	100.000000	0.000000	0.000000	0.000000		
23	0.0440	4.51	100.000000	0.000000	0.000000	0.000000		
24	0.0370	4.76	100.000000	0.000000	0.000000	0.000000		
25	0.0310	5.01	100.000000	0.000000	0.000000	0.000000		
26	0.0156	6.00	100.000000	0.000000	0.000000	0.000000		
27	0.0100	6.64	100.000000	0.000000	0.000000	0.000000		
28	0.0078	7.00	100.000000	0.000000	0.000000	0.000000		
29	0.0039	8.00	100.000000	0.000000	0.000000	0.000000		
30	0.0020	8.97	100.000000	0.000000	0.000000	0.000000		
31	0.0010	9.99	100.000000	0.000000	0.000000	0.000000		
32	0.0007	10.48	100.000000	0.000000	0.000000	0.000000		
33	0.0005	10.99	100.000000	0.000000	0.000000	0.000000		
34	0.0002	12.02	100.000000	0.000000	0.000000	0.000000		
35	0.0001	13.02	100.000000	0.000000	0.000000	0.000000		
36	0.0001	14.02	100.000000	0.000000	0.000000	0.000000		
37	0.0001	14.29	100.000000	0.000000	0.000000	0.000000		
	Sums:			100.00	100.00			

Grainsize Statistics
Percentiles

	phi	*mm*
5	1.24	0.422
16	1.55	0.341
25	1.72	0.303
50	2.09	0.236
75	2.45	0.183
84	2.62	0.163
95	2.94	0.131

Column: 43
Sample ID: 2014-12-12lw

Folks' Graphic Statistics

	Mean (Mz)	Sorting (σI)	Skewness (SkI)	Kurtosis (KG)	Mean *mm*
phi	2.086	0.523	0.004	0.958	0.235

Table II.43: *Results summary for sample 43: High intertidal zone, mid transect, Wainamu Beach. Sample collected on the 12th of December, 2014.*

Column: 44 **Density:** 2650
Volume: 0.010
Sample ID: 2014-12-12mh

Malvern data Phi	Malvern data Micron	Vol %	Equivalent Cum wt (g)
-1.00	2000.00	0	0.0
-0.75	1680.00	0	0.0
-0.50	1410.00	0	0.0
-0.25	1190.00	0	0.0
0.00	1000.00	0	0.0
0.25	840.00	0	0.0
0.49	710.00	0	0.0
0.76	590.00	0	0.0
1.00	500.00	0.010992	0.0
1.25	420.00	0.353505	0.1
1.51	350.00	2.90938	0.8
1.74	300.00	8.335202	2.2
2.00	250.00	20.003589	5.3
2.25	210.00	36.115534	9.6
2.50	177.00	54.365287	14.4
2.75	149.00	71.886068	19.0
3.00	125.00	85.871483	22.8
3.25	105.00	94.574797	25.1
3.51	88.00	98.72798	26.2
3.76	74.00	99.941433	26.5
3.99	63.00	100	26.5
4.24	53.00	100	26.5
4.51	44.00	100	26.5
4.76	37.00	100	26.5
5.01	31.00	100	26.5
6.00	15.60	100	26.5
6.64	10.00	100	26.5
7.00	7.80	100	26.5
8.00	3.90	100	26.5
8.97	2.00	100	26.5
9.99	0.98	100	26.5
10.48	0.70	100	26.5
10.99	0.49	100	26.5
12.02	0.24	100	26.5
13.02	0.12	100	26.5
14.02	0.06	100	26.5
14.29	0.05	100	26.5

Total weight: 26.5

	mm	phi	Cum wt (g)	Int wt (g)	Int wt%	Cum % finer	Modes	
1	2.0000	-1.00	0.000000	0.000000	0.000000	100.000000		
2	1.6800	-0.75	0.000000	0.000000	0.000000	100.000000		
3	1.4100	-0.50	0.000000	0.000000	0.000000	100.000000		
4	1.1900	-0.25	0.000000	0.000000	0.000000	100.000000		
5	1.0000	0.00	0.000000	0.000000	0.000000	100.000000		8
6	0.8400	0.25	0.000000	0.000000	0.000000	100.000000		
7	0.7100	0.49	0.000000	0.000000	0.000000	100.000000		
8	0.5900	0.76	0.000000	0.000000	0.000000	100.000000		
9	0.5000	1.00	0.010992	0.010992	0.010992	99.989008		
10	0.4200	1.25	0.353505	0.342513	0.342513	99.646495		
11	0.3500	1.51	2.909380	2.555875	2.555875	97.090620		
12	0.3000	1.74	8.335202	5.425822	5.425822	91.664798		
13	0.2500	2.00	20.003589	11.668387	11.668387	79.996411		
14	0.2100	2.25	36.115534	16.111945	16.111945	63.884466		
15	0.1770	2.50	54.365287	18.249753	18.249753	45.634713	mode at 2.374859	
16	0.1490	2.75	71.886068	17.520781	17.520781	28.113932		
17	0.1250	3.00	85.871483	13.985415	13.985415	14.128517		
18	0.1050	3.25	94.574797	8.703314	8.703314	5.425203		
19	0.0880	3.51	98.727980	4.153183	4.153183	1.272020		
20	0.0740	3.76	99.941433	1.213453	1.213453	0.058567		
21	0.0630	3.99	100.000000	0.058567	0.058567	0.000000		
22	0.0530	4.24	100.000000	0.000000	0.000000	0.000000		
23	0.0440	4.51	100.000000	0.000000	0.000000	0.000000		
24	0.0370	4.76	100.000000	0.000000	0.000000	0.000000		
25	0.0310	5.01	100.000000	0.000000	0.000000	0.000000		
26	0.0156	6.00	100.000000	0.000000	0.000000	0.000000		
27	0.0100	6.64	100.000000	0.000000	0.000000	0.000000		
28	0.0078	7.00	100.000000	0.000000	0.000000	0.000000		
29	0.0039	8.00	100.000000	0.000000	0.000000	0.000000		
30	0.0020	8.97	100.000000	0.000000	0.000000	0.000000		
31	0.0010	9.99	100.000000	0.000000	0.000000	0.000000		
32	0.0007	10.48	100.000000	0.000000	0.000000	0.000000		
33	0.0005	10.99	100.000000	0.000000	0.000000	0.000000		
34	0.0002	12.02	100.000000	0.000000	0.000000	0.000000		
35	0.0001	13.02	100.000000	0.000000	0.000000	0.000000		
36	0.0001	14.02	100.000000	0.000000	0.000000	0.000000		
37	0.0001	14.29	100.000000	0.000000	0.000000	0.000000		
	Sums:			100.00	100.00			

Column: 44
Sample ID: 2014-12-12mh

Folks' Graphic Statistics

	Mean (Mz)	Sorting (σI)	Skewness (SkI)	Kurtosis (KG)	Mean *mm*
phi	2.438	0.518	-0.001	0.948	0.184

Grainsize Statistics
Percentiles

	phi	*mm*
5	1.60	0.330
16	1.91	0.266
25	2.08	0.237
50	2.44	0.184
75	2.80	0.143
84	2.97	0.128
95	3.28	0.103

Table II.44: *Results summary for sample 44: Low intertidal zone, eastern transect, Wainamu Beach. Sample collected on the 12th of December, 2014.*

Column: 45 **Density:** 2650
Volume: 0.010
Sample ID: 2014-12-12LE

Malvern data Phi	Malvern data Micron	Vol %	Equivalent Cum wt (g)
-1.00	2000.00	0	0.0
-0.75	1680.00	0.108317	0.0
-0.50	1410.00	0.337309	0.1
-0.25	1190.00	0.456942	0.1
0.00	1000.00	0.456942	0.1
0.25	840.00	0.456942	0.1
0.49	710.00	0.456942	0.1
0.76	590.00	0.474219	0.1
1.00	500.00	1.358568	0.4
1.25	420.00	4.376381	1.2
1.51	350.00	11.124092	2.9
1.74	300.00	20.260368	5.4
2.00	250.00	34.724821	9.2
2.25	210.00	50.718949	13.4
2.50	177.00	66.265403	17.6
2.75	149.00	79.695946	21.1
3.00	125.00	89.714717	23.8
3.25	105.00	95.727949	25.4
3.51	88.00	98.556246	26.1
3.76	74.00	99.316667	26.3
3.99	63.00	99.345977	26.3
4.24	53.00	99.345977	26.3
4.51	44.00	99.345977	26.3
4.76	37.00	99.345977	26.3
5.01	31.00	99.345977	26.3
6.00	15.60	99.345977	26.3
6.64	10.00	99.345977	26.3
7.00	7.80	99.385122	26.3
8.00	3.90	99.820713	26.5
8.97	2.00	99.874222	26.5
9.99	0.98	99.874222	26.5
10.48	0.70	99.874222	26.5
10.99	0.49	99.874222	26.5
12.02	0.24	100	26.5
13.02	0.12	100	26.5
14.02	0.06	100	26.5
14.29	0.05	100	26.5

Total weight: 26.5

	mm	phi	Cum wt (g)	Int wt (g)	Int wt%	Cum % finer	Modes
1	2.0000	-1.00	0.000000	0.000000	0.000000	100.000000	
2	1.6800	-0.75	0.108317	0.108317	0.108317	99.891683	
3	1.4100	-0.50	0.337309	0.228992	0.228992	99.662691	mode at -0.62208
4	1.1900	-0.25	0.456942	0.119633	0.119633	99.543058	
5	1.0000	0.00	0.456942	0.000000	0.000000	99.543058	8
6	0.8400	0.25	0.456942	0.000000	0.000000	99.543058	
7	0.7100	0.49	0.456942	0.000000	0.000000	99.543058	
8	0.5900	0.76	0.474219	0.017277	0.017277	99.525781	
9	0.5000	1.00	1.358568	0.884349	0.884349	98.641432	
10	0.4200	1.25	4.376381	3.017813	3.017813	95.623619	
11	0.3500	1.51	11.124092	6.747711	6.747711	88.875908	
12	0.3000	1.74	20.260368	9.136276	9.136276	79.739632	
13	0.2500	2.00	34.724821	14.464453	14.464453	65.275179	
14	0.2100	2.25	50.718949	15.994128	15.994128	49.281051	mode at 2.125769
15	0.1770	2.50	66.265403	15.546454	15.546454	33.734597	
16	0.1490	2.75	79.695946	13.430543	13.430543	20.304054	
17	0.1250	3.00	89.714717	10.018771	10.018771	10.285283	
18	0.1050	3.25	95.727949	6.013232	6.013232	4.272051	
19	0.0880	3.51	98.556246	2.828297	2.828297	1.443754	
20	0.0740	3.76	99.316667	0.760421	0.760421	0.683333	
21	0.0630	3.99	99.345977	0.029310	0.029310	0.654023	
22	0.0530	4.24	99.345977	0.000000	0.000000	0.654023	
23	0.0440	4.51	99.345977	0.000000	0.000000	0.654023	
24	0.0370	4.76	99.345977	0.000000	0.000000	0.654023	
25	0.0310	5.01	99.345977	0.000000	0.000000	0.654023	
26	0.0156	6.00	99.345977	0.000000	0.000000	0.654023	
27	0.0100	6.64	99.345977	0.000000	0.000000	0.654023	
28	0.0078	7.00	99.385122	0.039145	0.039145	0.614878	
29	0.0039	8.00	99.820713	0.435591	0.435591	0.179287	mode at 7.50231
30	0.0020	8.97	99.874222	0.053509	0.053509	0.125778	
31	0.0010	9.99	99.874222	0.000000	0.000000	0.125778	
32	0.0007	10.48	99.874222	0.000000	0.000000	0.125778	
33	0.0005	10.99	99.874222	0.000000	0.000000	0.125778	
34	0.0002	12.02	100.000000	0.125778	0.125778	0.000000	mode at 11.5098
35	0.0001	13.02	100.000000	0.000000	0.000000	0.000000	
36	0.0001	14.02	100.000000	0.000000	0.000000	0.000000	
37	0.0001	14.29	100.000000	0.000000	0.000000	0.000000	
		Sums:		100.00	100.00		

Grainsize Statistics
Percentiles

	phi	*mm*
5	1.28	0.413
16	1.63	0.322
25	1.82	0.283
50	2.24	0.212
75	2.66	0.158
84	2.86	0.138
95	3.22	0.107

Column: 45
Sample ID: 2014-12-12LE

Folks' Graphic Statistics

	Mean (Mz)	Sorting (σI)	Skewness (SkI)	Kurtosis (KG)	Mean *mm*
phi	2.243	0.600	0.008	0.953	0.211

Table II.45: *Results summary for sample 45: High intertidal zone, eastern transect, Wainamu Beach. Sample collected on the 12th of December, 2014.*

Column: 46 **Density:** 2650
Volume: 0.010
Sample ID: 2014-12-12HE

Malvern data Phi	Malvern data Micron	Vol %	Equivalent Cum wt (g)
-1.00	2000.00	0	0.0
-0.75	1680.00	0	0.0
-0.50	1410.00	0	0.0
-0.25	1190.00	0	0.0
0.00	1000.00	0	0.0
0.25	840.00	0	0.0
0.49	710.00	0	0.0
0.76	590.00	0	0.0
1.00	500.00	0.008596	0.0
1.25	420.00	0.292371	0.1
1.51	350.00	2.518108	0.7
1.74	300.00	7.420983	2.0
2.00	250.00	18.314912	4.9
2.25	210.00	33.837936	9.0
2.50	177.00	51.936646	13.8
2.75	149.00	69.801419	18.5
3.00	125.00	84.458723	22.4
3.25	105.00	93.843877	24.9
3.51	88.00	98.473833	26.1
3.76	74.00	99.906418	26.5
3.99	63.00	100	26.5
4.24	53.00	100	26.5
4.51	44.00	100	26.5
4.76	37.00	100	26.5
5.01	31.00	100	26.5
6.00	15.60	100	26.5
6.64	10.00	100	26.5
7.00	7.80	100	26.5
8.00	3.90	100	26.5
8.97	2.00	100	26.5
9.99	0.98	100	26.5
10.48	0.70	100	26.5
10.99	0.49	100	26.5
12.02	0.24	100	26.5
13.02	0.12	100	26.5
14.02	0.06	100	26.5
14.29	0.05	100	26.5
		Total weight:	26.5

	mm	phi	Cum wt (g)	Int wt (g)	Int wt%	Cum % finer	Modes	
1	2.0000	-1.00	0.000000	0.000000	0.000000	100.000000		
2	1.6800	-0.75	0.000000	0.000000	0.000000	100.000000		
3	1.4100	-0.50	0.000000	0.000000	0.000000	100.000000		
4	1.1900	-0.25	0.000000	0.000000	0.000000	100.000000		
5	1.0000	0.00	0.000000	0.000000	0.000000	100.000000		8
6	0.8400	0.25	0.000000	0.000000	0.000000	100.000000		
7	0.7100	0.49	0.000000	0.000000	0.000000	100.000000		
8	0.5900	0.76	0.000000	0.000000	0.000000	100.000000		
9	0.5000	1.00	0.008596	0.008596	0.008596	99.991404		
10	0.4200	1.25	0.292371	0.283775	0.283775	99.707629		
11	0.3500	1.51	2.518108	2.225737	2.225737	97.481892		
12	0.3000	1.74	7.420983	4.902875	4.902875	92.579017		
13	0.2500	2.00	18.314912	10.893929	10.893929	81.685088		
14	0.2100	2.25	33.837936	15.523024	15.523024	66.162064		
15	0.1770	2.50	51.936646	18.098710	18.098710	48.063354	mode at 2.374859	
16	0.1490	2.75	69.801419	17.864773	17.864773	30.198581		
17	0.1250	3.00	84.458723	14.657304	14.657304	15.541277		
18	0.1050	3.25	93.843877	9.385154	9.385154	6.156123		
19	0.0880	3.51	98.473833	4.629956	4.629956	1.526167		
20	0.0740	3.76	99.906418	1.432585	1.432585	0.093582		
21	0.0630	3.99	100.000000	0.093582	0.093582	0.000000		
22	0.0530	4.24	100.000000	0.000000	0.000000	0.000000		
23	0.0440	4.51	100.000000	0.000000	0.000000	0.000000		
24	0.0370	4.76	100.000000	0.000000	0.000000	0.000000		
25	0.0310	5.01	100.000000	0.000000	0.000000	0.000000		
26	0.0156	6.00	100.000000	0.000000	0.000000	0.000000		
27	0.0100	6.64	100.000000	0.000000	0.000000	0.000000		
28	0.0078	7.00	100.000000	0.000000	0.000000	0.000000		
29	0.0039	8.00	100.000000	0.000000	0.000000	0.000000		
30	0.0020	8.97	100.000000	0.000000	0.000000	0.000000		
31	0.0010	9.99	100.000000	0.000000	0.000000	0.000000		
32	0.0007	10.48	100.000000	0.000000	0.000000	0.000000		
33	0.0005	10.99	100.000000	0.000000	0.000000	0.000000		
34	0.0002	12.02	100.000000	0.000000	0.000000	0.000000		
35	0.0001	13.02	100.000000	0.000000	0.000000	0.000000		
36	0.0001	14.02	100.000000	0.000000	0.000000	0.000000		
37	0.0001	14.29	100.000000	0.000000	0.000000	0.000000		
		Sums:		100.00	100.00			

Column: 46
Sample ID: 2014-12-12HE

Folks' Graphic Statistics

	Mean (Mz)	Sorting (σI)	Skewness (SkI)	Kurtosis (KG)	Mean *mm*
phi	2.469	0.518	-0.004	0.950	0.181

Grainsize Statistics
Percentiles

	phi	*mm*
5	1.63	0.324
16	1.94	0.260
25	2.11	0.232
50	2.47	0.180
75	2.84	0.140
84	2.99	0.126
95	3.32	0.100

Table II.46: *Results summary for sample 46: Mid intertidal zone, eastern transect, Wainamu Beach. Sample collected on the 12th of December, 2014.*

Column: 47 **Density:** 2650
Volume: 0.010
Sample ID: 2014-12-12ME

Malvern data Phi	Malvern data Micron	Vol %	Equivalent Cum wt (g)
-1.00	2000.00	0	0.0
-0.75	1680.00	0	0.0
-0.50	1410.00	0	0.0
-0.25	1190.00	0	0.0
0.00	1000.00	0	0.0
0.25	840.00	0	0.0
0.49	710.00	0	0.0
0.76	590.00	0	0.0
1.00	500.00	0.434698	0.1
1.25	420.00	2.79133	0.7
1.51	350.00	9.231644	2.4
1.74	300.00	18.857154	5.0
2.00	250.00	34.782385	9.2
2.25	210.00	52.347501	13.9
2.50	177.00	68.592841	18.2
2.75	149.00	81.289303	21.5
3.00	125.00	89.324736	23.7
3.25	105.00	93.047615	24.7
3.51	88.00	94.160944	25.0
3.76	74.00	94.234715	25.0
3.99	63.00	94.234715	25.0
4.24	53.00	94.234715	25.0
4.51	44.00	94.246277	25.0
4.76	37.00	94.458371	25.0
5.01	31.00	94.932669	25.2
6.00	15.60	96.769285	25.6
6.64	10.00	97.555621	25.9
7.00	7.80	98.059197	26.0
8.00	3.90	99.427188	26.3
8.97	2.00	100	26.5
9.99	0.98	100	26.5
10.48	0.70	100	26.5
10.99	0.49	100	26.5
12.02	0.24	100	26.5
13.02	0.12	100	26.5
14.02	0.06	100	26.5
14.29	0.05	100	26.5

Total weight: 26.5

	mm	phi	Cum wt (g)	Int wt (g)	Int wt%	Cum % finer	Modes
1	2.0000	-1.00	0.000000	0.000000	0.000000	100.000000	
2	1.6800	-0.75	0.000000	0.000000	0.000000	100.000000	
3	1.4100	-0.50	0.000000	0.000000	0.000000	100.000000	
4	1.1900	-0.25	0.000000	0.000000	0.000000	100.000000	
5	1.0000	0.00	0.000000	0.000000	0.000000	100.000000	8
6	0.8400	0.25	0.000000	0.000000	0.000000	100.000000	
7	0.7100	0.49	0.000000	0.000000	0.000000	100.000000	
8	0.5900	0.76	0.000000	0.000000	0.000000	100.000000	
9	0.5000	1.00	0.434698	0.434698	0.434698	99.565302	
10	0.4200	1.25	2.791330	2.356632	2.356632	97.208670	
11	0.3500	1.51	9.231644	6.440314	6.440314	90.768356	
12	0.3000	1.74	18.857154	9.625510	9.625510	81.142846	
13	0.2500	2.00	34.782385	15.925231	15.925231	65.217615	
14	0.2100	2.25	52.347501	17.565116	17.565116	47.652499	mode at 2.125769
15	0.1770	2.50	68.592841	16.245340	16.245340	31.407159	
16	0.1490	2.75	81.289303	12.696462	12.696462	18.710697	
17	0.1250	3.00	89.324736	8.035433	8.035433	10.675264	
18	0.1050	3.25	93.047615	3.722879	3.722879	6.952385	
19	0.0880	3.51	94.160944	1.113329	1.113329	5.839056	
20	0.0740	3.76	94.234715	0.073771	0.073771	5.765285	
21	0.0630	3.99	94.234715	0.000000	0.000000	5.765285	
22	0.0530	4.24	94.234715	0.000000	0.000000	5.765285	
23	0.0440	4.51	94.246277	0.011562	0.011562	5.753723	
24	0.0370	4.76	94.458371	0.212094	0.212094	5.541629	
25	0.0310	5.01	94.932669	0.474298	0.474298	5.067331	
26	0.0156	6.00	96.769285	1.836616	1.836616	3.230715	mode at 5.506949
27	0.0100	6.64	97.555621	0.786336	0.786336	2.444379	
28	0.0078	7.00	98.059197	0.503576	0.503576	1.940803	
29	0.0039	8.00	99.427188	1.367991	1.367991	0.572812	mode at 7.50231
30	0.0020	8.97	100.000000	0.572812	0.572812	0.000000	
31	0.0010	9.99	100.000000	0.000000	0.000000	0.000000	
32	0.0007	10.48	100.000000	0.000000	0.000000	0.000000	
33	0.0005	10.99	100.000000	0.000000	0.000000	0.000000	
34	0.0002	12.02	100.000000	0.000000	0.000000	0.000000	
35	0.0001	13.02	100.000000	0.000000	0.000000	0.000000	
36	0.0001	14.02	100.000000	0.000000	0.000000	0.000000	
37	0.0001	14.29	100.000000	0.000000	0.000000	0.000000	
		Sums:		100.00	100.00		

Grainsize Statistics
Percentiles

	phi	*mm*
5	1.34	0.395
16	1.67	0.314
25	1.84	0.280
50	2.22	0.215
75	2.62	0.162
84	2.83	0.140
95	5.05	0.030

Column: 47
Sample ID: 2014-12-12ME

Folks' Graphic Statistics

	Mean (Mz)	Sorting (σI)	Skewness (SkI)	Kurtosis (KG)	Mean *mm*
phi	2.240	0.852	0.293	1.935	0.212

Table II.47: *Results summary for sample 47: Mid intertidal zone, western transect, Wainamu Beach. Sample collected on the 12th of December, 2014.*

Column: 48 **Density:** 2650
Volume: 0.010
Sample ID: 2014-12-12mw

Malvern data Phi	**Malvern data** Micron	Vol %	Equivalent Cum wt (g)
-1.00	2000.00	0	0.0
-0.75	1680.00	0	0.0
-0.50	1410.00	0	0.0
-0.25	1190.00	0	0.0
0.00	1000.00	0	0.0
0.25	840.00	0	0.0
0.49	710.00	0	0.0
0.76	590.00	0	0.0
1.00	500.00	0	0.0
1.25	420.00	0	0.0
1.51	350.00	0.039044	0.0
1.74	300.00	0.883496	0.2
2.00	250.00	4.953504	1.3
2.25	210.00	13.974224	3.7
2.50	177.00	28.408571	7.5
2.75	149.00	47.027418	12.5
3.00	125.00	66.632907	17.7
3.25	105.00	82.772323	21.9
3.51	88.00	93.415561	24.8
3.76	74.00	98.426924	26.1
3.99	63.00	99.904688	26.5
4.24	53.00	100	26.5
4.51	44.00	100	26.5
4.76	37.00	100	26.5
5.01	31.00	100	26.5
6.00	15.60	100	26.5
6.64	10.00	100	26.5
7.00	7.80	100	26.5
8.00	3.90	100	26.5
8.97	2.00	100	26.5
9.99	0.98	100	26.5
10.48	0.70	100	26.5
10.99	0.49	100	26.5
12.02	0.24	100	26.5
13.02	0.12	100	26.5
14.02	0.06	100	26.5
14.29	0.05	100	26.5
		Total weight:	26.5

	mm	phi	Cum wt (g)	Int wt (g)	Int wt%	Cum % finer	Modes	
1	2.0000	-1.00	0.000000	0.000000	0.000000	100.000000		
2	1.6800	-0.75	0.000000	0.000000	0.000000	100.000000		
3	1.4100	-0.50	0.000000	0.000000	0.000000	100.000000		
4	1.1900	-0.25	0.000000	0.000000	0.000000	100.000000		
5	1.0000	0.00	0.000000	0.000000	0.000000	100.000000		8
6	0.8400	0.25	0.000000	0.000000	0.000000	100.000000		
7	0.7100	0.49	0.000000	0.000000	0.000000	100.000000		
8	0.5900	0.76	0.000000	0.000000	0.000000	100.000000		
9	0.5000	1.00	0.000000	0.000000	0.000000	100.000000		
10	0.4200	1.25	0.000000	0.000000	0.000000	100.000000		
11	0.3500	1.51	0.039044	0.039044	0.039044	99.960956		
12	0.3000	1.74	0.883496	0.844452	0.844452	99.116504		
13	0.2500	2.00	4.953504	4.070008	4.070008	95.046496		
14	0.2100	2.25	13.974224	9.020720	9.020720	86.025776		
15	0.1770	2.50	28.408571	14.434347	14.434347	71.591429		
16	0.1490	2.75	47.027418	18.618847	18.618847	52.972582		
17	0.1250	3.00	66.632907	19.605489	19.605489	33.367093	mode at 2.873308	
18	0.1050	3.25	82.772323	16.139416	16.139416	17.227677		
19	0.0880	3.51	93.415561	10.643238	10.643238	6.584439		
20	0.0740	3.76	98.426924	5.011363	5.011363	1.573076		
21	0.0630	3.99	99.904688	1.477764	1.477764	0.095312		
22	0.0530	4.24	100.000000	0.095312	0.095312	0.000000		
23	0.0440	4.51	100.000000	0.000000	0.000000	0.000000		
24	0.0370	4.76	100.000000	0.000000	0.000000	0.000000		
25	0.0310	5.01	100.000000	0.000000	0.000000	0.000000		
26	0.0156	6.00	100.000000	0.000000	0.000000	0.000000		
27	0.0100	6.64	100.000000	0.000000	0.000000	0.000000		
28	0.0078	7.00	100.000000	0.000000	0.000000	0.000000		
29	0.0039	8.00	100.000000	0.000000	0.000000	0.000000		
30	0.0020	8.97	100.000000	0.000000	0.000000	0.000000		
31	0.0010	9.99	100.000000	0.000000	0.000000	0.000000		
32	0.0007	10.48	100.000000	0.000000	0.000000	0.000000		
33	0.0005	10.99	100.000000	0.000000	0.000000	0.000000		
34	0.0002	12.02	100.000000	0.000000	0.000000	0.000000		
35	0.0001	13.02	100.000000	0.000000	0.000000	0.000000		
36	0.0001	14.02	100.000000	0.000000	0.000000	0.000000		
37	0.0001	14.29	100.000000	0.000000	0.000000	0.000000		
	Sums:			100.00	100.00			

Grainsize Statistics
Percentiles

	phi	*mm*
5	2.00	0.250
16	2.29	0.205
25	2.44	0.184
50	2.79	0.145
75	3.13	0.114
84	3.28	0.103
95	3.59	0.083

Column: 48
Sample ID: 2014-12-12mw

Folks' Graphic Statistics

	Mean (Mz)	Sorting (σI)	Skewness (SkI)	Kurtosis (KG)	Mean *mm*
phi	2.784	0.489	0.004	0.940	0.145

Table II.48: *Results summary for sample 48: Low intertidal zone, mid transect, Wainamu Beach. Sample collected on the 12th of December, 2014.*

Column: 49 **Density:** 2650
Volume: 0.010
Sample ID: 2014-12-12LM

Malvern data Phi	Malvern data Micron	Vol %	Equivalent Cum wt (g)
-1.00	2000.00	0	0.0
-0.75	1680.00	0	0.0
-0.50	1410.00	0	0.0
-0.25	1190.00	0	0.0
0.00	1000.00	0	0.0
0.25	840.00	0	0.0
0.49	710.00	0	0.0
0.76	590.00	0	0.0
1.00	500.00	0.539416	0.1
1.25	420.00	3.156874	0.8
1.51	350.00	10.159808	2.7
1.74	300.00	20.532212	5.4
2.00	250.00	37.576818	10.0
2.25	210.00	56.247477	14.9
2.50	177.00	73.396981	19.5
2.75	149.00	86.702817	23.0
3.00	125.00	95.049111	25.2
3.25	105.00	98.8534	26.2
3.51	88.00	99.949678	26.5
3.76	74.00	100	26.5
3.99	63.00	100	26.5
4.24	53.00	100	26.5
4.51	44.00	100	26.5
4.76	37.00	100	26.5
5.01	31.00	100	26.5
6.00	15.60	100	26.5
6.64	10.00	100	26.5
7.00	7.80	100	26.5
8.00	3.90	100	26.5
8.97	2.00	100	26.5
9.99	0.98	100	26.5
10.48	0.70	100	26.5
10.99	0.49	100	26.5
12.02	0.24	100	26.5
13.02	0.12	100	26.5
14.02	0.06	100	26.5
14.29	0.05	100	26.5
		Total weight:	26.5

	mm	phi	Cum wt (g)	Int wt (g)	Int wt%	Cum % finer	Modes
1	2.0000	-1.00	0.000000	0.000000	0.000000	100.000000	
2	1.6800	-0.75	0.000000	0.000000	0.000000	100.000000	
3	1.4100	-0.50	0.000000	0.000000	0.000000	100.000000	
4	1.1900	-0.25	0.000000	0.000000	0.000000	100.000000	
5	1.0000	0.00	0.000000	0.000000	0.000000	100.000000	8
6	0.8400	0.25	0.000000	0.000000	0.000000	100.000000	
7	0.7100	0.49	0.000000	0.000000	0.000000	100.000000	
8	0.5900	0.76	0.000000	0.000000	0.000000	100.000000	
9	0.5000	1.00	0.539416	0.539416	0.539416	99.460584	
10	0.4200	1.25	3.156874	2.617458	2.617458	96.843126	
11	0.3500	1.51	10.159808	7.002934	7.002934	89.840192	
12	0.3000	1.74	20.532212	10.372404	10.372404	79.467788	
13	0.2500	2.00	37.576818	17.044606	17.044606	62.423182	
14	0.2100	2.25	56.247477	18.670659	18.670659	43.752523	mode at 2.125769
15	0.1770	2.50	73.396981	17.149504	17.149504	26.603019	
16	0.1490	2.75	86.702817	13.305836	13.305836	13.297183	
17	0.1250	3.00	95.049111	8.346294	8.346294	4.950889	
18	0.1050	3.25	98.853400	3.804289	3.804289	1.146600	
19	0.0880	3.51	99.949678	1.096278	1.096278	0.050322	
20	0.0740	3.76	100.000000	0.050322	0.050322	0.000000	
21	0.0630	3.99	100.000000	0.000000	0.000000	0.000000	
22	0.0530	4.24	100.000000	0.000000	0.000000	0.000000	
23	0.0440	4.51	100.000000	0.000000	0.000000	0.000000	
24	0.0370	4.76	100.000000	0.000000	0.000000	0.000000	
25	0.0310	5.01	100.000000	0.000000	0.000000	0.000000	
26	0.0156	6.00	100.000000	0.000000	0.000000	0.000000	
27	0.0100	6.64	100.000000	0.000000	0.000000	0.000000	
28	0.0078	7.00	100.000000	0.000000	0.000000	0.000000	
29	0.0039	8.00	100.000000	0.000000	0.000000	0.000000	
30	0.0020	8.97	100.000000	0.000000	0.000000	0.000000	
31	0.0010	9.99	100.000000	0.000000	0.000000	0.000000	
32	0.0007	10.48	100.000000	0.000000	0.000000	0.000000	
33	0.0005	10.99	100.000000	0.000000	0.000000	0.000000	
34	0.0002	12.02	100.000000	0.000000	0.000000	0.000000	
35	0.0001	13.02	100.000000	0.000000	0.000000	0.000000	
36	0.0001	14.02	100.000000	0.000000	0.000000	0.000000	
37	0.0001	14.29	100.000000	0.000000	0.000000	0.000000	
	Sums:			100.00	100.00		

Grainsize Statistics
Percentiles

	phi	*mm*
5	1.32	0.400
16	1.64	0.321
25	1.81	0.286
50	2.17	0.223
75	2.53	0.173
84	2.70	0.154
95	3.00	0.125

Column: 49
Sample ID: 2014-12-12LM

Folks' Graphic Statistics

	Mean (Mz)	Sorting (σI)	Skewness (SkI)	Kurtosis (KG)	Mean *mm*
phi	2.168	0.518	-0.004	0.952	0.223

Table II.49: *Results summary for sample 49: High intertidal zone, western transect, Wainamu Beach. Sample collected on the 12th of December, 2014.*

Column: 50 **Density:** 2650
Volume: 0.010
Sample ID: 2014-12-12HW

Malvern data Phi	Malvern data Micron	Vol %	Equivalent Cum wt (g)
-1.00	2000.00	0	0.0
-0.75	1680.00	0.354528	0.1
-0.50	1410.00	1.096866	0.3
-0.25	1190.00	2.057851	0.5
0.00	1000.00	3.049606	0.8
0.25	840.00	3.755867	1.0
0.49	710.00	3.835635	1.0
0.76	590.00	3.835635	1.0
1.00	500.00	3.843593	1.0
1.25	420.00	4.335654	1.1
1.51	350.00	6.707819	1.8
1.74	300.00	11.297359	3.0
2.00	250.00	20.705197	5.5
2.25	210.00	33.676244	8.9
2.50	177.00	48.947427	13.0
2.75	149.00	64.793929	17.2
3.00	125.00	79.083726	21.0
3.25	105.00	89.694496	23.8
3.51	88.00	96.268659	25.5
3.76	74.00	99.230329	26.3
3.99	63.00	99.987082	26.5
4.24	53.00	100	26.5
4.51	44.00	100	26.5
4.76	37.00	100	26.5
5.01	31.00	100	26.5
6.00	15.60	100	26.5
6.64	10.00	100	26.5
7.00	7.80	100	26.5
8.00	3.90	100	26.5
8.97	2.00	100	26.5
9.99	0.98	100	26.5
10.48	0.70	100	26.5
10.99	0.49	100	26.5
12.02	0.24	100	26.5
13.02	0.12	100	26.5
14.02	0.06	100	26.5
14.29	0.05	100	26.5
		Total weight:	26.5

	mm	phi	Cum wt (g)	Int wt (g)	Int wt%	Cum % finer	Modes
1	2.0000	-1.00	0.000000	0.000000	0.000000	100.000000	
2	1.6800	-0.75	0.354528	0.354528	0.354528	99.645472	
3	1.4100	-0.50	1.096866	0.742338	0.742338	98.903134	
4	1.1900	-0.25	2.057851	0.960985	0.960985	97.942149	
5	1.0000	0.00	3.049606	0.991755	0.991755	96.950394	mode at -0.12548 8
6	0.8400	0.25	3.755867	0.706261	0.706261	96.244133	
7	0.7100	0.49	3.835635	0.079768	0.079768	96.164365	
8	0.5900	0.76	3.835635	0.000000	0.000000	96.164365	
9	0.5000	1.00	3.843593	0.007958	0.007958	96.156407	
10	0.4200	1.25	4.335654	0.492061	0.492061	95.664346	
11	0.3500	1.51	6.707819	2.372165	2.372165	93.292181	
12	0.3000	1.74	11.297359	4.589540	4.589540	88.702641	
13	0.2500	2.00	20.705197	9.407838	9.407838	79.294803	
14	0.2100	2.25	33.676244	12.971047	12.971047	66.323756	
15	0.1770	2.50	48.947427	15.271183	15.271183	51.052573	
16	0.1490	2.75	64.793929	15.846502	15.846502	35.206071	mode at 2.622397
17	0.1250	3.00	79.083726	14.289797	14.289797	20.916274	
18	0.1050	3.25	89.694496	10.610770	10.610770	10.305504	
19	0.0880	3.51	96.268659	6.574163	6.574163	3.731341	
20	0.0740	3.76	99.230329	2.961670	2.961670	0.769671	
21	0.0630	3.99	99.987082	0.756753	0.756753	0.012918	
22	0.0530	4.24	100.000000	0.012918	0.012918	0.000000	
23	0.0440	4.51	100.000000	0.000000	0.000000	0.000000	
24	0.0370	4.76	100.000000	0.000000	0.000000	0.000000	
25	0.0310	5.01	100.000000	0.000000	0.000000	0.000000	
26	0.0156	6.00	100.000000	0.000000	0.000000	0.000000	
27	0.0100	6.64	100.000000	0.000000	0.000000	0.000000	
28	0.0078	7.00	100.000000	0.000000	0.000000	0.000000	
29	0.0039	8.00	100.000000	0.000000	0.000000	0.000000	
30	0.0020	8.97	100.000000	0.000000	0.000000	0.000000	
31	0.0010	9.99	100.000000	0.000000	0.000000	0.000000	
32	0.0007	10.48	100.000000	0.000000	0.000000	0.000000	
33	0.0005	10.99	100.000000	0.000000	0.000000	0.000000	
34	0.0002	12.02	100.000000	0.000000	0.000000	0.000000	
35	0.0001	13.02	100.000000	0.000000	0.000000	0.000000	
36	0.0001	14.02	100.000000	0.000000	0.000000	0.000000	
37	0.0001	14.29	100.000000	0.000000	0.000000	0.000000	
		Sums:		100.00	100.00		

Grainsize Statistics
Percentiles

	phi	mm
5	1.33	0.399
16	1.87	0.274
25	2.08	0.236
50	2.51	0.175
75	2.93	0.131
84	3.12	0.115
95	3.46	0.091

Column: 50
Sample ID: 2014-12-12HW

Folks' Graphic Statistics

	Mean (Mz)	Sorting (σI)	Skewness (SkI)	Kurtosis (KG)	Mean *mm*
phi	2.500	0.635	-0.076	1.035	0.177

Table II.50: *Results summary for sample 50: High intertidal zone, western transect, Wainamu Beach..*
Sample collected on the 16th of July, 2014.

Column: 51 **Density:** 2650
Volume: 0.010
Sample ID: 2014-7-16HW

Malvern data Phi	Malvern data Micron	Vol %	Equivalent Cum wt (g)
-1.00	2000.00	0	0.0
-0.75	1680.00	0	0.0
-0.50	1410.00	0	0.0
-0.25	1190.00	0	0.0
0.00	1000.00	0	0.0
0.25	840.00	0	0.0
0.49	710.00	0	0.0
0.76	590.00	0	0.0
1.00	500.00	0.006886	0.0
1.25	420.00	0.617115	0.2
1.51	350.00	3.339887	0.9
1.74	300.00	8.419383	2.2
2.00	250.00	18.561026	4.9
2.25	210.00	32.268484	8.6
2.50	177.00	48.174541	12.8
2.75	149.00	64.49665	17.1
3.00	125.00	79.079948	21.0
3.25	105.00	89.81399	23.8
3.51	88.00	96.391702	25.5
3.76	74.00	99.298822	26.3
3.99	63.00	99.989914	26.5
4.24	53.00	100	26.5
4.51	44.00	100	26.5
4.76	37.00	100	26.5
5.01	31.00	100	26.5
6.00	15.60	100	26.5
6.64	10.00	100	26.5
7.00	7.80	100	26.5
8.00	3.90	100	26.5
8.97	2.00	100	26.5
9.99	0.98	100	26.5
10.48	0.70	100	26.5
10.99	0.49	100	26.5
12.02	0.24	100	26.5
13.02	0.12	100	26.5
14.02	0.06	100	26.5
14.29	0.05	100	26.5
		Total weight:	26.5

	mm	phi	Cum wt (g)	Int wt (g)	Int wt%	Cum % finer	Modes
1	2.0000	-1.00	0.000000	0.000000	0.000000	100.000000	
2	1.6800	-0.75	0.000000	0.000000	0.000000	100.000000	
3	1.4100	-0.50	0.000000	0.000000	0.000000	100.000000	
4	1.1900	-0.25	0.000000	0.000000	0.000000	100.000000	
5	1.0000	0.00	0.000000	0.000000	0.000000	100.000000	8
6	0.8400	0.25	0.000000	0.000000	0.000000	100.000000	
7	0.7100	0.49	0.000000	0.000000	0.000000	100.000000	
8	0.5900	0.76	0.000000	0.000000	0.000000	100.000000	
9	0.5000	1.00	0.006886	0.006886	0.006886	99.993114	
10	0.4200	1.25	0.617115	0.610229	0.610229	99.382885	
11	0.3500	1.51	3.339887	2.722772	2.722772	96.660113	
12	0.3000	1.74	8.419383	5.079496	5.079496	91.580617	
13	0.2500	2.00	18.561026	10.141643	10.141643	81.438974	
14	0.2100	2.25	32.268484	13.707458	13.707458	67.731516	
15	0.1770	2.50	48.174541	15.906057	15.906057	51.825459	
16	0.1490	2.75	64.496650	16.322109	16.322109	35.503350	mode at 2.622397
17	0.1250	3.00	79.079948	14.583298	14.583298	20.920052	
18	0.1050	3.25	89.813990	10.734042	10.734042	10.186010	
19	0.0880	3.51	96.391702	6.577712	6.577712	3.608298	
20	0.0740	3.76	99.298822	2.907120	2.907120	0.701178	
21	0.0630	3.99	99.989914	0.691092	0.691092	0.010086	
22	0.0530	4.24	100.000000	0.010086	0.010086	0.000000	
23	0.0440	4.51	100.000000	0.000000	0.000000	0.000000	
24	0.0370	4.76	100.000000	0.000000	0.000000	0.000000	
25	0.0310	5.01	100.000000	0.000000	0.000000	0.000000	
26	0.0156	6.00	100.000000	0.000000	0.000000	0.000000	
27	0.0100	6.64	100.000000	0.000000	0.000000	0.000000	
28	0.0078	7.00	100.000000	0.000000	0.000000	0.000000	
29	0.0039	8.00	100.000000	0.000000	0.000000	0.000000	
30	0.0020	8.97	100.000000	0.000000	0.000000	0.000000	
31	0.0010	9.99	100.000000	0.000000	0.000000	0.000000	
32	0.0007	10.48	100.000000	0.000000	0.000000	0.000000	
33	0.0005	10.99	100.000000	0.000000	0.000000	0.000000	
34	0.0002	12.02	100.000000	0.000000	0.000000	0.000000	
35	0.0001	13.02	100.000000	0.000000	0.000000	0.000000	
36	0.0001	14.02	100.000000	0.000000	0.000000	0.000000	
37	0.0001	14.29	100.000000	0.000000	0.000000	0.000000	
	Sums:			100.00	100.00		

Grainsize Statistics
Percentiles

	phi	*mm*
5	1.59	0.333
16	1.93	0.262
25	2.12	0.230
50	2.53	0.174
75	2.93	0.131
84	3.12	0.115
95	3.45	0.091

Column: 51
Sample ID: 2014-7-16HW

Folks' Graphic Statistics

	Mean (Mz)	Sorting (σI)	Skewness (SkI)	Kurtosis (KG)	Mean *mm*
phi	2.525	0.578	-0.005	0.943	0.174

Table II.51: *Results summary for sample 51: Low intertidal zone, mid transect, Wainamu Beach. Sample collected on the 16th of July, 2014.*

Column: 52 **Density:** 2650
Volume: 0.010
Sample ID: 2014-7-16LM

Malvern data Phi	Malvern data Micron	Vol %	Equivalent Cum wt (g)
-1.00	2000.00	0	0.0
-0.75	1680.00	0	0.0
-0.50	1410.00	0	0.0
-0.25	1190.00	0	0.0
0.00	1000.00	0	0.0
0.25	840.00	0	0.0
0.49	710.00	0	0.0
0.76	590.00	0	0.0
1.00	500.00	0.599854	0.2
1.25	420.00	3.229377	0.9
1.51	350.00	9.668633	2.6
1.74	300.00	18.778382	5.0
2.00	250.00	33.582765	8.9
2.25	210.00	50.208225	13.3
2.50	177.00	66.458806	17.6
2.75	149.00	80.449869	21.3
3.00	125.00	90.743202	24.0
3.25	105.00	96.745332	25.6
3.51	88.00	99.405847	26.3
3.76	74.00	99.994748	26.5
3.99	63.00	100	26.5
4.24	53.00	100	26.5
4.51	44.00	100	26.5
4.76	37.00	100	26.5
5.01	31.00	100	26.5
6.00	15.60	100	26.5
6.64	10.00	100	26.5
7.00	7.80	100	26.5
8.00	3.90	100	26.5
8.97	2.00	100	26.5
9.99	0.98	100	26.5
10.48	0.70	100	26.5
10.99	0.49	100	26.5
12.02	0.24	100	26.5
13.02	0.12	100	26.5
14.02	0.06	100	26.5
14.29	0.05	100	26.5
	Total weight:		26.5

Column: 52
Sample ID: 2014-7-16LM

Folks' Graphic Statistics

	Mean (Mz)	Sorting (σI)	Skewness (SkI)	Kurtosis (KG)	Mean *mm*
phi	2.251	0.572	0.004	0.947	0.210

	mm	phi	Cum wt (g)	Int wt (g)	Int wt%	Cum % finer	Modes
1	2.0000	-1.00	0.000000	0.000000	0.000000	100.000000	
2	1.6800	-0.75	0.000000	0.000000	0.000000	100.000000	
3	1.4100	-0.50	0.000000	0.000000	0.000000	100.000000	
4	1.1900	-0.25	0.000000	0.000000	0.000000	100.000000	
5	1.0000	0.00	0.000000	0.000000	0.000000	100.000000	8
6	0.8400	0.25	0.000000	0.000000	0.000000	100.000000	
7	0.7100	0.49	0.000000	0.000000	0.000000	100.000000	
8	0.5900	0.76	0.000000	0.000000	0.000000	100.000000	
9	0.5000	1.00	0.599854	0.599854	0.599854	99.400146	
10	0.4200	1.25	3.229377	2.629523	2.629523	96.770623	
11	0.3500	1.51	9.668633	6.439256	6.439256	90.331367	
12	0.3000	1.74	18.778382	9.109749	9.109749	81.221618	
13	0.2500	2.00	33.582765	14.804383	14.804383	66.417235	
14	0.2100	2.25	50.208225	16.625460	16.625460	49.791775	mode at 2.125769
15	0.1770	2.50	66.458806	16.250581	16.250581	33.541194	
16	0.1490	2.75	80.449869	13.991063	13.991063	19.550131	
17	0.1250	3.00	90.743202	10.293333	10.293333	9.256798	
18	0.1050	3.25	96.745332	6.002130	6.002130	3.254668	
19	0.0880	3.51	99.405847	2.660515	2.660515	0.594153	
20	0.0740	3.76	99.994748	0.588901	0.588901	0.005252	
21	0.0630	3.99	100.000000	0.005252	0.005252	0.000000	
22	0.0530	4.24	100.000000	0.000000	0.000000	0.000000	
23	0.0440	4.51	100.000000	0.000000	0.000000	0.000000	
24	0.0370	4.76	100.000000	0.000000	0.000000	0.000000	
25	0.0310	5.01	100.000000	0.000000	0.000000	0.000000	
26	0.0156	6.00	100.000000	0.000000	0.000000	0.000000	
27	0.0100	6.64	100.000000	0.000000	0.000000	0.000000	
28	0.0078	7.00	100.000000	0.000000	0.000000	0.000000	
29	0.0039	8.00	100.000000	0.000000	0.000000	0.000000	
30	0.0020	8.97	100.000000	0.000000	0.000000	0.000000	
31	0.0010	9.99	100.000000	0.000000	0.000000	0.000000	
32	0.0007	10.48	100.000000	0.000000	0.000000	0.000000	
33	0.0005	10.99	100.000000	0.000000	0.000000	0.000000	
34	0.0002	12.02	100.000000	0.000000	0.000000	0.000000	
35	0.0001	13.02	100.000000	0.000000	0.000000	0.000000	
36	0.0001	14.02	100.000000	0.000000	0.000000	0.000000	
37	0.0001	14.29	100.000000	0.000000	0.000000	0.000000	
	Sums:			100.00	100.00		

Grainsize Statistics
Percentiles

	phi	*mm*
5	1.32	0.399
16	1.67	0.314
25	1.85	0.278
50	2.25	0.210
75	2.65	0.159
84	2.83	0.140
95	3.18	0.110

Table II.52: *Results summary for sample 52: Mid intertidal zone, mid transect, Wainamu Beach..*
Sample collected on the 16th of July, 2014.

Column: 53 **Density:** 2650
Volume: 0.010
Sample ID: 2014-7-16MM

Malvern data Phi	Malvern data Micron	Vol %	Equivalent Cum wt (g)
-1.00	2000.00	0	0.0
-0.75	1680.00	0	0.0
-0.50	1410.00	0	0.0
-0.25	1190.00	0	0.0
0.00	1000.00	0	0.0
0.25	840.00	0	0.0
0.49	710.00	0	0.0
0.76	590.00	0	0.0
1.00	500.00	0.011221	0.0
1.25	420.00	0.68292	0.2
1.51	350.00	3.248672	0.9
1.74	300.00	7.958802	2.1
2.00	250.00	17.430333	4.6
2.25	210.00	30.481861	8.1
2.50	177.00	46.009852	12.2
2.75	149.00	62.391036	16.5
3.00	125.00	77.444516	20.5
3.25	105.00	88.823298	23.5
3.51	88.00	95.968255	25.4
3.76	74.00	99.199643	26.3
3.99	63.00	99.988062	26.5
4.24	53.00	100	26.5
4.51	44.00	100	26.5
4.76	37.00	100	26.5
5.01	31.00	100	26.5
6.00	15.60	100	26.5
6.64	10.00	100	26.5
7.00	7.80	100	26.5
8.00	3.90	100	26.5
8.97	2.00	100	26.5
9.99	0.98	100	26.5
10.48	0.70	100	26.5
10.99	0.49	100	26.5
12.02	0.24	100	26.5
13.02	0.12	100	26.5
14.02	0.06	100	26.5
14.29	0.05	100	26.5

Total weight: 26.5

	mm	phi	Cum wt (g)	Int wt (g)	Int wt%	Cum % finer	Modes	
1	2.0000	-1.00	0.000000	0.000000	0.000000	100.000000		
2	1.6800	-0.75	0.000000	0.000000	0.000000	100.000000		
3	1.4100	-0.50	0.000000	0.000000	0.000000	100.000000		
4	1.1900	-0.25	0.000000	0.000000	0.000000	100.000000		
5	1.0000	0.00	0.000000	0.000000	0.000000	100.000000		8
6	0.8400	0.25	0.000000	0.000000	0.000000	100.000000		
7	0.7100	0.49	0.000000	0.000000	0.000000	100.000000		
8	0.5900	0.76	0.000000	0.000000	0.000000	100.000000		
9	0.5000	1.00	0.011221	0.011221	0.011221	99.988779		
10	0.4200	1.25	0.682920	0.671699	0.671699	99.317080		
11	0.3500	1.51	3.248672	2.565752	2.565752	96.751328		
12	0.3000	1.74	7.958802	4.710130	4.710130	92.041198		
13	0.2500	2.00	17.430333	9.471531	9.471531	82.569667		
14	0.2100	2.25	30.481861	13.051528	13.051528	69.518139		
15	0.1770	2.50	46.009852	15.527991	15.527991	53.990148		
16	0.1490	2.75	62.391036	16.381184	16.381184	37.608964	mode at 2.622397	
17	0.1250	3.00	77.444516	15.053480	15.053480	22.555484		
18	0.1050	3.25	88.823298	11.378782	11.378782	11.176702		
19	0.0880	3.51	95.968255	7.144957	7.144957	4.031745		
20	0.0740	3.76	99.199643	3.231388	3.231388	0.800357		
21	0.0630	3.99	99.988062	0.788419	0.788419	0.011938		
22	0.0530	4.24	100.000000	0.011938	0.011938	0.000000		
23	0.0440	4.51	100.000000	0.000000	0.000000	0.000000		
24	0.0370	4.76	100.000000	0.000000	0.000000	0.000000		
25	0.0310	5.01	100.000000	0.000000	0.000000	0.000000		
26	0.0156	6.00	100.000000	0.000000	0.000000	0.000000		
27	0.0100	6.64	100.000000	0.000000	0.000000	0.000000		
28	0.0078	7.00	100.000000	0.000000	0.000000	0.000000		
29	0.0039	8.00	100.000000	0.000000	0.000000	0.000000		
30	0.0020	8.97	100.000000	0.000000	0.000000	0.000000		
31	0.0010	9.99	100.000000	0.000000	0.000000	0.000000		
32	0.0007	10.48	100.000000	0.000000	0.000000	0.000000		
33	0.0005	10.99	100.000000	0.000000	0.000000	0.000000		
34	0.0002	12.02	100.000000	0.000000	0.000000	0.000000		
35	0.0001	13.02	100.000000	0.000000	0.000000	0.000000		
36	0.0001	14.02	100.000000	0.000000	0.000000	0.000000		
37	0.0001	14.29	100.000000	0.000000	0.000000	0.000000		
	Sums:			100.00	100.00			

Column: 53
Sample ID: 2014-7-16MM

Folks' Graphic Statistics

	Mean (Mz)	Sorting (σI)	Skewness (SkI)	Kurtosis (KG)	Mean ***mm***
phi	2.555	0.580	-0.018	0.945	0.170

Grainsize Statistics
Percentiles

	phi	*mm*
5	1.60	0.331
16	1.96	0.257
25	2.15	0.226
50	2.56	0.170
75	2.96	0.129
84	3.14	0.113
95	3.47	0.090

Table II.53: *Results summary for sample 53: Low intertidal zone, western transect, Wainamu Beach. Sample collected on the 16th of July, 2014.*

Column: 54 **Density:** 2650
Volume: 0.010
Sample ID: 2014-7-16LW

Malvern data Phi	Malvern data Micron	Vol %	Equivalent Cum wt (g)
-1.00	2000.00	0	0.0
-0.75	1680.00	0	0.0
-0.50	1410.00	0	0.0
-0.25	1190.00	0	0.0
0.00	1000.00	0	0.0
0.25	840.00	0	0.0
0.49	710.00	0	0.0
0.76	590.00	0	0.0
1.00	500.00	0.00902	0.0
1.25	420.00	0.80233	0.2
1.51	350.00	4.490314	1.2
1.74	300.00	11.5888	3.1
2.00	250.00	25.65868	6.8
2.25	210.00	43.714304	11.6
2.50	177.00	62.684521	16.6
2.75	149.00	79.358003	21.0
3.00	125.00	91.225318	24.2
3.25	105.00	97.481268	25.8
3.51	88.00	99.758674	26.4
3.76	74.00	100	26.5
3.99	63.00	100	26.5
4.24	53.00	100	26.5
4.51	44.00	100	26.5
4.76	37.00	100	26.5
5.01	31.00	100	26.5
6.00	15.60	100	26.5
6.64	10.00	100	26.5
7.00	7.80	100	26.5
8.00	3.90	100	26.5
8.97	2.00	100	26.5
9.99	0.98	100	26.5
10.48	0.70	100	26.5
10.99	0.49	100	26.5
12.02	0.24	100	26.5
13.02	0.12	100	26.5
14.02	0.06	100	26.5
14.29	0.05	100	26.5
		Total weight:	26.5

	mm	phi	Cum wt (g)	Int wt (g)	Int wt%	Cum % finer	Modes	
1	2.0000	-1.00	0.000000	0.000000	0.000000	100.000000		
2	1.6800	-0.75	0.000000	0.000000	0.000000	100.000000		
3	1.4100	-0.50	0.000000	0.000000	0.000000	100.000000		
4	1.1900	-0.25	0.000000	0.000000	0.000000	100.000000		
5	1.0000	0.00	0.000000	0.000000	0.000000	100.000000		8
6	0.8400	0.25	0.000000	0.000000	0.000000	100.000000		
7	0.7100	0.49	0.000000	0.000000	0.000000	100.000000		
8	0.5900	0.76	0.000000	0.000000	0.000000	100.000000		
9	0.5000	1.00	0.009020	0.009020	0.009020	99.990980		
10	0.4200	1.25	0.802330	0.793310	0.793310	99.197670		
11	0.3500	1.51	4.490314	3.687984	3.687984	95.509686		
12	0.3000	1.74	11.588800	7.098486	7.098486	88.411200		
13	0.2500	2.00	25.658680	14.069880	14.069880	74.341320		
14	0.2100	2.25	43.714304	18.055624	18.055624	56.285696		
15	0.1770	2.50	62.684521	18.970217	18.970217	37.315479	mode at 2.374859	
16	0.1490	2.75	79.358003	16.673482	16.673482	20.641997		
17	0.1250	3.00	91.225318	11.867315	11.867315	8.774682		
18	0.1050	3.25	97.481268	6.255950	6.255950	2.518732		
19	0.0880	3.51	99.758674	2.277406	2.277406	0.241326		
20	0.0740	3.76	100.000000	0.241326	0.241326	0.000000		
21	0.0630	3.99	100.000000	0.000000	0.000000	0.000000		
22	0.0530	4.24	100.000000	0.000000	0.000000	0.000000		
23	0.0440	4.51	100.000000	0.000000	0.000000	0.000000		
24	0.0370	4.76	100.000000	0.000000	0.000000	0.000000		
25	0.0310	5.01	100.000000	0.000000	0.000000	0.000000		
26	0.0156	6.00	100.000000	0.000000	0.000000	0.000000		
27	0.0100	6.64	100.000000	0.000000	0.000000	0.000000		
28	0.0078	7.00	100.000000	0.000000	0.000000	0.000000		
29	0.0039	8.00	100.000000	0.000000	0.000000	0.000000		
30	0.0020	8.97	100.000000	0.000000	0.000000	0.000000		
31	0.0010	9.99	100.000000	0.000000	0.000000	0.000000		
32	0.0007	10.48	100.000000	0.000000	0.000000	0.000000		
33	0.0005	10.99	100.000000	0.000000	0.000000	0.000000		
34	0.0002	12.02	100.000000	0.000000	0.000000	0.000000		
35	0.0001	13.02	100.000000	0.000000	0.000000	0.000000		
36	0.0001	14.02	100.000000	0.000000	0.000000	0.000000		
37	0.0001	14.29	100.000000	0.000000	0.000000	0.000000		
	Sums:			100.00	100.00			

Column: 54
Sample ID: 2014-7-16LW

Folks' Graphic Statistics

	Mean (Mz)	Sorting (σI)	Skewness (SkI)	Kurtosis (KG)	Mean *mm*
phi	2.333	0.502	0.004	0.957	0.198

Grainsize Statistics
Percentiles

	phi	*mm*
5	1.53	0.346
16	1.82	0.283
25	1.99	0.252
50	2.33	0.198
75	2.68	0.156
84	2.85	0.139
95	3.15	0.113

Table II.54: *Results summary for sample 54: High intertidal zone, mid transect, Wainamu Beach. Sample collected on the 16th of July, 2014.*

Column: 55 **Density:** 2650
Volume: 0.010
Sample ID: 2014-7-16HM

Malvern data Phi	Malvern data Micron	Vol %	Equivalent Cum wt (g)
-1.00	2000.00	0	0.0
-0.75	1680.00	0	0.0
-0.50	1410.00	0	0.0
-0.25	1190.00	0	0.0
0.00	1000.00	0	0.0
0.25	840.00	0	0.0
0.49	710.00	0	0.0
0.76	590.00	0	0.0
1.00	500.00	0.026843	0.0
1.25	420.00	1.333765	0.4
1.51	350.00	5.474234	1.5
1.74	300.00	12.293408	3.3
2.00	250.00	24.689134	6.5
2.25	210.00	40.091651	10.6
2.50	177.00	56.611988	15.0
2.75	149.00	72.252336	19.1
3.00	125.00	85.054002	22.5
3.25	105.00	93.581056	24.8
3.51	88.00	98.172423	26.0
3.76	74.00	99.852698	26.5
3.99	63.00	100	26.5
4.24	53.00	100	26.5
4.51	44.00	100	26.5
4.76	37.00	100	26.5
5.01	31.00	100	26.5
6.00	15.60	100	26.5
6.64	10.00	100	26.5
7.00	7.80	100	26.5
8.00	3.90	100	26.5
8.97	2.00	100	26.5
9.99	0.98	100	26.5
10.48	0.70	100	26.5
10.99	0.49	100	26.5
12.02	0.24	100	26.5
13.02	0.12	100	26.5
14.02	0.06	100	26.5
14.29	0.05	100	26.5
		Total weight:	26.5

	mm	phi	Cum wt (g)	Int wt (g)	Int wt%	Cum % finer	Modes	
1	2.0000	-1.00	0.000000	0.000000	0.000000	100.000000		
2	1.6800	-0.75	0.000000	0.000000	0.000000	100.000000		
3	1.4100	-0.50	0.000000	0.000000	0.000000	100.000000		
4	1.1900	-0.25	0.000000	0.000000	0.000000	100.000000		
5	1.0000	0.00	0.000000	0.000000	0.000000	100.000000		8
6	0.8400	0.25	0.000000	0.000000	0.000000	100.000000		
7	0.7100	0.49	0.000000	0.000000	0.000000	100.000000		
8	0.5900	0.76	0.000000	0.000000	0.000000	100.000000		
9	0.5000	1.00	0.026843	0.026843	0.026843	99.973157		
10	0.4200	1.25	1.333765	1.306922	1.306922	98.666235		
11	0.3500	1.51	5.474234	4.140469	4.140469	94.525766		
12	0.3000	1.74	12.293408	6.819174	6.819174	87.706592		
13	0.2500	2.00	24.689134	12.395726	12.395726	75.310866		
14	0.2100	2.25	40.091651	15.402517	15.402517	59.908349		
15	0.1770	2.50	56.611988	16.520337	16.520337	43.388012	mode at 2.374859	
16	0.1490	2.75	72.252336	15.640348	15.640348	27.747664		
17	0.1250	3.00	85.054002	12.801666	12.801666	14.945998		
18	0.1050	3.25	93.581056	8.527054	8.527054	6.418944		
19	0.0880	3.51	98.172423	4.591367	4.591367	1.827577		
20	0.0740	3.76	99.852698	1.680275	1.680275	0.147302		
21	0.0630	3.99	100.000000	0.147302	0.147302	0.000000		
22	0.0530	4.24	100.000000	0.000000	0.000000	0.000000		
23	0.0440	4.51	100.000000	0.000000	0.000000	0.000000		
24	0.0370	4.76	100.000000	0.000000	0.000000	0.000000		
25	0.0310	5.01	100.000000	0.000000	0.000000	0.000000		
26	0.0156	6.00	100.000000	0.000000	0.000000	0.000000		
27	0.0100	6.64	100.000000	0.000000	0.000000	0.000000		
28	0.0078	7.00	100.000000	0.000000	0.000000	0.000000		
29	0.0039	8.00	100.000000	0.000000	0.000000	0.000000		
30	0.0020	8.97	100.000000	0.000000	0.000000	0.000000		
31	0.0010	9.99	100.000000	0.000000	0.000000	0.000000		
32	0.0007	10.48	100.000000	0.000000	0.000000	0.000000		
33	0.0005	10.99	100.000000	0.000000	0.000000	0.000000		
34	0.0002	12.02	100.000000	0.000000	0.000000	0.000000		
35	0.0001	13.02	100.000000	0.000000	0.000000	0.000000		
36	0.0001	14.02	100.000000	0.000000	0.000000	0.000000		
37	0.0001	14.29	100.000000	0.000000	0.000000	0.000000		
	Sums:			100.00	100.00			

Column: 55
Sample ID: 2014-7-16HM

Folks' Graphic Statistics

	Mean (Mz)	Sorting (σI)	Skewness (SkI)	Kurtosis (KG)	Mean *mm*
phi	2.398	0.571	0.002	0.950	0.190

Grainsize Statistics
Percentiles

	phi	*mm*
5	1.48	0.357
16	1.82	0.284
25	2.01	0.249
50	2.40	0.190
75	2.80	0.143
84	2.98	0.127
95	3.33	0.099

Table II.55: *Results summary for sample 55: Low intertidal zone, eastern transect, Wainamu Beach. Sample collected on the 16th of July, 2014.*

Column: 56 **Density:** 2650
Volume: 0.010
Sample ID: 2014-7-16LE

Malvern data Phi	Malvern data Micron	Vol %	Equivalent Cum wt (g)
-1.00	2000.00	0	0.0
-0.75	1680.00	0	0.0
-0.50	1410.00	0	0.0
-0.25	1190.00	0	0.0
0.00	1000.00	0	0.0
0.25	840.00	0	0.0
0.49	710.00	0	0.0
0.76	590.00	0.00549	0.0
1.00	500.00	0.697481	0.2
1.25	420.00	3.589387	1.0
1.51	350.00	10.372808	2.7
1.74	300.00	19.623161	5.2
2.00	250.00	34.09657	9.0
2.25	210.00	49.663778	13.2
2.50	177.00	64.167892	17.0
2.75	149.00	75.968962	20.1
3.00	125.00	84.065623	22.3
3.25	105.00	88.385482	23.4
3.51	88.00	90.088379	23.9
3.76	74.00	90.414542	24.0
3.99	63.00	90.419955	24.0
4.24	53.00	90.419955	24.0
4.51	44.00	90.715566	24.0
4.76	37.00	91.362072	24.2
5.01	31.00	92.22968	24.4
6.00	15.60	94.956618	25.2
6.64	10.00	96.119064	25.5
7.00	7.80	96.846342	25.7
8.00	3.90	98.768019	26.2
8.97	2.00	99.716287	26.4
9.99	0.98	100	26.5
10.48	0.70	100	26.5
10.99	0.49	100	26.5
12.02	0.24	100	26.5
13.02	0.12	100	26.5
14.02	0.06	100	26.5
14.29	0.05	100	26.5

Total weight: 26.5

	mm	phi	Cum wt (g)	Int wt (g)	Int wt%	Cum % finer	Modes
1	2.0000	-1.00	0.000000	0.000000	0.000000	100.000000	
2	1.6800	-0.75	0.000000	0.000000	0.000000	100.000000	
3	1.4100	-0.50	0.000000	0.000000	0.000000	100.000000	
4	1.1900	-0.25	0.000000	0.000000	0.000000	100.000000	
5	1.0000	0.00	0.000000	0.000000	0.000000	100.000000	
6	0.8400	0.25	0.000000	0.000000	0.000000	100.000000	
7	0.7100	0.49	0.000000	0.000000	0.000000	100.000000	
8	0.5900	0.76	0.005490	0.005490	0.005490	99.994510	
9	0.5000	1.00	0.697481	0.691991	0.691991	99.302519	
10	0.4200	1.25	3.589387	2.891906	2.891906	96.410613	
11	0.3500	1.51	10.372808	6.783421	6.783421	89.627192	
12	0.3000	1.74	19.623161	9.250353	9.250353	80.376839	
13	0.2500	2.00	34.096570	14.473409	14.473409	65.903430	
14	0.2100	2.25	49.663778	15.567208	15.567208	50.336222	mode at 2.125769
15	0.1770	2.50	64.167892	14.504114	14.504114	35.832108	
16	0.1490	2.75	75.968962	11.801070	11.801070	24.031038	
17	0.1250	3.00	84.065623	8.096661	8.096661	15.934377	
18	0.1050	3.25	88.385482	4.319859	4.319859	11.614518	
19	0.0880	3.51	90.088379	1.702897	1.702897	9.911621	
20	0.0740	3.76	90.414542	0.326163	0.326163	9.585458	
21	0.0630	3.99	90.419955	0.005413	0.005413	9.580045	
22	0.0530	4.24	90.419955	0.000000	0.000000	9.580045	
23	0.0440	4.51	90.715566	0.295611	0.295611	9.284434	
24	0.0370	4.76	91.362072	0.646506	0.646506	8.637928	
25	0.0310	5.01	92.229680	0.867608	0.867608	7.770320	
26	0.0156	6.00	94.956618	2.726938	2.726938	5.043382	mode at 5.506949
27	0.0100	6.64	96.119064	1.162446	1.162446	3.880936	
28	0.0078	7.00	96.846342	0.727278	0.727278	3.153658	
29	0.0039	8.00	98.768019	1.921677	1.921677	1.231981	mode at 7.50231
30	0.0020	8.97	99.716287	0.948268	0.948268	0.283713	
31	0.0010	9.99	100.000000	0.283713	0.283713	0.000000	
32	0.0007	10.48	100.000000	0.000000	0.000000	0.000000	
33	0.0005	10.99	100.000000	0.000000	0.000000	0.000000	
34	0.0002	12.02	100.000000	0.000000	0.000000	0.000000	
35	0.0001	13.02	100.000000	0.000000	0.000000	0.000000	
36	0.0001	14.02	100.000000	0.000000	0.000000	0.000000	
37	0.0001	14.29	100.000000	0.000000	0.000000	0.000000	
	Sums:			100.00	100.00		

Grainsize Statistics
Percentiles

	phi	*mm*
5	1.31	0.404
16	1.65	0.319
25	1.83	0.280
50	2.26	0.209
75	2.73	0.151
84	3.00	0.125
95	6.03	0.015

Column: 56
Sample ID: 2014-7-16LE

Folks' Graphic Statistics

	Mean (Mz)	Sorting (σI)	Skewness (SkI)	Kurtosis (KG)	Mean *mm*
phi	2.302	1.052	0.348	2.170	0.203

Table II.56: *Results summary for sample 56: High intertidal zone, eastern transect, Wainamu Beach. Sample collected on the 16th of July, 2014.*

Column: 57 **Density:** 2650
Volume: 0.010
Sample ID: 2014-7-16HE*

Malvern data Phi	Malvern data Micron	Vol %	Equivalent Cum wt (g)
-1.00	2000.00	0	0.0
-0.75	1680.00	0	0.0
-0.50	1410.00	0	0.0
-0.25	1190.00	0	0.0
0.00	1000.00	0	0.0
0.25	840.00	0	0.0
0.49	710.00	0	0.0
0.76	590.00	0	0.0
1.00	500.00	0.007132	0.0
1.25	420.00	0.679207	0.2
1.51	350.00	3.888257	1.0
1.74	300.00	10.150881	2.7
2.00	250.00	22.800757	6.0
2.25	210.00	39.497168	10.5
2.50	177.00	57.742146	15.3
2.75	149.00	74.6931	19.8
3.00	125.00	87.766558	23.3
3.25	105.00	95.572468	25.3
3.51	88.00	99.079218	26.3
3.76	74.00	99.977704	26.5
3.99	63.00	100	26.5
4.24	53.00	100	26.5
4.51	44.00	100	26.5
4.76	37.00	100	26.5
5.01	31.00	100	26.5
6.00	15.60	100	26.5
6.64	10.00	100	26.5
7.00	7.80	100	26.5
8.00	3.90	100	26.5
8.97	2.00	100	26.5
9.99	0.98	100	26.5
10.48	0.70	100	26.5
10.99	0.49	100	26.5
12.02	0.24	100	26.5
13.02	0.12	100	26.5
14.02	0.06	100	26.5
14.29	0.05	100	26.5
		Total weight:	26.5

	mm	phi	Cum wt (g)	Int wt (g)	Int wt%	Cum % finer	Modes	
1	2.0000	-1.00	0.000000	0.000000	0.000000	100.000000		
2	1.6800	-0.75	0.000000	0.000000	0.000000	100.000000		
3	1.4100	-0.50	0.000000	0.000000	0.000000	100.000000		
4	1.1900	-0.25	0.000000	0.000000	0.000000	100.000000		
5	1.0000	0.00	0.000000	0.000000	0.000000	100.000000		8
6	0.8400	0.25	0.000000	0.000000	0.000000	100.000000		
7	0.7100	0.49	0.000000	0.000000	0.000000	100.000000		
8	0.5900	0.76	0.000000	0.000000	0.000000	100.000000		
9	0.5000	1.00	0.007132	0.007132	0.007132	99.992868		
10	0.4200	1.25	0.679207	0.672075	0.672075	99.320793		
11	0.3500	1.51	3.888257	3.209050	3.209050	96.111743		
12	0.3000	1.74	10.150881	6.262624	6.262624	89.849119		
13	0.2500	2.00	22.800757	12.649876	12.649876	77.199243		
14	0.2100	2.25	39.497168	16.696411	16.696411	60.502832		
15	0.1770	2.50	57.742146	18.244978	18.244978	42.257854	mode at 2.374859	
16	0.1490	2.75	74.693100	16.950954	16.950954	25.306900		
17	0.1250	3.00	87.766558	13.073458	13.073458	12.233442		
18	0.1050	3.25	95.572468	7.805910	7.805910	4.427532		
19	0.0880	3.51	99.079218	3.506750	3.506750	0.920782		
20	0.0740	3.76	99.977704	0.898486	0.898486	0.022296		
21	0.0630	3.99	100.000000	0.022296	0.022296	0.000000		
22	0.0530	4.24	100.000000	0.000000	0.000000	0.000000		
23	0.0440	4.51	100.000000	0.000000	0.000000	0.000000		
24	0.0370	4.76	100.000000	0.000000	0.000000	0.000000		
25	0.0310	5.01	100.000000	0.000000	0.000000	0.000000		
26	0.0156	6.00	100.000000	0.000000	0.000000	0.000000		
27	0.0100	6.64	100.000000	0.000000	0.000000	0.000000		
28	0.0078	7.00	100.000000	0.000000	0.000000	0.000000		
29	0.0039	8.00	100.000000	0.000000	0.000000	0.000000		
30	0.0020	8.97	100.000000	0.000000	0.000000	0.000000		
31	0.0010	9.99	100.000000	0.000000	0.000000	0.000000		
32	0.0007	10.48	100.000000	0.000000	0.000000	0.000000		
33	0.0005	10.99	100.000000	0.000000	0.000000	0.000000		
34	0.0002	12.02	100.000000	0.000000	0.000000	0.000000		
35	0.0001	13.02	100.000000	0.000000	0.000000	0.000000		
36	0.0001	14.02	100.000000	0.000000	0.000000	0.000000		
37	0.0001	14.29	100.000000	0.000000	0.000000	0.000000		
	Sums:			100.00	100.00			

Column: 57
Sample ID: 2014-7-16HE*

Folks' Graphic Statistics

	Mean (Mz)	Sorting (σI)	Skewness (SkI)	Kurtosis (KG)	Mean *mm*
phi	2.393	0.522	-0.001	0.956	0.190

Grainsize Statistics
Percentiles

	phi	*mm*
5	1.55	0.341
16	1.86	0.276
25	2.03	0.244
50	2.39	0.190
75	2.75	0.148
84	2.93	0.131
95	3.23	0.106

Table II.57: *Results summary for sample 57: Mid intertidal zone, western transect, Wainamu Beach. Sample collected on the 16th of July, 2014.*

Column: 58 **Density:** 2650
Volume: 0.010
Sample ID: 2014-7-16MW*

Malvern data Phi	Malvern data Micron	Vol %	Equivalent Cum wt (g)
-1.00	2000.00	0	0.0
-0.75	1680.00	0	0.0
-0.50	1410.00	0	0.0
-0.25	1190.00	0	0.0
0.00	1000.00	0	0.0
0.25	840.00	0	0.0
0.49	710.00	0	0.0
0.76	590.00	0	0.0
1.00	500.00	0	0.0
1.25	420.00	0.214689	0.1
1.51	350.00	2.149043	0.6
1.74	300.00	6.527446	1.7
2.00	250.00	16.48348	4.4
2.25	210.00	31.081526	8.2
2.50	177.00	48.683015	12.9
2.75	149.00	66.741929	17.7
3.00	125.00	82.215939	21.8
3.25	105.00	92.610157	24.5
3.51	88.00	98.026058	26.0
3.76	74.00	99.841087	26.5
3.99	63.00	100	26.5
4.24	53.00	100	26.5
4.51	44.00	100	26.5
4.76	37.00	100	26.5
5.01	31.00	100	26.5
6.00	15.60	100	26.5
6.64	10.00	100	26.5
7.00	7.80	100	26.5
8.00	3.90	100	26.5
8.97	2.00	100	26.5
9.99	0.98	100	26.5
10.48	0.70	100	26.5
10.99	0.49	100	26.5
12.02	0.24	100	26.5
13.02	0.12	100	26.5
14.02	0.06	100	26.5
14.29	0.05	100	26.5
		Total weight:	26.5

	mm	phi	Cum wt (g)	Int wt (g)	Int wt%	Cum % finer	Modes	
1	2.0000	-1.00	0.000000	0.000000	0.000000	100.000000		
2	1.6800	-0.75	0.000000	0.000000	0.000000	100.000000		
3	1.4100	-0.50	0.000000	0.000000	0.000000	100.000000		
4	1.1900	-0.25	0.000000	0.000000	0.000000	100.000000		
5	1.0000	0.00	0.000000	0.000000	0.000000	100.000000		8
6	0.8400	0.25	0.000000	0.000000	0.000000	100.000000		
7	0.7100	0.49	0.000000	0.000000	0.000000	100.000000		
8	0.5900	0.76	0.000000	0.000000	0.000000	100.000000		
9	0.5000	1.00	0.000000	0.000000	0.000000	100.000000		
10	0.4200	1.25	0.214689	0.214689	0.214689	99.785311		
11	0.3500	1.51	2.149043	1.934354	1.934354	97.850957		
12	0.3000	1.74	6.527446	4.378403	4.378403	93.472554		
13	0.2500	2.00	16.483480	9.956034	9.956034	83.516520		
14	0.2100	2.25	31.081526	14.598046	14.598046	68.918474		
15	0.1770	2.50	48.683015	17.601489	17.601489	51.316985		
16	0.1490	2.75	66.741929	18.058914	18.058914	33.258071	mode at 2.622397	
17	0.1250	3.00	82.215939	15.474010	15.474010	17.784061		
18	0.1050	3.25	92.610157	10.394218	10.394218	7.389843		
19	0.0880	3.51	98.026058	5.415901	5.415901	1.973942		
20	0.0740	3.76	99.841087	1.815029	1.815029	0.158913		
21	0.0630	3.99	100.000000	0.158913	0.158913	0.000000		
22	0.0530	4.24	100.000000	0.000000	0.000000	0.000000		
23	0.0440	4.51	100.000000	0.000000	0.000000	0.000000		
24	0.0370	4.76	100.000000	0.000000	0.000000	0.000000		
25	0.0310	5.01	100.000000	0.000000	0.000000	0.000000		
26	0.0156	6.00	100.000000	0.000000	0.000000	0.000000		
27	0.0100	6.64	100.000000	0.000000	0.000000	0.000000		
28	0.0078	7.00	100.000000	0.000000	0.000000	0.000000		
29	0.0039	8.00	100.000000	0.000000	0.000000	0.000000		
30	0.0020	8.97	100.000000	0.000000	0.000000	0.000000		
31	0.0010	9.99	100.000000	0.000000	0.000000	0.000000		
32	0.0007	10.48	100.000000	0.000000	0.000000	0.000000		
33	0.0005	10.99	100.000000	0.000000	0.000000	0.000000		
34	0.0002	12.02	100.000000	0.000000	0.000000	0.000000		
35	0.0001	13.02	100.000000	0.000000	0.000000	0.000000		
36	0.0001	14.02	100.000000	0.000000	0.000000	0.000000		
37	0.0001	14.29	100.000000	0.000000	0.000000	0.000000		
	Sums:			100.00	100.00			

Grainsize Statistics
Percentiles

	phi	*mm*
5	1.66	0.317
16	1.99	0.252
25	2.15	0.226
50	2.52	0.175
75	2.88	0.136
84	3.04	0.121
95	3.36	0.097

Column: 58
Sample ID: 2014-7-16MW*

Folks' Graphic Statistics

	Mean (Mz)	Sorting (σI)	Skewness (SkI)	Kurtosis (KG)	Mean *mm*
phi	2.516	0.522	-0.004	0.950	0.175

Table II.58: *Results summary for sample 58: Mid intertidal zone, northern transect, Northern Ngarunui Beach. Sample collected on the 6th of February, 2015.*

Column: 59 **Density:** 2650
Volume: 0.010
Sample ID: 6-2-2015nm

Malvern data Phi	Malvern data Micron	Vol %	Equivalent Cum wt (g)
-1.00	2000.00	0	0.0
-0.75	1680.00	0	0.0
-0.50	1410.00	0	0.0
-0.25	1190.00	0	0.0
0.00	1000.00	0	0.0
0.25	840.00	0	0.0
0.49	710.00	0	0.0
0.76	590.00	0.369335	0.1
1.00	500.00	2.552916	0.7
1.25	420.00	8.753681	2.3
1.51	350.00	21.026593	5.6
1.74	300.00	35.754133	9.5
2.00	250.00	55.774217	14.8
2.25	210.00	73.798865	19.6
2.50	177.00	87.282048	23.1
2.75	149.00	95.474033	25.3
3.00	125.00	99.144147	26.3
3.25	105.00	99.943741	26.5
3.51	88.00	100	26.5
3.76	74.00	100	26.5
3.99	63.00	100	26.5
4.24	53.00	100	26.5
4.51	44.00	100	26.5
4.76	37.00	100	26.5
5.01	31.00	100	26.5
6.00	15.60	100	26.5
6.64	10.00	100	26.5
7.00	7.80	100	26.5
8.00	3.90	100	26.5
8.97	2.00	100	26.5
9.99	0.98	100	26.5
10.48	0.70	100	26.5
10.99	0.49	100	26.5
12.02	0.24	100	26.5
13.02	0.12	100	26.5
14.02	0.06	100	26.5
14.29	0.05	100	26.5

Total weight: 26.5

	mm	phi	Cum wt (g)	Int wt (g)	Int wt%	Cum % finer	Modes	
1	2.0000	-1.00	0.000000	0.000000	0.000000	100.000000		
2	1.6800	-0.75	0.000000	0.000000	0.000000	100.000000		
3	1.4100	-0.50	0.000000	0.000000	0.000000	100.000000		
4	1.1900	-0.25	0.000000	0.000000	0.000000	100.000000		
5	1.0000	0.00	0.000000	0.000000	0.000000	100.000000		8
6	0.8400	0.25	0.000000	0.000000	0.000000	100.000000		
7	0.7100	0.49	0.000000	0.000000	0.000000	100.000000		
8	0.5900	0.76	0.369335	0.369335	0.369335	99.630665		
9	0.5000	1.00	2.552916	2.183581	2.183581	97.447084		
10	0.4200	1.25	8.753681	6.200765	6.200765	91.246319		
11	0.3500	1.51	21.026593	12.272912	12.272912	78.973407		
12	0.3000	1.74	35.754133	14.727540	14.727540	64.245867		
13	0.2500	2.00	55.774217	20.020084	20.020084	44.225783	mode at 1.868483	
14	0.2100	2.25	73.798865	18.024648	18.024648	26.201135		
15	0.1770	2.50	87.282048	13.483183	13.483183	12.717952		
16	0.1490	2.75	95.474033	8.191985	8.191985	4.525967		
17	0.1250	3.00	99.144147	3.670114	3.670114	0.855853		
18	0.1050	3.25	99.943741	0.799594	0.799594	0.056259		
19	0.0880	3.51	100.000000	0.056259	0.056259	0.000000		
20	0.0740	3.76	100.000000	0.000000	0.000000	0.000000		
21	0.0630	3.99	100.000000	0.000000	0.000000	0.000000		
22	0.0530	4.24	100.000000	0.000000	0.000000	0.000000		
23	0.0440	4.51	100.000000	0.000000	0.000000	0.000000		
24	0.0370	4.76	100.000000	0.000000	0.000000	0.000000		
25	0.0310	5.01	100.000000	0.000000	0.000000	0.000000		
26	0.0156	6.00	100.000000	0.000000	0.000000	0.000000		
27	0.0100	6.64	100.000000	0.000000	0.000000	0.000000		
28	0.0078	7.00	100.000000	0.000000	0.000000	0.000000		
29	0.0039	8.00	100.000000	0.000000	0.000000	0.000000		
30	0.0020	8.97	100.000000	0.000000	0.000000	0.000000		
31	0.0010	9.99	100.000000	0.000000	0.000000	0.000000		
32	0.0007	10.48	100.000000	0.000000	0.000000	0.000000		
33	0.0005	10.99	100.000000	0.000000	0.000000	0.000000		
34	0.0002	12.02	100.000000	0.000000	0.000000	0.000000		
35	0.0001	13.02	100.000000	0.000000	0.000000	0.000000		
36	0.0001	14.02	100.000000	0.000000	0.000000	0.000000		
37	0.0001	14.29	100.000000	0.000000	0.000000	0.000000		
		Sums:		100.00	100.00			

Grainsize Statistics
Percentiles

	phi	*mm*
5	1.10	0.467
16	1.41	0.377
25	1.57	0.336
50	1.92	0.263
75	2.27	0.207
84	2.44	0.185
95	2.73	0.150

Column: 59
Sample ID: 6-2-2015nm

Folks' Graphic Statistics

	Mean (Mz)	Sorting (σI)	Skewness (SkI)	Kurtosis (KG)	Mean *mm*
phi	1.923	0.505	-0.007	0.958	0.264

Table II.59: *Results summary for sample 59: Mid intertidal zone, southern transect, Northern Ngarunui Beach. Sample collected on the 6th of February, 2015.*

Column: 60 **Density:** 2650
Volume: 0.010
Sample ID: 6-2-2015sm

Malvern data Phi	Malvern data Micron	Vol %	Equivalent Cum wt (g)
-1.00	2000.00	0	0.0
-0.75	1680.00	0	0.0
-0.50	1410.00	0	0.0
-0.25	1190.00	0	0.0
0.00	1000.00	0	0.0
0.25	840.00	0	0.0
0.49	710.00	0	0.0
0.76	590.00	0.251012	0.1
1.00	500.00	1.953871	0.5
1.25	420.00	7.086943	1.9
1.51	350.00	17.767363	4.7
1.74	300.00	31.18703	8.3
2.00	250.00	50.371043	13.3
2.25	210.00	68.715808	18.2
2.50	177.00	83.43767	22.1
2.75	149.00	93.234211	24.7
3.00	125.00	98.237832	26.0
3.25	105.00	99.860168	26.5
3.51	88.00	100	26.5
3.76	74.00	100	26.5
3.99	63.00	100	26.5
4.24	53.00	100	26.5
4.51	44.00	100	26.5
4.76	37.00	100	26.5
5.01	31.00	100	26.5
6.00	15.60	100	26.5
6.64	10.00	100	26.5
7.00	7.80	100	26.5
8.00	3.90	100	26.5
8.97	2.00	100	26.5
9.99	0.98	100	26.5
10.48	0.70	100	26.5
10.99	0.49	100	26.5
12.02	0.24	100	26.5
13.02	0.12	100	26.5
14.02	0.06	100	26.5
14.29	0.05	100	26.5
		Total weight:	26.5

	mm	phi	Cum wt (g)	Int wt (g)	Int wt%	Cum % finer	Modes	
1	2.0000	-1.00	0.000000	0.000000	0.000000	100.000000		
2	1.6800	-0.75	0.000000	0.000000	0.000000	100.000000		
3	1.4100	-0.50	0.000000	0.000000	0.000000	100.000000		
4	1.1900	-0.25	0.000000	0.000000	0.000000	100.000000		
5	1.0000	0.00	0.000000	0.000000	0.000000	100.000000		8
6	0.8400	0.25	0.000000	0.000000	0.000000	100.000000		
7	0.7100	0.49	0.000000	0.000000	0.000000	100.000000		
8	0.5900	0.76	0.251012	0.251012	0.251012	99.748988		
9	0.5000	1.00	1.953871	1.702859	1.702859	98.046129		
10	0.4200	1.25	7.086943	5.133072	5.133072	92.913057		
11	0.3500	1.51	17.767363	10.680420	10.680420	82.232637		
12	0.3000	1.74	31.187030	13.419667	13.419667	68.812970		
13	0.2500	2.00	50.371043	19.184013	19.184013	49.628957	mode at 1.868483	
14	0.2100	2.25	68.715808	18.344765	18.344765	31.284192		
15	0.1770	2.50	83.437670	14.721862	14.721862	16.562330		
16	0.1490	2.75	93.234211	9.796541	9.796541	6.765789		
17	0.1250	3.00	98.237832	5.003621	5.003621	1.762168		
18	0.1050	3.25	99.860168	1.622336	1.622336	0.139832		
19	0.0880	3.51	100.000000	0.139832	0.139832	0.000000		
20	0.0740	3.76	100.000000	0.000000	0.000000	0.000000		
21	0.0630	3.99	100.000000	0.000000	0.000000	0.000000		
22	0.0530	4.24	100.000000	0.000000	0.000000	0.000000		
23	0.0440	4.51	100.000000	0.000000	0.000000	0.000000		
24	0.0370	4.76	100.000000	0.000000	0.000000	0.000000		
25	0.0310	5.01	100.000000	0.000000	0.000000	0.000000		
26	0.0156	6.00	100.000000	0.000000	0.000000	0.000000		
27	0.0100	6.64	100.000000	0.000000	0.000000	0.000000		
28	0.0078	7.00	100.000000	0.000000	0.000000	0.000000		
29	0.0039	8.00	100.000000	0.000000	0.000000	0.000000		
30	0.0020	8.97	100.000000	0.000000	0.000000	0.000000		
31	0.0010	9.99	100.000000	0.000000	0.000000	0.000000		
32	0.0007	10.48	100.000000	0.000000	0.000000	0.000000		
33	0.0005	10.99	100.000000	0.000000	0.000000	0.000000		
34	0.0002	12.02	100.000000	0.000000	0.000000	0.000000		
35	0.0001	13.02	100.000000	0.000000	0.000000	0.000000		
36	0.0001	14.02	100.000000	0.000000	0.000000	0.000000		
37	0.0001	14.29	100.000000	0.000000	0.000000	0.000000		
	Sums:			100.00	100.00			

Grainsize Statistics
Percentiles

	phi	*mm*
5	1.15	0.451
16	1.47	0.361
25	1.63	0.322
50	1.99	0.251
75	2.36	0.195
84	2.51	0.175
95	2.84	0.140

Column: 60
Sample ID: 6-2-2015sm

Folks' Graphic Statistics

	Mean (Mz)	Sorting (σI)	Skewness (SkI)	Kurtosis (KG)	Mean *mm*
phi	1.993	0.516	-0.004	0.957	0.251

Table II.60: *Results summary for sample 60: Low intertidal zone, southern transect, Northern Ngarunui Beach. Sample collected on the 6th of February, 2015.*

Column: 61 **Density:** 2650
Volume: 0.010
Sample ID: 6-2-2015sl

Malvern data Phi	Malvern data Micron	Vol %	Equivalent Cum wt (g)
-1.00	2000.00	0	0.0
-0.75	1680.00	0	0.0
-0.50	1410.00	0	0.0
-0.25	1190.00	0	0.0
0.00	1000.00	0	0.0
0.25	840.00	0	0.0
0.49	710.00	0	0.0
0.76	590.00	0.362861	0.1
1.00	500.00	2.111499	0.6
1.25	420.00	7.047231	1.9
1.51	350.00	17.189534	4.6
1.74	300.00	30.024128	8.0
2.00	250.00	48.676277	12.9
2.25	210.00	66.928904	17.7
2.50	177.00	81.977424	21.7
2.75	149.00	92.321971	24.5
3.00	125.00	97.844265	25.9
3.25	105.00	99.78051	26.4
3.51	88.00	100	26.5
3.76	74.00	100	26.5
3.99	63.00	100	26.5
4.24	53.00	100	26.5
4.51	44.00	100	26.5
4.76	37.00	100	26.5
5.01	31.00	100	26.5
6.00	15.60	100	26.5
6.64	10.00	100	26.5
7.00	7.80	100	26.5
8.00	3.90	100	26.5
8.97	2.00	100	26.5
9.99	0.98	100	26.5
10.48	0.70	100	26.5
10.99	0.49	100	26.5
12.02	0.24	100	26.5
13.02	0.12	100	26.5
14.02	0.06	100	26.5
14.29	0.05	100	26.5
	Total weight:		26.5

	mm	phi	Cum wt (g)	Int wt (g)	Int wt%	Cum % finer	Modes
1	2.0000	-1.00	0.000000	0.000000	0.000000	100.000000	
2	1.6800	-0.75	0.000000	0.000000	0.000000	100.000000	
3	1.4100	-0.50	0.000000	0.000000	0.000000	100.000000	
4	1.1900	-0.25	0.000000	0.000000	0.000000	100.000000	
5	1.0000	0.00	0.000000	0.000000	0.000000	100.000000	8
6	0.8400	0.25	0.000000	0.000000	0.000000	100.000000	
7	0.7100	0.49	0.000000	0.000000	0.000000	100.000000	
8	0.5900	0.76	0.362861	0.362861	0.362861	99.637139	
9	0.5000	1.00	2.111499	1.748638	1.748638	97.888501	
10	0.4200	1.25	7.047231	4.935732	4.935732	92.952769	
11	0.3500	1.51	17.189534	10.142303	10.142303	82.810466	
12	0.3000	1.74	30.024128	12.834594	12.834594	69.975872	
13	0.2500	2.00	48.676277	18.652149	18.652149	51.323723	mode at 1.868483
14	0.2100	2.25	66.928904	18.252627	18.252627	33.071096	
15	0.1770	2.50	81.977424	15.048520	15.048520	18.022576	
16	0.1490	2.75	92.321971	10.344547	10.344547	7.678029	
17	0.1250	3.00	97.844265	5.522294	5.522294	2.155735	
18	0.1050	3.25	99.780510	1.936245	1.936245	0.219490	
19	0.0880	3.51	100.000000	0.219490	0.219490	0.000000	
20	0.0740	3.76	100.000000	0.000000	0.000000	0.000000	
21	0.0630	3.99	100.000000	0.000000	0.000000	0.000000	
22	0.0530	4.24	100.000000	0.000000	0.000000	0.000000	
23	0.0440	4.51	100.000000	0.000000	0.000000	0.000000	
24	0.0370	4.76	100.000000	0.000000	0.000000	0.000000	
25	0.0310	5.01	100.000000	0.000000	0.000000	0.000000	
26	0.0156	6.00	100.000000	0.000000	0.000000	0.000000	
27	0.0100	6.64	100.000000	0.000000	0.000000	0.000000	
28	0.0078	7.00	100.000000	0.000000	0.000000	0.000000	
29	0.0039	8.00	100.000000	0.000000	0.000000	0.000000	
30	0.0020	8.97	100.000000	0.000000	0.000000	0.000000	
31	0.0010	9.99	100.000000	0.000000	0.000000	0.000000	
32	0.0007	10.48	100.000000	0.000000	0.000000	0.000000	
33	0.0005	10.99	100.000000	0.000000	0.000000	0.000000	
34	0.0002	12.02	100.000000	0.000000	0.000000	0.000000	
35	0.0001	13.02	100.000000	0.000000	0.000000	0.000000	
36	0.0001	14.02	100.000000	0.000000	0.000000	0.000000	
37	0.0001	14.29	100.000000	0.000000	0.000000	0.000000	
	Sums:			100.00	100.00		

Grainsize Statistics
Percentiles

	phi	*mm*
5	1.15	0.451
16	1.48	0.358
25	1.65	0.319
50	2.02	0.247
75	2.38	0.192
84	2.55	0.171
95	2.87	0.137

Column: 61
Sample ID: 6-2-2015sl

Folks' Graphic Statistics

	Mean (Mz)	Sorting (σI)	Skewness (SkI)	Kurtosis (KG)	Mean *mm*
phi	2.016	0.527	-0.009	0.962	0.247

Table II.61: *Results summary for sample 61: Low intertidal zone, northern transect, Northern Ngarunui Beach. Sample collected on the 6th of February, 2015.*

Column: 62 **Density:** 2650
Volume: 0.010
Sample ID: 6-2-2015nl

Malvern data Phi	Malvern data Micron	Vol %	Equivalent Cum wt (g)
-1.00	2000.00	0	0.0
-0.75	1680.00	0	0.0
-0.50	1410.00	0	0.0
-0.25	1190.00	0	0.0
0.00	1000.00	0	0.0
0.25	840.00	0	0.0
0.49	710.00	0	0.0
0.76	590.00	0.412869	0.1
1.00	500.00	2.551537	0.7
1.25	420.00	8.478608	2.2
1.51	350.00	20.191136	5.4
1.74	300.00	34.362504	9.1
2.00	250.00	53.918927	14.3
2.25	210.00	71.92416	19.1
2.50	177.00	85.795811	22.7
2.75	149.00	94.58174	25.1
3.00	125.00	98.766156	26.2
3.25	105.00	99.932915	26.5
3.51	88.00	100	26.5
3.76	74.00	100	26.5
3.99	63.00	100	26.5
4.24	53.00	100	26.5
4.51	44.00	100	26.5
4.76	37.00	100	26.5
5.01	31.00	100	26.5
6.00	15.60	100	26.5
6.64	10.00	100	26.5
7.00	7.80	100	26.5
8.00	3.90	100	26.5
8.97	2.00	100	26.5
9.99	0.98	100	26.5
10.48	0.70	100	26.5
10.99	0.49	100	26.5
12.02	0.24	100	26.5
13.02	0.12	100	26.5
14.02	0.06	100	26.5
14.29	0.05	100	26.5

Total weight: 26.5

Column: 62
Sample ID: 6-2-2015nl

Folks' Graphic Statistics

	Mean (Mz)	Sorting (σI)	Skewness (SkI)	Kurtosis (KG)	Mean mm
phi	1.945	0.514	-0.009	0.955	0.260

	mm	phi	Cum wt (g)	Int wt (g)	Int wt%	Cum % finer	Modes	
1	2.0000	-1.00	0.000000	0.000000	0.000000	100.000000		
2	1.6800	-0.75	0.000000	0.000000	0.000000	100.000000		
3	1.4100	-0.50	0.000000	0.000000	0.000000	100.000000		
4	1.1900	-0.25	0.000000	0.000000	0.000000	100.000000		
5	1.0000	0.00	0.000000	0.000000	0.000000	100.000000		8
6	0.8400	0.25	0.000000	0.000000	0.000000	100.000000		
7	0.7100	0.49	0.000000	0.000000	0.000000	100.000000		
8	0.5900	0.76	0.412869	0.412869	0.412869	99.587131		
9	0.5000	1.00	2.551537	2.138668	2.138668	97.448463		
10	0.4200	1.25	8.478608	5.927071	5.927071	91.521392		
11	0.3500	1.51	20.191136	11.712528	11.712528	79.808864		
12	0.3000	1.74	34.362504	14.171368	14.171368	65.637496		
13	0.2500	2.00	53.918927	19.556423	19.556423	46.081073	mode at 1.868483	
14	0.2100	2.25	71.924160	18.005233	18.005233	28.075840		
15	0.1770	2.50	85.795811	13.871651	13.871651	14.204189		
16	0.1490	2.75	94.581740	8.785929	8.785929	5.418260		
17	0.1250	3.00	98.766156	4.184416	4.184416	1.233844		
18	0.1050	3.25	99.932915	1.166759	1.166759	0.067085		
19	0.0880	3.51	100.000000	0.067085	0.067085	0.000000		
20	0.0740	3.76	100.000000	0.000000	0.000000	0.000000		
21	0.0630	3.99	100.000000	0.000000	0.000000	0.000000		
22	0.0530	4.24	100.000000	0.000000	0.000000	0.000000		
23	0.0440	4.51	100.000000	0.000000	0.000000	0.000000		
24	0.0370	4.76	100.000000	0.000000	0.000000	0.000000		
25	0.0310	5.01	100.000000	0.000000	0.000000	0.000000		
26	0.0156	6.00	100.000000	0.000000	0.000000	0.000000		
27	0.0100	6.64	100.000000	0.000000	0.000000	0.000000		
28	0.0078	7.00	100.000000	0.000000	0.000000	0.000000		
29	0.0039	8.00	100.000000	0.000000	0.000000	0.000000		
30	0.0020	8.97	100.000000	0.000000	0.000000	0.000000		
31	0.0010	9.99	100.000000	0.000000	0.000000	0.000000		
32	0.0007	10.48	100.000000	0.000000	0.000000	0.000000		
33	0.0005	10.99	100.000000	0.000000	0.000000	0.000000		
34	0.0002	12.02	100.000000	0.000000	0.000000	0.000000		
35	0.0001	13.02	100.000000	0.000000	0.000000	0.000000		
36	0.0001	14.02	100.000000	0.000000	0.000000	0.000000		
37	0.0001	14.29	100.000000	0.000000	0.000000	0.000000		
	Sums:			100.00	100.00			

Grainsize Statistics
Percentiles

	phi	*mm*
5	1.10	0.465
16	1.42	0.374
25	1.59	0.332
50	1.95	0.259
75	2.31	0.202
84	2.47	0.181
95	2.77	0.146

Table II.62: *Results summary for sample 62: High intertidal zone, mid transect, Wainamu Beach. Sample collected on the 28th of November, 2014.*

Column: 63 **Density:** 2650
Volume: 0.010
Sample ID: 2014-11-28mh

Malvern data Phi	Malvern data Micron	Vol %	Equivalent Cum wt (g)
-1.00	2000.00	0	0.0
-0.75	1680.00	0	0.0
-0.50	1410.00	0	0.0
-0.25	1190.00	0	0.0
0.00	1000.00	0	0.0
0.25	840.00	0	0.0
0.49	710.00	0	0.0
0.76	590.00	0	0.0
1.00	500.00	0	0.0
1.25	420.00	0.072547	0.0
1.51	350.00	1.201626	0.3
1.74	300.00	4.220276	1.1
2.00	250.00	11.89792	3.2
2.25	210.00	24.279479	6.4
2.50	177.00	40.525676	10.7
2.75	149.00	58.656394	15.5
3.00	125.00	75.677198	20.1
3.25	105.00	88.397296	23.4
3.51	88.00	96.043812	25.5
3.76	74.00	99.250062	26.3
3.99	63.00	99.988746	26.5
4.24	53.00	100	26.5
4.51	44.00	100	26.5
4.76	37.00	100	26.5
5.01	31.00	100	26.5
6.00	15.60	100	26.5
6.64	10.00	100	26.5
7.00	7.80	100	26.5
8.00	3.90	100	26.5
8.97	2.00	100	26.5
9.99	0.98	100	26.5
10.48	0.70	100	26.5
10.99	0.49	100	26.5
12.02	0.24	100	26.5
13.02	0.12	100	26.5
14.02	0.06	100	26.5
14.29	0.05	100	26.5
		Total weight:	26.5

	mm	phi	Cum wt (g)	Int wt (g)	Int wt%	Cum % finer	Modes
1	2.0000	-1.00	0.000000	0.000000	0.000000	100.000000	
2	1.6800	-0.75	0.000000	0.000000	0.000000	100.000000	
3	1.4100	-0.50	0.000000	0.000000	0.000000	100.000000	
4	1.1900	-0.25	0.000000	0.000000	0.000000	100.000000	
5	1.0000	0.00	0.000000	0.000000	0.000000	100.000000	8
6	0.8400	0.25	0.000000	0.000000	0.000000	100.000000	
7	0.7100	0.49	0.000000	0.000000	0.000000	100.000000	
8	0.5900	0.76	0.000000	0.000000	0.000000	100.000000	
9	0.5000	1.00	0.000000	0.000000	0.000000	100.000000	
10	0.4200	1.25	0.072547	0.072547	0.072547	99.927453	
11	0.3500	1.51	1.201626	1.129079	1.129079	98.798374	
12	0.3000	1.74	4.220276	3.018650	3.018650	95.779724	
13	0.2500	2.00	11.897920	7.677644	7.677644	88.102080	
14	0.2100	2.25	24.279479	12.381559	12.381559	75.720521	
15	0.1770	2.50	40.525676	16.246197	16.246197	59.474324	
16	0.1490	2.75	58.656394	18.130718	18.130718	41.343606	mode at 2.622397
17	0.1250	3.00	75.677198	17.020804	17.020804	24.322802	
18	0.1050	3.25	88.397296	12.720098	12.720098	11.602704	
19	0.0880	3.51	96.043812	7.646516	7.646516	3.956188	
20	0.0740	3.76	99.250062	3.206250	3.206250	0.749938	
21	0.0630	3.99	99.988746	0.738684	0.738684	0.011254	
22	0.0530	4.24	100.000000	0.011254	0.011254	0.000000	
23	0.0440	4.51	100.000000	0.000000	0.000000	0.000000	
24	0.0370	4.76	100.000000	0.000000	0.000000	0.000000	
25	0.0310	5.01	100.000000	0.000000	0.000000	0.000000	
26	0.0156	6.00	100.000000	0.000000	0.000000	0.000000	
27	0.0100	6.64	100.000000	0.000000	0.000000	0.000000	
28	0.0078	7.00	100.000000	0.000000	0.000000	0.000000	
29	0.0039	8.00	100.000000	0.000000	0.000000	0.000000	
30	0.0020	8.97	100.000000	0.000000	0.000000	0.000000	
31	0.0010	9.99	100.000000	0.000000	0.000000	0.000000	
32	0.0007	10.48	100.000000	0.000000	0.000000	0.000000	
33	0.0005	10.99	100.000000	0.000000	0.000000	0.000000	
34	0.0002	12.02	100.000000	0.000000	0.000000	0.000000	
35	0.0001	13.02	100.000000	0.000000	0.000000	0.000000	
36	0.0001	14.02	100.000000	0.000000	0.000000	0.000000	
37	0.0001	14.29	100.000000	0.000000	0.000000	0.000000	
	Sums:			100.00	100.00		

Column: 63
Sample ID: 2014-11-28mh

Folks' Graphic Statistics

	Mean (Mz)	Sorting (σI)	Skewness (SkI)	Kurtosis (KG)	Mean *mm*
phi	2.625	0.529	-0.010	0.962	0.162

Grainsize Statistics
Percentiles

	phi	*mm*
5	1.76	0.294
16	2.08	0.236
25	2.26	0.208
50	2.63	0.162
75	2.99	0.126
84	3.16	0.112
95	3.47	0.090

Table II.63: *Results summary for sample 63: Low intertidal zone, western transect, Wainamu Beach. Sample collected on the 28th of November, 2014.*

Column: 64 **Density:** 2650
Volume: 0.010
Sample ID: 2014-11-28wl

Malvern data Phi	Malvern data Micron	Vol %	Equivalent Cum wt (g)
-1.00	2000.00	0	0.0
-0.75	1680.00	0	0.0
-0.50	1410.00	0	0.0
-0.25	1190.00	0	0.0
0.00	1000.00	0	0.0
0.25	840.00	0	0.0
0.49	710.00	0	0.0
0.76	590.00	0	0.0
1.00	500.00	0.223295	0.1
1.25	420.00	2.221138	0.6
1.51	350.00	7.754973	2.1
1.74	300.00	16.178596	4.3
2.00	250.00	30.552463	8.1
2.25	210.00	47.332184	12.5
2.50	177.00	64.208299	17.0
2.75	149.00	79.043443	20.9
3.00	125.00	90.104781	23.9
3.25	105.00	96.583008	25.6
3.51	88.00	99.425033	26.3
3.76	74.00	100	26.5
3.99	63.00	100	26.5
4.24	53.00	100	26.5
4.51	44.00	100	26.5
4.76	37.00	100	26.5
5.01	31.00	100	26.5
6.00	15.60	100	26.5
6.64	10.00	100	26.5
7.00	7.80	100	26.5
8.00	3.90	100	26.5
8.97	2.00	100	26.5
9.99	0.98	100	26.5
10.48	0.70	100	26.5
10.99	0.49	100	26.5
12.02	0.24	100	26.5
13.02	0.12	100	26.5
14.02	0.06	100	26.5
14.29	0.05	100	26.5
		Total weight:	26.5

	mm	phi	Cum wt (g)	Int wt (g)	Int wt%	Cum % finer	Modes	
1	2.0000	-1.00	0.000000	0.000000	0.000000	100.000000		
2	1.6800	-0.75	0.000000	0.000000	0.000000	100.000000		
3	1.4100	-0.50	0.000000	0.000000	0.000000	100.000000		
4	1.1900	-0.25	0.000000	0.000000	0.000000	100.000000		
5	1.0000	0.00	0.000000	0.000000	0.000000	100.000000		8
6	0.8400	0.25	0.000000	0.000000	0.000000	100.000000		
7	0.7100	0.49	0.000000	0.000000	0.000000	100.000000		
8	0.5900	0.76	0.000000	0.000000	0.000000	100.000000		
9	0.5000	1.00	0.223295	0.223295	0.223295	99.776705		
10	0.4200	1.25	2.221138	1.997843	1.997843	97.778862		
11	0.3500	1.51	7.754973	5.533835	5.533835	92.245027		
12	0.3000	1.74	16.178596	8.423623	8.423623	83.821404		
13	0.2500	2.00	30.552463	14.373867	14.373867	69.447537		
14	0.2100	2.25	47.332184	16.779721	16.779721	52.667816		
15	0.1770	2.50	64.208299	16.876115	16.876115	35.791701	mode at 2.374859	
16	0.1490	2.75	79.043443	14.835144	14.835144	20.956557		
17	0.1250	3.00	90.104781	11.061338	11.061338	9.895219		
18	0.1050	3.25	96.583008	6.478227	6.478227	3.416992		
19	0.0880	3.51	99.425033	2.842025	2.842025	0.574967		
20	0.0740	3.76	100.000000	0.574967	0.574967	0.000000		
21	0.0630	3.99	100.000000	0.000000	0.000000	0.000000		
22	0.0530	4.24	100.000000	0.000000	0.000000	0.000000		
23	0.0440	4.51	100.000000	0.000000	0.000000	0.000000		
24	0.0370	4.76	100.000000	0.000000	0.000000	0.000000		
25	0.0310	5.01	100.000000	0.000000	0.000000	0.000000		
26	0.0156	6.00	100.000000	0.000000	0.000000	0.000000		
27	0.0100	6.64	100.000000	0.000000	0.000000	0.000000		
28	0.0078	7.00	100.000000	0.000000	0.000000	0.000000		
29	0.0039	8.00	100.000000	0.000000	0.000000	0.000000		
30	0.0020	8.97	100.000000	0.000000	0.000000	0.000000		
31	0.0010	9.99	100.000000	0.000000	0.000000	0.000000		
32	0.0007	10.48	100.000000	0.000000	0.000000	0.000000		
33	0.0005	10.99	100.000000	0.000000	0.000000	0.000000		
34	0.0002	12.02	100.000000	0.000000	0.000000	0.000000		
35	0.0001	13.02	100.000000	0.000000	0.000000	0.000000		
36	0.0001	14.02	100.000000	0.000000	0.000000	0.000000		
37	0.0001	14.29	100.000000	0.000000	0.000000	0.000000		
	Sums:			100.00	100.00			

Column: 64
Sample ID: 2014-11-28wl

Folks' Graphic Statistics

	Mean (Mz)	Sorting (σI)	Skewness (SkI)	Kurtosis (KG)	Mean *mm*
phi	2.294	0.556	0.003	0.949	0.204

Grainsize Statistics
Percentiles

	phi	*mm*
5	1.38	0.383
16	1.73	0.301
25	1.90	0.268
50	2.29	0.204
75	2.68	0.156
84	2.86	0.138
95	3.19	0.110

Table II.64: *Results summary for sample 64: High intertidal zone, western transect, Wainamu Beach. Sample collected on the 28th of November, 2014.*

Column: 65 **Density:** 2650
Volume: 0.010
Sample ID: 2014-11-28wh

Malvern data Phi	Malvern data Micron	Vol %	Equivalent Cum wt (g)
-1.00	2000.00	0	0.0
-0.75	1680.00	0	0.0
-0.50	1410.00	0	0.0
-0.25	1190.00	0	0.0
0.00	1000.00	0	0.0
0.25	840.00	0	0.0
0.49	710.00	0	0.0
0.76	590.00	0	0.0
1.00	500.00	0.015376	0.0
1.25	420.00	0.382491	0.1
1.51	350.00	2.558249	0.7
1.74	300.00	6.800607	1.8
2.00	250.00	15.706162	4.2
2.25	210.00	28.288794	7.5
2.50	177.00	43.531691	11.5
2.75	149.00	59.890584	15.9
3.00	125.00	75.239696	19.9
3.25	105.00	87.175848	23.1
3.51	88.00	94.99887	25.2
3.76	74.00	98.804798	26.2
3.99	63.00	99.973944	26.5
4.24	53.00	100	26.5
4.51	44.00	100	26.5
4.76	37.00	100	26.5
5.01	31.00	100	26.5
6.00	15.60	100	26.5
6.64	10.00	100	26.5
7.00	7.80	100	26.5
8.00	3.90	100	26.5
8.97	2.00	100	26.5
9.99	0.98	100	26.5
10.48	0.70	100	26.5
10.99	0.49	100	26.5
12.02	0.24	100	26.5
13.02	0.12	100	26.5
14.02	0.06	100	26.5
14.29	0.05	100	26.5
	Total weight:		26.5

	mm	phi	Cum wt (g)	Int wt (g)	Int wt%	Cum % finer	Modes
1	2.0000	-1.00	0.000000	0.000000	0.000000	100.000000	
2	1.6800	-0.75	0.000000	0.000000	0.000000	100.000000	
3	1.4100	-0.50	0.000000	0.000000	0.000000	100.000000	
4	1.1900	-0.25	0.000000	0.000000	0.000000	100.000000	
5	1.0000	0.00	0.000000	0.000000	0.000000	100.000000	8
6	0.8400	0.25	0.000000	0.000000	0.000000	100.000000	
7	0.7100	0.49	0.000000	0.000000	0.000000	100.000000	
8	0.5900	0.76	0.000000	0.000000	0.000000	100.000000	
9	0.5000	1.00	0.015376	0.015376	0.015376	99.984624	
10	0.4200	1.25	0.382491	0.367115	0.367115	99.617509	
11	0.3500	1.51	2.558249	2.175758	2.175758	97.441751	
12	0.3000	1.74	6.800607	4.242358	4.242358	93.199393	
13	0.2500	2.00	15.706162	8.905555	8.905555	84.293838	
14	0.2100	2.25	28.288794	12.582632	12.582632	71.711206	
15	0.1770	2.50	43.531691	15.242897	15.242897	56.468309	
16	0.1490	2.75	59.890584	16.358893	16.358893	40.109416	mode at 2.622397
17	0.1250	3.00	75.239696	15.349112	15.349112	24.760304	
18	0.1050	3.25	87.175848	11.936152	11.936152	12.824152	
19	0.0880	3.51	94.998870	7.823022	7.823022	5.001130	
20	0.0740	3.76	98.804798	3.805928	3.805928	1.195202	
21	0.0630	3.99	99.973944	1.169146	1.169146	0.026056	
22	0.0530	4.24	100.000000	0.026056	0.026056	0.000000	
23	0.0440	4.51	100.000000	0.000000	0.000000	0.000000	
24	0.0370	4.76	100.000000	0.000000	0.000000	0.000000	
25	0.0310	5.01	100.000000	0.000000	0.000000	0.000000	
26	0.0156	6.00	100.000000	0.000000	0.000000	0.000000	
27	0.0100	6.64	100.000000	0.000000	0.000000	0.000000	
28	0.0078	7.00	100.000000	0.000000	0.000000	0.000000	
29	0.0039	8.00	100.000000	0.000000	0.000000	0.000000	
30	0.0020	8.97	100.000000	0.000000	0.000000	0.000000	
31	0.0010	9.99	100.000000	0.000000	0.000000	0.000000	
32	0.0007	10.48	100.000000	0.000000	0.000000	0.000000	
33	0.0005	10.99	100.000000	0.000000	0.000000	0.000000	
34	0.0002	12.02	100.000000	0.000000	0.000000	0.000000	
35	0.0001	13.02	100.000000	0.000000	0.000000	0.000000	
36	0.0001	14.02	100.000000	0.000000	0.000000	0.000000	
37	0.0001	14.29	100.000000	0.000000	0.000000	0.000000	
		Sums:		100.00	100.00		

Grainsize Statistics
Percentiles

	phi	*mm*
5	1.64	0.320
16	2.01	0.249
25	2.19	0.220
50	2.60	0.165
75	3.00	0.125
84	3.18	0.110
95	3.51	0.088

Column: 65
Sample ID: 2014-11-28wh

Folks' Graphic Statistics

	Mean (Mz)	Sorting (σI)	Skewness (SkI)	Kurtosis (KG)	Mean *mm*
phi	2.596	0.577	-0.013	0.943	0.165

Table II.65: *Results summary for sample 65: Low intertidal zone, eastern transect, Wainamu Beach. Sample collected on the 28th of November, 2014.*

Column: 66 **Density:** 2650
Volume: 0.010
Sample ID: 2014-11-28el

Malvern data Phi	Malvern data Micron	Vol %	Equivalent Cum wt (g)
-1.00	2000.00	0	0.0
-0.75	1680.00	0	0.0
-0.50	1410.00	0	0.0
-0.25	1190.00	0	0.0
0.00	1000.00	0	0.0
0.25	840.00	0	0.0
0.49	710.00	0	0.0
0.76	590.00	0	0.0
1.00	500.00	0.498488	0.1
1.25	420.00	2.700384	0.7
1.51	350.00	8.188446	2.2
1.74	300.00	16.121137	4.3
2.00	250.00	29.385275	7.8
2.25	210.00	44.862453	11.9
2.50	177.00	60.731766	16.1
2.75	149.00	75.257531	19.9
3.00	125.00	86.846575	23.0
3.25	105.00	94.416851	25.0
3.51	88.00	98.430546	26.1
3.76	74.00	99.877601	26.5
3.99	63.00	100	26.5
4.24	53.00	100	26.5
4.51	44.00	100	26.5
4.76	37.00	100	26.5
5.01	31.00	100	26.5
6.00	15.60	100	26.5
6.64	10.00	100	26.5
7.00	7.80	100	26.5
8.00	3.90	100	26.5
8.97	2.00	100	26.5
9.99	0.98	100	26.5
10.48	0.70	100	26.5
10.99	0.49	100	26.5
12.02	0.24	100	26.5
13.02	0.12	100	26.5
14.02	0.06	100	26.5
14.29	0.05	100	26.5

Total weight: 26.5

	mm	phi	Cum wt (g)	Int wt (g)	Int wt%	Cum % finer	Modes
1	2.0000	-1.00	0.000000	0.000000	0.000000	100.000000	
2	1.6800	-0.75	0.000000	0.000000	0.000000	100.000000	
3	1.4100	-0.50	0.000000	0.000000	0.000000	100.000000	
4	1.1900	-0.25	0.000000	0.000000	0.000000	100.000000	
5	1.0000	0.00	0.000000	0.000000	0.000000	100.000000	8
6	0.8400	0.25	0.000000	0.000000	0.000000	100.000000	
7	0.7100	0.49	0.000000	0.000000	0.000000	100.000000	
8	0.5900	0.76	0.000000	0.000000	0.000000	100.000000	
9	0.5000	1.00	0.498488	0.498488	0.498488	99.501512	
10	0.4200	1.25	2.700384	2.201896	2.201896	97.299616	
11	0.3500	1.51	8.188446	5.488062	5.488062	91.811554	
12	0.3000	1.74	16.121137	7.932691	7.932691	83.878863	
13	0.2500	2.00	29.385275	13.264138	13.264138	70.614725	
14	0.2100	2.25	44.862453	15.477178	15.477178	55.137547	
15	0.1770	2.50	60.731766	15.869313	15.869313	39.268234	mode at 2.374859
16	0.1490	2.75	75.257531	14.525765	14.525765	24.742469	
17	0.1250	3.00	86.846575	11.589044	11.589044	13.153425	
18	0.1050	3.25	94.416851	7.570276	7.570276	5.583149	
19	0.0880	3.51	98.430546	4.013695	4.013695	1.569454	
20	0.0740	3.76	99.877601	1.447055	1.447055	0.122399	
21	0.0630	3.99	100.000000	0.122399	0.122399	0.000000	
22	0.0530	4.24	100.000000	0.000000	0.000000	0.000000	
23	0.0440	4.51	100.000000	0.000000	0.000000	0.000000	
24	0.0370	4.76	100.000000	0.000000	0.000000	0.000000	
25	0.0310	5.01	100.000000	0.000000	0.000000	0.000000	
26	0.0156	6.00	100.000000	0.000000	0.000000	0.000000	
27	0.0100	6.64	100.000000	0.000000	0.000000	0.000000	
28	0.0078	7.00	100.000000	0.000000	0.000000	0.000000	
29	0.0039	8.00	100.000000	0.000000	0.000000	0.000000	
30	0.0020	8.97	100.000000	0.000000	0.000000	0.000000	
31	0.0010	9.99	100.000000	0.000000	0.000000	0.000000	
32	0.0007	10.48	100.000000	0.000000	0.000000	0.000000	
33	0.0005	10.99	100.000000	0.000000	0.000000	0.000000	
34	0.0002	12.02	100.000000	0.000000	0.000000	0.000000	
35	0.0001	13.02	100.000000	0.000000	0.000000	0.000000	
36	0.0001	14.02	100.000000	0.000000	0.000000	0.000000	
37	0.0001	14.29	100.000000	0.000000	0.000000	0.000000	
		Sums:		100.00	100.00		

Column: 66
Sample ID: 2014-11-28el

Folks' Graphic Statistics

	Mean (Mz)	Sorting (σI)	Skewness (SkI)	Kurtosis (KG)	Mean *mm*
phi	2.334	0.593	0.000	0.952	0.198

Grainsize Statistics
Percentiles

	phi	*mm*
5	1.36	0.389
16	1.73	0.301
25	1.91	0.266
50	2.33	0.199
75	2.74	0.149
84	2.94	0.131
95	3.29	0.102

Table II.66: *Results summary for sample 66: Low intertidal zone, mid transect, Wainamu Beach. Sample collected on the 28th of November, 2014.*

Column: 67 **Density:** 2650
Volume: 0.010
Sample ID: 2014-11-28ml

Malvern data Phi	Malvern data Micron	Vol %	Equivalent Cum wt (g)
-1.00	2000.00	0	0.0
-0.75	1680.00	0	0.0
-0.50	1410.00	0	0.0
-0.25	1190.00	0	0.0
0.00	1000.00	0	0.0
0.25	840.00	0	0.0
0.49	710.00	0	0.0
0.76	590.00	0	0.0
1.00	500.00	0.483402	0.1
1.25	420.00	3.05661	0.8
1.51	350.00	10.053065	2.7
1.74	300.00	20.460313	5.4
2.00	250.00	37.576635	10.0
2.25	210.00	56.314429	14.9
2.50	177.00	73.498414	19.5
2.75	149.00	86.798243	23.0
3.00	125.00	95.11116	25.2
3.25	105.00	98.879972	26.2
3.51	88.00	99.952219	26.5
3.76	74.00	100	26.5
3.99	63.00	100	26.5
4.24	53.00	100	26.5
4.51	44.00	100	26.5
4.76	37.00	100	26.5
5.01	31.00	100	26.5
6.00	15.60	100	26.5
6.64	10.00	100	26.5
7.00	7.80	100	26.5
8.00	3.90	100	26.5
8.97	2.00	100	26.5
9.99	0.98	100	26.5
10.48	0.70	100	26.5
10.99	0.49	100	26.5
12.02	0.24	100	26.5
13.02	0.12	100	26.5
14.02	0.06	100	26.5
14.29	0.05	100	26.5
		Total weight:	26.5

Column: 67
Sample ID: 2014-11-28ml

Folks' Graphic Statistics

	Mean (Mz)	Sorting (σI)	Skewness (SkI)	Kurtosis (KG)	Mean *mm*
phi	2.168	0.517	-0.003	0.952	0.223

	mm	phi	Cum wt (g)	Int wt (g)	Int wt%	Cum % finer	Modes
1	2.0000	-1.00	0.000000	0.000000	0.000000	100.000000	
2	1.6800	-0.75	0.000000	0.000000	0.000000	100.000000	
3	1.4100	-0.50	0.000000	0.000000	0.000000	100.000000	
4	1.1900	-0.25	0.000000	0.000000	0.000000	100.000000	
5	1.0000	0.00	0.000000	0.000000	0.000000	100.000000	8
6	0.8400	0.25	0.000000	0.000000	0.000000	100.000000	
7	0.7100	0.49	0.000000	0.000000	0.000000	100.000000	
8	0.5900	0.76	0.000000	0.000000	0.000000	100.000000	
9	0.5000	1.00	0.483402	0.483402	0.483402	99.516598	
10	0.4200	1.25	3.056610	2.573208	2.573208	96.943390	
11	0.3500	1.51	10.053065	6.996455	6.996455	89.946935	
12	0.3000	1.74	20.460313	10.407248	10.407248	79.539687	
13	0.2500	2.00	37.576635	17.116322	17.116322	62.423365	
14	0.2100	2.25	56.314429	18.737794	18.737794	43.685571	mode at 2.125769
15	0.1770	2.50	73.498414	17.183985	17.183985	26.501586	
16	0.1490	2.75	86.798243	13.299829	13.299829	13.201757	
17	0.1250	3.00	95.111160	8.312917	8.312917	4.888840	
18	0.1050	3.25	98.879972	3.768812	3.768812	1.120028	
19	0.0880	3.51	99.952219	1.072247	1.072247	0.047781	
20	0.0740	3.76	100.000000	0.047781	0.047781	0.000000	
21	0.0630	3.99	100.000000	0.000000	0.000000	0.000000	
22	0.0530	4.24	100.000000	0.000000	0.000000	0.000000	
23	0.0440	4.51	100.000000	0.000000	0.000000	0.000000	
24	0.0370	4.76	100.000000	0.000000	0.000000	0.000000	
25	0.0310	5.01	100.000000	0.000000	0.000000	0.000000	
26	0.0156	6.00	100.000000	0.000000	0.000000	0.000000	
27	0.0100	6.64	100.000000	0.000000	0.000000	0.000000	
28	0.0078	7.00	100.000000	0.000000	0.000000	0.000000	
29	0.0039	8.00	100.000000	0.000000	0.000000	0.000000	
30	0.0020	8.97	100.000000	0.000000	0.000000	0.000000	
31	0.0010	9.99	100.000000	0.000000	0.000000	0.000000	
32	0.0007	10.48	100.000000	0.000000	0.000000	0.000000	
33	0.0005	10.99	100.000000	0.000000	0.000000	0.000000	
34	0.0002	12.02	100.000000	0.000000	0.000000	0.000000	
35	0.0001	13.02	100.000000	0.000000	0.000000	0.000000	
36	0.0001	14.02	100.000000	0.000000	0.000000	0.000000	
37	0.0001	14.29	100.000000	0.000000	0.000000	0.000000	
		Sums:		100.00	100.00		

Grainsize Statistics
Percentiles

	phi	*mm*
5	1.32	0.399
16	1.64	0.320
25	1.81	0.286
50	2.17	0.223
75	2.53	0.174
84	2.69	0.154
95	3.00	0.125

Table II.67: *Results summary for sample 67: Mid intertidal zone, western transect, Wainamu Beach. Sample collected on the 28th of November, 2014.*

Column: 68 **Density:** 2650
Volume: 0.010
Sample ID: 2014-11-28wm

Malvern data Phi	Malvern data Micron	Vol %	Equivalent Cum wt (g)
-1.00	2000.00	0	0.0
-0.75	1680.00	0	0.0
-0.50	1410.00	0	0.0
-0.25	1190.00	0	0.0
0.00	1000.00	0	0.0
0.25	840.00	0	0.0
0.49	710.00	0	0.0
0.76	590.00	0	0.0
1.00	500.00	0	0.0
1.25	420.00	0	0.0
1.51	350.00	0	0.0
1.74	300.00	0.017242	0.0
2.00	250.00	0.68511	0.2
2.25	210.00	4.817851	1.3
2.50	177.00	15.876287	4.2
2.75	149.00	35.334424	9.4
3.00	125.00	59.639883	15.8
3.25	105.00	80.700364	21.4
3.51	88.00	93.740184	24.8
3.76	74.00	98.854835	26.2
3.99	63.00	99.944784	26.5
4.24	53.00	100	26.5
4.51	44.00	100	26.5
4.76	37.00	100	26.5
5.01	31.00	100	26.5
6.00	15.60	100	26.5
6.64	10.00	100	26.5
7.00	7.80	100	26.5
8.00	3.90	100	26.5
8.97	2.00	100	26.5
9.99	0.98	100	26.5
10.48	0.70	100	26.5
10.99	0.49	100	26.5
12.02	0.24	100	26.5
13.02	0.12	100	26.5
14.02	0.06	100	26.5
14.29	0.05	100	26.5

Total weight: 26.5

Column: 68
Sample ID: 2014-11-28wm

	mm	phi	Cum wt (g)	Int wt (g)	Int wt%	Cum % finer	Modes
1	2.0000	-1.00	0.000000	0.000000	0.000000	100.000000	
2	1.6800	-0.75	0.000000	0.000000	0.000000	100.000000	
3	1.4100	-0.50	0.000000	0.000000	0.000000	100.000000	
4	1.1900	-0.25	0.000000	0.000000	0.000000	100.000000	
5	1.0000	0.00	0.000000	0.000000	0.000000	100.000000	8
6	0.8400	0.25	0.000000	0.000000	0.000000	100.000000	
7	0.7100	0.49	0.000000	0.000000	0.000000	100.000000	
8	0.5900	0.76	0.000000	0.000000	0.000000	100.000000	
9	0.5000	1.00	0.000000	0.000000	0.000000	100.000000	
10	0.4200	1.25	0.000000	0.000000	0.000000	100.000000	
11	0.3500	1.51	0.000000	0.000000	0.000000	100.000000	
12	0.3000	1.74	0.017242	0.017242	0.017242	99.982758	
13	0.2500	2.00	0.685110	0.667868	0.667868	99.314890	
14	0.2100	2.25	4.817851	4.132741	4.132741	95.182149	
15	0.1770	2.50	15.876287	11.058436	11.058436	84.123713	
16	0.1490	2.75	35.334424	19.458137	19.458137	64.665576	
17	0.1250	3.00	59.639883	24.305459	24.305459	40.360117	mode at 2.873308
18	0.1050	3.25	80.700364	21.060481	21.060481	19.299636	
19	0.0880	3.51	93.740184	13.039820	13.039820	6.259816	
20	0.0740	3.76	98.854835	5.114651	5.114651	1.145165	
21	0.0630	3.99	99.944784	1.089949	1.089949	0.055216	
22	0.0530	4.24	100.000000	0.055216	0.055216	0.000000	
23	0.0440	4.51	100.000000	0.000000	0.000000	0.000000	
24	0.0370	4.76	100.000000	0.000000	0.000000	0.000000	
25	0.0310	5.01	100.000000	0.000000	0.000000	0.000000	
26	0.0156	6.00	100.000000	0.000000	0.000000	0.000000	
27	0.0100	6.64	100.000000	0.000000	0.000000	0.000000	
28	0.0078	7.00	100.000000	0.000000	0.000000	0.000000	
29	0.0039	8.00	100.000000	0.000000	0.000000	0.000000	
30	0.0020	8.97	100.000000	0.000000	0.000000	0.000000	
31	0.0010	9.99	100.000000	0.000000	0.000000	0.000000	
32	0.0007	10.48	100.000000	0.000000	0.000000	0.000000	
33	0.0005	10.99	100.000000	0.000000	0.000000	0.000000	
34	0.0002	12.02	100.000000	0.000000	0.000000	0.000000	
35	0.0001	13.02	100.000000	0.000000	0.000000	0.000000	
36	0.0001	14.02	100.000000	0.000000	0.000000	0.000000	
37	0.0001	14.29	100.000000	0.000000	0.000000	0.000000	
	Sums:			100.00	100.00		

Grainsize Statistics
Percentiles

	phi	*mm*
5	2.26	0.209
16	2.50	0.177
25	2.61	0.163
50	2.90	0.134
75	3.18	0.110
84	3.32	0.100
95	3.57	0.084

Folks' Graphic Statistics

	Mean (Mz)	Sorting (σI)	Skewness (SkI)	Kurtosis (KG)	Mean *mm*
phi	2.905	0.403	0.020	0.946	0.133

Table II.68: *Results summary for sample 68: High intertidal zone, eastern transect, Wainamu Beach. Sample collected on the 28th of November, 2014.*

Column: 69 **Density:** 2650
Volume: 0.010
Sample ID: 2014-11-28eh

Malvern data Phi	Malvern data Micron	Vol %	Equivalent Cum wt (g)
-1.00	2000.00	0	0.0
-0.75	1680.00	0	0.0
-0.50	1410.00	0	0.0
-0.25	1190.00	0	0.0
0.00	1000.00	0	0.0
0.25	840.00	0	0.0
0.49	710.00	0	0.0
0.76	590.00	0	0.0
1.00	500.00	0	0.0
1.25	420.00	0.208285	0.1
1.51	350.00	2.041195	0.5
1.74	300.00	5.956552	1.6
2.00	250.00	14.568767	3.9
2.25	210.00	27.092658	7.2
2.50	177.00	42.511293	11.3
2.75	149.00	59.191302	15.7
3.00	125.00	74.873206	19.8
3.25	105.00	87.040864	23.1
3.51	88.00	94.975489	25.2
3.76	74.00	98.809089	26.2
3.99	63.00	99.974303	26.5
4.24	53.00	100	26.5
4.51	44.00	100	26.5
4.76	37.00	100	26.5
5.01	31.00	100	26.5
6.00	15.60	100	26.5
6.64	10.00	100	26.5
7.00	7.80	100	26.5
8.00	3.90	100	26.5
8.97	2.00	100	26.5
9.99	0.98	100	26.5
10.48	0.70	100	26.5
10.99	0.49	100	26.5
12.02	0.24	100	26.5
13.02	0.12	100	26.5
14.02	0.06	100	26.5
14.29	0.05	100	26.5
		Total weight:	26.5

	mm	phi	Cum wt (g)	Int wt (g)	Int wt%	Cum % finer	Modes	
1	2.0000	-1.00	0.000000	0.000000	0.000000	100.000000		
2	1.6800	-0.75	0.000000	0.000000	0.000000	100.000000		
3	1.4100	-0.50	0.000000	0.000000	0.000000	100.000000		
4	1.1900	-0.25	0.000000	0.000000	0.000000	100.000000		
5	1.0000	0.00	0.000000	0.000000	0.000000	100.000000		8
6	0.8400	0.25	0.000000	0.000000	0.000000	100.000000		
7	0.7100	0.49	0.000000	0.000000	0.000000	100.000000		
8	0.5900	0.76	0.000000	0.000000	0.000000	100.000000		
9	0.5000	1.00	0.000000	0.000000	0.000000	100.000000		
10	0.4200	1.25	0.208285	0.208285	0.208285	99.791715		
11	0.3500	1.51	2.041195	1.832910	1.832910	97.958805		
12	0.3000	1.74	5.956552	3.915357	3.915357	94.043448		
13	0.2500	2.00	14.568767	8.612215	8.612215	85.431233		
14	0.2100	2.25	27.092658	12.523891	12.523891	72.907342		
15	0.1770	2.50	42.511293	15.418635	15.418635	57.488707		
16	0.1490	2.75	59.191302	16.680009	16.680009	40.808698	mode at 2.622397	
17	0.1250	3.00	74.873206	15.681904	15.681904	25.126794		
18	0.1050	3.25	87.040864	12.167658	12.167658	12.959136		
19	0.0880	3.51	94.975489	7.934625	7.934625	5.024511		
20	0.0740	3.76	98.809089	3.833600	3.833600	1.190911		
21	0.0630	3.99	99.974303	1.165214	1.165214	0.025697		
22	0.0530	4.24	100.000000	0.025697	0.025697	0.000000		
23	0.0440	4.51	100.000000	0.000000	0.000000	0.000000		
24	0.0370	4.76	100.000000	0.000000	0.000000	0.000000		
25	0.0310	5.01	100.000000	0.000000	0.000000	0.000000		
26	0.0156	6.00	100.000000	0.000000	0.000000	0.000000		
27	0.0100	6.64	100.000000	0.000000	0.000000	0.000000		
28	0.0078	7.00	100.000000	0.000000	0.000000	0.000000		
29	0.0039	8.00	100.000000	0.000000	0.000000	0.000000		
30	0.0020	8.97	100.000000	0.000000	0.000000	0.000000		
31	0.0010	9.99	100.000000	0.000000	0.000000	0.000000		
32	0.0007	10.48	100.000000	0.000000	0.000000	0.000000		
33	0.0005	10.99	100.000000	0.000000	0.000000	0.000000		
34	0.0002	12.02	100.000000	0.000000	0.000000	0.000000		
35	0.0001	13.02	100.000000	0.000000	0.000000	0.000000		
36	0.0001	14.02	100.000000	0.000000	0.000000	0.000000		
37	0.0001	14.29	100.000000	0.000000	0.000000	0.000000		
	Sums:			100.00	100.00			

Column: 69
Sample ID: 2014-11-28eh

Folks' Graphic Statistics

	Mean (Mz)	Sorting (σI)	Skewness (SkI)	Kurtosis (KG)	Mean *mm*
phi	2.609	0.567	-0.009	0.943	0.164

Grainsize Statistics
Percentiles

	phi	*mm*
5	1.68	0.312
16	2.03	0.245
25	2.21	0.216
50	2.61	0.164
75	3.00	0.125
84	3.19	0.110
95	3.51	0.088

Table II.69: *Results summary for sample 69: Mid intertidal zone, mid transect, Wainamu Beach. Sample collected on the 28th of November, 2014.*

Column: 70 **Density:** 2650
Volume: 0.010
Sample ID: 2014-11-28mm

Malvern data Phi	Malvern data Micron	Vol %	Equivalent Cum wt (g)
-1.00	2000.00	0	0.0
-0.75	1680.00	0.317057	0.1
-0.50	1410.00	0.980865	0.3
-0.25	1190.00	1.851578	0.5
0.00	1000.00	2.786537	0.7
0.25	840.00	3.510988	0.9
0.49	710.00	3.800557	1.0
0.76	590.00	3.812712	1.0
1.00	500.00	3.822749	1.0
1.25	420.00	4.251644	1.1
1.51	350.00	6.233432	1.7
1.74	300.00	10.148756	2.7
2.00	250.00	18.439869	4.9
2.25	210.00	30.334261	8.0
2.50	177.00	44.952791	11.9
2.75	149.00	60.834114	16.1
3.00	125.00	75.86139	20.1
3.25	105.00	87.585684	23.2
3.51	88.00	95.241945	25.2
3.76	74.00	98.914015	26.2
3.99	63.00	99.978167	26.5
4.24	53.00	100	26.5
4.51	44.00	100	26.5
4.76	37.00	100	26.5
5.01	31.00	100	26.5
6.00	15.60	100	26.5
6.64	10.00	100	26.5
7.00	7.80	100	26.5
8.00	3.90	100	26.5
8.97	2.00	100	26.5
9.99	0.98	100	26.5
10.48	0.70	100	26.5
10.99	0.49	100	26.5
12.02	0.24	100	26.5
13.02	0.12	100	26.5
14.02	0.06	100	26.5
14.29	0.05	100	26.5

Total weight: 26.5

	mm	phi	Cum wt (g)	Int wt (g)	Int wt%	Cum % finer	Modes
1	2.0000	-1.00	0.000000	0.000000	0.000000	100.000000	
2	1.6800	-0.75	0.317057	0.317057	0.317057	99.682943	
3	1.4100	-0.50	0.980865	0.663808	0.663808	99.019135	
4	1.1900	-0.25	1.851578	0.870713	0.870713	98.148422	
5	1.0000	0.00	2.786537	0.934959	0.934959	97.213463	mode at -0.12548 8
6	0.8400	0.25	3.510988	0.724451	0.724451	96.489012	
7	0.7100	0.49	3.800557	0.289569	0.289569	96.199443	
8	0.5900	0.76	3.812712	0.012155	0.012155	96.187288	
9	0.5000	1.00	3.822749	0.010037	0.010037	96.177251	
10	0.4200	1.25	4.251644	0.428895	0.428895	95.748356	
11	0.3500	1.51	6.233432	1.981788	1.981788	93.766568	
12	0.3000	1.74	10.148756	3.915324	3.915324	89.851244	
13	0.2500	2.00	18.439869	8.291113	8.291113	81.560131	
14	0.2100	2.25	30.334261	11.894392	11.894392	69.665739	
15	0.1770	2.50	44.952791	14.618530	14.618530	55.047209	
16	0.1490	2.75	60.834114	15.881323	15.881323	39.165886	mode at 2.622397
17	0.1250	3.00	75.861390	15.027276	15.027276	24.138610	
18	0.1050	3.25	87.585684	11.724294	11.724294	12.414316	
19	0.0880	3.51	95.241945	7.656261	7.656261	4.758055	
20	0.0740	3.76	98.914015	3.672070	3.672070	1.085985	
21	0.0630	3.99	99.978167	1.064152	1.064152	0.021833	
22	0.0530	4.24	100.000000	0.021833	0.021833	0.000000	
23	0.0440	4.51	100.000000	0.000000	0.000000	0.000000	
24	0.0370	4.76	100.000000	0.000000	0.000000	0.000000	
25	0.0310	5.01	100.000000	0.000000	0.000000	0.000000	
26	0.0156	6.00	100.000000	0.000000	0.000000	0.000000	
27	0.0100	6.64	100.000000	0.000000	0.000000	0.000000	
28	0.0078	7.00	100.000000	0.000000	0.000000	0.000000	
29	0.0039	8.00	100.000000	0.000000	0.000000	0.000000	
30	0.0020	8.97	100.000000	0.000000	0.000000	0.000000	
31	0.0010	9.99	100.000000	0.000000	0.000000	0.000000	
32	0.0007	10.48	100.000000	0.000000	0.000000	0.000000	
33	0.0005	10.99	100.000000	0.000000	0.000000	0.000000	
34	0.0002	12.02	100.000000	0.000000	0.000000	0.000000	
35	0.0001	13.02	100.000000	0.000000	0.000000	0.000000	
36	0.0001	14.02	100.000000	0.000000	0.000000	0.000000	
37	0.0001	14.29	100.000000	0.000000	0.000000	0.000000	
		Sums:		100.00	100.00		

Column: 70
Sample ID: 2014-11-28mm

Folks' Graphic Statistics

	Mean (Mz)	Sorting (σI)	Skewness (SkI)	Kurtosis (KG)	Mean *mm*
phi	2.558	0.638	-0.094	1.039	0.170

Grainsize Statistics
Percentiles

	phi	*mm*
5	1.35	0.392
16	1.92	0.264
25	2.14	0.227
50	2.58	0.168
75	2.99	0.126
84	3.17	0.111
95	3.50	0.088

Table II.70: *Results summary for sample 70: Mid intertidal zone, eastern transect, Wainamu Beach. Sample collected on the 28th of November, 2014.*

Column: 71 **Density:** 2650
Volume: 0.010
Sample ID: 2014-11-28em

Malvern data Phi	Malvern data Micron	Vol %	Equivalent Cum wt (g)
-1.00	2000.00	0	0.0
-0.75	1680.00	0.015706	0.0
-0.50	1410.00	0.015706	0.0
-0.25	1190.00	0.015706	0.0
0.00	1000.00	0.015706	0.0
0.25	840.00	0.015706	0.0
0.49	710.00	0.015706	0.0
0.76	590.00	0.027182	0.0
1.00	500.00	1.105431	0.3
1.25	420.00	4.674188	1.2
1.51	350.00	12.463073	3.3
1.74	300.00	22.723693	6.0
2.00	250.00	38.480738	10.2
2.25	210.00	55.265821	14.6
2.50	177.00	70.874008	18.8
2.75	149.00	83.622983	22.2
3.00	125.00	92.440556	24.5
3.25	105.00	97.172842	25.8
3.51	88.00	98.989075	26.2
3.76	74.00	99.19586	26.3
3.99	63.00	99.19586	26.3
4.24	53.00	99.19586	26.3
4.51	44.00	99.19586	26.3
4.76	37.00	99.19586	26.3
5.01	31.00	99.19586	26.3
6.00	15.60	99.19586	26.3
6.64	10.00	99.19586	26.3
7.00	7.80	99.339622	26.3
8.00	3.90	99.869552	26.5
8.97	2.00	100	26.5
9.99	0.98	100	26.5
10.48	0.70	100	26.5
10.99	0.49	100	26.5
12.02	0.24	100	26.5
13.02	0.12	100	26.5
14.02	0.06	100	26.5
14.29	0.05	100	26.5
		Total weight:	26.5

	mm	phi	Cum wt (g)	Int wt (g)	Int wt%	Cum % finer	Modes	
1	2.0000	-1.00	0.000000	0.000000	0.000000	100.000000		
2	1.6800	-0.75	0.015706	0.015706	0.015706	99.984294	mode at -0.87423	
3	1.4100	-0.50	0.015706	0.000000	0.000000	99.984294		
4	1.1900	-0.25	0.015706	0.000000	0.000000	99.984294		
5	1.0000	0.00	0.015706	0.000000	0.000000	99.984294		8
6	0.8400	0.25	0.015706	0.000000	0.000000	99.984294		
7	0.7100	0.49	0.015706	0.000000	0.000000	99.984294		
8	0.5900	0.76	0.027182	0.011476	0.011476	99.972818		
9	0.5000	1.00	1.105431	1.078249	1.078249	98.894569		
10	0.4200	1.25	4.674188	3.568757	3.568757	95.325812		
11	0.3500	1.51	12.463073	7.788885	7.788885	87.536927		
12	0.3000	1.74	22.723693	10.260620	10.260620	77.276307		
13	0.2500	2.00	38.480738	15.757045	15.757045	61.519262		
14	0.2100	2.25	55.265821	16.785083	16.785083	44.734179	mode at 2.125769	
15	0.1770	2.50	70.874008	15.608187	15.608187	29.125992		
16	0.1490	2.75	83.622983	12.748975	12.748975	16.377017		
17	0.1250	3.00	92.440556	8.817573	8.817573	7.559444		
18	0.1050	3.25	97.172842	4.732286	4.732286	2.827158		
19	0.0880	3.51	98.989075	1.816233	1.816233	1.010925		
20	0.0740	3.76	99.195860	0.206785	0.206785	0.804140		
21	0.0630	3.99	99.195860	0.000000	0.000000	0.804140		
22	0.0530	4.24	99.195860	0.000000	0.000000	0.804140		
23	0.0440	4.51	99.195860	0.000000	0.000000	0.804140		
24	0.0370	4.76	99.195860	0.000000	0.000000	0.804140		
25	0.0310	5.01	99.195860	0.000000	0.000000	0.804140		
26	0.0156	6.00	99.195860	0.000000	0.000000	0.804140		
27	0.0100	6.64	99.195860	0.000000	0.000000	0.804140		
28	0.0078	7.00	99.339622	0.143762	0.143762	0.660378		
29	0.0039	8.00	99.869552	0.529930	0.529930	0.130448	mode at 7.50231	
30	0.0020	8.97	100.000000	0.130448	0.130448	0.000000		
31	0.0010	9.99	100.000000	0.000000	0.000000	0.000000		
32	0.0007	10.48	100.000000	0.000000	0.000000	0.000000		
33	0.0005	10.99	100.000000	0.000000	0.000000	0.000000		
34	0.0002	12.02	100.000000	0.000000	0.000000	0.000000		
35	0.0001	13.02	100.000000	0.000000	0.000000	0.000000		
36	0.0001	14.02	100.000000	0.000000	0.000000	0.000000		
37	0.0001	14.29	100.000000	0.000000	0.000000	0.000000		
		Sums:		100.00	100.00			

Grainsize Statistics
Percentiles

	phi	*mm*
5	1.26	0.417
16	1.59	0.332
25	1.77	0.292
50	2.17	0.222
75	2.58	0.167
84	2.76	0.148
95	3.14	0.114

Column: 71
Sample ID: 2014-11-28em

Folks' Graphic Statistics

	Mean (Mz)	Sorting (σI)	Skewness (SkI)	Kurtosis (KG)	Mean *mm*
phi	2.174	0.575	0.016	0.955	0.222

Table II.71: *Results summary for sample 71: Mid intertidal zone, mid transect, Northern Ngarunui Beach. Sample collected on the 15th of August, 2014.*

Column: 72 **Density:** 2650
Volume: 0.010
Sample ID: 2014-8-15mm

Malvern data Phi	Malvern data Micron	Vol %	Equivalent Cum wt (g)
-1.00	2000.00	0	0.0
-0.75	1680.00	0	0.0
-0.50	1410.00	0	0.0
-0.25	1190.00	0	0.0
0.00	1000.00	0	0.0
0.25	840.00	0	0.0
0.49	710.00	0.423441	0.1
0.76	590.00	3.089668	0.8
1.00	500.00	9.010566	2.4
1.25	420.00	20.07095	5.3
1.51	350.00	36.568964	9.7
1.74	300.00	52.684612	14.0
2.00	250.00	71.043268	18.8
2.25	210.00	84.966273	22.5
2.50	177.00	93.79899	24.9
2.75	149.00	98.272156	26.0
3.00	125.00	99.821644	26.5
3.25	105.00	100	26.5
3.51	88.00	100	26.5
3.76	74.00	100	26.5
3.99	63.00	100	26.5
4.24	53.00	100	26.5
4.51	44.00	100	26.5
4.76	37.00	100	26.5
5.01	31.00	100	26.5
6.00	15.60	100	26.5
6.64	10.00	100	26.5
7.00	7.80	100	26.5
8.00	3.90	100	26.5
8.97	2.00	100	26.5
9.99	0.98	100	26.5
10.48	0.70	100	26.5
10.99	0.49	100	26.5
12.02	0.24	100	26.5
13.02	0.12	100	26.5
14.02	0.06	100	26.5
14.29	0.05	100	26.5
		Total weight:	26.5

	mm	phi	Cum wt (g)	Int wt (g)	Int wt%	Cum % finer	Modes
1	2.0000	-1.00	0.000000	0.000000	0.000000	100.000000	
2	1.6800	-0.75	0.000000	0.000000	0.000000	100.000000	
3	1.4100	-0.50	0.000000	0.000000	0.000000	100.000000	
4	1.1900	-0.25	0.000000	0.000000	0.000000	100.000000	
5	1.0000	0.00	0.000000	0.000000	0.000000	100.000000	8
6	0.8400	0.25	0.000000	0.000000	0.000000	100.000000	
7	0.7100	0.49	0.423441	0.423441	0.423441	99.576559	
8	0.5900	0.76	3.089668	2.666227	2.666227	96.910332	
9	0.5000	1.00	9.010566	5.920898	5.920898	90.989434	
10	0.4200	1.25	20.070950	11.060384	11.060384	79.929050	
11	0.3500	1.51	36.568964	16.498014	16.498014	63.431036	mode at 1.383056
12	0.3000	1.74	52.684612	16.115648	16.115648	47.315388	
13	0.2500	2.00	71.043268	18.358656	18.358656	28.956732	mode at 1.868483
14	0.2100	2.25	84.966273	13.923005	13.923005	15.033727	
15	0.1770	2.50	93.798990	8.832717	8.832717	6.201010	
16	0.1490	2.75	98.272156	4.473166	4.473166	1.727844	
17	0.1250	3.00	99.821644	1.549488	1.549488	0.178356	
18	0.1050	3.25	100.000000	0.178356	0.178356	0.000000	
19	0.0880	3.51	100.000000	0.000000	0.000000	0.000000	
20	0.0740	3.76	100.000000	0.000000	0.000000	0.000000	
21	0.0630	3.99	100.000000	0.000000	0.000000	0.000000	
22	0.0530	4.24	100.000000	0.000000	0.000000	0.000000	
23	0.0440	4.51	100.000000	0.000000	0.000000	0.000000	
24	0.0370	4.76	100.000000	0.000000	0.000000	0.000000	
25	0.0310	5.01	100.000000	0.000000	0.000000	0.000000	
26	0.0156	6.00	100.000000	0.000000	0.000000	0.000000	
27	0.0100	6.64	100.000000	0.000000	0.000000	0.000000	
28	0.0078	7.00	100.000000	0.000000	0.000000	0.000000	
29	0.0039	8.00	100.000000	0.000000	0.000000	0.000000	
30	0.0020	8.97	100.000000	0.000000	0.000000	0.000000	
31	0.0010	9.99	100.000000	0.000000	0.000000	0.000000	
32	0.0007	10.48	100.000000	0.000000	0.000000	0.000000	
33	0.0005	10.99	100.000000	0.000000	0.000000	0.000000	
34	0.0002	12.02	100.000000	0.000000	0.000000	0.000000	
35	0.0001	13.02	100.000000	0.000000	0.000000	0.000000	
36	0.0001	14.02	100.000000	0.000000	0.000000	0.000000	
37	0.0001	14.29	100.000000	0.000000	0.000000	0.000000	
		Sums:		100.00	100.00		

Grainsize Statistics
Percentiles

	phi	*mm*
5	0.84	0.559
16	1.16	0.448
25	1.33	0.398
50	1.70	0.308
75	2.07	0.238
84	2.23	0.213
95	2.56	0.169

Column: 72
Sample ID: 2014-8-15mm

Folks' Graphic Statistics

	Mean (Mz)	Sorting (σI)	Skewness (SkI)	Kurtosis (KG)	Mean *mm*
phi	1.698	0.530	-0.002	0.955	0.308

Table II.72: *Results summary for sample 72: High intertidal zone, northern transect, Northern Ngarunui Beach. Sample collected on the 15th of August, 2014.*

Column: 73 **Density:** 2650
Volume: 0.010
Sample ID: 2014-8-15hn

Malvern data Phi	Malvern data Micron	Vol %	Equivalent Cum wt (g)
-1.00	2000.00	0	0.0
-0.75	1680.00	0	0.0
-0.50	1410.00	0	0.0
-0.25	1190.00	0	0.0
0.00	1000.00	0	0.0
0.25	840.00	0	0.0
0.49	710.00	0	0.0
0.76	590.00	0.343044	0.1
1.00	500.00	2.251776	0.6
1.25	420.00	7.665742	2.0
1.51	350.00	18.565811	4.9
1.74	300.00	31.997483	8.5
2.00	250.00	50.945234	13.5
2.25	210.00	68.910075	18.3
2.50	177.00	83.298801	22.1
2.75	149.00	92.946195	24.6
3.00	125.00	98.004217	26.0
3.25	105.00	99.776813	26.4
3.51	88.00	100	26.5
3.76	74.00	100	26.5
3.99	63.00	100	26.5
4.24	53.00	100	26.5
4.51	44.00	100	26.5
4.76	37.00	100	26.5
5.01	31.00	100	26.5
6.00	15.60	100	26.5
6.64	10.00	100	26.5
7.00	7.80	100	26.5
8.00	3.90	100	26.5
8.97	2.00	100	26.5
9.99	0.98	100	26.5
10.48	0.70	100	26.5
10.99	0.49	100	26.5
12.02	0.24	100	26.5
13.02	0.12	100	26.5
14.02	0.06	100	26.5
14.29	0.05	100	26.5
		Total weight:	26.5

	mm	phi	Cum wt (g)	Int wt (g)	Int wt%	Cum % finer	Modes
1	2.0000	-1.00	0.000000	0.000000	0.000000	100.000000	
2	1.6800	-0.75	0.000000	0.000000	0.000000	100.000000	
3	1.4100	-0.50	0.000000	0.000000	0.000000	100.000000	
4	1.1900	-0.25	0.000000	0.000000	0.000000	100.000000	
5	1.0000	0.00	0.000000	0.000000	0.000000	100.000000	8
6	0.8400	0.25	0.000000	0.000000	0.000000	100.000000	
7	0.7100	0.49	0.000000	0.000000	0.000000	100.000000	
8	0.5900	0.76	0.343044	0.343044	0.343044	99.656956	
9	0.5000	1.00	2.251776	1.908732	1.908732	97.748224	
10	0.4200	1.25	7.665742	5.413966	5.413966	92.334258	
11	0.3500	1.51	18.565811	10.900069	10.900069	81.434189	
12	0.3000	1.74	31.997483	13.431672	13.431672	68.002517	
13	0.2500	2.00	50.945234	18.947751	18.947751	49.054766	mode at 1.868483
14	0.2100	2.25	68.910075	17.964841	17.964841	31.089925	
15	0.1770	2.50	83.298801	14.388726	14.388726	16.701199	
16	0.1490	2.75	92.946195	9.647394	9.647394	7.053805	
17	0.1250	3.00	98.004217	5.058022	5.058022	1.995783	
18	0.1050	3.25	99.776813	1.772596	1.772596	0.223187	
19	0.0880	3.51	100.000000	0.223187	0.223187	0.000000	
20	0.0740	3.76	100.000000	0.000000	0.000000	0.000000	
21	0.0630	3.99	100.000000	0.000000	0.000000	0.000000	
22	0.0530	4.24	100.000000	0.000000	0.000000	0.000000	
23	0.0440	4.51	100.000000	0.000000	0.000000	0.000000	
24	0.0370	4.76	100.000000	0.000000	0.000000	0.000000	
25	0.0310	5.01	100.000000	0.000000	0.000000	0.000000	
26	0.0156	6.00	100.000000	0.000000	0.000000	0.000000	
27	0.0100	6.64	100.000000	0.000000	0.000000	0.000000	
28	0.0078	7.00	100.000000	0.000000	0.000000	0.000000	
29	0.0039	8.00	100.000000	0.000000	0.000000	0.000000	
30	0.0020	8.97	100.000000	0.000000	0.000000	0.000000	
31	0.0010	9.99	100.000000	0.000000	0.000000	0.000000	
32	0.0007	10.48	100.000000	0.000000	0.000000	0.000000	
33	0.0005	10.99	100.000000	0.000000	0.000000	0.000000	
34	0.0002	12.02	100.000000	0.000000	0.000000	0.000000	
35	0.0001	13.02	100.000000	0.000000	0.000000	0.000000	
36	0.0001	14.02	100.000000	0.000000	0.000000	0.000000	
37	0.0001	14.29	100.000000	0.000000	0.000000	0.000000	
	Sums:			100.00	100.00		

Column: 73
Sample ID: 2014-8-15hn

Folks' Graphic Statistics

	Mean (Mz)	Sorting (σI)	Skewness (SkI)	Kurtosis (KG)	Mean *mm*
phi	1.985	0.527	-0.001	0.960	0.253

Grainsize Statistics
Percentiles

	phi	*mm*
5	1.13	0.458
16	1.45	0.365
25	1.62	0.325
50	1.99	0.252
75	2.36	0.195
84	2.52	0.175
95	2.85	0.139

Table II.73: *Results summary for sample 73: Low intertidal zone, mid transect, Northern Ngarunui Beach. Sample collected on the 15th of August, 2014.*

Column: 74 **Density:** 2650
Volume: 0.010
Sample ID: 2014-8-15lm

Malvern data Phi	Malvern data Micron	Vol %	Equivalent Cum wt (g)
-1.00	2000.00	0	0.0
-0.75	1680.00	0	0.0
-0.50	1410.00	0	0.0
-0.25	1190.00	0	0.0
0.00	1000.00	0	0.0
0.25	840.00	0.086281	0.0
0.49	710.00	0.960012	0.3
0.76	590.00	4.639173	1.2
1.00	500.00	11.795152	3.1
1.25	420.00	24.180822	6.4
1.51	350.00	41.624137	11.0
1.74	300.00	57.889722	15.3
2.00	250.00	75.577087	20.0
2.25	210.00	88.246903	23.4
2.50	177.00	95.712462	25.4
2.75	149.00	99.085594	26.3
3.00	125.00	99.938975	26.5
3.25	105.00	100	26.5
3.51	88.00	100	26.5
3.76	74.00	100	26.5
3.99	63.00	100	26.5
4.24	53.00	100	26.5
4.51	44.00	100	26.5
4.76	37.00	100	26.5
5.01	31.00	100	26.5
6.00	15.60	100	26.5
6.64	10.00	100	26.5
7.00	7.80	100	26.5
8.00	3.90	100	26.5
8.97	2.00	100	26.5
9.99	0.98	100	26.5
10.48	0.70	100	26.5
10.99	0.49	100	26.5
12.02	0.24	100	26.5
13.02	0.12	100	26.5
14.02	0.06	100	26.5
14.29	0.05	100	26.5
		Total weight:	26.5

	mm	phi	Cum wt (g)	Int wt (g)	Int wt%	Cum % finer	Modes	
1	2.0000	-1.00	0.000000	0.000000	0.000000	100.000000		
2	1.6800	-0.75	0.000000	0.000000	0.000000	100.000000		
3	1.4100	-0.50	0.000000	0.000000	0.000000	100.000000		
4	1.1900	-0.25	0.000000	0.000000	0.000000	100.000000		
5	1.0000	0.00	0.000000	0.000000	0.000000	100.000000		8
6	0.8400	0.25	0.086281	0.086281	0.086281	99.913719		
7	0.7100	0.49	0.960012	0.873731	0.873731	99.039988		
8	0.5900	0.76	4.639173	3.679161	3.679161	95.360827		
9	0.5000	1.00	11.795152	7.155979	7.155979	88.204848		
10	0.4200	1.25	24.180822	12.385670	12.385670	75.819178		
11	0.3500	1.51	41.624137	17.443315	17.443315	58.375863	mode at 1.383056	
12	0.3000	1.74	57.889722	16.265585	16.265585	42.110278		
13	0.2500	2.00	75.577087	17.687365	17.687365	24.422913	mode at 1.868483	
14	0.2100	2.25	88.246903	12.669816	12.669816	11.753097		
15	0.1770	2.50	95.712462	7.465559	7.465559	4.287538		
16	0.1490	2.75	99.085594	3.373132	3.373132	0.914406		
17	0.1250	3.00	99.938975	0.853381	0.853381	0.061025		
18	0.1050	3.25	100.000000	0.061025	0.061025	0.000000		
19	0.0880	3.51	100.000000	0.000000	0.000000	0.000000		
20	0.0740	3.76	100.000000	0.000000	0.000000	0.000000		
21	0.0630	3.99	100.000000	0.000000	0.000000	0.000000		
22	0.0530	4.24	100.000000	0.000000	0.000000	0.000000		
23	0.0440	4.51	100.000000	0.000000	0.000000	0.000000		
24	0.0370	4.76	100.000000	0.000000	0.000000	0.000000		
25	0.0310	5.01	100.000000	0.000000	0.000000	0.000000		
26	0.0156	6.00	100.000000	0.000000	0.000000	0.000000		
27	0.0100	6.64	100.000000	0.000000	0.000000	0.000000		
28	0.0078	7.00	100.000000	0.000000	0.000000	0.000000		
29	0.0039	8.00	100.000000	0.000000	0.000000	0.000000		
30	0.0020	8.97	100.000000	0.000000	0.000000	0.000000		
31	0.0010	9.99	100.000000	0.000000	0.000000	0.000000		
32	0.0007	10.48	100.000000	0.000000	0.000000	0.000000		
33	0.0005	10.99	100.000000	0.000000	0.000000	0.000000		
34	0.0002	12.02	100.000000	0.000000	0.000000	0.000000		
35	0.0001	13.02	100.000000	0.000000	0.000000	0.000000		
36	0.0001	14.02	100.000000	0.000000	0.000000	0.000000		
37	0.0001	14.29	100.000000	0.000000	0.000000	0.000000		
	Sums:			100.00	100.00			

Column: 74
Sample ID: 2014-8-15lm

Folks' Graphic Statistics

	Mean (Mz)	Sorting (σI)	Skewness (SkI)	Kurtosis (KG)	Mean *mm*
phi	1.627	0.528	-0.006	0.958	0.324

Grainsize Statistics
Percentiles

	phi	*mm*
5	0.77	0.585
16	1.09	0.471
25	1.26	0.416
50	1.63	0.323
75	1.99	0.251
84	2.17	0.223
95	2.47	0.180

Table II.74: *Results summary for sample 74: High intertidal zone, southern transect, Northern Ngarunui Beach. Sample collected on the 15th of August, 2014.*

Column: 75 **Density:** 2650
Volume: 0.010
Sample ID: 2014-8-15hs

Malvern data Phi	Malvern data Micron	Vol %	Equivalent Cum wt (g)
-1.00	2000.00	0	0.0
-0.75	1680.00	0	0.0
-0.50	1410.00	0	0.0
-0.25	1190.00	0	0.0
0.00	1000.00	0	0.0
0.25	840.00	0	0.0
0.49	710.00	0.145282	0.0
0.76	590.00	1.906335	0.5
1.00	500.00	6.258075	1.7
1.25	420.00	14.775876	3.9
1.51	350.00	28.154246	7.5
1.74	300.00	42.122887	11.2
2.00	250.00	59.602598	15.8
2.25	210.00	74.809014	19.8
2.50	177.00	86.429034	22.9
2.75	149.00	94.126753	24.9
3.00	125.00	98.259167	26.0
3.25	105.00	99.821369	26.5
3.51	88.00	100	26.5
3.76	74.00	100	26.5
3.99	63.00	100	26.5
4.24	53.00	100	26.5
4.51	44.00	100	26.5
4.76	37.00	100	26.5
5.01	31.00	100	26.5
6.00	15.60	100	26.5
6.64	10.00	100	26.5
7.00	7.80	100	26.5
8.00	3.90	100	26.5
8.97	2.00	100	26.5
9.99	0.98	100	26.5
10.48	0.70	100	26.5
10.99	0.49	100	26.5
12.02	0.24	100	26.5
13.02	0.12	100	26.5
14.02	0.06	100	26.5
14.29	0.05	100	26.5

Total weight: 26.5

	mm	phi	Cum wt (g)	Int wt (g)	Int wt%	Cum % finer	Modes
1	2.0000	-1.00	0.000000	0.000000	0.000000	100.000000	
2	1.6800	-0.75	0.000000	0.000000	0.000000	100.000000	
3	1.4100	-0.50	0.000000	0.000000	0.000000	100.000000	
4	1.1900	-0.25	0.000000	0.000000	0.000000	100.000000	
5	1.0000	0.00	0.000000	0.000000	0.000000	100.000000	8
6	0.8400	0.25	0.000000	0.000000	0.000000	100.000000	
7	0.7100	0.49	0.145282	0.145282	0.145282	99.854718	
8	0.5900	0.76	1.906335	1.761053	1.761053	98.093665	
9	0.5000	1.00	6.258075	4.351740	4.351740	93.741925	
10	0.4200	1.25	14.775876	8.517801	8.517801	85.224124	
11	0.3500	1.51	28.154246	13.378370	13.378370	71.845754	
12	0.3000	1.74	42.122887	13.968641	13.968641	57.877113	
13	0.2500	2.00	59.602598	17.479711	17.479711	40.397402	mode at 1.868483
14	0.2100	2.25	74.809014	15.206416	15.206416	25.190986	
15	0.1770	2.50	86.429034	11.620020	11.620020	13.570966	
16	0.1490	2.75	94.126753	7.697719	7.697719	5.873247	
17	0.1250	3.00	98.259167	4.132414	4.132414	1.740833	
18	0.1050	3.25	99.821369	1.562202	1.562202	0.178631	
19	0.0880	3.51	100.000000	0.178631	0.178631	0.000000	
20	0.0740	3.76	100.000000	0.000000	0.000000	0.000000	
21	0.0630	3.99	100.000000	0.000000	0.000000	0.000000	
22	0.0530	4.24	100.000000	0.000000	0.000000	0.000000	
23	0.0440	4.51	100.000000	0.000000	0.000000	0.000000	
24	0.0370	4.76	100.000000	0.000000	0.000000	0.000000	
25	0.0310	5.01	100.000000	0.000000	0.000000	0.000000	
26	0.0156	6.00	100.000000	0.000000	0.000000	0.000000	
27	0.0100	6.64	100.000000	0.000000	0.000000	0.000000	
28	0.0078	7.00	100.000000	0.000000	0.000000	0.000000	
29	0.0039	8.00	100.000000	0.000000	0.000000	0.000000	
30	0.0020	8.97	100.000000	0.000000	0.000000	0.000000	
31	0.0010	9.99	100.000000	0.000000	0.000000	0.000000	
32	0.0007	10.48	100.000000	0.000000	0.000000	0.000000	
33	0.0005	10.99	100.000000	0.000000	0.000000	0.000000	
34	0.0002	12.02	100.000000	0.000000	0.000000	0.000000	
35	0.0001	13.02	100.000000	0.000000	0.000000	0.000000	
36	0.0001	14.02	100.000000	0.000000	0.000000	0.000000	
37	0.0001	14.29	100.000000	0.000000	0.000000	0.000000	
		Sums:		100.00	100.00		

Column: 75
Sample ID: 2014-8-15hs

Folks' Graphic Statistics

	Mean (Mz)	Sorting (σI)	Skewness (SkI)	Kurtosis (KG)	Mean *mm*
phi	1.859	0.576	0.010	0.954	0.276

Grainsize Statistics
Percentiles

	phi	*mm*
5	0.93	0.525
16	1.28	0.413
25	1.45	0.365
50	1.86	0.276
75	2.26	0.209
84	2.45	0.183
95	2.80	0.144

Table II.75: *Results summary for sample 75: High intertidal zone, mid transect, Northern Ngarunui Beach. Sample collected on the 15th of August, 2014.*

Column: 76 **Density:** 2650
Volume: 0.010
Sample ID: 2014-8-15mh

Malvern data Phi	Malvern data Micron	Vol %	Equivalent Cum wt (g)
-1.00	2000.00	0	0.0
-0.75	1680.00	0	0.0
-0.50	1410.00	0	0.0
-0.25	1190.00	0	0.0
0.00	1000.00	0	0.0
0.25	840.00	0	0.0
0.49	710.00	0	0.0
0.76	590.00	0.432489	0.1
1.00	500.00	2.55228	0.7
1.25	420.00	8.355801	2.2
1.51	350.00	19.784531	5.2
1.74	300.00	33.614593	8.9
2.00	250.00	52.760526	14.0
2.25	210.00	70.53348	18.7
2.50	177.00	84.457201	22.4
2.75	149.00	93.573867	24.8
3.00	125.00	98.230135	26.0
3.25	105.00	99.810996	26.4
3.51	88.00	100	26.5
3.76	74.00	100	26.5
3.99	63.00	100	26.5
4.24	53.00	100	26.5
4.51	44.00	100	26.5
4.76	37.00	100	26.5
5.01	31.00	100	26.5
6.00	15.60	100	26.5
6.64	10.00	100	26.5
7.00	7.80	100	26.5
8.00	3.90	100	26.5
8.97	2.00	100	26.5
9.99	0.98	100	26.5
10.48	0.70	100	26.5
10.99	0.49	100	26.5
12.02	0.24	100	26.5
13.02	0.12	100	26.5
14.02	0.06	100	26.5
14.29	0.05	100	26.5
		Total weight:	26.5

	mm	phi	Cum wt (g)	Int wt (g)	Int wt%	Cum % finer	Modes
1	2.0000	-1.00	0.000000	0.000000	0.000000	100.000000	
2	1.6800	-0.75	0.000000	0.000000	0.000000	100.000000	
3	1.4100	-0.50	0.000000	0.000000	0.000000	100.000000	
4	1.1900	-0.25	0.000000	0.000000	0.000000	100.000000	
5	1.0000	0.00	0.000000	0.000000	0.000000	100.000000	8
6	0.8400	0.25	0.000000	0.000000	0.000000	100.000000	
7	0.7100	0.49	0.000000	0.000000	0.000000	100.000000	
8	0.5900	0.76	0.432489	0.432489	0.432489	99.567511	
9	0.5000	1.00	2.552280	2.119791	2.119791	97.447720	
10	0.4200	1.25	8.355801	5.803521	5.803521	91.644199	
11	0.3500	1.51	19.784531	11.428730	11.428730	80.215469	
12	0.3000	1.74	33.614593	13.830062	13.830062	66.385407	
13	0.2500	2.00	52.760526	19.145933	19.145933	47.239474	mode at 1.868483
14	0.2100	2.25	70.533480	17.772954	17.772954	29.466520	
15	0.1770	2.50	84.457201	13.923721	13.923721	15.542799	
16	0.1490	2.75	93.573867	9.116666	9.116666	6.426133	
17	0.1250	3.00	98.230135	4.656268	4.656268	1.769865	
18	0.1050	3.25	99.810996	1.580861	1.580861	0.189004	
19	0.0880	3.51	100.000000	0.189004	0.189004	0.000000	
20	0.0740	3.76	100.000000	0.000000	0.000000	0.000000	
21	0.0630	3.99	100.000000	0.000000	0.000000	0.000000	
22	0.0530	4.24	100.000000	0.000000	0.000000	0.000000	
23	0.0440	4.51	100.000000	0.000000	0.000000	0.000000	
24	0.0370	4.76	100.000000	0.000000	0.000000	0.000000	
25	0.0310	5.01	100.000000	0.000000	0.000000	0.000000	
26	0.0156	6.00	100.000000	0.000000	0.000000	0.000000	
27	0.0100	6.64	100.000000	0.000000	0.000000	0.000000	
28	0.0078	7.00	100.000000	0.000000	0.000000	0.000000	
29	0.0039	8.00	100.000000	0.000000	0.000000	0.000000	
30	0.0020	8.97	100.000000	0.000000	0.000000	0.000000	
31	0.0010	9.99	100.000000	0.000000	0.000000	0.000000	
32	0.0007	10.48	100.000000	0.000000	0.000000	0.000000	
33	0.0005	10.99	100.000000	0.000000	0.000000	0.000000	
34	0.0002	12.02	100.000000	0.000000	0.000000	0.000000	
35	0.0001	13.02	100.000000	0.000000	0.000000	0.000000	
36	0.0001	14.02	100.000000	0.000000	0.000000	0.000000	
37	0.0001	14.29	100.000000	0.000000	0.000000	0.000000	
		Sums:		100.00	100.00		

Column: 76
Sample ID: 2014-8-15mh

Folks' Graphic Statistics

	Mean (Mz)	Sorting (σI)	Skewness (SkI)	Kurtosis (KG)	Mean *mm*
phi	1.960	0.526	-0.001	0.962	0.257

Grainsize Statistics
Percentiles

	phi	*mm*
5	1.11	0.465
16	1.43	0.372
25	1.60	0.330
50	1.96	0.257
75	2.33	0.199
84	2.49	0.178
95	2.82	0.141

Table II.76: *Results summary for sample 76: Mid intertidal zone, southern transect, Northern Ngarunui Beach. Sample collected on the 15th of August, 2014.*

Column: 77 **Density:** 2650
Volume: 0.010
Sample ID: 2014-8-15ms

Malvern data Phi	Malvern data Micron	Vol %	Equivalent Cum wt (g)
-1.00	2000.00	0	0.0
-0.75	1680.00	0	0.0
-0.50	1410.00	0	0.0
-0.25	1190.00	0	0.0
0.00	1000.00	0	0.0
0.25	840.00	0	0.0
0.49	710.00	0.549393	0.1
0.76	590.00	3.892042	1.0
1.00	500.00	11.039556	2.9
1.25	420.00	23.836373	6.3
1.51	350.00	41.985612	11.1
1.74	300.00	58.769828	15.6
2.00	250.00	76.693087	20.3
2.25	210.00	89.183399	23.6
2.50	177.00	96.277467	25.5
2.75	149.00	99.304937	26.3
3.00	125.00	99.978142	26.5
3.25	105.00	100	26.5
3.51	88.00	100	26.5
3.76	74.00	100	26.5
3.99	63.00	100	26.5
4.24	53.00	100	26.5
4.51	44.00	100	26.5
4.76	37.00	100	26.5
5.01	31.00	100	26.5
6.00	15.60	100	26.5
6.64	10.00	100	26.5
7.00	7.80	100	26.5
8.00	3.90	100	26.5
8.97	2.00	100	26.5
9.99	0.98	100	26.5
10.48	0.70	100	26.5
10.99	0.49	100	26.5
12.02	0.24	100	26.5
13.02	0.12	100	26.5
14.02	0.06	100	26.5
14.29	0.05	100	26.5
		Total weight:	26.5

	mm	phi	Cum wt (g)	Int wt (g)	Int wt%	Cum % finer	Modes
1	2.0000	-1.00	0.000000	0.000000	0.000000	100.000000	
2	1.6800	-0.75	0.000000	0.000000	0.000000	100.000000	
3	1.4100	-0.50	0.000000	0.000000	0.000000	100.000000	
4	1.1900	-0.25	0.000000	0.000000	0.000000	100.000000	
5	1.0000	0.00	0.000000	0.000000	0.000000	100.000000	8
6	0.8400	0.25	0.000000	0.000000	0.000000	100.000000	
7	0.7100	0.49	0.549393	0.549393	0.549393	99.450607	
8	0.5900	0.76	3.892042	3.342649	3.342649	96.107958	
9	0.5000	1.00	11.039556	7.147514	7.147514	88.960444	
10	0.4200	1.25	23.836373	12.796817	12.796817	76.163627	
11	0.3500	1.51	41.985612	18.149239	18.149239	58.014388	mode at 1.383056
12	0.3000	1.74	58.769828	16.784216	16.784216	41.230172	
13	0.2500	2.00	76.693087	17.923259	17.923259	23.306913	mode at 1.868483
14	0.2100	2.25	89.183399	12.490312	12.490312	10.816601	
15	0.1770	2.50	96.277467	7.094068	7.094068	3.722533	
16	0.1490	2.75	99.304937	3.027470	3.027470	0.695063	
17	0.1250	3.00	99.978142	0.673205	0.673205	0.021858	
18	0.1050	3.25	100.000000	0.021858	0.021858	0.000000	
19	0.0880	3.51	100.000000	0.000000	0.000000	0.000000	
20	0.0740	3.76	100.000000	0.000000	0.000000	0.000000	
21	0.0630	3.99	100.000000	0.000000	0.000000	0.000000	
22	0.0530	4.24	100.000000	0.000000	0.000000	0.000000	
23	0.0440	4.51	100.000000	0.000000	0.000000	0.000000	
24	0.0370	4.76	100.000000	0.000000	0.000000	0.000000	
25	0.0310	5.01	100.000000	0.000000	0.000000	0.000000	
26	0.0156	6.00	100.000000	0.000000	0.000000	0.000000	
27	0.0100	6.64	100.000000	0.000000	0.000000	0.000000	
28	0.0078	7.00	100.000000	0.000000	0.000000	0.000000	
29	0.0039	8.00	100.000000	0.000000	0.000000	0.000000	
30	0.0020	8.97	100.000000	0.000000	0.000000	0.000000	
31	0.0010	9.99	100.000000	0.000000	0.000000	0.000000	
32	0.0007	10.48	100.000000	0.000000	0.000000	0.000000	
33	0.0005	10.99	100.000000	0.000000	0.000000	0.000000	
34	0.0002	12.02	100.000000	0.000000	0.000000	0.000000	
35	0.0001	13.02	100.000000	0.000000	0.000000	0.000000	
36	0.0001	14.02	100.000000	0.000000	0.000000	0.000000	
37	0.0001	14.29	100.000000	0.000000	0.000000	0.000000	
		Sums:		100.00	100.00		

Grainsize Statistics
Percentiles

	phi	*mm*
5	0.80	0.575
16	1.10	0.467
25	1.27	0.415
50	1.62	0.325
75	1.98	0.254
84	2.15	0.226
95	2.45	0.183

Column: 77
Sample ID: 2014-8-15ms

Folks' Graphic Statistics

	Mean (Mz)	Sorting (σI)	Skewness (SkI)	Kurtosis (KG)	Mean *mm*
phi	1.622	0.513	0.005	0.960	0.325

Table II.77: *Results summary for sample 77: Low intertidal zone, northern transect, Northern Ngarunui Beach. Sample collected on the 15th of August, 2014.*

Column: 78 **Density:** 2650
Volume: 0.010
Sample ID: 2014-8-15ln

Malvern data Phi	Malvern data Micron	Vol %	Equivalent Cum wt (g)
-1.00	2000.00	0	0.0
-0.75	1680.00	0	0.0
-0.50	1410.00	0	0.0
-0.25	1190.00	0	0.0
0.00	1000.00	0	0.0
0.25	840.00	0	0.0
0.49	710.00	0.41859	0.1
0.76	590.00	3.063163	0.8
1.00	500.00	8.6221	2.3
1.25	420.00	18.605431	4.9
1.51	350.00	33.293358	8.8
1.74	300.00	47.853125	12.7
2.00	250.00	65.209678	17.3
2.25	210.00	79.534604	21.1
2.50	177.00	89.85484	23.8
2.75	149.00	96.175892	25.5
3.00	125.00	99.189908	26.3
3.25	105.00	99.935006	26.5
3.51	88.00	100	26.5
3.76	74.00	100	26.5
3.99	63.00	100	26.5
4.24	53.00	100	26.5
4.51	44.00	100	26.5
4.76	37.00	100	26.5
5.01	31.00	100	26.5
6.00	15.60	100	26.5
6.64	10.00	100	26.5
7.00	7.80	100	26.5
8.00	3.90	100	26.5
8.97	2.00	100	26.5
9.99	0.98	100	26.5
10.48	0.70	100	26.5
10.99	0.49	100	26.5
12.02	0.24	100	26.5
13.02	0.12	100	26.5
14.02	0.06	100	26.5
14.29	0.05	100	26.5
		Total weight:	26.5

	mm	phi	Cum wt (g)	Int wt (g)	Int wt%	Cum % finer	Modes	
1	2.0000	-1.00	0.000000	0.000000	0.000000	100.000000		
2	1.6800	-0.75	0.000000	0.000000	0.000000	100.000000		
3	1.4100	-0.50	0.000000	0.000000	0.000000	100.000000		
4	1.1900	-0.25	0.000000	0.000000	0.000000	100.000000		
5	1.0000	0.00	0.000000	0.000000	0.000000	100.000000		8
6	0.8400	0.25	0.000000	0.000000	0.000000	100.000000		
7	0.7100	0.49	0.418590	0.418590	0.418590	99.581410		
8	0.5900	0.76	3.063163	2.644573	2.644573	96.936837		
9	0.5000	1.00	8.622100	5.558937	5.558937	91.377900		
10	0.4200	1.25	18.605431	9.983331	9.983331	81.394569		
11	0.3500	1.51	33.293358	14.687927	14.687927	66.706642	mode at 1.383056	
12	0.3000	1.74	47.853125	14.559767	14.559767	52.146875		
13	0.2500	2.00	65.209678	17.356553	17.356553	34.790322	mode at 1.868483	
14	0.2100	2.25	79.534604	14.324926	14.324926	20.465396		
15	0.1770	2.50	89.854840	10.320236	10.320236	10.145160		
16	0.1490	2.75	96.175892	6.321052	6.321052	3.824108		
17	0.1250	3.00	99.189908	3.014016	3.014016	0.810092		
18	0.1050	3.25	99.935006	0.745098	0.745098	0.064994		
19	0.0880	3.51	100.000000	0.064994	0.064994	0.000000		
20	0.0740	3.76	100.000000	0.000000	0.000000	0.000000		
21	0.0630	3.99	100.000000	0.000000	0.000000	0.000000		
22	0.0530	4.24	100.000000	0.000000	0.000000	0.000000		
23	0.0440	4.51	100.000000	0.000000	0.000000	0.000000		
24	0.0370	4.76	100.000000	0.000000	0.000000	0.000000		
25	0.0310	5.01	100.000000	0.000000	0.000000	0.000000		
26	0.0156	6.00	100.000000	0.000000	0.000000	0.000000		
27	0.0100	6.64	100.000000	0.000000	0.000000	0.000000		
28	0.0078	7.00	100.000000	0.000000	0.000000	0.000000		
29	0.0039	8.00	100.000000	0.000000	0.000000	0.000000		
30	0.0020	8.97	100.000000	0.000000	0.000000	0.000000		
31	0.0010	9.99	100.000000	0.000000	0.000000	0.000000		
32	0.0007	10.48	100.000000	0.000000	0.000000	0.000000		
33	0.0005	10.99	100.000000	0.000000	0.000000	0.000000		
34	0.0002	12.02	100.000000	0.000000	0.000000	0.000000		
35	0.0001	13.02	100.000000	0.000000	0.000000	0.000000		
36	0.0001	14.02	100.000000	0.000000	0.000000	0.000000		
37	0.0001	14.29	100.000000	0.000000	0.000000	0.000000		
	Sums:			100.00	100.00			

Column: 78
Sample ID: 2014-8-15ln

Folks' Graphic Statistics

	Mean (Mz)	Sorting (σI)	Skewness (SkI)	Kurtosis (KG)	Mean *mm*
phi	1.771	0.574	0.004	0.944	0.293

Grainsize Statistics
Percentiles

	phi	*mm*
5	0.84	0.557
16	1.19	0.440
25	1.37	0.388
50	1.77	0.293
75	2.17	0.222
84	2.36	0.195
95	2.70	0.154

Table II.78: *Results summary for sample 78: Low intertidal zone, southern transect, Northern Ngarunui Beach. Sample collected on the 15th of August, 2014.*

Column: 79 **Density:** 2650
Volume: 0.010
Sample ID: 2014-8-15ls

Malvern data Phi	Malvern data Micron	Vol %	Equivalent Cum wt (g)
-1.00	2000.00	0	0.0
-0.75	1680.00	0	0.0
-0.50	1410.00	0	0.0
-0.25	1190.00	0	0.0
0.00	1000.00	0	0.0
0.25	840.00	0	0.0
0.49	710.00	0.820355	0.2
0.76	590.00	4.668865	1.2
1.00	500.00	11.747061	3.1
1.25	420.00	23.407474	6.2
1.51	350.00	39.38151	10.4
1.74	300.00	54.30185	14.4
2.00	250.00	71.101048	18.8
2.25	210.00	84.118318	22.3
2.50	177.00	92.857615	24.6
2.75	149.00	97.734494	25.9
3.00	125.00	99.713754	26.4
3.25	105.00	100	26.5
3.51	88.00	100	26.5
3.76	74.00	100	26.5
3.99	63.00	100	26.5
4.24	53.00	100	26.5
4.51	44.00	100	26.5
4.76	37.00	100	26.5
5.01	31.00	100	26.5
6.00	15.60	100	26.5
6.64	10.00	100	26.5
7.00	7.80	100	26.5
8.00	3.90	100	26.5
8.97	2.00	100	26.5
9.99	0.98	100	26.5
10.48	0.70	100	26.5
10.99	0.49	100	26.5
12.02	0.24	100	26.5
13.02	0.12	100	26.5
14.02	0.06	100	26.5
14.29	0.05	100	26.5
		Total weight:	26.5

	mm	phi	Cum wt (g)	Int wt (g)	Int wt%	Cum % finer	Modes	
1	2.0000	-1.00	0.000000	0.000000	0.000000	100.000000		
2	1.6800	-0.75	0.000000	0.000000	0.000000	100.000000		
3	1.4100	-0.50	0.000000	0.000000	0.000000	100.000000		
4	1.1900	-0.25	0.000000	0.000000	0.000000	100.000000		
5	1.0000	0.00	0.000000	0.000000	0.000000	100.000000		8
6	0.8400	0.25	0.000000	0.000000	0.000000	100.000000		
7	0.7100	0.49	0.820355	0.820355	0.820355	99.179645		
8	0.5900	0.76	4.668865	3.848510	3.848510	95.331135		
9	0.5000	1.00	11.747061	7.078196	7.078196	88.252939		
10	0.4200	1.25	23.407474	11.660413	11.660413	76.592526		
11	0.3500	1.51	39.381510	15.974036	15.974036	60.618490	mode at 1.383056	
12	0.3000	1.74	54.301850	14.920340	14.920340	45.698150		
13	0.2500	2.00	71.101048	16.799198	16.799198	28.898952	mode at 1.868483	
14	0.2100	2.25	84.118318	13.017270	13.017270	15.881682		
15	0.1770	2.50	92.857615	8.739297	8.739297	7.142385		
16	0.1490	2.75	97.734494	4.876879	4.876879	2.265506		
17	0.1250	3.00	99.713754	1.979260	1.979260	0.286246		
18	0.1050	3.25	100.000000	0.286246	0.286246	0.000000		
19	0.0880	3.51	100.000000	0.000000	0.000000	0.000000		
20	0.0740	3.76	100.000000	0.000000	0.000000	0.000000		
21	0.0630	3.99	100.000000	0.000000	0.000000	0.000000		
22	0.0530	4.24	100.000000	0.000000	0.000000	0.000000		
23	0.0440	4.51	100.000000	0.000000	0.000000	0.000000		
24	0.0370	4.76	100.000000	0.000000	0.000000	0.000000		
25	0.0310	5.01	100.000000	0.000000	0.000000	0.000000		
26	0.0156	6.00	100.000000	0.000000	0.000000	0.000000		
27	0.0100	6.64	100.000000	0.000000	0.000000	0.000000		
28	0.0078	7.00	100.000000	0.000000	0.000000	0.000000		
29	0.0039	8.00	100.000000	0.000000	0.000000	0.000000		
30	0.0020	8.97	100.000000	0.000000	0.000000	0.000000		
31	0.0010	9.99	100.000000	0.000000	0.000000	0.000000		
32	0.0007	10.48	100.000000	0.000000	0.000000	0.000000		
33	0.0005	10.99	100.000000	0.000000	0.000000	0.000000		
34	0.0002	12.02	100.000000	0.000000	0.000000	0.000000		
35	0.0001	13.02	100.000000	0.000000	0.000000	0.000000		
36	0.0001	14.02	100.000000	0.000000	0.000000	0.000000		
37	0.0001	14.29	100.000000	0.000000	0.000000	0.000000		
	Sums:			100.00	100.00			

Column: 79
Sample ID: 2014-8-15ls

Folks' Graphic Statistics

	Mean (Mz)	Sorting (σI)	Skewness (SkI)	Kurtosis (KG)	Mean *mm*
phi	1.671	0.567	0.007	0.943	0.314

Grainsize Statistics
Percentiles

	phi	*mm*
5	0.77	0.585
16	1.09	0.469
25	1.28	0.412
50	1.67	0.314
75	2.08	0.237
84	2.25	0.210
95	2.61	0.164

Table II.79: *Results summary for sample 79: Mid intertidal zone, northern transect, Northern Ngarunui Beach. Sample collected on the 15th of August, 2014.*

Column: 80 **Density:** 2650
Volume: 0.010
Sample ID: 2014-8-15nm

Malvern data Phi	Malvern data Micron	Vol %	Equivalent Cum wt (g)
-1.00	2000.00	0	0.0
-0.75	1680.00	0	0.0
-0.50	1410.00	0	0.0
-0.25	1190.00	0	0.0
0.00	1000.00	0	0.0
0.25	840.00	0	0.0
0.49	710.00	0.645332	0.2
0.76	590.00	3.850676	1.0
1.00	500.00	10.045185	2.7
1.25	420.00	20.700213	5.5
1.51	350.00	35.904138	9.5
1.74	300.00	50.62512	13.4
2.00	250.00	67.789801	18.0
2.25	210.00	81.606478	21.6
2.50	177.00	91.27415	24.2
2.75	149.00	96.963359	25.7
3.00	125.00	99.49171	26.4
3.25	105.00	99.991323	26.5
3.51	88.00	100	26.5
3.76	74.00	100	26.5
3.99	63.00	100	26.5
4.24	53.00	100	26.5
4.51	44.00	100	26.5
4.76	37.00	100	26.5
5.01	31.00	100	26.5
6.00	15.60	100	26.5
6.64	10.00	100	26.5
7.00	7.80	100	26.5
8.00	3.90	100	26.5
8.97	2.00	100	26.5
9.99	0.98	100	26.5
10.48	0.70	100	26.5
10.99	0.49	100	26.5
12.02	0.24	100	26.5
13.02	0.12	100	26.5
14.02	0.06	100	26.5
14.29	0.05	100	26.5
		Total weight:	26.5

	mm	phi	Cum wt (g)	Int wt (g)	Int wt%	Cum % finer	Modes	
1	2.0000	-1.00	0.000000	0.000000	0.000000	100.000000		
2	1.6800	-0.75	0.000000	0.000000	0.000000	100.000000		
3	1.4100	-0.50	0.000000	0.000000	0.000000	100.000000		
4	1.1900	-0.25	0.000000	0.000000	0.000000	100.000000		
5	1.0000	0.00	0.000000	0.000000	0.000000	100.000000		8
6	0.8400	0.25	0.000000	0.000000	0.000000	100.000000		
7	0.7100	0.49	0.645332	0.645332	0.645332	99.354668		
8	0.5900	0.76	3.850676	3.205344	3.205344	96.149324		
9	0.5000	1.00	10.045185	6.194509	6.194509	89.954815		
10	0.4200	1.25	20.700213	10.655028	10.655028	79.299787		
11	0.3500	1.51	35.904138	15.203925	15.203925	64.095862	mode at 1.383056	
12	0.3000	1.74	50.625120	14.720982	14.720982	49.374880		
13	0.2500	2.00	67.789801	17.164681	17.164681	32.210199	mode at 1.868483	
14	0.2100	2.25	81.606478	13.816677	13.816677	18.393522		
15	0.1770	2.50	91.274150	9.667672	9.667672	8.725850		
16	0.1490	2.75	96.963359	5.689209	5.689209	3.036641		
17	0.1250	3.00	99.491710	2.528351	2.528351	0.508290		
18	0.1050	3.25	99.991323	0.499613	0.499613	0.008677		
19	0.0880	3.51	100.000000	0.008677	0.008677	0.000000		
20	0.0740	3.76	100.000000	0.000000	0.000000	0.000000		
21	0.0630	3.99	100.000000	0.000000	0.000000	0.000000		
22	0.0530	4.24	100.000000	0.000000	0.000000	0.000000		
23	0.0440	4.51	100.000000	0.000000	0.000000	0.000000		
24	0.0370	4.76	100.000000	0.000000	0.000000	0.000000		
25	0.0310	5.01	100.000000	0.000000	0.000000	0.000000		
26	0.0156	6.00	100.000000	0.000000	0.000000	0.000000		
27	0.0100	6.64	100.000000	0.000000	0.000000	0.000000		
28	0.0078	7.00	100.000000	0.000000	0.000000	0.000000		
29	0.0039	8.00	100.000000	0.000000	0.000000	0.000000		
30	0.0020	8.97	100.000000	0.000000	0.000000	0.000000		
31	0.0010	9.99	100.000000	0.000000	0.000000	0.000000		
32	0.0007	10.48	100.000000	0.000000	0.000000	0.000000		
33	0.0005	10.99	100.000000	0.000000	0.000000	0.000000		
34	0.0002	12.02	100.000000	0.000000	0.000000	0.000000		
35	0.0001	13.02	100.000000	0.000000	0.000000	0.000000		
36	0.0001	14.02	100.000000	0.000000	0.000000	0.000000		
37	0.0001	14.29	100.000000	0.000000	0.000000	0.000000		
	Sums:			100.00	100.00			

Column: 80
Sample ID: 2014-8-15nm

Folks' Graphic Statistics

	Mean (Mz)	Sorting (σI)	Skewness (SkI)	Kurtosis (KG)	Mean ***mm***
phi	1.727	0.574	0.002	0.944	0.302

Grainsize Statistics
Percentiles

	phi	***mm***
5	0.81	0.572
16	1.14	0.454
25	1.33	0.399
50	1.73	0.302
75	2.13	0.228
84	2.31	0.201
95	2.66	0.158

Table II.80: *Results summary for sample 80: High intertidal zone, mid transect, Northern Ngarunui Beach. Sample collected on the 30th of August, 2014.*

Column: 81 **Density:** 2650
Volume: 0.010
Sample ID: 2014-8-30hm

Malvern data Phi	Malvern data Micron	Vol %	Equivalent Cum wt (g)
-1.00	2000.00	0	0.0
-0.75	1680.00	0	0.0
-0.50	1410.00	0	0.0
-0.25	1190.00	0	0.0
0.00	1000.00	0	0.0
0.25	840.00	0	0.0
0.49	710.00	0	0.0
0.76	590.00	0.244789	0.1
1.00	500.00	1.951694	0.5
1.25	420.00	7.162421	1.9
1.51	350.00	18.069787	4.8
1.74	300.00	31.776857	8.4
2.00	250.00	51.273467	13.6
2.25	210.00	69.721921	18.5
2.50	177.00	84.296746	22.3
2.75	149.00	93.783688	24.9
3.00	125.00	98.473524	26.1
3.25	105.00	99.894969	26.5
3.51	88.00	100	26.5
3.76	74.00	100	26.5
3.99	63.00	100	26.5
4.24	53.00	100	26.5
4.51	44.00	100	26.5
4.76	37.00	100	26.5
5.01	31.00	100	26.5
6.00	15.60	100	26.5
6.64	10.00	100	26.5
7.00	7.80	100	26.5
8.00	3.90	100	26.5
8.97	2.00	100	26.5
9.99	0.98	100	26.5
10.48	0.70	100	26.5
10.99	0.49	100	26.5
12.02	0.24	100	26.5
13.02	0.12	100	26.5
14.02	0.06	100	26.5
14.29	0.05	100	26.5
		Total weight:	26.5

	mm	phi	Cum wt (g)	Int wt (g)	Int wt%	Cum % finer	Modes	
1	2.0000	-1.00	0.000000	0.000000	0.000000	100.000000		
2	1.6800	-0.75	0.000000	0.000000	0.000000	100.000000		
3	1.4100	-0.50	0.000000	0.000000	0.000000	100.000000		
4	1.1900	-0.25	0.000000	0.000000	0.000000	100.000000		
5	1.0000	0.00	0.000000	0.000000	0.000000	100.000000		8
6	0.8400	0.25	0.000000	0.000000	0.000000	100.000000		
7	0.7100	0.49	0.000000	0.000000	0.000000	100.000000		
8	0.5900	0.76	0.244789	0.244789	0.244789	99.755211		
9	0.5000	1.00	1.951694	1.706905	1.706905	98.048306		
10	0.4200	1.25	7.162421	5.210727	5.210727	92.837579		
11	0.3500	1.51	18.069787	10.907366	10.907366	81.930213		
12	0.3000	1.74	31.776857	13.707070	13.707070	68.223143		
13	0.2500	2.00	51.273467	19.496610	19.496610	48.726533	mode at 1.868483	
14	0.2100	2.25	69.721921	18.448454	18.448454	30.278079		
15	0.1770	2.50	84.296746	14.574825	14.574825	15.703254		
16	0.1490	2.75	93.783688	9.486942	9.486942	6.216312		
17	0.1250	3.00	98.473524	4.689836	4.689836	1.526476		
18	0.1050	3.25	99.894969	1.421445	1.421445	0.105031		
19	0.0880	3.51	100.000000	0.105031	0.105031	0.000000		
20	0.0740	3.76	100.000000	0.000000	0.000000	0.000000		
21	0.0630	3.99	100.000000	0.000000	0.000000	0.000000		
22	0.0530	4.24	100.000000	0.000000	0.000000	0.000000		
23	0.0440	4.51	100.000000	0.000000	0.000000	0.000000		
24	0.0370	4.76	100.000000	0.000000	0.000000	0.000000		
25	0.0310	5.01	100.000000	0.000000	0.000000	0.000000		
26	0.0156	6.00	100.000000	0.000000	0.000000	0.000000		
27	0.0100	6.64	100.000000	0.000000	0.000000	0.000000		
28	0.0078	7.00	100.000000	0.000000	0.000000	0.000000		
29	0.0039	8.00	100.000000	0.000000	0.000000	0.000000		
30	0.0020	8.97	100.000000	0.000000	0.000000	0.000000		
31	0.0010	9.99	100.000000	0.000000	0.000000	0.000000		
32	0.0007	10.48	100.000000	0.000000	0.000000	0.000000		
33	0.0005	10.99	100.000000	0.000000	0.000000	0.000000		
34	0.0002	12.02	100.000000	0.000000	0.000000	0.000000		
35	0.0001	13.02	100.000000	0.000000	0.000000	0.000000		
36	0.0001	14.02	100.000000	0.000000	0.000000	0.000000		
37	0.0001	14.29	100.000000	0.000000	0.000000	0.000000		
	Sums:			100.00	100.00			

Column: 81
Sample ID: 2014-8-30hm

Folks' Graphic Statistics

	Mean (Mz)	Sorting (σI)	Skewness (SkI)	Kurtosis (KG)	Mean *mm*
phi	1.980	0.509	-0.006	0.956	0.253

Grainsize Statistics
Percentiles

	phi	*mm*
5	1.15	0.452
16	1.46	0.362
25	1.63	0.324
50	1.98	0.253
75	2.34	0.197
84	2.49	0.178
95	2.81	0.142

Table II.81: *Results summary for sample 81: Mid intertidal zone, mid transect, Northern Ngarunui Beach. Sample collected on the 30th of August, 2014.*

Column: 82 **Density:** 2650
Volume: 0.010
Sample ID: 2014-8-30mm

Malvern data Phi	Malvern data Micron	Vol %	Equivalent Cum wt (g)
-1.00	2000.00	0	0.0
-0.75	1680.00	0	0.0
-0.50	1410.00	0	0.0
-0.25	1190.00	0	0.0
0.00	1000.00	0	0.0
0.25	840.00	0.703413	0.2
0.49	710.00	4.221915	1.1
0.76	590.00	12.690916	3.4
1.00	500.00	24.716465	6.5
1.25	420.00	40.904416	10.8
1.51	350.00	59.132722	15.7
1.74	300.00	73.258454	19.4
2.00	250.00	86.312554	22.9
2.25	210.00	94.298083	25.0
2.50	177.00	98.33128	26.1
2.75	149.00	99.801369	26.4
3.00	125.00	100	26.5
3.25	105.00	100	26.5
3.51	88.00	100	26.5
3.76	74.00	100	26.5
3.99	63.00	100	26.5
4.24	53.00	100	26.5
4.51	44.00	100	26.5
4.76	37.00	100	26.5
5.01	31.00	100	26.5
6.00	15.60	100	26.5
6.64	10.00	100	26.5
7.00	7.80	100	26.5
8.00	3.90	100	26.5
8.97	2.00	100	26.5
9.99	0.98	100	26.5
10.48	0.70	100	26.5
10.99	0.49	100	26.5
12.02	0.24	100	26.5
13.02	0.12	100	26.5
14.02	0.06	100	26.5
14.29	0.05	100	26.5

Total weight: 26.5

Column: 82
Sample ID: 2014-8-30mm

Folks' Graphic Statistics

	Mean (Mz)	Sorting (σI)	Skewness (SkI)	Kurtosis (KG)	Mean *mm*
phi	1.388	0.551	0.020	0.948	0.382

	mm	phi	Cum wt (g)	Int wt (g)	Int wt%	Cum % finer	Modes
1	2.0000	-1.00	0.000000	0.000000	0.000000	100.000000	
2	1.6800	-0.75	0.000000	0.000000	0.000000	100.000000	
3	1.4100	-0.50	0.000000	0.000000	0.000000	100.000000	
4	1.1900	-0.25	0.000000	0.000000	0.000000	100.000000	
5	1.0000	0.00	0.000000	0.000000	0.000000	100.000000	8
6	0.8400	0.25	0.703413	0.703413	0.703413	99.296587	
7	0.7100	0.49	4.221915	3.518502	3.518502	95.778085	
8	0.5900	0.76	12.690916	8.469001	8.469001	87.309084	
9	0.5000	1.00	24.716465	12.025549	12.025549	75.283535	
10	0.4200	1.25	40.904416	16.187951	16.187951	59.095584	
11	0.3500	1.51	59.132722	18.228306	18.228306	40.867278	mode at 1.383056
12	0.3000	1.74	73.258454	14.125732	14.125732	26.741546	
13	0.2500	2.00	86.312554	13.054100	13.054100	13.687446	
14	0.2100	2.25	94.298083	7.985529	7.985529	5.701917	
15	0.1770	2.50	98.331280	4.033197	4.033197	1.668720	
16	0.1490	2.75	99.801369	1.470089	1.470089	0.198631	
17	0.1250	3.00	100.000000	0.198631	0.198631	0.000000	
18	0.1050	3.25	100.000000	0.000000	0.000000	0.000000	
19	0.0880	3.51	100.000000	0.000000	0.000000	0.000000	
20	0.0740	3.76	100.000000	0.000000	0.000000	0.000000	
21	0.0630	3.99	100.000000	0.000000	0.000000	0.000000	
22	0.0530	4.24	100.000000	0.000000	0.000000	0.000000	
23	0.0440	4.51	100.000000	0.000000	0.000000	0.000000	
24	0.0370	4.76	100.000000	0.000000	0.000000	0.000000	
25	0.0310	5.01	100.000000	0.000000	0.000000	0.000000	
26	0.0156	6.00	100.000000	0.000000	0.000000	0.000000	
27	0.0100	6.64	100.000000	0.000000	0.000000	0.000000	
28	0.0078	7.00	100.000000	0.000000	0.000000	0.000000	
29	0.0039	8.00	100.000000	0.000000	0.000000	0.000000	
30	0.0020	8.97	100.000000	0.000000	0.000000	0.000000	
31	0.0010	9.99	100.000000	0.000000	0.000000	0.000000	
32	0.0007	10.48	100.000000	0.000000	0.000000	0.000000	
33	0.0005	10.99	100.000000	0.000000	0.000000	0.000000	
34	0.0002	12.02	100.000000	0.000000	0.000000	0.000000	
35	0.0001	13.02	100.000000	0.000000	0.000000	0.000000	
36	0.0001	14.02	100.000000	0.000000	0.000000	0.000000	
37	0.0001	14.29	100.000000	0.000000	0.000000	0.000000	
	Sums:			100.00	100.00		

Grainsize Statistics
Percentiles

	phi	*mm*
5	0.52	0.698
16	0.83	0.564
25	1.00	0.498
50	1.38	0.383
75	1.77	0.293
84	1.95	0.258
95	2.29	0.204

Table II.82: *Results summary for sample 82: Low intertidal zone, mid transect, Northern Ngarunui Beach. Sample collected on the 30th of August, 2014.*

Column: 83 **Density:** 2650
Volume: 0.010
Sample ID: 2014-8-30lm

Malvern data Phi	**Malvern data Micron**	**Vol %**	**Equivalent Cum wt (g)**
-1.00	2000.00	0	0.0
-0.75	1680.00	0	0.0
-0.50	1410.00	0	0.0
-0.25	1190.00	0	0.0
0.00	1000.00	0.258093	0.1
0.25	840.00	2.496152	0.7
0.49	710.00	7.508424	2.0
0.76	590.00	16.775884	4.4
1.00	500.00	28.110346	7.4
1.25	420.00	42.189191	11.2
1.51	350.00	57.602701	15.3
1.74	300.00	69.81415	18.5
2.00	250.00	81.953208	21.7
2.25	210.00	90.494701	24.0
2.50	177.00	95.882289	25.4
2.75	149.00	98.771474	26.2
3.00	125.00	99.875148	26.5
3.25	105.00	100	26.5
3.51	88.00	100	26.5
3.76	74.00	100	26.5
3.99	63.00	100	26.5
4.24	53.00	100	26.5
4.51	44.00	100	26.5
4.76	37.00	100	26.5
5.01	31.00	100	26.5
6.00	15.60	100	26.5
6.64	10.00	100	26.5
7.00	7.80	100	26.5
8.00	3.90	100	26.5
8.97	2.00	100	26.5
9.99	0.98	100	26.5
10.48	0.70	100	26.5
10.99	0.49	100	26.5
12.02	0.24	100	26.5
13.02	0.12	100	26.5
14.02	0.06	100	26.5
14.29	0.05	100	26.5
		Total weight:	26.5

	mm	**phi**	**Cum wt (g)**	**Int wt (g)**	**Int wt%**	**Cum % finer**	**Modes**	
1	2.0000	-1.00	0.000000	0.000000	0.000000	100.000000		
2	1.6800	-0.75	0.000000	0.000000	0.000000	100.000000		
3	1.4100	-0.50	0.000000	0.000000	0.000000	100.000000		
4	1.1900	-0.25	0.000000	0.000000	0.000000	100.000000		
5	1.0000	0.00	0.258093	0.258093	0.258093	99.741907		8
6	0.8400	0.25	2.496152	2.238059	2.238059	97.503848		
7	0.7100	0.49	7.508424	5.012272	5.012272	92.491576		
8	0.5900	0.76	16.775884	9.267460	9.267460	83.224116		
9	0.5000	1.00	28.110346	11.334462	11.334462	71.889654		
10	0.4200	1.25	42.189191	14.078845	14.078845	57.810809		
11	0.3500	1.51	57.602701	15.413510	15.413510	42.397299	mode at 1.383056	
12	0.3000	1.74	69.814150	12.211449	12.211449	30.185850		
13	0.2500	2.00	81.953208	12.139058	12.139058	18.046792		
14	0.2100	2.25	90.494701	8.541493	8.541493	9.505299		
15	0.1770	2.50	95.882289	5.387588	5.387588	4.117711		
16	0.1490	2.75	98.771474	2.889185	2.889185	1.228526		
17	0.1250	3.00	99.875148	1.103674	1.103674	0.124852		
18	0.1050	3.25	100.000000	0.124852	0.124852	0.000000		
19	0.0880	3.51	100.000000	0.000000	0.000000	0.000000		
20	0.0740	3.76	100.000000	0.000000	0.000000	0.000000		
21	0.0630	3.99	100.000000	0.000000	0.000000	0.000000		
22	0.0530	4.24	100.000000	0.000000	0.000000	0.000000		
23	0.0440	4.51	100.000000	0.000000	0.000000	0.000000		
24	0.0370	4.76	100.000000	0.000000	0.000000	0.000000		
25	0.0310	5.01	100.000000	0.000000	0.000000	0.000000		
26	0.0156	6.00	100.000000	0.000000	0.000000	0.000000		
27	0.0100	6.64	100.000000	0.000000	0.000000	0.000000		
28	0.0078	7.00	100.000000	0.000000	0.000000	0.000000		
29	0.0039	8.00	100.000000	0.000000	0.000000	0.000000		
30	0.0020	8.97	100.000000	0.000000	0.000000	0.000000		
31	0.0010	9.99	100.000000	0.000000	0.000000	0.000000		
32	0.0007	10.48	100.000000	0.000000	0.000000	0.000000		
33	0.0005	10.99	100.000000	0.000000	0.000000	0.000000		
34	0.0002	12.02	100.000000	0.000000	0.000000	0.000000		
35	0.0001	13.02	100.000000	0.000000	0.000000	0.000000		
36	0.0001	14.02	100.000000	0.000000	0.000000	0.000000		
37	0.0001	14.29	100.000000	0.000000	0.000000	0.000000		
		Sums:		100.00	100.00			

Grainsize Statistics
Percentiles

	phi	***mm***
5	0.37	0.772
16	0.74	0.599
25	0.93	0.523
50	1.38	0.383
75	1.85	0.278
84	2.06	0.240
95	2.46	0.182

Column: 83
Sample ID: 2014-8-30lm

Folks' Graphic Statistics

	Mean (Mz)	Sorting (σI)	Skewness (SkI)	Kurtosis (KG)	Mean ***mm***
phi	1.395	0.646	0.026	0.934	0.380

Table II.83: *Results summary for sample 83: Low intertidal zone, northern transect, Northern Ngarunui Beach. Sample collected on the 30th of August, 2014.*

Column: 84 **Density:** 2650
Volume: 0.010
Sample ID: 2014-8-30ln

Malvern data Phi	Malvern data Micron	Vol %	Equivalent Cum wt (g)
-1.00	2000.00	0	0.0
-0.75	1680.00	0	0.0
-0.50	1410.00	0.018477	0.0
-0.25	1190.00	0.341125	0.1
0.00	1000.00	2.049329	0.5
0.25	840.00	5.785448	1.5
0.49	710.00	11.924076	3.2
0.76	590.00	21.816534	5.8
1.00	500.00	33.110102	8.8
1.25	420.00	46.639262	12.4
1.51	350.00	61.161967	16.2
1.74	300.00	72.556799	19.2
2.00	250.00	83.813884	22.2
2.25	210.00	91.670369	24.3
2.50	177.00	96.553093	25.6
2.75	149.00	99.095954	26.3
3.00	125.00	99.916606	26.5
3.25	105.00	100	26.5
3.51	88.00	100	26.5
3.76	74.00	100	26.5
3.99	63.00	100	26.5
4.24	53.00	100	26.5
4.51	44.00	100	26.5
4.76	37.00	100	26.5
5.01	31.00	100	26.5
6.00	15.60	100	26.5
6.64	10.00	100	26.5
7.00	7.80	100	26.5
8.00	3.90	100	26.5
8.97	2.00	100	26.5
9.99	0.98	100	26.5
10.48	0.70	100	26.5
10.99	0.49	100	26.5
12.02	0.24	100	26.5
13.02	0.12	100	26.5
14.02	0.06	100	26.5
14.29	0.05	100	26.5
		Total weight:	26.5

	mm	phi	Cum wt (g)	Int wt (g)	Int wt%	Cum % finer	Modes	
1	2.0000	-1.00	0.000000	0.000000	0.000000	100.000000		
2	1.6800	-0.75	0.000000	0.000000	0.000000	100.000000		
3	1.4100	-0.50	0.018477	0.018477	0.018477	99.981523		
4	1.1900	-0.25	0.341125	0.322648	0.322648	99.658875		
5	1.0000	0.00	2.049329	1.708204	1.708204	97.950671		8
6	0.8400	0.25	5.785448	3.736119	3.736119	94.214552		
7	0.7100	0.49	11.924076	6.138628	6.138628	88.075924		
8	0.5900	0.76	21.816534	9.892458	9.892458	78.183466		
9	0.5000	1.00	33.110102	11.293568	11.293568	66.889898		
10	0.4200	1.25	46.639262	13.529160	13.529160	53.360738		
11	0.3500	1.51	61.161967	14.522705	14.522705	38.838033	mode at 1.383056	
12	0.3000	1.74	72.556799	11.394832	11.394832	27.443201		
13	0.2500	2.00	83.813884	11.257085	11.257085	16.186116		
14	0.2100	2.25	91.670369	7.856485	7.856485	8.329631		
15	0.1770	2.50	96.553093	4.882724	4.882724	3.446907		
16	0.1490	2.75	99.095954	2.542861	2.542861	0.904046		
17	0.1250	3.00	99.916606	0.820652	0.820652	0.083394		
18	0.1050	3.25	100.000000	0.083394	0.083394	0.000000		
19	0.0880	3.51	100.000000	0.000000	0.000000	0.000000		
20	0.0740	3.76	100.000000	0.000000	0.000000	0.000000		
21	0.0630	3.99	100.000000	0.000000	0.000000	0.000000		
22	0.0530	4.24	100.000000	0.000000	0.000000	0.000000		
23	0.0440	4.51	100.000000	0.000000	0.000000	0.000000		
24	0.0370	4.76	100.000000	0.000000	0.000000	0.000000		
25	0.0310	5.01	100.000000	0.000000	0.000000	0.000000		
26	0.0156	6.00	100.000000	0.000000	0.000000	0.000000		
27	0.0100	6.64	100.000000	0.000000	0.000000	0.000000		
28	0.0078	7.00	100.000000	0.000000	0.000000	0.000000		
29	0.0039	8.00	100.000000	0.000000	0.000000	0.000000		
30	0.0020	8.97	100.000000	0.000000	0.000000	0.000000		
31	0.0010	9.99	100.000000	0.000000	0.000000	0.000000		
32	0.0007	10.48	100.000000	0.000000	0.000000	0.000000		
33	0.0005	10.99	100.000000	0.000000	0.000000	0.000000		
34	0.0002	12.02	100.000000	0.000000	0.000000	0.000000		
35	0.0001	13.02	100.000000	0.000000	0.000000	0.000000		
36	0.0001	14.02	100.000000	0.000000	0.000000	0.000000		
37	0.0001	14.29	100.000000	0.000000	0.000000	0.000000		
	Sums:			100.00	100.00			

Grainsize Statistics
Percentiles

	phi	*mm*
5	0.20	0.871
16	0.60	0.658
25	0.83	0.563
50	1.31	0.403
75	1.79	0.288
84	2.01	0.249
95	2.42	0.187

Column: 84
Sample ID: 2014-8-30ln

Folks' Graphic Statistics

	Mean (Mz)	Sorting (σI)	Skewness (SkI)	Kurtosis (KG)	Mean *mm*
phi	1.308	0.687	-0.007	0.943	0.404

Table II.84: *Results summary for sample 84: Low intertidal zone, southern transect, Northern Ngarunui Beach. Sample collected on the 30th of August, 2014.*

Column: 85 **Density:** 2650
Volume: 0.010
Sample ID: 2014-8-30ls

Malvern data Phi	Malvern data Micron	Vol %	Equivalent Cum wt (g)
-1.00	2000.00	0	0.0
-0.75	1680.00	0	0.0
-0.50	1410.00	0	0.0
-0.25	1190.00	0	0.0
0.00	1000.00	0.124751	0.0
0.25	840.00	1.44505	0.4
0.49	710.00	4.928885	1.3
0.76	590.00	12.312557	3.3
1.00	500.00	22.399156	5.9
1.25	420.00	36.120671	9.6
1.51	350.00	52.324228	13.9
1.74	300.00	65.850669	17.5
2.00	250.00	79.711747	21.1
2.25	210.00	89.543287	23.7
2.50	177.00	95.632484	25.3
2.75	149.00	98.754307	26.2
3.00	125.00	99.873624	26.5
3.25	105.00	100	26.5
3.51	88.00	100	26.5
3.76	74.00	100	26.5
3.99	63.00	100	26.5
4.24	53.00	100	26.5
4.51	44.00	100	26.5
4.76	37.00	100	26.5
5.01	31.00	100	26.5
6.00	15.60	100	26.5
6.64	10.00	100	26.5
7.00	7.80	100	26.5
8.00	3.90	100	26.5
8.97	2.00	100	26.5
9.99	0.98	100	26.5
10.48	0.70	100	26.5
10.99	0.49	100	26.5
12.02	0.24	100	26.5
13.02	0.12	100	26.5
14.02	0.06	100	26.5
14.29	0.05	100	26.5
		Total weight:	26.5

	mm	phi	Cum wt (g)	Int wt (g)	Int wt%	Cum % finer	Modes	
1	2.0000	-1.00	0.000000	0.000000	0.000000	100.000000		
2	1.6800	-0.75	0.000000	0.000000	0.000000	100.000000		
3	1.4100	-0.50	0.000000	0.000000	0.000000	100.000000		
4	1.1900	-0.25	0.000000	0.000000	0.000000	100.000000		
5	1.0000	0.00	0.124751	0.124751	0.124751	99.875249		8
6	0.8400	0.25	1.445050	1.320299	1.320299	98.554950		
7	0.7100	0.49	4.928885	3.483835	3.483835	95.071115		
8	0.5900	0.76	12.312557	7.383672	7.383672	87.687443		
9	0.5000	1.00	22.399156	10.086599	10.086599	77.600844		
10	0.4200	1.25	36.120671	13.721515	13.721515	63.879329		
11	0.3500	1.51	52.324228	16.203557	16.203557	47.675772	mode at 1.383056	
12	0.3000	1.74	65.850669	13.526441	13.526441	34.149331		
13	0.2500	2.00	79.711747	13.861078	13.861078	20.288253	mode at 1.868483	
14	0.2100	2.25	89.543287	9.831540	9.831540	10.456713		
15	0.1770	2.50	95.632484	6.089197	6.089197	4.367516		
16	0.1490	2.75	98.754307	3.121823	3.121823	1.245693		
17	0.1250	3.00	99.873624	1.119317	1.119317	0.126376		
18	0.1050	3.25	100.000000	0.126376	0.126376	0.000000		
19	0.0880	3.51	100.000000	0.000000	0.000000	0.000000		
20	0.0740	3.76	100.000000	0.000000	0.000000	0.000000		
21	0.0630	3.99	100.000000	0.000000	0.000000	0.000000		
22	0.0530	4.24	100.000000	0.000000	0.000000	0.000000		
23	0.0440	4.51	100.000000	0.000000	0.000000	0.000000		
24	0.0370	4.76	100.000000	0.000000	0.000000	0.000000		
25	0.0310	5.01	100.000000	0.000000	0.000000	0.000000		
26	0.0156	6.00	100.000000	0.000000	0.000000	0.000000		
27	0.0100	6.64	100.000000	0.000000	0.000000	0.000000		
28	0.0078	7.00	100.000000	0.000000	0.000000	0.000000		
29	0.0039	8.00	100.000000	0.000000	0.000000	0.000000		
30	0.0020	8.97	100.000000	0.000000	0.000000	0.000000		
31	0.0010	9.99	100.000000	0.000000	0.000000	0.000000		
32	0.0007	10.48	100.000000	0.000000	0.000000	0.000000		
33	0.0005	10.99	100.000000	0.000000	0.000000	0.000000		
34	0.0002	12.02	100.000000	0.000000	0.000000	0.000000		
35	0.0001	13.02	100.000000	0.000000	0.000000	0.000000		
36	0.0001	14.02	100.000000	0.000000	0.000000	0.000000		
37	0.0001	14.29	100.000000	0.000000	0.000000	0.000000		
		Sums:		100.00	100.00			

Column: 85
Sample ID: 2014-8-30ls

Folks' Graphic Statistics

	Mean (Mz)	Sorting (σI)	Skewness (SkI)	Kurtosis (KG)	Mean ***mm***
phi	1.478	0.615	0.006	0.938	0.359

Grainsize Statistics
Percentiles

	phi	***mm***
5	0.50	0.709
16	0.85	0.555
25	1.05	0.484
50	1.48	0.359
75	1.91	0.266
84	2.11	0.232
95	2.47	0.180

Table II.85: *Results summary for sample 85: Mid intertidal zone, southern transect, Northern Ngarunui Beach. Sample collected on the 30th of August, 2014.*

Column: 86 **Density:** 2650
Volume: 0.010
Sample ID: 2014-8-30sm

Malvern data Phi	Malvern data Micron	Vol %	Equivalent Cum wt (g)
-1.00	2000.00	0	0.0
-0.75	1680.00	0	0.0
-0.50	1410.00	0	0.0
-0.25	1190.00	0	0.0
0.00	1000.00	0.22005	0.1
0.25	840.00	2.724157	0.7
0.49	710.00	9.146803	2.4
0.76	590.00	21.685578	5.7
1.00	500.00	36.984866	9.8
1.25	420.00	55.002199	14.6
1.51	350.00	72.648504	19.3
1.74	300.00	84.499852	22.4
2.00	250.00	93.788608	24.9
2.25	210.00	98.276897	26.0
2.50	177.00	99.824961	26.5
2.75	149.00	100	26.5
3.00	125.00	100	26.5
3.25	105.00	100	26.5
3.51	88.00	100	26.5
3.76	74.00	100	26.5
3.99	63.00	100	26.5
4.24	53.00	100	26.5
4.51	44.00	100	26.5
4.76	37.00	100	26.5
5.01	31.00	100	26.5
6.00	15.60	100	26.5
6.64	10.00	100	26.5
7.00	7.80	100	26.5
8.00	3.90	100	26.5
8.97	2.00	100	26.5
9.99	0.98	100	26.5
10.48	0.70	100	26.5
10.99	0.49	100	26.5
12.02	0.24	100	26.5
13.02	0.12	100	26.5
14.02	0.06	100	26.5
14.29	0.05	100	26.5
		Total weight:	26.5

Column: 86
Sample ID: 2014-8-30sm

Folks' Graphic Statistics

	Mean (Mz)	Sorting (σI)	Skewness (SkI)	Kurtosis (KG)	Mean mm
phi	1.183	0.534	0.014	0.951	0.440

	mm	phi	Cum wt (g)	Int wt (g)	Int wt%	Cum % finer	Modes
1	2.0000	-1.00	0.000000	0.000000	0.000000	100.000000	
2	1.6800	-0.75	0.000000	0.000000	0.000000	100.000000	
3	1.4100	-0.50	0.000000	0.000000	0.000000	100.000000	
4	1.1900	-0.25	0.000000	0.000000	0.000000	100.000000	
5	1.0000	0.00	0.220050	0.220050	0.220050	99.779950	8
6	0.8400	0.25	2.724157	2.504107	2.504107	97.275843	
7	0.7100	0.49	9.146803	6.422646	6.422646	90.853197	
8	0.5900	0.76	21.685578	12.538775	12.538775	78.314422	
9	0.5000	1.00	36.984866	15.299288	15.299288	63.015134	
10	0.4200	1.25	55.002199	18.017333	18.017333	44.997801	mode at 1.125769
11	0.3500	1.51	72.648504	17.646305	17.646305	27.351496	
12	0.3000	1.74	84.499852	11.851348	11.851348	15.500148	
13	0.2500	2.00	93.788608	9.288756	9.288756	6.211392	
14	0.2100	2.25	98.276897	4.488289	4.488289	1.723103	
15	0.1770	2.50	99.824961	1.548064	1.548064	0.175039	
16	0.1490	2.75	100.000000	0.175039	0.175039	0.000000	
17	0.1250	3.00	100.000000	0.000000	0.000000	0.000000	
18	0.1050	3.25	100.000000	0.000000	0.000000	0.000000	
19	0.0880	3.51	100.000000	0.000000	0.000000	0.000000	
20	0.0740	3.76	100.000000	0.000000	0.000000	0.000000	
21	0.0630	3.99	100.000000	0.000000	0.000000	0.000000	
22	0.0530	4.24	100.000000	0.000000	0.000000	0.000000	
23	0.0440	4.51	100.000000	0.000000	0.000000	0.000000	
24	0.0370	4.76	100.000000	0.000000	0.000000	0.000000	
25	0.0310	5.01	100.000000	0.000000	0.000000	0.000000	
26	0.0156	6.00	100.000000	0.000000	0.000000	0.000000	
27	0.0100	6.64	100.000000	0.000000	0.000000	0.000000	
28	0.0078	7.00	100.000000	0.000000	0.000000	0.000000	
29	0.0039	8.00	100.000000	0.000000	0.000000	0.000000	
30	0.0020	8.97	100.000000	0.000000	0.000000	0.000000	
31	0.0010	9.99	100.000000	0.000000	0.000000	0.000000	
32	0.0007	10.48	100.000000	0.000000	0.000000	0.000000	
33	0.0005	10.99	100.000000	0.000000	0.000000	0.000000	
34	0.0002	12.02	100.000000	0.000000	0.000000	0.000000	
35	0.0001	13.02	100.000000	0.000000	0.000000	0.000000	
36	0.0001	14.02	100.000000	0.000000	0.000000	0.000000	
37	0.0001	14.29	100.000000	0.000000	0.000000	0.000000	
	Sums:			100.00	100.00		

Grainsize Statistics
Percentiles

	phi	*mm*
5	0.34	0.791
16	0.64	0.642
25	0.81	0.569
50	1.18	0.441
75	1.56	0.339
84	1.73	0.302
95	2.07	0.239

Table II.86: *Results summary for sample 86: High intertidal zone, northern transect, Northern Ngarunui Beach. Sample collected on the 30th of August, 2014.*

Column: 87 **Density:** 2650
Volume: 0.010
Sample ID: 2014-8-30hn

Malvern data Phi	Malvern data Micron	Vol %	Equivalent Cum wt (g)
-1.00	2000.00	0	0.0
-0.75	1680.00	0	0.0
-0.50	1410.00	0	0.0
-0.25	1190.00	0	0.0
0.00	1000.00	0	0.0
0.25	840.00	0	0.0
0.49	710.00	0	0.0
0.76	590.00	0.282201	0.1
1.00	500.00	2.308381	0.6
1.25	420.00	8.826878	2.3
1.51	350.00	22.62014	6.0
1.74	300.00	39.425095	10.4
2.00	250.00	61.584474	16.3
2.25	210.00	79.976767	21.2
2.50	177.00	91.995198	24.4
2.75	149.00	97.92643	26.0
3.00	125.00	99.810627	26.4
3.25	105.00	100	26.5
3.51	88.00	100	26.5
3.76	74.00	100	26.5
3.99	63.00	100	26.5
4.24	53.00	100	26.5
4.51	44.00	100	26.5
4.76	37.00	100	26.5
5.01	31.00	100	26.5
6.00	15.60	100	26.5
6.64	10.00	100	26.5
7.00	7.80	100	26.5
8.00	3.90	100	26.5
8.97	2.00	100	26.5
9.99	0.98	100	26.5
10.48	0.70	100	26.5
10.99	0.49	100	26.5
12.02	0.24	100	26.5
13.02	0.12	100	26.5
14.02	0.06	100	26.5
14.29	0.05	100	26.5
		Total weight:	26.5

	mm	phi	Cum wt (g)	Int wt (g)	Int wt%	Cum % finer	Modes	
1	2.0000	-1.00	0.000000	0.000000	0.000000	100.000000		
2	1.6800	-0.75	0.000000	0.000000	0.000000	100.000000		
3	1.4100	-0.50	0.000000	0.000000	0.000000	100.000000		
4	1.1900	-0.25	0.000000	0.000000	0.000000	100.000000		
5	1.0000	0.00	0.000000	0.000000	0.000000	100.000000		8
6	0.8400	0.25	0.000000	0.000000	0.000000	100.000000		
7	0.7100	0.49	0.000000	0.000000	0.000000	100.000000		
8	0.5900	0.76	0.282201	0.282201	0.282201	99.717799		
9	0.5000	1.00	2.308381	2.026180	2.026180	97.691619		
10	0.4200	1.25	8.826878	6.518497	6.518497	91.173122		
11	0.3500	1.51	22.620140	13.793262	13.793262	77.379860		
12	0.3000	1.74	39.425095	16.804955	16.804955	60.574905		
13	0.2500	2.00	61.584474	22.159379	22.159379	38.415526	mode at 1.868483	
14	0.2100	2.25	79.976767	18.392293	18.392293	20.023233		
15	0.1770	2.50	91.995198	12.018431	12.018431	8.004802		
16	0.1490	2.75	97.926430	5.931232	5.931232	2.073570		
17	0.1250	3.00	99.810627	1.884197	1.884197	0.189373		
18	0.1050	3.25	100.000000	0.189373	0.189373	0.000000		
19	0.0880	3.51	100.000000	0.000000	0.000000	0.000000		
20	0.0740	3.76	100.000000	0.000000	0.000000	0.000000		
21	0.0630	3.99	100.000000	0.000000	0.000000	0.000000		
22	0.0530	4.24	100.000000	0.000000	0.000000	0.000000		
23	0.0440	4.51	100.000000	0.000000	0.000000	0.000000		
24	0.0370	4.76	100.000000	0.000000	0.000000	0.000000		
25	0.0310	5.01	100.000000	0.000000	0.000000	0.000000		
26	0.0156	6.00	100.000000	0.000000	0.000000	0.000000		
27	0.0100	6.64	100.000000	0.000000	0.000000	0.000000		
28	0.0078	7.00	100.000000	0.000000	0.000000	0.000000		
29	0.0039	8.00	100.000000	0.000000	0.000000	0.000000		
30	0.0020	8.97	100.000000	0.000000	0.000000	0.000000		
31	0.0010	9.99	100.000000	0.000000	0.000000	0.000000		
32	0.0007	10.48	100.000000	0.000000	0.000000	0.000000		
33	0.0005	10.99	100.000000	0.000000	0.000000	0.000000		
34	0.0002	12.02	100.000000	0.000000	0.000000	0.000000		
35	0.0001	13.02	100.000000	0.000000	0.000000	0.000000		
36	0.0001	14.02	100.000000	0.000000	0.000000	0.000000		
37	0.0001	14.29	100.000000	0.000000	0.000000	0.000000		
		Sums:		100.00	100.00			

Grainsize Statistics
Percentiles

	phi	*mm*
5	1.10	0.465
16	1.39	0.382
25	1.55	0.342
50	1.86	0.275
75	2.18	0.220
84	2.33	0.198
95	2.62	0.162

Column: 87
Sample ID: 2014-8-30hn

Folks' Graphic Statistics

	Mean (Mz)	Sorting (σI)	Skewness (SkI)	Kurtosis (KG)	Mean *mm*
phi	1.862	0.467	0.000	0.977	0.275

Table II.87: *Results summary for sample 87: Mid intertidal zone, northern transect, Northern Ngarunui Beach. Sample collected on the 30th of August, 2014.*

Column: 88 **Density:** 2650
Volume: 0.010
Sample ID: 2014-8-30nm

Malvern data Phi	Malvern data Micron	Vol %	Equivalent Cum wt (g)
-1.00	2000.00	0	0.0
-0.75	1680.00	0	0.0
-0.50	1410.00	0	0.0
-0.25	1190.00	0	0.0
0.00	1000.00	0	0.0
0.25	840.00	0.161686	0.0
0.49	710.00	1.730035	0.5
0.76	590.00	7.130549	1.9
1.00	500.00	16.665648	4.4
1.25	420.00	31.765222	8.4
1.51	350.00	51.114192	13.5
1.74	300.00	67.499913	17.9
2.00	250.00	83.471321	22.1
2.25	210.00	93.404357	24.8
2.50	177.00	98.25617	26.0
2.75	149.00	99.842186	26.5
3.00	125.00	100	26.5
3.25	105.00	100	26.5
3.51	88.00	100	26.5
3.76	74.00	100	26.5
3.99	63.00	100	26.5
4.24	53.00	100	26.5
4.51	44.00	100	26.5
4.76	37.00	100	26.5
5.01	31.00	100	26.5
6.00	15.60	100	26.5
6.64	10.00	100	26.5
7.00	7.80	100	26.5
8.00	3.90	100	26.5
8.97	2.00	100	26.5
9.99	0.98	100	26.5
10.48	0.70	100	26.5
10.99	0.49	100	26.5
12.02	0.24	100	26.5
13.02	0.12	100	26.5
14.02	0.06	100	26.5
14.29	0.05	100	26.5

Total weight: 26.5

Column: 88
Sample ID: 2014-8-30nm

Folks' Graphic Statistics

	Mean (Mz)	Sorting (σI)	Skewness (SkI)	Kurtosis (KG)	Mean *mm*
phi	1.499	0.512	-0.004	0.952	0.354

	mm	phi	Cum wt (g)	Int wt (g)	Int wt%	Cum % finer	Modes
1	2.0000	-1.00	0.000000	0.000000	0.000000	100.000000	
2	1.6800	-0.75	0.000000	0.000000	0.000000	100.000000	
3	1.4100	-0.50	0.000000	0.000000	0.000000	100.000000	
4	1.1900	-0.25	0.000000	0.000000	0.000000	100.000000	
5	1.0000	0.00	0.000000	0.000000	0.000000	100.000000	8
6	0.8400	0.25	0.161686	0.161686	0.161686	99.838314	
7	0.7100	0.49	1.730035	1.568349	1.568349	98.269965	
8	0.5900	0.76	7.130549	5.400514	5.400514	92.869451	
9	0.5000	1.00	16.665648	9.535099	9.535099	83.334352	
10	0.4200	1.25	31.765222	15.099574	15.099574	68.234778	
11	0.3500	1.51	51.114192	19.348970	19.348970	48.885808	mode at 1.383056
12	0.3000	1.74	67.499913	16.385721	16.385721	32.500087	
13	0.2500	2.00	83.471321	15.971408	15.971408	16.528679	
14	0.2100	2.25	93.404357	9.933036	9.933036	6.595643	
15	0.1770	2.50	98.256170	4.851813	4.851813	1.743830	
16	0.1490	2.75	99.842186	1.586016	1.586016	0.157814	
17	0.1250	3.00	100.000000	0.157814	0.157814	0.000000	
18	0.1050	3.25	100.000000	0.000000	0.000000	0.000000	
19	0.0880	3.51	100.000000	0.000000	0.000000	0.000000	
20	0.0740	3.76	100.000000	0.000000	0.000000	0.000000	
21	0.0630	3.99	100.000000	0.000000	0.000000	0.000000	
22	0.0530	4.24	100.000000	0.000000	0.000000	0.000000	
23	0.0440	4.51	100.000000	0.000000	0.000000	0.000000	
24	0.0370	4.76	100.000000	0.000000	0.000000	0.000000	
25	0.0310	5.01	100.000000	0.000000	0.000000	0.000000	
26	0.0156	6.00	100.000000	0.000000	0.000000	0.000000	
27	0.0100	6.64	100.000000	0.000000	0.000000	0.000000	
28	0.0078	7.00	100.000000	0.000000	0.000000	0.000000	
29	0.0039	8.00	100.000000	0.000000	0.000000	0.000000	
30	0.0020	8.97	100.000000	0.000000	0.000000	0.000000	
31	0.0010	9.99	100.000000	0.000000	0.000000	0.000000	
32	0.0007	10.48	100.000000	0.000000	0.000000	0.000000	
33	0.0005	10.99	100.000000	0.000000	0.000000	0.000000	
34	0.0002	12.02	100.000000	0.000000	0.000000	0.000000	
35	0.0001	13.02	100.000000	0.000000	0.000000	0.000000	
36	0.0001	14.02	100.000000	0.000000	0.000000	0.000000	
37	0.0001	14.29	100.000000	0.000000	0.000000	0.000000	
	Sums:			100.00	100.00		

Grainsize Statistics
Percentiles

	phi	*mm*
5	0.66	0.635
16	0.98	0.506
25	1.14	0.454
50	1.50	0.354
75	1.86	0.275
84	2.01	0.248
95	2.33	0.199

Table II.88: *Results summary for sample 88: High intertidal zone, southern transect, Northern Ngarunui Beach. Sample collected on the 30th of August, 2014.*

Column: 89 **Density:** 2650
Volume: 0.010
Sample ID: 2014-8-30sh

Malvern data Phi	Malvern data Micron	Vol %	Equivalent Cum wt (g)
-1.00	2000.00	0	0.0
-0.75	1680.00	0	0.0
-0.50	1410.00	0	0.0
-0.25	1190.00	0	0.0
0.00	1000.00	0	0.0
0.25	840.00	0	0.0
0.49	710.00	0.357463	0.1
0.76	590.00	3.098674	0.8
1.00	500.00	9.451695	2.5
1.25	420.00	21.357979	5.7
1.51	350.00	38.872598	10.3
1.74	300.00	55.583327	14.7
2.00	250.00	74.00171	19.6
2.25	210.00	87.333983	23.1
2.50	177.00	95.277986	25.2
2.75	149.00	98.93661	26.2
3.00	125.00	99.911921	26.5
3.25	105.00	100	26.5
3.51	88.00	100	26.5
3.76	74.00	100	26.5
3.99	63.00	100	26.5
4.24	53.00	100	26.5
4.51	44.00	100	26.5
4.76	37.00	100	26.5
5.01	31.00	100	26.5
6.00	15.60	100	26.5
6.64	10.00	100	26.5
7.00	7.80	100	26.5
8.00	3.90	100	26.5
8.97	2.00	100	26.5
9.99	0.98	100	26.5
10.48	0.70	100	26.5
10.99	0.49	100	26.5
12.02	0.24	100	26.5
13.02	0.12	100	26.5
14.02	0.06	100	26.5
14.29	0.05	100	26.5
		Total weight:	26.5

	mm	phi	Cum wt (g)	Int wt (g)	Int wt%	Cum % finer	Modes	
1	2.0000	-1.00	0.000000	0.000000	0.000000	100.000000		
2	1.6800	-0.75	0.000000	0.000000	0.000000	100.000000		
3	1.4100	-0.50	0.000000	0.000000	0.000000	100.000000		
4	1.1900	-0.25	0.000000	0.000000	0.000000	100.000000		
5	1.0000	0.00	0.000000	0.000000	0.000000	100.000000		8
6	0.8400	0.25	0.000000	0.000000	0.000000	100.000000		
7	0.7100	0.49	0.357463	0.357463	0.357463	99.642537		
8	0.5900	0.76	3.098674	2.741211	2.741211	96.901326		
9	0.5000	1.00	9.451695	6.353021	6.353021	90.548305		
10	0.4200	1.25	21.357979	11.906284	11.906284	78.642021		
11	0.3500	1.51	38.872598	17.514619	17.514619	61.127402	mode at 1.383056	
12	0.3000	1.74	55.583327	16.710729	16.710729	44.416673		
13	0.2500	2.00	74.001710	18.418383	18.418383	25.998290	mode at 1.868483	
14	0.2100	2.25	87.333983	13.332273	13.332273	12.666017		
15	0.1770	2.50	95.277986	7.944003	7.944003	4.722014		
16	0.1490	2.75	98.936610	3.658624	3.658624	1.063390		
17	0.1250	3.00	99.911921	0.975311	0.975311	0.088079		
18	0.1050	3.25	100.000000	0.088079	0.088079	0.000000		
19	0.0880	3.51	100.000000	0.000000	0.000000	0.000000		
20	0.0740	3.76	100.000000	0.000000	0.000000	0.000000		
21	0.0630	3.99	100.000000	0.000000	0.000000	0.000000		
22	0.0530	4.24	100.000000	0.000000	0.000000	0.000000		
23	0.0440	4.51	100.000000	0.000000	0.000000	0.000000		
24	0.0370	4.76	100.000000	0.000000	0.000000	0.000000		
25	0.0310	5.01	100.000000	0.000000	0.000000	0.000000		
26	0.0156	6.00	100.000000	0.000000	0.000000	0.000000		
27	0.0100	6.64	100.000000	0.000000	0.000000	0.000000		
28	0.0078	7.00	100.000000	0.000000	0.000000	0.000000		
29	0.0039	8.00	100.000000	0.000000	0.000000	0.000000		
30	0.0020	8.97	100.000000	0.000000	0.000000	0.000000		
31	0.0010	9.99	100.000000	0.000000	0.000000	0.000000		
32	0.0007	10.48	100.000000	0.000000	0.000000	0.000000		
33	0.0005	10.99	100.000000	0.000000	0.000000	0.000000		
34	0.0002	12.02	100.000000	0.000000	0.000000	0.000000		
35	0.0001	13.02	100.000000	0.000000	0.000000	0.000000		
36	0.0001	14.02	100.000000	0.000000	0.000000	0.000000		
37	0.0001	14.29	100.000000	0.000000	0.000000	0.000000		
	Sums:			100.00	100.00			

Grainsize Statistics
Percentiles

	phi	*mm*
5	0.83	0.561
16	1.14	0.454
25	1.31	0.404
50	1.66	0.316
75	2.02	0.247
84	2.19	0.219
95	2.49	0.178

Column: 89
Sample ID: 2014-8-30sh

Folks' Graphic Statistics

	Mean (Mz)	Sorting (σI)	Skewness (SkI)	Kurtosis (KG)	Mean *mm*
phi	1.663	0.514	0.000	0.953	0.316

Table II.89: *Results summary for sample 89: Low intertidal zone, southern transect, Northern Ngarunui Beach. Sample collected on the 27th of September, 2014.*

Column: 90 **Density:** 2650
Volume: 0.010
Sample ID: 2014-9-27sl

Malvern data Phi	Malvern data Micron	Vol %	Equivalent Cum wt (g)
-1.00	2000.00	0	0.0
-0.75	1680.00	0.497526	0.1
-0.50	1410.00	1.750108	0.5
-0.25	1190.00	4.086356	1.1
0.00	1000.00	8.229043	2.2
0.25	840.00	14.722581	3.9
0.49	710.00	23.444328	6.2
0.76	590.00	35.540401	9.4
1.00	500.00	47.738479	12.7
1.25	420.00	60.810619	16.1
1.51	350.00	73.382422	19.4
1.74	300.00	82.312878	21.8
2.00	250.00	90.345142	23.9
2.25	210.00	95.431977	25.3
2.50	177.00	98.306845	26.1
2.75	149.00	99.657331	26.4
3.00	125.00	100	26.5
3.25	105.00	100	26.5
3.51	88.00	100	26.5
3.76	74.00	100	26.5
3.99	63.00	100	26.5
4.24	53.00	100	26.5
4.51	44.00	100	26.5
4.76	37.00	100	26.5
5.01	31.00	100	26.5
6.00	15.60	100	26.5
6.64	10.00	100	26.5
7.00	7.80	100	26.5
8.00	3.90	100	26.5
8.97	2.00	100	26.5
9.99	0.98	100	26.5
10.48	0.70	100	26.5
10.99	0.49	100	26.5
12.02	0.24	100	26.5
13.02	0.12	100	26.5
14.02	0.06	100	26.5
14.29	0.05	100	26.5
		Total weight:	26.5

	mm	phi	Cum wt (g)	Int wt (g)	Int wt%	Cum % finer	Modes	
1	2.0000	-1.00	0.000000	0.000000	0.000000	100.000000		
2	1.6800	-0.75	0.497526	0.497526	0.497526	99.502474		
3	1.4100	-0.50	1.750108	1.252582	1.252582	98.249892		
4	1.1900	-0.25	4.086356	2.336248	2.336248	95.913644		
5	1.0000	0.00	8.229043	4.142687	4.142687	91.770957		8
6	0.8400	0.25	14.722581	6.493538	6.493538	85.277419		
7	0.7100	0.49	23.444328	8.721747	8.721747	76.555672		
8	0.5900	0.76	35.540401	12.096073	12.096073	64.459599		
9	0.5000	1.00	47.738479	12.198078	12.198078	52.261521		
10	0.4200	1.25	60.810619	13.072140	13.072140	39.189381	mode at 1.125769	
11	0.3500	1.51	73.382422	12.571803	12.571803	26.617578		
12	0.3000	1.74	82.312878	8.930456	8.930456	17.687122		
13	0.2500	2.00	90.345142	8.032264	8.032264	9.654858		
14	0.2100	2.25	95.431977	5.086835	5.086835	4.568023		
15	0.1770	2.50	98.306845	2.874868	2.874868	1.693155		
16	0.1490	2.75	99.657331	1.350486	1.350486	0.342669		
17	0.1250	3.00	100.000000	0.342669	0.342669	0.000000		
18	0.1050	3.25	100.000000	0.000000	0.000000	0.000000		
19	0.0880	3.51	100.000000	0.000000	0.000000	0.000000		
20	0.0740	3.76	100.000000	0.000000	0.000000	0.000000		
21	0.0630	3.99	100.000000	0.000000	0.000000	0.000000		
22	0.0530	4.24	100.000000	0.000000	0.000000	0.000000		
23	0.0440	4.51	100.000000	0.000000	0.000000	0.000000		
24	0.0370	4.76	100.000000	0.000000	0.000000	0.000000		
25	0.0310	5.01	100.000000	0.000000	0.000000	0.000000		
26	0.0156	6.00	100.000000	0.000000	0.000000	0.000000		
27	0.0100	6.64	100.000000	0.000000	0.000000	0.000000		
28	0.0078	7.00	100.000000	0.000000	0.000000	0.000000		
29	0.0039	8.00	100.000000	0.000000	0.000000	0.000000		
30	0.0020	8.97	100.000000	0.000000	0.000000	0.000000		
31	0.0010	9.99	100.000000	0.000000	0.000000	0.000000		
32	0.0007	10.48	100.000000	0.000000	0.000000	0.000000		
33	0.0005	10.99	100.000000	0.000000	0.000000	0.000000		
34	0.0002	12.02	100.000000	0.000000	0.000000	0.000000		
35	0.0001	13.02	100.000000	0.000000	0.000000	0.000000		
36	0.0001	14.02	100.000000	0.000000	0.000000	0.000000		
37	0.0001	14.29	100.000000	0.000000	0.000000	0.000000		
	Sums:			100.00	100.00			

Grainsize Statistics
Percentiles

	phi	*mm*
5	-0.20	1.145
16	0.29	0.820
25	0.53	0.693
50	1.04	0.485
75	1.55	0.340
84	1.79	0.289
95	2.23	0.213

Column: 90
Sample ID: 2014-9-27sl

Folks' Graphic Statistics

	Mean (Mz)	Sorting (σI)	Skewness (SkI)	Kurtosis (KG)	Mean *mm*
phi	1.041	0.744	-0.013	0.969	0.486

Table II.90: *Results summary for sample 90: Low intertidal zone, mid transect, Northern Ngarunui Beach. Sample collected on the 27th of September, 2014.*

Column: 91 **Density:** 2650
Volume: 0.010
Sample ID: 2014-9-27ml

Malvern data Phi	Malvern data Micron	Vol %	Equivalent Cum wt (g)
-1.00	2000.00	0	0.0
-0.75	1680.00	0	0.0
-0.50	1410.00	0	0.0
-0.25	1190.00	0	0.0
0.00	1000.00	0.242896	0.1
0.25	840.00	2.379725	0.6
0.49	710.00	7.629809	2.0
0.76	590.00	18.171131	4.8
1.00	500.00	31.618024	8.4
1.25	420.00	48.359568	12.8
1.51	350.00	65.957606	17.5
1.74	300.00	78.795101	20.9
2.00	250.00	89.95947	23.8
2.25	210.00	96.292458	25.5
2.50	177.00	99.164889	26.3
2.75	149.00	99.9713	26.5
3.00	125.00	100	26.5
3.25	105.00	100	26.5
3.51	88.00	100	26.5
3.76	74.00	100	26.5
3.99	63.00	100	26.5
4.24	53.00	100	26.5
4.51	44.00	100	26.5
4.76	37.00	100	26.5
5.01	31.00	100	26.5
6.00	15.60	100	26.5
6.64	10.00	100	26.5
7.00	7.80	100	26.5
8.00	3.90	100	26.5
8.97	2.00	100	26.5
9.99	0.98	100	26.5
10.48	0.70	100	26.5
10.99	0.49	100	26.5
12.02	0.24	100	26.5
13.02	0.12	100	26.5
14.02	0.06	100	26.5
14.29	0.05	100	26.5
		Total weight:	26.5

	mm	phi	Cum wt (g)	Int wt (g)	Int wt%	Cum % finer	Modes	
1	2.0000	-1.00	0.000000	0.000000	0.000000	100.000000		
2	1.6800	-0.75	0.000000	0.000000	0.000000	100.000000		
3	1.4100	-0.50	0.000000	0.000000	0.000000	100.000000		
4	1.1900	-0.25	0.000000	0.000000	0.000000	100.000000		
5	1.0000	0.00	0.242896	0.242896	0.242896	99.757104		8
6	0.8400	0.25	2.379725	2.136829	2.136829	97.620275		
7	0.7100	0.49	7.629809	5.250084	5.250084	92.370191		
8	0.5900	0.76	18.171131	10.541322	10.541322	81.828869		
9	0.5000	1.00	31.618024	13.446893	13.446893	68.381976		
10	0.4200	1.25	48.359568	16.741544	16.741544	51.640432		
11	0.3500	1.51	65.957606	17.598038	17.598038	34.042394	mode at 1.383056	
12	0.3000	1.74	78.795101	12.837495	12.837495	21.204899		
13	0.2500	2.00	89.959470	11.164369	11.164369	10.040530		
14	0.2100	2.25	96.292458	6.332988	6.332988	3.707542		
15	0.1770	2.50	99.164889	2.872431	2.872431	0.835111		
16	0.1490	2.75	99.971300	0.806411	0.806411	0.028700		
17	0.1250	3.00	100.000000	0.028700	0.028700	0.000000		
18	0.1050	3.25	100.000000	0.000000	0.000000	0.000000		
19	0.0880	3.51	100.000000	0.000000	0.000000	0.000000		
20	0.0740	3.76	100.000000	0.000000	0.000000	0.000000		
21	0.0630	3.99	100.000000	0.000000	0.000000	0.000000		
22	0.0530	4.24	100.000000	0.000000	0.000000	0.000000		
23	0.0440	4.51	100.000000	0.000000	0.000000	0.000000		
24	0.0370	4.76	100.000000	0.000000	0.000000	0.000000		
25	0.0310	5.01	100.000000	0.000000	0.000000	0.000000		
26	0.0156	6.00	100.000000	0.000000	0.000000	0.000000		
27	0.0100	6.64	100.000000	0.000000	0.000000	0.000000		
28	0.0078	7.00	100.000000	0.000000	0.000000	0.000000		
29	0.0039	8.00	100.000000	0.000000	0.000000	0.000000		
30	0.0020	8.97	100.000000	0.000000	0.000000	0.000000		
31	0.0010	9.99	100.000000	0.000000	0.000000	0.000000		
32	0.0007	10.48	100.000000	0.000000	0.000000	0.000000		
33	0.0005	10.99	100.000000	0.000000	0.000000	0.000000		
34	0.0002	12.02	100.000000	0.000000	0.000000	0.000000		
35	0.0001	13.02	100.000000	0.000000	0.000000	0.000000		
36	0.0001	14.02	100.000000	0.000000	0.000000	0.000000		
37	0.0001	14.29	100.000000	0.000000	0.000000	0.000000		
		Sums:		100.00	100.00			

Column: 91
Sample ID: 2014-9-27ml

Folks' Graphic Statistics

	Mean (Mz)	Sorting (σI)	Skewness (SkI)	Kurtosis (KG)	Mean ***mm***
phi	1.281	0.565	0.012	0.950	0.412

Grainsize Statistics
Percentiles

	phi	***mm***
5	0.37	0.772
16	0.71	0.613
25	0.88	0.542
50	1.28	0.413
75	1.67	0.314
84	1.86	0.276
95	2.20	0.218

Table II.91: *Results summary for sample 91: Mid intertidal zone, northern transect, Northern Ngarunui Beach. Sample collected on the 27th of September, 2014.*

Column: 92 **Density:** 2650
Volume: 0.010
Sample ID: 2014-9-27nm

Malvern data Phi	Malvern data Micron	Vol %	Equivalent Cum wt (g)
-1.00	2000.00	0	0.0
-0.75	1680.00	0	0.0
-0.50	1410.00	0	0.0
-0.25	1190.00	0	0.0
0.00	1000.00	0	0.0
0.25	840.00	0	0.0
0.49	710.00	0.018964	0.0
0.76	590.00	1.00815	0.3
1.00	500.00	4.511549	1.2
1.25	420.00	12.760046	3.4
1.51	350.00	27.210683	7.2
1.74	300.00	43.063984	11.4
2.00	250.00	62.95399	16.7
2.25	210.00	79.466607	21.1
2.50	177.00	90.852968	24.1
2.75	149.00	97.153404	25.7
3.00	125.00	99.614703	26.4
3.25	105.00	100	26.5
3.51	88.00	100	26.5
3.76	74.00	100	26.5
3.99	63.00	100	26.5
4.24	53.00	100	26.5
4.51	44.00	100	26.5
4.76	37.00	100	26.5
5.01	31.00	100	26.5
6.00	15.60	100	26.5
6.64	10.00	100	26.5
7.00	7.80	100	26.5
8.00	3.90	100	26.5
8.97	2.00	100	26.5
9.99	0.98	100	26.5
10.48	0.70	100	26.5
10.99	0.49	100	26.5
12.02	0.24	100	26.5
13.02	0.12	100	26.5
14.02	0.06	100	26.5
14.29	0.05	100	26.5
		Total weight:	26.5

	mm	phi	Cum wt (g)	Int wt (g)	Int wt%	Cum % finer	Modes	
1	2.0000	-1.00	0.000000	0.000000	0.000000	100.000000		
2	1.6800	-0.75	0.000000	0.000000	0.000000	100.000000		
3	1.4100	-0.50	0.000000	0.000000	0.000000	100.000000		
4	1.1900	-0.25	0.000000	0.000000	0.000000	100.000000		
5	1.0000	0.00	0.000000	0.000000	0.000000	100.000000		8
6	0.8400	0.25	0.000000	0.000000	0.000000	100.000000		
7	0.7100	0.49	0.018964	0.018964	0.018964	99.981036		
8	0.5900	0.76	1.008150	0.989186	0.989186	98.991850		
9	0.5000	1.00	4.511549	3.503399	3.503399	95.488451		
10	0.4200	1.25	12.760046	8.248497	8.248497	87.239954		
11	0.3500	1.51	27.210683	14.450637	14.450637	72.789317		
12	0.3000	1.74	43.063984	15.853301	15.853301	56.936016		
13	0.2500	2.00	62.953990	19.890006	19.890006	37.046010	mode at 1.868483	
14	0.2100	2.25	79.466607	16.512617	16.512617	20.533393		
15	0.1770	2.50	90.852968	11.386361	11.386361	9.147032		
16	0.1490	2.75	97.153404	6.300436	6.300436	2.846596		
17	0.1250	3.00	99.614703	2.461299	2.461299	0.385297		
18	0.1050	3.25	100.000000	0.385297	0.385297	0.000000		
19	0.0880	3.51	100.000000	0.000000	0.000000	0.000000		
20	0.0740	3.76	100.000000	0.000000	0.000000	0.000000		
21	0.0630	3.99	100.000000	0.000000	0.000000	0.000000		
22	0.0530	4.24	100.000000	0.000000	0.000000	0.000000		
23	0.0440	4.51	100.000000	0.000000	0.000000	0.000000		
24	0.0370	4.76	100.000000	0.000000	0.000000	0.000000		
25	0.0310	5.01	100.000000	0.000000	0.000000	0.000000		
26	0.0156	6.00	100.000000	0.000000	0.000000	0.000000		
27	0.0100	6.64	100.000000	0.000000	0.000000	0.000000		
28	0.0078	7.00	100.000000	0.000000	0.000000	0.000000		
29	0.0039	8.00	100.000000	0.000000	0.000000	0.000000		
30	0.0020	8.97	100.000000	0.000000	0.000000	0.000000		
31	0.0010	9.99	100.000000	0.000000	0.000000	0.000000		
32	0.0007	10.48	100.000000	0.000000	0.000000	0.000000		
33	0.0005	10.99	100.000000	0.000000	0.000000	0.000000		
34	0.0002	12.02	100.000000	0.000000	0.000000	0.000000		
35	0.0001	13.02	100.000000	0.000000	0.000000	0.000000		
36	0.0001	14.02	100.000000	0.000000	0.000000	0.000000		
37	0.0001	14.29	100.000000	0.000000	0.000000	0.000000		
		Sums:		100.00	100.00			

Column: 92
Sample ID: 2014-9-27nm

Folks' Graphic Statistics

	Mean (Mz)	Sorting (σI)	Skewness (SkI)	Kurtosis (KG)	Mean *mm*
phi	1.830	0.509	0.007	0.952	0.281

Grainsize Statistics
Percentiles

	phi	*mm*
5	1.01	0.495
16	1.31	0.403
25	1.47	0.360
50	1.83	0.282
75	2.18	0.220
84	2.35	0.196
95	2.66	0.158

Table II.92: *Results summary for sample 92: High intertidal zone, southern transect, Northern Ngarunui Beach. Sample collected on the 27th of September, 2014.*

Column: 93 **Density:** 2650
Volume: 0.010
Sample ID: 2014-9-27sh

Malvern data Phi	Malvern data Micron	Vol %	Equivalent Cum wt (g)
-1.00	2000.00	0	0.0
-0.75	1680.00	0	0.0
-0.50	1410.00	0	0.0
-0.25	1190.00	0	0.0
0.00	1000.00	0	0.0
0.25	840.00	0	0.0
0.49	710.00	0	0.0
0.76	590.00	0.56504	0.1
1.00	500.00	2.756671	0.7
1.25	420.00	8.085155	2.1
1.51	350.00	17.947491	4.8
1.74	300.00	29.701387	7.9
2.00	250.00	46.364865	12.3
2.25	210.00	62.876681	16.7
2.50	177.00	77.264597	20.5
2.75	149.00	88.280291	23.4
3.00	125.00	95.367884	25.3
3.25	105.00	98.824455	26.2
3.51	88.00	99.94141	26.5
3.76	74.00	100	26.5
3.99	63.00	100	26.5
4.24	53.00	100	26.5
4.51	44.00	100	26.5
4.76	37.00	100	26.5
5.01	31.00	100	26.5
6.00	15.60	100	26.5
6.64	10.00	100	26.5
7.00	7.80	100	26.5
8.00	3.90	100	26.5
8.97	2.00	100	26.5
9.99	0.98	100	26.5
10.48	0.70	100	26.5
10.99	0.49	100	26.5
12.02	0.24	100	26.5
13.02	0.12	100	26.5
14.02	0.06	100	26.5
14.29	0.05	100	26.5
		Total weight:	26.5

	mm	phi	Cum wt (g)	Int wt (g)	Int wt%	Cum % finer	Modes	
1	2.0000	-1.00	0.000000	0.000000	0.000000	100.000000		
2	1.6800	-0.75	0.000000	0.000000	0.000000	100.000000		
3	1.4100	-0.50	0.000000	0.000000	0.000000	100.000000		
4	1.1900	-0.25	0.000000	0.000000	0.000000	100.000000		
5	1.0000	0.00	0.000000	0.000000	0.000000	100.000000		8
6	0.8400	0.25	0.000000	0.000000	0.000000	100.000000		
7	0.7100	0.49	0.000000	0.000000	0.000000	100.000000		
8	0.5900	0.76	0.565040	0.565040	0.565040	99.434960		
9	0.5000	1.00	2.756671	2.191631	2.191631	97.243329		
10	0.4200	1.25	8.085155	5.328484	5.328484	91.914845		
11	0.3500	1.51	17.947491	9.862336	9.862336	82.052509		
12	0.3000	1.74	29.701387	11.753896	11.753896	70.298613		
13	0.2500	2.00	46.364865	16.663478	16.663478	53.635135	mode at 1.868483	
14	0.2100	2.25	62.876681	16.511816	16.511816	37.123319		
15	0.1770	2.50	77.264597	14.387916	14.387916	22.735403		
16	0.1490	2.75	88.280291	11.015694	11.015694	11.719709		
17	0.1250	3.00	95.367884	7.087593	7.087593	4.632116		
18	0.1050	3.25	98.824455	3.456571	3.456571	1.175545		
19	0.0880	3.51	99.941410	1.116955	1.116955	0.058590		
20	0.0740	3.76	100.000000	0.058590	0.058590	0.000000		
21	0.0630	3.99	100.000000	0.000000	0.000000	0.000000		
22	0.0530	4.24	100.000000	0.000000	0.000000	0.000000		
23	0.0440	4.51	100.000000	0.000000	0.000000	0.000000		
24	0.0370	4.76	100.000000	0.000000	0.000000	0.000000		
25	0.0310	5.01	100.000000	0.000000	0.000000	0.000000		
26	0.0156	6.00	100.000000	0.000000	0.000000	0.000000		
27	0.0100	6.64	100.000000	0.000000	0.000000	0.000000		
28	0.0078	7.00	100.000000	0.000000	0.000000	0.000000		
29	0.0039	8.00	100.000000	0.000000	0.000000	0.000000		
30	0.0020	8.97	100.000000	0.000000	0.000000	0.000000		
31	0.0010	9.99	100.000000	0.000000	0.000000	0.000000		
32	0.0007	10.48	100.000000	0.000000	0.000000	0.000000		
33	0.0005	10.99	100.000000	0.000000	0.000000	0.000000		
34	0.0002	12.02	100.000000	0.000000	0.000000	0.000000		
35	0.0001	13.02	100.000000	0.000000	0.000000	0.000000		
36	0.0001	14.02	100.000000	0.000000	0.000000	0.000000		
37	0.0001	14.29	100.000000	0.000000	0.000000	0.000000		
		Sums:		100.00	100.00			

Grainsize Statistics
Percentiles

	phi	*mm*
5	1.11	0.465
16	1.46	0.363
25	1.65	0.319
50	2.06	0.241
75	2.46	0.182
84	2.65	0.159
95	2.99	0.126

Column: 93
Sample ID: 2014-9-27sh

Folks' Graphic Statistics

	Mean (Mz)	Sorting (σI)	Skewness (SkI)	Kurtosis (KG)	Mean *mm*
phi	2.056	0.582	-0.004	0.950	0.240

Table II.93: *Results summary for sample 93: Mid intertidal zone, southern transect, Northern Ngarunui Beach. Sample collected on the 27th of September, 2014.*

Column: 94 **Density:** 2650
Volume: 0.010
Sample ID: 2014-9-27sm

Malvern data Phi	Malvern data Micron	Vol %	Equivalent Cum wt (g)
-1.00	2000.00	0	0.0
-0.75	1680.00	0	0.0
-0.50	1410.00	0.028984	0.0
-0.25	1190.00	0.384571	0.1
0.00	1000.00	2.158114	0.6
0.25	840.00	6.508222	1.7
0.49	710.00	14.210357	3.8
0.76	590.00	27.042252	7.2
1.00	500.00	41.50813	11.0
1.25	420.00	57.886263	15.3
1.51	350.00	73.714846	19.5
1.74	300.00	84.455515	22.4
2.00	250.00	93.171032	24.7
2.25	210.00	97.729742	25.9
2.50	177.00	99.588937	26.4
2.75	149.00	100	26.5
3.00	125.00	100	26.5
3.25	105.00	100	26.5
3.51	88.00	100	26.5
3.76	74.00	100	26.5
3.99	63.00	100	26.5
4.24	53.00	100	26.5
4.51	44.00	100	26.5
4.76	37.00	100	26.5
5.01	31.00	100	26.5
6.00	15.60	100	26.5
6.64	10.00	100	26.5
7.00	7.80	100	26.5
8.00	3.90	100	26.5
8.97	2.00	100	26.5
9.99	0.98	100	26.5
10.48	0.70	100	26.5
10.99	0.49	100	26.5
12.02	0.24	100	26.5
13.02	0.12	100	26.5
14.02	0.06	100	26.5
14.29	0.05	100	26.5
		Total weight:	26.5

	mm	phi	Cum wt (g)	Int wt (g)	Int wt%	Cum % finer	Modes	
1	2.0000	-1.00	0.000000	0.000000	0.000000	100.000000		
2	1.6800	-0.75	0.000000	0.000000	0.000000	100.000000		
3	1.4100	-0.50	0.028984	0.028984	0.028984	99.971016		
4	1.1900	-0.25	0.384571	0.355587	0.355587	99.615429		
5	1.0000	0.00	2.158114	1.773543	1.773543	97.841886		8
6	0.8400	0.25	6.508222	4.350108	4.350108	93.491778		
7	0.7100	0.49	14.210357	7.702135	7.702135	85.789643		
8	0.5900	0.76	27.042252	12.831895	12.831895	72.957748		
9	0.5000	1.00	41.508130	14.465878	14.465878	58.491870		
10	0.4200	1.25	57.886263	16.378133	16.378133	42.113737	mode at 1.125769	
11	0.3500	1.51	73.714846	15.828583	15.828583	26.285154		
12	0.3000	1.74	84.455515	10.740669	10.740669	15.544485		
13	0.2500	2.00	93.171032	8.715517	8.715517	6.828968		
14	0.2100	2.25	97.729742	4.558710	4.558710	2.270258		
15	0.1770	2.50	99.588937	1.859195	1.859195	0.411063		
16	0.1490	2.75	100.000000	0.411063	0.411063	0.000000		
17	0.1250	3.00	100.000000	0.000000	0.000000	0.000000		
18	0.1050	3.25	100.000000	0.000000	0.000000	0.000000		
19	0.0880	3.51	100.000000	0.000000	0.000000	0.000000		
20	0.0740	3.76	100.000000	0.000000	0.000000	0.000000		
21	0.0630	3.99	100.000000	0.000000	0.000000	0.000000		
22	0.0530	4.24	100.000000	0.000000	0.000000	0.000000		
23	0.0440	4.51	100.000000	0.000000	0.000000	0.000000		
24	0.0370	4.76	100.000000	0.000000	0.000000	0.000000		
25	0.0310	5.01	100.000000	0.000000	0.000000	0.000000		
26	0.0156	6.00	100.000000	0.000000	0.000000	0.000000		
27	0.0100	6.64	100.000000	0.000000	0.000000	0.000000		
28	0.0078	7.00	100.000000	0.000000	0.000000	0.000000		
29	0.0039	8.00	100.000000	0.000000	0.000000	0.000000		
30	0.0020	8.97	100.000000	0.000000	0.000000	0.000000		
31	0.0010	9.99	100.000000	0.000000	0.000000	0.000000		
32	0.0007	10.48	100.000000	0.000000	0.000000	0.000000		
33	0.0005	10.99	100.000000	0.000000	0.000000	0.000000		
34	0.0002	12.02	100.000000	0.000000	0.000000	0.000000		
35	0.0001	13.02	100.000000	0.000000	0.000000	0.000000		
36	0.0001	14.02	100.000000	0.000000	0.000000	0.000000		
37	0.0001	14.29	100.000000	0.000000	0.000000	0.000000		
		Sums:		100.00	100.00			

Grainsize Statistics
Percentiles

	phi	*mm*
5	0.16	0.892
16	0.53	0.692
25	0.72	0.608
50	1.13	0.457
75	1.54	0.344
84	1.73	0.302
95	2.10	0.233

Column: 94
Sample ID: 2014-9-27sm

Folks' Graphic Statistics

	Mean (Mz)	Sorting (σI)	Skewness (SkI)	Kurtosis (KG)	Mean *mm*
phi	1.130	0.592	0.000	0.965	0.457

Table II.94: *Results summary for sample 94: Mid intertidal zone, mid transect, Northern Ngarunui Beach. Sample collected on the 27th of September, 2014.*

Column: 95 **Density:** 2650
Volume: 0.010
Sample ID: 2014-9-27mm

Malvern data Phi	Malvern data Micron	Vol %	Equivalent Cum wt (g)
-1.00	2000.00	0	0.0
-0.75	1680.00	0	0.0
-0.50	1410.00	0	0.0
-0.25	1190.00	0	0.0
0.00	1000.00	0	0.0
0.25	840.00	0.214415	0.1
0.49	710.00	1.872214	0.5
0.76	590.00	6.868377	1.8
1.00	500.00	15.086811	4.0
1.25	420.00	27.728956	7.3
1.51	350.00	44.12637	11.7
1.74	300.00	58.791197	15.6
2.00	250.00	74.678615	19.8
2.25	210.00	86.528072	22.9
2.50	177.00	94.190697	25.0
2.75	149.00	98.282184	26.0
3.00	125.00	99.816098	26.5
3.25	105.00	100	26.5
3.51	88.00	100	26.5
3.76	74.00	100	26.5
3.99	63.00	100	26.5
4.24	53.00	100	26.5
4.51	44.00	100	26.5
4.76	37.00	100	26.5
5.01	31.00	100	26.5
6.00	15.60	100	26.5
6.64	10.00	100	26.5
7.00	7.80	100	26.5
8.00	3.90	100	26.5
8.97	2.00	100	26.5
9.99	0.98	100	26.5
10.48	0.70	100	26.5
10.99	0.49	100	26.5
12.02	0.24	100	26.5
13.02	0.12	100	26.5
14.02	0.06	100	26.5
14.29	0.05	100	26.5
		Total weight:	26.5

Column: 95
Sample ID: 2014-9-27mm

Folks' Graphic Statistics

	Mean (Mz)	Sorting (σI)	Skewness (SkI)	Kurtosis (KG)	Mean *mm*
phi	1.607	0.581	0.004	0.955	0.328

	mm	phi	Cum wt (g)	Int wt (g)	Int wt%	Cum % finer	Modes	
1	2.0000	-1.00	0.000000	0.000000	0.000000	100.000000		
2	1.6800	-0.75	0.000000	0.000000	0.000000	100.000000		
3	1.4100	-0.50	0.000000	0.000000	0.000000	100.000000		
4	1.1900	-0.25	0.000000	0.000000	0.000000	100.000000		
5	1.0000	0.00	0.000000	0.000000	0.000000	100.000000		8
6	0.8400	0.25	0.214415	0.214415	0.214415	99.785585		
7	0.7100	0.49	1.872214	1.657799	1.657799	98.127786		
8	0.5900	0.76	6.868377	4.996163	4.996163	93.131623		
9	0.5000	1.00	15.086811	8.218434	8.218434	84.913189		
10	0.4200	1.25	27.728956	12.642145	12.642145	72.271044		
11	0.3500	1.51	44.126370	16.397414	16.397414	55.873630	mode at 1.383056	
12	0.3000	1.74	58.791197	14.664827	14.664827	41.208803		
13	0.2500	2.00	74.678615	15.887418	15.887418	25.321385	mode at 1.868483	
14	0.2100	2.25	86.528072	11.849457	11.849457	13.471928		
15	0.1770	2.50	94.190697	7.662625	7.662625	5.809303		
16	0.1490	2.75	98.282184	4.091487	4.091487	1.717816		
17	0.1250	3.00	99.816098	1.533914	1.533914	0.183902		
18	0.1050	3.25	100.000000	0.183902	0.183902	0.000000		
19	0.0880	3.51	100.000000	0.000000	0.000000	0.000000		
20	0.0740	3.76	100.000000	0.000000	0.000000	0.000000		
21	0.0630	3.99	100.000000	0.000000	0.000000	0.000000		
22	0.0530	4.24	100.000000	0.000000	0.000000	0.000000		
23	0.0440	4.51	100.000000	0.000000	0.000000	0.000000		
24	0.0370	4.76	100.000000	0.000000	0.000000	0.000000		
25	0.0310	5.01	100.000000	0.000000	0.000000	0.000000		
26	0.0156	6.00	100.000000	0.000000	0.000000	0.000000		
27	0.0100	6.64	100.000000	0.000000	0.000000	0.000000		
28	0.0078	7.00	100.000000	0.000000	0.000000	0.000000		
29	0.0039	8.00	100.000000	0.000000	0.000000	0.000000		
30	0.0020	8.97	100.000000	0.000000	0.000000	0.000000		
31	0.0010	9.99	100.000000	0.000000	0.000000	0.000000		
32	0.0007	10.48	100.000000	0.000000	0.000000	0.000000		
33	0.0005	10.99	100.000000	0.000000	0.000000	0.000000		
34	0.0002	12.02	100.000000	0.000000	0.000000	0.000000		
35	0.0001	13.02	100.000000	0.000000	0.000000	0.000000		
36	0.0001	14.02	100.000000	0.000000	0.000000	0.000000		
37	0.0001	14.29	100.000000	0.000000	0.000000	0.000000		
		Sums:		100.00	100.00			

Grainsize Statistics
Percentiles

	phi	*mm*
5	0.66	0.632
16	1.02	0.494
25	1.20	0.436
50	1.60	0.329
75	2.01	0.249
84	2.20	0.218
95	2.55	0.171

Table II.95: *Results summary for sample 95: High intertidal zone, northern transect, Northern Ngarunui Beach. Sample collected on the 27th of September, 2014.*

Column: 96 **Density:** 2650
Volume: 0.010
Sample ID: 2014-9-27nh

Malvern data Phi	Malvern data Micron	Vol %	Equivalent Cum wt (g)
-1.00	2000.00	0	0.0
-0.75	1680.00	0	0.0
-0.50	1410.00	0	0.0
-0.25	1190.00	0	0.0
0.00	1000.00	0	0.0
0.25	840.00	0	0.0
0.49	710.00	0	0.0
0.76	590.00	0.005668	0.0
1.00	500.00	0.262779	0.1
1.25	420.00	2.109691	0.6
1.51	350.00	7.193762	1.9
1.74	300.00	15.020346	4.0
2.00	250.00	28.609974	7.6
2.25	210.00	44.825716	11.9
2.50	177.00	61.550632	16.3
2.75	149.00	76.700528	20.3
3.00	125.00	88.427379	23.4
3.25	105.00	95.651102	25.3
3.51	88.00	99.082642	26.3
3.76	74.00	99.979974	26.5
3.99	63.00	100	26.5
4.24	53.00	100	26.5
4.51	44.00	100	26.5
4.76	37.00	100	26.5
5.01	31.00	100	26.5
6.00	15.60	100	26.5
6.64	10.00	100	26.5
7.00	7.80	100	26.5
8.00	3.90	100	26.5
8.97	2.00	100	26.5
9.99	0.98	100	26.5
10.48	0.70	100	26.5
10.99	0.49	100	26.5
12.02	0.24	100	26.5
13.02	0.12	100	26.5
14.02	0.06	100	26.5
14.29	0.05	100	26.5
		Total weight:	26.5

	mm	phi	Cum wt (g)	Int wt (g)	Int wt%	Cum % finer	Modes	
1	2.0000	-1.00	0.000000	0.000000	0.000000	100.000000		
2	1.6800	-0.75	0.000000	0.000000	0.000000	100.000000		
3	1.4100	-0.50	0.000000	0.000000	0.000000	100.000000		
4	1.1900	-0.25	0.000000	0.000000	0.000000	100.000000		
5	1.0000	0.00	0.000000	0.000000	0.000000	100.000000		8
6	0.8400	0.25	0.000000	0.000000	0.000000	100.000000		
7	0.7100	0.49	0.000000	0.000000	0.000000	100.000000		
8	0.5900	0.76	0.005668	0.005668	0.005668	99.994332		
9	0.5000	1.00	0.262779	0.257111	0.257111	99.737221		
10	0.4200	1.25	2.109691	1.846912	1.846912	97.890309		
11	0.3500	1.51	7.193762	5.084071	5.084071	92.806238		
12	0.3000	1.74	15.020346	7.826584	7.826584	84.979654		
13	0.2500	2.00	28.609974	13.589628	13.589628	71.390026		
14	0.2100	2.25	44.825716	16.215742	16.215742	55.174284		
15	0.1770	2.50	61.550632	16.724916	16.724916	38.449368	mode at 2.374859	
16	0.1490	2.75	76.700528	15.149896	15.149896	23.299472		
17	0.1250	3.00	88.427379	11.726851	11.726851	11.572621		
18	0.1050	3.25	95.651102	7.223723	7.223723	4.348898		
19	0.0880	3.51	99.082642	3.431540	3.431540	0.917358		
20	0.0740	3.76	99.979974	0.897332	0.897332	0.020026		
21	0.0630	3.99	100.000000	0.020026	0.020026	0.000000		
22	0.0530	4.24	100.000000	0.000000	0.000000	0.000000		
23	0.0440	4.51	100.000000	0.000000	0.000000	0.000000		
24	0.0370	4.76	100.000000	0.000000	0.000000	0.000000		
25	0.0310	5.01	100.000000	0.000000	0.000000	0.000000		
26	0.0156	6.00	100.000000	0.000000	0.000000	0.000000		
27	0.0100	6.64	100.000000	0.000000	0.000000	0.000000		
28	0.0078	7.00	100.000000	0.000000	0.000000	0.000000		
29	0.0039	8.00	100.000000	0.000000	0.000000	0.000000		
30	0.0020	8.97	100.000000	0.000000	0.000000	0.000000		
31	0.0010	9.99	100.000000	0.000000	0.000000	0.000000		
32	0.0007	10.48	100.000000	0.000000	0.000000	0.000000		
33	0.0005	10.99	100.000000	0.000000	0.000000	0.000000		
34	0.0002	12.02	100.000000	0.000000	0.000000	0.000000		
35	0.0001	13.02	100.000000	0.000000	0.000000	0.000000		
36	0.0001	14.02	100.000000	0.000000	0.000000	0.000000		
37	0.0001	14.29	100.000000	0.000000	0.000000	0.000000		
		Sums:		100.00	100.00			

Grainsize Statistics
Percentiles

	phi	*mm*
5	1.40	0.379
16	1.76	0.296
25	1.93	0.262
50	2.33	0.199
75	2.72	0.152
84	2.90	0.134
95	3.23	0.107

Column: 96
Sample ID: 2014-9-27nh

Folks' Graphic Statistics

	Mean (Mz)	Sorting (σI)	Skewness (SkI)	Kurtosis (KG)	Mean *mm*
phi	2.329	0.564	-0.005	0.950	0.199

Table II.96: *Results summary for sample 96: Low intertidal zone, northern transect, Northern Ngarunui Beach. Sample collected on the 27th of September, 2014.*

Column: 97 **Density:** 2650
Volume: 0.010
Sample ID: 2014-9-27nl

Malvern data Phi	Malvern data Micron	Vol %	Equivalent Cum wt (g)
-1.00	2000.00	0	0.0
-0.75	1680.00	0	0.0
-0.50	1410.00	0	0.0
-0.25	1190.00	0	0.0
0.00	1000.00	0	0.0
0.25	840.00	0.120299	0.0
0.49	710.00	1.456149	0.4
0.76	590.00	6.303237	1.7
1.00	500.00	15.118531	4.0
1.25	420.00	29.40346	7.8
1.51	350.00	48.141448	12.8
1.74	300.00	64.425938	17.1
2.00	250.00	80.853963	21.4
2.25	210.00	91.629734	24.3
2.50	177.00	97.361756	25.8
2.75	149.00	99.602903	26.4
3.00	125.00	100	26.5
3.25	105.00	100	26.5
3.51	88.00	100	26.5
3.76	74.00	100	26.5
3.99	63.00	100	26.5
4.24	53.00	100	26.5
4.51	44.00	100	26.5
4.76	37.00	100	26.5
5.01	31.00	100	26.5
6.00	15.60	100	26.5
6.64	10.00	100	26.5
7.00	7.80	100	26.5
8.00	3.90	100	26.5
8.97	2.00	100	26.5
9.99	0.98	100	26.5
10.48	0.70	100	26.5
10.99	0.49	100	26.5
12.02	0.24	100	26.5
13.02	0.12	100	26.5
14.02	0.06	100	26.5
14.29	0.05	100	26.5

Total weight: 26.5

	mm	phi	Cum wt (g)	Int wt (g)	Int wt%	Cum % finer	Modes
1	2.0000	-1.00	0.000000	0.000000	0.000000	100.000000	
2	1.6800	-0.75	0.000000	0.000000	0.000000	100.000000	
3	1.4100	-0.50	0.000000	0.000000	0.000000	100.000000	
4	1.1900	-0.25	0.000000	0.000000	0.000000	100.000000	
5	1.0000	0.00	0.000000	0.000000	0.000000	100.000000	8
6	0.8400	0.25	0.120299	0.120299	0.120299	99.879701	
7	0.7100	0.49	1.456149	1.335850	1.335850	98.543851	
8	0.5900	0.76	6.303237	4.847088	4.847088	93.696763	
9	0.5000	1.00	15.118531	8.815294	8.815294	84.881469	
10	0.4200	1.25	29.403460	14.284929	14.284929	70.596540	
11	0.3500	1.51	48.141448	18.737988	18.737988	51.858552	mode at 1.383056
12	0.3000	1.74	64.425938	16.284490	16.284490	35.574062	
13	0.2500	2.00	80.853963	16.428025	16.428025	19.146037	mode at 1.868483
14	0.2100	2.25	91.629734	10.775771	10.775771	8.370266	
15	0.1770	2.50	97.361756	5.732022	5.732022	2.638244	
16	0.1490	2.75	99.602903	2.241147	2.241147	0.397097	
17	0.1250	3.00	100.000000	0.397097	0.397097	0.000000	
18	0.1050	3.25	100.000000	0.000000	0.000000	0.000000	
19	0.0880	3.51	100.000000	0.000000	0.000000	0.000000	
20	0.0740	3.76	100.000000	0.000000	0.000000	0.000000	
21	0.0630	3.99	100.000000	0.000000	0.000000	0.000000	
22	0.0530	4.24	100.000000	0.000000	0.000000	0.000000	
23	0.0440	4.51	100.000000	0.000000	0.000000	0.000000	
24	0.0370	4.76	100.000000	0.000000	0.000000	0.000000	
25	0.0310	5.01	100.000000	0.000000	0.000000	0.000000	
26	0.0156	6.00	100.000000	0.000000	0.000000	0.000000	
27	0.0100	6.64	100.000000	0.000000	0.000000	0.000000	
28	0.0078	7.00	100.000000	0.000000	0.000000	0.000000	
29	0.0039	8.00	100.000000	0.000000	0.000000	0.000000	
30	0.0020	8.97	100.000000	0.000000	0.000000	0.000000	
31	0.0010	9.99	100.000000	0.000000	0.000000	0.000000	
32	0.0007	10.48	100.000000	0.000000	0.000000	0.000000	
33	0.0005	10.99	100.000000	0.000000	0.000000	0.000000	
34	0.0002	12.02	100.000000	0.000000	0.000000	0.000000	
35	0.0001	13.02	100.000000	0.000000	0.000000	0.000000	
36	0.0001	14.02	100.000000	0.000000	0.000000	0.000000	
37	0.0001	14.29	100.000000	0.000000	0.000000	0.000000	
		Sums:		100.00	100.00		

Column: 97
Sample ID: 2014-9-27nl

Folks' Graphic Statistics

	Mean (Mz)	Sorting (σI)	Skewness (SkI)	Kurtosis (KG)	Mean *mm*
phi	1.543	0.523	0.006	0.955	0.343

Grainsize Statistics
Percentiles

	phi	*mm*
5	0.69	0.620
16	1.02	0.495
25	1.17	0.443
50	1.54	0.344
75	1.91	0.267
84	2.07	0.238
95	2.40	0.190

Table II.97: *Results summary for sample 97: High intertidal zone, mid transect, Northern Ngarunui Beach. Sample collected on the 27th of September, 2014.*

Column: 98 **Density:** 2650
Volume: 0.010
Sample ID: 2014-9-27mh

Malvern data Phi	Malvern data Micron	Vol %	Equivalent Cum wt (g)
-1.00	2000.00	0	0.0
-0.75	1680.00	0	0.0
-0.50	1410.00	0	0.0
-0.25	1190.00	0	0.0
0.00	1000.00	0	0.0
0.25	840.00	0	0.0
0.49	710.00	0	0.0
0.76	590.00	0.164217	0.0
1.00	500.00	1.075905	0.3
1.25	420.00	3.830206	1.0
1.51	350.00	9.919925	2.6
1.74	300.00	18.249655	4.8
2.00	250.00	31.700596	8.4
2.25	210.00	46.991323	12.5
2.50	177.00	62.377706	16.5
2.75	149.00	76.275734	20.2
3.00	125.00	87.281871	23.1
3.25	105.00	94.475003	25.0
3.51	88.00	98.342136	26.1
3.76	74.00	99.808588	26.4
3.99	63.00	99.993231	26.5
4.24	53.00	100	26.5
4.51	44.00	100	26.5
4.76	37.00	100	26.5
5.01	31.00	100	26.5
6.00	15.60	100	26.5
6.64	10.00	100	26.5
7.00	7.80	100	26.5
8.00	3.90	100	26.5
8.97	2.00	100	26.5
9.99	0.98	100	26.5
10.48	0.70	100	26.5
10.99	0.49	100	26.5
12.02	0.24	100	26.5
13.02	0.12	100	26.5
14.02	0.06	100	26.5
14.29	0.05	100	26.5
		Total weight:	26.5

	mm	phi	Cum wt (g)	Int wt (g)	Int wt%	Cum % finer	Modes	
1	2.0000	-1.00	0.000000	0.000000	0.000000	100.000000		
2	1.6800	-0.75	0.000000	0.000000	0.000000	100.000000		
3	1.4100	-0.50	0.000000	0.000000	0.000000	100.000000		
4	1.1900	-0.25	0.000000	0.000000	0.000000	100.000000		
5	1.0000	0.00	0.000000	0.000000	0.000000	100.000000		8
6	0.8400	0.25	0.000000	0.000000	0.000000	100.000000		
7	0.7100	0.49	0.000000	0.000000	0.000000	100.000000		
8	0.5900	0.76	0.164217	0.164217	0.164217	99.835783		
9	0.5000	1.00	1.075905	0.911688	0.911688	98.924095		
10	0.4200	1.25	3.830206	2.754301	2.754301	96.169794		
11	0.3500	1.51	9.919925	6.089719	6.089719	90.080075		
12	0.3000	1.74	18.249655	8.329730	8.329730	81.750345		
13	0.2500	2.00	31.700596	13.450941	13.450941	68.299404		
14	0.2100	2.25	46.991323	15.290727	15.290727	53.008677		
15	0.1770	2.50	62.377706	15.386383	15.386383	37.622294	mode at 2.374859	
16	0.1490	2.75	76.275734	13.898028	13.898028	23.724266		
17	0.1250	3.00	87.281871	11.006137	11.006137	12.718129		
18	0.1050	3.25	94.475003	7.193132	7.193132	5.524997		
19	0.0880	3.51	98.342136	3.867133	3.867133	1.657864		
20	0.0740	3.76	99.808588	1.466452	1.466452	0.191412		
21	0.0630	3.99	99.993231	0.184643	0.184643	0.006769		
22	0.0530	4.24	100.000000	0.006769	0.006769	0.000000		
23	0.0440	4.51	100.000000	0.000000	0.000000	0.000000		
24	0.0370	4.76	100.000000	0.000000	0.000000	0.000000		
25	0.0310	5.01	100.000000	0.000000	0.000000	0.000000		
26	0.0156	6.00	100.000000	0.000000	0.000000	0.000000		
27	0.0100	6.64	100.000000	0.000000	0.000000	0.000000		
28	0.0078	7.00	100.000000	0.000000	0.000000	0.000000		
29	0.0039	8.00	100.000000	0.000000	0.000000	0.000000		
30	0.0020	8.97	100.000000	0.000000	0.000000	0.000000		
31	0.0010	9.99	100.000000	0.000000	0.000000	0.000000		
32	0.0007	10.48	100.000000	0.000000	0.000000	0.000000		
33	0.0005	10.99	100.000000	0.000000	0.000000	0.000000		
34	0.0002	12.02	100.000000	0.000000	0.000000	0.000000		
35	0.0001	13.02	100.000000	0.000000	0.000000	0.000000		
36	0.0001	14.02	100.000000	0.000000	0.000000	0.000000		
37	0.0001	14.29	100.000000	0.000000	0.000000	0.000000		
		Sums:		100.00	100.00			

Column: 98
Sample ID: 2014-9-27mh

Folks' Graphic Statistics

	Mean (Mz)	Sorting (σI)	Skewness (SkI)	Kurtosis (KG)	Mean *mm*
phi	2.300	0.613	-0.002	0.951	0.203

Grainsize Statistics
Percentiles

	phi	*mm*
5	1.30	0.406
16	1.68	0.313
25	1.87	0.274
50	2.30	0.203
75	2.72	0.151
84	2.92	0.132
95	3.29	0.103

Table II.98: *Results summary for sample 98: High intertidal zone, southern transect, Northern Ngarunui Beach. Sample collected on the 25th of October, 2014.*

Column: 99 **Density:** 2650
Volume: 0.010
Sample ID: 2014-10-25sh

Malvern data Phi	Malvern data Micron	Vol %	Equivalent Cum wt (g)
-1.00	2000.00	0	0.0
-0.75	1680.00	0	0.0
-0.50	1410.00	0	0.0
-0.25	1190.00	0	0.0
0.00	1000.00	0	0.0
0.25	840.00	0	0.0
0.49	710.00	0	0.0
0.76	590.00	0.297728	0.1
1.00	500.00	1.694139	0.4
1.25	420.00	5.483687	1.5
1.51	350.00	13.158021	3.5
1.74	300.00	23.011396	6.1
2.00	250.00	38.034136	10.1
2.25	210.00	54.133159	14.3
2.50	177.00	69.370965	18.4
2.75	149.00	82.203769	21.8
3.00	125.00	91.522955	24.3
3.25	105.00	96.946059	25.7
3.51	88.00	99.388995	26.3
3.76	74.00	99.987952	26.5
3.99	63.00	100	26.5
4.24	53.00	100	26.5
4.51	44.00	100	26.5
4.76	37.00	100	26.5
5.01	31.00	100	26.5
6.00	15.60	100	26.5
6.64	10.00	100	26.5
7.00	7.80	100	26.5
8.00	3.90	100	26.5
8.97	2.00	100	26.5
9.99	0.98	100	26.5
10.48	0.70	100	26.5
10.99	0.49	100	26.5
12.02	0.24	100	26.5
13.02	0.12	100	26.5
14.02	0.06	100	26.5
14.29	0.05	100	26.5
		Total weight:	26.5

	mm	phi	Cum wt (g)	Int wt (g)	Int wt%	Cum % finer	Modes	
1	2.0000	-1.00	0.000000	0.000000	0.000000	100.000000		
2	1.6800	-0.75	0.000000	0.000000	0.000000	100.000000		
3	1.4100	-0.50	0.000000	0.000000	0.000000	100.000000		
4	1.1900	-0.25	0.000000	0.000000	0.000000	100.000000		
5	1.0000	0.00	0.000000	0.000000	0.000000	100.000000		8
6	0.8400	0.25	0.000000	0.000000	0.000000	100.000000		
7	0.7100	0.49	0.000000	0.000000	0.000000	100.000000		
8	0.5900	0.76	0.297728	0.297728	0.297728	99.702272		
9	0.5000	1.00	1.694139	1.396411	1.396411	98.305861		
10	0.4200	1.25	5.483687	3.789548	3.789548	94.516313		
11	0.3500	1.51	13.158021	7.674334	7.674334	86.841979		
12	0.3000	1.74	23.011396	9.853375	9.853375	76.988604		
13	0.2500	2.00	38.034136	15.022740	15.022740	61.965864		
14	0.2100	2.25	54.133159	16.099023	16.099023	45.866841	mode at 2.125769	
15	0.1770	2.50	69.370965	15.237806	15.237806	30.629035		
16	0.1490	2.75	82.203769	12.832804	12.832804	17.796231		
17	0.1250	3.00	91.522955	9.319186	9.319186	8.477045		
18	0.1050	3.25	96.946059	5.423104	5.423104	3.053941		
19	0.0880	3.51	99.388995	2.442936	2.442936	0.611005		
20	0.0740	3.76	99.987952	0.598957	0.598957	0.012048		
21	0.0630	3.99	100.000000	0.012048	0.012048	0.000000		
22	0.0530	4.24	100.000000	0.000000	0.000000	0.000000		
23	0.0440	4.51	100.000000	0.000000	0.000000	0.000000		
24	0.0370	4.76	100.000000	0.000000	0.000000	0.000000		
25	0.0310	5.01	100.000000	0.000000	0.000000	0.000000		
26	0.0156	6.00	100.000000	0.000000	0.000000	0.000000		
27	0.0100	6.64	100.000000	0.000000	0.000000	0.000000		
28	0.0078	7.00	100.000000	0.000000	0.000000	0.000000		
29	0.0039	8.00	100.000000	0.000000	0.000000	0.000000		
30	0.0020	8.97	100.000000	0.000000	0.000000	0.000000		
31	0.0010	9.99	100.000000	0.000000	0.000000	0.000000		
32	0.0007	10.48	100.000000	0.000000	0.000000	0.000000		
33	0.0005	10.99	100.000000	0.000000	0.000000	0.000000		
34	0.0002	12.02	100.000000	0.000000	0.000000	0.000000		
35	0.0001	13.02	100.000000	0.000000	0.000000	0.000000		
36	0.0001	14.02	100.000000	0.000000	0.000000	0.000000		
37	0.0001	14.29	100.000000	0.000000	0.000000	0.000000		
		Sums:		100.00	100.00			

Column: 99
Sample ID: 2014-10-25sh

Grainsize Statistics
Percentiles

	phi	*mm*
5	1.22	0.429
16	1.58	0.335
25	1.77	0.293
50	2.19	0.220
75	2.61	0.164
84	2.80	0.144
95	3.16	0.112

Folks' Graphic Statistics

	Mean (Mz)	Sorting (σI)	Skewness (SkI)	Kurtosis (KG)	Mean *mm*
phi	2.187	0.598	0.002	0.953	0.220

Table II.99: *Results summary for sample 99: Low intertidal zone, mid transect, Northern Ngarunui Beach. Sample collected on the 25th of October, 2014.*

Column: 100 **Density:** 2650
Volume: 0.010
Sample ID: 2014-10-25ml

Malvern data Phi	Malvern data Micron	Vol %	Equivalent Cum wt (g)
-1.00	2000.00	0	0.0
-0.75	1680.00	0	0.0
-0.50	1410.00	0.048822	0.0
-0.25	1190.00	1.120845	0.3
0.00	1000.00	4.673721	1.2
0.25	840.00	12.094527	3.2
0.49	710.00	23.378756	6.2
0.76	590.00	39.632311	10.5
1.00	500.00	55.626383	14.7
1.25	420.00	71.49117	18.9
1.51	350.00	84.757955	22.5
1.74	300.00	92.460921	24.5
2.00	250.00	97.62188	25.9
2.25	210.00	99.600338	26.4
2.50	177.00	100	26.5
2.75	149.00	100	26.5
3.00	125.00	100	26.5
3.25	105.00	100	26.5
3.51	88.00	100	26.5
3.76	74.00	100	26.5
3.99	63.00	100	26.5
4.24	53.00	100	26.5
4.51	44.00	100	26.5
4.76	37.00	100	26.5
5.01	31.00	100	26.5
6.00	15.60	100	26.5
6.64	10.00	100	26.5
7.00	7.80	100	26.5
8.00	3.90	100	26.5
8.97	2.00	100	26.5
9.99	0.98	100	26.5
10.48	0.70	100	26.5
10.99	0.49	100	26.5
12.02	0.24	100	26.5
13.02	0.12	100	26.5
14.02	0.06	100	26.5
14.29	0.05	100	26.5

Total weight: 26.5

	mm	phi	Cum wt (g)	Int wt (g)	Int wt%	Cum % finer	Modes	
1	2.0000	-1.00	0.000000	0.000000	0.000000	100.000000		
2	1.6800	-0.75	0.000000	0.000000	0.000000	100.000000		
3	1.4100	-0.50	0.048822	0.048822	0.048822	99.951178		
4	1.1900	-0.25	1.120845	1.072023	1.072023	98.879155		
5	1.0000	0.00	4.673721	3.552876	3.552876	95.326279		8
6	0.8400	0.25	12.094527	7.420806	7.420806	87.905473		
7	0.7100	0.49	23.378756	11.284229	11.284229	76.621244		
8	0.5900	0.76	39.632311	16.253555	16.253555	60.367689	mode at 0.627661	
9	0.5000	1.00	55.626383	15.994072	15.994072	44.373617		
10	0.4200	1.25	71.491170	15.864787	15.864787	28.508830		
11	0.3500	1.51	84.757955	13.266785	13.266785	15.242045		
12	0.3000	1.74	92.460921	7.702966	7.702966	7.539079		
13	0.2500	2.00	97.621880	5.160959	5.160959	2.378120		
14	0.2100	2.25	99.600338	1.978458	1.978458	0.399662		
15	0.1770	2.50	100.000000	0.399662	0.399662	0.000000		
16	0.1490	2.75	100.000000	0.000000	0.000000	0.000000		
17	0.1250	3.00	100.000000	0.000000	0.000000	0.000000		
18	0.1050	3.25	100.000000	0.000000	0.000000	0.000000		
19	0.0880	3.51	100.000000	0.000000	0.000000	0.000000		
20	0.0740	3.76	100.000000	0.000000	0.000000	0.000000		
21	0.0630	3.99	100.000000	0.000000	0.000000	0.000000		
22	0.0530	4.24	100.000000	0.000000	0.000000	0.000000		
23	0.0440	4.51	100.000000	0.000000	0.000000	0.000000		
24	0.0370	4.76	100.000000	0.000000	0.000000	0.000000		
25	0.0310	5.01	100.000000	0.000000	0.000000	0.000000		
26	0.0156	6.00	100.000000	0.000000	0.000000	0.000000		
27	0.0100	6.64	100.000000	0.000000	0.000000	0.000000		
28	0.0078	7.00	100.000000	0.000000	0.000000	0.000000		
29	0.0039	8.00	100.000000	0.000000	0.000000	0.000000		
30	0.0020	8.97	100.000000	0.000000	0.000000	0.000000		
31	0.0010	9.99	100.000000	0.000000	0.000000	0.000000		
32	0.0007	10.48	100.000000	0.000000	0.000000	0.000000		
33	0.0005	10.99	100.000000	0.000000	0.000000	0.000000		
34	0.0002	12.02	100.000000	0.000000	0.000000	0.000000		
35	0.0001	13.02	100.000000	0.000000	0.000000	0.000000		
36	0.0001	14.02	100.000000	0.000000	0.000000	0.000000		
37	0.0001	14.29	100.000000	0.000000	0.000000	0.000000		
		Sums:		100.00	100.00			

Column: 100
Sample ID: 2014-10-25ml

Folks' Graphic Statistics

	Mean (Mz)	Sorting (σI)	Skewness (SkI)	Kurtosis (KG)	Mean *mm*
phi	0.917	0.572	0.014	0.950	0.530

Grainsize Statistics
Percentiles

	phi	*mm*
5	0.01	0.992
16	0.34	0.793
25	0.52	0.697
50	0.92	0.530
75	1.32	0.400
84	1.50	0.354
95	1.87	0.274

Table II.100: *Results summary for sample 100: Mid intertidal zone, mid transect, Northern Ngarunui Beach. Sample collected on the 25th of October, 2014.*

Column: 101 **Density:** 2650
Volume: 0.010
Sample ID: 2014-10-25mm

Malvern data Phi	Malvern data Micron	Vol %	Equivalent Cum wt (g)
-1.00	2000.00	0	0.0
-0.75	1680.00	0	0.0
-0.50	1410.00	0	0.0
-0.25	1190.00	0	0.0
0.00	1000.00	0	0.0
0.25	840.00	0	0.0
0.49	710.00	0.341834	0.1
0.76	590.00	2.982662	0.8
1.00	500.00	9.156789	2.4
1.25	420.00	20.849856	5.5
1.51	350.00	38.248978	10.1
1.74	300.00	55.015359	14.6
2.00	250.00	73.641021	19.5
2.25	210.00	87.192679	23.1
2.50	177.00	95.271478	25.2
2.75	149.00	98.966658	26.2
3.00	125.00	99.924126	26.5
3.25	105.00	100	26.5
3.51	88.00	100	26.5
3.76	74.00	100	26.5
3.99	63.00	100	26.5
4.24	53.00	100	26.5
4.51	44.00	100	26.5
4.76	37.00	100	26.5
5.01	31.00	100	26.5
6.00	15.60	100	26.5
6.64	10.00	100	26.5
7.00	7.80	100	26.5
8.00	3.90	100	26.5
8.97	2.00	100	26.5
9.99	0.98	100	26.5
10.48	0.70	100	26.5
10.99	0.49	100	26.5
12.02	0.24	100	26.5
13.02	0.12	100	26.5
14.02	0.06	100	26.5
14.29	0.05	100	26.5

Total weight: 26.5

	mm	phi	Cum wt (g)	Int wt (g)	Int wt%	Cum % finer	Modes	
1	2.0000	-1.00	0.000000	0.000000	0.000000	100.000000		
2	1.6800	-0.75	0.000000	0.000000	0.000000	100.000000		
3	1.4100	-0.50	0.000000	0.000000	0.000000	100.000000		
4	1.1900	-0.25	0.000000	0.000000	0.000000	100.000000		
5	1.0000	0.00	0.000000	0.000000	0.000000	100.000000		8
6	0.8400	0.25	0.000000	0.000000	0.000000	100.000000		
7	0.7100	0.49	0.341834	0.341834	0.341834	99.658166		
8	0.5900	0.76	2.982662	2.640828	2.640828	97.017338		
9	0.5000	1.00	9.156789	6.174127	6.174127	90.843211		
10	0.4200	1.25	20.849856	11.693067	11.693067	79.150144		
11	0.3500	1.51	38.248978	17.399122	17.399122	61.751022	mode at 1.383056	
12	0.3000	1.74	55.015359	16.766381	16.766381	44.984641		
13	0.2500	2.00	73.641021	18.625662	18.625662	26.358979	mode at 1.868483	
14	0.2100	2.25	87.192679	13.551658	13.551658	12.807321		
15	0.1770	2.50	95.271478	8.078799	8.078799	4.728522		
16	0.1490	2.75	98.966658	3.695180	3.695180	1.033342		
17	0.1250	3.00	99.924126	0.957468	0.957468	0.075874		
18	0.1050	3.25	100.000000	0.075874	0.075874	0.000000		
19	0.0880	3.51	100.000000	0.000000	0.000000	0.000000		
20	0.0740	3.76	100.000000	0.000000	0.000000	0.000000		
21	0.0630	3.99	100.000000	0.000000	0.000000	0.000000		
22	0.0530	4.24	100.000000	0.000000	0.000000	0.000000		
23	0.0440	4.51	100.000000	0.000000	0.000000	0.000000		
24	0.0370	4.76	100.000000	0.000000	0.000000	0.000000		
25	0.0310	5.01	100.000000	0.000000	0.000000	0.000000		
26	0.0156	6.00	100.000000	0.000000	0.000000	0.000000		
27	0.0100	6.64	100.000000	0.000000	0.000000	0.000000		
28	0.0078	7.00	100.000000	0.000000	0.000000	0.000000		
29	0.0039	8.00	100.000000	0.000000	0.000000	0.000000		
30	0.0020	8.97	100.000000	0.000000	0.000000	0.000000		
31	0.0010	9.99	100.000000	0.000000	0.000000	0.000000		
32	0.0007	10.48	100.000000	0.000000	0.000000	0.000000		
33	0.0005	10.99	100.000000	0.000000	0.000000	0.000000		
34	0.0002	12.02	100.000000	0.000000	0.000000	0.000000		
35	0.0001	13.02	100.000000	0.000000	0.000000	0.000000		
36	0.0001	14.02	100.000000	0.000000	0.000000	0.000000		
37	0.0001	14.29	100.000000	0.000000	0.000000	0.000000		
		Sums:		100.00	100.00			

Grainsize Statistics
Percentiles

	phi	*mm*
5	0.84	0.559
16	1.15	0.451
25	1.31	0.402
50	1.67	0.314
75	2.03	0.246
84	2.19	0.219
95	2.49	0.178

Column: 101
Sample ID: 2014-10-25mm

Folks' Graphic Statistics

	Mean (Mz)	Sorting (σI)	Skewness (SkI)	Kurtosis (KG)	Mean *mm*
phi	1.670	0.511	-0.004	0.952	0.314

Table II.101: *Results summary for sample 101: Low intertidal zone, northern transect, Northern Ngarunui Beach. Sample collected on the 25th of October, 2014.*

Column: 102 **Density:** 2650
Volume: 0.010
Sample ID: 2014-10-25nl

Malvern data Phi	Malvern data Micron	Vol %	Equivalent Cum wt (g)
-1.00	2000.00	0	0.0
-0.75	1680.00	0	0.0
-0.50	1410.00	0	0.0
-0.25	1190.00	0	0.0
0.00	1000.00	0	0.0
0.25	840.00	0	0.0
0.49	710.00	0.210757	0.1
0.76	590.00	2.4258	0.6
1.00	500.00	8.048633	2.1
1.25	420.00	19.147713	5.1
1.51	350.00	36.15933	9.6
1.74	300.00	52.930042	14.0
2.00	250.00	71.950268	19.1
2.25	210.00	86.092514	22.8
2.50	177.00	94.718605	25.1
2.75	149.00	98.781455	26.2
3.00	125.00	99.893695	26.5
3.25	105.00	100	26.5
3.51	88.00	100	26.5
3.76	74.00	100	26.5
3.99	63.00	100	26.5
4.24	53.00	100	26.5
4.51	44.00	100	26.5
4.76	37.00	100	26.5
5.01	31.00	100	26.5
6.00	15.60	100	26.5
6.64	10.00	100	26.5
7.00	7.80	100	26.5
8.00	3.90	100	26.5
8.97	2.00	100	26.5
9.99	0.98	100	26.5
10.48	0.70	100	26.5
10.99	0.49	100	26.5
12.02	0.24	100	26.5
13.02	0.12	100	26.5
14.02	0.06	100	26.5
14.29	0.05	100	26.5
		Total weight:	26.5

	mm	phi	Cum wt (g)	Int wt (g)	Int wt%	Cum % finer	Modes
1	2.0000	-1.00	0.000000	0.000000	0.000000	100.000000	
2	1.6800	-0.75	0.000000	0.000000	0.000000	100.000000	
3	1.4100	-0.50	0.000000	0.000000	0.000000	100.000000	
4	1.1900	-0.25	0.000000	0.000000	0.000000	100.000000	
5	1.0000	0.00	0.000000	0.000000	0.000000	100.000000	
6	0.8400	0.25	0.000000	0.000000	0.000000	100.000000	
7	0.7100	0.49	0.210757	0.210757	0.210757	99.789243	
8	0.5900	0.76	2.425800	2.215043	2.215043	97.574200	
9	0.5000	1.00	8.048633	5.622833	5.622833	91.951367	
10	0.4200	1.25	19.147713	11.099080	11.099080	80.852287	
11	0.3500	1.51	36.159330	17.011617	17.011617	63.840670	mode at 1.383056
12	0.3000	1.74	52.930042	16.770712	16.770712	47.069958	
13	0.2500	2.00	71.950268	19.020226	19.020226	28.049732	mode at 1.868483
14	0.2100	2.25	86.092514	14.142246	14.142246	13.907486	
15	0.1770	2.50	94.718605	8.626091	8.626091	5.281395	
16	0.1490	2.75	98.781455	4.062850	4.062850	1.218545	
17	0.1250	3.00	99.893695	1.112240	1.112240	0.106305	
18	0.1050	3.25	100.000000	0.106305	0.106305	0.000000	
19	0.0880	3.51	100.000000	0.000000	0.000000	0.000000	
20	0.0740	3.76	100.000000	0.000000	0.000000	0.000000	
21	0.0630	3.99	100.000000	0.000000	0.000000	0.000000	
22	0.0530	4.24	100.000000	0.000000	0.000000	0.000000	
23	0.0440	4.51	100.000000	0.000000	0.000000	0.000000	
24	0.0370	4.76	100.000000	0.000000	0.000000	0.000000	
25	0.0310	5.01	100.000000	0.000000	0.000000	0.000000	
26	0.0156	6.00	100.000000	0.000000	0.000000	0.000000	
27	0.0100	6.64	100.000000	0.000000	0.000000	0.000000	
28	0.0078	7.00	100.000000	0.000000	0.000000	0.000000	
29	0.0039	8.00	100.000000	0.000000	0.000000	0.000000	
30	0.0020	8.97	100.000000	0.000000	0.000000	0.000000	
31	0.0010	9.99	100.000000	0.000000	0.000000	0.000000	
32	0.0007	10.48	100.000000	0.000000	0.000000	0.000000	
33	0.0005	10.99	100.000000	0.000000	0.000000	0.000000	
34	0.0002	12.02	100.000000	0.000000	0.000000	0.000000	
35	0.0001	13.02	100.000000	0.000000	0.000000	0.000000	
36	0.0001	14.02	100.000000	0.000000	0.000000	0.000000	
37	0.0001	14.29	100.000000	0.000000	0.000000	0.000000	
		Sums:		100.00	100.00		

Column: 102
Sample ID: 2014-10-25nl

Folks' Graphic Statistics

	Mean (Mz)	Sorting (σI)	Skewness (SkI)	Kurtosis (KG)	Mean *mm*
phi	1.698	0.508	-0.004	0.947	0.308

Grainsize Statistics
Percentiles

	phi	*mm*
5	0.87	0.547
16	1.18	0.441
25	1.34	0.394
50	1.70	0.308
75	2.05	0.241
84	2.21	0.215
95	2.52	0.175

Table II.102: *Results summary for sample 102: High intertidal zone, northern transect, Northern Ngarunui Beach. Sample collected on the 25th of October, 2014.*

Column:	103	**Density:**	2650
		Volume:	0.010
Sample ID:	2014-10-25nh		

Malvern data Phi	**Malvern data** Micron	Vol %	Equivalent Cum wt (g)
-1.00	2000.00	0	0.0
-0.75	1680.00	0	0.0
-0.50	1410.00	0	0.0
-0.25	1190.00	0	0.0
0.00	1000.00	0	0.0
0.25	840.00	0	0.0
0.49	710.00	0	0.0
0.76	590.00	0.152865	0.0
1.00	500.00	1.42893	0.4
1.25	420.00	5.585096	1.5
1.51	350.00	14.87104	3.9
1.74	300.00	27.209316	7.2
2.00	250.00	45.784291	12.1
2.25	210.00	64.482749	17.1
2.50	177.00	80.255652	21.3
2.75	149.00	91.343156	24.2
3.00	125.00	97.431097	25.8
3.25	105.00	99.682825	26.4
3.51	88.00	100	26.5
3.76	74.00	100	26.5
3.99	63.00	100	26.5
4.24	53.00	100	26.5
4.51	44.00	100	26.5
4.76	37.00	100	26.5
5.01	31.00	100	26.5
6.00	15.60	100	26.5
6.64	10.00	100	26.5
7.00	7.80	100	26.5
8.00	3.90	100	26.5
8.97	2.00	100	26.5
9.99	0.98	100	26.5
10.48	0.70	100	26.5
10.99	0.49	100	26.5
12.02	0.24	100	26.5
13.02	0.12	100	26.5
14.02	0.06	100	26.5
14.29	0.05	100	26.5
		Total weight:	26.5

	mm	phi	Cum wt (g)	Int wt (g)	Int wt%	Cum % finer	Modes	
1	2.0000	-1.00	0.000000	0.000000	0.000000	100.000000		
2	1.6800	-0.75	0.000000	0.000000	0.000000	100.000000		
3	1.4100	-0.50	0.000000	0.000000	0.000000	100.000000		
4	1.1900	-0.25	0.000000	0.000000	0.000000	100.000000		
5	1.0000	0.00	0.000000	0.000000	0.000000	100.000000		8
6	0.8400	0.25	0.000000	0.000000	0.000000	100.000000		
7	0.7100	0.49	0.000000	0.000000	0.000000	100.000000		
8	0.5900	0.76	0.152865	0.152865	0.152865	99.847135		
9	0.5000	1.00	1.428930	1.276065	1.276065	98.571070		
10	0.4200	1.25	5.585096	4.156166	4.156166	94.414904		
11	0.3500	1.51	14.871040	9.285944	9.285944	85.128960		
12	0.3000	1.74	27.209316	12.338276	12.338276	72.790684		
13	0.2500	2.00	45.784291	18.574975	18.574975	54.215709		
14	0.2100	2.25	64.482749	18.698458	18.698458	35.517251	mode at 2.125769	
15	0.1770	2.50	80.255652	15.772903	15.772903	19.744348		
16	0.1490	2.75	91.343156	11.087504	11.087504	8.656844		
17	0.1250	3.00	97.431097	6.087941	6.087941	2.568903		
18	0.1050	3.25	99.682825	2.251728	2.251728	0.317175		
19	0.0880	3.51	100.000000	0.317175	0.317175	0.000000		
20	0.0740	3.76	100.000000	0.000000	0.000000	0.000000		
21	0.0630	3.99	100.000000	0.000000	0.000000	0.000000		
22	0.0530	4.24	100.000000	0.000000	0.000000	0.000000		
23	0.0440	4.51	100.000000	0.000000	0.000000	0.000000		
24	0.0370	4.76	100.000000	0.000000	0.000000	0.000000		
25	0.0310	5.01	100.000000	0.000000	0.000000	0.000000		
26	0.0156	6.00	100.000000	0.000000	0.000000	0.000000		
27	0.0100	6.64	100.000000	0.000000	0.000000	0.000000		
28	0.0078	7.00	100.000000	0.000000	0.000000	0.000000		
29	0.0039	8.00	100.000000	0.000000	0.000000	0.000000		
30	0.0020	8.97	100.000000	0.000000	0.000000	0.000000		
31	0.0010	9.99	100.000000	0.000000	0.000000	0.000000		
32	0.0007	10.48	100.000000	0.000000	0.000000	0.000000		
33	0.0005	10.99	100.000000	0.000000	0.000000	0.000000		
34	0.0002	12.02	100.000000	0.000000	0.000000	0.000000		
35	0.0001	13.02	100.000000	0.000000	0.000000	0.000000		
36	0.0001	14.02	100.000000	0.000000	0.000000	0.000000		
37	0.0001	14.29	100.000000	0.000000	0.000000	0.000000		
		Sums:		100.00	100.00			

Grainsize Statistics
Percentiles

	phi	*mm*
5	1.22	0.430
16	1.53	0.345
25	1.70	0.308
50	2.06	0.240
75	2.42	0.187
84	2.58	0.167
95	2.90	0.134

Column: 103
Sample ID: 2014-10-25nh

Folks' Graphic Statistics

	Mean (Mz)	Sorting (σI)	Skewness (SkI)	Kurtosis (KG)	Mean *mm*
phi	2.058	0.517	0.002	0.959	0.240

Table II.103: *Results summary for sample 103: Mid intertidal zone, northern transect, Northern Ngarunui Beach. Sample collected on the 25th of October, 2014.*

Column: 104 **Density:** 2650
Volume: 0.010
Sample ID: 2014-10-25nm

Malvern data Phi	Malvern data Micron	Vol %	Equivalent Cum wt (g)
-1.00	2000.00	0	0.0
-0.75	1680.00	0	0.0
-0.50	1410.00	0	0.0
-0.25	1190.00	0	0.0
0.00	1000.00	0.210117	0.1
0.25	840.00	1.293326	0.3
0.49	710.00	3.704428	1.0
0.76	590.00	8.714292	2.3
1.00	500.00	15.835758	4.2
1.25	420.00	26.289848	7.0
1.51	350.00	40.010794	10.6
1.74	300.00	52.895909	14.0
2.00	250.00	67.974314	18.0
2.25	210.00	80.503491	21.3
2.50	177.00	89.786415	23.8
2.75	149.00	95.766835	25.4
3.00	125.00	98.855807	26.2
3.25	105.00	99.905958	26.5
3.51	88.00	100	26.5
3.76	74.00	100	26.5
3.99	63.00	100	26.5
4.24	53.00	100	26.5
4.51	44.00	100	26.5
4.76	37.00	100	26.5
5.01	31.00	100	26.5
6.00	15.60	100	26.5
6.64	10.00	100	26.5
7.00	7.80	100	26.5
8.00	3.90	100	26.5
8.97	2.00	100	26.5
9.99	0.98	100	26.5
10.48	0.70	100	26.5
10.99	0.49	100	26.5
12.02	0.24	100	26.5
13.02	0.12	100	26.5
14.02	0.06	100	26.5
14.29	0.05	100	26.5
	Total weight:		26.5

	mm	phi	Cum wt (g)	Int wt (g)	Int wt%	Cum % finer	Modes	
1	2.0000	-1.00	0.000000	0.000000	0.000000	100.000000		
2	1.6800	-0.75	0.000000	0.000000	0.000000	100.000000		
3	1.4100	-0.50	0.000000	0.000000	0.000000	100.000000		
4	1.1900	-0.25	0.000000	0.000000	0.000000	100.000000		
5	1.0000	0.00	0.210117	0.210117	0.210117	99.789883		8
6	0.8400	0.25	1.293326	1.083209	1.083209	98.706674		
7	0.7100	0.49	3.704428	2.411102	2.411102	96.295572		
8	0.5900	0.76	8.714292	5.009864	5.009864	91.285708		
9	0.5000	1.00	15.835758	7.121466	7.121466	84.164242		
10	0.4200	1.25	26.289848	10.454090	10.454090	73.710152		
11	0.3500	1.51	40.010794	13.720946	13.720946	59.989206	mode at 1.383056	
12	0.3000	1.74	52.895909	12.885115	12.885115	47.104091		
13	0.2500	2.00	67.974314	15.078405	15.078405	32.025686	mode at 1.868483	
14	0.2100	2.25	80.503491	12.529177	12.529177	19.496509		
15	0.1770	2.50	89.786415	9.282924	9.282924	10.213585		
16	0.1490	2.75	95.766835	5.980420	5.980420	4.233165		
17	0.1250	3.00	98.855807	3.088972	3.088972	1.144193		
18	0.1050	3.25	99.905958	1.050151	1.050151	0.094042		
19	0.0880	3.51	100.000000	0.094042	0.094042	0.000000		
20	0.0740	3.76	100.000000	0.000000	0.000000	0.000000		
21	0.0630	3.99	100.000000	0.000000	0.000000	0.000000		
22	0.0530	4.24	100.000000	0.000000	0.000000	0.000000		
23	0.0440	4.51	100.000000	0.000000	0.000000	0.000000		
24	0.0370	4.76	100.000000	0.000000	0.000000	0.000000		
25	0.0310	5.01	100.000000	0.000000	0.000000	0.000000		
26	0.0156	6.00	100.000000	0.000000	0.000000	0.000000		
27	0.0100	6.64	100.000000	0.000000	0.000000	0.000000		
28	0.0078	7.00	100.000000	0.000000	0.000000	0.000000		
29	0.0039	8.00	100.000000	0.000000	0.000000	0.000000		
30	0.0020	8.97	100.000000	0.000000	0.000000	0.000000		
31	0.0010	9.99	100.000000	0.000000	0.000000	0.000000		
32	0.0007	10.48	100.000000	0.000000	0.000000	0.000000		
33	0.0005	10.99	100.000000	0.000000	0.000000	0.000000		
34	0.0002	12.02	100.000000	0.000000	0.000000	0.000000		
35	0.0001	13.02	100.000000	0.000000	0.000000	0.000000		
36	0.0001	14.02	100.000000	0.000000	0.000000	0.000000		
37	0.0001	14.29	100.000000	0.000000	0.000000	0.000000		
	Sums:			100.00	100.00			

Grainsize Statistics
Percentiles

	phi	*mm*
5	0.56	0.677
16	1.00	0.499
25	1.22	0.429
50	1.69	0.311
75	2.14	0.227
84	2.34	0.197
95	2.71	0.152

Column: 104
Sample ID: 2014-10-25nm

Folks' Graphic Statistics

	Mean (Mz)	Sorting (σI)	Skewness (SkI)	Kurtosis (KG)	Mean *mm*
phi	1.678	0.661	-0.032	0.958	0.312

Table II.104: *Results summary for sample 104: High intertidal zone, mid transect, Northern Ngarunui Beach. Sample collected on the 25th of October, 2014.*

Column: 105 **Density:** 2650 **Volume:** 0.010

Sample ID: 2014-10-25mh

Malvern data Phi	Malvern data Micron	Vol %	Equivalent Cum wt (g)
-1.00	2000.00	0	0.0
-0.75	1680.00	0	0.0
-0.50	1410.00	0	0.0
-0.25	1190.00	0	0.0
0.00	1000.00	0.009657	0.0
0.25	840.00	0.123307	0.0
0.49	710.00	0.461345	0.1
0.76	590.00	1.556478	0.4
1.00	500.00	3.794471	1.0
1.25	420.00	8.326454	2.2
1.51	350.00	16.33675	4.3
1.74	300.00	26.029038	6.9
2.00	250.00	40.442348	10.7
2.25	210.00	55.786549	14.8
2.50	177.00	70.365499	18.6
2.75	149.00	82.740563	21.9
3.00	125.00	91.797881	24.3
3.25	105.00	97.087629	25.7
3.51	88.00	99.453039	26.4
3.76	74.00	99.994544	26.5
3.99	63.00	100	26.5
4.24	53.00	100	26.5
4.51	44.00	100	26.5
4.76	37.00	100	26.5
5.01	31.00	100	26.5
6.00	15.60	100	26.5
6.64	10.00	100	26.5
7.00	7.80	100	26.5
8.00	3.90	100	26.5
8.97	2.00	100	26.5
9.99	0.98	100	26.5
10.48	0.70	100	26.5
10.99	0.49	100	26.5
12.02	0.24	100	26.5
13.02	0.12	100	26.5
14.02	0.06	100	26.5
14.29	0.05	100	26.5

Total weight: 26.5

	mm	phi	Cum wt (g)	Int wt (g)	Int wt%	Cum % finer	Modes
1	2.0000	-1.00	0.000000	0.000000	0.000000	100.000000	
2	1.6800	-0.75	0.000000	0.000000	0.000000	100.000000	
3	1.4100	-0.50	0.000000	0.000000	0.000000	100.000000	
4	1.1900	-0.25	0.000000	0.000000	0.000000	100.000000	
5	1.0000	0.00	0.009657	0.009657	0.009657	99.990343	8
6	0.8400	0.25	0.123307	0.113650	0.113650	99.876693	
7	0.7100	0.49	0.461345	0.338038	0.338038	99.538655	
8	0.5900	0.76	1.556478	1.095133	1.095133	98.443522	
9	0.5000	1.00	3.794471	2.237993	2.237993	96.205529	
10	0.4200	1.25	8.326454	4.531983	4.531983	91.673546	
11	0.3500	1.51	16.336750	8.010296	8.010296	83.663250	
12	0.3000	1.74	26.029038	9.692288	9.692288	73.970962	
13	0.2500	2.00	40.442348	14.413310	14.413310	59.557652	
14	0.2100	2.25	55.786549	15.344201	15.344201	44.213451	mode at 2.125769
15	0.1770	2.50	70.365499	14.578950	14.578950	29.634501	
16	0.1490	2.75	82.740563	12.375064	12.375064	17.259437	
17	0.1250	3.00	91.797881	9.057318	9.057318	8.202119	
18	0.1050	3.25	97.087629	5.289748	5.289748	2.912371	
19	0.0880	3.51	99.453039	2.365410	2.365410	0.546961	
20	0.0740	3.76	99.994544	0.541505	0.541505	0.005456	
21	0.0630	3.99	100.000000	0.005456	0.005456	0.000000	
22	0.0530	4.24	100.000000	0.000000	0.000000	0.000000	
23	0.0440	4.51	100.000000	0.000000	0.000000	0.000000	
24	0.0370	4.76	100.000000	0.000000	0.000000	0.000000	
25	0.0310	5.01	100.000000	0.000000	0.000000	0.000000	
26	0.0156	6.00	100.000000	0.000000	0.000000	0.000000	
27	0.0100	6.64	100.000000	0.000000	0.000000	0.000000	
28	0.0078	7.00	100.000000	0.000000	0.000000	0.000000	
29	0.0039	8.00	100.000000	0.000000	0.000000	0.000000	
30	0.0020	8.97	100.000000	0.000000	0.000000	0.000000	
31	0.0010	9.99	100.000000	0.000000	0.000000	0.000000	
32	0.0007	10.48	100.000000	0.000000	0.000000	0.000000	
33	0.0005	10.99	100.000000	0.000000	0.000000	0.000000	
34	0.0002	12.02	100.000000	0.000000	0.000000	0.000000	
35	0.0001	13.02	100.000000	0.000000	0.000000	0.000000	
36	0.0001	14.02	100.000000	0.000000	0.000000	0.000000	
37	0.0001	14.29	100.000000	0.000000	0.000000	0.000000	
		Sums:		100.00	100.00		

Column: 105

Sample ID: 2014-10-25mh

Folks' Graphic Statistics

	Mean (Mz)	Sorting (σI)	Skewness (SkI)	Kurtosis (KG)	Mean *mm*
phi	2.147	0.636	-0.034	0.974	0.226

Grainsize Statistics

Percentiles

	phi	*mm*
5	1.07	0.477
16	1.50	0.353
25	1.71	0.305
50	2.16	0.224
75	2.59	0.166
84	2.78	0.145
95	3.15	0.112

Table II.105: *Results summary for sample 105: Mid intertidal zone, southern transect, Northern Ngarunui Beach. Sample collected on the 25th of October, 2014.*

Column: 106 **Density:** 2650 **Volume:** 0.010

Sample ID: 2014-10-25sm

Malvern data Phi	Malvern data Micron	Vol %	Equivalent Cum wt (g)
-1.00	2000.00	0	0.0
-0.75	1680.00	0	0.0
-0.50	1410.00	0	0.0
-0.25	1190.00	0	0.0
0.00	1000.00	0	0.0
0.25	840.00	0	0.0
0.49	710.00	0.130138	0.0
0.76	590.00	1.612118	0.4
1.00	500.00	5.655151	1.5
1.25	420.00	14.267302	3.8
1.51	350.00	28.625157	7.6
1.74	300.00	44.03272	11.7
2.00	250.00	63.228688	16.8
2.25	210.00	79.231591	21.0
2.50	177.00	90.431886	24.0
2.75	149.00	96.812394	25.7
3.00	125.00	99.466035	26.4
3.25	105.00	99.976785	26.5
3.51	88.00	100	26.5
3.76	74.00	100	26.5
3.99	63.00	100	26.5
4.24	53.00	100	26.5
4.51	44.00	100	26.5
4.76	37.00	100	26.5
5.01	31.00	100	26.5
6.00	15.60	100	26.5
6.64	10.00	100	26.5
7.00	7.80	100	26.5
8.00	3.90	100	26.5
8.97	2.00	100	26.5
9.99	0.98	100	26.5
10.48	0.70	100	26.5
10.99	0.49	100	26.5
12.02	0.24	100	26.5
13.02	0.12	100	26.5
14.02	0.06	100	26.5
14.29	0.05	100	26.5
		Total weight:	26.5

	mm	phi	Cum wt (g)	Int wt (g)	Int wt%	Cum % finer	Modes	
1	2.0000	-1.00	0.000000	0.000000	0.000000	100.000000		
2	1.6800	-0.75	0.000000	0.000000	0.000000	100.000000		
3	1.4100	-0.50	0.000000	0.000000	0.000000	100.000000		
4	1.1900	-0.25	0.000000	0.000000	0.000000	100.000000		
5	1.0000	0.00	0.000000	0.000000	0.000000	100.000000		8
6	0.8400	0.25	0.000000	0.000000	0.000000	100.000000		
7	0.7100	0.49	0.130138	0.130138	0.130138	99.869862		
8	0.5900	0.76	1.612118	1.481980	1.481980	98.387882		
9	0.5000	1.00	5.655151	4.043033	4.043033	94.344849		
10	0.4200	1.25	14.267302	8.612151	8.612151	85.732698		
11	0.3500	1.51	28.625157	14.357855	14.357855	71.374843		
12	0.3000	1.74	44.032720	15.407563	15.407563	55.967280		
13	0.2500	2.00	63.228688	19.195968	19.195968	36.771312	mode at 1.868483	
14	0.2100	2.25	79.231591	16.002903	16.002903	20.768409		
15	0.1770	2.50	90.431886	11.200295	11.200295	9.568114		
16	0.1490	2.75	96.812394	6.380508	6.380508	3.187606		
17	0.1250	3.00	99.466035	2.653641	2.653641	0.533965		
18	0.1050	3.25	99.976785	0.510750	0.510750	0.023215		
19	0.0880	3.51	100.000000	0.023215	0.023215	0.000000		
20	0.0740	3.76	100.000000	0.000000	0.000000	0.000000		
21	0.0630	3.99	100.000000	0.000000	0.000000	0.000000		
22	0.0530	4.24	100.000000	0.000000	0.000000	0.000000		
23	0.0440	4.51	100.000000	0.000000	0.000000	0.000000		
24	0.0370	4.76	100.000000	0.000000	0.000000	0.000000		
25	0.0310	5.01	100.000000	0.000000	0.000000	0.000000		
26	0.0156	6.00	100.000000	0.000000	0.000000	0.000000		
27	0.0100	6.64	100.000000	0.000000	0.000000	0.000000		
28	0.0078	7.00	100.000000	0.000000	0.000000	0.000000		
29	0.0039	8.00	100.000000	0.000000	0.000000	0.000000		
30	0.0020	8.97	100.000000	0.000000	0.000000	0.000000		
31	0.0010	9.99	100.000000	0.000000	0.000000	0.000000		
32	0.0007	10.48	100.000000	0.000000	0.000000	0.000000		
33	0.0005	10.99	100.000000	0.000000	0.000000	0.000000		
34	0.0002	12.02	100.000000	0.000000	0.000000	0.000000		
35	0.0001	13.02	100.000000	0.000000	0.000000	0.000000		
36	0.0001	14.02	100.000000	0.000000	0.000000	0.000000		
37	0.0001	14.29	100.000000	0.000000	0.000000	0.000000		
		Sums:		100.00	100.00			

Grainsize Statistics
Percentiles

	phi	*mm*
5	0.96	0.514
16	1.28	0.411
25	1.45	0.366
50	1.82	0.283
75	2.19	0.220
84	2.36	0.195
95	2.68	0.156

Column: 106
Sample ID: 2014-10-25sm

Folks' Graphic Statistics

	Mean (Mz)	Sorting (σI)	Skewness (SkI)	Kurtosis (KG)	Mean *mm*
phi	1.820	0.528	0.001	0.954	0.283

Table II.106: *Results summary for sample 106: Mid intertidal zone, mid transect, Northern Ngarunui Beach. Sample collected on the 25th of October, 2014.*

Column: 107 **Density:** 2650
Volume: 0.010
Sample ID: 2014-10-25mm*

Malvern data Phi	Malvern data Micron	Vol %	Equivalent Cum wt (g)
-1.00	2000.00	0	0.0
-0.75	1680.00	0	0.0
-0.50	1410.00	0	0.0
-0.25	1190.00	0	0.0
0.00	1000.00	0	0.0
0.25	840.00	0	0.0
0.49	710.00	0.245069	0.1
0.76	590.00	2.794315	0.7
1.00	500.00	9.075305	2.4
1.25	420.00	21.103642	5.6
1.51	350.00	38.972209	10.3
1.74	300.00	56.056387	14.9
2.00	250.00	74.787998	19.8
2.25	210.00	88.141647	23.4
2.50	177.00	95.865655	25.4
2.75	149.00	99.216516	26.3
3.00	125.00	99.974311	26.5
3.25	105.00	100	26.5
3.51	88.00	100	26.5
3.76	74.00	100	26.5
3.99	63.00	100	26.5
4.24	53.00	100	26.5
4.51	44.00	100	26.5
4.76	37.00	100	26.5
5.01	31.00	100	26.5
6.00	15.60	100	26.5
6.64	10.00	100	26.5
7.00	7.80	100	26.5
8.00	3.90	100	26.5
8.97	2.00	100	26.5
9.99	0.98	100	26.5
10.48	0.70	100	26.5
10.99	0.49	100	26.5
12.02	0.24	100	26.5
13.02	0.12	100	26.5
14.02	0.06	100	26.5
14.29	0.05	100	26.5
		Total weight:	26.5

	mm	phi	Cum wt (g)	Int wt (g)	Int wt%	Cum % finer	Modes
1	2.0000	-1.00	0.000000	0.000000	0.000000	100.000000	
2	1.6800	-0.75	0.000000	0.000000	0.000000	100.000000	
3	1.4100	-0.50	0.000000	0.000000	0.000000	100.000000	
4	1.1900	-0.25	0.000000	0.000000	0.000000	100.000000	
5	1.0000	0.00	0.000000	0.000000	0.000000	100.000000	8
6	0.8400	0.25	0.000000	0.000000	0.000000	100.000000	
7	0.7100	0.49	0.245069	0.245069	0.245069	99.754931	
8	0.5900	0.76	2.794315	2.549246	2.549246	97.205685	
9	0.5000	1.00	9.075305	6.280990	6.280990	90.924695	
10	0.4200	1.25	21.103642	12.028337	12.028337	78.896358	
11	0.3500	1.51	38.972209	17.868567	17.868567	61.027791	mode at 1.383056
12	0.3000	1.74	56.056387	17.084178	17.084178	43.943613	
13	0.2500	2.00	74.787998	18.731611	18.731611	25.212002	mode at 1.868483
14	0.2100	2.25	88.141647	13.353649	13.353649	11.858353	
15	0.1770	2.50	95.865655	7.724008	7.724008	4.134345	
16	0.1490	2.75	99.216516	3.350861	3.350861	0.783484	
17	0.1250	3.00	99.974311	0.757795	0.757795	0.025689	
18	0.1050	3.25	100.000000	0.025689	0.025689	0.000000	
19	0.0880	3.51	100.000000	0.000000	0.000000	0.000000	
20	0.0740	3.76	100.000000	0.000000	0.000000	0.000000	
21	0.0630	3.99	100.000000	0.000000	0.000000	0.000000	
22	0.0530	4.24	100.000000	0.000000	0.000000	0.000000	
23	0.0440	4.51	100.000000	0.000000	0.000000	0.000000	
24	0.0370	4.76	100.000000	0.000000	0.000000	0.000000	
25	0.0310	5.01	100.000000	0.000000	0.000000	0.000000	
26	0.0156	6.00	100.000000	0.000000	0.000000	0.000000	
27	0.0100	6.64	100.000000	0.000000	0.000000	0.000000	
28	0.0078	7.00	100.000000	0.000000	0.000000	0.000000	
29	0.0039	8.00	100.000000	0.000000	0.000000	0.000000	
30	0.0020	8.97	100.000000	0.000000	0.000000	0.000000	
31	0.0010	9.99	100.000000	0.000000	0.000000	0.000000	
32	0.0007	10.48	100.000000	0.000000	0.000000	0.000000	
33	0.0005	10.99	100.000000	0.000000	0.000000	0.000000	
34	0.0002	12.02	100.000000	0.000000	0.000000	0.000000	
35	0.0001	13.02	100.000000	0.000000	0.000000	0.000000	
36	0.0001	14.02	100.000000	0.000000	0.000000	0.000000	
37	0.0001	14.29	100.000000	0.000000	0.000000	0.000000	
		Sums:		100.00	100.00		

Column: 107
Sample ID: 2014-10-25mm*

Folks' Graphic Statistics

	Mean (Mz)	Sorting (σI)	Skewness (SkI)	Kurtosis (KG)	Mean ***mm***
phi	1.659	0.503	0.001	0.958	0.317

Grainsize Statistics
Percentiles

	phi	***mm***
5	0.85	0.557
16	1.14	0.452
25	1.31	0.404
50	1.66	0.317
75	2.00	0.249
84	2.17	0.222
95	2.47	0.180

Table II.107: *Results summary for sample 107: High intertidal zone, western transect, Moonlight Bay. Sample collected on the 22nd of September, 2014.*

Column: 108 **Density:** 2650
Volume: 0.010
Sample ID: 2014-9-22wh

Malvern data Phi	Malvern data Micron	Vol %	Equivalent Cum wt (g)
-1.00	2000.00	0	0.0
-0.75	1680.00	0	0.0
-0.50	1410.00	0.023889	0.0
-0.25	1190.00	0.791053	0.2
0.00	1000.00	3.480228	0.9
0.25	840.00	8.861936	2.3
0.49	710.00	16.971875	4.5
0.76	590.00	29.076221	7.7
1.00	500.00	41.984921	11.1
1.25	420.00	56.482908	15.0
1.51	350.00	70.977654	18.8
1.74	300.00	81.493787	21.6
2.00	250.00	90.898266	24.1
2.25	210.00	96.541503	25.6
2.50	177.00	99.270107	26.3
2.75	149.00	100	26.5
3.00	125.00	100	26.5
3.25	105.00	100	26.5
3.51	88.00	100	26.5
3.76	74.00	100	26.5
3.99	63.00	100	26.5
4.24	53.00	100	26.5
4.51	44.00	100	26.5
4.76	37.00	100	26.5
5.01	31.00	100	26.5
6.00	15.60	100	26.5
6.64	10.00	100	26.5
7.00	7.80	100	26.5
8.00	3.90	100	26.5
8.97	2.00	100	26.5
9.99	0.98	100	26.5
10.48	0.70	100	26.5
10.99	0.49	100	26.5
12.02	0.24	100	26.5
13.02	0.12	100	26.5
14.02	0.06	100	26.5
14.29	0.05	100	26.5
		Total weight:	26.5

	mm	phi	Cum wt (g)	Int wt (g)	Int wt%	Cum % finer	Modes
1	2.0000	-1.00	0.000000	0.000000	0.000000	100.000000	
2	1.6800	-0.75	0.000000	0.000000	0.000000	100.000000	
3	1.4100	-0.50	0.023889	0.023889	0.023889	99.976111	
4	1.1900	-0.25	0.791053	0.767164	0.767164	99.208947	
5	1.0000	0.00	3.480228	2.689175	2.689175	96.519772	
6	0.8400	0.25	8.861936	5.381708	5.381708	91.138064	
7	0.7100	0.49	16.971875	8.109939	8.109939	83.028125	
8	0.5900	0.76	29.076221	12.104346	12.104346	70.923779	
9	0.5000	1.00	41.984921	12.908700	12.908700	58.015079	
10	0.4200	1.25	56.482908	14.497987	14.497987	43.517092	mode at 1.125769
11	0.3500	1.51	70.977654	14.494746	14.494746	29.022346	
12	0.3000	1.74	81.493787	10.516133	10.516133	18.506213	
13	0.2500	2.00	90.898266	9.404479	9.404479	9.101734	
14	0.2100	2.25	96.541503	5.643237	5.643237	3.458497	
15	0.1770	2.50	99.270107	2.728604	2.728604	0.729893	
16	0.1490	2.75	100.000000	0.729893	0.729893	0.000000	
17	0.1250	3.00	100.000000	0.000000	0.000000	0.000000	
18	0.1050	3.25	100.000000	0.000000	0.000000	0.000000	
19	0.0880	3.51	100.000000	0.000000	0.000000	0.000000	
20	0.0740	3.76	100.000000	0.000000	0.000000	0.000000	
21	0.0630	3.99	100.000000	0.000000	0.000000	0.000000	
22	0.0530	4.24	100.000000	0.000000	0.000000	0.000000	
23	0.0440	4.51	100.000000	0.000000	0.000000	0.000000	
24	0.0370	4.76	100.000000	0.000000	0.000000	0.000000	
25	0.0310	5.01	100.000000	0.000000	0.000000	0.000000	
26	0.0156	6.00	100.000000	0.000000	0.000000	0.000000	
27	0.0100	6.64	100.000000	0.000000	0.000000	0.000000	
28	0.0078	7.00	100.000000	0.000000	0.000000	0.000000	
29	0.0039	8.00	100.000000	0.000000	0.000000	0.000000	
30	0.0020	8.97	100.000000	0.000000	0.000000	0.000000	
31	0.0010	9.99	100.000000	0.000000	0.000000	0.000000	
32	0.0007	10.48	100.000000	0.000000	0.000000	0.000000	
33	0.0005	10.99	100.000000	0.000000	0.000000	0.000000	
34	0.0002	12.02	100.000000	0.000000	0.000000	0.000000	
35	0.0001	13.02	100.000000	0.000000	0.000000	0.000000	
36	0.0001	14.02	100.000000	0.000000	0.000000	0.000000	
37	0.0001	14.29	100.000000	0.000000	0.000000	0.000000	
		Sums:		100.00	100.00		

Column: 108
Sample ID: 2014-9-22wh

Folks' Graphic Statistics

	Mean (Mz)	Sorting (σI)	Skewness (SkI)	Kurtosis (KG)	Mean *mm*
phi	1.137	0.655	-0.008	0.932	0.455

Grainsize Statistics
Percentiles

	phi	*mm*
5	0.07	0.952
16	0.47	0.724
25	0.67	0.628
50	1.14	0.454
75	1.60	0.330
84	1.81	0.286
95	2.18	0.220

Table II.108: *Results summary for sample 108: High intertidal zone, eastern transect, Moonlight Bay. Sample collected on the 22nd of September, 2014.*

Column: 109 **Density:** 2650
Volume: 0.010
Sample ID: 2014-9-22eh

Malvern data Phi	Malvern data Micron	Vol %	Equivalent Cum wt (g)
-1.00	2000.00	0	0.0
-0.75	1680.00	1.623864	0.4
-0.50	1410.00	5.236563	1.4
-0.25	1190.00	10.783567	2.9
0.00	1000.00	18.547	4.9
0.25	840.00	28.024188	7.4
0.49	710.00	38.1234	10.1
0.76	590.00	49.495454	13.1
1.00	500.00	59.254984	15.7
1.25	420.00	68.649574	18.2
1.51	350.00	77.172253	20.5
1.74	300.00	83.162134	22.0
2.00	250.00	88.684192	23.5
2.25	210.00	92.371531	24.5
2.50	177.00	94.610987	25.1
2.75	149.00	95.765754	25.4
3.00	125.00	96.178453	25.5
3.25	105.00	96.220577	25.5
3.51	88.00	96.220577	25.5
3.76	74.00	96.220577	25.5
3.99	63.00	96.296719	25.5
4.24	53.00	96.482306	25.6
4.51	44.00	96.734928	25.6
4.76	37.00	96.974335	25.7
5.01	31.00	97.199223	25.8
6.00	15.60	97.980284	26.0
6.64	10.00	98.55281	26.1
7.00	7.80	98.869171	26.2
8.00	3.90	99.580626	26.4
8.97	2.00	99.983212	26.5
9.99	0.98	100	26.5
10.48	0.70	100	26.5
10.99	0.49	100	26.5
12.02	0.24	100	26.5
13.02	0.12	100	26.5
14.02	0.06	100	26.5
14.29	0.05	100	26.5

Total weight: 26.5

	mm	phi	Cum wt (g)	Int wt (g)	Int wt%	Cum % finer	Modes
1	2.0000	-1.00	0.000000	0.000000	0.000000	100.000000	
2	1.6800	-0.75	1.623864	1.623864	1.623864	98.376136	
3	1.4100	-0.50	5.236563	3.612699	3.612699	94.763437	
4	1.1900	-0.25	10.783567	5.547004	5.547004	89.216433	
5	1.0000	0.00	18.547000	7.763433	7.763433	81.453000	8
6	0.8400	0.25	28.024188	9.477188	9.477188	71.975812	
7	0.7100	0.49	38.123400	10.099212	10.099212	61.876600	
8	0.5900	0.76	49.495454	11.372054	11.372054	50.504546	mode at 0.627661
9	0.5000	1.00	59.254984	9.759530	9.759530	40.745016	
10	0.4200	1.25	68.649574	9.394590	9.394590	31.350426	
11	0.3500	1.51	77.172253	8.522679	8.522679	22.827747	
12	0.3000	1.74	83.162134	5.989881	5.989881	16.837866	
13	0.2500	2.00	88.684192	5.522058	5.522058	11.315808	
14	0.2100	2.25	92.371531	3.687339	3.687339	7.628469	
15	0.1770	2.50	94.610987	2.239456	2.239456	5.389013	
16	0.1490	2.75	95.765754	1.154767	1.154767	4.234246	
17	0.1250	3.00	96.178453	0.412699	0.412699	3.821547	
18	0.1050	3.25	96.220577	0.042124	0.042124	3.779423	
19	0.0880	3.51	96.220577	0.000000	0.000000	3.779423	
20	0.0740	3.76	96.220577	0.000000	0.000000	3.779423	
21	0.0630	3.99	96.296719	0.076142	0.076142	3.703281	
22	0.0530	4.24	96.482306	0.185587	0.185587	3.517694	
23	0.0440	4.51	96.734928	0.252622	0.252622	3.265072	mode at 4.372108
24	0.0370	4.76	96.974335	0.239407	0.239407	3.025665	
25	0.0310	5.01	97.199223	0.224888	0.224888	2.800777	
26	0.0156	6.00	97.980284	0.781061	0.781061	2.019716	mode at 5.506949
27	0.0100	6.64	98.552810	0.572526	0.572526	1.447190	
28	0.0078	7.00	98.869171	0.316361	0.316361	1.130829	
29	0.0039	8.00	99.580626	0.711455	0.711455	0.419374	mode at 7.50231
30	0.0020	8.97	99.983212	0.402586	0.402586	0.016788	
31	0.0010	9.99	100.000000	0.016788	0.016788	0.000000	
32	0.0007	10.48	100.000000	0.000000	0.000000	0.000000	
33	0.0005	10.99	100.000000	0.000000	0.000000	0.000000	
34	0.0002	12.02	100.000000	0.000000	0.000000	0.000000	
35	0.0001	13.02	100.000000	0.000000	0.000000	0.000000	
36	0.0001	14.02	100.000000	0.000000	0.000000	0.000000	
37	0.0001	14.29	100.000000	0.000000	0.000000	0.000000	
		Sums:		100.00	100.00		

Column: 109
Sample ID: 2014-9-22eh

Folks' Graphic Statistics

	Mean (Mz)	Sorting (σI)	Skewness (SkI)	Kurtosis (KG)	Mean *mm*
phi	0.823	0.934	0.124	0.994	0.565

Grainsize Statistics
Percentiles

	phi	*mm*
5	-0.51	1.426
16	-0.08	1.059
25	0.17	0.888
50	0.77	0.585
75	1.45	0.367
84	1.78	0.292
95	2.58	0.167

Table II.109: *Results summary for sample 109: Mid intertidal zone, western transect, Moonlight Bay. Sample collected on the 22nd of September, 2014.*

Column: 110 **Density:** 2650
Volume: 0.010
Sample ID: 2014-9-22wm

Malvern data Phi	Malvern data Micron	Vol %	Equivalent Cum wt (g)
-1.00	2000.00	0	0.0
-0.75	1680.00	0.048975	0.0
-0.50	1410.00	0.165003	0.0
-0.25	1190.00	0.342757	0.1
0.00	1000.00	0.564276	0.1
0.25	840.00	0.860479	0.2
0.49	710.00	1.39647	0.4
0.76	590.00	2.83764	0.8
1.00	500.00	5.719238	1.5
1.25	420.00	11.443208	3.0
1.51	350.00	21.124394	5.6
1.74	300.00	32.078691	8.5
2.00	250.00	46.884582	12.4
2.25	210.00	60.705315	16.1
2.50	177.00	71.848169	19.0
2.75	149.00	79.48981	21.1
3.00	125.00	83.624165	22.2
3.25	105.00	85.054325	22.5
3.51	88.00	85.198588	22.6
3.76	74.00	85.198588	22.6
3.99	63.00	85.198588	22.6
4.24	53.00	85.198588	22.6
4.51	44.00	85.537033	22.7
4.76	37.00	86.158474	22.8
5.01	31.00	86.939986	23.0
6.00	15.60	89.843306	23.8
6.64	10.00	91.808668	24.3
7.00	7.80	93.028788	24.7
8.00	3.90	96.114821	25.5
8.97	2.00	97.923687	25.9
9.99	0.98	98.891723	26.2
10.48	0.70	99.235109	26.3
10.99	0.49	99.601906	26.4
12.02	0.24	100	26.5
13.02	0.12	100	26.5
14.02	0.06	100	26.5
14.29	0.05	100	26.5

Total weight: 26.5

	mm	phi	Cum wt (g)	Int wt (g)	Int wt%	Cum % finer	Modes
1	2.0000	-1.00	0.000000	0.000000	0.000000	100.000000	
2	1.6800	-0.75	0.048975	0.048975	0.048975	99.951025	
3	1.4100	-0.50	0.165003	0.116028	0.116028	99.834997	
4	1.1900	-0.25	0.342757	0.177754	0.177754	99.657243	
5	1.0000	0.00	0.564276	0.221519	0.221519	99.435724	8
6	0.8400	0.25	0.860479	0.296203	0.296203	99.139521	
7	0.7100	0.49	1.396470	0.535991	0.535991	98.603530	
8	0.5900	0.76	2.837640	1.441170	1.441170	97.162360	
9	0.5000	1.00	5.719238	2.881598	2.881598	94.280762	
10	0.4200	1.25	11.443208	5.723970	5.723970	88.556792	
11	0.3500	1.51	21.124394	9.681186	9.681186	78.875606	
12	0.3000	1.74	32.078691	10.954297	10.954297	67.921309	
13	0.2500	2.00	46.884582	14.805891	14.805891	53.115418	mode at 1.868483
14	0.2100	2.25	60.705315	13.820733	13.820733	39.294685	
15	0.1770	2.50	71.848169	11.142854	11.142854	28.151831	
16	0.1490	2.75	79.489810	7.641641	7.641641	20.510190	
17	0.1250	3.00	83.624165	4.134355	4.134355	16.375835	
18	0.1050	3.25	85.054325	1.430160	1.430160	14.945675	
19	0.0880	3.51	85.198588	0.144263	0.144263	14.801412	
20	0.0740	3.76	85.198588	0.000000	0.000000	14.801412	
21	0.0630	3.99	85.198588	0.000000	0.000000	14.801412	
22	0.0530	4.24	85.198588	0.000000	0.000000	14.801412	
23	0.0440	4.51	85.537033	0.338445	0.338445	14.462967	
24	0.0370	4.76	86.158474	0.621441	0.621441	13.841526	
25	0.0310	5.01	86.939986	0.781512	0.781512	13.060014	
26	0.0156	6.00	89.843306	2.903320	2.903320	10.156694	mode at 5.506949
27	0.0100	6.64	91.808668	1.965362	1.965362	8.191332	
28	0.0078	7.00	93.028788	1.220120	1.220120	6.971212	
29	0.0039	8.00	96.114821	3.086033	3.086033	3.885179	mode at 7.50231
30	0.0020	8.97	97.923687	1.808866	1.808866	2.076313	
31	0.0010	9.99	98.891723	0.968036	0.968036	1.108277	
32	0.0007	10.48	99.235109	0.343386	0.343386	0.764891	
33	0.0005	10.99	99.601906	0.366797	0.366797	0.398094	
34	0.0002	12.02	100.000000	0.398094	0.398094	0.000000	mode at 11.5098
35	0.0001	13.02	100.000000	0.000000	0.000000	0.000000	
36	0.0001	14.02	100.000000	0.000000	0.000000	0.000000	
37	0.0001	14.29	100.000000	0.000000	0.000000	0.000000	
		Sums:		100.00	100.00		

Grainsize Statistics
Percentiles

	phi	*mm*
5	0.94	0.521
16	1.38	0.385
25	1.59	0.331
50	2.06	0.240
75	2.60	0.165
84	3.07	0.119
95	7.64	0.005

Column: 110
Sample ID: 2014-9-22wm

Folks' Graphic Statistics

	Mean (Mz)	Sorting (σI)	Skewness (SkI)	Kurtosis (KG)	Mean *mm*
phi	2.166	1.438	0.430	2.726	0.223

Table II.110: *Results summary for sample 110: Low intertidal zone, eastern transect, Moonlight Bay. Sample collected on the 22nd of September, 2014.*

Column: 111 **Density:** 2650
Volume: 0.010
Sample ID: 2014-9-22el

Malvern data Phi	Malvern data Micron	Vol %	Equivalent Cum wt (g)
-1.00	2000.00	0	0.0
-0.75	1680.00	0.196167	0.1
-0.50	1410.00	0.717149	0.2
-0.25	1190.00	1.577867	0.4
0.00	1000.00	2.863268	0.8
0.25	840.00	4.51605	1.2
0.49	710.00	6.366413	1.7
0.76	590.00	8.578689	2.3
1.00	500.00	10.635176	2.8
1.25	420.00	12.853744	3.4
1.51	350.00	15.241875	4.0
1.74	300.00	17.331537	4.6
2.00	250.00	19.880784	5.3
2.25	210.00	22.353599	5.9
2.50	177.00	24.744738	6.6
2.75	149.00	27.063085	7.2
3.00	125.00	29.319138	7.8
3.25	105.00	31.491145	8.3
3.51	88.00	33.709099	8.9
3.76	74.00	36.000932	9.5
3.99	63.00	38.299486	10.1
4.24	53.00	40.978546	10.9
4.51	44.00	44.071661	11.7
4.76	37.00	47.062111	12.5
5.01	31.00	50.121511	13.3
6.00	15.60	60.864995	16.1
6.64	10.00	66.961072	17.7
7.00	7.80	70.315894	18.6
8.00	3.90	79.853408	21.2
8.97	2.00	88.228834	23.4
9.99	0.98	94.176988	25.0
10.48	0.70	96.284723	25.5
10.99	0.49	98.203065	26.0
12.02	0.24	99.98668	26.5
13.02	0.12	100	26.5
14.02	0.06	100	26.5
14.29	0.05	100	26.5
		Total weight:	26.5

	mm	phi	Cum wt (g)	Int wt (g)	Int wt%	Cum % finer	Modes	
1	2.0000	-1.00	0.000000	0.000000	0.000000	100.000000		
2	1.6800	-0.75	0.196167	0.196167	0.196167	99.803833		
3	1.4100	-0.50	0.717149	0.520982	0.520982	99.282851		
4	1.1900	-0.25	1.577867	0.860718	0.860718	98.422133		
5	1.0000	0.00	2.863268	1.285401	1.285401	97.136732		8
6	0.8400	0.25	4.516050	1.652782	1.652782	95.483950		
7	0.7100	0.49	6.366413	1.850363	1.850363	93.633587		
8	0.5900	0.76	8.578689	2.212276	2.212276	91.421311	mode at 0.627661	
9	0.5000	1.00	10.635176	2.056487	2.056487	89.364824		
10	0.4200	1.25	12.853744	2.218568	2.218568	87.146256		
11	0.3500	1.51	15.241875	2.388131	2.388131	84.758125	mode at 1.383056	
12	0.3000	1.74	17.331537	2.089662	2.089662	82.668463		
13	0.2500	2.00	19.880784	2.549247	2.549247	80.119216	mode at 1.868483	
14	0.2100	2.25	22.353599	2.472815	2.472815	77.646401		
15	0.1770	2.50	24.744738	2.391139	2.391139	75.255262		
16	0.1490	2.75	27.063085	2.318347	2.318347	72.936915		
17	0.1250	3.00	29.319138	2.256053	2.256053	70.680862		
18	0.1050	3.25	31.491145	2.172007	2.172007	68.508855		
19	0.0880	3.51	33.709099	2.217954	2.217954	66.290901		
20	0.0740	3.76	36.000932	2.291833	2.291833	63.999068		
21	0.0630	3.99	38.299486	2.298554	2.298554	61.700514		
22	0.0530	4.24	40.978546	2.679060	2.679060	59.021454		
23	0.0440	4.51	44.071661	3.093115	3.093115	55.928339	mode at 4.372108	
24	0.0370	4.76	47.062111	2.990450	2.990450	52.937889		
25	0.0310	5.01	50.121511	3.059400	3.059400	49.878489		
26	0.0156	6.00	60.864995	10.743484	10.743484	39.135005	mode at 5.506949	
27	0.0100	6.64	66.961072	6.096077	6.096077	33.038928		
28	0.0078	7.00	70.315894	3.354822	3.354822	29.684106		
29	0.0039	8.00	79.853408	9.537514	9.537514	20.146592	mode at 7.50231	
30	0.0020	8.97	88.228834	8.375426	8.375426	11.771166		
31	0.0010	9.99	94.176988	5.948154	5.948154	5.823012		
32	0.0007	10.48	96.284723	2.107735	2.107735	3.715277		
33	0.0005	10.99	98.203065	1.918342	1.918342	1.796935		
34	0.0002	12.02	99.986680	1.783615	1.783615	0.013320		
35	0.0001	13.02	100.000000	0.013320	0.013320	0.000000		
36	0.0001	14.02	100.000000	0.000000	0.000000	0.000000		
37	0.0001	14.29	100.000000	0.000000	0.000000	0.000000		
	Sums:			100.00	100.00			

Column: 111
Sample ID: 2014-9-22el

Folks' Graphic Statistics

	Mean (Mz)	Sorting (σI)	Skewness (SkI)	Kurtosis (KG)	Mean *mm*
phi	5.025	3.216	0.030	0.814	0.031

Grainsize Statistics
Percentiles

	phi	*mm*
5	0.31	0.804
16	1.60	0.331
25	2.53	0.174
50	5.00	0.031
75	7.49	0.006
84	8.48	0.003
95	10.18	0.001

Table II.111: *Results summary for sample 111: Low intertidal zone, western transect, Moonlight Bay. Sample collected on the 22nd of September, 2014.*

Column:	112	**Density:**	2650
		Volume:	0.010
Sample ID:	2014-9-22wl		

Malvern data Phi	**Malvern data Micron**	**Vol %**	**Equivalent Cum wt (g)**
-1.00	2000.00	0	0.0
-0.75	1680.00	0.189273	0.1
-0.50	1410.00	0.605896	0.2
-0.25	1190.00	1.20504	0.3
0.00	1000.00	1.993473	0.5
0.25	840.00	2.935428	0.8
0.49	710.00	4.066854	1.1
0.76	590.00	5.895919	1.6
1.00	500.00	8.544214	2.3
1.25	420.00	13.015805	3.4
1.51	350.00	20.084294	5.3
1.74	300.00	28.058111	7.4
2.00	250.00	39.327835	10.4
2.25	210.00	50.875432	13.5
2.50	177.00	61.596056	16.3
2.75	149.00	70.620174	18.7
3.00	125.00	77.286917	20.5
3.25	105.00	81.31361	21.5
3.51	88.00	83.256143	22.1
3.76	74.00	83.820503	22.2
3.99	63.00	83.846738	22.2
4.24	53.00	83.846738	22.2
4.51	44.00	84.053196	22.3
4.76	37.00	84.563159	22.4
5.01	31.00	85.316439	22.6
6.00	15.60	88.649795	23.5
6.64	10.00	90.845502	24.1
7.00	7.80	92.180161	24.4
8.00	3.90	95.636635	25.3
8.97	2.00	97.668076	25.9
9.99	0.98	98.735099	26.2
10.48	0.70	99.113313	26.3
10.99	0.49	99.506449	26.4
12.02	0.24	100	26.5
13.02	0.12	100	26.5
14.02	0.06	100	26.5
14.29	0.05	100	26.5
		Total weight:	26.5

	mm	**phi**	**Cum wt (g)**	**Int wt (g)**	**Int wt%**	**Cum % finer**	**Modes**
1	2.0000	-1.00	0.000000	0.000000	0.000000	100.000000	
2	1.6800	-0.75	0.189273	0.189273	0.189273	99.810727	
3	1.4100	-0.50	0.605896	0.416623	0.416623	99.394104	
4	1.1900	-0.25	1.205040	0.599144	0.599144	98.794960	
5	1.0000	0.00	1.993473	0.788433	0.788433	98.006527	8
6	0.8400	0.25	2.935428	0.941955	0.941955	97.064572	
7	0.7100	0.49	4.066854	1.131426	1.131426	95.933146	
8	0.5900	0.76	5.895919	1.829065	1.829065	94.104081	
9	0.5000	1.00	8.544214	2.648295	2.648295	91.455786	
10	0.4200	1.25	13.015805	4.471591	4.471591	86.984195	
11	0.3500	1.51	20.084294	7.068489	7.068489	79.915706	
12	0.3000	1.74	28.058111	7.973817	7.973817	71.941889	
13	0.2500	2.00	39.327835	11.269724	11.269724	60.672165	
14	0.2100	2.25	50.875432	11.547597	11.547597	49.124568	mode at 2.125769
15	0.1770	2.50	61.596056	10.720624	10.720624	38.403944	
16	0.1490	2.75	70.620174	9.024118	9.024118	29.379826	
17	0.1250	3.00	77.286917	6.666743	6.666743	22.713083	
18	0.1050	3.25	81.313610	4.026693	4.026693	18.686390	
19	0.0880	3.51	83.256143	1.942533	1.942533	16.743857	
20	0.0740	3.76	83.820503	0.564360	0.564360	16.179497	
21	0.0630	3.99	83.846738	0.026235	0.026235	16.153262	
22	0.0530	4.24	83.846738	0.000000	0.000000	16.153262	
23	0.0440	4.51	84.053196	0.206458	0.206458	15.946804	
24	0.0370	4.76	84.563159	0.509963	0.509963	15.436841	
25	0.0310	5.01	85.316439	0.753280	0.753280	14.683561	
26	0.0156	6.00	88.649795	3.333356	3.333356	11.350205	mode at 5.506949
27	0.0100	6.64	90.845502	2.195707	2.195707	9.154498	
28	0.0078	7.00	92.180161	1.334659	1.334659	7.819839	
29	0.0039	8.00	95.636635	3.456474	3.456474	4.363365	mode at 7.50231
30	0.0020	8.97	97.668076	2.031441	2.031441	2.331924	
31	0.0010	9.99	98.735099	1.067023	1.067023	1.264901	
32	0.0007	10.48	99.113313	0.378214	0.378214	0.886687	
33	0.0005	10.99	99.506449	0.393136	0.393136	0.493551	
34	0.0002	12.02	100.000000	0.493551	0.493551	0.000000	mode at 11.5098
35	0.0001	13.02	100.000000	0.000000	0.000000	0.000000	
36	0.0001	14.02	100.000000	0.000000	0.000000	0.000000	
37	0.0001	14.29	100.000000	0.000000	0.000000	0.000000	
		Sums:		100.00	100.00		

Grainsize Statistics
Percentiles

	phi	***mm***
5	0.63	0.646
16	1.36	0.389
25	1.65	0.318
50	2.23	0.213
75	2.91	0.133
84	4.44	0.046
95	7.82	0.004

Column: 112
Sample ID: 2014-9-22wl

Folks' Graphic Statistics

	Mean (Mz)	Sorting (σI)	Skewness (SkI)	Kurtosis (KG)	Mean ***mm***
phi	2.677	1.858	0.494	2.335	0.156

Table II.112: *Results summary for sample 112: Mid intertidal zone, eastern transect, Moonlight Bay. Sample collected on the 22nd of September, 2014.*

Column: 113 **Density:** 2650
Volume: 0.010
Sample ID: 2014-9-22em

Malvern data Phi	Malvern data Micron	Vol %	Equivalent Cum wt (g)
-1.00	2000.00	0	0.0
-0.75	1680.00	0.123359	0.0
-0.50	1410.00	0.787389	0.2
-0.25	1190.00	2.541432	0.7
0.00	1000.00	6.096267	1.6
0.25	840.00	11.833099	3.1
0.49	710.00	19.468155	5.2
0.76	590.00	29.911926	7.9
1.00	500.00	40.409668	10.7
1.25	420.00	51.781782	13.7
1.51	350.00	62.983287	16.7
1.74	300.00	71.187161	18.9
2.00	250.00	78.816479	20.9
2.25	210.00	83.819979	22.2
2.50	177.00	86.730977	23.0
2.75	149.00	88.117272	23.4
3.00	125.00	88.475545	23.4
3.25	105.00	88.475545	23.4
3.51	88.00	88.475545	23.4
3.76	74.00	88.475545	23.4
3.99	63.00	88.60477	23.5
4.24	53.00	88.899626	23.6
4.51	44.00	89.29502	23.7
4.76	37.00	89.682935	23.8
5.01	31.00	90.079552	23.9
6.00	15.60	91.957432	24.4
6.64	10.00	93.693663	24.8
7.00	7.80	94.731142	25.1
8.00	3.90	97.170528	25.8
8.97	2.00	98.53969	26.1
9.99	0.98	99.296907	26.3
10.48	0.70	99.565223	26.4
10.99	0.49	99.823456	26.5
12.02	0.24	100	26.5
13.02	0.12	100	26.5
14.02	0.06	100	26.5
14.29	0.05	100	26.5
		Total weight:	26.5

	mm	phi	Cum wt (g)	Int wt (g)	Int wt%	Cum % finer	Modes
1	2.0000	-1.00	0.000000	0.000000	0.000000	100.000000	
2	1.6800	-0.75	0.123359	0.123359	0.123359	99.876641	
3	1.4100	-0.50	0.787389	0.664030	0.664030	99.212611	
4	1.1900	-0.25	2.541432	1.754043	1.754043	97.458568	
5	1.0000	0.00	6.096267	3.554835	3.554835	93.903733	8
6	0.8400	0.25	11.833099	5.736832	5.736832	88.166901	
7	0.7100	0.49	19.468155	7.635056	7.635056	80.531845	
8	0.5900	0.76	29.911926	10.443771	10.443771	70.088074	
9	0.5000	1.00	40.409668	10.497742	10.497742	59.590332	
10	0.4200	1.25	51.781782	11.372114	11.372114	48.218218	mode at 1.125769
11	0.3500	1.51	62.983287	11.201505	11.201505	37.016713	
12	0.3000	1.74	71.187161	8.203874	8.203874	28.812839	
13	0.2500	2.00	78.816479	7.629318	7.629318	21.183521	
14	0.2100	2.25	83.819979	5.003500	5.003500	16.180021	
15	0.1770	2.50	86.730977	2.910998	2.910998	13.269023	
16	0.1490	2.75	88.117272	1.386295	1.386295	11.882728	
17	0.1250	3.00	88.475545	0.358273	0.358273	11.524455	
18	0.1050	3.25	88.475545	0.000000	0.000000	11.524455	
19	0.0880	3.51	88.475545	0.000000	0.000000	11.524455	
20	0.0740	3.76	88.475545	0.000000	0.000000	11.524455	
21	0.0630	3.99	88.604770	0.129225	0.129225	11.395230	
22	0.0530	4.24	88.899626	0.294856	0.294856	11.100374	
23	0.0440	4.51	89.295020	0.395394	0.395394	10.704980	mode at 4.372108
24	0.0370	4.76	89.682935	0.387915	0.387915	10.317065	
25	0.0310	5.01	90.079552	0.396617	0.396617	9.920448	
26	0.0156	6.00	91.957432	1.877880	1.877880	8.042568	mode at 5.506949
27	0.0100	6.64	93.693663	1.736231	1.736231	6.306337	
28	0.0078	7.00	94.731142	1.037479	1.037479	5.268858	
29	0.0039	8.00	97.170528	2.439386	2.439386	2.829472	mode at 7.50231
30	0.0020	8.97	98.539690	1.369162	1.369162	1.460310	
31	0.0010	9.99	99.296907	0.757217	0.757217	0.703093	
32	0.0007	10.48	99.565223	0.268316	0.268316	0.434777	
33	0.0005	10.99	99.823456	0.258233	0.258233	0.176544	
34	0.0002	12.02	100.000000	0.176544	0.176544	0.000000	
35	0.0001	13.02	100.000000	0.000000	0.000000	0.000000	
36	0.0001	14.02	100.000000	0.000000	0.000000	0.000000	
37	0.0001	14.29	100.000000	0.000000	0.000000	0.000000	
		Sums:		100.00	100.00		

Column: 113
Sample ID: 2014-9-22em

Folks' Graphic Statistics

	Mean (Mz)	Sorting (σI)	Skewness (SkI)	Kurtosis (KG)	Mean *mm*
phi	1.288	1.560	0.381	2.390	0.410

Grainsize Statistics
Percentiles

	phi	*mm*
5	-0.08	1.055
16	0.38	0.766
25	0.64	0.644
50	1.21	0.432
75	1.87	0.274
84	2.27	0.208
95	7.11	0.007

Table II.113: *Results summary for sample 113: High intertidal zone, western transect, Moonlight Bay. Sample collected on the 23rd of September, 2014.*

Column: 114 **Density:** 2650
Volume: 0.010
Sample ID: 2014-9-23wh

Malvern data Phi	Malvern data Micron	Vol %	Equivalent Cum wt (g)
-1.00	2000.00	0	0.0
-0.75	1680.00	0	0.0
-0.50	1410.00	0.180016	0.0
-0.25	1190.00	1.476218	0.4
0.00	1000.00	4.701261	1.2
0.25	840.00	10.596836	2.8
0.49	710.00	19.097427	5.1
0.76	590.00	31.45031	8.3
1.00	500.00	44.384498	11.8
1.25	420.00	58.700255	15.6
1.51	350.00	72.811438	19.3
1.74	300.00	82.907243	22.0
2.00	250.00	91.793723	24.3
2.25	210.00	97.005218	25.7
2.50	177.00	99.428594	26.3
2.75	149.00	100	26.5
3.00	125.00	100	26.5
3.25	105.00	100	26.5
3.51	88.00	100	26.5
3.76	74.00	100	26.5
3.99	63.00	100	26.5
4.24	53.00	100	26.5
4.51	44.00	100	26.5
4.76	37.00	100	26.5
5.01	31.00	100	26.5
6.00	15.60	100	26.5
6.64	10.00	100	26.5
7.00	7.80	100	26.5
8.00	3.90	100	26.5
8.97	2.00	100	26.5
9.99	0.98	100	26.5
10.48	0.70	100	26.5
10.99	0.49	100	26.5
12.02	0.24	100	26.5
13.02	0.12	100	26.5
14.02	0.06	100	26.5
14.29	0.05	100	26.5
	Total weight:		26.5

	mm	phi	Cum wt (g)	Int wt (g)	Int wt%	Cum % finer	Modes	
1	2.0000	-1.00	0.000000	0.000000	0.000000	100.000000		
2	1.6800	-0.75	0.000000	0.000000	0.000000	100.000000		
3	1.4100	-0.50	0.180016	0.180016	0.180016	99.819984		
4	1.1900	-0.25	1.476218	1.296202	1.296202	98.523782		
5	1.0000	0.00	4.701261	3.225043	3.225043	95.298739		8
6	0.8400	0.25	10.596836	5.895575	5.895575	89.403164		
7	0.7100	0.49	19.097427	8.500591	8.500591	80.902573		
8	0.5900	0.76	31.450310	12.352883	12.352883	68.549690		
9	0.5000	1.00	44.384498	12.934188	12.934188	55.615502		
10	0.4200	1.25	58.700255	14.315757	14.315757	41.299745	mode at 1.125769	
11	0.3500	1.51	72.811438	14.111183	14.111183	27.188562		
12	0.3000	1.74	82.907243	10.095805	10.095805	17.092757		
13	0.2500	2.00	91.793723	8.886480	8.886480	8.206277		
14	0.2100	2.25	97.005218	5.211495	5.211495	2.994782		
15	0.1770	2.50	99.428594	2.423376	2.423376	0.571406		
16	0.1490	2.75	100.000000	0.571406	0.571406	0.000000		
17	0.1250	3.00	100.000000	0.000000	0.000000	0.000000		
18	0.1050	3.25	100.000000	0.000000	0.000000	0.000000		
19	0.0880	3.51	100.000000	0.000000	0.000000	0.000000		
20	0.0740	3.76	100.000000	0.000000	0.000000	0.000000		
21	0.0630	3.99	100.000000	0.000000	0.000000	0.000000		
22	0.0530	4.24	100.000000	0.000000	0.000000	0.000000		
23	0.0440	4.51	100.000000	0.000000	0.000000	0.000000		
24	0.0370	4.76	100.000000	0.000000	0.000000	0.000000		
25	0.0310	5.01	100.000000	0.000000	0.000000	0.000000		
26	0.0156	6.00	100.000000	0.000000	0.000000	0.000000		
27	0.0100	6.64	100.000000	0.000000	0.000000	0.000000		
28	0.0078	7.00	100.000000	0.000000	0.000000	0.000000		
29	0.0039	8.00	100.000000	0.000000	0.000000	0.000000		
30	0.0020	8.97	100.000000	0.000000	0.000000	0.000000		
31	0.0010	9.99	100.000000	0.000000	0.000000	0.000000		
32	0.0007	10.48	100.000000	0.000000	0.000000	0.000000		
33	0.0005	10.99	100.000000	0.000000	0.000000	0.000000		
34	0.0002	12.02	100.000000	0.000000	0.000000	0.000000		
35	0.0001	13.02	100.000000	0.000000	0.000000	0.000000		
36	0.0001	14.02	100.000000	0.000000	0.000000	0.000000		
37	0.0001	14.29	100.000000	0.000000	0.000000	0.000000		
	Sums:			100.00	100.00			

Grainsize Statistics
Percentiles

	phi	*mm*
5	0.01	0.991
16	0.41	0.755
25	0.62	0.650
50	1.10	0.467
75	1.56	0.338
84	1.77	0.293
95	2.15	0.225

Column: 114
Sample ID: 2014-9-23wh

Folks' Graphic Statistics

	Mean (Mz)	Sorting (σI)	Skewness (SkI)	Kurtosis (KG)	Mean *mm*
phi	1.091	0.665	-0.015	0.933	0.469

Table II.114: *Results summary for sample 114: Mid intertidal zone, western transect, Moonlight Bay. Sample collected on the 23rd of September, 2014.*

Column: 115 **Density:** 2650
Volume: 0.010
Sample ID: 2014-9-23mw

Malvern data Phi	Malvern data Micron	Vol %	Equivalent Cum wt (g)
-1.00	2000.00	0	0.0
-0.75	1680.00	0	0.0
-0.50	1410.00	0	0.0
-0.25	1190.00	0	0.0
0.00	1000.00	0	0.0
0.25	840.00	0.015307	0.0
0.49	710.00	0.150914	0.0
0.76	590.00	0.955162	0.3
1.00	500.00	3.172998	0.8
1.25	420.00	8.397805	2.2
1.51	350.00	18.197422	4.8
1.74	300.00	29.899558	7.9
2.00	250.00	46.023218	12.2
2.25	210.00	60.861145	16.1
2.50	177.00	72.241373	19.1
2.75	149.00	79.368142	21.0
3.00	125.00	82.69275	21.9
3.25	105.00	83.582991	22.1
3.51	88.00	83.634096	22.2
3.76	74.00	83.634096	22.2
3.99	63.00	83.634096	22.2
4.24	53.00	83.634096	22.2
4.51	44.00	84.129328	22.3
4.76	37.00	84.944298	22.5
5.01	31.00	85.931378	22.8
6.00	15.60	89.431698	23.7
6.64	10.00	91.648413	24.3
7.00	7.80	92.962261	24.6
8.00	3.90	96.136234	25.5
8.97	2.00	97.929355	26.0
9.99	0.98	98.896827	26.2
10.48	0.70	99.235723	26.3
10.99	0.49	99.581516	26.4
12.02	0.24	100	26.5
13.02	0.12	100	26.5
14.02	0.06	100	26.5
14.29	0.05	100	26.5

Total weight: 26.5

Column: 115
Sample ID: 2014-9-23mw

	mm	phi	Cum wt (g)	Int wt (g)	Int wt%	Cum % finer	Modes
1	2.0000	-1.00	0.000000	0.000000	0.000000	100.000000	
2	1.6800	-0.75	0.000000	0.000000	0.000000	100.000000	
3	1.4100	-0.50	0.000000	0.000000	0.000000	100.000000	
4	1.1900	-0.25	0.000000	0.000000	0.000000	100.000000	
5	1.0000	0.00	0.000000	0.000000	0.000000	100.000000	8
6	0.8400	0.25	0.015307	0.015307	0.015307	99.984693	
7	0.7100	0.49	0.150914	0.135607	0.135607	99.849086	
8	0.5900	0.76	0.955162	0.804248	0.804248	99.044838	
9	0.5000	1.00	3.172998	2.217836	2.217836	96.827002	
10	0.4200	1.25	8.397805	5.224807	5.224807	91.602195	
11	0.3500	1.51	18.197422	9.799617	9.799617	81.802578	
12	0.3000	1.74	29.899558	11.702136	11.702136	70.100442	
13	0.2500	2.00	46.023218	16.123660	16.123660	53.976782	mode at 1.868483
14	0.2100	2.25	60.861145	14.837927	14.837927	39.138855	
15	0.1770	2.50	72.241373	11.380228	11.380228	27.758627	
16	0.1490	2.75	79.368142	7.126769	7.126769	20.631858	
17	0.1250	3.00	82.692750	3.324608	3.324608	17.307250	
18	0.1050	3.25	83.582991	0.890241	0.890241	16.417009	
19	0.0880	3.51	83.634096	0.051105	0.051105	16.365904	
20	0.0740	3.76	83.634096	0.000000	0.000000	16.365904	
21	0.0630	3.99	83.634096	0.000000	0.000000	16.365904	
22	0.0530	4.24	83.634096	0.000000	0.000000	16.365904	
23	0.0440	4.51	84.129328	0.495232	0.495232	15.870672	
24	0.0370	4.76	84.944298	0.814970	0.814970	15.055702	
25	0.0310	5.01	85.931378	0.987080	0.987080	14.068622	
26	0.0156	6.00	89.431698	3.500320	3.500320	10.568302	mode at 5.506949
27	0.0100	6.64	91.648413	2.216715	2.216715	8.351587	
28	0.0078	7.00	92.962261	1.313848	1.313848	7.037739	
29	0.0039	8.00	96.136234	3.173973	3.173973	3.863766	mode at 7.50231
30	0.0020	8.97	97.929355	1.793121	1.793121	2.070645	
31	0.0010	9.99	98.896827	0.967472	0.967472	1.103173	
32	0.0007	10.48	99.235723	0.338896	0.338896	0.764277	
33	0.0005	10.99	99.581516	0.345793	0.345793	0.418484	
34	0.0002	12.02	100.000000	0.418484	0.418484	0.000000	mode at 11.5098
35	0.0001	13.02	100.000000	0.000000	0.000000	0.000000	
36	0.0001	14.02	100.000000	0.000000	0.000000	0.000000	
37	0.0001	14.29	100.000000	0.000000	0.000000	0.000000	
		Sums:		100.00	100.00		

Grainsize Statistics
Percentiles

	phi	*mm*
5	1.09	0.470
16	1.46	0.365
25	1.64	0.320
50	2.07	0.239
75	2.59	0.166
84	4.44	0.046
95	7.64	0.005

Folks' Graphic Statistics

	Mean (Mz)	Sorting (σI)	Skewness (SkI)	Kurtosis (KG)	Mean *mm*
phi	2.653	1.739	0.645	2.827	0.159

Table II.115: *Results summary for sample 115: High intertidal zone, eastern transect, Moonlight Bay. Sample collected on the 23rd of September, 2014.*

Column: 116 **Density:** 2650
Volume: 0.010
Sample ID: 2014-9-23eh

Malvern data Phi	Malvern data Micron	Vol %	Equivalent Cum wt (g)
-1.00	2000.00	0	0.0
-0.75	1680.00	1.293191	0.3
-0.50	1410.00	4.18775	1.1
-0.25	1190.00	8.659881	2.3
0.00	1000.00	14.966719	4.0
0.25	840.00	22.783408	6.0
0.49	710.00	31.354021	8.3
0.76	590.00	41.49429	11.0
1.00	500.00	50.810415	13.5
1.25	420.00	60.522423	16.0
1.51	350.00	70.122967	18.6
1.74	300.00	77.389556	20.5
2.00	250.00	84.498469	22.4
2.25	210.00	89.471167	23.7
2.50	177.00	92.573339	24.5
2.75	149.00	94.175744	25.0
3.00	125.00	94.69934	25.1
3.25	105.00	94.716708	25.1
3.51	88.00	94.716708	25.1
3.76	74.00	94.716708	25.1
3.99	63.00	94.794681	25.1
4.24	53.00	95.032543	25.2
4.51	44.00	95.377344	25.3
4.76	37.00	95.702883	25.4
5.01	31.00	95.996383	25.4
6.00	15.60	96.897974	25.7
6.64	10.00	97.595881	25.9
7.00	7.80	98.019974	26.0
8.00	3.90	99.078807	26.3
8.97	2.00	99.737613	26.4
9.99	0.98	100	26.5
10.48	0.70	100	26.5
10.99	0.49	100	26.5
12.02	0.24	100	26.5
13.02	0.12	100	26.5
14.02	0.06	100	26.5
14.29	0.05	100	26.5

Total weight: 26.5

	mm	phi	Cum wt (g)	Int wt (g)	Int wt%	Cum % finer	Modes
1	2.0000	-1.00	0.000000	0.000000	0.000000	100.000000	
2	1.6800	-0.75	1.293191	1.293191	1.293191	98.706809	
3	1.4100	-0.50	4.187750	2.894559	2.894559	95.812250	
4	1.1900	-0.25	8.659881	4.472131	4.472131	91.340119	
5	1.0000	0.00	14.966719	6.306838	6.306838	85.033281	8
6	0.8400	0.25	22.783408	7.816689	7.816689	77.216592	
7	0.7100	0.49	31.354021	8.570613	8.570613	68.645979	
8	0.5900	0.76	41.494290	10.140269	10.140269	58.505710	mode at 0.627661
9	0.5000	1.00	50.810415	9.316125	9.316125	49.189585	
10	0.4200	1.25	60.522423	9.712008	9.712008	39.477577	mode at 1.125769
11	0.3500	1.51	70.122967	9.600544	9.600544	29.877033	
12	0.3000	1.74	77.389556	7.266589	7.266589	22.610444	
13	0.2500	2.00	84.498469	7.108913	7.108913	15.501531	
14	0.2100	2.25	89.471167	4.972698	4.972698	10.528833	
15	0.1770	2.50	92.573339	3.102172	3.102172	7.426661	
16	0.1490	2.75	94.175744	1.602405	1.602405	5.824256	
17	0.1250	3.00	94.699340	0.523596	0.523596	5.300660	
18	0.1050	3.25	94.716708	0.017368	0.017368	5.283292	
19	0.0880	3.51	94.716708	0.000000	0.000000	5.283292	
20	0.0740	3.76	94.716708	0.000000	0.000000	5.283292	
21	0.0630	3.99	94.794681	0.077973	0.077973	5.205319	
22	0.0530	4.24	95.032543	0.237862	0.237862	4.967457	
23	0.0440	4.51	95.377344	0.344801	0.344801	4.622656	mode at 4.372108
24	0.0370	4.76	95.702883	0.325539	0.325539	4.297117	
25	0.0310	5.01	95.996383	0.293500	0.293500	4.003617	
26	0.0156	6.00	96.897974	0.901591	0.901591	3.102026	mode at 5.506949
27	0.0100	6.64	97.595881	0.697907	0.697907	2.404119	
28	0.0078	7.00	98.019974	0.424093	0.424093	1.980026	
29	0.0039	8.00	99.078807	1.058833	1.058833	0.921193	mode at 7.50231
30	0.0020	8.97	99.737613	0.658806	0.658806	0.262387	
31	0.0010	9.99	100.000000	0.262387	0.262387	0.000000	
32	0.0007	10.48	100.000000	0.000000	0.000000	0.000000	
33	0.0005	10.99	100.000000	0.000000	0.000000	0.000000	
34	0.0002	12.02	100.000000	0.000000	0.000000	0.000000	
35	0.0001	13.02	100.000000	0.000000	0.000000	0.000000	
36	0.0001	14.02	100.000000	0.000000	0.000000	0.000000	
37	0.0001	14.29	100.000000	0.000000	0.000000	0.000000	
		Sums:		100.00	100.00		

Column: 116
Sample ID: 2014-9-23eh

Folks' Graphic Statistics

	Mean (Mz)	Sorting (σI)	Skewness (SkI)	Kurtosis (KG)	Mean ***mm***
phi	0.998	1.192	0.207	1.414	0.501

Grainsize Statistics
Percentiles

	phi	***mm***
5	-0.45	1.367
16	0.03	0.977
25	0.31	0.804
50	0.98	0.507
75	1.66	0.316
84	1.98	0.253
95	4.20	0.054

Table II.116: *Results summary for sample 116: Mid intertidal zone, eastern transect, Moonlight Bay. Sample collected on the 23rd of September, 2014.*

Column: 117 **Density:** 2650
Volume: 0.010
Sample ID: 2014-9-23me

Malvern data Phi	Malvern data Micron	Vol %	Equivalent Cum wt (g)		mm	phi	Cum wt (g)	Int wt (g)	Int wt%	Cum % finer	Modes	
-1.00	2000.00	0	0.0	1	2.0000	-1.00	0.000000	0.000000	0.000000	100.000000		
-0.75	1680.00	0.350108	0.1	2	1.6800	-0.75	0.350108	0.350108	0.350108	99.649892		
-0.50	1410.00	1.377527	0.4	3	1.4100	-0.50	1.377527	1.027419	1.027419	98.622473		
-0.25	1190.00	3.477345	0.9	4	1.1900	-0.25	3.477345	2.099818	2.099818	96.522655		
0.00	1000.00	7.240181	1.9	5	1.0000	0.00	7.240181	3.762836	3.762836	92.759819		8
0.25	840.00	12.98498	3.4	6	0.8400	0.25	12.984980	5.744799	5.744799	87.015020		
0.49	710.00	20.479863	5.4	7	0.7100	0.49	20.479863	7.494883	7.494883	79.520137		
0.76	590.00	30.73347	8.1	8	0.5900	0.76	30.733470	10.253607	10.253607	69.266530		
1.00	500.00	41.164604	10.9	9	0.5000	1.00	41.164604	10.431134	10.431134	58.835396		
1.25	420.00	52.674497	14.0	10	0.4200	1.25	52.674497	11.509893	11.509893	47.325503		
1.51	350.00	64.2688	17.0	11	0.3500	1.51	64.268800	11.594303	11.594303	35.731200	mode at 1.383056	
1.74	300.00	72.948946	19.3	12	0.3000	1.74	72.948946	8.680146	8.680146	27.051054		
2.00	250.00	81.19079	21.5	13	0.2500	2.00	81.190790	8.241844	8.241844	18.809210		
2.25	210.00	86.705992	23.0	14	0.2100	2.25	86.705992	5.515202	5.515202	13.294008		
2.50	177.00	89.967139	23.8	15	0.1770	2.50	89.967139	3.261147	3.261147	10.032861		
2.75	149.00	91.533266	24.3	16	0.1490	2.75	91.533266	1.566127	1.566127	8.466734		
3.00	125.00	91.930653	24.4	17	0.1250	3.00	91.930653	0.397387	0.397387	8.069347		
3.25	105.00	91.930653	24.4	18	0.1050	3.25	91.930653	0.000000	0.000000	8.069347		
3.51	88.00	91.930653	24.4	19	0.0880	3.51	91.930653	0.000000	0.000000	8.069347		
3.76	74.00	91.930653	24.4	20	0.0740	3.76	91.930653	0.000000	0.000000	8.069347		
3.99	63.00	92.034696	24.4	21	0.0630	3.99	92.034696	0.104043	0.104043	7.965304		
4.24	53.00	92.312402	24.5	22	0.0530	4.24	92.312402	0.277706	0.277706	7.687598		
4.51	44.00	92.70092	24.6	23	0.0440	4.51	92.700920	0.388518	0.388518	7.299080	mode at 4.372108	
4.76	37.00	93.074723	24.7	24	0.0370	4.76	93.074723	0.373803	0.373803	6.925277		
5.01	31.00	93.43529	24.8	25	0.0310	5.01	93.435290	0.360567	0.360567	6.564710		
6.00	15.60	94.879771	25.1	26	0.0156	6.00	94.879771	1.444481	1.444481	5.120229	mode at 5.506949	
6.64	10.00	96.118539	25.5	27	0.0100	6.64	96.118539	1.238768	1.238768	3.881461		
7.00	7.80	96.842439	25.7	28	0.0078	7.00	96.842439	0.723900	0.723900	3.157561		
8.00	3.90	98.482125	26.1	29	0.0039	8.00	98.482125	1.639686	1.639686	1.517875	mode at 7.50231	
8.97	2.00	99.343531	26.3	30	0.0020	8.97	99.343531	0.861406	0.861406	0.656469		
9.99	0.98	99.767223	26.4	31	0.0010	9.99	99.767223	0.423692	0.423692	0.232777		
10.48	0.70	99.909652	26.5	32	0.0007	10.48	99.909652	0.142429	0.142429	0.090348		
10.99	0.49	100	26.5	33	0.0005	10.99	100.000000	0.090348	0.090348	0.000000		
12.02	0.24	100	26.5	34	0.0002	12.02	100.000000	0.000000	0.000000	0.000000		
13.02	0.12	100	26.5	35	0.0001	13.02	100.000000	0.000000	0.000000	0.000000		
14.02	0.06	100	26.5	36	0.0001	14.02	100.000000	0.000000	0.000000	0.000000		
14.29	0.05	100	26.5	37	0.0001	14.29	100.000000	0.000000	0.000000	0.000000		
						Sums:		100.00	100.00			

Total weight: 26.5

Column: 117
Sample ID: 2014-9-23me

Folks' Graphic Statistics

	Mean (Mz)	Sorting (σI)	Skewness (SkI)	Kurtosis (KG)	Mean *mm*
phi	1.223	1.386	0.310	2.139	0.428

Grainsize Statistics
Percentiles

	phi	*mm*
5	-0.15	1.109
16	0.35	0.785
25	0.61	0.654
50	1.19	0.437
75	1.80	0.287
84	2.13	0.229
95	6.06	0.015

Table II.117: *Results summary for sample 117: Low intertidal zone, eastern transect, Moonlight Bay. Sample collected on the 23rd of September, 2014.*

Column: 118 **Density:** 2650
Volume: 0.010
Sample ID: 2014-9-23el

Malvern data Phi	Malvern data Micron	Vol %	Equivalent Cum wt (g)
-1.00	2000.00	0	0.0
-0.75	1680.00	0.279629	0.1
-0.50	1410.00	0.961129	0.3
-0.25	1190.00	2.132839	0.6
0.00	1000.00	3.959285	1.0
0.25	840.00	6.421515	1.7
0.49	710.00	9.286832	2.5
0.76	590.00	12.796163	3.4
1.00	500.00	16.051376	4.3
1.25	420.00	19.431823	5.1
1.51	350.00	22.787438	6.0
1.74	300.00	25.426826	6.7
2.00	250.00	28.288462	7.5
2.25	210.00	30.758	8.2
2.50	177.00	32.936644	8.7
2.75	149.00	34.915961	9.3
3.00	125.00	36.768159	9.7
3.25	105.00	38.524749	10.2
3.51	88.00	40.324335	10.7
3.76	74.00	42.205648	11.2
3.99	63.00	44.113311	11.7
4.24	53.00	46.354669	12.3
4.51	44.00	48.95996	13.0
4.76	37.00	51.499031	13.6
5.01	31.00	54.126921	14.3
6.00	15.60	63.77329	16.9
6.64	10.00	69.536671	18.4
7.00	7.80	72.723664	19.3
8.00	3.90	81.589205	21.6
8.97	2.00	89.192572	23.6
9.99	0.98	94.698844	25.1
10.48	0.70	96.677541	25.6
10.99	0.49	98.460779	26.1
12.02	0.24	100	26.5
13.02	0.12	100	26.5
14.02	0.06	100	26.5
14.29	0.05	100	26.5

Total weight: 26.5

	mm	phi	Cum wt (g)	Int wt (g)	Int wt%	Cum % finer	Modes
1	2.0000	-1.00	0.000000	0.000000	0.000000	100.000000	
2	1.6800	-0.75	0.279629	0.279629	0.279629	99.720371	
3	1.4100	-0.50	0.961129	0.681500	0.681500	99.038871	
4	1.1900	-0.25	2.132839	1.171710	1.171710	97.867161	
5	1.0000	0.00	3.959285	1.826446	1.826446	96.040715	8
6	0.8400	0.25	6.421515	2.462230	2.462230	93.578485	
7	0.7100	0.49	9.286832	2.865317	2.865317	90.713168	
8	0.5900	0.76	12.796163	3.509331	3.509331	87.203837	mode at 0.627661
9	0.5000	1.00	16.051376	3.255213	3.255213	83.948624	
10	0.4200	1.25	19.431823	3.380447	3.380447	80.568177	mode at 1.125769
11	0.3500	1.51	22.787438	3.355615	3.355615	77.212562	
12	0.3000	1.74	25.426826	2.639388	2.639388	74.573174	
13	0.2500	2.00	28.288462	2.861636	2.861636	71.711538	mode at 1.868483
14	0.2100	2.25	30.758000	2.469538	2.469538	69.242000	
15	0.1770	2.50	32.936644	2.178644	2.178644	67.063356	
16	0.1490	2.75	34.915961	1.979317	1.979317	65.084039	
17	0.1250	3.00	36.768159	1.852198	1.852198	63.231841	
18	0.1050	3.25	38.524749	1.756590	1.756590	61.475251	
19	0.0880	3.51	40.324335	1.799586	1.799586	59.675665	
20	0.0740	3.76	42.205648	1.881313	1.881313	57.794352	
21	0.0630	3.99	44.113311	1.907663	1.907663	55.886689	
22	0.0530	4.24	46.354669	2.241358	2.241358	53.645331	
23	0.0440	4.51	48.959960	2.605291	2.605291	51.040040	mode at 4.372108
24	0.0370	4.76	51.499031	2.539071	2.539071	48.500969	
25	0.0310	5.01	54.126921	2.627890	2.627890	45.873079	
26	0.0156	6.00	63.773290	9.646369	9.646369	36.226710	mode at 5.506949
27	0.0100	6.64	69.536671	5.763381	5.763381	30.463329	
28	0.0078	7.00	72.723664	3.186993	3.186993	27.276336	
29	0.0039	8.00	81.589205	8.865541	8.865541	18.410795	mode at 7.50231
30	0.0020	8.97	89.192572	7.603367	7.603367	10.807428	
31	0.0010	9.99	94.698844	5.506272	5.506272	5.301156	
32	0.0007	10.48	96.677541	1.978697	1.978697	3.322459	
33	0.0005	10.99	98.460779	1.783238	1.783238	1.539221	
34	0.0002	12.02	100.000000	1.539221	1.539221	0.000000	
35	0.0001	13.02	100.000000	0.000000	0.000000	0.000000	
36	0.0001	14.02	100.000000	0.000000	0.000000	0.000000	
37	0.0001	14.29	100.000000	0.000000	0.000000	0.000000	
		Sums:		100.00	100.00		

Grainsize Statistics
Percentiles

	phi	*mm*
5	0.11	0.929
16	1.00	0.501
25	1.70	0.308
50	4.61	0.041
75	7.26	0.007
84	8.31	0.003
95	10.07	0.001

Column: 118
Sample ID: 2014-9-23el

Folks' Graphic Statistics

	Mean (Mz)	Sorting (σI)	Skewness (SkI)	Kurtosis (KG)	Mean *mm*
phi	4.638	3.337	0.054	0.735	0.040

Table II.118: *Results summary for sample 118: Low intertidal zone, western transect, Moonlight Bay. Sample collected on the 23rd of September, 2014.*

Column: 119 **Density:** 2650
Volume: 0.010
Sample ID: 2014-9-23wl

Malvern data Phi	Malvern data Micron	Vol %	Equivalent Cum wt (g)
-1.00	2000.00	0	0.0
-0.75	1680.00	0.174385	0.0
-0.50	1410.00	0.605774	0.2
-0.25	1190.00	1.321497	0.4
0.00	1000.00	2.409268	0.6
0.25	840.00	3.886639	1.0
0.49	710.00	5.767213	1.5
0.76	590.00	8.642679	2.3
1.00	500.00	12.336406	3.3
1.25	420.00	17.897955	4.7
1.51	350.00	25.941693	6.9
1.74	300.00	34.501796	9.1
2.00	250.00	46.104624	12.2
2.25	210.00	57.601291	15.3
2.50	177.00	67.990205	18.0
2.75	149.00	76.516843	20.3
3.00	125.00	82.643449	21.9
3.25	105.00	86.208953	22.8
3.51	88.00	87.821136	23.3
3.76	74.00	88.184159	23.4
3.99	63.00	88.190827	23.4
4.24	53.00	88.190827	23.4
4.51	44.00	88.337634	23.4
4.76	37.00	88.763841	23.5
5.01	31.00	89.391473	23.7
6.00	15.60	91.98548	24.4
6.64	10.00	93.603851	24.8
7.00	7.80	94.599605	25.1
8.00	3.90	97.198195	25.8
8.97	2.00	98.684681	26.2
9.99	0.98	99.376862	26.3
10.48	0.70	99.601342	26.4
10.99	0.49	99.830352	26.5
12.02	0.24	100	26.5
13.02	0.12	100	26.5
14.02	0.06	100	26.5
14.29	0.05	100	26.5

Total weight: 26.5

	mm	phi	Cum wt (g)	Int wt (g)	Int wt%	Cum % finer	Modes
1	2.0000	-1.00	0.000000	0.000000	0.000000	100.000000	
2	1.6800	-0.75	0.174385	0.174385	0.174385	99.825615	
3	1.4100	-0.50	0.605774	0.431389	0.431389	99.394226	
4	1.1900	-0.25	1.321497	0.715723	0.715723	98.678503	
5	1.0000	0.00	2.409268	1.087771	1.087771	97.590732	8
6	0.8400	0.25	3.886639	1.477371	1.477371	96.113361	
7	0.7100	0.49	5.767213	1.880574	1.880574	94.232787	
8	0.5900	0.76	8.642679	2.875466	2.875466	91.357321	
9	0.5000	1.00	12.336406	3.693727	3.693727	87.663594	
10	0.4200	1.25	17.897955	5.561549	5.561549	82.102045	
11	0.3500	1.51	25.941693	8.043738	8.043738	74.058307	
12	0.3000	1.74	34.501796	8.560103	8.560103	65.498204	
13	0.2500	2.00	46.104624	11.602828	11.602828	53.895376	mode at 1.868483
14	0.2100	2.25	57.601291	11.496667	11.496667	42.398709	
15	0.1770	2.50	67.990205	10.388914	10.388914	32.009795	
16	0.1490	2.75	76.516843	8.526638	8.526638	23.483157	
17	0.1250	3.00	82.643449	6.126606	6.126606	17.356551	
18	0.1050	3.25	86.208953	3.565504	3.565504	13.791047	
19	0.0880	3.51	87.821136	1.612183	1.612183	12.178864	
20	0.0740	3.76	88.184159	0.363023	0.363023	11.815841	
21	0.0630	3.99	88.190827	0.006668	0.006668	11.809173	
22	0.0530	4.24	88.190827	0.000000	0.000000	11.809173	
23	0.0440	4.51	88.337634	0.146807	0.146807	11.662366	
24	0.0370	4.76	88.763841	0.426207	0.426207	11.236159	
25	0.0310	5.01	89.391473	0.627632	0.627632	10.608527	
26	0.0156	6.00	91.985480	2.594007	2.594007	8.014520	mode at 5.506949
27	0.0100	6.64	93.603851	1.618371	1.618371	6.396149	
28	0.0078	7.00	94.599605	0.995754	0.995754	5.400395	
29	0.0039	8.00	97.198195	2.598590	2.598590	2.801805	mode at 7.50231
30	0.0020	8.97	98.684681	1.486486	1.486486	1.315319	
31	0.0010	9.99	99.376862	0.692181	0.692181	0.623138	
32	0.0007	10.48	99.601342	0.224480	0.224480	0.398658	
33	0.0005	10.99	99.830352	0.229010	0.229010	0.169648	mode at 10.73764
34	0.0002	12.02	100.000000	0.169648	0.169648	0.000000	
35	0.0001	13.02	100.000000	0.000000	0.000000	0.000000	
36	0.0001	14.02	100.000000	0.000000	0.000000	0.000000	
37	0.0001	14.29	100.000000	0.000000	0.000000	0.000000	
		Sums:		100.00	100.00		

Column: 119
Sample ID: 2014-9-23wl

Folks' Graphic Statistics

	Mean (Mz)	Sorting (σI)	Skewness (SkI)	Kurtosis (KG)	Mean ***mm***
phi	2.116	1.507	0.274	2.274	0.231

Grainsize Statistics
Percentiles

	phi	***mm***
5	0.40	0.760
16	1.17	0.446
25	1.48	0.358
50	2.09	0.236
75	2.70	0.154
84	3.10	0.117
95	7.16	0.007

APPENDIX II: SEDIMENT TEXTURAL ANALYSIS

II.0 SEDIMENT TEXTURAL SIZE CLASSES AND DISTRIBUTIONS

Tables of summary statistics including textural size class and description, Wentworth size class, logarithmic method of moments parameters and logarithmic graphical measures after Ward (1974) are presented.

Derived grain size distribution histograms and cumulative frequency (both arithmetic and probability scale) plots of percent finer than are also presented for visual assessment.

All Moonlight Bay samples contained size fractions that were larger than 2 mm.

1.20777	WL	22/09/2014
1.13882	WH	
1.086957	EH	
1.14297	EM	
1.095197	EL	
1.174377	WM	
1.247466	WL	23/09/2014
1.08642	EH	
1.175177	ME	
1.132253	HW	
1.162771	MW	
1.106929	EL	

Table II.1: *Graphical and statistical parameters, textural description and size classes for sample 1: Mid intertidal zone, mid transect, Northern Ngarunui Beach. Sample collected on the 20th of July, 2014.*

Textural description	**Textural size classes**
Moderately well sorted, Near symmetrical skewed, Mesokurtic	Sand = 100 000%Fines = 0.000% Silt = 0.000%Clay = 0.000%
Moments method parameters (µm)	**Graphical method parameters. After Folk (1980) (ϕ)**
Mean = 287.466 Standard deviation (sd) = 100.209 Skewness (Sk_I)=0.829 Kurtosis (K_G) = 3.557	Mean (M_z) = 1.888 d (0.5) = 1.889 Sorting (σ_I) = 0.512 Skewness (Sk_I) = -0.004 Kurtosis (K_G) = 0.965 Mean (mm) = 0.270 Mean (µm) = 270.217
Wentworth size class Medium sand	

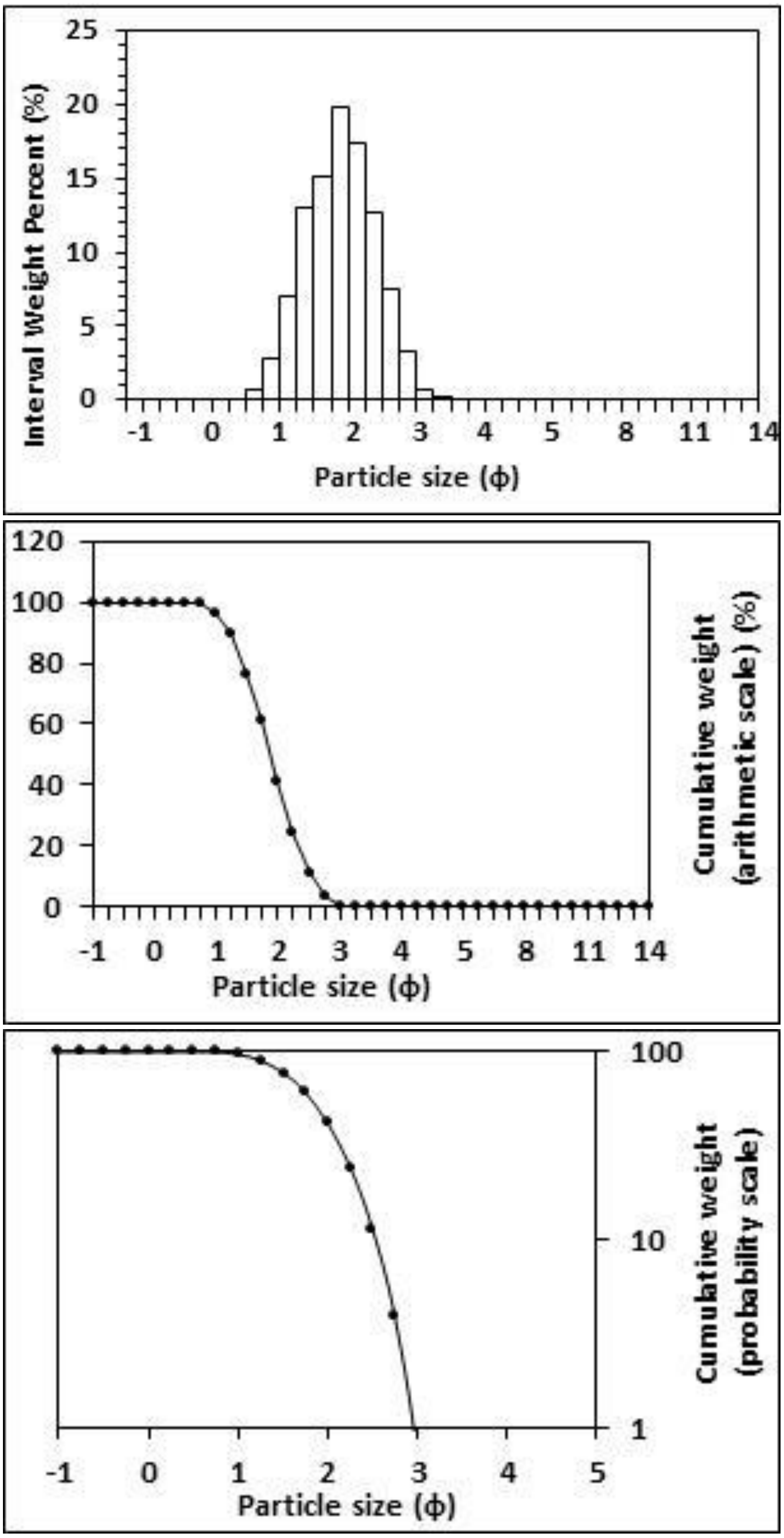

Figures II.1, II.2 and II.3: Histogram of grain size distribution and cumulative frequency graphs (arithmetic scale and probability scale) for sample 1: Mid intertidal zone, mid transect, Northern Ngarunui Beach. Sample collected on the 20th of July, 2014.

Table II.2: *Graphical and statistical parameters, textural description and size classes for sample 2: High intertidal zone, mid transect, Northern Ngarunui Beach. Sample collected on the 20th of July, 2014.*

Textural description	**Textural size classes**
Well sorted, Near symmetrical skewed, Mesokurtic	Sand = 100 000%Fines = 0.000% Silt = 0.000%Clay = 0.000%
Moment method parameters (µm) Mean = 239.063 Standard deviation (sd) = 76.844 Skewness (Sk_I)= 0.807 Kurtosis (K_G) = 3.604	**Graphical method parameters. After Folk (1980) (ϕ)** Mean (M_z) = 2.144 d (0.5) = 2.143 Sorting (σ_I) = 0.473 Skewness (Sk_I) = -0.002 Kurtosis (K_G) = 0.977 Mean (mm) = 0.226 Mean (µm) = 226.272
Wentworth size class Fine sand	

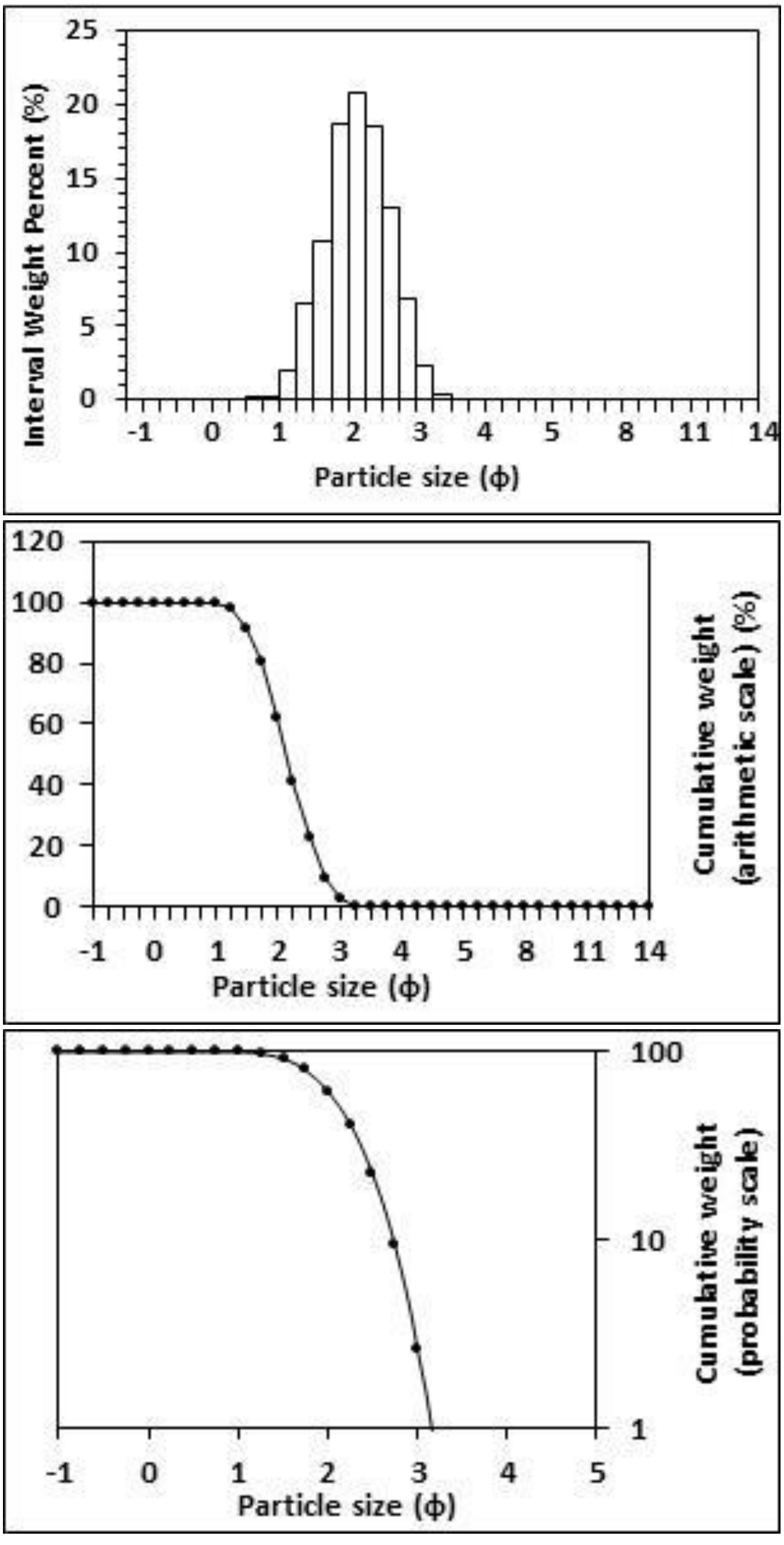

Figures II.4, II.5 and II.6: Histogram of grain size distribution and cumulative frequency graphs (arithmetic scale and probability scale) for sample 2: High intertidal zone, mid transect, Northern Ngarunui Beach. Sample collected on the 20th of July, 2014

Table II.3: *Graphical and statistical parameters, textural description and size classes for sample 3: Mid intertidal zone, northern transect, Northern Ngarunui Beach. Sample collected on the 20th of July, 2014.*

<table>
<tr><td>Textural description
Well sorted,
Near symmetrical skewed,
Mesokurtic</td><td>Textural size classes
Sand = 100 000%Fines = 0.000%
Silt = 0.000%Clay = 0.000%</td></tr>
<tr><td>Moment method parameters (μm)
Mean = 316.317
Standard deviation (sd) = 100.429
Skewness (Sk_I)= 0.756
Kurtosis (K_G) = 3.448</td><td rowspan="2">Graphical method parameters. After Folk (1980) (ϕ)
Mean (M_z) = 1.738
d (0.5) = 1.735
Sorting (σ_I) = 0.459
Skewness (Sk_I) = -0.008
Kurtosis (K_G) = 0.933
Mean (mm) = 0.300
Mean (μm) = 299.834</td></tr>
<tr><td>Wentworth size class
Medium sand</td></tr>
</table>

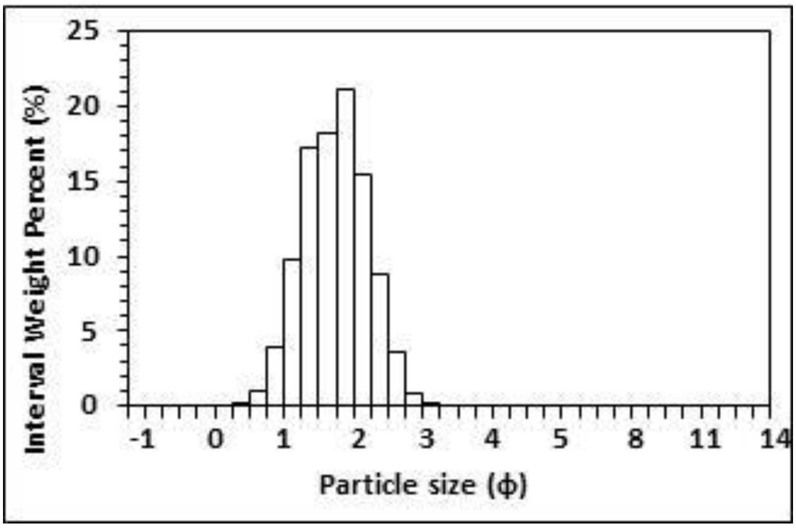

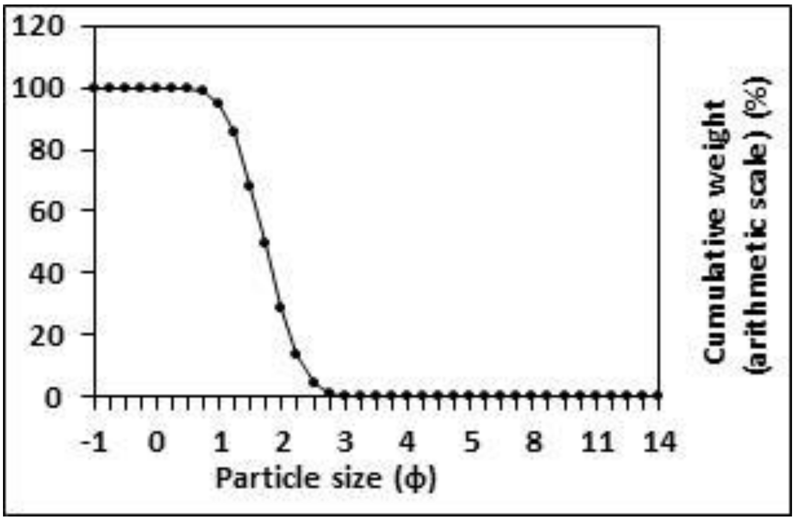

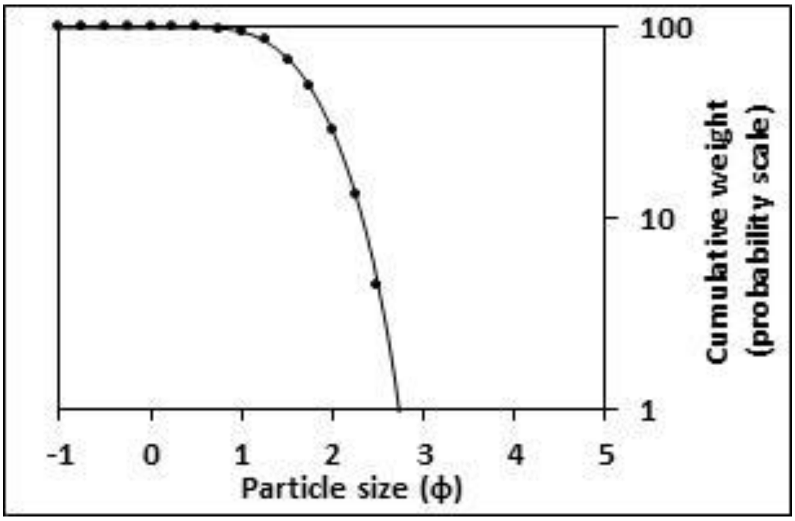

Figures II.7, II.8 and II.9: Histogram of grain size distribution and cumulative frequency graphs (arithmetic scale and probability scale) for sample 3: Mid intertidal zone, northern transect, Northern Ngarunui Beach. Sample collected on the 20th of July, 2014.

Table II.4: *Graphical and statistical parameters, textural description and size classes for sample 4: High intertidal zone, southern transect, Northern Ngarunui Beach. Sample collected on the 20th of July, 2014.*

Textural description	**Textural size classes**
Well sorted, Near symmetrical skewed, Mesokurtic	Sand = 100 000%Fines = 0.000% Silt = 0.000%Clay = 0.000%
Moment method parameters (µm)	**Graphical method parameters. After Folk (1980) (ϕ)**
Mean = 238.635 Standard deviation (sd) = 77.071 Skewness (Sk_I)= 0.804 Kurtosis (K_G) = 3.591	Mean (M_z) = 2.147 d (0.5) = 2.146 Sorting (σ_I) = 0.476 Skewness (Sk_I) = -0.001 Kurtosis (K_G) = 0.977
Wentworth size class Fine sand	Mean (mm) = 0.226 Mean (µm) = 225.778

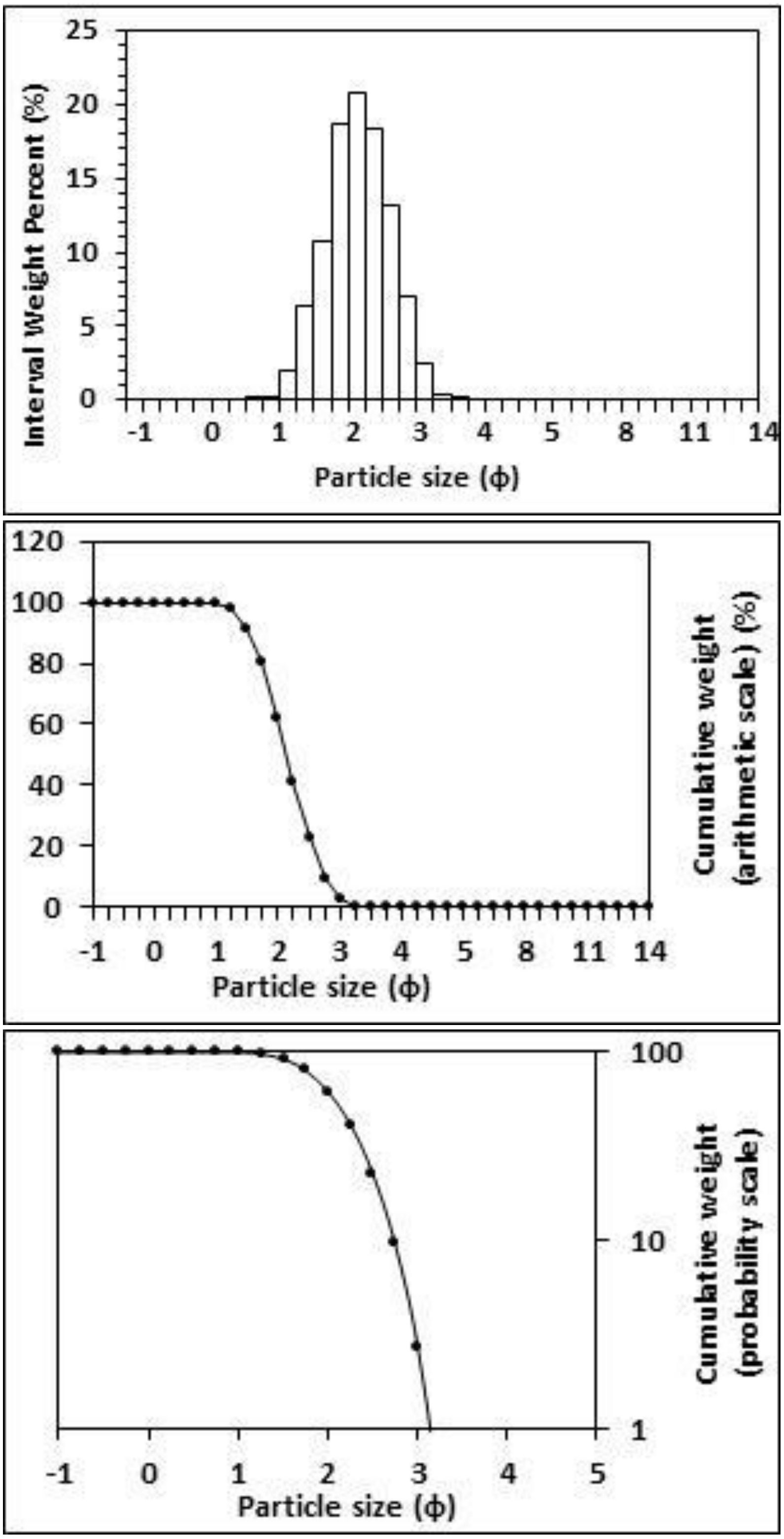

Figures II.10, II.1 and II.2: Histogram of grain size distribution and cumulative frequency graphs (arithmetic scale and probability scale) for sample 35: High intertidal zone, southern transect, Northern Ngarunui Beach. Sample collected on the 20th of July, 2014.

Table II.5: *Graphical and statistical parameters, textural description and size classes for sample 5: High intertidal zone, northern transect, Northern Ngarunui Beach. Sample collected on the 20th of July, 2014.*

Textural description	**Textural size classes**
Well sorted, Near symmetrical skewed, Mesokurtic	Sand = 100 000%Fines = 0.000% Silt = 0.000%Clay = 0.000%
Moment method parameters (µm)	**Graphical method parameters. After Folk (1980) (ϕ)**
Mean = 255.345 Standard deviation (sd) = 79.608 Skewness (Sk_I)= 0.757 Kurtosis (K_G) 3.438	Mean (M_z) = 2.040 d(0.5) = 2.044 Sorting (σ_I) = 0.454 Skewness (Sk_I) = -0.010 Kurtosis (K_G) = 0.961 Mean (mm) = 0.243 Mean (µm) = 243.137
Wentworth size class Fine sand	

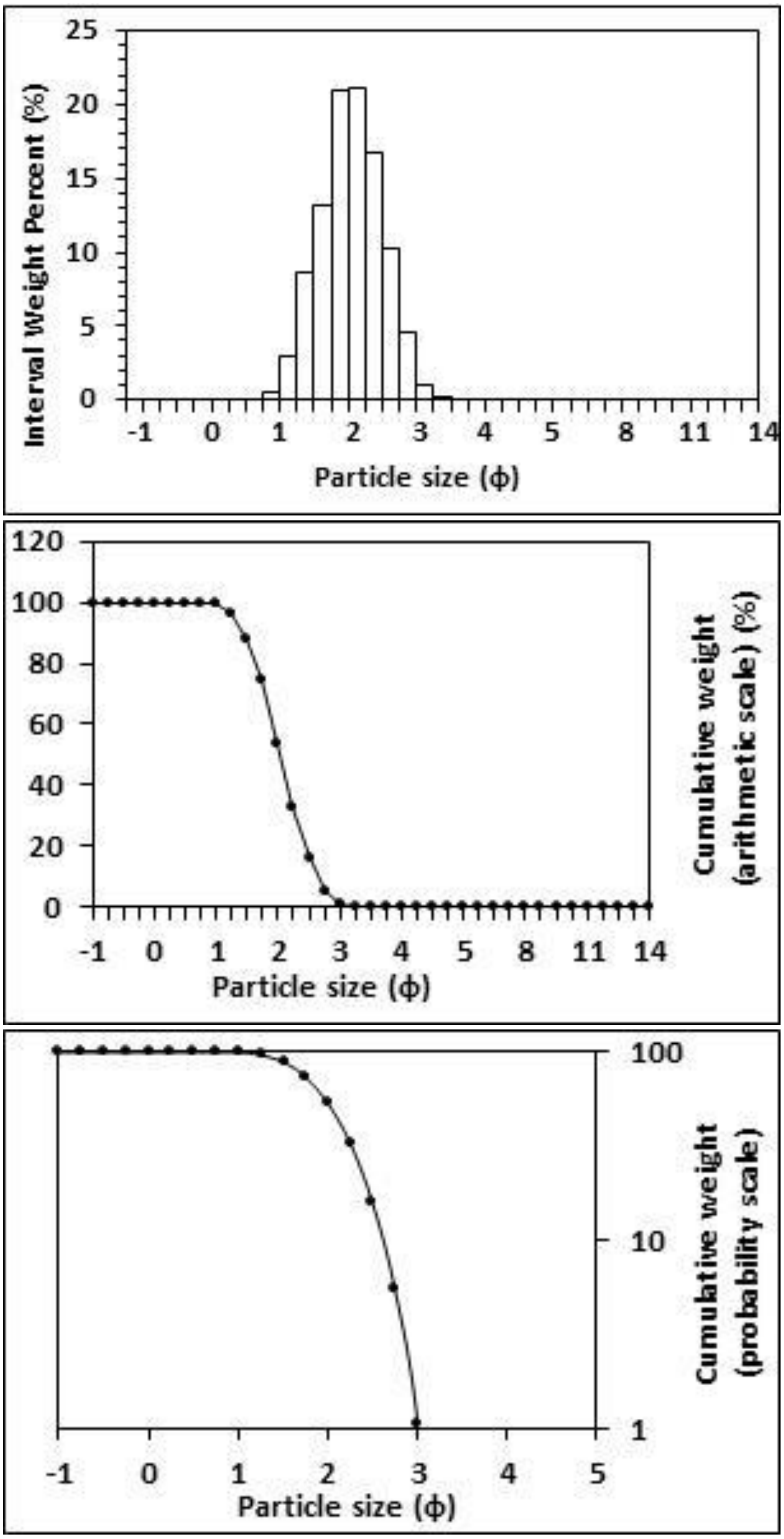

Figures II.13, II.4 and II.5: Histogram of grain size distribution and cumulative frequency graphs (arithmetic scale and probability scale) for sample 5: High intertidal zone, northern transect, Northern Ngarunui Beach. Sample collected on the 20th of July, 2014.

Table II.6: *Graphical and statistical parameters, textural description and size classes for sample 6: Mid intertidal zone, southern transect, Northern Ngarunui Beach. Sample collected on the 20th of July, 2014.*

Textural description	**Textural size classes**
Moderately well sorted, Near symmetrical skewed, Mesokurtic	Sand = 100 000%Fines = 0.000% Silt = 0.000%Clay = 0.000%
Moment method parameters (µm) Mean = 294.170 Standard deviation (sd) = 102.236 Skewness (Sk_I)= 0.800 Kurtosis (K_G) = 3.464	**Graphical method parameters. After Folk (1980) (ϕ)** Mean (M_z) = 1.855 d(0.5) = 1.854 Sorting (σ_I) = 0.512 Skewness (Sk_I) = 0.005 Kurtosis (K_G) = 0.960 Mean (mm) = 0.276 Mean (µm) = 276.386
Wentworth size class Medium sand	

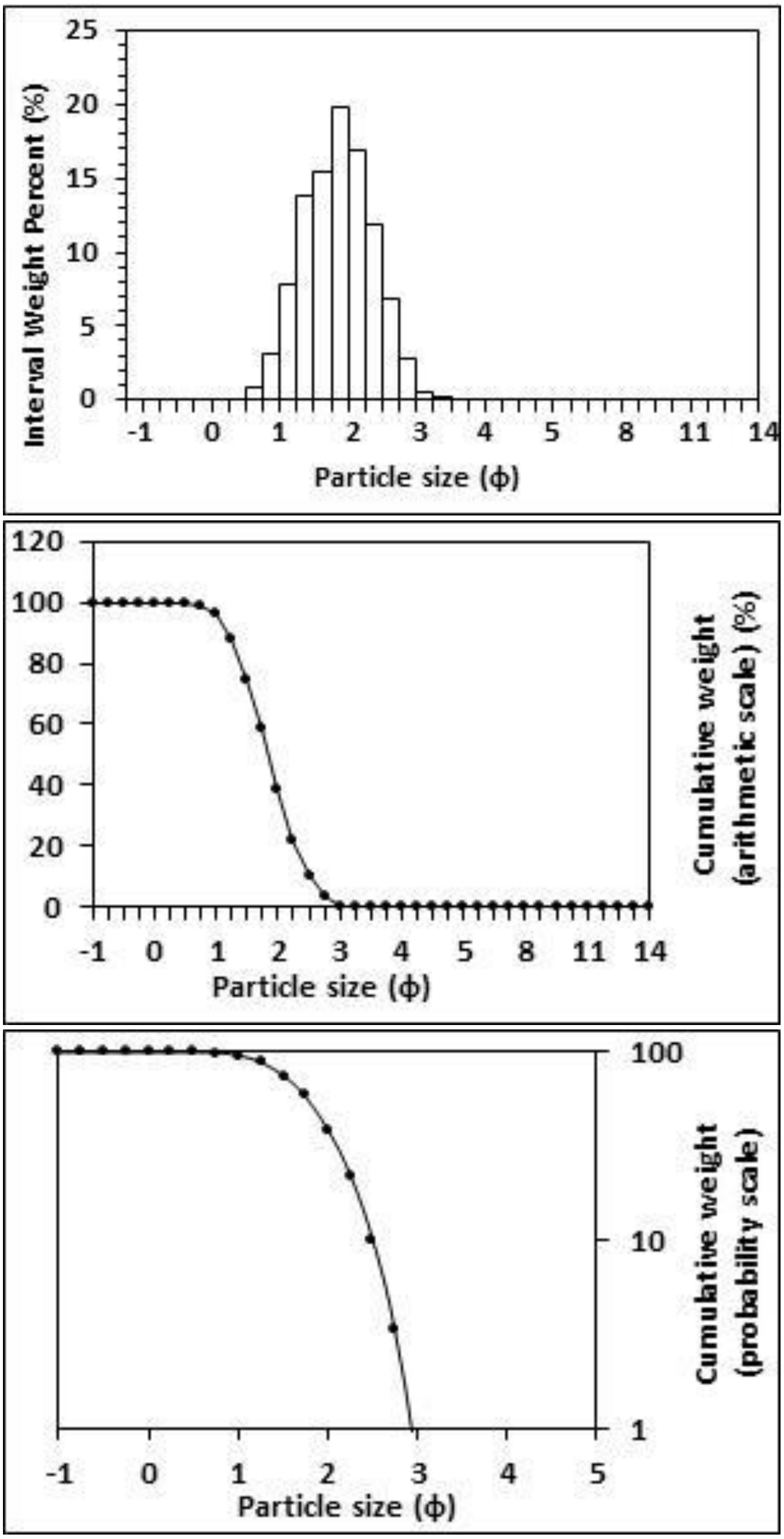

Figures II.16, II.17 and II.18: Histogram of grain size distribution and cumulative frequency graphs (arithmetic scale and probability scale) for sample 6: Mid intertidal zone, southern transect, Northern Ngarunui Beach. Sample collected on the 20th of July, 2014.

Table II.7: *Graphical and statistical parameters, textural description and size classes for sample 7: High intertidal zone, eastern transect, Wainamu Beach. Sample collected on the 16th of July, 2014.*

Textural description	**Textural size classes**
Moderately well sorted, Near symmetrical skewed, Mesokurtic	Sand = 100 000%Fines = 0.000% Silt = 0.000%Clay = 0.000%
Moment method parameters (µm) Mean = 207.341 Standard deviation (sd) = 73.749 Skewness (Sk_I)= 0.834 Kurtosis (K_G) = 3.552	**Graphical method parameters. After Folk (1980) (ϕ)** Mean (M_z) = 2.364 d(0.5) = 2.364 Sorting (σ_I) = 0.521 Skewness (Sk_I) = 0.003 Kurtosis (K_G) = 0.959 Mean (mm) = 0.194 Mean (µm) = 194.309
Wentworth size class Fine sand	

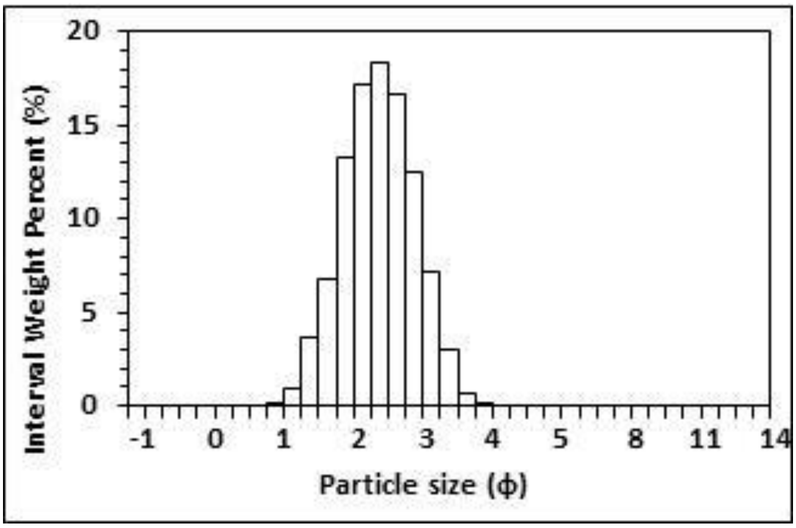

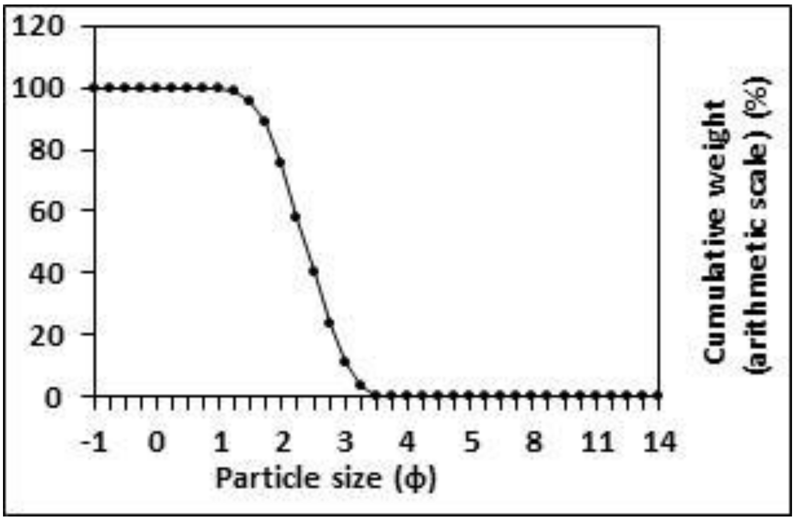

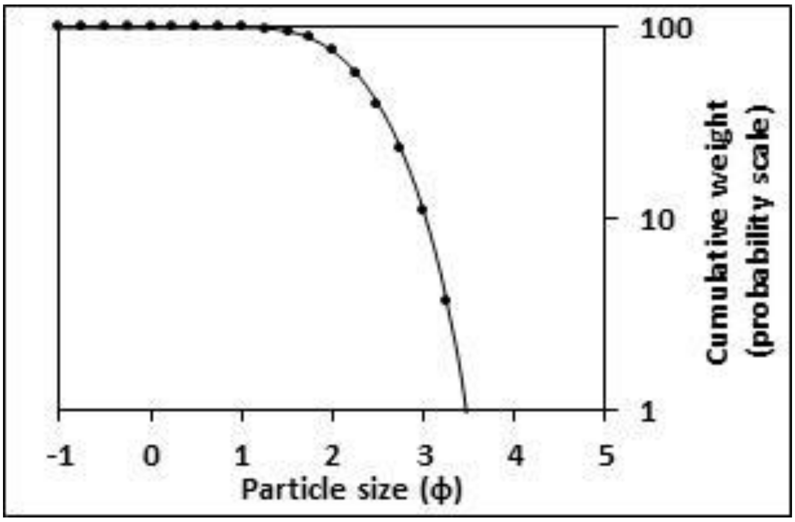

Figures II.19, II.20 and II.21: Histogram of grain size distribution and cumulative frequency graphs (arithmetic scale and probability scale) for sample 7: High intertidal zone, eastern transect, Wainamu Beach. Sample collected on the 16th of July, 2014.

Table II.8: *Graphical and statistical parameters, textural description and size classes for sample 8: Mid intertidal zone, western transect, Wainamu Beach. Sample collected on the 16th of July, 2014.*

Textural description	**Textural size classes**
Moderately well sorted, Near symmetrical skewed, Mesokurtic	Sand = 100 000%Fines = 0.000% Silt = 0.000%Clay = 0.000%
Moment method parameters (µm)	**Graphical method parameters. After Folk (1980) (ϕ)**
Mean = 190.102 Standard deviation (sd) = 68.825 Skewness (Sk_I)= 0.889 Kurtosis (K_G) = 3.739	Mean (M_z) = 2.491 d(0.5) = 2.494 Sorting (σ_I) = 0.527 Skewness (Sk_I) = -0.008 Kurtosis (K_G) = 0.951 Mean (mm) = 0.178 Mean (µm) = 177.892
Wentworth size class Fine sand	

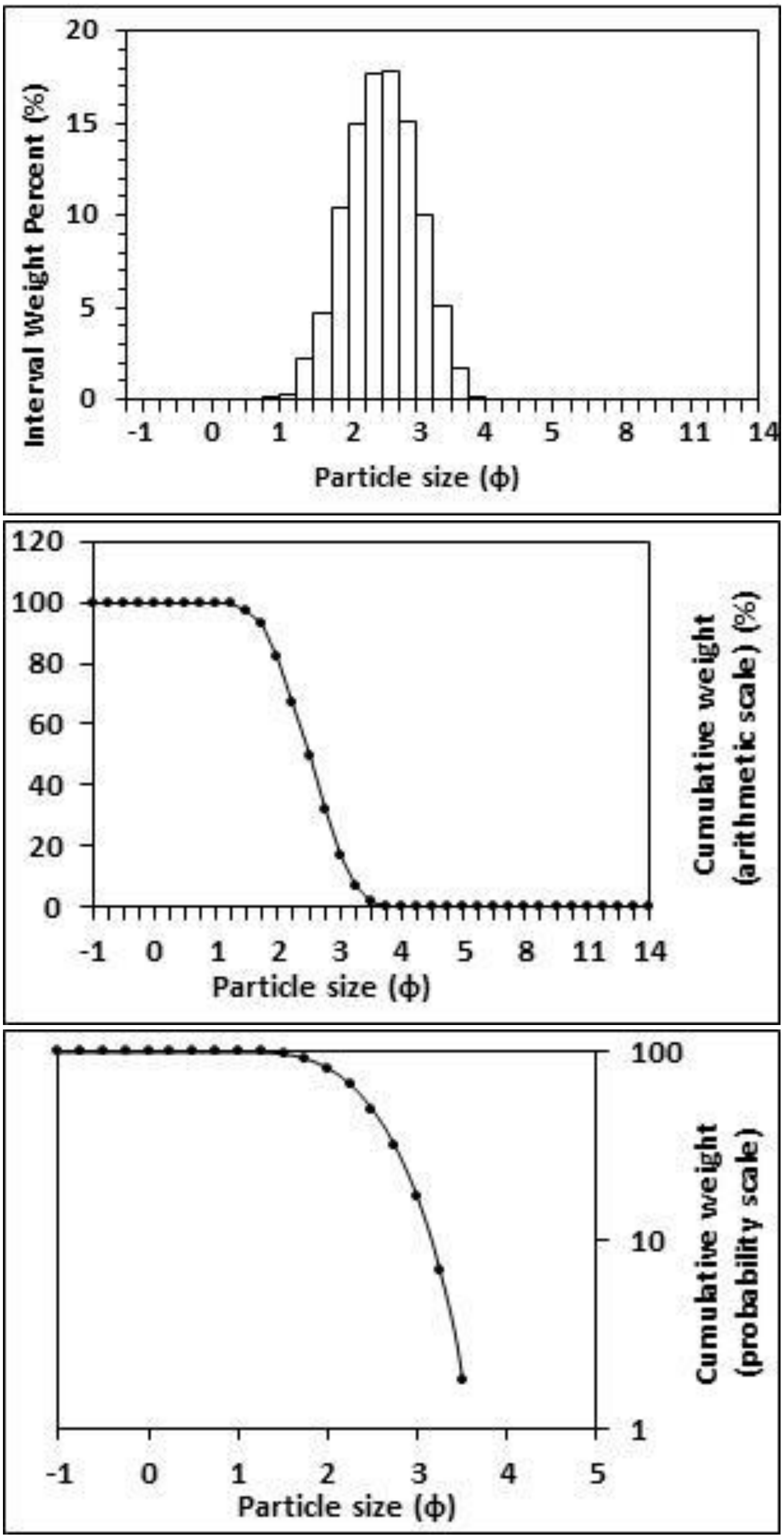

Figures II.22, II.23 and II.24: Histogram of grain size distribution and cumulative frequency graphs (arithmetic scale and probability scale) for sample 8: Mid intertidal zone, western transect, Wainamu Beach. Sample collected on the 16th of July, 2014.

Table II.9: *Graphical and statistical parameters, textural description and size classes for sample 9: Low intertidal zone, mid transect, Northern Ngarunui Beach. Sample collected on the 6th of February, 2015.*

Textural description	**Textural size classes**
Moderately well sorted, Near symmetrical skewed, Mesokurtic	Sand = 100 000%Fines = 0.000% Silt = 0.000%Clay = 0.000%
Moment method parameters **(µm)** Mean = 276.703 Standard deviation (sd) = 97.981 Skewness (Sk_I)= 0.840 Kurtosis (K_G) = 3.602	**Graphical method parameters.** **After Folk (1980) (ϕ)** Mean (M_z) = 1.943 d(0.5) = 1.945 Sorting (σ_I) = 0.519 Skewness (Sk_I) = -0.007 Kurtosis (K_G) = 0.956 Mean (mm) = 0.260 Mean (µm) = 260.061
Wentworth size class Medium sand	

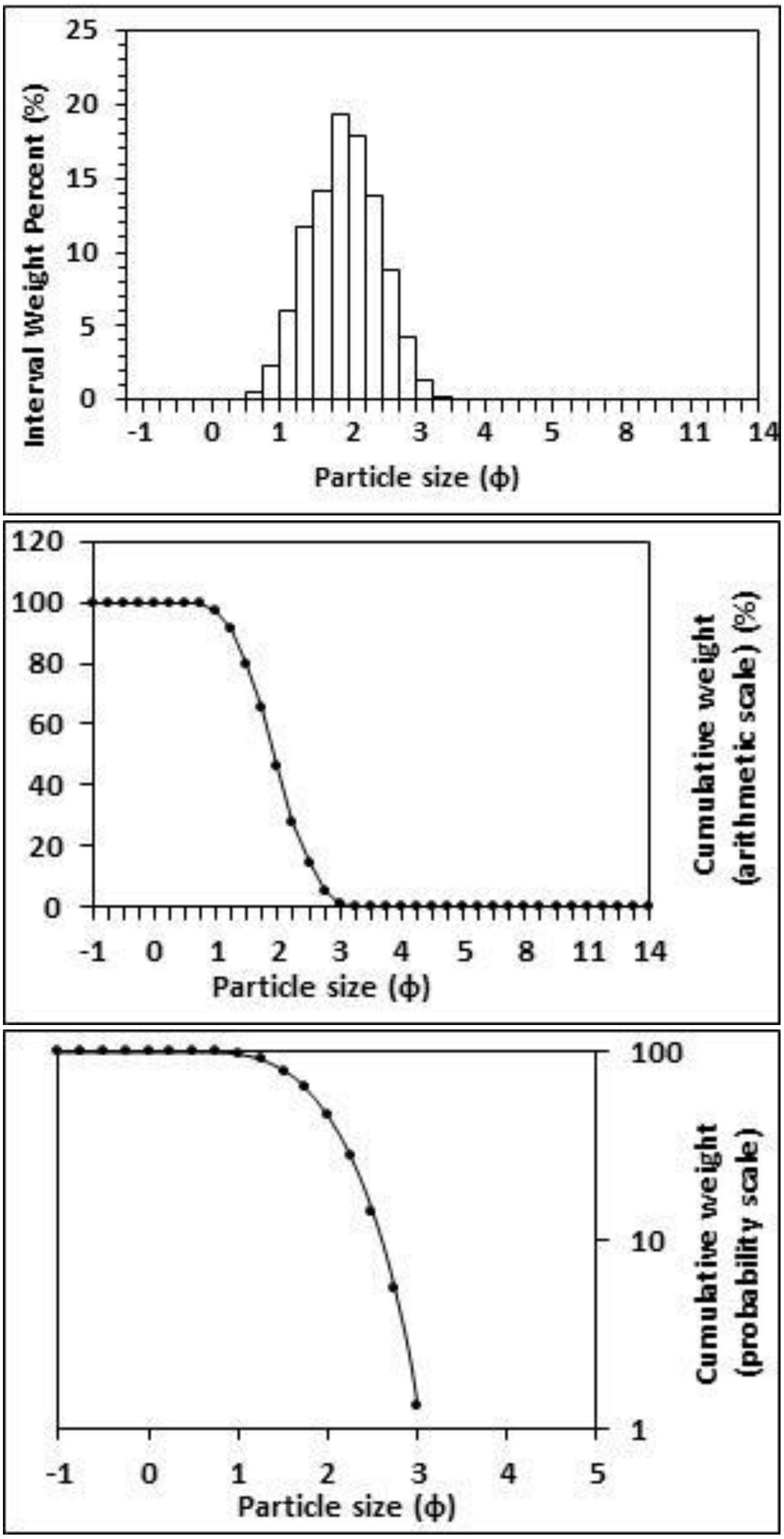

Figures II.25, II.26 and II.27: Histogram of grain size distribution and cumulative frequency graphs (arithmetic scale and probability scale) for sample 9: Low intertidal zone, mid transect, Northern Ngarunui Beach. Sample collected on the 6th of February, 2015.

Table II.10: *Graphical and statistical parameters, textural description and size classes for sample 10: High intertidal zone, mid transect, Northern Ngarunui Beach. Sample collected on the 6th of February, 2015.*

Textural description	**Textural size classes**
Moderately well sorted, Near symmetrical skewed, Mesokurtic	Sand = 100 000%Fines = 0.000% Silt = 0.000%Clay = 0.000%
Moment method parameters (µm) Mean = 240.095 Standard deviation (sd) = 84.829 Skewness (Sk_I)= 0.822 Kurtosis (K_G) = 3.521 **Wentworth size class** Fine sand	**Graphical method parameters. After Folk (1980) (ϕ)** Mean (M_z) = 2.151 d(0.5) = 2.150 Sorting (σ_I) = 0.518 Skewness (Sk_I) = -0.001 Kurtosis (K_G) = 0.959 Mean (mm) = 0.225 Mean (µm) = 225.231

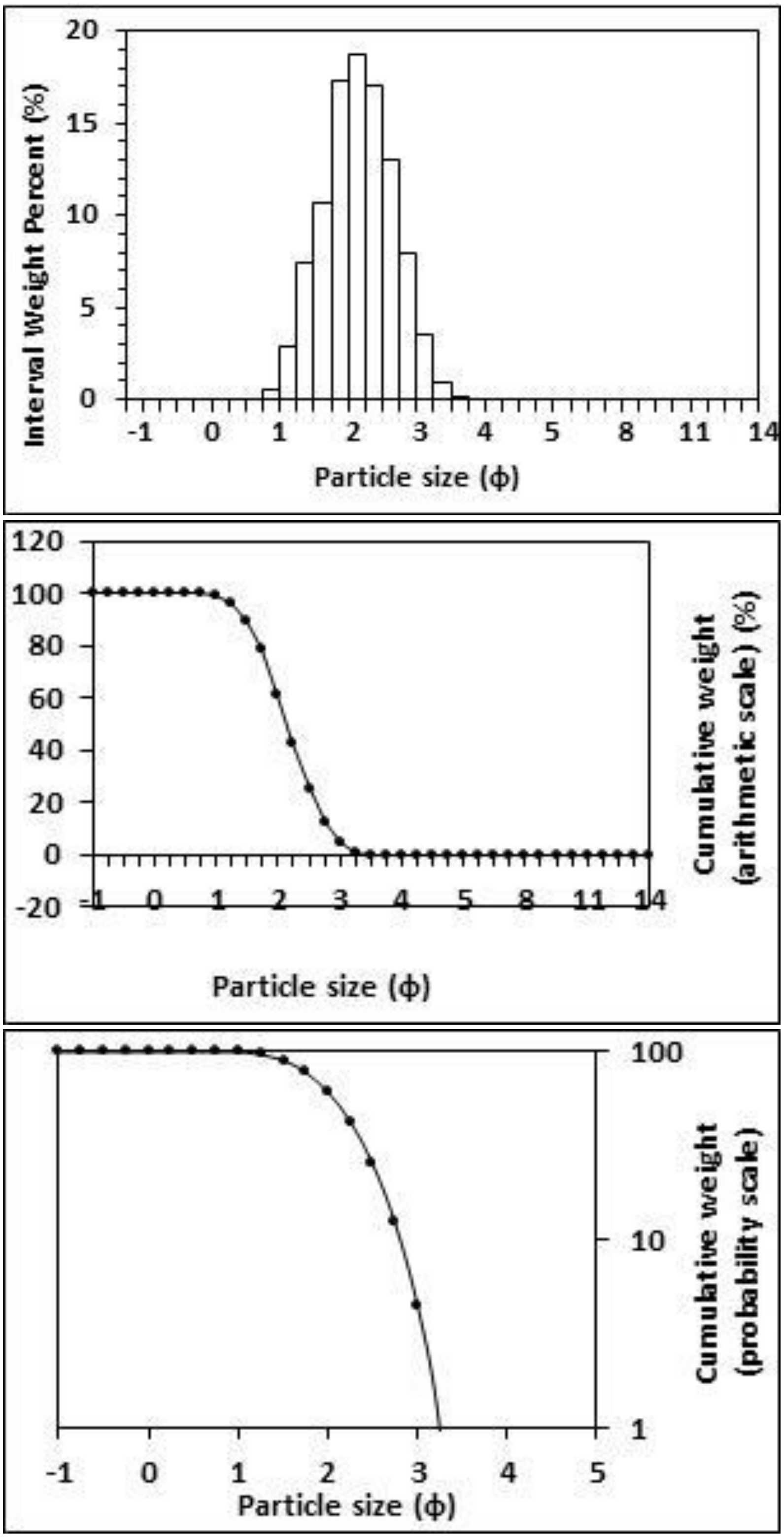

Figures II.28, II.29 and II.30: Histogram of grain size distribution and cumulative frequency graphs (arithmetic scale and probability scale) for sample 10: High intertidal zone, mid transect, Northern Ngarunui Beach. Sample collected on the 6th of February, 2015.

Table II.11: *Graphical and statistical parameters, textural description and size classes for sample 11: High intertidal zone, southern transect, Northern Ngarunui Beach. Sample collected on the 6th of February, 2015.*

Textural description	**Textural size classes**
Moderately well sorted, Near symmetrical skewed, Mesokurtic	Sand = 100 000%Fines = 0.000% Silt = 0.000%Clay = 0.000%
Moment method parameters (µm)	**Graphical method parameters. After Folk (1980) (ϕ)**
Mean = 260.571 Standard deviation (sd) = 91.125 Skewness (Sk_I)= 0.818 Kurtosis (K_G) = 3.521	Mean (M_z) = 2.034 d(0.5) = 2.031 Sorting (σ_I) = 0.512 Skewness (Sk_I) = 0.007 Kurtosis (K_G) = 0.955 Mean (mm) = 0.244 Mean (µm) = 244.151
Wentworth size class Fine sand	

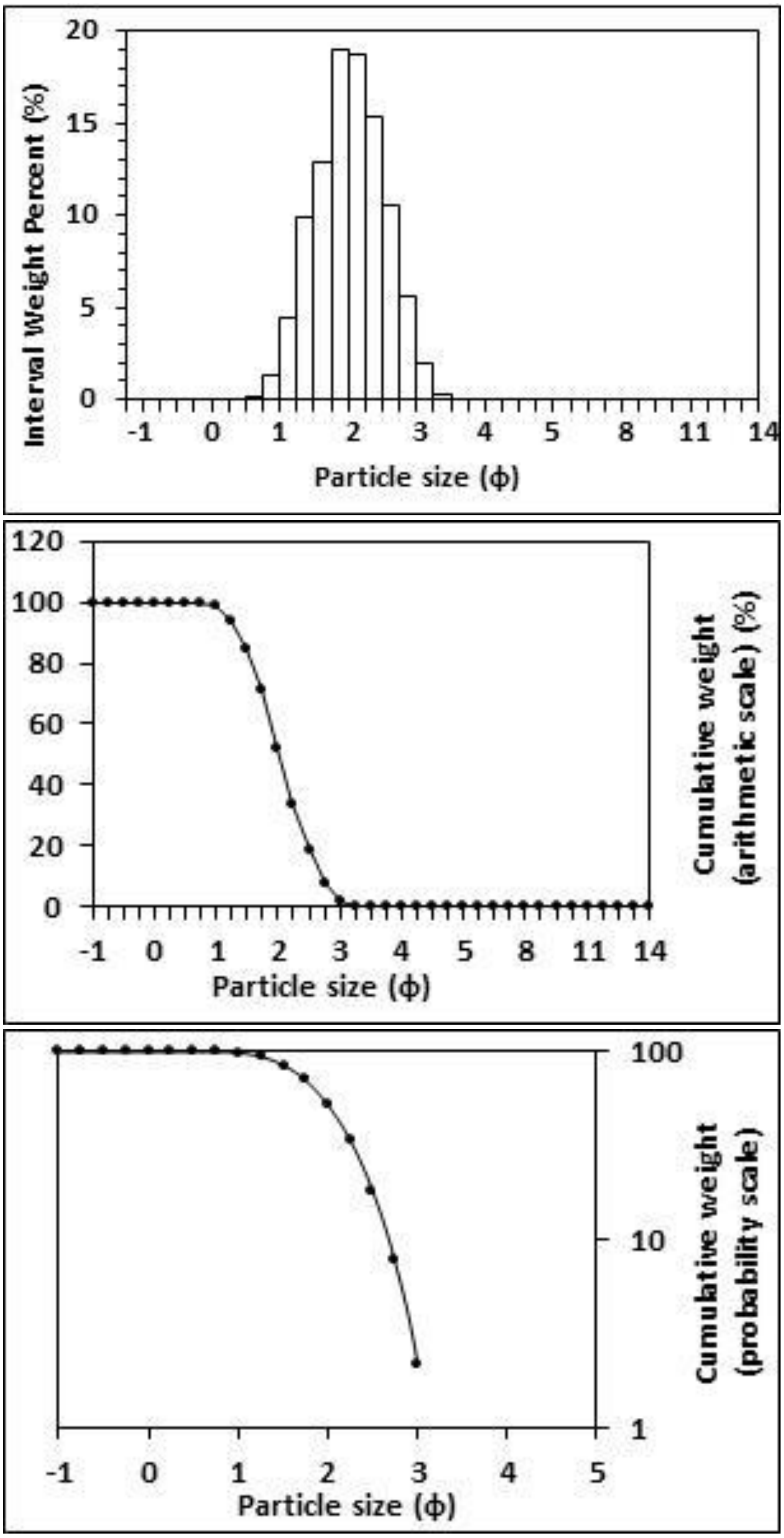

Figures II.31, II.32 and II.33: Histogram of grain size distribution and cumulative frequency graphs (arithmetic scale and probability scale) for sample 11: High intertidal zone, southern transect, Northern Ngarunui Beach. Sample collected on the 6th of February, 2015.

Table II.12: *Graphical and statistical parameters, textural description and size classes for sample 12: High intertidal zone, northern transect, Northern Ngarunui Beach. Sample collected on the 6th of February, 2015.*

Textural description	**Textural size classes**
Moderately well sorted, Near symmetrical skewed, Mesokurtic	Sand = 100 000%Fines = 0.000% Silt = 0.000%Clay = 0.000%
Moment method parameters (µm)	**Graphical method parameters. After Folk (1980) (ϕ)**
Mean = 210.810 Standard deviation (sd) = 75.293 Skewness (Sk_I)= 0.847 Kurtosis (K_G) = 3.600	Mean (M_z) = 2.341 d(0.5) = 2.341 Sorting (σ_I) = 0.522 Skewness (Sk_I) = 0.005 Kurtosis (K_G) = 0.955 Mean (mm) = 0.197 Mean (µm) = 197.326
Wentworth size class Fine sand	

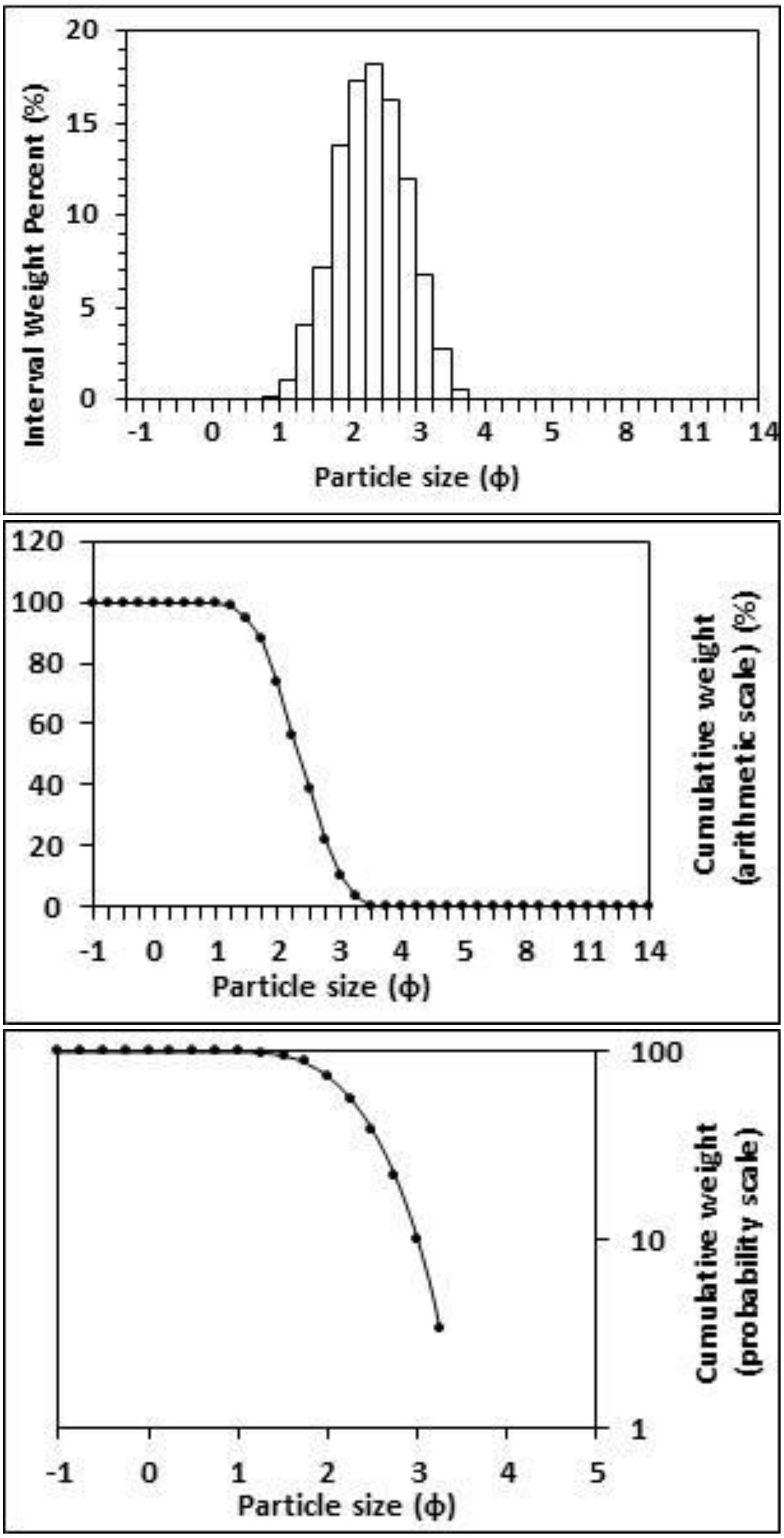

Figures II.34, II.35 and II.36: Histogram of grain size distribution and cumulative frequency graphs (arithmetic scale and probability scale) for sample 12: High intertidal zone, northern transect, Northern Ngarunui Beach. Sample collected on the 6th of February, 2015.

Table II.13: *Graphical and statistical parameters, textural description and size classes for sample 13: Mid intertidal zone, mid transect, Northern Ngarunui Beach. Sample collected on the 6th of February, 2015.*

Textural description	**Textural size classes**
Well sorted, Near symmetrical skewed, Mesokurtic	Sand = 100 000%Fines = 0.000% Silt = 0.000%Clay = 0.000%
Moment method parameters (μm) Mean = 266.141 Standard deviation (sd) = 85.526 Skewness (Sk_I)= 0.785 Kurtosis (K_G) = 3.529	**Graphical method parameters. After Folk (1980) (ϕ)** Mean (M_z) = 1.989 d(0.5) = 1.987 Sorting (σ_I) = 0.463 Skewness (Sk_I) = 0.003 Kurtosis (K_G) = 0.943 Mean (mm) = 0.252 Mean (μm) = 251.863
Wentworth size class Medium sand	

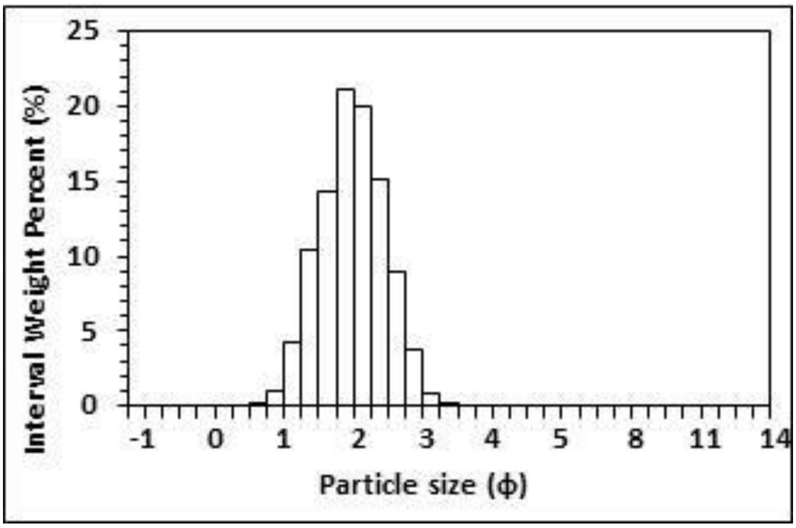

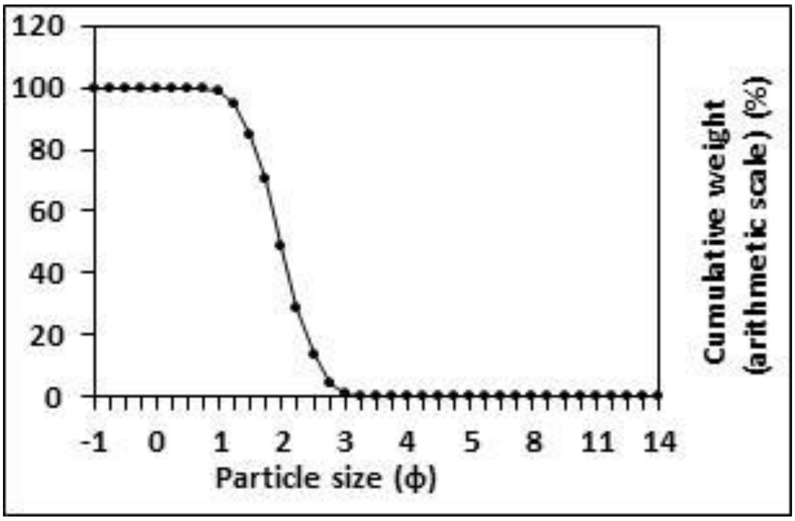

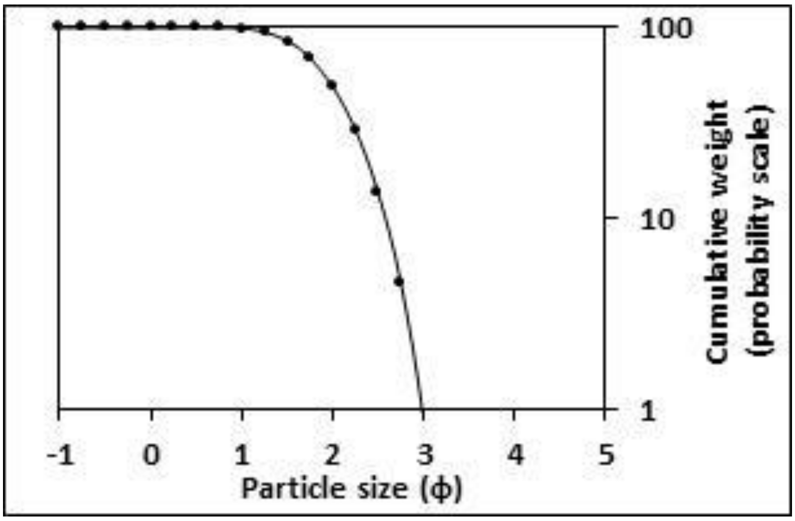

Figures II.37, II.38 and II.39: Histogram of grain size distribution and cumulative frequency graphs (arithmetic scale and probability scale) for sample 13: Mid intertidal zone, mid transect, Northern Ngarunui Beach. Sample collected on the 6th of February, 2015.

Table II.14: *Graphical and statistical parameters, textural description and size classes for sample 14: High intertidal zone, northern transect, Northern Ngarunui Beach. Sample collected on the 27th of November, 2014.*

Textural description	**Textural size classes**
Well sorted, Near symmetrical skewed, Mesokurtic	Sand = 100 000%Fines = 0.000% Silt = 0.000%Clay = 0.000%
Moment method parameters (µm) Mean = 251.706 Standard deviation (sd) = 79.334 Skewness (Sk_I)= 0.775 Kurtosis (K_G) = 3.491	**Graphical method parameters. After Folk (1980) (ϕ)** Mean (M_z) = 2.064 d(0.5) = 2.067 Sorting (σ_I) = 0.462 Skewness (Sk_I) = -0.006 Kurtosis (K_G) = 0.970 Mean (mm) = 0.239 Mean (µm) = 239.143
Wentworth size class Fine sand	

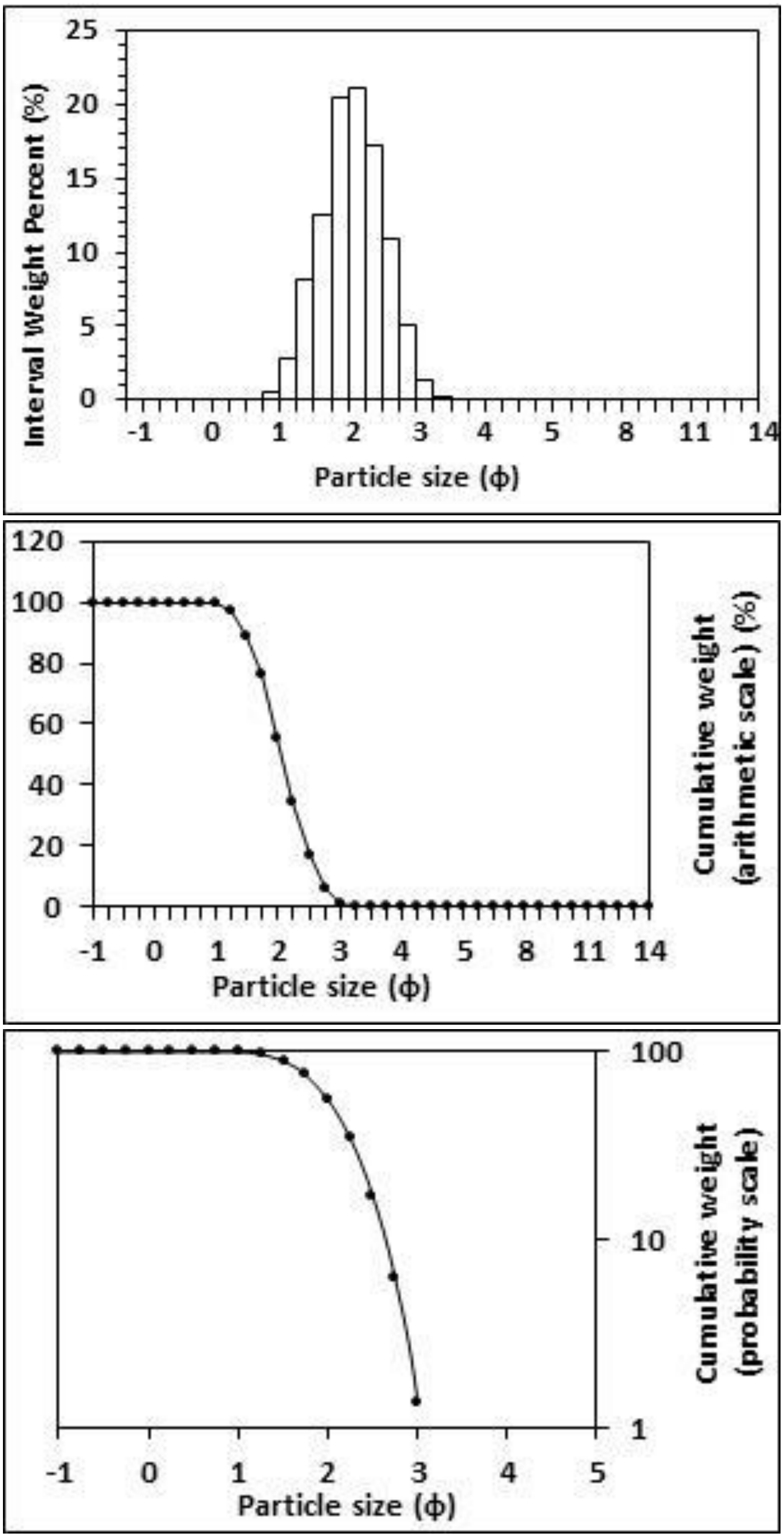

Figures II.40, II.41 and II.42: Histogram of grain size distribution and cumulative frequency graphs (arithmetic scale and probability scale) for sample 14: High intertidal zone, northern transect, Northern Ngarunui Beach. Sample collected on the 27th of November, 2014.

Table II.15: *Graphical and statistical parameters, textural description and size classes for sample 15: Mid intertidal zone, northern transect, Northern Ngarunui Beach. Sample collected on the 27th of November, 2014.*

Textural description	**Textural size classes**
Moderately well sorted, Near symmetrical skewed, Mesokurtic	Sand = 100 000%Fines = 0.000% Silt = 0.000%Clay = 0.000%
Moment method parameters (µm) Mean = 315.833 Standard deviation (sd) = 111.146 Skewness (Sk_I)= 0.836 Kurtosis (K_G) = 3.576	**Graphical method parameters. After Folk (1980) (ϕ)** Mean (M_z) = 1.755 d(0.5) = 1.756 Sorting (σ_I) = 0.513 Skewness (Sk_I) = -0.001 Kurtosis (K_G) = 0.950 Mean (mm) = 0.296 Mean (µm) = 296.226
Wentworth size class Medium sand	

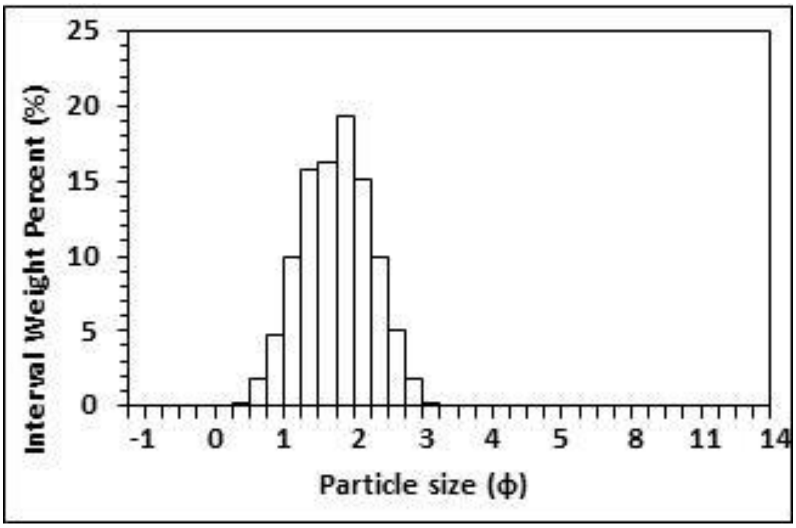

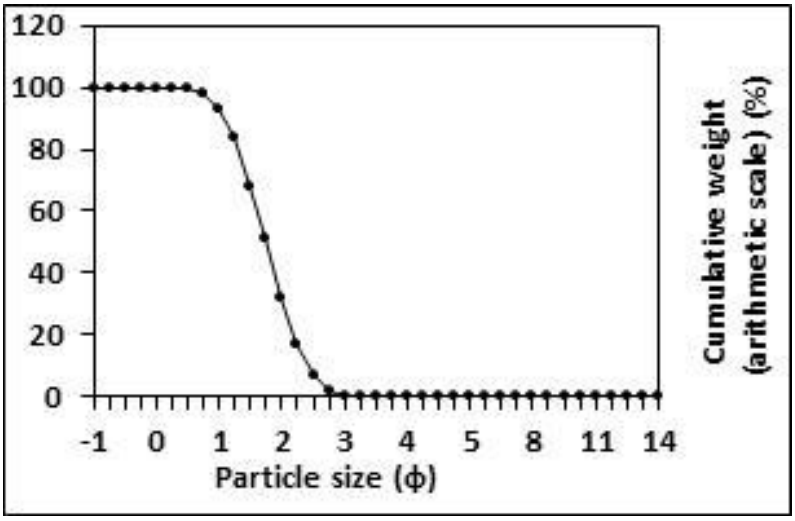

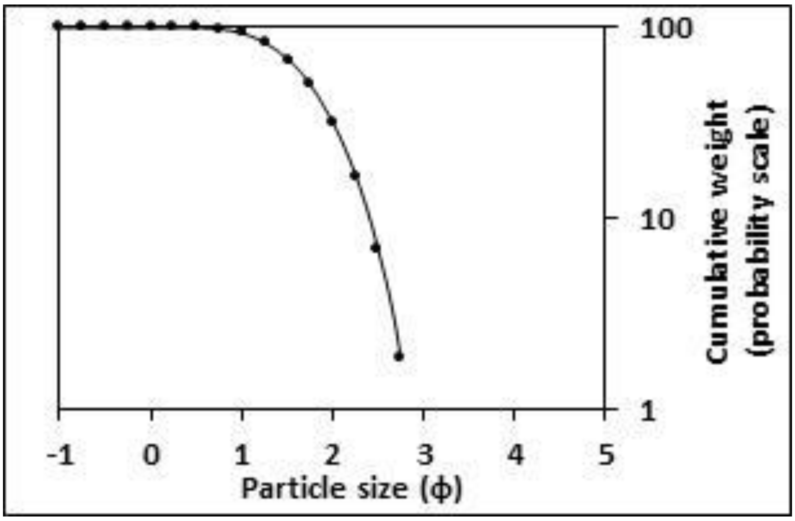

Figures II.43, II.44 and II.45: Histogram of grain size distribution and cumulative frequency graphs (arithmetic scale and probability scale) for sample 15: Mid intertidal zone, northern transect, Northern Ngarunui Beach. Sample collected on the 27th of November, 2014.

Table II.16: *Graphical and statistical parameters, textural description and size classes for sample 16: High intertidal zone, southern transect, Northern Ngarunui Beach. Sample collected on the 27th of November, 2014.*

Textural description	**Textural size classes**
Moderately well sorted, Near symmetrical skewed, Mesokurtic	Sand = 100 000%Fines = 0.000% Silt = 0.000%Clay = 0.000%
Moment method parameters (µm) Mean = 309.414 Standard deviation (sd) = 110.364 Skewness (Sk_I)= 0.851 Kurtosis (K_G) = 3.643	**Graphical method parameters. After Folk (1980) (ϕ)** Mean (M_z) = 1.789 d(0.5) = 1.787 Sorting (σ_I) = 0.521 Skewness (Sk_I) = 0.006 Kurtosis (K_G) = 0.951 Mean (mm) = 0.289 Mean (µm) = 289.295
Wentworth size class Medium sand	

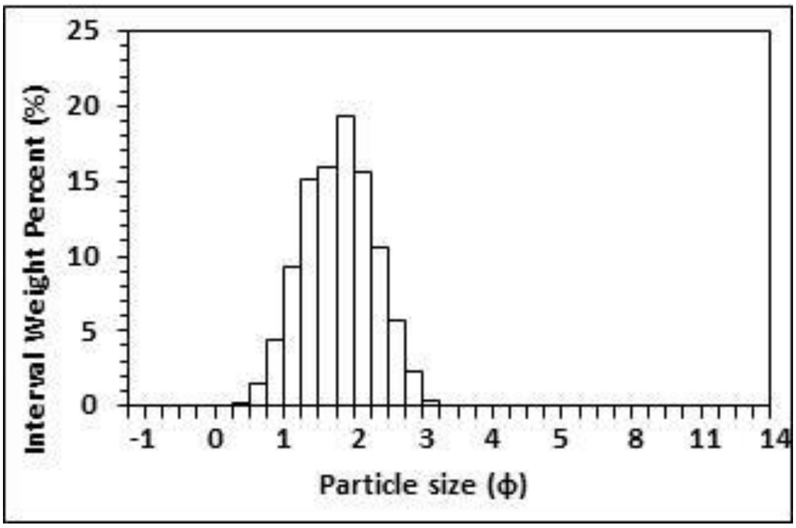

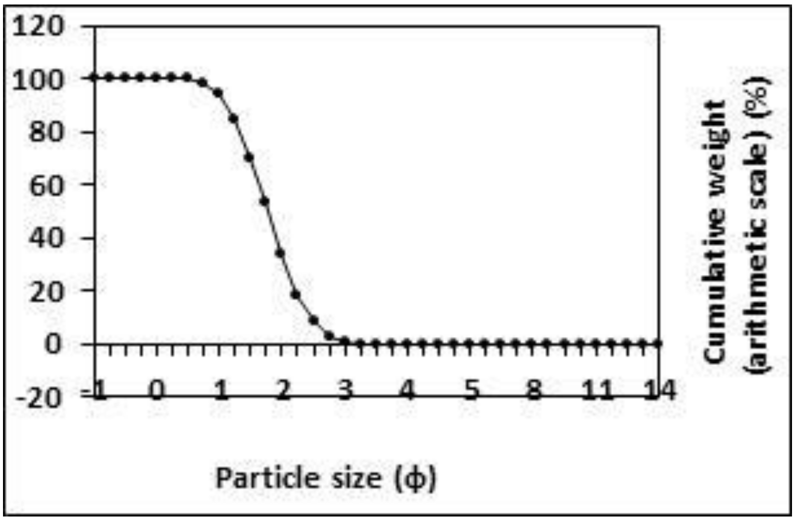

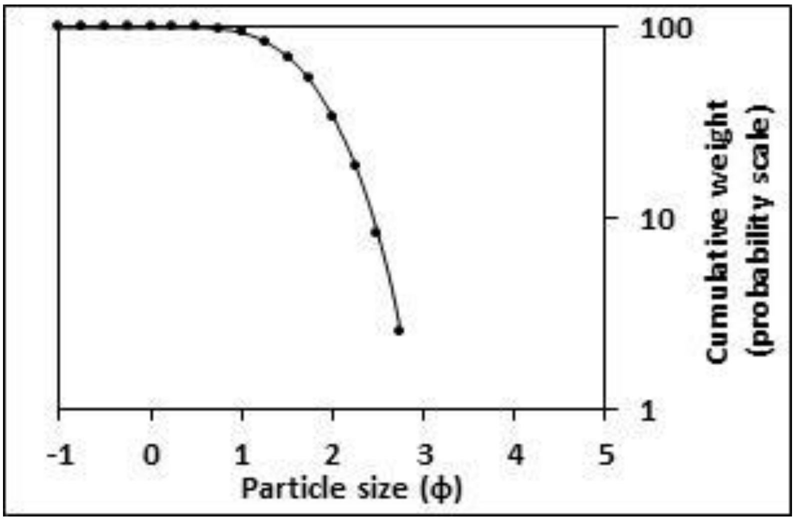

Figures II.46, II.47 and II.48: Histogram of grain size distribution and cumulative frequency graphs (arithmetic scale and probability scale) for sample 16: High intertidal zone, southern transect, Northern Ngarunui Beach. Sample collected on the 27th of November, 2014.

Table II.17: *Graphical and statistical parameters, textural description and size classes for sample 17: Mid intertidal zone, southern transect, Northern Ngarunui Beach. Sample collected on the 27th of November, 2014.*

Textural description	**Textural size classes**
Moderately well sorted, Near symmetrical skewed, Mesokurtic	Sand = 100 000%Fines = 0.000% Silt = 0.000%Clay = 0.000%
Moment method parameters (μm) Mean = 333.022 Standard deviation (sd) = 121.209 Skewness (Sk_I)= 0.851 Kurtosis (K_G) = 0.889	**Graphical method parameters. After Folk (1980) (ϕ)** Mean (M_z) = 1.681 d(0.5) = 1.685 Sorting (σ_I) = 0.529 Skewness (Sk_I) = -0.011 Kurtosis (K_G) = 0.952 Mean (mm) = 0.312 Mean (μm) = 311.765
Wentworth size class Medium sand	

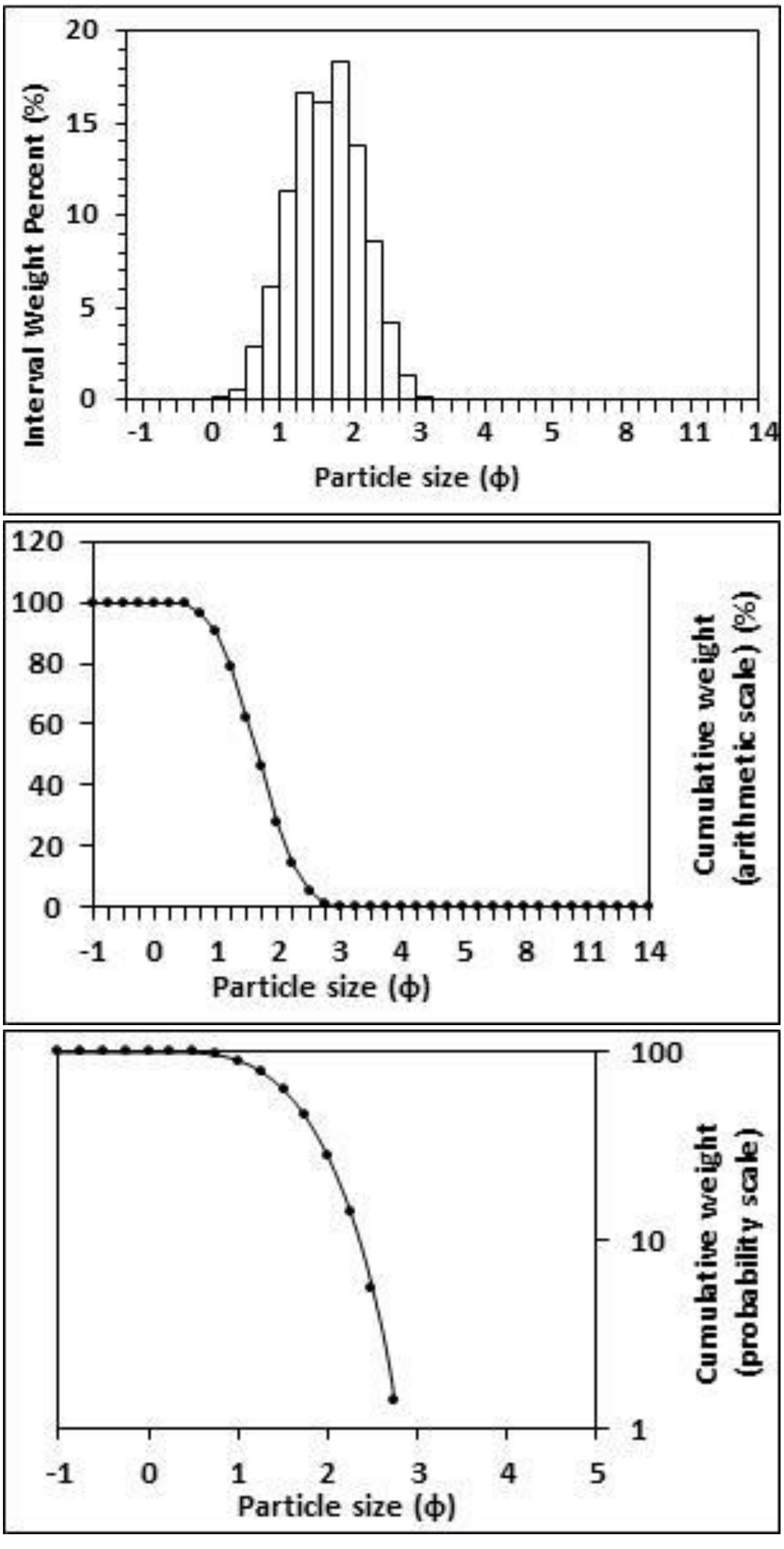

Figures II.49, II.50 and II.51: Histogram of grain size distribution and cumulative frequency graphs (arithmetic scale and probability scale) for sample 17: Mid intertidal zone, southern transect, Northern Ngarunui Beach. Sample collected on the 27th of November, 2014.

Table II.18: *Graphical and statistical parameters, textural description and size classes for sample 18: Low intertidal zone, mid transect, Northern Ngarunui Beach. Sample collected on the 27th of November, 2014.*

Textural description	**Textural size classes**
Moderately well sorted, Near symmetrical skewed, Mesokurtic	Sand = 100 000%Fines = 0.000% Silt = 0.000%Clay = 0.000%
Moment method parameters (µm)	**Graphical method parameters. After Folk (1980) (ϕ)**
Mean = 536.678 Standard deviation (sd) = 235.886 Skewness (Sk_I)= 1.218 Kurtosis (K_G) = 5.047	Mean (M_z) = 1.035 d(0.5) = 1.039 Sorting (σ_I) = 0.618 Skewness (Sk_I) = -0.015 Kurtosis (K_G) = 0.955 Mean (mm) = 0.488 Mean (µm) = 488.161
Wentworth size class Medium sand	

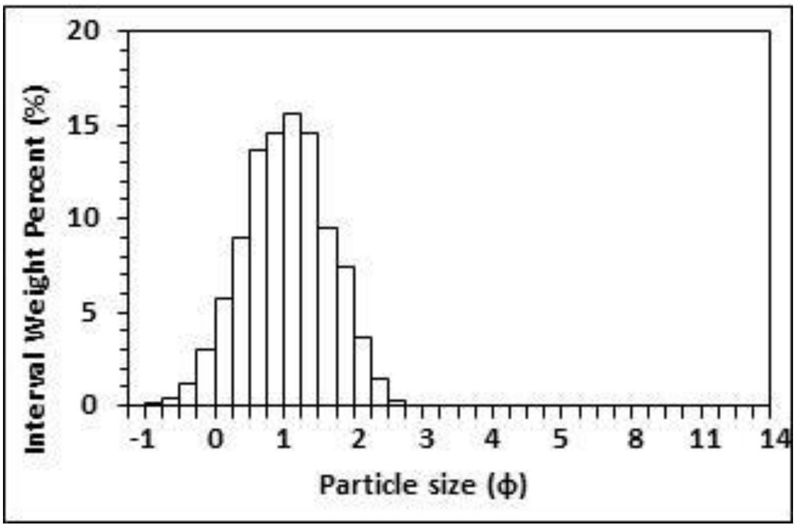

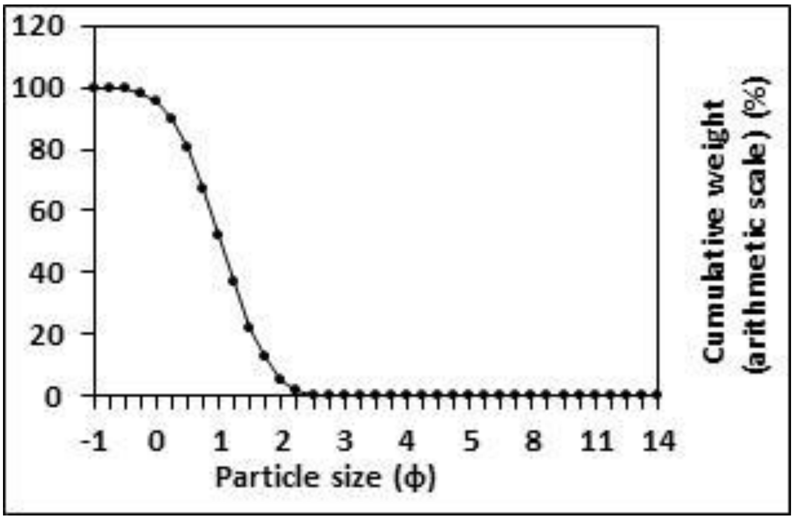

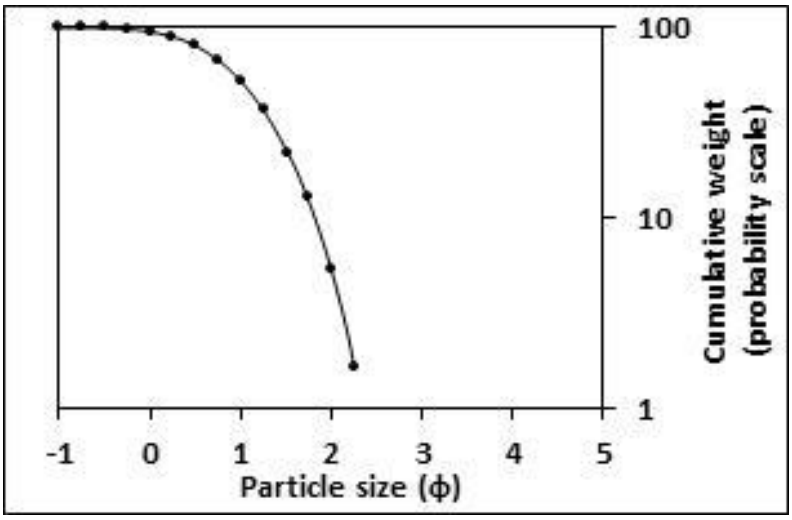

Figures II.52, II.53 and II.54: Histogram of grain size distribution and cumulative frequency graphs (arithmetic scale and probability scale) for sample 18: Low intertidal zone, mid transect, Northern Ngarunui Beach. Sample collected on the 27th of November, 2014.

Table II.19: *Graphical and statistical parameters, textural description and size classes for sample 19: Low intertidal zone, southern transect, Northern Ngarunui Beach. Sample collected on the 27th of November, 2014.*

Textural description	**Textural size classes**
Moderately well sorted, Near symmetrical skewed, Mesokurtic	Sand = 100 000%Fines = 0.000% Silt = 0.000%Clay = 0.000%
Moment method parameters (µm)	**Graphical method parameters. After Folk (1980) (ϕ)**
Mean = 349.441 Standard deviation (sd) = 144.341 Skewness (Sk_I)= 1.006 Kurtosis (K_G) = 3.999	Mean (M_z) = 1.639 d(0.5) = 1.644 Sorting (σ_I) = 0.597 Skewness (Sk_I) = -0.014 Kurtosis (K_G) = 0.959 Mean (mm) = 0.321 Mean (µm) = 320.990
Wentworth size class Medium sand	

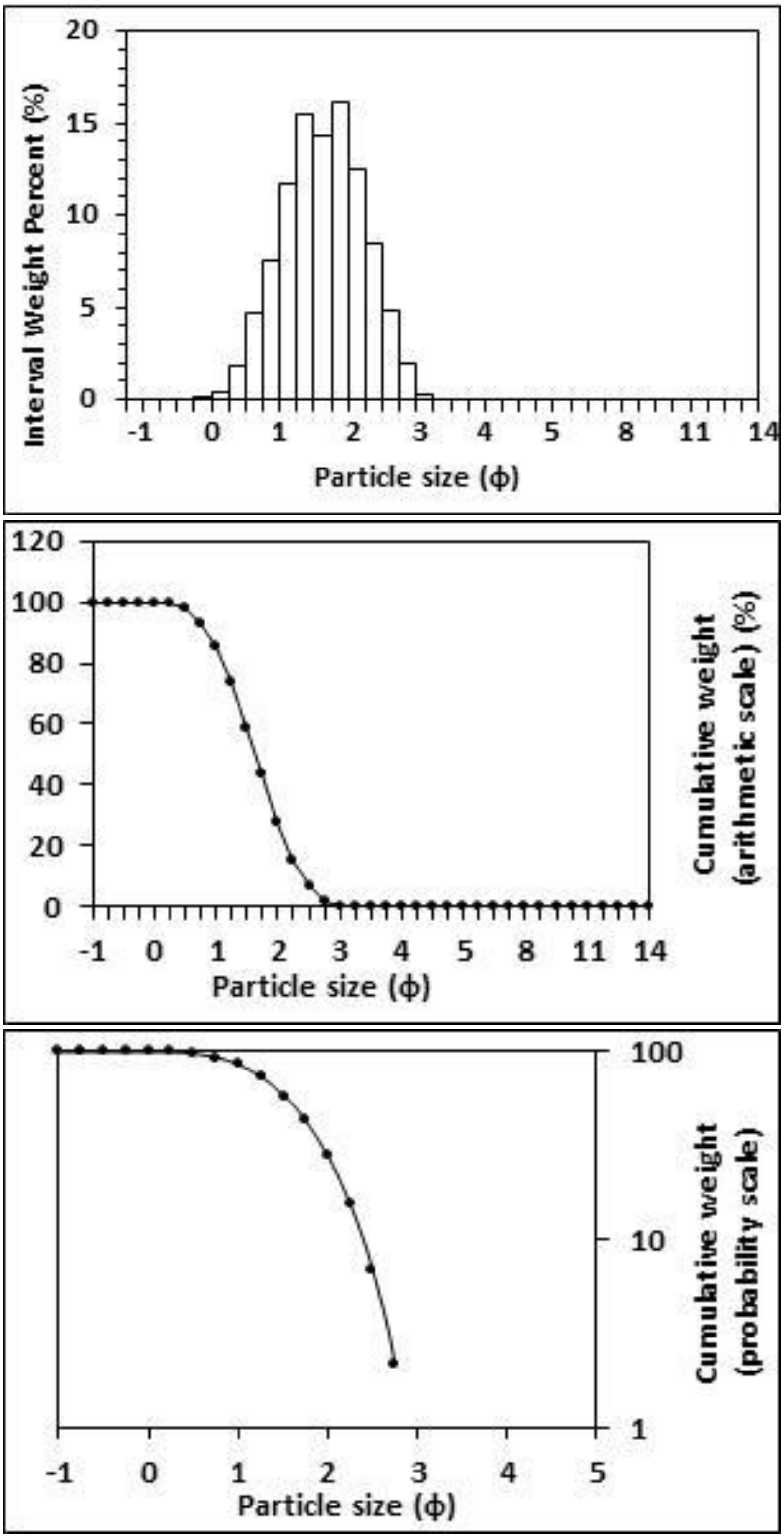

Figures II.55, II.56 and II.57: Histogram of grain size distribution and cumulative frequency graphs (arithmetic scale and probability scale) for sample 19: Low intertidal zone, southern transect, Northern Ngarunui Beach. Sample collected on the 27th of November, 2014.

Table II.20: *Graphical and statistical parameters, textural description and size classes for sample 20: Low intertidal zone, northern transect, Northern Ngarunui Beach. Sample collected on the 27th of November, 2014.*

Textural description	**Textural size classes**
Moderately well sorted, Near symmetrical skewed, Mesokurtic	Sand = 100 000%Fines = 0.000% Silt = 0.000%Clay = 0.000%
Moment method parameters (µm)	**Graphical method parameters. After Folk (1980) (ϕ)**
Mean = 369.912 Standard deviation (sd) = 201.777 Skewness (Sk_I)= 2.334 Kurtosis (K_G) = 11.905	Mean (M_z) = 1.623 d(0.5) = 1.645 Sorting (σ_I) = 0.665 Skewness (Sk_I) = -0.071 Kurtosis (K_G) = 0.995 Mean (mm) = 0.325 Mean (µm) = 324.684
Wentworth size class Medium sand	

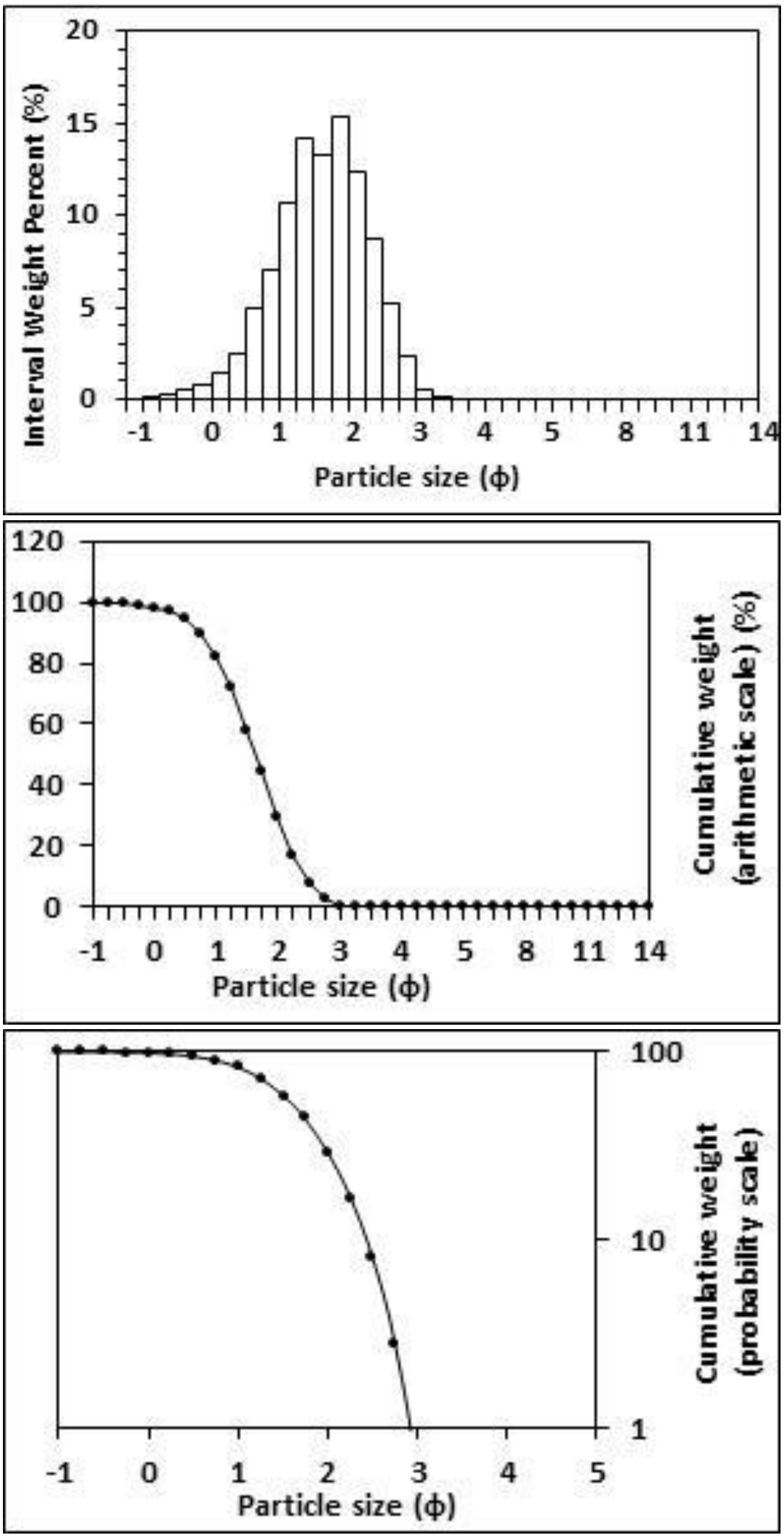

Figures II.58, II.59 and II.60: Histogram of grain size distribution and cumulative frequency graphs (arithmetic scale and probability scale) for sample 20: Low intertidal zone, northern transect, Northern Ngarunui Beach. Sample collected on the 27th of November, 2014.

Table II.21: *Graphical and statistical parameters, textural description and size classes for sample 21: Mid intertidal zone, mid transect, Northern Ngarunui Beach. Sample collected on the 27th of November, 2014.*

Textural description	**Textural size classes**
Moderately well sorted, Near symmetrical skewed, Mesokurtic	Sand = 100 000%Fines = 0.000% Silt = 0.000%Clay = 0.000%
Moment method parameters (µm) Mean = 316.207 Standard deviation (sd) = 116.182 Skewness (Sk_I)= 0.954 Kurtosis (K_G) 3.959	**Graphical method parameters. After Folk (1980) (ϕ)** Mean (M_z) = 1.762 d(0.5) = 1.765 Sorting (σ_I) = 0.530 Skewness (Sk_I) = -0.014 Kurtosis (K_G) = 0.958 Mean (mm) = 0.295 Mean (µm) = 294.838
Wentworth size class Medium sand	

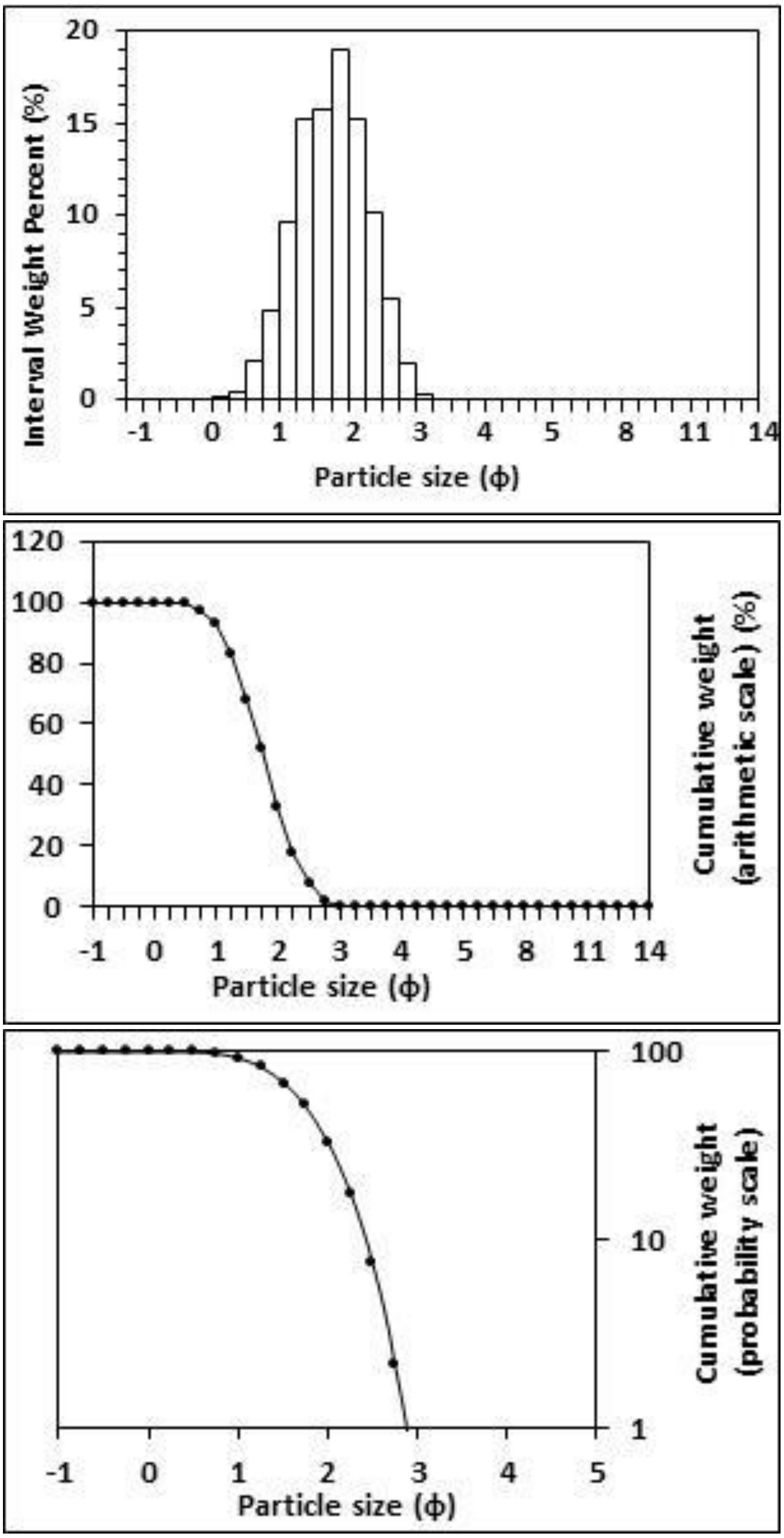

Figures II.61, II.62 and II.63: Histogram of grain size distribution and cumulative frequency graphs (arithmetic scale and probability scale) for sample 21: Mid intertidal zone, mid transect, Northern Ngarunui Beach. Sample collected on the 27th of November, 2014.

Table II.22: *Graphical and statistical parameters, textural description and size classes for sample 22: Mid intertidal zone, eastern transect, Wainamu Beach. Sample collected on the 15th of July, 2014.*

Textural description	**Textural size classes**
Moderately well sorted, Fine skewed, Mesokurtic	Sand = 95.489%, Fines = 4.511% Silt = 4.025%, Clay = 0.485%
Moment method parameters (µm) Mean = 222.871 Standard deviation (sd) = 93.536 Skewness (Sk_I)= 0.329 Kurtosis (K_G) 3.605	**Graphical method parameters. After Folk (1980) (ϕ)** Mean (M_z) = 2.248 d(0.5) = 2.230 Sorting (σ_I) = 0.607 Skewness (Sk_I) = 0.104 Kurtosis (K_G) = 1.101 Mean (mm) = 0.211 Mean (µm) = 210.531
Wentworth size class Fine sand	

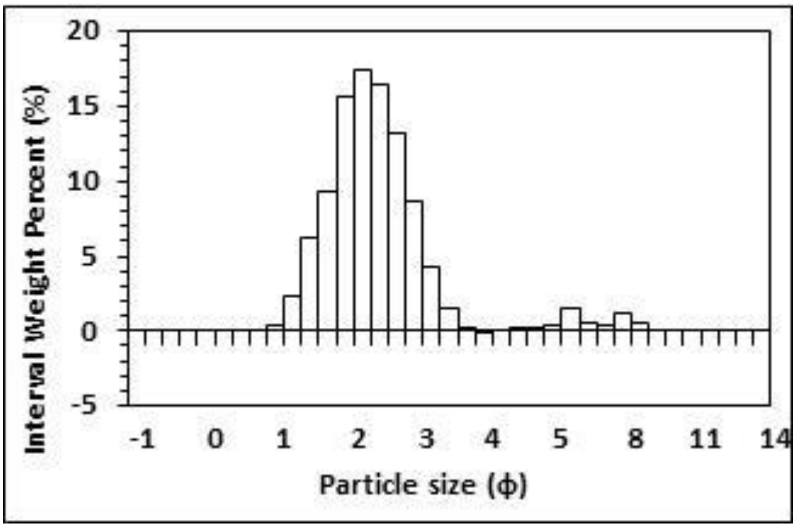

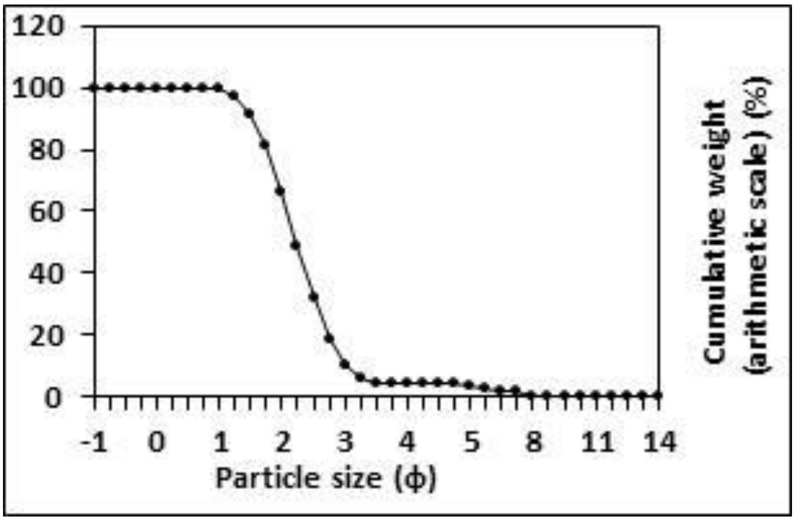

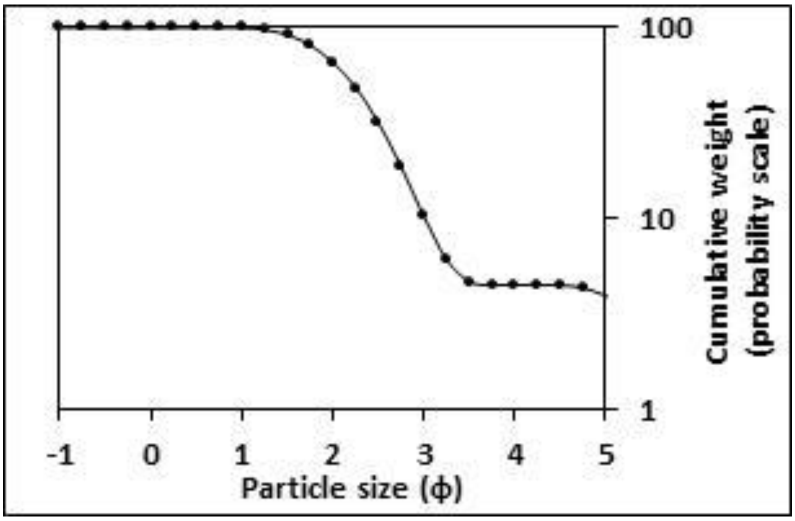

Figures II.64, II.65 and II.66: Histogram of grain size distribution and cumulative frequency graphs (arithmetic scale and probability scale) for sample 22: Mid intertidal zone, eastern transect, Wainamu Beach. Sample collected on the 15th of July, 2014.

Table II.23: *Graphical and statistical parameters, textural description and size classes for sample 23: High intertidal zone, mid transect, Wainamu Beach. Sample collected on the 15th of July, 2014.*

Textural description	**Textural size classes**
Moderately well sorted, Near symmetrical skewed, Mesokurtic	Sand = 100 000%Fines = 0.000% Silt = 0.000%Clay = 0.000%
Moment method parameters (µm) Mean = 196.764 Standard deviation (sd) = 71.028 Skewness (Sk_I)= 0.855 Kurtosis (K_G) 3.626 **Wentworth size class** Fine sand	**Graphical method parameters. After Folk (1980) (ϕ)** Mean (M_z) = 2.438 d(0.5 = 2.441 Sorting (σ_I) = 0.528 Skewness (Sk_I) = -0.004 Kurtosis (K_G) = 0.951 Mean (mm) = 0.184 Mean (µm) = 184.487

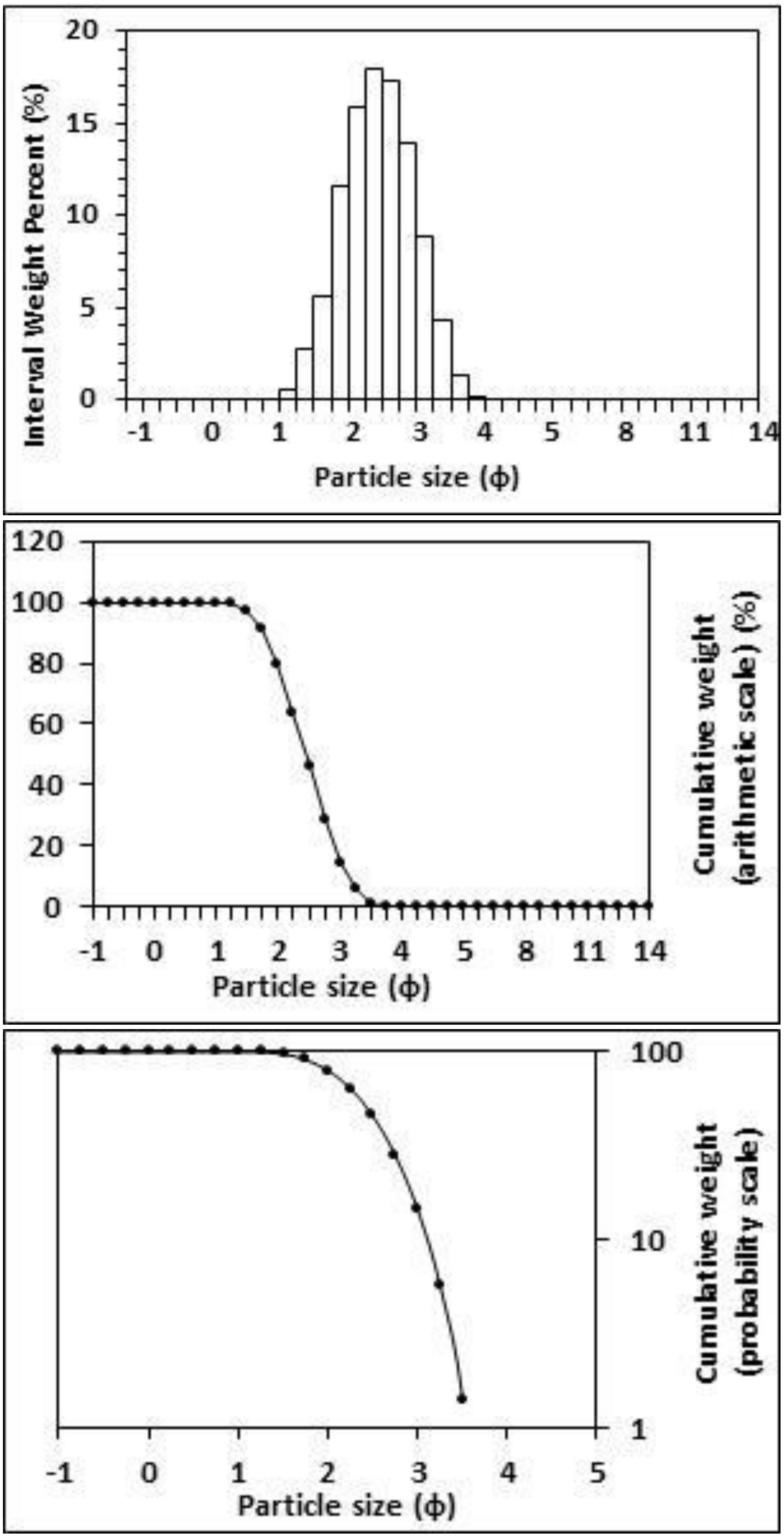

Figures II.67, II.68 and II.69: Histogram of grain size distribution and cumulative frequency graphs (arithmetic scale and probability scale) for sample 23: High intertidal zone, mid transect, Wainamu Beach. Sample collected on the 15th of July, 2014.

Table II.24: *Graphical and statistical parameters, textural description and size classes for sample 24: Mid intertidal zone, mid transect, Wainamu Beach. Sample collected on the 15th of July, 2014.*

<table>
<tr><td>Textural description

Moderately well sorted,

Near symmetrical skewed,

Mesokurtic</td><td>Textural size classes

Sand = 100 000%Fines = 0.000%

Silt = 0.000%Clay = 0.000%</td></tr>
<tr><td>Moment method parameters

(µm)

Mean = 224.774

Standard deviation (sd) = 87.772

Skewness (Sk_I)= 0.886

Kurtosis (K_G) 3.618</td><td rowspan="2">Graphical method parameters.

After Folk (1980) (ϕ)

Mean (M_z) = 2.267

d(0.5) = 2.264

Sorting (σ_I) = 0.574

Skewness (Sk_I) = 0.002

Kurtosis (K_G) = 0.947

Mean (mm) = 0.208

Mean (µm) = 207.818</td></tr>
<tr><td>Wentworth size class

Fine sand</td></tr>
</table>

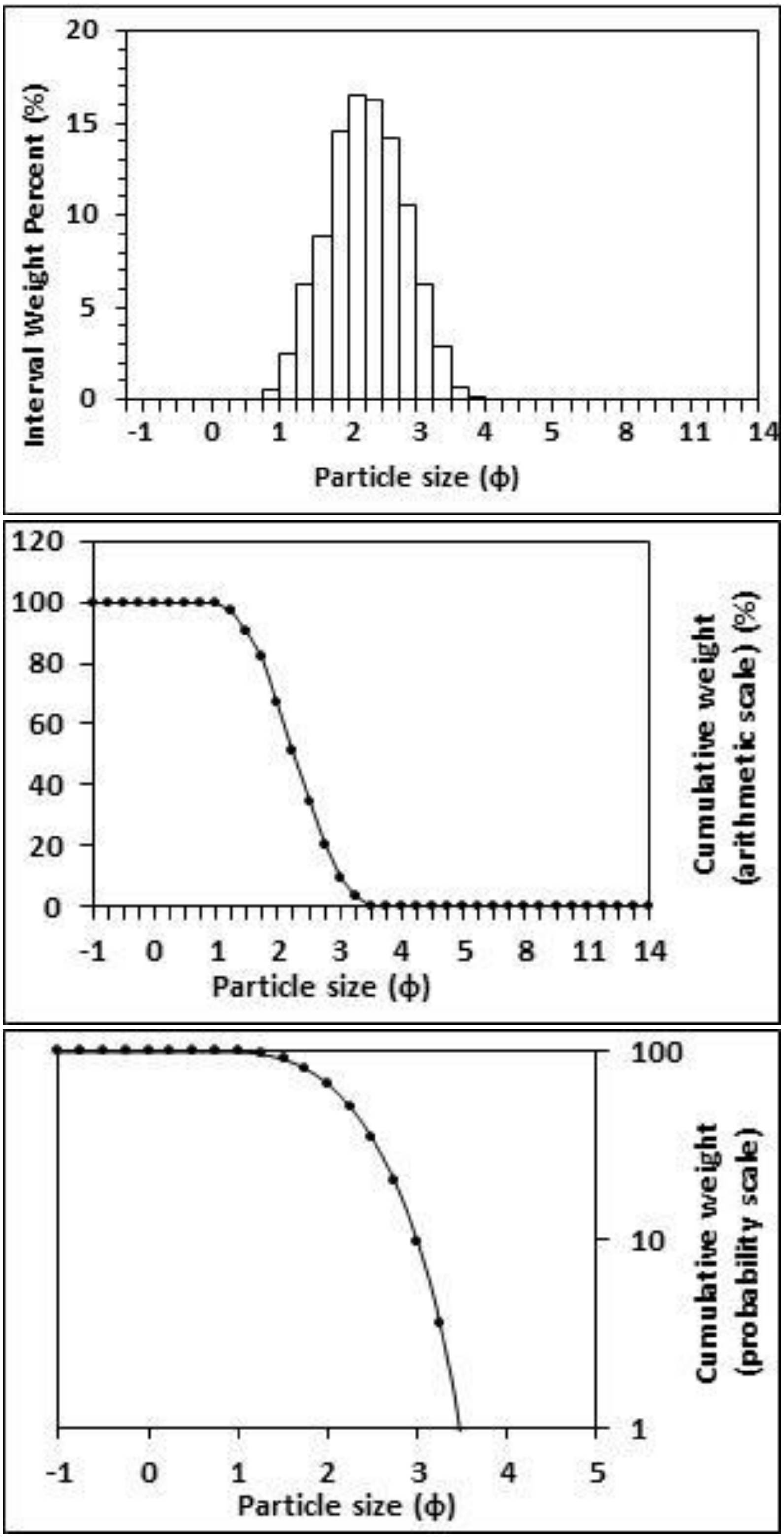

Figures II.70, II.71 and II.72: Histogram of grain size distribution and cumulative frequency graphs (arithmetic scale and probability scale) for sample 24: Mid intertidal zone, mid transect, Wainamu Beach. Sample collected on the 15th of July, 2014.

Table II.25: *Graphical and statistical parameters, textural description and size classes for sample 25: Mid intertidal zone, western transect, Wainamu Beach. Sample collected on the 15th of July, 2014.*

Textural description	**Textural size classes**
Moderately well sorted, Near symmetrical skewed, Mesokurtic	Sand = 100 000%Fines = 0.000% Silt = 0.000%Clay = 0.000%
Moment method parameters (µm)	**Graphical method parameters. After Folk (1980) (ϕ)**
Mean = 191.186 Standard deviation (sd) = 69.317 Skewness (Sk_I)= 0.885 Kurtosis (K_G) 3.733	Mean (M_z) = 2.482 d(0.5) = 2.485 Sorting (σ_I) = 0.528 Skewness (Sk_I) = -0.007 Kurtosis (K_G) = 0.951 Mean (mm) = 0.179 Mean (µm) = 179.019
Wentworth size class Fine sand	

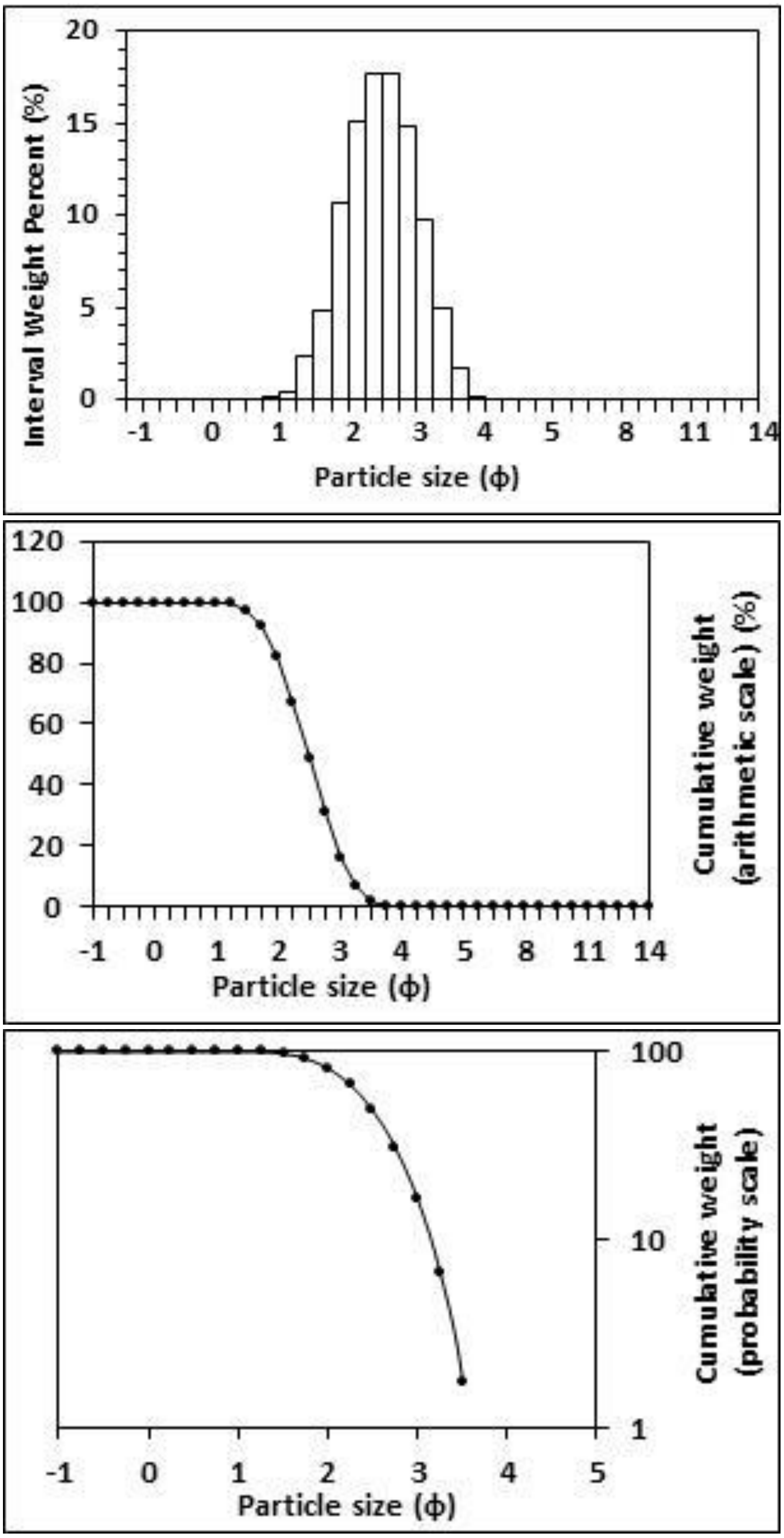

Figures II.73, II.74 and II.75: Histogram of grain size distribution and cumulative frequency graphs (arithmetic scale and probability scale) for sample 25: Mid intertidal zone, western transect, Wainamu Beach. Sample collected on the 15th of July, 2014.

Table II.26: *Graphical and statistical parameters, textural description and size classes for sample 26: Low intertidal zone, mid transect, Wainamu Beach. Sample collected on the 15th of July, 2014.*

Textural description	**Textural size classes**
Moderately well sorted, Near symmetrical skewed, Mesokurtic	Sand = 100 000%Fines = 0.000% Silt = 0.000%Clay = 0.000%
Moment method parameters (µm) Mean = 227.820 Standard deviation (sd) = 88.009 Skewness (Sk_I)= 0.858 Kurtosis (K_G) 3.532 **Wentworth size class** Fine sand	**Graphical method parameters. After Folk (1980) (ϕ)** Mean (M_z) = 2.244 d(0.5) = 2.241 Sorting (σ_I) = 0.570 Skewness (Sk_I) = 0.007 Kurtosis (K_G) = 0.946 Mean (mm) = 0.211 Mean (µm) = 211.123

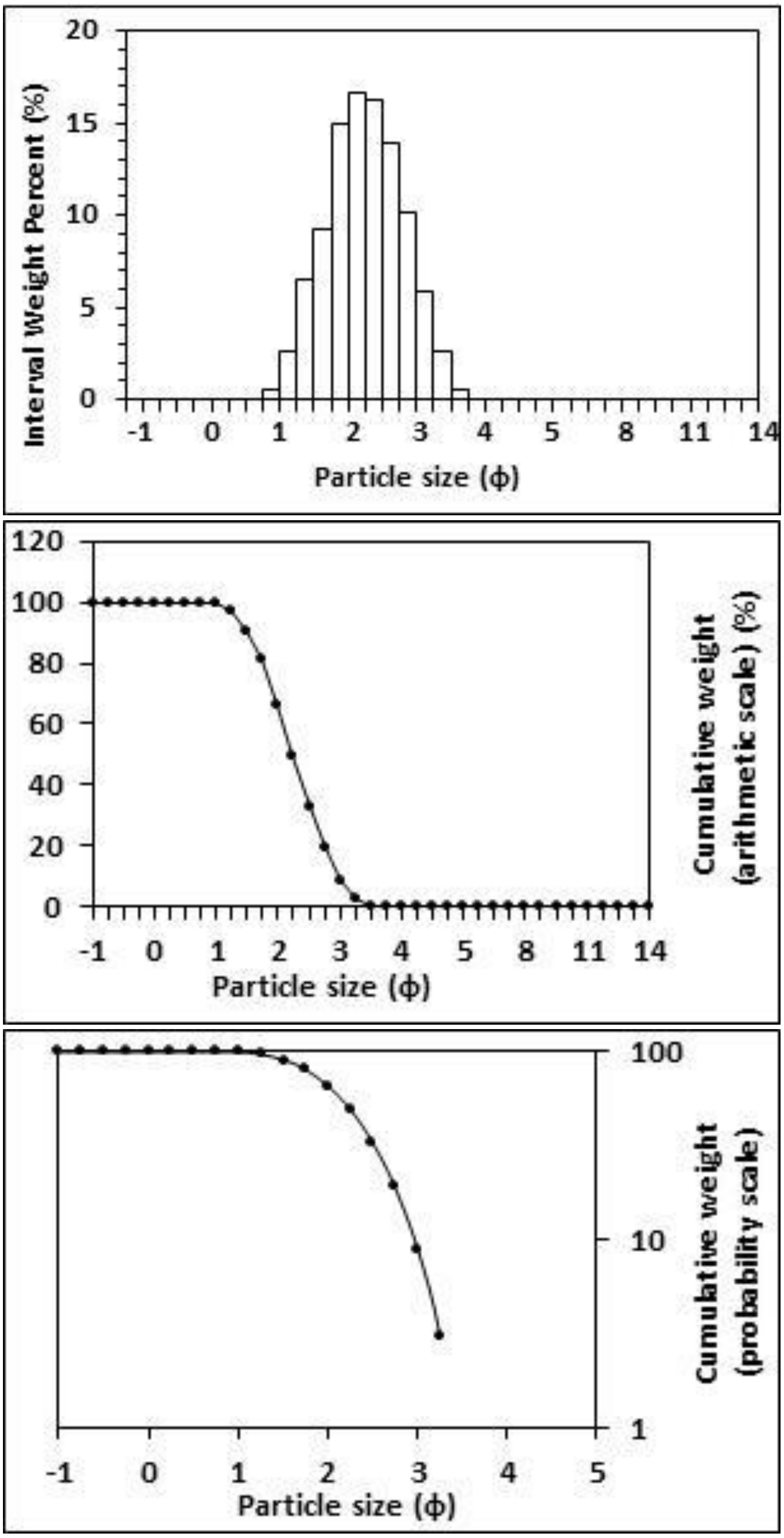

Figures II.76, II.77 and II.78: Histogram of grain size distribution and cumulative frequency graphs (arithmetic scale and probability scale) for sample 26: Low intertidal zone, mid transect, Wainamu Beach. Sample collected on the 15th of July, 2014.

Table I.27: *Graphical and statistical parameters, textural description and size classes for sample 27: High intertidal zone, eastern transect, Wainamu Beach. Sample collected on the 15th of July, 2014.*

Textural description	**Textural size classes**
Moderately well sorted, Near symmetrical skewed, Mesokurtic	Sand = 100 000%Fines = 0.000% Silt = 0.000%Clay = 0.000%
Moment method parameters (µm)	**Graphical method parameters. After Folk (1980) (ϕ)**
Mean = 221.646 Standard deviation (sd) = 77.009 Skewness (Sk_I)= 0.798 Kurtosis (K_G) 3.460	Mean (M_z) = 2.265 d(0.5) = 2.263 Sorting (σ_I) = 0.510 Skewness (Sk_I) = 0.006 Kurtosis (K_G) = 0.953 Mean (mm) = 0.208 Mean (µm) = 208.107
Wentworth size class Fine sand	

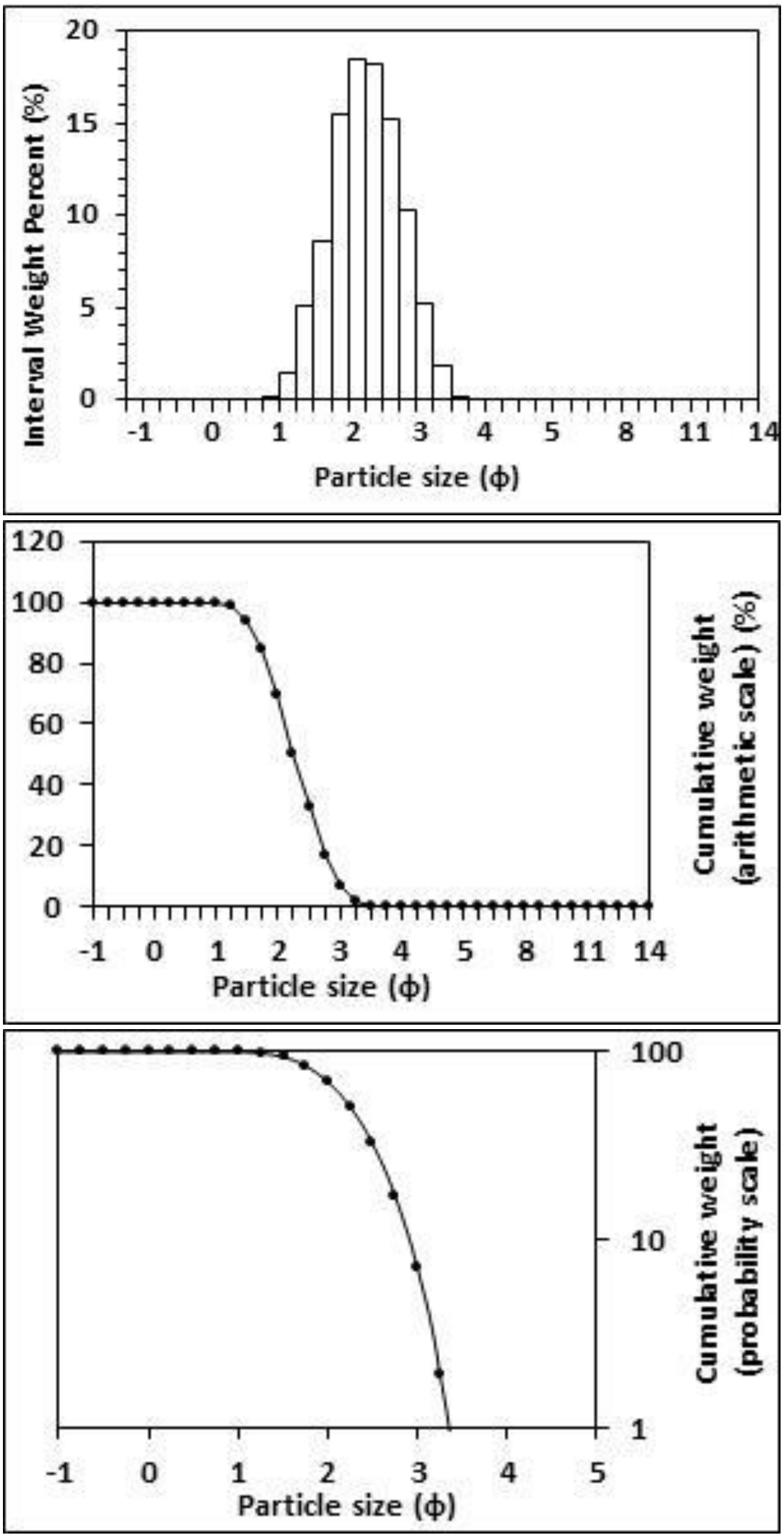

Figures II.79, II.80 and II.81: Histogram of grain size distribution and cumulative frequency graphs (arithmetic scale and probability scale) for sample 27: High intertidal zone, eastern transect, Wainamu Beach. Sample collected on the 15th of July, 2014.

Table II.28: *Graphical and statistical parameters, textural description and size classes for sample 28: Low intertidal zone, western transect, Wainamu Beach. Sample collected on the 15th of July, 2014.*

Textural description	**Textural size classes**
Moderately well sorted, Near symmetrical skewed, Mesokurtic	Sand = 100 000%Fines = 0.000% Silt = 0.000%Clay = 0.000%
Moment method parameters (µm)	**Graphical method parameters. After Folk (1980) (ϕ)**
Mean = 201.797 Standard deviation (sd) = 70.025 Skewness (Sk_I)= 0.816 Kurtosis (K_G) 3.533	Mean (M_z) = 2.397 d(0.5) = 2.398 Sorting (σ_I) = 0.510 Skewness (Sk_I) = -0.001 Kurtosis (K_G) = 0.962 Mean (mm) = 0.190 Mean (µm) = 189.817
Wentworth size class Fine sand	

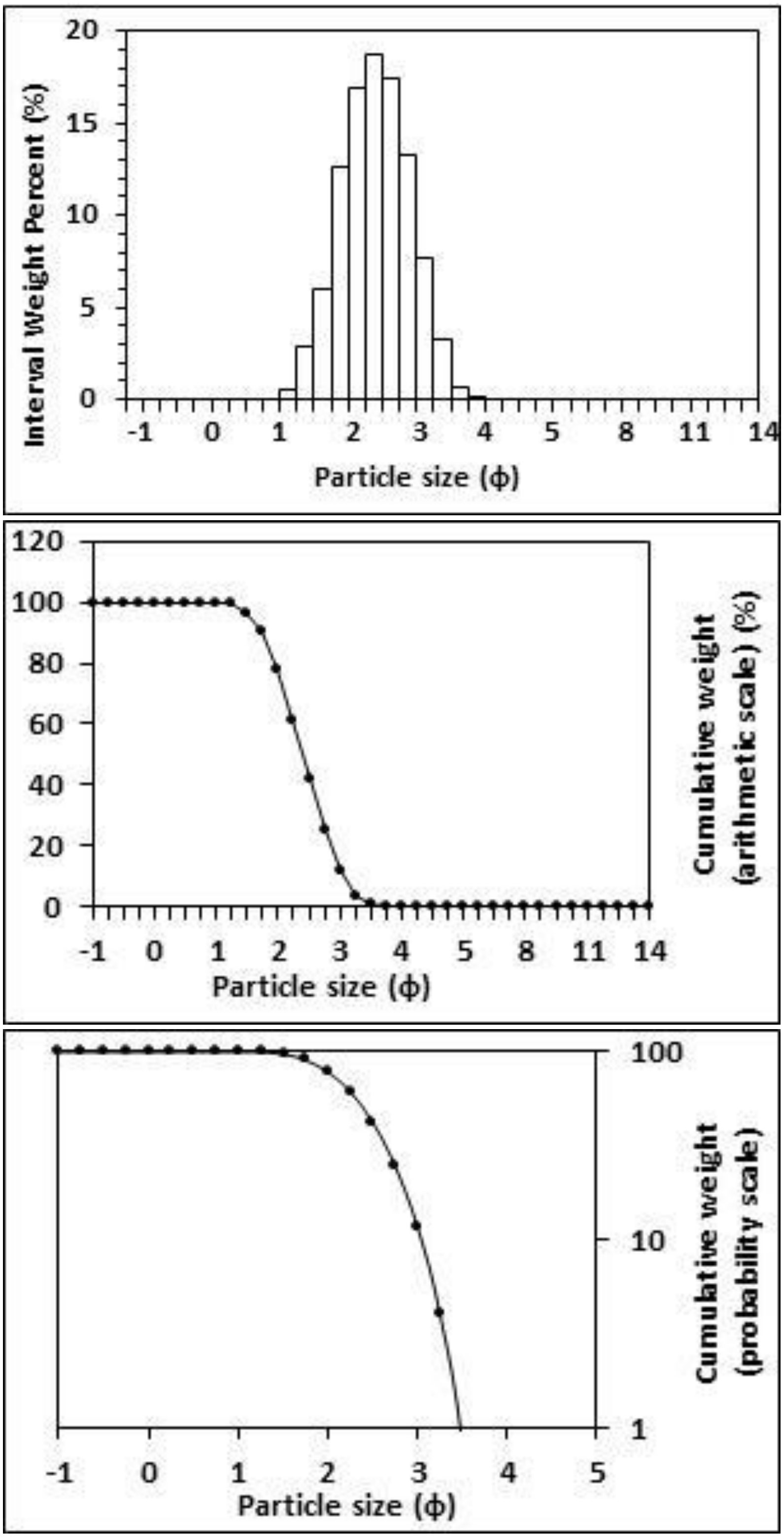

Figures II.82, II.83and II.84: Histogram of grain size distribution and cumulative frequency graphs (arithmetic scale and probability scale) for sample 28: Low intertidal zone, western transect, Wainamu Beach. Sample collected on the 15th of July, 2014.

Table II.29: *Graphical and statistical parameters, textural description and size classes for sample 29: Low intertidal zone, Transect 1, Southern Ngarunui Beach. Sample collected on the 10th of February, 2015.*

Textural description	**Textural size classes**
Well sorted, Near symmetrical skewed, Mesokurtic	Sand = 100 000%Fines = 0.000% Silt = 0.000%Clay = 0.000%
Moment method parameters (µm) Mean = 257.540 Standard deviation (sd) = 87.589 Skewness (Sk_I)= 0.790 Kurtosis (K_G) 3.434	**Graphical method parameters. After Folk (1980) (ϕ)** Mean (M_z) = 2.045 d(0.5) = 2.044 Sorting (σ_I) = 0.497 Skewness (Sk_I) = 0.010 Kurtosis (K_G) = 0.947 Mean (mm) = 0.242 Mean (µm) = 242.240
Wentworth size class Fine sand	

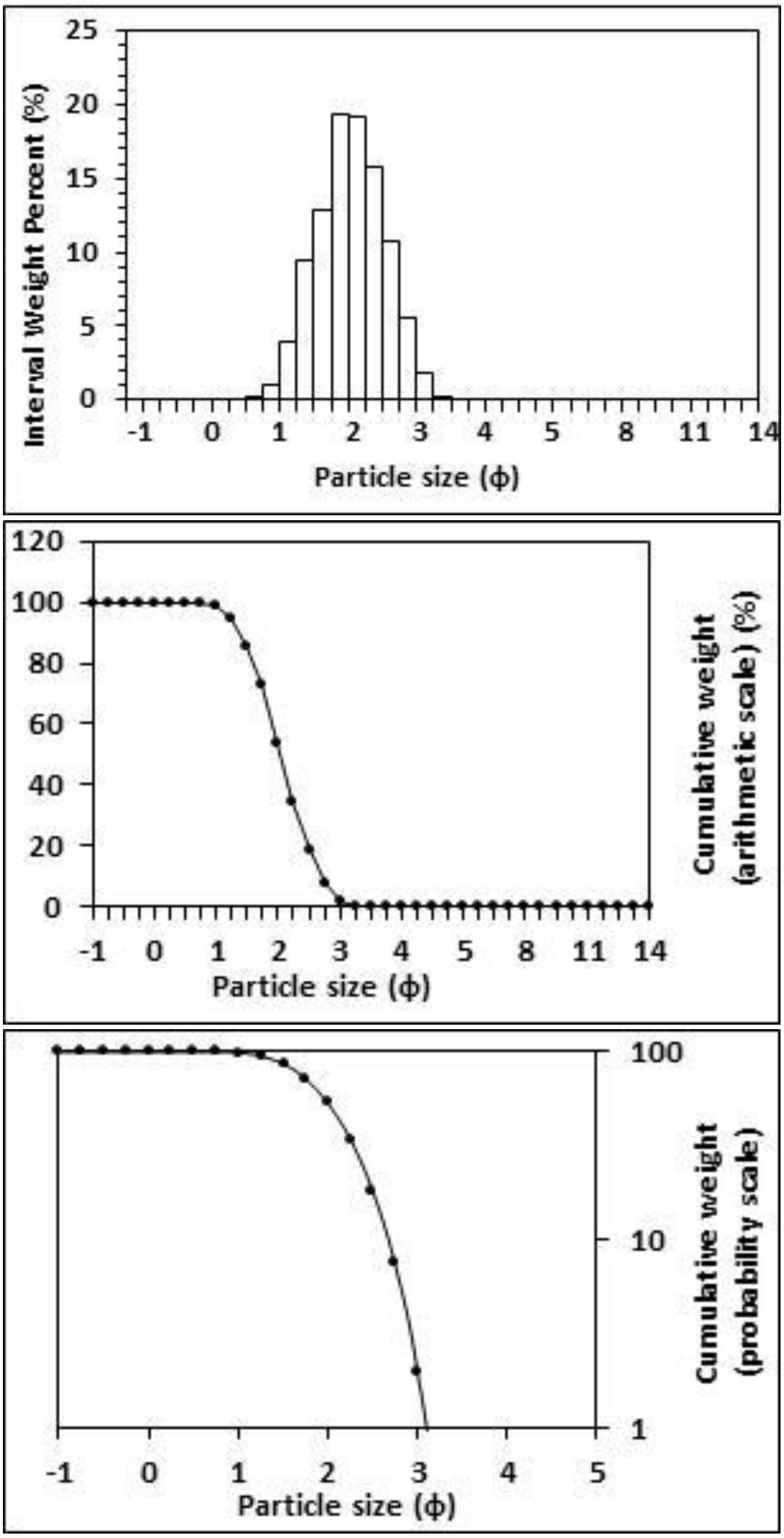

Figures II.85, II.86 and II.87: Histogram of grain size distribution and cumulative frequency graphs (arithmetic scale and probability scale) for sample 29: Low intertidal zone, Transect 1, Southern Ngarunui Beach. Sample collected on the 10th of February, 2015.

Table II.30: *Graphical and statistical parameters, textural description and size classes for sample 30: Low intertidal zone, Transect 2, Southern Ngarunui Beach. Sample collected on the 10th of February, 2015.*

Textural description	**Textural size classes**
Moderately well sorted, Near symmetrical skewed, Mesokurtic	Sand = 100 000%Fines = 0.000% Silt = 0.000%Clay = 0.000%
Moment method parameters (μm) Mean = 315.435 Standard deviation (sd) = 113.221 Skewness (Sk_I)= 0.833 Kurtosis (K_G) 3.567	**Graphical method parameters. After Folk (1980) (ϕ)** Mean (M_z) = 1.761 d(0.5) = 1.759 Sorting (σ_I) = 0.526 Skewness (Sk_I) = 0.005 Kurtosis (K_G) = 0.953 Mean (mm) = 0.295 Mean (μm) = 295.077
Wentworth size class Medium sand	

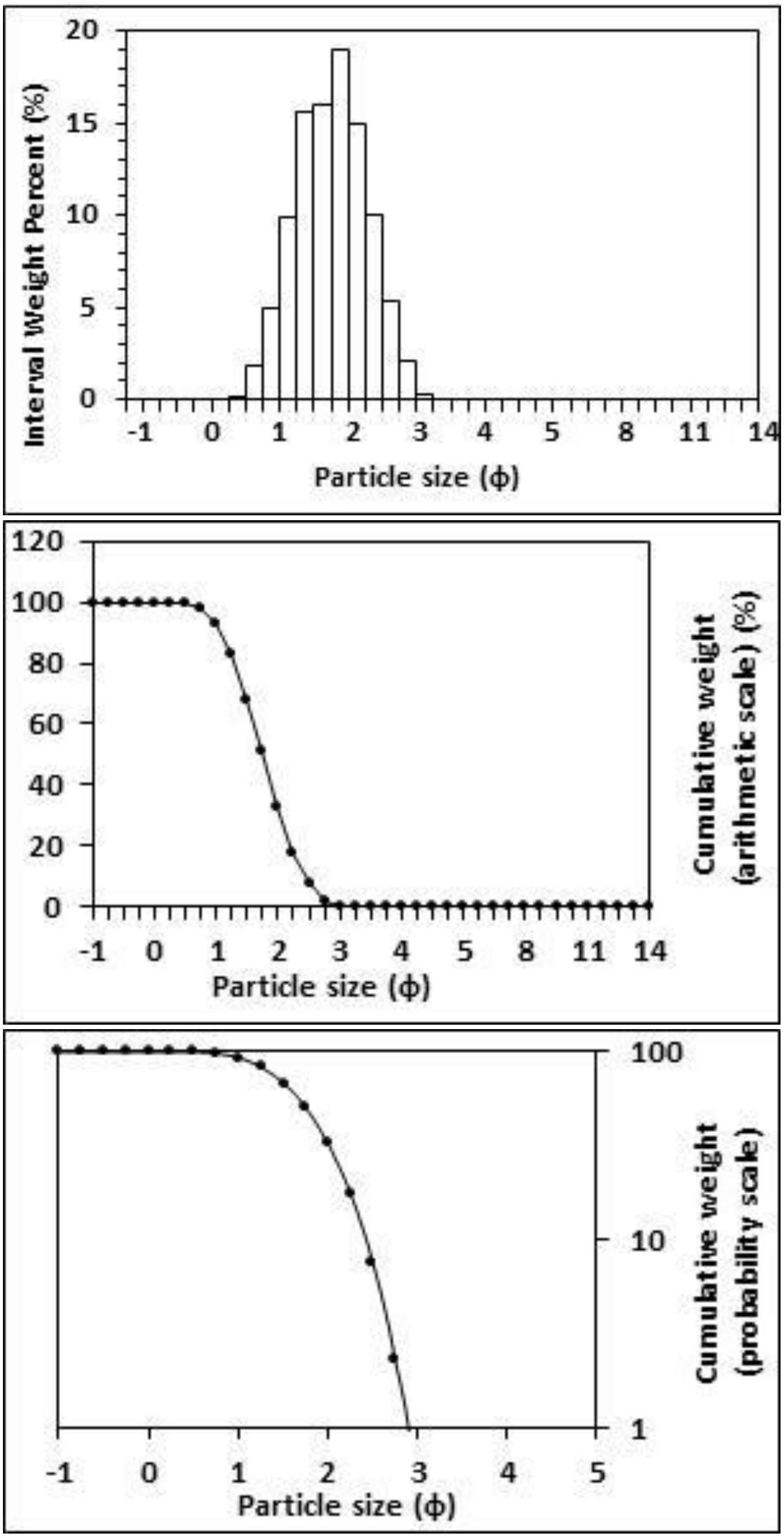

Figures II.88, II.89 and II.90: Histogram of grain size distribution and cumulative frequency graphs (arithmetic scale and probability scale) for sample 30: Low intertidal zone, Transect 2, Southern Ngarunui Beach. Sample collected on the 10th of February, 2015.

Table II.31: *Graphical and statistical parameters, textural description and size classes for sample 31: High intertidal zone, Transect 4, Southern Ngarunui Beach. Sample collected on the 10th of February, 2015.*

Textural description	**Textural size classes**
Moderately well sorted, Near symmetrical skewed, Mesokurtic	Sand = 100 000%Fines = 0.000% Silt = 0.000%Clay = 0.000%
Moment method parameters (µm)	**Graphical method parameters. After Folk (1980) (ϕ)**
Mean = 266.543 Standard deviation (sd) = 92.931 Skewness (Sk_I)= 0.825 Kurtosis (K_G) 3.556 **Wentworth size class** Medium sand	Mean (M_z) = 1.996 d(0.5) = 1.998 Sorting (σ_I) = 0.510 Skewness (Sk_I) = -0.003 Kurtosis (K_G) = 0.955 Mean (mm) = 0.251 Mean (µm) = 250.621

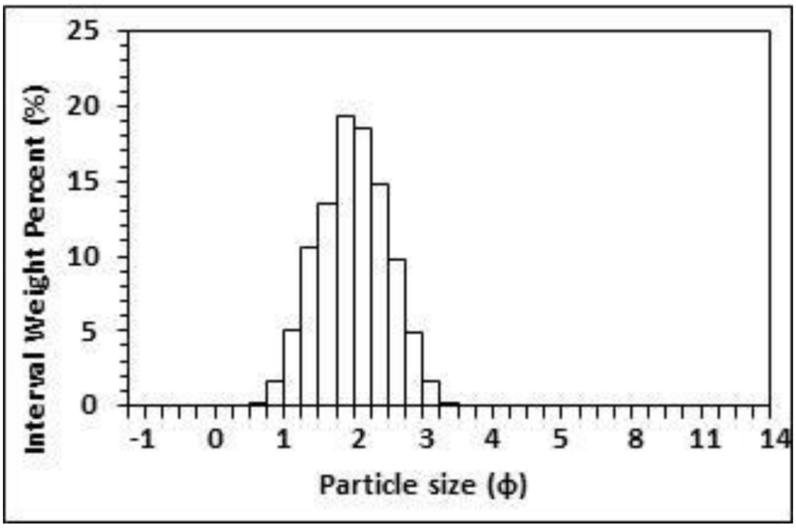

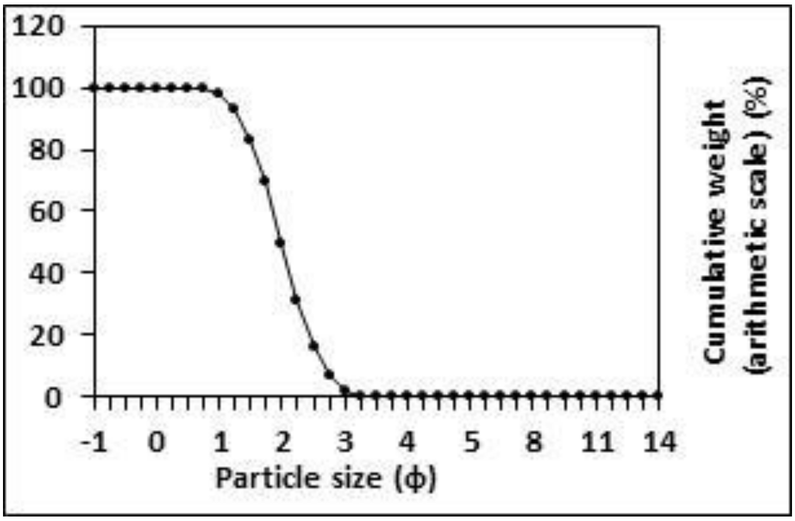

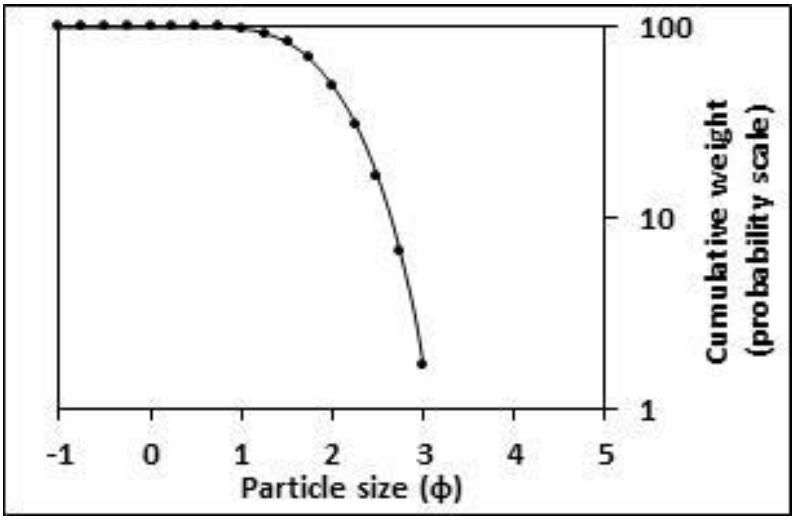

Figures II.91, II.92 and II.93: Histogram of grain size distribution and cumulative frequency graphs (arithmetic scale and probability scale) for sample 31: High intertidal zone, Transect 4, Southern Ngarunui Beach. Sample collected on the 10th of February, 2015.

Table II.32: *Graphical and statistical parameters, textural description and size classes for sample 32: High intertidal zone, Transect 1, Southern Ngarunui Beach. Sample collected on the 10th of February, 2015.*

Textural description	**Textural size classes**
Moderately well sorted, Near symmetrical skewed, Mesokurtic	Sand = 100 000%Fines = 0.000% Silt = 0.000%Clay = 0.000%
Moment method parameters (µm)	**Graphical method parameters. After Folk (1980) (ϕ)**
Mean = 255.341 Standard deviation (sd) = 88.731 Skewness (Sk_I)= 0.821 Kurtosis (K_G) 3.522	Mean (M_z) = 2.062 d(0.5) = 2.061 Sorting (σ_I) = 0.508 Skewness (Sk_I) = 0.007 Kurtosis (K_G) = 0.952 Mean (mm) = 0.239 Mean (µm) = 239.480
Wentworth size class Fine sand	

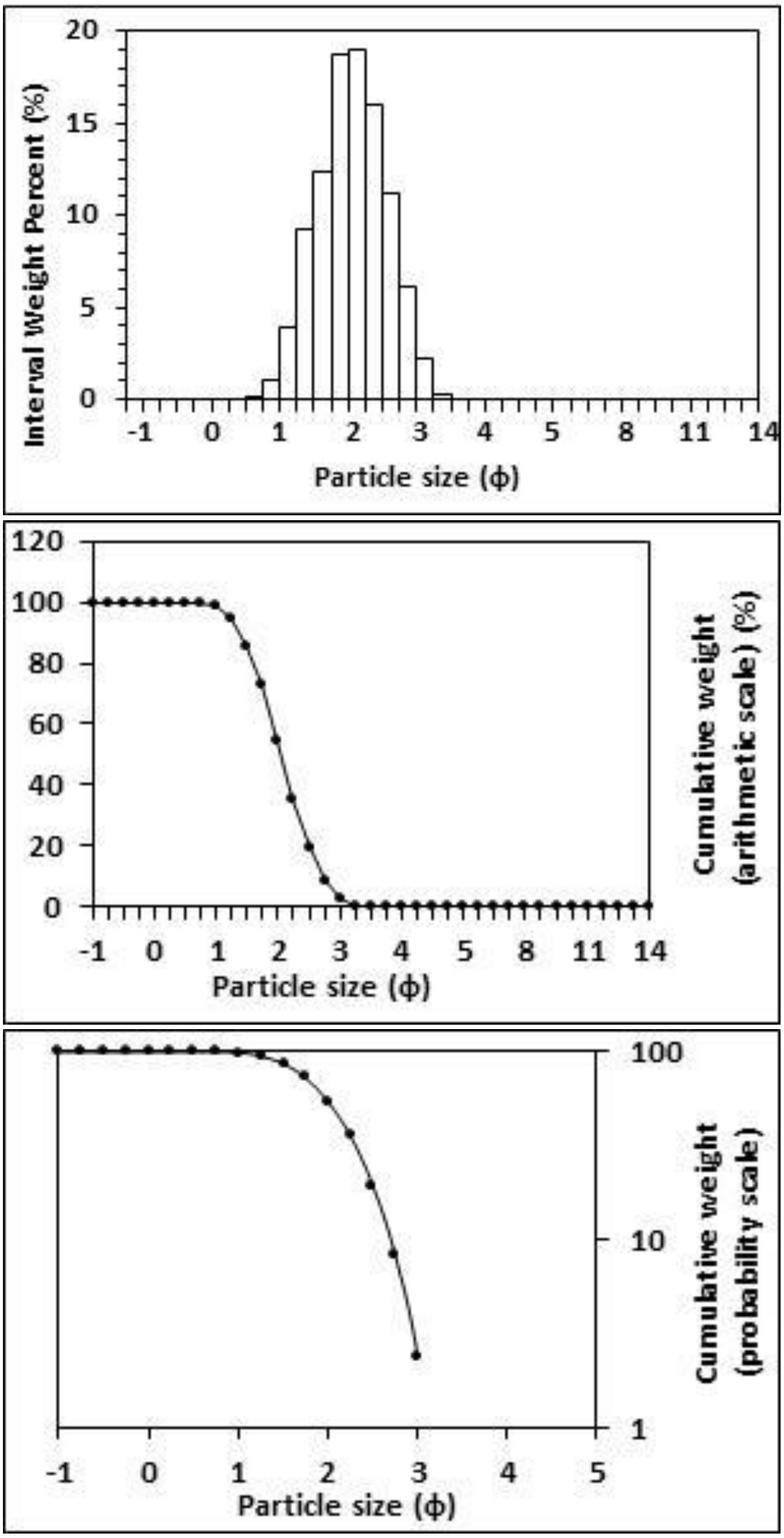

Figures II.94, II.95 and II.96: Histogram of grain size distribution and cumulative frequency graphs (arithmetic scale and probability scale) for sample 32: High intertidal zone, Transect 1, Southern Ngarunui Beach. Sample collected on the 10th of February, 2015.

Table II.33: *Graphical and statistical parameters, textural description and size classes for sample 33: High intertidal zone, Transect 2, Southern Ngarunui Beach. Sample collected on the 10th of February, 2015.*

Textural description	**Textural size classes**
Well sorted, Near symmetrical skewed, Mesokurtic	Sand = 100 000%Fines = 0.000% Silt = 0.000%Clay = 0.000%
Moment method parameters (µm) Mean = 244.945 Standard deviation (sd) = 78.507 Skewness (Sk_I)= 0.788 Kurtosis (K_G) 3.531	**Graphical method parameters. After Folk (1980) (ϕ)** Mean (M_z) = 2.108 d(0.5) = 2.107 Sorting (σ_I) = 0.473 Skewness (Sk_I) = -0.000 Kurtosis (K_G) = 0.975 Mean (mm) = 0.232 Mean (µm) = 232.040
Wentworth size class Fine sand	

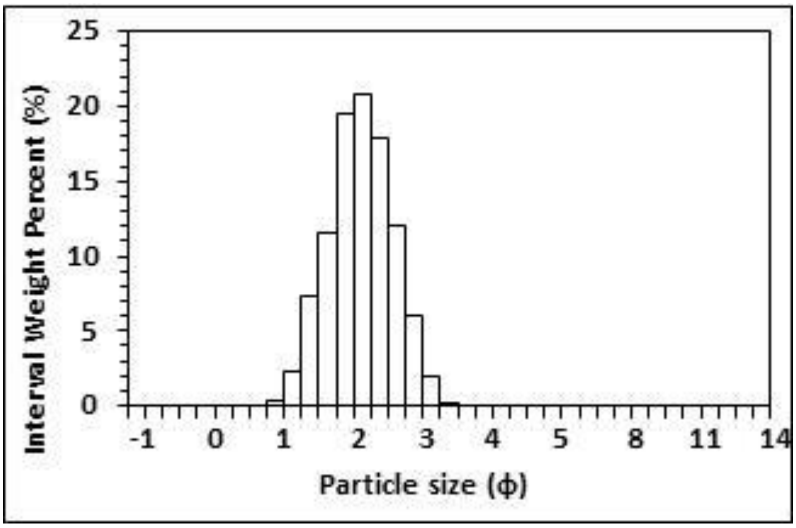

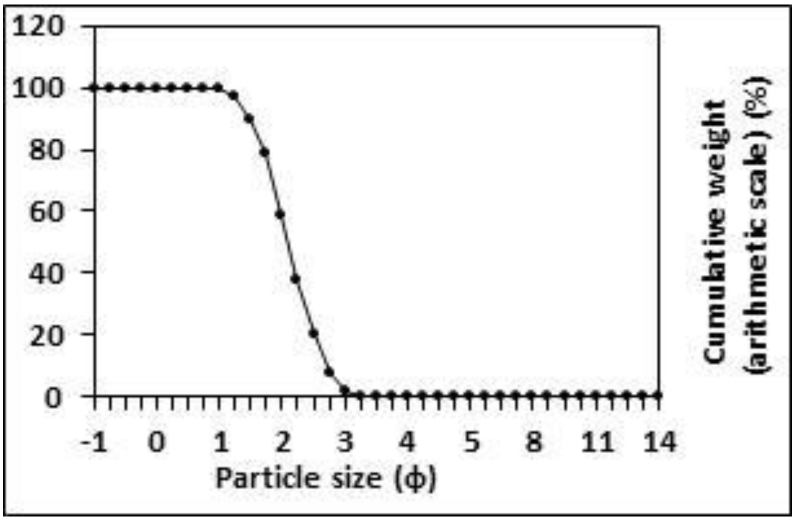

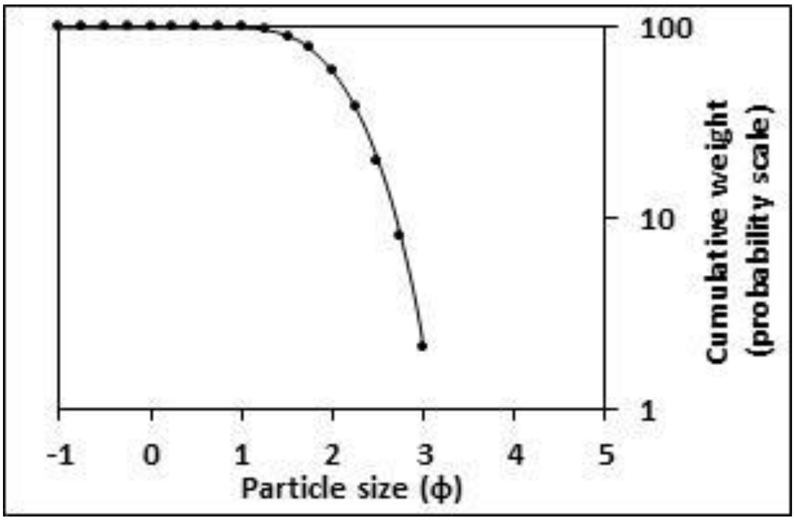

Figures II.97, II.98 and II.99: Histogram of grain size distribution and cumulative frequency graphs (arithmetic scale and probability scale) for sample 33: High intertidal zone, Transect 2, Southern Ngarunui Beach. Sample collected on the 10th of February, 2015.

uptoTable II.34: *Graphical and statistical parameters, textural description and size classes for sample 34: High intertidal zone, Transect 3, Southern Ngarunui Beach. Sample collected on the 10th of February, 2015.*

Textural description	**Textural size classes**
Well sorted, Near symmetrical skewed, Mesokurtic	Sand = 100 000%Fines = 0.000% Silt = 0.000%Clay = 0.000%
Moment method parameters (µm) Mean = 261.245 Standard deviation (sd) = 84.013 Skewness (SkI) = 0.781 Kurtosis (KG) = 3.511 **Wentworth size class** Fine sand	**Graphical method parameters. After Folk (1980) (ϕ)** Mean (Mz) = 2.014 d(0.5) = 2.015 Sorting (σI) = 0.464 Skewness (SkI) = 0.000 Kurtosis (KG) = 0.945 Mean (mm) = 0.248 Mean (µm) = 247.633

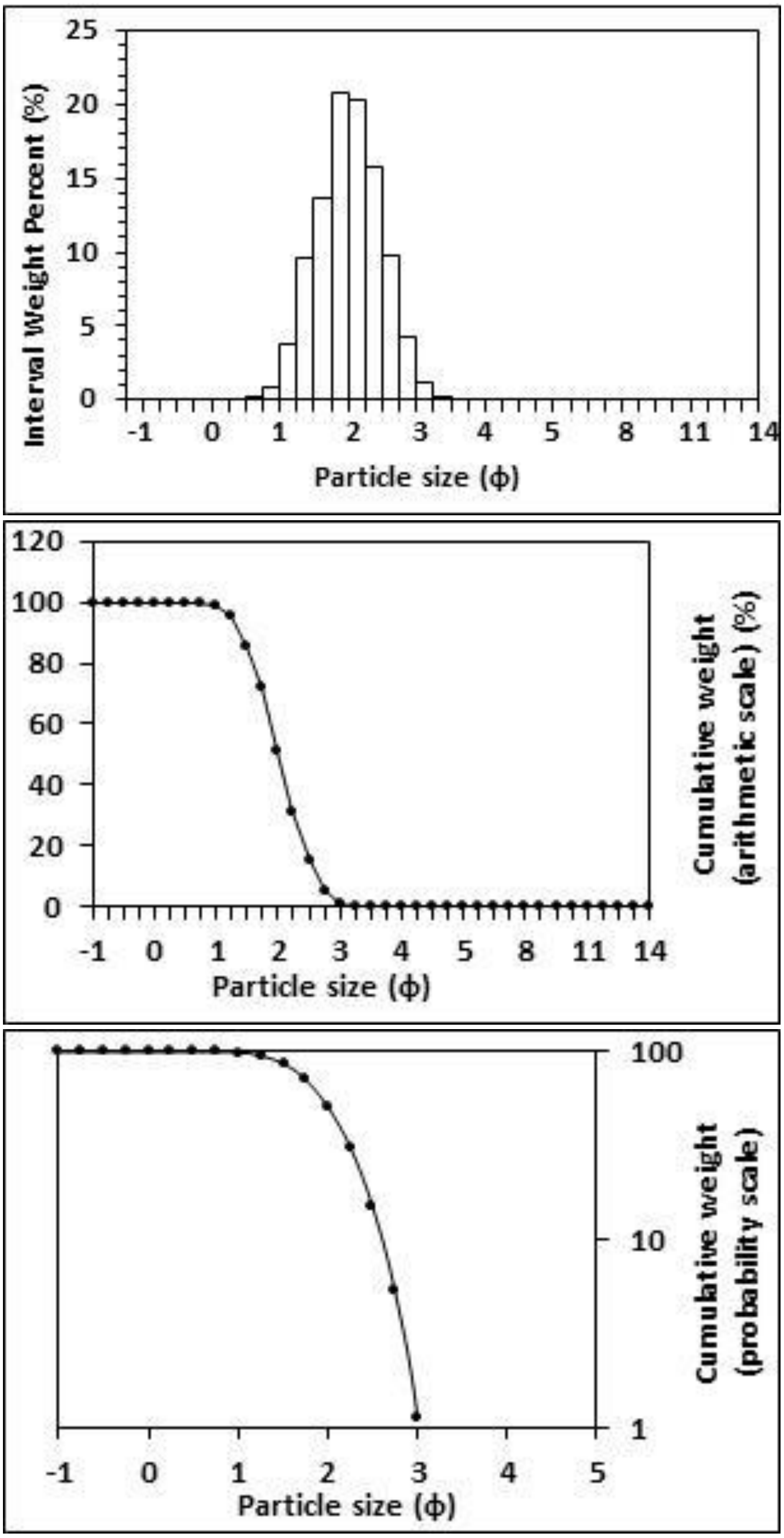

Figures II.100, II.101 and II.102: Histogram of grain size distribution and cumulative frequency graphs (arithmetic scale and probability scale) for sample 34: High intertidal zone, Transect 3, Southern Ngarunui Beach. Sample collected on the 10th of February, 2015.

Table II.35: *Graphical and statistical parameters, textural description and size classes for sample 35: Low intertidal zone, Transect 3, Southern Ngarunui Beach. Sample collected on the 10th of February, 2015.*

Textural description	**Textural size classes**
Moderately well sorted, Near symmetrical skewed, Mesokurtic	Sand = 100 000%Fines = 0.000% Silt = 0.000%Clay = 0.000%
Moment method parameters (µm) Mean = 306.168 Standard deviation (sd) = 114.908 Skewness (SkI)= 0.942 Kurtosis (KG) 3.883	**Graphical method parameters. After Folk (1980) (ϕ)** Mean (Mz) = 1.815 d(0.5) = 1.815 Sorting (σI) = 0.543 Skewness (SkI) = -0.008 Kurtosis (KG) = 0.957 Mean (mm) = 0.284 Mean (µm) = 284.269
Wentworth size class Medium sand	

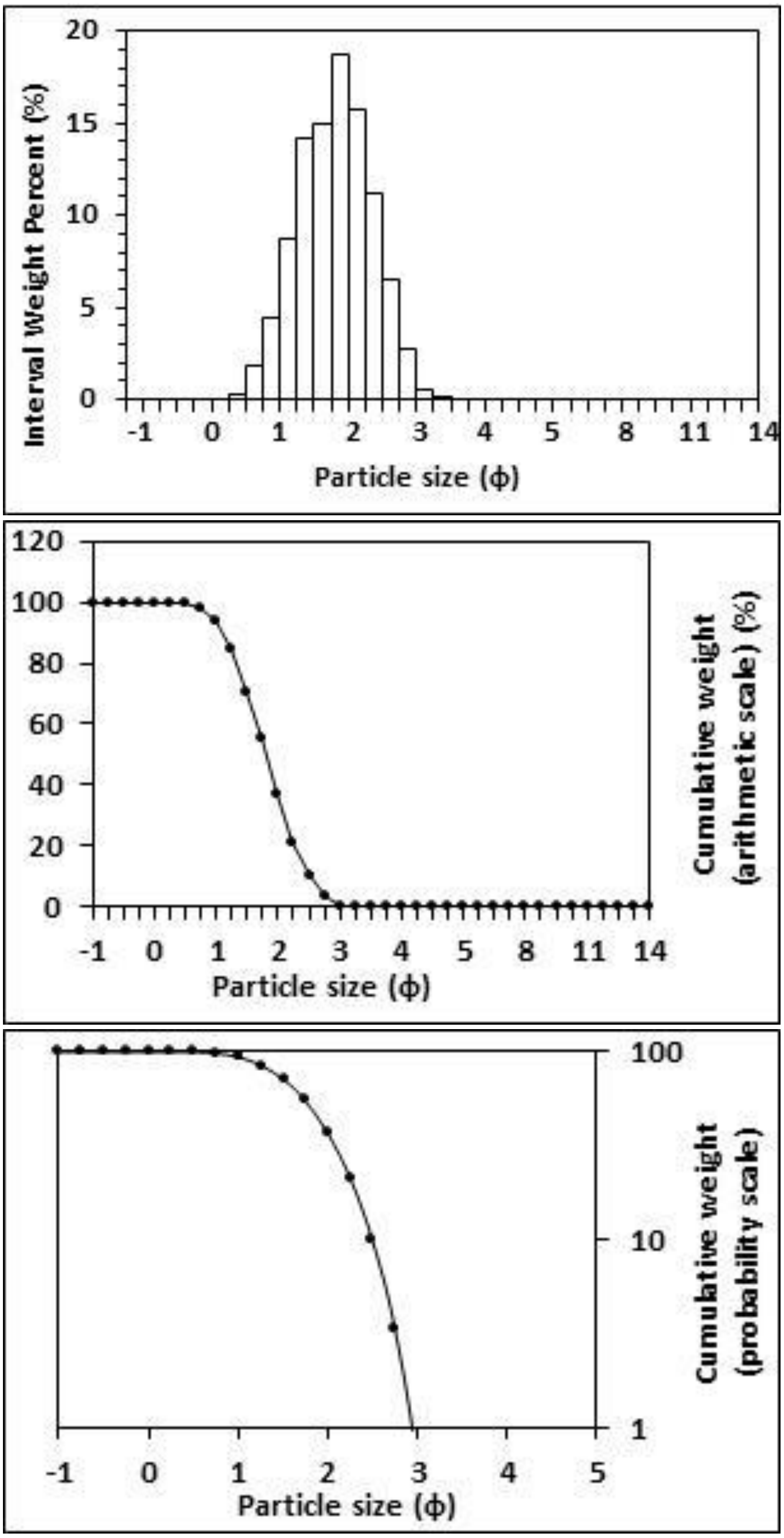

Figures II.103, II.104 and II.105: Histogram of grain size distribution and cumulative frequency graphs (arithmetic scale and probability scale) for sample 35: Low intertidal zone, Transect 3, Southern Ngarunui Beach. Sample collected on the 10th of February, 2015.

Table II.36: *Graphical and statistical parameters, textural description and size classes for sample 36: Mid intertidal zone, Transect 3, Southern Ngarunui Beach. Sample collected on the 10th of February, 2015.*

Textural description	**Textural size classes**
Moderately well sorted, Near symmetrical skewed, Mesokurtic	Sand = 100 000%Fines = 0.000% Silt = 0.000%Clay = 0.000%
Moment method parameters (µm)	**Graphical method parameters. After Folk (1980) (ϕ)**
Mean = 338.607 Standard deviation (sd) = 126.382 Skewness (SkI) = 0.935 Kurtosis (KG) = 3.896	Mean (Mz) = 1.663 d(0.5) = 1.667 Sorting (σI) = 0.539 Skewness (SkI) = -0.011 Kurtosis (KG) = 0.953 Mean (mm) = 0.316 Mean (µm) = 315.887
Wentworth size class Medium sand	

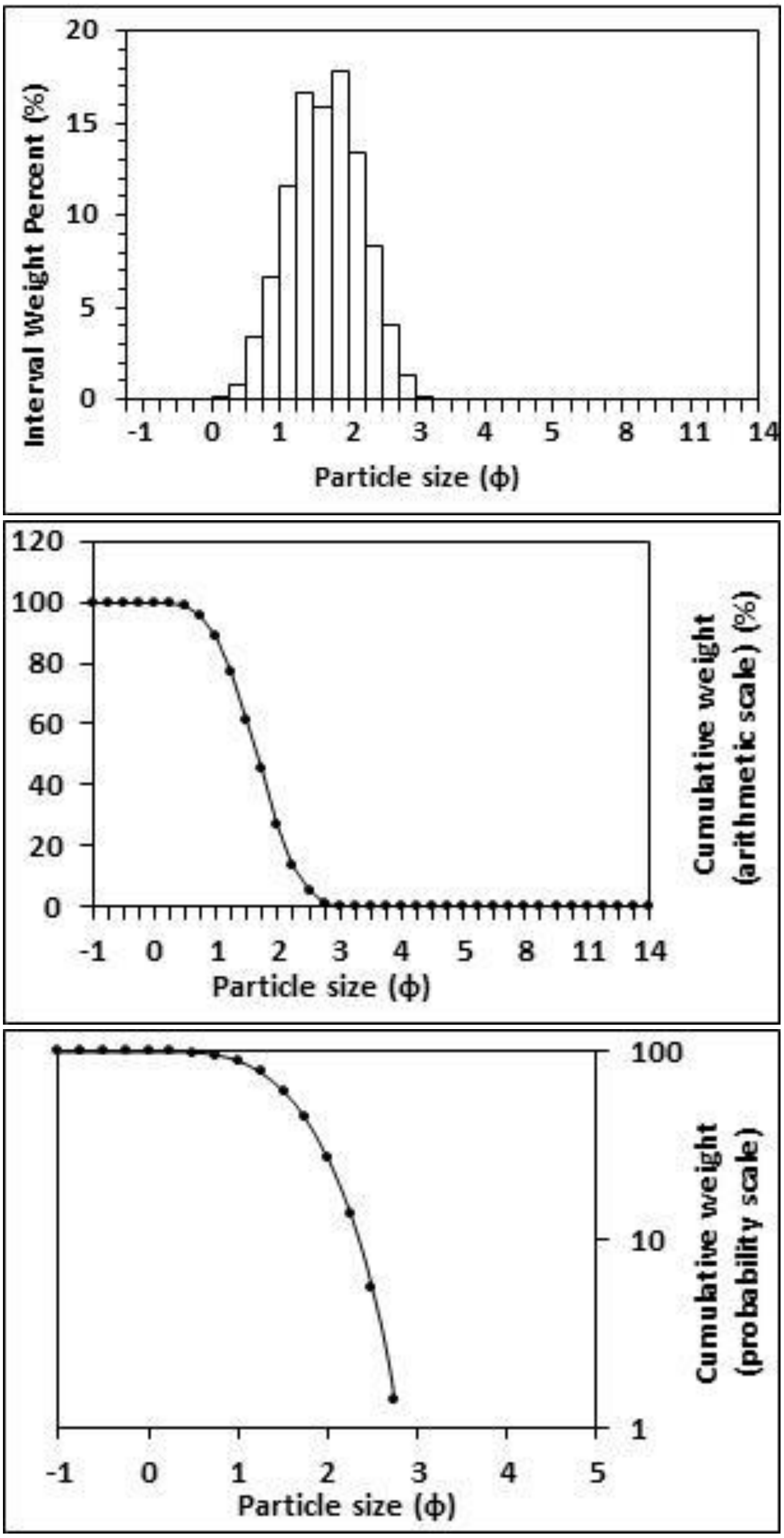

Figures II.106, II.107 and II.108: Histogram of grain size distribution and cumulative frequency graphs (arithmetic scale and probability scale) for sample 36: Mid intertidal zone, Transect 3, Southern Ngarunui Beach. Sample collected on the 10th of February, 2015.

Table II.37: *Graphical and statistical parameters, textural description and size classes for sample 37: Mid intertidal zone, Transect 1, Southern Ngarunui Beach. Sample collected on the 10th of February, 2015.*

Textural description	**Textural size classes**
Moderately well sorted, Near symmetrical skewed, Mesokurtic	Sand = 100 000%Fines = 0.000% Silt = 0.000%Clay = 0.000%
Moments method parameters (µm) Mean = 325.845 Standard deviation (sd) = 118.320 Skewness (SkI) = 0.892 Kurtosis (KG) = 3.713	**Graphical method parameters. After Folk (1980) (ϕ)** Mean (Mz) = 1.712 d (0.5) = 1.717 Sorting (σI) = 0.527 Skewness (SkI) = -0.014 Kurtosis (KG) = 0.953 Mean (mm) = 0.305 Mean (µm) = 305.259
Wentworth size class Medium sand	

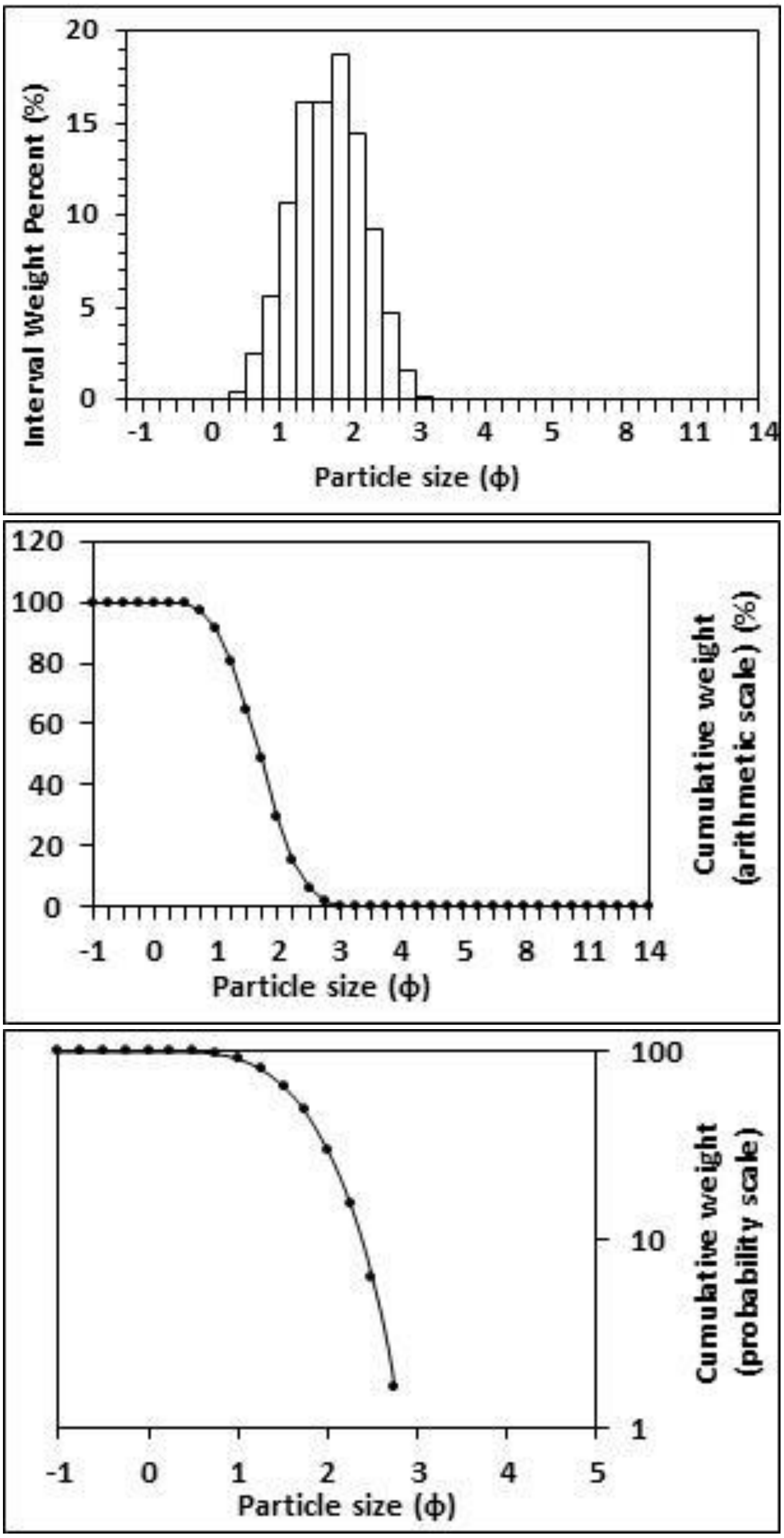

Figures II.109, II.10 and II.111: Histogram of grain size distribution and cumulative frequency graphs (arithmetic scale and probability scale) for sample 37: Mid intertidal zone, Transect 1, Southern Ngarunui Beach. Sample collected on the 10th of February, 2015.

Table II.38: *Graphical and statistical parameters, textural description and size classes for sample 38: Mid intertidal zone, Transect 2, Southern Ngarunui Beach. Sample collected on the 10th of February, 2015.*

Textural description	**Textural size classes**
Moderately well sorted, Near symmetrical skewed, Mesokurtic	Sand = 100 000%Fines = 0.000% Silt = 0.000%Clay = 0.000%
Moment method parameters (µm)	**Graphical method parameters. After Folk (1980) (ϕ)**
Mean = 327.889 Standard deviation (sd) = 118.390 Skewness (SkI) = 0.873 Kurtosis (KG) = 3.657	Mean (Mz) = 1.702 d(0.5) = 1.706 Sorting (SI) = 0.526 Skewness (SkI) = -0.011 Kurtosis (KG) = 0.952 Mean (mm) = 0.307 Mean (µm) = 307.349
Wentworth size class Medium sand	

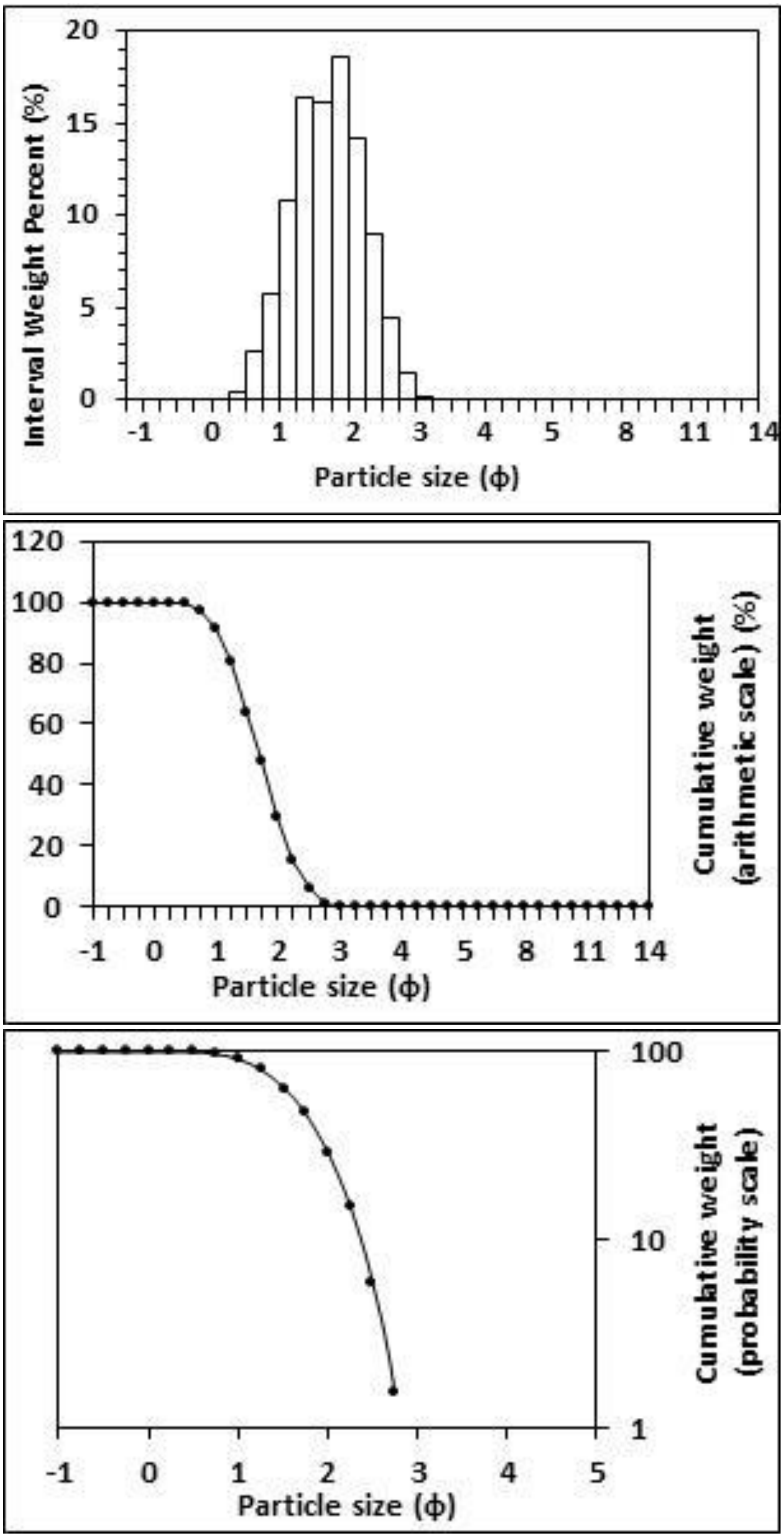

Figures II.112, II.113 and II.114: Histogram of grain size distribution and cumulative frequency graphs (arithmetic scale and probability scale) for sample 38: Mid intertidal zone, Transect 2, Southern Ngarunui Beach. Sample collected on the 10th of February, 2015.

Table II.39: *Graphical and statistical parameters, textural description and size classes for sample 39: Mid intertidal zone, Transect 4, Southern Ngarunui Beach. Sample collected on the 10th of February, 2015.*

Textural description	**Textural size classes**
Moderately well sorted, Near symmetrical skewed, Mesokurtic	Sand = 100 000%Fines = 0.000% Silt = 0.000%Clay = 0.000%
Moment method parameters (µm)	**Graphical method parameters. After Folk (1980) (ϕ)**
Mean = 354.938 Standard deviation (sd) = 142.801 Skewness (SkI) = 0.944 Kurtosis (KG) = 3.774	Mean (Mz) = 1.613 d(0.5) = 1.615 Sorting (SI) = 0.585 Skewness (SkI) = -0.009 Kurtosis (KG) = 0.955 Mean (mm) = 0.327 Mean (µm) = 326.822
Wentworth size class Medium sand	

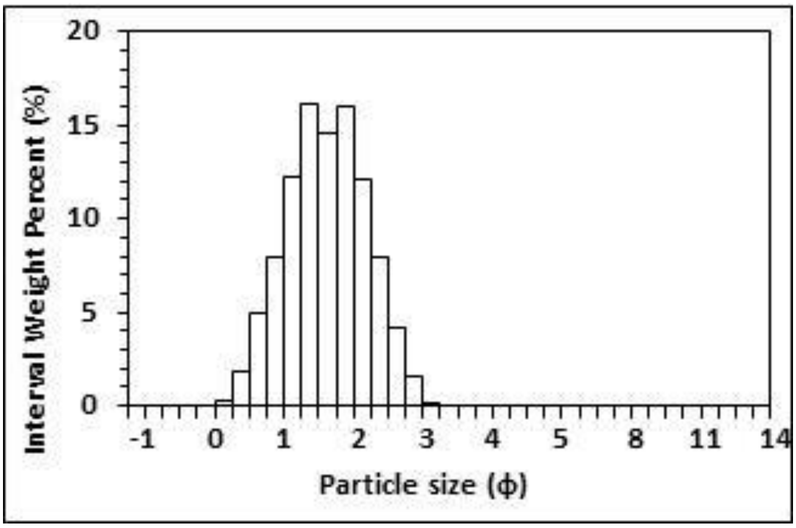

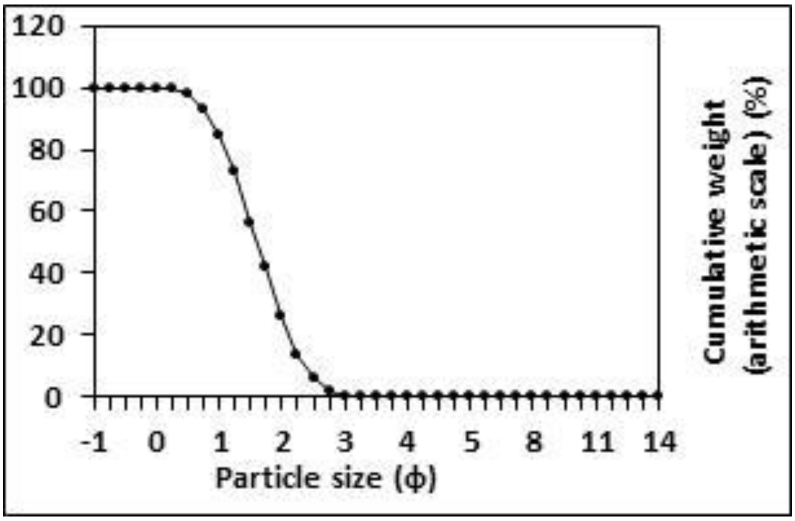

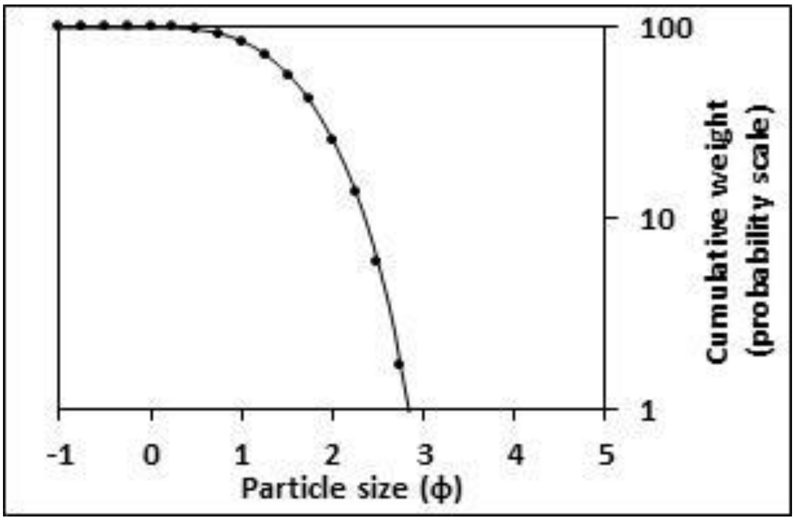

Figures II.115, II.116 and II.117: Histogram of grain size distribution and cumulative frequency graphs (arithmetic scale and probability scale) for sample 39: Mid intertidal zone, Transect 4, Southern Ngarunui Beach. Sample collected on the 10th of February, 2015.

Table II.40: *Graphical and statistical parameters, textural description and size classes for sample 40: Low intertidal zone, Transect 4, Southern Ngarunui Beach. Sample collected on the 10th of February, 2015.*

Textural description	**Textural size classes**
Moderately sorted, Coarsely skewed, Mesokurtic	Sand = 100 000%Fines = 0.000% Silt = 0.000%Clay = 0.000%
Moment method parameters (µm) Mean = 489.141 Standard deviation (sd) = 314.849 Skewness (SkI) = 1.706 Kurtosis (KG) = 6.206	**Graphical method parameters. After Folk (1980) (ϕ)** Mean (Mz) = 1.298 d(0.5) = 1.346 Sorting (SI) = 0.847 Skewness (SkI) = -0.107 Kurtosis (KG) = 0.976 Mean (mm) = 0.407 Mean (µm) = 406.801
Wentworth size class Medium sand	

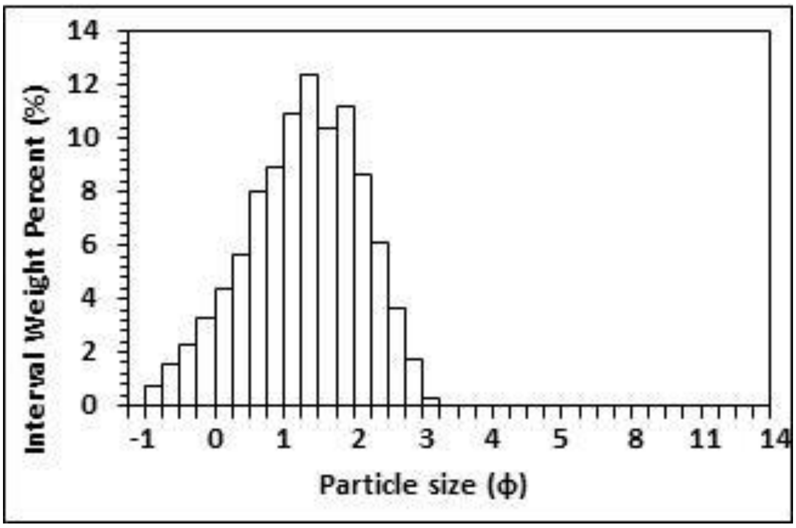

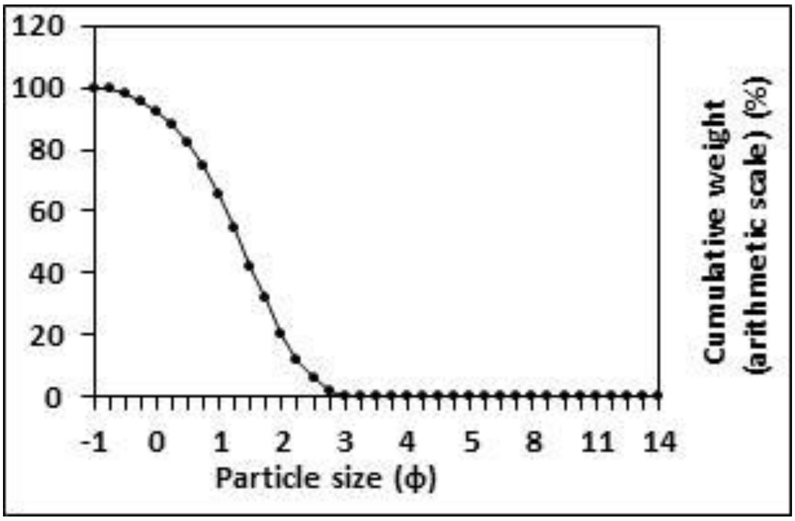

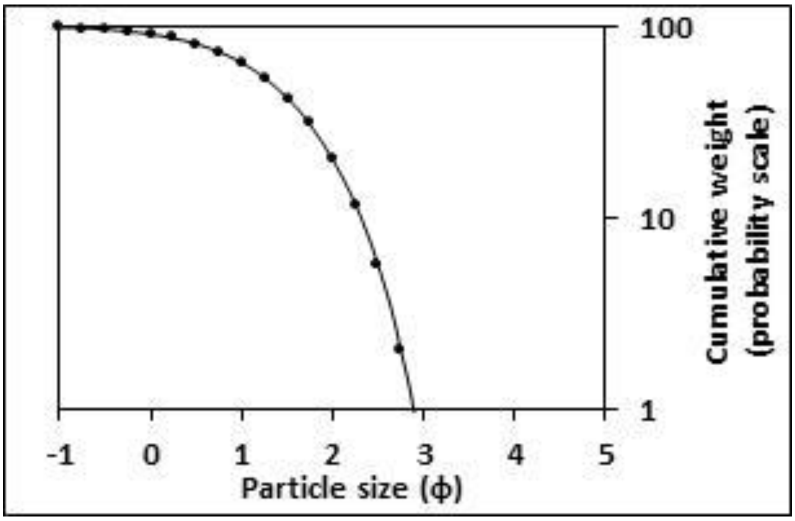

Figures II.118, II.119 and II.20: Histogram of grain size distribution and cumulative frequency graphs (arithmetic scale and probability scale) for sample 40: Low intertidal zone, Transect 4, Southern Ngarunui Beach. Sample collected on the 10th of February, 2015.

Table II.41: *Graphical and statistical parameters, textural description and size classes for sample 41: Mid intertidal zone, mid transect, Wainamu Beach. Sample collected on the 12th of December, 2014.*

Textural description	**Textural size classes**
Moderately well sorted, Near symmetrical skewed, Mesokurtic	Sand = 99.993% Fines = 0.007% Silt = 0.007% Clay = 0.000%
Moment method parameters (μm) Mean = 184.767 Standard deviation (sd) = 72.528 Skewness (SkI) = 0.954 Kurtosis (KG) = 3.831	**Graphical method parameters. After Folk (1980) (ϕ)** Mean (Mz) = 2.552 d(0.5) = 2.554 Sorting (SI) = 0.570 Skewness (SkI) = -0.012 Kurtosis (KG) = 0.945 Mean (mm) = 0.171 Mean (μm) = 170.573
Wentworth size class Fine sand	

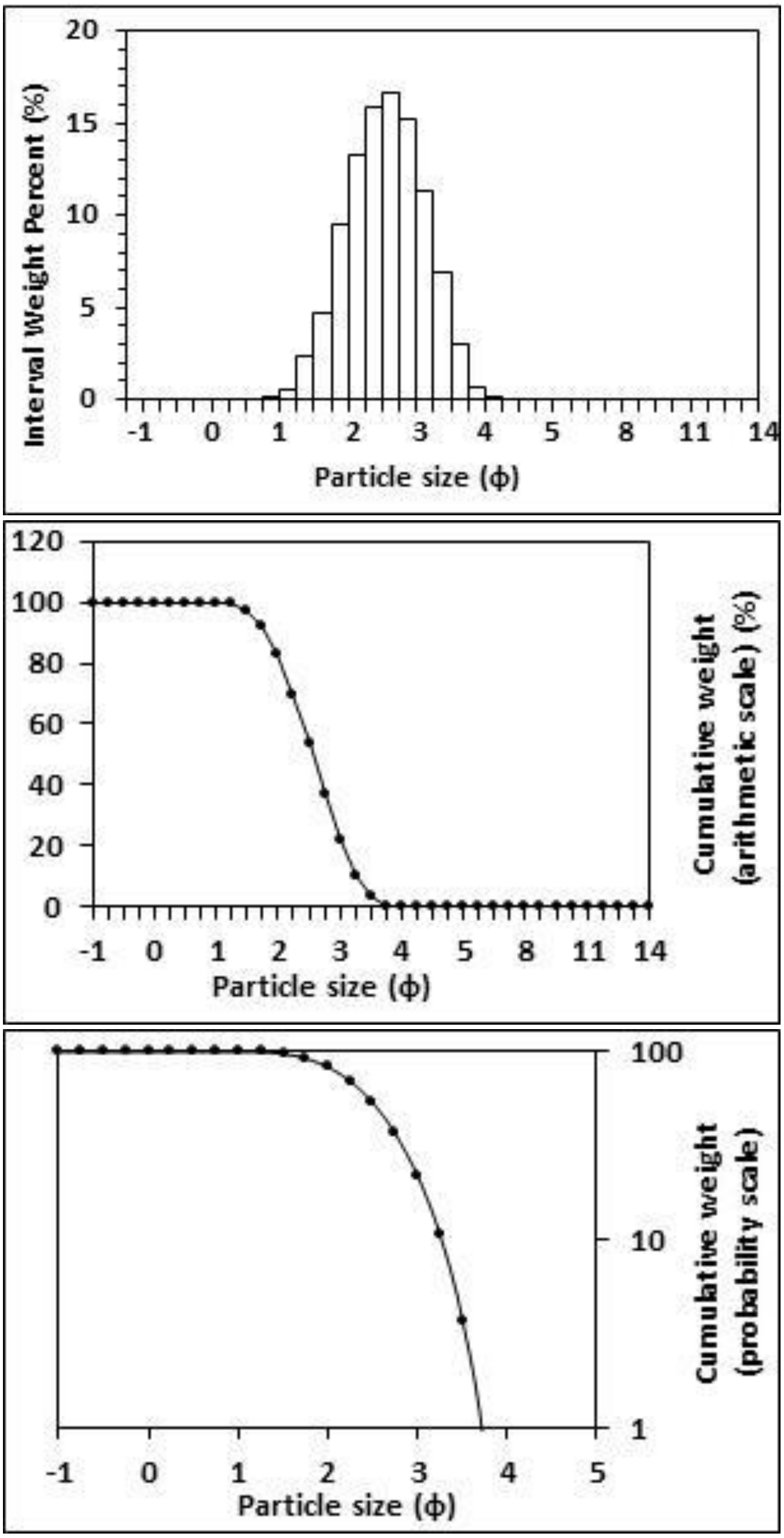

Figures II.121, II.122 and II.123: Histogram of grain size distribution and cumulative frequency graphs (arithmetic scale and probability scale) for sample 41: Mid intertidal zone, mid transect, Wainamu Beach. Sample collected on the 12th of December, 2014.

Table II.42: *Graphical and statistical parameters, textural description and size classes for sample 42: Low intertidal zone, western transect, Wainamu Beach. Sample collected on the 12th of December, 2014.*

Textural description	**Textural size classes**
Moderately well sorted, Near symmetrical skewed, Mesokurtic	Sand = 100 000%Fines = 0.000% Silt = 0.000%Clay = 0.000%
Moment method parameters (µm)	**Graphical method parameters. After Folk (1980) (ϕ)**
Mean = 252.057 Standard deviation (sd) = 90.641 Skewness (SkI) = 0.874 Kurtosis (KG) = 3.705	Mean (Mz) = 2.086 d(0.5) = 2.085 Sorting (SI) = 0.523 Skewness (SkI) = 0.004 Kurtosis (KG) = 0.958 Mean (mm) = 0.235 Mean (µm) = 235.466
Wentworth size class Fine sand	

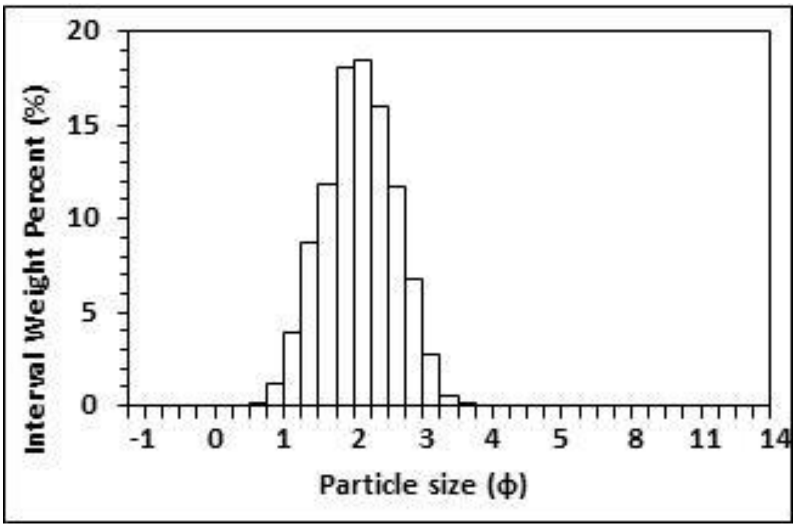

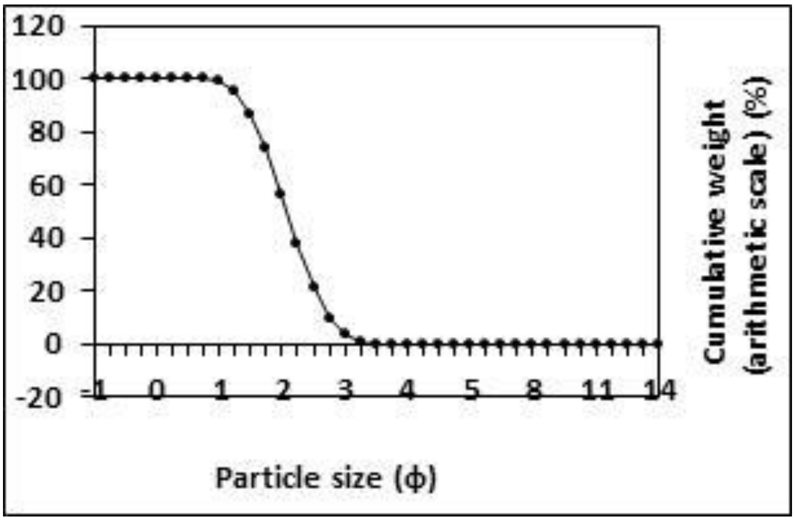

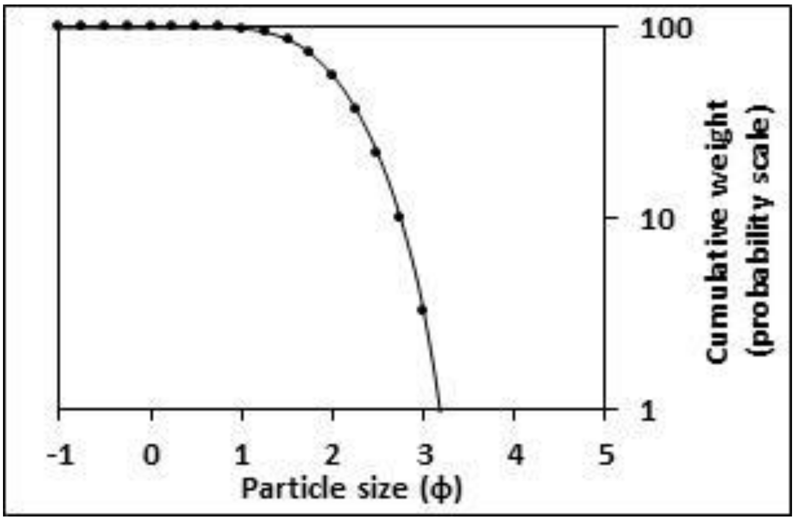

Figures II.124, II.125 and II.126 Histogram of grain size distribution and cumulative frequency graphs (arithmetic scale and probability scale) for sample 42: Low intertidal zone, western transect, Wainamu Beach. Sample collected on the 12th of December, 2014.

Table II.43: *Graphical and statistical parameters, textural description and size classes for sample 43: High intertidal zone, mid transect, Wainamu Beach. Sample collected on the 12th of December, 2014.*

Textural description	**Textural size classes**
Moderately well sorted, Near symmetrical skewed, Mesokurtic	Sand = 100 000%Fines = 0.000% Silt = 0.000%Clay = 0.000%
Moment method parameters (µm) Mean = 196.327 Standard deviation (sd) = 69.378 Skewness (SkI) = 0.821 Kurtosis (KG) = 3.552 **Wentworth size class** Fine sand	**Graphical method parameters. After Folk (1980) (ϕ)** Mean (Mz) = 2.438 d(0.5) = 2.439 Sorting (SI) = 0.518 Skewness (SkI) = -0.001 Kurtosis (KG) = 0.948 Mean (mm) = 0.184 Mean (µm) = 184.496

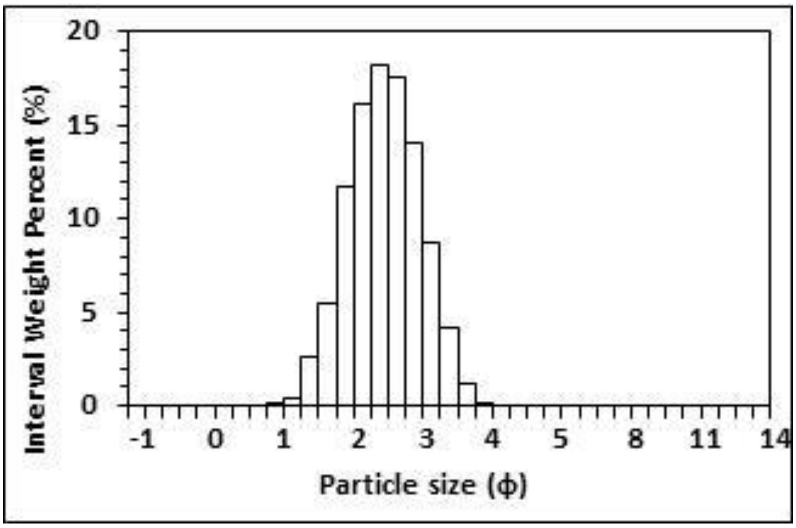

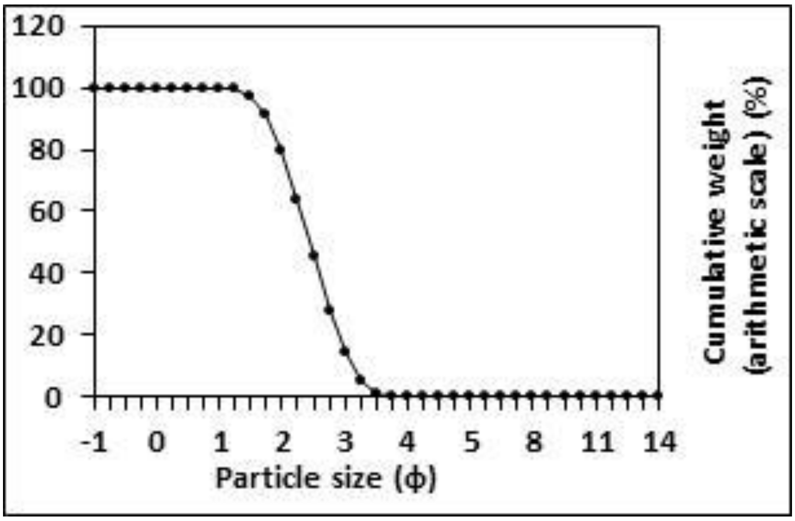

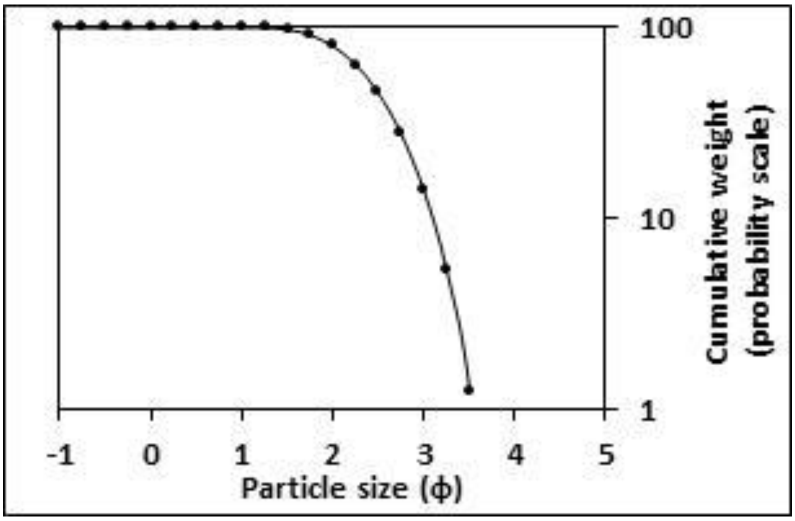

Figures II.127, II.128 and II.129: Histogram of grain size distribution and cumulative frequency graphs (arithmetic scale and probability scale) for sample 43: High intertidal zone, mid transect, Wainamu Beach. Sample collected on the 12th of December, 2014.

Table II.44: *Graphical and statistical parameters, textural description and size classes for sample 44: Low intertidal zone, eastern transect, Wainamu Beach. Sample collected on the 12th of December, 2014.*

Textural description	**Textural size classes**
Moderately well sorted, Near symmetrical skewed, Mesokurtic	Sand = 99.346 % Fines = 0.654% Silt = 0.475% Clay = 0.179%
Moment method parameters (μm)	**Graphical method parameters. After Folk (1980) (ϕ)**
Mean = 234.147 Standard deviation (sd) = 129.797 Skewness (SkI) = 5.302 Kurtosis (KG) = 55.576	Mean (Mz) = 2.243 d(0.5) = 2.240 Sorting (SI) = 0.600 Skewness (SkI) = 0.008 Kurtosis (KG) = 0.953 Mean (mm) = 0.211 Mean (μm) = 211.248
Wentworth size class Fine sand	

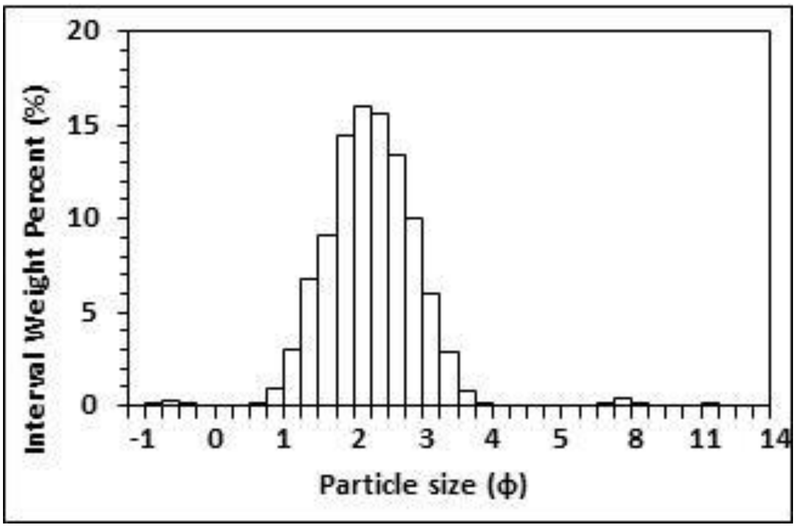

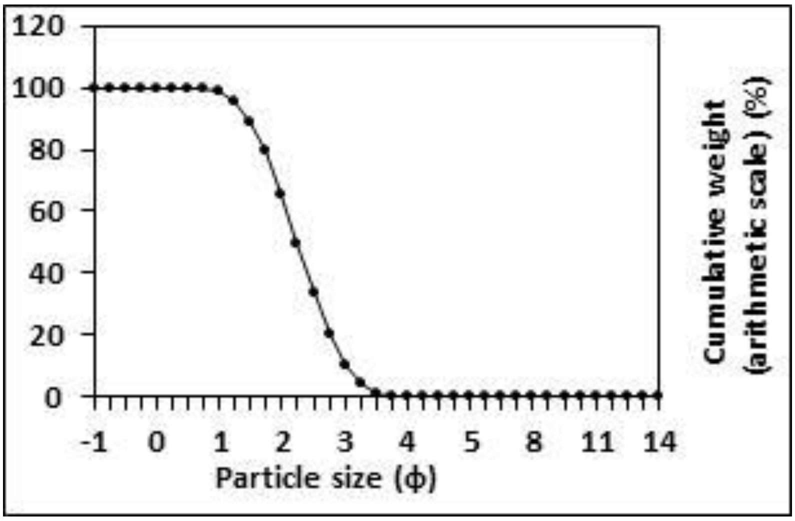

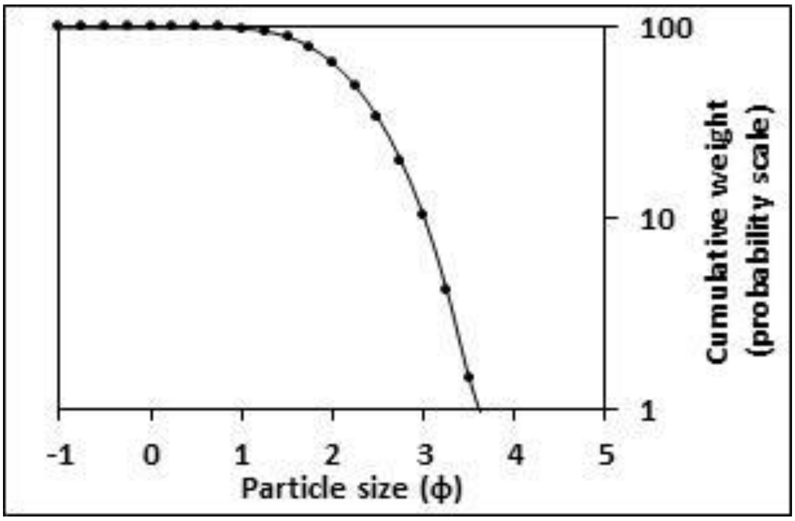

Figures II.130, II.131 and II.132: Histogram of grain size distribution and cumulative frequency graphs (arithmetic scale and probability scale) for sample 44: Low intertidal zone, eastern transect, Wainamu Beach. Sample collected on the 12th of December, 2014.

Table II.45: *Graphical and statistical parameters, textural description and size classes for sample 45: High intertidal zone, eastern transect, Wainamu Beach. Sample collected on the 12th of December, 2014.*

Textural description	**Textural size classes**
Moderately well sorted, Near symmetrical skewed, Mesokurtic	Sand = 100 000%Fines = 0.000% Silt = 0.000%Clay = 0.000%
Moment method parameters (µm) Mean = 192.223 Standard deviation (sd) = 68.183 Skewness (SkI) = 0.846 Kurtosis (KG) = 3.630	**Graphical method parameters. After Folk (1980) (ϕ)** Mean (Mz) = 2.469 d(0.5) = 2.472 Sorting (SI) = 0.518 Skewness (SkI) = -0.004 Kurtosis (KG) = 0.950 Mean (mm) = 0.181 Mean (µm) = 180.576
Wentworth size class Fine sand	

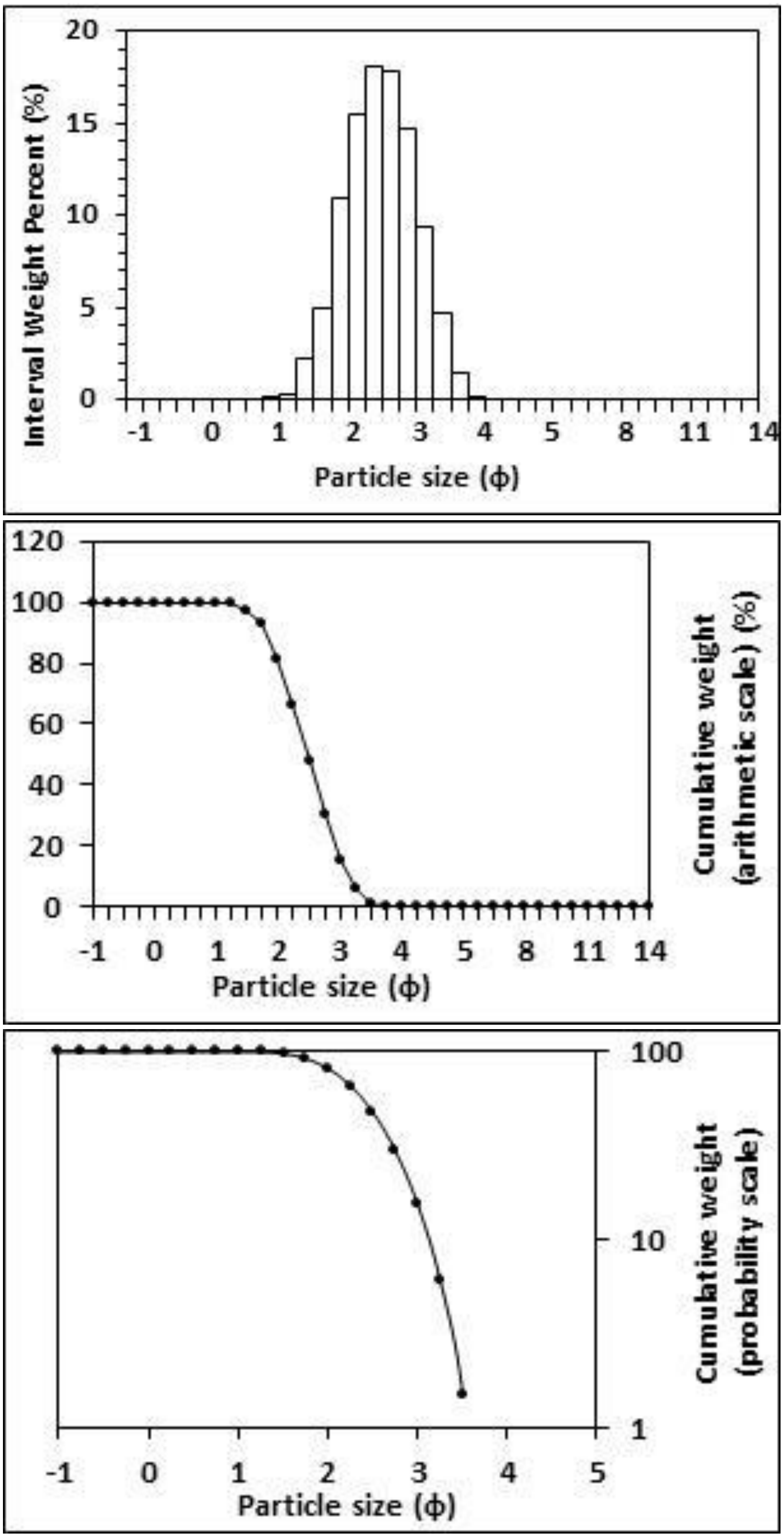

Figures II.133, II.134 and II .135: Histogram of grain size distribution and cumulative frequency graphs (arithmetic scale and probability scale) for sample 45: High intertidal zone, eastern transect, Wainamu Beach. Sample collected on the 12th of December, 2014.

Table II.46: *Graphical and statistical parameters, textural description and size classes for sample 46: Mid intertidal zone, eastern transect, Wainamu Beach. Sample collected on the 12th of December, 2014.*

Textural description	**Textural size classes**
Moderately sorted, Fine skewed, Very leptokurtic	Sand = 94.235% Fines = 5.765% Silt = 5.192% Clay = 0.573%
Moment method parameters (µm) Mean = 222.959 Standard deviation (sd) = 95.927 Skewness (SkI) = 0.214 Kurtosis (KG) = 3.530	**Graphical method parameters. After Folk (1980) (ϕ)** Mean (Mz) = 2.240 d(0.5) = 2.218 Sorting (SI) = 0.852 Skewness (SkI) = 0.293 Kurtosis (KG) = 1.935 Mean (mm) = 0.212 Mean (µm) = 211.639
Wentworth size class Fine sand	

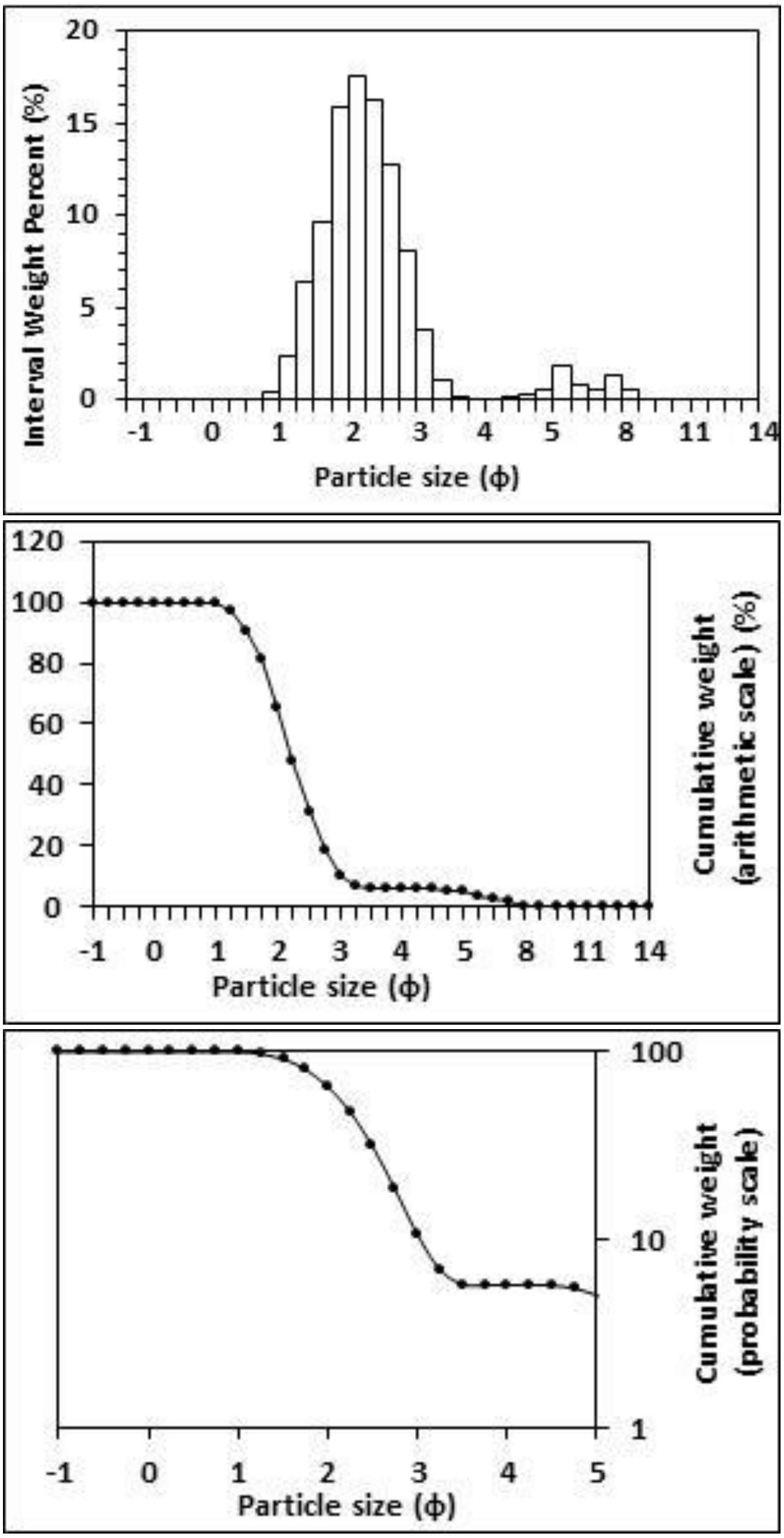

Figures II.136, II.137 and II.138: Histogram of grain size distribution and cumulative frequency graphs (arithmetic scale and probability scale) for sample 46: Mid intertidal zone, eastern transect, Wainamu Beach. Sample collected on the 12th of December, 2014.

Table II.47: *Graphical and statistical parameters, textural description and size classes for sample 47: Mid intertidal zone, western transect, Wainamu Beach. Sample collected on the 12th of December, 2014.*

Textural description	**Textural size classes**
Well sorted, Near symmetrical skewed, Mesokurtic	Sand = 99.905% Fines = 0.095% Silt = 0.095% Clay = 0.000%
Moment method parameters (µm) Mean = 153.931 Standard deviation (sd) = 51.603 Skewness (SkI) = 0.786 Kurtosis (KG) = 3.426	**Graphical method parameters. After Folk (1980) (ϕ)** Mean (Mz) = 2.784 d(0.5) = 2.785 Sorting (SI) = 0.489 Skewness (SkI) = 0.004 Kurtosis (KG) = 0.940 Mean (mm) = 0.145 Mean (µm) = 145.185
Wentworth size class Fine sand	

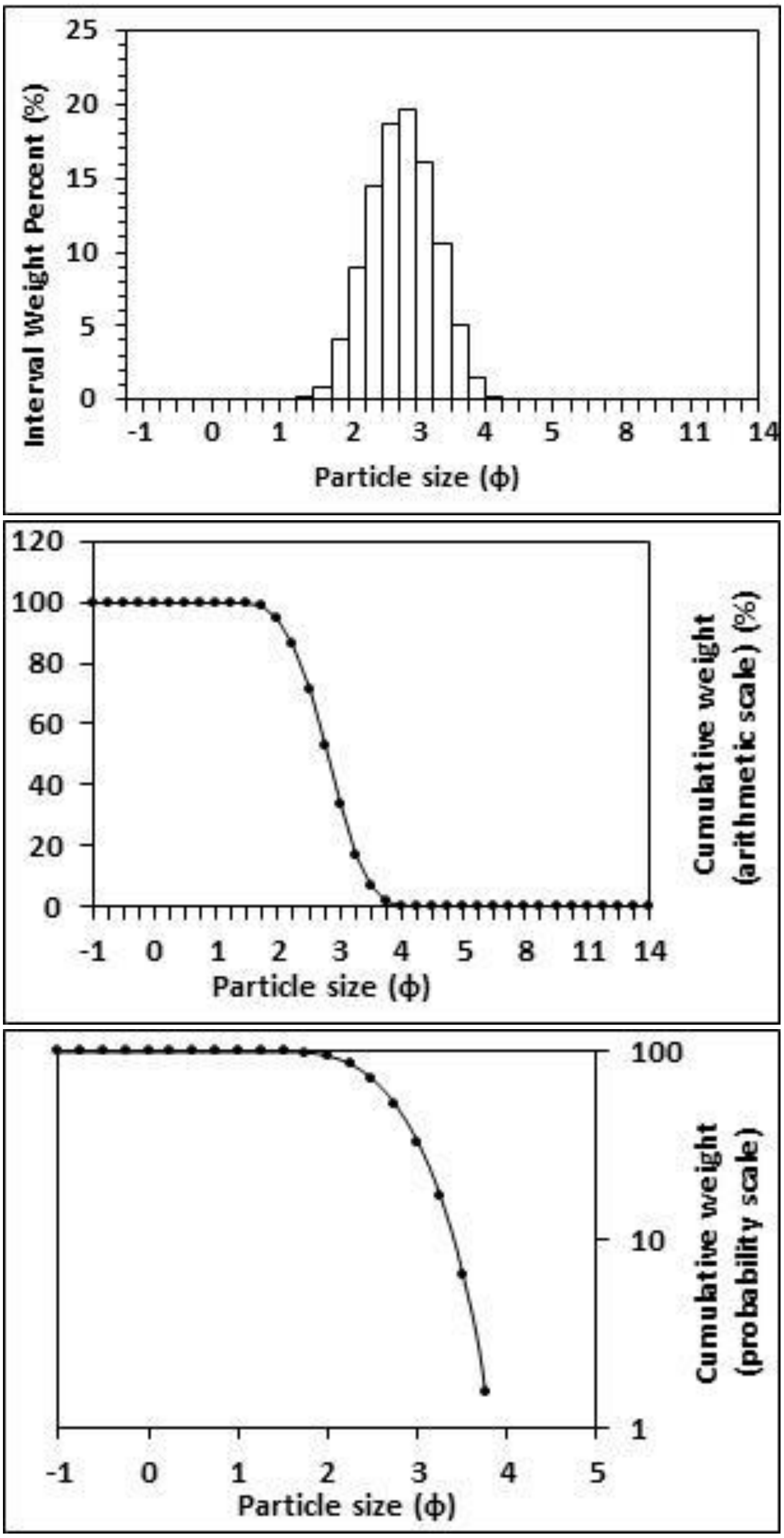

Figures II.139, II.140 and II.141: Histogram of grain size distribution and cumulative frequency graphs (arithmetic scale and probability scale) for sample 47: Mid intertidal zone, western transect, Wainamu Beach. Sample collected on the 12th of December, 2014.

Table II.48: *Graphical and statistical parameters, textural description and size classes for sample 48: Low intertidal zone, mid transect, Wainamu Beach. Sample collected on the 12th of December, 2014.*

Textural description	**Textural size classes**
Moderately well sorted, Near symmetrical skewed, Mesokurtic	Sand = 100 000%Fines = 0.000% Silt = 0.000%Clay = 0.000%
Moment method parameters (µm) Mean = 237.248 Standard deviation (sd) = 84.192 Skewness (SkI) = 0.832 Kurtosis (KG) =3.561	**Graphical method parameters. After Folk (1980) (ϕ)** Mean (Mz) = 2.168 d(0.5) = 2.167 Sorting (SI) = 0.518 Skewness (SkI) = -0.004 Kurtosis (KG) = 0.952 Mean (mm) = 0.223 Mean (µm) = 222.554
Wentworth size class Fine sand	

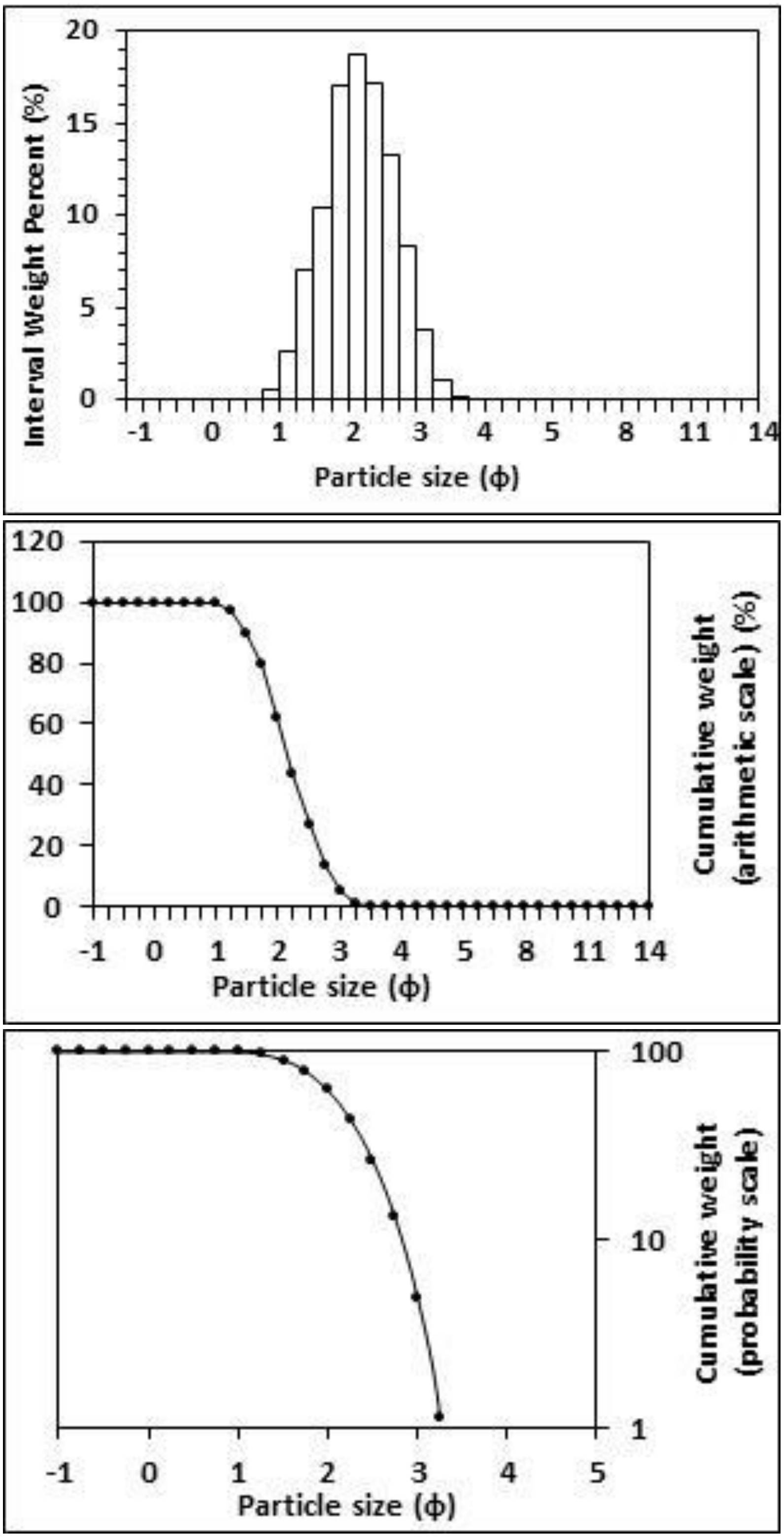

Figures II.142, II.143 and II.144: Histogram of grain size distribution and cumulative frequency graphs (arithmetic scale and probability scale) for sample 48: Low intertidal zone, mid transect, Wainamu Beach. Sample collected on the 12th of December, 2014.

Table II.49: *Graphical and statistical parameters, textural description and size classes for sample 49: High intertidal zone, western transect, Wainamu Beach. Sample collected on the 12th of December, 2014.*

Textural description	**Textural size classes**
Moderately well sorted, Near symmetrical skewed, Mesokurtic	Sand = 99.987% Fines = 0.013% Silt = 0.013% Clay = 0.000%
Moment method parameters (µm)	**Graphical method parameters. After Folk (1980) (ɸ)**
Mean = 226.949 Standard deviation (sd) = 225.979 Skewness (SkI) = 4.538 Kurtosis (KG) = 25.531	Mean (Mz) = 2.500 d(0.5) = 2.515 Sorting (SI) = 0.635 Skewness (SkI) = -0.076 Kurtosis (KG) = 1.035 Mean (mm) = 0.177 Mean (µm) = 176.790
Wentworth size class Fine sand	

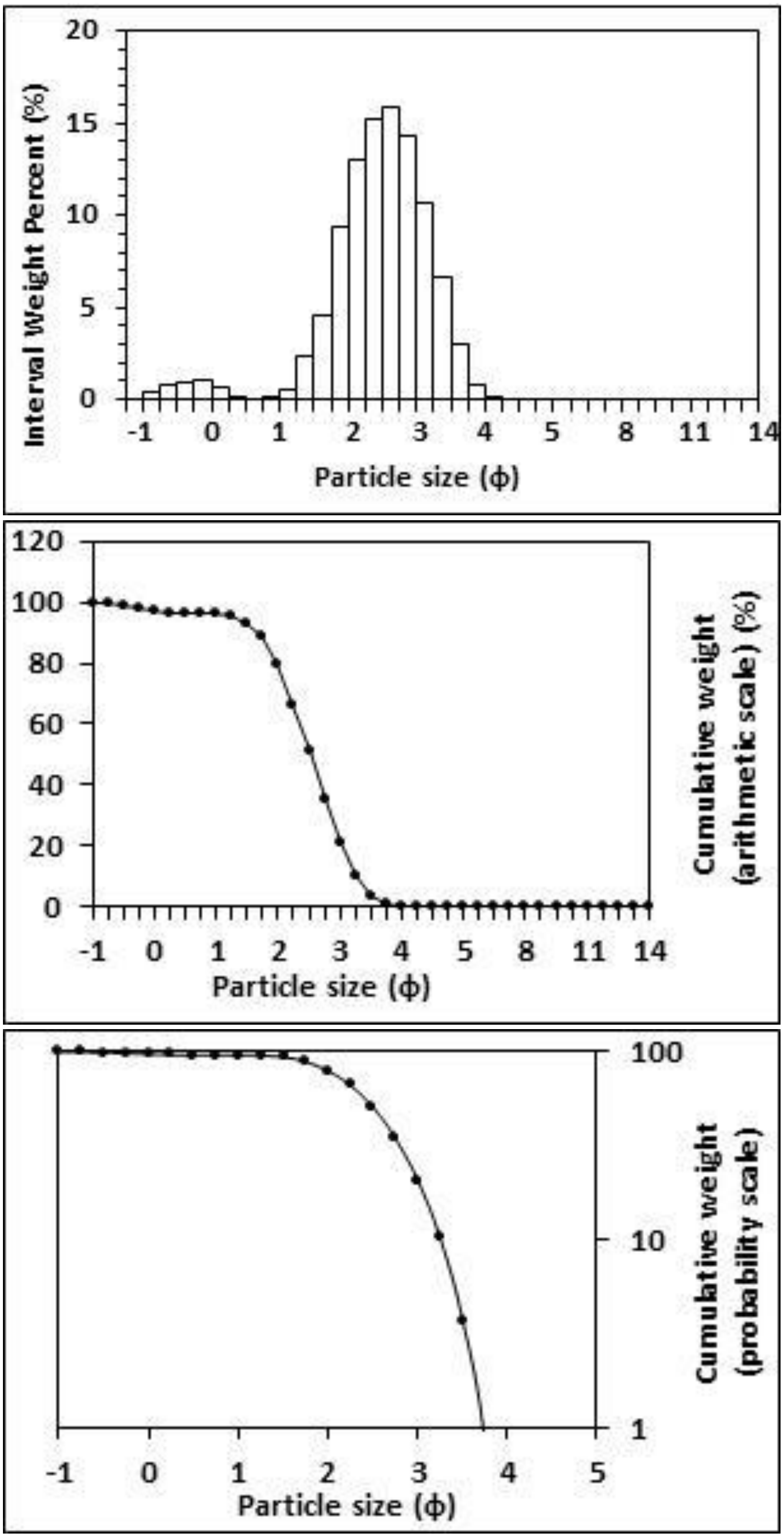

Figures II.145, II.146 and II.147: Histogram of grain size distribution and cumulative frequency graphs (arithmetic scale and probability scale) for sample 49: High intertidal zone, western transect, Wainamu Beach. Sample collected on the 12th of December, 2014.

Table II.50: *Graphical and statistical parameters, textural description and size classes for sample 50: High intertidal zone, western transect, Wainamu Beach.*
Sample collected on the 16th of July, 2014.

Textural description	**Textural size classes**
Moderately well sorted, Near symmetrical skewed, Mesokurtic	Sand = 99.990% Fines = 0.010% Silt = 0.010% Clay = 0.000%
Moment method parameters (µm) Mean = 188.140 Standard deviation (sd) = 74.309 Skewness (SkI) = 0.920 Kurtosis (KG) = 3.719 **Wentworth size class** Fine sand	**Graphical method parameters. After Folk (1980) (ϕ)** Mean (Mz) = 2.525 d(0.5) = 2.526 Sorting (SI) = 0.578 Skewness (SkI) = -0.005 Kurtosis (KG) = 0.943 Mean (mm) = 0.174 Mean (µm) = 173.746

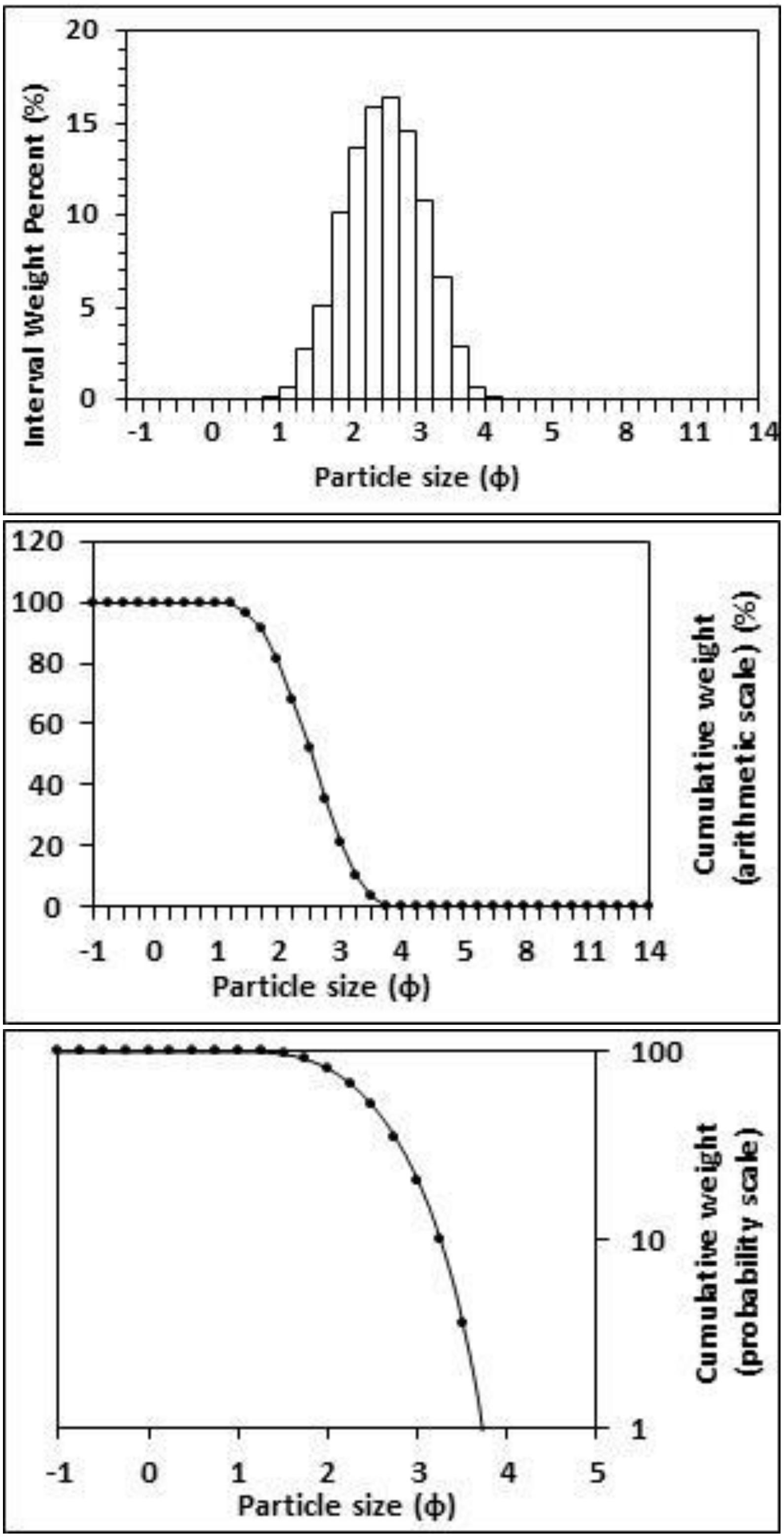

Figures II.148, II.149 and II.150: Histogram of grain size distribution and cumulative frequency graphs (arithmetic scale and probability scale) for sample 50: High intertidal zone, western transect, Wainamu Beach. Sample collected on the 16th of July, 2014.

Table II.51: *Graphical and statistical parameters, textural description and size classes for sample 51: Low intertidal zone, mid transect, Wainamu Beach. Sample collected on the 16th of July, 2014.*

Textural description	**Textural size classes**
Moderately well sorted, Near symmetrical skewed, Mesokurtic	Sand = 100 000%Fines = 0.000% Silt = 0.000%Clay = 0.000%
Moment method parameters (µm) Mean = 227.016 Standard deviation (sd) = 88.211 Skewness (SkI) = 0.876 Kurtosis (KG) = 3.589	**Graphical method parameters. After Folk (1980) (ϕ)** Mean (Mz) = 2.251 d(0.5) = 2.248 Sorting (SI) = 0.572 Skewness (SkI) = 0.004 Kurtosis (KG) = 0.947 Mean (mm) = 0.210 Mean (µm) = 210.150
Wentworth size class Fine sand	

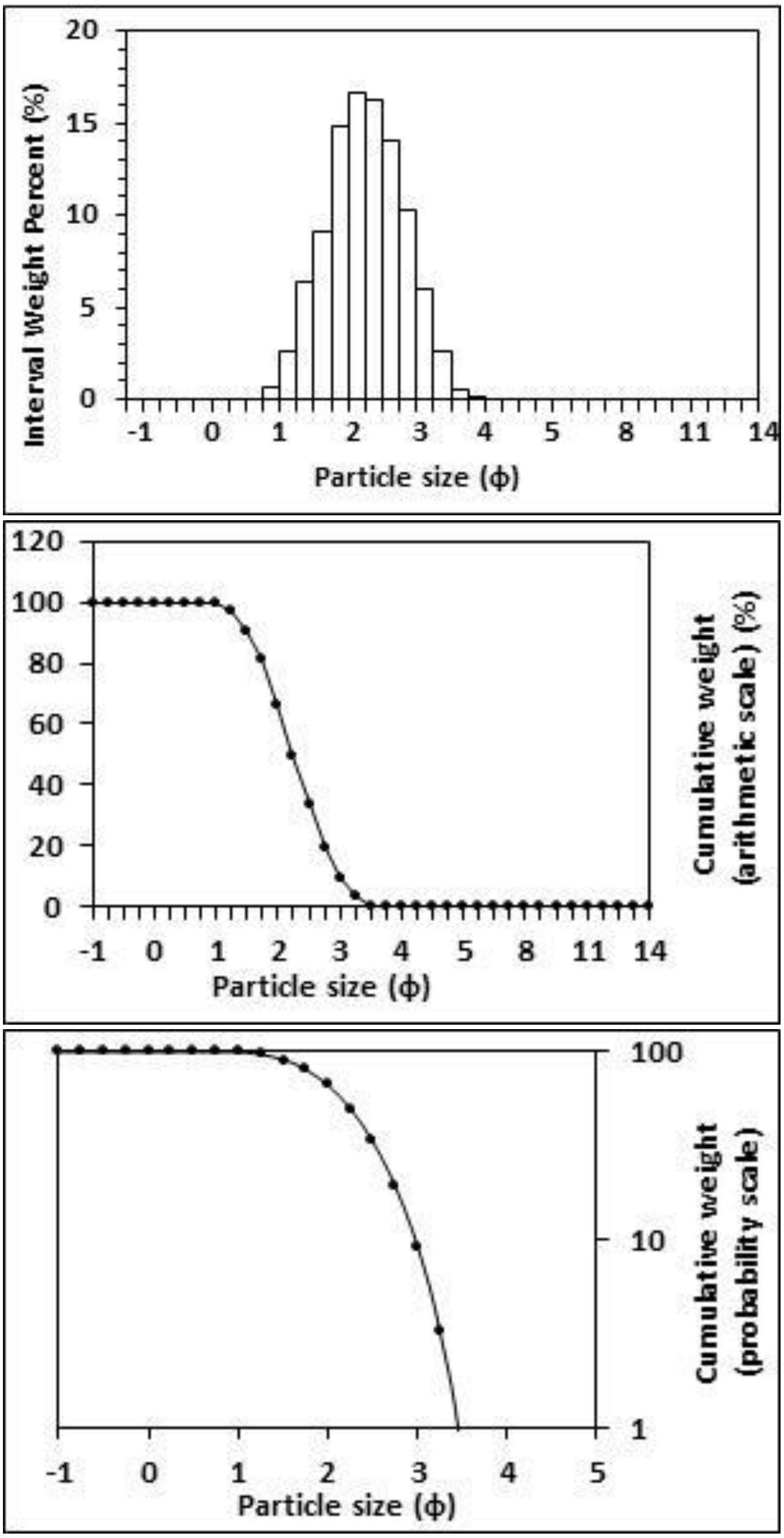

Figures II.151, II.152 and II.153: Histogram of grain size distribution and cumulative frequency graphs (arithmetic scale and probability scale) for sample 51: Low intertidal zone, mid transect, Wainamu Beach. Sample collected on the 16th of July, 2014.

Table II.52: *Graphical and statistical parameters, textural description and size classes for sample 52: Mid intertidal zone, mid transect, Wainamu Beach. Sample collected on the 16th of July, 2014.*

Textural description	**Textural size classes**
Moderately well sorted, Near symmetrical skewed, Mesokurtic	Sand = 99.988% Fines = 0.012% Silt = 0.012% Clay = 0.000%
Moment method parameters (µm) Mean = 184.918 Standard deviation (sd) = 74.273 Skewness (SkI) = 0.990 Kurtosis (KG) = 3.928 **Wentworth size class** Fine sand	**Graphical method parameters. After Folk (1980) (ϕ)** Mean (Mz) = 2.555 d(0.5) = 2.559 Sorting (SI) = 0.580 Skewness (SkI) = -0.018 Kurtosis (KG) = 0.945 Mean (mm) = 0.170 Mean (µm) = 170.208

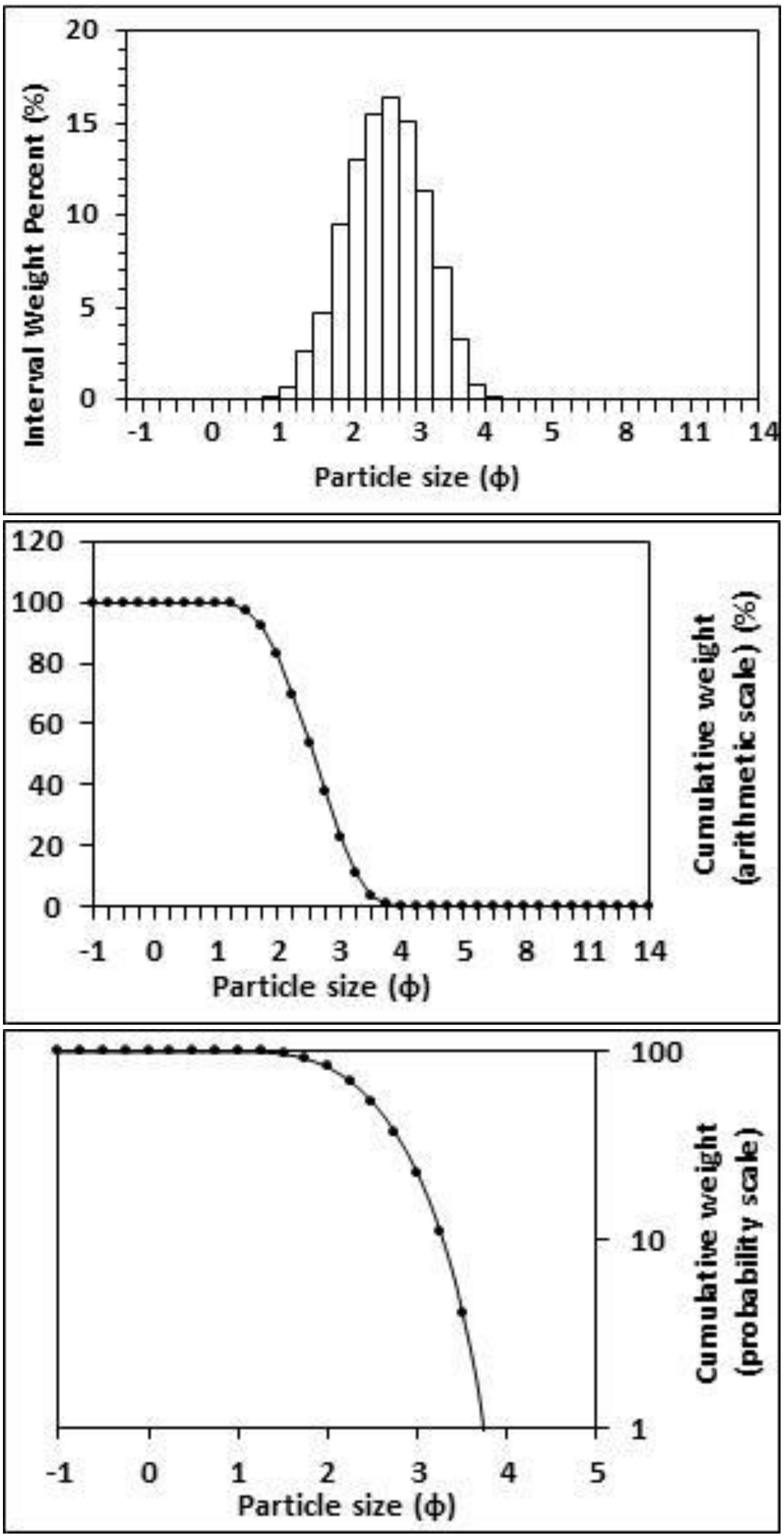

Figures II.154, II.155 and II.156: Histogram of grain size distribution and cumulative frequency graphs (arithmetic scale and probability scale) for sample 52: Mid intertidal zone, mid transect, Wainamu Beach. Sample collected on the 16th of July, 2014.

Table II.53: *Graphical and statistical parameters, textural description and size classes for sample 53: Low intertidal zone, western transect, Wainamu Beach. Sample collected on the 16th of July, 2014.*

Textural description	**Textural size classes**
Moderately well sorted, Near symmetrical skewed, Mesokurtic	Sand = 100 000%Fines = 0.000% Silt = 0.000%Clay = 0.000%
Moment method parameters (µm) Mean = 210.918 Standard deviation (sd) = 72.045 Skewness (SkI) = 0.808 Kurtosis (KG) = 3.499	**Graphical method parameters. After Folk (1980) (ϕ)** Mean (Mz) = 2.333 d(0.5) = 2.333 Sorting (SI) = 0.502 Skewness (SkI) = 0.004 Kurtosis (KG) = 0.957 Mean (mm) = 0.198 Mean (µm) = 198.497
Wentworth size class Fine sand	

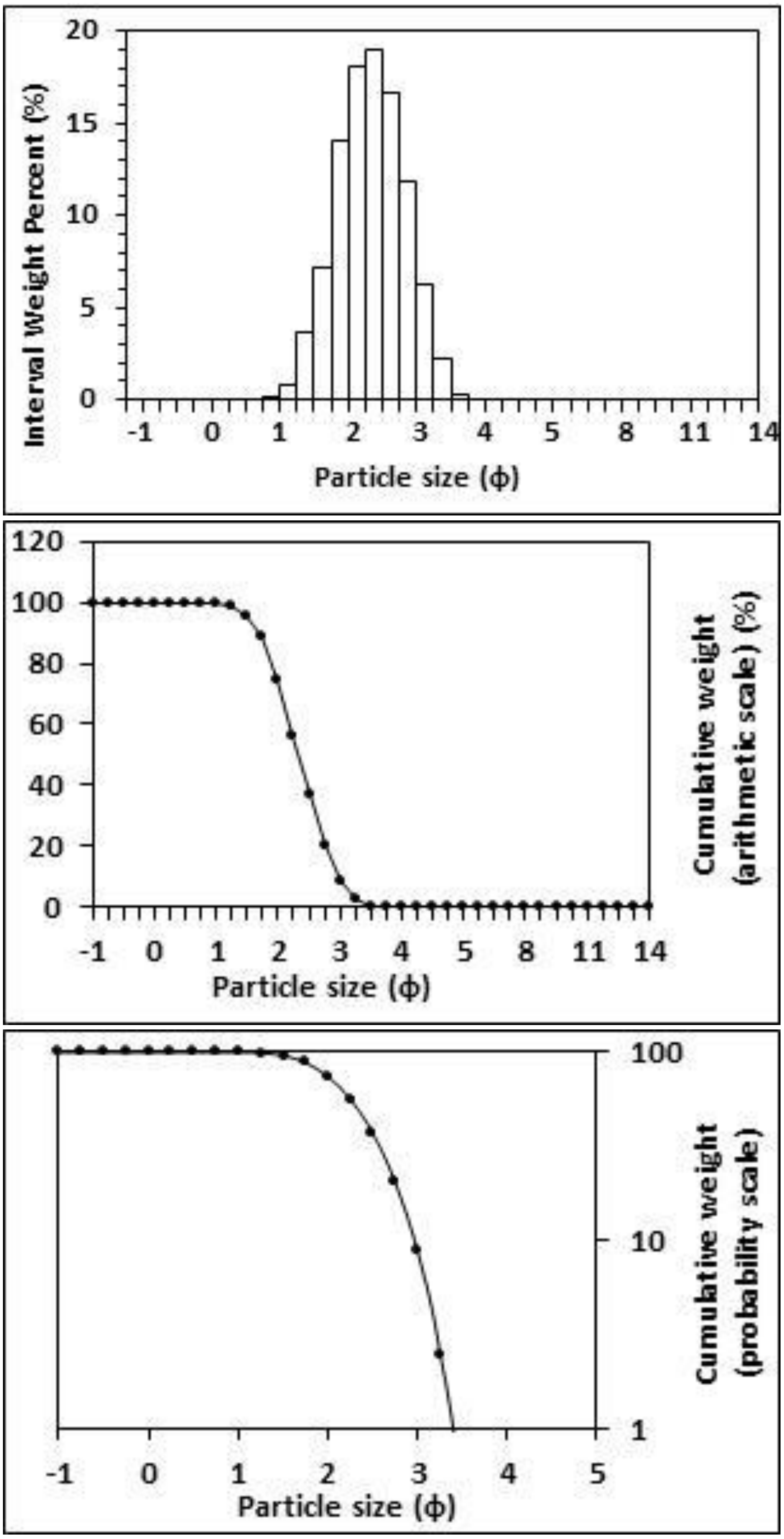

Figures II.157, II.158 and II.159: Histogram of grain size distribution and cumulative frequency graphs (arithmetic scale and probability scale) for sample 53: Low intertidal zone, western transect, Wainamu Beach. Sample collected on the 16th of July, 2014.

Table II.54: *Graphical and statistical parameters, textural description and size classes for sample 54: High intertidal zone, mid transect, Wainamu Beach. Sample collected on the 16th of July, 2014.*

Textural description	**Textural size classes**
Moderately well sorted, Near symmetrical skewed, Mesokurtic	Sand = 100 000%Fines = 0.000% Silt = 0.000%Clay = 0.000%
Moment method parameters (µm) Mean = 204.473 Standard deviation (sd) = 79.463 Skewness (SkI) = 0.863 Kurtosis (KG) = 3.513	**Graphical method parameters. After Folk (1980) (ϕ)** Mean (Mz) = 2.398 d(0.5) = 2.399 Sorting (SI) = 0.571 Skewness (SkI) = 0.002 Kurtosis (KG) = 0.950 Mean (mm) = 0.190 Mean (µm) = 189.718
Wentworth size class Fine sand	

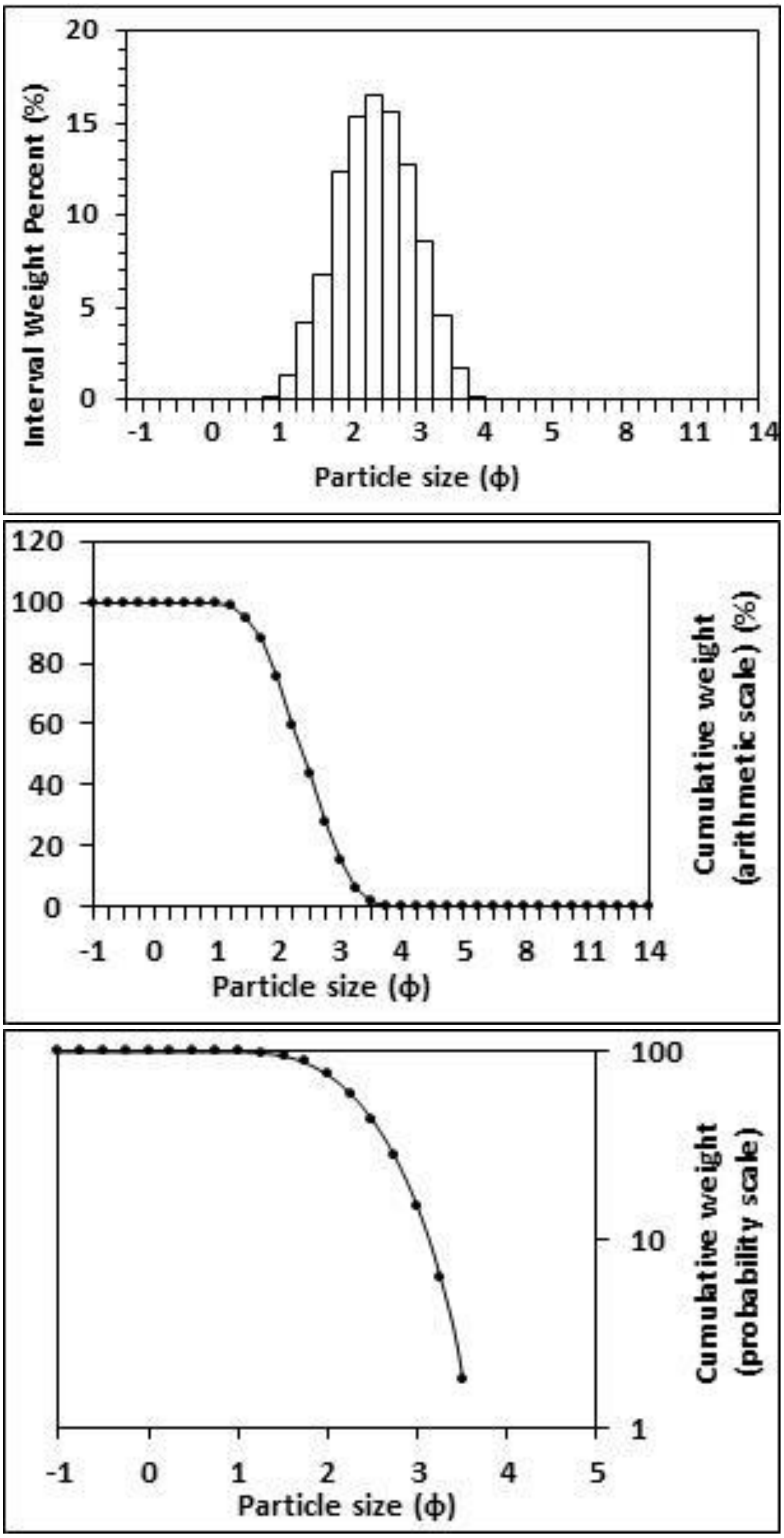

Figures II.160, II.161 and II.162: Histogram of grain size distribution and cumulative frequency graphs (arithmetic scale and probability scale) for sample 54: High intertidal zone, mid transect, Wainamu Beach. Sample collected on the 16th of July, 2014.

Table II.55: *Graphical and statistical parameters, textural description and size classes for sample 55: Low intertidal zone, eastern transect, Wainamu Beach. Sample collected on the 16th of July, 2014.*

Textural description	**Textural size classes**
Poorly sorted, Strongly fine skewed, Very leptokurtic	Sand = 90.420% Fines = 9.580% Silt = 8.348% Clay = 1.232%
Moment method parameters (µm) Mean = 215.862 Standard deviation (sd) = 107.192 Skewness (SkI) = 0.208 Kurtosis (KG) = 3.187	**Graphical method parameters. After Folk (1980) (ϕ)** Mean (Mz) = 2.302 d(0.5) = 2.257 Sorting (SI) = 1.052 Skewness (SkI) = 0.348 Kurtosis (KG) = 2.170 Mean (mm) = 0.203 Mean (µm) = 202.826
Wentworth size class Fine sand	

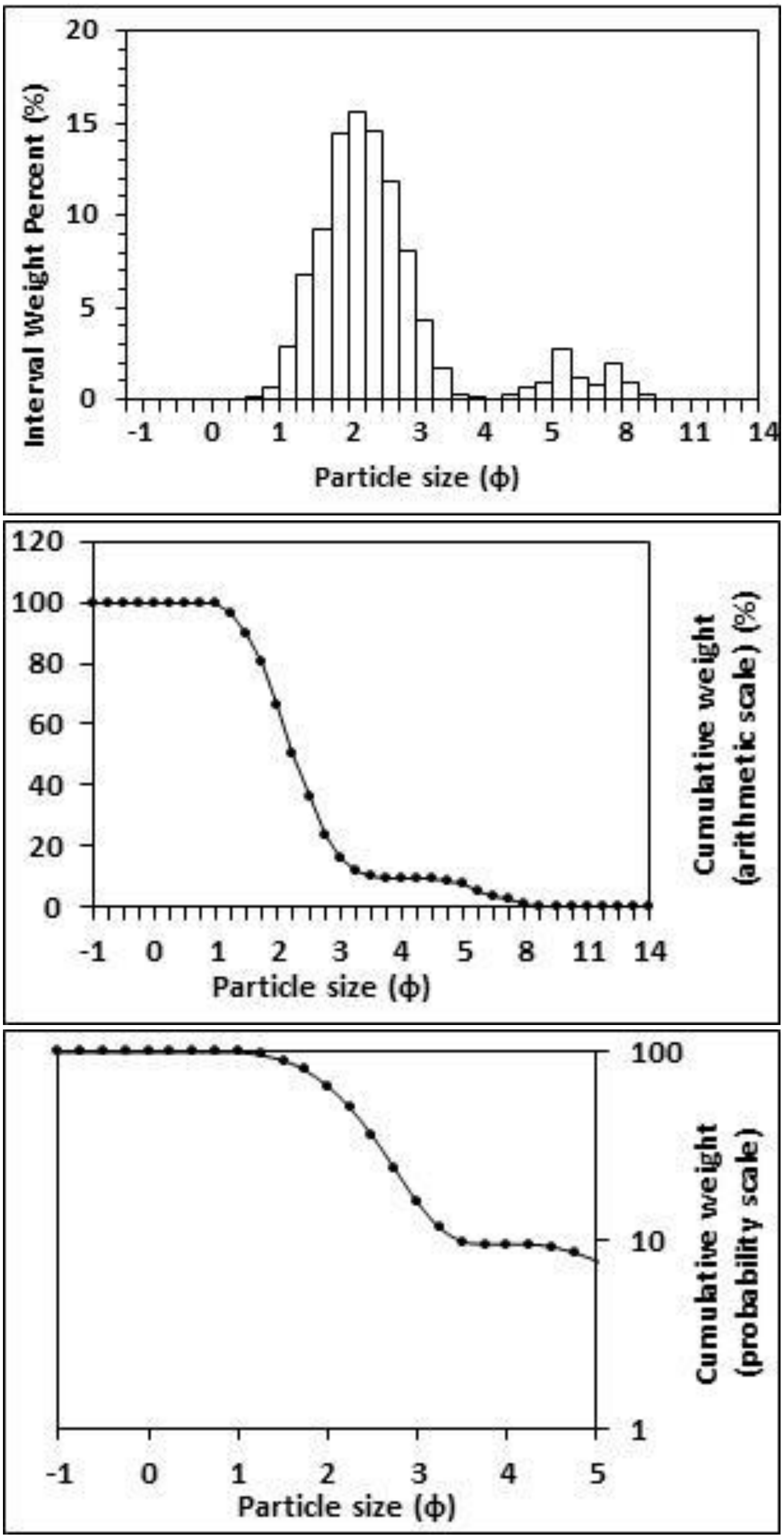

Figures II.163, II.164 and II.165: Histogram of grain size distribution and cumulative frequency graphs (arithmetic scale and probability scale) for sample 55: Low intertidal zone, eastern transect, Wainamu Beach. Sample collected on the 16th of July, 2014.

Table II.56: *Graphical and statistical parameters, textural description and size classes for sample 56: High intertidal zone, eastern transect, Wainamu Beach. Sample collected on the 16th of July, 2014.*

Textural description	**Textural size classes**
Moderately well sorted, Near symmetrical skewed, Mesokurtic	Sand = 100 000%Fines = 0.000% Silt = 0.000%Clay = 0.000%
Moment method parameters (µm) Mean = 202.976 Standard deviation (sd) = 72.263 Skewness (SkI) = 0.832 Kurtosis (KG) = 3.560	**Graphical method parameters. After Folk (1980) (ϕ)** Mean (Mz) = 2.393 d(0.5) = 2.394 Sorting (SI) = 0.522 Skewness (SkI) = -0.001 Kurtosis (KG) = 0.956 Mean (mm) = 0.190 Mean (µm) =190.381
Wentworth size class Fine sand	

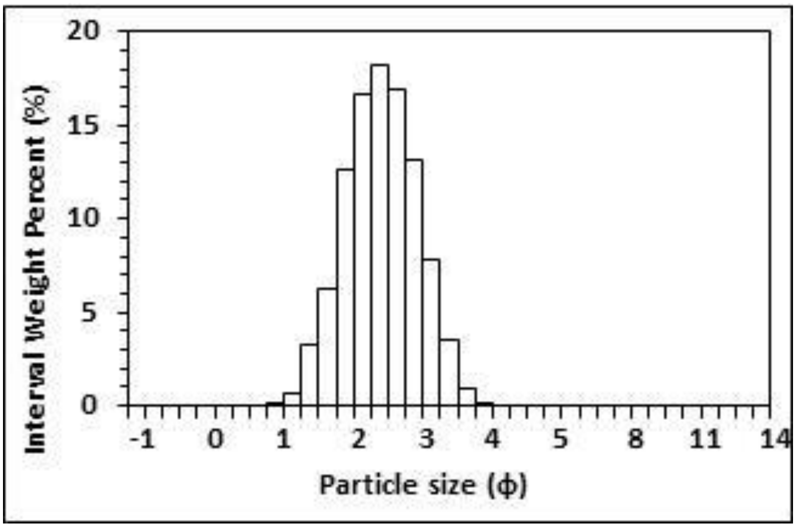

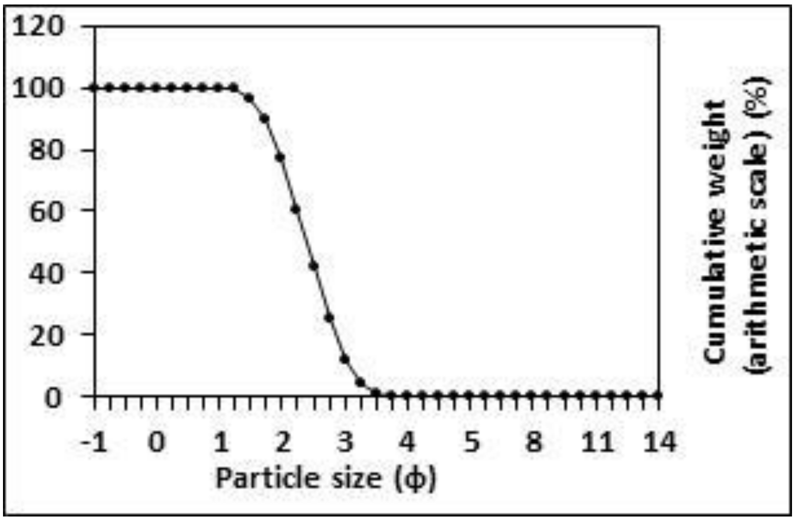

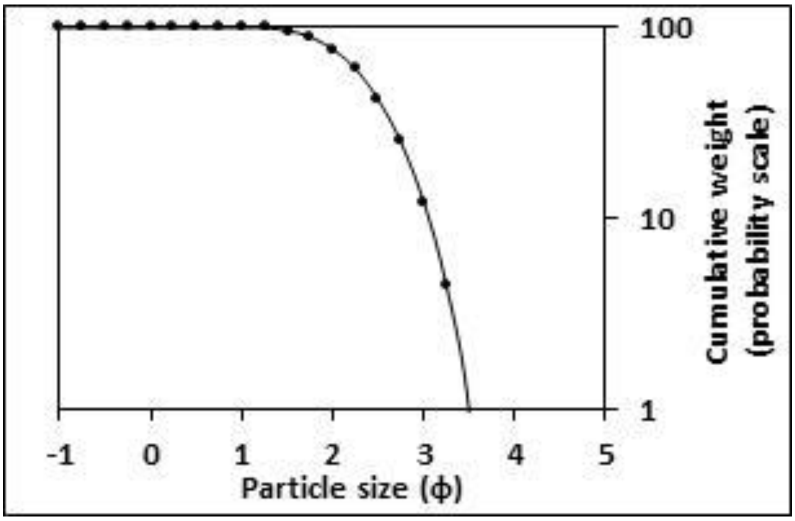

Figures II.166, II.167 and II.168: Histogram of grain size distribution and cumulative frequency graphs (arithmetic scale and probability scale) for sample 56: High intertidal zone, eastern transect, Wainamu Beach. Sample collected on the 16th of July, 2014.

Table II.57: *Graphical and statistical parameters, textural description and size classes for sample 57: Mid intertidal zone, western transect, Wainamu Beach. Sample collected on the 16th of July, 2014.*

Textural description	**Textural size classes**
Moderately well sorted, Near symmetrical skewed, Mesokurtic	Sand = 100 000%Fines = 0.000% Silt = 0.000%Clay = 0.000%
Moment method parameters (µm) Mean = 187.072 Standard deviation (sd) = 67.082 Skewness (SkI) = 0.869 Kurtosis (KG) = 3.654	**Graphical method parameters. After Folk (1980) (ϕ)** Mean (Mz) = 2.516 d(0.5) = 2.516 Sorting (SI) = 0.522 Skewness (SkI) = -0.004 Kurtosis (KG) = 0.950 Mean (mm) = 0.175 Mean (µm) = 174.880
Wentworth size class Fine sand	

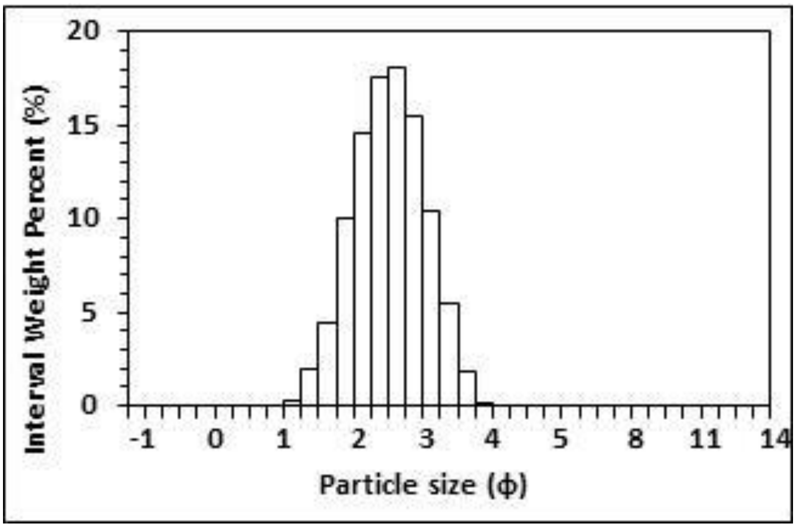

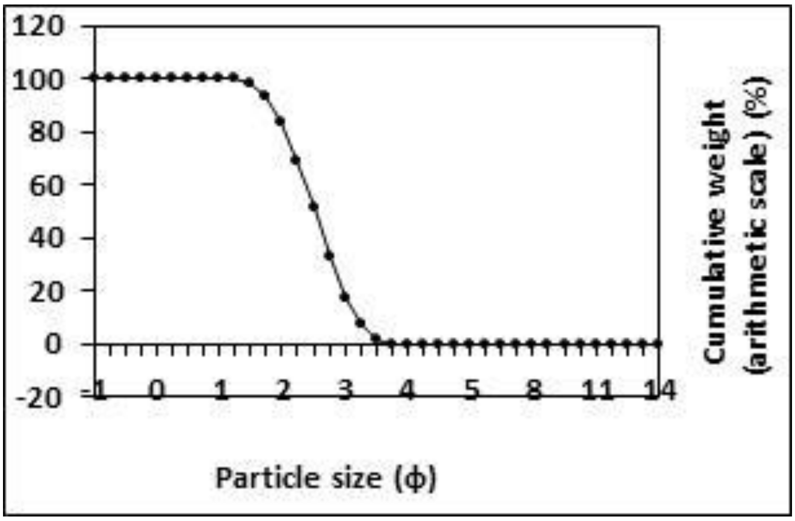

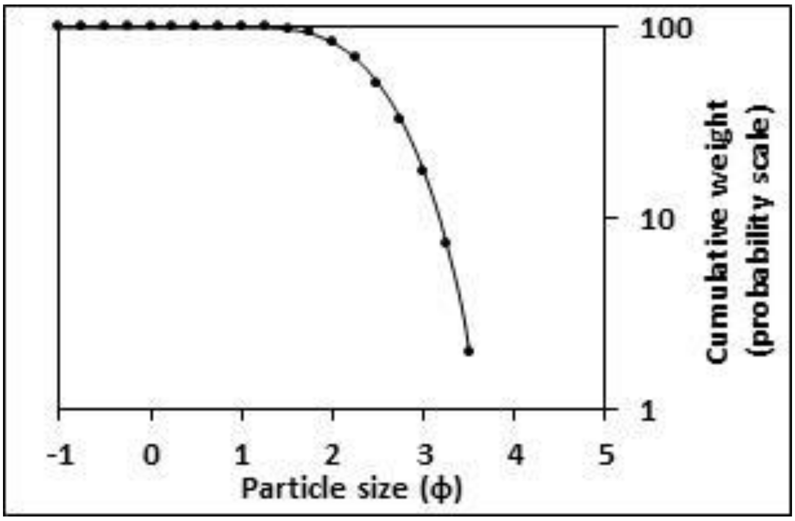

Figures II.169, II.170 and II.171: Histogram of grain size distribution and cumulative frequency graphs (arithmetic scale and probability scale) for sample 57: Mid intertidal zone, western transect, Wainamu Beach. Sample collected on the 16th of July, 2014.

Table II.58: *Graphical and statistical parameters, textural description and size classes for sample 58: Mid intertidal zone, northern transect, Northern Ngarunui Beach. Sample collected on the 6th of February, 2015.*

Textural description	**Textural size classes**
Moderately well sorted, Near symmetrical skewed, Mesokurtic	Sand = 100 000%Fines = 0.000% Silt = 0.000%Clay = 0.000%
Moment method parameters (μm) Mean = 279.897 Standard deviation (sd) = 96.293 Skewness (SkI) = 0.813 Kurtosis (KG) = 3.533	**Graphical method parameters. After Folk (1980) (ϕ)** Mean (Mz) = 1.923 d(0.5) = 1.924 Sorting (SI) = 0.505 Skewness (SkI) = -0.007 Kurtosis (KG) = 0.958 Mean (mm) = 0.264 Mean (μm) = 263.698
Wentworth size class Medium sand	

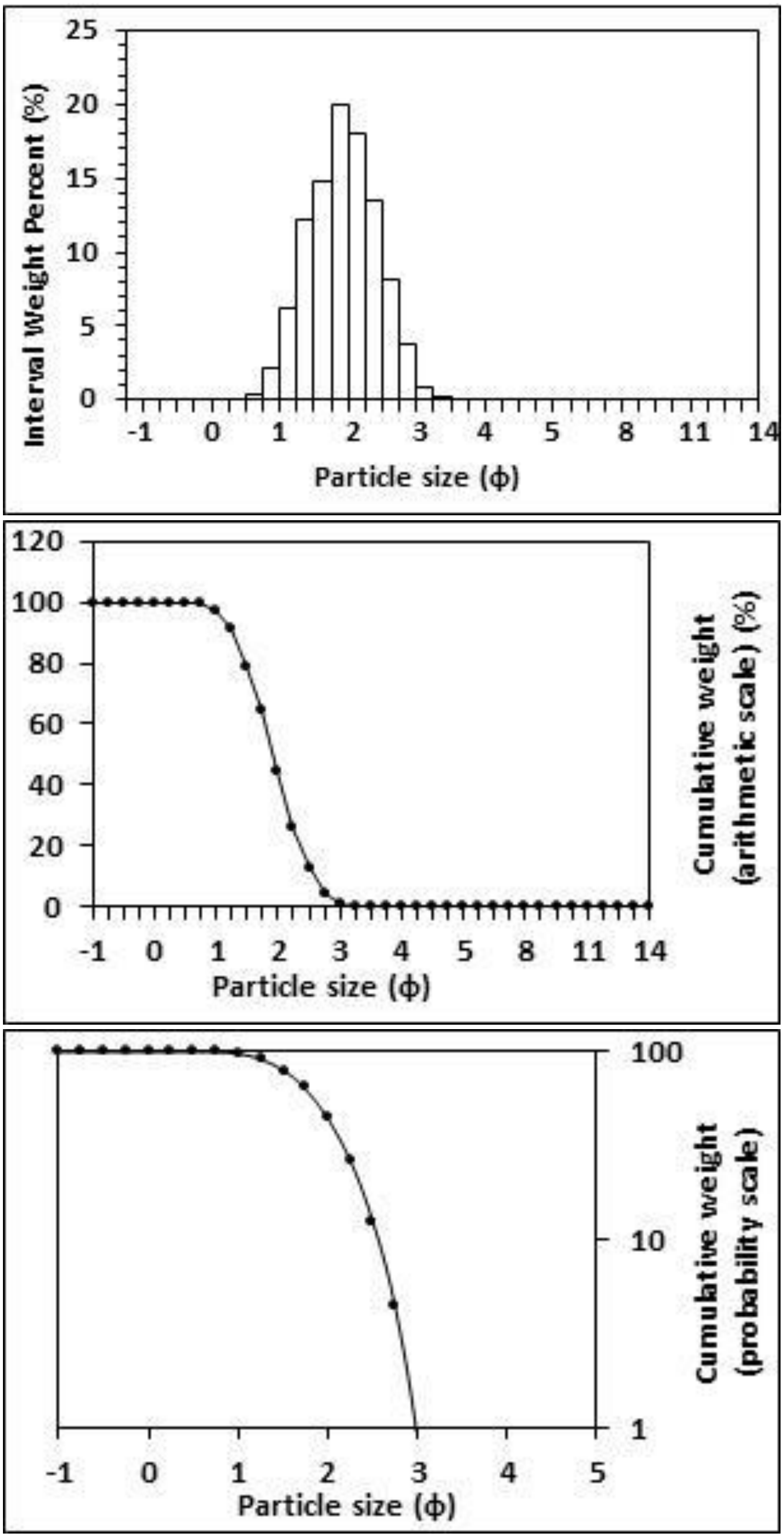

Figures II.172, II.173 and II.174: Histogram of grain size distribution and cumulative frequency graphs (arithmetic scale and probability scale) for sample 58: Mid intertidal zone, northern transect, Northern Ngarunui Beach. Sample collected on the 6th of February, 2015.

Table II.59: *Graphical and statistical parameters, textural description and size classes for sample 59: Mid intertidal zone, southern transect, Northern Ngarunui Beach. Sample collected on the 6th of February, 2015.*

Textural description	**Textural size classes**
Moderately well sorted, Near symmetrical skewed, Mesokurtic	Sand = 100 000%Fines = 0.000% Silt = 0.000%Clay = 0.000%
Moment method parameters (µm) Mean = 267.518 Standard deviation (sd) = 94.414 Skewness (SkI) = 0.846 Kurtosis (KG) = 3.623 **Wentworth size class** Medium sand	**Graphical method parameters. After Folk (1980) (ϕ)** Mean (Mz) = 1.993 d(0.5) = 1.995 Sorting (SI) = 0.516 Skewness (SkI) = -0.004 Kurtosis (KG) = 0.957 Mean (mm) = 0.251 Mean (µm) = 251.251

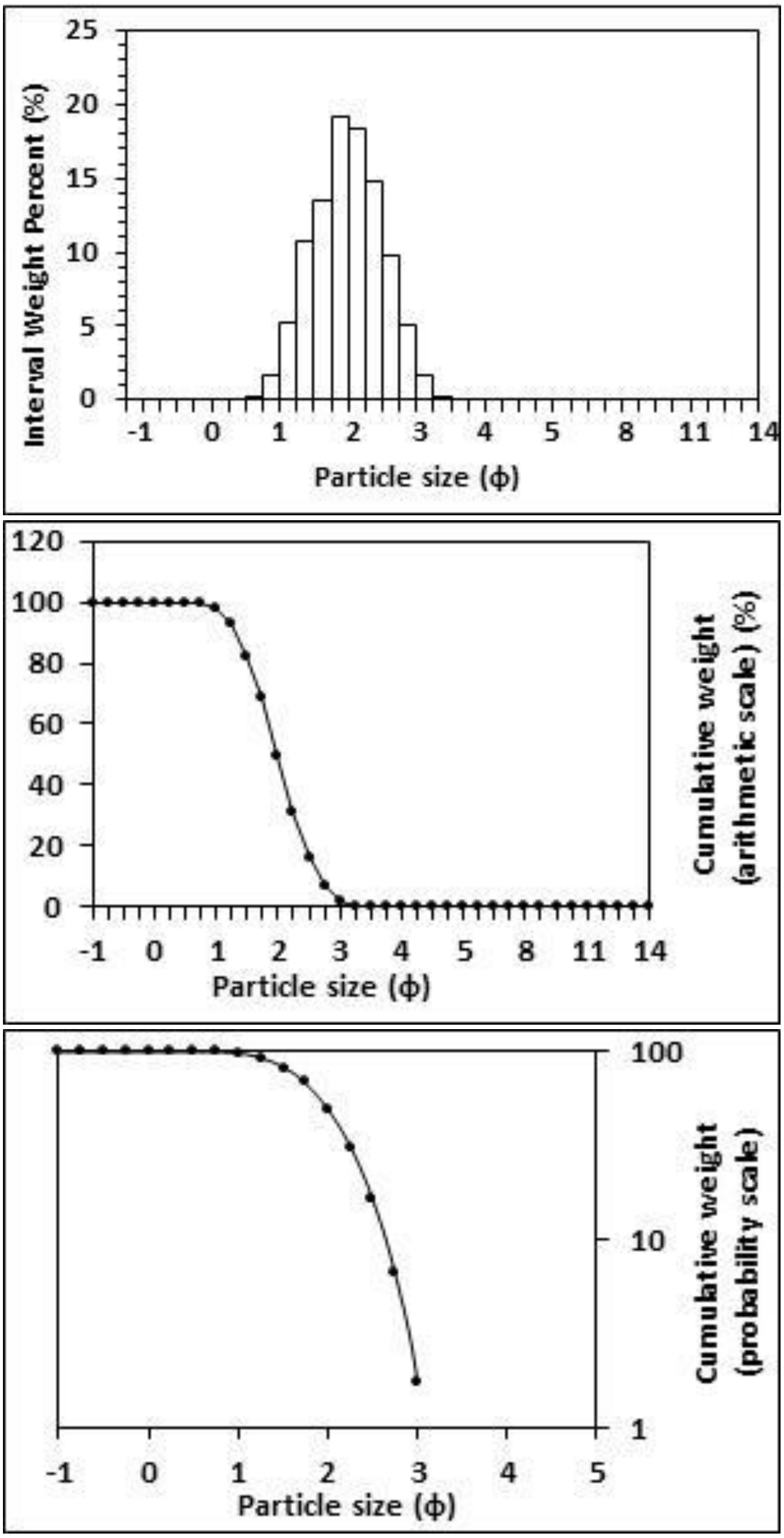

Figures II.175, II.176 and II.177: Histogram of grain size distribution and cumulative frequency graphs (arithmetic scale and probability scale) for sample 59: Mid intertidal zone, southern transect, Northern Ngarunui Beach. Sample collected on the 6th of February, 2015.

Table II.60: *Graphical and statistical parameters, textural description and size classes for sample 60: Low intertidal zone, southern transect, Northern Ngarunui Beach. Sample collected on the 6th of February, 2015.*

Textural description	**Textural size classes**
Moderately well sorted, Near symmetrical skewed, Mesokurtic	Sand = 100 000%Fines = 0.000% Silt = 0.000%Clay = 0.000%
Moment method parameters (μm) Mean = 264.612 Standard deviation (sd) = 95.909 Skewness (SkI) = 0.914 Kurtosis (KG) = 3.833 **Wentworth size class** Fine sand	**Graphical method parameters. After Folk (1980) (ϕ)** Mean (Mz) = 2.016 d(0.5) = 2.018 Sorting (SI) = 0.527 Skewness (SkI) = -0.009 Kurtosis (KG) = 0.962 Mean (mm) = 0.247 Mean (μm) = 247.202

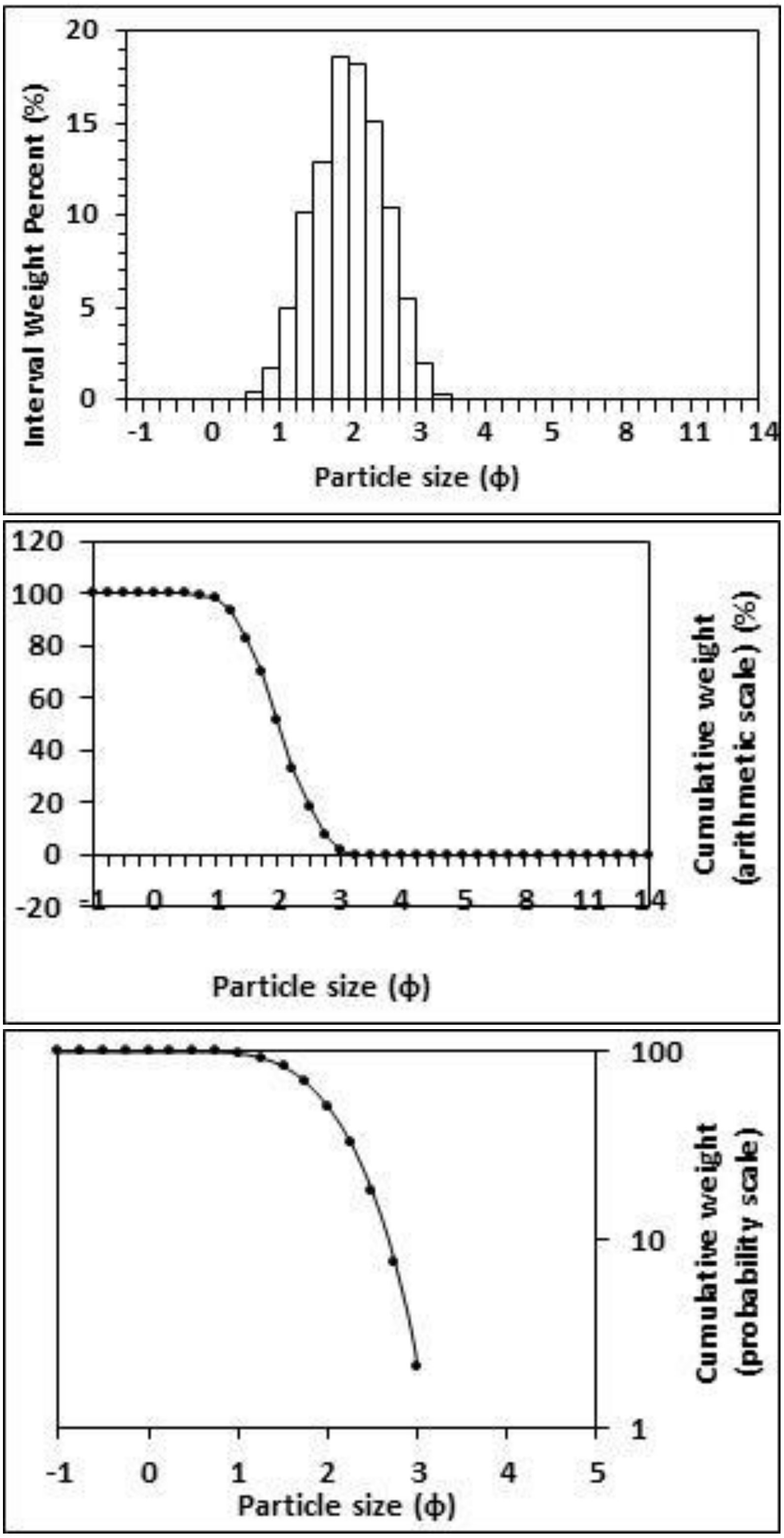

Figures II.178, II.179 and II.180: Histogram of grain size distribution and cumulative frequency graphs (arithmetic scale and probability scale) for sample 60: Low intertidal zone, southern transect, Northern Ngarunui Beach. Sample collected on the 6th of February, 2015.

Table II.61: *Graphical and statistical parameters, textural description and size classes for sample 61: Low intertidal zone, northern transect, Northern Ngarunui Beach. Sample collected on the 6th of February, 2015.*

Textural description	**Textural size classes**
Moderately well sorted, Near symmetrical skewed, Mesokurtic	Sand = 100 000%Fines = 0.000% Silt = 0.000%Clay = 0.000%
Moment method parameters (µm) Mean = 276.248 Standard deviation (sd) = 97.176 Skewness (SkI) = 0.845 Kurtosis (KG) = 3.622	**Graphical method parameters. After Folk (1980) (ϕ)** Mean (Mz) = 1.945 d(0.5) = 1.947 Sorting (SI) = 0.514 Skewness (SkI) = -0.009 Kurtosis (KG) = 0.955 Mean (mm) = 0.260 Mean (µm) = 259.775
Wentworth size class Medium sand	

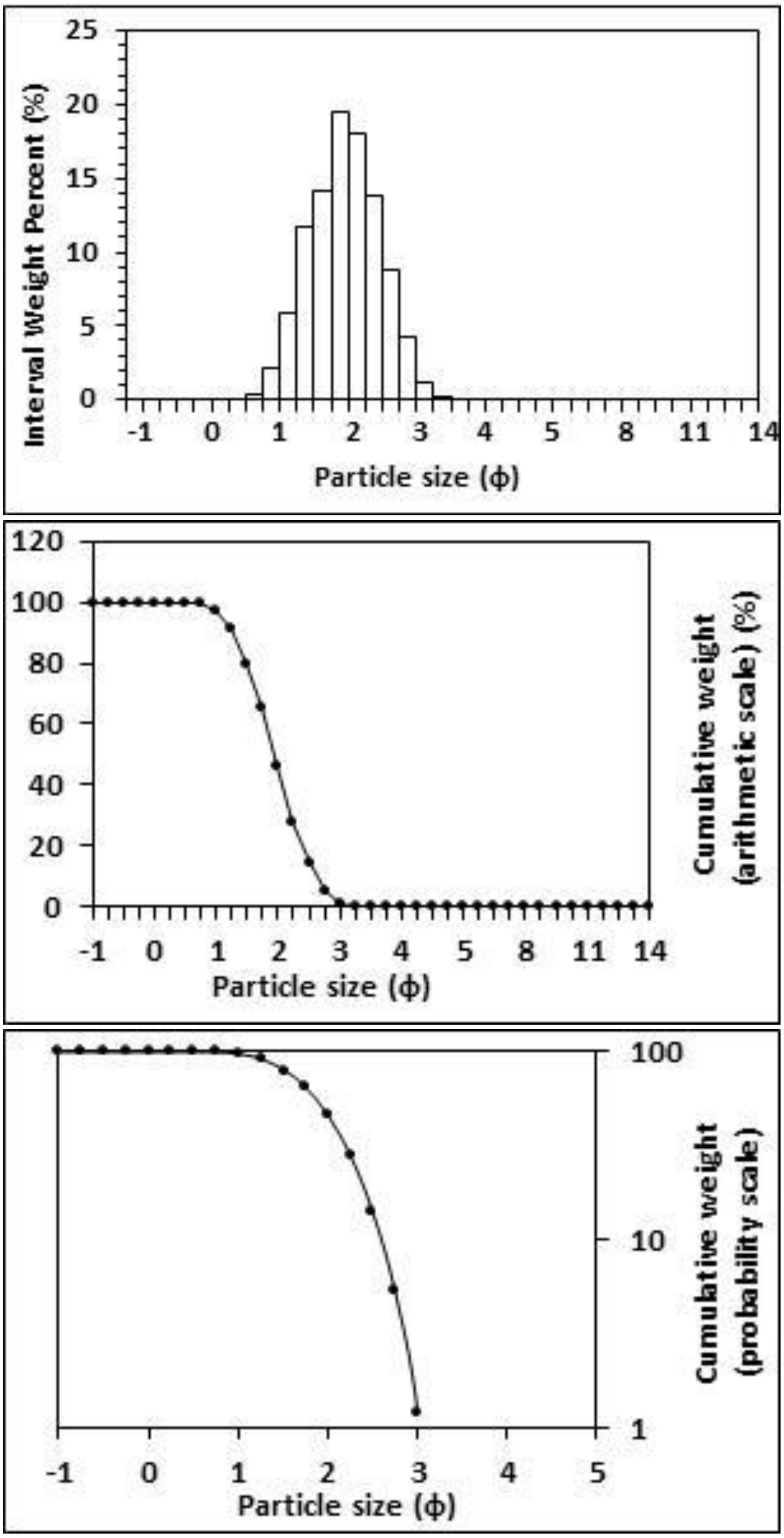

Figures II.181, II.182 and II.183: Histogram of grain size distribution and cumulative frequency graphs (arithmetic scale and probability scale) for sample 61: Low intertidal zone, northern transect, Northern Ngarunui Beach. Sample collected on the 6th of February, 2015.

Table II.62: *Graphical and statistical parameters, textural description and size classes for sample 62: High intertidal zone, mid transect, Wainamu Beach. Sample collected on the 28th of November, 2014.*

Textural description	**Textural size classes**
Moderately well sorted, Near symmetrical skewed, Mesokurtic	Sand = 99.989% Fines = 0.011% Silt = 0.011% Clay = 0.000%
Moment method parameters (µm)	**Graphical method parameters. After Folk (1980) (ϕ)**
Mean = 173.507 Standard deviation (sd) = 63.256 Skewness (SkI) = 0.908 Kurtosis (KG) = 3.782	Mean (Mz) = 2.625 d(0.5) = 2.628 Sorting (SI) = 0.529 Skewness (SkI) = -0.010 Kurtosis (KG) = 0.962 Mean (mm) = 0.162 Mean (µm) = 162.070
Wentworth size class Fine sand	

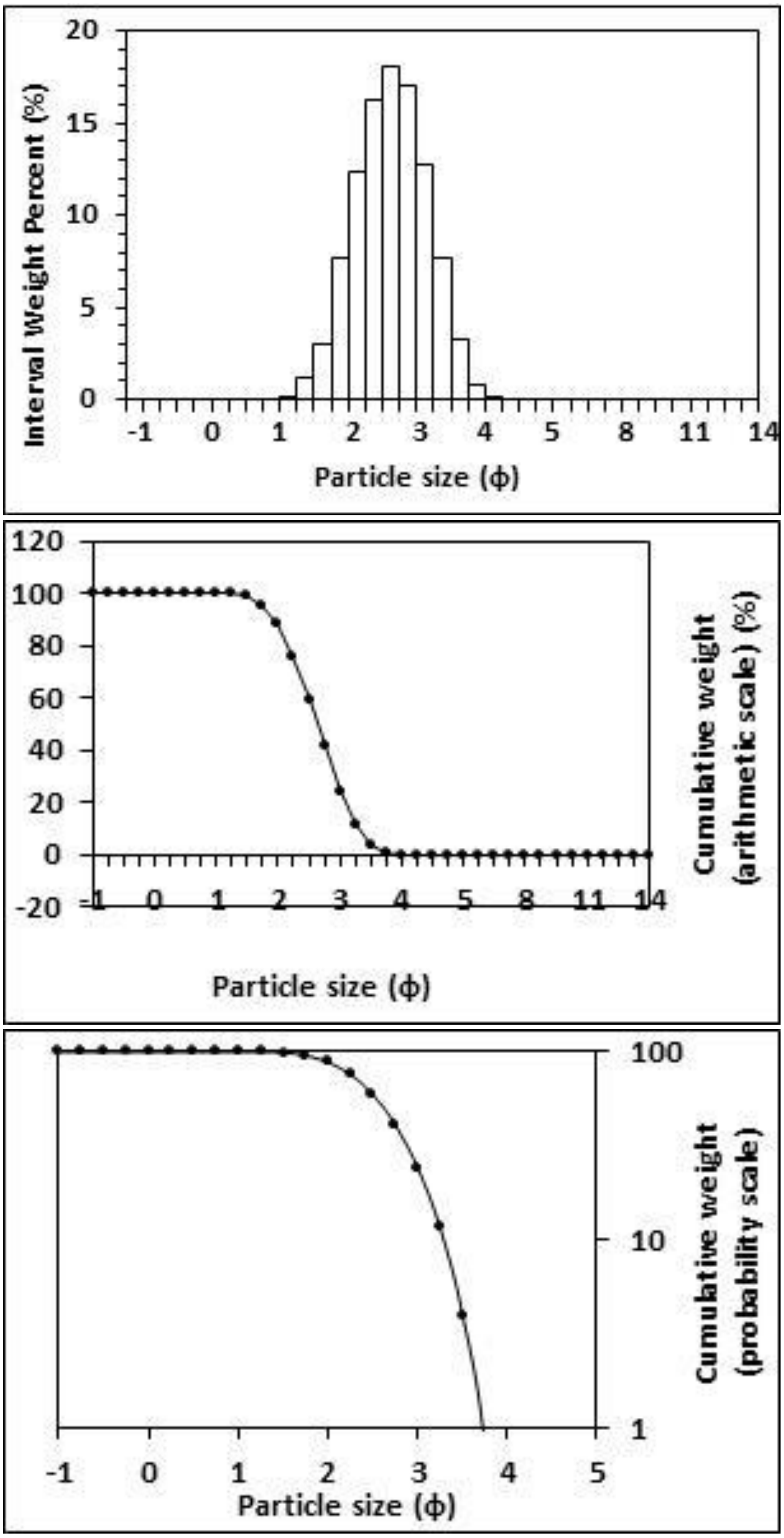

Figures II.184, II.185 and II.186: Histogram of grain size distribution and cumulative frequency graphs (arithmetic scale and probability scale) for sample 62: High intertidal zone, mid transect, Wainamu Beach. Sample collected on the 28th of November, 2014.

Table II.63: *Graphical and statistical parameters, textural description and size classes for sample 63: Low intertidal zone, western transect, Wainamu Beach. Sample collected on the 28th of November, 2014.*

Textural description	**Textural size classes**
Moderately well sorted, Near symmetrical skewed, Mesokurtic	Sand = 100 000%Fines = 0.000% Silt = 0.000%Clay = 0.000%
Moment method parameters (µm)	**Graphical method parameters. After Folk (1980) (ϕ)**
Mean = 219.859 Standard deviation (sd) = 83.035 Skewness (SkI) = 0.853 Kurtosis (KG) = 3.525	Mean (Mz) = 2.294 d(0.5) = 2.291 Sorting (SI) = 0.556 Skewness (SkI) = 0.003 Kurtosis (KG) = 0.949 Mean (mm) = 0.204 Mean (µm) = 203.865
Wentworth size class Fine sand	

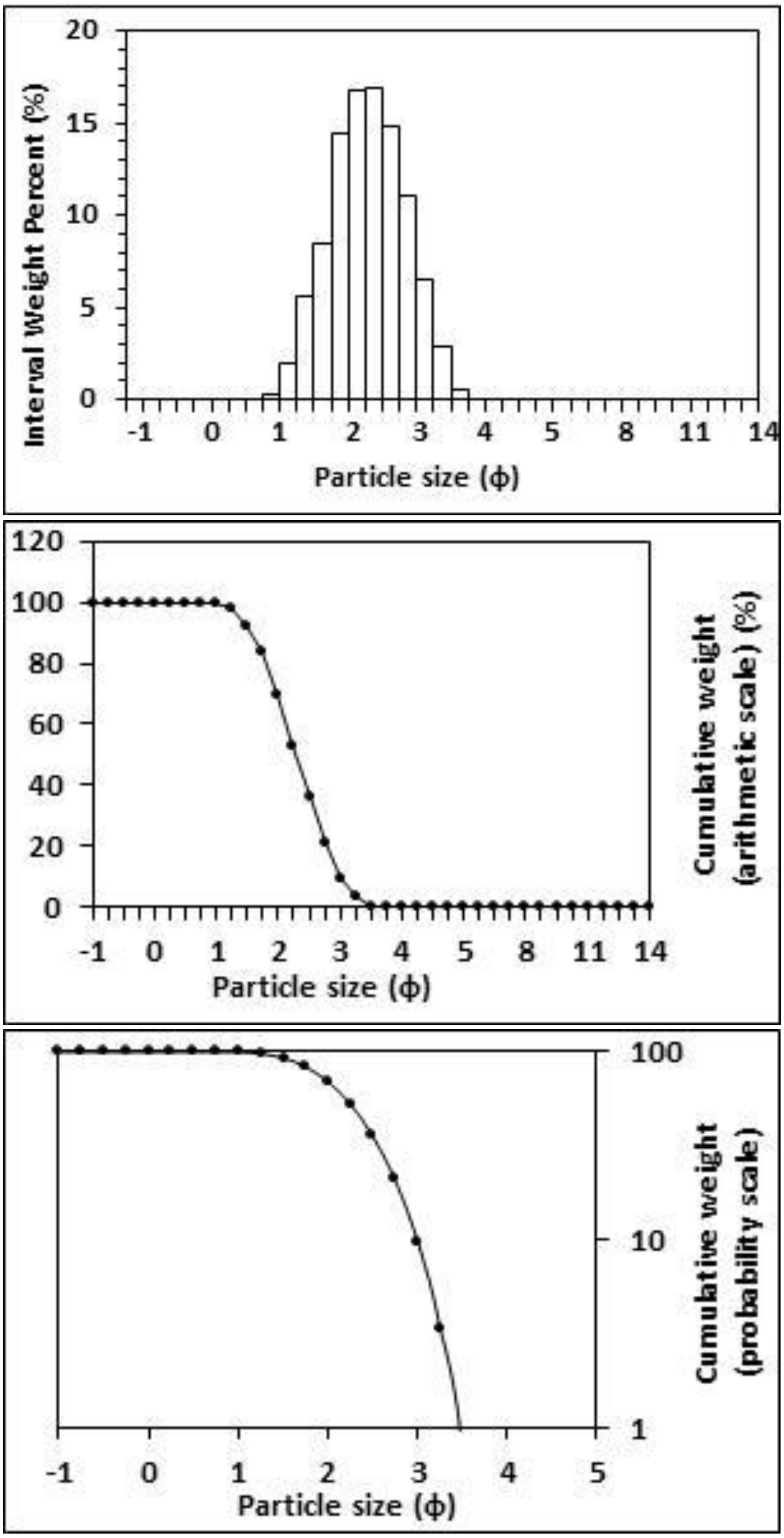

Figures II.187, II.188 and II.189: Histogram of grain size distribution and cumulative frequency graphs (arithmetic scale and probability scale) for sample 63: Low intertidal zone, western transect, Wainamu Beach. Sample collected on the 28th of November, 2014.

Table II.64: *Graphical and statistical parameters, textural description and size classes for sample 64: High intertidal zone, western transect, Wainamu Beach. Sample collected on the 28th of November, 2014.*

Textural description	**Textural size classes**
Moderately well sorted, Near symmetrical skewed, Mesokurtic	Sand = 99.9734% Fines = 0.0261% Silt = 0.026% Clay = 0.000%
Moment method parameters (µm)	**Graphical method parameters. After Folk (1980) (ϕ)**
Mean = 179.730 Standard deviation (sd) = 71.859 Skewness (SkI) = 0.961 Kurtosis (KG) = 3.859	Mean (Mz) = 2.596 d(0.5) = 2.596 Sorting (SI) = 0.577 Skewness (SkI) = -0.013 Kurtosis (KG) = 0.943 Mean (mm) = 0.165 Mean (µm) = 165.439
Wentworth size class Fine sand	

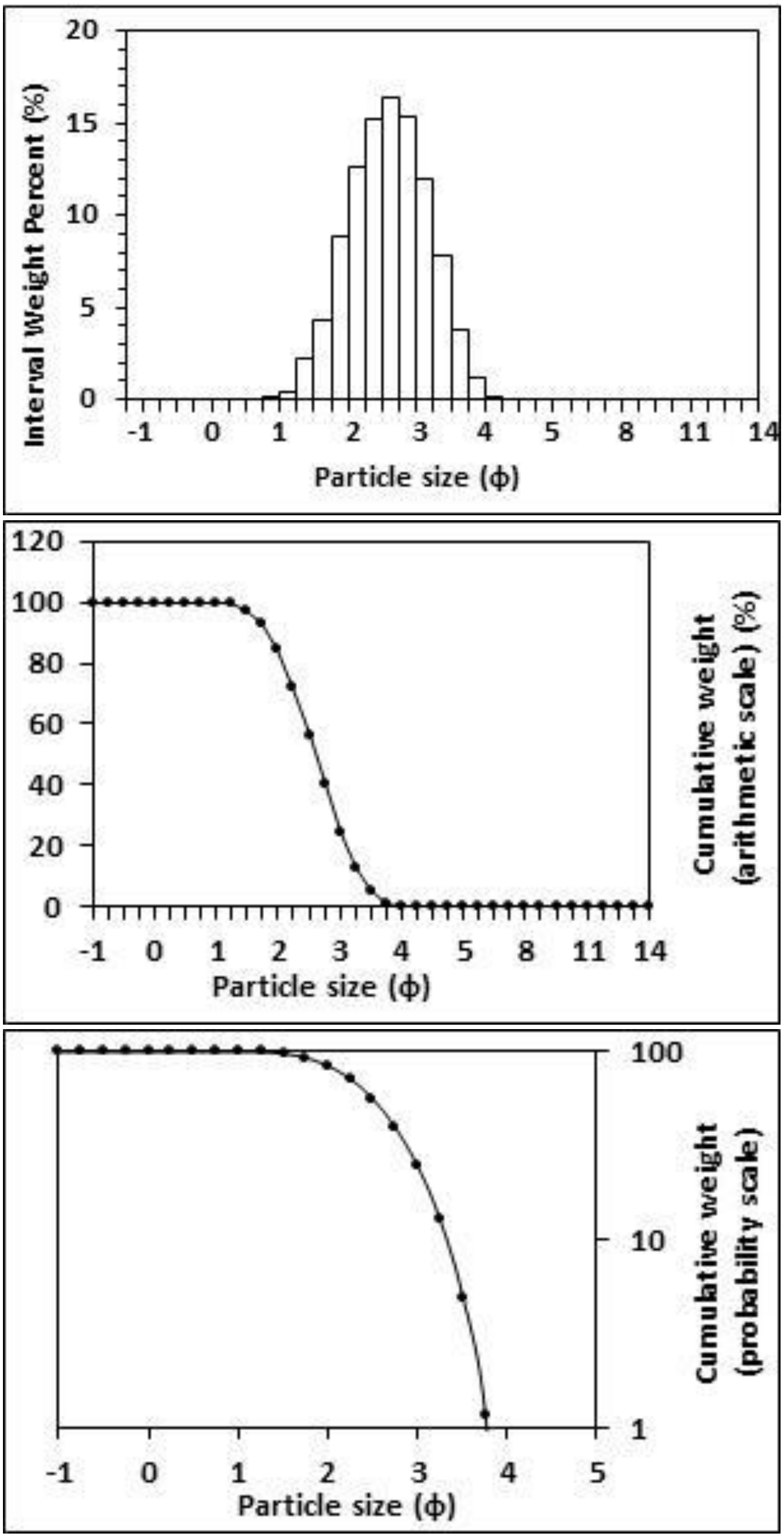

Figures II.190, II.191and II.192: Histogram of grain size distribution and cumulative frequency graphs (arithmetic scale and probability scale) for sample 64: High intertidal zone, western transect, Wainamu Beach. Sample collected on the 28th of November, 2014.

Table II.65: *Graphical and statistical parameters, textural description and size classes for sample 65: Low intertidal zone, eastern transect, Wainamu Beach. Sample collected on the 28th of November, 2014.*

Textural description	**Textural size classes**
Moderately well sorted, Near symmetrical skewed, Mesokurtic	Sand = 100 000%Fines = 0.000% Silt = 0.000%Clay = 0.000%
Moment method parameters (µm) Mean = 215.926 Standard deviation (sd) = 87.749 Skewness (SkI) = 0.929 Kurtosis (KG) = 3.734 **Wentworth size class** Fine sand	**Graphical method parameters. After Folk (1980) (ϕ)** Mean (Mz) = 2.334 d(0.5) = 2.331 Sorting (SI) = 0.593 Skewness (SkI) = 0.000 Kurtosis (KG) = 0.952 Mean (mm) = 0.198 Mean (µm) = 198.301

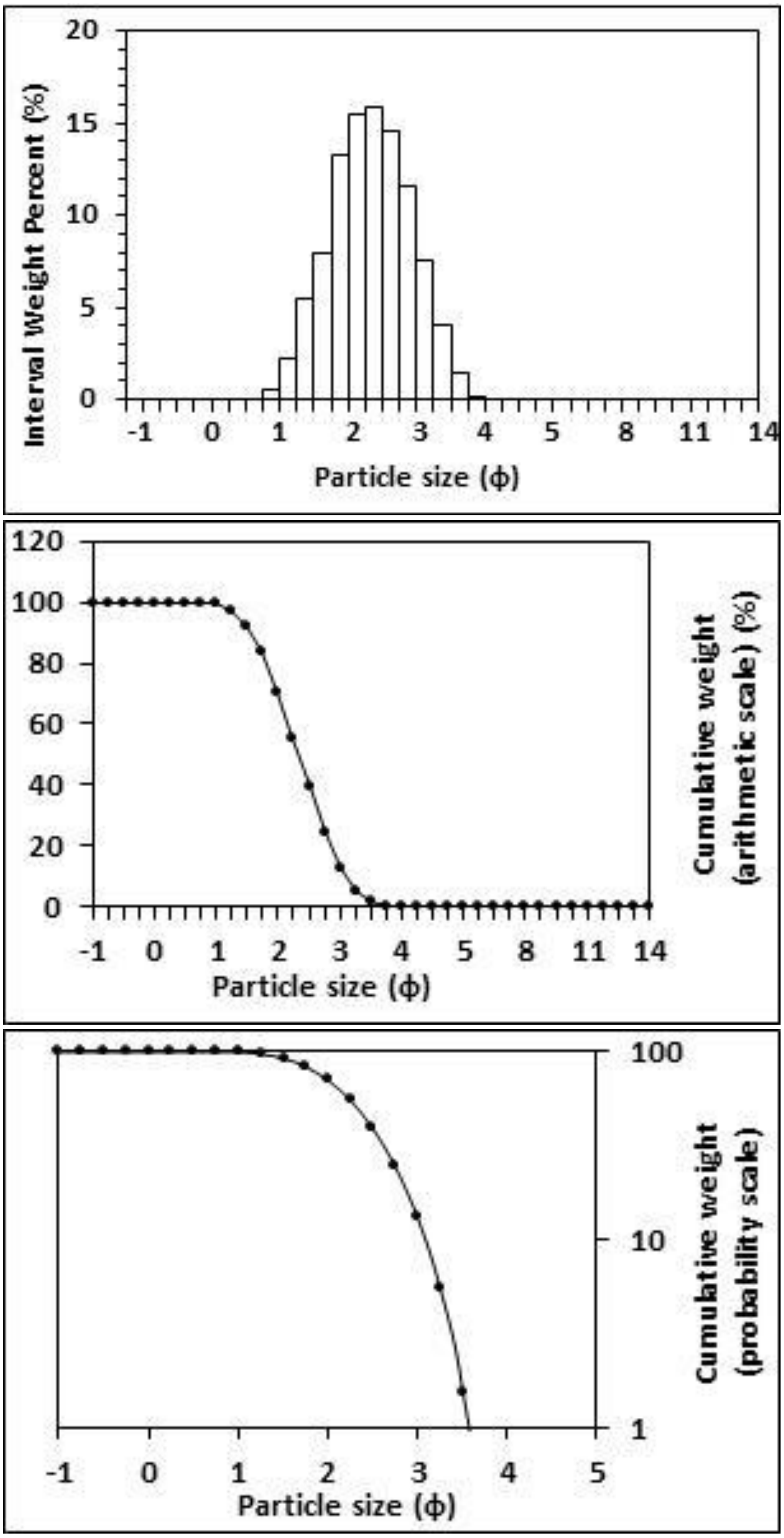

Figures II.193, II.194 and II.195: Histogram of grain size distribution and cumulative frequency graphs (arithmetic scale and probability scale) for sample 65: Low intertidal zone, eastern transect, Wainamu Beach. Sample collected on the 28th of November, 2014.

Table II.66: *Graphical and statistical parameters, textural description and size classes for sample 66: Low intertidal zone, mid transect, Wainamu Beach. Sample collected on the 28th of November, 2014.*

Textural description	**Textural size classes**
Moderately well sorted, Near symmetrical skewed, Mesokurtic	Sand = 100 000%Fines = 0.000% Silt = 0.000%Clay = 0.000%
Moment method parameters (µm) Mean = 237.124 Standard deviation (sd) = 83.678 Skewness (SkI) = 0.819 Kurtosis (KG) = 3.524 **Wentworth size class** Fine sand	**Graphical method parameters. After Folk (1980) (ϕ)** Mean (Mz) = 2.168 d(0.5) = 2.167 Sorting (SI) = 0.517 Skewness (SkI) = -0.003 Kurtosis (KG) = 0.952 Mean (mm) = 0.223 Mean (µm) = 222.582

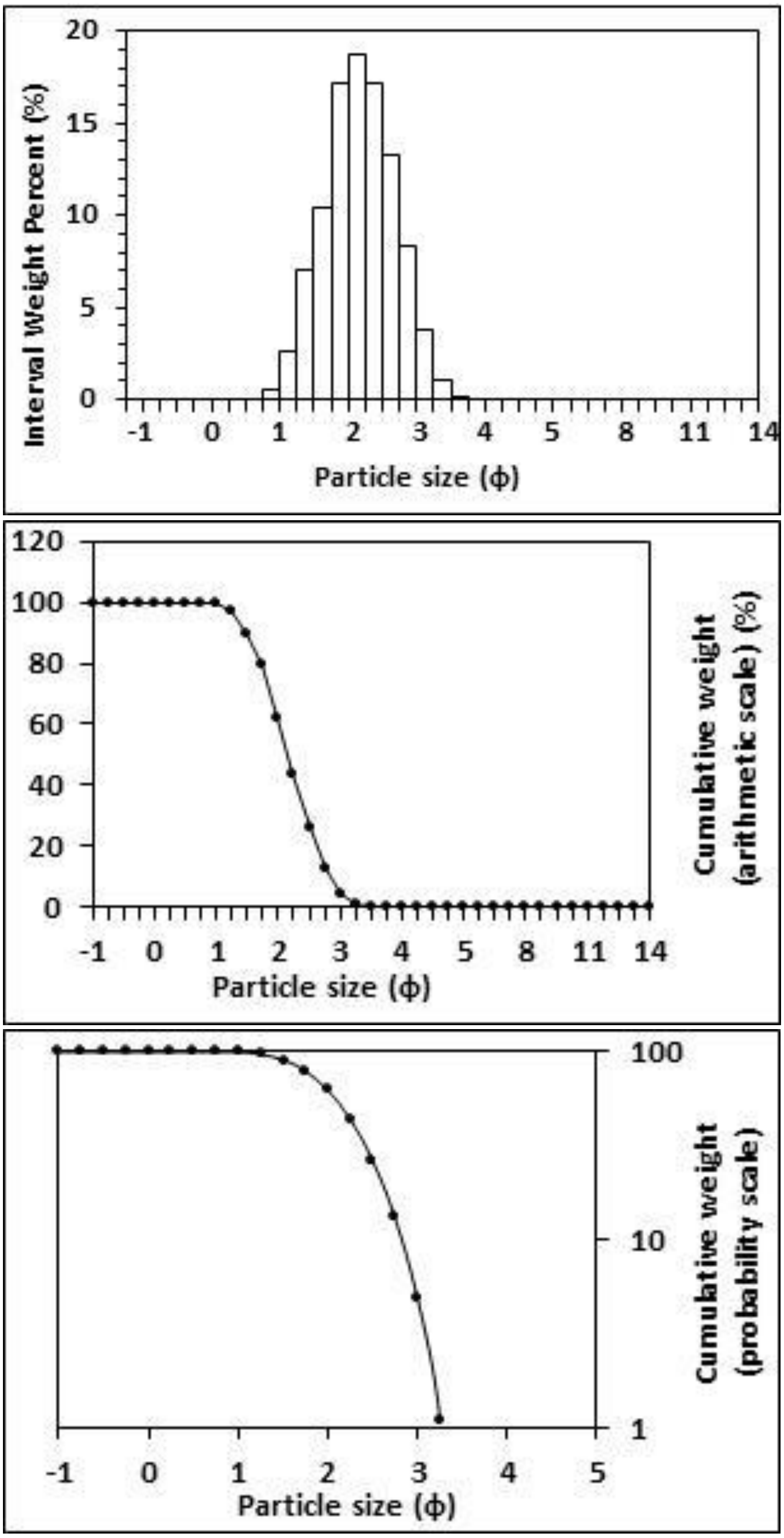

Figures II.196, II.197 and II.198: Histogram of grain size distribution and cumulative frequency graphs (arithmetic scale and probability scale) for sample 66: Low intertidal zone, mid transect, Wainamu Beach. Sample collected on the 28th of November, 2014.

Table II.67: *Graphical and statistical parameters, textural description and size classes for sample 67: Mid intertidal zone, western transect, Wainamu Beach. Sample collected on the 28th of November, 2014.*

Textural description	**Textural size classes**
Well sorted, Near symmetrical skewed, Mesokurtic	Sand = 99.945% Fines = 0.055% Silt = 0.055% Clay = 0.000%
Moment method parameters (µm) Mean = 139.536 Standard deviation (sd) = 38.725 Skewness (SkI) = 0.693 Kurtosis (KG) = 3.399 **Wentworth size class** Fine sand	**Graphical method parameters. After Folk (1980) (ϕ)** Mean (Mz) = 2.905 d(0.5) = 2.900 Sorting (SI) = 0.403 Skewness (SkI) = 0.020 Kurtosis (KG) = 0.946 Mean (mm) = 0.133 Mean (µm) = 133.500

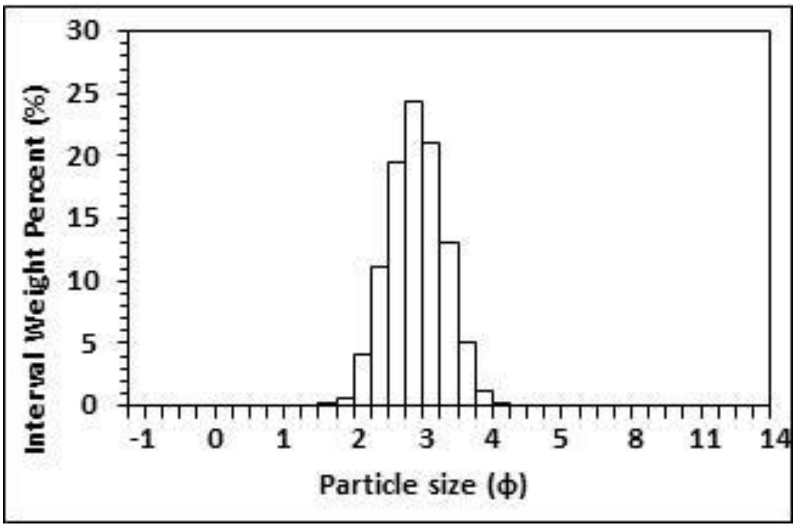

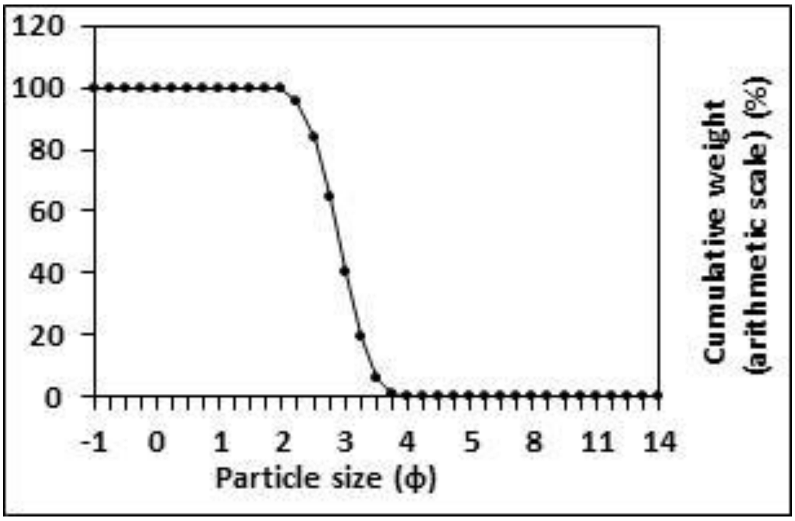

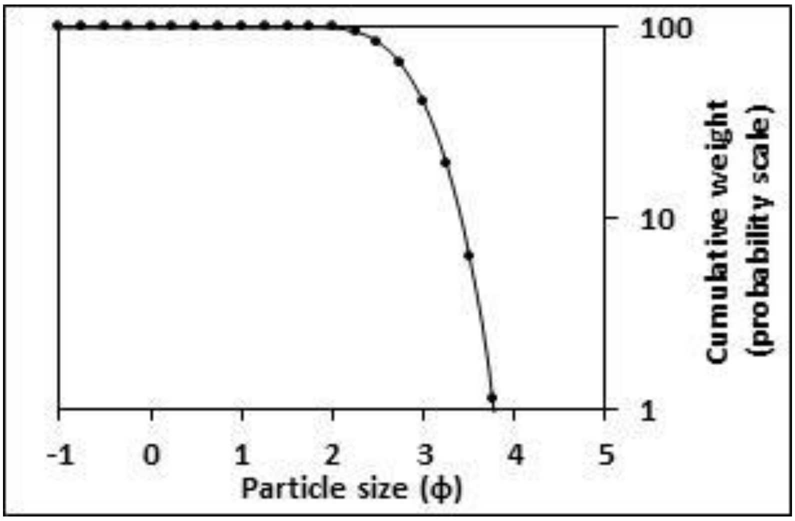

Figures II.199, II.200 and II.201: Histogram of grain size distribution and cumulative frequency graphs (arithmetic scale and probability scale) for sample 67: Mid intertidal zone, western transect, Wainamu Beach. Sample collected on the 28th of November, 2014.

Table II.68: *Graphical and statistical parameters, textural description and size classes for sample 68: High intertidal zone, eastern transect, Wainamu Beach. Sample collected on the 28th of November, 2014.*

Textural description	**Textural size classes**
Moderately well sorted, Near symmetrical skewed, Mesokurtic	Sand = 99.974% Fines = 0.026% Silt = 0.026% Clay = 0.000%
Moment method parameters (µm) Mean = 177.304 Standard deviation (sd) = 69.267 Skewness (SkI) = 0.918 Kurtosis (KG) = 3.714 **Wentworth size class** Fine sand	**Graphical method parameters. After Folk (1980) (ϕ)** Mean (Mz) = 2.609 d(0.5) = 2.610 Sorting (SI) = 0.567 Skewness (SkI) = -0.009 Kurtosis (KG) = 0.943 Mean (mm) = 0.164 Mean (µm) = 163.907

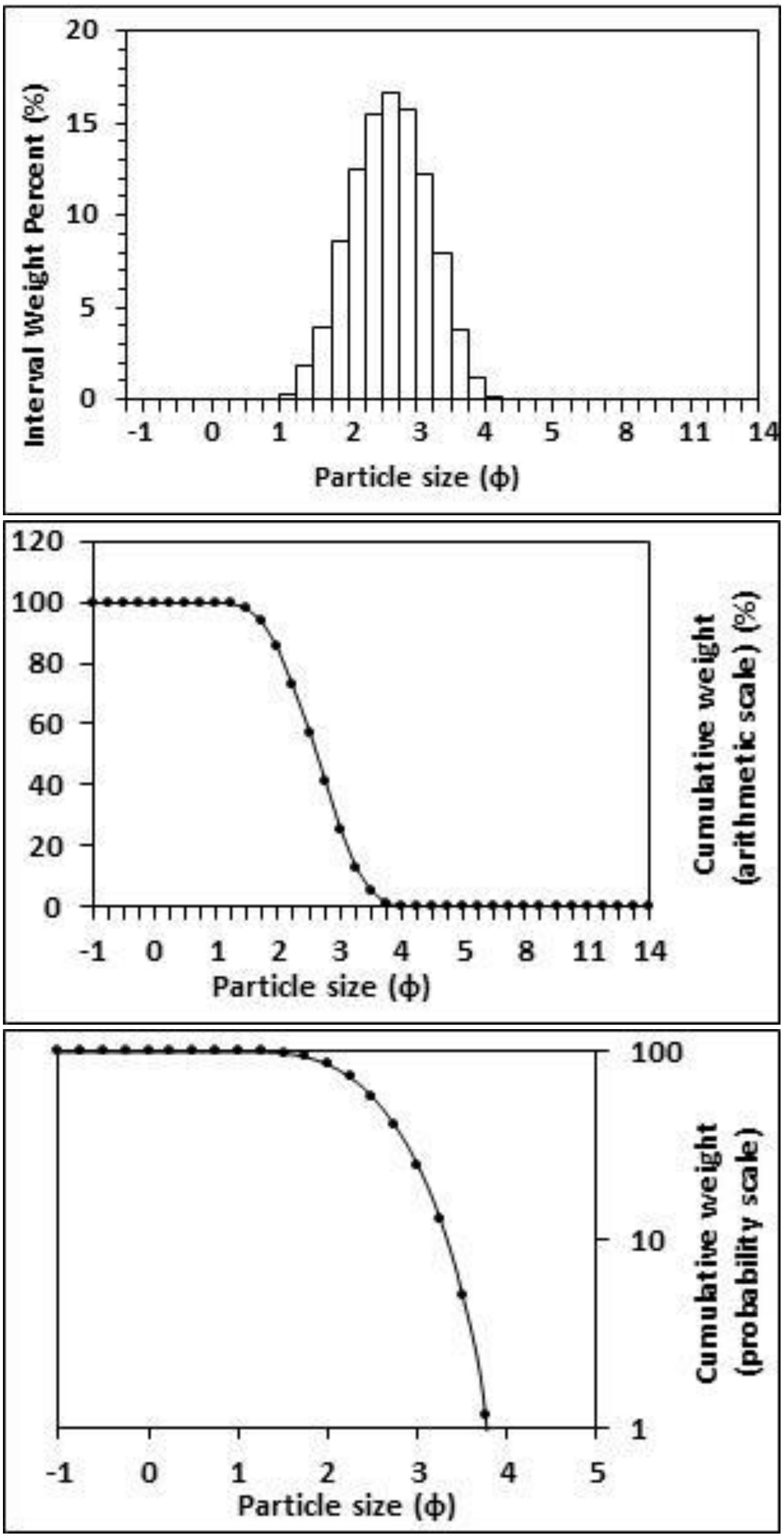

Figures II.202, II.203 and II.204: Histogram of grain size distribution and cumulative frequency graphs (arithmetic scale and probability scale) for sample 68: High intertidal zone, eastern transect, Wainamu Beach. Sample collected on the 28th of November, 2014.

Table II.69: *Graphical and statistical parameters, textural description and size classes for sample 69: Mid intertidal zone, mid transect, Wainamu Beach. Sample collected on the 28th of November, 2014.*

Textural description	**Textural size classes**
Moderately well sorted, Near symmetrical skewed, Mesokurtic	Sand = 99.978% Fines = 0.022% Silt = 0.022% Clay = 0.000%
Moment method parameters (µm) Mean = 218.523 Standard deviation (sd) = 219.810 Skewness (SkI) = 4.617 Kurtosis (KG) = 26.570 **Wentworth size class** Fine sand	**Graphical method parameters. After Folk (1980) (ϕ)** Mean (Mz) = 2.558 d(0.5) = 2.577 Sorting (SI) = 0.638 Skewness (SkI) = -0.094 Kurtosis (KG) = 1.039 Mean (mm) = 0.170 Mean (µm) = 169.797

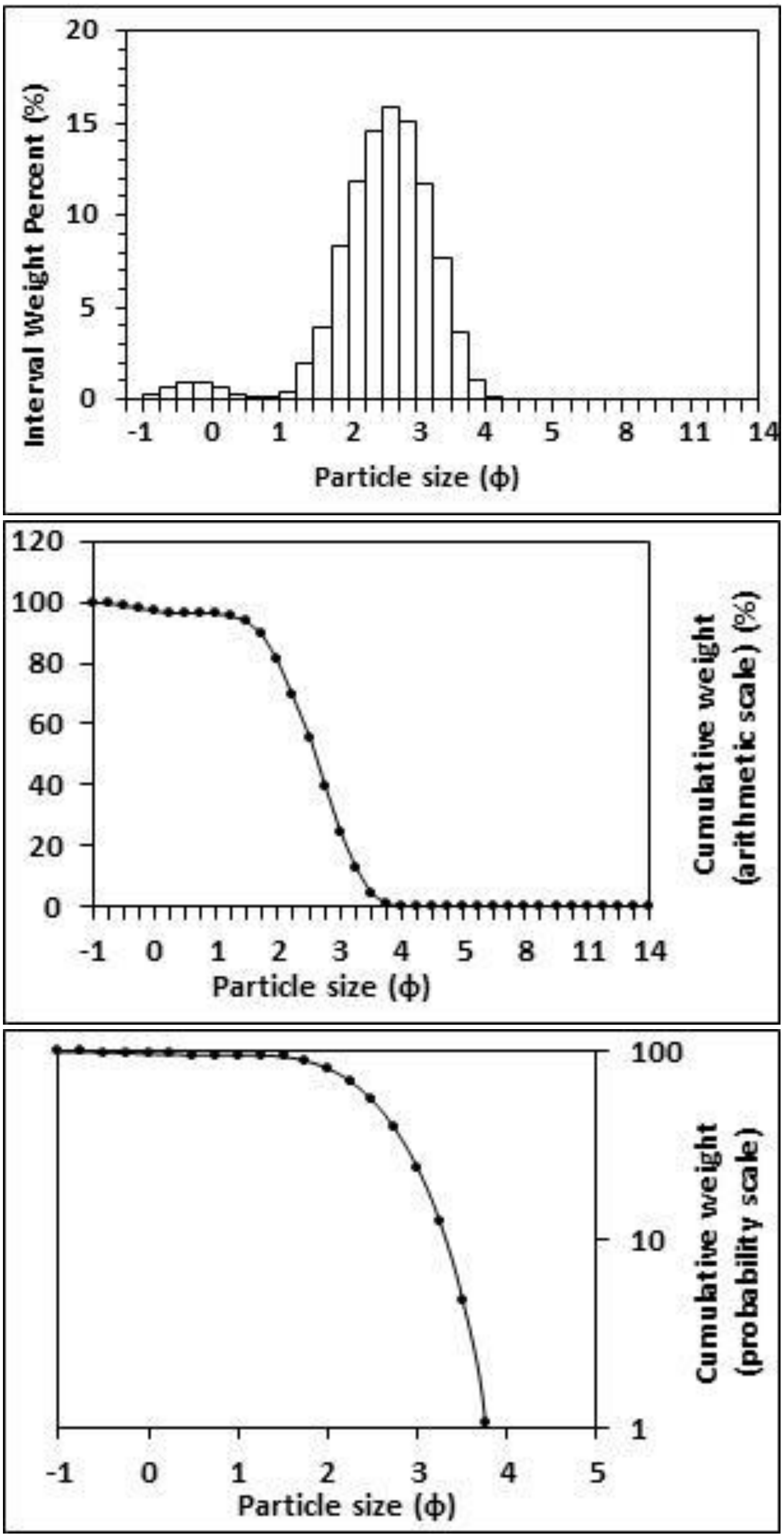

Figures II.205, II.206 and II.207: Histogram of grain size distribution and cumulative frequency graphs (arithmetic scale and probability scale) for sample 69: Mid intertidal zone, mid transect, Wainamu Beach. Sample collected on the 28th of November, 2014.

Table II.70: *Graphical and statistical parameters, textural description and size classes for sample 70: Mid intertidal zone, eastern transect, Wainamu Beach. Sample collected on the 28th of November, 2014.*

Textural description	**Textural size classes**
Moderately well sorted, Near symmetrical skewed, Mesokurtic	Sand = 99.196% Fines = 0.804% Silt = 0.674% Clay = 0.130%
Moment method parameters (µm)	**Graphical method parameters. After Folk (1980) (ϕ)**
Mean = 238.401 Standard deviation (sd) = 96.814 Skewness (SkI) = 1.390 Kurtosis (KG) = 14.994	Mean (Mz) = 2.174 d(0.5) = 2.173 Sorting (SI) = 0.575 Skewness (SkI) = 0.016 Kurtosis (KG) = 0.955 Mean (mm) = 0.222 Mean (µm) = 221.631
Wentworth size class Fine sand	

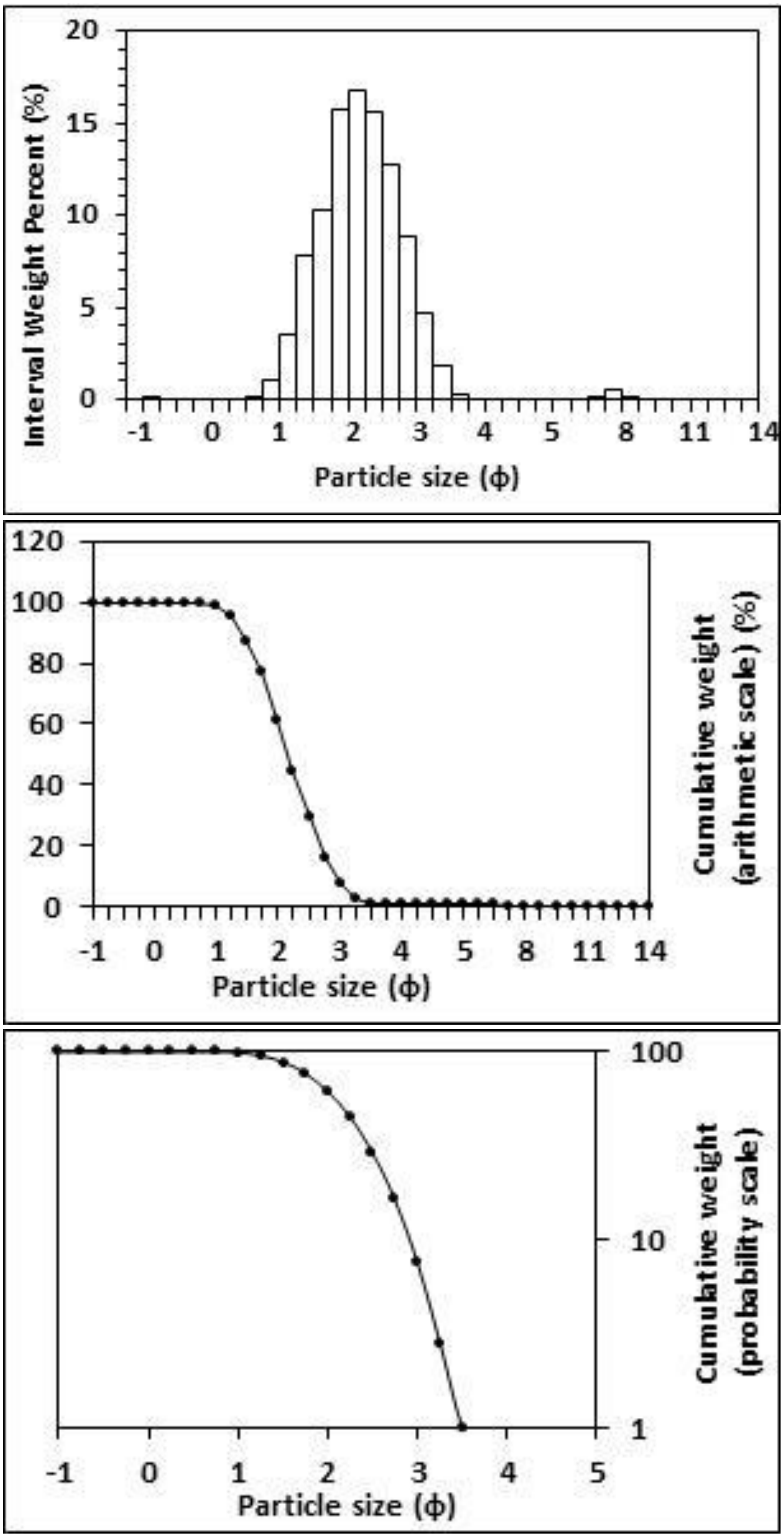

Figures II.208, II.209 and II.210: Histogram of grain size distribution and cumulative frequency graphs (arithmetic scale and probability scale) for sample 70: Mid intertidal zone, eastern transect, Wainamu Beach. Sample collected on the 28th of November, 2014.

Table II.71: *Graphical and statistical parameters, textural description and size classes for sample 71: Mid intertidal zone, mid transect, Northern Ngarunui Beach. Sample collected on the 15th of August, 2014.*

Textural description	**Textural size classes**
Moderately well sorted, Near symmetrical skewed, Mesokurtic	Sand = 100 000%Fines = 0.000% Silt = 0.000%Clay = 0.000%
Moment method parameters (µm) Mean = 328.872 Standard deviation (sd) = 119.068 Skewness (SkI) = 0.842 Kurtosis (KG) = 3.572	**Graphical method parameters. After Folk (1980) (ϕ)** Mean (Mz) = 1.698 d(0.5) = 1.700 Sorting (SI) = 0.530 Skewness (SkI) = -0.002 Kurtosis (KG) = 0.955 Mean (mm) = 0.308 Mean (µm) = 308.287
Wentworth size class Medium sand	

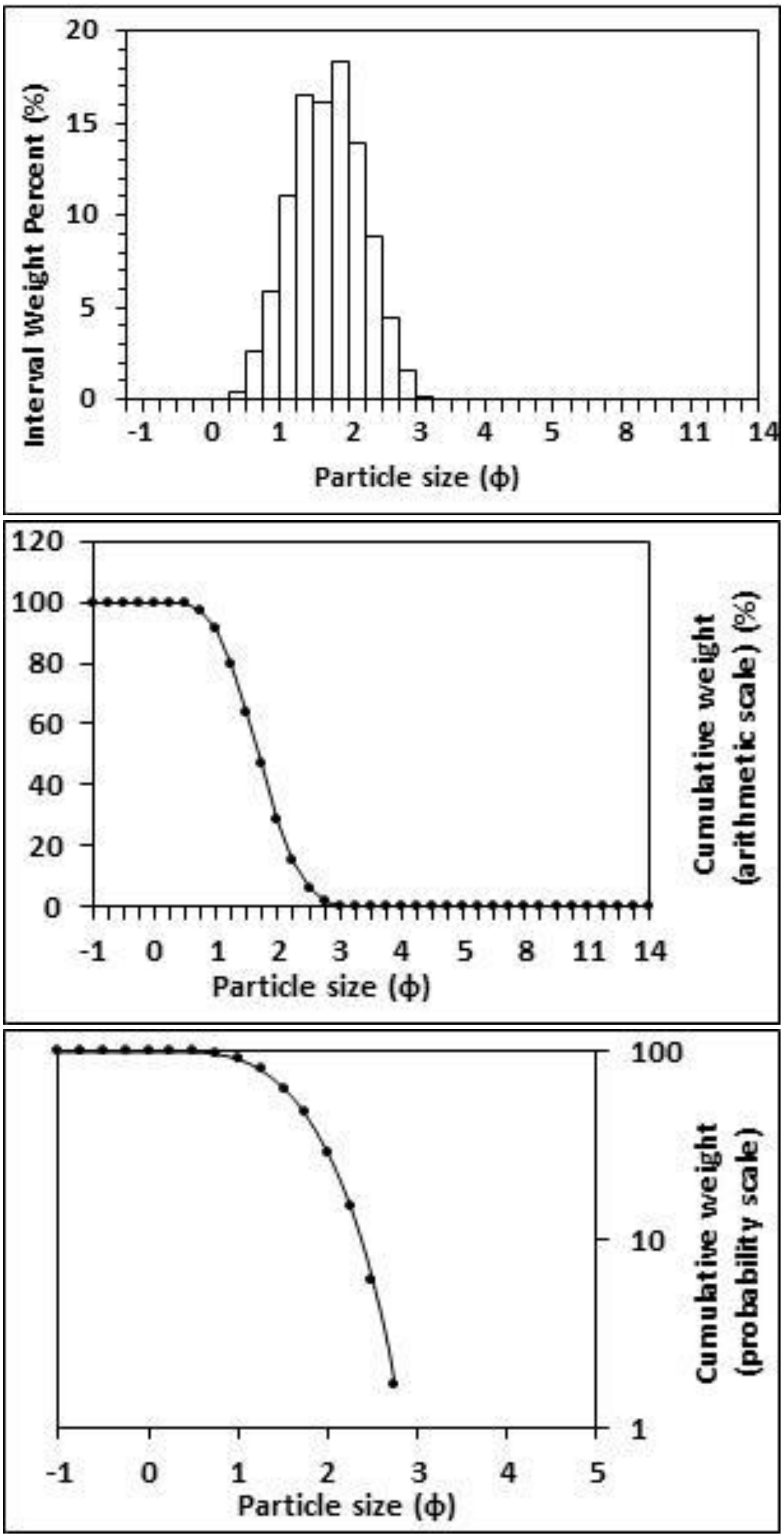

Figures II.211, II.212 and II.213: Histogram of grain size distribution and cumulative frequency graphs (arithmetic scale and probability scale) for sample 71: Mid intertidal zone, mid transect, Northern Ngarunui Beach. Sample collected on the 15th of August, 2014.

Table II.72: *Graphical and statistical parameters, textural description and size classes for sample 72: High intertidal zone, northern transect, Northern Ngarunui Beach. Sample collected on the 15th of August, 2014.*

Textural description	**Textural size classes**
Moderately well sorted, Near symmetrical skewed, Mesokurtic	Sand = 100 000%Fines = 0.000% Silt = 0.000%Clay = 0.000%
Moment method parameters (µm) Mean = 269.331 Standard deviation (sd) = 96.784 Skewness (SkI) = 0.852 Kurtosis (KG) = 3.644 **Wentworth size class** Medium sand	**Graphical method parameters. After Folk (1980) (ϕ)** Mean (Mz) = 1.985 d(0.5) = 1.987 Sorting (SI) = 0.527 Skewness (SkI) = -0.001 Kurtosis (KG) = 0.960 Mean (mm) = 0.253 Mean (µm) = 252.568

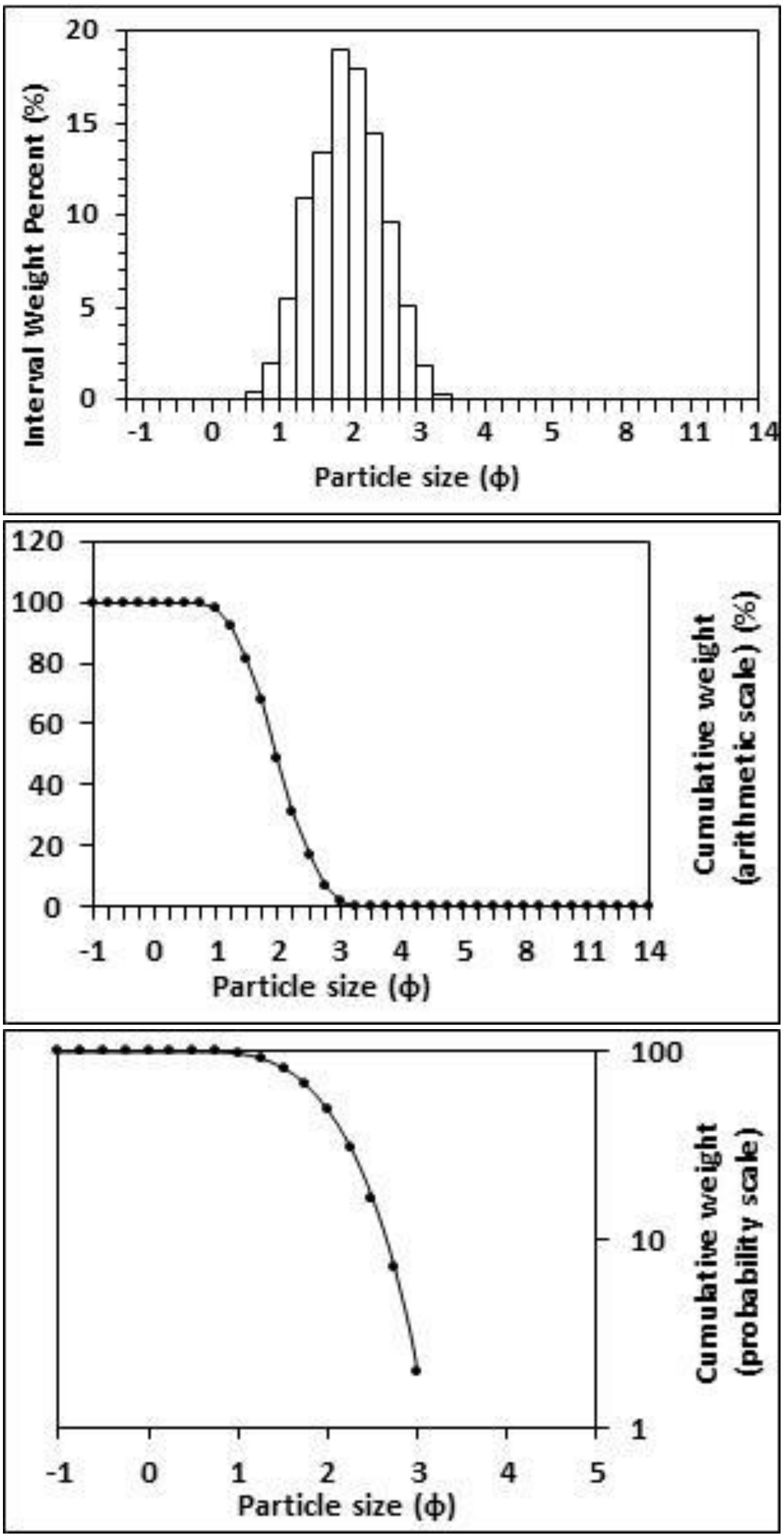

Figures II.214, II.215 and II.216: Histogram of grain size distribution and cumulative frequency graphs (arithmetic scale and probability scale) for sample 72: High intertidal zone, northern transect, Northern Ngarunui Beach. Sample collected on the 15th of August, 2014.

Table II.73: *Graphical and statistical parameters, textural description and size classes for sample 73: Low intertidal zone, mid transect, Northern Ngarunui Beach. Sample collected on the 15th of August, 2014.*

Textural description	**Textural size classes**
Moderately well sorted, Near symmetrical skewed, Mesokurtic	Sand = 100 000%Fines = 0.000% Silt = 0.000%Clay = 0.000%
Moments method parameters (µm) Mean = 346.438 Standard deviation (sd) = 126.255 Skewness (SkI) = 0.896 Kurtosis (KG) = 3.770 **Wentworth size class** Medium sand	**Graphical method parameters. After Folk (1980) (ϕ)** Mean (Mz) = 1.627 d (0.5) = 1.629 Sorting (σI) = 0.528 Skewness (SkI) = -0.006 Kurtosis (KG) = 0.958 Mean (mm) = 0.324 Mean (µm) = 323.708

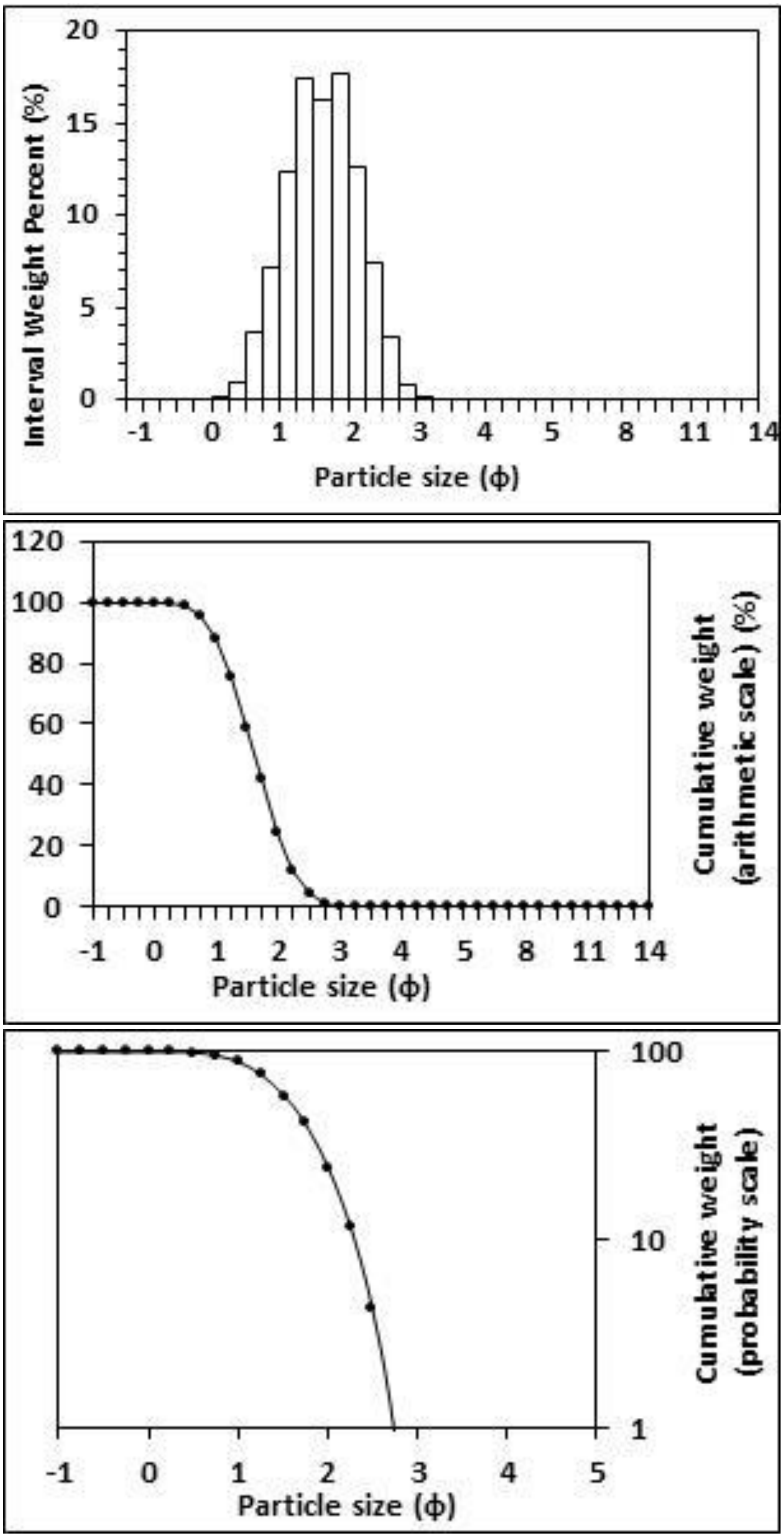

Figures II.217, II.218 and II.219: Histogram of grain size distribution and cumulative frequency graphs (arithmetic scale and probability scale) for sample 73: Low intertidal zone, mid transect, Northern Ngarunui Beach. Sample collected on the 15th of August, 2014.

Table II.74: *Graphical and statistical parameters, textural description and size classes for sample 74: High intertidal zone, southern transect, Northern Ngarunui Beach. Sample collected on the 15th of August, 2014.*

Textural description	**Textural size classes**
Moderately well sorted, Near symmetrical skewed, Mesokurtic	Sand = 100 000%Fines = 0.000% Silt = 0.000%Clay = 0.000%
Moment method parameters (μm) Mean = 298.083 Standard deviation (sd) = 116.840 Skewness (SkI) = 0.863 Kurtosis (KG) = 3.565 **Wentworth size class** Medium sand	**Graphical method parameters. After Folk (1980) (ϕ)** Mean (Mz) = 1.859 d(0.5) = 1.856 Sorting (SI) = 0.576 Skewness (SkI) = 0.010 Kurtosis (KG) = 0.954 Mean (mm) = 0.276 Mean (μm) = 275.621

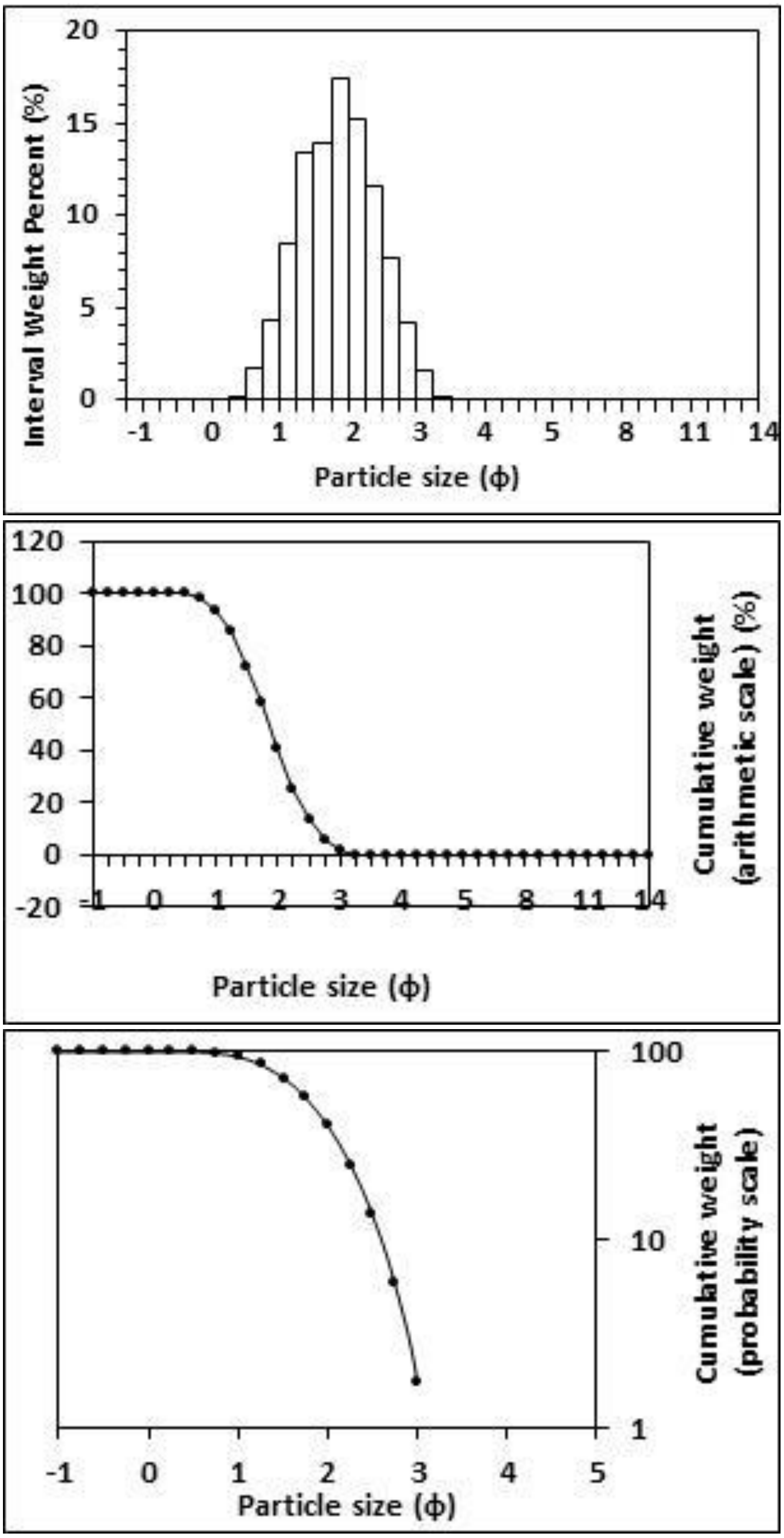

Figures II.220, II.221 and II.222: Histogram of grain size distribution and cumulative frequency graphs (arithmetic scale and probability scale) for sample 74: High intertidal zone, southern transect, Northern Ngarunui Beach. Sample collected on the 15th of August, 2014.

Table II.75: *Graphical and statistical parameters, textural description and size classes for sample 75: High intertidal zone, mid transect, Northern Ngarunui Beach. Sample collected on the 15th of August, 2014.*

<table>
<tr><td>Textural description

Moderately well sorted,

Near symmetrical skewed,

Mesokurtic</td><td>Textural size classes

Sand = 100 000%Fines = 0.000%

Silt = 0.000%Clay = 0.000%</td></tr>
<tr><td>Moment method parameters (µm)

Mean = 273.720

Standard deviation (sd) = 98.218

Skewness (SkI) = 0.846

Kurtosis (KG) = 3.634</td><td rowspan="2">Graphical method parameters. After Folk (1980) (ϕ)

Mean (Mz) = 1.960

d(0.5) = 1.962

Sorting (SI) = 0.526

Skewness (SkI) = -0.001

Kurtosis (KG) = 0.962

Mean (mm) = 0.257

Mean (µm) = 257.051</td></tr>
<tr><td>Wentworth size class

Medium sand</td></tr>
</table>

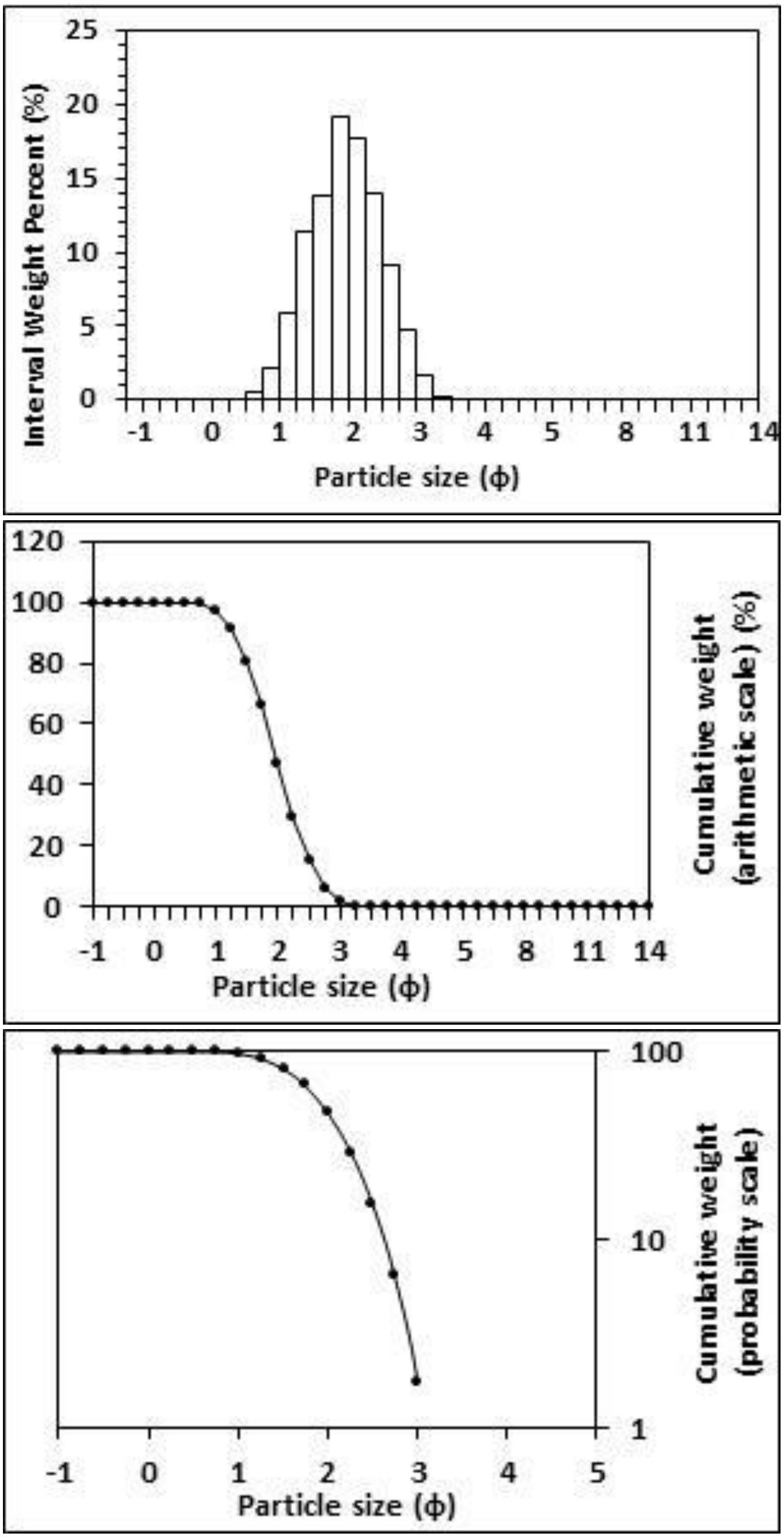

Figures II.223, II.224 and II.225: Histogram of grain size distribution and cumulative frequency graphs (arithmetic scale and probability scale) for sample 75: High intertidal zone, mid transect, Northern Ngarunui Beach. Sample collected on the 15th of August, 2014.

Table II.76: *Graphical and statistical parameters, textural description and size classes for sample 76: Mid intertidal zone, southern transect, Northern Ngarunui Beach. Sample collected on the 15th of August, 2014.*

Textural description	**Textural size classes**
Moderately well sorted, Near symmetrical skewed, Mesokurtic	Sand = 100 000%Fines = 0.000% Silt = 0.000%Clay = 0.000%
Moment method parameters (µm) Mean = 345.854 Standard deviation (sd) = 120.405 Skewness (SkI) = 0.791 Kurtosis (KG) = 3.423	**Graphical method parameters. After Folk (1980) (ϕ)** Mean (Mz) = 1.622 d(0.5) = 1.621 Sorting (SI) = 0.513 Skewness (SkI) = 0.005 Kurtosis (KG) = 0.960 Mean (mm) = 0.325 Mean (µm) = 324.928
Wentworth size class Medium sand	

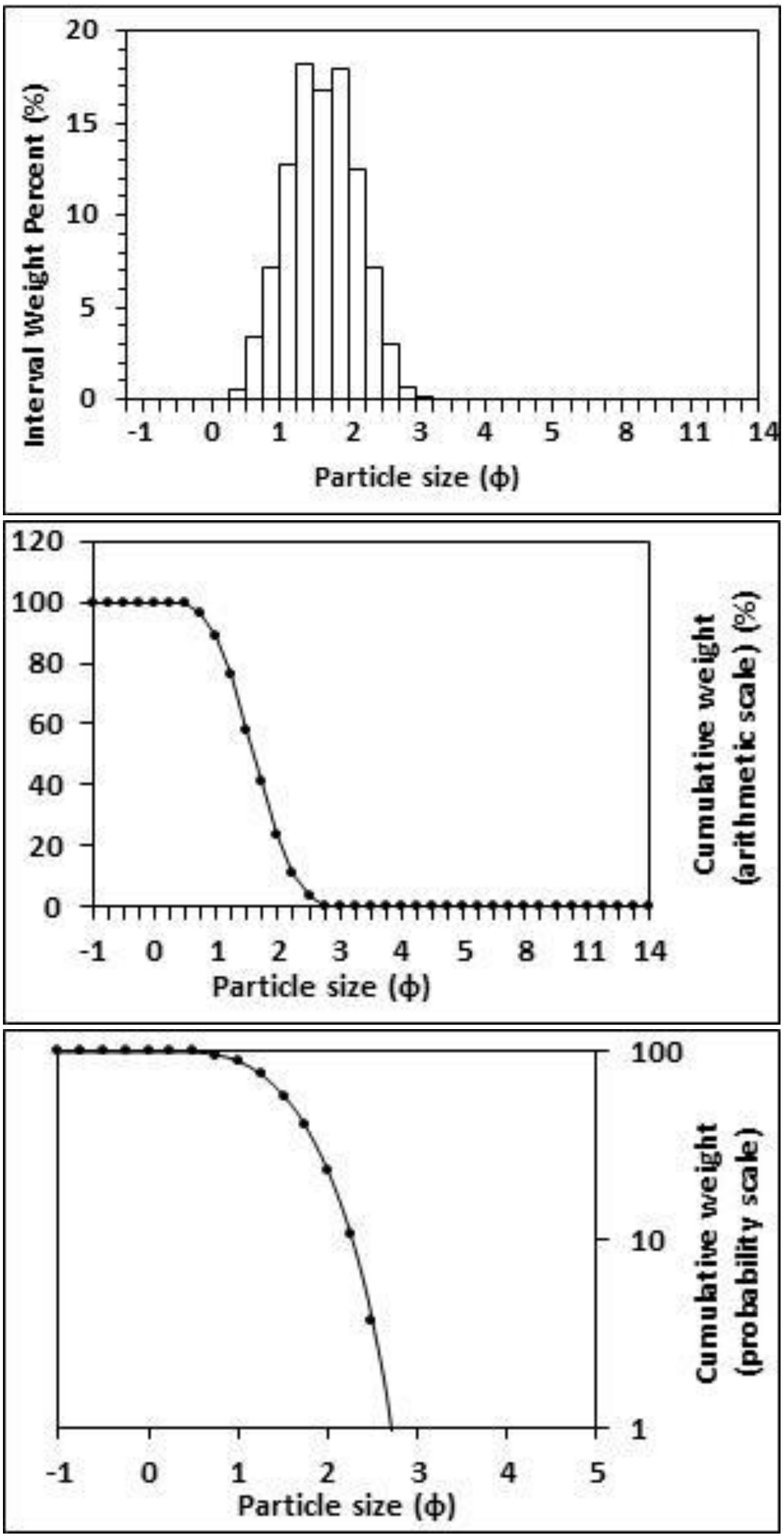

Figures II.226, II.227 and II.228: Histogram of grain size distribution and cumulative frequency graphs (arithmetic scale and probability scale) for sample 76: Mid intertidal zone, southern transect, Northern Ngarunui Beach. Sample collected on the 15th of August, 2014.

Table II.77: *Graphical and statistical parameters, textural description and size classes for sample 77: Low intertidal zone, northern transect, Northern Ngarunui Beach. Sample collected on the 15th of August, 2014.*

Textural description	**Textural size classes**
Moderately well sorted, Near symmetrical skewed, Mesokurtic	Sand = 100 000%Fines = 0.000% Silt = 0.000%Clay = 0.000%
Moment method parameters (µm) Mean = 316.521 Standard deviation (sd) = 123.312 Skewness (SkI) = 0.865 Kurtosis (KG) = 3.553 **Wentworth size class** Medium sand	**Graphical method parameters. After Folk (1980) (ϕ)** Mean (Mz) = 1.771 d(0.5) = 1.770 Sorting (SI) = 0.574 Skewness (SkI) = 0.004 Kurtosis (KG) = 0.944 Mean (mm) = 0.293 Mean (µm) = 292.962

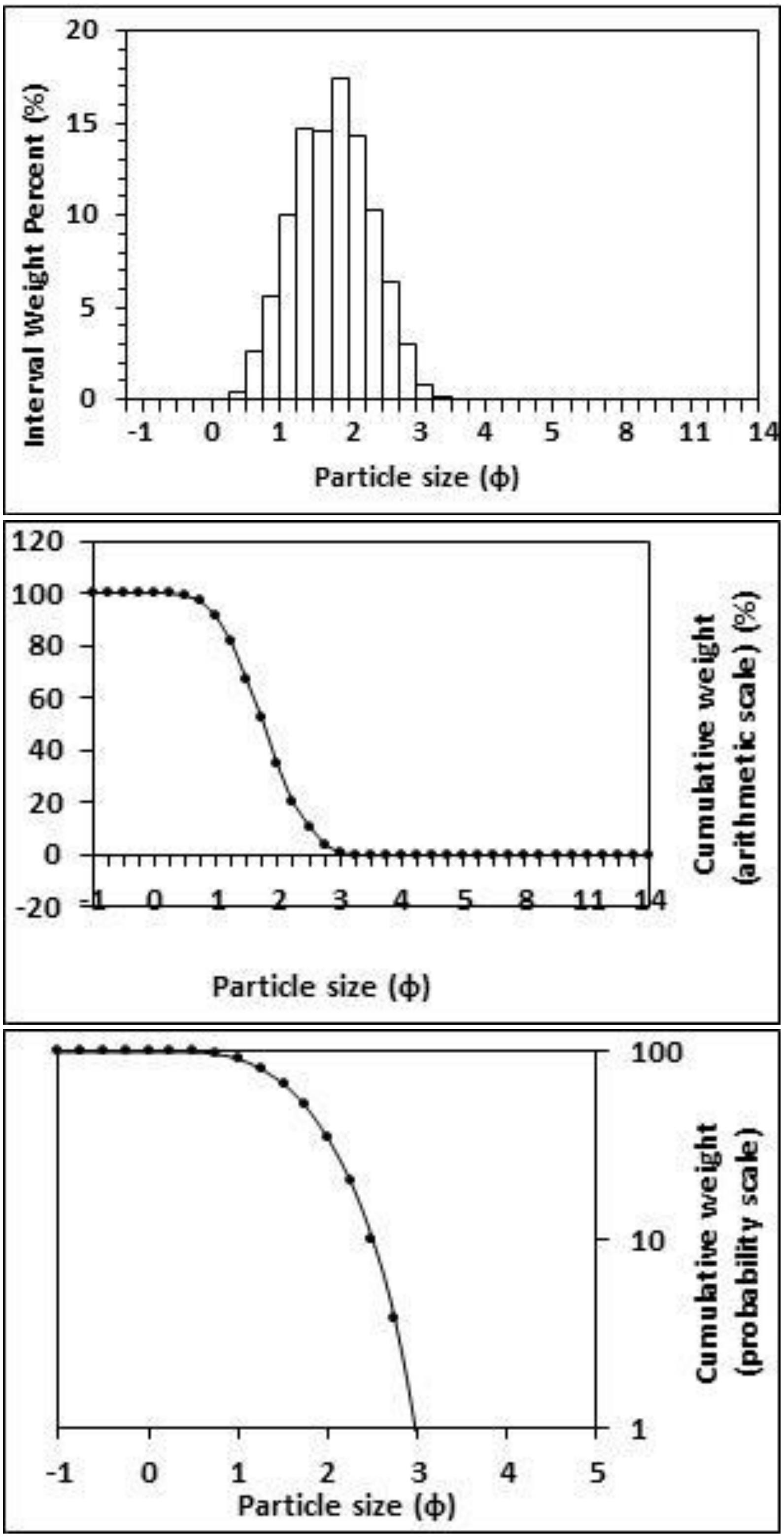

Figures II.229, II.230 and II.231: Histogram of grain size distribution and cumulative frequency graphs (arithmetic scale and probability scale) for sample 77: Low intertidal zone, northern transect, Northern Ngarunui Beach. Sample collected on the 15th of August, 2014.

Table II.78: *Graphical and statistical parameters, textural description and size classes for sample 78: Low intertidal zone, southern transect, Northern Ngarunui Beach. Sample collected on the 15th of August, 2014.*

Textural description	**Textural size classes**
Moderately well sorted, Near symmetrical skewed, Mesokurtic	Sand = 100 000%Fines = 0.000% Silt = 0.000%Clay = 0.000%
Moment method parameters (µm) Mean = 337.616 Standard deviation (sd) = 130.018 Skewness (SkI) = 0.821 Kurtosis (KG) = 3.383	**Graphical method parameters. After Folk (1980) (ϕ)** Mean (Mz) = 1.671 d(0.5) = 1.673 Sorting (SI) = 0.567 Skewness (SkI) = 0.007 Kurtosis (KG) = 0.943 Mean (mm) = 0.314 Mean (µm) = 313.974
Wentworth size class Medium sand	

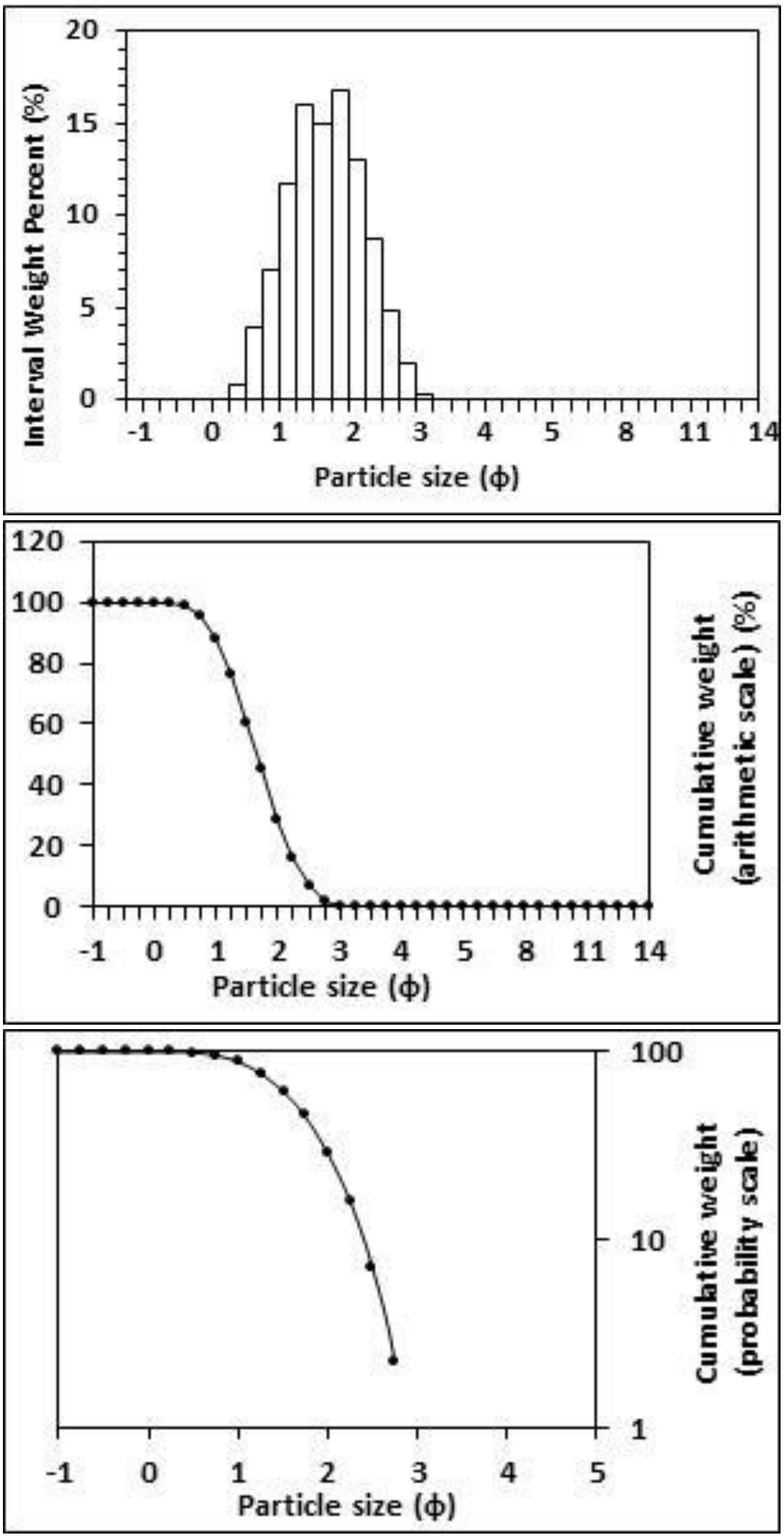

Figures II.232, II.233 and II.234: Histogram of grain size distribution and cumulative frequency graphs (arithmetic scale and probability scale) for sample 78: Low intertidal zone, southern transect, Northern Ngarunui Beach. Sample collected on the 15th of August, 2014.

Table II.79: *Graphical and statistical parameters, textural description and size classes for sample 79: Mid intertidal zone, northern transect, Northern Ngarunui Beach. Sample collected on the 15th of August, 2014.*

Textural description	**Textural size classes**
Moderately well sorted, Near symmetrical skewed, Mesokurtic	Sand = 100 000%Fines = 0.000% Silt = 0.000%Clay = 0.000%
Moment method parameters (μm)	**Graphical method parameters. After Folk (1980) (ϕ)**
Mean = 325.996 Standard deviation (sd) = 127.036 Skewness (SkI) = 0.867 Kurtosis (KG) = 3.530	Mean (Mz) = 1.727 d(0.5) = 1.728 Sorting (SI) = 0.574 Skewness (SkI) = 0.002 Kurtosis (KG) = 0.944 Mean (mm) = 0.302 Mean (μm) = 302.100
Wentworth size class Medium sand	

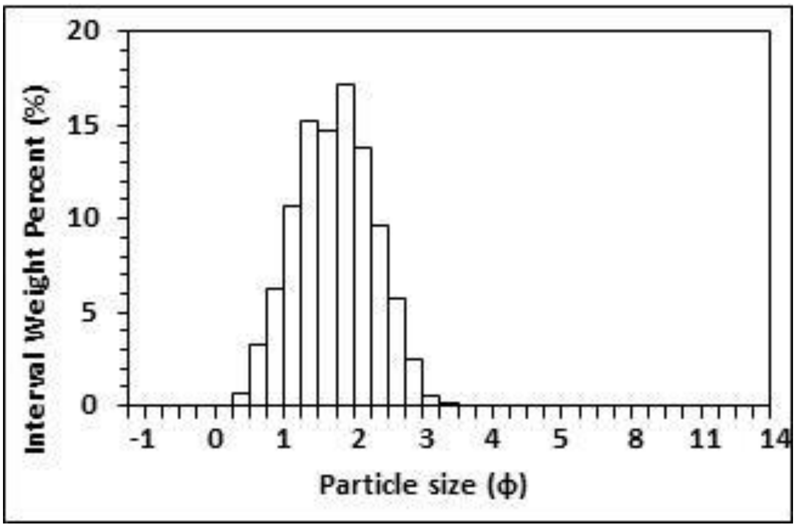

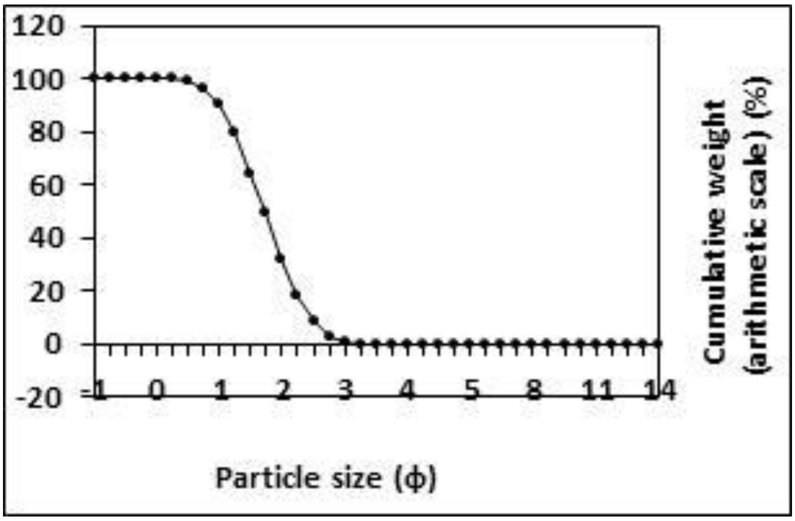

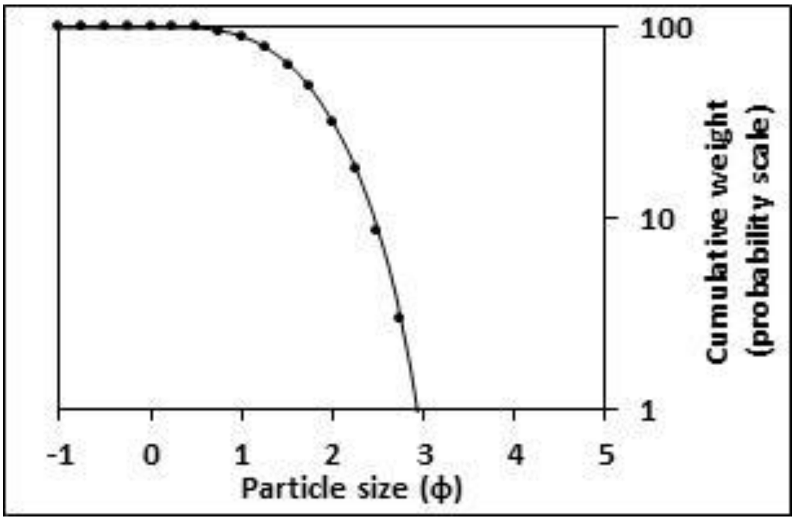

Figures II.235, II.236 and II.237: Histogram of grain size distribution and cumulative frequency graphs (arithmetic scale and probability scale) for sample 79: Mid intertidal zone, northern transect, Northern Ngarunui Beach. Sample collected on the 15th of August, 2014.

Table II.80: *Graphical and statistical parameters, textural description and size classes for sample 80: High intertidal zone, mid transect, Northern Ngarunui Beach. Sample collected on the 30th of August, 2014.*

Textural description	**Textural size classes**
Moderately well sorted, Near symmetrical skewed, Mesokurtic	Sand = 100 000%Fines = 0.000% Silt = 0.000%Clay = 0.000%
Moment method parameters (µm) Mean = 269.279 Standard deviation (sd) = 93.936 Skewness (SkI) = 0.835 Kurtosis (KG) = 3.604	**Graphical method parameters. After Folk (1980) (ϕ)** Mean (Mz) = 1.980 d(0.5) = 1.983 Sorting (SI) = 0.509 Skewness (SkI) = -0.006 Kurtosis (KG) = 0.956 Mean (mm) = 0.253 Mean (µm) = 253.453
Wentworth size class Medium sand	

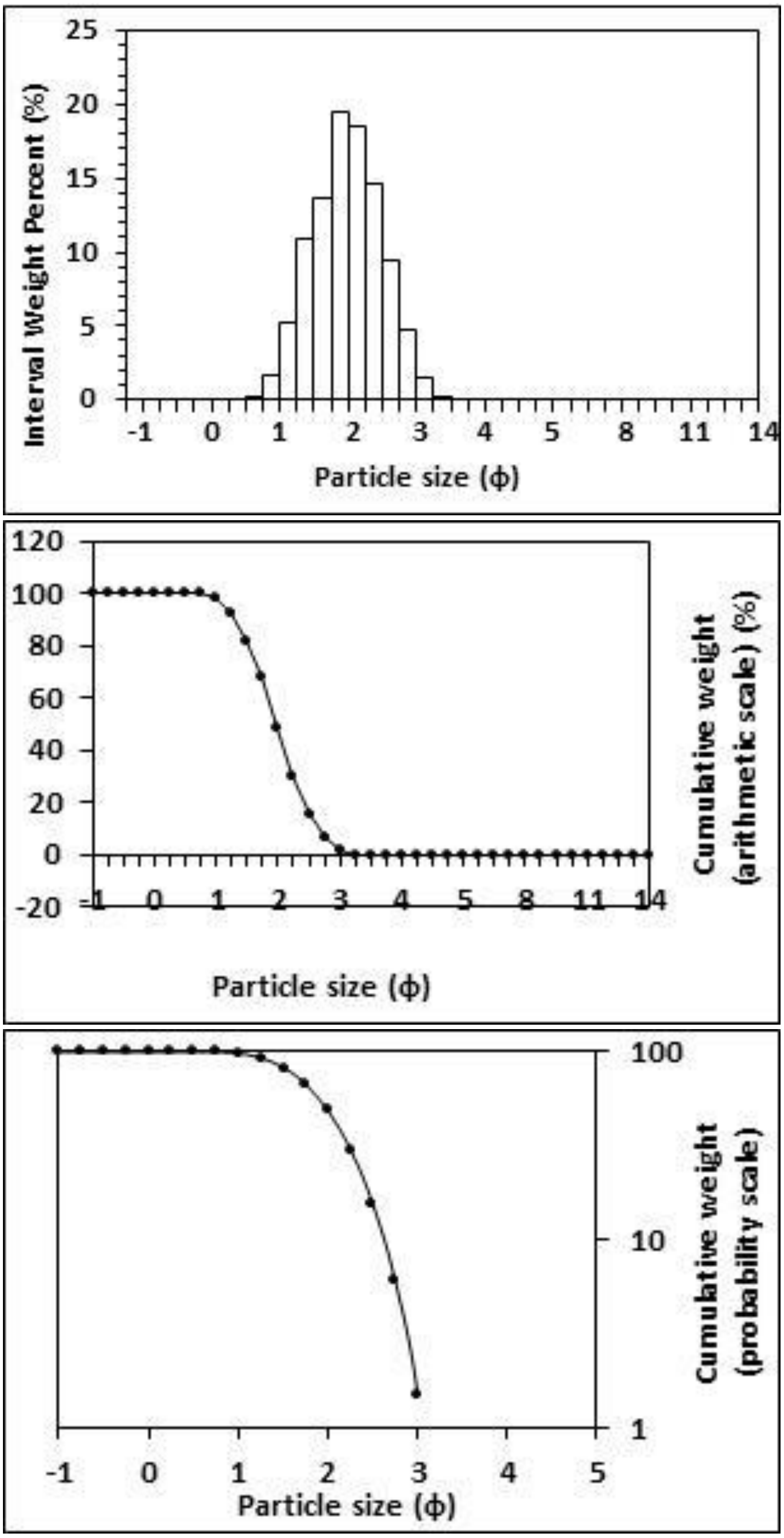

Figures II.238, II.239 and II.240: Histogram of grain size distribution and cumulative frequency graphs (arithmetic scale and probability scale) for sample 80: High intertidal zone, mid transect, Northern Ngarunui Beach. Sample collected on the 30th of August, 2014.

Table II.81: *Graphical and statistical parameters, textural description and size classes for sample 81: Mid intertidal zone, mid transect, Northern Ngarunui Beach. Sample collected on the 30th of August, 2014.*

Textural description	**Textural size classes**
Moderately well sorted, Near symmetrical skewed, Mesokurtic	Sand = 100 000%Fines = 0.000% Silt = 0.000%Clay = 0.000%
Moment method parameters (µm) Mean = 409.618 Standard deviation (sd) = 151.749 Skewness (SkI) = 0.747 Kurtosis (KG) = 3.235	**Graphical method parameters. After Folk (1980) (ϕ)** Mean (Mz) = 1.388 d(0.5) = 1.383 Sorting (SI) = 0.551 Skewness (SkI) = 0.020 Kurtosis (KG) = 0.948 Mean (mm) = 0.382 Mean (µm) = 382.173
Wentworth size class Medium sand	

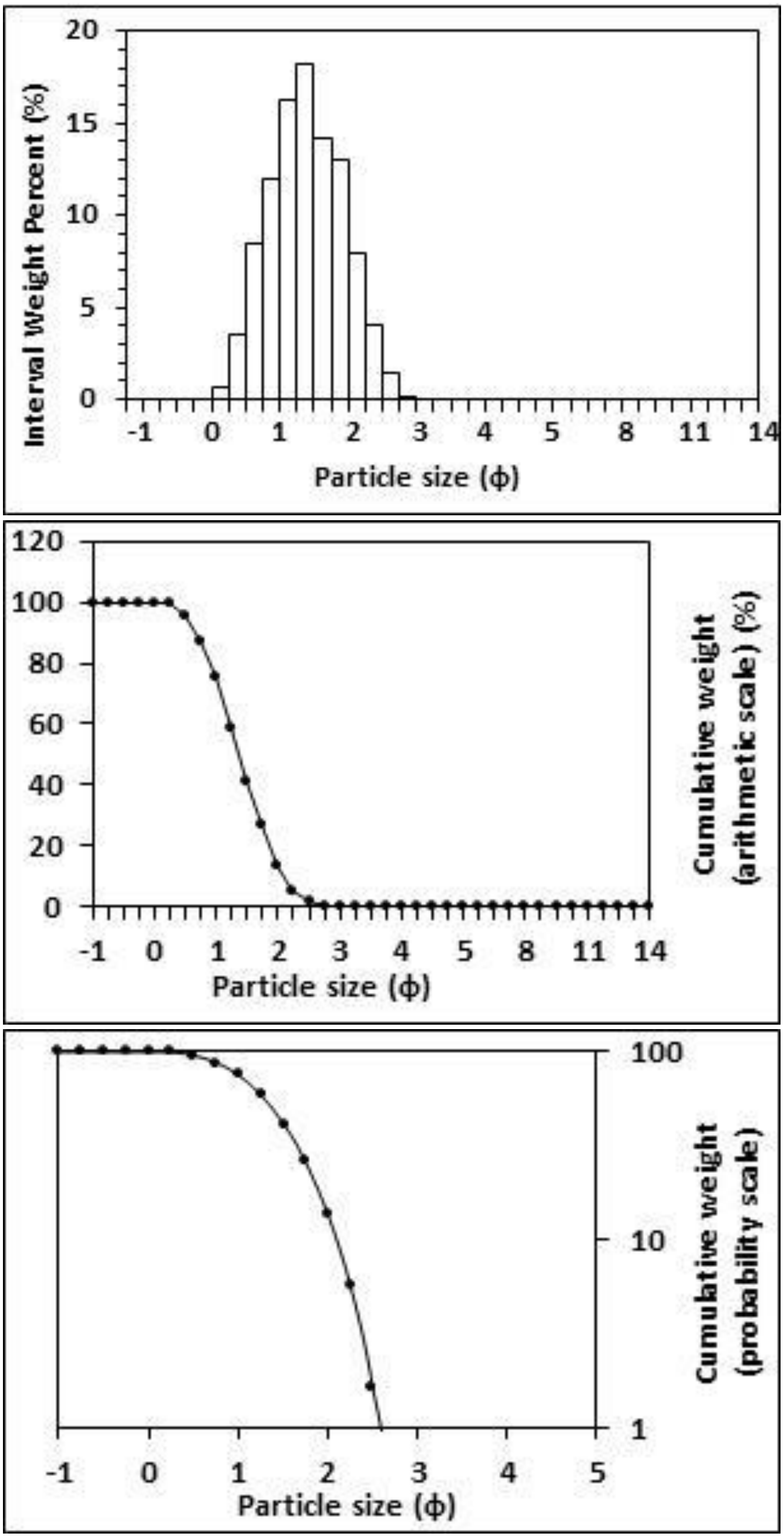

Figures II.241, II.242 and II.243: Histogram of grain size distribution and cumulative frequency graphs (arithmetic scale and probability scale) for sample 81: Mid intertidal zone, mid transect, Northern Ngarunui Beach. Sample collected on the 30th of August, 2014.

Table II.82: *Graphical and statistical parameters, textural description and size classes for sample 82: Low intertidal zone, mid transect, Northern Ngarunui Beach. Sample collected on the 30th of August, 2014.*

Textural description	**Textural size classes**
Moderately well sorted, Near symmetrical skewed, Mesokurtic	Sand = 100 000%Fines = 0.000% Silt = 0.000%Clay = 0.000%
Moment method parameters (µm) Mean = 417.882 Standard deviation (sd) = 180.502 Skewness (SkI) = 0.838 Kurtosis (KG) =3.376 **Wentworth size class** Medium sand	**Graphical method parameters. After Folk (1980) (ϕ)** Mean (Mz) = 1.395 d(0.5) = 1.385 Sorting (SI) = 0.646 Skewness (SkI) = 0.026 Kurtosis (KG) = 0.934 Mean (mm) = 0.380 Mean (µm) = 380.336

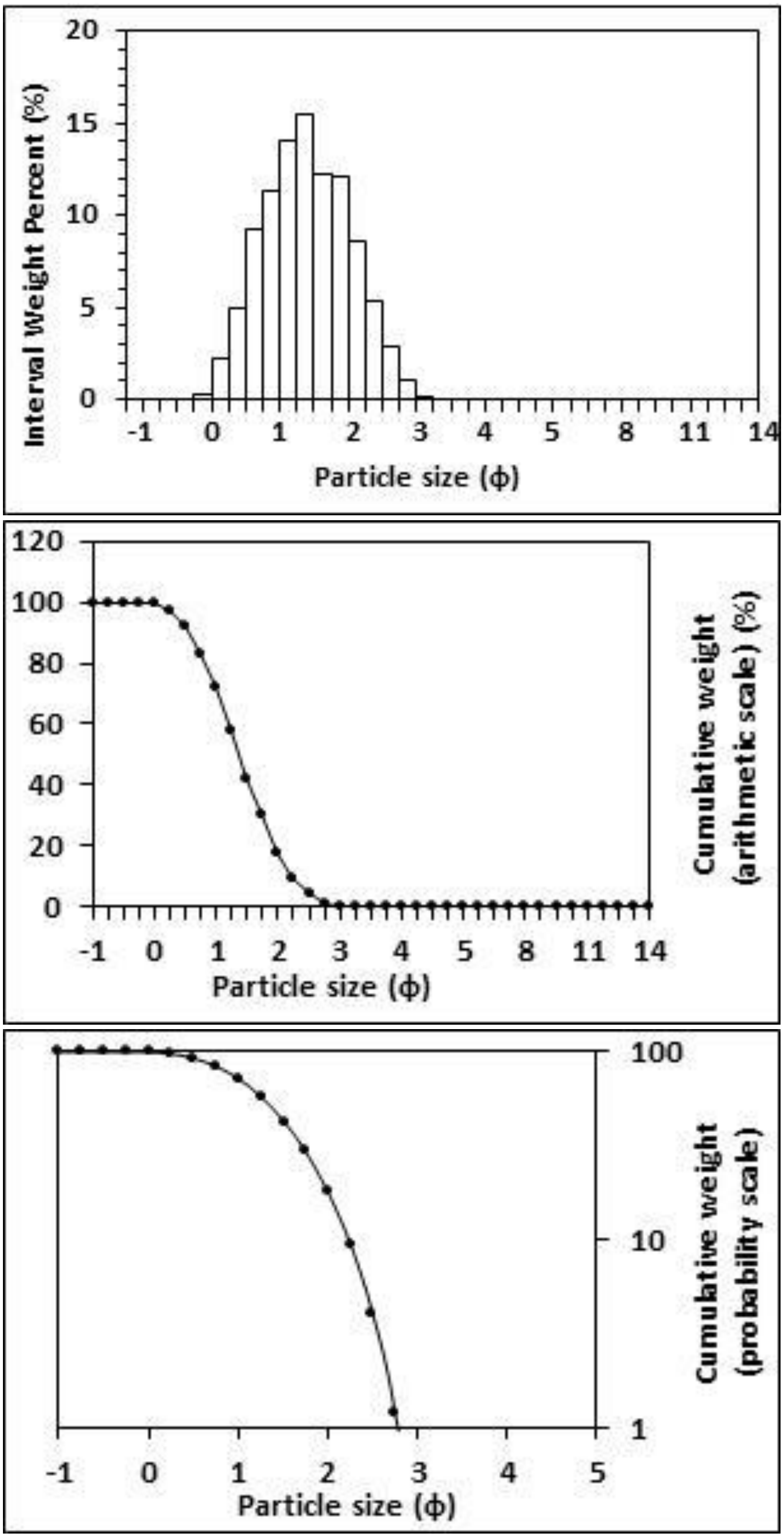

Figures II.244, II.245 and II.246: Histogram of grain size distribution and cumulative frequency graphs (arithmetic scale and probability scale) for sample 82: Low intertidal zone, mid transect, Northern Ngarunui Beach. Sample collected on the 30th of August, 2014.

Table II.83: *Graphical and statistical parameters, textural description and size classes for sample 83: Low intertidal zone, northern transect, Northern Ngarunui Beach. Sample collected on the 30th of August, 2014.*

Textural description	**Textural size classes**
Moderately well sorted, Near symmetrical skewed, Mesokurtic	Sand = 100 000%Fines = 0.000% Silt = 0.000%Clay = 0.000%
Moment method parameters (µm) Mean = 450.002 Standard deviation (sd) = 212.684 Skewness (SkI) = 1.068 Kurtosis (KG) = 4.093 **Wentworth size class** Medium sand	**Graphical method parameters. After Folk (1980) (ϕ)** Mean (Mz) = 1.308 d(0.5) = 1.312 Sorting (SI) = 0.687 Skewness (SkI) = -0.007 Kurtosis (KG) = 0.943 Mean (mm) = 0.404 Mean (µm) = 404.018

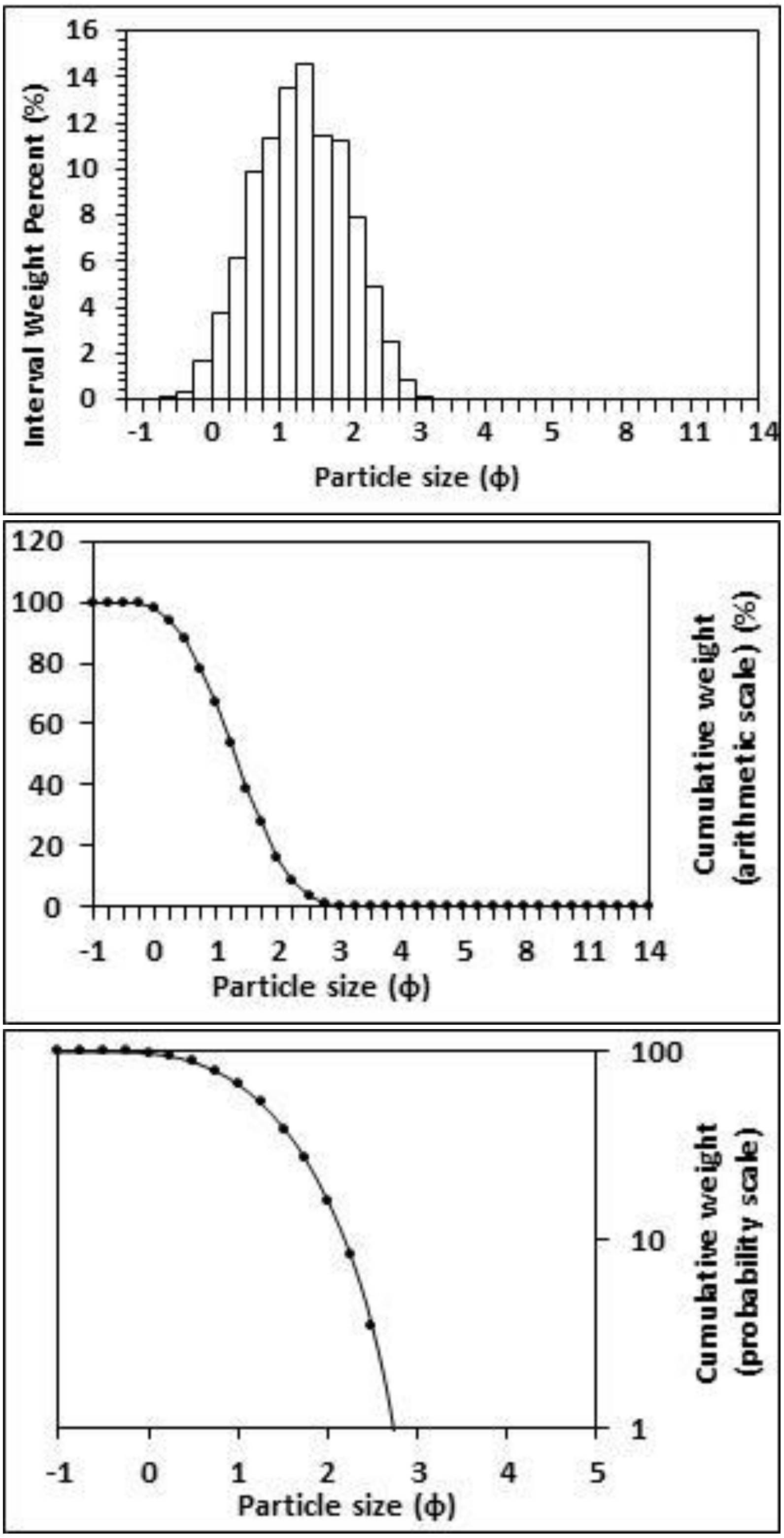

Figures II.247, II.248 and II.249: Histogram of grain size distribution and cumulative frequency graphs (arithmetic scale and probability scale) for sample 83: Low intertidal zone, northern transect, Northern Ngarunui Beach. Sample collected on the 30th of August, 2014.

Table II.84: *Graphical and statistical parameters, textural description and size classes for sample 84: Low intertidal zone, southern transect, Northern Ngarunui Beach. Sample collected on the 30th of August, 2014.*

Textural description	**Textural size classes**
Moderately well sorted, Near symmetrical skewed, Mesokurtic	Sand = 100 000%Fines = 0.000% Silt = 0.000%Clay = 0.000%
Moment method parameters (µm) Mean = 392.222 Standard deviation (sd) = 165.143 Skewness (SkI) = 0.942 Kurtosis (KG) = 3.756	**Graphical method parameters. After Folk (1980) (ϕ)** Mean (Mz) = 1.478 d(0.5) = 1.477 Sorting (SI) = 0.615 Skewness (SkI) = 0.006 Kurtosis (KG) = 0.938 Mean (mm) = 0.359 Mean (µm) = 358.898
Wentworth size class Medium sand	

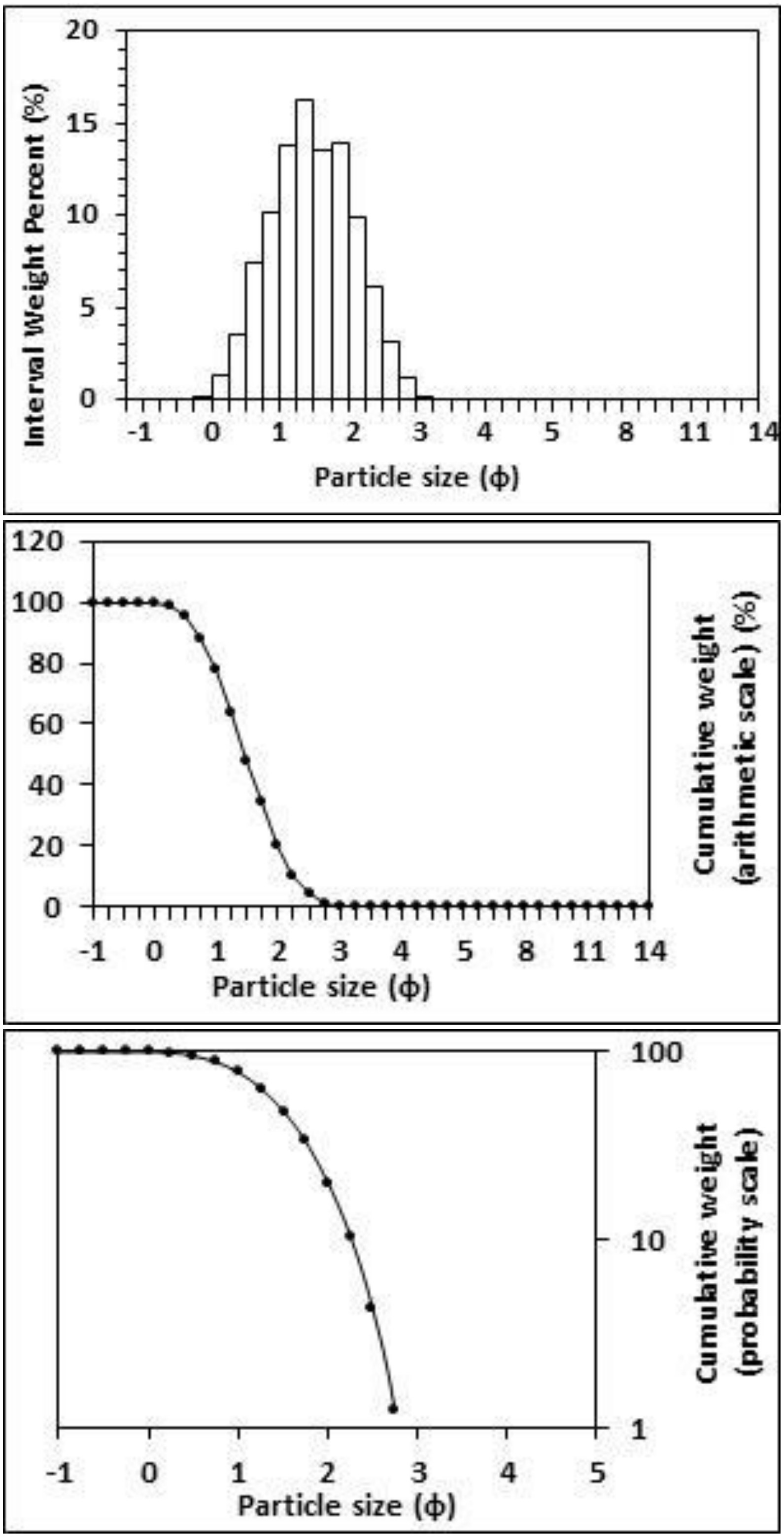

Figures II.250, II.251 and II.252: Histogram of grain size distribution and cumulative frequency graphs (arithmetic scale and probability scale) for sample 84: Low intertidal zone, southern transect, Northern Ngarunui Beach. Sample collected on the 30th of August, 2014.

Table II.85: *Graphical and statistical parameters, textural description and size classes for sample 85: Mid intertidal zone, southern transect, Northern Ngarunui Beach. Sample collected on the 30th of August, 2014.*

Textural description	**Textural size classes**
Moderately well sorted, Near symmetrical skewed, Mesokurtic	Sand = 100 000%Fines = 0.000% Silt = 0.000%Clay = 0.000%
Moment method parameters (µm) Mean = 468.589 Standard deviation (sd) = 167.561 Skewness (SkI) = 0.723 Kurtosis (KG) = 3.203 **Wentworth size class** Medium sand	**Graphical method parameters. After Folk (1980) (ϕ)** Mean (Mz) = 1.183 d(0.5) = 1.182 Sorting (SI) = 0.534 Skewness (SkI) = 0.014 Kurtosis (KG) = 0.951 Mean (mm) = 0.440 Mean (µm) = 440.395

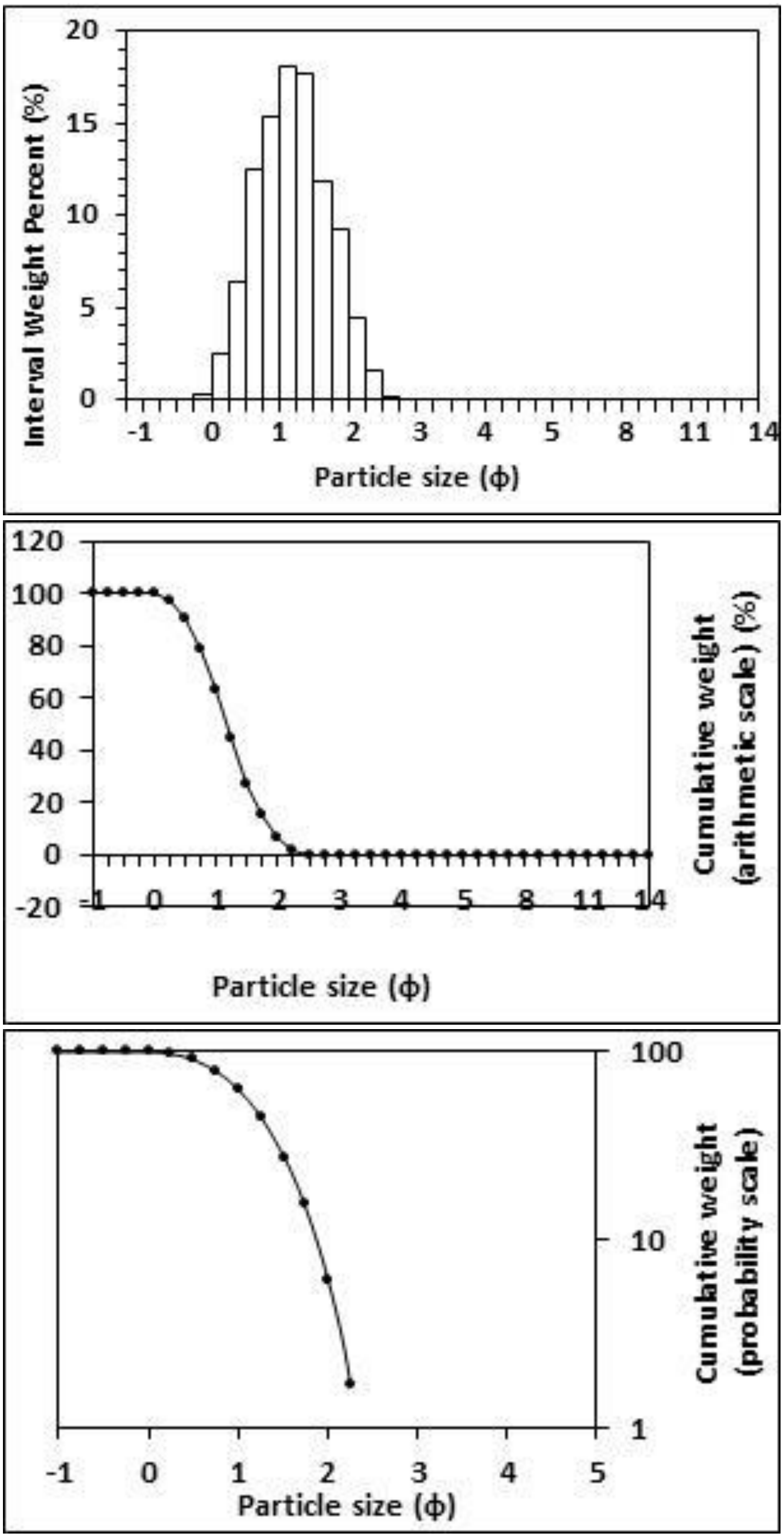

Figures II.253, II.254 and II.255: Histogram of grain size distribution and cumulative frequency graphs (arithmetic scale and probability scale) for sample 85: Mid intertidal zone, southern transect, Northern Ngarunui Beach. Sample collected on the 30th of August, 2014.

Table II.86: *Graphical and statistical parameters, textural description and size classes for sample 86: High intertidal zone, northern transect, Northern Ngarunui Beach. Sample collected on the 30th of August, 2014.*

<table>
<tr><td>Textural description
Well sorted,
Near symmetrical skewed,
Mesokurtic</td><td>Textural size classes
Sand = 100 000%Fines = 0.000%
Silt = 0.000%Clay = 0.000%</td></tr>
<tr><td>Moment method parameters (µm)
Mean = 289.546
Standard deviation (sd) = 91.129
Skewness (SkI) = 0.763
Kurtosis (KG) = 3.486</td><td rowspan="2">Graphical method parameters. After Folk (1980) (ϕ)
Mean (Mz) = 1.862
d(0.5) = 1.862
Sorting (SI) = 0.467
Skewness (SkI) = 0.000
Kurtosis (KG) = 0.977
Mean (mm) = 0.275
Mean (µm) = 275.163</td></tr>
<tr><td>Wentworth size class
Medium sand</td></tr>
</table>

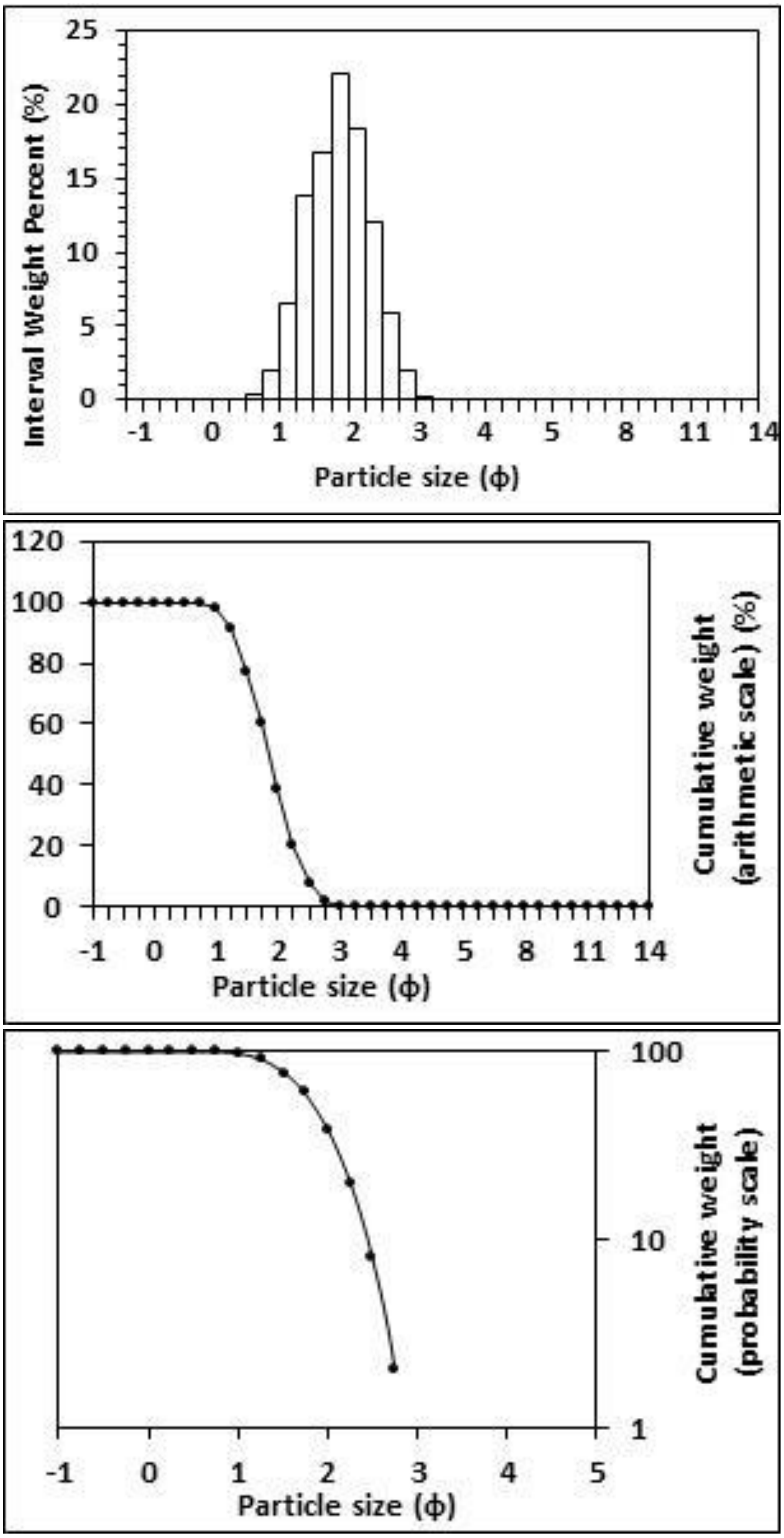

Figures II.256, II.257 and II.258: Histogram of grain size distribution and cumulative frequency graphs (arithmetic scale and probability scale) for sample 86: High intertidal zone, northern transect, Northern Ngarunui Beach. Sample collected on the 30th of August, 2014.

Table II.87: *Graphical and statistical parameters, textural description and size classes for sample 87: Mid intertidal zone, northern transect, Northern Ngarunui Beach. Sample collected on the 30th of August, 2014.*

Textural description	**Textural size classes**
Moderately well sorted, Near symmetrical skewed, Mesokurtic	Sand = 100 000%Fines = 0.000% Silt = 0.000%Clay = 0.000%
Moment method parameters (μm) Mean = 376.874 Standard deviation (sd) = 132.030 Skewness (SkI) = 0.828 Kurtosis (KG) =3.543	**Graphical method parameters. After Folk (1980) (ϕ)** Mean (Mz) = 1.499 d(0.5) = 1.499 Sorting (SI) = 0.512 Skewness (SkI) = -0.004 Kurtosis (KG) = 0.952 Mean (mm) = 0.354 Mean (μm) = 353.868
Wentworth size class Medium sand	

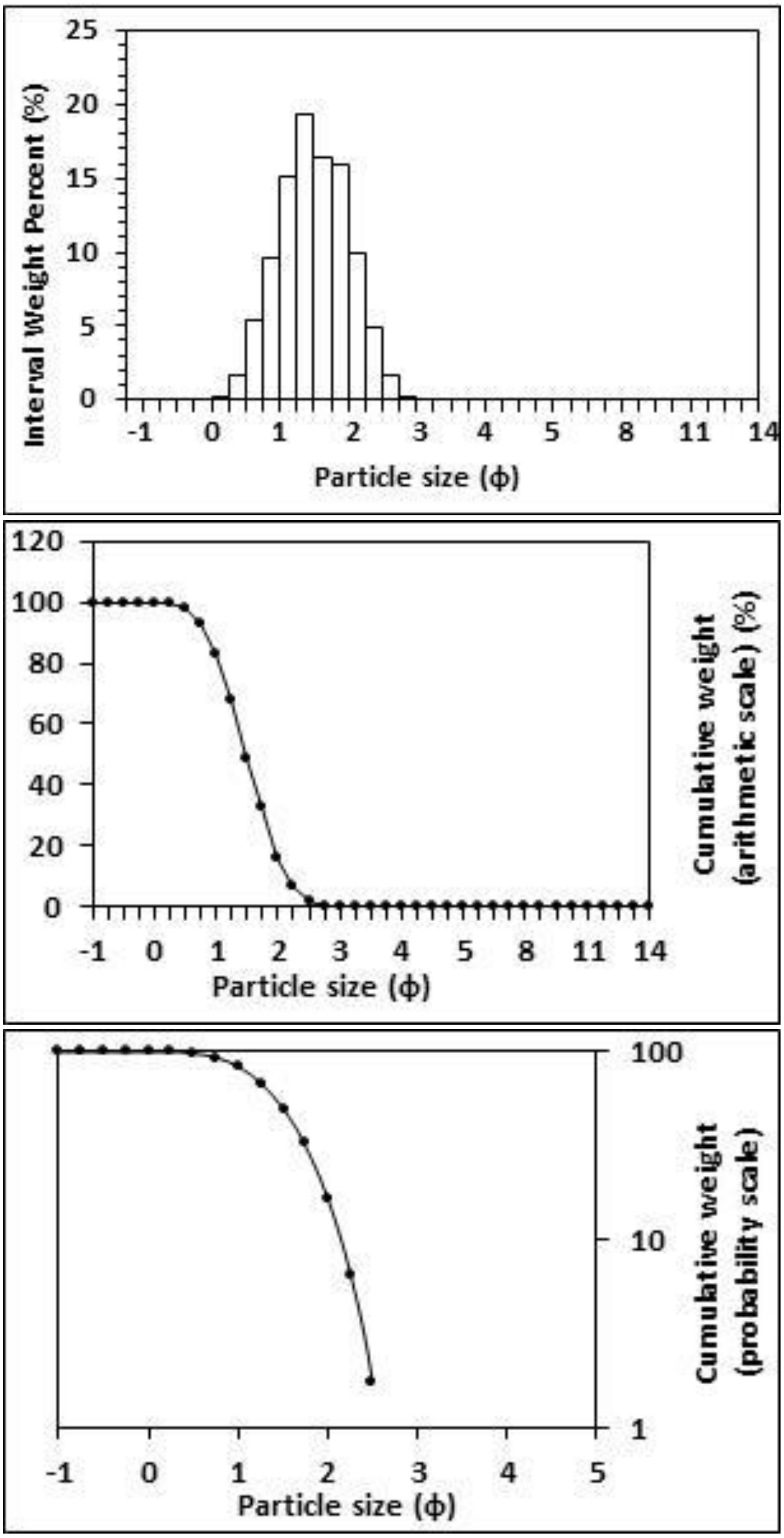

Figures II.259, II.260 and II.261: Histogram of grain size distribution and cumulative frequency graphs (arithmetic scale and probability scale) for sample 87: Mid intertidal zone, northern transect, Northern Ngarunui Beach. Sample collected on the 30th of August, 2014.

Table II.88: *Graphical and statistical parameters, textural description and size classes for sample 88: High intertidal zone, southern transect, Northern Ngarunui Beach. Sample collected on the 30th of August, 2014.*

Textural description	**Textural size classes**
Moderately well sorted, Near symmetrical skewed, Mesokurtic	Sand = 100 000%Fines = 0.000% Silt = 0.000%Clay = 0.000%
Moment method parameters (µm)	**Graphical method parameters. After Folk (1980) (ϕ)**
Mean = 335.810 Standard deviation (sd) = 117.298 Skewness (SkI) = 0.793 Kurtosis (KG) = 3.449	Mean (Mz) = 1.663 d(0.5) = 1.663 Sorting (SI) = 0.514 Skewness (SkI) = 0.000 Kurtosis (KG) = 0.953 Mean (mm) = 0.316 Mean (µm) = 315.735
Wentworth size class Medium sand	

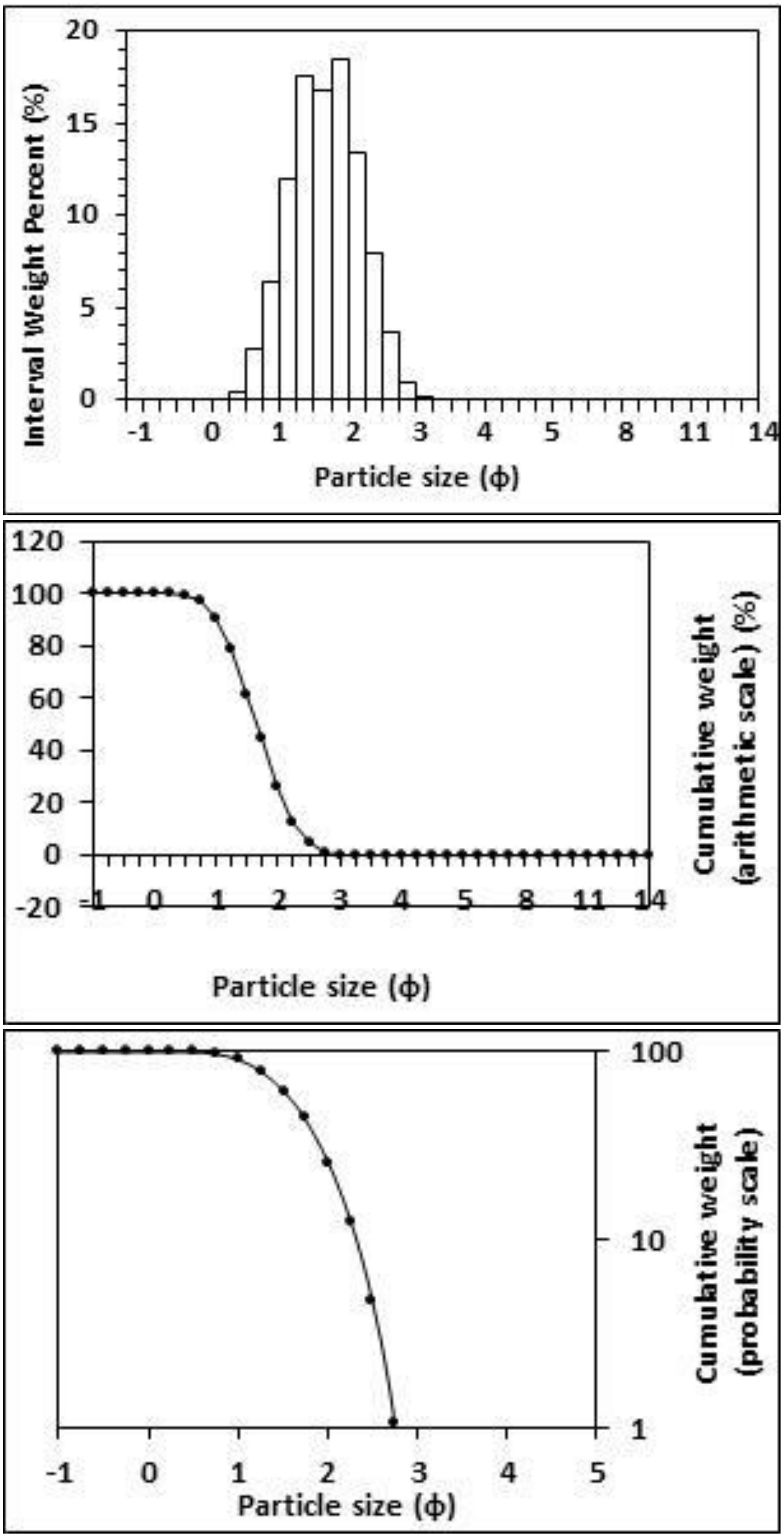

Figures II.262, II.263 and II.264: Histogram of grain size distribution and cumulative frequency graphs (arithmetic scale and probability scale) for sample 88: High intertidal zone, southern transect, Northern Ngarunui Beach. Sample collected on the 30th of August, 2014.

Table II.89: *Graphical and statistical parameters, textural description and size classes for sample 89: Low intertidal zone, southern transect, Northern Ngarunui Beach. Sample collected on the 27th of September, 2014.*

Textural description	**Textural size classes**
Moderately sorted, Near symmetrical skewed, Mesokurtic	Sand = 100 000%Fines = 0.000% Silt = 0.000%Clay = 0.000%
Moment method parameters (µm) Mean = 556.258 Standard deviation (sd) = 295.215 Skewness (SkI) =1.361 Kurtosis (KG) = 5.246	**Graphical method parameters. After Folk (1980) (ϕ)** Mean (Mz) = 1.041 d(0.5) = 1.044 Sorting (SI) = 0.744 Skewness (SkI) = -0.013 Kurtosis (KG) = 0.969 Mean (mm) = 0.486 Mean (µm) = 486.013
Wentworth size class Medium sand	

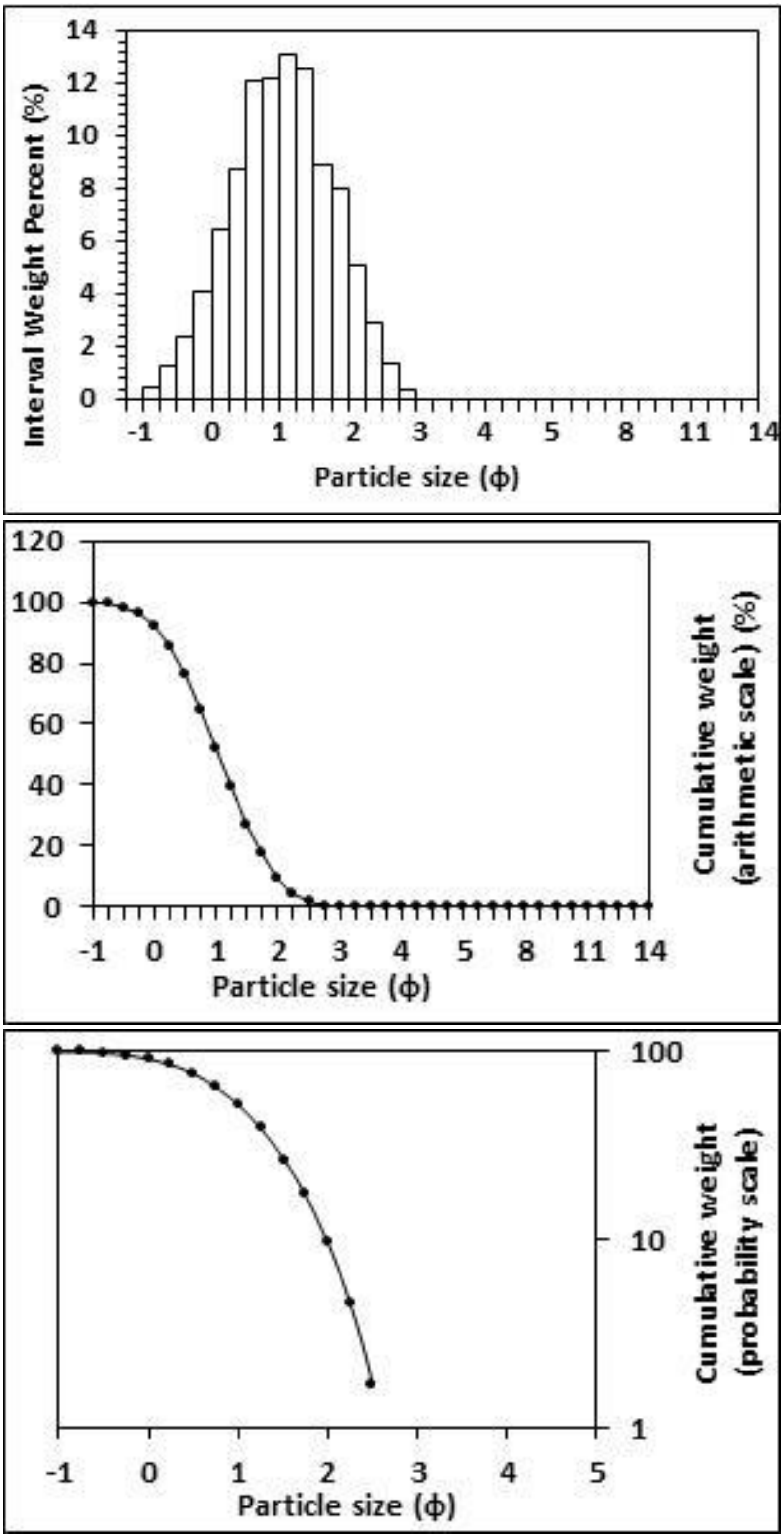

Figures II.265, II.266 and II.267: Histogram of grain size distribution and cumulative frequency graphs (arithmetic scale and probability scale) for sample 89: Low intertidal zone, southern transect, Northern Ngarunui Beach. Sample collected on the 27th of September, 2014.

Table II.90: *Graphical and statistical parameters, textural description and size classes for sample 90: Low intertidal zone, mid transect, Northern Ngarunui Beach. Sample collected on the 27th of September, 2014.*

Textural description	**Textural size classes**
Moderately well sorted, Near symmetrical skewed, Mesokurtic	Sand = 100 000%Fines = 0.000% Silt = 0.000%Clay = 0.000%
Moment method parameters (µm)	**Graphical method parameters. After Folk (1980) (ϕ)**
Mean = 443.476 Standard deviation (sd) = 168.808 Skewness (SkI) = 0.818 Kurtosis (KG) = 3.440	Mean (Mz) = 1.281 d(0.5) = 1.276 Sorting (SI) = 0.565 Skewness (SkI) = 0.012 Kurtosis (KG) = 0.950 Mean (mm) = 0.412 Mean (µm) = 411.619
Wentworth size class Medium sand	

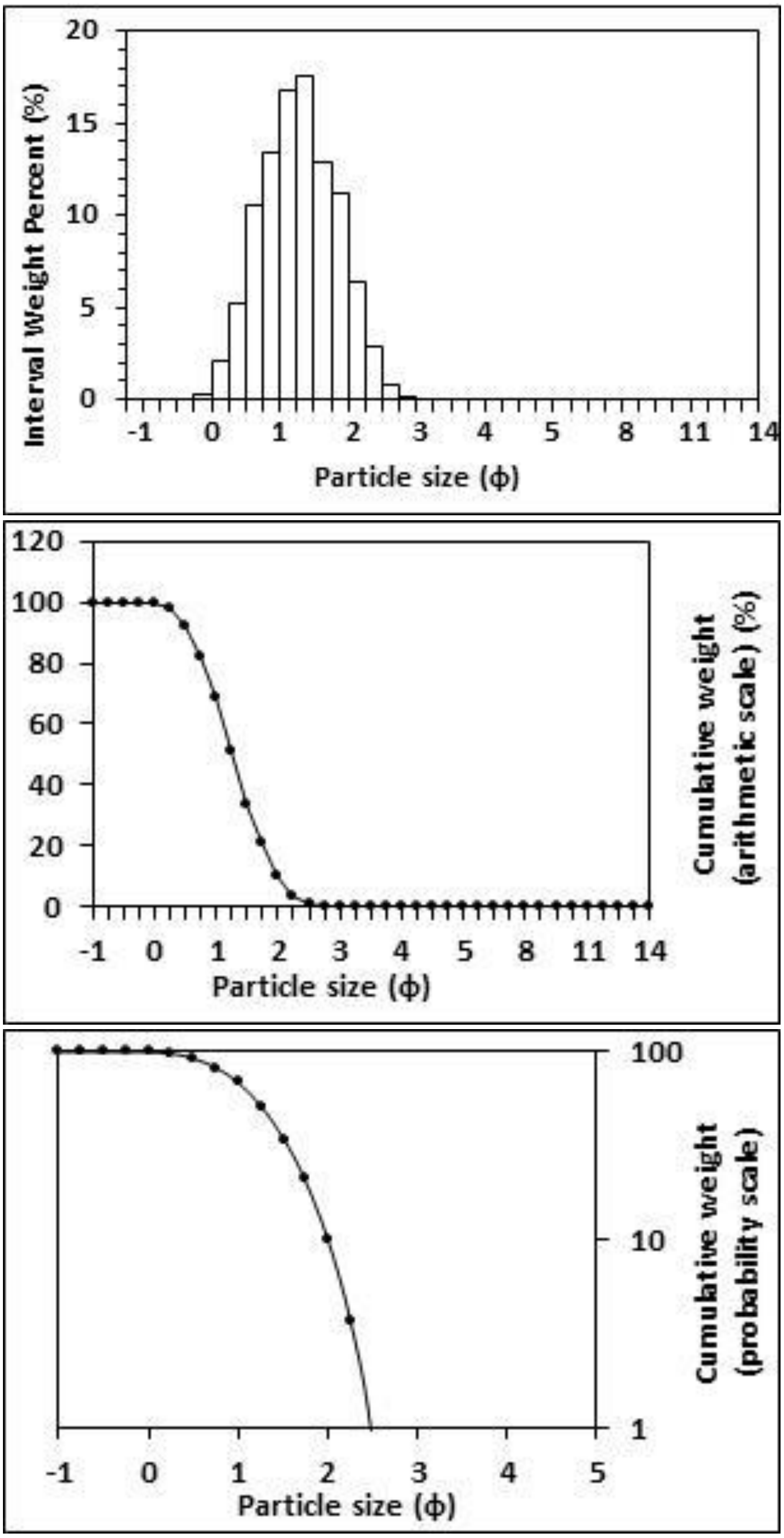

Figures II.268, II.269 and II.270: Histogram of grain size distribution and cumulative frequency graphs (arithmetic scale and probability scale) for sample 90: Low intertidal zone, mid transect, Northern Ngarunui Beach. Sample collected on the 27th of September, 2014.

Table II.91: *Graphical and statistical parameters, textural description and size classes for sample 91: Mid intertidal zone, northern transect, Northern Ngarunui Beach. Sample collected on the 27th of September, 2014.*

Textural description	**Textural size classes**
Moderately well sorted, Near symmetrical skewed, Mesokurtic	Sand = 100 000%Fines = 0.000% Silt = 0.000%Clay = 0.000%
Moment method parameters (µm) Mean = 299.565 Standard deviation (sd) = 103.948 Skewness (SkI) = 0.812 Kurtosis (KG) = 3.515	**Graphical method parameters. After Folk (1980) (ϕ)** Mean (Mz) = 1.830 d(0.5) = 1.829 Sorting (SI) = 0.509 Skewness (SkI) = 0.007 Kurtosis (KG) = 0.952 Mean (mm) = 0.281 Mean (µm) = 281.333
Wentworth size class Medium sand	

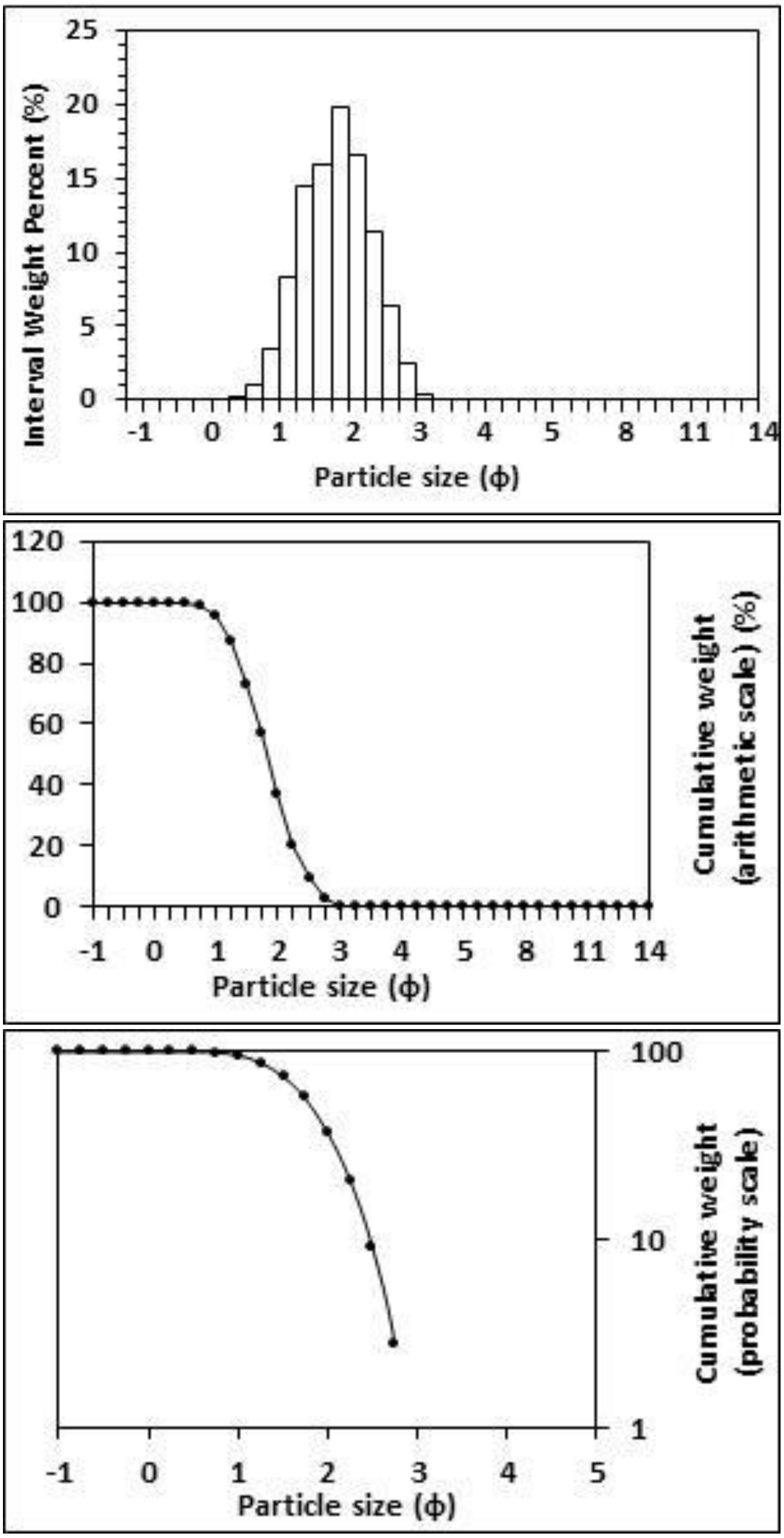

Figures II.271, II.272 and II.273: Histogram of grain size distribution and cumulative frequency graphs (arithmetic scale and probability scale) for sample 91: Mid intertidal zone, northern transect, Northern Ngarunui Beach. Sample collected on the 27th of September, 2014.

Table II.92: *Graphical and statistical parameters, textural description and size classes for sample 92: High intertidal zone, southern transect, Northern Ngarunui Beach. Sample collected on the 27th of September, 2014.*

Textural description	**Textural size classes**
Moderately well sorted, Near symmetrical skewed, Mesokurtic	Sand = 100 000%Fines = 0.000% Silt = 0.000%Clay = 0.000%
Moment method parameters (μm)	**Graphical method parameters. After Folk (1980) (ϕ)**
Mean = 260.707 Standard deviation (sd) = 103.843 Skewness (SkI) = 0.924 Kurtosis (KG) = 3.755	Mean (Mz) = 2.056 d(0.5) = 2.055 Sorting (SI) = 0.582 Skewness (SkI) = -0.004 Kurtosis (KG) = 0.950 Mean (mm) = 0.240 Mean (μm) = 240.477
Wentworth size class Fine sand	

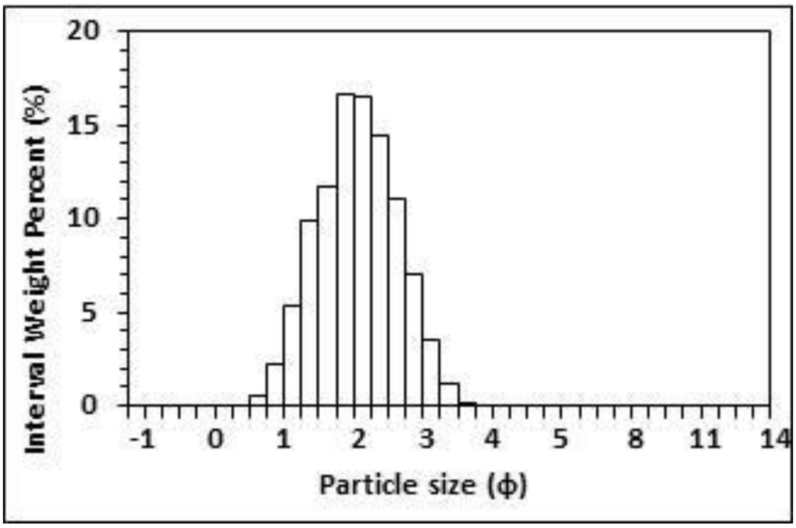

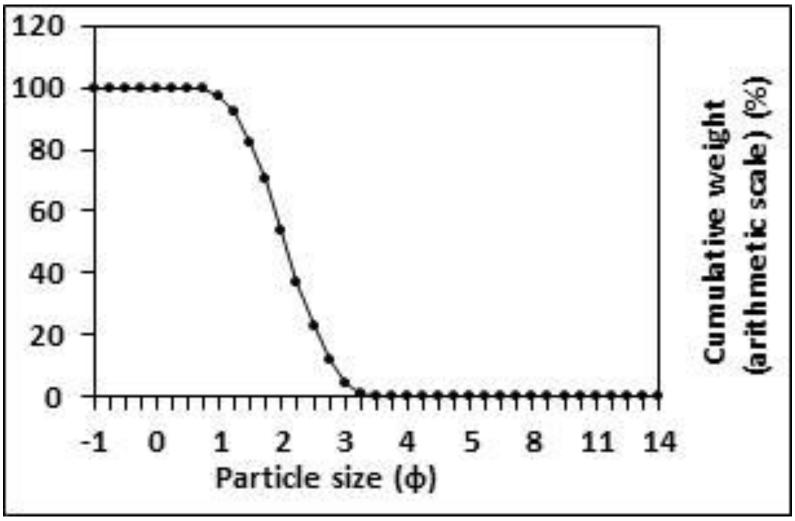

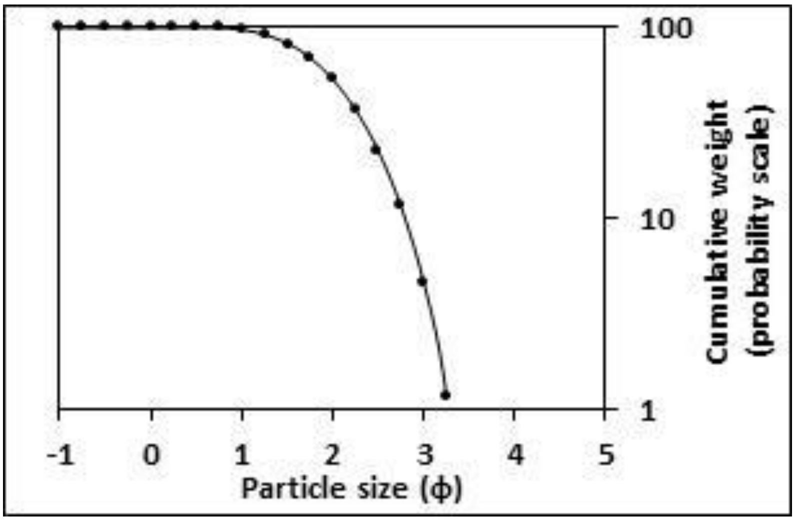

Figures II.274, II.275 and II.276: Histogram of grain size distribution and cumulative frequency graphs (arithmetic scale and probability scale) for sample 92: High intertidal zone, southern transect, Northern Ngarunui Beach. Sample collected on the 27th of September, 2014.

Table II.93: *Graphical and statistical parameters, textural description and size classes for sample 93: Mid intertidal zone, southern transect, Northern Ngarunui Beach. Sample collected on the 27th of September, 2014.*

<table>
<tr><td>Textural description

Moderately well sorted,

Near symmetrical skewed,

Mesokurtic</td><td>Textural size classes

Sand = 100 000%Fines = 0.000%

Silt = 0.000%Clay = 0.000%</td></tr>
<tr><td>Moment method parameters

(µm)

Mean = 496.357

Standard deviation (sd) = 202.805

Skewness (SkI) = 0.983

Kurtosis (KG) = 4.027</td><td rowspan="2">Graphical method parameters.

After Folk (1980) (ϕ)

Mean (Mz) = 1.130

d(0.5) = 1.130

Sorting (SI) = 0.592

Skewness (SkI) = 0.000

Kurtosis (KG) = 0.965

Mean (mm) = 0.457

Mean (µm) = 456.988</td></tr>
<tr><td>Wentworth size class

Medium sand</td></tr>
</table>

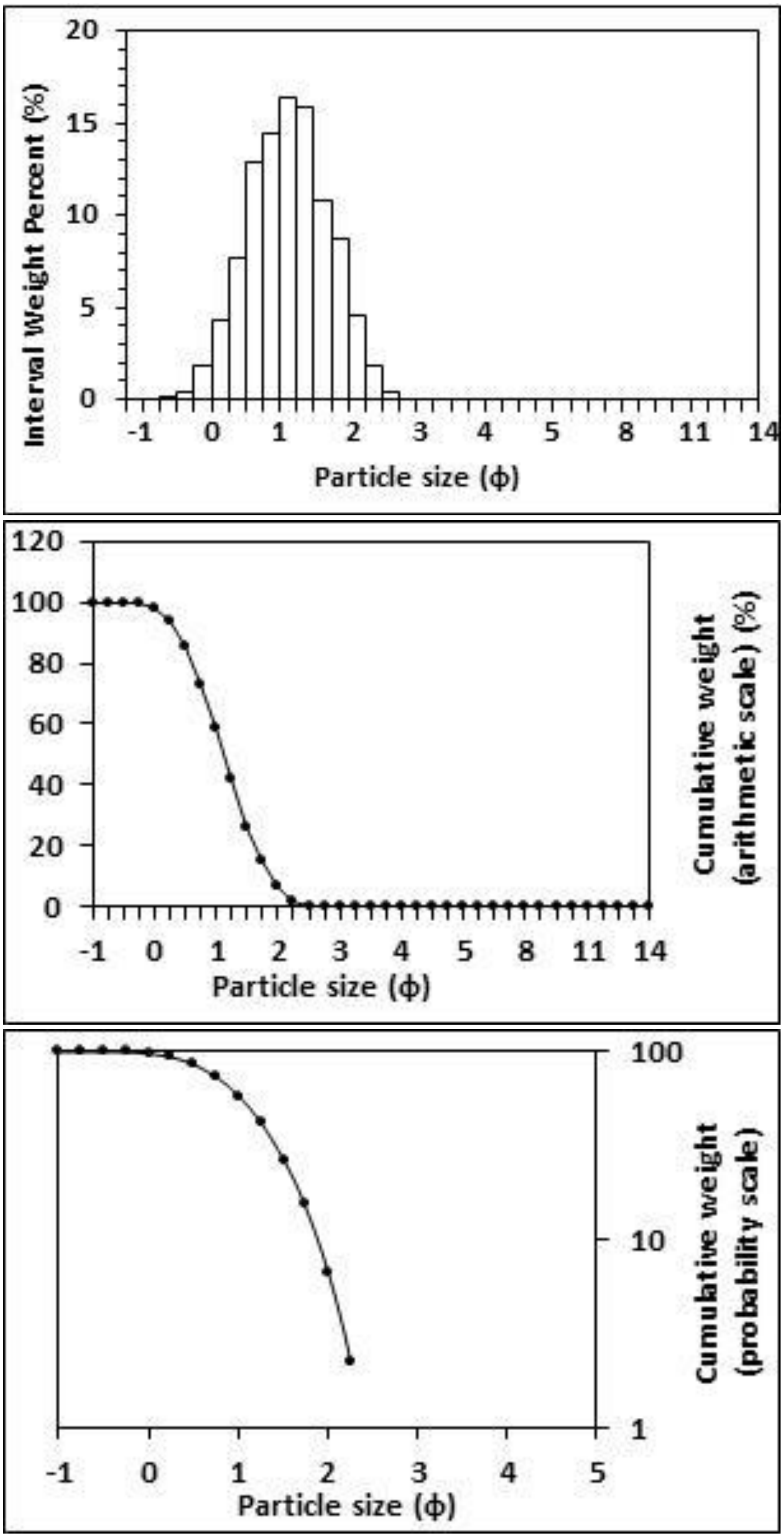

Figures II.277, II.278 and II.279: Histogram of grain size distribution and cumulative frequency graphs (arithmetic scale and probability scale) for sample 93: Mid intertidal zone, southern transect, Northern Ngarunui Beach. Sample collected on the 27th of September, 2014.

Table II.94: *Graphical and statistical parameters, textural description and size classes for sample 94: Mid intertidal zone, mid transect, Northern Ngarunui Beach. Sample collected on the 27th of September, 2014.*

Textural description	**Textural size classes**
Moderately well sorted, Near symmetrical skewed, Mesokurtic	Sand = 100 000%Fines = 0.000% Silt = 0.000%Clay = 0.000%
Moment method parameters (µm)	**Graphical method parameters. After Folk (1980) (ϕ)**
Mean = 355.784 Standard deviation (sd) = 140.735 Skewness (SkI) = 0.880 Kurtosis (KG) = 3.598	Mean (Mz) = 1.607 d(0.5) = 1.604 Sorting (SI) = 0.581 Skewness (SkI) = 0.004 Kurtosis (KG) = 0.955 Mean (mm) = 0.328 Mean (µm) = 328.380
Wentworth size class Medium sand	

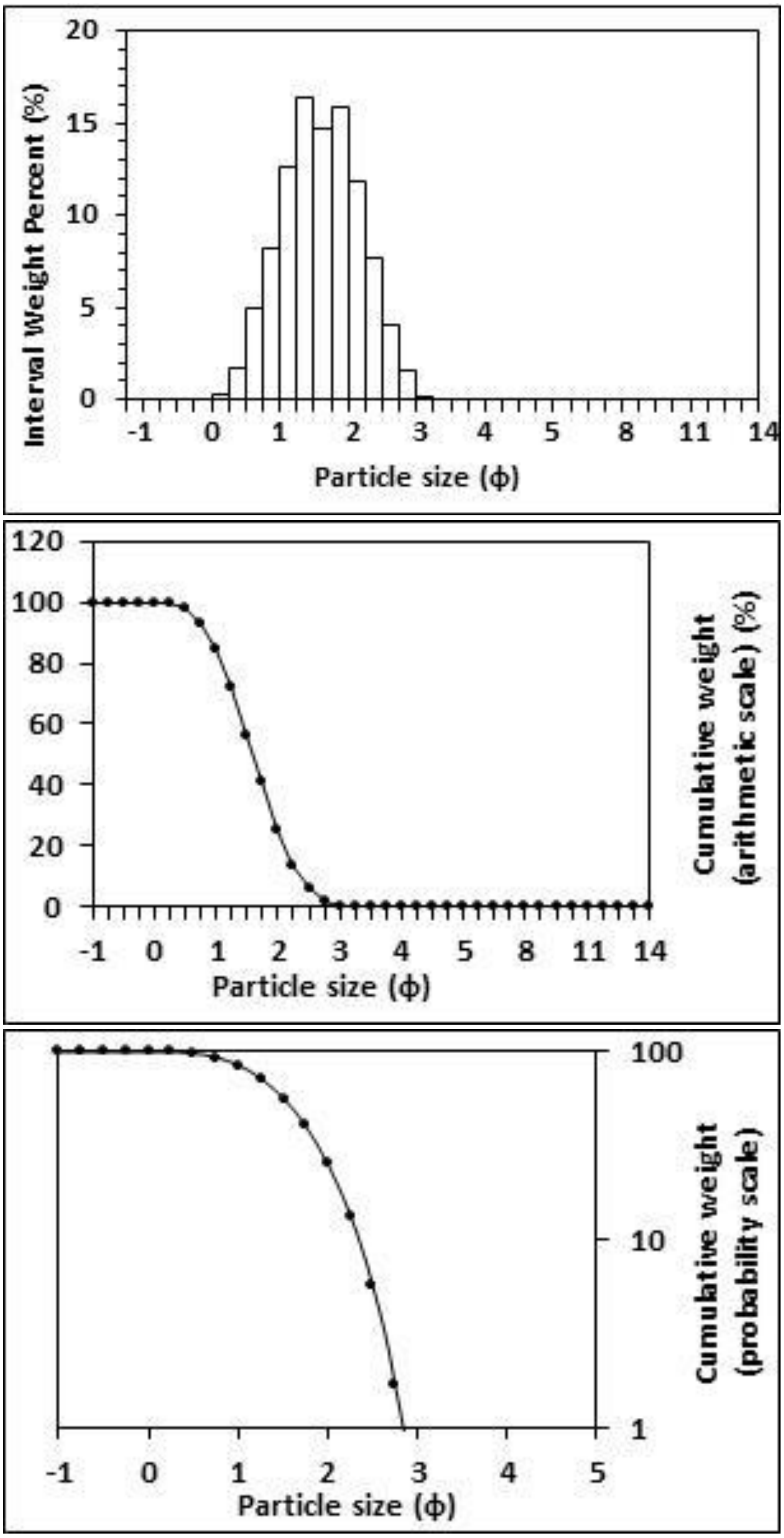

Figures II.280, II.281 and II.282: Histogram of grain size distribution and cumulative frequency graphs (arithmetic scale and probability scale) for sample 94: Mid intertidal zone, mid transect, Northern Ngarunui Beach. Sample collected on the 27th of September, 2014.

Table II.95: *Graphical and statistical parameters, textural description and size classes for sample 95: High intertidal zone, northern transect, Northern Ngarunui Beach. Sample collected on the 27th of September, 2014.*

Textural description	**Textural size classes**
Moderately well sorted, Near symmetrical skewed, Mesokurtic	Sand = 100 000%Fines = 0.000% Silt = 0.000%Clay = 0.000%
Moment method parameters (µm)	**Graphical method parameters. After Folk (1980) (ϕ)**
Mean = 215.094 Standard deviation (sd) = 83.135 Skewness (SkI) = 0.906 Kurtosis (KG) = 3.706	Mean (Mz) = 2.329 d(0.5) = 2.328 Sorting (SI) = 0.564 Skewness (SkI) = -0.005 Kurtosis (KG) = 0.950 Mean (mm) = 0.199 Mean (µm) = 198.971
Wentworth size class Fine sand	

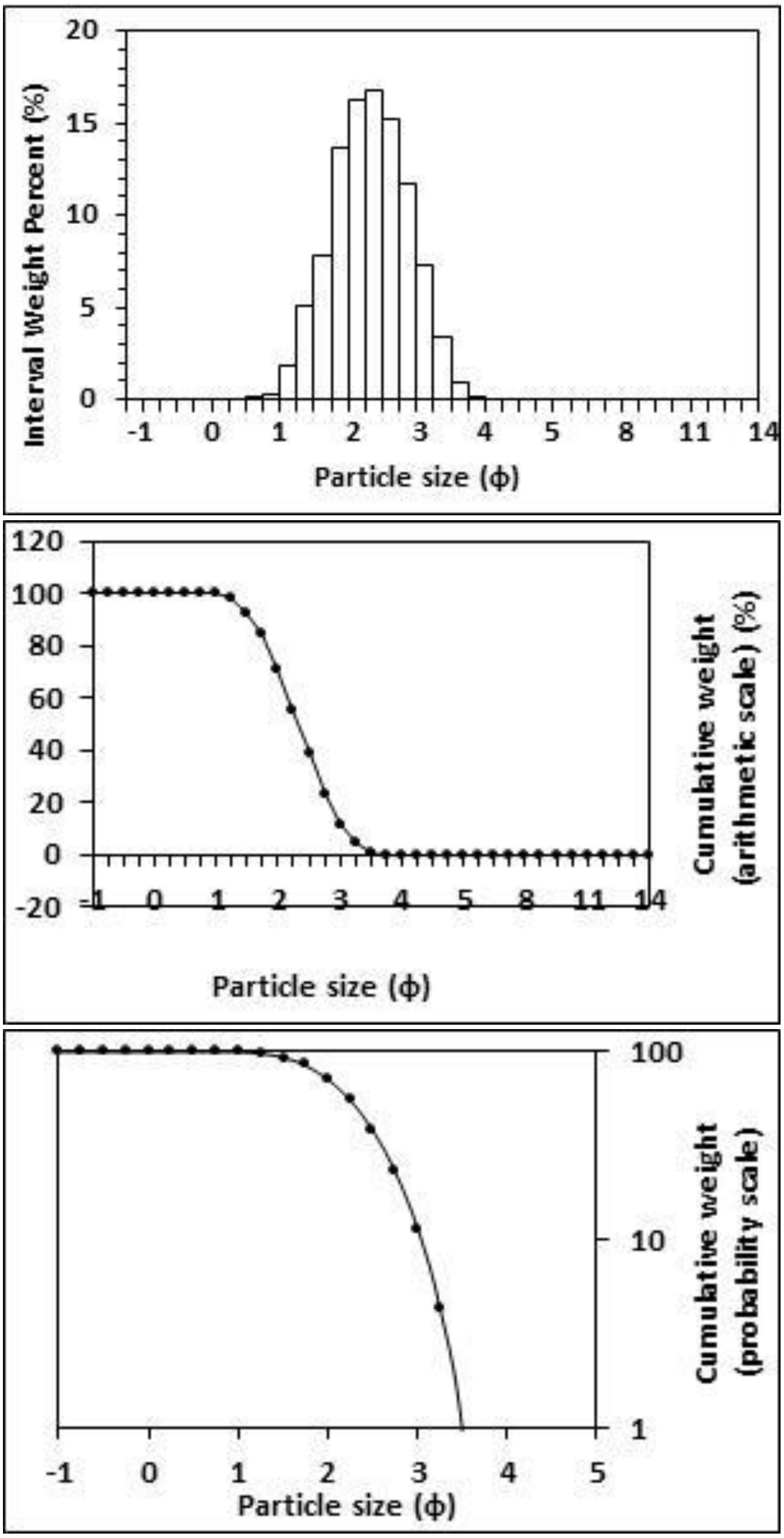

Figures II.283, II.284 and II.285: Histogram of grain size distribution and cumulative frequency graphs (arithmetic scale and probability scale) for sample 95: High intertidal zone, northern transect, Northern Ngarunui Beach. Sample collected on the 27th of September, 2014.

Table II.96: *Graphical and statistical parameters, textural description and size classes for sample 96: Low intertidal zone, northern transect, Northern Ngarunui Beach. Sample collected on the 27th of September, 2014.*

Textural description	**Textural size classes**
Moderately well sorted, Near symmetrical skewed, Mesokurtic	Sand = 100 000%Fines = 0.000% Silt = 0.000%Clay = 0.000%
Moment method parameters (µm)	**Graphical method parameters. After Folk (1980) (ϕ)**
Mean = 367.035 Standard deviation (sd) = 130.886 Skewness (SkI) = 0.832 Kurtosis (KG) = 3.559	Mean (Mz) = 1.543 d(0.5) = 1.540 Sorting (SI) = 0.523 Skewness (SkI) = 0.006 Kurtosis (KG) = 0.955 Mean (mm) = 0.343 Mean (µm) = 343.178
Wentworth size class Medium sand	

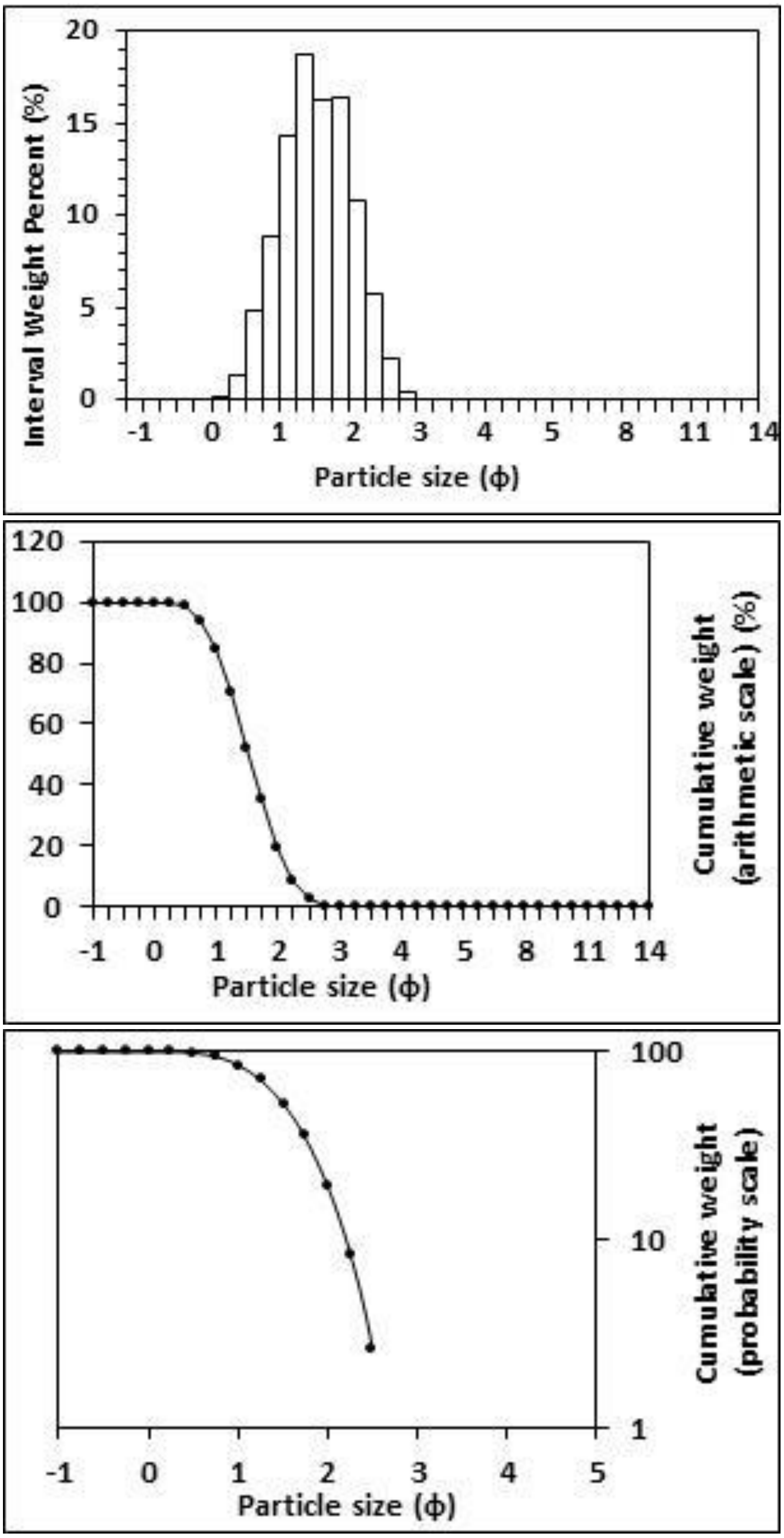

Figures II.286, II.287 and II.288: Histogram of grain size distribution and cumulative frequency graphs (arithmetic scale and probability scale) for sample 96: Low intertidal zone, northern transect, Northern Ngarunui Beach. Sample collected on the 27th of September, 2014.

Table II.97: *Graphical and statistical parameters, textural description and size classes for sample 97: High intertidal zone, mid transect, Northern Ngarunui Beach. Sample collected on the 27th of September, 2014.*

Textural description	**Textural size classes**
Moderately well sorted, Near symmetrical skewed, Mesokurtic	Sand = 99.993% Fines = 0.007% Silt = 0.007% Clay = 0.000%
Moment method parameters (µm) Mean = 222.209 Standard deviation (sd) = 94.206 Skewness (SkI) = 1.034 Kurtosis (KG) = 4.175 **Wentworth size class** Fine sand	**Graphical method parameters. After Folk (1980) (ϕ)** Mean (Mz) = 2.300 d(0.5) = 2.300 Sorting (SI) = 0.613 Skewness (SkI) = -0.002 Kurtosis (KG) = 0.951 Mean (mm) = 0.203 Mean (µm) = 203.011

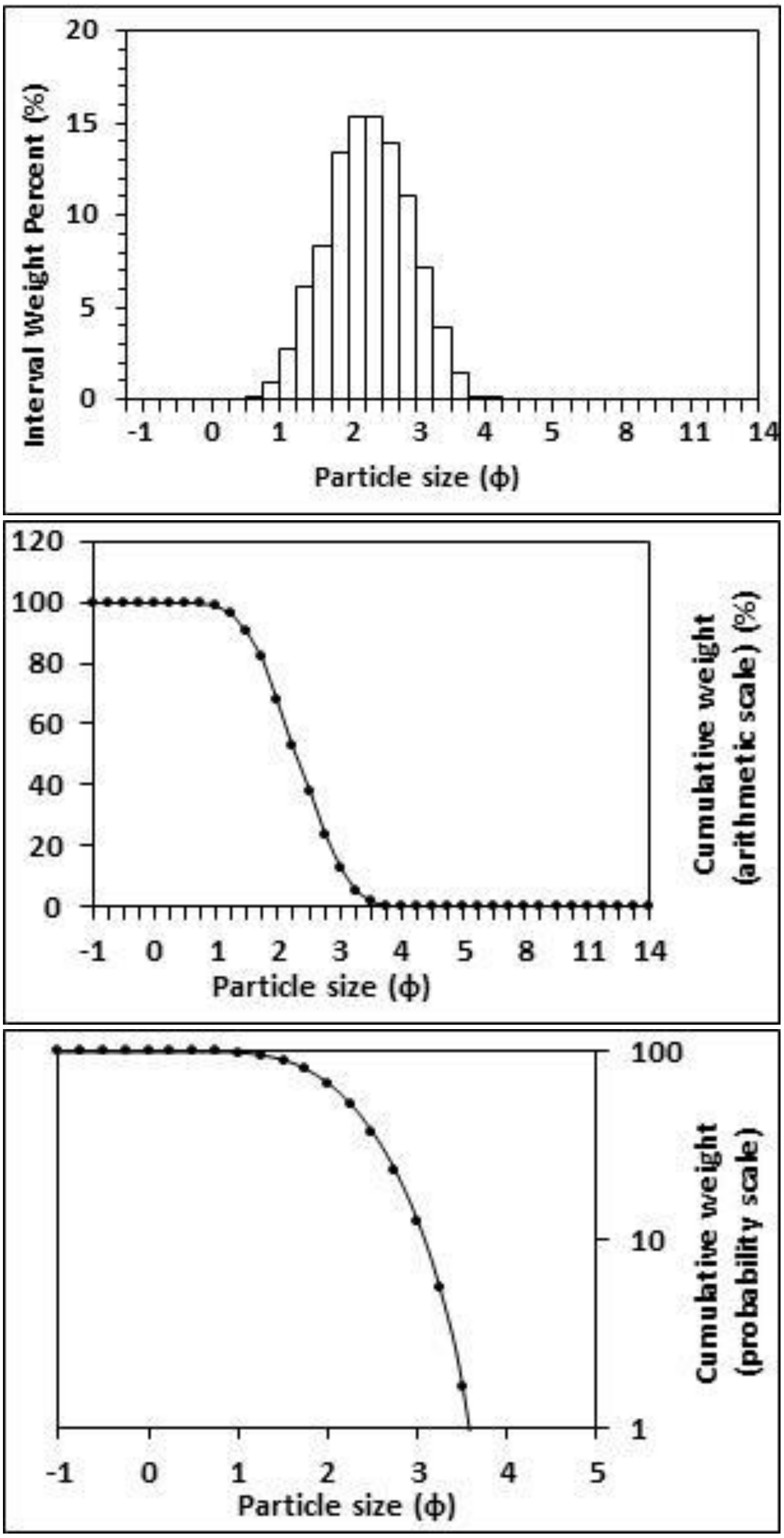

Figures II.289, II.290 and II.291: Histogram of grain size distribution and cumulative frequency graphs (arithmetic scale and probability scale) for sample 97: High intertidal zone, mid transect, Northern Ngarunui Beach. Sample collected on the 27th of September, 2014.

Table II.98: *Graphical and statistical parameters, textural description and size classes for sample 98: High intertidal zone, southern transect, Northern Ngarunui Beach. Sample collected on the 25th of October, 2014.*

Textural description	**Textural size classes**
Moderately well sorted, Near symmetrical skewed, Mesokurtic	Sand = 100 000%Fines = 0.000% Silt = 0.000%Clay = 0.000%
Moment method parameters (µm)	**Graphical method parameters. After Folk (1980) (ϕ)**
Mean = 239.145 Standard deviation (sd) = 98.706 Skewness (SkI) = 0.990 Kurtosis (KG) = 3.998	Mean (Mz) = 2.187 d(0.5) = 2.187 Sorting (SI) = 0.598 Skewness (SkI) = 0.002 Kurtosis (KG) = 0.953 Mean (mm) = 0.220 Mean (µm) = 219.601
Wentworth size class Fine sand	

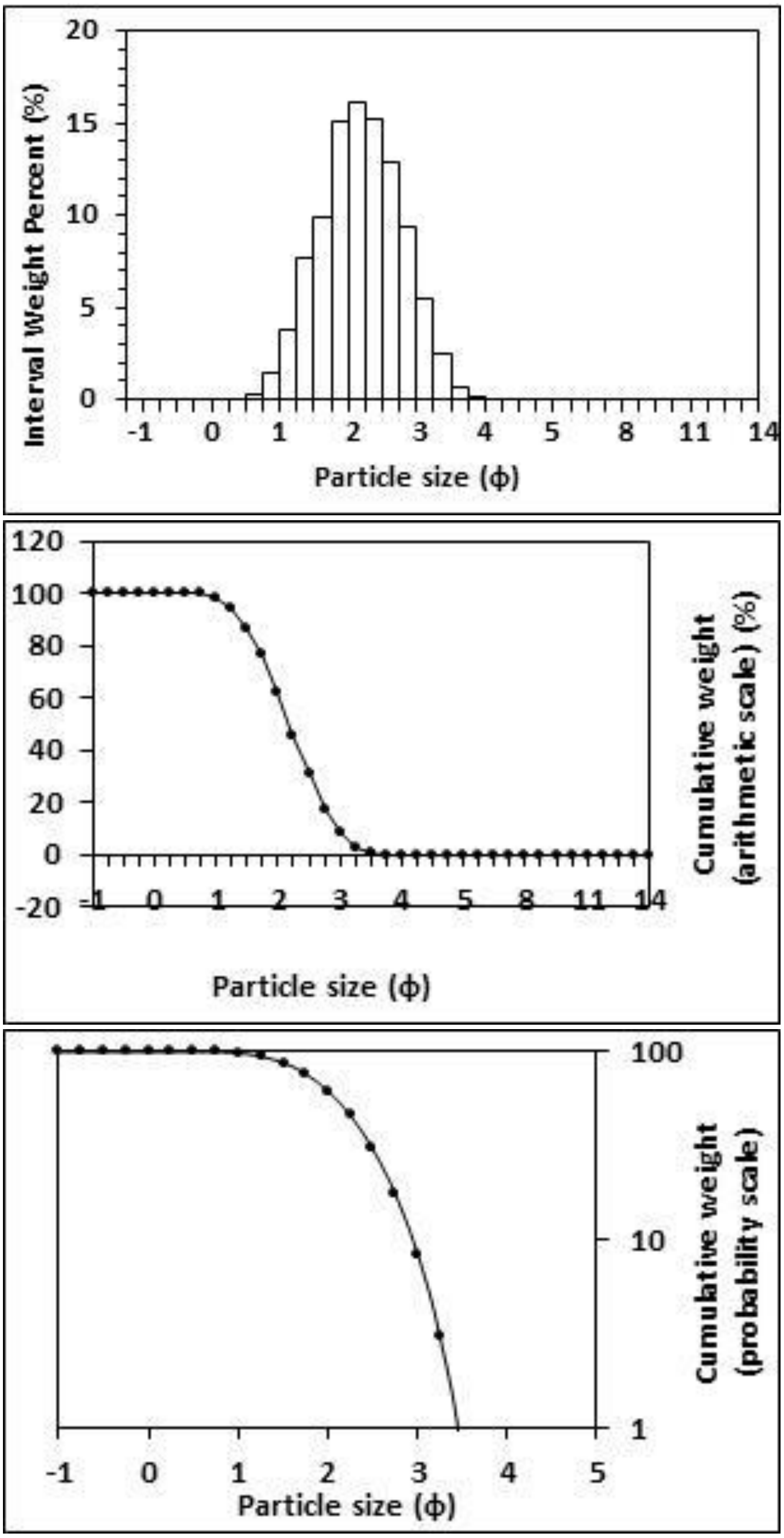

Figures II.292, II.293and II. 294: Histogram of grain size distribution and cumulative frequency graphs (arithmetic scale and probability scale) for sample 98: High intertidal zone, southern transect, Northern Ngarunui Beach. Sample collected on the 25th of October, 2014.

Table II.99: *Graphical and statistical parameters, textural description and size classes for sample 99: Low intertidal zone, mid transect, Northern Ngarunui Beach. Sample collected on the 25th of October, 2014.*

Textural description	**Textural size classes**
Moderately well sorted, Near symmetrical skewed, Mesokurtic	Sand = 100 000%Fines = 0.000% Silt = 0.000%Clay = 0.000%
Moment method parameters (µm) Mean = 570.741 Standard deviation (sd) = 222.195 Skewness (SkI) = 0.856 Kurtosis (KG) = 3.556	**Graphical method parameters. After Folk (1980) (ϕ)** Mean (Mz) = 0.917 d(0.5) = 0.916 Sorting (SI) = 0.572 Skewness (SkI) = 0.014 Kurtosis (KG) = 0.950 Mean (mm) = 0.530 Mean (µm) = 529.605
Wentworth size class Coarse sand	

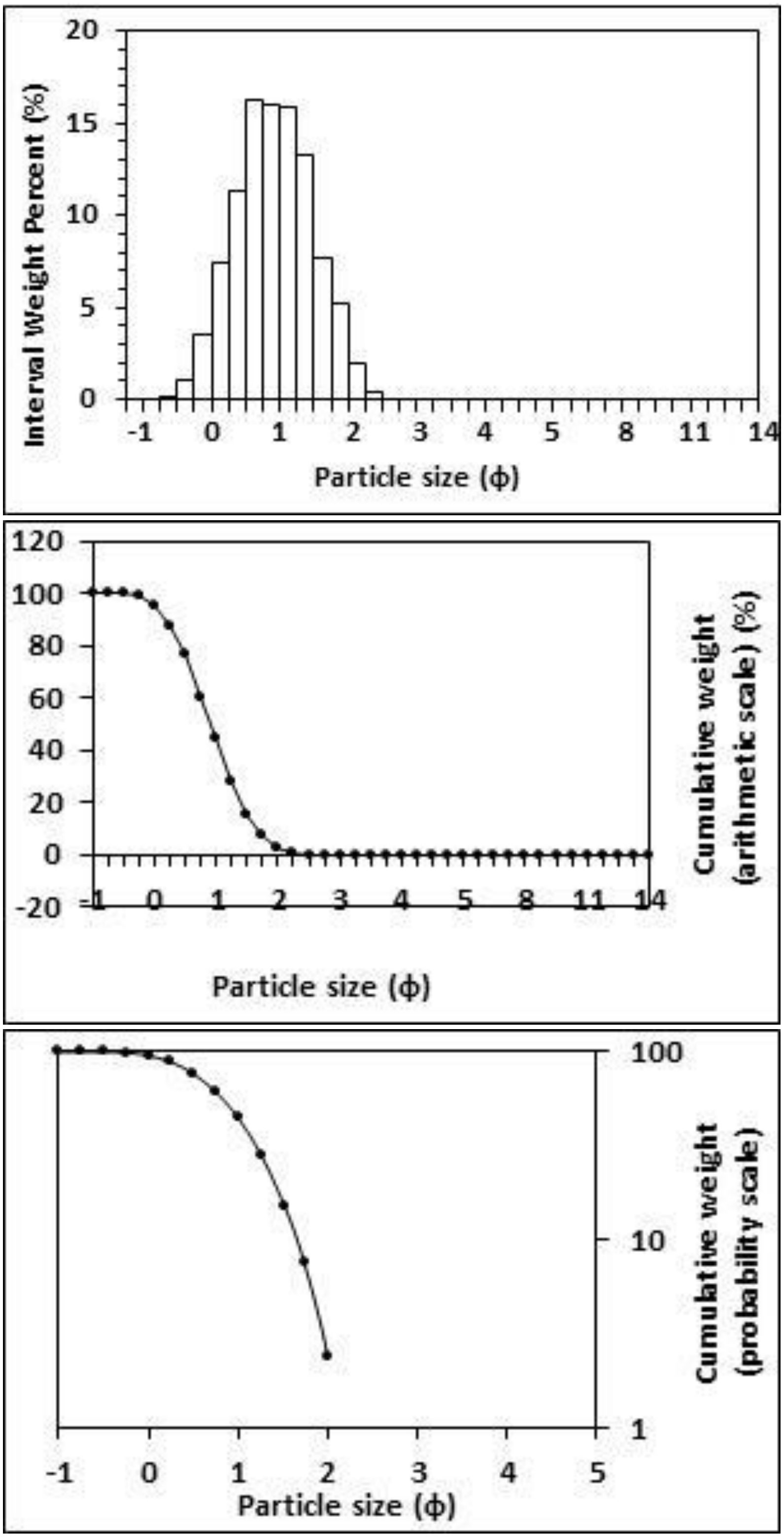

Figures II.295, II.296 and II.297: Histogram of grain size distribution and cumulative frequency graphs (arithmetic scale and probability scale) for sample 99: Low intertidal zone, mid transect, Northern Ngarunui Beach. Sample collected on the 25th of October, 2014.

Table II.100: *Graphical and statistical parameters, textural description and size classes for sample 100: Mid intertidal zone, mid transect, Northern Ngarunui Beach. Sample collected on the 25th of October, 2014.*

Textural description	**Textural size classes**
Moderately well sorted, Near symmetrical skewed, Mesokurtic	Sand = 100 000%Fines = 0.000% Silt = 0.000%Clay = 0.000%
Moment method parameters (µm) Mean = 334.173 Standard deviation (sd) = 116.492 Skewness (SkI) = 0.807 Kurtosis (KG) = 3.487 **Wentworth size class** Medium sand	**Graphical method parameters. After Folk (1980) (ϕ)** Mean (Mz) = 1.670 d(0.5) = 1.670 Sorting (SI) = 0.511 Skewness (SkI) = -0.004 Kurtosis (KG) = 0.952 Mean (mm) = 0.314 Mean (µm) = 314.259

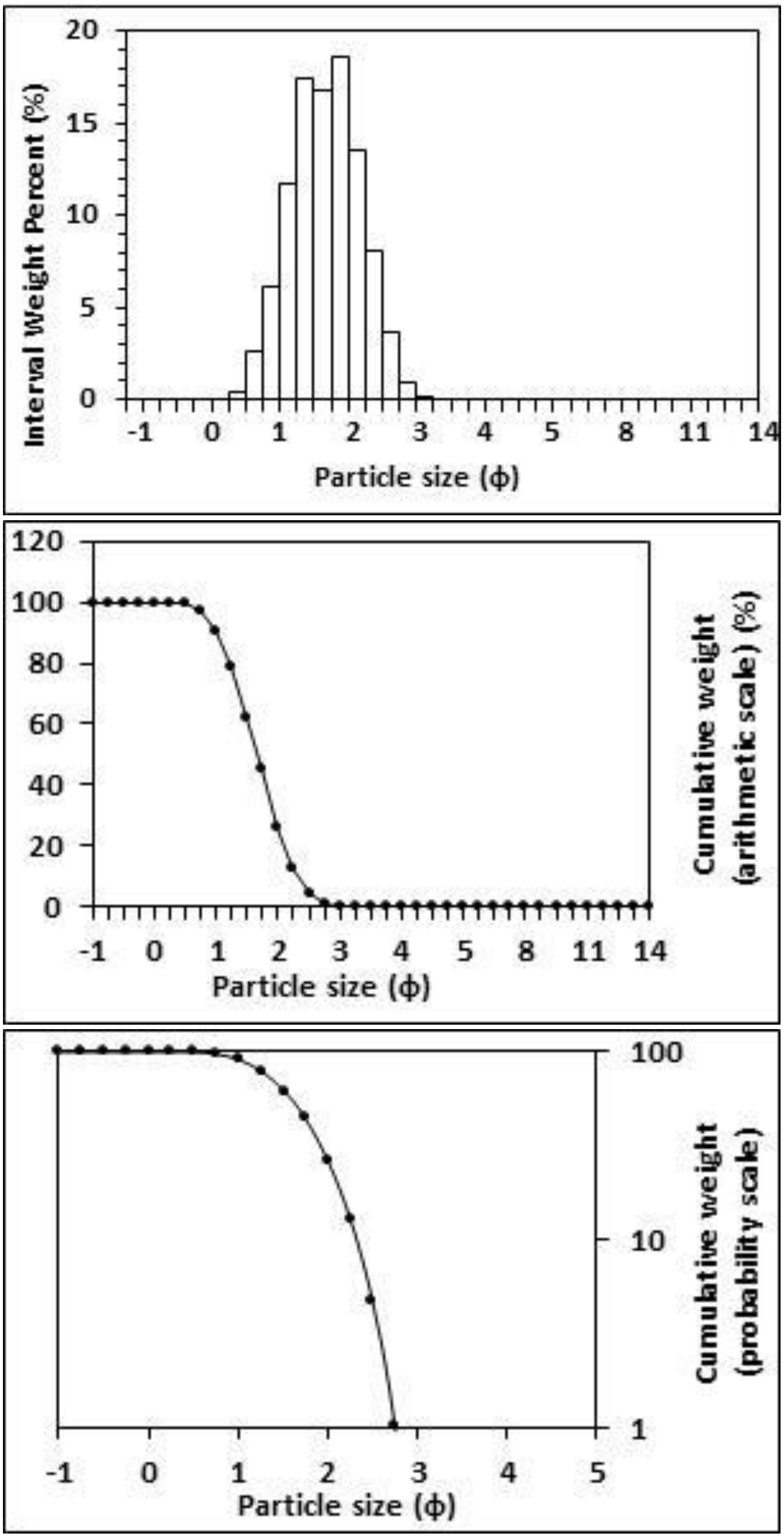

Figures II.298, II.299and II.300: Histogram of grain size distribution and cumulative frequency graphs (arithmetic scale and probability scale) for sample 100: Mid intertidal zone, mid transect, Northern Ngarunui Beach. Sample collected on the 25th of October, 2014.

Table II.101: *Graphical and statistical parameters, textural description and size classes for sample 101: Low intertidal zone, northern transect, Northern Ngarunui Beach. Sample collected on the 25th of October, 2014.*

Textural description	**Textural size classes**
Moderately well sorted, Near symmetrical skewed, Mesokurtic	Sand = 100 000%Fines = 0.000% Silt = 0.000%Clay = 0.000%
Moment method parameters (µm)	**Graphical method parameters. After Folk (1980) (ϕ)**
Mean = 327.524 Standard deviation (sd) = 113.430 Skewness (SkI) = 0.799 Kurtosis (KG) = 3.470	Mean (Mz) = 1.698 d(0.5) = 1.698 Sorting (SI) = 0.508 Skewness (SkI) = -0.004 Kurtosis (KG) = 0.947 Mean (mm) = 0.308 Mean (µm) = 308.310
Wentworth size class Medium sand	

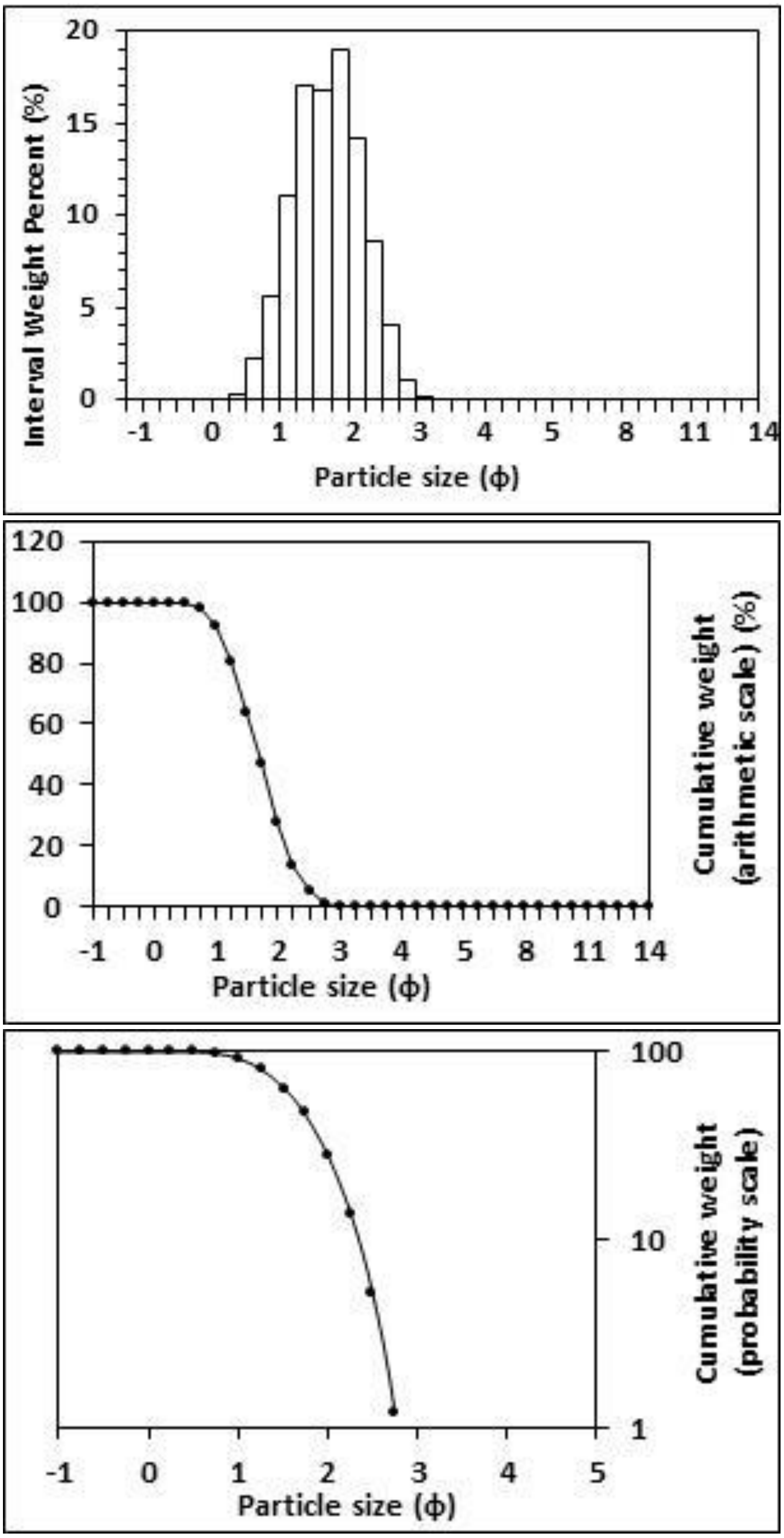

Figures II.301, II.302 and II.303: Histogram of grain size distribution and cumulative frequency graphs (arithmetic scale and probability scale) for sample 101: Low intertidal zone, northern transect, Northern Ngarunui Beach. Sample collected on the 25th of October, 2014.

Table II.102: *Graphical and statistical parameters, textural description and size classes for sample 102: High intertidal zone, northern transect, Northern Ngarunui Beach. Sample collected on the 25th of October, 2014.*

Textural description	**Textural size classes**
Moderately well sorted, Near symmetrical skewed, Mesokurtic	Sand = 100 000%Fines = 0.000% Silt = 0.000%Clay = 0.000%
Moment method parameters (µm) Mean = 256.834 Standard deviation (sd) = 91.234 Skewness (SkI) = 0.876 Kurtosis (KG) = 3.725	**Graphical method parameters. After Folk (1980) (ϕ)** Mean (Mz) = 2.058 d(0.5) = 2.057 Sorting (SI) = 0.517 Skewness (SkI) = 0.002 Kurtosis (KG) = 0.959 Mean (mm) = 0.240 Mean (µm) = 240.165
Wentworth size class Fine sand	

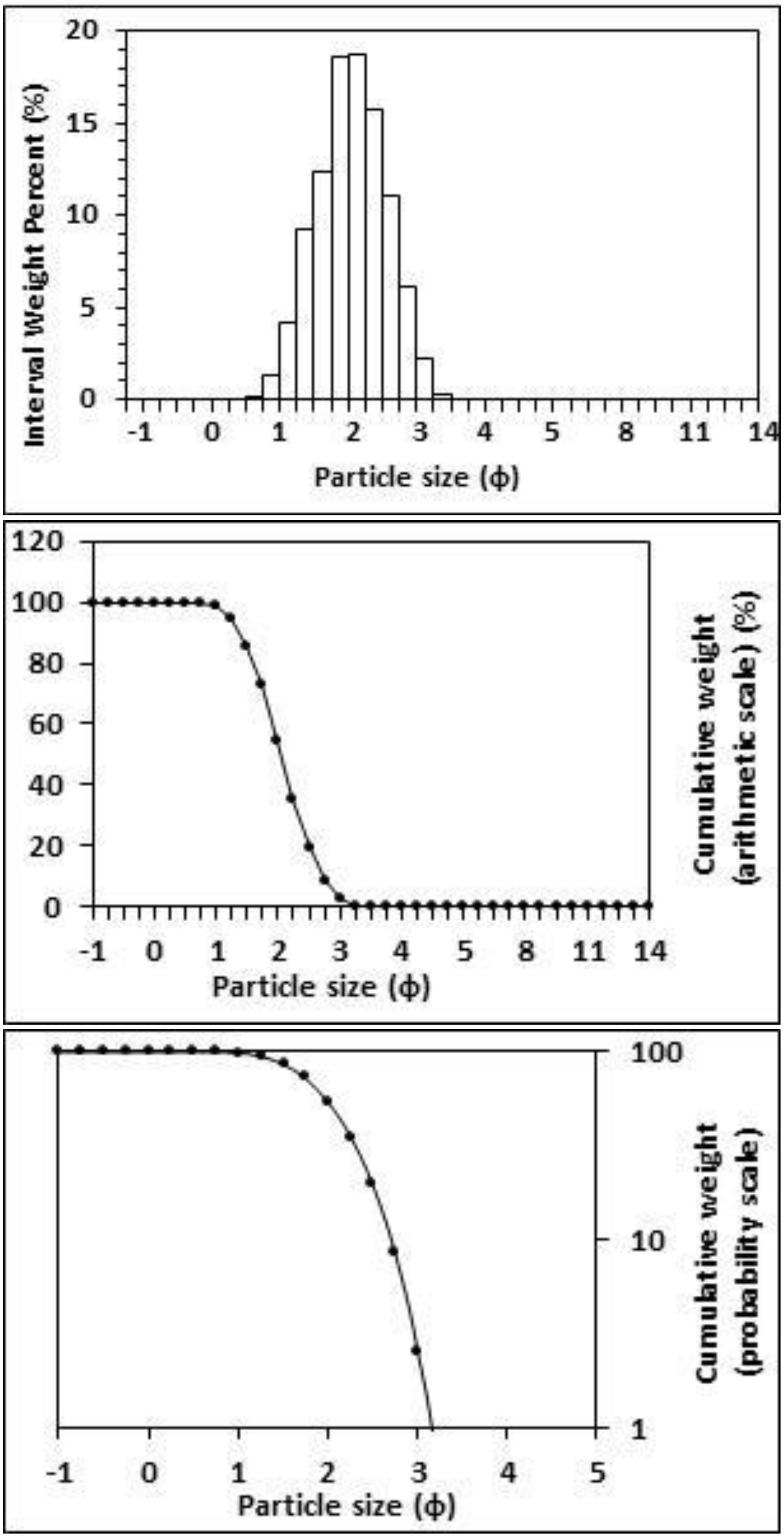

Figures II.304, II.305 and II.306: Histogram of grain size distribution and cumulative frequency graphs (arithmetic scale and probability scale) for sample 102: High intertidal zone, northern transect, Northern Ngarunui Beach. Sample collected on the 25th of October, 2014.

Table II.103: *Graphical and statistical parameters, textural description and size classes for sample 103: Mid intertidal zone, northern transect, Northern Ngarunui Beach. Sample collected on the 25th of October, 2014.*

Textural description	**Textural size classes**
Moderately well sorted, Near symmetrical skewed, Mesokurtic	Sand = 100 000%Fines = 0.000% Silt = 0.000%Clay = 0.000%
Moment method parameters (µm) Mean = 348.643 Standard deviation (sd) = 163.793 Skewness (SkI) = 1.225 Kurtosis (KG) = 4.709	**Graphical method parameters. After Folk (1980) (ϕ)** Mean (Mz) = 1.678 d(0.5) = 1.687 Sorting (SI) = 0.661 Skewness (SkI) = -0.032 Kurtosis (KG) = 0.958 Mean (mm) = 0.312 Mean (µm) = 312.416
Wentworth size class Medium sand	

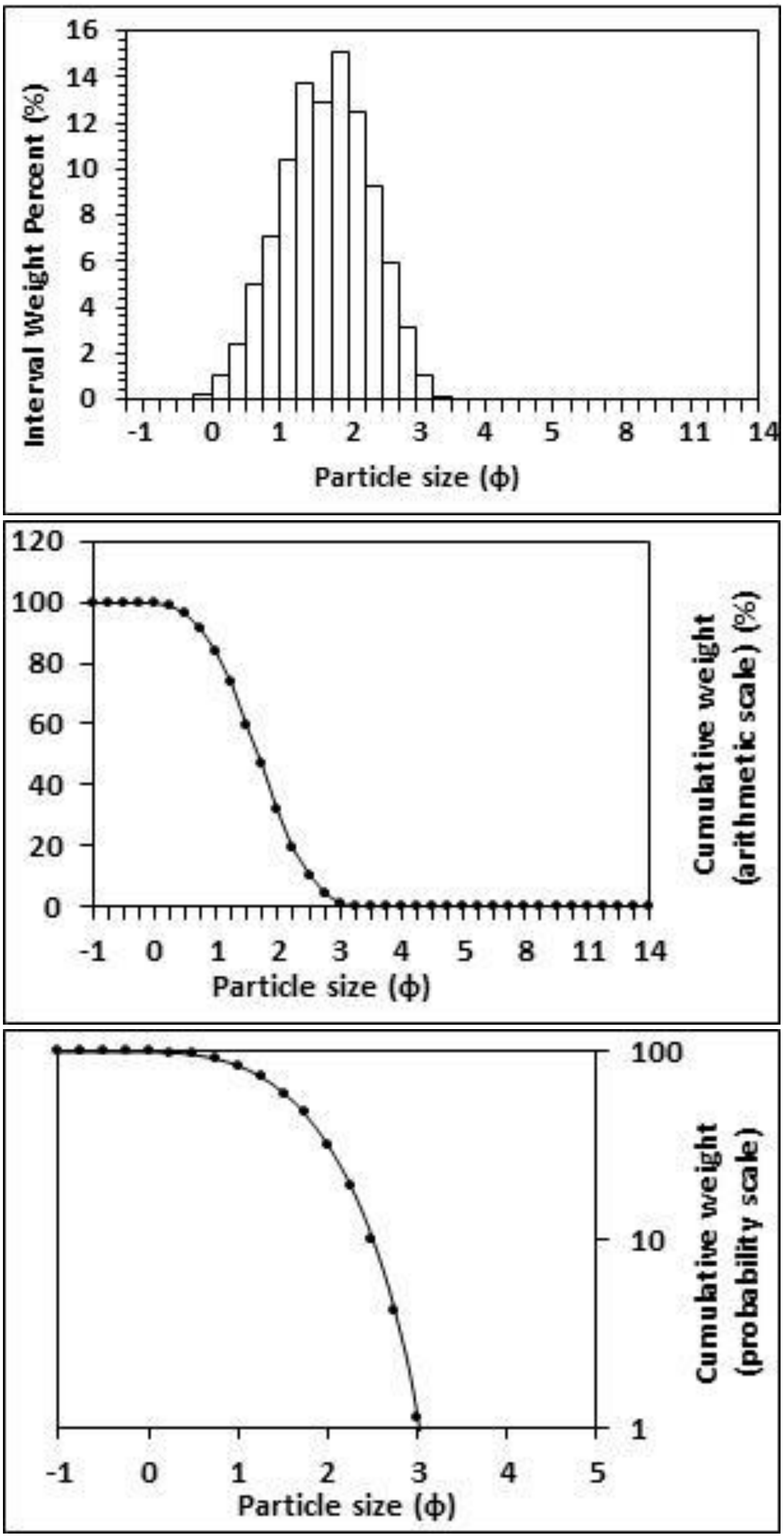

Figures II.307, II.308 and II.309: Histogram of grain size distribution and cumulative frequency graphs (arithmetic scale and probability scale) for sample 103: Mid intertidal zone, northern transect, Northern Ngarunui Beach. Sample collected on the 25th of October, 2014.

Table II.104: *Graphical and statistical parameters, textural description and size classes for sample 104: High intertidal zone, mid transect, Northern Ngarunui Beach. Sample collected on the 25th of October, 2014.*

Textural description	**Textural size classes**
Moderately well sorted, Near symmetrical skewed, Mesokurtic	Sand = 100 000%Fines = 0.000% Silt = 0.000%Clay = 0.000%
Moment method parameters (µm)	**Graphical method parameters. After Folk (1980) (ϕ)**
Mean = 250.800 Standard deviation (sd) = 116.626 Skewness (SkI) = 1.456 Kurtosis (KG) = 6.237	Mean (Mz) = 2.147 d(0.5) = 2.157 Sorting (SI) = 0.636 Skewness (SkI) = -0.034 Kurtosis (KG) = 0.974 Mean (mm) = 0.226 Mean (µm) = 225.727
Wentworth size class Fine sand	

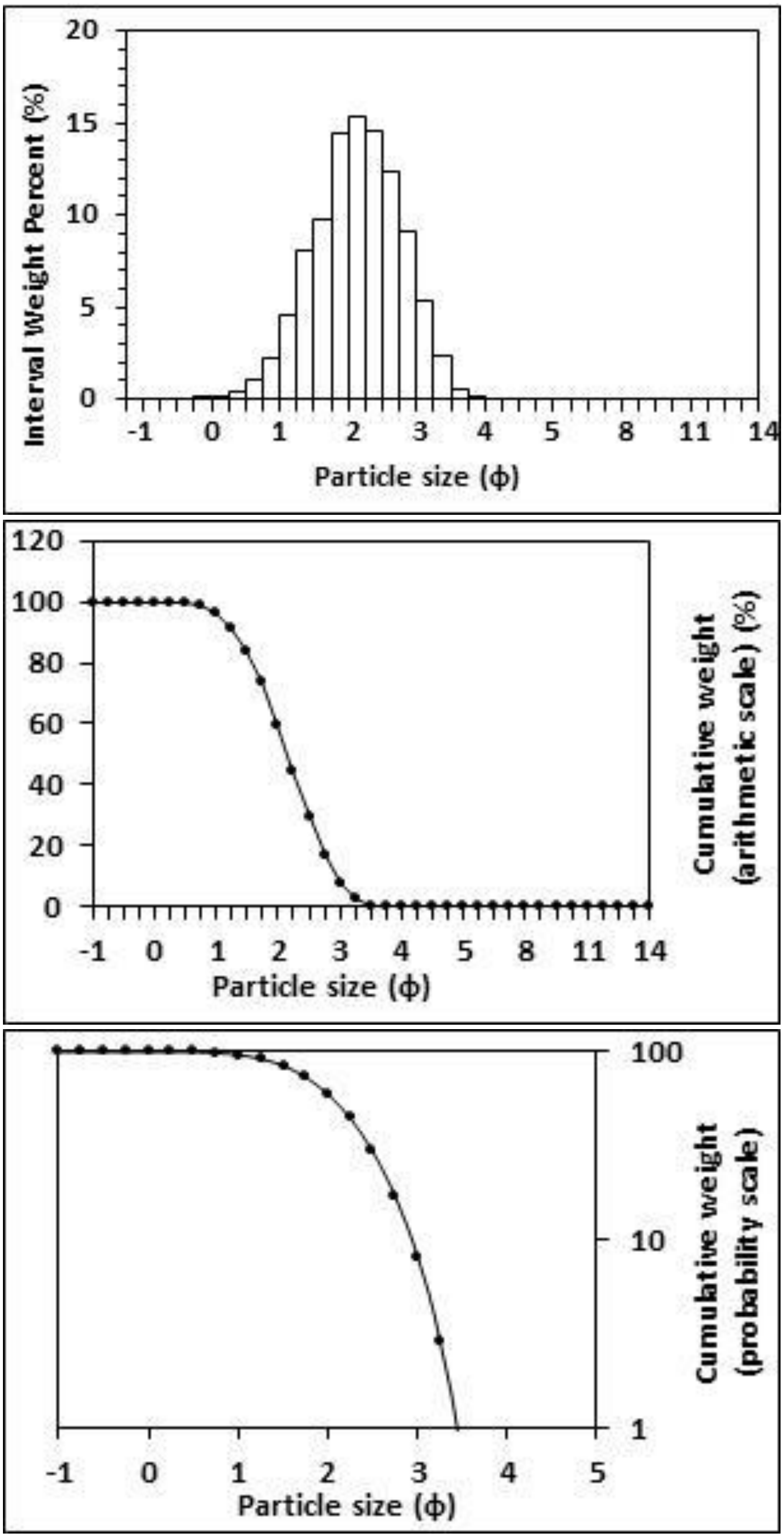

Figures II.310, II.311 and II.312: Histogram of grain size distribution and cumulative frequency graphs (arithmetic scale and probability scale) for sample 104: High intertidal zone, mid transect, Northern Ngarunui Beach. Sample collected on the 25th of October, 2014.

Table II.105: *Graphical and statistical parameters, textural description and size classes for sample 105: Mid intertidal zone, southern transect, Northern Ngarunui Beach. Sample collected on the 25th of October, 2014.*

Textural description	**Textural size classes**
Moderately well sorted, Near symmetrical skewed, Mesokurtic	Sand = 100 000%Fines = 0.000% Silt = 0.000%Clay = 0.000%
Moment method parameters (µm) Mean = 303.558 Standard deviation (sd) = 110.105 Skewness (SkI) = 0.882 Kurtosis (KG) = 3.719	**Graphical method parameters. After Folk (1980) (ϕ)** Mean (Mz) = 1.820 d(0.5) = 1.819 Sorting (SI) = 0.528 Skewness (SkI) = 0.001 Kurtosis (KG) = 0.954 Mean (mm) = 0.283 Mean (µm) = 283.315
Wentworth size class Medium sand	

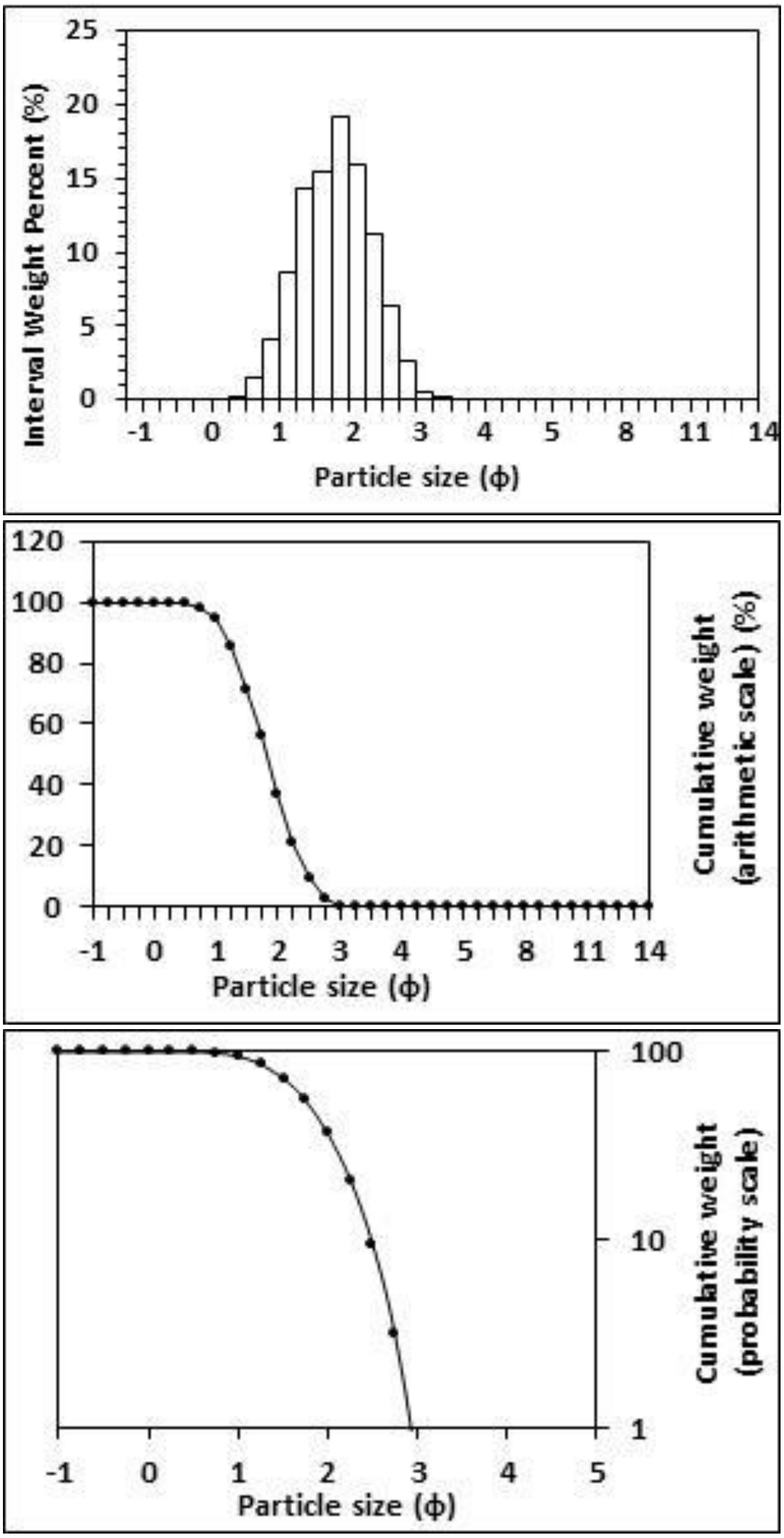

Figures II.313, II.314 and II.315: Histogram of grain size distribution and cumulative frequency graphs (arithmetic scale and probability scale) for sample 105: Mid intertidal zone, southern transect, Northern Ngarunui Beach. Sample collected on the 25th of October, 2014.

Table II.106: *Graphical and statistical parameters, textural description and size classes for sample 106: Mid intertidal zone, mid transect, Northern Ngarunui Beach. Sample collected on the 25th of October, 2014.*

<table>
<tr><td>Textural description
Moderately well sorted,
Near symmetrical skewed,
Mesokurtic</td><td>Textural size classes
Sand = 100 000%Fines = 0.000%
Silt = 0.000%Clay = 0.000%</td></tr>
<tr><td>Moment method parameters
(µm)
Mean = 336.050
Standard deviation (sd) = 114.499
Skewness (SkI) = 0.771
Kurtosis (KG) = 3.385</td><td rowspan="2">Graphical method parameters.
After Folk (1980) (ϕ)
Mean (Mz) = 1.659
d(0.5) = 1.658
Sorting (SI) = 0.503
Skewness (SkI) = 0.001
Kurtosis (KG) = 0.958
Mean (mm) = 0.317
Mean (µm) = 316.698</td></tr>
<tr><td>Wentworth size class
Medium sand</td></tr>
</table>

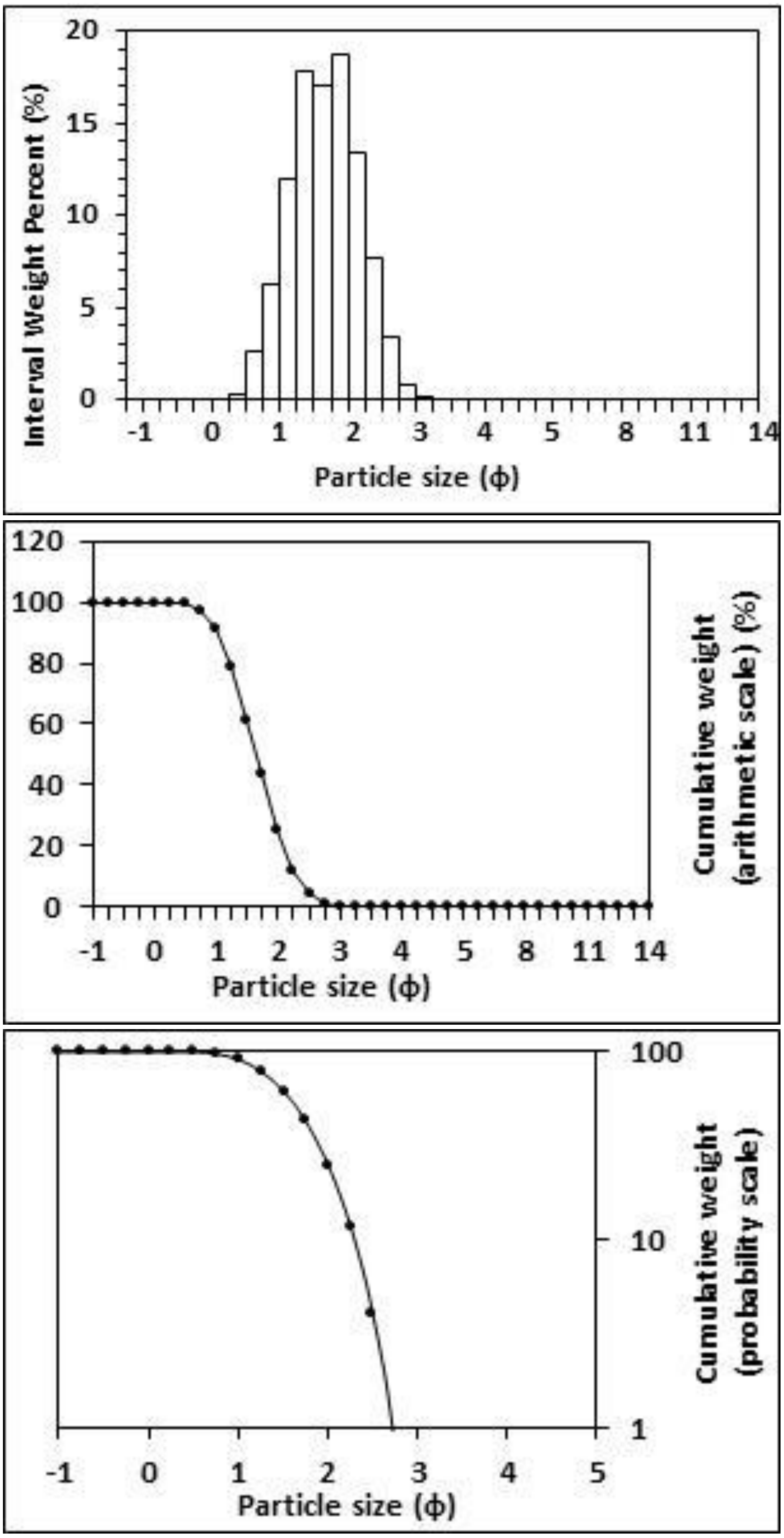

Figures II.316, II.317 and II.318: Histogram of grain size distribution and cumulative frequency graphs (arithmetic scale and probability scale) for sample 106: Mid intertidal zone, mid transect, Northern Ngarunui Beach. Sample collected on the 25th of October, 2014.

Table II.107: *Graphical and statistical parameters, textural description and size classes for sample 107: High intertidal zone, western transect, Moonlight Bay. Sample collected on the 22nd of September, 2014.*

Textural description	**Textural size classes**
Moderately well sorted, Near symmetrical skewed, Mesokurtic	Sand = 100 000%Fines = 0.000% Silt = 0.000%Clay = 0.000%
Moment method parameters (μm)	**Graphical method parameters. After Folk (1980) (ϕ)**
Mean = 503.167 Standard deviation (sd) = 225.675 Skewness (SkI) = 0.995 Kurtosis (KG) = 3.798 **Wentworth size class** Medium sand	Mean (Mz) = 1.137 d(0.5) = 1.139 Sorting (SI) = 0.655 Skewness (SkI) = -0.008 Kurtosis (KG) = 0.932 Mean (mm) = 0.455 Mean (μm) = 454.687

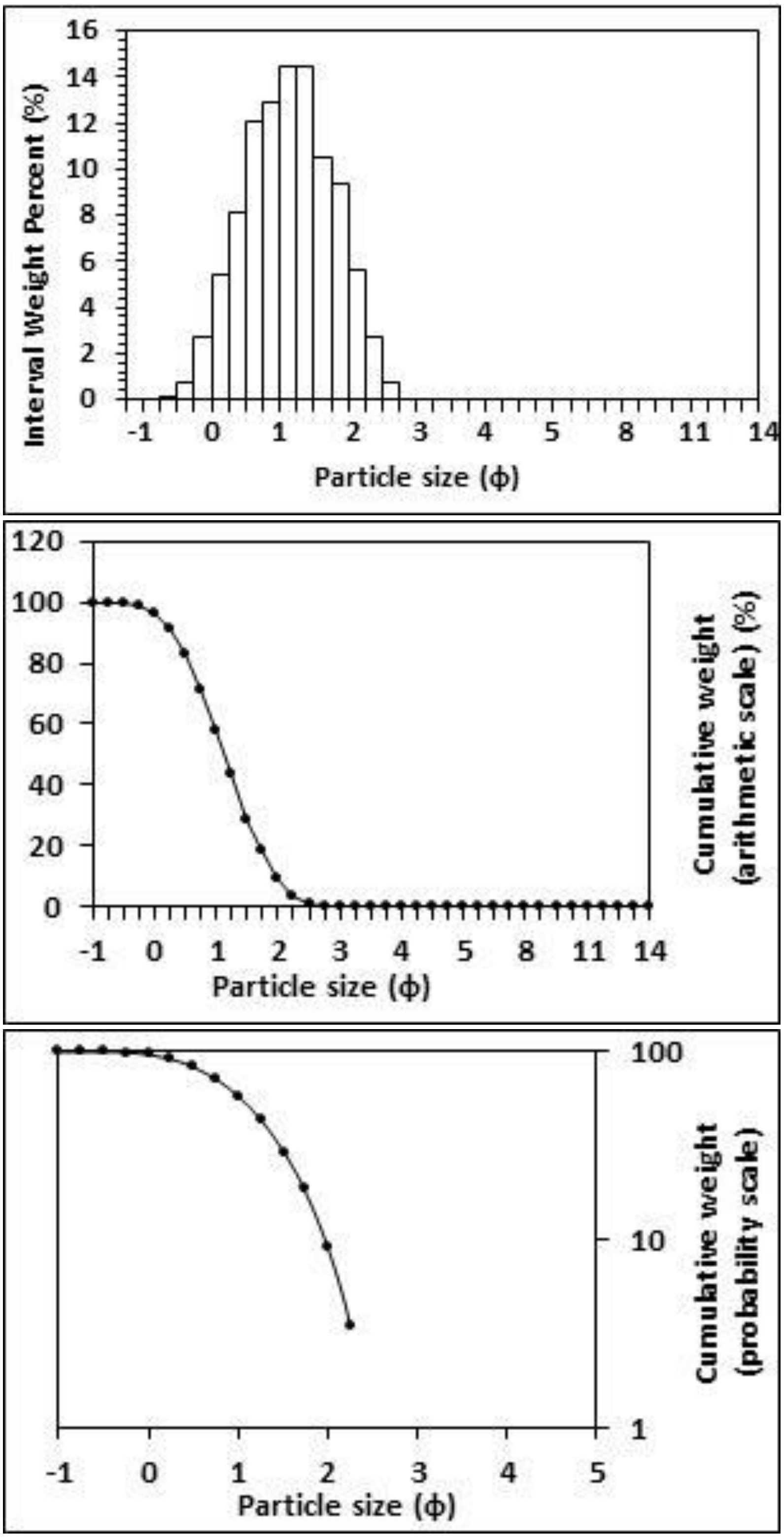

Figures II.319, II.320 and II.321: Histogram of grain size distribution and cumulative frequency graphs (arithmetic scale and probability scale) for sample 107: High intertidal zone, western transect, Moonlight Bay. Sample collected on the 22nd of September, 2014.

Table II.108: *Graphical and statistical parameters, textural description and size classes for sample 108: High intertidal zone, eastern transect, Moonlight Bay. Sample collected on the 22nd of September, 2014.*

Textural description	**Textural size classes**
Moderately sorted, Fine skewed, Mesokurtic	Sand = 96.297% Fines = 3.703% Silt = 3.284% Clay = 0.419%
Moment method parameters (µm) Mean = 662.166 Standard deviation (sd) = 392.058 Skewness (SkI) = 0.800 Kurtosis (KG) = 3.305	**Graphical method parameters. After Folk (1980) (ϕ)** Mean (Mz) = 0.823 d(0.5) = 0.774 Sorting (SI) = 0.934 Skewness (SkI) = 0.124 Kurtosis (KG) = 0.994 Mean (mm) = 0.565 Mean (µm) = 565.383
Wentworth size class Coarse sand	

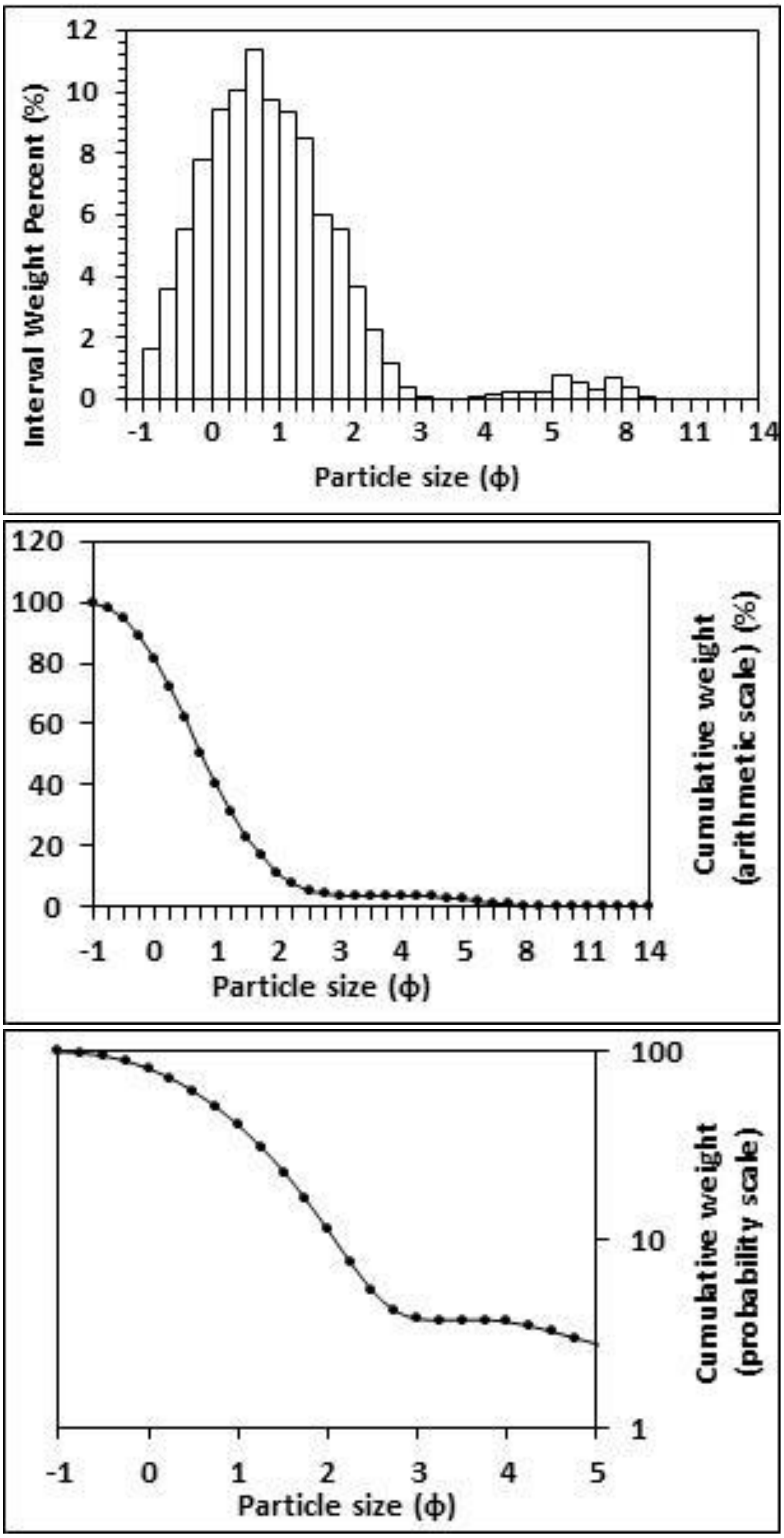

Figures II.322, II.323 and II.324: Histogram of grain size distribution and cumulative frequency graphs (arithmetic scale and probability scale) for sample 108: High intertidal zone, eastern transect, Moonlight Bay. Sample collected on the 22nd of September, 2014.

Table II.109: *Graphical and statistical parameters, textural description and size classes for sample 109: Mid intertidal zone, western transect, Moonlight Bay. Sample collected on the 22nd of September, 2014.*

Textural description	**Textural size classes**
Poorly sorted, Strongly fine skewed, Very leptokurtic	Sand = 85.199% Fines = 14.801% Silt = 10.916% Clay = 3.885%
Moments method parameters (µm) Mean = 254.528 Standard deviation (sd) = 171.603 Skewness (SkI) = 1.876 Kurtosis (KG) = 13.533 **Wentworth size class** Fine sand	**Graphical method parameters. After Folk (1980) (ϕ)** Mean (Mz) = 2.166 d (0.5) = 2.057 Sorting (σI) = 1.438 Skewness (SkI) = 0.430 Kurtosis (KG) = 2.726 Mean (mm) = 0.223 Mean (µm) = 222.820

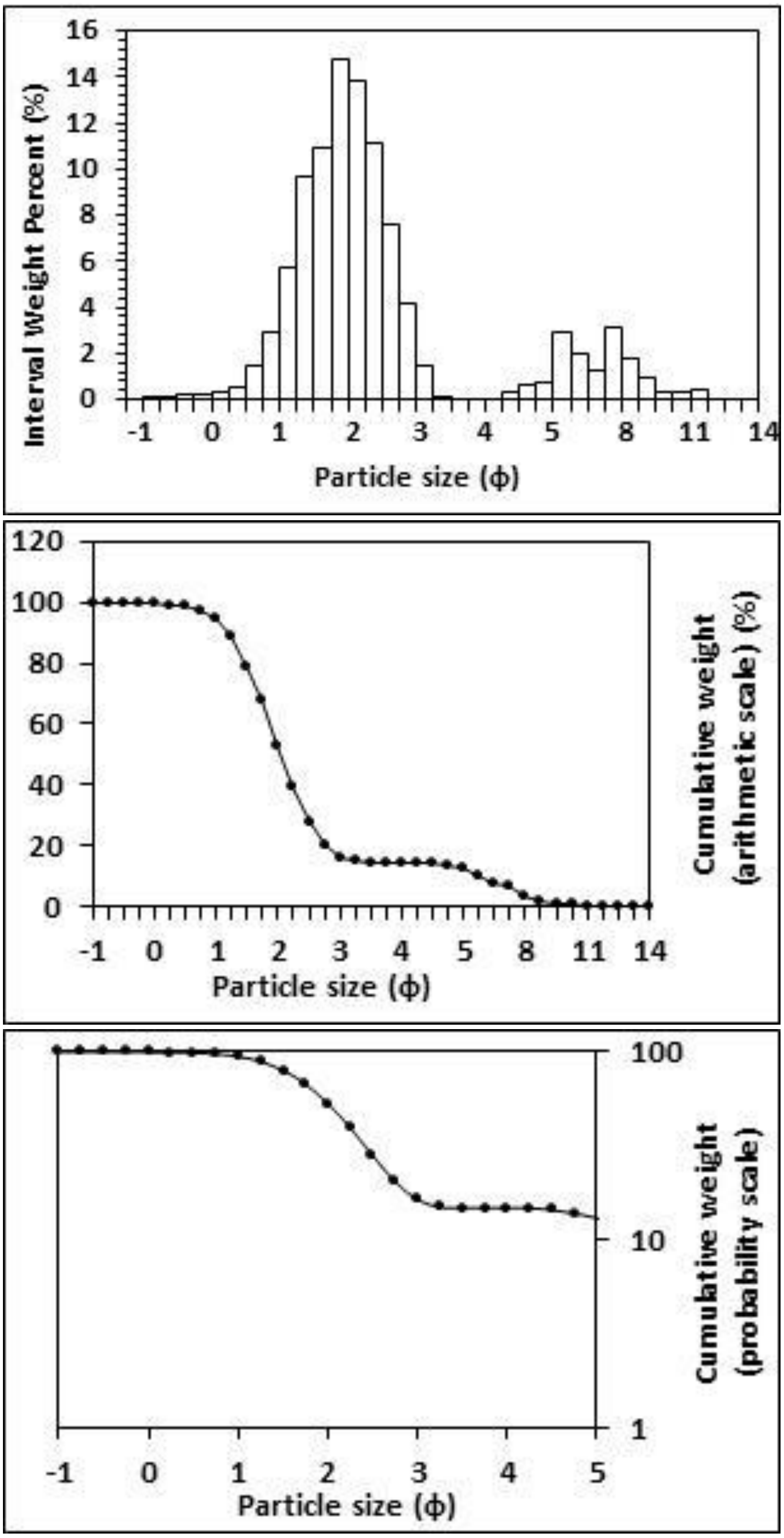

Figures II.325, II.326 and II.327: Histogram of grain size distribution and cumulative frequency graphs (arithmetic scale and probability scale) for sample 109: Mid intertidal zone, western transect, Moonlight Bay. Sample collected on the 22nd of September, 2014.

Table II.110: *Graphical and statistical parameters, textural description and size classes for sample 110: Low intertidal zone, eastern transect, Moonlight Bay. Sample collected on the 22nd of September, 2014.*

Textural description	**Textural size classes**
Very poorly sorted, Near symmetrical skewed, Platykurtic	Sand = 38.299% Fines = 61.701% Silt = 41.554% Clay = 20.147%
Moment method parameters (µm) Mean = 160.328 Standard deviation (sd) = 283.858 Skewness (SkI) = 2.655 Kurtosis (KG) = 10.707 **Wentworth size class** Medium silt	**Graphical method parameters. After Folk (1980) (ϕ)** Mean (Mz) = 5.025 d(0.5) = 5.001 Sorting (SI) = 3.216 Skewness (SkI) = 0.030 Kurtosis (KG) = 0.814 Mean (mm) = 0.031 Mean (µm) = 30.706

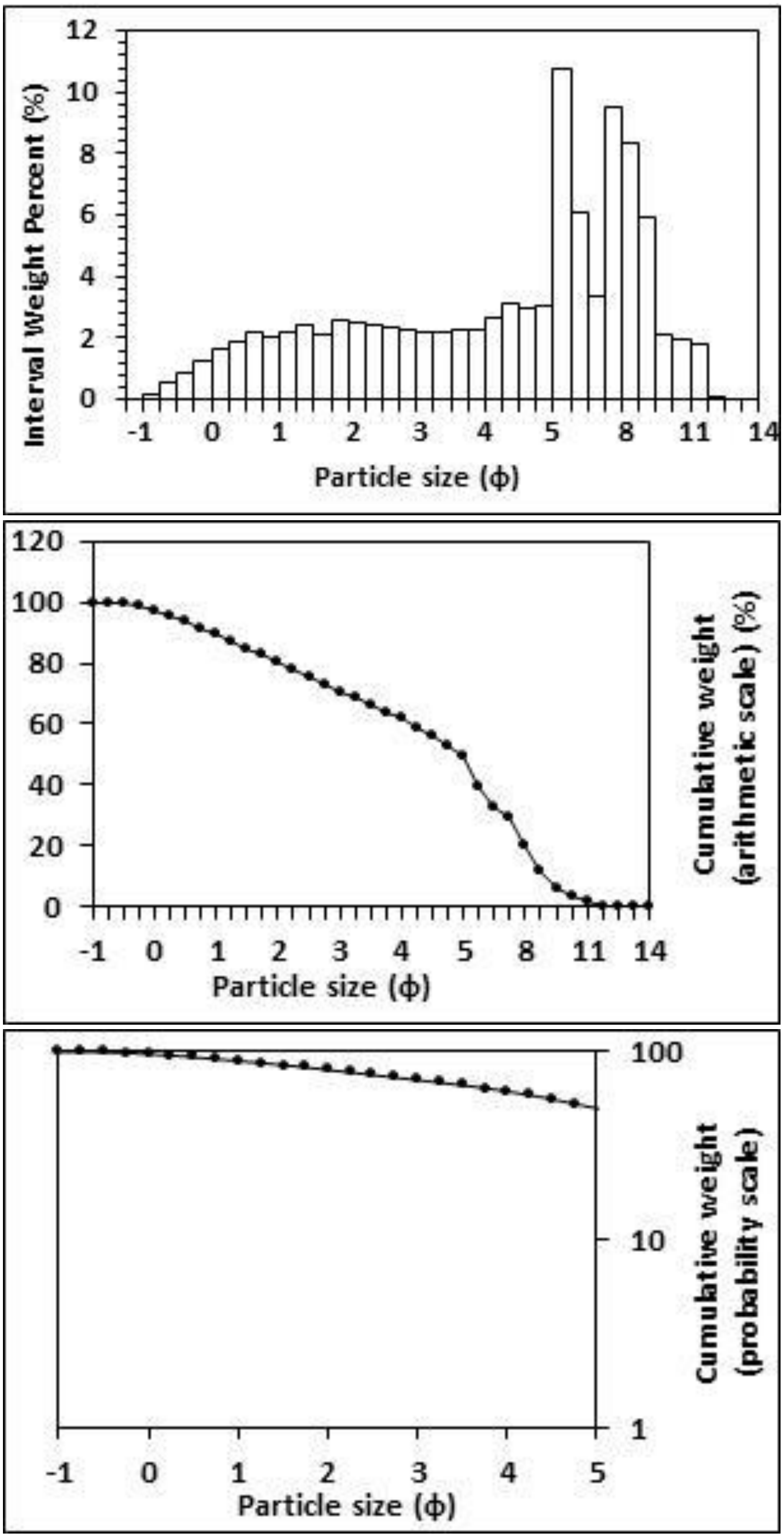

Figures II.328, II.329 and II.330: Histogram of grain size distribution and cumulative frequency graphs (arithmetic scale and probability scale) for sample 110: Low intertidal zone, eastern transect, Moonlight Bay. Sample collected on the 22nd of September, 2014.

Table II.111: *Graphical and statistical parameters, textural description and size classes for sample 111: Low intertidal zone, western transect, Moonlight Bay. Sample collected on the 22nd of September, 2014.*

Textural description	**Textural size classes**
Poorly sorted, Strongly fine skewed, Very leptokurtic	Sand = 83.847% Fines = 16.153% Silt = 11.790% Clay = 4.363%
Moment method parameters (µm) Mean = 254.940 Standard deviation (sd) = 229.682 Skewness (SkI) = 2.638 Kurtosis (KG) = 13.864	**Graphical method parameters. After Folk (1980) (ϕ)** Mean (Mz) = 2.677 d(0.5) = 2.232 Sorting (SI) = 1.858 Skewness (SkI) = 0.494 Kurtosis (KG) = 2.335 Mean (mm) = 0.156 Mean (µm) = 156.322
Wentworth size class Fine sand	

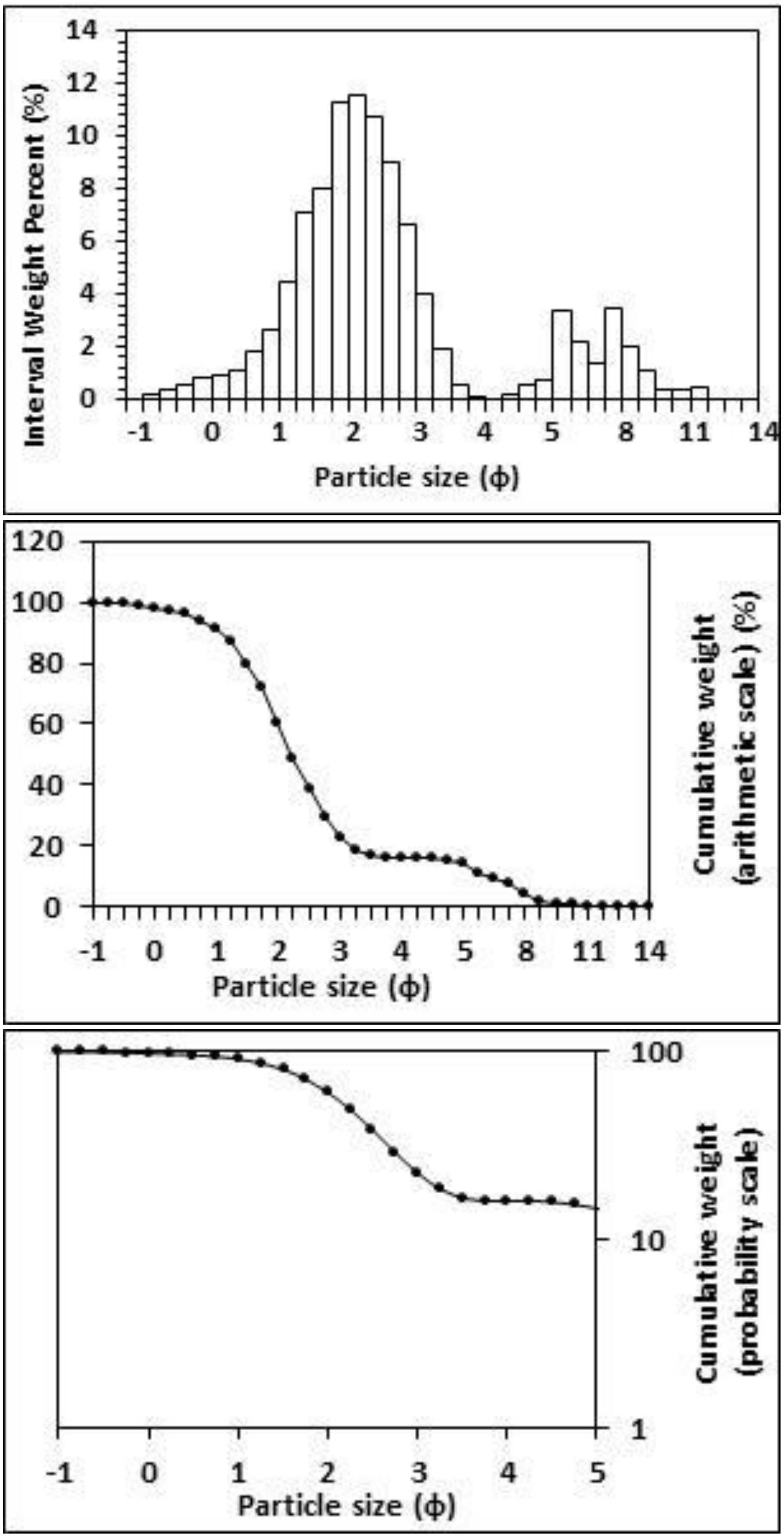

Figures II.331, II.332 and II.333: Histogram of grain size distribution and cumulative frequency graphs (arithmetic scale and probability scale) for sample 111: Low intertidal zone, western transect, Moonlight Bay. Sample collected on the 22nd of September, 2014.

Table II.112: *Graphical and statistical parameters, textural description and size classes for sample 112: Mid intertidal zone, eastern transect, Moonlight Bay. Sample collected on the 22nd of September, 2014.*

Textural description	**Textural size classes**
Poorly sorted, Strongly fine skewed, Very leptokurtic	Sand = 88.605% Fines = 11.395% Silt = 8.566% Clay = 2.829%
Moment method parameters (µm) Mean = 475.971 Standard deviation (sd) = 307.881 Skewness (SkI) = 0.783 Kurtosis (KG) = 3.913	**Graphical method parameters. After Folk (1980) (ϕ)** Mean (Mz) = 1.288 d(0.5) = 1.212 Sorting (SI) = 1.560 Skewness (SkI) = 0.381 Kurtosis (KG) = 2.390 Mean (mm) = 0.410 Mean (µm) = 409.628
Wentworth size class Medium sand	

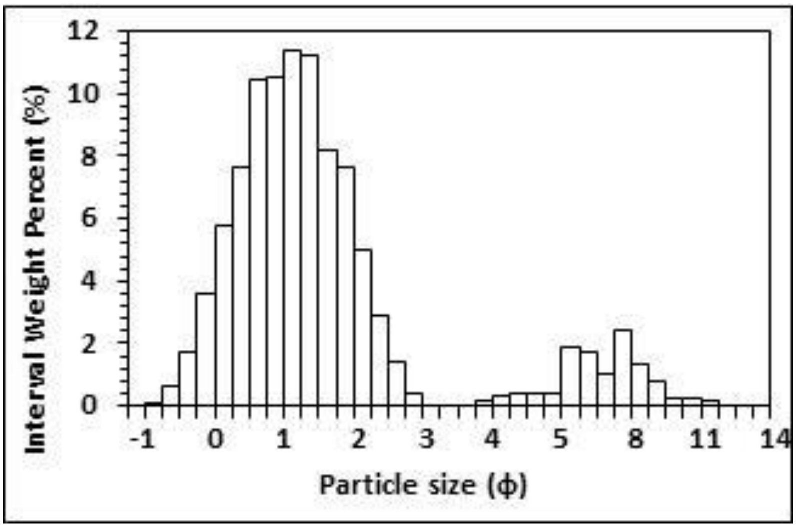

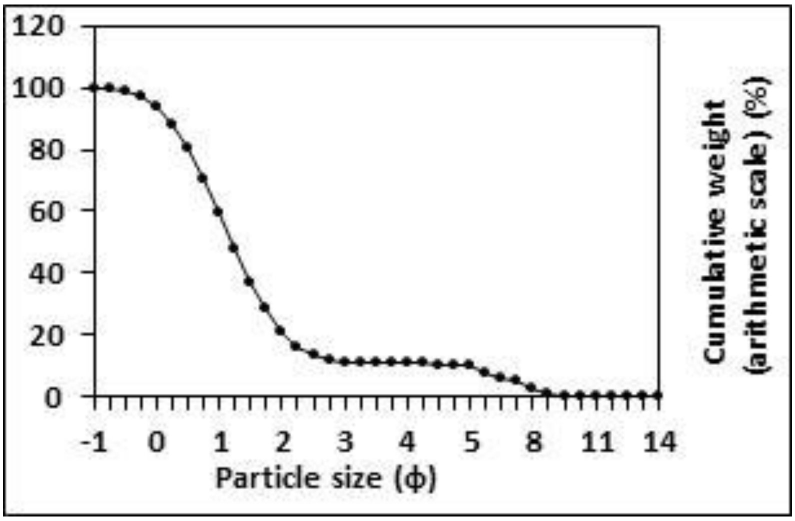

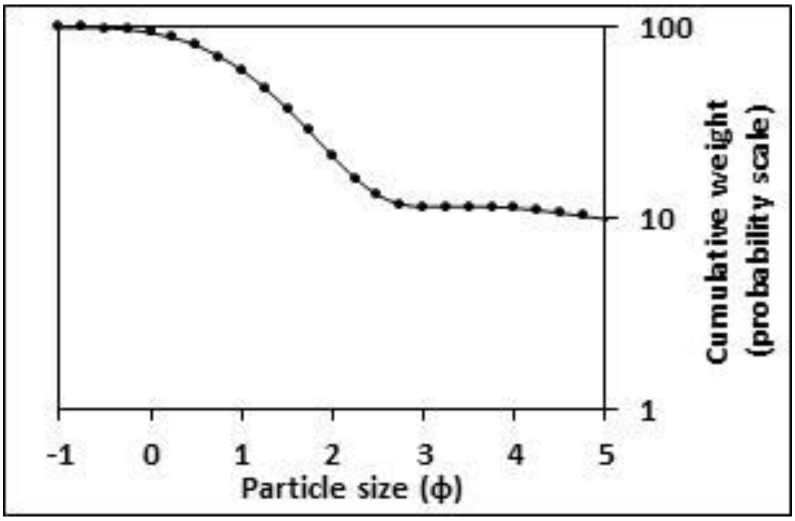

Figures II.334, II.335 and II.336: Histogram of grain size distribution and cumulative frequency graphs (arithmetic scale and probability scale) for sample 112: Mid intertidal zone, eastern transect, Moonlight Bay. Sample collected on the 22nd of September, 2014.

Table II.113: *Graphical and statistical parameters, textural description and size classes for sample 113: High intertidal zone, western transect, Moonlight Bay. Sample collected on the 23rd of September, 2014.*

Textural description	**Textural size classes**
Moderately well sorted, Near symmetrical skewed, Mesokurtic	Sand = 100 000%Fines = 0.000% Silt = 0.000%Clay = 0.000%
Moment method parameters (µm) Mean = 520.887 Standard deviation (sd) = 239.839 Skewness (SkI) = 1.067 Kurtosis (KG) = 4.054 **Wentworth size class** Medium sand	**Graphical method parameters. After Folk (1980) (ϕ)** Mean (Mz) = 1.091 d(0.5) = 1.099 Sorting (SI) = 0.665 Skewness (SkI) = -0.015 Kurtosis (KG) = 0.933 Mean (mm) = 0.469 Mean (µm) = 469.360

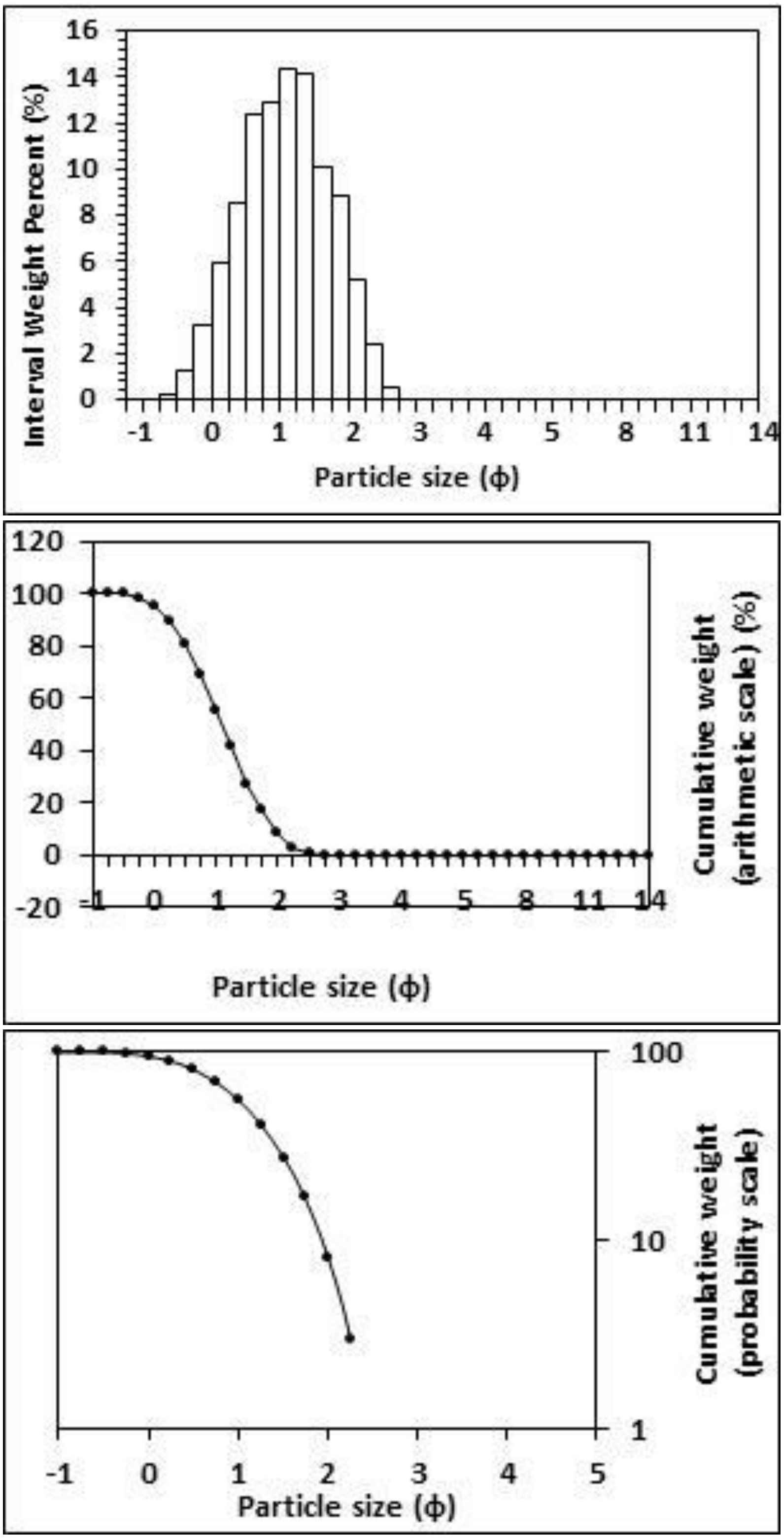

Figures II.337, II.338 and II.339: Histogram of grain size distribution and cumulative frequency graphs (arithmetic scale and probability scale) for sample 113: High intertidal zone, western transect, Moonlight Bay. Sample collected on the 23rd of September, 2014.

Table II.114: *Graphical and statistical parameters, textural description and size classes for sample 114: Mid intertidal zone, western transect, Moonlight Bay. Sample collected on the 23rd of September, 2014.*

Textural description	**Textural size classes**
Poorly sorted, Strongly fine skewed, Very leptokurtic	Sand = 83.634% Fines = 16.366% Silt = 12.502% Clay = 3.864%
Moment method parameters (µm) Mean = 238.415 Standard deviation (sd) = 137.965 Skewness (SkI) = 0.179 Kurtosis (KG) = 3.250	**Graphical method parameters. After Folk (1980) (ϕ)** Mean (Mz) = 2.653 d(0.5) = 2.067 Sorting (SI) = 1.739 Skewness (SkI) = 0.645 Kurtosis (KG) = 2.827 Mean (mm) = 0.159 Mean (µm) = 158.980
Wentworth size class Fine sand	

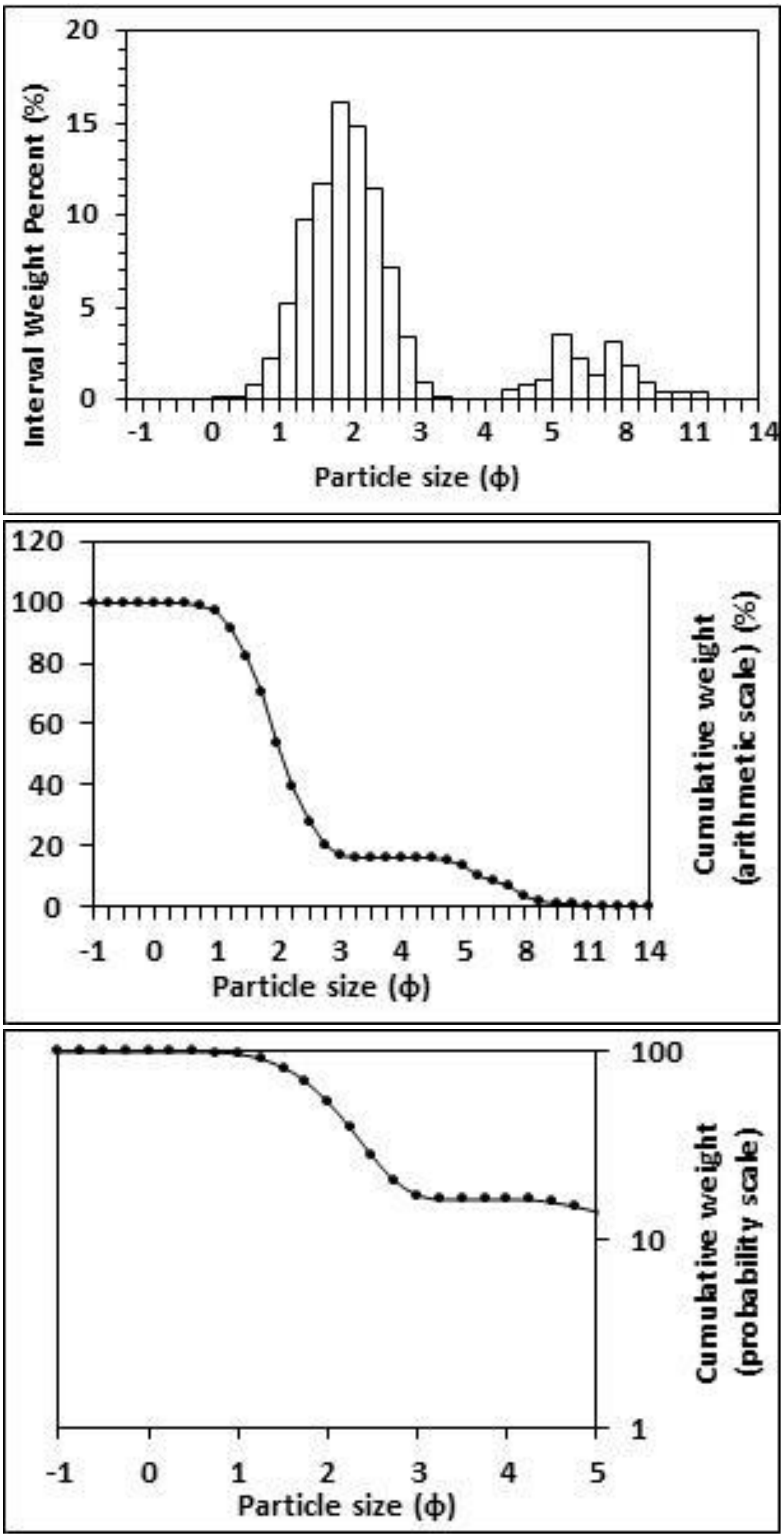

Figures II.340, II.341 and II.342 Histogram of grain size distribution and cumulative frequency graphs (arithmetic scale and probability scale) for sample 114: Mid intertidal zone, western transect, Moonlight Bay. Sample collected on the 23rd of September, 2014.

Table II.115: *Graphical and statistical parameters, textural description and size classes for sample 115: High intertidal zone, eastern transect, Moonlight Bay. Sample collected on the 23rd of September, 2014.*

Textural description	**Textural size classes**
Poorly sorted, Fine skewed, Leptokurtic	Sand = 94.795% Fines = 5.205% Silt = 4.284% Clay = 0.921%
Moment method parameters (µm)	**Graphical method parameters. After Folk (1980) (ϕ)**
Mean = 597.339 Standard deviation (sd) = 384.187 Skewness (SkI) = 0.956 Kurtosis (KG) = 3.661	Mean (Mz) = 0.998 d(0.5) = 0.979 Sorting (SI) = 1.192 Skewness (SkI) = 0.207 Kurtosis (KG) = 1.414 Mean (mm) = 0.501 Mean (µm) = 500.690
Wentworth size class Coarse sand	

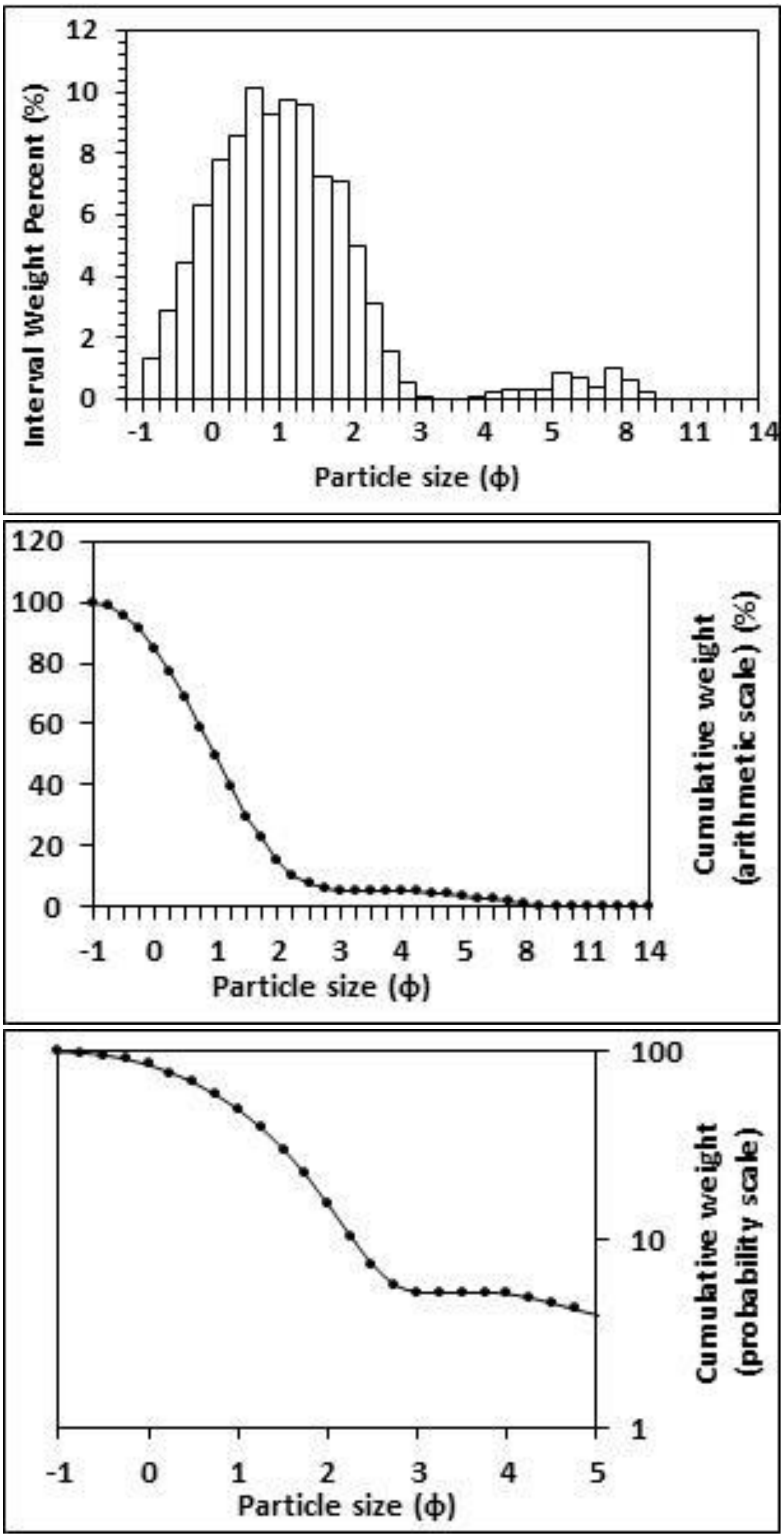

Figures II.343, II.344 and II.345: Histogram of grain size distribution and cumulative frequency graphs (arithmetic scale and probability scale) for sample 115: High intertidal zone, eastern transect, Moonlight Bay. Sample collected on the 23rd of September, 2014.

Table I.116: *Graphical and statistical parameters, textural description and size classes for sample 116: Mid intertidal zone, eastern transect, Moonlight Bay. Sample collected on the 23rd of September, 2014.*

Textural description	**Textural size classes**
Poorly sorted, Strongly fine skewed, Very leptokurtic	Sand = 92.035% Fines = 7.965% Silt = 6.447% Clay = 1.518%
Moment method parameters (µm) Mean = 497.187 Standard deviation (sd) = 315.195 Skewness (SkI) = 1.032 Kurtosis (KG) = 4.566	**Graphical method parameters. After Folk (1980) (ϕ)** Mean (Mz) = 1.223 d(0.5) = 1.193 Sorting (SI) = 1.386 Skewness (SkI) = 0.310 Kurtosis (KG) = 2.139 Mean (mm) = 0.428 Mean (µm) = 428.259
Wentworth size class Medium sand	

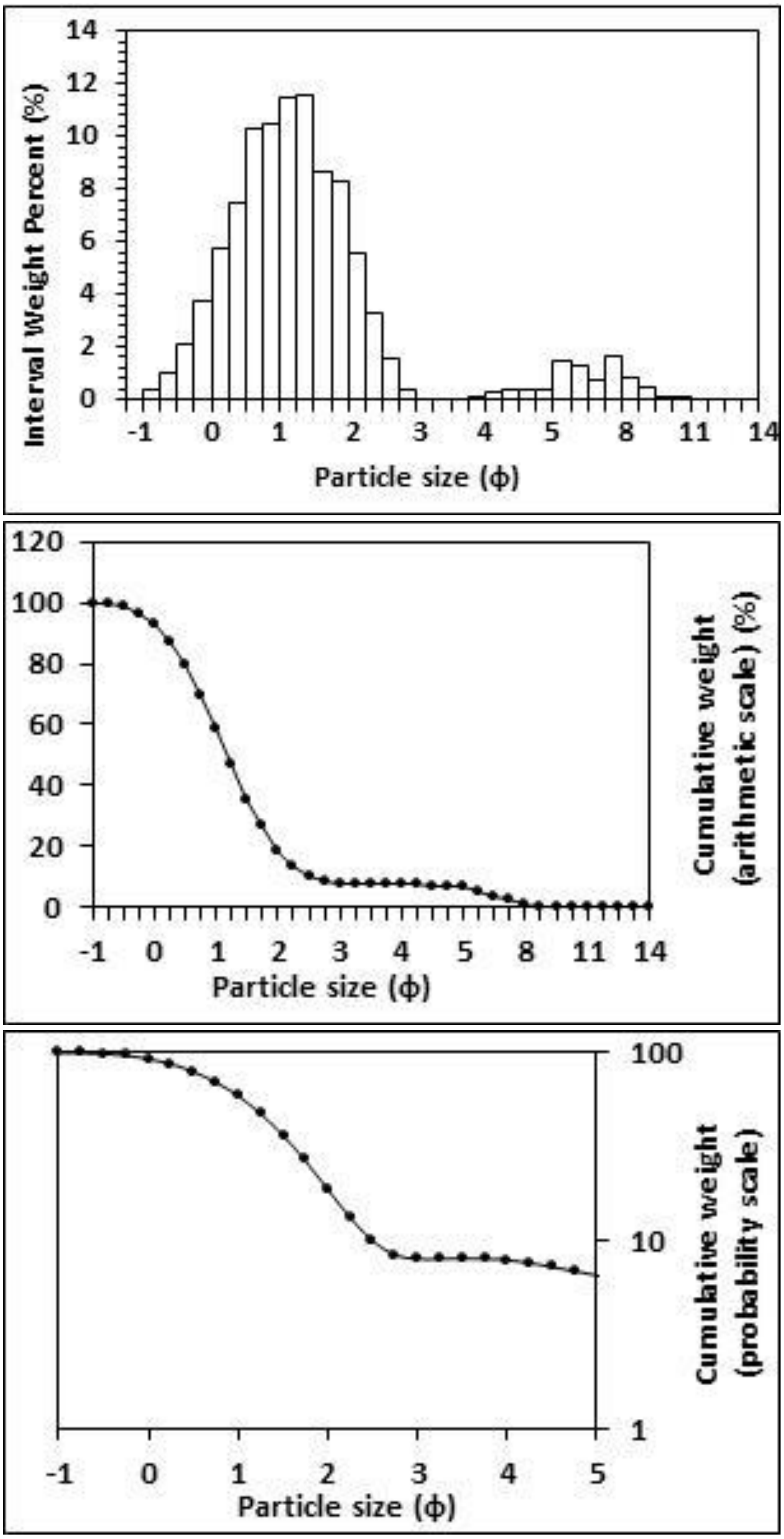

Figures II.346, II.347 and II.348: Histogram of grain size distribution and cumulative frequency graphs (arithmetic scale and probability scale) for sample 116: Mid intertidal zone, eastern transect, Moonlight Bay. Sample collected on the 23rd of September, 2014.

Table II.117: *Graphical and statistical parameters, textural description and size classes for sample 117: Low intertidal zone, eastern transect, Moonlight Bay. Sample collected on the 23rd of September, 2014.*

Textural description	**Textural size classes**
Very poorly sorted, Near symmetrical skewed, Platykurtic	Sand = 44.113% Fines = 55.887% Silt = 37.476% Clay = 18.411%
Moment method parameters (μm) Mean = 212.092 Standard deviation (sd) = 325.520 Skewness (SkI) = 2.032 Kurtosis (KG) = 7.166 **Wentworth size class** Coarse silt	**Graphical method parameters. After Folk (1980) (ϕ)** Mean (Mz) = 4.638 d(0.5) = 4.609 Sorting (SI) = 3.337 Skewness (SkI) = 0.054 Kurtosis (KG) = 0.735 Mean (mm) = 0.040 Mean (μm) = 40.174

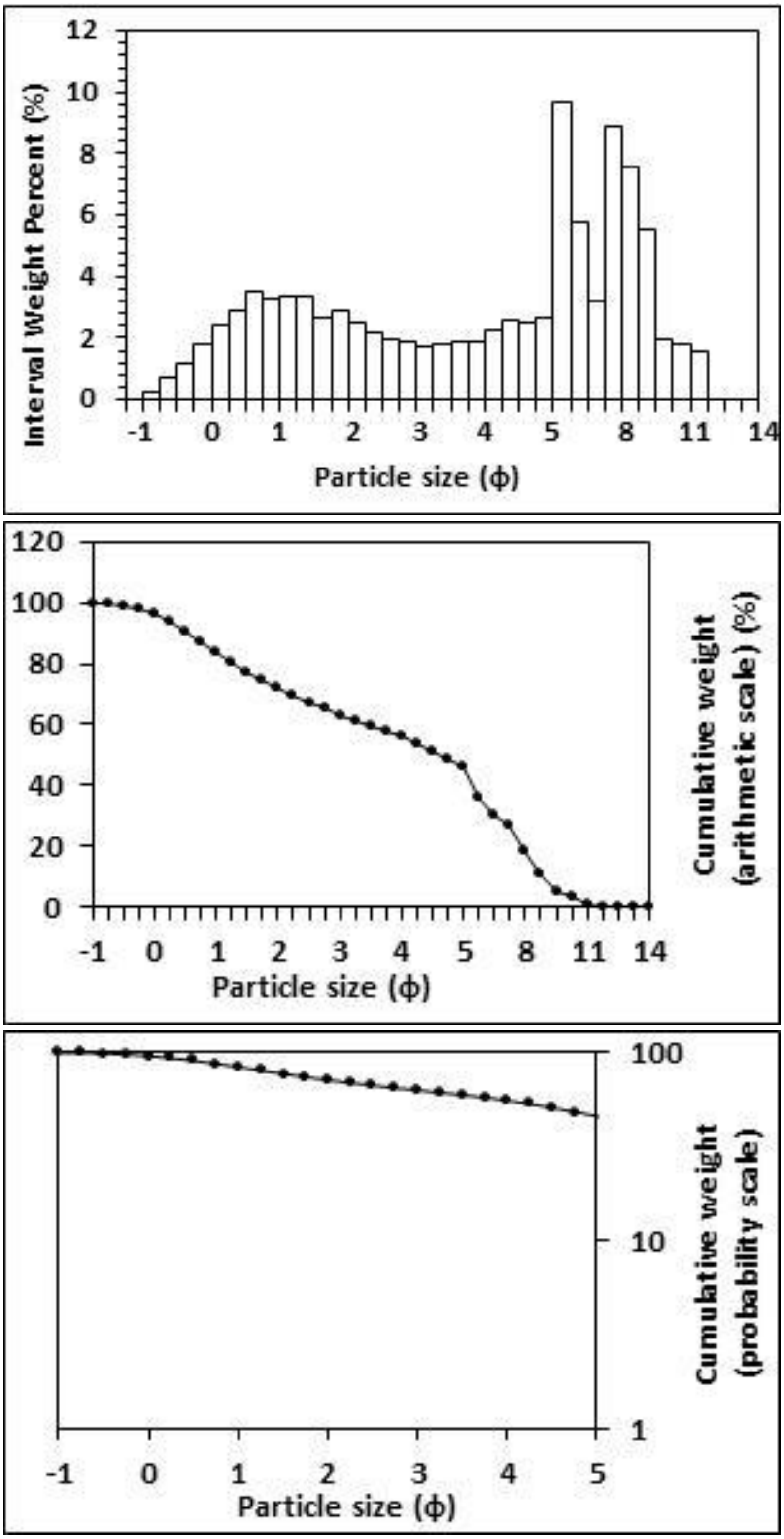

Figures II.349, II.350 and II.351: Histogram of grain size distribution and cumulative frequency graphs (arithmetic scale and probability scale) for sample 117: Low intertidal zone, eastern transect, Moonlight Bay. Sample collected on the 23rd of September, 2014.

Table II.118: *Graphical and statistical parameters, textural description and size classes for sample 118: Low intertidal zone, western transect, Moonlight Bay. Sample collected on the 23rd of September, 2014.*

Textural description	**Textural size classes**
Poorly sorted, Fine skewed, Very leptokurtic	Sand = 88.191% Fines = 11.809% Silt = 9.007% Clay = 2.802%
Moment method parameters (µm) Mean = 290.715 Standard deviation (sd) = 243.558 Skewness (SkI) = 2.264 Kurtosis (KG) = 10.679	**Graphical method parameters. After Folk (1980) (ϕ)** Mean (Mz) = 2.116 d(0.5) = 2.085 Sorting (SI) = 1.507 Skewness (SkI) = 0.274 Kurtosis (KG) = 2.274 Mean (mm) = 0.231 Mean (µm) = 230.759
Wentworth size class Fine sand	

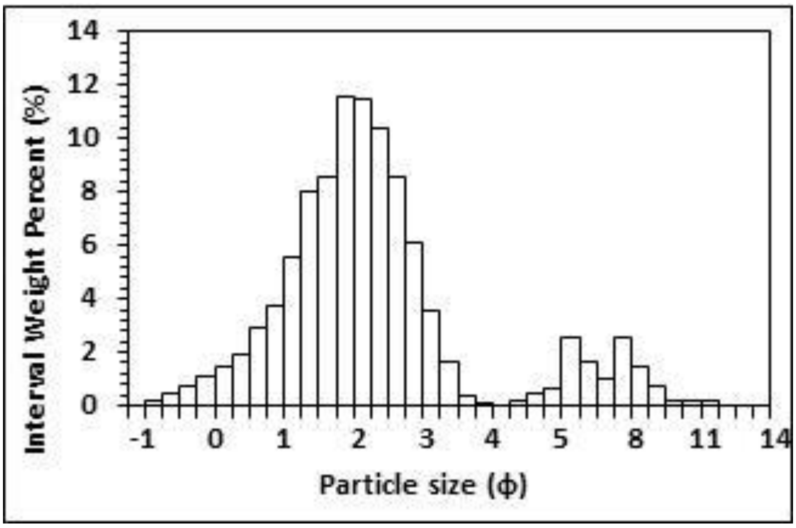

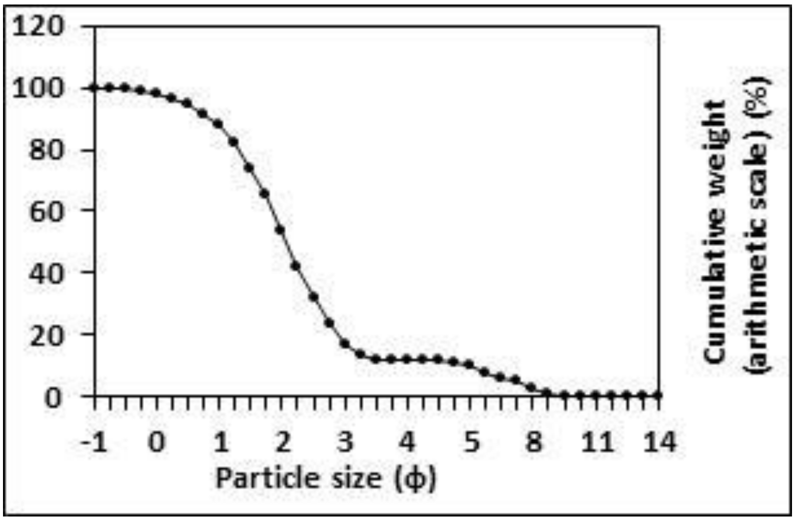

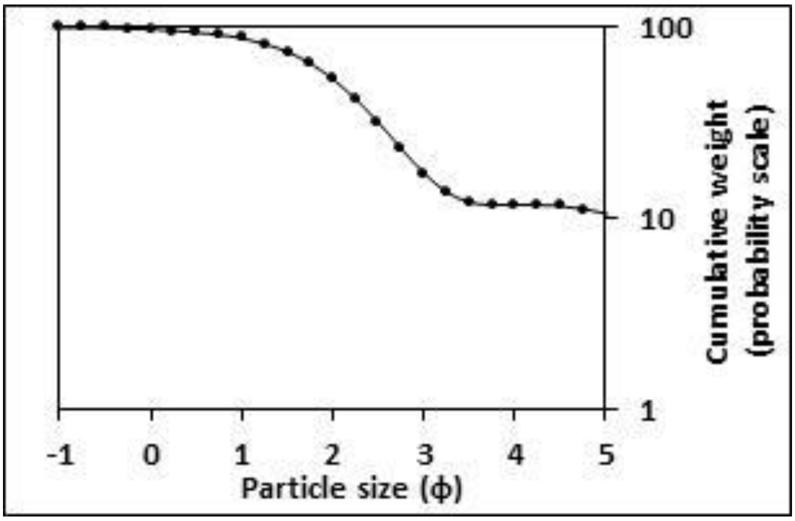

Figures II.352, II.353 and II.354: Histogram of grain size distribution and cumulative frequency graphs (arithmetic scale and probability scale) for sample 118: Low intertidal zone, western transect, Moonlight Bay. Sample collected on the 23rd of September, 2014.

APPENDIX III: CONTROL POINT LOCATIONS AND CHECKS

III.0 CONTROL POINT LOCATIONS AND CHECKS FOR CONSISTENCY

Locations of control points and control point checks are provided below as well as some consistency checks for rod locations.

	MOTURIKI NIWA/UNI					MOTURIKI			
	WGS84		Mount Eden Circuit 2000			WGS84		Mount Eden Circuit 2000	
	Latitude	Longitude	Northing (m)	Easting (m)		Latitude	Longitude	Northing (m)	Easting (m)
LINZ Marks									
B4BT						37° 48 06.875' S	174° 52 21.577' E	697656.594	409553.886
B4BT_GNSS						37° 48 06.875' S	174° 52 21.577' E	697656.594	409553.886
b4bt_topo_check						37° 48 06.876' S	174° 52 21.579' E	697656.565	409553.939
B4BT						37° 48 06.875' S	174° 52 21.577' E	697656.594	409553.886
B4BT_GNSS						37° 48 06.875' S	174° 52 21.577' E	697656.594	409553.886
B4BT_check						37° 48 06.876' S	174° 52 21.578' E	697656.549	409553.899
BEIG									
beig_check									
BEIG_GNSS									
Bench Marks									
BM1_front	37° 48.7979' S	174° 49.9236' E	696396.08	405977.66	**BM1_front_check**	37° 48 47.870' S	174° 49 55.415' E	696396.161	405977.701
BM1_back	37° 48.8003' S	174° 49.9288' E	696391.66	405985.41	**BM1_mot_check**	**37° 48 48.014' S**	**174° 49 55.732' E**	**696391.726**	**405985.451**
BM2_front	37° 48.9198' S	174° 49.8575' E	696170.54	405880.51	**BM2_front_check**	37° 48 55.188' S	174° 49 51.454 E	696170.623	405880.675
BM2_back	37° 48.9217' S	174° 49.8616' E	696167.03	405886.59					
BM3_front	37° 49.0191' S	174° 49.7944' E	695986.94	405787.91	**BM3_front_check**	37° 49 01.146' S	174° 49 47.673' E	695987.009	405788.061
BM3_back	37° 49.0201' S	174° 49.7962' E	695985.23	405790.48					
BM4_front	37° 49.1342' S	174° 49.7038' E	695774.18	405654.83	**BM4_front_check**	37° 49 08.051' S	174° 49 42.237' E	695774.245	405654.984
BM4_back	37° 49.1400' S	174° 49.7131' E	695763.42	405668.44					
Ground Control Points									
cp1						37° 49 17.239' S	174° 49 32.135' E	695491.16	405407.753
cp3a						37° 49 10.972' S	174° 49 39.640' E	695684.231	405591.412
cp4						37° 49 08.166' S	174° 49 41.713' E	695770.707	405642.163
cp5							CP5 is missing		
cp6						37° 49 01.087' S	174° 49 47.497' E	695988.826	405783.76
cp7						37° 48 54.163' S	174° 49 52.146' E	696202.203	405897.609
cp8						37° 48 49.237' S	174° 49 54.853' E	696354.033	405963.922
cp9						37° 48 43.834' S	174° 49 58.036' E	696520.527	406041.902
cp10						37° 48 39.220' S	174° 50 00.127' E	696662.725	406093.144
cp11						37° 48 32.407' S	174° 50 04.957' E	696872.695	406211.445
cp12						37° 48 29.335' S	174° 50 08.373' E	696967.326	406295.058
cp13						37° 48 23.743' S	174° 50 20.397' E	697139.478	406589.299
cp14_carpark						37° 48 20.826' S	174° 50 26.908' E	697229.295	406748.608
cp15_kitesurf						37° 48 14.469 S	174° 50 40.261' E	697424.976	407075.387
cp16_picnic_area						37° 48 15.030' S	174° 50 46.520' E	697407.569	407228.473
cp17_marae						37° 48 17.068' S	174° 50 58.955' E	697344.455	407532.586
cp18_airfield						37° 48 20.075' S	174° 51 10.061' E	697251.494	407804.156

	MEAN SEA LEVEL				UNCALIBRATED							
	WGS84		Mount Eden Circuit 2000		WGS84		Mount Eden Circuit 2000		Moturiki 1953 NIWA/UNI	Moturiki 1953	Mean Sea Level (msl)	uncalibrated control points
	Latitude	Longitude	Northing (m)	Easting (m)	Latitude	Longitude	Northing (m)	Easting (m)	Elevation (m)	Elevation (m)	Elevation (m)	Elevation (m)
LINZ Marks												
B4BT										38		
B4BT_GNSS										38		
b4bt_topo_check										37.915		
B4BT										38		
B4BT_GNSS										38		
B4BT_check	37° 48 06.874' S	174° 52 21.578' E	697656.621	409553.904						37.989	37.84	
BEIG	37° 48 36.272' S	174° 51 08.545' E	696752.213	407766.584							7.8	
beig_check	37° 48 36.271' S	174° 51 08.545' E	696752.252	407766.603							7.811	
BEIG_GNSS	37° 48 36.272' S	174° 51 08.545' E	696752.213	407766.584							7.8	
Bench Marks												
BM1_front	37° 48 47.868' S	174° 49 55.415' E	696396.216	405977.712					6.919	6.992	6.864	
BM1_back	37° 48 48.012' S	174° 49 55.733' E	696391.767	405985.469					10.528	10.595	10.497	
BM2_front	37° 48 55.186' S	174° 49 51.452' E	696170.674	405880.609					6.978	7.044	6.917	
BM2_back									8.377			
BM3_front	37° 49 01.145' S	174° 49 47.671' E	695987.061	405788.017					6.473	6.553	6.393	
BM3_back									6.095			
BM4_front	37° 49 08.049' S	174° 49 42.235' E	695774.312	405654.923					7.227	7.27	7.166	
BM4_back									7.035			
Ground Control Points												
cp1	37° 49 17.239' S	174° 49 32.134' E	695491.17	405407.714	37° 49 17.223' S	174° 49 32.134' E	695491.648	405407.728		3.421	3.145	3.023
cp3a	37° 49 10.970' S	174° 49 39.638' E	695684.284	405591.354	37° 49 10.957' S	174° 49 39.638' E	695684.704	405591.36		8.971	8.857	8.608
cp4	37° 49 08.164' S	174° 49 41.710' E	695770.774	405642.096	37° 49 08.150' S	174° 49 41.711' E	695771.201	405642.111		6.889	6.82	6.521
cp5	37° 49 04.377' S	174° 49 44.840' E	695887.455	405718.715	37° 49 04.363' S	174° 49 44.840' E	695887.875	405718.712			6.002	5.74
cp6	37° 49 01.085' S	174° 49 42.235' E	695988.891	405783.686	37° 49 01.072' S	174° 49 47.494' E	695989.311	405783.697		5.475	5.364	5.098
cp7	37° 48 54.162' S	174° 49 52.146' E	696202.25	405897.611	37° 48 54.148' S	174° 49 52.146' E	696202.674	405897.625		10.509	10.368	10.077
cp8	37° 48 49.236' S	174° 49 54.854' E	696354.063	405963.944	37° 48 49.222' S	174° 49 54.853' E	696354.481	405963.938		11.941	11.812	11.541
cp9	37° 48 43.833' S	174° 49 58.036' E	696520.572	406041.905	37° 48 43.819' S	174° 49 58.037' E	696520.992	406041.921		14.203	14.091	13.758
cp10	37° 48 39.219' S	174° 50 00.128' E	696662.759	406093.168	37° 48 39.206' S	174° 50 00.129' E	696663.173	406093.18		6.452	6.449	6.073
cp11	37° 48 32.406' S	174° 50 04.958' E	696872.714	406211.454	37° 48 32.392' S	174° 50 04.959' E	696873.14	406211.479		11.141	11.086	10.741
cp12	37° 48 29.334' S	174° 50 08.373' E	696967.351	406295.056	37° 48 29.320' S	174° 50 08.374' E	696967.78	406295.08		3.963	3.834	3.543
cp13	37° 48 23.742' S	174° 50 20.398' E	697139.51	406589.305	37° 48 23.728' S	174° 50 20.399' E	697139.943	406589.334		7.275	7.197	6.886
cp14_carpark	37° 48 20.825' S	174° 50 26.910' E	697229.322	406748.655	37° 48 20.811' S	174° 50 26.909' E	697229.736	406748.641		8.014	7.941	7.642
cp15_kitesur	37° 48 14.466' S	174° 50 40.261' E	697425.088	407075.393	37° 48 14.452' S	174° 50 40.260' E	697425.522	407075.37		6.781	6.839	6.531
cp16_picnic_	37° 48 15.027' S	174° 50 46.520' E	697407.636	407228.465	37° 48 15.014' S	174° 50 46.520' E	697408.054	407228.476		5.05	4.985	4.7
cp17_marae	37° 48 17.067' S	174° 50 58.955' E	697344.491	407532.582	37° 48 17.053' S	174° 50 58.955' E	697344.904	407532.581		3.779	3.702	3.418
cp18_airfield	37° 48 20.075' S	174° 51 10.062' E	697251.505	407804.17	37° 48 20.061' S	174° 51 10.062' E	697251.936	407804.175		4.527	4.493	4.18

Site Calibration

Jobs > New > c_points-msl (GD2000/Mount Eden2000)

Measure > VRS > site calibration

→ No points!!!

> Exit general survey

Settings > survey styles > VRS > site calibration

Default settings

□ fix horizontal.scale to 1.0	□ auto calibrate
Vertical adjustment	
Horizontal plane	
Observation	
Observation type:	
Observed control point:	
Max. horiz. Resids. 0.010m	

Max vert, resids	0.02m	Min horiz. Scale	0.99999
Max horiz. resids	9.00001	Max slope	10.000ppm

Calibration point name > Add

Method

Add suffix > _GNSS

Key In > Points

Point Name	BEIG
Northing	N – 6966 752.213 m
Easting	E – 407 766.584 m
Code	-
Elevation	7.8 m
check □ control point	
Store > Esc	

Measure > VRS > Measure points (from internet)

Data Source > VRS > UNI

Key point select control point > Store > Esc

Measure > VRS > Measure > Calibrate point

Store > Apply (used horiz/vert)

Measure

→Measure > measure points

Tried topo point cp16_topo_msl and obs control point cp16_ocp_msl

> Exit

Review Job

cp16_topo_msl

N: 697407.608 m

E: 407228.453 m

Elevation: 4.890 m

obs control point cp16_ocp_msl

cp16_topo_msl

N: 697407.607 m

E: 407228.455 m

Elevation: 4.880 m

Measure > Site calibration

> Select point > Apply

To test if calibrated we set up a new job called test and measured cp16_test

N: 697408.053 m

E: 407228.460 m

Elevation: 4.649 m

This was a good indicator that in fact the sites were calibrated

Testing site calibration using Moturiki datum

New job > cpts > Mot_dat

Key In > details of control points   Select control points □ check

Measure > VRS > Measure > Calibrate point

Store > Apply site calibration

Measure

→Measure > measure points > Exit

B4BT_test (test as topo point)   37.98 m

B4BT_test2 (test as obs control point)   37.991 m

cp16_mot_topo

N: 697407.584 m

E: 407228.460 m

Elevation: 5.080 m

cp16_mot_obc

N: 697407.587 m

E: 407228.459 m

Elevation: 5.079 m

New Job test plain to validate whether calibration worked

cp16_obc_plain

N: 697408.043 m

E: 407228.484 m

Elevation: 4.646 m

cp16_topo_plain

N: 697408.039 m

E: 407228.484 m

Elevation: 4.645 m

Justine’s work

11/02/2013 Survey – GPS without site calibration

Vert. Adjust.	Geoid model
Projection	Transverse Mercator
Ellipsoid	6378137.000 m

Control points 07/02/2013 (accuracy ≈ 4 mm horiz / ≈7 mm vert)

Height adjust	No adjustment
Ellipsoid	6378137.000 m
Projection	Tranverse Mercator
Vert. Adjust.	Geoid model

Field Work Datum Calibration 13th February, 2013

Control point	Northing (m)	Easting (m)	Elevation (m)	
cp1	695 491.648	405407.728	3.023	Horiz precision: 0.005 m Vert precision: 0.009 m
cp2	-	-	-	
cp3	695 684.704	405 591.360	8.608	
cp4	695 771.201	405 642.111	6.521	
cp5	695 887.875	405 718.712	5.740	
cp6	659 89.311	405 783.697	5.098	
cp7	696 202.674	405 897.625	10.077	
cp8	696 354.481	405 963.938	11.541	
cp9	695 620.992	406 041.921	13.758	
cp10	696 663.173	406 093.180	6.073	
cp11	696 873.140	406 211.479	10.741	
cp12	696 967.780	406 295.080	3.543	
cp13	697 139.943	406 589.334	6.886	
cp14 carpark	697 229.736	406 748.641	7.642	
cp15 Kitesurf	697 425.522	407 075.370	6.531	

cp16 picnic	697 408.054	407 228.476	4.700	
cp17 marae	697 344.904	407 532.581	3.418	
cp18 airfield	697 251.936	407 804.175	4.180	
cp19 airfield	697258.7	408113.4	3.248	New Point

Name	Northing	Easting	Elevation (m)
b4bt_topo_check	697656.565	409553.939	37.915
cp1_moturiki	695491.160	405407.753	3.421
cp3_ moturiki	695684.231	405591.412	8.971
cp4_ moturiki	695770.707	405642.163	6.889
BM4_front_check	695774.245	405654.984	7.27
cp5_ moturiki	695988.826	405783.76	5.475
BM3_front_check	695987.009	405788.061	6.553
BM2_front_check	696170.623	405880.675	7.044

BEIG	linz mark	696752.2	407766.6	7.8
BEIG_GNSS		696752.2	407766.6	7.8
OCP_CHECK_START1		696752.2	407766.6	7.796
TP_CHECK_START1		696752.2	407766.6	7.796
CP7_BW_2014		696202.2	405897.6	10.328
CP7_BW_2014_TP1		696202.2	405897.6	10.332
CP7_BW_2014_TP2		696202.2	405897.6	10.331
T2_2014		696164	405856.9	6.143
T2_2014_TP_CHECK		696164	405856.9	6.142
BM3_FRONT_2014		695987	405788	6.386
BM3_FRONT2014_TP		695987	405788	6.389
BM2_FRONT_2014		696170.7	405880.6	6.901

BW_BS_SHORT	696182.2	405882.3	8.349
CP18_2014	697251.5	407804.2	4.493
CP18_2014_TOPO	697251.5	407804.2	4.481
CP19_2014	697258.7	408113.4	3.248
CP19_2014_TOPO	697258.6	408113.4	3.246
BEIG_OCP_END	696752.2	407766.6	7.822
BEIG_TP_END	696752.2	407766.6	7.809

2013 GPS DATA ANALYSIS					
BEIG	696752.213	407766.584	7.8	m	Linz mark, calibrated to point
OCP_CHECK_START1	696752.215	407766.58	7.796	m	Start of survey check, calibration accurate to 4mm in vertical (c
	0.002	**-0.004**	**-0.004**	**m**	
	0.20	**-0.40**	**-0.40**	**cm**	
	2.0	**-4.0**	**-4.0**	**mm**	
BEIG	696752.213	407766.584	7.8	m	Linz mark, calibrated to point
BEIG_OCP_END	696752.214	407766.582	7.822	m	End survey observed control point
	0.001	**-0.002**	**0.022**	**m**	
	0.10	**-0.20**	**2.20**	**cm**	
	1.0	**-2.0**	**22.0**	**mm**	
BEIG	696752.213	407766.584	7.8	m	Linz mark
BEIG_TP_END	696752.208	407766.581	7.809	m	Topo point as a check at end of survey
	-0.005	**-0.003**	**0.009**	**m**	
	-0.50	**-0.30**	**0.90**	**cm**	
	-5.0	**-3.0**	**9.0**	**mm**	
CP7_BW_2014	696202.239	405897.6	10.328	m	2014 data
cp7_bw_msl	696202.25	405897.611	10.368	m	2013 data
	0.011	**0.011**	**0.04**	**m**	
	1.10	**1.10**	**4.00**	**cm**	
	11.0	**11.0**	**40.0**	**mm**	
CP7_BW_2014	696202.239	405897.6	10.328	m	Observed control point data 2014
CP7_BW_2014_TP2	696202.233	405897.601	10.331	m	Topo point data check 2014
	-0.006	**0.001**	**0.003**	**m**	
	-0.60	**0.10**	**0.30**	**cm**	
	-6.0	**1.0**	**3.0**	**mm**	
T2_2014	696163.978	405856.857	6.143	m	Measured mark 28th July 2014
GW_marker2	696163.998	405856.874	6.167	m	Mark established for GW experiment
	0.02	**0.017**	**0.024**	**m**	
	2.00	**1.70**	**2.40**	**cm**	
	20.0	**17.0**	**24.0**	**mm**	
T2_2014	696163.978	405856.857	6.143	m	Observed control point data 2014
T2_2014_TP_CHECK	696163.999	405856.853	6.142	m	Topo point data check 2014
	0.021	**-0.004**	**-0.001**	**m**	
	2.10	**-0.40**	**-0.10**	**cm**	
	21.0	**-4.0**	**-1.0**	**mm**	
BM3_FRONT_2014	695987.04	405787.985	6.386	**m**	2014 data
BM3_front_msl	695987.061	405788.017	6.393	**m**	2013 data
	0.021	**0.032**	**0.007**	**m**	
	2.10	**3.20**	**0.70**	**cm**	
	21.0	**32.0**	**7.0**	**mm**	
BM3_FRONT_2014	695987.04	405787.985	6.386	**m**	Observed control point data 2014
BM3_FRONT2014_TP	695987.033	405787.992	6.389	**m**	Topo point data check 2014
	-0.007	**0.007**	**0.003**	**m**	
	-0.70	**0.70**	**0.30**	**cm**	
	-7.0	**7.0**	**3.0**	**mm**	
BM2_FRONT_2014	696170.656	405880.579	6.901	**m**	2014 data
BM2_front_msl	696170.674	405880.609	6.917	**m**	2013 data
	0.018	**0.03**	**0.016**	**m**	
	1.80	**3.00**	**1.60**	**cm**	
	18.0	**30.0**	**16.0**	**mm**	
CP18_2014	697251.493	407804.173	4.493	**m**	2014 data
cp18_air_msl	697251.505	407804.17	4.493	**m**	2013 data
	0.012	**-0.003**	**0**	**m**	
	1.20	**-0.30**	**0.00**	**cm**	
	12.0	**-3.0**	**0.0**	**mm**	
CP19_2014	697258.652	408113.423	3.248	**m**	Observed control point data
CP19_2014_TOPO	697258.649	408113.423	3.246	**m**	Quick topo point for data check
	-0.003	**0**	**-0.002**	**m**	
	-0.30	**0.00**	**-0.20**	**cm**	
	-3.0	**0.0**	**-2.0**	**mm**	
BW_BS_SHORT	696182.186	405882.273	8.349	**m**	Mark used by Justy in testing Total Station

T2_15/08/2014	696163.978	405856.857	6.143	m	Measured mark 28th July 2014
GW_marker2	696163.978	405856.857	6.143	m	Mark established for GW experiment
	0	**0**	**0**	**m**	
	0.00	**0.00**	**0.00**	**cm**	
	0.0	**0.0**	**0.0**	**mm**	Start of survey check, calibration accurate to 4mm in vertical (observed control point)
BM3_from report	695987.061	405788.017	6.393	m	Observed control point data 2014
BM3_15/08/2014	695986.99	405787.932	6.431	m	Survey back site used - BM3 in TS
	-0.071	**-0.085**	**0.038**	**m**	
	-7.10	**-8.50**	**3.80**	**cm**	
	-71.0	**-85.0**	**38.0**	**mm**	
CP7_BM5_15/08/14	696199.724	405894.868	9.997	m	CP7-check for the previous day 14/08/2014
CP7_				m	Profile 1_Rod_HN
	-696199.724	**-405894.868**	**-9.997**	**m**	
	-69619972.40	**-40589486.80**	**-999.70**	**cm**	
	-696199724.0	**-405894868.0**	**-9997.0**	**mm**	
CP7_BM6_15/08/14	696202.661	405897.23	10.321	m	CP7-check for the previous day 14/08/2014
HN_14_14/08/2014				m	Profile 1_Rod_HN
	-696202.661	**-405897.23**	**-10.321**	**m**	
	-69620266.10	**-40589723.00**	**-1032.10**	**cm**	
	-696202661.0	**-405897230.0**	**-10321.0**	**mm**	

20140728					
BEIG	696752.213	407766.584	7.8	m	Linz mark, calibrated to point
OCP_CHECK_START1	696752.215	407766.58	7.796	m	Start of survey check, calibration accurate to 4mm in vertical (observed control point)
	0.002	**-0.004**	**-0.004**	**m**	
	0.20	**-0.40**	**-0.40**	**cm**	
	2.0	**-4.0**	**-4.0**	**mm**	
BEIG	696752.213	407766.584	7.8	m	Linz mark, calibrated to point
BEIG_OCP_END	696752.214	407766.582	7.822	m	End survey observed control point
	0.001	**-0.002**	**0.022**	**m**	
	0.10	**-0.20**	**2.20**	**cm**	
	1.0	**-2.0**	**22.0**	**mm**	
BEIG	696752.213	407766.584	7.8	m	Linz mark
BEIG_TP_END	696752.208	407766.581	7.809	m	Topo point as a check at end of survey
	-0.005	**-0.003**	**0.009**	**m**	
	-0.50	**-0.30**	**0.90**	**cm**	
	-5.0	**-3.0**	**9.0**	**mm**	
CP7_BW_2014	696202.239	405897.6	10.328	m	2014 data
cp7_bw_msl	696202.25	405897.611	10.368	m	2013 data
	0.011	**0.011**	**0.04**	**m**	
	1.10	**1.10**	**4.00**	**cm**	
	11.0	**11.0**	**40.0**	**mm**	
CP7_BW_2014	696202.239	405897.6	10.328	m	Observed control point data 2014
CP7_BW_2014_TP2	696202.233	405897.601	10.331	m	Topo point data check 2014
	-0.006	**0.001**	**0.003**	**m**	
	-0.60	**0.10**	**0.30**	**cm**	
	-6.0	**1.0**	**3.0**	**mm**	
T2_2014	696163.978	405856.857	6.143	m	Measured mark 28th July 2014
GW_marker2	696163.998	405856.874	6.167	m	Mark established for GW experiment
	0.02	**0.017**	**0.024**	**m**	
	2.00	**1.70**	**2.40**	**cm**	
	20.0	**17.0**	**24.0**	**mm**	
T2_2014	696163.978	405856.857	6.143	m	Observed control point data 2014
T2_2014_TP_CHECK	696163.999	405856.853	6.142	m	Topo point data check 2014
	0.021	**-0.004**	**-0.001**	**m**	
	2.10	**-0.40**	**-0.10**	**cm**	
	21.0	**-4.0**	**-1.0**	**mm**	
BM3_FRONT_2014	695987.04	405787.985	6.386	**m**	2014 data
BM3_front_msl	695987.061	405788.017	6.393	**m**	2013 data
	0.021	**0.032**	**0.007**	**m**	
	2.10	**3.20**	**0.70**	**cm**	
	21.0	**32.0**	**7.0**	**mm**	
BM3_FRONT_2014	695987.04	405787.985	6.386	**m**	Observed control point data 2014
BM3_FRONT2014_TP	695987.033	405787.992	6.389	**m**	Topo point data check 2014
	-0.007	**0.007**	**0.003**	**m**	
	-0.70	**0.70**	**0.30**	**cm**	
	-7.0	**7.0**	**3.0**	**mm**	
BM2_FRONT_2014	696170.656	405880.579	6.901	**m**	2014 data
BM2_front_msl	696170.674	405880.609	6.917	**m**	2013 data
	0.018	**0.03**	**0.016**	**m**	
	1.80	**3.00**	**1.60**	**cm**	
	18.0	**30.0**	**16.0**	**mm**	
CP18_2014	697251.493	407804.173	4.493	**m**	2014 data
cp18_air_msl	697251.505	407804.17	4.493	**m**	2013 data
	0.012	**-0.003**	**0**	**m**	
	1.20	**-0.30**	**0.00**	**cm**	
	12.0	**-3.0**	**0.0**	**mm**	
CP19_2014	697258.652	408113.423	3.248	**m**	Observed control point data
CP19_2014_TOPO	697258.649	408113.423	3.246	**m**	Quick topo point for data check
	-0.003	**0**	**-0.002**	**m**	
	-0.30	**0.00**	**-0.20**	**cm**	
	-3.0	**0.0**	**-2.0**	**mm**	
BW_BS_SHORT	696182.186	405882.273	8.349	**m**	Mark used by Justy in testing Total Station

T2_Amir_29/08/2014	696163.978	405856.857	6.143	m	Measured mark 29th August 2014
GW_marker_T2_2014	696163.978	405856.857	6.143	m	Mark established for GW experiment
	0	**0**	**0**	**m**	
	0.00	**0.00**	**0.00**	**cm**	
	0.0	**0.0**	**0.0**	**mm**	
BM3_from report	695987.061	405788.017	6.393	m	Observed control point data 2014
BM3_2014_dod exp	695987.061	405788.017	6.393	m	Survey back site used - BM3 in TS
	0	**0**	**0**	**m**	
	0.00	**0.00**	**0.00**	**cm**	
	0.0	**0.0**	**0.0**	**mm**	
HN_14_29/08/2014	696241.532	405828.88	2.273	m	Linz mark
HN_14_30/08/2014	696241.663	405829.188	1.16	m	Topo point as a check at end of survey
	0.131	**0.308**	**-1.113**	**m**	
	13.10	**30.80**	**-111.30**	**cm**	
	131.0	**308.0**	**-1113.0**	**mm**	
MN_51_29/08/2014				m	Observed control point data 2014
MN_51_30/08/2014				m	Topo point data check 2014
	0	**0**	**0**	**m**	
	0.00	**0.00**	**0.00**	**cm**	
	0.0	**0.0**	**0.0**	**mm**	
LN_48_29/08/2014	696275.207	405736.378	0.453	m	2014 data
LN_48_30/08/2014	696274.819	405736.177	-0.643	m	2013 data
	-0.388	**-0.201**	**-1.096**	**m**	
	-38.80	**-20.10**	**-109.60**	**cm**	
	-388.0	**-201.0**	**-1096.0**	**mm**	
HM_51_29/08/2014	696097.732	405795.24	2.741	m	Observed control point data 2014
HM_51_30/08/2014	696097.875	405795.06	1.637	m	Topo point data check 2014
	0.143	**-0.18**	**-1.104**	**m**	
	14.30	**-18.00**	**-110.40**	**cm**	
	143.0	**-180.0**	**-1104.0**	**mm**	
MM_59_29/08/2014	696118.814	405753.664	1.251	m	Measured mark 28th July 2014
MM_59_30/08/2014	696119.036	405753.544	0.133	m	Mark established for GW experiment
	0.222	**-0.12**	**-1.118**	**m**	
	22.20	**-12.00**	**-111.80**	**cm**	
	222.0	**-120.0**	**-1118.0**	**mm**	
BM3_59_29/08/2014	695986.895	405788.266	7.467	m	Observed control point data 2014
BM3_2014_dod exp	695987.061	405788.017	6.393	m	Topo point data check 2014
	0.166	**-0.249**	**-1.074**	**m**	
	16.60	**-24.90**	**-107.40**	**cm**	
	166.0	**-249.0**	**-1074.0**	**mm**	
CP729	696202.234	405897.629	11.369	**m**	2014 data
cp7 old control p0oint val	696202.239	405897.6	10.328	**m**	2013 data
	0.005	**-0.029**	**-1.041**	**m**	
	0.50	**-2.90**	**-104.10**	**cm**	
	5.0	**-29.0**	**-1041.0**	**mm**	
BM3_FRONT_2014	695987.04	405787.985	6.386	**m**	Observed control point data 2014
BM3_FRONT2014_TP	695987.033	405787.992	6.389	**m**	Topo point data check 2014
	-0.007	**0.007**	**0.003**	**m**	
	-0.70	**0.70**	**0.30**	**cm**	
	-7.0	**7.0**	**3.0**	**mm**	
BM2_FRONT_2014	696170.656	405880.579	6.901	**m**	2014 data
BM2_front_msl	696170.674	405880.609	6.917	**m**	2013 data
	0.018	**0.03**	**0.016**	**m**	
	1.80	**3.00**	**1.60**	**cm**	
	18.0	**30.0**	**16.0**	**mm**	
CP18_2014	697251.493	407804.173	4.493	**m**	2014 data
cp18_air_msl	697251.505	407804.17	4.493	**m**	2013 data
	0.012	**-0.003**	**0**	**m**	
	1.20	**-0.30**	**0.00**	**cm**	
	12.0	**-3.0**	**0.0**	**mm**	
CP19_2014	697258.652	408113.423	3.248	**m**	Observed control point data
CP19_2014_TOPO	697258.649	408113.423	3.246	**m**	Quick topo point for data check
	-0.003	**0**	**-0.002**	**m**	
	-0.30	**0.00**	**-0.20**	**cm**	
	-3.0	**0.0**	**-2.0**	**mm**	
BW_BS_SHORT	696182.186	405882.273	8.349	**m**	Mark used by Justy in testing Total Station

T2_2014	696163.978	405856.857	6.143	m	Measured mark 28th July 2014
GW_marker2	696163.978	405856.857	6.143	m	Mark established for GW experiment
	0	0	0	m	
	0.00	0.00	0.00	cm	
	0.0	0.0	0.0	mm	Start of survey check, calibration accurate to 4mm in vertical (observed control point)
BM3_from report	695987.061	405788.017	6.393	m	Observed control point data 2014
BM3_2014_dod exp	695987.061	405788.017	6.393	m	Survey back site used - BM3 in TS
	0	0	0	m	
	0.00	0.00	0.00	cm	
	0.0	0.0	0.0	mm	
HN_CP7-2_20/07/14	696240.9	405828.3	1.022	m	Profile 1_Rod_HN
HN_14_14/08/2014	696237.9	405840	1.401	m	Profile 1_Rod_HN
	-3	11.7	0.379	m	
	-300.00	1170.00	37.90	cm	
	-3000.0	11700.0	379.0	mm	
MN_CP7-20_20/07/14	696256.562	405766.011	-0.177	m	Profile 1_Rod_MN
MN_31_14/08/2014	696255.097	405798.179	0.214	m	Profile 1_Rod_MN
	-1.465	32.168	0.391	m	
	-146.50	3216.80	39.10	cm	
	-1465.0	32168.0	391.0	mm	
LN_CP7-41_20/07/14	696272.671	405691.234	-0.75	m	Profile 1_Rod_LN
LN_48_14/08/2014	696275.839	405751.336	-0.662	m	Profile 1_Rod_LN
	3.168	60.102	0.088	m	
	316.80	6010.20	8.80	cm	
	3168.0	60102.0	88.0	mm	
HM_CP7-43_20/07/14	696094.413	405803.116	1.428	m	Profile 2_Rod_HM
HM_51_14/08/2014	696098.784	405786.965	1.193	m	Profile 2_Rod_HM
	4.371	-16.151	-0.235	m	
	437.10	-1615.10	-23.50	cm	
	4371.0	-16151.0	-235.0	mm	
MM_CP7-60_20/07/14	696108.243	405749.972	0.127	m	Profile 2_Rod_MM
MM_59_14/08/2014	696108.451	405755.354	0.258	m	Profile 2_Rod_MM
	0.208	5.382	0.131	m	
	20.80	538.20	13.10	cm	
	208.0	5382.0	131.0	mm	
LM_CP7-79_20/07/14	696112.9	405688.6	-0.802	m	Profile 2_Rod_LM
LM_71_14/08/2014	696120.538	405714.632	-0.476	m	Profile 2_Rod_LM
	7.638	26.032	0.326	m	
	763.80	2603.20	32.60	cm	
	7638.0	26032.0	326.0	mm	
HS_CP7-81_20/07/14	695982.5	405668.2	-0.733	m	Profile 3_Rod_HS
HS__14/08/2014				m	Profile 3_Rod_HS
	-695982.5	-405668.2	0.733	m	
	-69598250.00	-40566820.00	73.30	cm	
	-695982500.0	-405668200.0	733.0	mm	
MS_CP7-60_20/07/14	696108.243	405749.972	0.127	m	Profile 2_Rod_MS
MS_59_14/08/2014	696108.451	405755.354	0.258	m	Profile 2_Rod_MM
	0.208	5.382	0.131	m	
	20.80	538.20	13.10	cm	
	208.0	5382.0	131.0	mm	
LS_CP7-79_20/07/14	696112.9	405688.6	-0.802	m	Profile 2_Rod_LS
LS_71_14/08/2014	696120.538	405714.632	-0.476	m	Profile 2_Rod_LS
	7.638	26.032	0.326	m	
	763.80	2603.20	32.60	cm	
	7638.0	26032.0	326.0	mm	
BM2_FRONT_2014	696170.656	405880.579	6.901	m	2014 data
BM2_front_msl	696170.674	405880.609	6.917	m	2013 data
	0.018	0.03	0.016	m	
	1.80	3.00	1.60	cm	
	18.0	30.0	16.0	mm	
BW_BS_SHORT	696182.186	405882.273	8.349	m	Mark used by Justy in testing Total Station

BEIG	696752.213	407766.584	7.8	m	Linz mark, calibrated to point
OCP_CHECK_START1	696752.215	407766.58	7.796	m	Start of survey check, calibration accurate to 4mm in vertical (observed control point)
	0.002	**-0.004**	**-0.004**	**m**	
	0.20	**-0.40**	**-0.40**	**cm**	
	2.0	**-4.0**	**-4.0**	**mm**	
BEIG	696752.213	407766.584	7.8	m	Linz mark, calibrated to point
BEIG_OCP_END	696752.214	407766.582	7.822	m	End survey observed control point
	0.001	**-0.002**	**0.022**	**m**	
	0.10	**-0.20**	**2.20**	**cm**	
	1.0	**-2.0**	**22.0**	**mm**	
BEIG	696752.213	407766.584	7.8	m	Linz mark
BEIG_TP_END	696752.208	407766.581	7.809	m	Topo point as a check at end of survey
	-0.005	**-0.003**	**0.009**	**m**	
	-0.50	**-0.30**	**0.90**	**cm**	
	-5.0	**-3.0**	**9.0**	**mm**	
CP7_BW_2014	696202.239	405897.6	10.328	m	2014 data
cp7_bw_msl	696202.25	405897.611	10.368	m	2013 data
	0.011	**0.011**	**0.04**	**m**	
	1.10	**1.10**	**4.00**	**cm**	
	11.0	**11.0**	**40.0**	**mm**	
CP7_BW_2014	696202.239	405897.6	10.328	m	Observed control point data 2014
CP7_BW_2014_TP2	696202.233	405897.601	10.331	m	Topo point data check 2014
	-0.006	**0.001**	**0.003**	**m**	
	-0.60	**0.10**	**0.30**	**cm**	
	-6.0	**1.0**	**3.0**	**mm**	
T2_2014	696163.978	405856.857	6.143	m	Measured mark 28th July 2014
GW_marker2	696163.998	405856.874	6.167	m	Mark established for GW experiment
	0.02	**0.017**	**0.024**	**m**	
	2.00	**1.70**	**2.40**	**cm**	
	20.0	**17.0**	**24.0**	**mm**	
T2_2014	696163.978	405856.857	6.143	m	Observed control point data 2014
T2_2014_TP_CHECK	696163.999	405856.853	6.142	m	Topo point data check 2014
	0.021	**-0.004**	**-0.001**	**m**	
	2.10	**-0.40**	**-0.10**	**cm**	
	21.0	**-4.0**	**-1.0**	**mm**	
BM3_FRONT_2014	695987.04	405787.985	6.386	**m**	2014 data
BM3_front_msl	695987.061	405788.017	6.393	**m**	2013 data
	0.021	**0.032**	**0.007**	**m**	
	2.10	**3.20**	**0.70**	**cm**	
	21.0	**32.0**	**7.0**	**mm**	
BM3_FRONT_2014	695987.04	405787.985	6.386	**m**	Observed control point data 2014
BM3_FRONT2014_TP	695987.033	405787.992	6.389	**m**	Topo point data check 2014
	-0.007	**0.007**	**0.003**	**m**	
	-0.70	**0.70**	**0.30**	**cm**	
	-7.0	**7.0**	**3.0**	**mm**	
BM2_FRONT_2014	696170.656	405880.579	6.901	**m**	2014 data
BM2_front_msl	696170.674	405880.609	6.917	**m**	2013 data
	0.018	**0.03**	**0.016**	**m**	
	1.80	**3.00**	**1.60**	**cm**	
	18.0	**30.0**	**16.0**	**mm**	
CP18_2014	697251.493	407804.173	4.493	**m**	2014 data
cp18_air_msl	697251.505	407804.17	4.493	**m**	2013 data
	0.012	**-0.003**	**0**	**m**	
	1.20	**-0.30**	**0.00**	**cm**	
	12.0	**-3.0**	**0.0**	**mm**	
CP19_2014	697258.652	408113.423	3.248	**m**	Observed control point data
CP19_2014_TOPO	697258.649	408113.423	3.246	**m**	Quick topo point for data check
	-0.003	**0**	**-0.002**	**m**	
	-0.30	**0.00**	**-0.20**	**cm**	
	-3.0	**0.0**	**-2.0**	**mm**	
BW_BS_SHORT	696182.186	405882.273	8.349	**m**	Mark used by Justy in testing Total Station

T2_Amir_30/08/2014	696163.978	405856.857	6.143	m	Measured mark 30th August 2014
GW_marker_T2_2014	696163.978	405856.857	6.143	m	Mark established for GW experiment
	0	**0**	**0**	**m**	
	0.00	**0.00**	**0.00**	**cm**	
	0.0	**0.0**	**0.0**	**mm**	
BM3_from report	695987.061	405788.017	6.393	m	Observed control point data
BM3__30/08/2014	695987.061	405788.017	6.393	m	Survey back site used - (BM3 in TS)
	0	**0**	**0**	**m**	
	0.00	**0.00**	**0.00**	**cm**	
	0.0	**0.0**	**0.0**	**mm**	
HN_99_29/08/2014	696242.586	405825.932	2.17	m	Profile 1_Rod_HN
HN_93_30/08/2014	696241.663	405829.188	1.16	m	Profile 1_Rod_HN
	-0.923	**3.256**	**-1.01**	**m**	
	-92.30	**325.60**	**-101.00**	**cm**	
	-923.0	**3256.0**	**-1010.0**	**mm**	
MN_83_29/08/2014	696258.881	405787.041	1.139	m	Profile 1_Rod_MN
MN_80_30/08/2014	696258.822	405786.916	0.02	m	Profile 1_Rod_MN
	-0.059	**-0.125**	**-1.119**	**m**	
	-5.90	**-12.50**	**-111.90**	**cm**	
	-59.0	**-125.0**	**-1119.0**	**mm**	
LN_61_29/08/2014	696275.207	405736.378	0.453	m	Profile 1_Rod_LN
LN_61_30/08/2014	696274.819	405736.177	-0.643	m	Profile 1_Rod_LN
	-0.388	**-0.201**	**-1.096**	**m**	
	-38.80	**-20.10**	**-109.60**	**cm**	
	-388.0	**-201.0**	**-1096.0**	**mm**	
HM_36_29/08/2014	696097.732	405795.24	2.741	m	Profile 2_Rod_HM
HM_60_30/08/2014	696097.875	405795.06	1.637	m	Profile 2_Rod_HM
	0.143	**-0.18**	**-1.104**	**m**	
	14.30	**-18.00**	**-110.40**	**cm**	
	143.0	**-180.0**	**-1104.0**	**mm**	
MM_48_29/08/2014	696118.814	405753.664	1.251	m	Profile 2_Rod_MM
MM_46_30/08/2014	696119.036	405753.544	0.133	m	Profile 2_Rod_MM
	0.222	**-0.12**	**-1.118**	**m**	
	22.20	**-12.00**	**-111.80**	**cm**	
	222.0	**-120.0**	**-1118.0**	**mm**	
LM_60_29/08/2014	696139.394	405712.489	0.438	**m**	Profile 2_Rod_LM
LM_33_30/08/2014	696139.508	405712.435	-0.663	**m**	Profile 2_Rod_LM
	0.114	**-0.054**	**-1.101**	**m**	
	11.40	**-5.40**	**-110.10**	**cm**	
	114.0	**-54.0**	**-1101.0**	**mm**	
HS_103_29/08/2014	696004.767	405753.868	2.56	**m**	Profile 3_Rod_HS
HS_4_30/08/2014	696004.949	405753.555	1.54	**m**	Profile 3_Rod_HS
	0.182	**-0.313**	**-1.02**	**m**	
	18.20	**-31.30**	**-102.00**	**cm**	
	182.0	**-313.0**	**-1020.0**	**mm**	
MS_17_29/08/2014	696017.1	405721.1	1.324	**m**	Profile 3_Rod_MS
MS_11_30/08/2014	696017.5	405729.8	0.448	**m**	Profile 3_Rod_MS
	0.4	**8.7**	**-0.876**	**m**	
	40.00	**870.00**	**-87.60**	**cm**	
	400.0	**8700.0**	**-876.0**	**mm**	
LS_35_29/08/2014	696049.239	405663.637	0.169	**m**	Profile 3_Rod_LS
LS_31_30/08/2014	696048.253	405662.828	-0.976	**m**	Profile 3_Rod_LS
	-0.986	**-0.809**	**-1.145**	**m**	
	-98.60	**-80.90**	**-114.50**	**cm**	
	-986.0	**-809.0**	**-1145.0**	**mm**	

START OF SURVEY CHECKS

BEIG	linz mark	696752.21	407766.58	7.80	m	LINZ MARK
beig_checkstart1		696752.21	407766.59	7.80	m	Measured mark using GPS
		0.00	**0.00**	**0.00**	**m**	
		-0.10	**0.10**	**0.30**	**cm**	
		-1.00	**1.00**	**3.00**	**mm**	

BEIG	linz mark	696752.21	407766.58	7.80	m	LINZ MARK
beig_checkstart2		696752.21	407766.58	7.80	m	Measured mark using GPS
		0.00	**0.00**	**0.00**	**m**	
		-0.20	**-0.20**	**0.00**	**cm**	
		-2.00	**-2.00**	**0.00**	**mm**	

BEIG	linz mark	696752.21	407766.58	7.80	m	LINZ MARK
beig_checkstart3		696752.21	407766.59	7.79	m	Measured mark using GPS
		0.00	**0.00**	**-0.01**	**m**	
		0.00	**0.20**	**-0.80**	**cm**	
		0.00	**2.00**	**-8.00**	**mm**	

BEIG	linz mark	696752.21	407766.58	7.80	m	LINZ MARK
beig_checkend0		696752.22	407766.60	7.88	m	Measured mark using GPS
		0.01	**0.02**	**0.08**	**m**	
		0.80	**1.90**	**7.60**	**cm**	
		8.00	**19.00**	**76.00**	**mm**	

BEIG	linz mark	696752.21	407766.58	7.80	m	LINZ MARK
beig_checkend1		696752.2	407766.6	7.853	m	Measured mark using GPS
		0.01	**0.02**	**0.05**	**m**	
		0.70	**2.00**	**5.30**	**cm**	
		7.00	**20.00**	**53.00**	**mm**	

BEIG	linz mark	696752.21	407766.58	7.80	m	LINZ MARK
beig_checkend		696752.2	407766.6	7.847	m	Measured mark using GPS
		0.01	**0.02**	**0.05**	**m**	
		0.70	**1.80**	**4.70**	**cm**	
		7.00	**18.00**	**47.00**	**mm**	

APPENDIX IV: 3D PROFILES

IV.0 3D PROFILES OF NGARUNUI BEACH

3D profiles of Ngarunui Beach are presented below.

5th February 2015

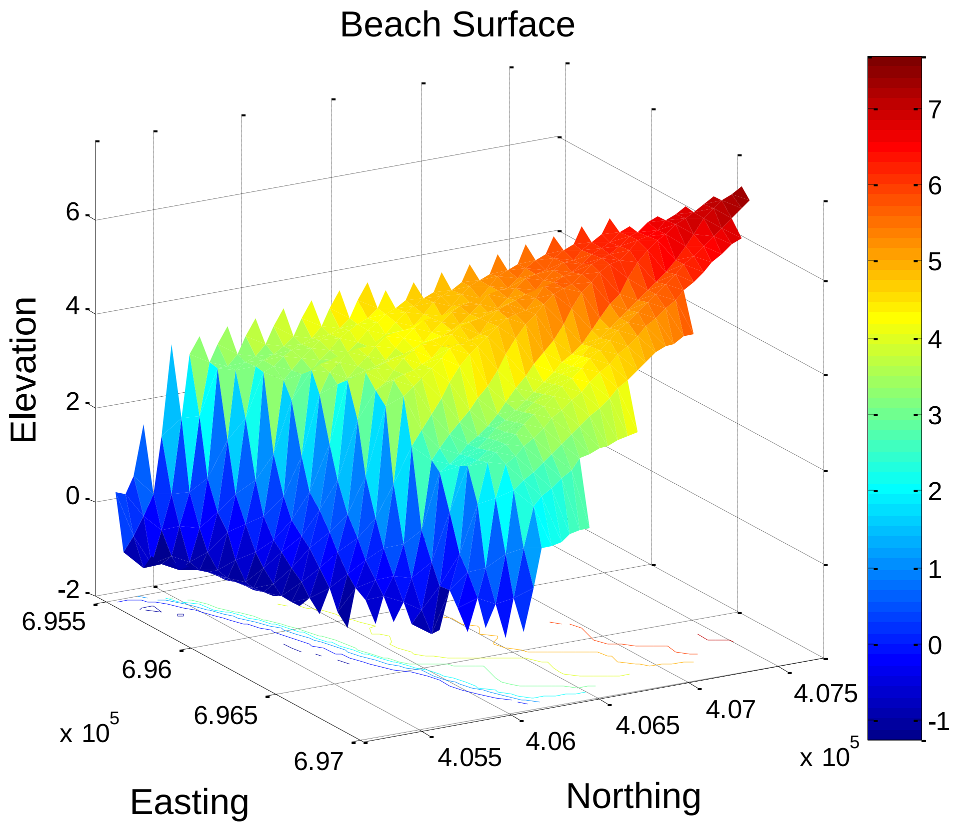

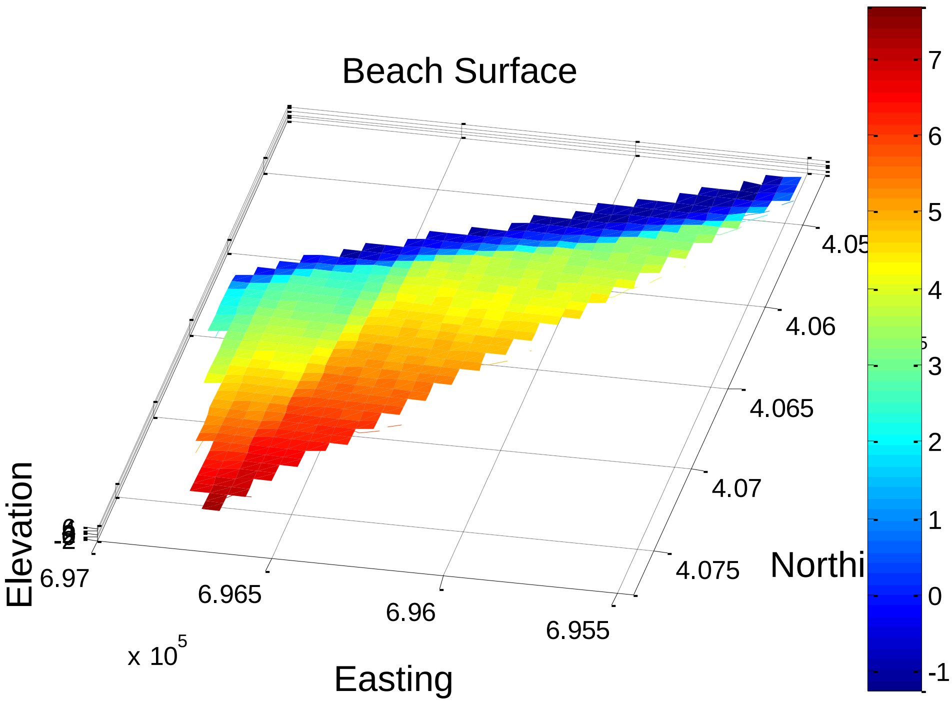
Beach Surface
Elevation
6.97
6.965
6.96
6.955
x 10^5
Easting
4.075
4.07
4.065
4.06
4.05
Northi
7
6
5
4
3
2
1
0
-1

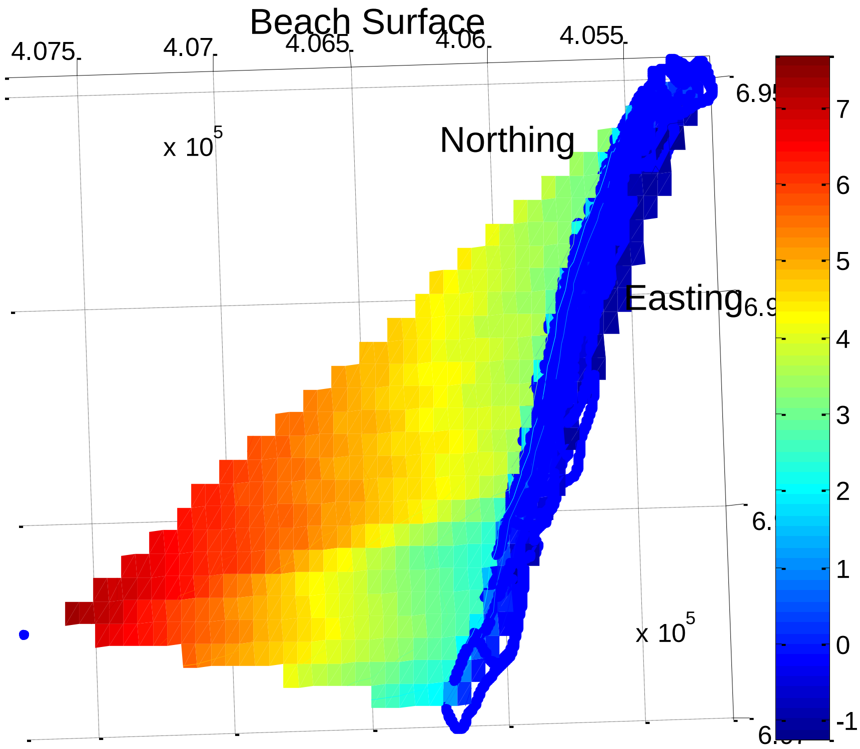
Beach Surface
4.075
4.07
4.065
4.06
4.055
x 10^5
Northing
Easting
x 10^5
7
6
5
4
3
2
1
0
-1

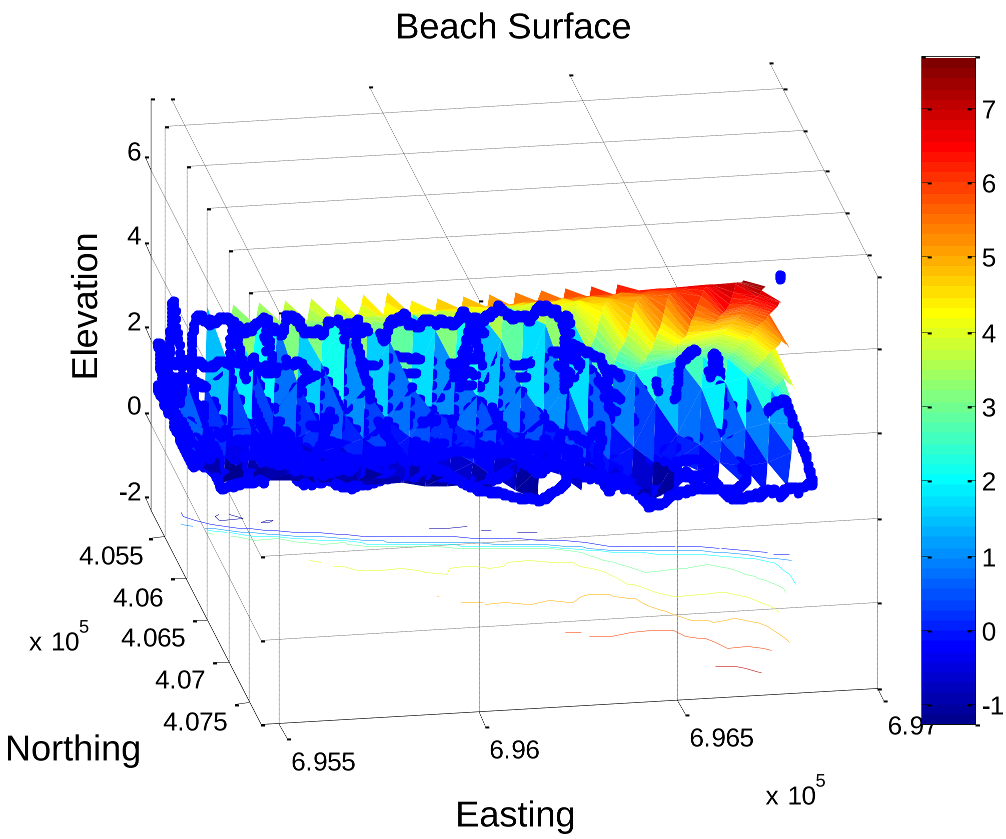
Beach Surface
Elevation
6
4
2
0
-2
4.055
4.06
x 10^5
4.065
4.07
4.075
Northing
6.955
6.96
6.965
6.97
x 10^5
Easting
7
6
5
4
3
2
1
0
-1

CP2

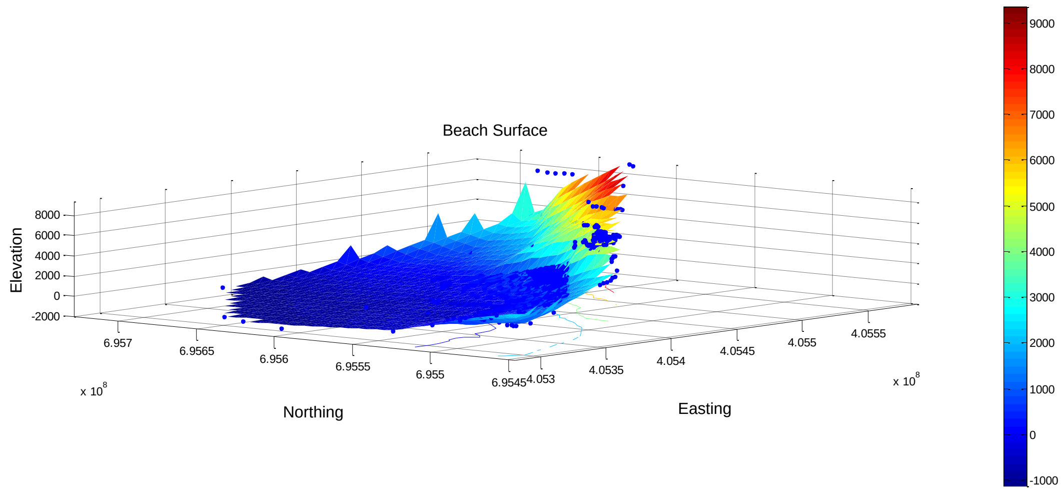
Beach Surface
Elevation
8000
6000
4000
2000
0
-2000
6.957
6.9565
6.956
6.9555
6.955
6.9545
x 10^8
Northing
4.053
4.0535
4.054
4.0545
4.055
4.0555
x 10^8
Easting
9000
8000
7000
6000
5000
4000
3000
2000
1000
0
-1000

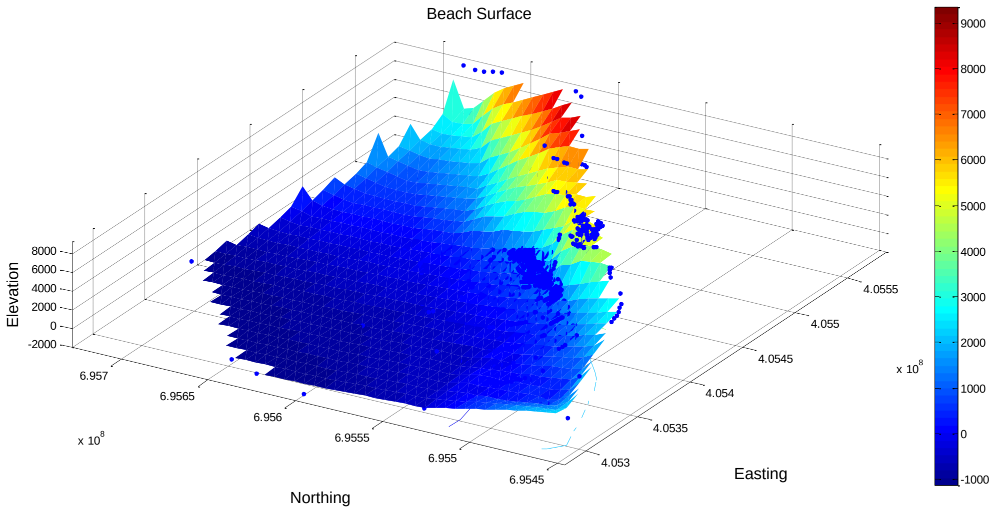
Beach Surface
Elevation
8000
6000
4000
2000
0
-2000
6.957
6.9565
6.956
6.9555
6.955
6.9545
x 10^8
Northing
4.053
4.0535
4.054
4.0545
4.055
4.0555
x 10^8
Easting
9000
8000
7000
6000
5000
4000
3000
2000
1000
0
-1000

VRS Beach

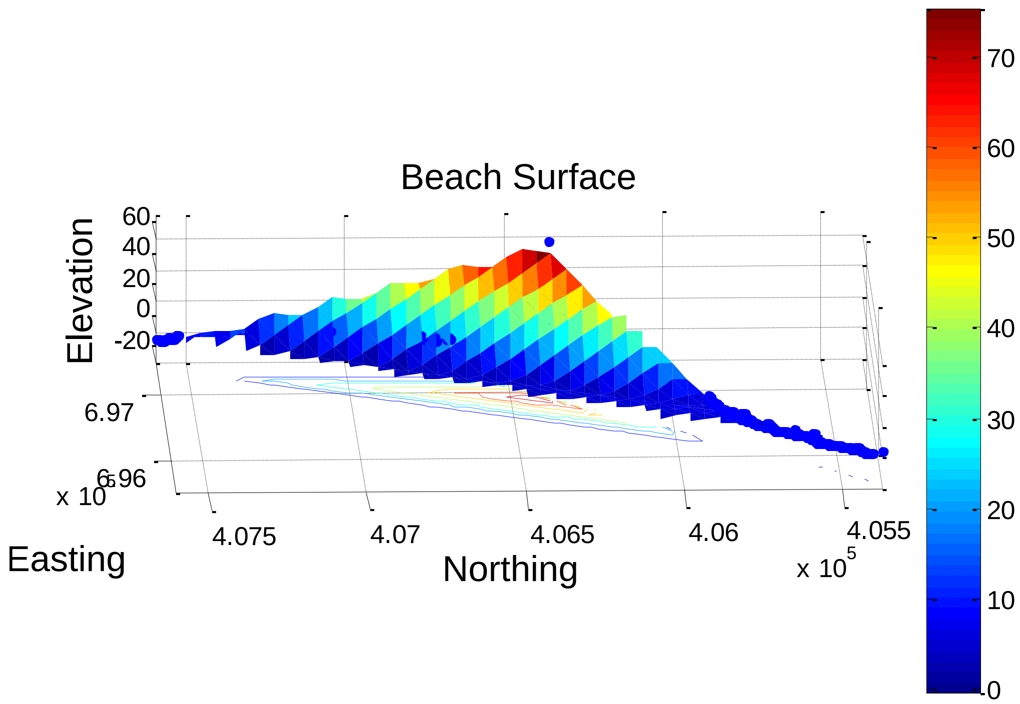
Beach Surface
Elevation
60
40
20
0
-20
6.97
6.96
x 10^5
Easting
4.075
4.07
4.065
4.06
4.055
Northing
x 10^5
70
60
50
40
30
20
10
0

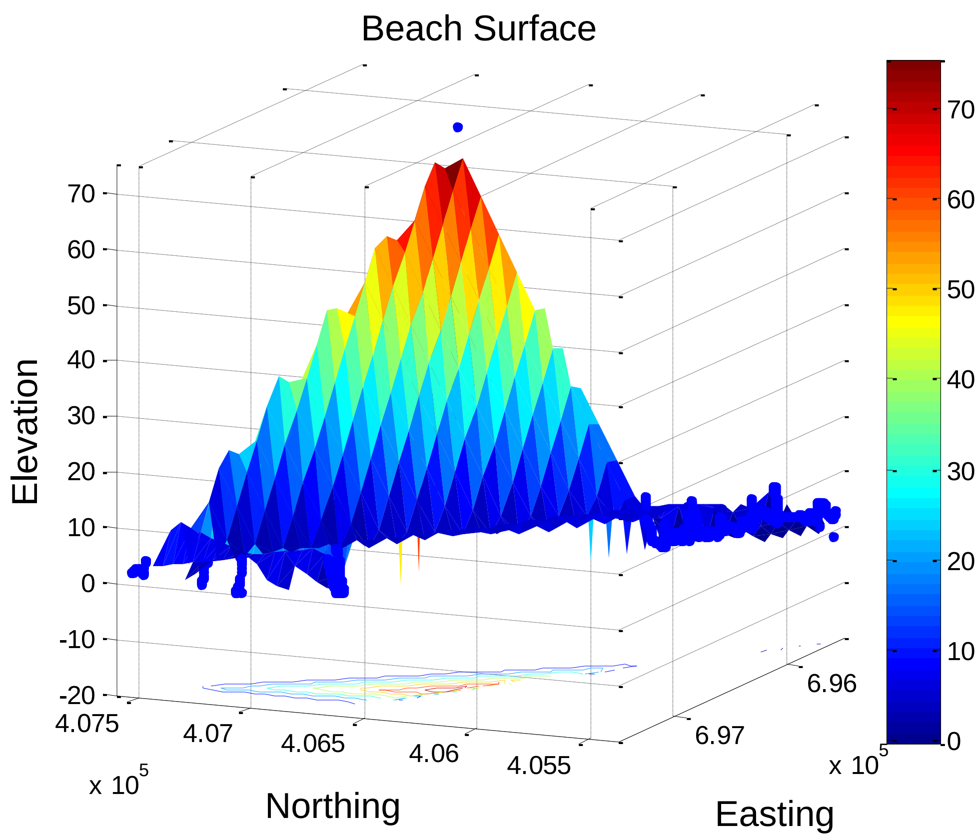
Beach Surface
Elevation
70
60
50
40
30
20
10
0
-10
-20
4.075
4.07
4.065
4.06
4.055
x 10^5
Northing
6.97
6.96
x 10^5
Easting
70
60
50
40
30
20
10
0

Transects

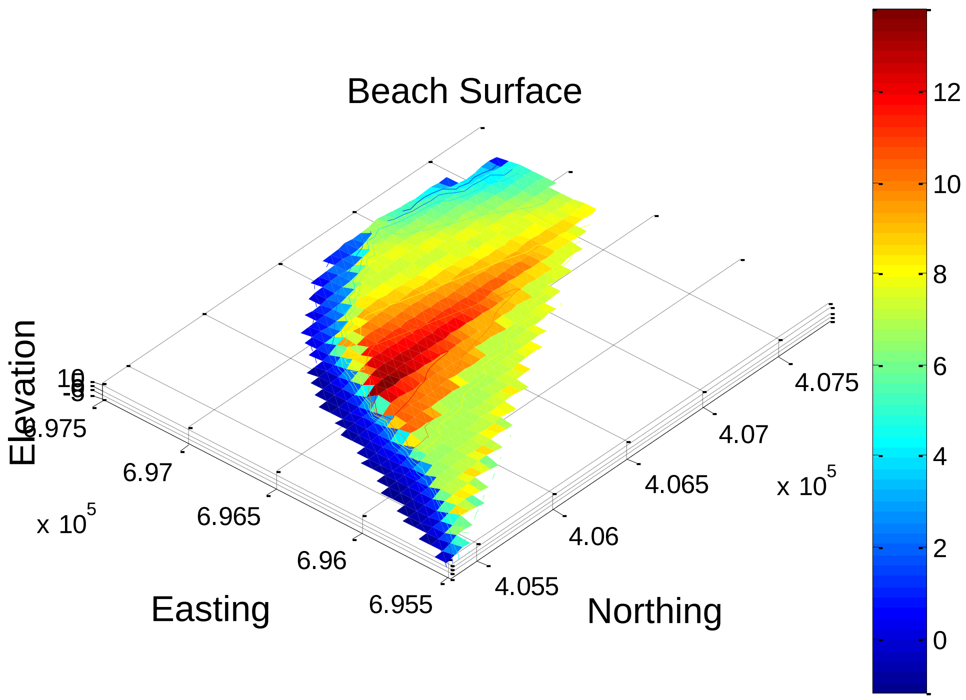
Beach Surface
Elevation
6.975
6.97
6.965
6.96
6.955
x 10^5
Easting
4.075
4.07
4.065
4.06
4.055
x 10^5
Northing
12
10
8
6
4
2
0

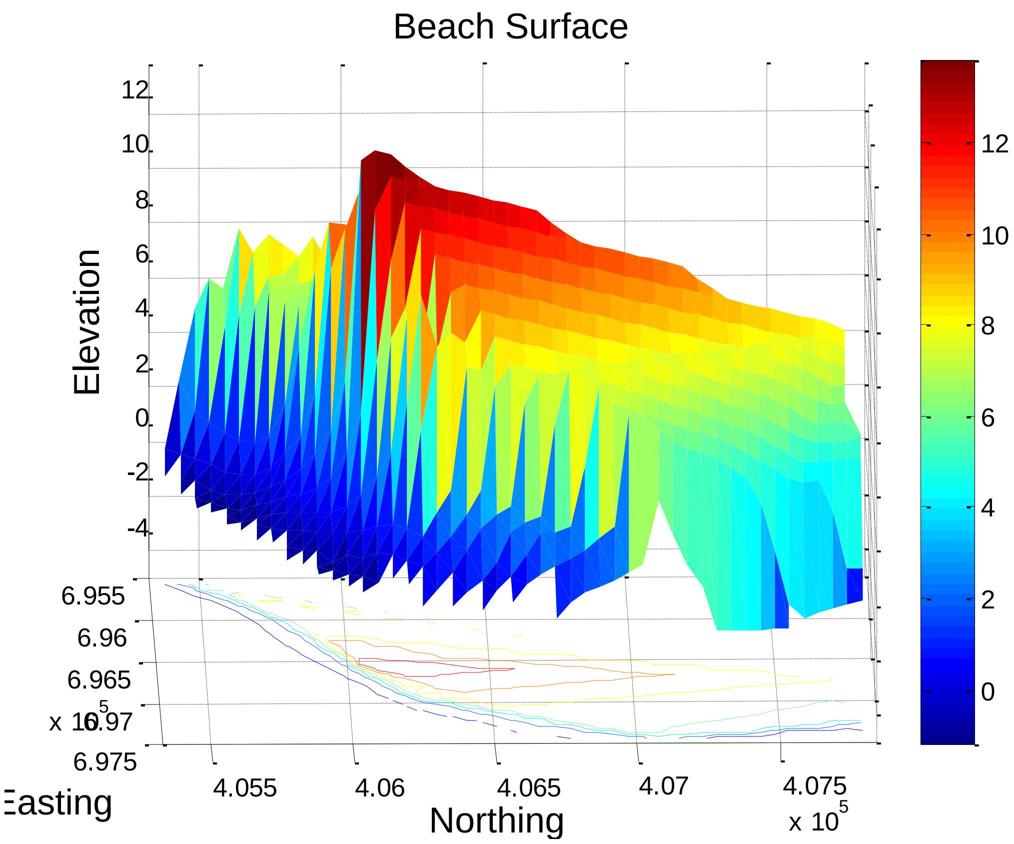
Beach Surface
Elevation
12
10
8
6
4
2
0
-2
-4
6.955
6.96
6.965
6.97
6.975
x 10^5
Easting
4.055
4.06
4.065
4.07
4.075
x 10^5
Northing
12
10
8
6
4
2
0

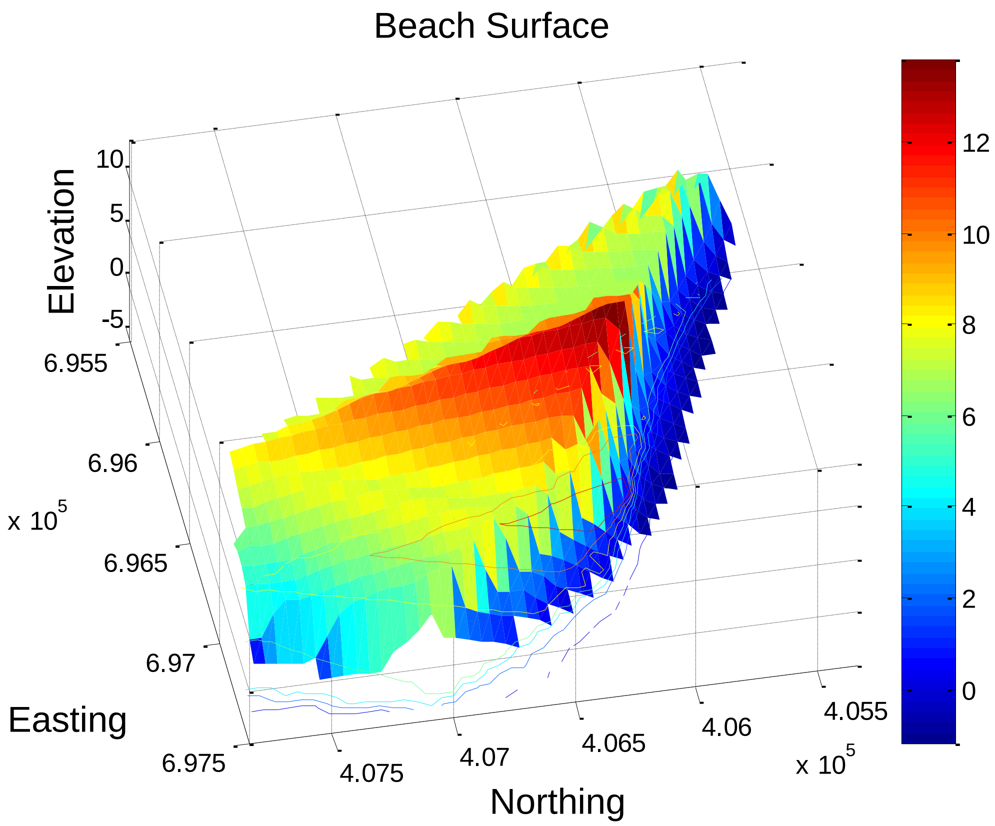
Beach Surface
Elevation
10
5
0
-5
6.955
6.96
6.965
6.97
6.975
x 10^5
Easting
4.075
4.07
4.065
4.06
4.055
x 10^5
Northing
12
10
8
6
4
2
0

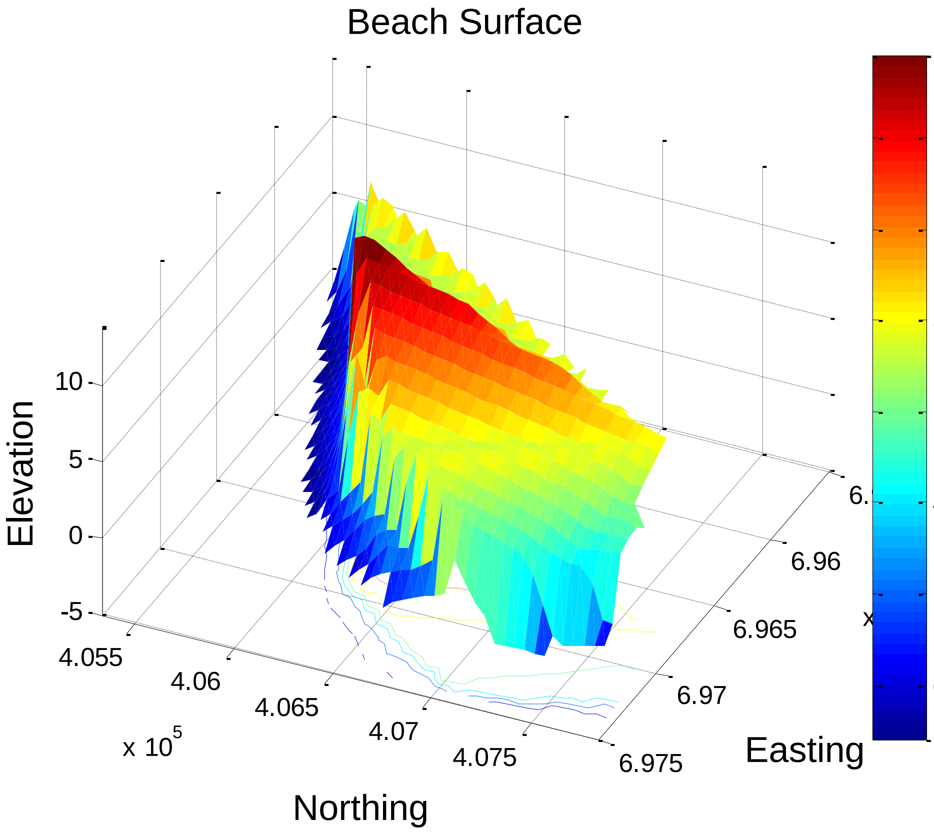
Beach Surface
Elevation
10
5
0
-5
4.055
4.06
4.065
4.07
4.075
x 10^5
Northing
6.96
6.965
6.97
6.975
Easting
12
10
8
6
4
2
0

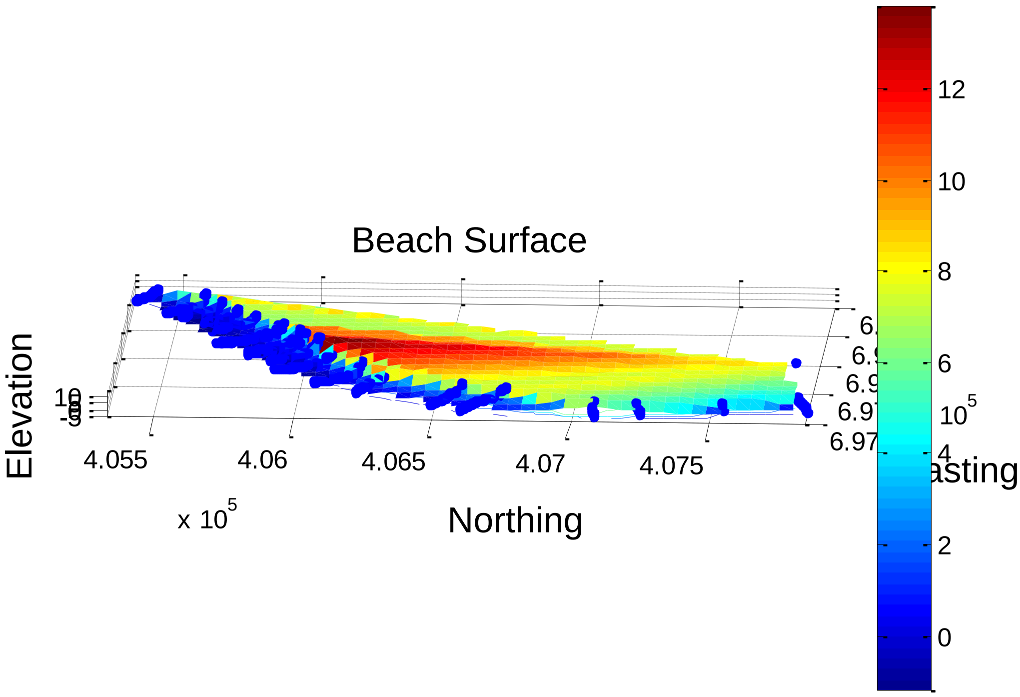
Beach Surface
Elevation
4.055
4.06
4.065
4.07
4.075
x 10^5
Northing
12
10
8
6
4
2
0

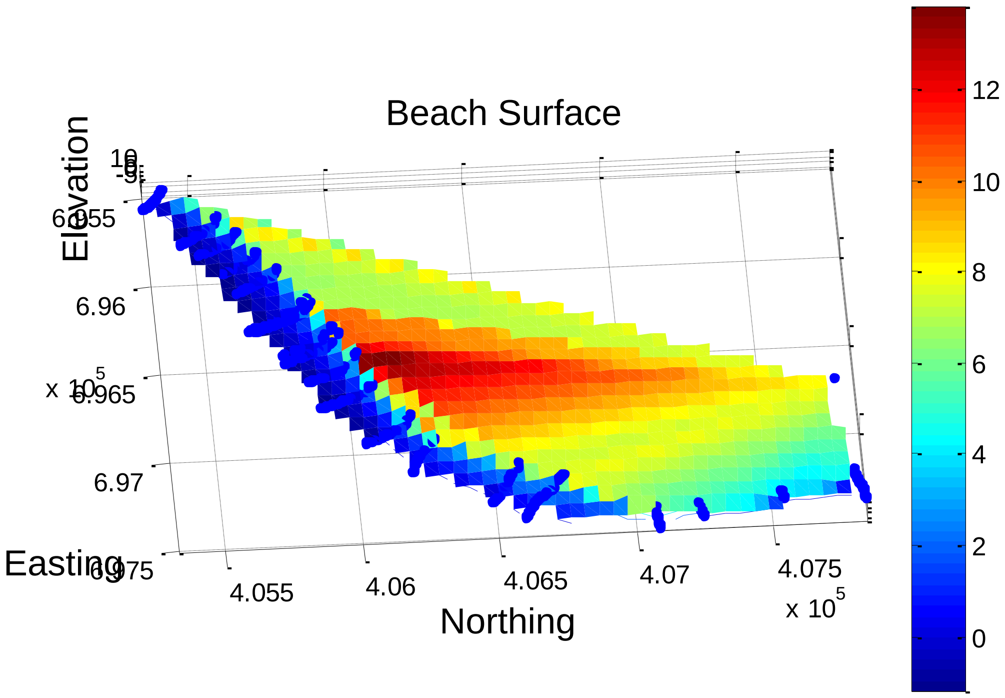

Beach Survey with Prism

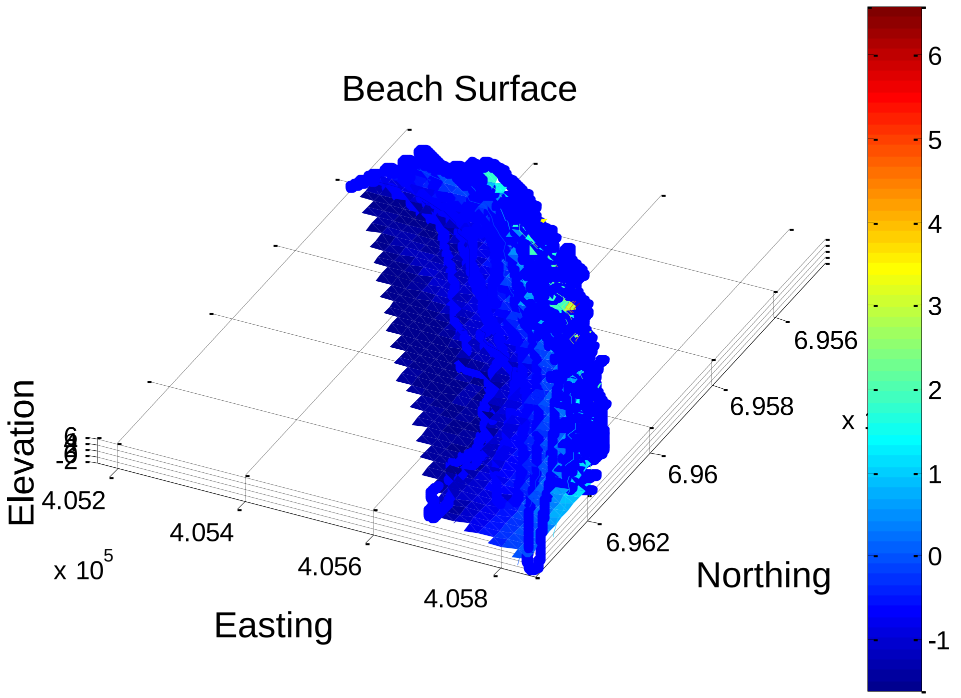

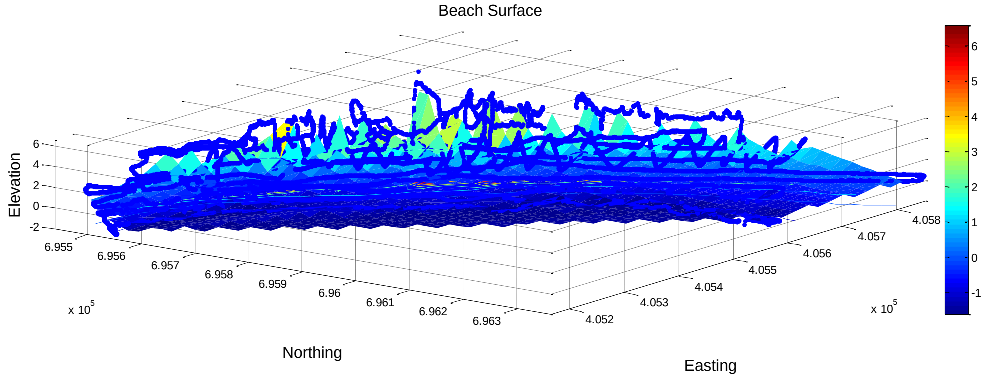

Beach Surface
Elevation
6
4
2
0
-2
6.955
6.956
6.957
6.958
6.959
6.96
6.961
6.962
6.963
x 10^5
Northing
4.052
4.053
4.054
4.055
4.056
4.057
4.058
x 10^5
Easting
6
5
4
3
2
1
0
-1

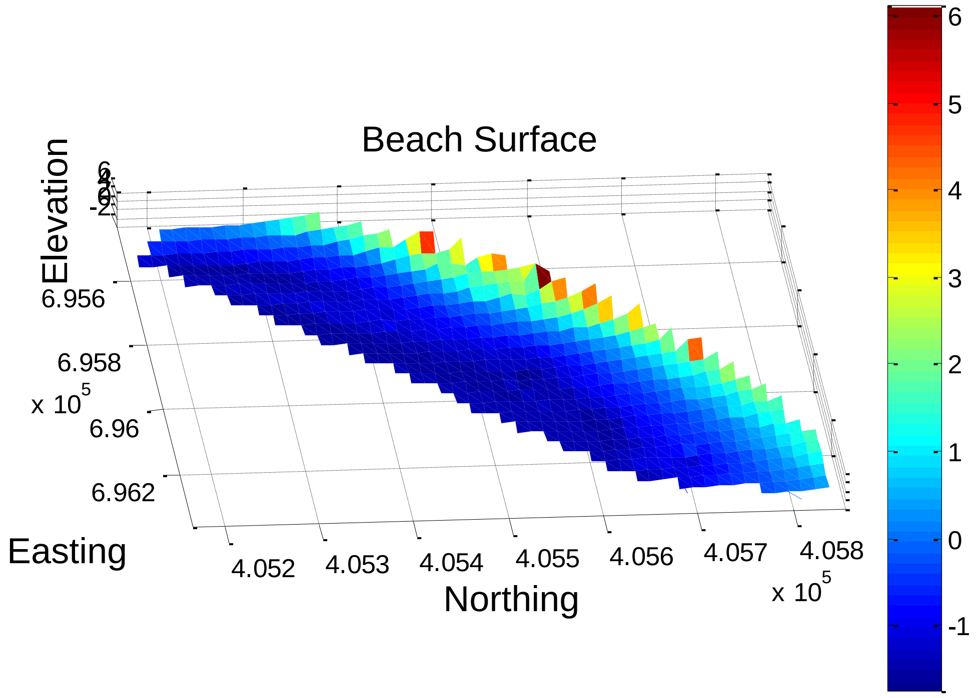

Beach Surface
Elevation
6.956
6.958
x 10^5
6.96
6.962
Easting
4.052
4.053
4.054
4.055
4.056
4.057
4.058
x 10^5
Northing
6
5
4
3
2
1
0
-1

Scan 57

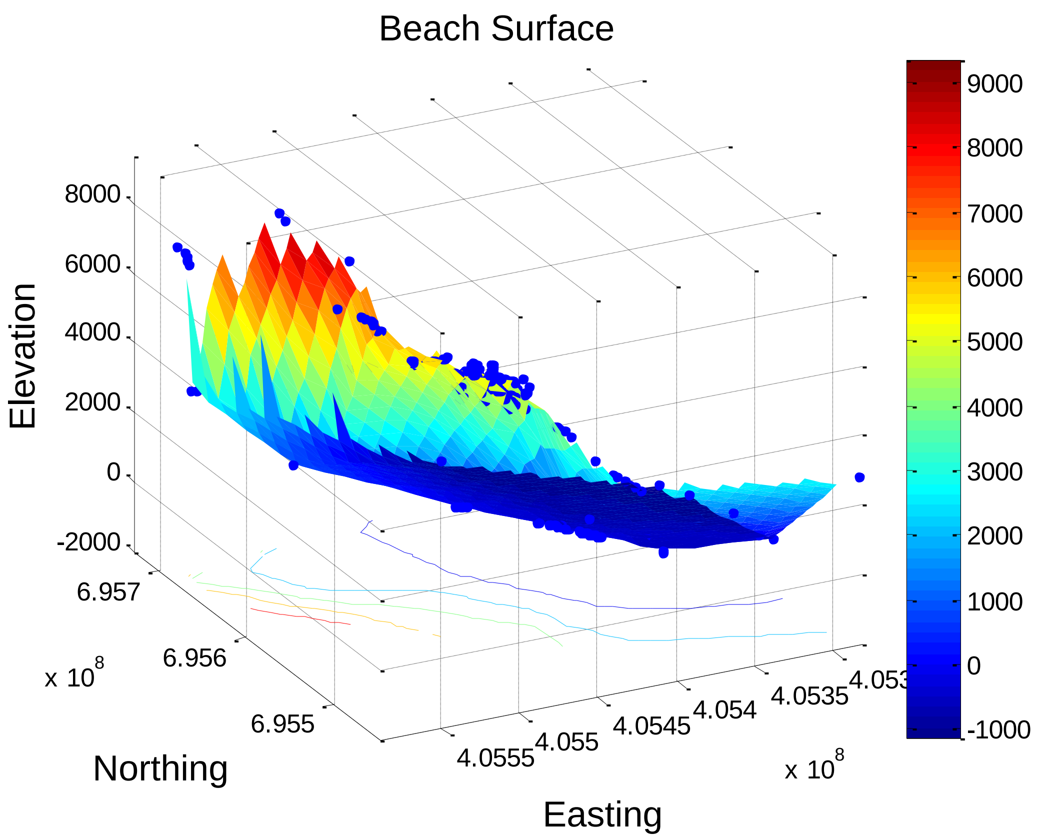

Scan 61

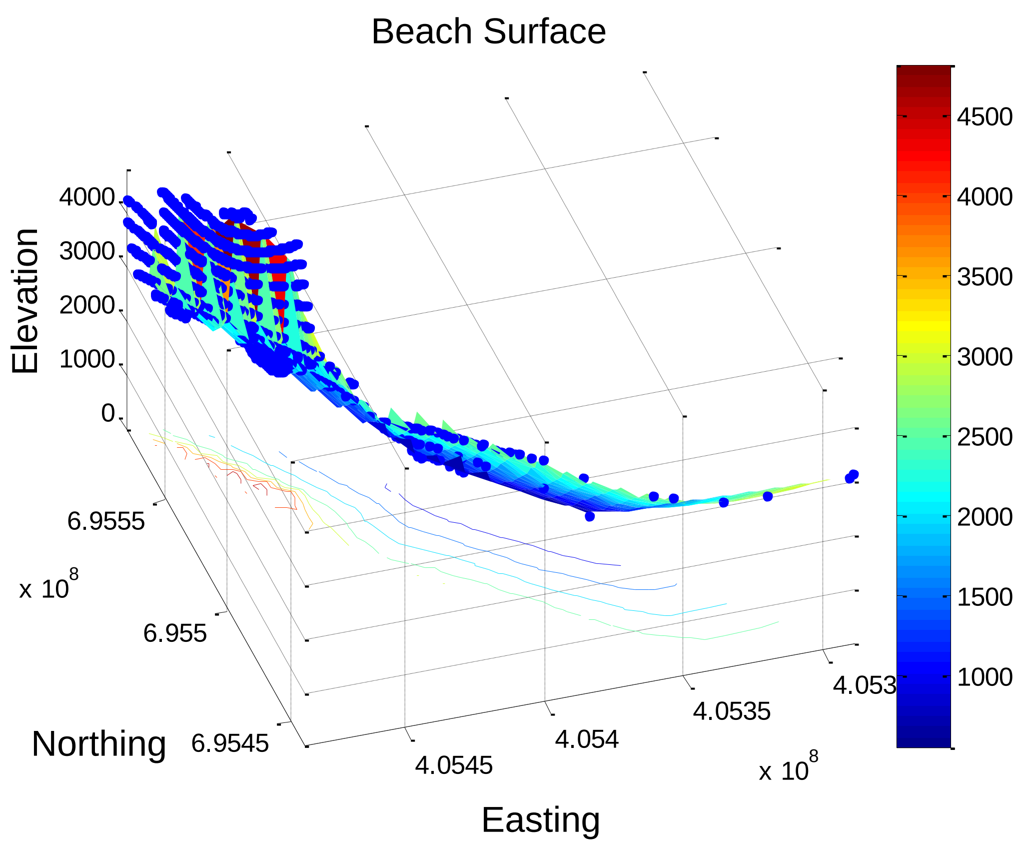

Scan 64

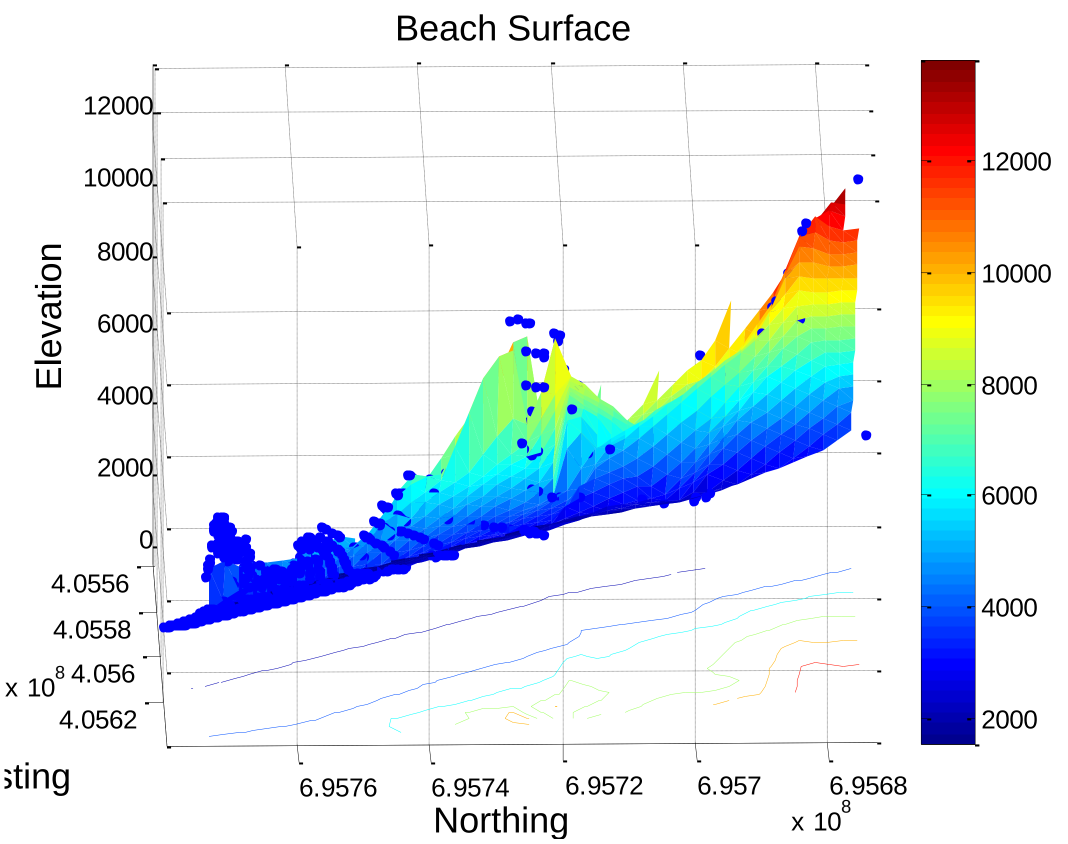
Beach Surface
Elevation
12000
10000
8000
6000
4000
2000
0
4.0556
4.0558
x 10^8 4.056
4.0562
sting
6.9576
6.9574
6.9572
6.957
6.9568
Northing
x 10^8
12000
10000
8000
6000
4000
2000

Scan 62

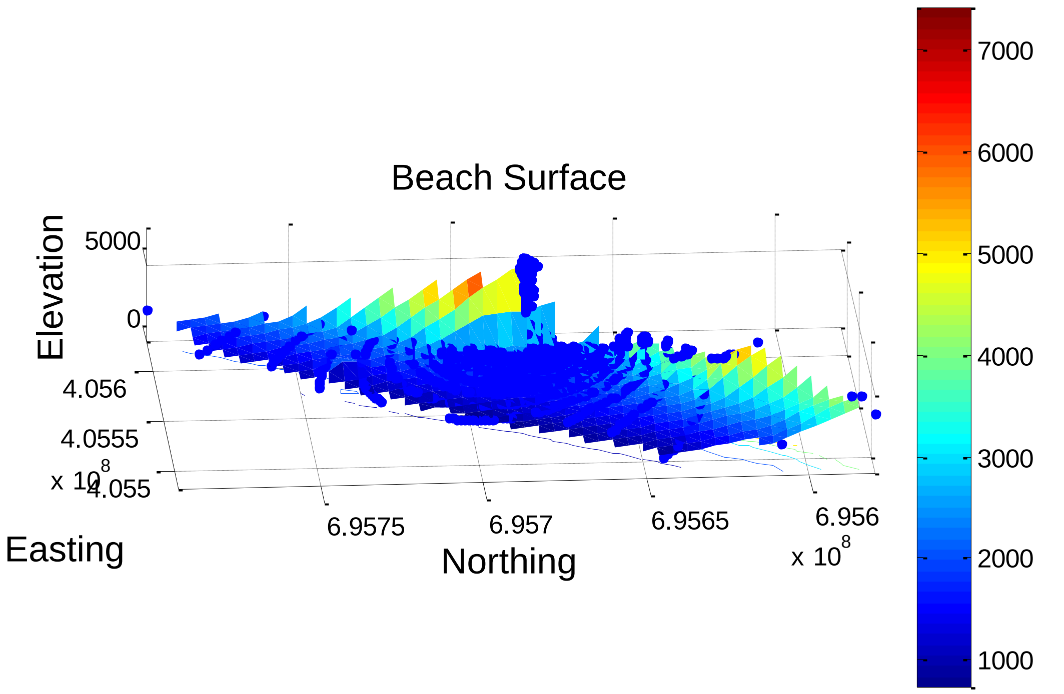
Beach Surface
Elevation
5000
0
4.056
4.0555
x 10^8 4.055
Easting
6.9575
6.957
6.9565
6.956
Northing
x 10^8
7000
6000
5000
4000
3000
2000
1000

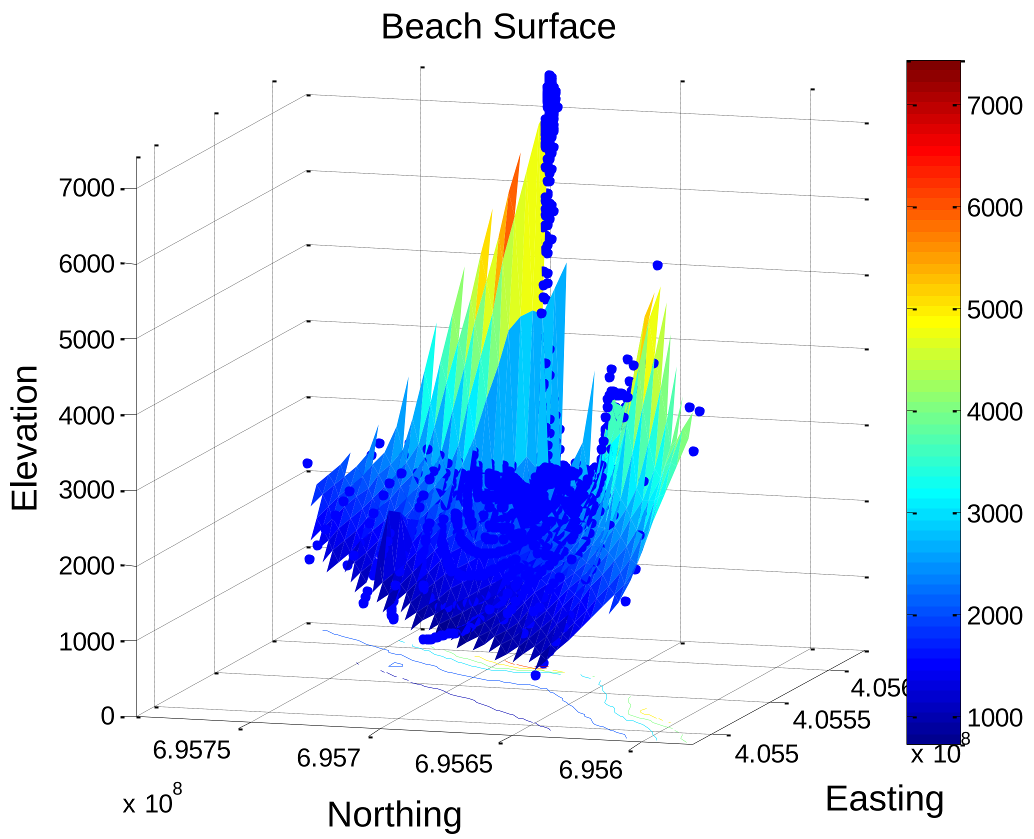
Beach Surface
Elevation
7000
6000
5000
4000
3000
2000
1000
0
6.9575
6.957
6.9565
6.956
x 10^8
Northing
4.055
4.0555
4.056
Easting
x 10^8

Scan 58 59 60

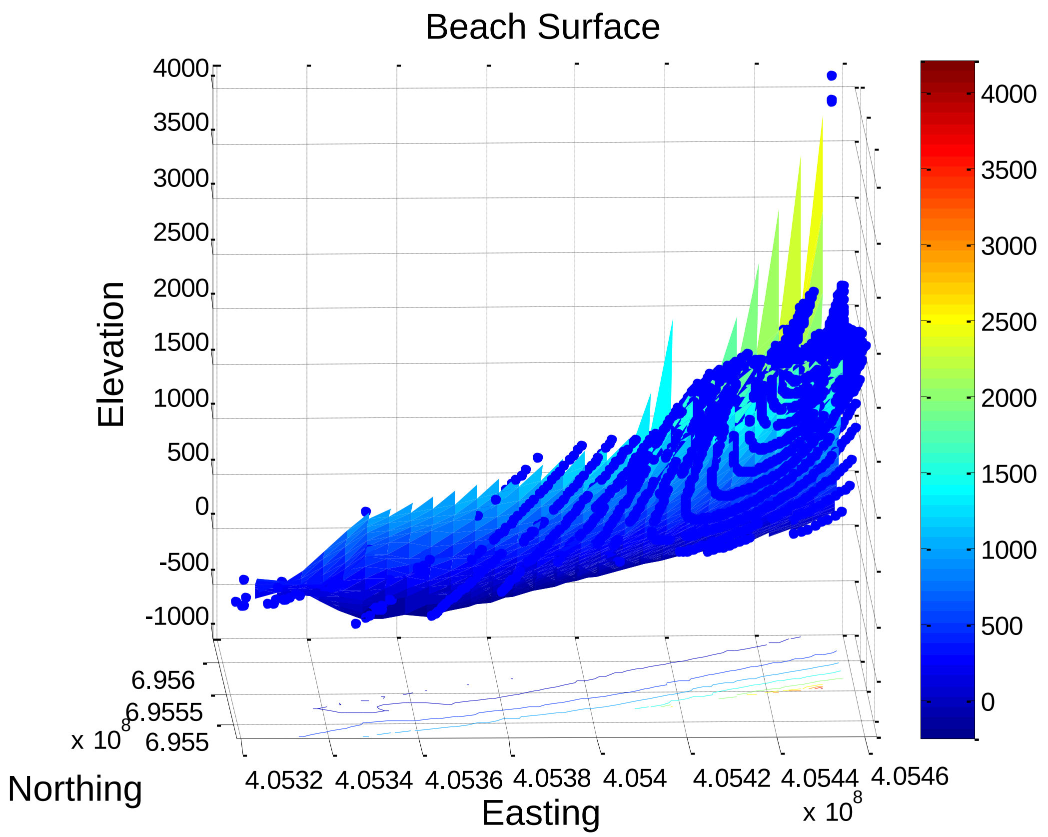
Beach Surface
Elevation
4000
3500
3000
2500
2000
1500
1000
500
0
-500
-1000
6.956
6.9555
6.955
x 10^8
Northing
4.0532
4.0534
4.0536
4.0538
4.054
4.0542
4.0544
4.0546
Easting
x 10^8

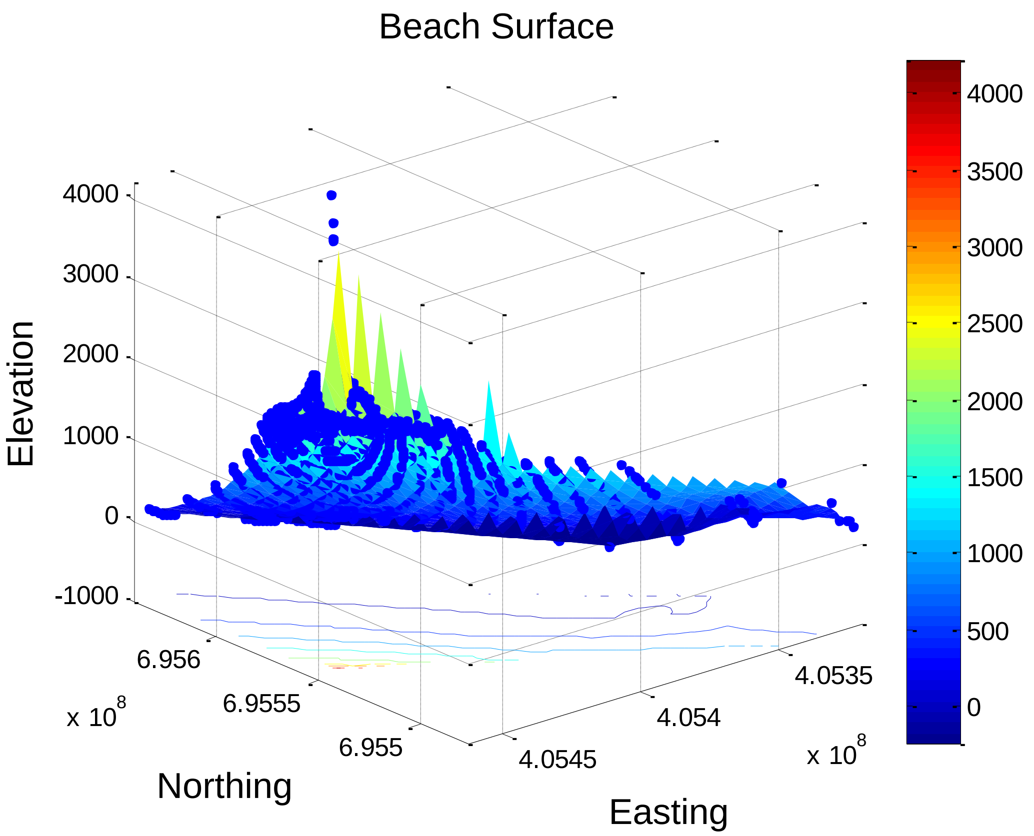
Beach Surface
Elevation
4000
3000
2000
1000
0
-1000
6.956
6.9555
6.955
x 10^8
Northing
4.0545
4.054
4.0535
x 10^8
Easting
4000
3500
3000
2500
2000
1500
1000
500
0

CP3

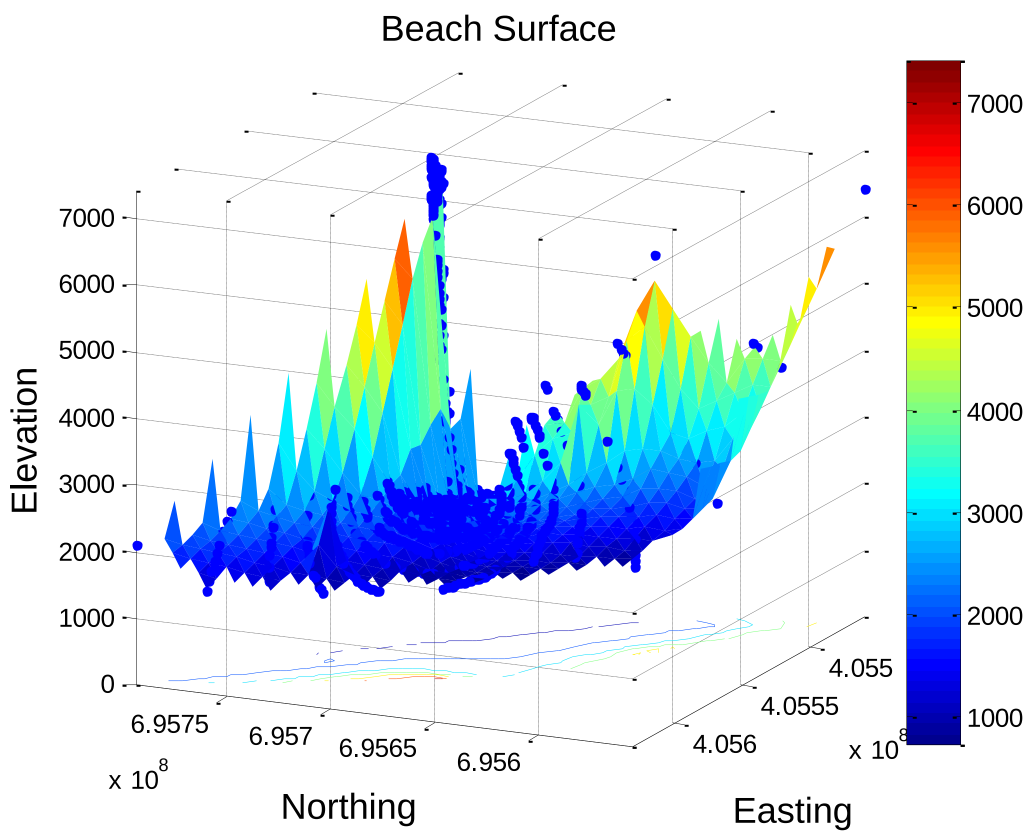
Beach Surface
Elevation
7000
6000
5000
4000
3000
2000
1000
0
6.9575
6.957
6.9565
6.956
x 10^8
Northing
4.056
4.0555
4.055
x 10^8
Easting
7000
6000
5000
4000
3000
2000
1000

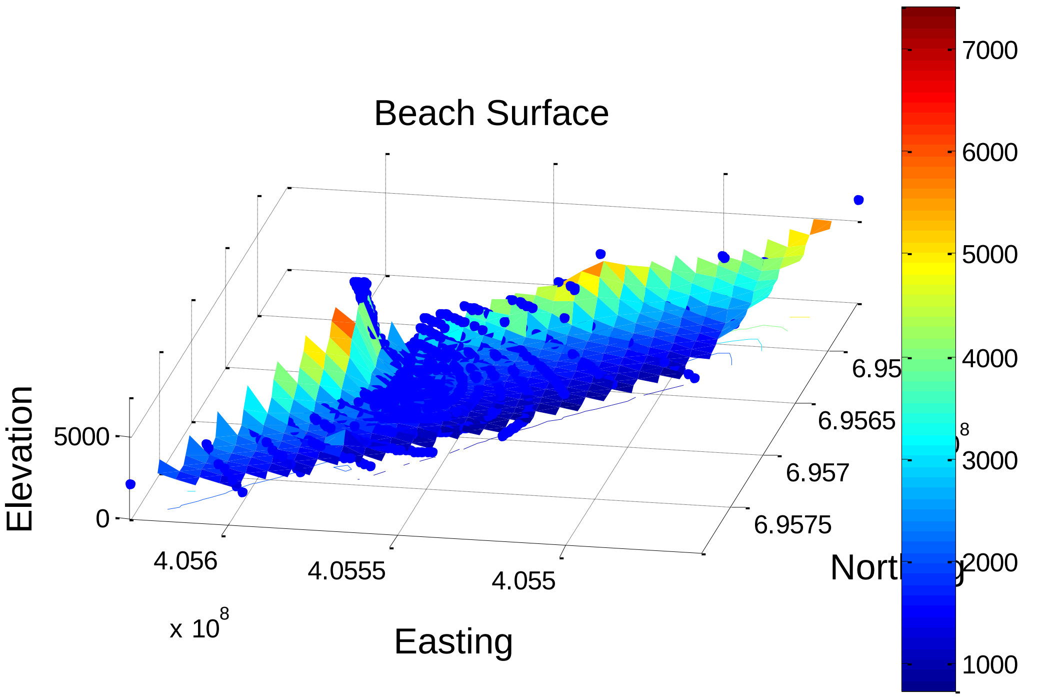
Beach Surface
Elevation
5000
0
4.056
4.0555
4.055
x 10^8
Easting
6.9565
6.957
6.9575
7000
6000
5000
4000
3000
2000
1000

CP4

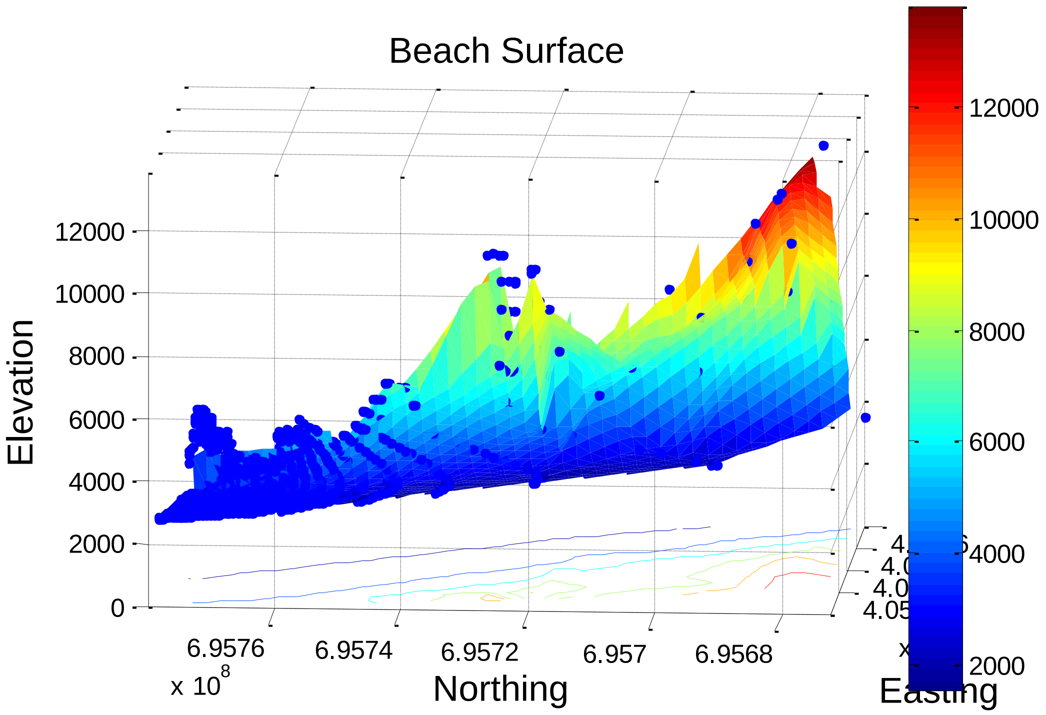
Beach Surface
Elevation
12000
10000
8000
6000
4000
2000
0
6.9576
6.9574
6.9572
6.957
6.9568
x 10^8
Northing
12000
10000
8000
6000
4000
2000

CP2aa

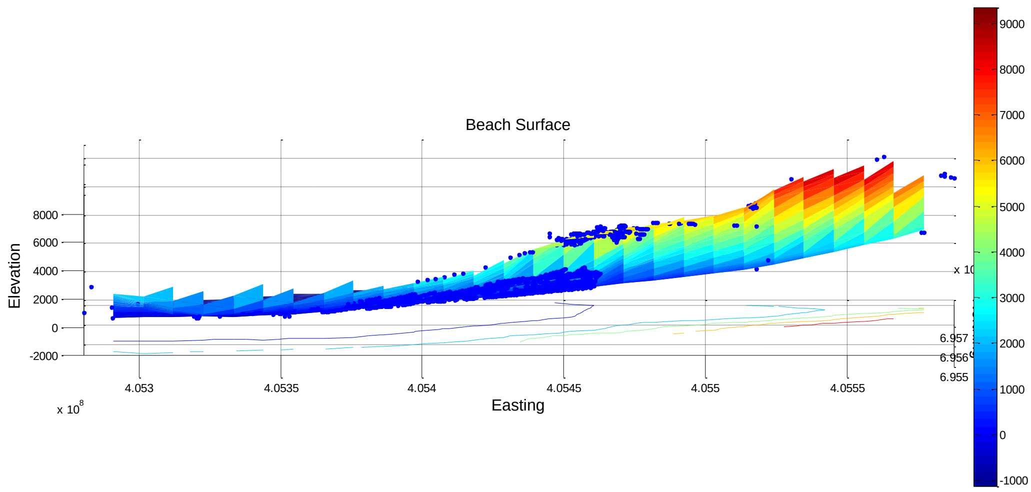
Beach Surface
Elevation
Easting
x 10^8
8000
6000
4000
2000
0
-2000
4.053
4.0535
4.054
4.0545
4.055
4.0555
6.957
6.956
6.955
9000
8000
7000
6000
5000
4000
3000
2000
1000
0
-1000

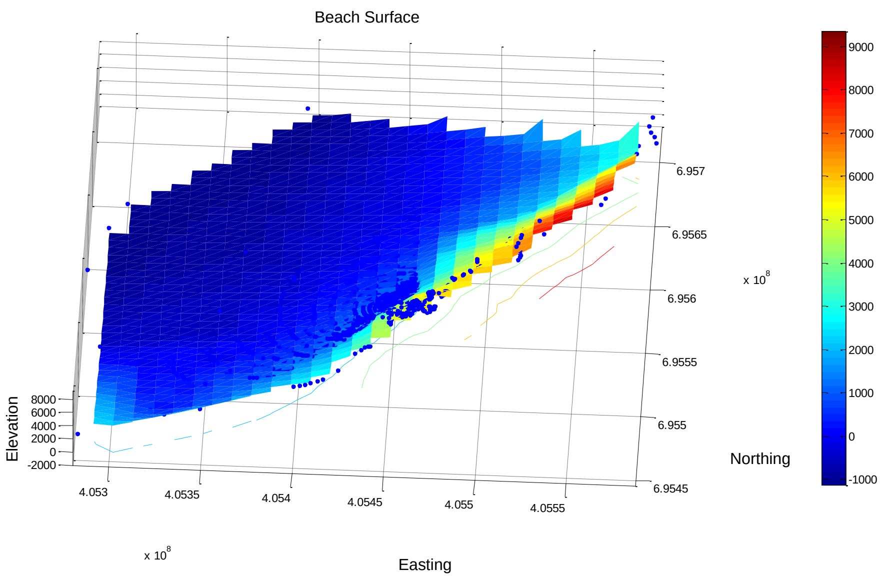
Beach Surface
Elevation
Easting
Northing
x 10^8
x 10^8
8000
6000
4000
2000
0
-2000
4.053
4.0535
4.054
4.0545
4.055
4.0555
6.957
6.9565
6.956
6.9555
6.955
6.9545
9000
8000
7000
6000
5000
4000
3000
2000
1000
0
-1000

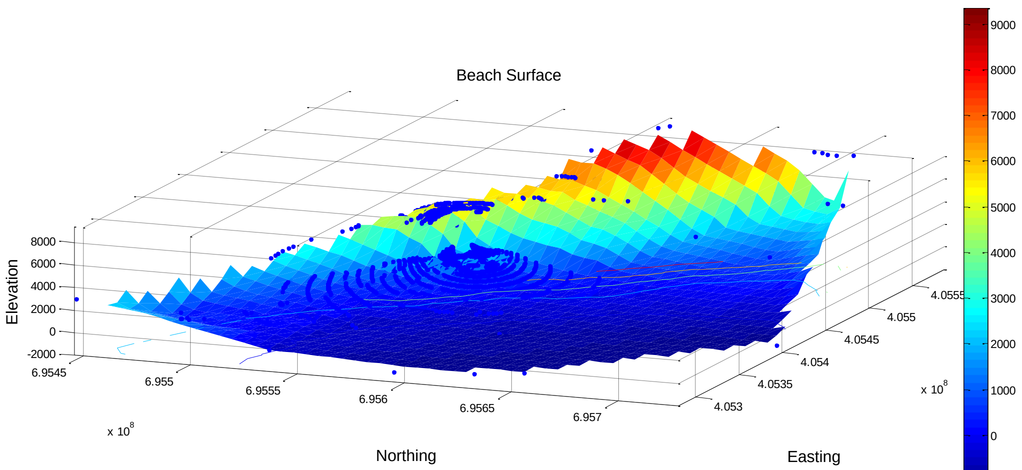
Beach Surface
Elevation
Northing
Easting
x 10^8
x 10^8
8000
6000
4000
2000
0
-2000
6.9545
6.955
6.9555
6.956
6.9565
6.957
4.053
4.0535
4.054
4.0545
4.055
4.0555
9000
8000
7000
6000
5000
4000
3000
2000
1000
0
-1000

CP2

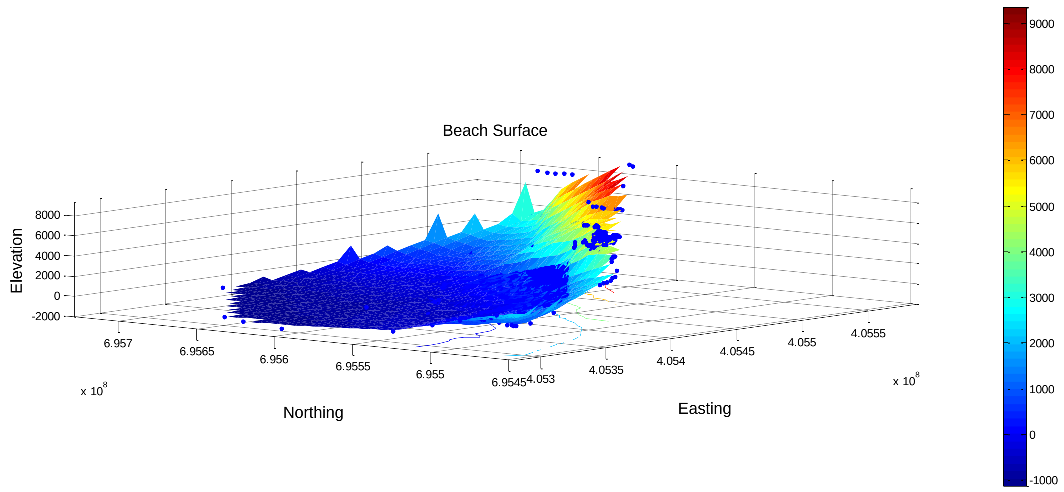
Beach Surface
Elevation
8000
6000
4000
2000
0
-2000
6.957
6.9565
6.956
6.9555
6.955
6.9545
x 10^8
Northing
4.053
4.0535
4.054
4.0545
4.055
4.0555
x 10^8
Easting
9000
8000
7000
6000
5000
4000
3000
2000
1000
0
-1000

CP Scans

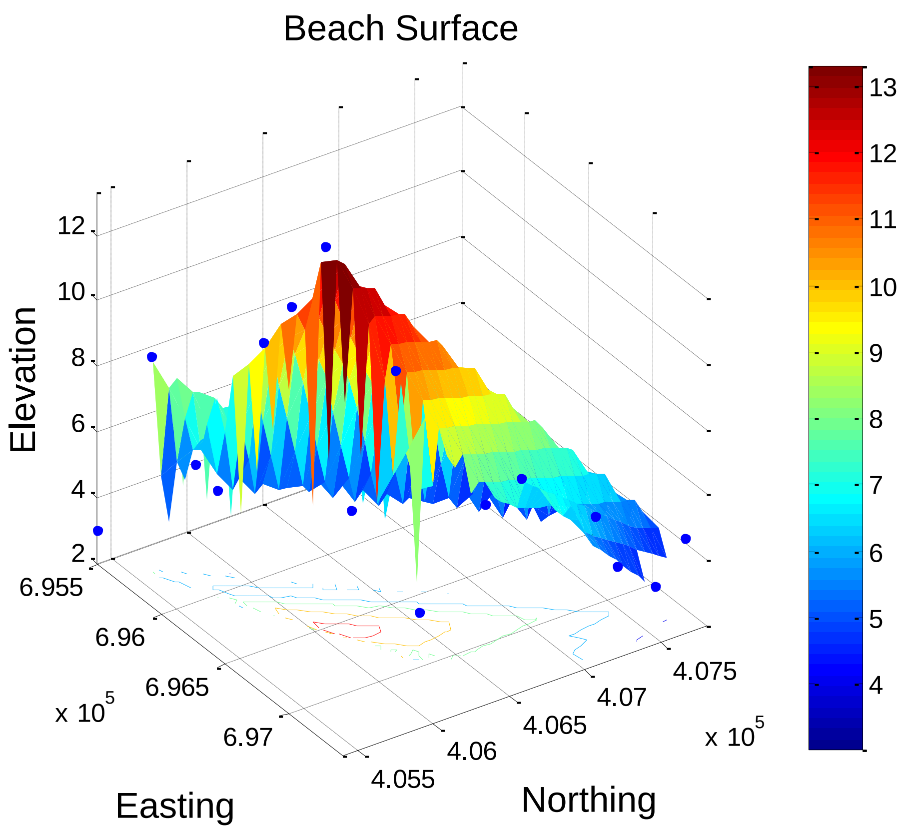
Beach Surface
Elevation
12
10
8
6
4
2
6.955
6.96
6.965
6.97
x 10^5
Easting
4.055
4.06
4.065
4.07
4.075
x 10^5
Northing
13
12
11
10
9
8
7
6
5
4

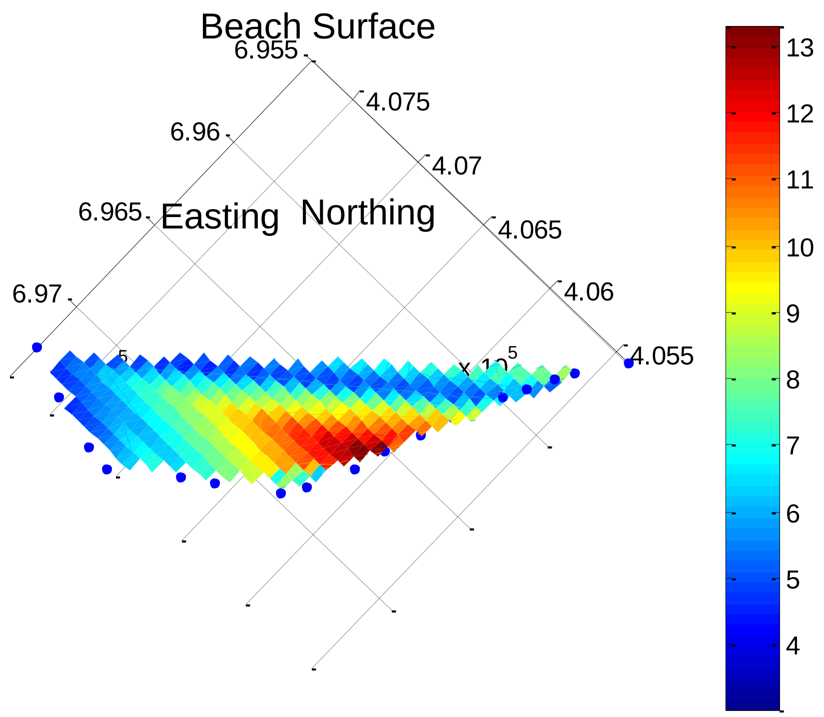
Beach Surface
6.955
6.96
6.965
6.97
Easting
Northing
4.075
4.07
4.065
4.06
4.055
13
12
11
10
9
8
7
6
5
4

Amir

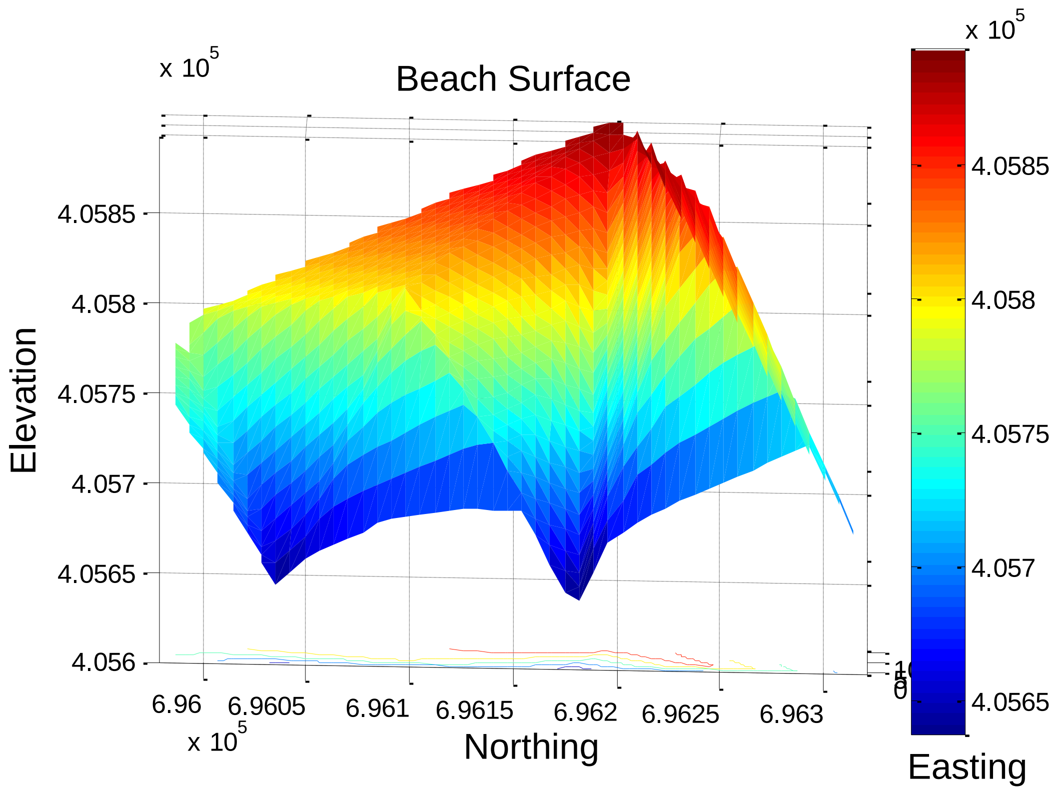
x 10^5
Beach Surface
Elevation
4.0585
4.058
4.0575
4.057
4.0565
4.056
6.96
6.9605
6.961
6.9615
6.962
6.9625
6.963
x 10^5
Northing
x 10^5
4.0585
4.058
4.0575
4.057
4.0565
Easting

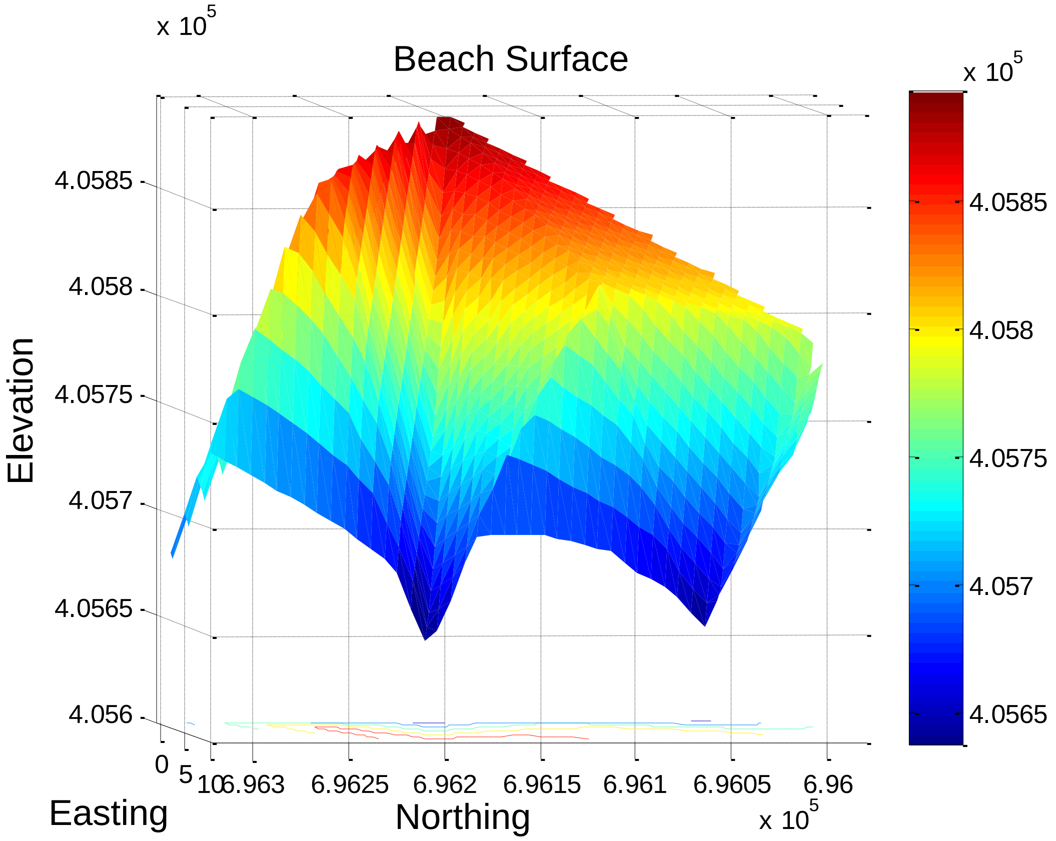
x 10^5
Beach Surface
x 10^5
4.0585
4.058
4.0575
4.057
4.0565
4.056
Elevation
0
5
10
6.963
6.9625
6.962
6.9615
6.961
6.9605
6.96
Easting
Northing
x 10^5
4.0585
4.058
4.0575
4.057
4.0565

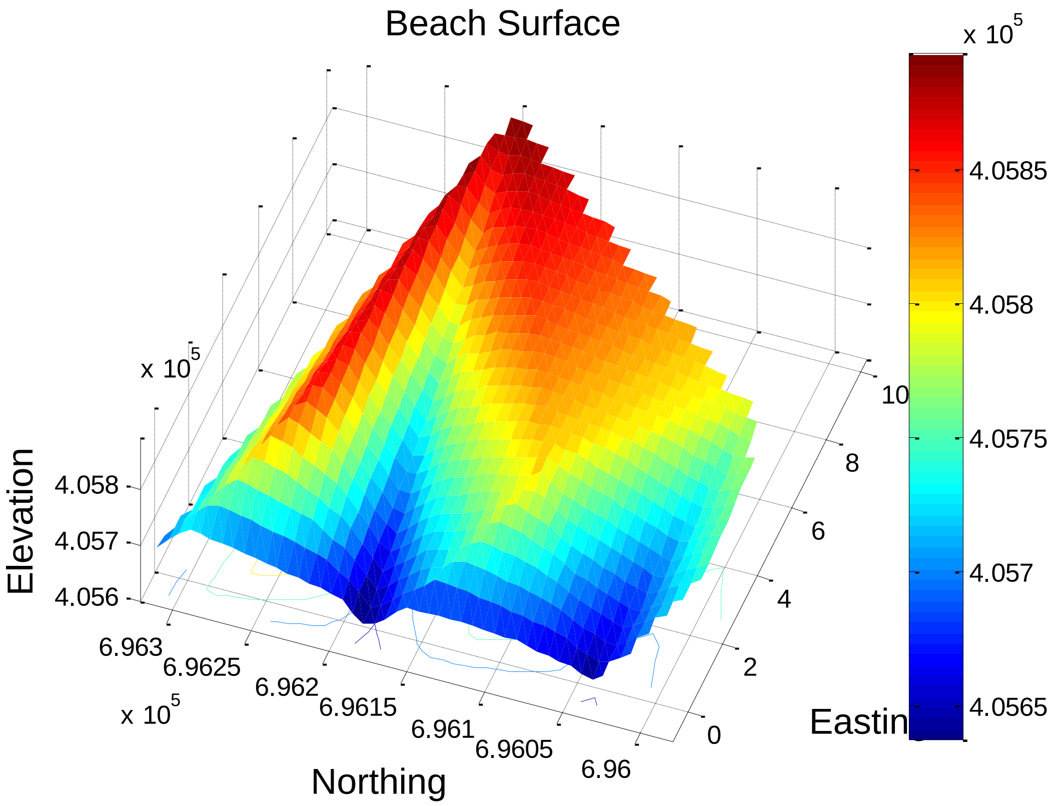
Beach Surface
x 10^5
x 10^5
4.058
4.057
4.056
Elevation
6.963
6.9625
6.962
6.9615
6.961
6.9605
6.96
x 10^5
Northing
10
8
6
4
2
0
Eastin
4.0585
4.058
4.0575
4.057
4.0565

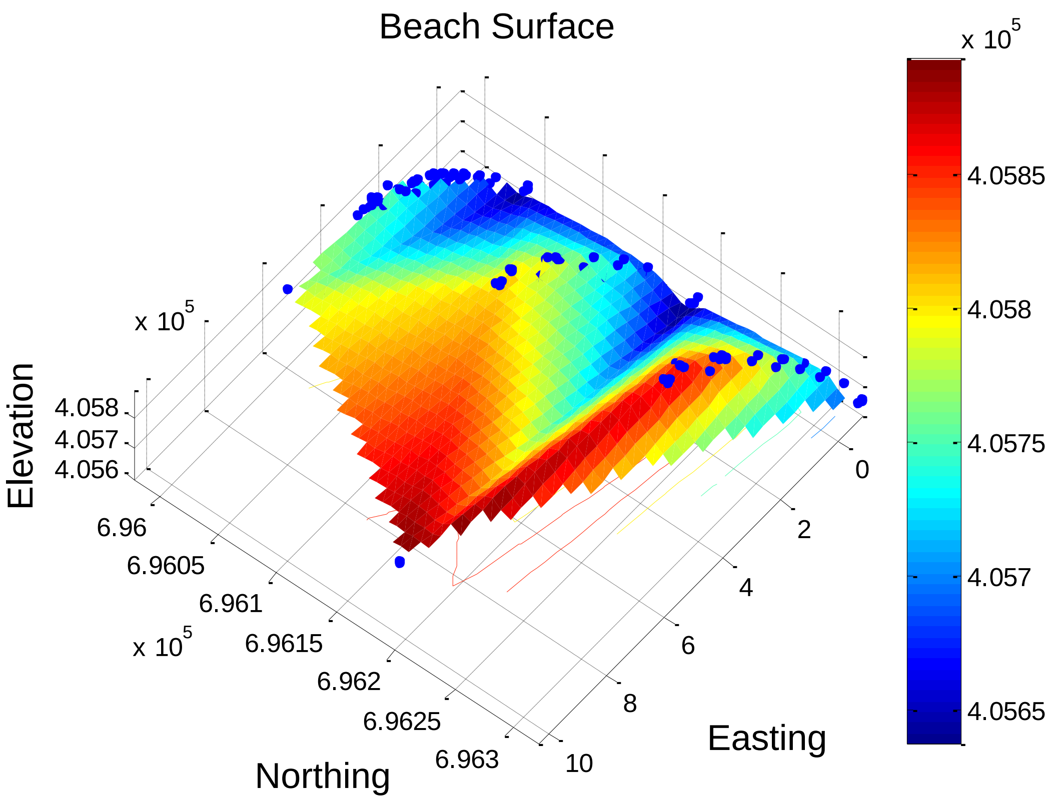
Beach Surface
x 10^5
4.0585
4.058
4.0575
4.057
4.0565
Elevation
x 10^5
4.058
4.057
4.056
6.96
6.9605
6.961
6.9615
6.962
6.9625
6.963
x 10^5
Northing
0
2
4
6
8
10
Easting

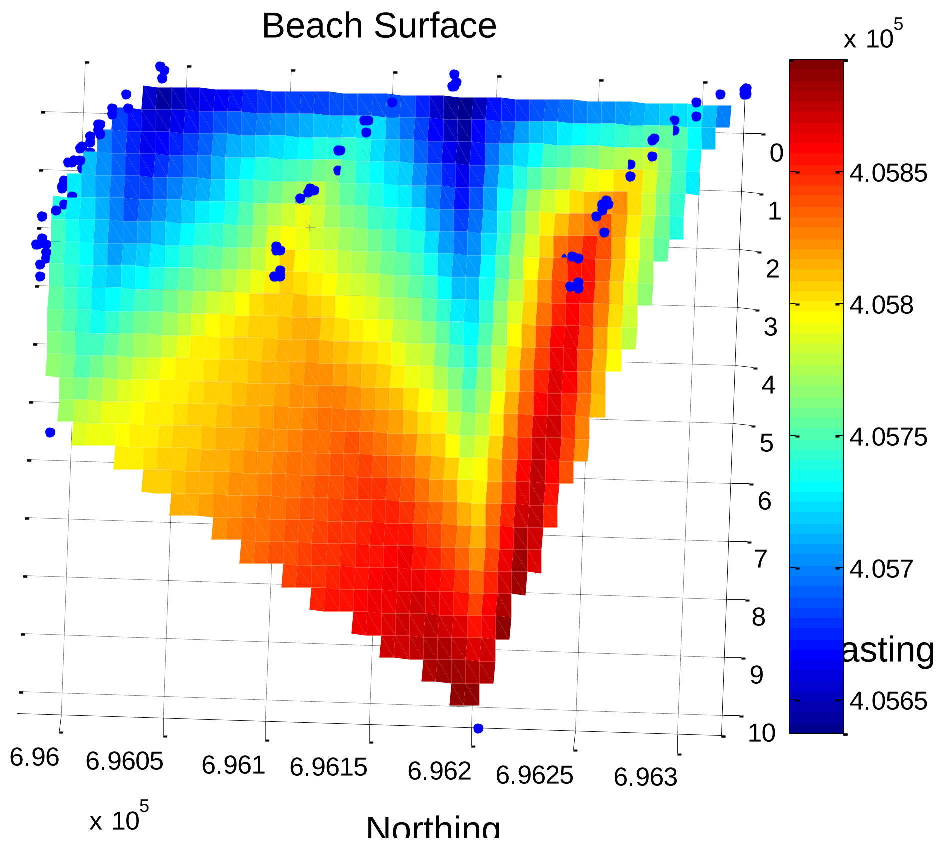
Beach Surface
x 10^5
4.0585
4.058
4.0575
4.057
4.0565
0
1
2
3
4
5
6
7
8
9
10
asting
6.96
6.9605
6.961
6.9615
6.962
6.9625
6.963
x 10^5
Northing

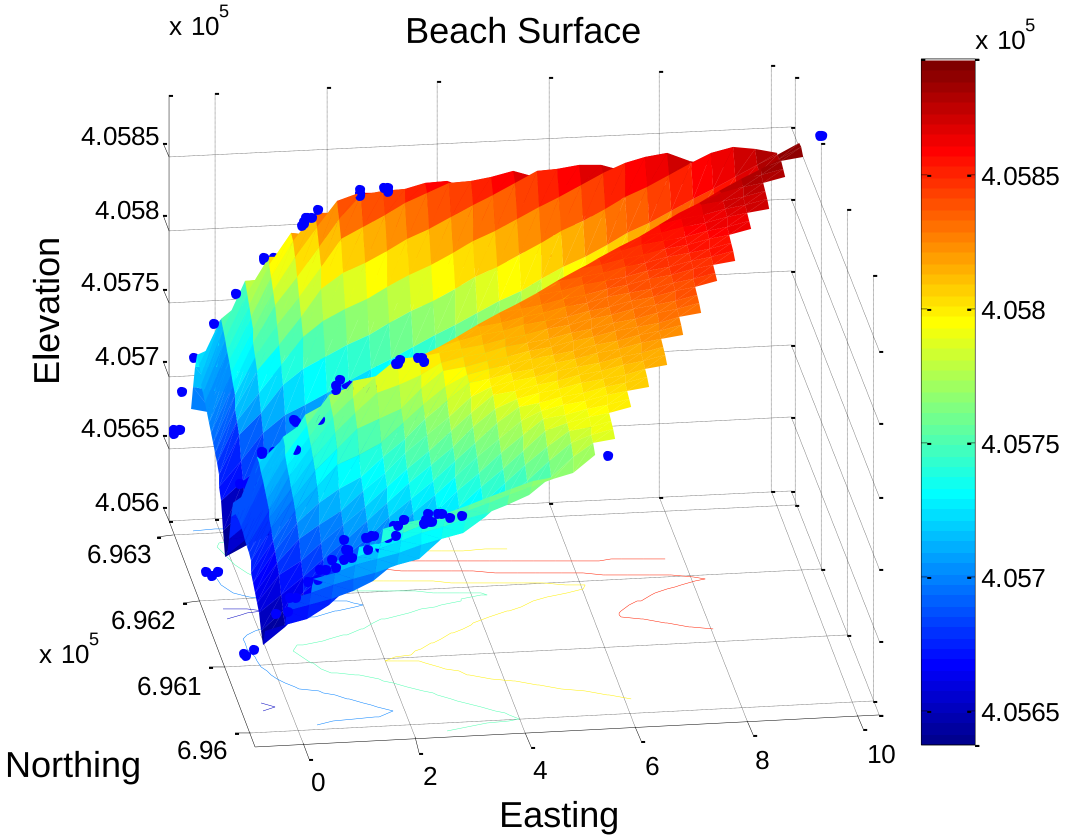
Beach Surface
x 10^5
4.0585
4.058
4.0575
4.057
4.0565
4.056
Elevation
6.963
6.962
6.961
6.96
x 10^5
Northing
0
2
4
6
8
10
Easting
x 10^5
4.0585
4.058
4.0575
4.057
4.0565

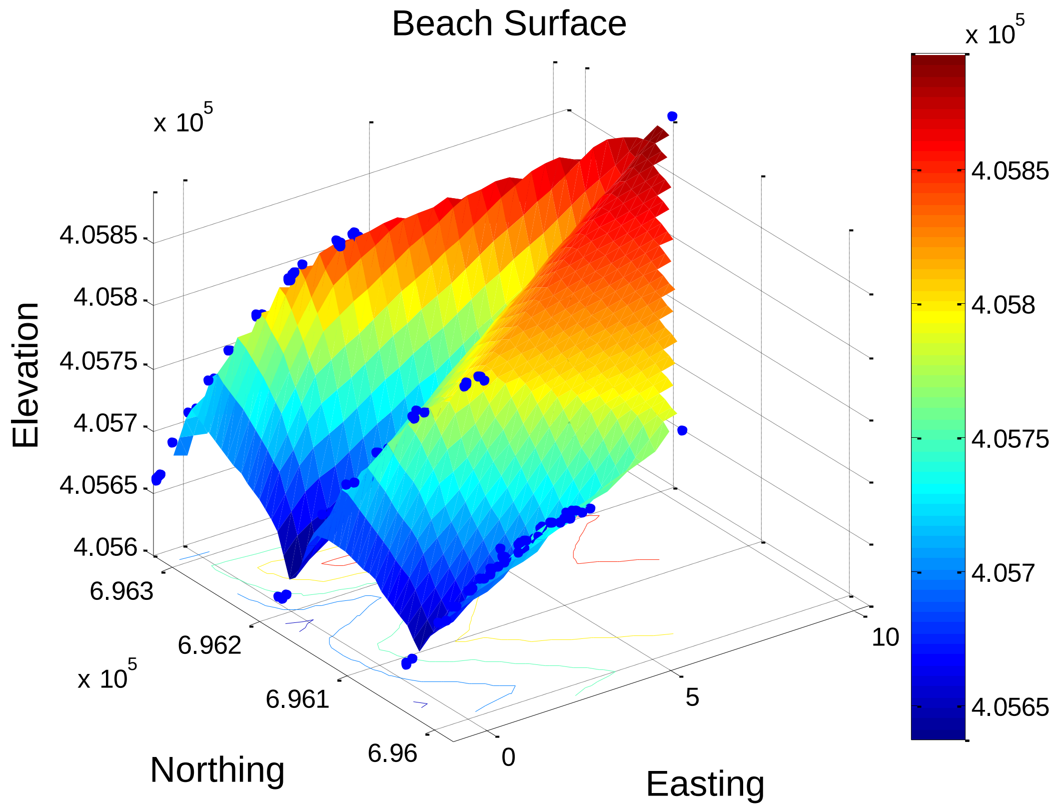
Beach Surface
x 10^5
4.0585
4.058
4.0575
4.057
4.0565
4.056
Elevation
6.963
6.962
6.961
6.96
x 10^5
Northing
0
5
10
Easting
x 10^5
4.0585
4.058
4.0575
4.057
4.0565

APPENDIX V: BEACH PROFILES

V.0 BEACH PROFILES

Beach profiles from Ngarunui Beach, Wainamu Beach and Moonlight Bay are presented below. Some of the profiles were not grounded to a control point. These free form profiles have been listed within the text. The rod locations in the free form profiles were estimated on the 14/15th of July. The other rod locations were known.

A line of best fit is included in each profile to estimate beach slope (tanβ) at each location.

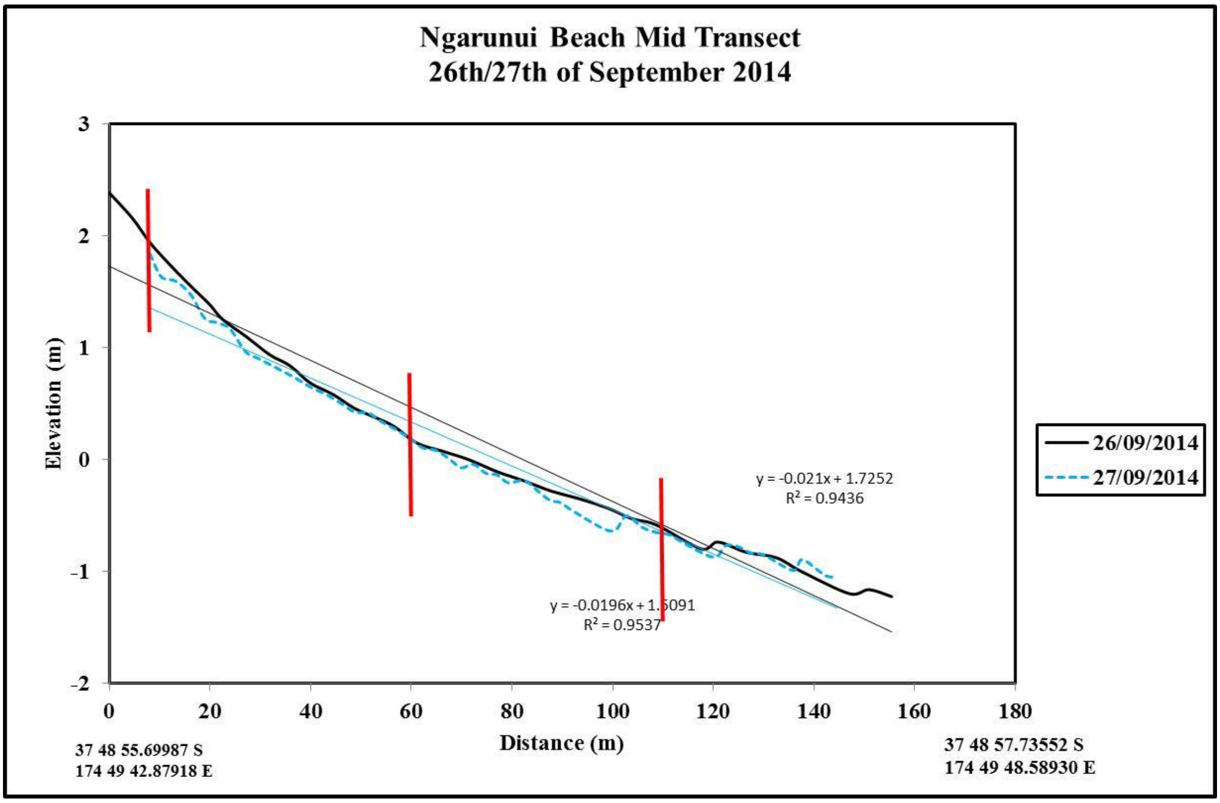

Ngarunui Beach Mid Transect
26th/27th of September 2014
Elevation (m)
Distance (m)
3
2
1
0
-1
-2
0
20
40
60
80
100
120
140
160
180
y = -0.021x + 1.7252
R² = 0.9436
y = -0.0196x + 1.5091
R² = 0.9537
26/09/2014
27/09/2014
37 48 55.69987 S
174 49 42.87918 E
37 48 57.73552 S
174 49 48.58930 E

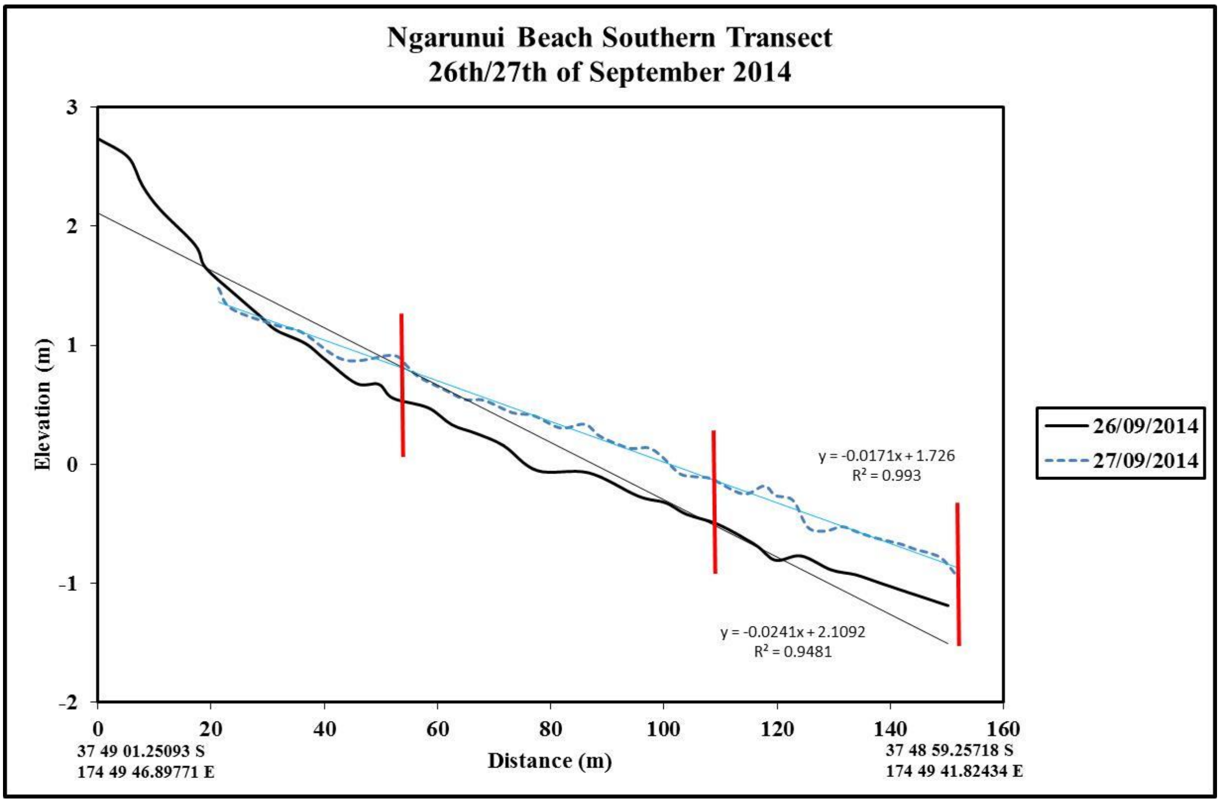

Ngarunui Beach Southern Transect
26th/27th of September 2014
Elevation (m)
Distance (m)
3
2
1
0
-1
-2
0
20
40
60
80
100
120
140
160
y = -0.0171x + 1.726
R² = 0.993
y = -0.0241x + 2.1092
R² = 0.9481
26/09/2014
27/09/2014
37 49 01.25093 S
174 49 46.89771 E
37 48 59.25718 S
174 49 41.82434 E

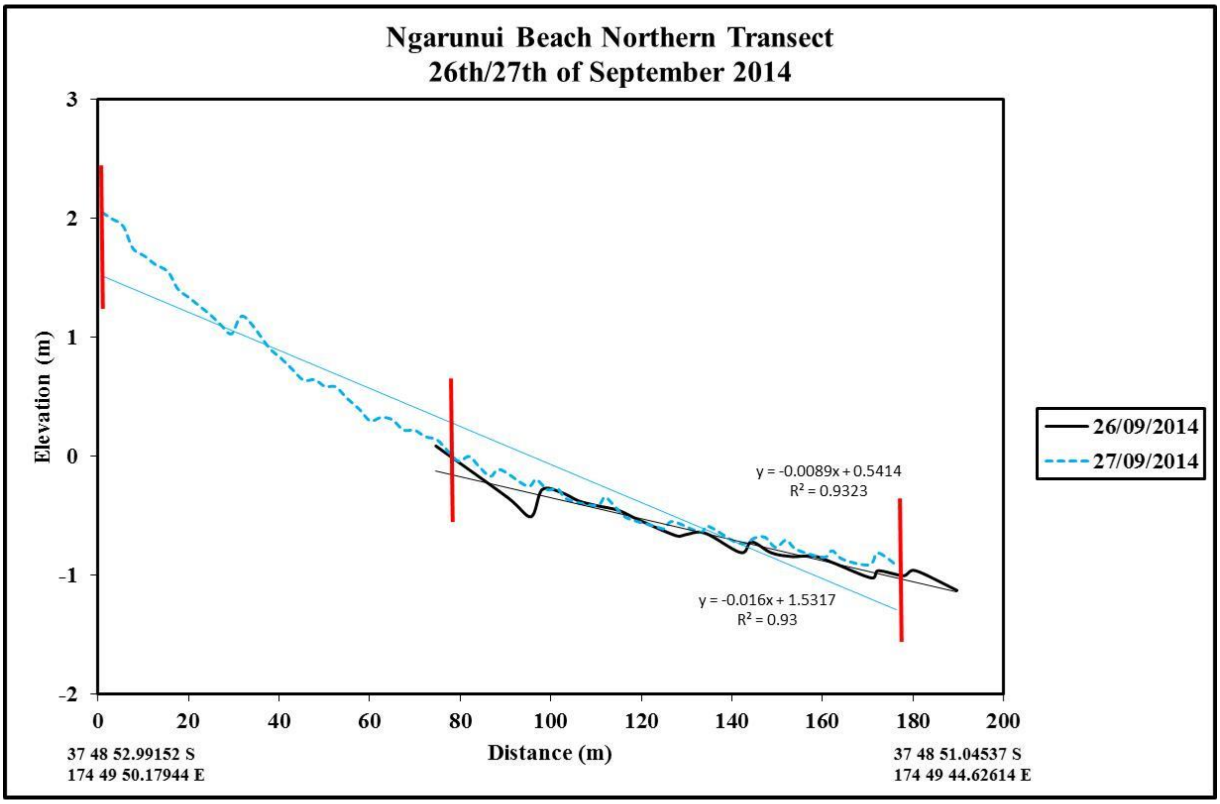

Ngarunui Beach Northern Transect
26th/27th of September 2014
Elevation (m)
Distance (m)
26/09/2014
27/09/2014
y = -0.0089x + 0.5414
R² = 0.9323
y = -0.016x + 1.5317
R² = 0.93
37 48 52.99152 S
174 49 50.17944 E
37 48 51.04537 S
174 49 44.62614 E

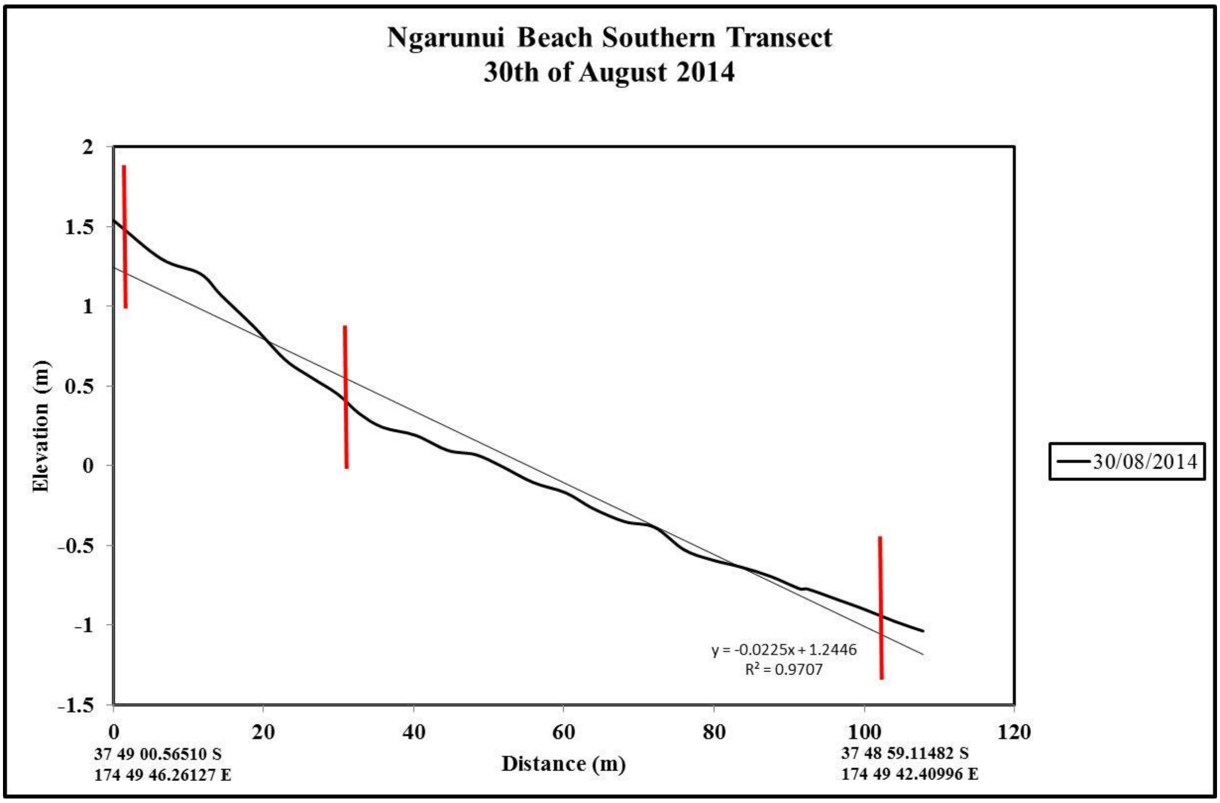

Ngarunui Beach Southern Transect
30th of August 2014
Elevation (m)
Distance (m)
30/08/2014
y = -0.0225x + 1.2446
R² = 0.9707
37 49 00.56510 S
174 49 46.26127 E
37 48 59.11482 S
174 49 42.40996 E

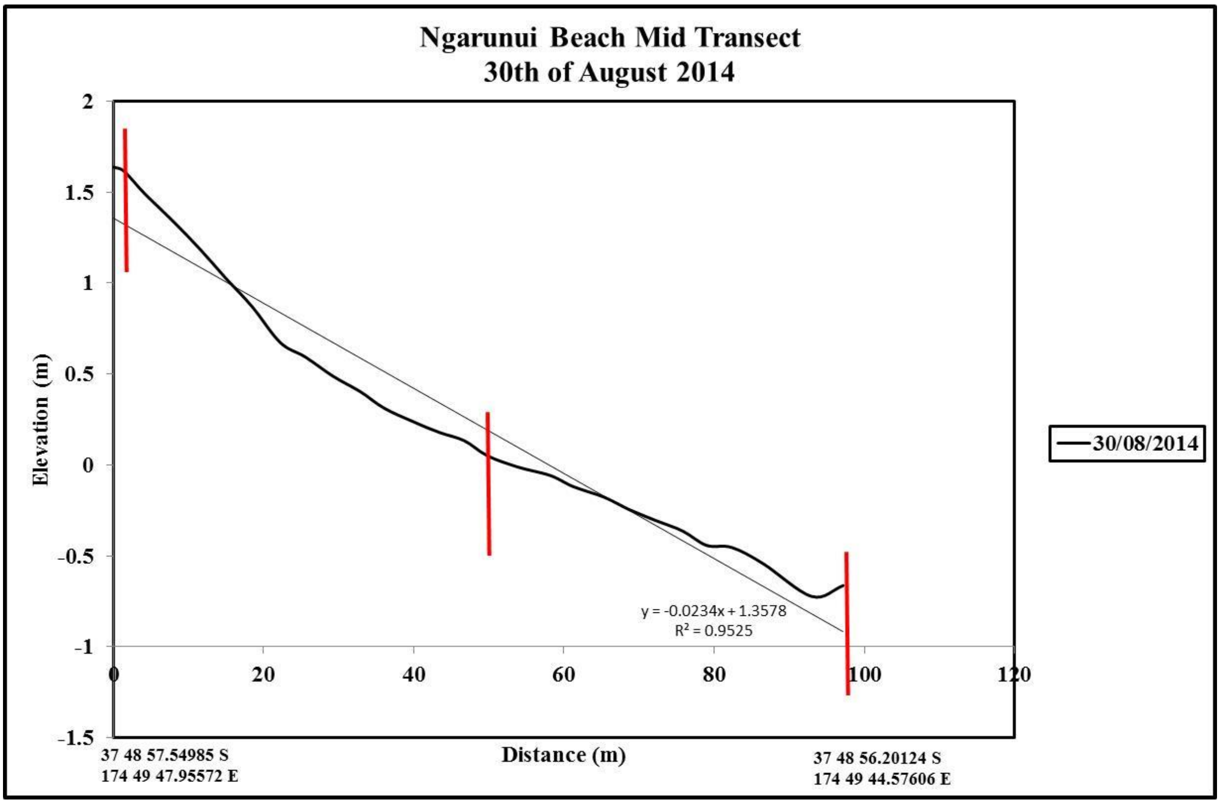
Ngarunui Beach Mid Transect
30th of August 2014
Elevation (m)
Distance (m)
2
1.5
1
0.5
0
-0.5
-1
-1.5
0
20
40
60
80
100
120
y = -0.0234x + 1.3578
R² = 0.9525
30/08/2014
37 48 57.54985 S
174 49 47.95572 E
37 48 56.20124 S
174 49 44.57606 E

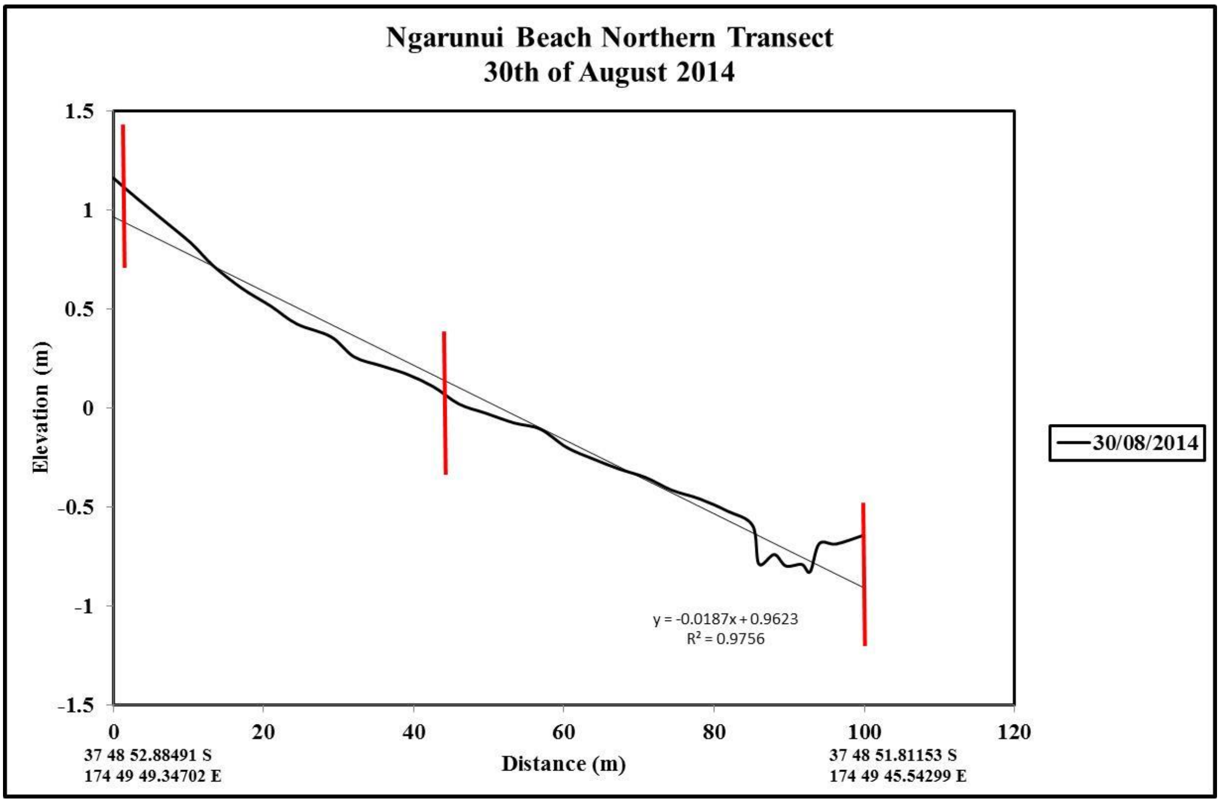
Ngarunui Beach Northern Transect
30th of August 2014
Elevation (m)
Distance (m)
1.5
1
0.5
0
-0.5
-1
-1.5
0
20
40
60
80
100
120
y = -0.0187x + 0.9623
R² = 0.9756
30/08/2014
37 48 52.88491 S
174 49 49.34702 E
37 48 51.81153 S
174 49 45.54299 E

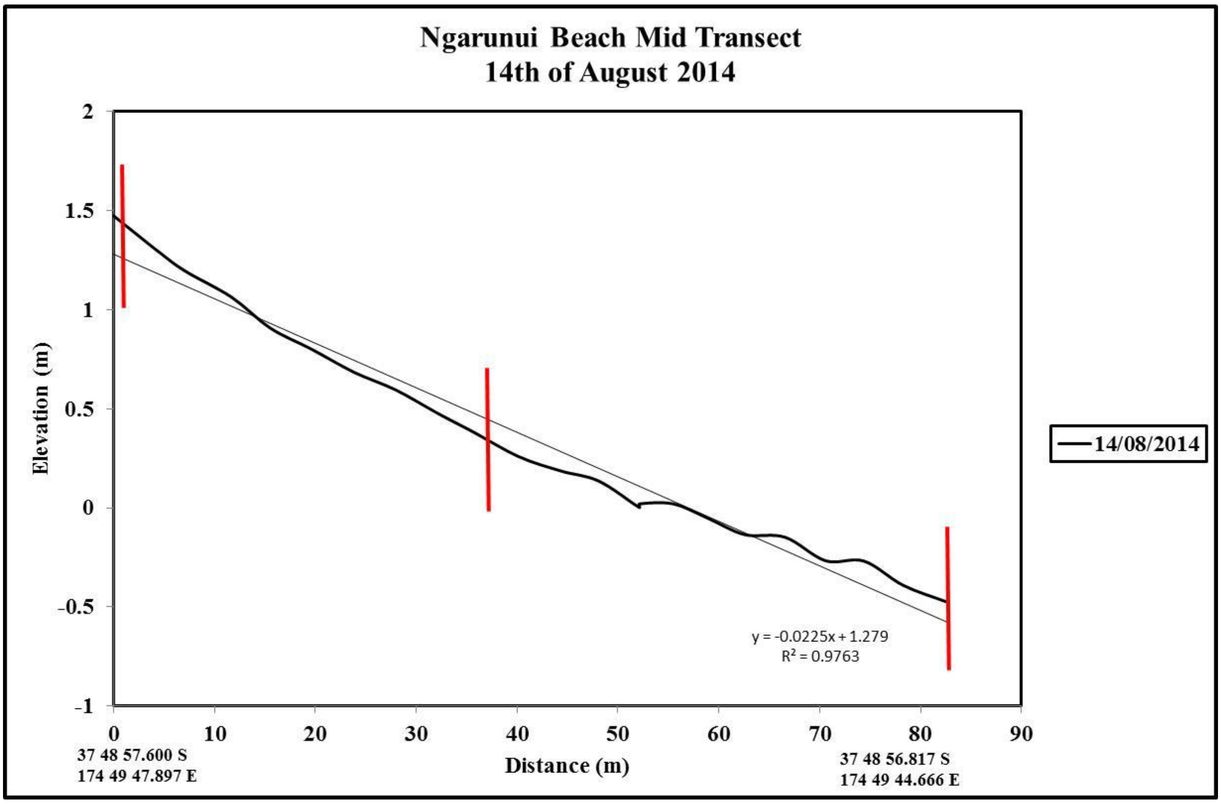
Ngarunui Beach Mid Transect
14th of August 2014
Elevation (m)
Distance (m)
2
1.5
1
0.5
0
-0.5
-1
0
10
20
30
40
50
60
70
80
90
y = -0.0225x + 1.279
R² = 0.9763
37 48 57.600 S
174 49 47.897 E
37 48 56.817 S
174 49 44.666 E
14/08/2014

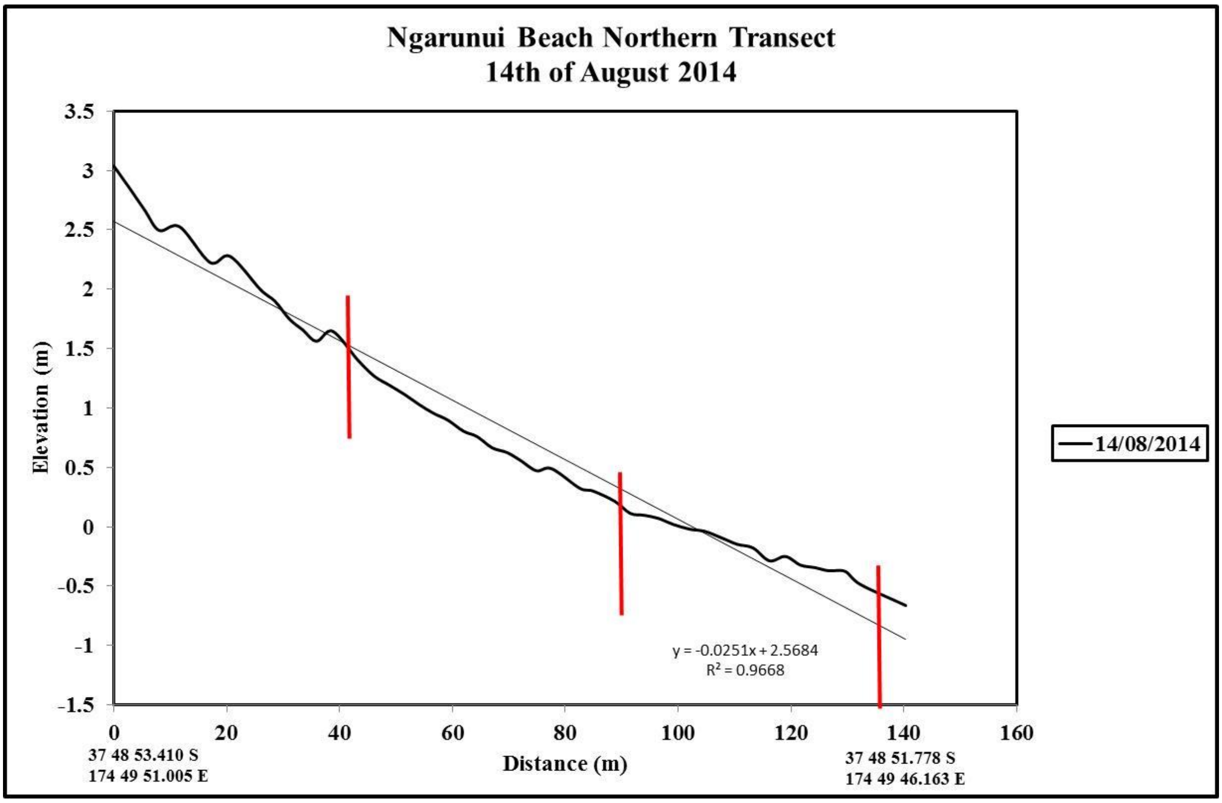
Ngarunui Beach Northern Transect
14th of August 2014
Elevation (m)
Distance (m)
3.5
3
2.5
2
1.5
1
0.5
0
-0.5
-1
-1.5
0
20
40
60
80
100
120
140
160
y = -0.0251x + 2.5684
R² = 0.9668
37 48 53.410 S
174 49 51.005 E
37 48 51.778 S
174 49 46.163 E
14/08/2014

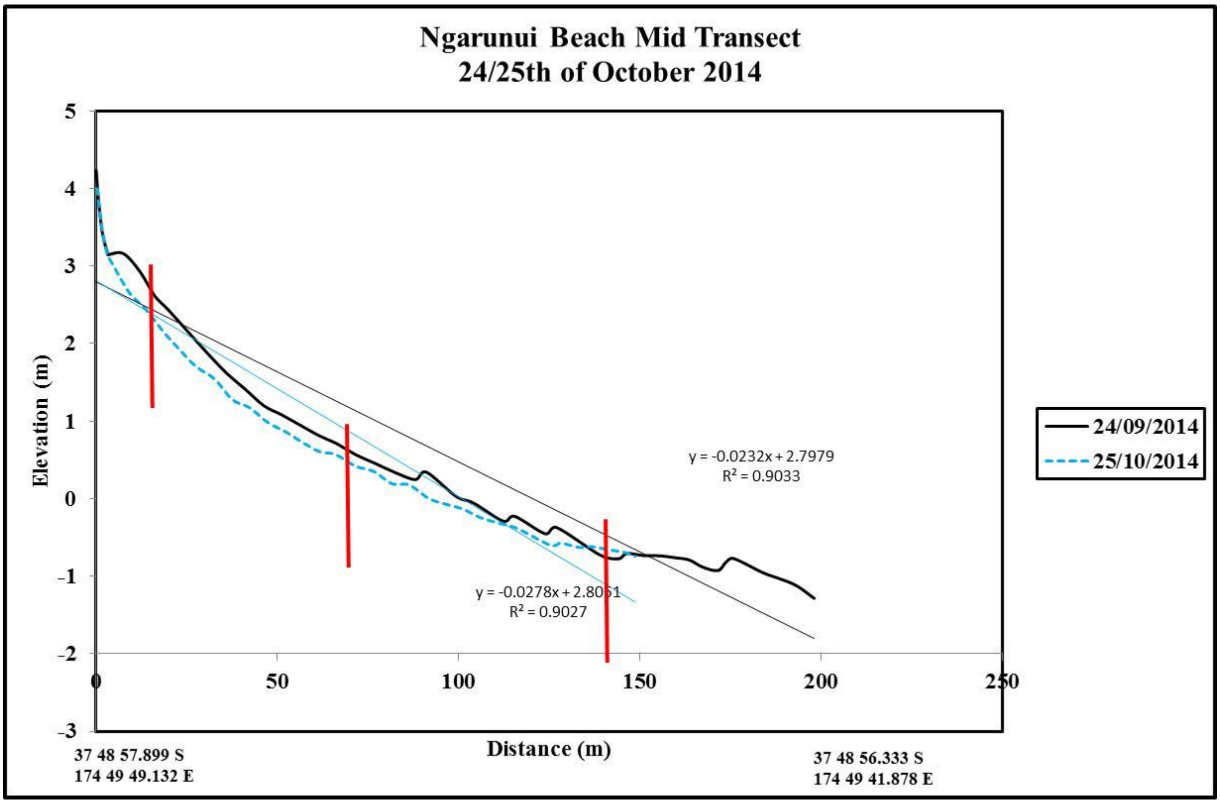
Ngarunui Beach Mid Transect
24/25th of October 2014
Elevation (m)
Distance (m)
24/09/2014
25/10/2014
y = -0.0232x + 2.7979
R² = 0.9033
y = -0.0278x + 2.8061
R² = 0.9027
37 48 57.899 S
174 49 49.132 E
37 48 56.333 S
174 49 41.878 E

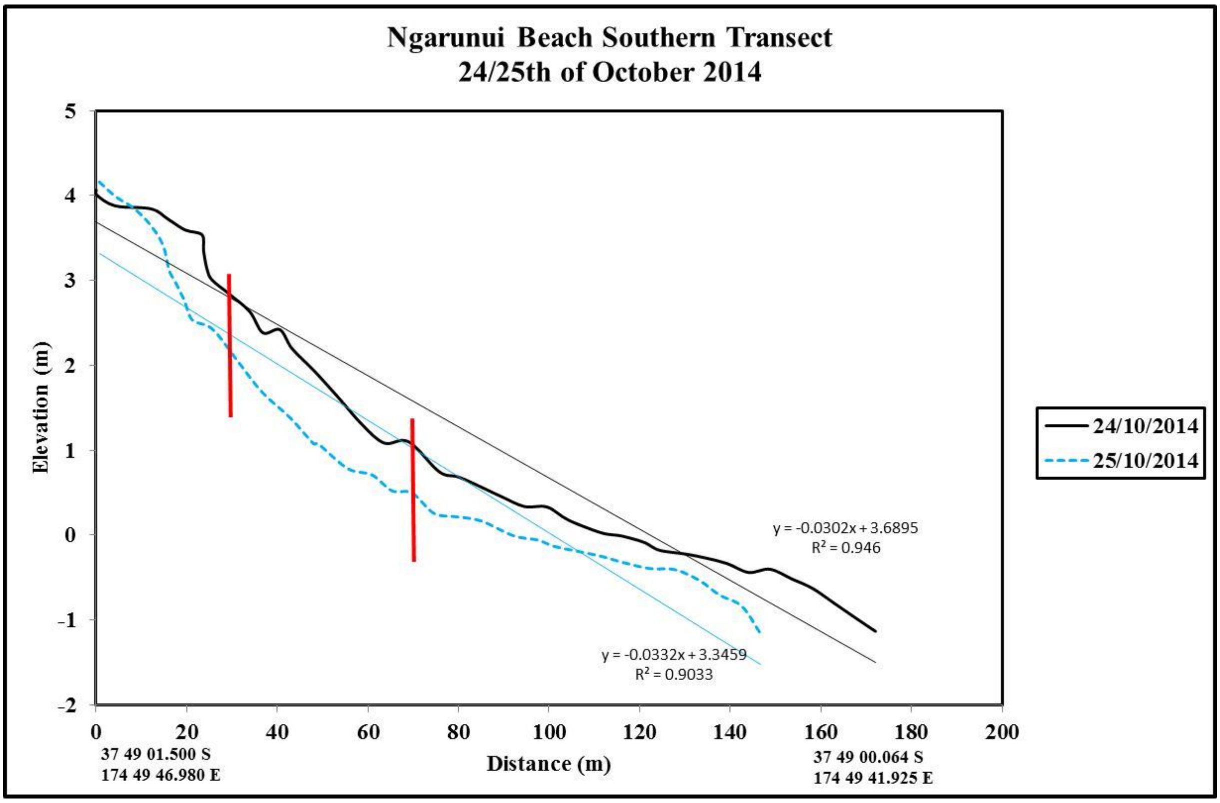
Ngarunui Beach Southern Transect
24/25th of October 2014
Elevation (m)
Distance (m)
24/10/2014
25/10/2014
y = -0.0302x + 3.6895
R² = 0.946
y = -0.0332x + 3.3459
R² = 0.9033
37 49 01.500 S
174 49 46.980 E
37 49 00.064 S
174 49 41.925 E

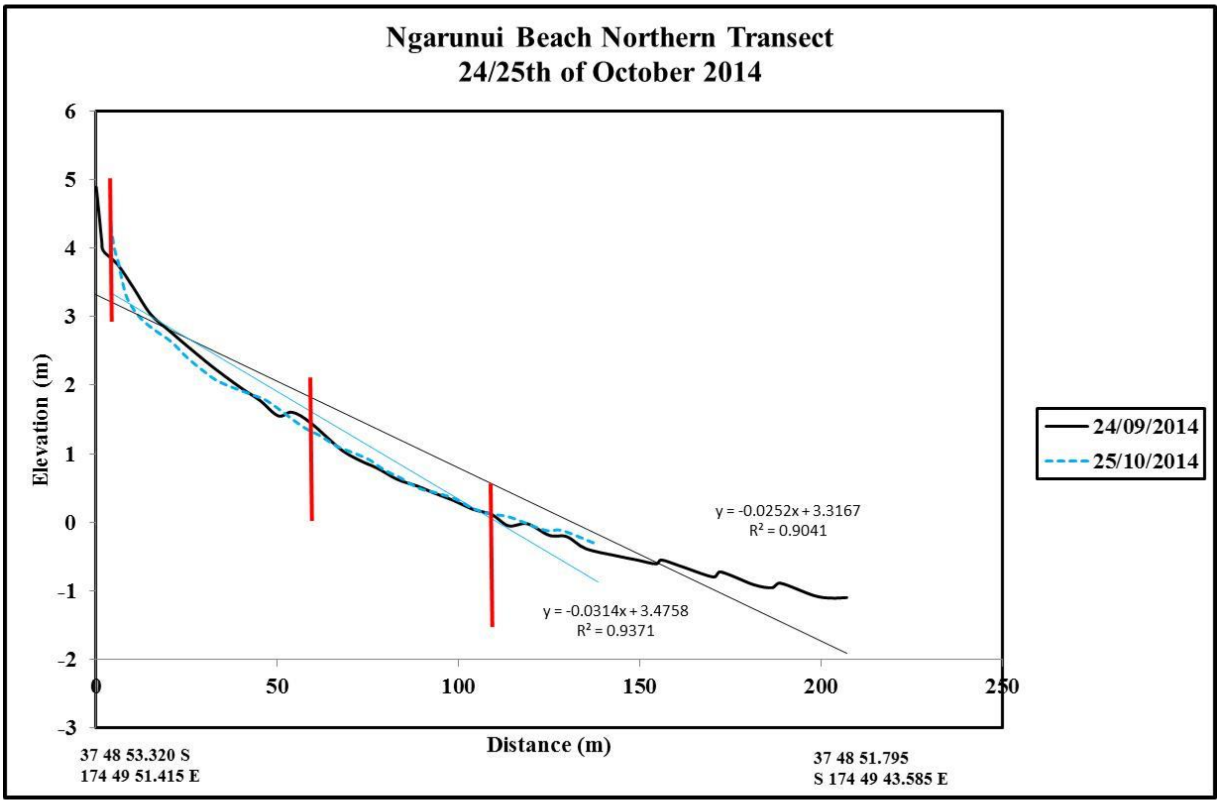
Ngarunui Beach Northern Transect
24/25th of October 2014
Elevation (m)
Distance (m)
24/09/2014
25/10/2014
y = -0.0252x + 3.3167
R² = 0.9041
y = -0.0314x + 3.4758
R² = 0.9371
37 48 53.320 S
174 49 51.415 E
37 48 51.795
S 174 49 43.585 E

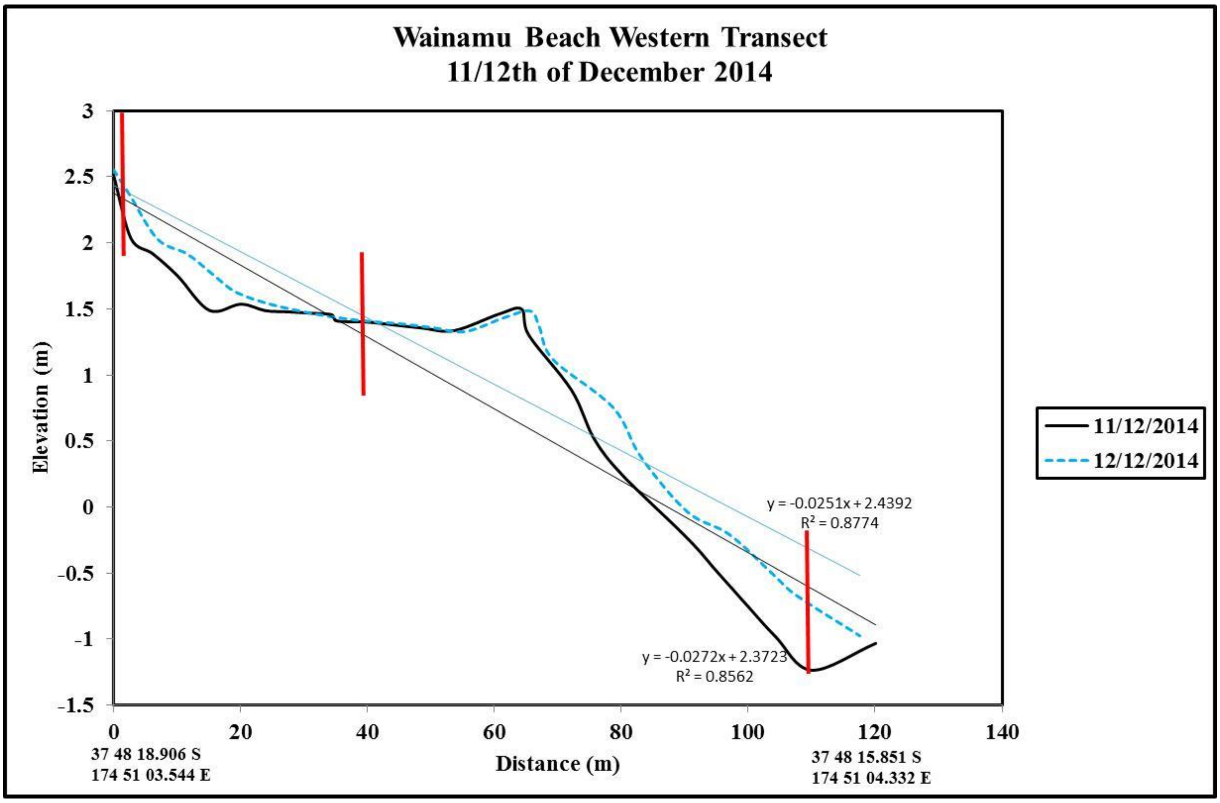
Wainamu Beach Western Transect
11/12th of December 2014
Elevation (m)
Distance (m)
11/12/2014
12/12/2014
y = -0.0251x + 2.4392
R² = 0.8774
y = -0.0272x + 2.3723
R² = 0.8562
37 48 18.906 S
174 51 03.544 E
37 48 15.851 S
174 51 04.332 E

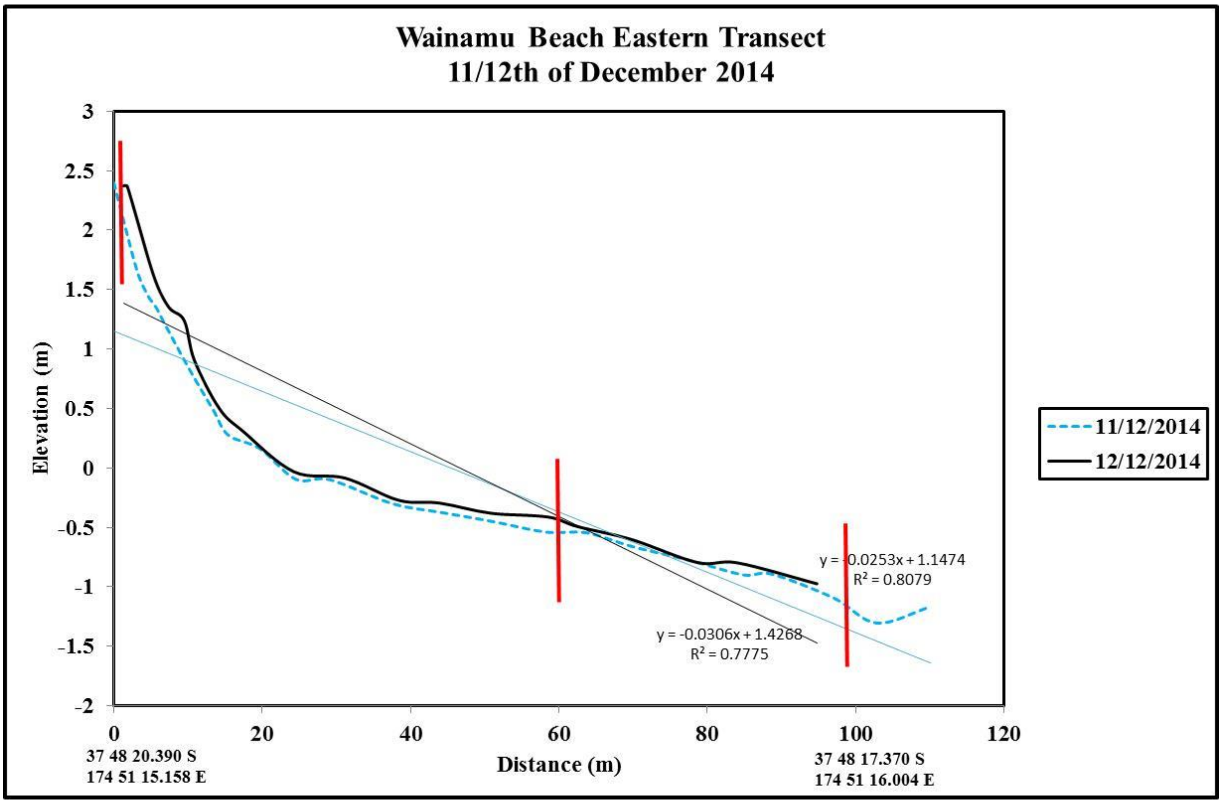
Wainamu Beach Eastern Transect
11/12th of December 2014
Elevation (m)
Distance (m)
3
2.5
2
1.5
1
0.5
0
-0.5
-1
-1.5
-2
0
20
40
60
80
100
120
37 48 20.390 S
174 51 15.158 E
37 48 17.370 S
174 51 16.004 E
y = -0.0253x + 1.1474
R² = 0.8079
y = -0.0306x + 1.4268
R² = 0.7775
11/12/2014
12/12/2014

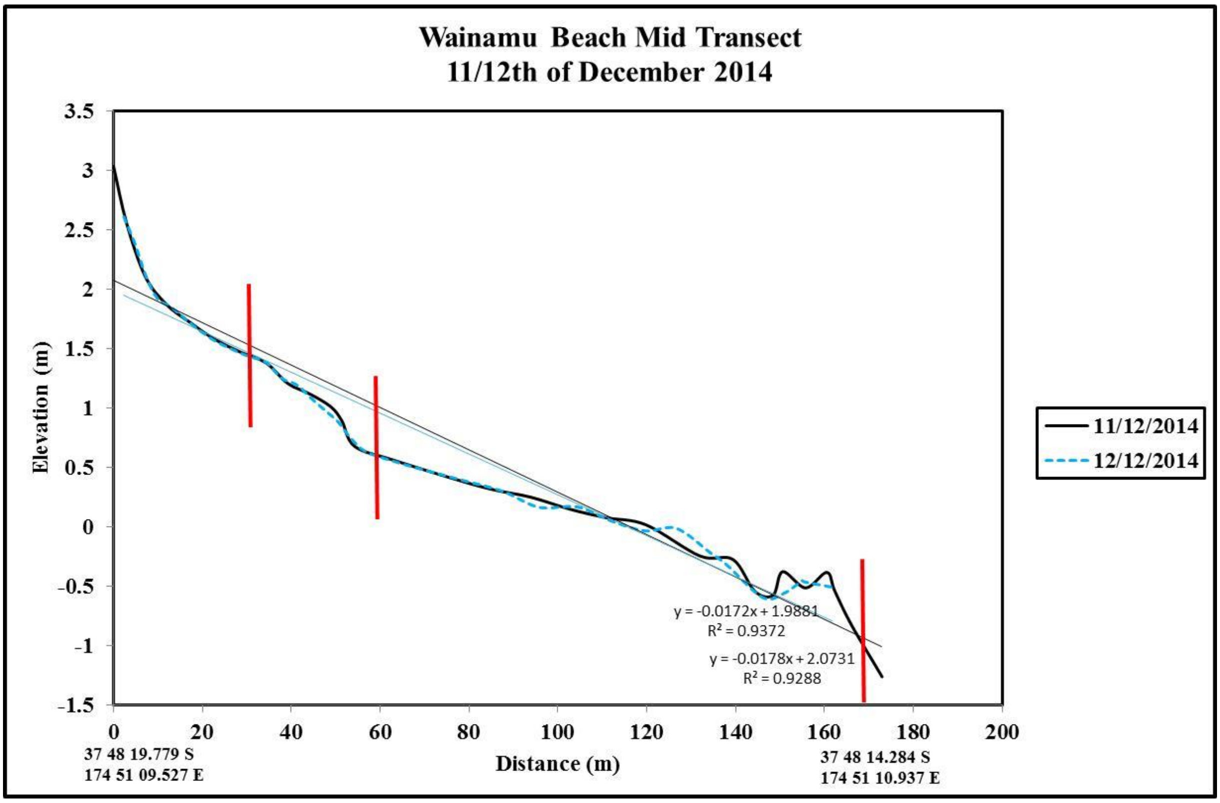
Wainamu Beach Mid Transect
11/12th of December 2014
Elevation (m)
Distance (m)
3.5
3
2.5
2
1.5
1
0.5
0
-0.5
-1
-1.5
0
20
40
60
80
100
120
140
160
180
200
37 48 19.779 S
174 51 09.527 E
37 48 14.284 S
174 51 10.937 E
y = -0.0172x + 1.9881
R² = 0.9372
y = -0.0178x + 2.0731
R² = 0.9288
11/12/2014
12/12/2014

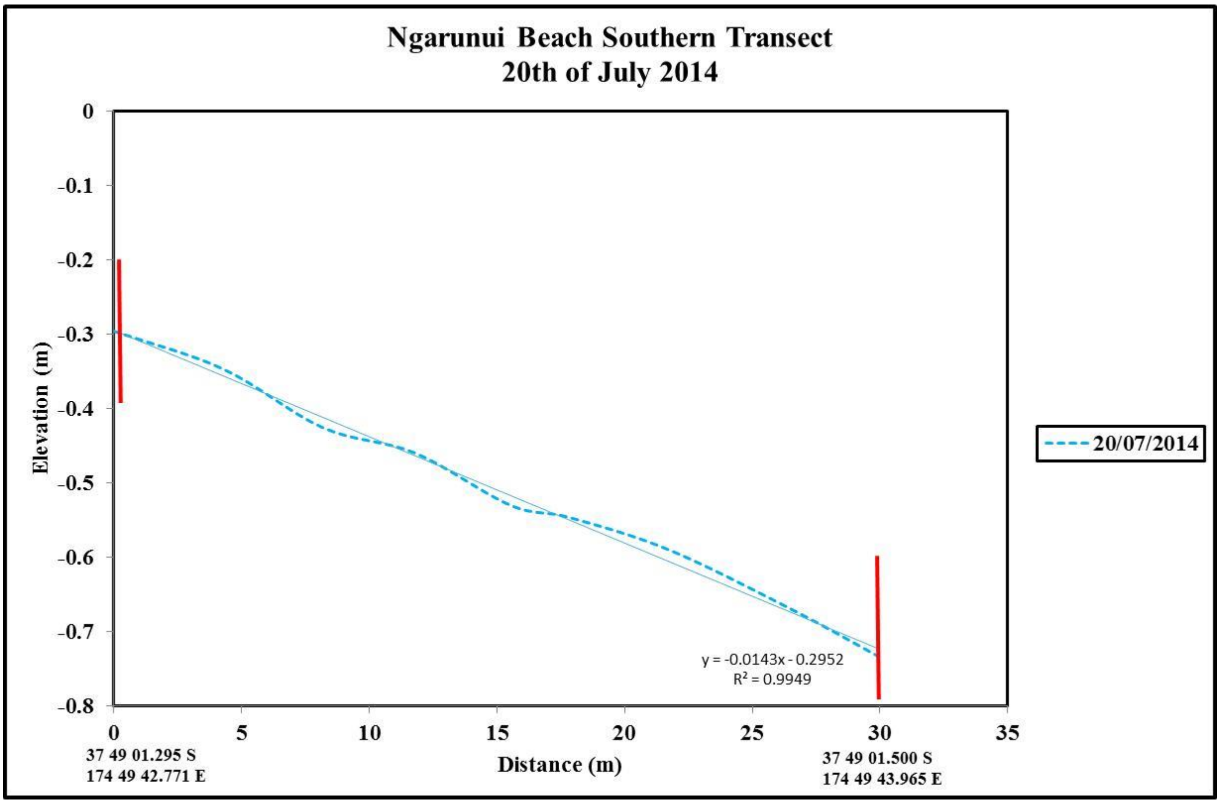
Ngarunui Beach Southern Transect
20th of July 2014
0
-0.1
-0.2
-0.3
-0.4
-0.5
-0.6
-0.7
-0.8
Elevation (m)
0
5
10
15
20
25
30
35
Distance (m)
37 49 01.295 S
174 49 42.771 E
37 49 01.500 S
174 49 43.965 E
y = -0.0143x - 0.2952
R² = 0.9949
20/07/2014

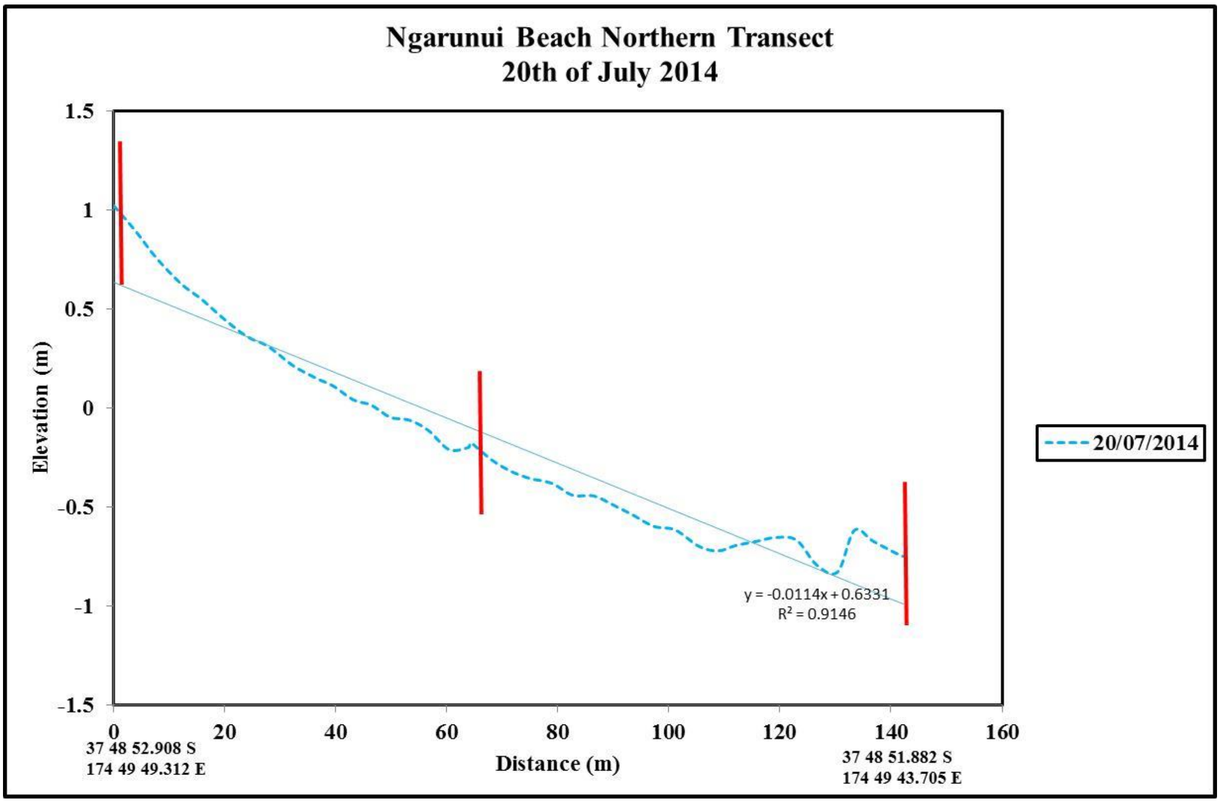
Ngarunui Beach Northern Transect
20th of July 2014
1.5
1
0.5
0
-0.5
-1
-1.5
Elevation (m)
0
20
40
60
80
100
120
140
160
Distance (m)
37 48 52.908 S
174 49 49.312 E
37 48 51.882 S
174 49 43.705 E
y = -0.0114x + 0.6331
R² = 0.9146
20/07/2014

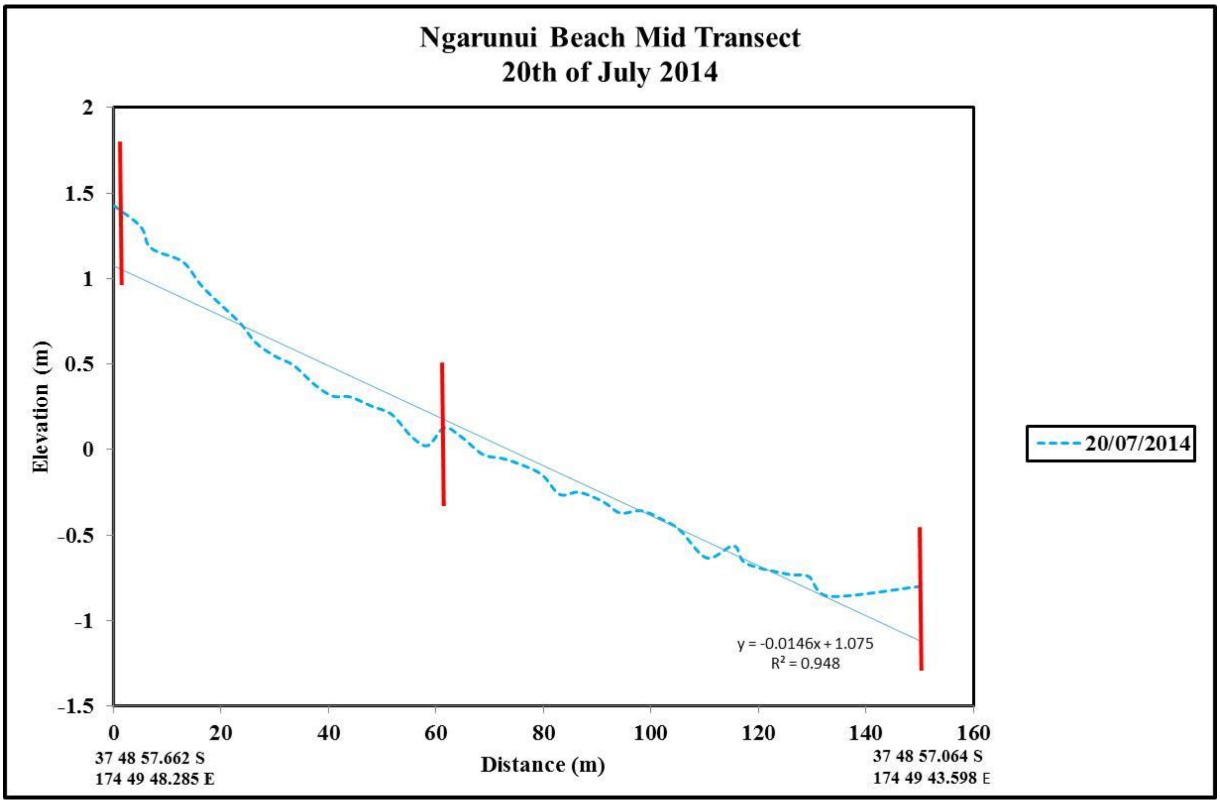
Ngarunui Beach Mid Transect
20th of July 2014
Elevation (m)
Distance (m)
20/07/2014
y = -0.0146x + 1.075
R² = 0.948
37 48 57.662 S
174 49 48.285 E
37 48 57.064 S
174 49 43.598 E

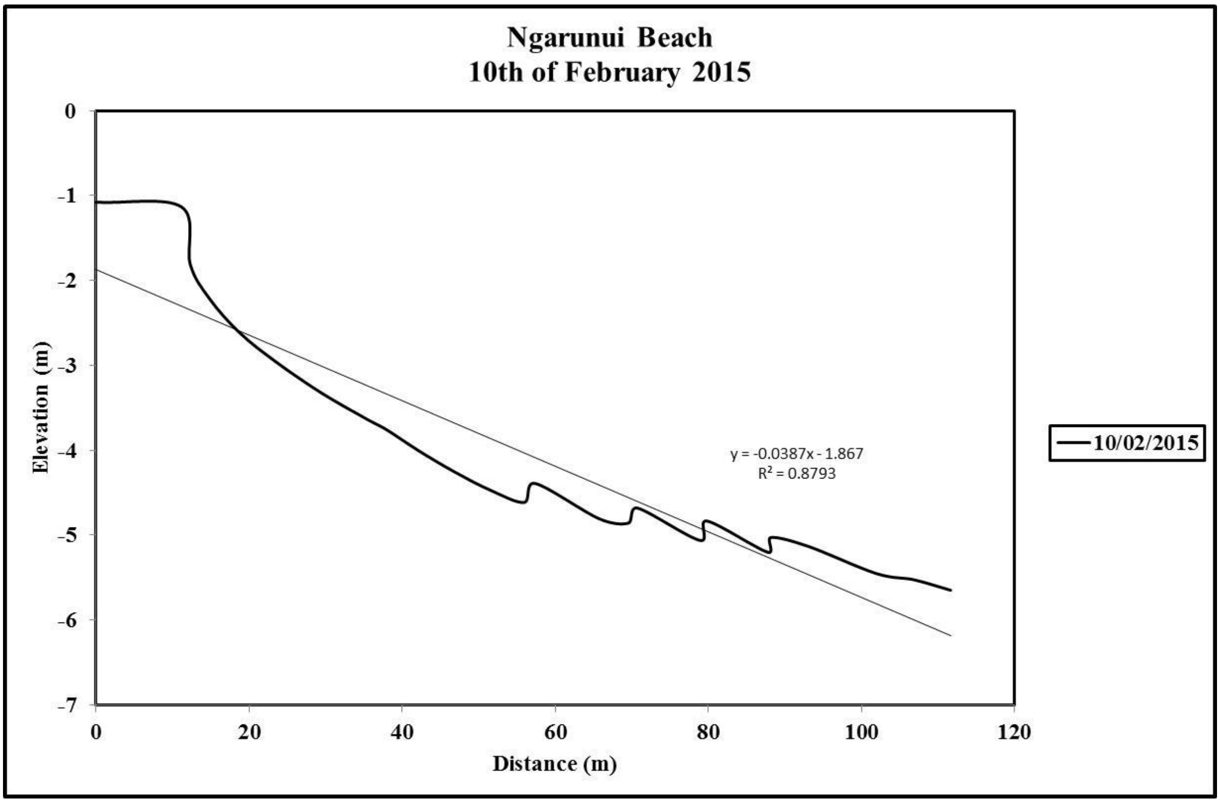
Ngarunui Beach
10th of February 2015
Elevation (m)
Distance (m)
10/02/2015
y = -0.0387x - 1.867
R² = 0.8793

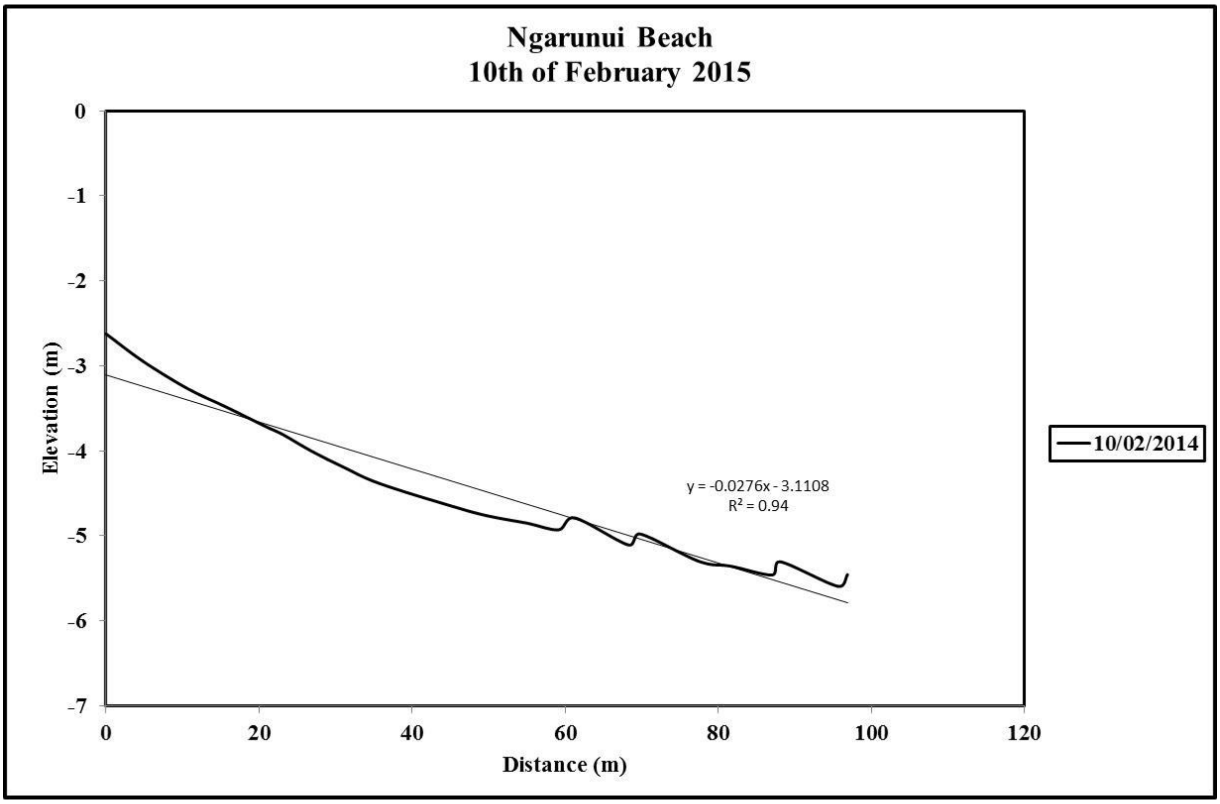
Ngarunui Beach
10th of February 2015
Elevation (m)
Distance (m)
0
-1
-2
-3
-4
-5
-6
-7
0
20
40
60
80
100
120
10/02/2014
y = -0.0276x - 3.1108
R² = 0.94

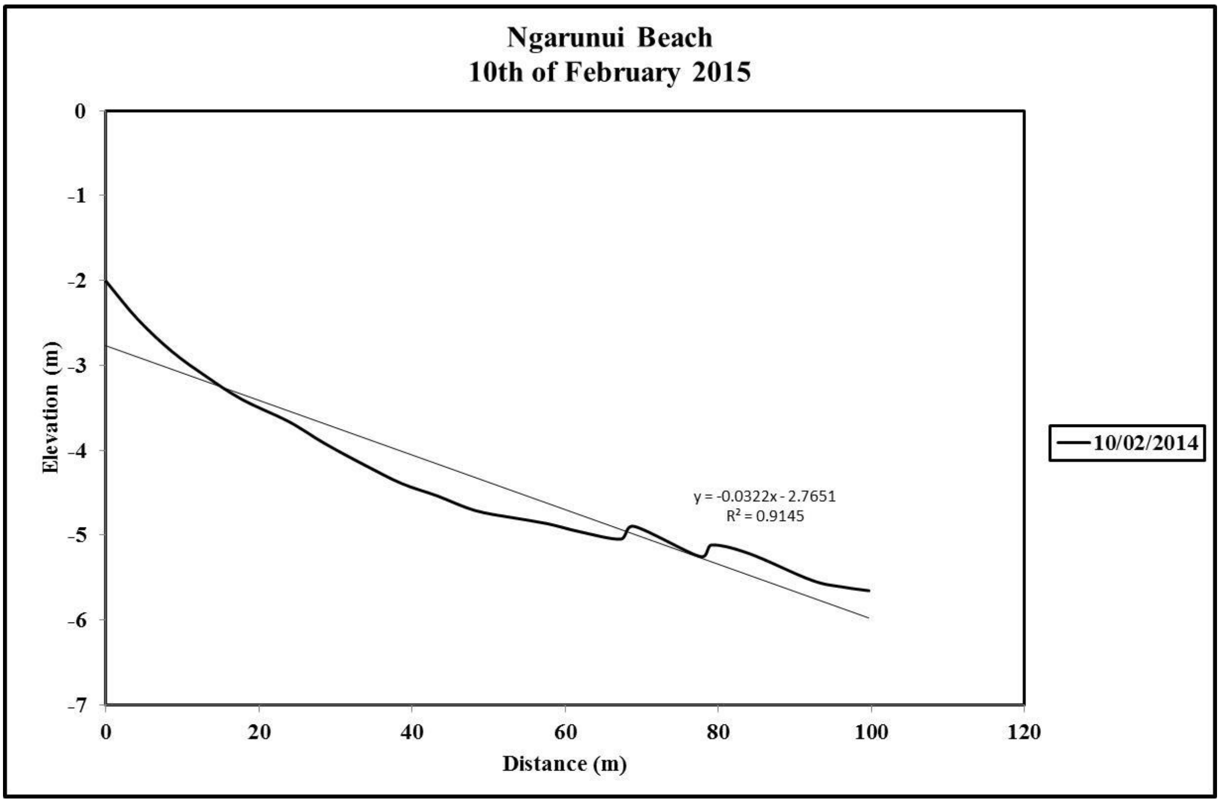
Ngarunui Beach
10th of February 2015
Elevation (m)
Distance (m)
0
-1
-2
-3
-4
-5
-6
-7
0
20
40
60
80
100
120
10/02/2014
y = -0.0322x - 2.7651
R² = 0.9145

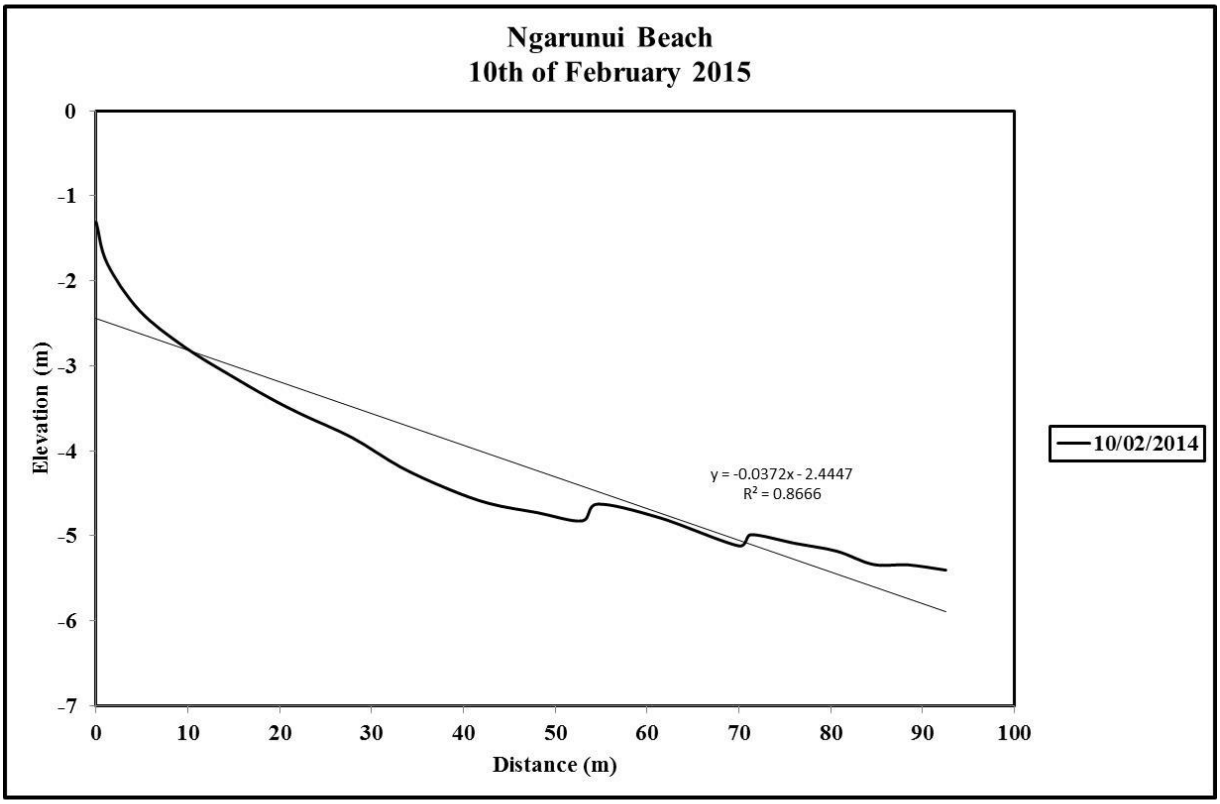
Ngarunui Beach
10th of February 2015
Elevation (m)
Distance (m)
0
-1
-2
-3
-4
-5
-6
-7
0
10
20
30
40
50
60
70
80
90
100
y = -0.0372x - 2.4447
R² = 0.8666
10/02/2014

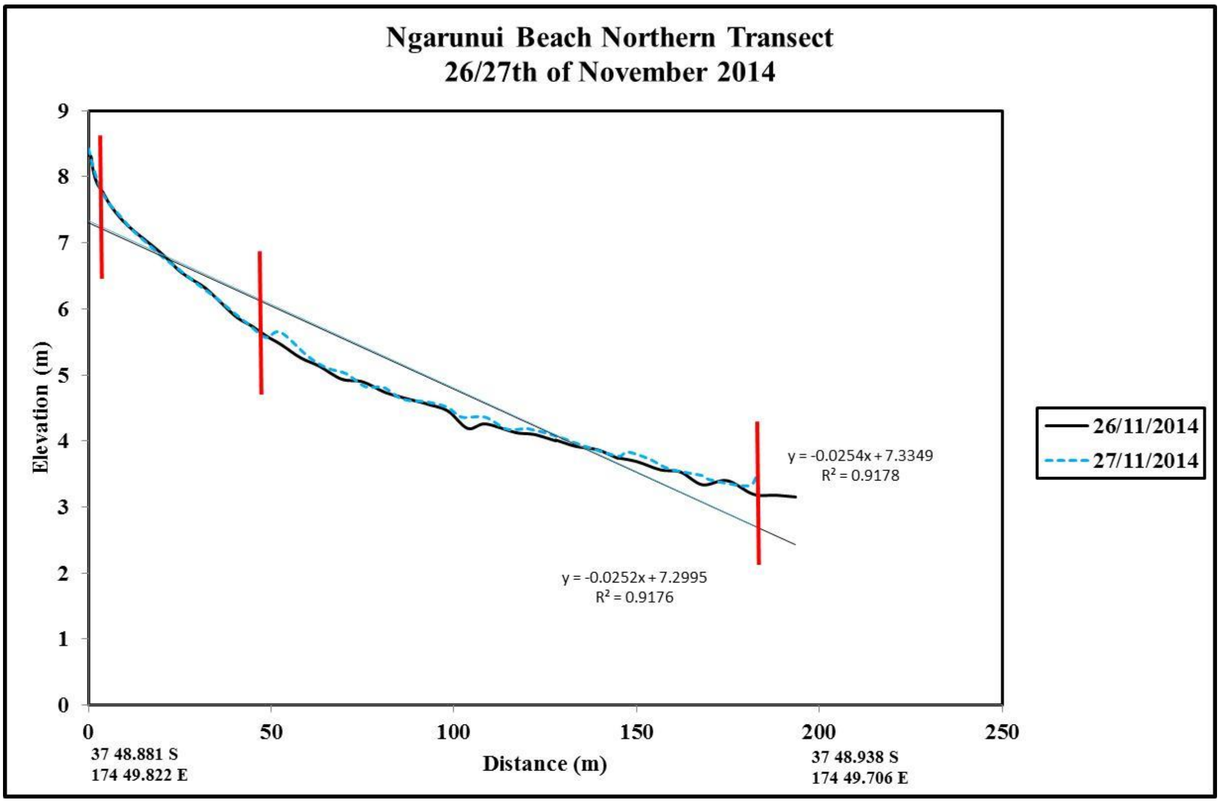
Ngarunui Beach Northern Transect
26/27th of November 2014
Elevation (m)
Distance (m)
0
1
2
3
4
5
6
7
8
9
0
50
100
150
200
250
y = -0.0254x + 7.3349
R² = 0.9178
y = -0.0252x + 7.2995
R² = 0.9176
26/11/2014
27/11/2014
37 48.881 S
174 49.822 E
37 48.938 S
174 49.706 E

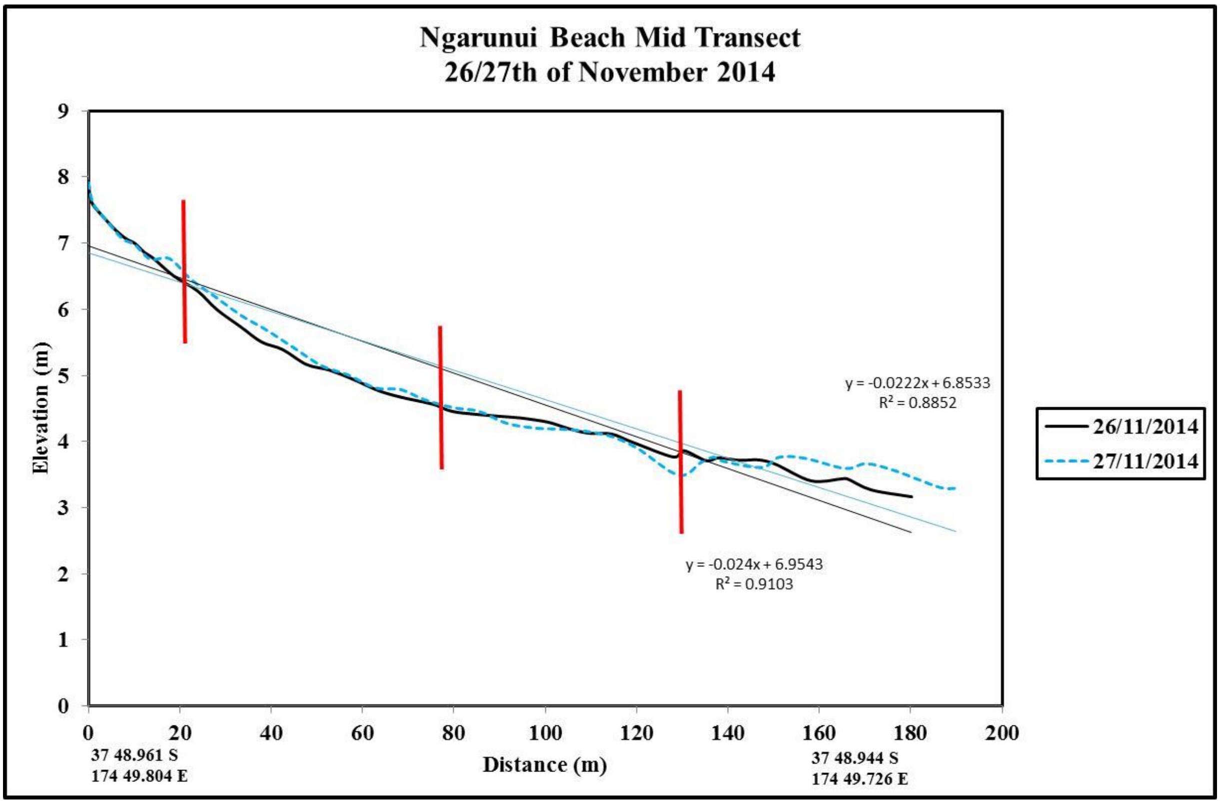
Ngarunui Beach Mid Transect
26/27th of November 2014
Elevation (m)
Distance (m)
37 48.961 S
174 49.804 E
37 48.944 S
174 49.726 E
y = -0.0222x + 6.8533
R² = 0.8852
y = -0.024x + 6.9543
R² = 0.9103
26/11/2014
27/11/2014

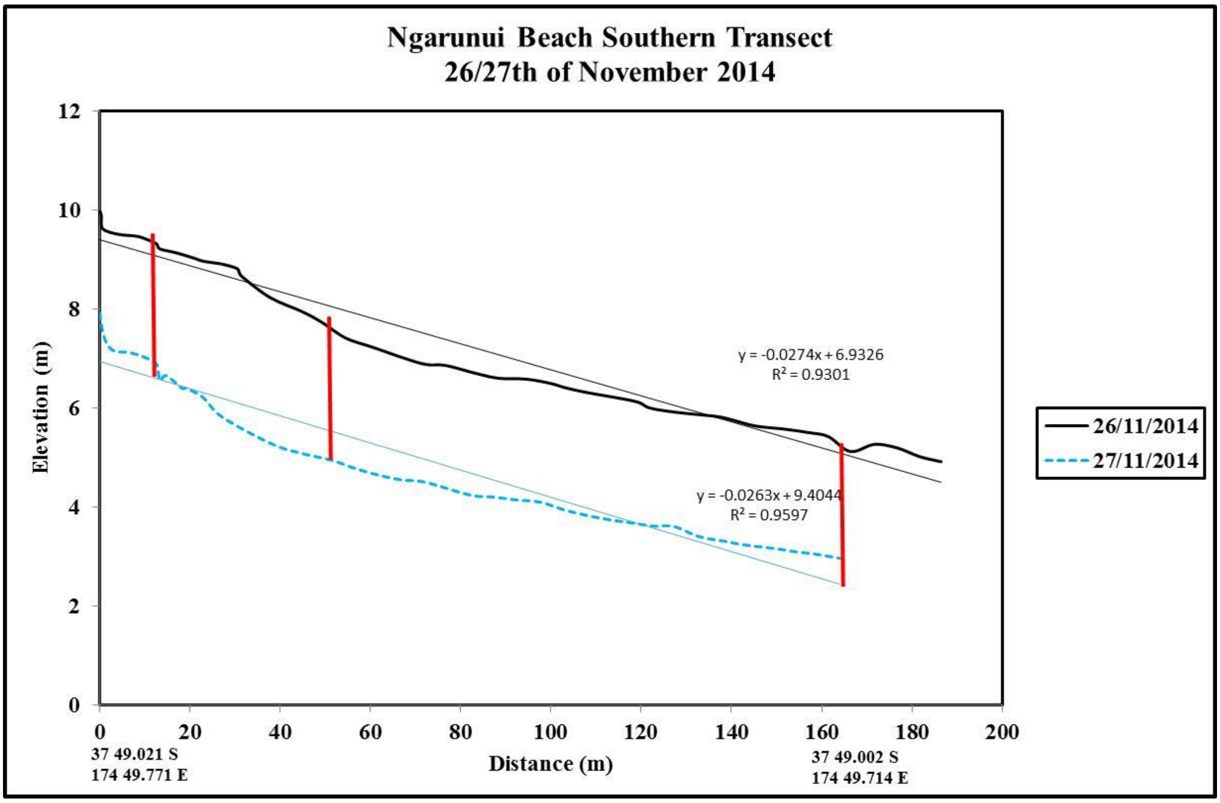
Ngarunui Beach Southern Transect
26/27th of November 2014
Elevation (m)
Distance (m)
37 49.021 S
174 49.771 E
37 49.002 S
174 49.714 E
y = -0.0274x + 6.9326
R² = 0.9301
y = -0.0263x + 9.4044
R² = 0.9597
26/11/2014
27/11/2014

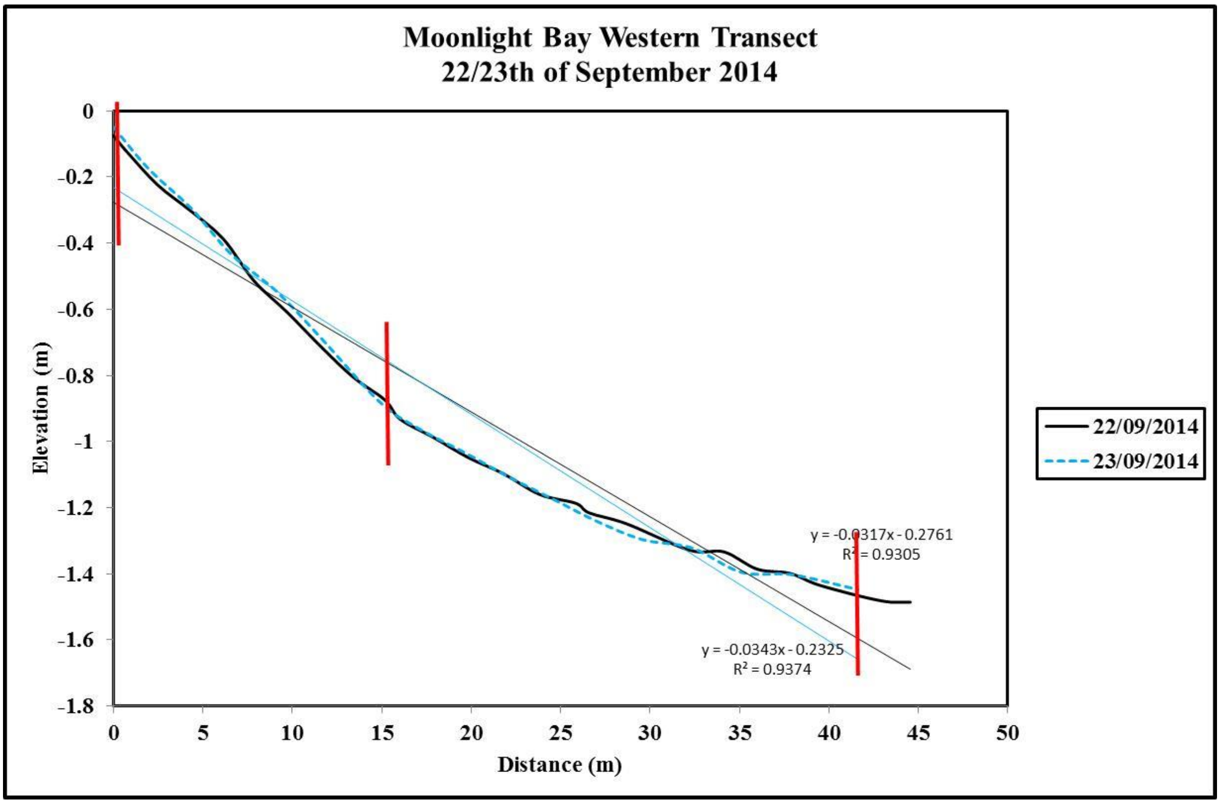
Moonlight Bay Western Transect
22/23th of September 2014
Elevation (m)
Distance (m)
22/09/2014
23/09/2014
y = -0.0317x - 0.2761
R² = 0.9305
y = -0.0343x - 0.2325
R² = 0.9374
0
-0.2
-0.4
-0.6
-0.8
-1
-1.2
-1.4
-1.6
-1.8
0 5 10 15 20 25 30 35 40 45 50

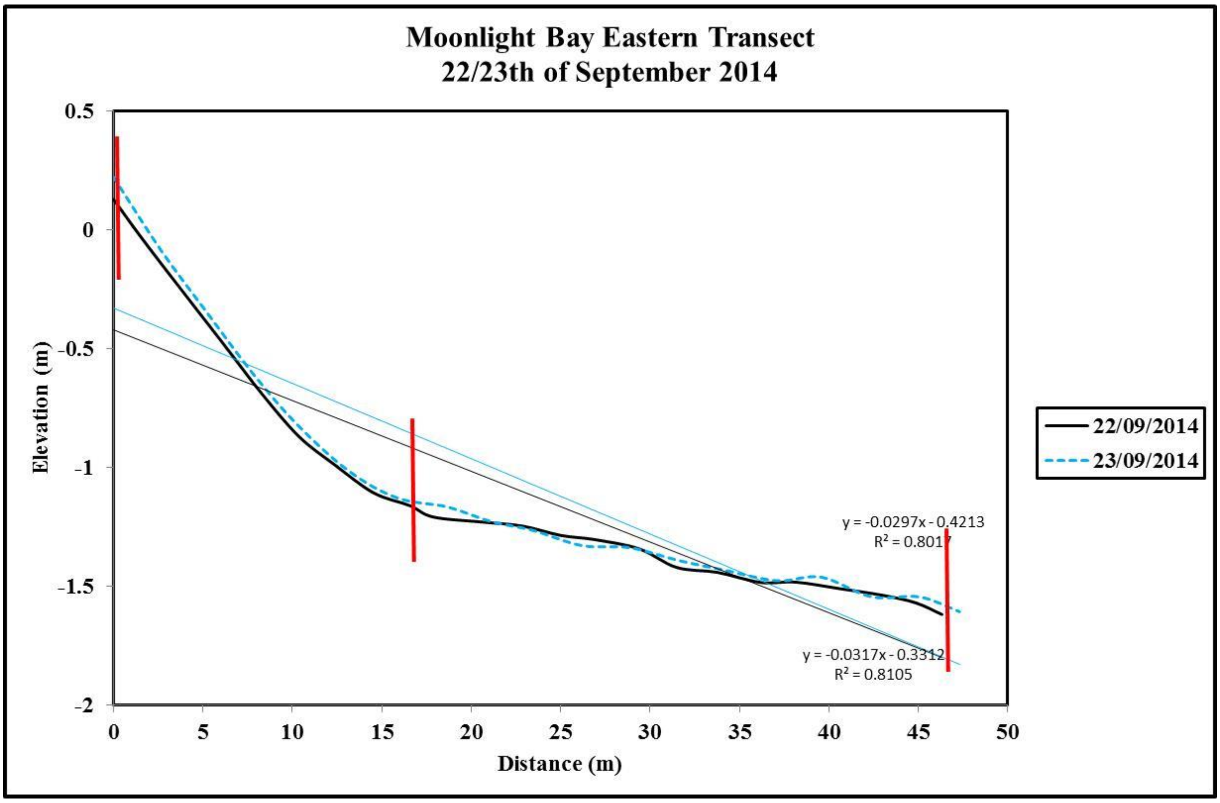
Moonlight Bay Eastern Transect
22/23th of September 2014
Elevation (m)
Distance (m)
22/09/2014
23/09/2014
y = -0.0297x - 0.4213
R² = 0.8017
y = -0.0317x - 0.3312
R² = 0.8105
0.5
0
-0.5
-1
-1.5
-2
0 5 10 15 20 25 30 35 40 45 50

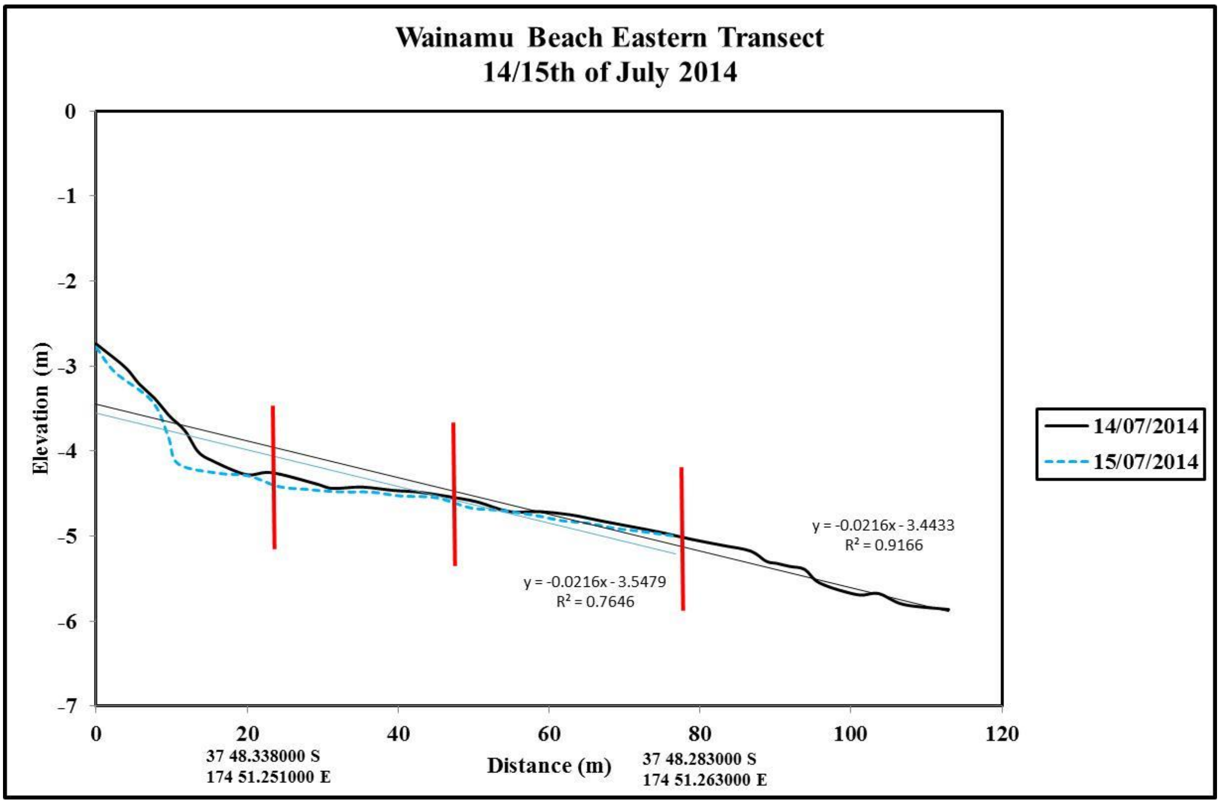
Wainamu Beach Eastern Transect
14/15th of July 2014
Elevation (m)
Distance (m)
0
-1
-2
-3
-4
-5
-6
-7
0
20
40
60
80
100
120
37 48.338000 S
174 51.251000 E
37 48.283000 S
174 51.263000 E
14/07/2014
15/07/2014
y = -0.0216x - 3.4433
R² = 0.9166
y = -0.0216x - 3.5479
R² = 0.7646

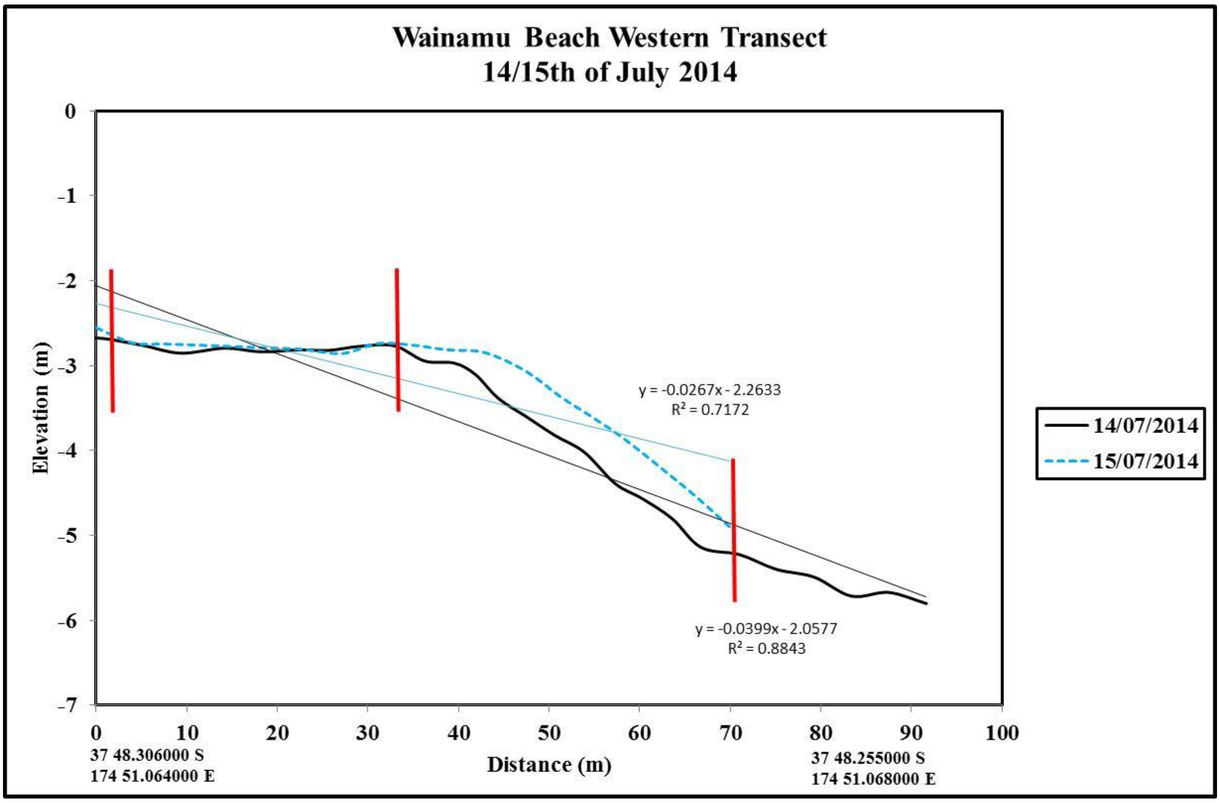
Wainamu Beach Western Transect
14/15th of July 2014
Elevation (m)
Distance (m)
0
-1
-2
-3
-4
-5
-6
-7
0
10
20
30
40
50
60
70
80
90
100
37 48.306000 S
174 51.064000 E
37 48.255000 S
174 51.068000 E
14/07/2014
15/07/2014
y = -0.0267x - 2.2633
R² = 0.7172
y = -0.0399x - 2.0577
R² = 0.8843

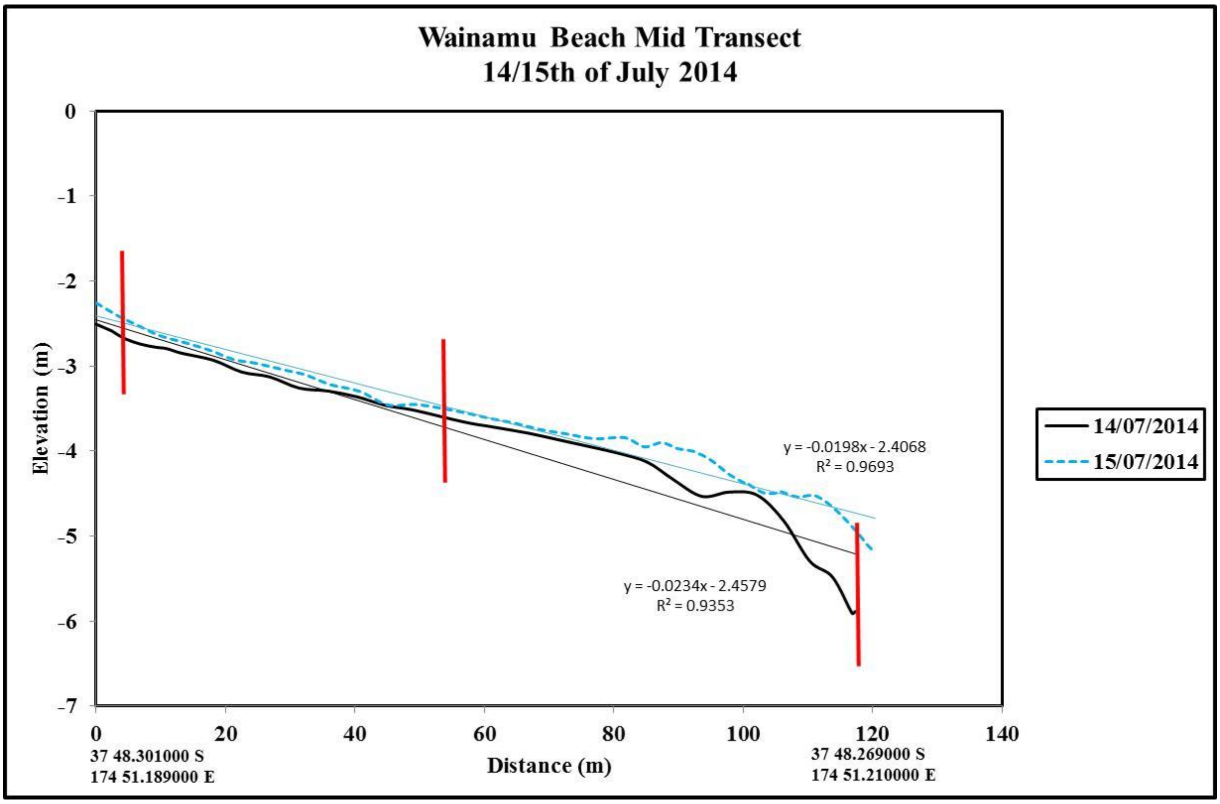

Wainamu Beach Mid Transect
14/15th of July 2014
Elevation (m)
Distance (m)
0
-1
-2
-3
-4
-5
-6
-7
0
20
40
60
80
100
120
140
37 48.301000 S
174 51.189000 E
37 48.269000 S
174 51.210000 E
y = -0.0198x - 2.4068
R² = 0.9693
y = -0.0234x - 2.4579
R² = 0.9353
14/07/2014
15/07/2014

APPENDIX VI: DEPTH OF DISTURBANCE MEASUREMENTS

VI. DEPTH OF DISTURBANCE MEASUREMENTS

DoD measurements are given in tables below.

NGARUNUI BEACH

19th AUGUST 2013

	Depth of disturbance (DoD) (mm)			***DoD difference (mm)***			
	Northern transect	***Mid transect***	***Southern transect***	***Difference N-M***	***Difference M-S***	***Average***	***s.d.***
Low tide position	64	76	42	12	34	61	17.24
Mid tide position	40	24	52	16	28	39	14.05
High tide position	n.d.	n.d.	n.d.				
Difference L-M	24	52	10				
Average	52	50	47				
s.d.	16.97	36.77	7.07				
	Erosion and deposition (mm)			***Erosional and depositional variation (mm)***			
Low tide position	(+) 15	(-) 20	0	35	20		
Mid tide position	(-) 23	(+) 10	0	33	10		
High tide position	n.d.	n.d.	n.d.				
Difference L-M	38	30	0				

21st JULY 2014

	Depth of disturbance (DoD) (mm)			***DoD difference (mm)***			
	Northern transect	***Mid transect***	***Southern transect***	***Difference N-M***	***Difference M-S***	***Average***	***s.d.***
Low tide position	335	30	25	305	5	130	177.55
Mid tide position	143	44	55	4	11	81	54.26
High tide position	n.d.	n.d.	n.d.	n.d.	n.d.		
Difference L-M	295	14	30				
Average	239	37	40				
s.d.	135.76	9.90	21.21				

	Erosion and deposition (mm)			***Erosional and depositional variation (mm)***	
Low tide position	(-) 295	(-) 27	(-) 25	268	2
Mid tide position	(-) 103	(-) 3	(-) 18	100	15
High tide position	n.d.	n.d.	n.d.	n.d.	n.d.
Difference L-M	192	24	7		

15th AUGUST 2014

	Depth of disturbance (DoD) (mm)			*DoD difference (mm)*			
	Northern transect	***Mid transect***	***Southern transect***	***Difference N-M***	***Difference M-S***	***Average***	***s.d.***
Low tide position	176	138	348 ** Fallen	38	210	157	26.87
Mid tide position	220	283	313 ** Bent	63	30	252	44.55
High tide position	98	114	55	16	59	89	30.51
Difference L-M	44	145	nd				
Difference M-H	122	169	nd				
Average	165	178	55				
s.d.	62	91	nd				
	Erosion and deposition (mm)			***Erosional and depositional variation (mm)***			
Low tide position	(-) 23	(-) 20	(-) 198 **Fallen	3	178		
Mid tide position	(-) 20	(-) 140 ** Bent	(+) 215** Bent	120	425		
High tide position	(+) 4	0	(+) 5	4	5		
Difference L-M	3	120	483				
Difference M-H	24	140	280				

30th AUGUST 2014

	Depth of disturbance (DoD) (mm)			*DoD difference (mm)*			
	Northern transect	***Mid transect***	***Southern transect***	***Difference N-M***	***Difference M-S***	***Average***	***s.d.***
Low tide position	44	62	42	18	20	49	11.02
Mid tide position	68	55	39	13	16	54	14.53
High tide position	(+) 5	(+) 15	(+) 16	10	1	12	6.08
Difference L-M	24	7	3				
Difference M-H	73	70	55				
Average	39	44	32.33				
s.d.	31.80	25.36	14.22				

	Erosion and deposition (mm)			*Erosional and depositional variation (mm)*	
Low tide position	0	(+) 30	(+) 20	30	10
Mid tide position	(-) 5	0	(-) 5	5	5
High tide position	(+) 40	(+) 20	(+) 38	20	18
Difference L-M	5	30	25		
Difference M-H	45	20	43		

27th SEPTEMBER 2014

	Depth of disturbance (DoD) (mm)			***DoD difference (mm)***			
	Northern transect	***Mid transect***	***Southern transect***	***Difference N-M***	***Difference M-S***	***Average***	***s.d.***
Low tide position	59	134	204	75	70	132	72.51
Mid tide position	43	70	150	27	80	88	55.64
High tide position	(+) 2	40	84	38	44	42	41.04
Difference L-M	16	64	54				
Difference M-H	45	30	66				
Average	25	81.33	146				
s.d.	29	48	60				
	Erosion and deposition (mm)			***Erosional and depositional variation (mm)***			
Low tide position	(+) 23	0	(-) 50	23	50		
Mid tide position	(+) 7	(+) 25	(+) 13	18	12		
High tide position	(+) 12	(-) 15	(-) 23	3	8		
Difference L-M	16	25	63				
Difference M-H	5	40	36				

25th OCTOBER 2014

	Depth of disturbance (DoD) (mm)			*DoD difference (mm)*			
	Northern transect	***Mid transect***	***Southern transect***	***Difference N-M***	***Difference M-S***	***Average***	***s.d.***
Low tide position	51	** Bent 211	n.d.	nd	n.d.	51	n.d.
Mid tide position	80	65	18	15	47	54.33	32.35
High tide position	28	10	(+) 15	18	25	18	9.29
Difference L-M	29	nd	n.d.				
Difference M-H	52	55	33				
Average	53	38	16.5				
s.d.	26.06	38.89	2.12				
	Erosion and deposition (mm)			***Erosional and depositional variation (mm)***			
Low tide position	0	(+) 56	n.d.	56	n.d.		
Mid tide position	(-) 75	(+) 10 *	(-) 70	85	80		
High tide position	(-) 14	(-) 4	(+) 19	10	23		
Difference L-M	75	46	n.d.				
Difference M-H	14	14	89				

<u>26th NOVEMBER 2014</u>

	Depth of disturbance (DoD) (mm)			*DoD difference (mm)*			
	Northern transect	***Mid transect***	***Southern transect***	***Difference N-M***	***Difference M-S***	***Average***	***s.d.***
Low tide position	56	110	43	54	67	70	35.53
Mid tide position	60	55	10	5	45	40	27.54
High tide position	29	n.d.	40	n.d.	n.d.	33	7.78
Difference L-M	4	55	33				
Difference M-H	31	n.d.	30				
Average	48	83	31				
s.d.	17	39	18				
	Erosion and deposition (mm)			***Erosional and depositional variation (mm)***			
Low tide position	0	(-) 25	(-) 10	29	15		
Mid tide position	(+) 4	(-) 16	(-) 30	20	14		
High tide position	(+) 4	n.d.	0	n.d.	n.d.		
Difference L-M	0	9	20				
Difference M-H	4	n.d.	30				

5th FEBRUARY 2015

	Depth of disturbance (DoD) (mm)			*DoD difference (mm)*			
	Northern transect	***Mid transect***	***Southern transect***	***Difference N-M***	***Difference M-S***	***Average***	***s.d.***
Low tide position	200	294 ** Fallen	266	4	28	233	46.67
Mid tide position	158	159	131	1	48	143	15.89
High tide position	92	122	170	30	48	128	39.34
Difference L-M	42	135	155				
Difference M-H	66	37	59				
Average	150	141	189				
s.d.	54.44	26.16	69.48				

	Erosion and deposition (mm)			*Erosional and depositional variation (mm)*	
Low tide position	(-) 50	(-) 120	(-) 110	70	10
Mid tide position	0	(-) 40	(+) 20	40	60
High tide position	(-) 73	(-) 64	(-) 120	9	56
Difference L-M	50	80	130		
Difference M-H	73	24	140		

NGARUNUI BEACH SOUTH

10th FEBRUARY 2015

	Depth of disturbance (DoD) (mm)				***DoD difference (mm)***				
	Transect 1	***Transect 2***	***Transect 3***	***Transect 4***	***Difference 1-2***	***Difference 2-3***	***Difference 3-4***	***Average***	***s.d***
Low tide position	30	23	28	n.d.	7	5	nd	27	3.6
Mid tide position	83	81	98	80	2	17	18	86	8.4
High tide position	60	65	65	67	5	0	2	64	2.9
Difference L-M	53	58	70	n.d.					
Difference M-H	23	16	33	13					
Average	58	56	64	73.5					
s.d.	27	30	35	9					

	Erosion and deposition (mm)				***Erosional and depositional variation (mm)***		
Low tide position	(+) 15	(+) 8	(+) 15	(+) 16	7	7	1
Mid tide position	(-) 20	(-) 6	0	(-) 5	14	6	5
High tide position	(+) 10	(+) 12	0	(+) 9	2	12	9
Difference L-M	35	14	15				
Difference M-H	30	18	0				

WAINAMU BEACH

14/15th JULY

	Depth of disturbance (DoD) (mm)			*DoD difference (mm)*			
	Western transect	***Mid transect***	***Eastern transect***	***Difference W-M***	***Difference M-E***	***Average***	***s.d.***
Low tide position	8	20	Lost	12	n.d.	14	8.49
Mid tide position	35	6	4	29	2	12	17.35
High tide position	Fallen	26	30	n.d.	4	28	2.83
Difference L-M	27	14	n.d.				
Difference M-H	n.d.	20	26				
Average	22	17	17				
s.d.	19	10	18				
	Erosion and deposition (mm)			***Erosional and depositional variation (mm)***			
Low tide position	0	0	Lost	0	n.d.		
Mid tide position	(+) 10	(-) 6	(-) 4	16	2		
High tide position	Fallen	(-) 14	(-) 10	n.d.	4		
Difference L-M	10	6	n.d.				
Difference M-H	n.d.	8	4				

15/16th JULY 2014

	Depth of disturbance (DoD) (mm)			*DoD difference (mm)*			
	Western transect	*Mid transect*	*Eastern transect*	*Difference W-M*	*Difference M-E*	*Average*	*s.d.*
Low tide position							
Mid tide position	12	12	4	0	8	9	4.62
High tide position	20	10	16	10	6	15	5.03
Difference L-M	12	12	4				
Difference M-H	8	-2	12				
Average	16	11	10				
s.d.	5.66	1.41	8.49				

	Erosion and deposition (mm)			*Erosional and depositional variation (mm)*	
Low tide position					
Mid tide position	(-) 12	(-) 12	(-) 4	0	8
High tide position	(-) 20	(-) 10	(-) 10	10	0
Difference L-M					
Difference M-H	8	2	4		

27/28th NOVEMBER

	Depth of disturbance (DoD) (mm)			*DoD difference (mm)*			
	Western transect	***Mid transect***	***Eastern transect***	***Difference W-M***	***Difference M-E***	***Average***	***s.d.***
Low tide position	n.d.	60	n.d.	n.d.	n.d.	60	n.d.
Mid tide position	0	10	16	10	6	9	8.08
High tide position	20	2	3	18	1	8.33	10.12
Difference L-M	n.d.	50	n.d.				
Difference M-H	20	8	13				
Average	10	24	10				
s.d.	14.14	31.43	9.19				
	Erosion and deposition (mm)			***Erosional and depositional variation (mm)***			
	n.d.	(-) 14	n.d.	n.d.	n.d.		
	0	(-) 10	(-) 16	10	6		
High tide position	(+) 4	0	0	4	0		
Difference L-M	n.d.	4	n.d.				
Difference M-H	4	10	16				

11/12th DECEMBER 2014

	Depth of disturbance (DoD) (mm)			***DoD difference (mm)***			
	Western transect	***Mid transect***	***Eastern transect***	***Difference W-M***	***Difference M-E***	***Average***	***s.d.***
Low tide position	8	16	0	8	16	8	8
Mid tide position	0	6	0	6	6	2	3.46
High tide position	0	5	0	5	5	2	2.89
Difference L-M	8	10	0				
Difference M-H	0	1	0				
Average	3	9	0				
s.d.	5	6	0				
	Erosion and deposition (mm)			***Erosional and depositional variation (mm)***			
Low tide position	(-) 8	(-) 13	0	5	13		
Mid tide position	0	(-) 6	0	6	6		
High tide position	0	0	0	0	0		
Difference L-M	8	7	0				
Difference M-H	0	6	0				

MOONLIGHT BAY

22/23th SEPTEMBER 2014

	Depth of disturbance (DoD) (mm)		***DoD difference (mm)***		
	Western transect	***Eastern transect***	***Difference W-E***	***Average***	***s.d.***
Low tide position	0	0	0	0	0
Mid tide position	0	0	0	0	0
High tide position	0	5	3	2.5	3.54
Difference L-M	0	0			
Difference M-H	0	5			
Average	0	1.67			
s.d.	0	2.89			

	Erosion an.d. deposition (mm)		***Erosional an.d. depositional variation (mm)***
Low tide position	0	0	0
Mid tide position	0	0	0
High tide position	0	5	0
Difference L-M	0	0	
Difference M-H	0	5	

APPENDIX VII: DEPTH OF DISTURBANCE MEASUREMENTS

VI. WAVE, TIDE AND WIND CONDITIONS

Tides times and heights for Raglan during DoD experiments.

Tides	***High***	***Low***	***High***	***Low***	***High***
18th September 2013	-	02:28 0.3 m	08:55 3.2 m	14:50 0.2 m	21:15 3.4 m
19th September 2013	-	03:16 0.1 m	09:42 3.4 m	15:36 0.1 m	21:59 3.5 m
14th July 2014	-	04:56 0.1 m	11:20 3.4 m	17:17 0.0 m	23:42 3.6 m
15th July 2014	-	05:46 0.0 m	12:10 3.4 m	18: 05 0.0 m	-
16th July 2014	00:31 3.5 m	06:36 0.1 m	13:00 3.3 m	18:54 0.2 m	-
20th July 2014	04:08 2.9 m	10:12 0.7 m	16:45 2.7 m	22:44 0.9 m	-
21st July 2014	05:11 2.7 m	11:16 0.8 m	17:54 2.7 m	23:53 0.9 m	-
14th August 2014	00:16 3.6 m	06:14 0.0 m	12:44 3.5 m	18:34 0.1 m	-
15th August 2014	01:04 3.5 m	07:00 0.1 m	13:31 3.3 m	19:21 0.3 m	-
29th August 2014	-	05:53 0.4 m	12:15 3.1 m	18:07 0.4 m	-
30th August 2014	00:28 3.1 m	06:30 0.4 m	12:50 3.1 m	18:46 0.5 m	-
22nd September 2014	-	02:32 0.7 m	08:52 3.0 m	14:48 0.6 m	21:10 3.1 m
23rd September 2014	-	03:07 0.5 m	09:31 3.1 m	15:22 0.5 m	21:46 3.2 m
26th September 2014	-	4:50 0.3 m	11:16 3.3 m	17:06 0.3 m	23:29 3.2 m
27th September 2014	-	05:26 0.3 m	11:51 3.2 m	17:44 0.3 m	-
24th October 2014	-	04:46 0.3 m	11:16 3.3 m	17:04 0.3 m	22:30 3.3 m
25th October 2014	-	05:24 0.2 m	11:53 3.3 m	17:43 0.3 m	-
27th November 2014	02:05 3.2 m	08:00 0.3 m	14:30 3.3 m	20:31 0.4 m	-
28th November 2014	02:57 3.1 m	08:51 0.4 m	15:22 3.2 m	20:31 0.4 m	
11th December 2014	01:44 2.9 m	07:38 0.6 m	14:02 3 m	21:24 0.5 m	-
12th December 2014	02:21 2.8 m	08:16 0.7 m	14:39 2.9 m	20:46 0.8 m	-
5th February 2015					
6th February 2015					
10th February 2015	14:53	21:02	-	-	-
11th February 2015	03:17 2.8 m	09:20 0.8 m	15:36 2.8 m	21:48 0.8 m	-

Wave climate and wind conditions for Ngarunui Beach and Raglan Bar during DoD experiments on the 9th of July, 2014.

Wave Climate	*Swell height (m) and Direction*	*Wave height (m) and Set face (m)*	*Period (s)*	*Wind Direction and Speed (kts)*	*Atmospheric Pressure (mba)*
18th September 2013	0.6 (SW)	1.2 (n.d.)	15-17	3-15 (SE-NE)	n.d.
19th September 2013	0.5 (SW)	1.1 (0.7-1.2)	13-17	3-15 (SE-NE)	n.d.
14th July 2014	1.5-1.7 (SW)	1.5-1.7 (1.8-2.2)	12-17	8-18 (SE-SW)	1007-1008 W
15th July 2014	1-1.5 (SW)	1-1.5 (2.2)	15	8-18 (E-S)	1009 M
16th July 2014	1 (SW)	1 (1.5)	13	8-18 (SW-E)	1004 M
20th July 2014	1-1.2 (W)	1-1.3 (2)	15-16	10-22 (SSE)	995 W 990 M
21st July 2014	1.5-1.7 (W-SW)	1.6-1.8 (2)	12-15	5-30 (SW-S)	1000 M 998 - 1000 M
14th August 2014	2-3 (W)	2.8-3.2 (2.8-3.2) 2 (1.5-2)	15-10	24-36 (W-SW)	1006 M 1005 W
15th August 2014	2 (SW)	2.6 (2.8)	13-15	18-32 (SW)	1010 M 1006-1010 W
29th August 2014	1-1.1 (SW-W)	n.d. (1.4-1.7)	14-18	20-30 (E)	1000 M 1027 – 1032 W
30th August 2014	1.1-1.3 (SW)	n.d. (1.8-2)	16-18	8-30 (E)	1025-1029 W
22nd September 2014	2-3 (W)	2.8-3.8 (2.8-3.8)	12-14	(SW-S)	996-1014 W 998 M
23rd September 2014				SW)	1016-1019 W 1018 M
26th September 2014	1.1-1.2 (SW)	1.1-1.3 (1.5-1.9)	13-15	5-20 (SE-NW)	1017 M 1016-1018 W
27th September 2014					1006-1015 W
24th October 2014	1 (SW)	0.6-0.9	12	17-21(SW)	1012 M 1013-1018 W
25th October 2014	1.2-1.5 (SW)	1.4-1.7 (1.8-2.1)	13-15	10-17 (SW)	997 M 1021-1024 W
26th November 2014					
27th November 2014	1-1.2 (SW)	1.4-1.8 (1.5-1.8)	13-15	10-20 (W)	1015 M 1013 M
11th December 2014	1-0.8 (W-SW)	1.5-1.25 (1.5-1.25)	8	10-20 (W)	1008-1010 W 1012 M
12th December 2014	0.7-0.8 (SW)	1.3 (1.3)	12	8-15 (SW)	1010-1011 W

10th February 2015	0.9-1.1 (SW)	1.1-1.3 (1.4-1.6)	13	10-20 (S-E)	1022 M 1021 – 1030 W
11th February 2015	1..3(SW)	1.3 (1.7)	13	23-0 (E)	1029-1031 W 1000 M

Wave conditions

19th August 2013	***Small to moderate wave conditions***
20th July 2014	***Small waves offshore, inconsistent swell.***
21st July 2014	***3-4 ft waves, some larger.***
14th August 2014	***Very large swell, mostly wind swell.***
29th August 2014	***Small surf, overcast, no rain.***
30th August 2014	***Clean surf, long lulled groundswell.***
22nd September 2014	***Storong onshore winds and big storm surf.***
23rd September 2014	***Short period and groundswell.***
27th September 2014	***2 ft crumbly lingering waves***
	Moderate – small swell, crumbly, messy
26th September 2014	***Still swell present , sea breeze rising later.***
27 th November 2014	***Small crumbly waves, front approaching with increasing swell, WSW turns WNW***
10th February 2015	***Small surf, long lulls between waves***
	Small swell, winds picking up and turning. Small mid-period swell.
15th July 2014	***Moderate sweels***
16th July 2014	***Small long period swell, light winds***
21st July 2014 20 ?	***Small, long period swell.***
21st July 21014??	***Moderate long swell.***
14th July 2014	***Gentle breeze, moderate swell***
11th December 2014	***Light winds. Small – moderate low period waves.***
12th December 2014	***Light onshore winds. Small short period wind waves and chop.***